Basics of precipitation measurement from space

Kenji Nakamura
Hydrospheric Atmospheric Research Center
Nagoya University

International Hydrological Programme
Precipitation Measurement from Space and its Applications
The Twenty-second IHP Training Course
18 November - 1 December, 2012

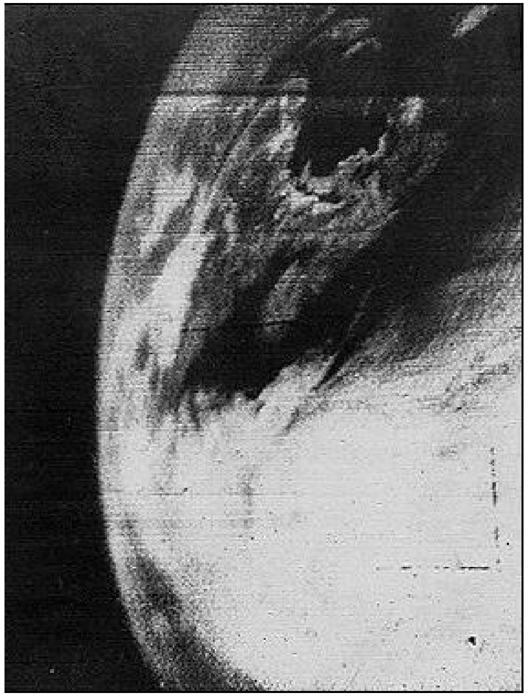

1957: First satellite Sputok

1960-65: TIROS-1, -10

(Television and Inra-Red Observation Satellite)

120-140 kg

1966-69: ESSA-1, -9

Operated by Environmental Science Service Administration

→ NOAA

1970-: NOAA series

From TIROS-1 in 1960

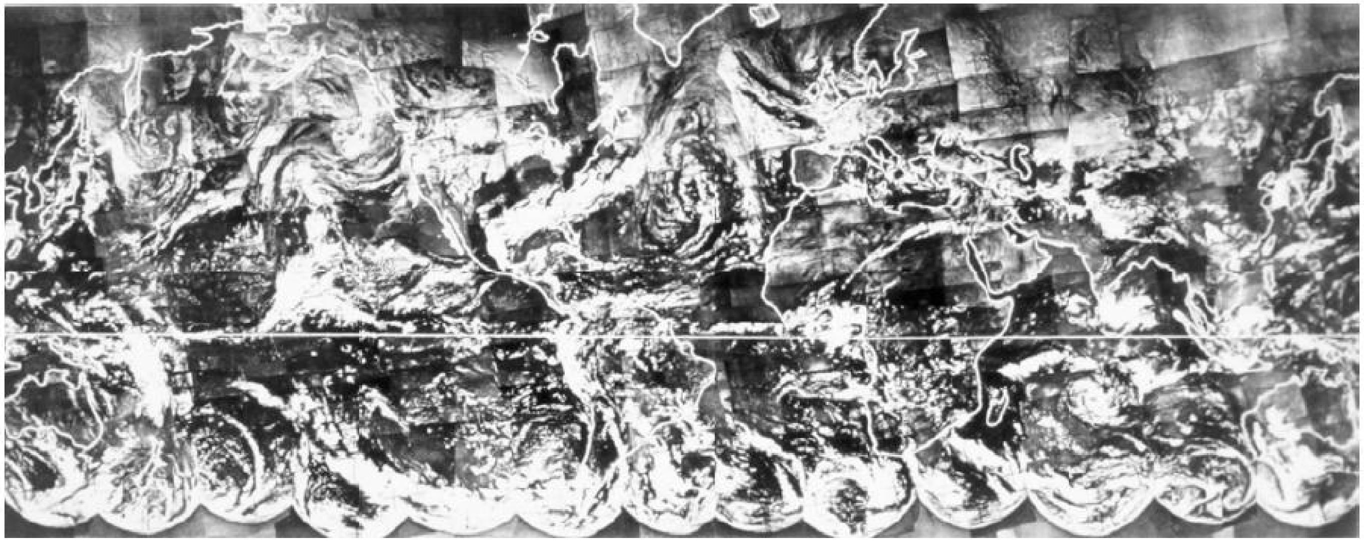

(composite image of clouds for 13 Feb. 1965 from TIROS-9 (Earth Observations from Space, 2008)

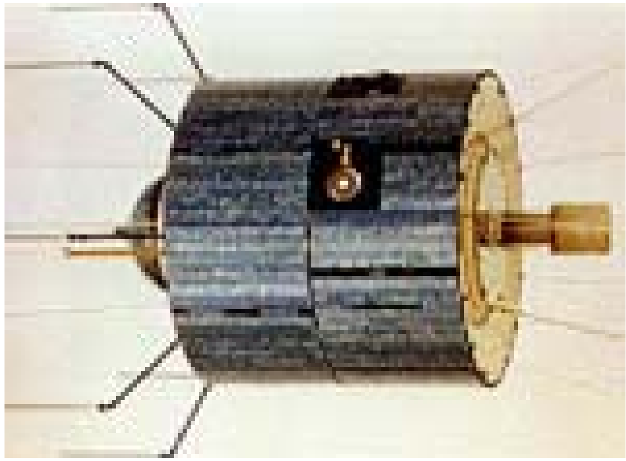

http://science.nasa.gov/missions/ats/

Applications Technology Satellite (ATS) (NASA)

ATS-1: Launch: 7 Dec, 1966.

- Geostationary orbit
- Spin stabilized
- Dry weight: 352 kg, Length: 1.35 m
- Communication text instruments
- Spin scan cloud camera: every 30 minutes
- Visible 1 channel
- Pixel: 4.6 km at nadir

ATS-3: Nov. 1967

- Visible 3 channels

From ATS-3 in 1970

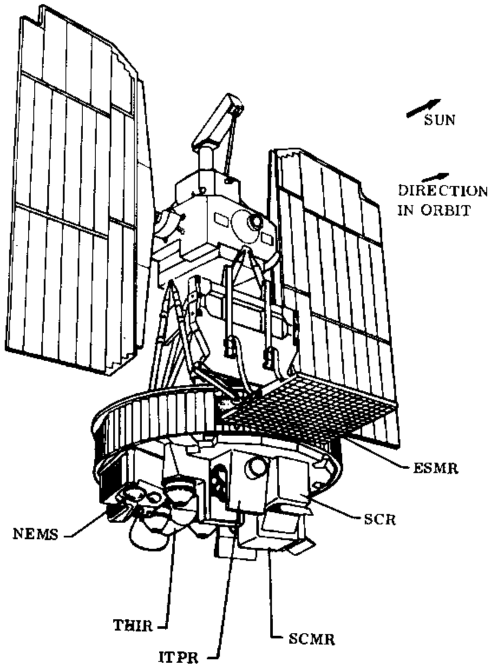

1964-1978: NIMBUS series (NASA)

Less than one month

Visible/infrared channels

1972: Nimbus-5, 10 years,

Electrically scanning Microwave Radiometer

(ESMR) (1.55 cm wavelength)

SST, snow cover, sea ice, first/multi-year ice, rainfall,

etc.

1978: Nimbus-7, > 9 years

Scanning Multichannel Microwave Radiometer

(SMMR)

0.8, 1.4, 1.7, 2.7, and 4.6 cm (H/V)

The Weddell Polynya as Seen with ESMR

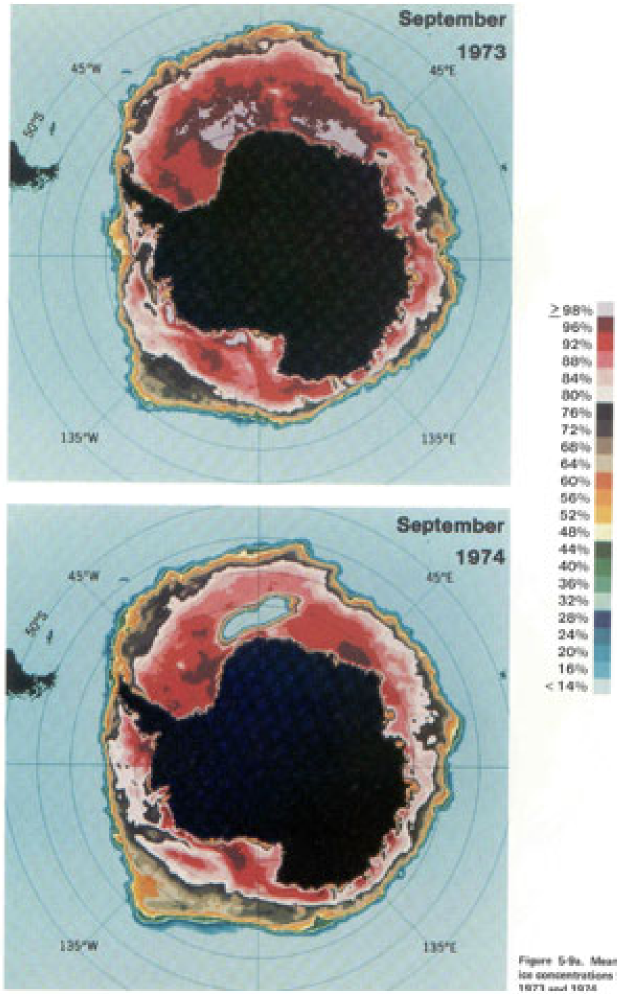

Figure 5-9a. Mean monthly ice concentrations for Septemb 1973 and 1974

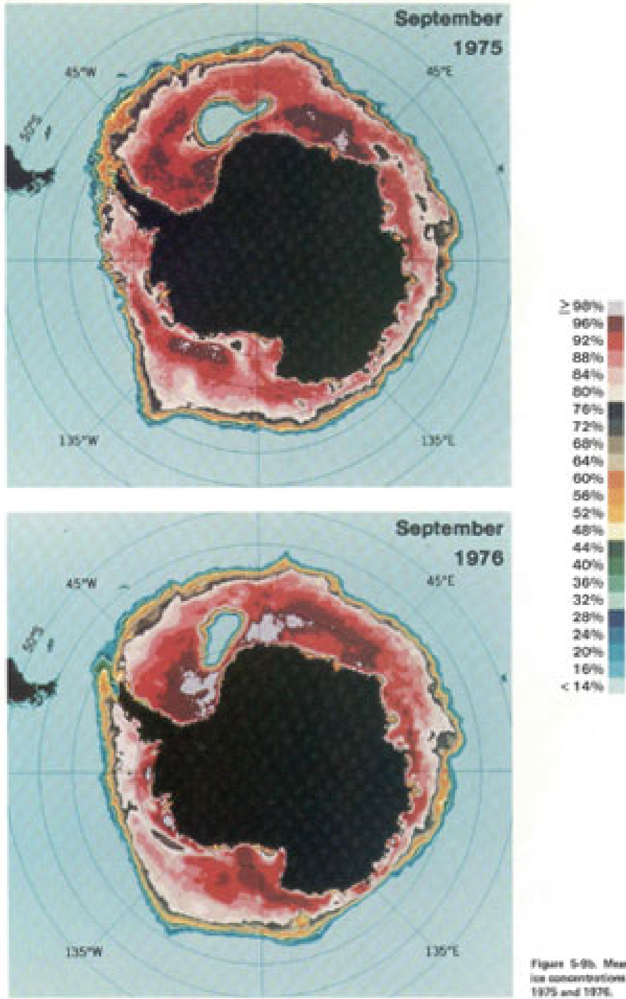

Figure 5-9b. Mean monthly sea ice concentrations for September 1975 and 1976.

Arctic sea ice distribution for 1980-2000 from microwave radiometers

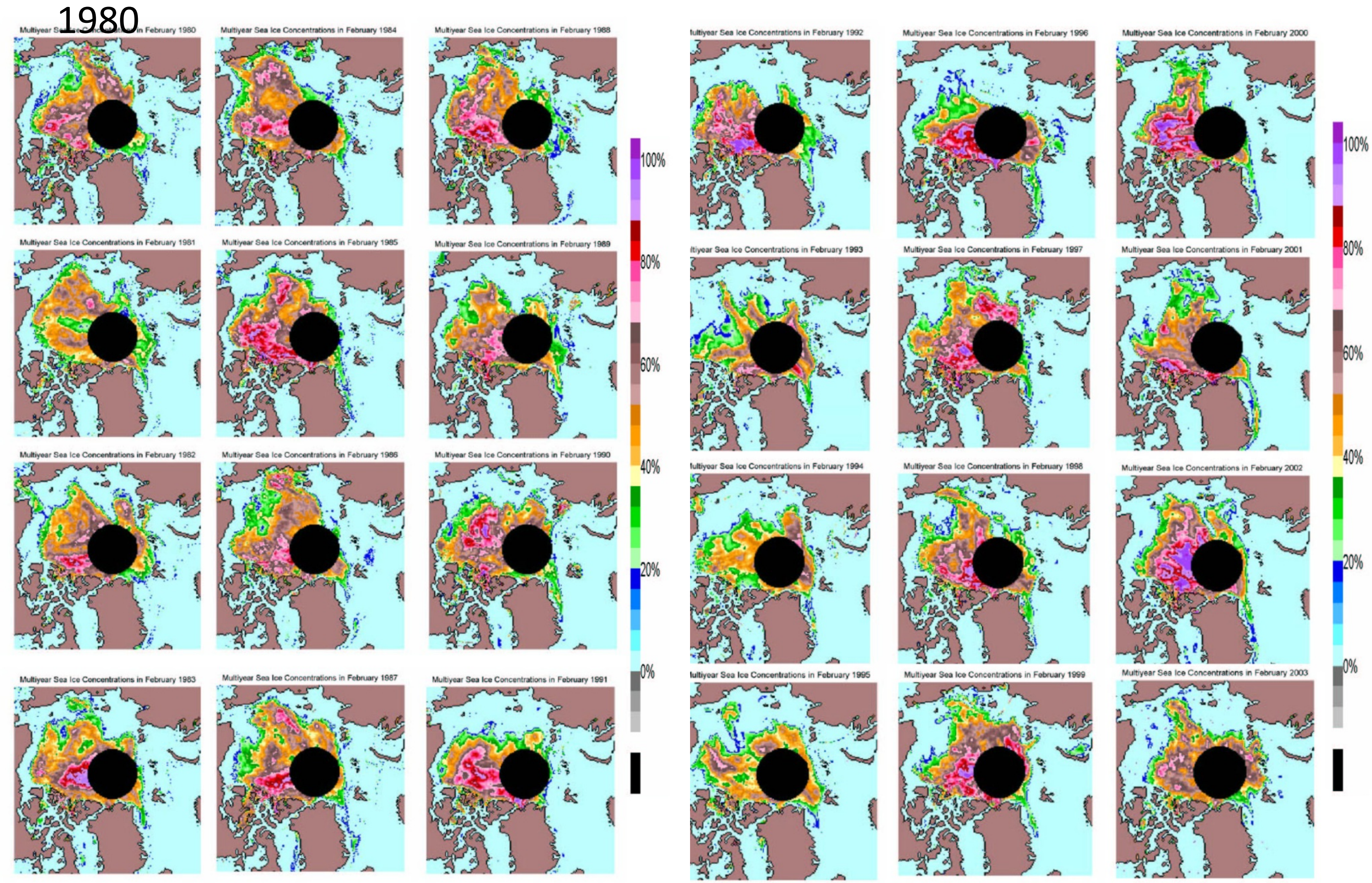

2000
(NASA)

SEASAT

Launched in 1978 by NASA

Operated for 105 days

Orbit: Altitude: 800 km,

Inclination: 108 degrees

Active microwave sensors:

- Altimeter: spacecraft height from ocean surface
- Sscatterometer: ocean surface wind
- Synthetic aperture radar (SAR): ocean surface
- SMMR: Sea surface temperature

VIS/IR radiometer:

cloud, land, water features

Earth observation from space

Remote sensing using optical waves or microwaves

Transparency of atmosphere

Exceptions: gravity mission, occultation technique

Orbit of satellite

Low Earth Orbit (LEO).

Altitude: 350-1000 km

Generally, polar orbit

Exceptions: TRMM, Megha-Tropique

Sensors: passive/active, optical/microwave

Geostationary Earth Orbit (GEO)

Altitude: 36,000 km

Above equator

Exception:

Sensors: optical, passive

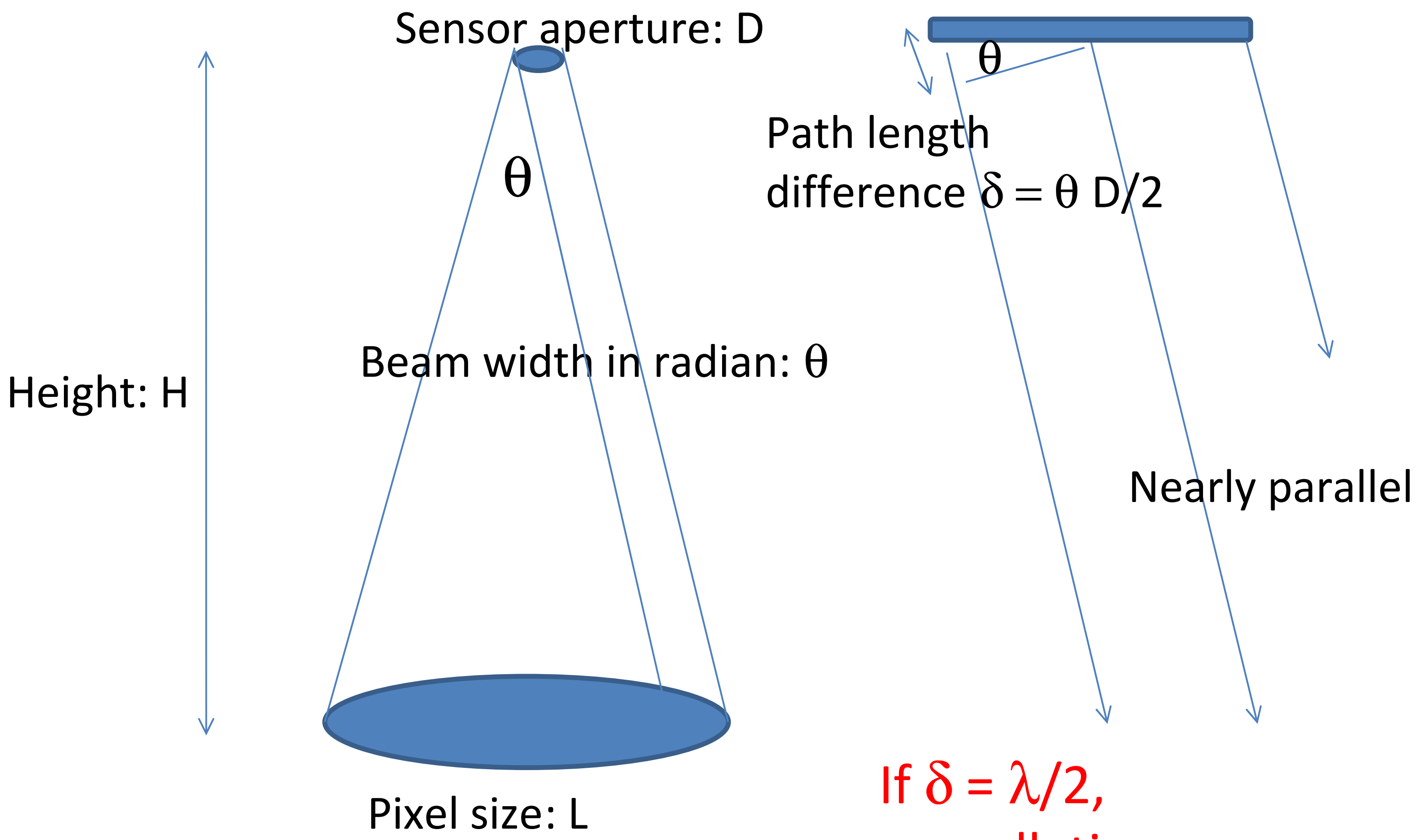

If $\delta = \lambda/2$,
cancellation occurs.

Beam width θ = c x λ / D

(c: order of 1)

Pixel size on the Earth's surface = c x Height x θ

Example:

Microwave of 10 GHz ($3 \times 10^9\ s^{-1}$)

Lambda = 300 M m s^{-1} / 10 GHz = 3 cm

Antenna size of 1 m

Satellite Height of 1000 km

→ Pixel size = c x 3 cm / 1 m x 1000 km = c x 30 km

Satellite Height of 36,000 km

→ Pixel size = c x 1000 km

Similarly for optical wave

Optical wave of 1 micrometer (1×10^{-6} m)

Aperture diameter of 10 cm

→ Pixel size = c x 1 micrometer / 10 cm x 36000 km = c x 360 m

Satellite Orbit

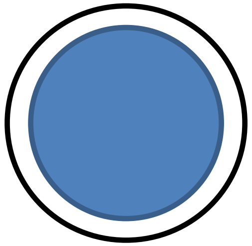

LEO: altitude:
350-1,000 km
Period: 90 min.

GPS: 20,200 km

GEO: 35,800 km
Period: 24 hours

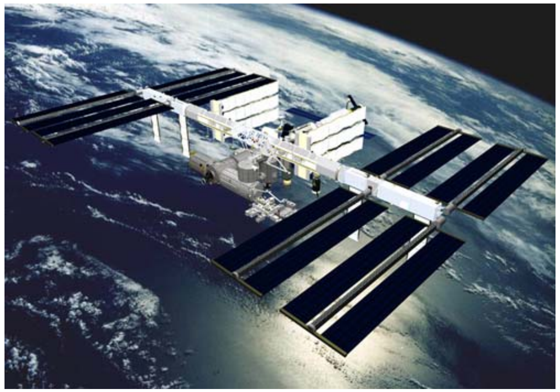

ISS at about 400 km altitude
(from JAXA website)

Instantaneous observation

Eclipse on 21 May 2012 (from JAXA website)

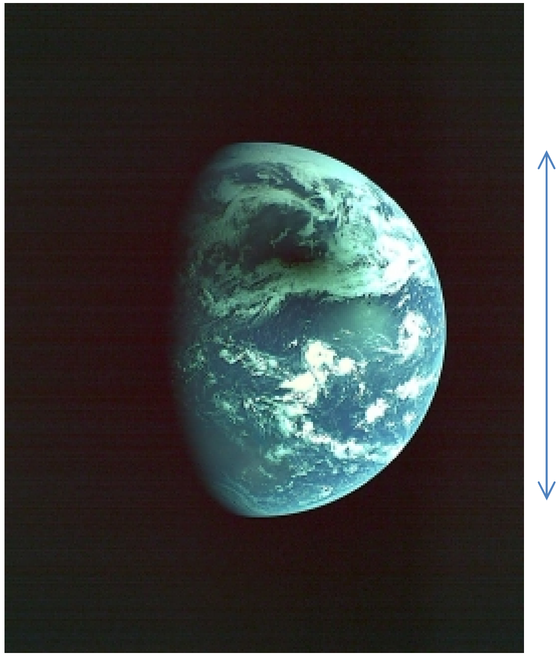

20
deg

Quasi-continuous observation

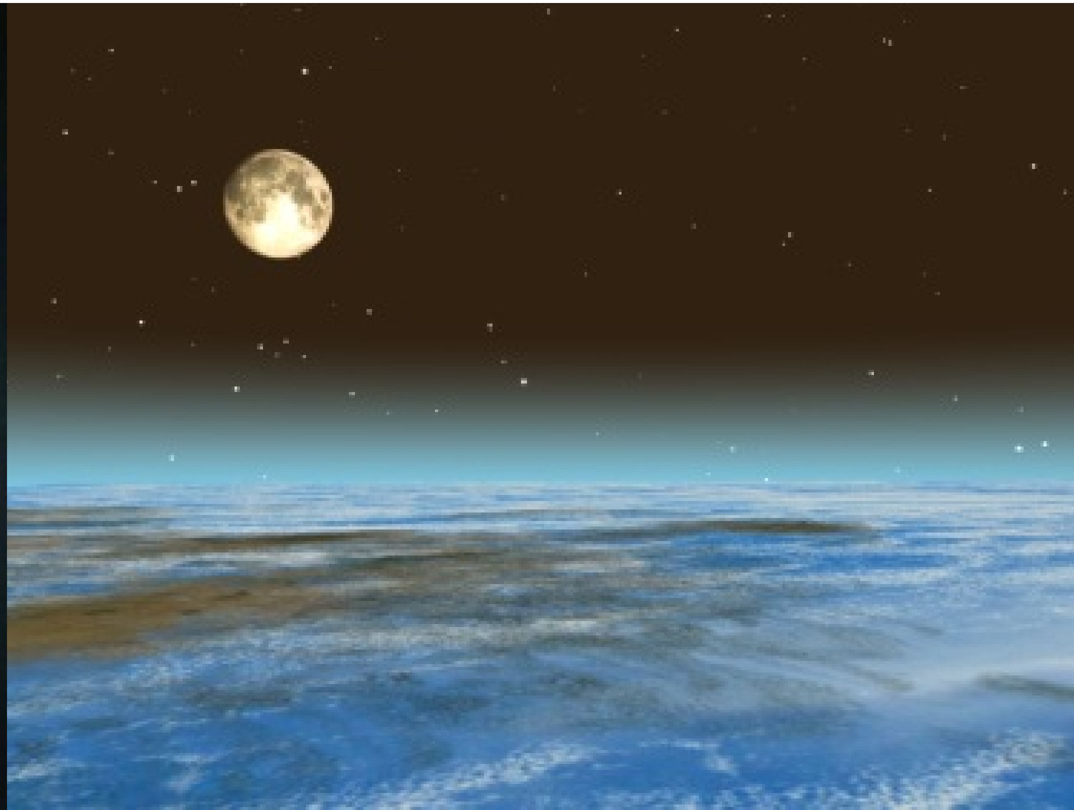

Eclipse by Earth.
Thin atmosphere

(http://www.jaxa.jp)

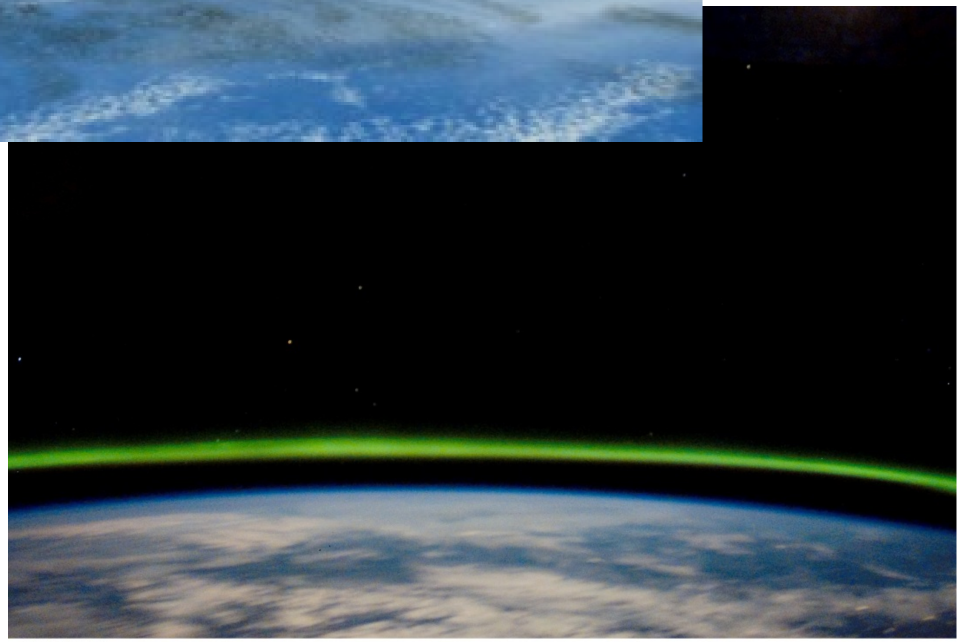

S123E008022

Aurola at 100-150km height. Green light is from atomic oxygen.

Newton's law

$$GMm/r^2 = mv^2/r$$

And

$$GM/r_e^2 = g,\ r_e = 6{,}400\text{ km},\ g = 10\text{ m s}^2,$$

Then

$$v = r_e \text{ root } (g/r)$$

For e

Example: near Earth's surface: v = 8 km/s

Period:

$$T = 2\pi r / v$$

Then

$$T = 2\pi\ (r/r_e) \text{ root } (r/g)$$

Example:

Near Earth's surface: T = 90 min.

r = 36,000 km: T = 24 hours

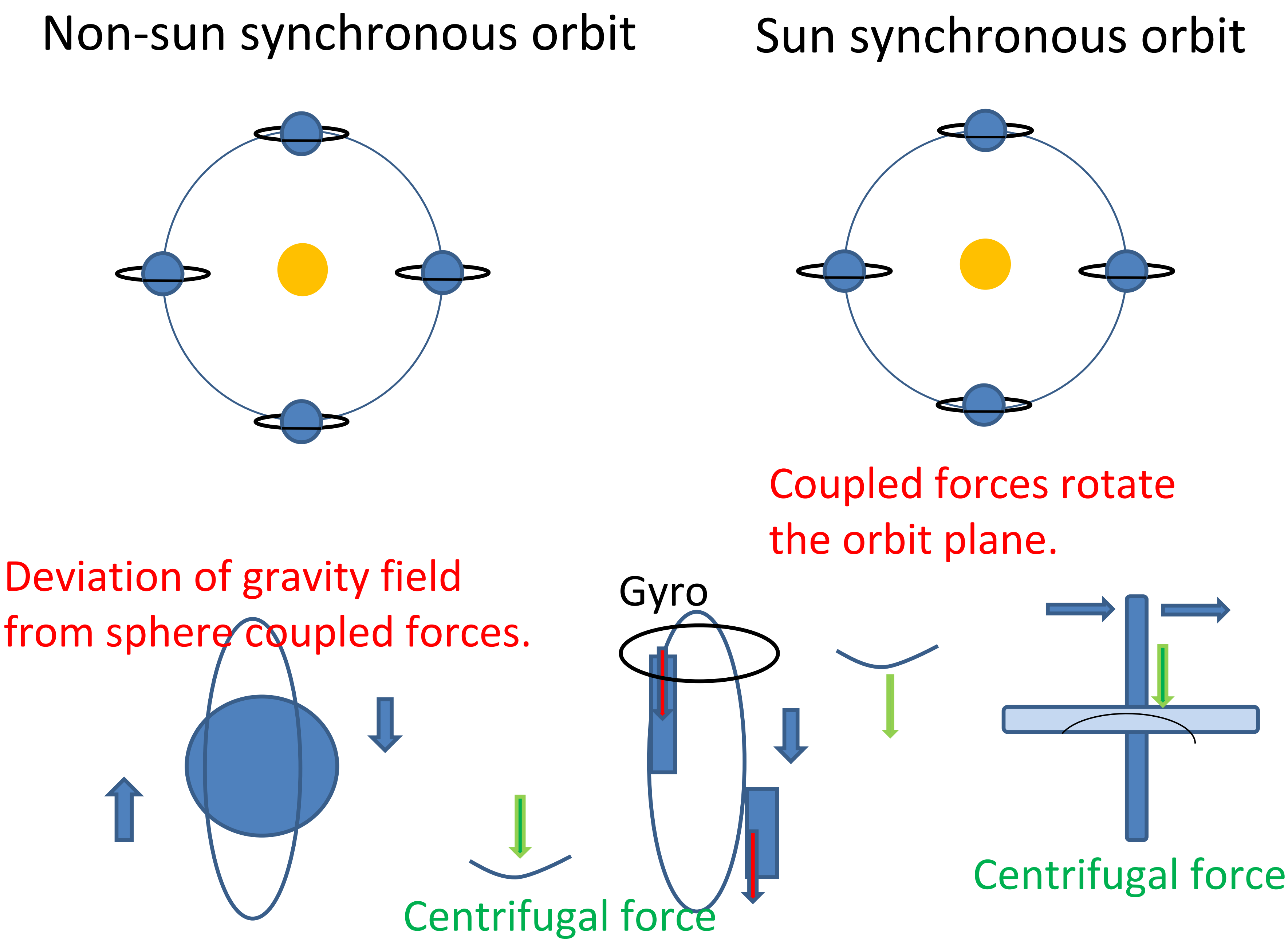
Non-sun synchronous orbit
Sun synchronous orbit
Coupled forces rotate
the orbit plane.
Deviation of gravity field
from sphere coupled forces.
Gyro
Centrifugal force
Centrifugal force

Rotation of the orbit plane:

-0.58 deg. $(R_e/r)^2$ x cos (i) / revolution

Solar movement:

360 degrees / year

For low orbit, 16 revolution / day

→ Roughly 1 degree / day

→ cos (i) = 0.11 → i = 97 degrees

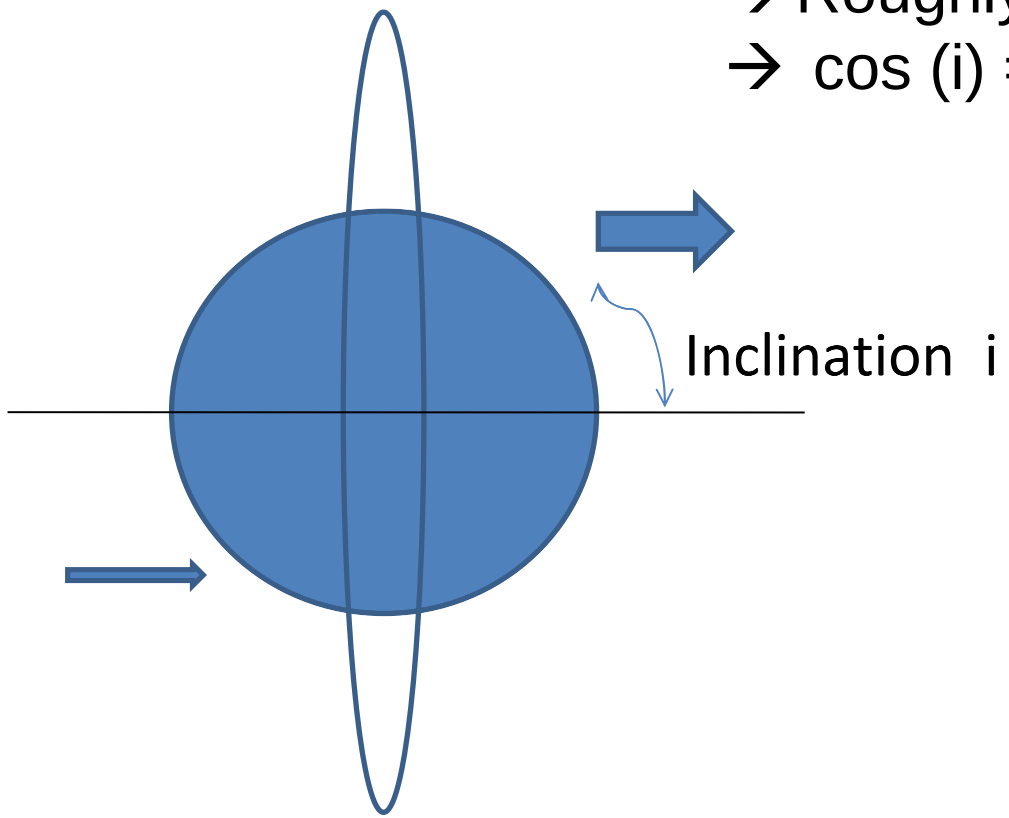

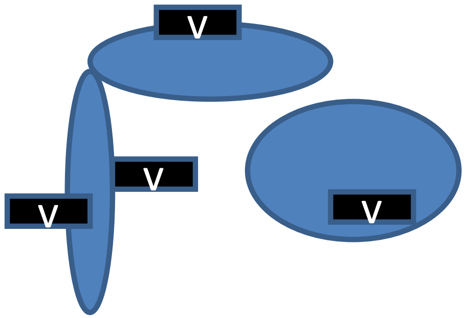

Three wheels for atitude control

GCOM-W1 Specifications

Senosr	Advanced Microwave radiometer2（AMSR2）
Designed life time	5 years
Launch	May 2012 H-IIA rocket
Weight	1910 kg
Size	With two deployable solar paddles 5.1 m (X)×17.5 m (Y)×3.4 m (Z)
Orbit	Sun synchromous revisiting
Altitude	699.6km (over equator)
Inclination	98.186 degs.
Ascending node local time	13:30 ± 15 min.

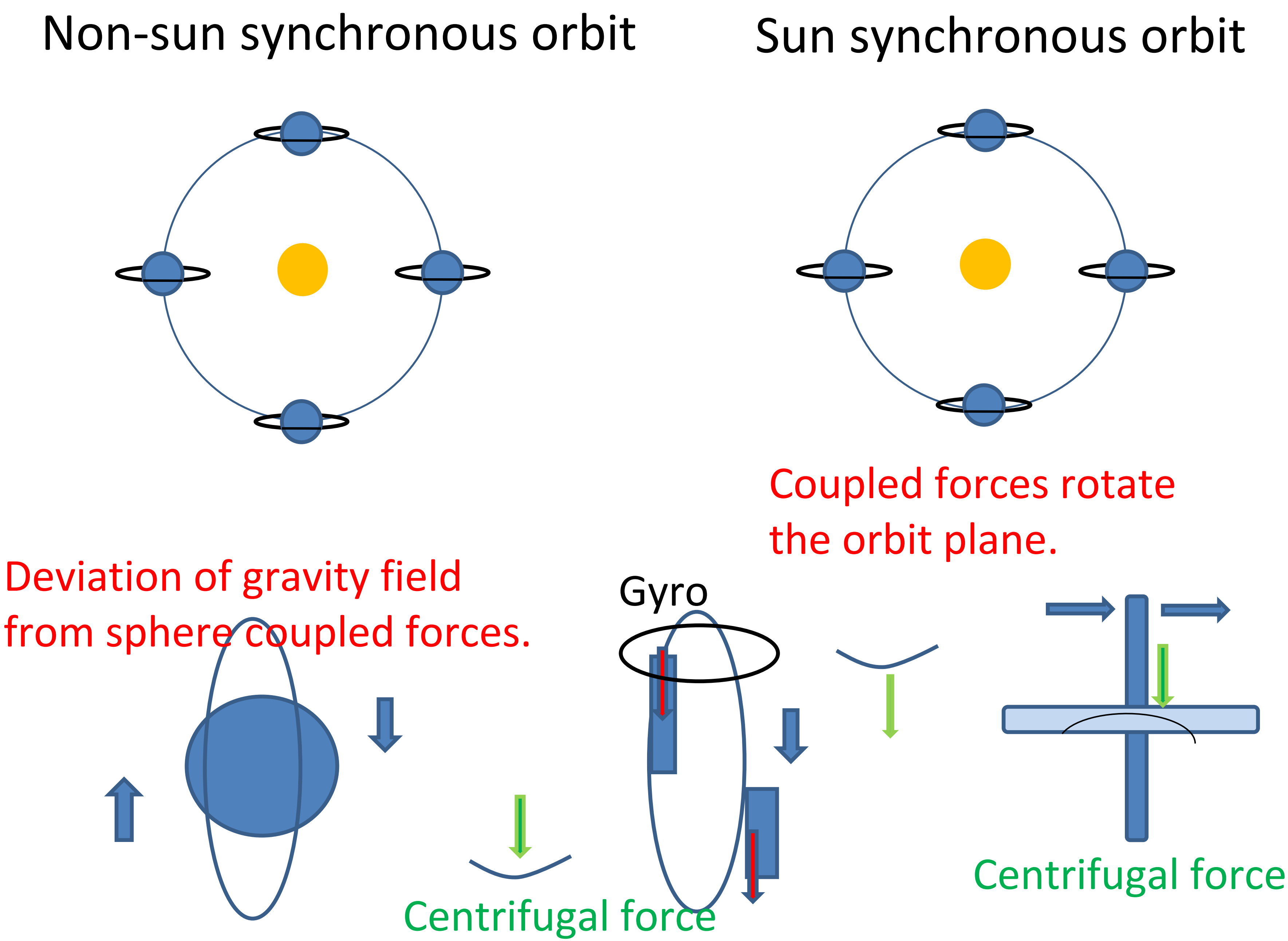
Non-sun synchronous orbit
Sun synchronous orbit
Coupled forces rotate
the orbit plane.
Deviation of gravity field
from sphere coupled forces.
Gyro
Centrifugal force
Centrifugal force

Rotation of the orbit plane:

-0.58 deg. $(R_e/r)^2$ x cos (i) / revolution

Solar movement:

360 degrees / year

For low orbit, 16 revolution / day

→ Roughly 1 degree / day

→ cos (i) = 0.11 → i = 97 degrees

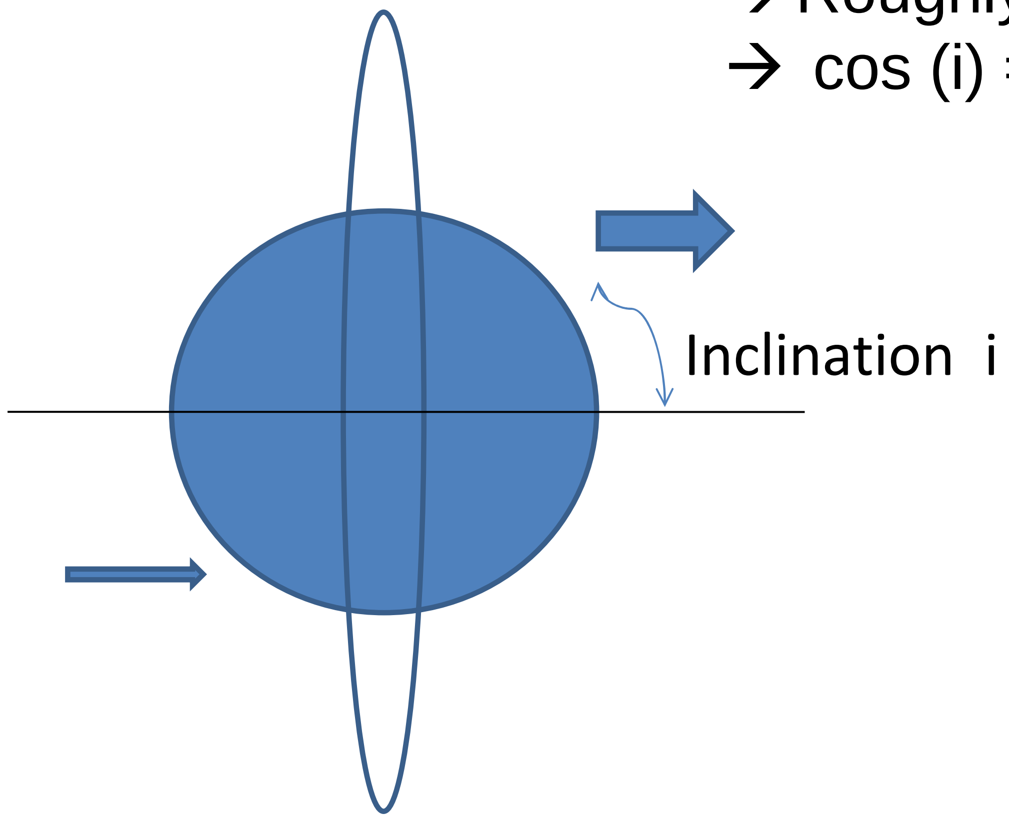

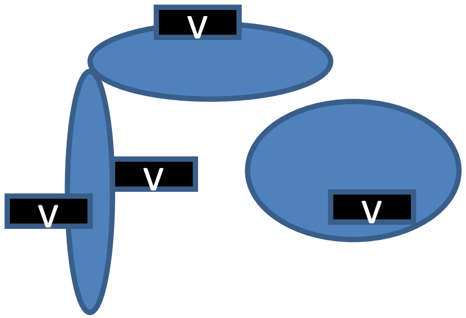

Three wheels for
atitude control

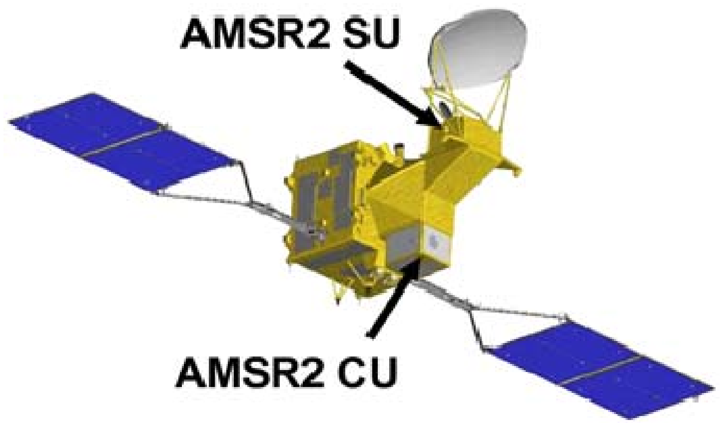

GCOM-W1主要諸元

項目	仕様
ミッション機器	高性能マイクロ波放射計2（AMSR2）
設計寿命	5年
打ち上げ予定	2012年1月 H-IIAロケット
質量	1910kg
衛星形状	2翼太陽電池パドルを有する 5.1m (X)×17.5m (Y)×3.4m (Z)(軌道上展開形状)
軌道種別	太陽同期準回帰軌道
軌道高度	699.6km (赤道上)
軌道傾斜角	98.186度
昇交点通過地方太陽時	13時30分 ±15分

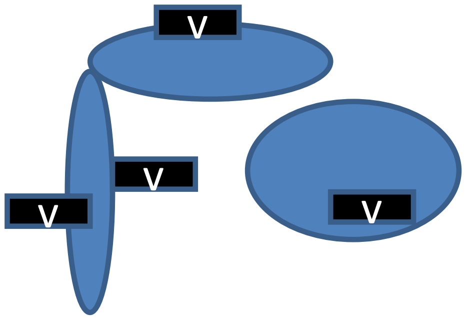

Three wheels for atitude control

GCOM-W1 Specifications

Senosr	Advanced Microwave radiometer2 (AMSR2)
Designed life time	5 years
Launch	May 2012 H-IIA rocket
Weight	1910 kg
Size	With two deployable solar paddles 5.1 m (X)×17.5 m (Y)×3.4 m (Z)
Orbit	Sun synchromous revisiting
Altitude	699.6km (over equator)
Inclination	98.186 degs.
Ascending node local time	13:30 ± 15 min.

TRMM 降雨レーダによる観測（１軌道）

1997年12月8日16:41-18:13（世界時）　　高度：2.0km

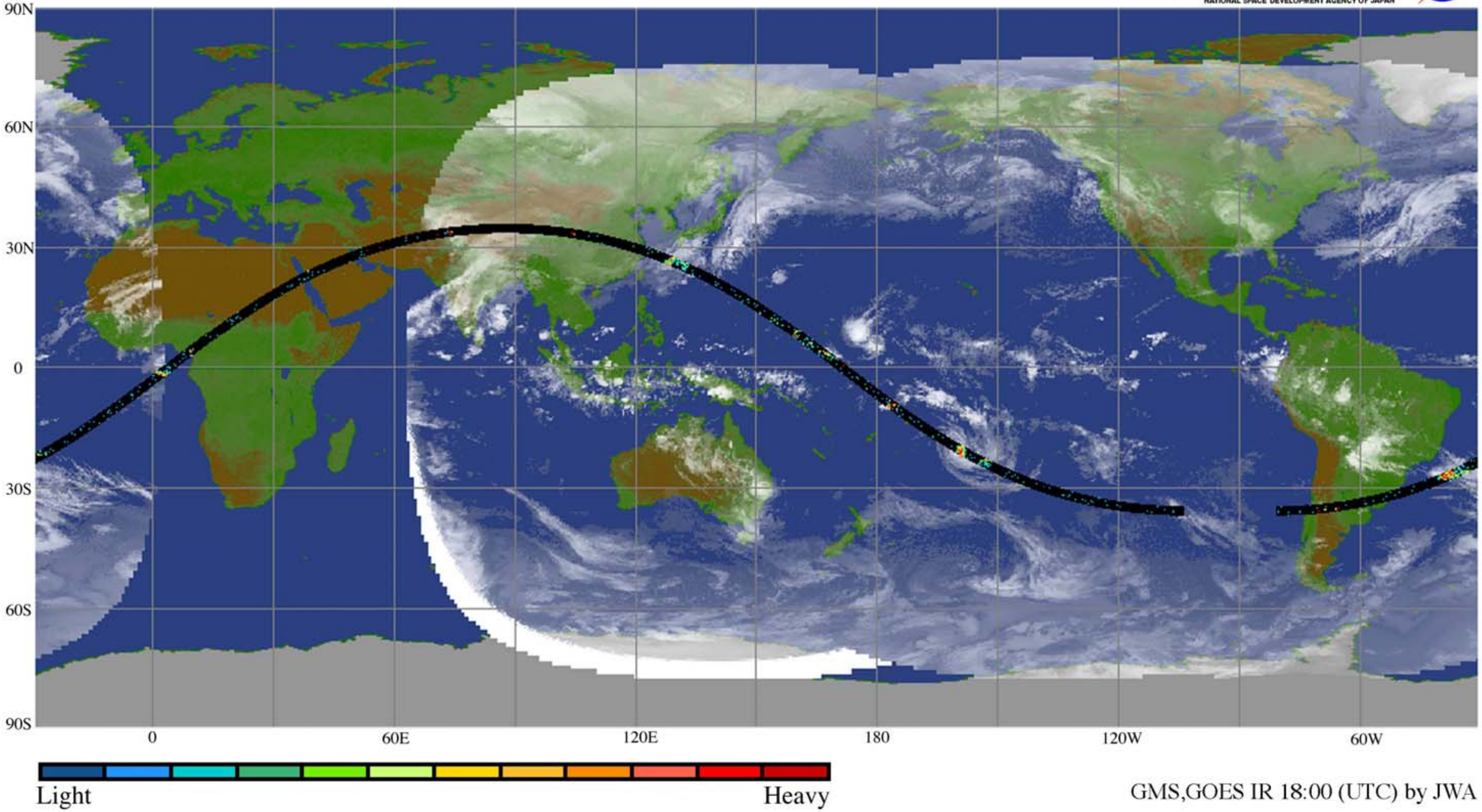

GMS,GOES IR 18:00 (UTC) by JWA

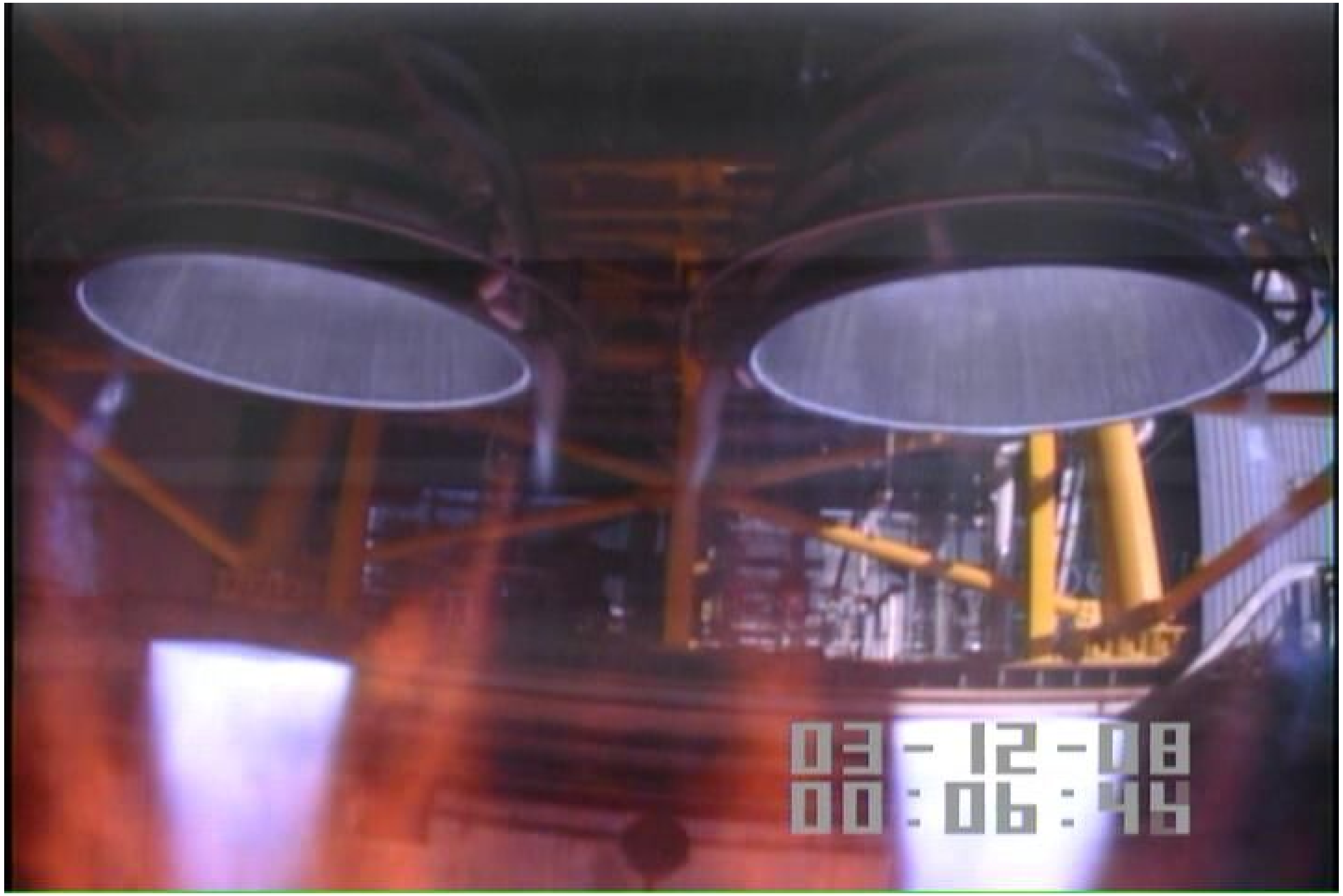
03-12-08
00:06:46

Rocket

m: fuel consumption

(M-m)v = ((M-m) – dm)(v + dv) + (v – w) dm,   w: velocity of gas

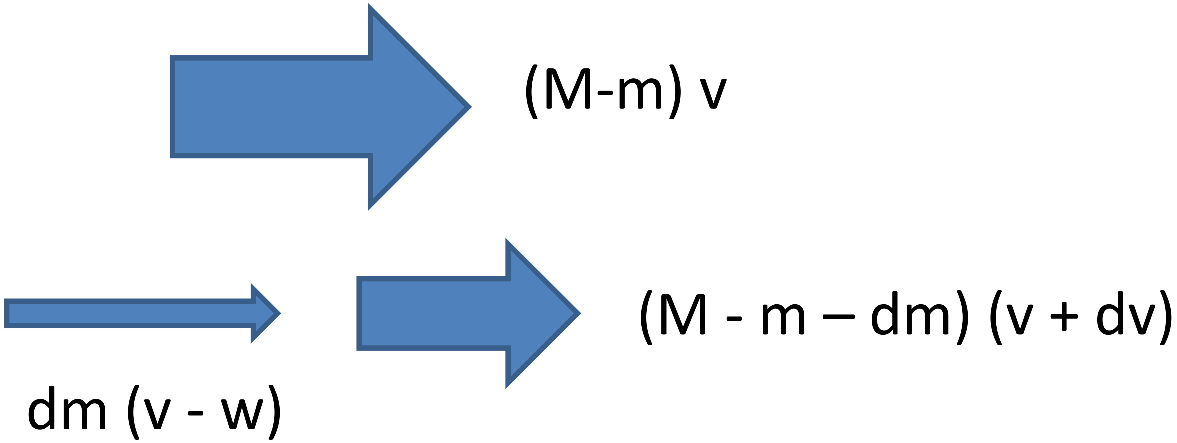

d v = w dm /(M - m)

→ $v-v_0 = w \log_e [m_0/(m_0-m_f)]$

(Tsiolkovskii's formula)

W (H_2/O_2): 4300 m/s (Isp (specific impulse) = w/g = 440 sec)

m0 = (30t) exp [(8 km/s) / (4300 m/s)] = 180t

Multi-Stage Rocket

$M = M_f + M_p$

$M = M_1 + M_2$, $M_f = M_{1f} + M_{2f}$

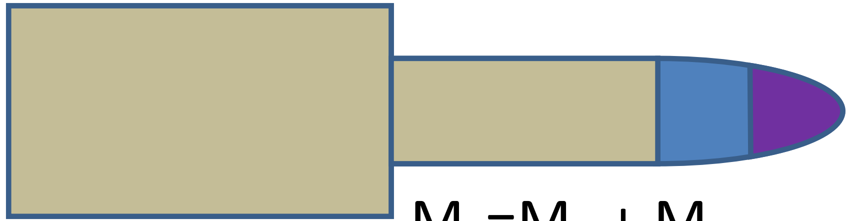

$M_2 = M_p + M_{2f}$

$M_1 = M_{1f} + M_2$

M_f: weight of fuel,

M_p: weight of payload

$$v = w \log_e [(M/(M-M_f)]$$
$$= w \log_e (M/M_p)$$

$$v1 = w \log_e (M/M_2)$$
$$v2 = v1 + w \log_e (M_2/M_{2p})$$
$$= w [\log_e (M/M_2) + \log_e (M_2/M_p)]$$
$$= w \log_e (M/M_p)$$

Multi-Stage Rocket

$M = M_1 + M_2$, $M_f = M_{1f} + M_{2f}$

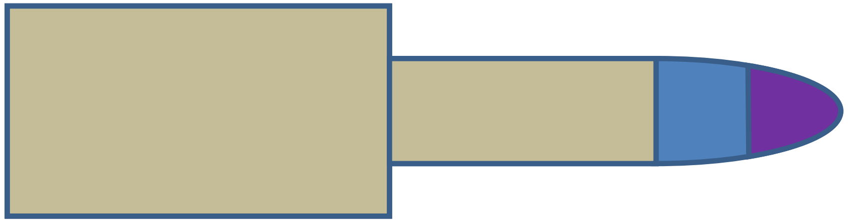

$M_1 = M_{1f} + M_2$

$M = M_1 + M_2$

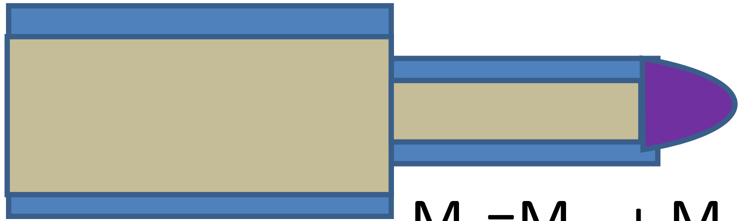

$M_2 = M_{2s} + M_p + M_{2f}$

$M_1 = M_{1f} + (M_{1s} + M_2)$

M_f: weight of fuel,

M_s: weight of structure,

M_p: weight of payload

$$v = w \log_e [(M/(M_{1s}+M_{2s}+M_p)]$$

$$v1 = w \log_e (M/(M_{1s} + M_2))$$

$$v2 = v1 + w \log_e (M_2/(M_{2s} + M_p))$$

$$= w \ \log_e [M/(M_{1s} + M_2) \times (M_2/(M_{2s}+M_p) \ ]$$

$$V2/V = w \log_e [(M_{1s}+M_{2s}+M_p) \ / \ [M_{1s} \ (M_{2s}+M_p)/M_2 \ +M_{2s}+M_p] \ ]> 1$$

Multi-Stage Rocket

$M = M_1 + M_2$

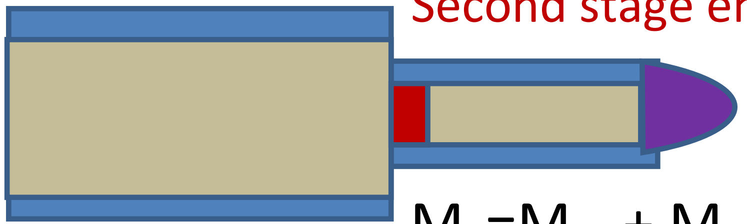

$M_2 = M_{2s} + M_p + M_{2f} + M_{2e}$

$M_1 = M_{1f} + (M_{1s} + M_2)$

$$v1 = w \log_e (M/(M_{1s} + M_2))$$
$$v2 = v1 + w \log_e (M_2/(M_{2s} + M_p + M_{2e}))$$
$$= w \log_e [M/(M_{1s} + M_2) \times (M_2/(M_{2s} + M_p + M_{2e})]$$

$$V2/V = w \log_e [(M_{1s} + M_{2s} + M_p) / [M_{1s} (M_{2s} + M_p + M_{2e})/M_2 + M_{2s} + M_p + M_{2e}]] > 1$$

GOES Precipitation Index (GPI)

Original: Arkin andMeisner, 1987, Mon. Wea. Rev., 115, 51-74.

Rain (mm) = Frac x 3 mm/hour
where

Frac: fractional coverage of GOES image with < 235 K
at around 11-12 micron.

Adjusted GPI (AGPI)
Incorporation of regional and seasonal biases.

Reference
Adler, R. F., G. J. Huffman, and P. R. Keehn 1994: Global rain estimates from microwave-adjusted geosynchronous IR data, *Remote Sens. Rev.*, **11**, 125-152.

GCOM-W1/AMSR2: a successor of

- GCOM-W1 (JFY 2011~) will carry microwave imager: AMSR2
  - Deployable main reflector system with 2.0m diameter
    - Achieve 20% finer resolution than AMSR-E with 1.6m reflector
  - Frequency channel set is identical to that of AMSR-E except 7.3GHz channel for Radio Frequency Interference mitigation
  - Two-point external calibration with the improved HTS (hot-load)
  - Add a redundant momentum wheel to increase reliability
- GCOM-W1 in the A-Train
  - GCOM-W1 will join the A-Train constellation
  - Participating in the A-Train will benefit
  - Precise inter-calibration between AMSR-E and AMSR2
  - Synergy with the other A-Train instruments for new Earth science research

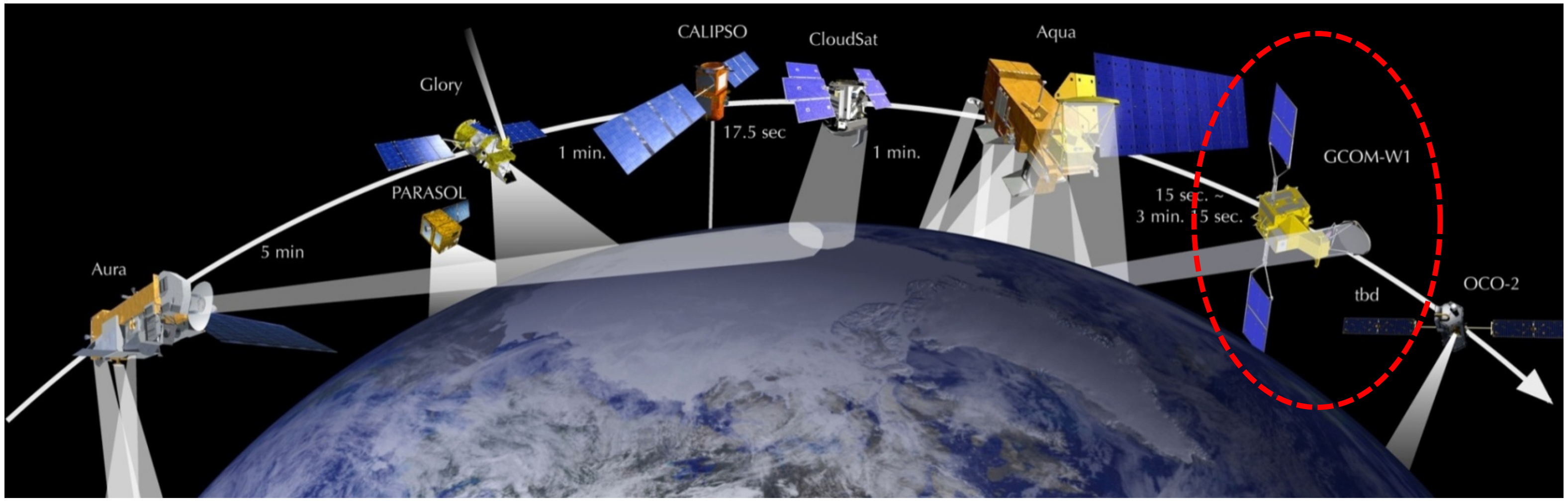

Tropical Rainfall Measuring Mission: TRMM

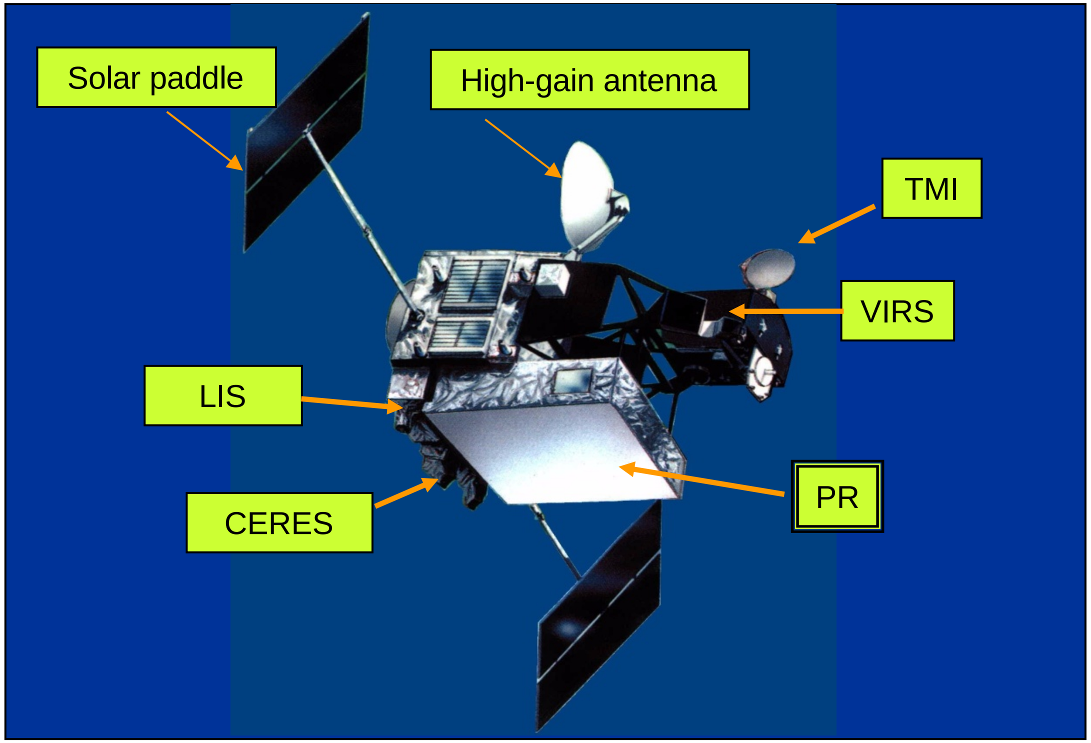

Orbit Altitude Inclination	Circular（Non-Sun Synchronous） 350km (402.5km since Aug. 2001) (±1.25km) 35 deg.
Sensor	**Precipitation Radar (PR)** TRMM Microwave Imager (TMI) Visible and Infrared Scanner (VIRS) Clouds and the Earth's Radiation Energy System (CERES) Lightning (LIS)

- ɔbservation of tropical rainfall (ðriving engine of global atmosphere)
- ʊʃ-ǝapan joint mission (ǝapanː PR, Launch, ʊʃː Bus, 4 sensors, operation)
- Launched in ŋov., 1997. ʃtill under operation
- First space-borne precipitation radar developed by CRL and ŋaʃða

NASDA NATIONAL SPACE DEVELOPMENT AGENCY OF JAPAN
CRL COMMUNICATIONS RESEARCH LABORATORY
NASA

Microwave radiometer (Examples of TRMM)

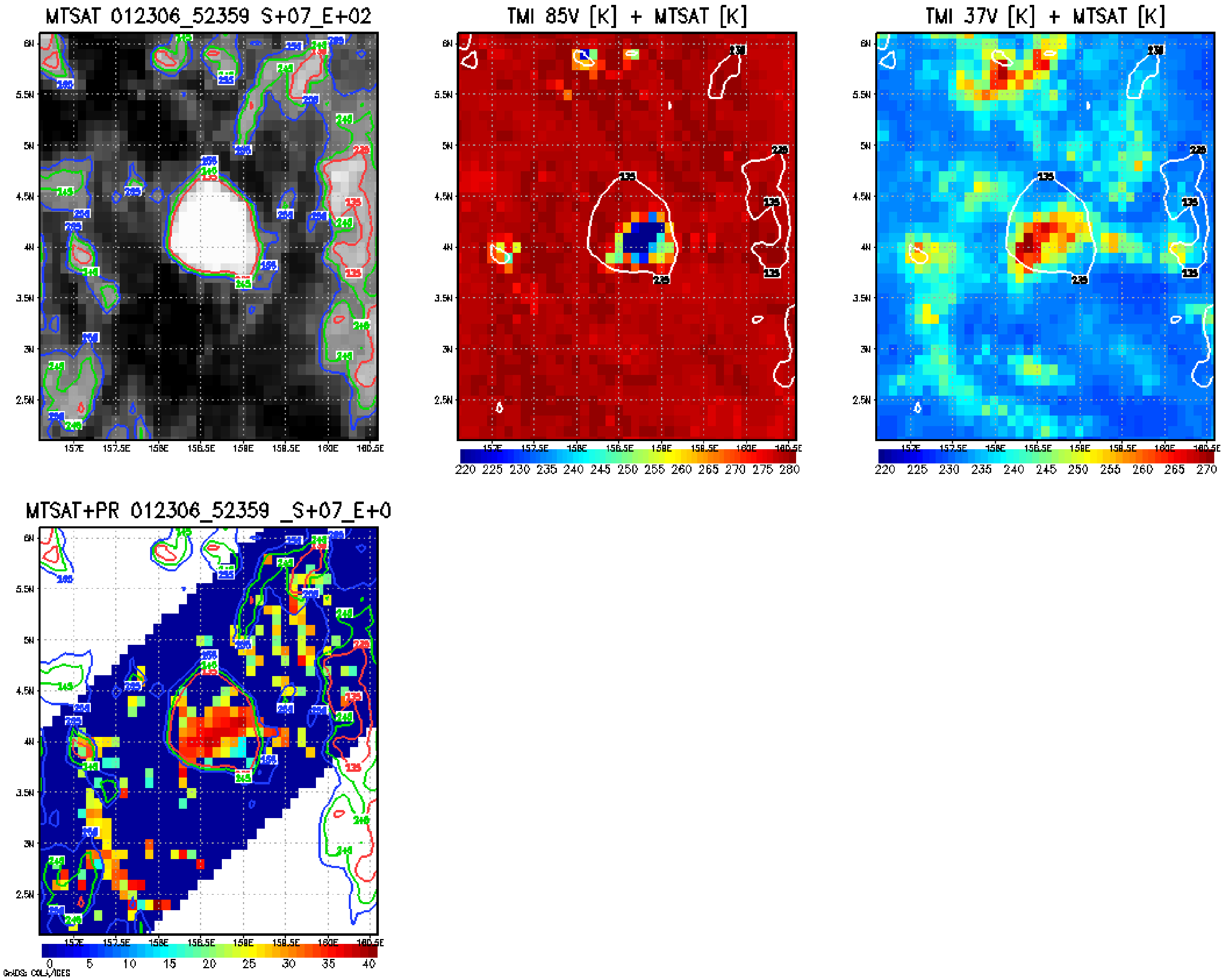

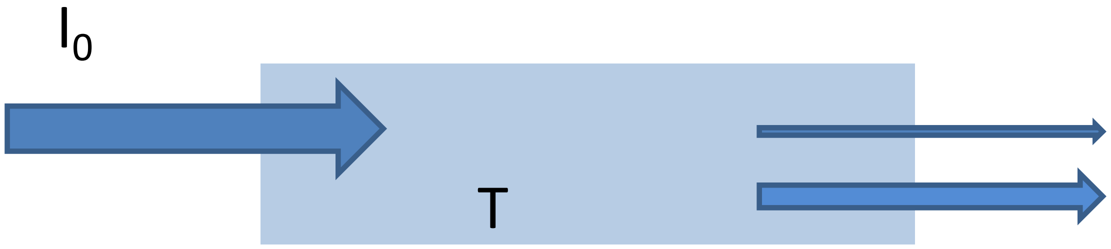

$I = I_0 – dI = I_0 – a\ dr$

$dI’ = e\ dr$

Local equilibrium → amount of absorption = amount emission

→ a = e: absorption coefficient = emissivity (Kirchhoff’s law)

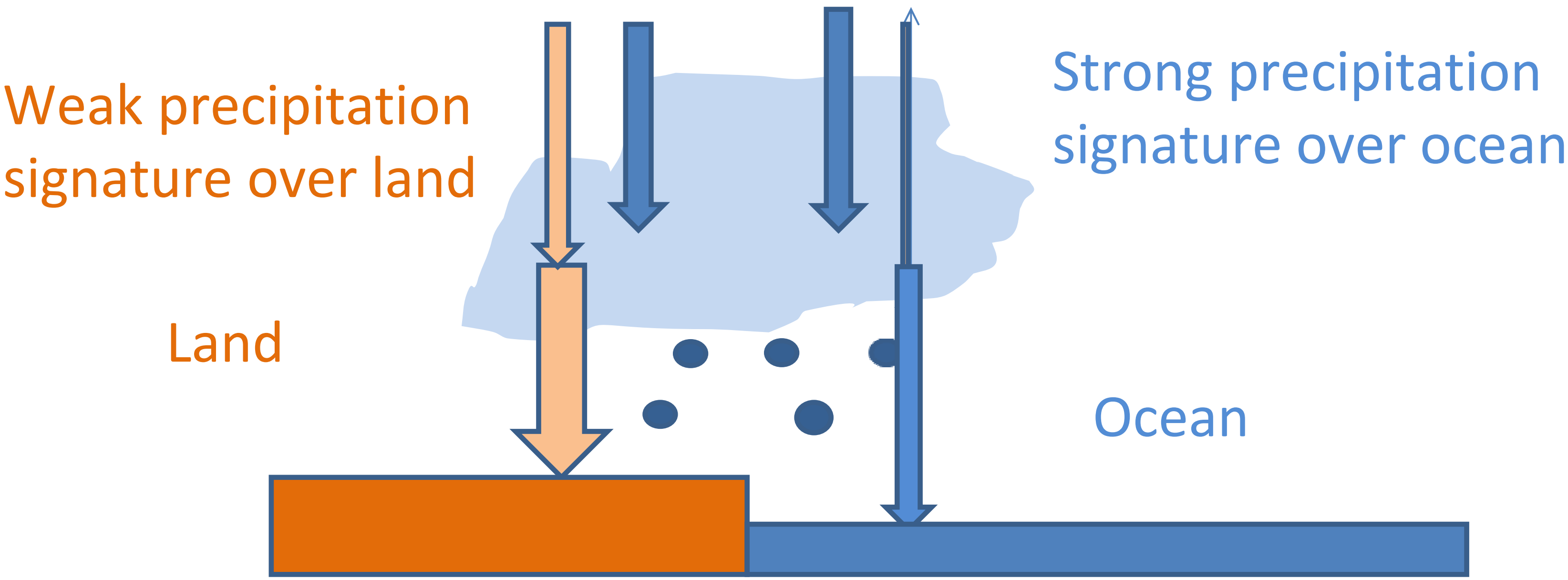

Blackbody radiation (Planck function) ($Wm^{-2}\ sr^{-1}\ m^{-1}$)

$$B_\lambda(T) = \frac{2hc^2}{\lambda^5}\frac{1}{e^{\frac{hc}{\lambda kT}} - 1}$$

$$B_\lambda(T) = \frac{c_1}{\lambda^5}\frac{1}{e^{\frac{c_2}{\lambda kT}} - 1}$$

$$c_1 = 1.191 \times 10^{-16}\mathrm{Wm^2sr^{-1}}、c_2 = 1.439 \times 10^{-2}\mathrm{mK}$$

Wien' law

$$\lambda_m T = 2898\ \mu\mathrm{mK}$$

Tropical Rainfall Measuring Mission (TRMM)

- *Major characteristics*
  - *Focused on rainfall observation. First instantaneous rainfall observation by three different sensors (PR, TMI, VIRS). PR, active sensor, can observe 3D structure of rainfall.*
  - *Targeting tropical and subtropical region, and chose non-sun-synchronous orbit (inc. angle 35 degree) to observe diurnal variation.*
- *Major achievement in Japan*
  - More than 14 years rain observation data archive
  - *Demonstration of high quality and high reliability of a satellite onboard precipitation radar*
  - *Improvement of MWR precipitation retrieval by PR 3D observation*
  - *Pioneering precipitation system climatology by PR observation*
  - *Operational use in NWP etc.*
  - *New products including all-weather SST, global soil moisture*

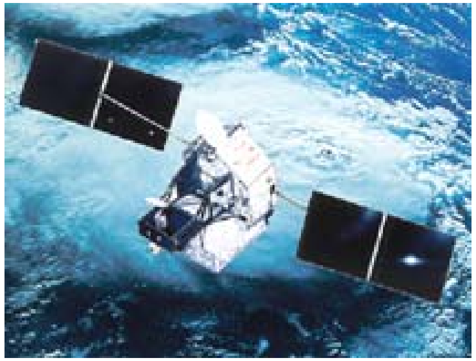

US-Japan joint mission

Japan: PR, launch

US: satellite, TMI, VIRS, CERES, LIS, operation

Launch	28 Nov. 1997 (JST)
Altitude	About 350km (since 2001, boosted to 402km to extend mission operation）
Inc. angle	About 35 degree, non-sun-synchronous orbit
Design life	3-year and 2month (still operating)
Instruments	Precipitation Radar (PR) TRMM Microwave Imager (TMI) Visible Infrared Scanner (VIRS) Lightning Imaging Sensor (LIS) CERES (not in operation)

TRMM Precipitation Radar

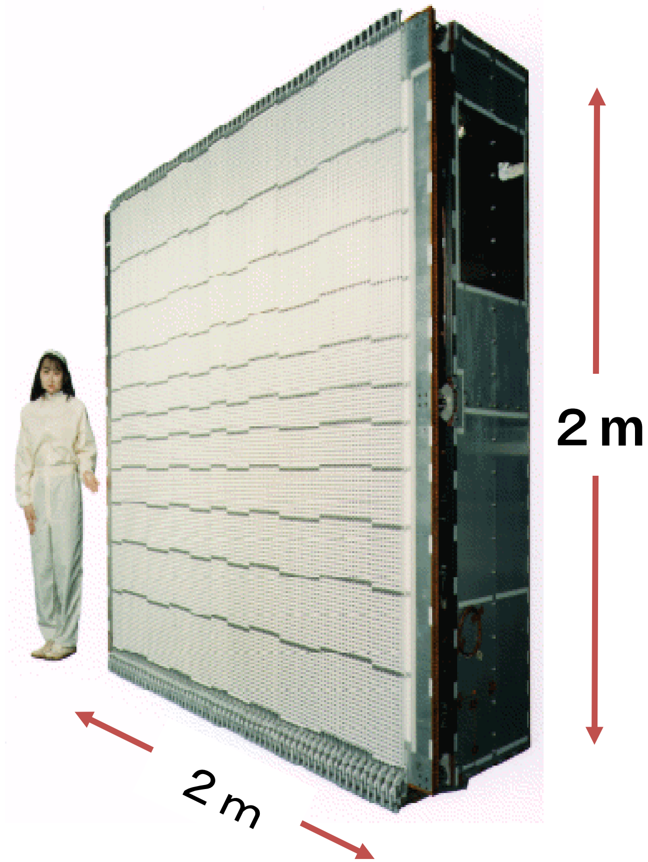

Radar type	Pulse radar
Antenna type	128-elem. WG slot array
Beam scanning	Active phased array
Frequency	13.796, 13.802 GHz
Polarization	Horizontal
TX/RX pulse width	1.57 / 1.67μsec
RX band width	0.6 MHz
Pulse rep. freq.	2776 Hz
Data rate	93.5 kbps
Mass	460 kg
Designed Life time	3 years
Sensitivity	< 0.5mm/h
Horizontal resolution	4.3 km (nadir)
Range resolution	250 m
# of indpdt samples	64 (fading noise < 0.7 dB)
Swath width	215km
Observable range	Surface to 15km

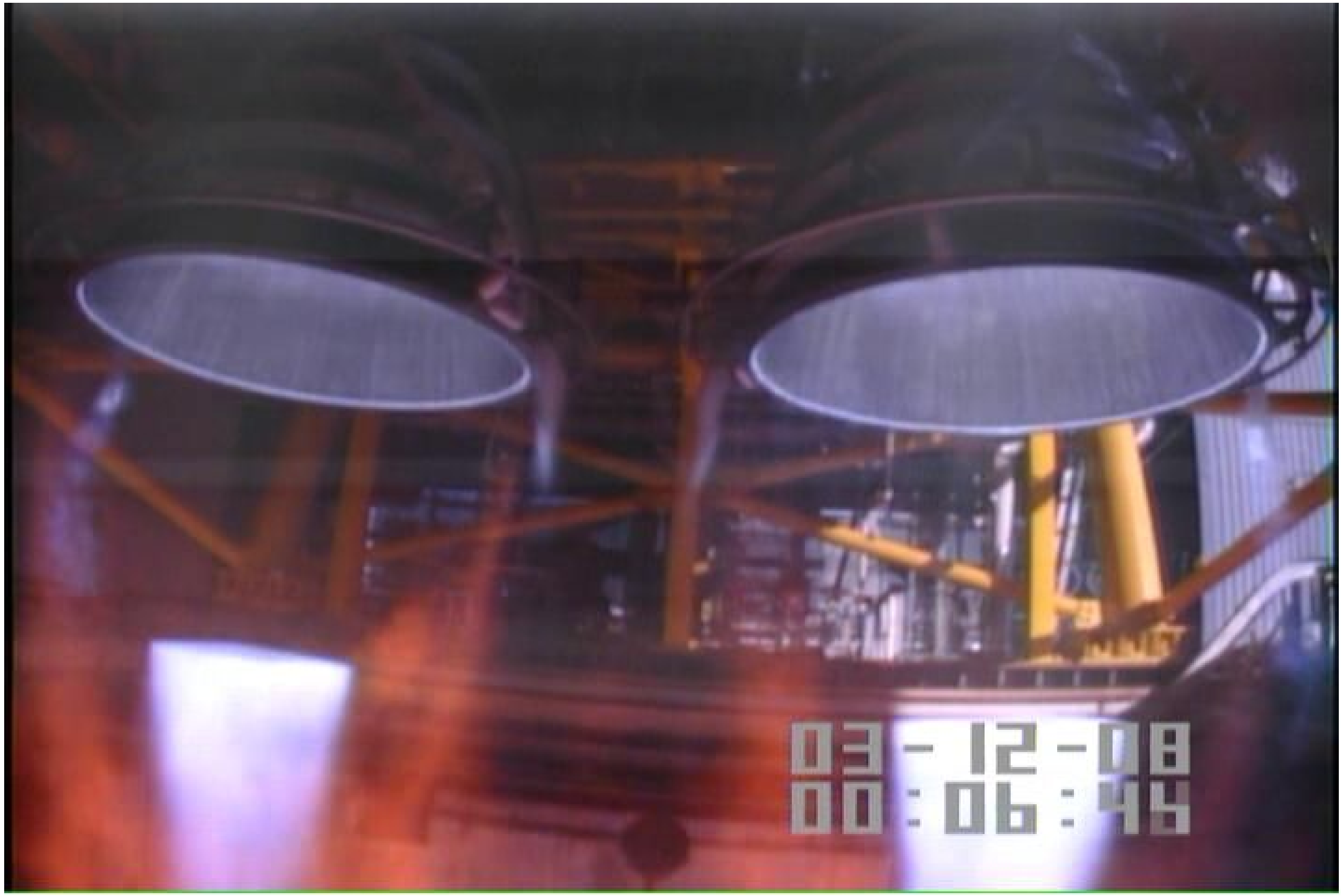
03 - 12 - 08
00 : 06 : 46

3-D Observation of a Typhoon by TRMM

TRMM PR 2A25 Rain

Aug. 2, 2000, 20:49-20:53 (Japanese local time)

Rain intensity at H=2 km

Vertical cross section through the eye and 3D structure

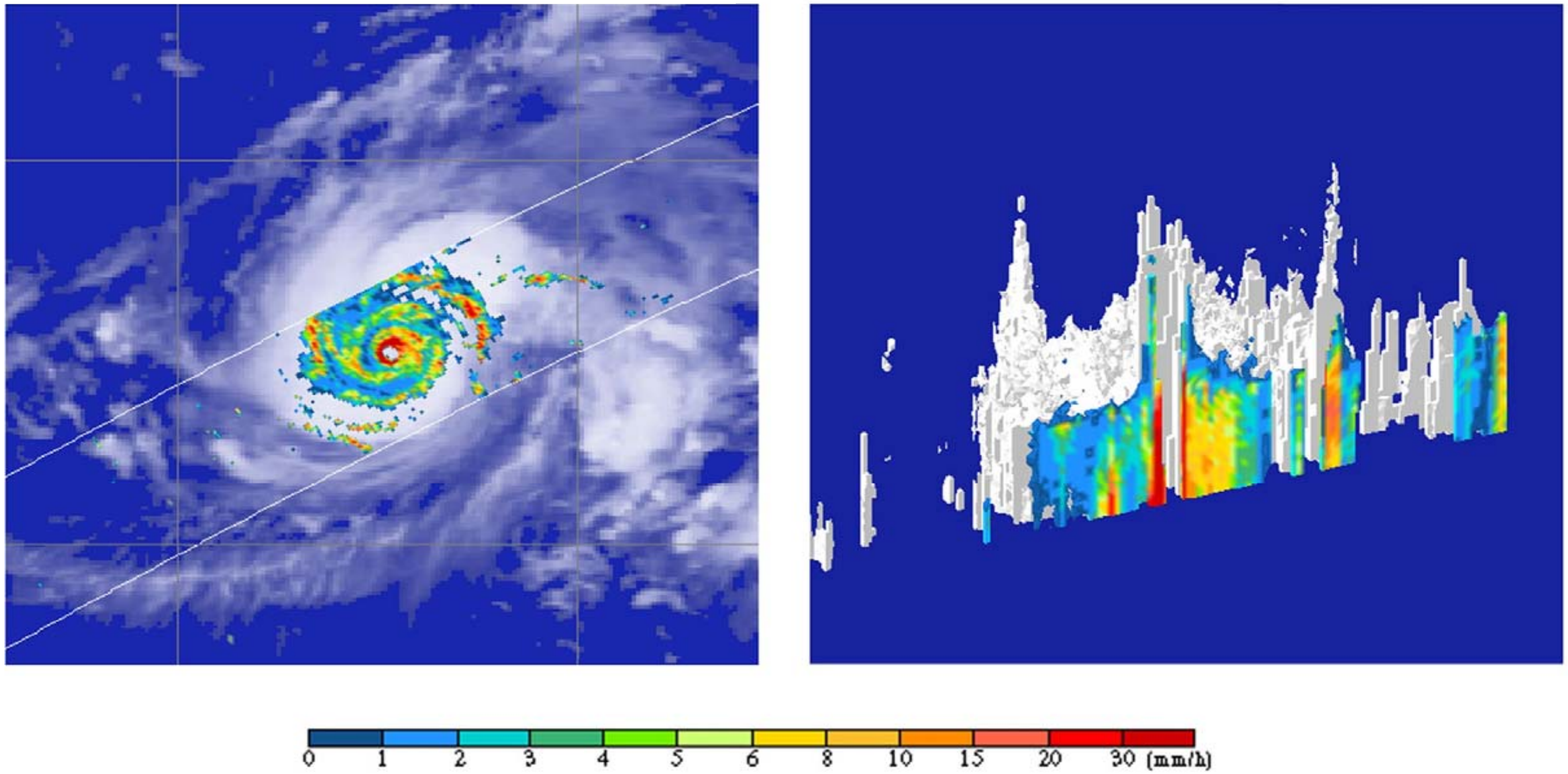

PR realized observation of 3D structure of rain over ocean where few observations had been available.

Global Monthly accumulated Rain by θRMM/PR (εstimated ʃurface Rain 1997/12 – 2010/05)

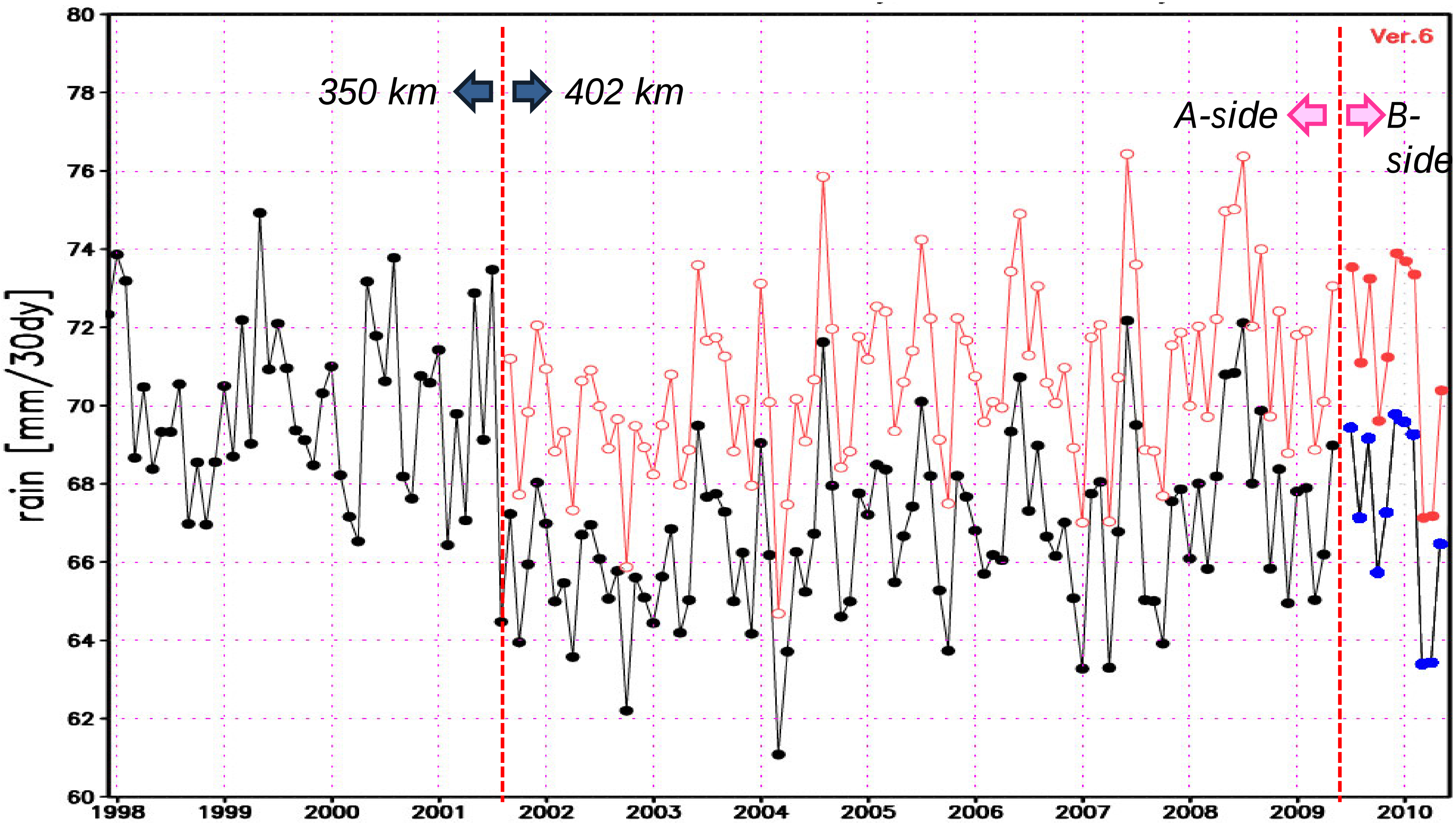

- *The total decrease in PR e_surface rain by altitude change is estimated to be 5.90% on average in a global scale.*
- *Data continuity was kept by calibration for B-side H/W.*

GSMaP_NRT: A proto-type for GPM

- Global rainfall map by merging TRMM, AMSR-E, and other satellite information.
- 0.1-degree lat/lon grid, hourly products.
- GSMaP near-real-time version (GSMaP_NRT) is distributed via internet
  – Available 4-hr after observation
  – Binary and text data has been freely available since Oct. 2008 via password protected ftp site.
  – Hourly browse images are also available.
  – SSMIS (F16, F17) has been introduced into the NRT system since June 2010.
  – Introduction of AMSU/MHS (NOAA N15/16/18/19, MetOp-A) into the NRT system is in preparation.
- Reanalysis of GSMaP (GSMaP_MVK) in latest version is underway.
  – Processing of 2007 data is completed, and it has been distributed to NRT registered users..
  – Use all available microwave imagers, including SSMIS, AMSU, and MHS.

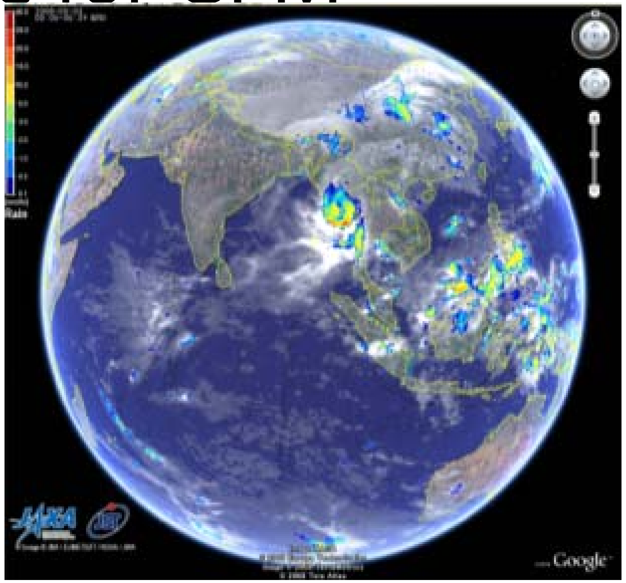

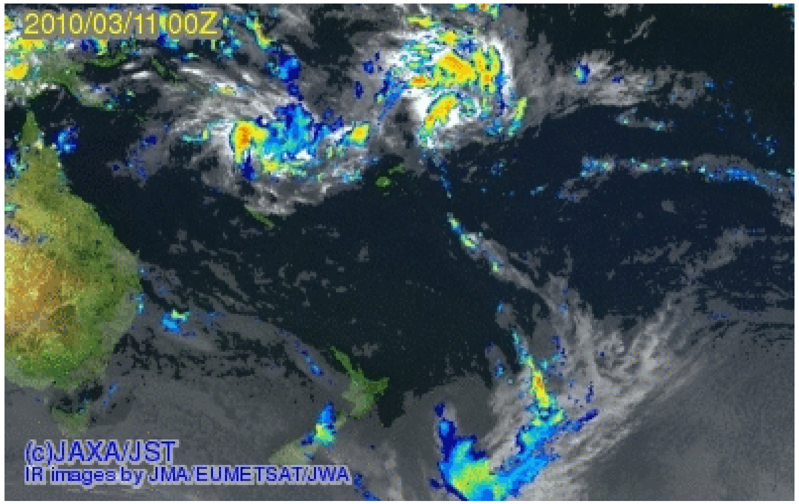

3-hourly animation of two Tropical Cyclones over the South Pacific in March 2010 by GSMaP_NRT.

http://sharaku.eorc.jaxa.jp/GSMaP/

Global Distribution of the Mean Storm Height Measured by the TRMM Precipitation Radar

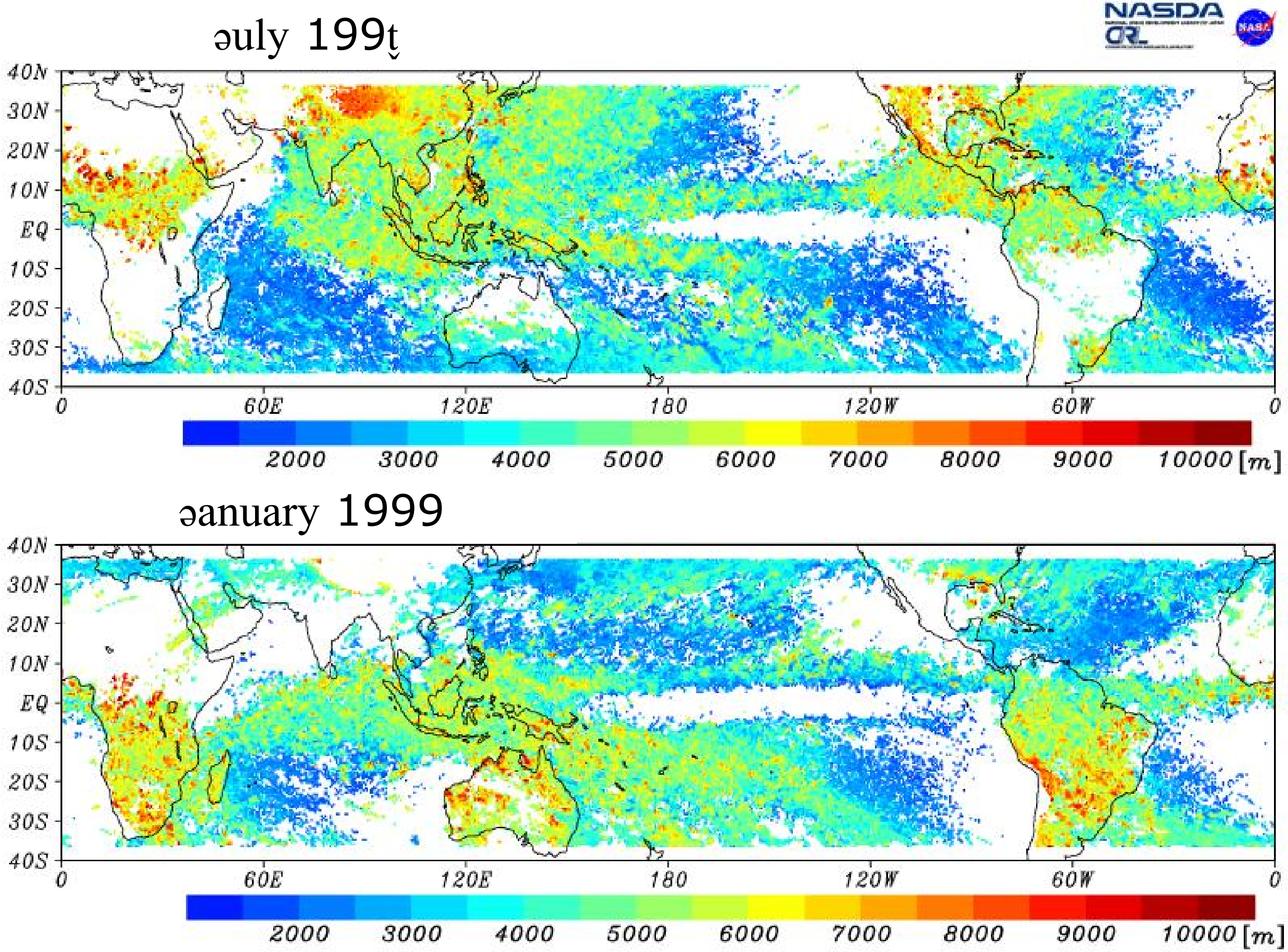

図10

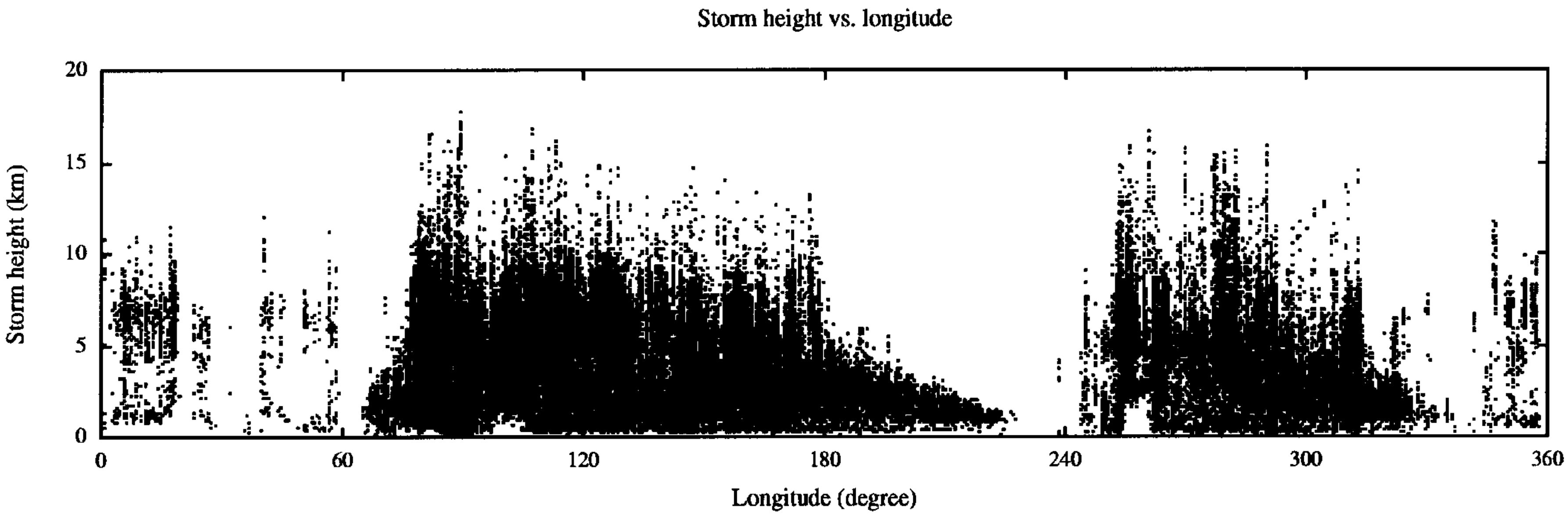
Storm height vs. longitude
Storm height (km)
Longitude (degree)
20
15
10
5
0
0
60
120
180
240
300
360

図11

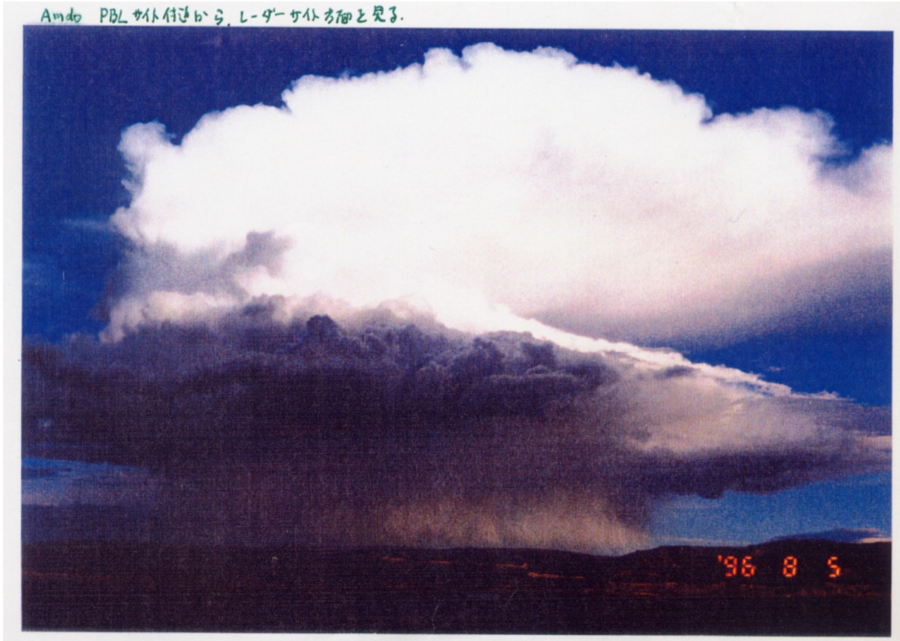

(by Endo and Koike)

7.5 km

2 km

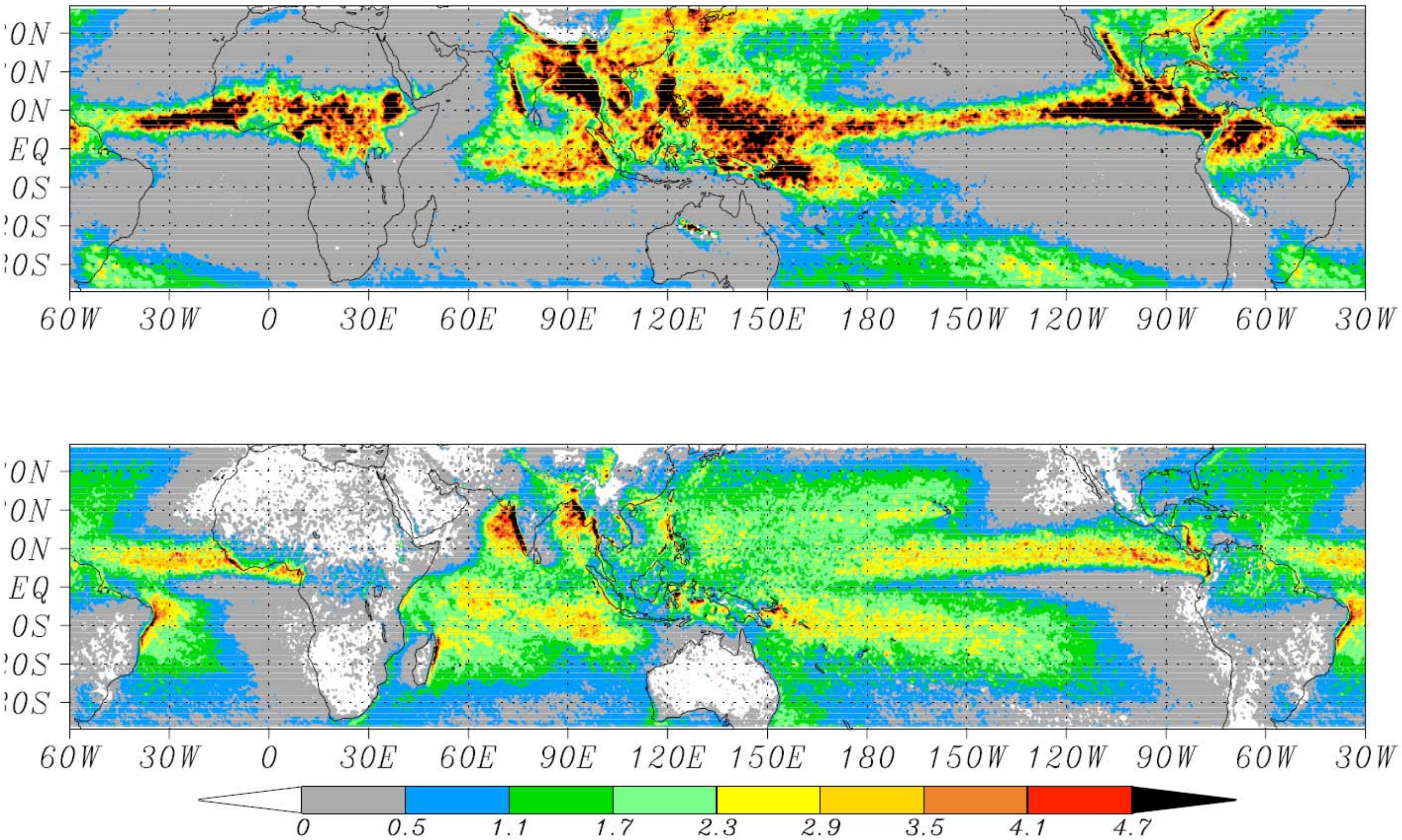

Latent heating from TRMM PR for 1998-2000.

(Takayabu et al.)

EarthCARE / Cloud Profiling Radar

εʃα εarth εxplorer Core Mission

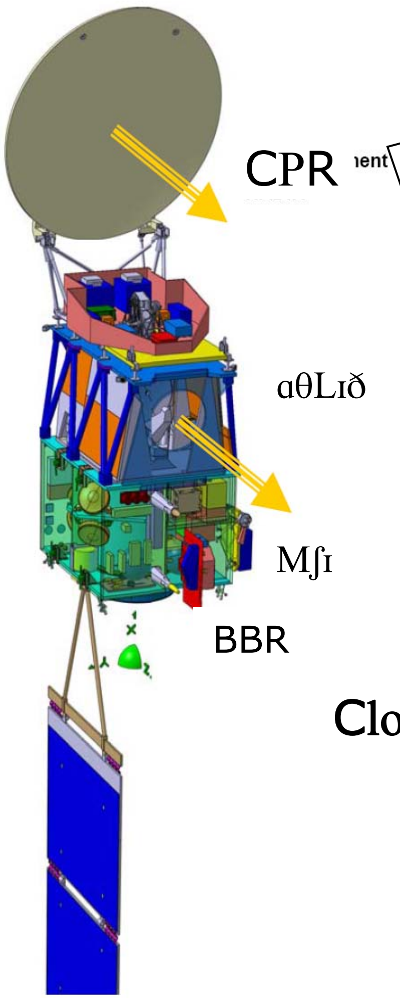

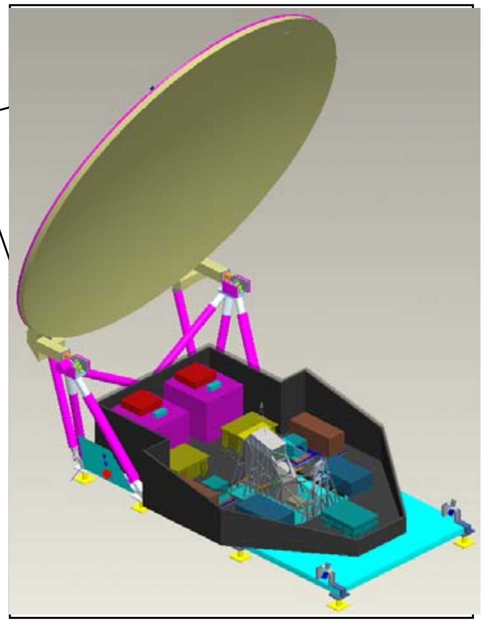

Cloud Profiling RαðαR(CPR)
əoint ðevelopment
of əαṱα/ŋɪCθ

Radar type	94 GHz Doppler Radar
Center frequency	94.05 GHz
Pulse width	3.3 micro second (equivalent to 500m vertical resolution)
Beam width	0.095 deg
Polarization	Circular
Transmit power	> 1.5 kW (Klystron spec.)
Height range	-0.5 ~ 20 km
Resolution	500 m (100 m sample); Vertical, 500m integration; Horizontal
Sensitivity*	-35 ~ +21 dBZ
Radiometric accuracy*	< 2.7 dB
Doppler measurement	Pulse Pair Method
Doppler range*	-10 ~ +10 m/s
Doppler accuracy*	< 1 m/s
Pulse repetition frequency	Variable; 6100~7500 Hz
Pointing accuracy	< 0.015 degree

*; at 10 km integration and 387 km orbit height

Concept of GPM

GPM = follow-on mission of the TRMM (Tropical Rainfall Measuring Mission)

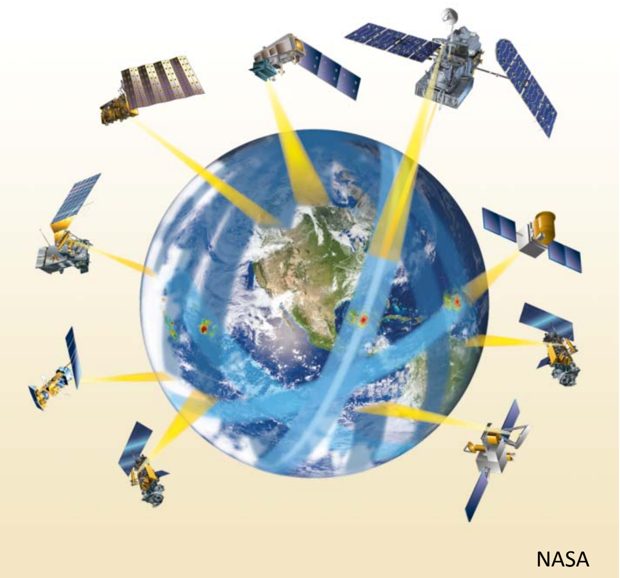

3-hourly global rainfall map

Core Observatory

- Dual-frequency Precipitation Radar (DPR)
- Microwave Imager (GMI)

✧Highly sensitive precipitation measurement

✧Calibration for constellation radiometers

JAXA and NICT: DPR
NASA : Spacecraft bus and GMI
JAXA: H2A Launcher

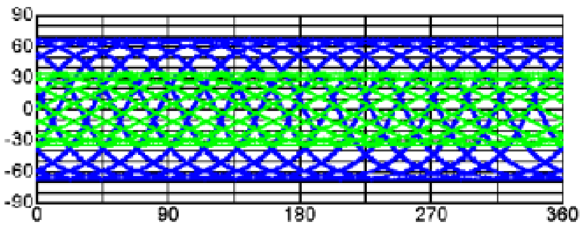

Blue: Inclination ~65º (GPM core)
Green: Inclination ~35º (TRMM)

Constellation Satellites

- Microwave Radio-meters installed on each satellite

✧Frequent precipitation measurement

Expected Partners:
NASA, NOAA, CNES-ISRO, China, others

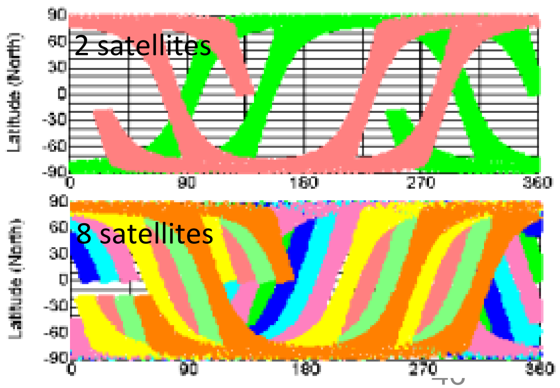

θime and space ınterval of the ðPR database

1-day orbit

Color: orbit num

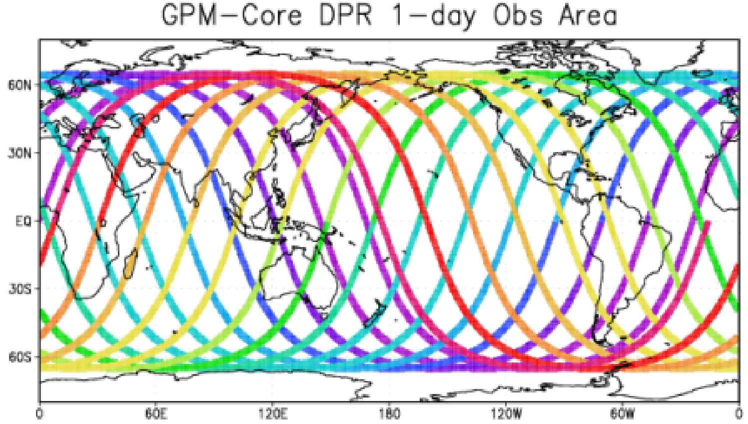

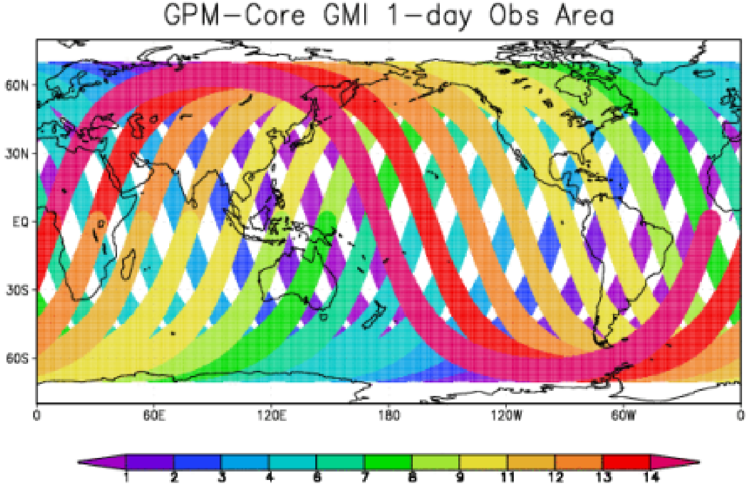

One-day orbit observations of DPR (upper) and GMI (lower)

The orbit data was calculated by Y.Iida (Osaka Prefecture Univ)

3-days orbit

Color: IFOV pixel num

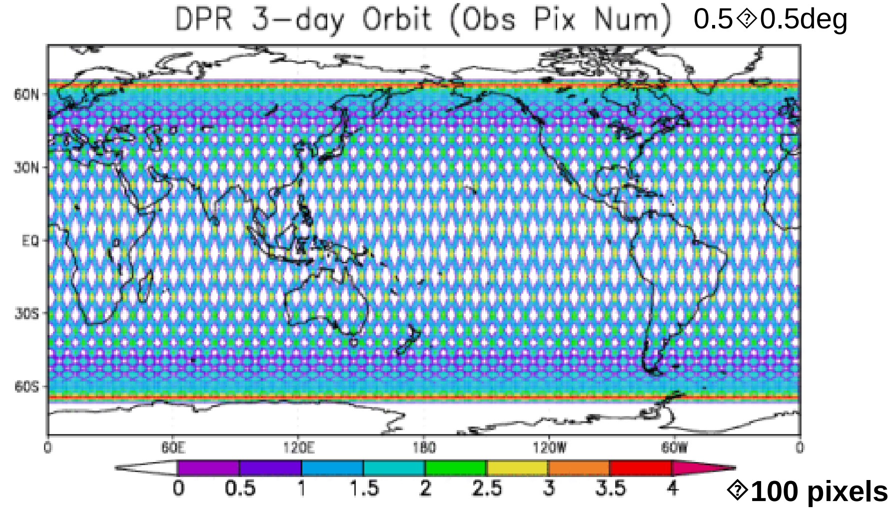

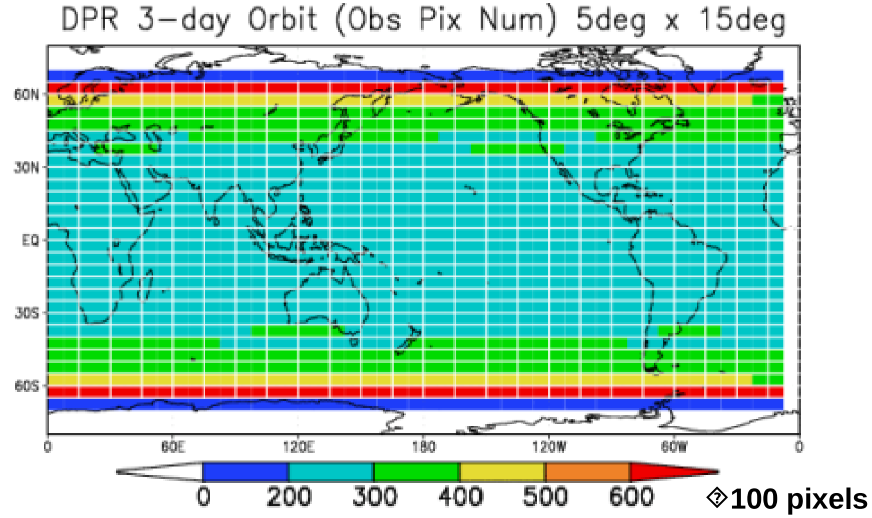

DPR dynamic database will be renewed in 15 deg × 5 deg grids every 3-10 days

Overview of GPM Core Observatory

Dual-frequency precipitation radar (DPR) consists of
Ku-band (13.6GHz) radar : KuPR
and
Ka-band (35.55GHz) radar : KaPR

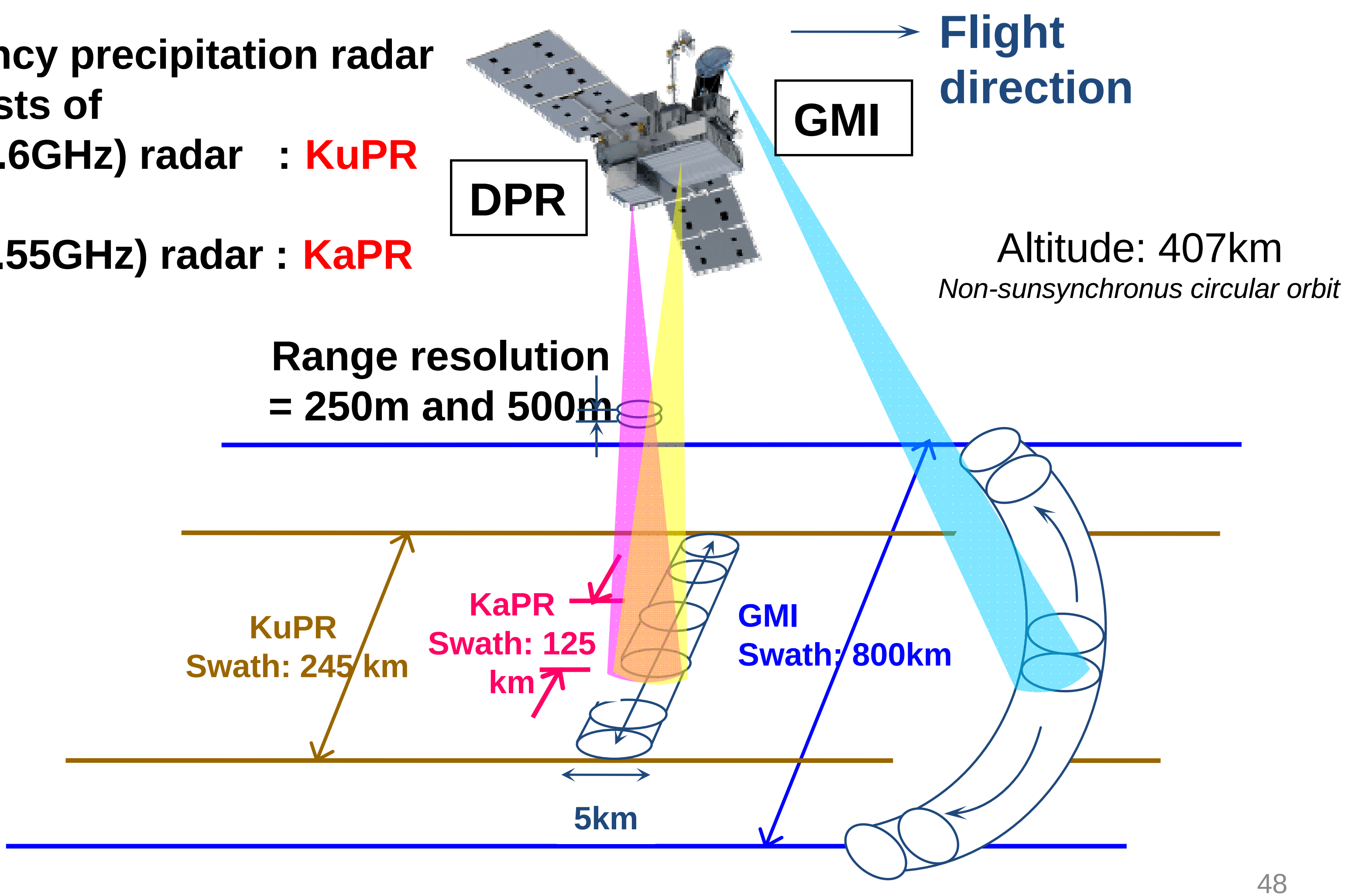

Scanning Method

KuPR footprint : Dz=250m
KaPR footprint (Matched with KuPR) : Dz=250m
KaPR footprint (Interlaced) : Dz=500m

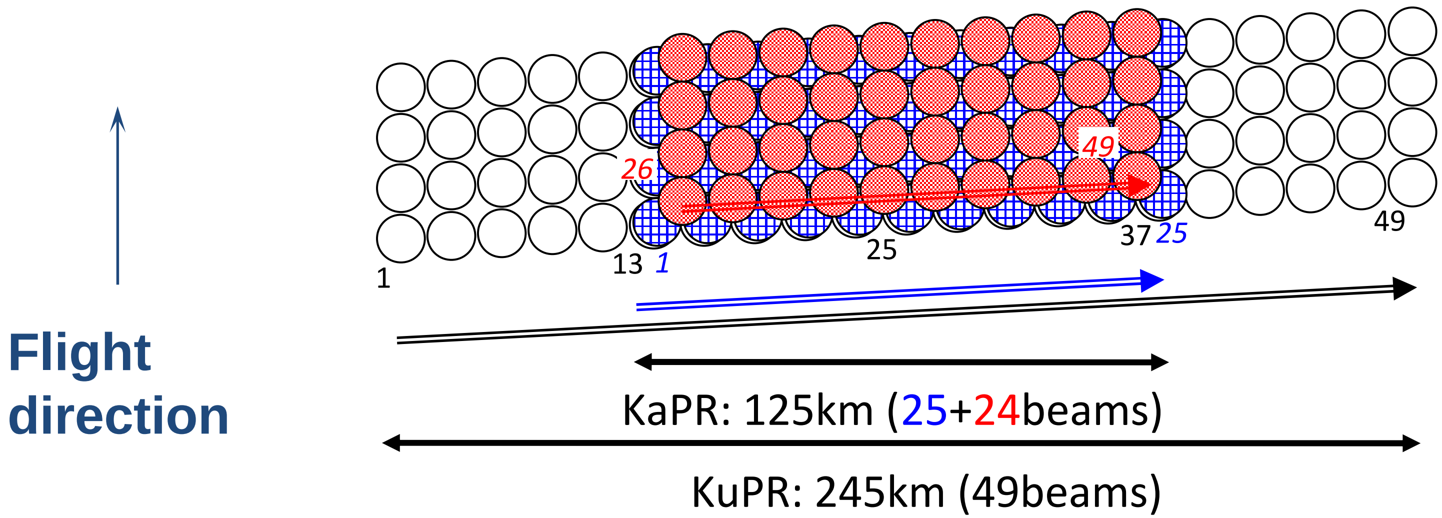

The synchronized matched beam ( ) is necessary for the dual-frequency algorithm.

In the interlacing scan area ( ), the KaPR can measure snow and light rain in a high-sensitivity mode with a double pulse width.

Precipitation Measurement by DPR

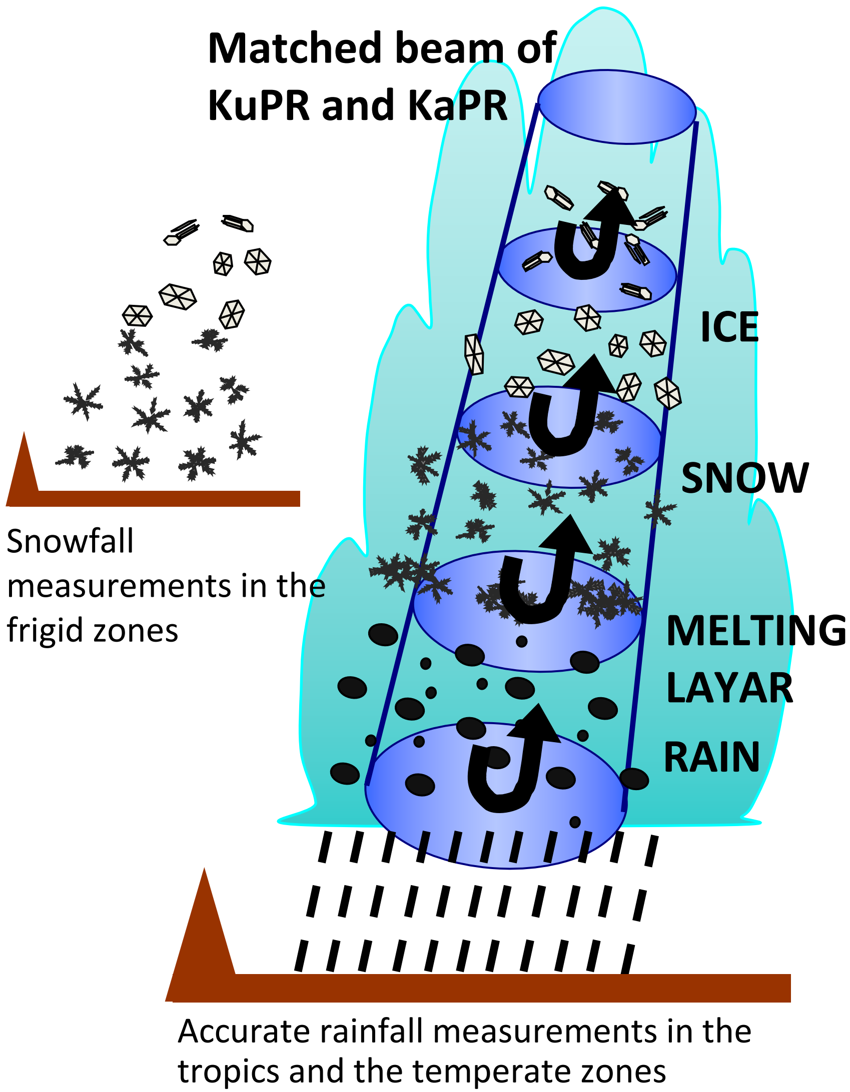

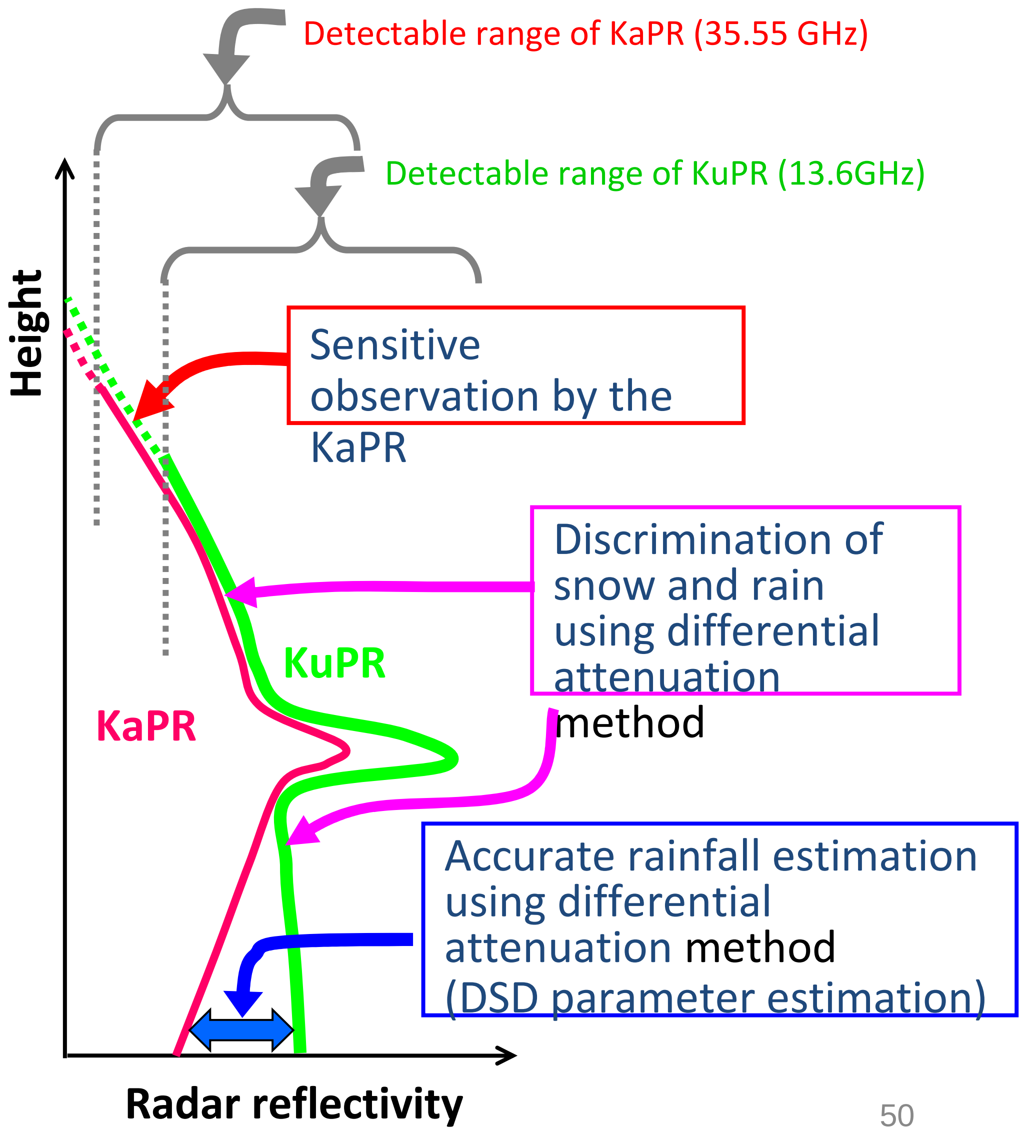

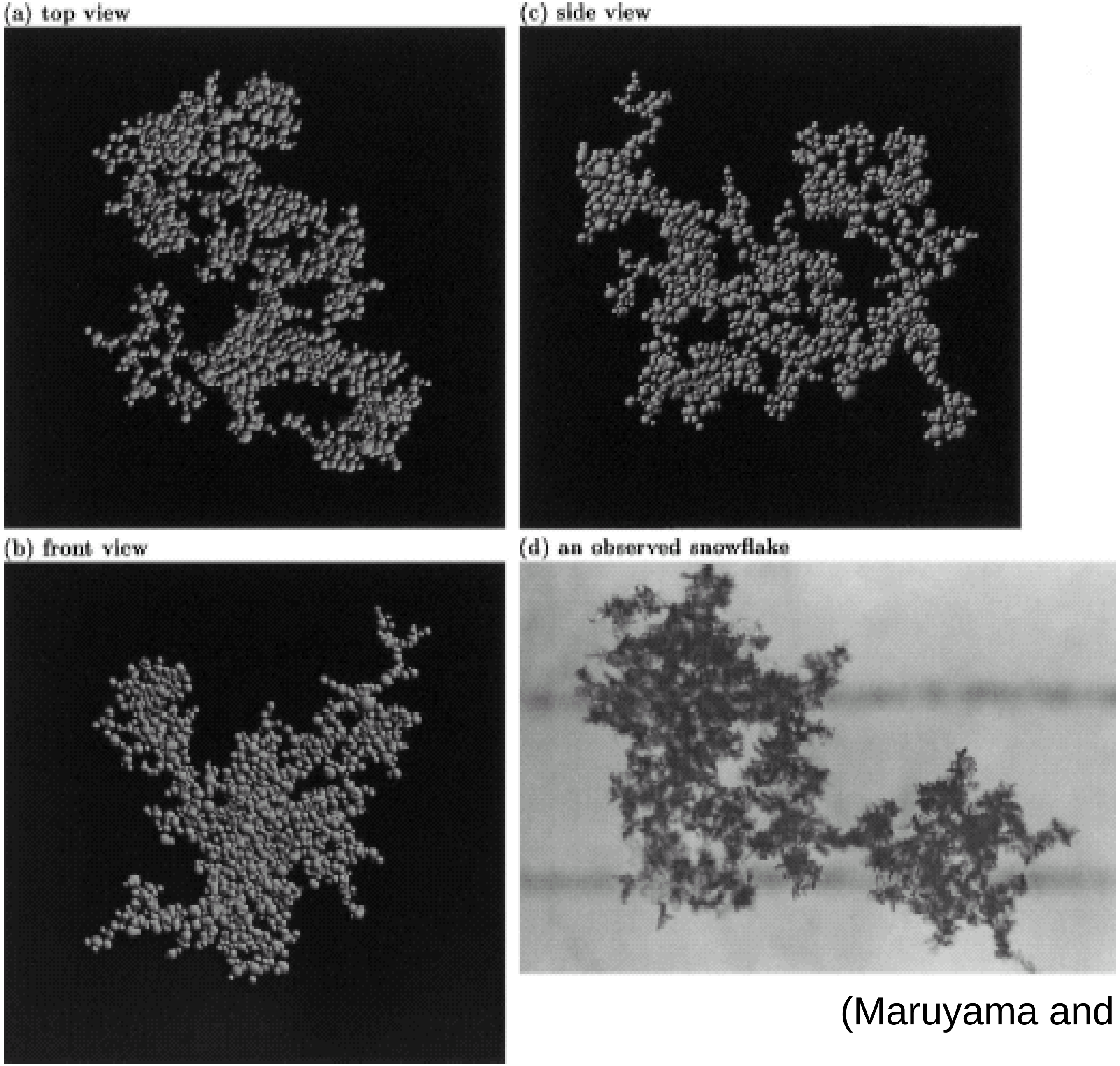

(Maruyama and Fujiyoshi, JAS, 2005)

FIG. 2. Images in 3D of a generated snowflake consisting of 1760 particles: (a) top view and (b) front view. (c) A picture of an observed snowflake is also shown for comparison; the two faint lines behind the observed snowflake are separated by 5 mm.

Radar measurement from space (1)

-- TRMM/PR and GPM/DPR rain retrieval algorithms--

Toshio Iguchi

Applied Electromagnetic Research Institute,

National Institute of Information and Communications Technology

International Hydrological Programme

Precipitation Measurement from Space and its Applications

The Twenty-second IHP Training Course

18 November - 1 December, 2012

Nagoya, Japan

Remote sensing of rain by radar

RADAR: RAdio Detection And Ranging

- Radar emits a known pulse of radio waves and measures its echoes from objects or targets.
- The time for the pulse to travel to the target gives the distance to the target.
- The direction of the radio waves gives the direction of the target.
- The echo power depends on the size and number of the targets.

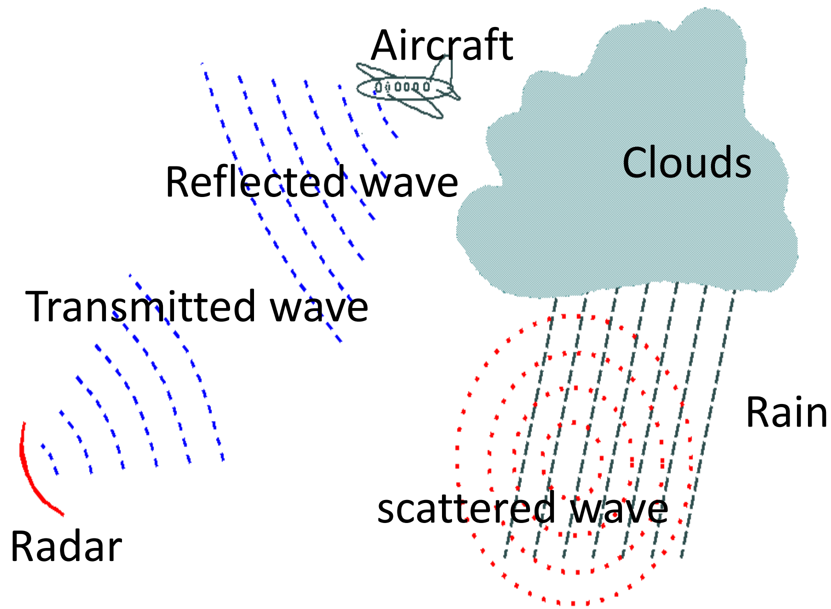

Current and future satellite missions carrying a precipitation or cloud radar

- Tropical Rainfall Measuring Mission (TRMM) / PR
  - November 1997 – present
  - Single frequency (13.8 GHz),
  - 250 km swath, >18 dBZ, 250 m v. res.
- Global Precipitation Measurement (GPM) / DPR
  - 2014 (launch)
  - Dual-frequency (13.6 GHz, 35.5GHz)
  - 250 km swath, >12dBZ (Ka, 125 km swath, 500 m vert. res)
- CloudSat/CPR
  - April 2006 – present
  - 94GHz, nadir only, > -30dBZ, 500 m vertical res.
- EarthCARE/CPR
  - 2015(launch)
  - 94GHz, nadir only, > -35dBZ, 500 m vertical res.
  - Doppler

Tropical Rainfall Measuring Mission: TRMM

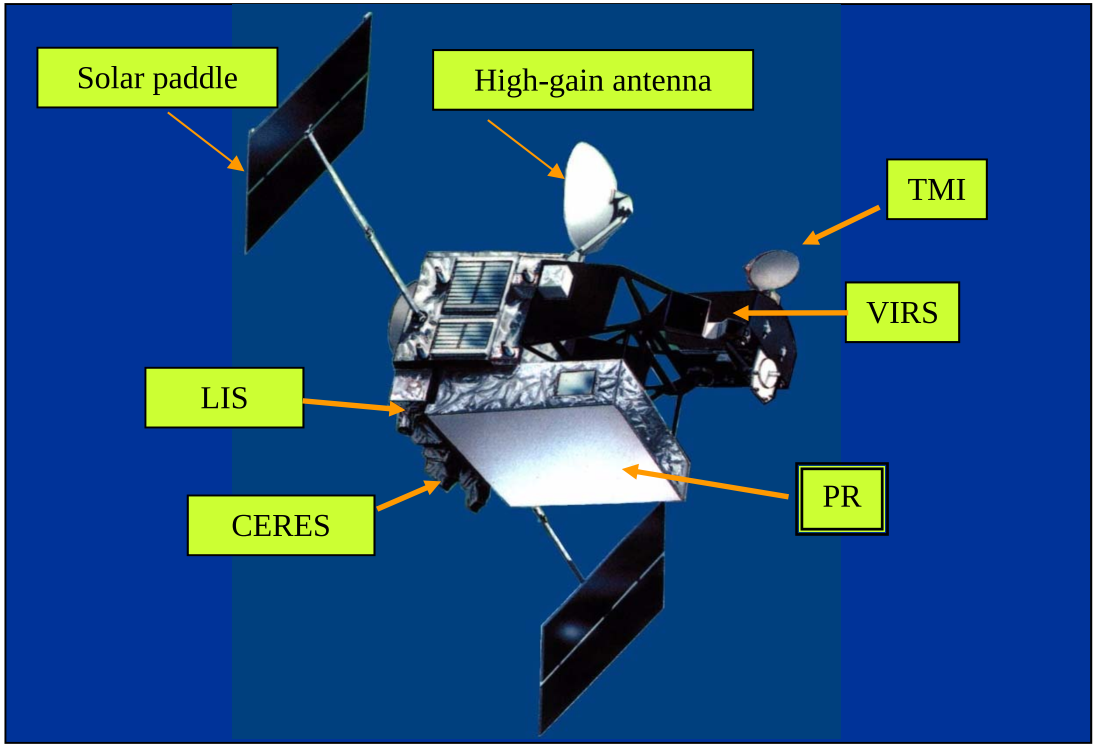

Orbit Altitude Inclination	Circular（Non-Sun Synchronous） 350km (402.5km since Aug. 2001) (±1.25km) 35 deg.
Sensor	**Precipitation Radar (PR)** TRMM Microwave Imager (TMI) Visible and Infrared Scanner (VIRS) Clouds and the Earth's Radiation Energy System (CERES) Lightning (LIS)

- Observation of tropical rainfall (Driving engine of global atmosphere)
- US-Japan joint mission (Japan: PR, Launch, US: Bus, 4 sensors, operation)
- Launched in Nov., 1997. Still under operation
- First space-borne precipitation radar developed by CRL and NASDA

NASDA NATIONAL SPACE DEVELOPMENT AGENCY OF JAPAN
CRL COMMUNICATIONS RESEARCH LABORATORY
NASA

TRMM Precipitation Radar

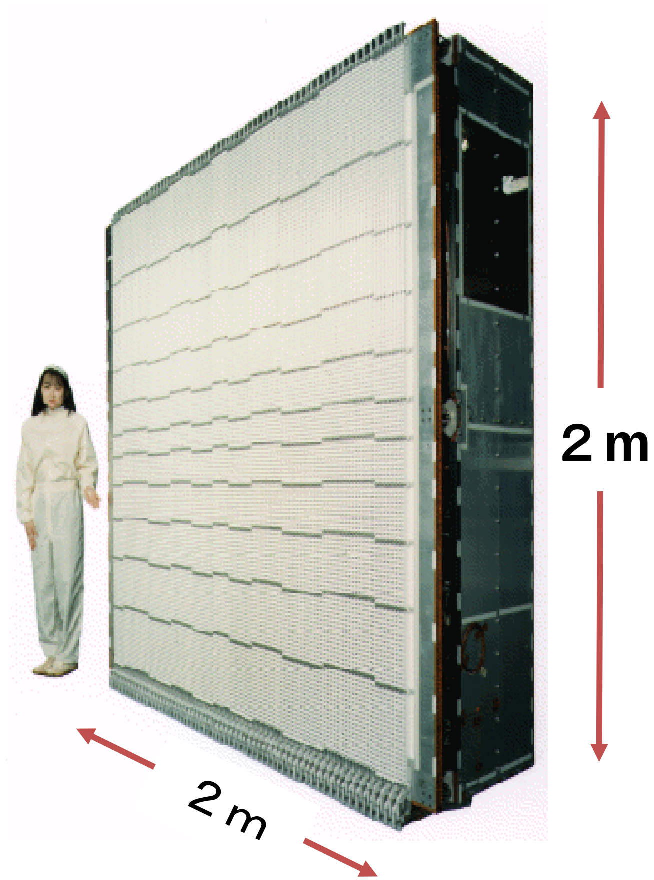

Radar type	Pulse radar
Antenna type	128-elem. WG slot array
Beam scanning	Active phased array
Frequency	13.796, 13.802 GHz
Polarization	Horizontal
TX/RX pulse width	1.57 / 1.67μsec
RX band width	0.6 MHz
Pulse rep. freq.	2776 Hz
Data rate	93.5 kbps
Mass	460 kg
Designed Life time	3 years
Sensitivity	< 0.5mm/h
Horizontal resolution	4.3 km (nadir)
Range resolution	250 m
# of indpdt samples	64 (fading noise < 0.7 dB)
Swath width	215km
Observable range	Surface to 15km

Concept of TRMM Rain Observation

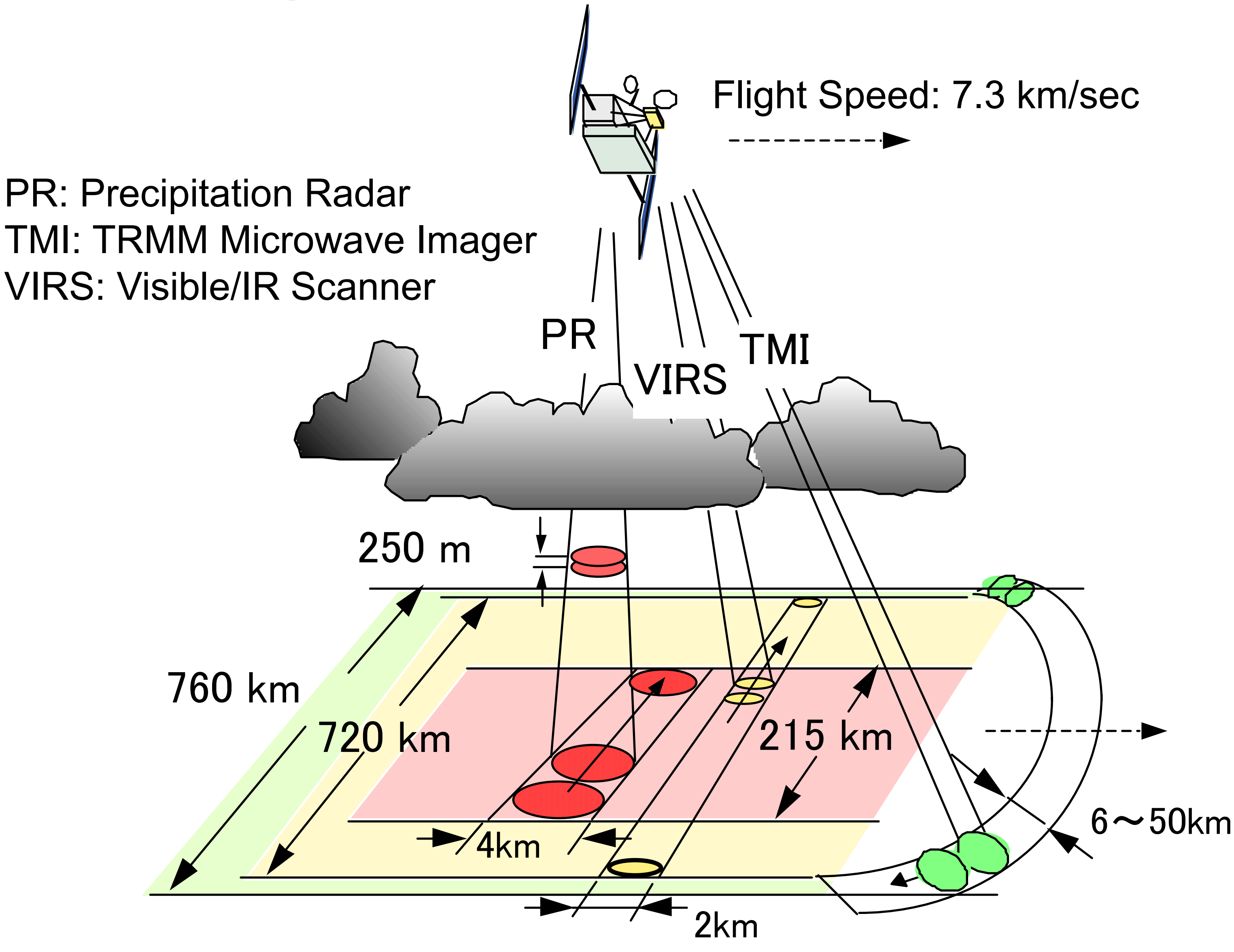

3-D Observation of a Typhoon by the PR

TRMM PR 2A25 Rain

Aug. 2, 2000, 20:49-20:53 (Japanese local time)

Rain intensity at H=2 km

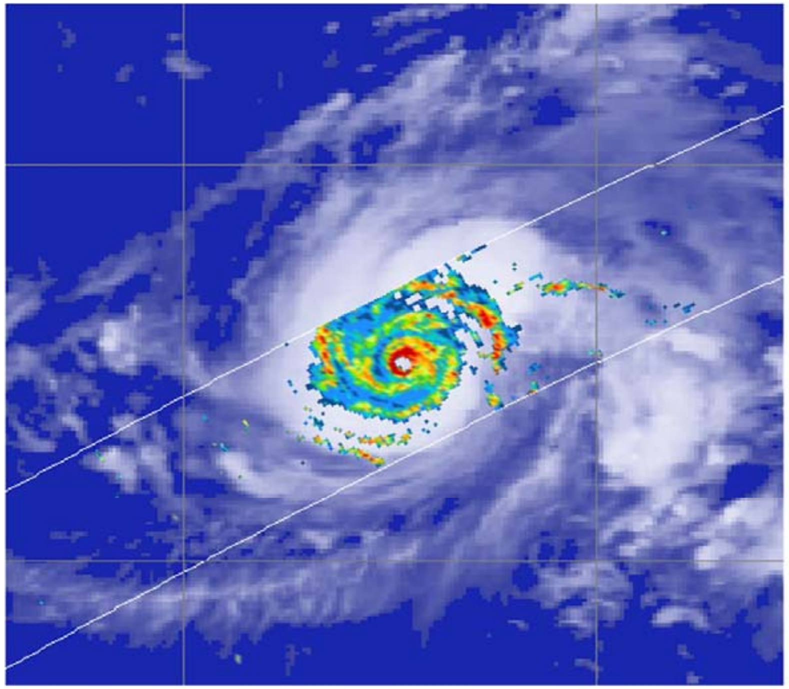

Vertical cross section through the eye and 3D structure

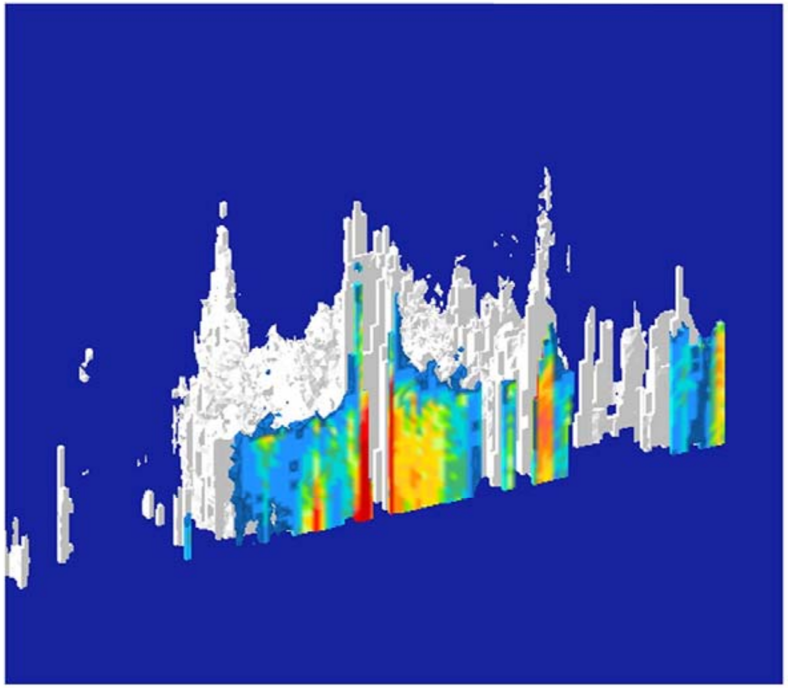

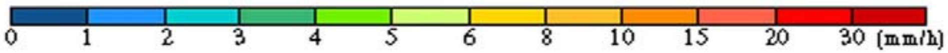

PR realized observation of 3D structure of rain over ocean where few observations had been available.

Monthly Rain Distributions estimated from the TRMM PR data in 1998 (El Nino year) and 1999

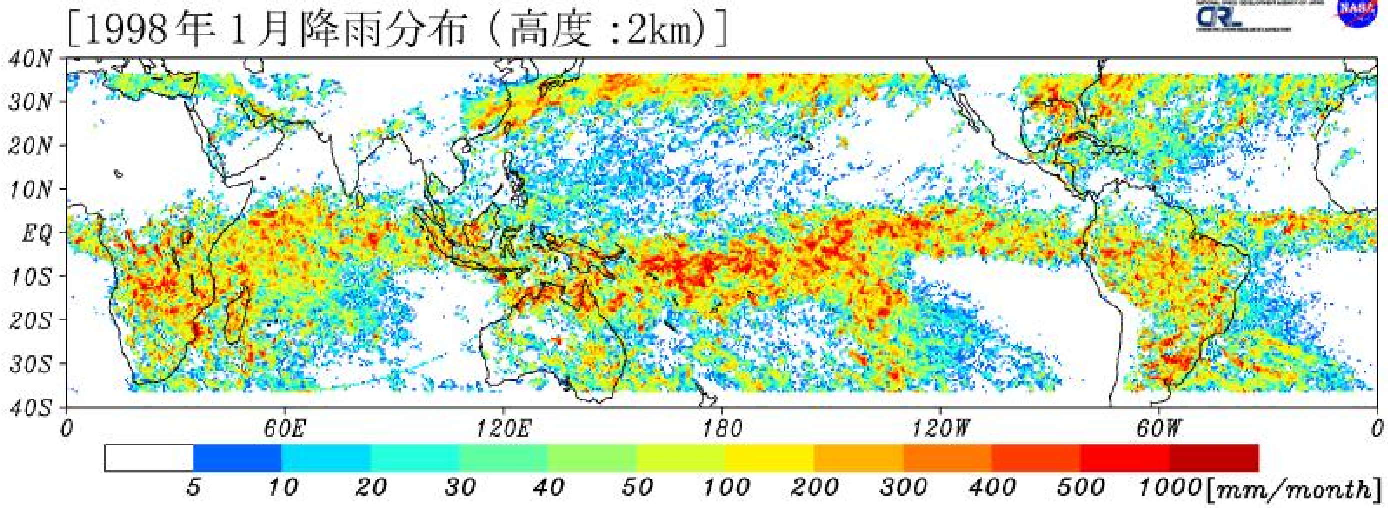

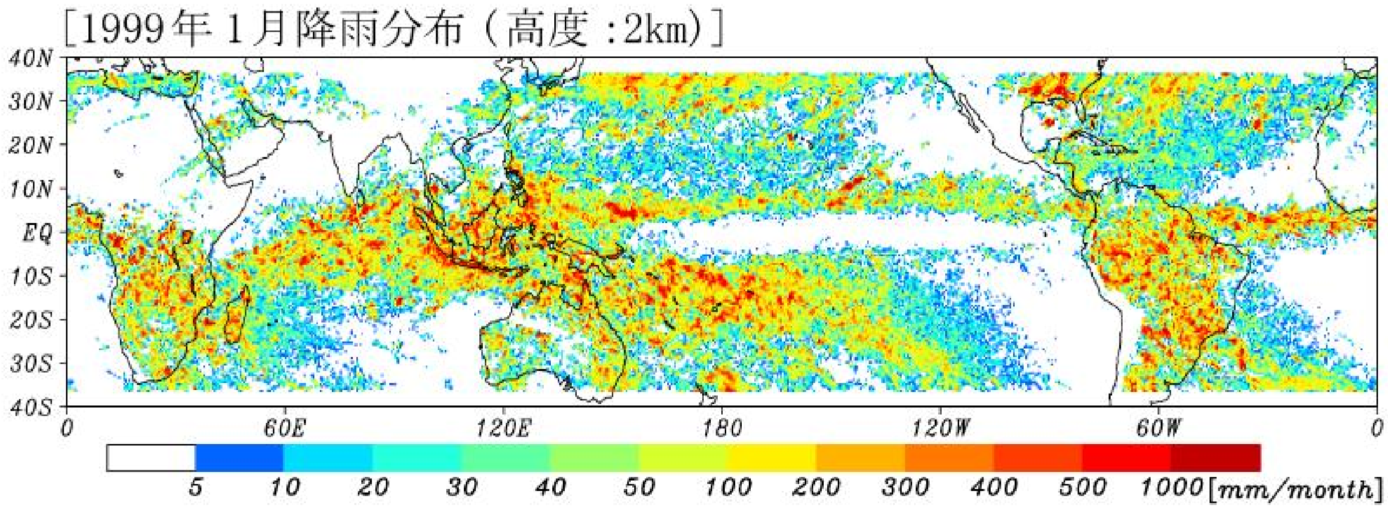

Strom Top Height Distribution measured with the TRMM Precipitation Radar

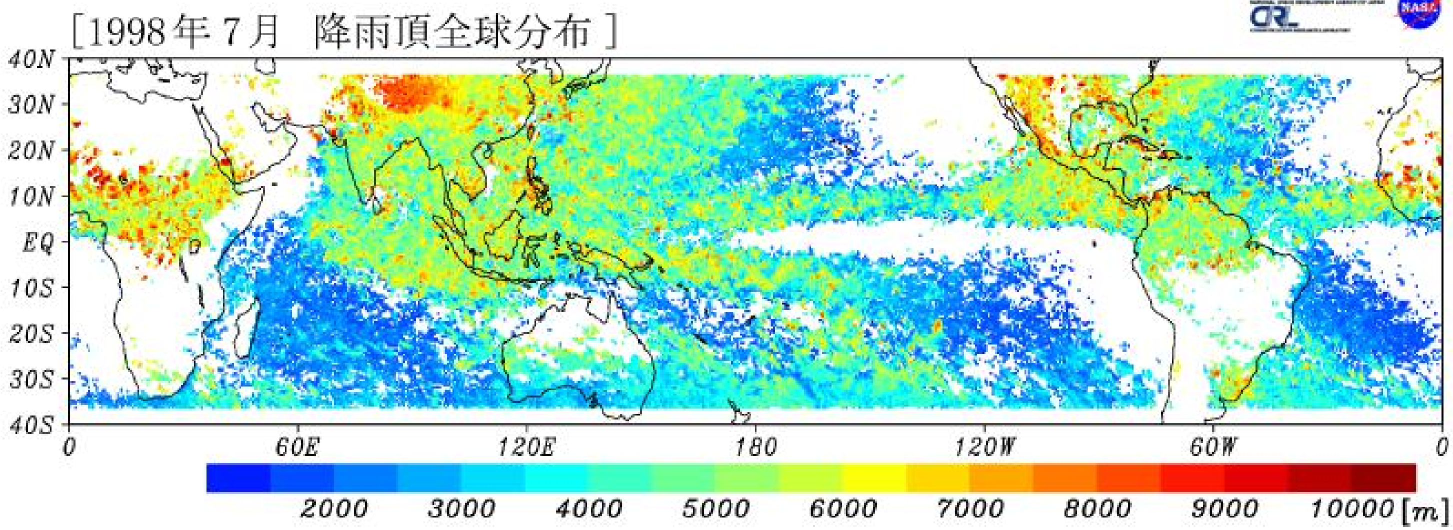

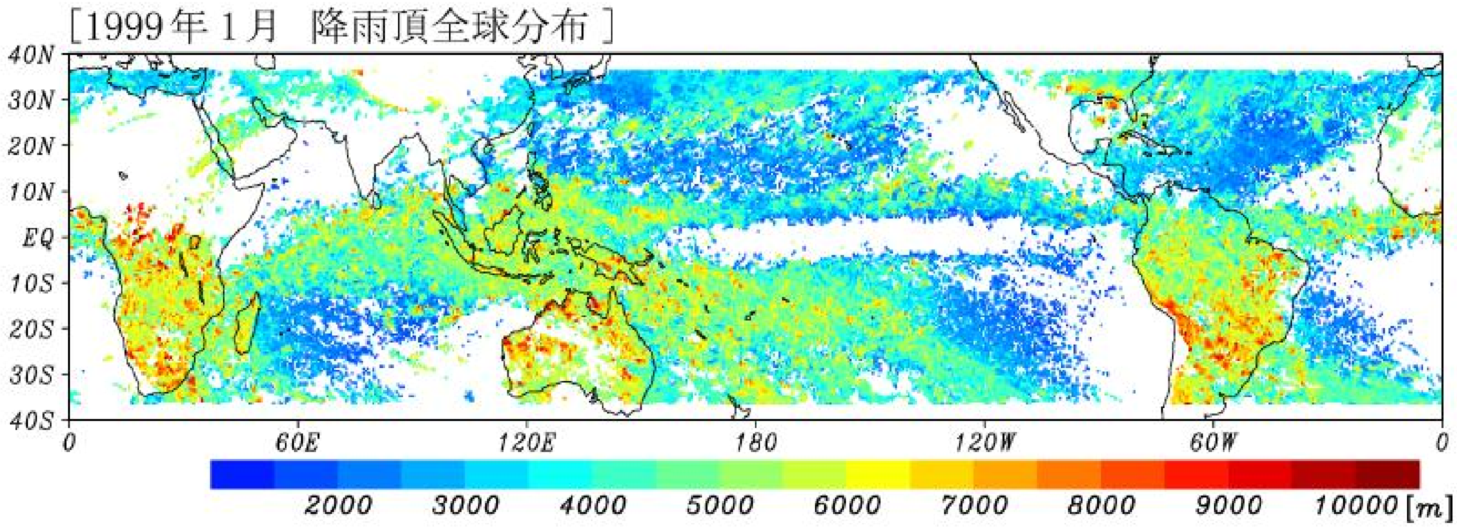

Peculiarities of satellite-borne radar

Differences from ground-based radar

- Hardware constraints
  - size, mass, power consumption
    - use of short waves -> attenuation
    - sensitivity
  - reliability
- Observation geometry
  - distance, angle
    - sensitivity, resolution
  - surface behind rain
    - surface clutter
  - moving platform (unless from a geostationary satellite)
    - difficulty in Doppler measurement

Peculiarities of space-borne radar

- Spacecraft constraints
  - Power (500 W)
  - Antenna dimensions (2 m)
  - Orbit (350 km)
- PR is a simple single-frequency radar
  - No Doppler
  - No polarimetry
- Observation geometry
  - large distance
  - nadir looking, surface echo (clutter)
  - high range resolution (250 m)
  - low horizontal resolution (4.5 km)
  - narrow swath (250 km)
- Use of short wavelength (13.8 GHz)
  - Attenuation correction
- Sparse sampling in time at a given location
- Various rain systems with different characteristics

Footprint size and wavelength

- Use of relatively high frequency (short wave) to realize a good horizontal resolution.
  - antenna beam width ~ $c_1\lambda/D$ (wavelength/diameter)
    - λ: wavelength of the electromagnetic wave
    - D: antenna diameter
    - c_1: a constant that depends on the antenna illumination (~1.2)
  - footprint size ~ $c_1 r\lambda/D$ (r: range to surface)
  - D < 2~3 m unless the antenna is developed on orbit
  - r > ~300 km.
  - -> use a small λ to make the footprint size ($c_1 r\lambda/D$) small.
  - to realize a 5 km footprint with a 2 m antenna from a 400km orbit, λ ~ 5*2/(1.2*400) m = 2.08 cm (= 14.4GHz)

Issues associated with short waves

- Attenuation
  - rain, snow, water vapor, cloud liquid water (liquid cloud droplets), and oxygen molecules
  - Correction methods:
    - Hitschfeld-Bordan method, Surface reference method
- Non-Rayleigh scattering effect
  - scattering cross section does not change proportionally to D^6
  - Drop size distribution model

PR Algorithm Flow and adjustable parameters

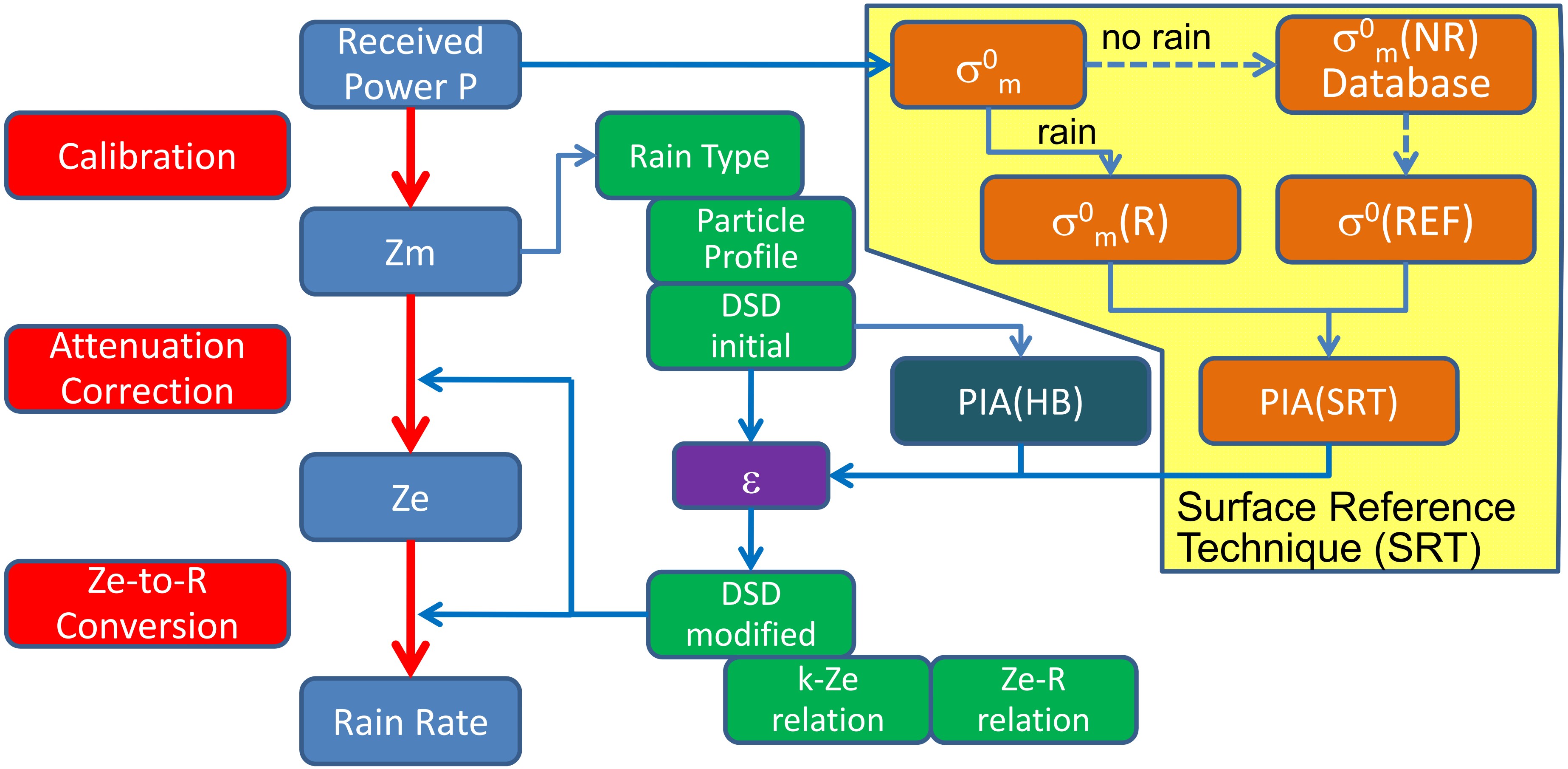

- Calibration
- Particle model
  - DSD parameters
  - particle profile
    - BB model
    - snow model

- Measurement errors
- PIA errors
- Rain profile in surface clutter
- Inhomogeneity

Radar Equation

$$P_r(r) = P_t \frac{G_t G_r \lambda^2 \theta_1 \theta_2 c\tau}{2^{10}\pi^2 \ln(2) r^2} \eta(r) \exp(-2\int_0^r k(s)\, ds)$$

$$\eta = \frac{1}{V}\sum_V \sigma_b = \int \sigma_b(D) N(D) dD$$

$$k = \frac{1}{V}\sum_V \sigma_t = \int \sigma_t(D) N(D)\, dD$$

$$Z_e = \frac{\lambda^4}{\pi^5 |K_w|^2}\eta, \qquad K = \frac{\epsilon_r - 1}{\epsilon_r + 2} = \frac{n^2 - 1}{n^2 + 2}$$

$$R = \frac{\pi}{6}\int D^3 v(D) N(D)\, dD \overset{\propto}{\approx} \int D^{3.67} N(D)\, dD$$

If $\lambda \gg \pi D$ (Rayleigh scattering),

$$\eta \propto \int D^6 N(D)\, dD = Z, \qquad k \propto \mathrm{Im}(-K) \int D^3 N(D)\, dD$$

Factors that may affect the rain estimates from space-borne radar

- Principles of radar measurement of rain
  - Conversion of received power (Pr) to apparent radar reflectivity factor (Zm) (Calibration of instrument)
  - Conversion of Zm into effective radar reflectivity factor (Ze) (attenuation correction)
  - Conversion from Ze to rain rate (R)
- Scattering and extinction characteristics of precipitation particles and their vertical distribution (Type of precipitation: rain, snow, groupel, hail, etc.)
  - Drop size distribution (DSD)
  - Phase state, density (Mixing formula)
  - Shape and canting angle
  - Temperature (refractive index)
- Fall velocity of precipitation particles (size, density, shape, vertical wind)
- Inhomogeneity of rain (Non-uniform distribution of rain)
- Scattering characteristics of sea and land surfaces
- Attenuation due to constituents other than precipitation itself
  - Clouds, water vapor, other gasses
- Effect of multiple scattering (Ka band and above)

Drop Size Distribution (DSD)

- Both *k-Ze* and *R-Ze* relations depend on DSD.
- Hitschfeld-Bordan's solution assumes a *k-Ze* relation.
- When the SRT is not applicable, the initial DSD determines the attenuation correction and the *Ze*-to-*R* conversion.
- When the SRT is applicable, α can be adjusted to match the H-B estimate of PIA to the SRT PIA. This in effect corresponds to adjusting the initial DSD.

Hitschfeld-Bordan solution

$$Z_m(r) = Z_e(r) \exp\left(-0.2 \ln 10 \int_0^r k(s)\, ds\right)$$

If $k = \alpha Z_e^{\beta}$, then

$$Z_e(r) = \frac{Z_m(r)}{\left(C_1 - 0.2 \ln(10) \beta \int_0^r \alpha(s) Z_m^{\beta}(s)\, ds\right)^{1/\beta}}$$

DSD variation in Indian rain

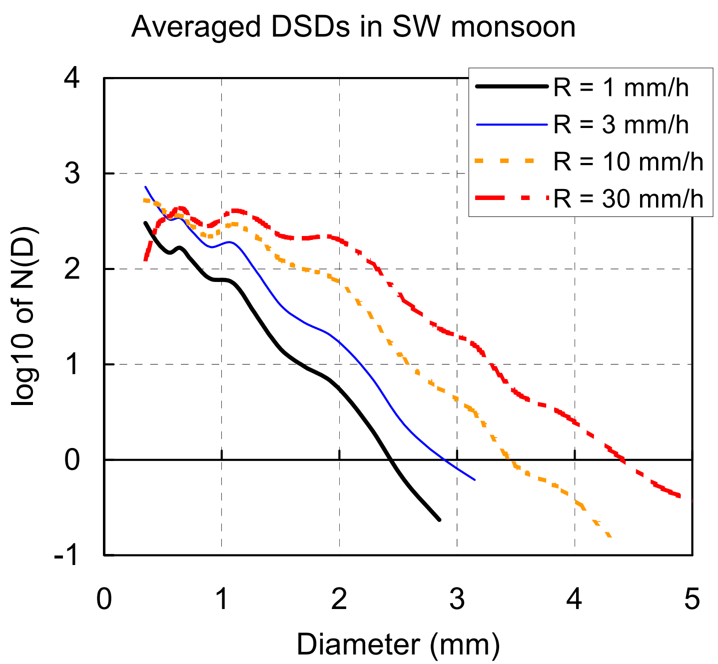

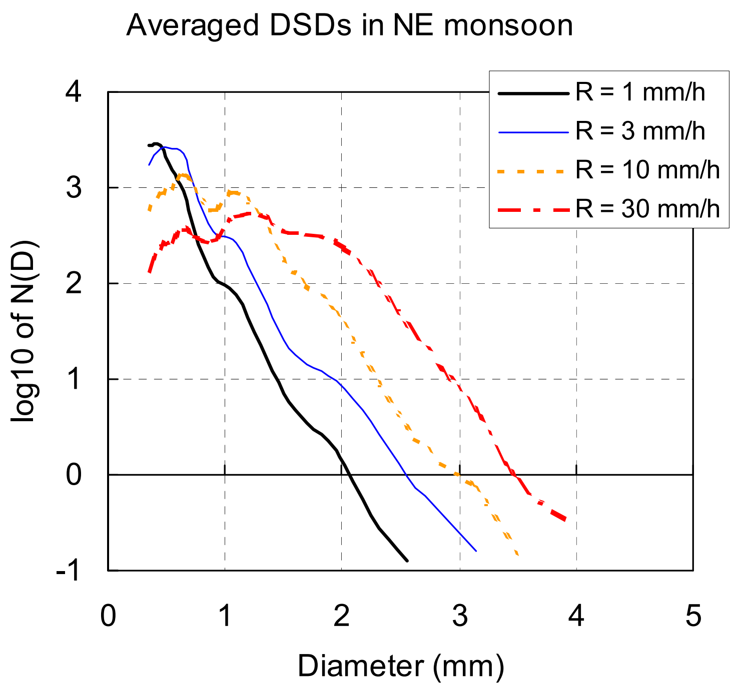

Averaged Dropsize Distribution during South-West (SW) and North-East (NE) monsoon seasons in Gadanki, south India in 1997 and 1999. SW and NE seasons are between May and October, and between November and December, respectively. DSDs within +/- 1 dB centered at the rain rate specified are averaged.

T. Kozu, K. K. Reddy and A.R. Jain
Oct. 20, 2000

Z-R relations
in SW and NE Indian monsoon seasons

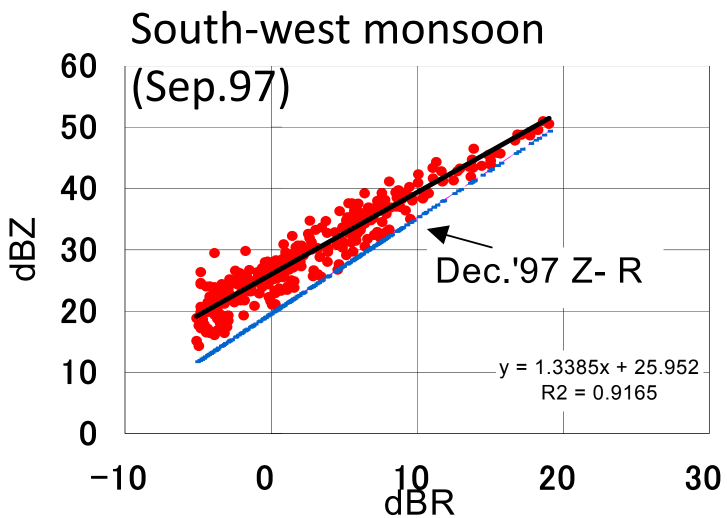

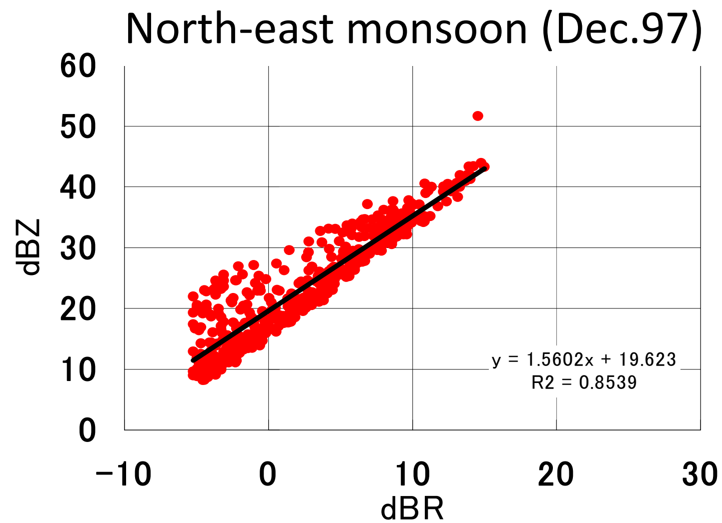

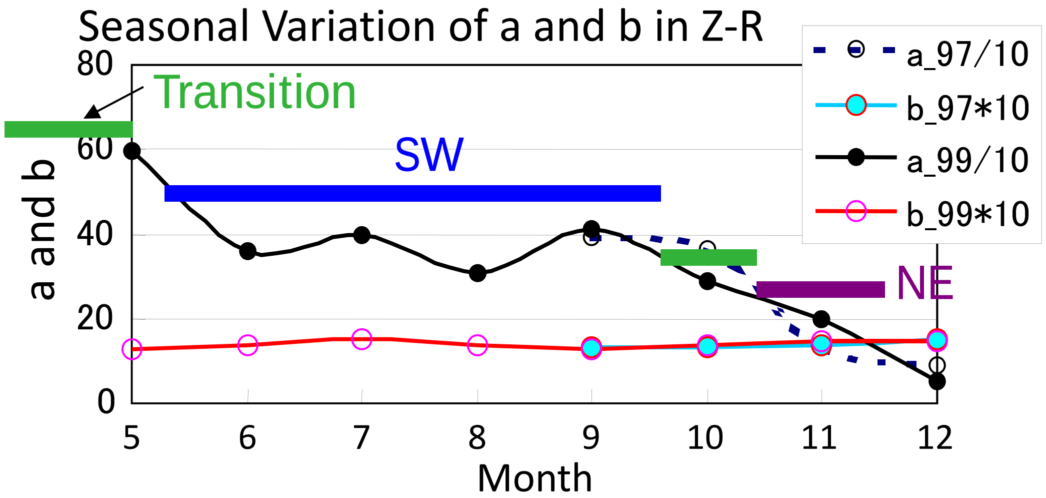

SW $Z = 405R^{1.29}$

NE $Z = 144R^{1.38}$

Strat/Conv separation:
Not significant

Surface Reference Technique

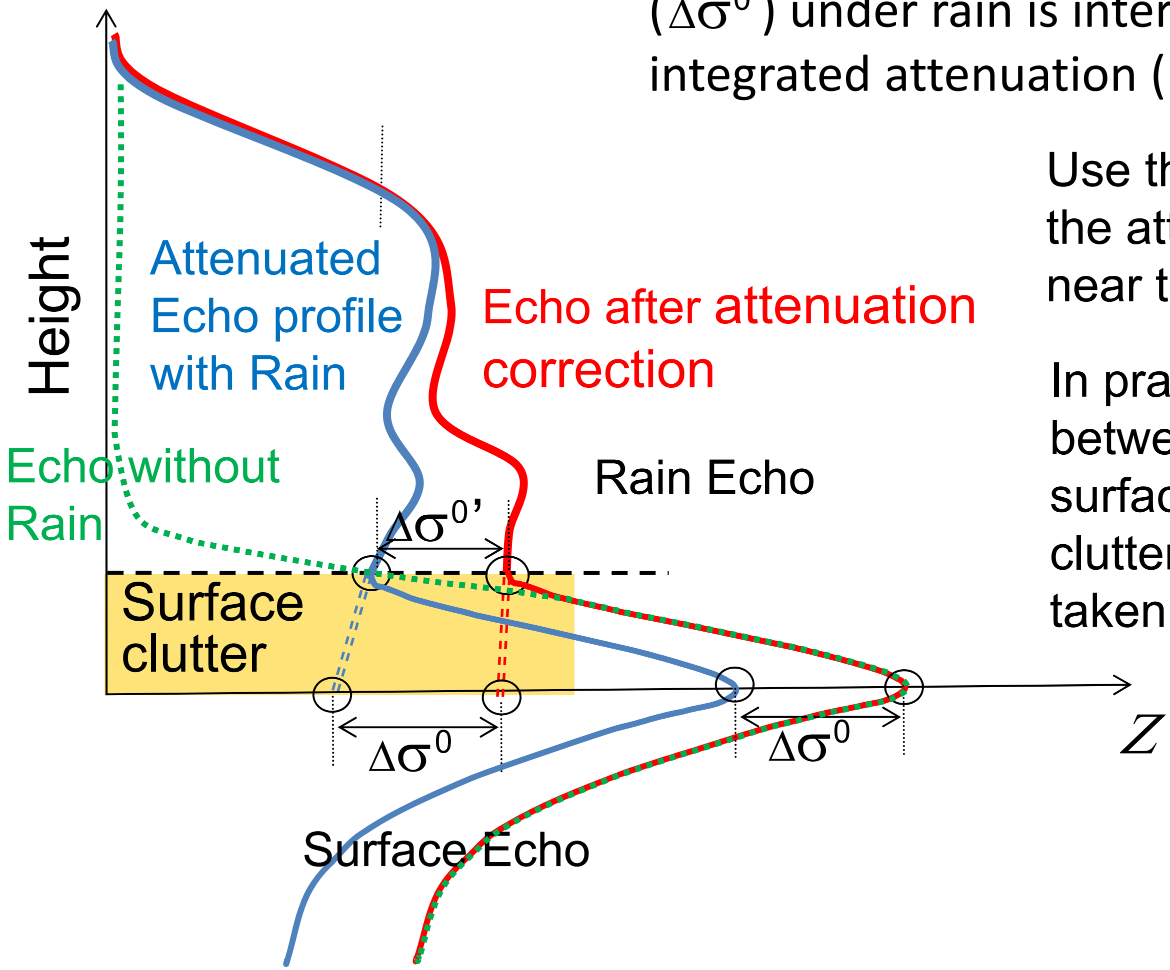

Decrease of the apparent surface echo ($\Delta\sigma^0$) under rain is interpreted as the path-integrated attenuation (PIA) due to rain.

Use this PIA to correct for the attenuation of rain echo near the surface.

In practice, the difference between the PIA to the surface and the PIA to the clutter-free bottom must be taken into account.

Rain and Surface Echoes

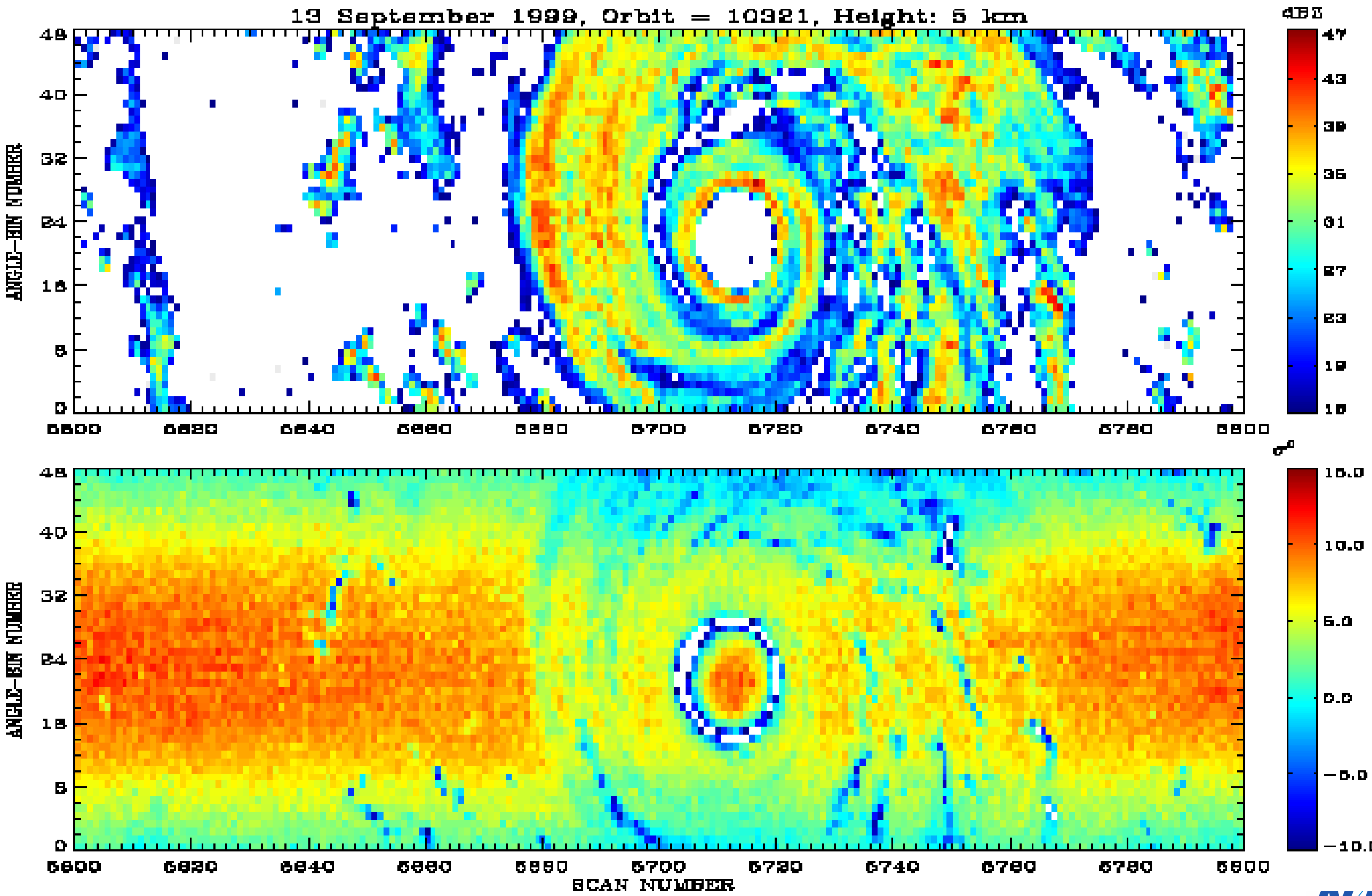

Vertical Cross Section of Radar Echo and Decrease of Apparent Surface Cross Section

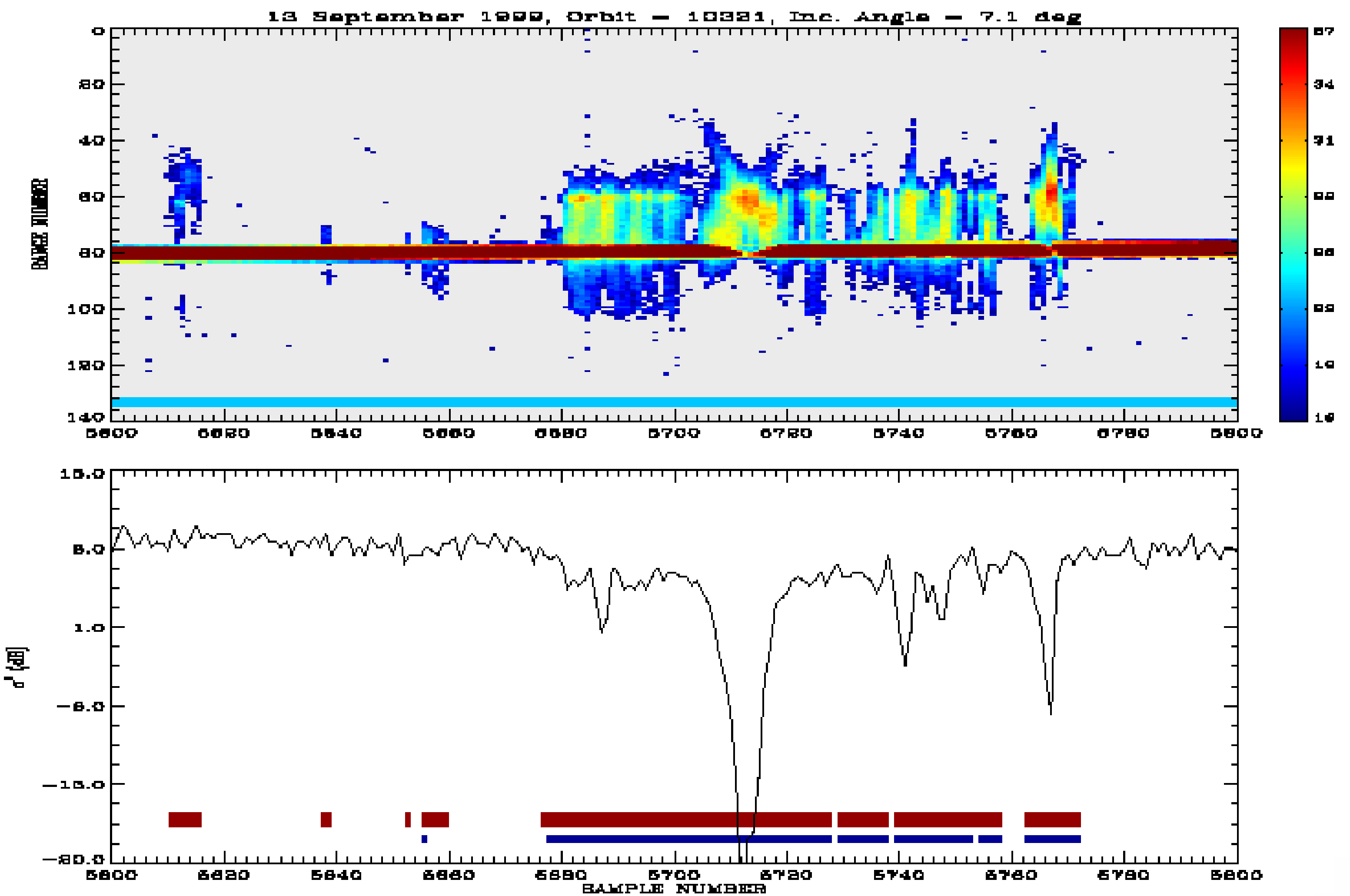

TRMM/PR Standard Algorithm

$$Z_m(r) = Z_e(r)\exp\left[-0.2\ln(10)\int_0^r k(s)\,ds\right]$$

$$k(r) = \alpha_0(r) Z_e(r)^{\beta_0}$$ *DSD assumed*

$$Z_e(r_s) = Z_m(r_s)/(1-\zeta)^{1/\beta_0}$$

$$\zeta = 0.2\beta_0 \ln(10)\int_0^{r_s} \alpha_0(s) Z_m(s)^{\beta_0}\,ds$$

$$\mathrm{PIA}_{\mathrm{HB}} = -\frac{10}{\beta_0}\log_{10}(1-\zeta)$$ Hitschfeld-Bordan (HB)

$$\mathrm{PIA}_{\mathrm{fin}} = -\frac{10}{\beta_0}\log_{10}(1-\varepsilon\zeta)$$ Bayesian

$$\mathrm{PIA}_{\mathrm{SRT}} = \sigma^0_{\mathrm{SRT}} - \sigma^0_m$$ Surface Reference Technique (SRT)

σ^0_{SRT} is an estimate of σ^0_e

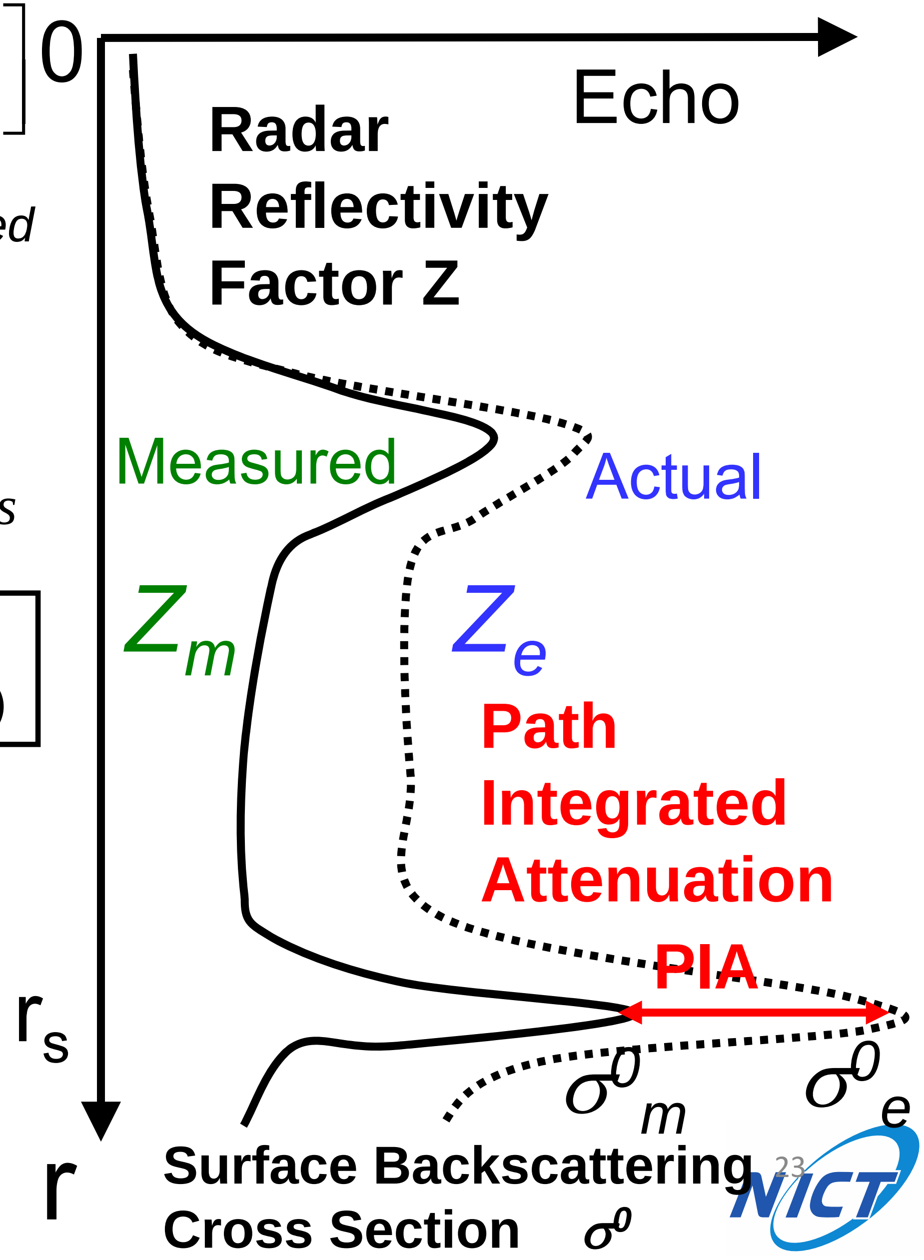

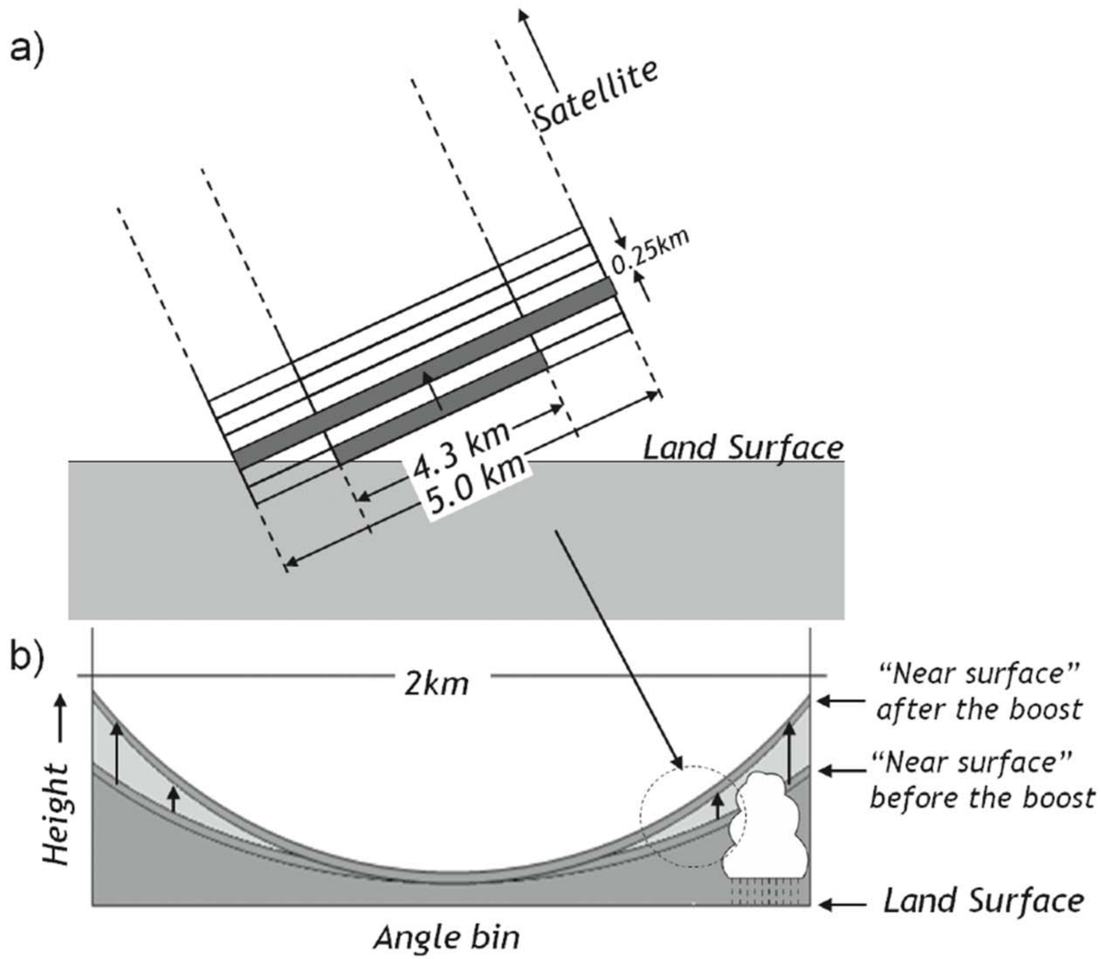

Shmizu et al. (2009)

Other issues due to the nature of the measurements

- main lobe and side lobe clutter obscuring the near surface echo, can contaminate meteorological echo
- Uncertain σ_0 in complex terrain
- *A priori* DSD assumed as a function of height. Appropriate?
- Single frequency measurements + unreliable PIA = limited independent DSD information

Rain-type count and BB count
- angle bin dependence -

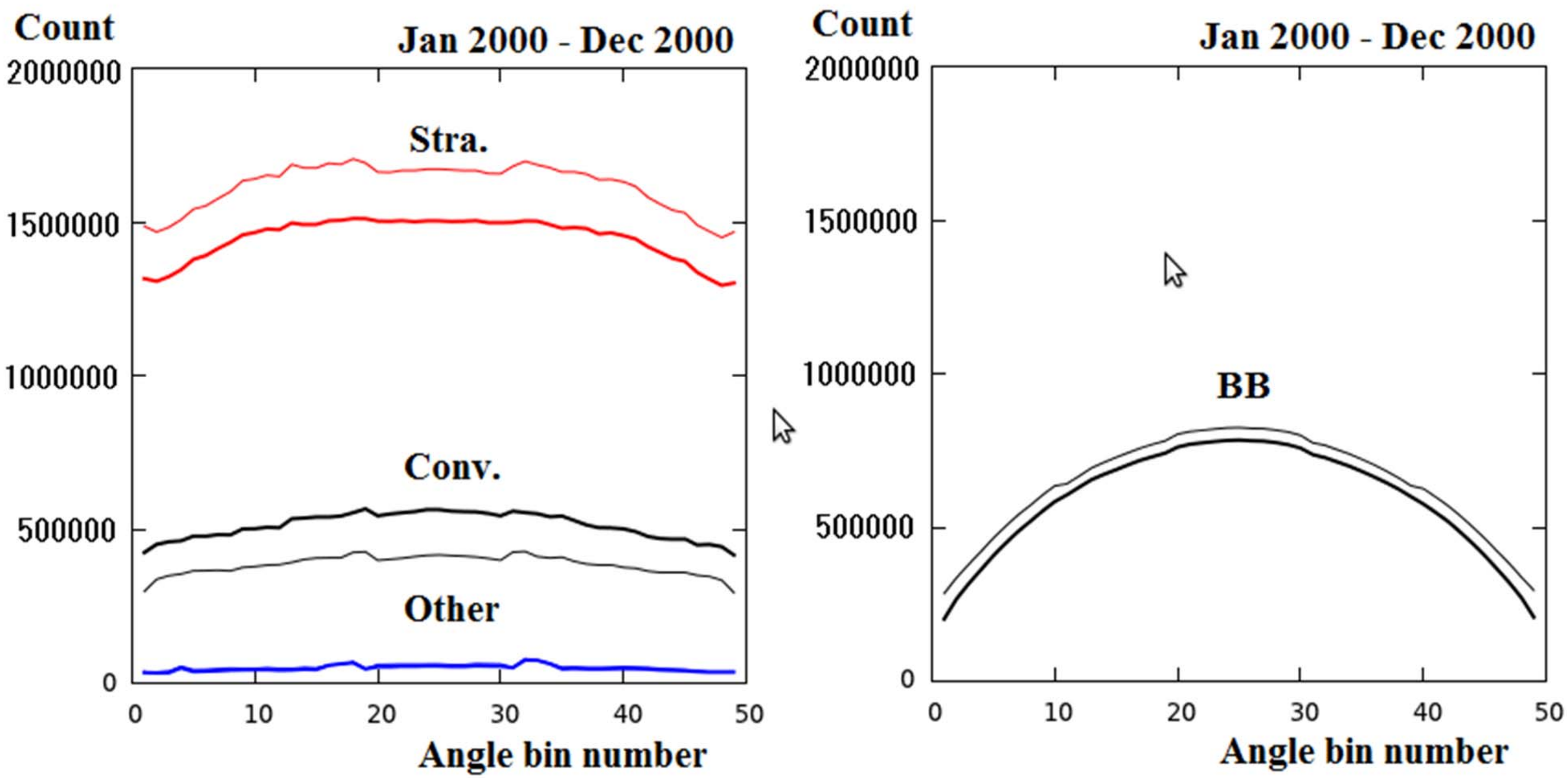

Thin: V6
Thick: V7 OAT

(Courtesy of J. Awaka)

k profiles for Z_e=40 dBZ

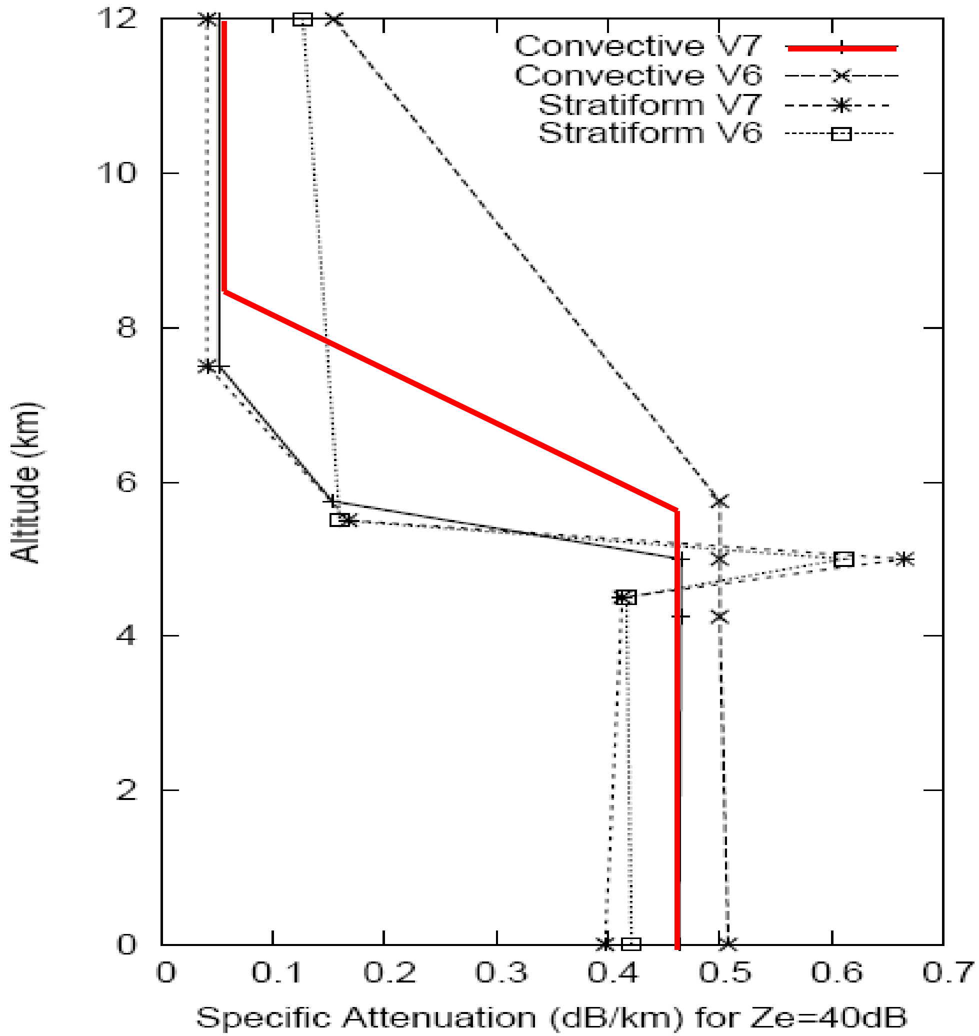

0 degree C height is assumed at 5 km
The lapse rate is assumed to be -6 degrees/km.

The assumed profile has been changed to the red line in V7 (ITE232).
(100% ice above the -20 degree level.)
It was the solid line before the change
(100% ice above the -15 degree level.)

Effect of non-uniform rain distribution

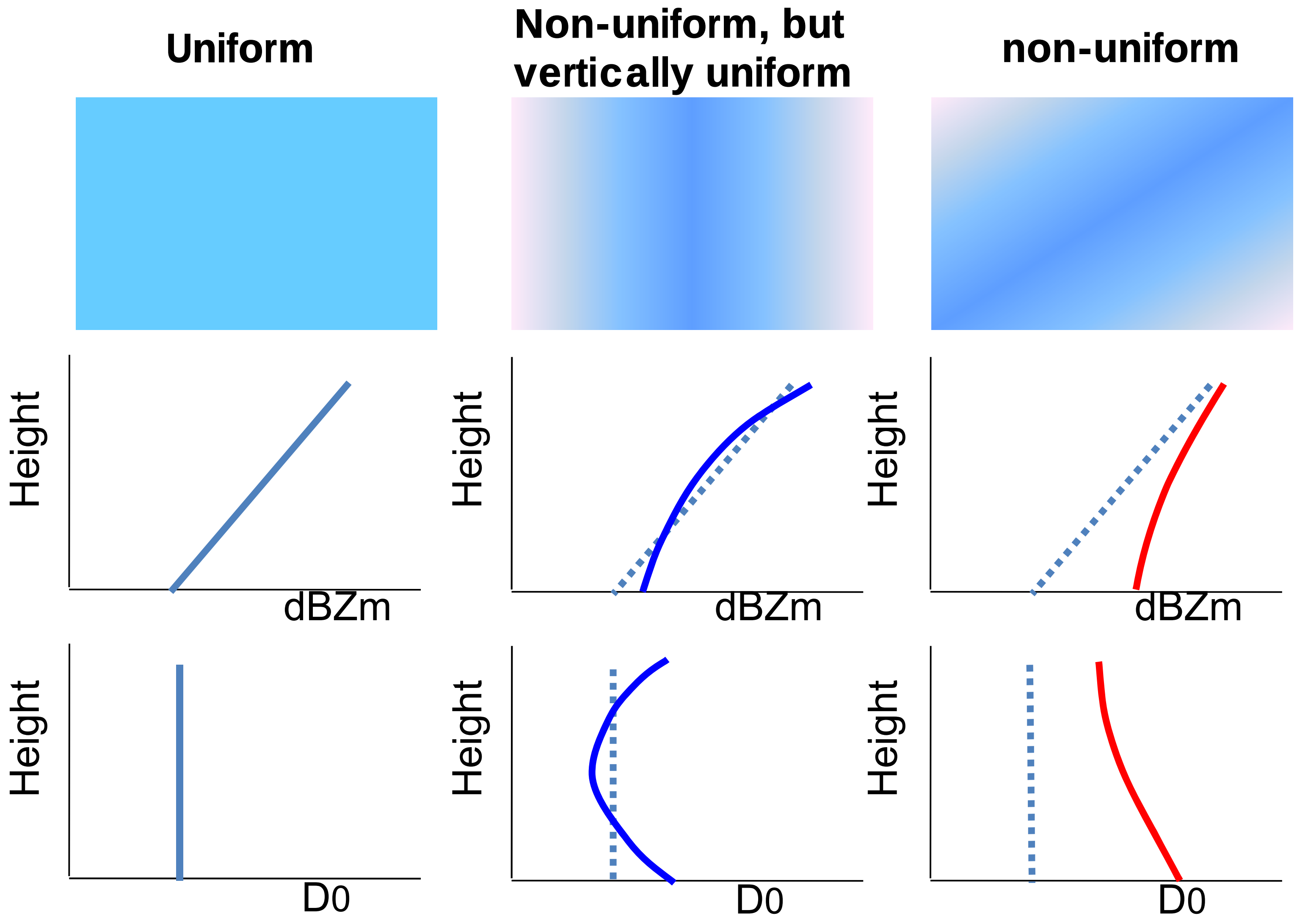

Reasons for Revisions

- Major reasons for the past revisions
  - Internal inconsistencies: angle-bin dependence,
  - Disagreement of rain estimates between PR and TMI.
  - Discrepancies between ground measurements and PR estimates were found to be not significant enough to motivate the revision until the revision for version 7
    - ground measurements had large errors and comparisons between satellite data and ground data on the same footings were not easy.
- Longevity of the TRMM satellite enables us to make climatological comparisons with ground data.
  - Comparisons using histograms of rain rates in addition to the comparisons with the total rain amount revealed underestimation of rain with PR at many places over land in various time intervals.

Agreement with TMI

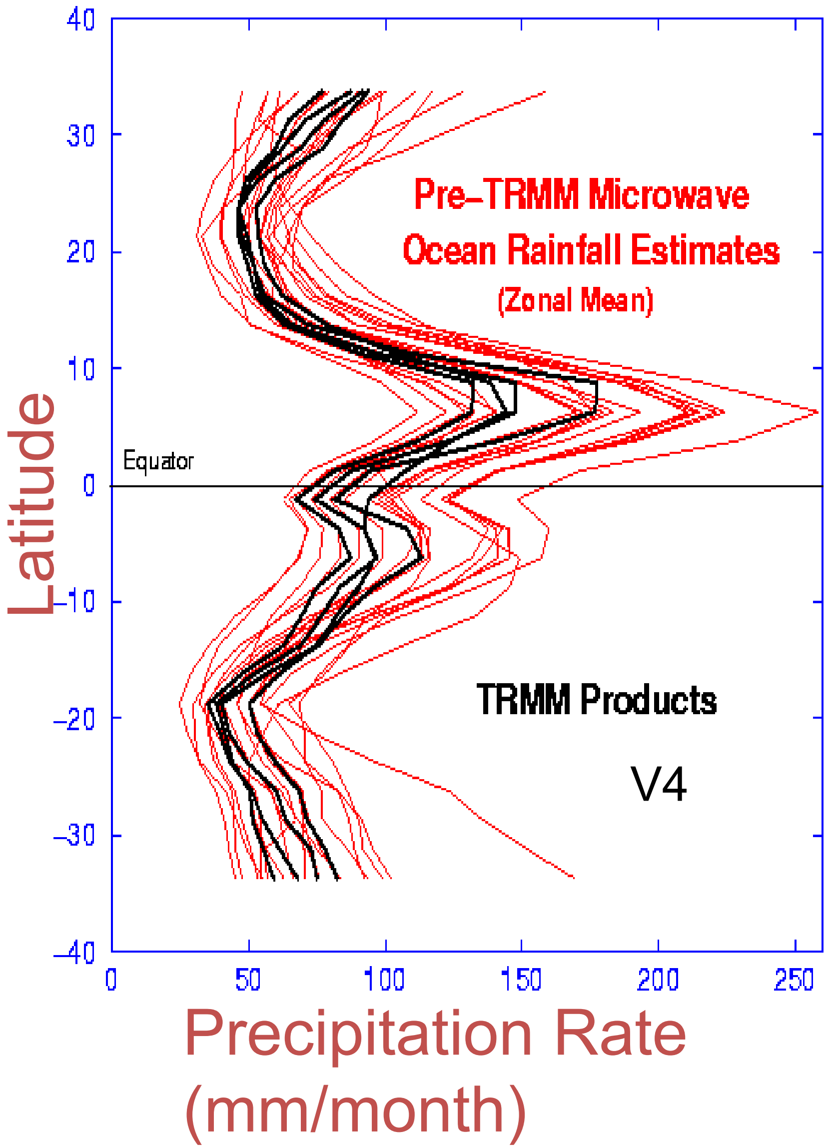

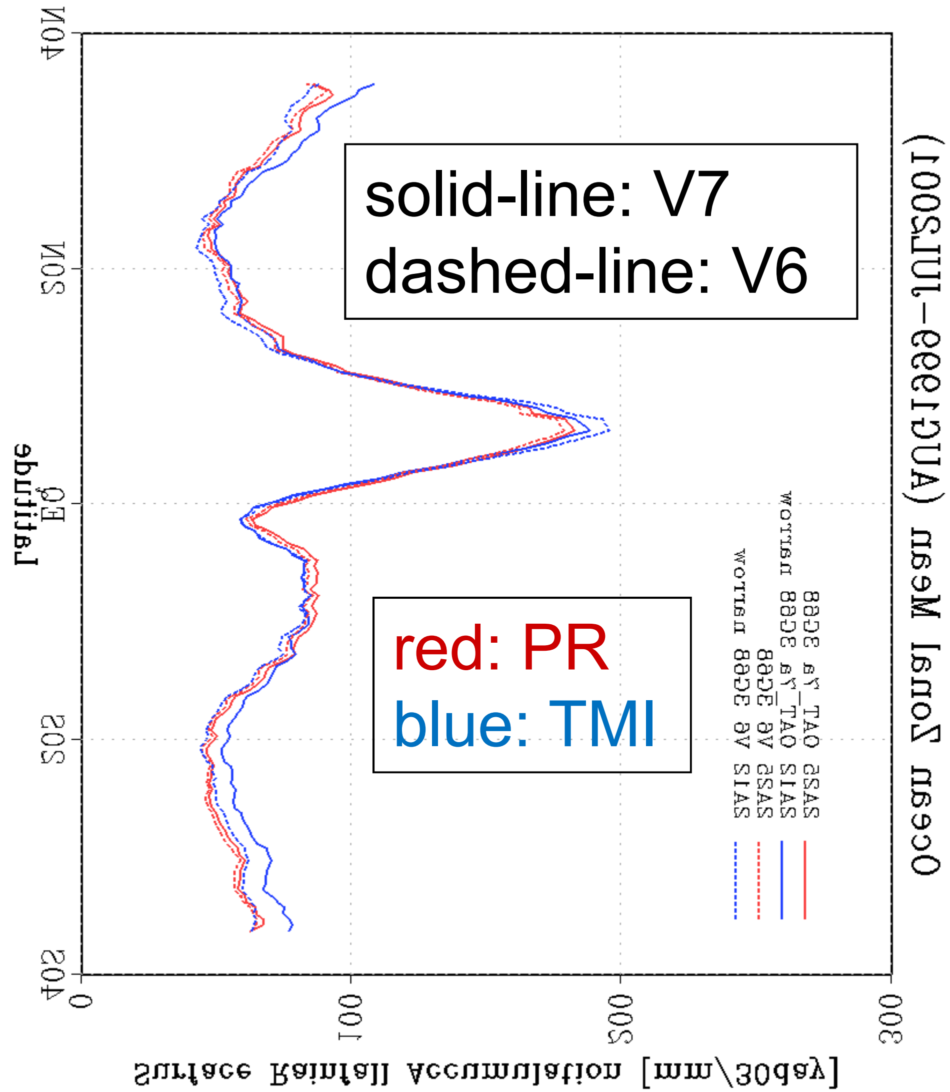

Future Issues

- ε-statistics shows a clear difference between rain over ocean and rain over land.
  - The current algorithm assumes common PSD parameters over ocean and land for each storm type.
  - A positive bias of ε often found over ocean and a negative bias over land suggest that there are more small drops than the assumed PSD over ocean and the opposite over land.
  - Possibility of defining regionally dependent PSD models from the knowledge we accumulated in the past.
- Orographic rain.
  - vertical structure of orographic rain may differ substantially from other types of rain.
  - Estimating surface rain from the rain echoes at altitude much higher than the surface involves a large error.
  - Poor performance of SRT in mountainous regions amplifies the issue.
- Non-uniformity of rain distribution within a footprint remains to be a very complex but important issue to be solved in the future.

Difference between radar and radiometer retrieval of rain

- Radar
  - well defined range information
    - Height information is very reliable.
  - Z-R relation scatters more than Tb-R relation
    - Echo power is more sensitive to DSD variation than Tb.
  - Number of wavelengths is very limited in practice.
- Radiometer
  - Needs to assume a vertical precipitation profile.
    - e. g., freezing height

Time series of monthly mean rainfall anomalies over Tropical ocean

－Comparison among different passive microwave algorithms－

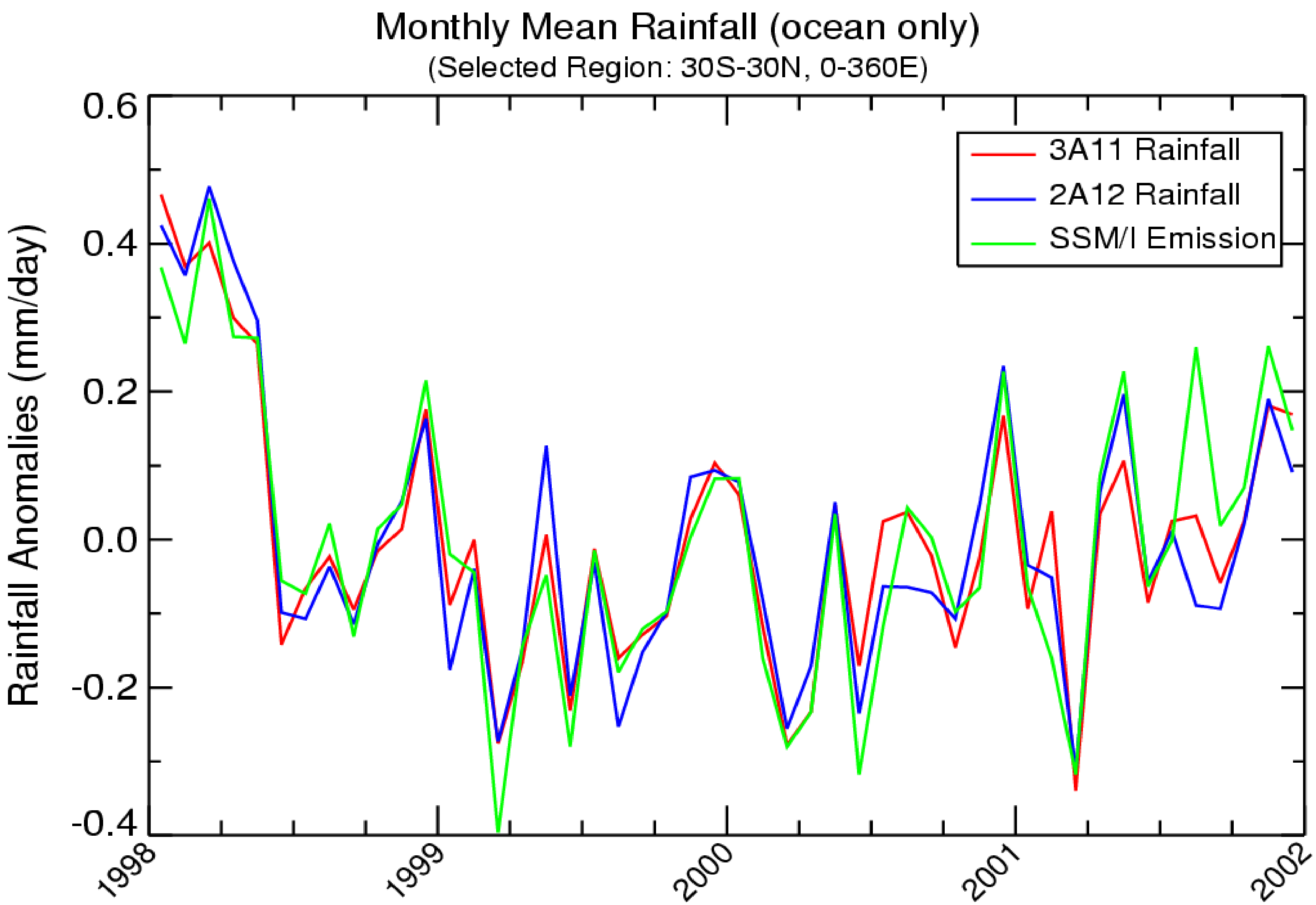

(W. Berg, et al.)

Time series of monthly mean rainfall anomalies over Tropical ocean

(TRMM Ocean Retrievals)

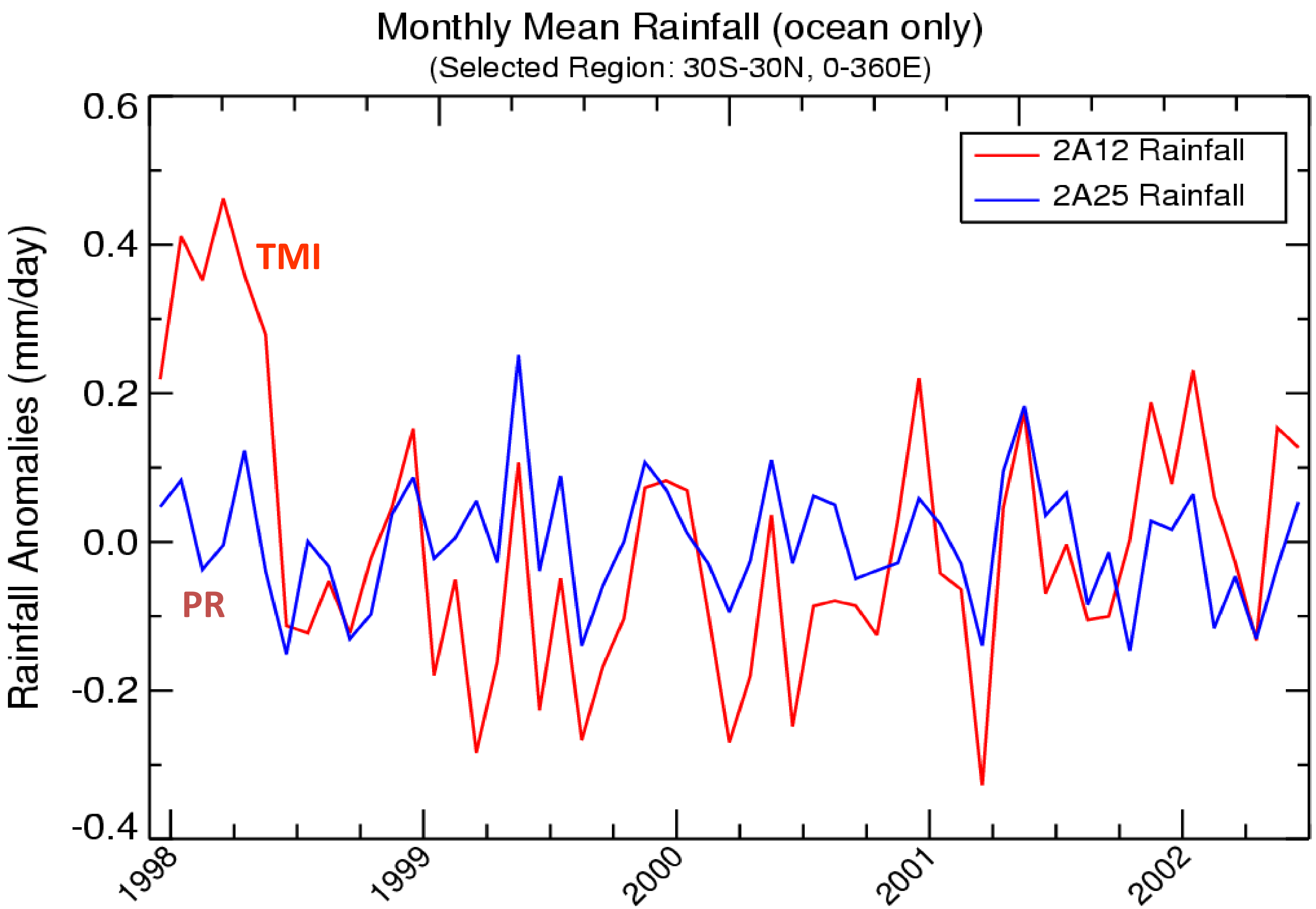

(W. Berg, et al.)

Passive Microwave Retrievals

Column integrated water vs rainfall rate

Tb's in the low frequency channels of a microwave radiometer are proportional to the column integrated rain water content.

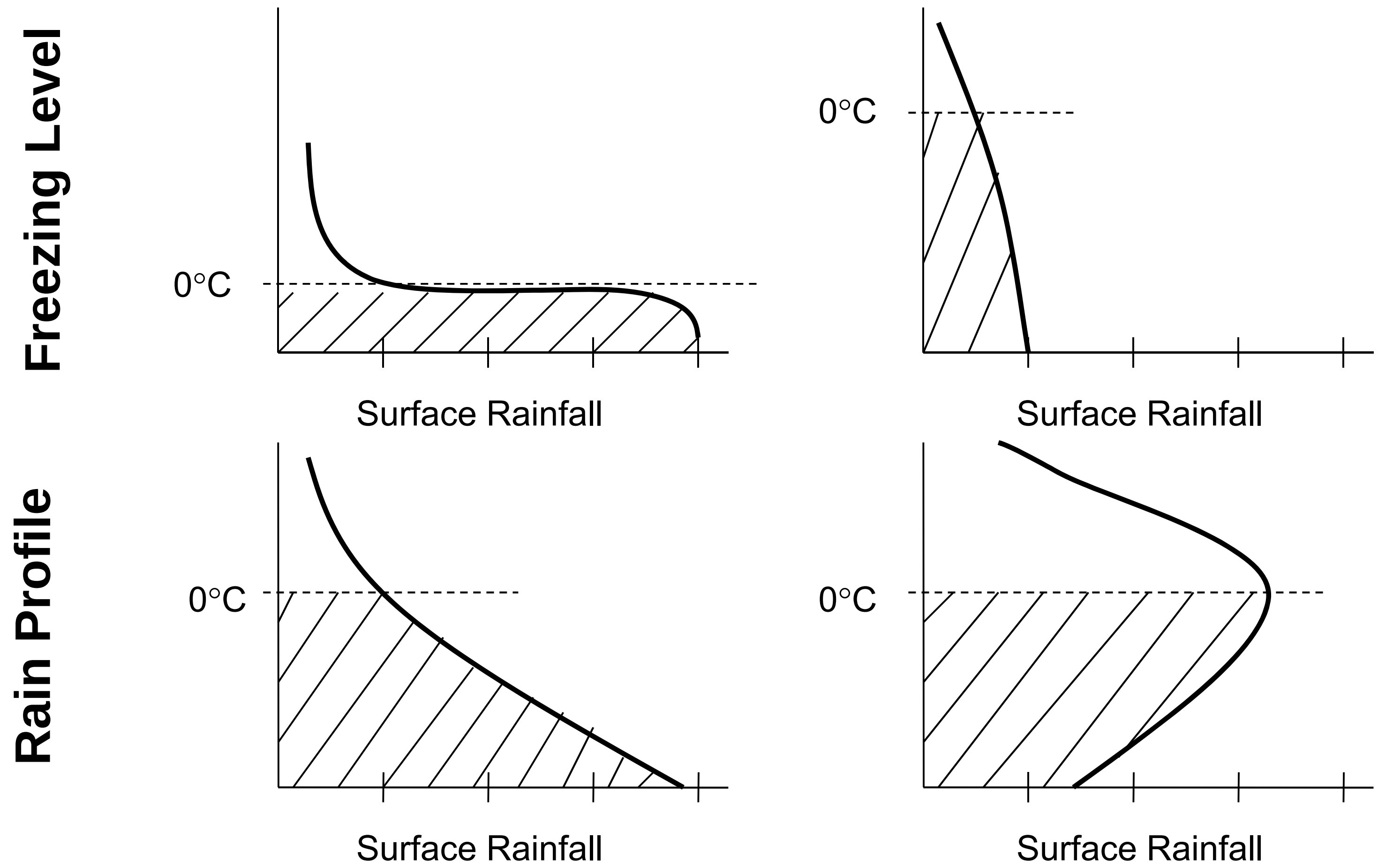

(Courtesy of W. Berg)

PR Bright-Band Height and TMI Freezing Height

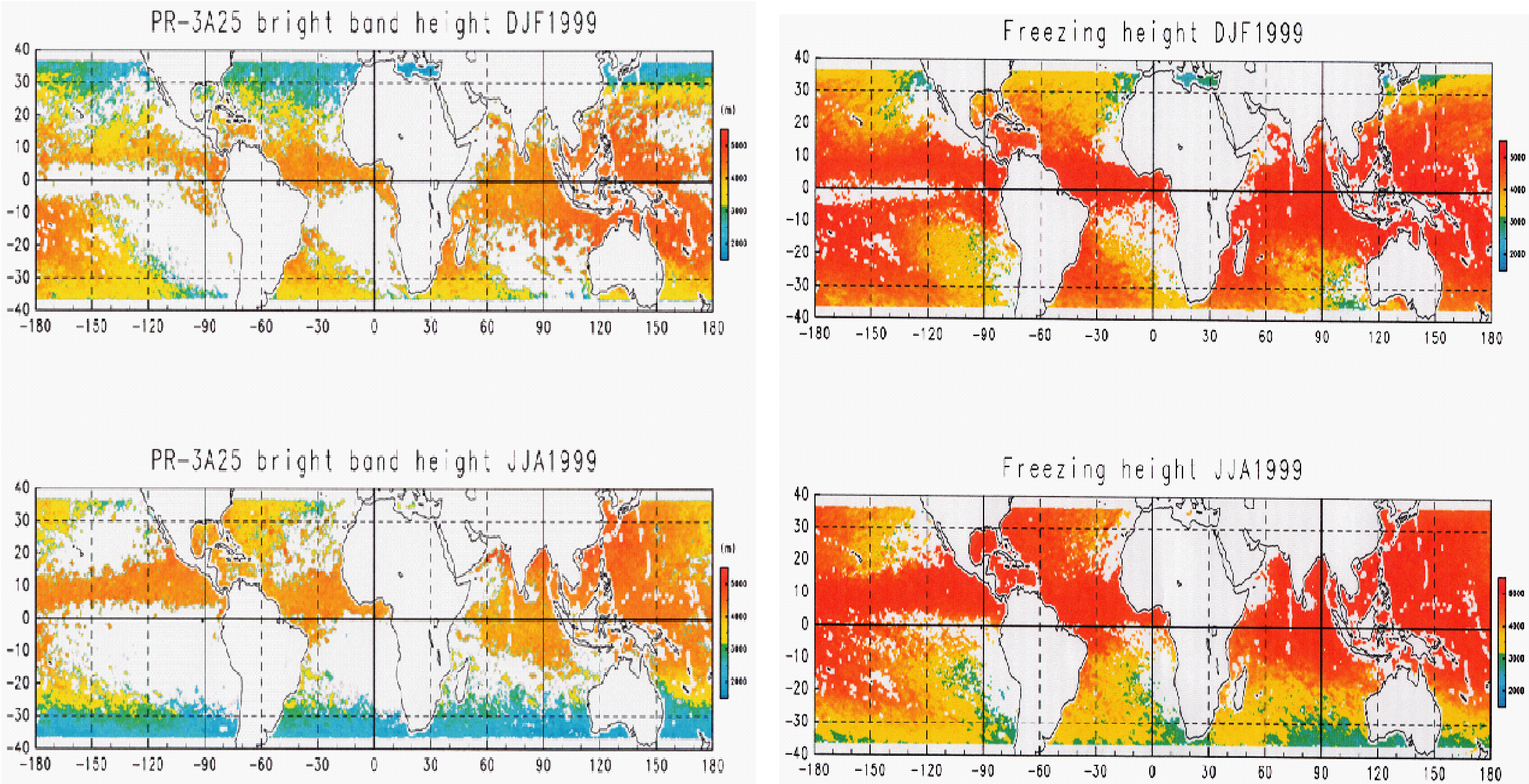

TMI Freezing Height – PR Bright Band Height

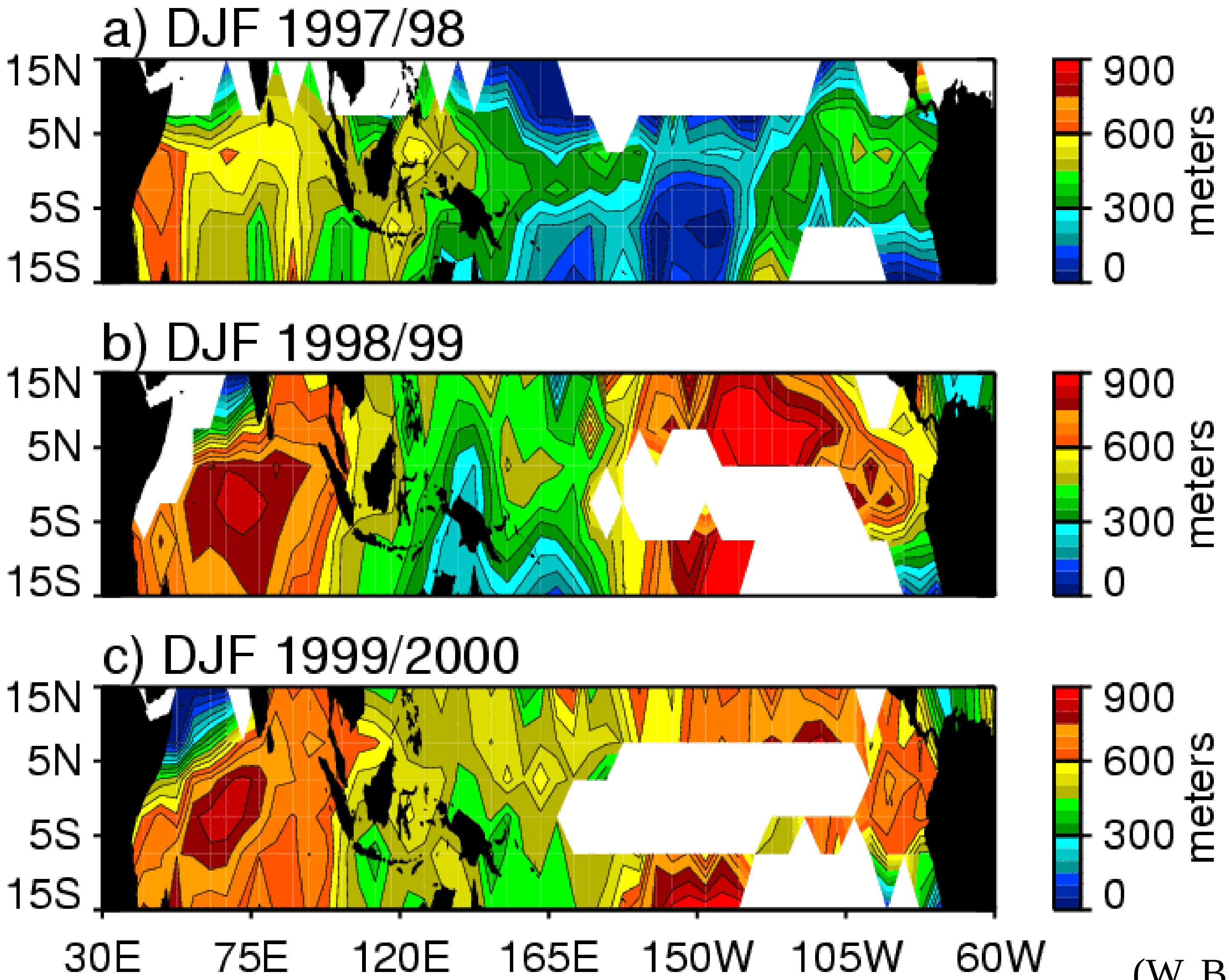

(W. Berg, et al.)

PR and TMI Regional Validation

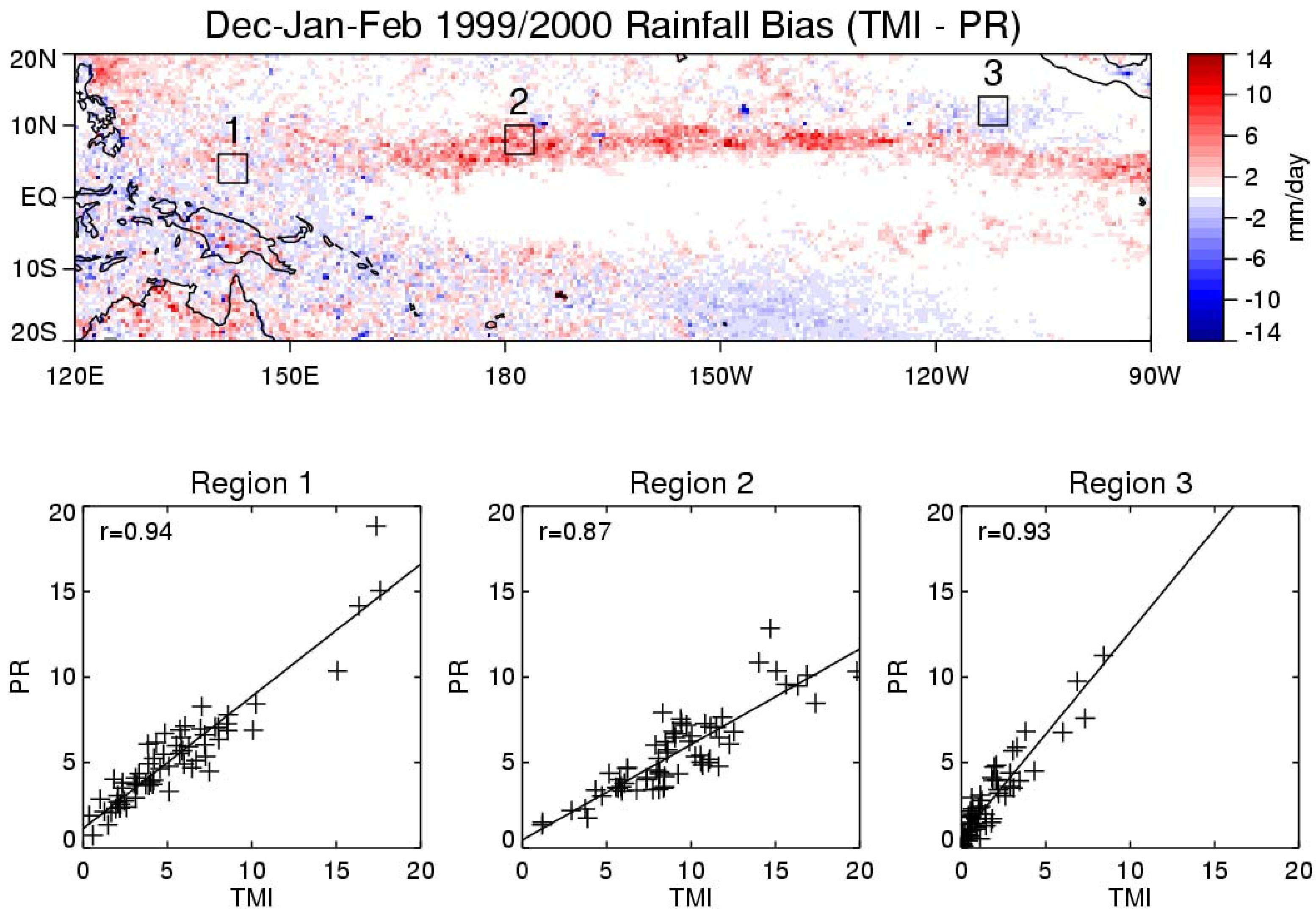

TMI V6, PR V5

(W. Berg, et al.)

GPM (Global Precipitation Measurement Mission)

Dual-frequency Precipitation Radar
二周波降水レーダ

GPM core satellite

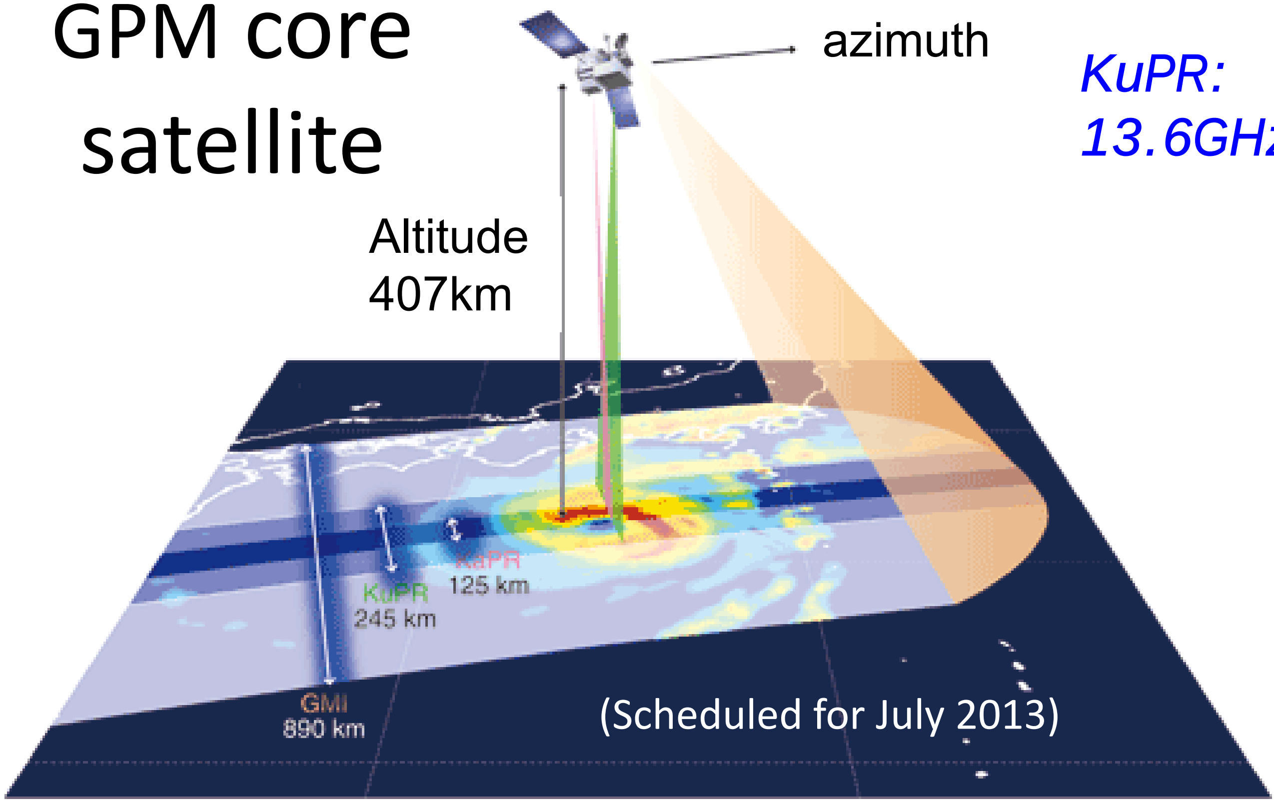

DPR (Dual-frequency Precipitation Radar)

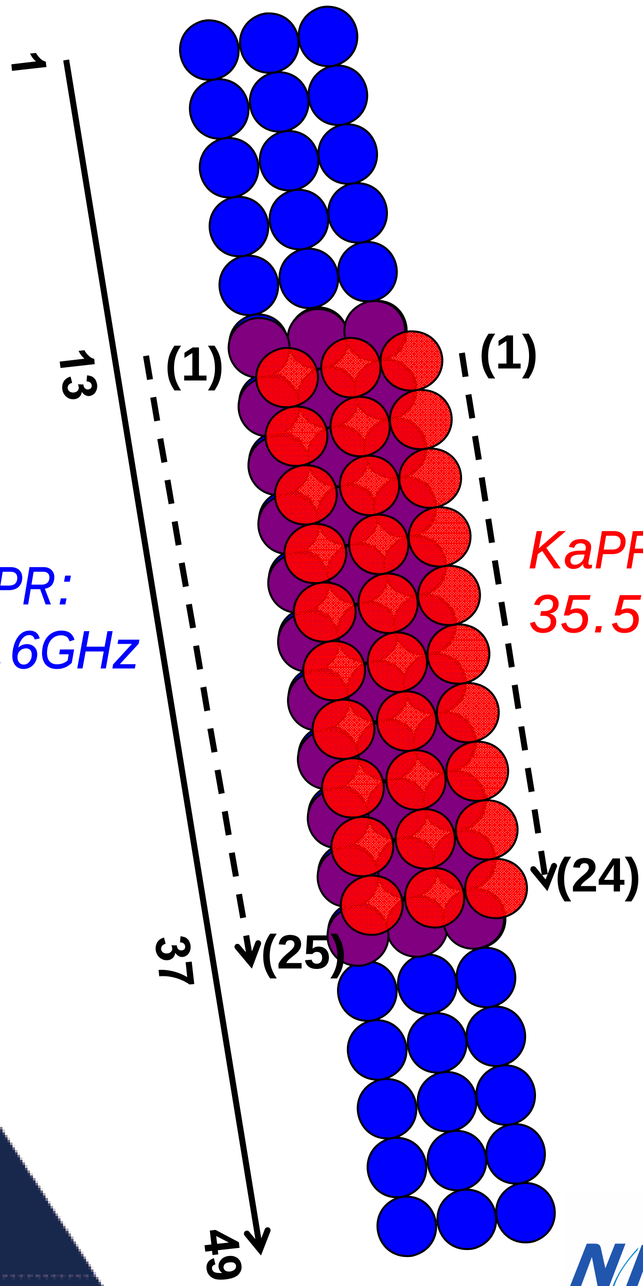

NICT

GPM Core Satellite

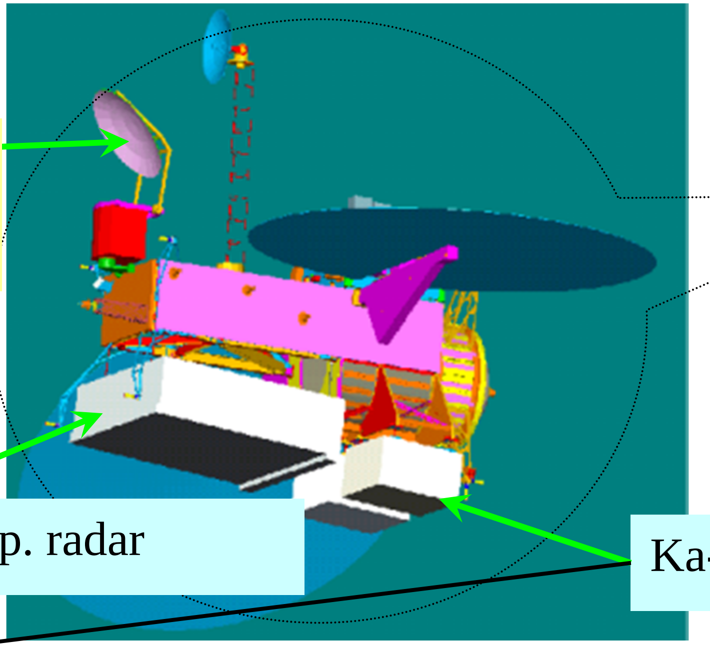

Microwave radiometer

Ku-band precip. radar

Ka-band precip. radar

Frequency	Ku-band (13.6 GHz), Ka-band (35.5 GHz)
Sensitivity	Ku-band --- same as TRMM PR (18 dBZ, Δz=250 m)
	Ka-band --- same as Ku-band (18 dBZ, Δz=250 m)
	--- 6 dB better than Ku-band (12 dBZ, Δz=500 m)
Swath width	245 km (Ku), >100 km (Ka)
Footprint	5 km

Frequency	10 GHz --- 85 GHz (5 bands, 9 channels) --- similar to TMI
Swath width	Approximately 900 km (Conical scan)
Footprint	40 x 60 km (10 GHz) --- 5 x 8 km (85 GHz)

Dual Frequency Precipitation Radar

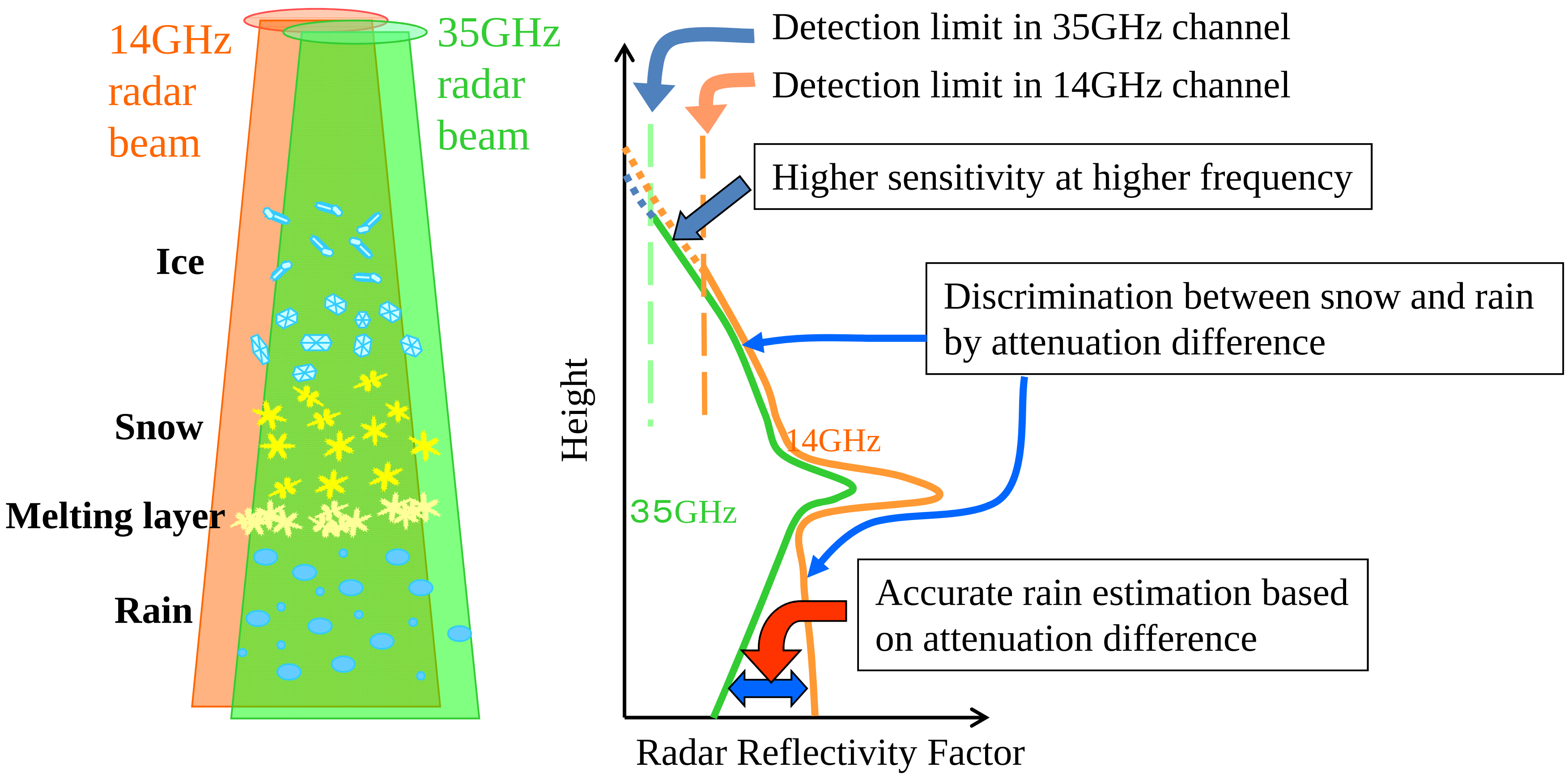

- Measure 3-D structure of rain as TRMM, but with better sensitivity
- Accumulate climatological precipitation data continuously since TRMM
- **Improve estimation accuracy with dual-frequency radar**
  - Identification of hydrometer type
  - Estimation of DSD parameters

NICT

Main Characteristics of DPR

Item	GPM DPR		TRMM PR
	KuPR	KaPR	
Antenna Type	Active Phased Array (128)	Active Phased Array (128)	Active Phased Array (128)
Frequency	13.597 & 13.603 GHz	35.547 & 35.553 GHz	13.796 & 13.802 GHz
Swath Width	245 km	120 km	215 km
Horizontal Reso	5 km (at nadir)	5 km (at nadir)	4.3 km (at nadir)
Tx Pulse Width	1.6 μs (x2)	1.6/3.2 μs (x2)	1.6 μs (x2)
Range Reso	250 m (1.67 μs)	250 m/500 m (1.67/3.34 μs)	250m
Observation Range	18 km to -5 km (mirror image around nadir)	18 km to -3 km (mirror image around nadir)	15km to -5km (mirror image at nadir)
PRF	VPRF (4206 Hz±170 Hz)	VPRF (4275 Hz±100 Hz)	Fixed PRF (2776Hz)
Sampling Num	104～112	108～112	64
Tx Peak Power	> 1013 W	> 146 W	> 500 W
Min Detect Ze (Rainfall Rate)	< 18 dBZ (< 0.5 mm/hr)	< 12 dBZ (500m res) (< 0.2 mm/hr)	< 18 dBZ (< 0.7 mm/hr)
Measure Accuracy	within ±1 dB	within ±1 dB	within ±1 dB
Data Rate	< 112 Kbps	< 78 Kbps	< 93.5 Kbps
Mass	< 365 kg	< 300 kg	< 465 kg
Power Consumption	< 383 W	< 297 W	< 250 W
Size	2.4×2.4×0.6 m	1.44 ×1.07×0.7 m	2.2×2.2×0.6 m

* Minimum detectable rainfall rate is defined by $Ze=200\ R^{1.6}$ (TRMM/PR: $Ze=372.4\ R^{1.54}$)

Beam Matching

- Dimensions and shape
  - **Same design for Ku and Ka antennas**

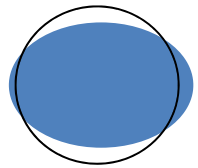

- Cross-track alignment
  - **Granularity of 5-bit Phase shifter:**
    - Res. = 2.4 m ($<\Delta\theta>=\theta w/(2^{(5-1)}x128)=\theta w/2048$)

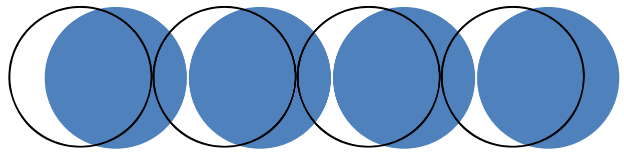

- Along-track alignment
  - **Hardware alignment (not adjustable)**
    - max. error: 0.02 deg=140 m
  - **Shift the pulse timing, e.g. 1 PRT = 0.25 ms = 1.8 m**

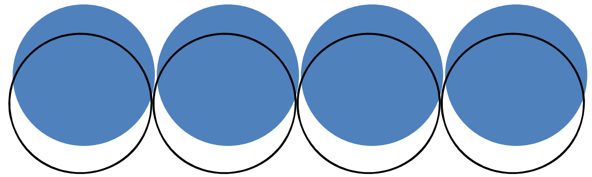

- Scan direction
  - **Hardware alignment (not adjustable)**
    - max. error: 0.02 deg=17 m at scan edge → not so significant

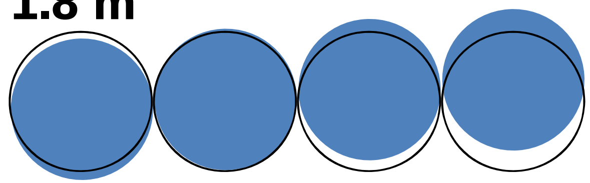

New Factors in DPR Algorithm

Compared with TRMM PR, DPR will provide

- More accurate estimates with higher sensitivity
- Increased number of output variables
  - E.g. Two DSD parameters at each range bin.

by assuming

- More detailed microphysical models

and using

- More complicated algorithm
  - Combination of different algorithms
    - Optimum weights and combination among Z_m(Ku), Z_m(Ka), SRT(Ka) and SRT(Ku) depend on region, height, rain rate, etc.

Assumptions in the DF algorithms

- DSD is parameterized by at most 2 free parameters.
  - e.g., N_0, Λ with known μ in Γ-distribution
- Phase state of particles is known.
  - Phase state is likely to be estimated from data.
- Temperature of rain drops is known.
  - Uncertainty of temperature is a source of error but not large.
- There is a condition that makes the solution stable.
  - SRT, N_0 constant, etc.
- Rain is uniformly distributed in IFOV.
- Attenuation is only caused by precipitating particles. (No attenuation by water vapor, cloud particles, etc. are considered.)
  - **Cloud liquid water: Att(Ka) = 10 * Att(Ku), up to 5 dB**
  - **Water vapor: Att(Ka) = 5 * Att(Ku), up to 1.5 dB near surface**
  - **Oxygen: Att(ka) = 5 * Att(Ku), 0.4 dB near surface**

Basic Idea of Meneghini's DF Algorithm

- $2N(+2)$ observables ($2N$ of Zm (and 2 of $\Delta\sigma^0$)) to estimate RR at N range gates.
  - If the relations among Z, R and k were constant, R would be overdetermined.
  - In fact, Z, R and k are functions of many parameters (DSD, phase, shape, temp., vertical air velocity, non-uniformity, etc.)
- Parameterize DSD with two variables.
  - E.g., N_0 and D_0、 N_0^* and D_0
- Estimate these two parameters at each gate.
  - $2N$ estimates from $2N(+2)$ observables
- All other parameters are fixed.
  - E.g. shape parameter in DSD, phase, temp, etc.
- Calculate R with the estimated parameters.
- Needs initial conditions (e.g., attenuations at a range)

DPR Rain Profiling Algorithm

- At each range, *r*,

$$Z_e(r;Ka)/Z_e(r;Ku) \Rightarrow D_0(r)$$

$$Z_e(r;Ku),\ D_0(r) \Rightarrow N_0(r)$$

$$D_0(r),\ N_0(r) \Rightarrow R(r),\ k(r;Ka),\ k(r;Ku)$$

- Range *r* to *r*+Δ*r*

$$k(r;Ka), Z_e(r;Ka), Z_m(r+\Delta r;Ka) \Rightarrow Z_e(r+\Delta r;Ka)$$

$$k(r;Ku), Z_e(r;Ku), Z_m(r+\Delta r;Ku) \Rightarrow Z_e(r+\Delta r;Ku)$$

- Iterate

Difference in Ze

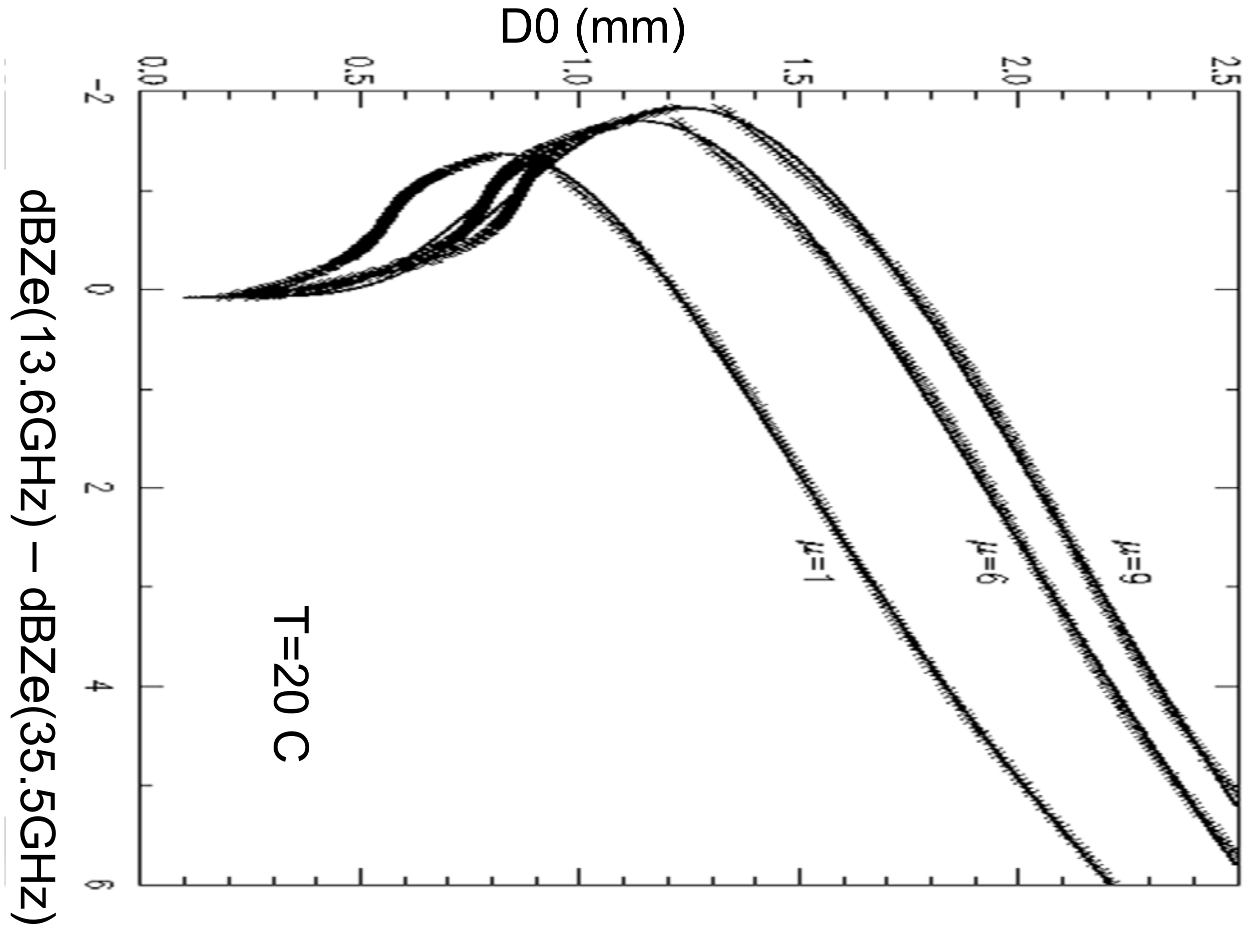

(Meneghini et al., 2002)

Characteristics of DF algorithm (Ze-ratio method)

- can estimate **two DSD parameters** at each range bin.
- generally works well under the given assumptions (SRT available, no NUBF effect, etc.)
  - Random noise or quantization error in P_r does not cause a serious bias error in retrieval.
- Issues:
  - Multiple solutions possible for liquid particles
  - **Choice of DSD model** (Closeness of model DSD to actual DSD)
    - Actual variation of DSD is rather large (A. Tokay, N. Adhikari)
  - separation of solid (ice) phase from liquid phase
  - inhomogeneity of rain within footprint
  - beam mismatching
  - attenuation caused by CLW and water vapor

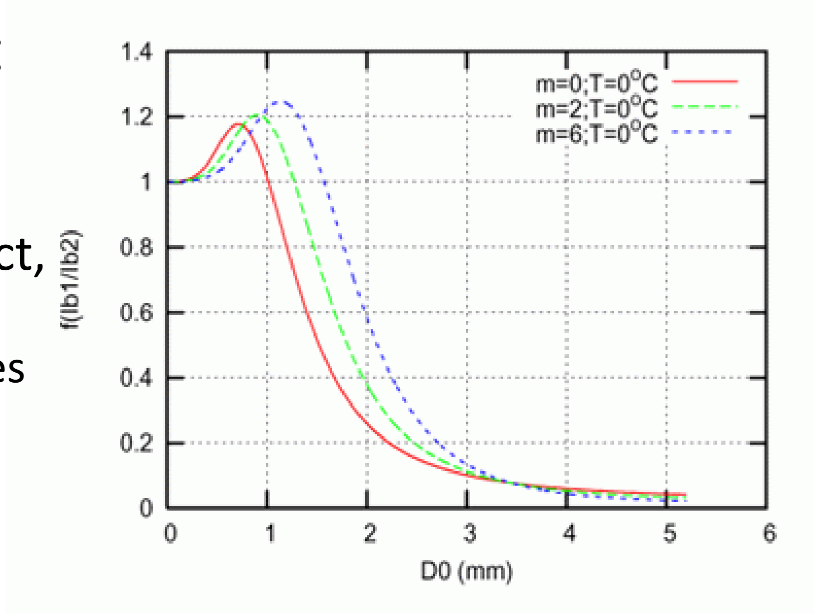

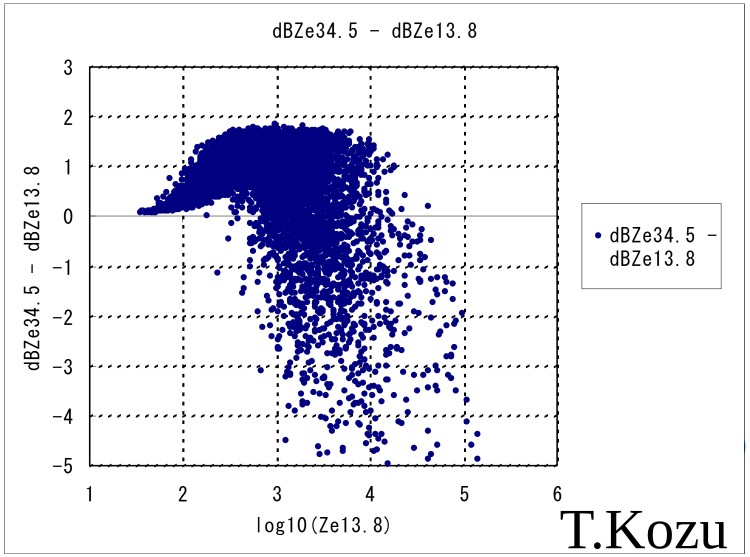

Basic Structure of DPR/L2 algorithm

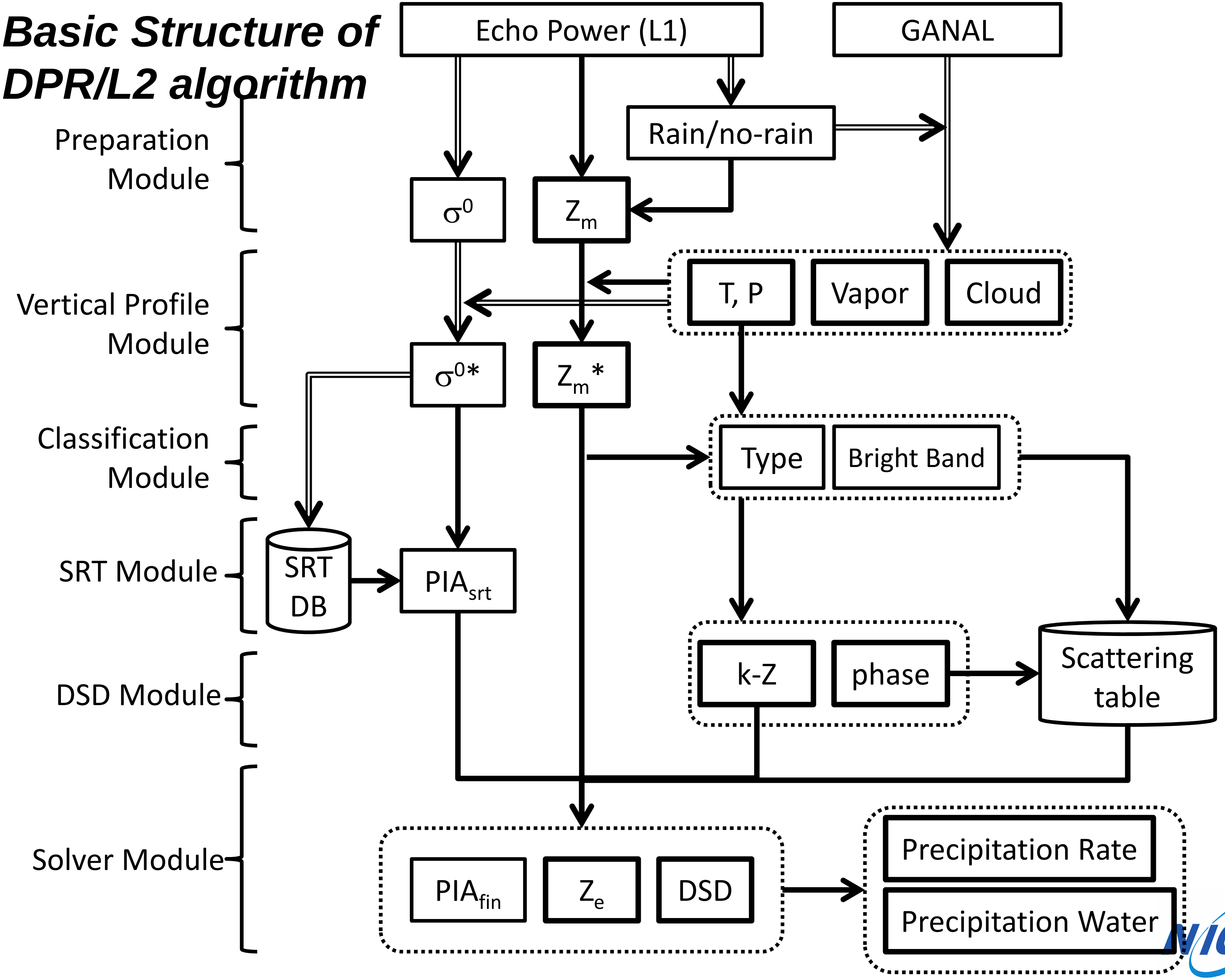

Issues with DPR algorithm

- Zm at 2 freq. are not necessarily always available at all range bins.
  - sensitivity difference
  - large attenuation in Ka band
  - limited applicable range in rain rate
- Effect of attenuation by clouds and water vapor
  - if the att. by clouds and WV are estimated accurately, PIA(Ka)-PIA(Ku) by precip. can be estimated well.
- A small bias in measurement may affect the estimates.
- Basic equations assume beam matching and uniformity of rain within IFOV.

Applicable Range of DF Algorithm

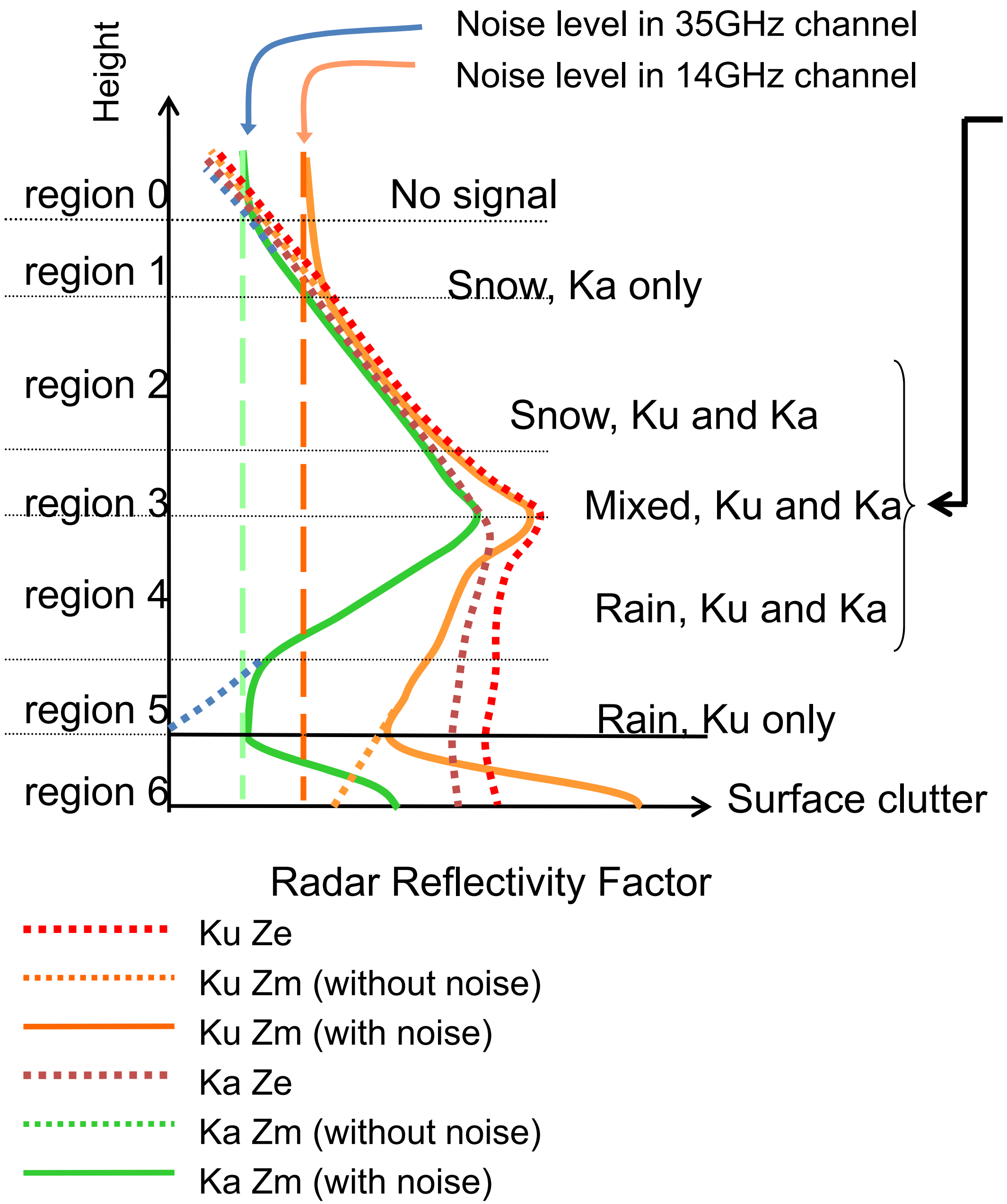

DF algorithm applicable in regions 2, 3, and 4.

Region 0: Nothing can be done.

Region 1: Use *Z*(Ka)-*R* relationship.
No attn. correction needed.

Region 2: Use DF algo. for snow.
Attn. by WV, CW.

Region 3: Use DF algo for mixed rain
Needs int. value at r3b or r3t

Region 4: Use DF algo for rain.
Needs int. value at r4b or r4t

Region 5: Use Ku SF algo for rain.
Needs init. value at r5b or r5

Region 6: Use a model profile

SRT gives attn. at r6b.

Region 5 appears only when Ka attn. is large.

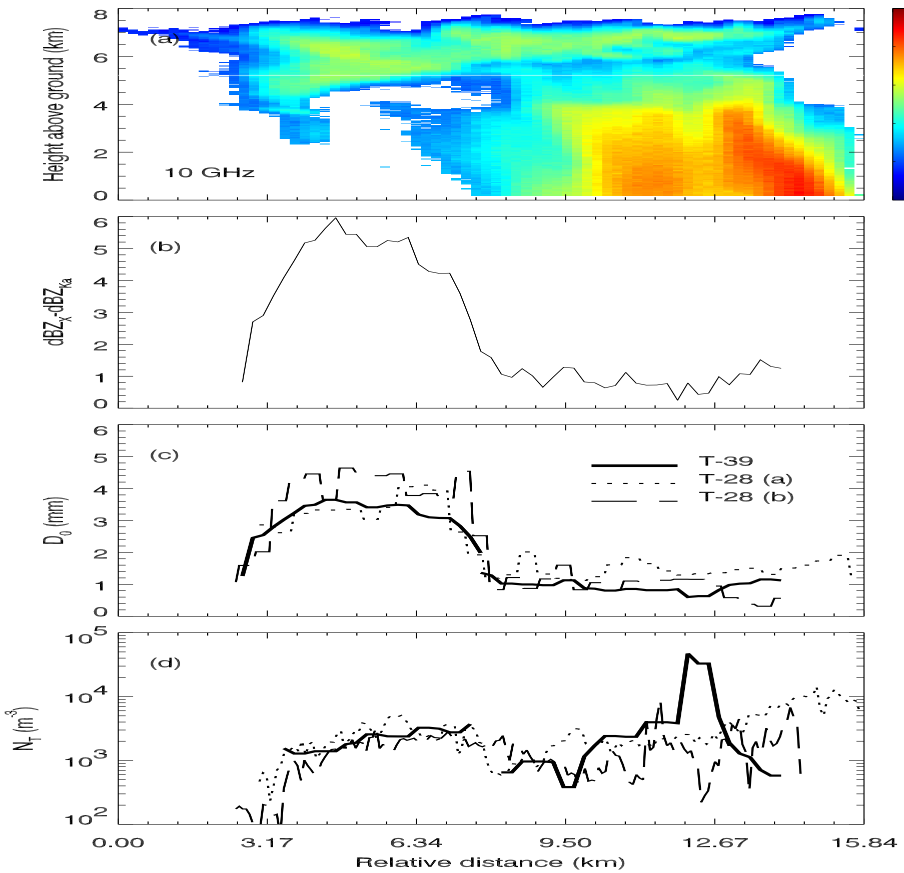

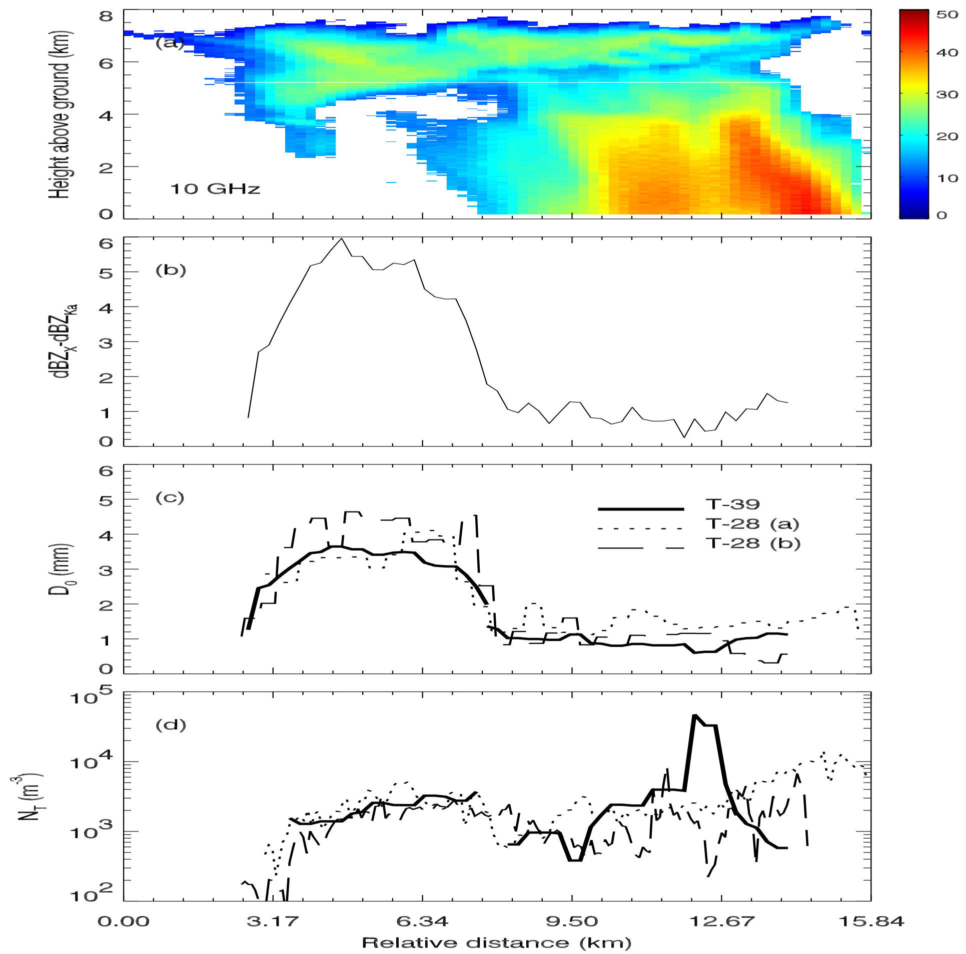

Airborne radar measurements over a weak convective cell and retrievals of the size distributions in comparisons with the in-situ particle measurements: (a) T-39 radar measured reflectivity at nadir along the flight track shown in Fig.2, (b) DFR of X and Ka bands at the altitude where the T-28 flew, as indicated by the white line in Fig.3a, (c) comparisons of D_0 between the radar estimated and the 2D-P measured results and (d) similar comparisons for N_T.

(Liao et al. 2003)

CloudSat CPR System Characteristics

- Nominal Frequency 94 GHz Pulse Width 3.3 µsec
- Minimum Detectable Z* < -29 dBZ PRF 4300 Hz
- Data Window 0-25 km Antenna Size 1.85 m
- Dynamic Range 70 dB Integration Time 0.16 sec
- Nadir Angle (since 15 Aug 2006***) 0.16°
- Vertical Resolution 500 m Cross-track Resolution 1.4 km
- Along-track Resolution** 1.7 km Data Rate 20 kbps

- *Equivalent radar reflectivity that gives a mean power equal to the standard deviation after integration and noise subtraction. Atmospheric attenuation is not included.
- **The along-track resolution is based on averaging the instantaneous footprint over the integration time. Based on purely geometric arguments, the along-track resolution would be approximately 2.5 km. However, a more rigorous convolution calculation gives an along-track resolution of 1.7 km, as shown in the table.
- ***Nadir angles were changed from approx. 1.71° to 0.0° on 7 July 2006 and from 0.0° to 0.16° on 15 August 2006

Heritage: APR-2 and ACR in Wakasa Bay (Japan), APR-2 and CRS/EDOP in TC4 (East Pac).

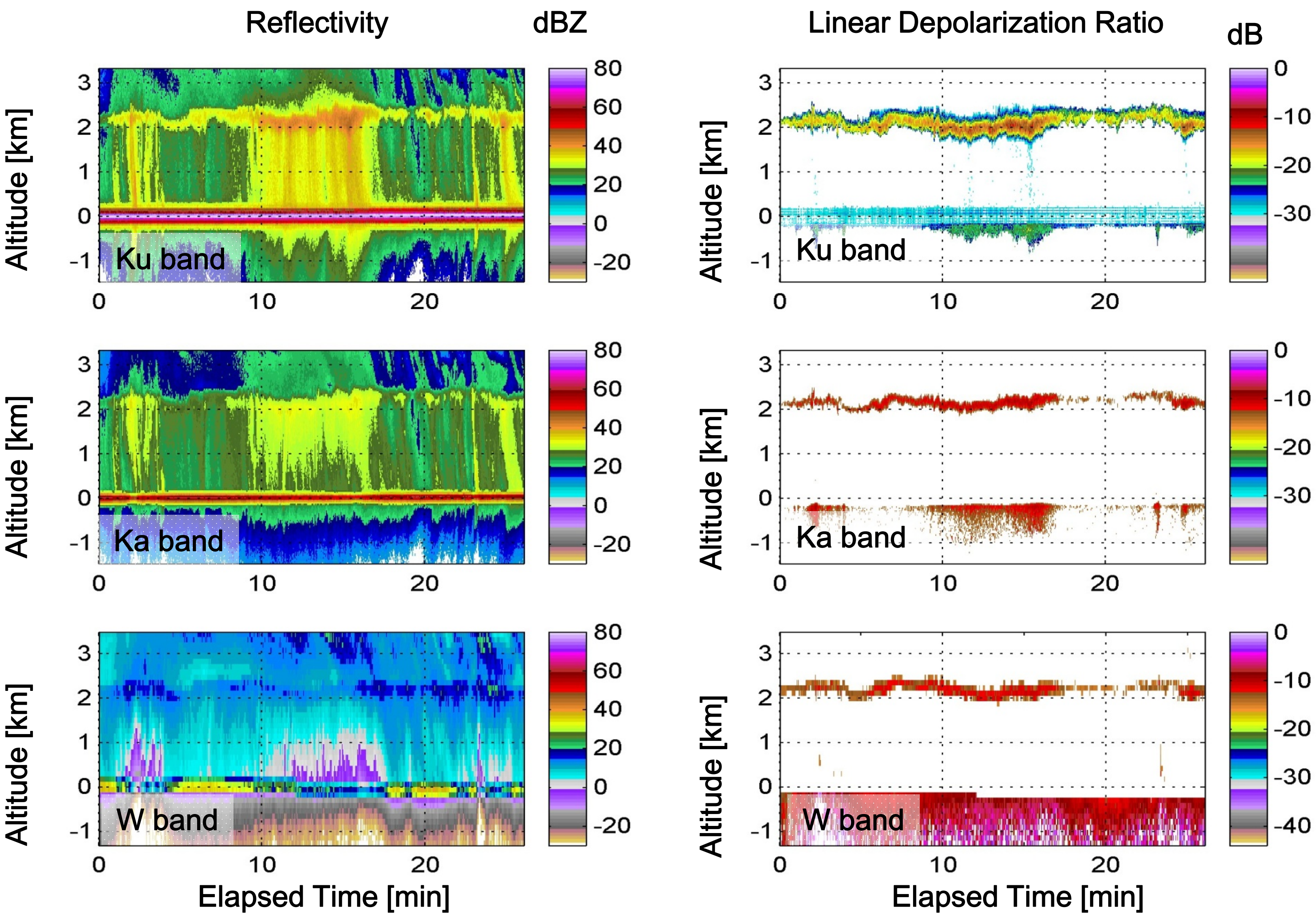

(courtesy: S. Tanelli)

What is EarthCARE ?

EarthCARE (Earth Clouds, Aerosols and Radiation Explore)

- Satellite mission selected as the sixth Earth Explorer Mission in 2004 of ESA
- European Space Agency (ESA) and Japanese (JAXA, NICT) collaboration
- Objective: global clouds and aerosol vertical observation for global radiation budget
- Launch: 2015 (?)
- Instrument:

  Cloud Profiling Radar (CPR)

  Atmospheric Lidar (ATLID)

  Multi-spectral Imager (MSI)

  Broad Band Radiometer (BBR)

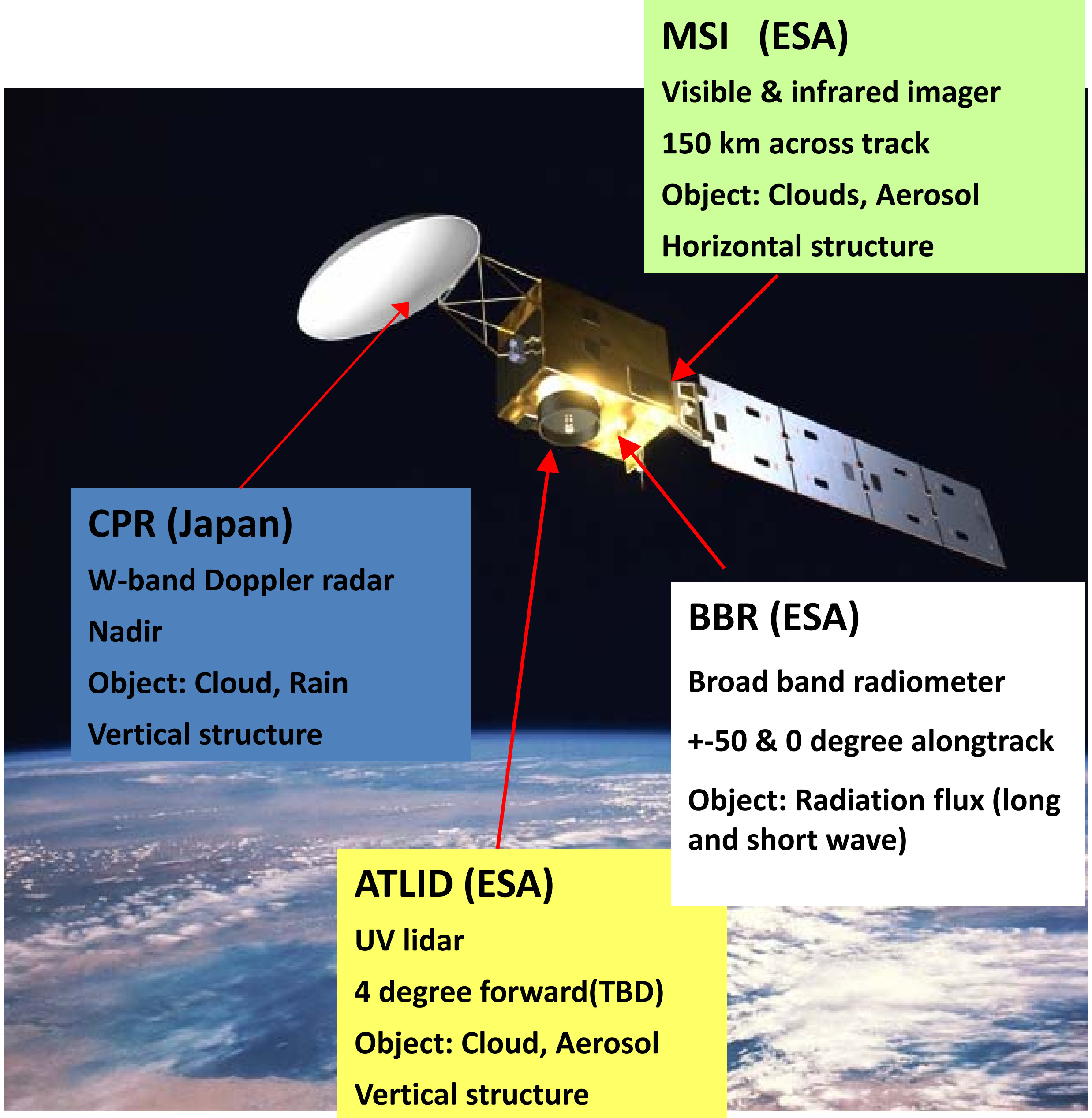

Orbit

- Sun-synchronous
- Inclination 97 degrees
- Altitude: 450 km (TBD)
- Local time: 13:30 descending node
- Period: 94 min
- Mission life: 3 years
- Revisit period: 10 - 30 days (TBD)

Satellite

- Mass: 1300 kg
- Power: 1100 W
- Data rate: up to 1500 kbit/sec

CPR structure and function

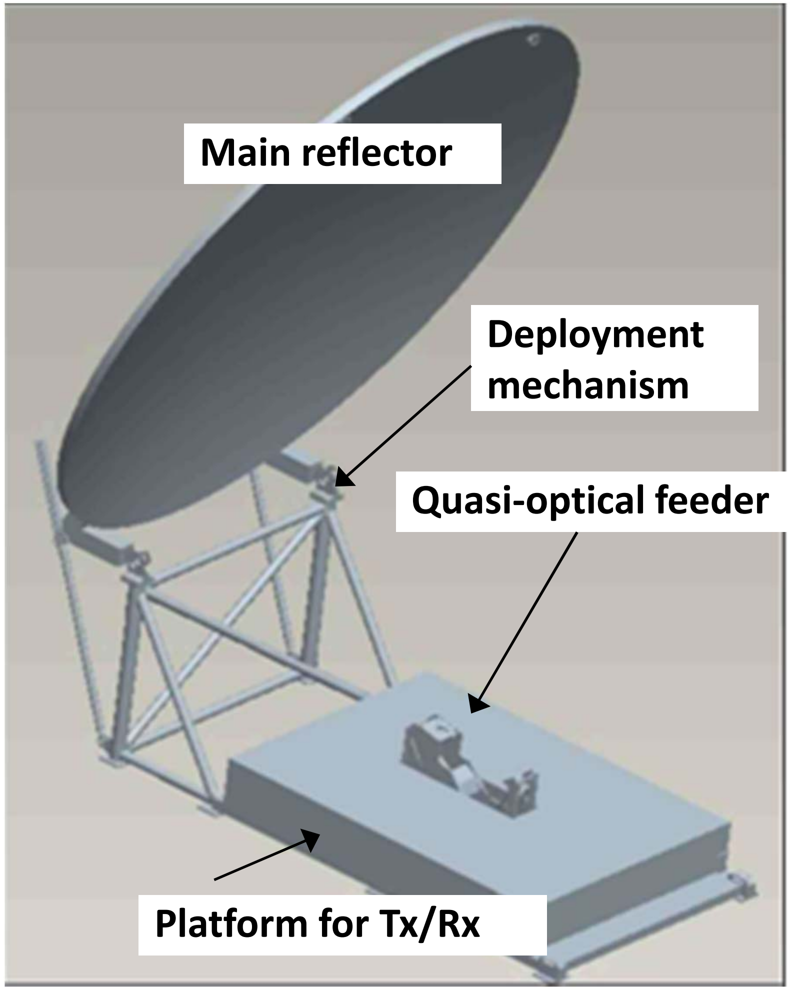

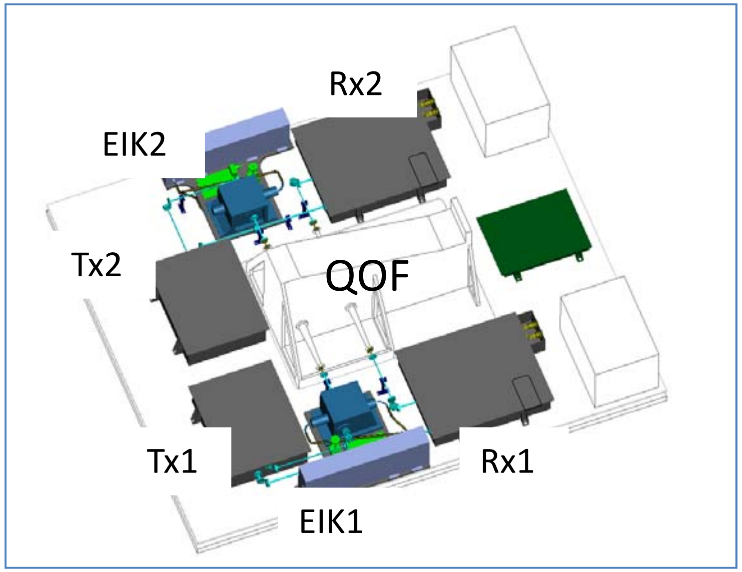

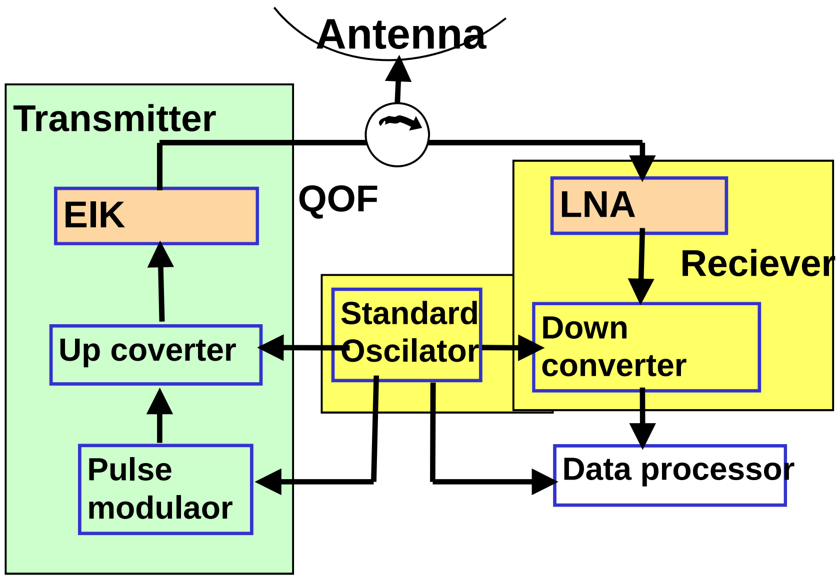

CPR specifications

Tx frequency	94.05 GHz
Tx peak power	1.5 kW (EOL)
Pulse width	3.3μs
Polarization	Circular
Antenna diameter	2.5 m
Beam footprint size	700 m
Beam direction	Nadir
Minimum sensitivity	-35 dBZ (10km average)
Data sampling	100 m (Vertical) 500 m (Horizontal)
Doppler measurement	Pulse pair

Difference from CloudSat CPR

- Higher sensitivity (about 10 dB) from bigger antenna and lower orbit

  minimum detection: -35dBZ at TOA (10km integration)

- Doppler function (pulse–pair method)
  vertical velocity measurement

  accuracy: 1 m/ s (10km integration -19dBZ echo)

- Variable PRF and height range
- Co-registration with Lidar and other sensors
- Circular polarization
- Less ground clutter effect
- Longer life transmit tube (EIK)

Spaceborne Atmospheric Radars

TRMM/PR – NICT/JAXA
Ku, Scanning , Tropical Rain

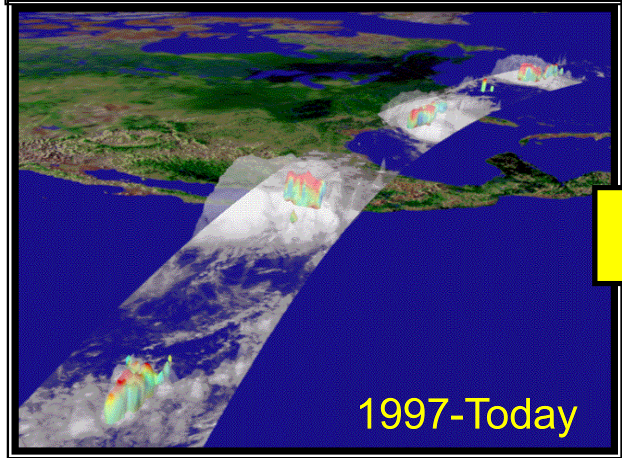

GPM/DPR – NICT/JAXA
Ku/Ka, Scanning, Precipitation

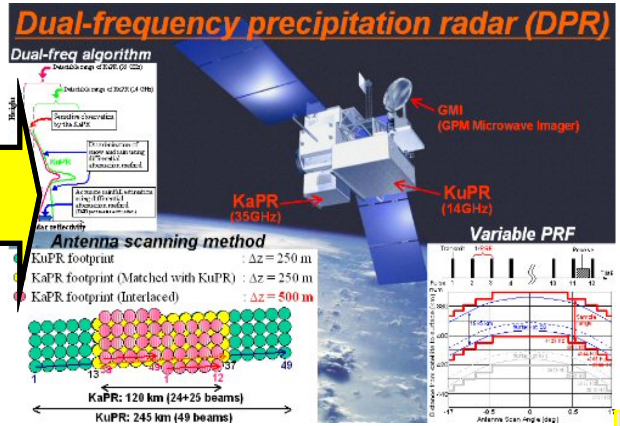

ACE Radar (one concept)
W/Ka, Scanning, Doppler

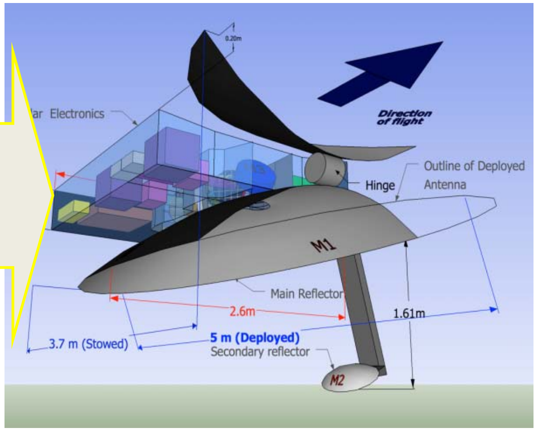

CloudSat/CPR – JPL/NASA
W, -30dBZ , Clouds

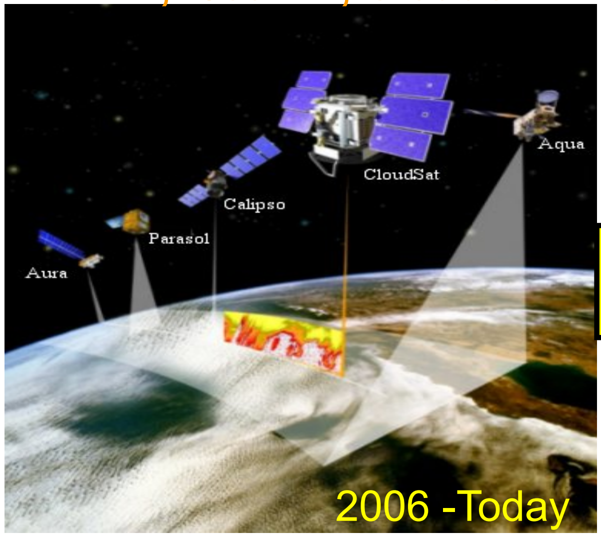

EarthCARE/CPR – NICT/JAXA
W, Doppler, Clouds

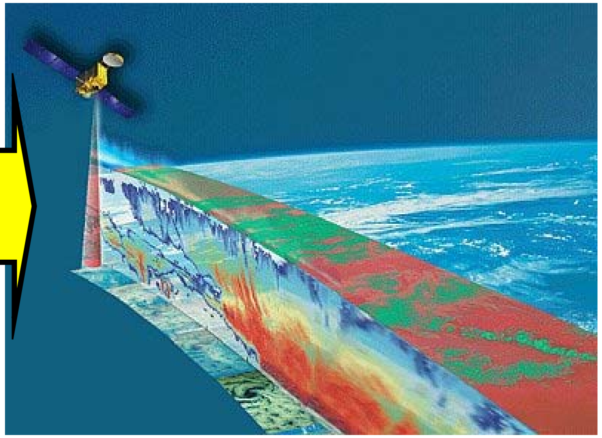

NASA/JAXA worshop on ACE Mission –
Lihue July 29-31 2008

NICT

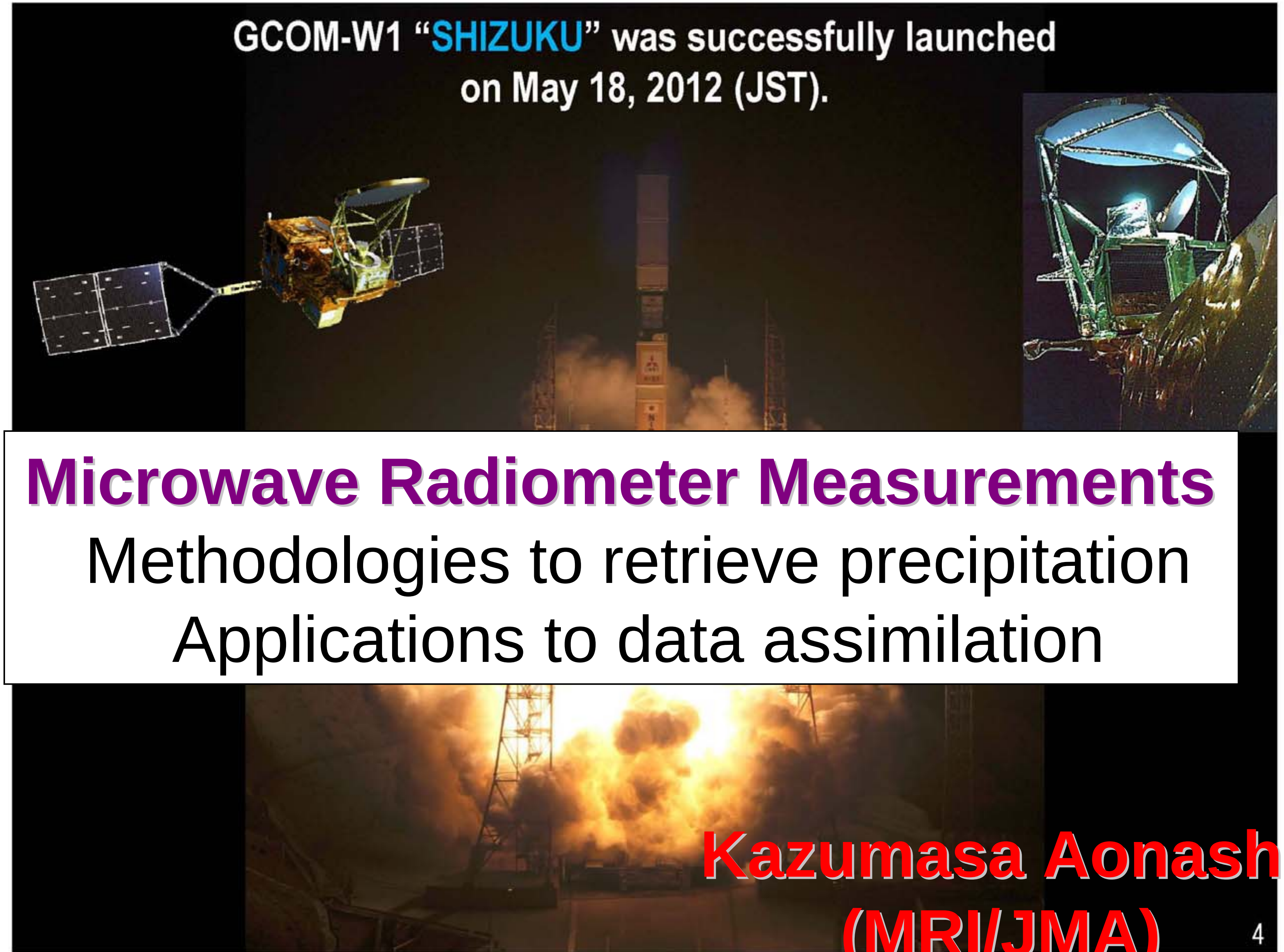

Microwave Radiometer Measurements

Methodologies to retrieve precipitation
Applications to data assimilation

Kazumasa Aonashi
(MRI/JMA)

Motivation: Needs for Precip. Remote-sensing




- Precipitation monitoring is very important to disaster prevention.
- Precipitation observation data are sparse, especially over oceans.

Heavy Precipitation observed with TRMM sensors
(MCS near Southern Kyushu, Jun. 13, 1998)

IR Ch4 TBB(K)

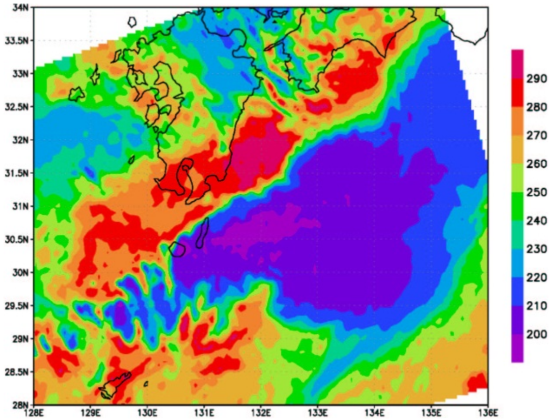

Radar Precip.

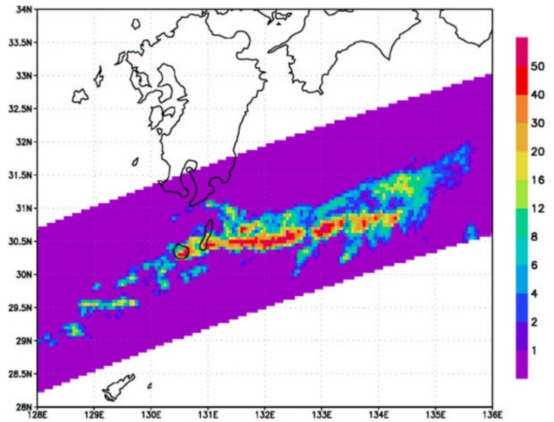

MWR TB (19V)

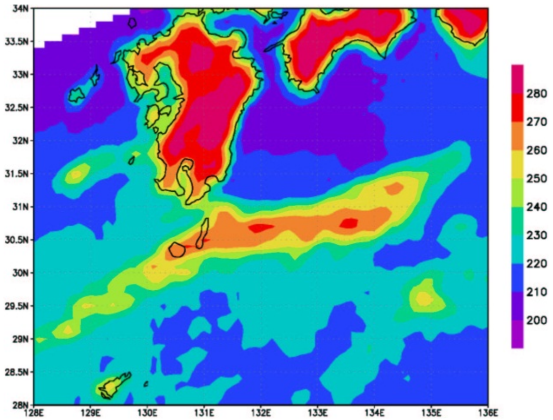

MWR TB (85V)

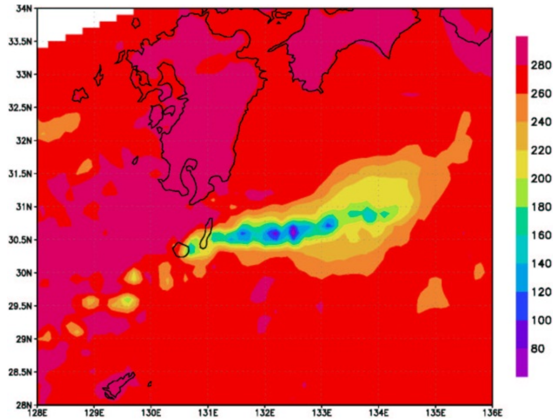

Correlation of satellite-estimated and Radar-estimated instantaneous rain rates vs normalized RMS differences (Ebert & Manton, 1998)

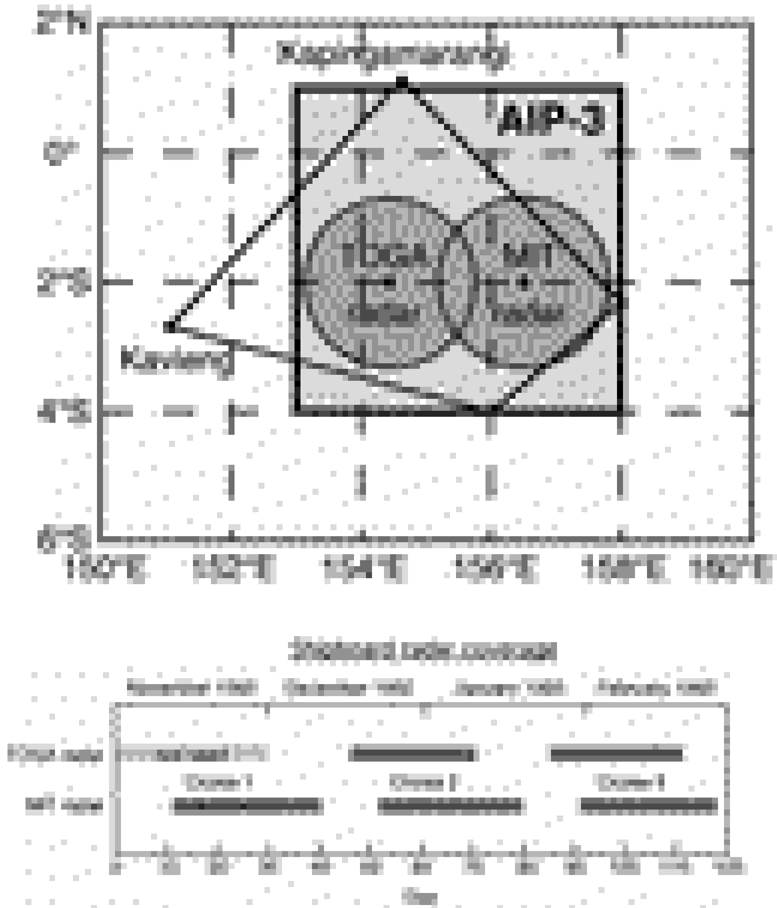

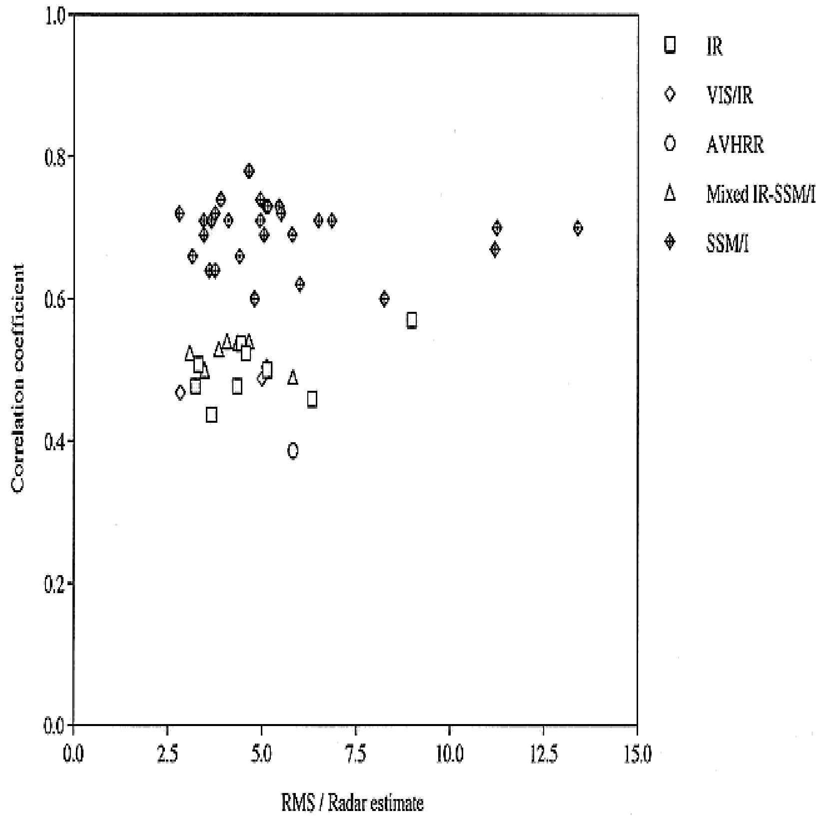

Application: TC monitorin Cyclone SIDR (Nov. 12-15, 2007）

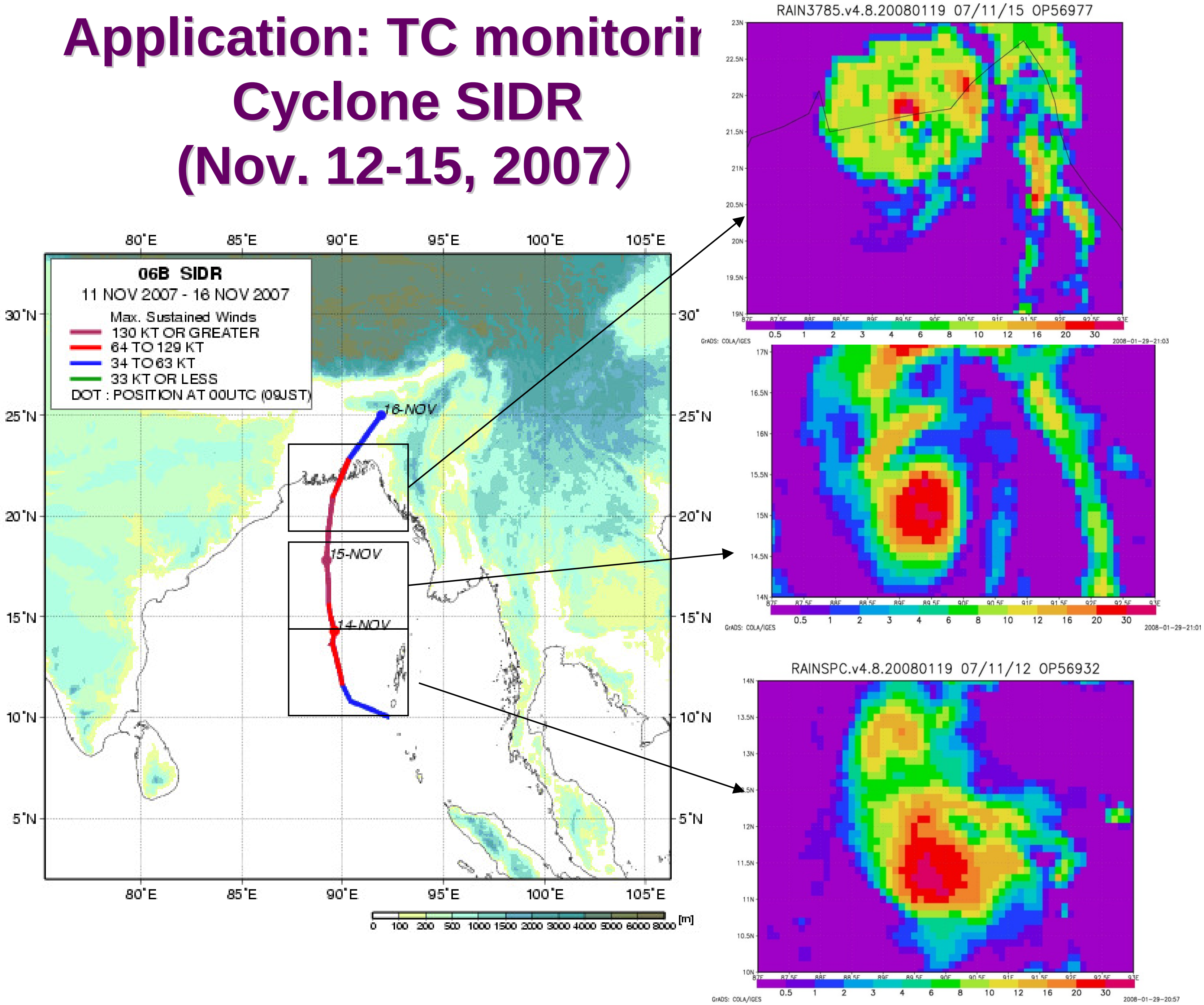

Time vs. Longitudinal Cross Section of GSMaP_SSM/I Precipitation (5S-5N)

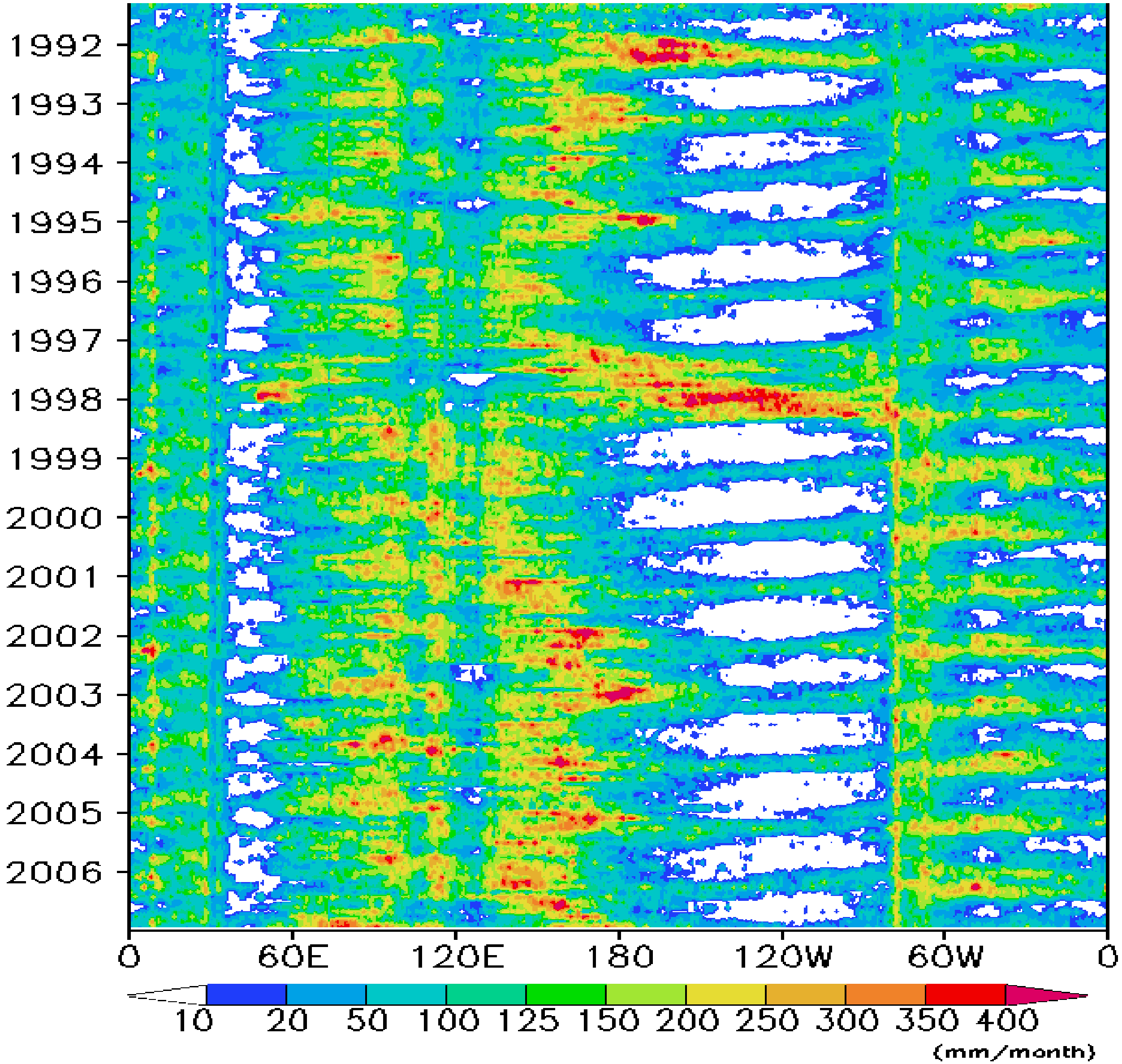

Application: Assimilation to NWP models

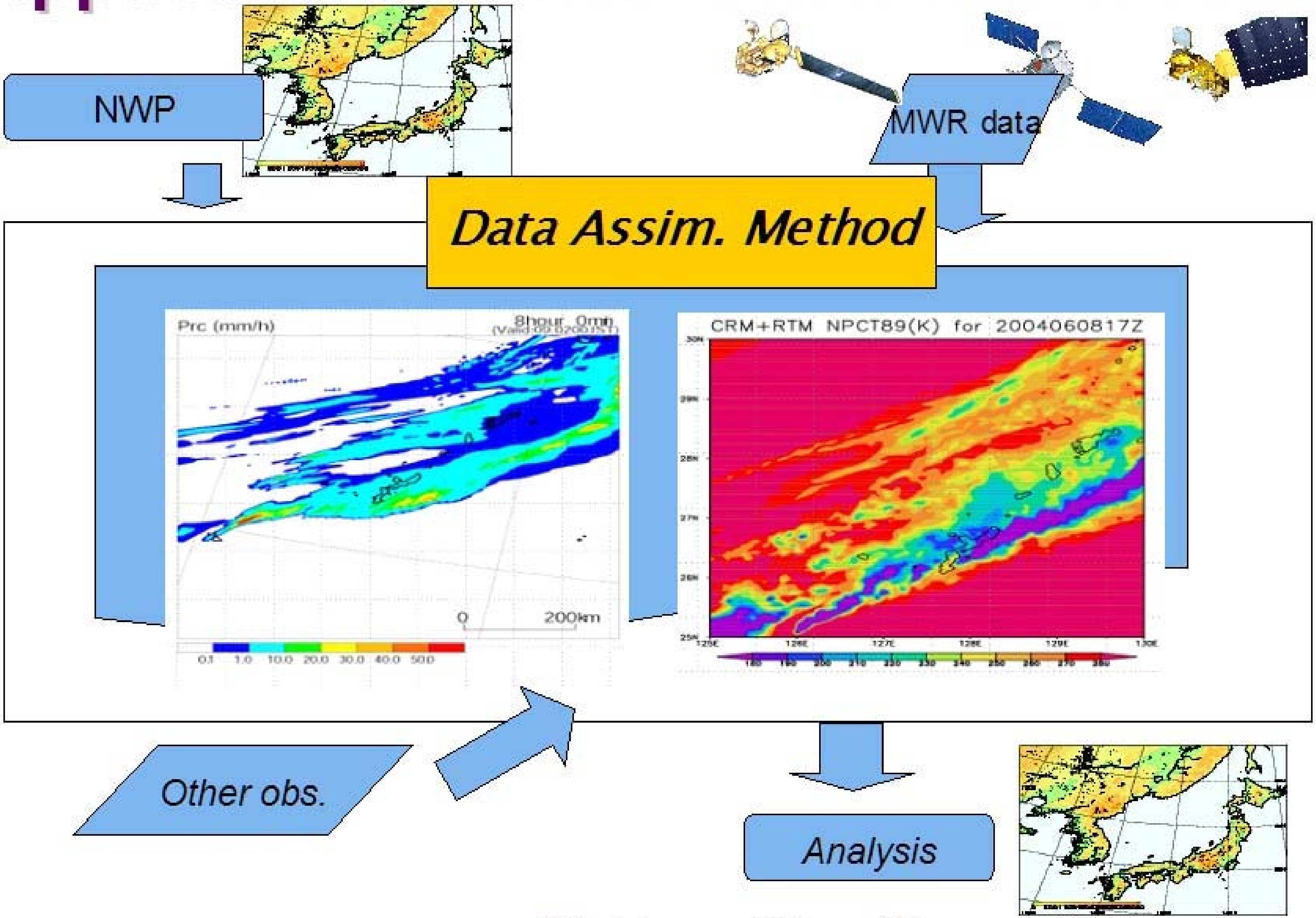

Outline

- Introduction
- Features of Microwave Radiometer Data
- Passive Microwave Precipitation Retrieval
- Data Assimilation using Microwave Radiometer Data

Global Rainfall Map Processing System at JAXA/EORC

Near real time and high-resolution global rainfall map based on satellite observation

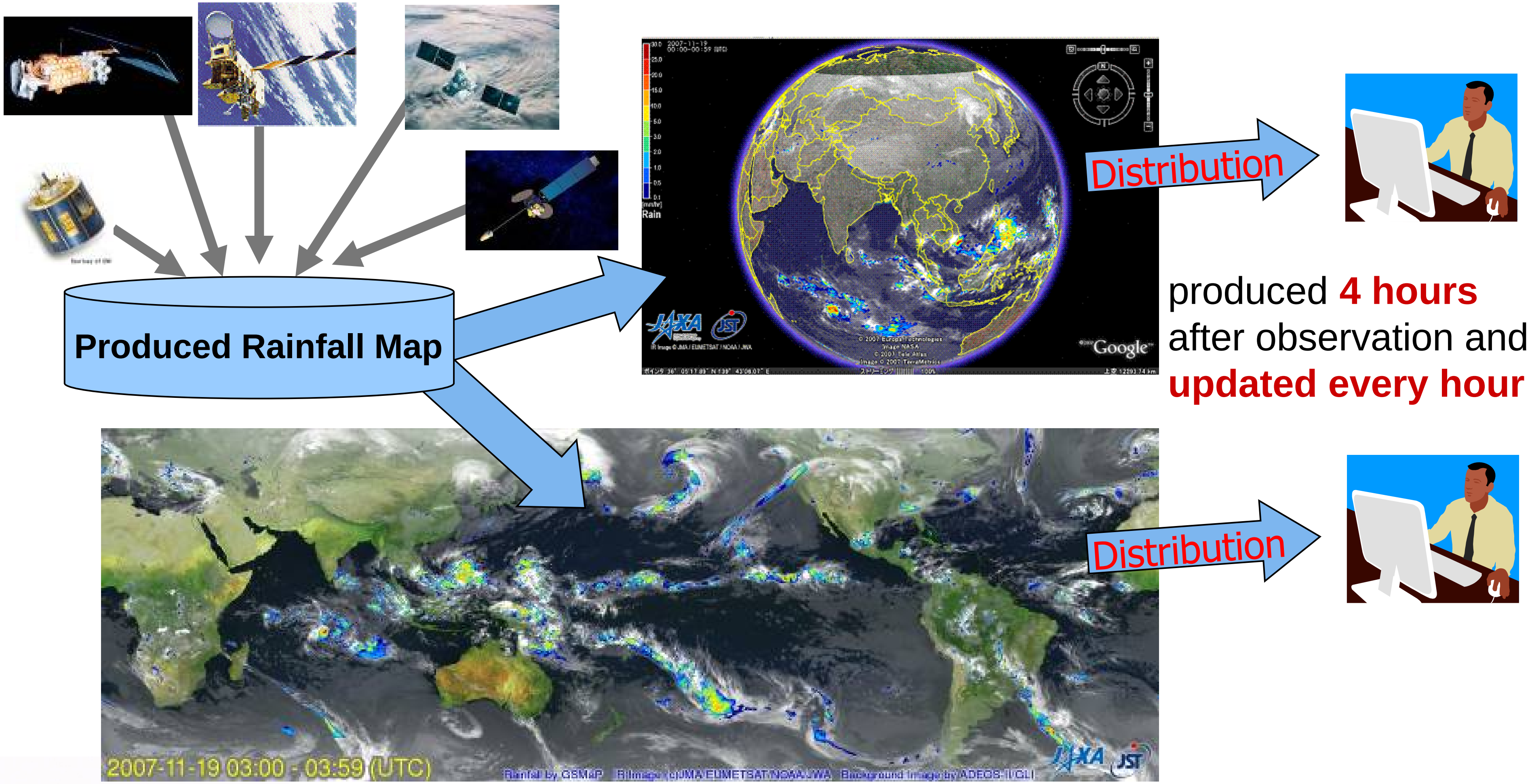

http://sharaku.eorc.jaxa.jp/GSMaP/

Multi-Satellite Precip Composite (GSMaP_MWR, daily precip)

TMI+AMSR+AMSR-E+SSM/I (F13, F14, F15), 0.25°×0.25°

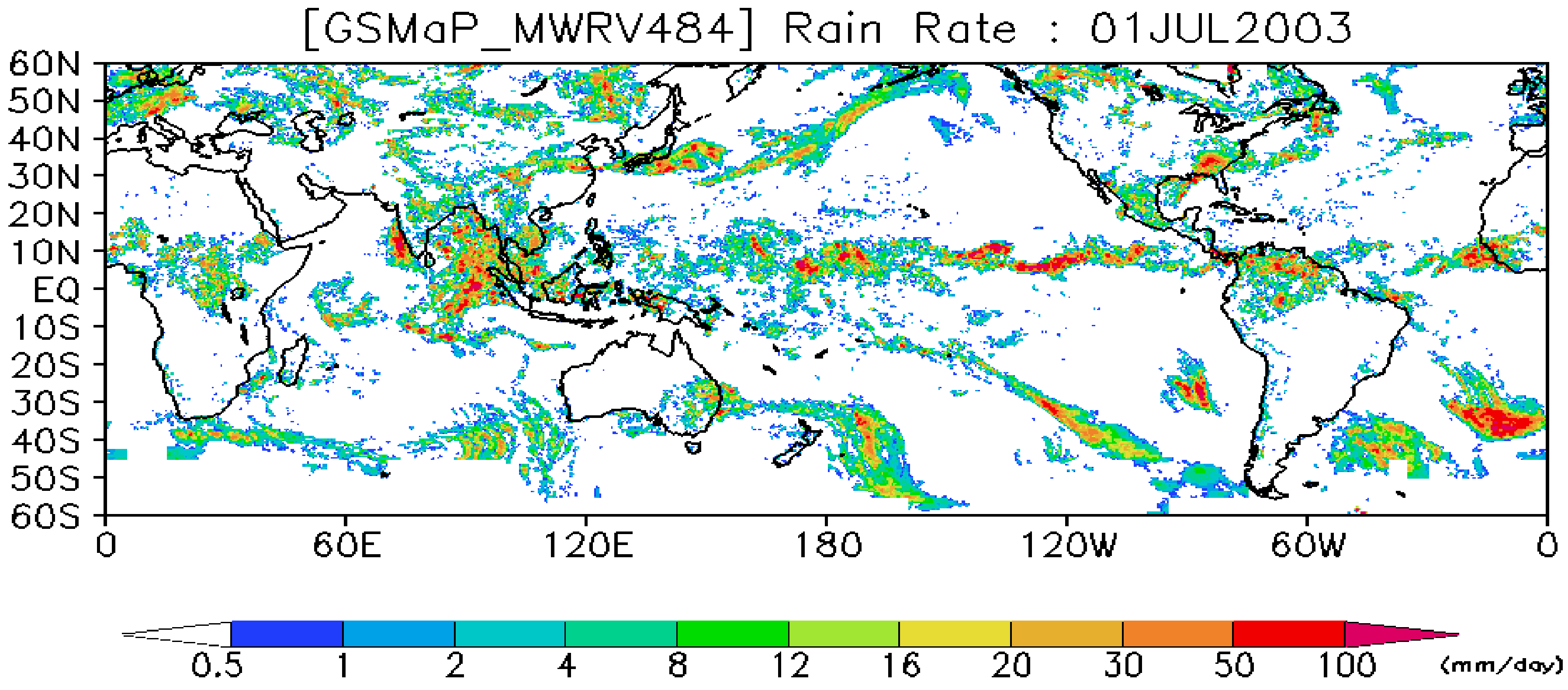

Outline

- Introduction
- Features of Microwave Radiometer Data
- Passive Microwave Precipitation Retrieval
- **Data Assimilation using Microwave Radiometer Data**

JMA operational Regional model

JMANHM (Saito et al,2001)
- Resolution: 5 km
- Grids: 400 x 400 x 38
- Time interval: 15 s

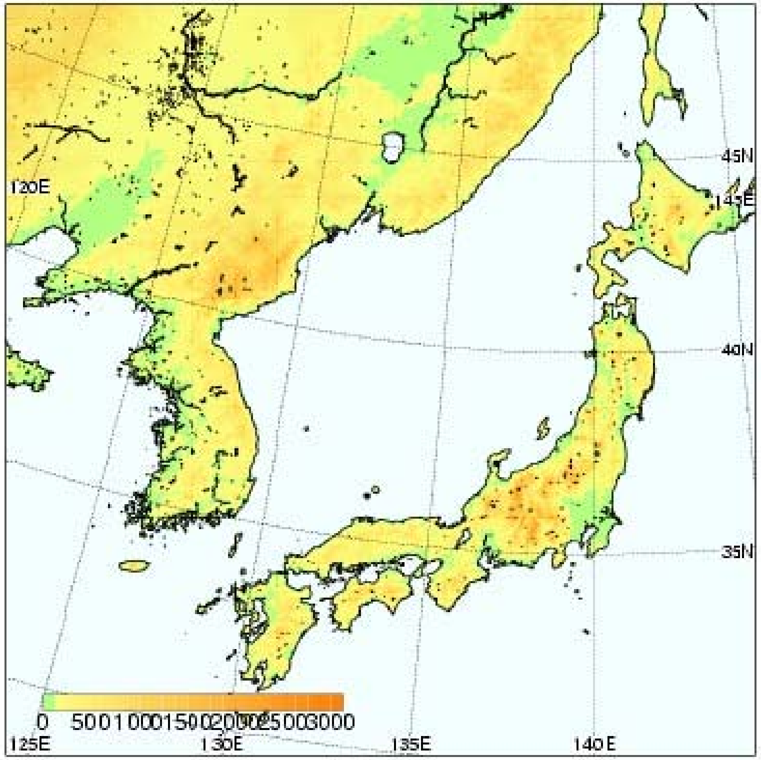

Explicitly forecasts species of water substances

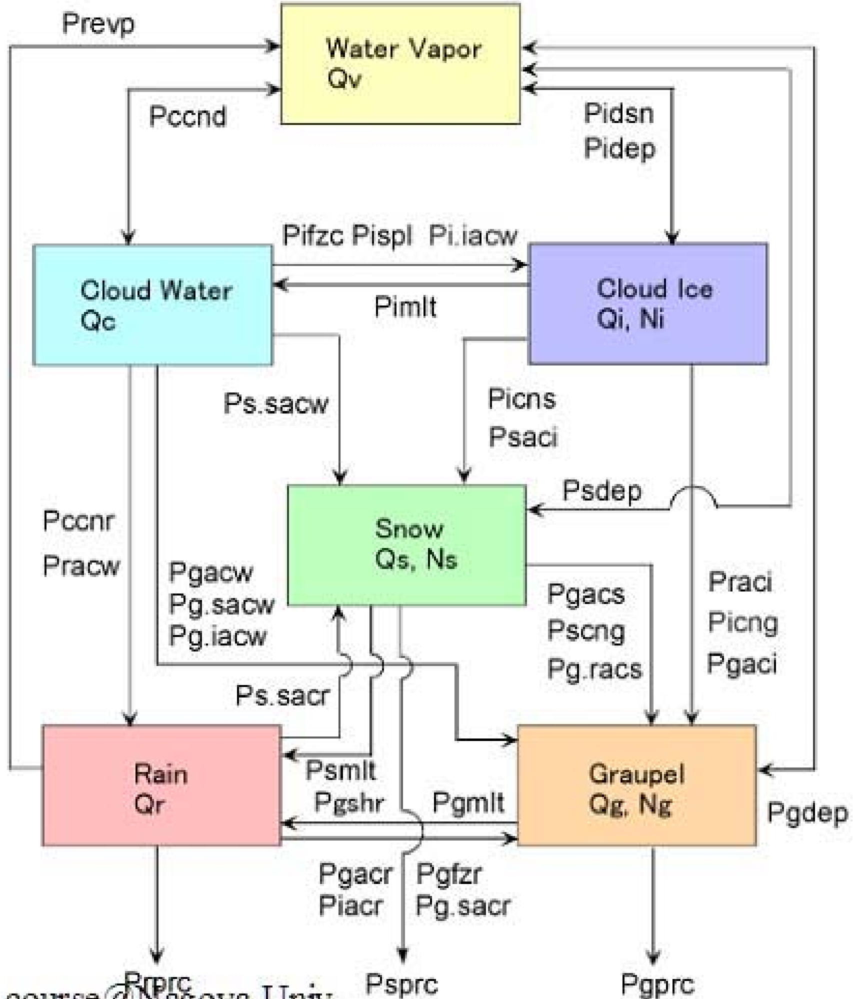

Microwave Radiometer Measurements

Features of Microwave Radiometer Data

Microwave properties of Precipitation

Satellite Microwave Radiometers (Imagers)

Microwave Range
Frequency　3－300GHz
（Wavelength 1 mm~10cm)

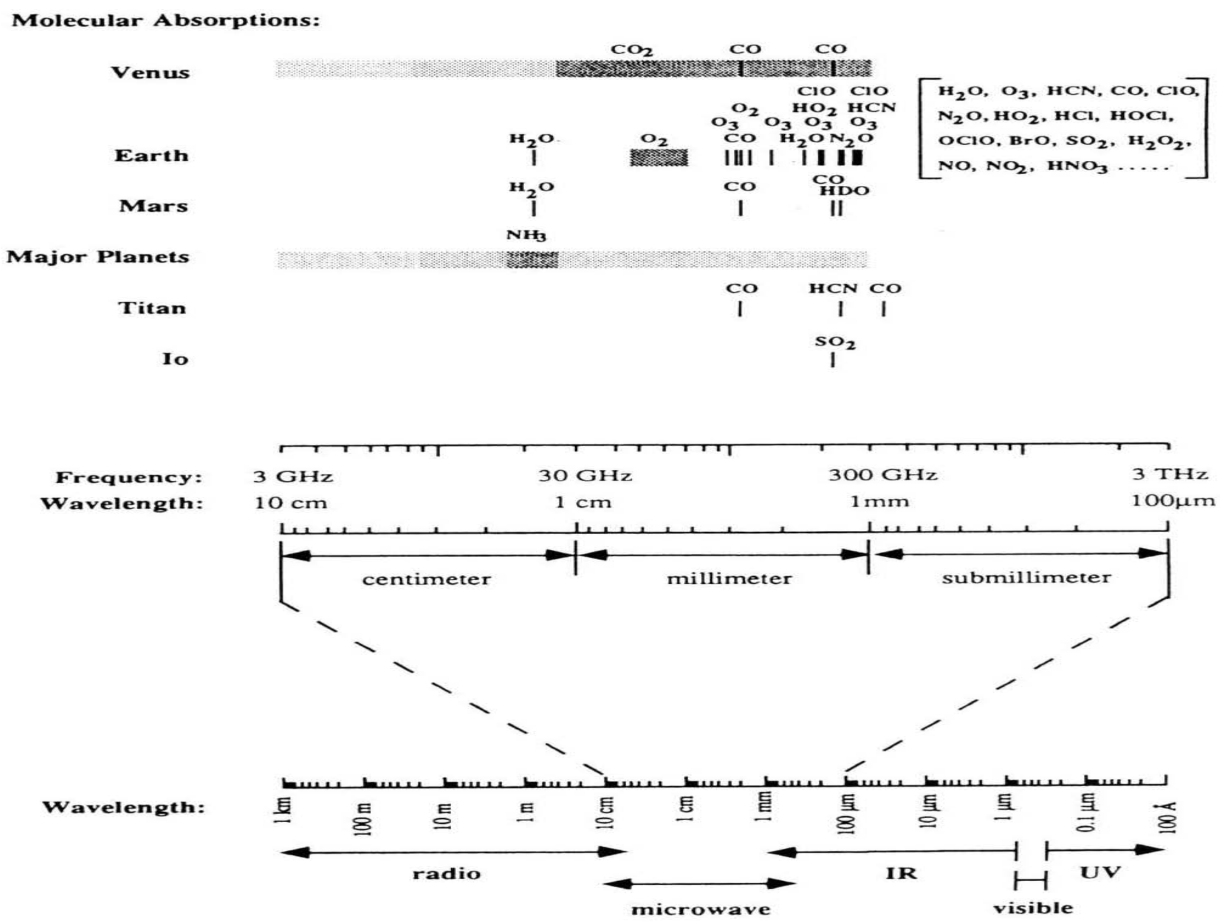

Satellite Observation (TRMM)

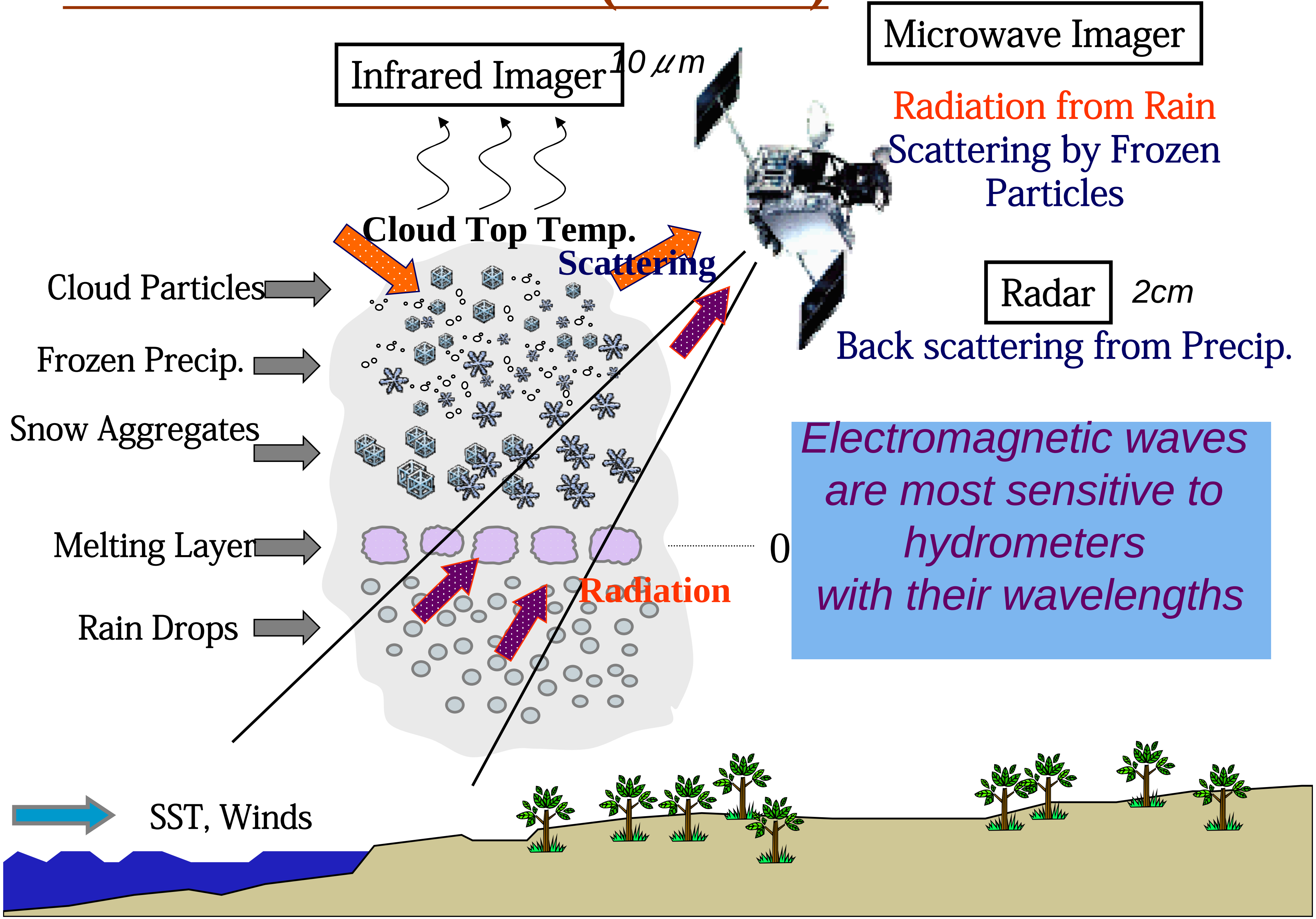

Electromagnetic waves are most sensitive to hydrometers with their wavelengths

Heavy Precipitation observed with TRMM sensors
(MCS near Southern Kyushu, Jun. 13, 1998)

IR Ch4 TBB(K)

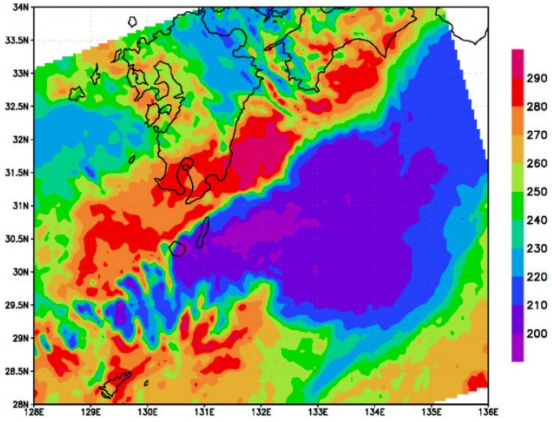

Radar Precip.

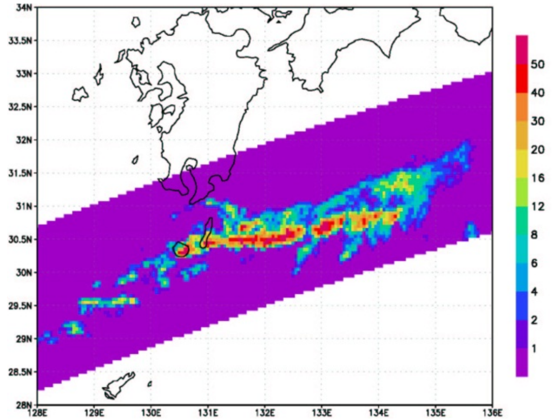

MWR TB (19V)

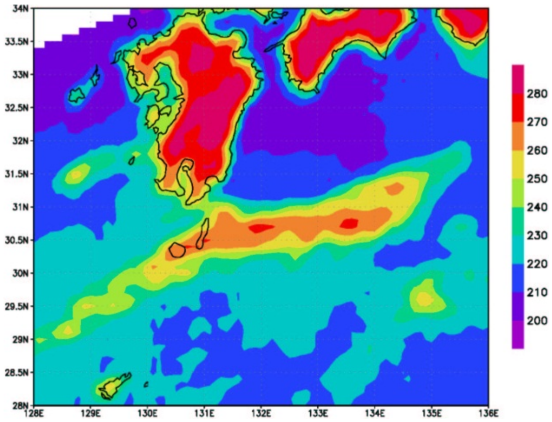

MWR TB (85V)

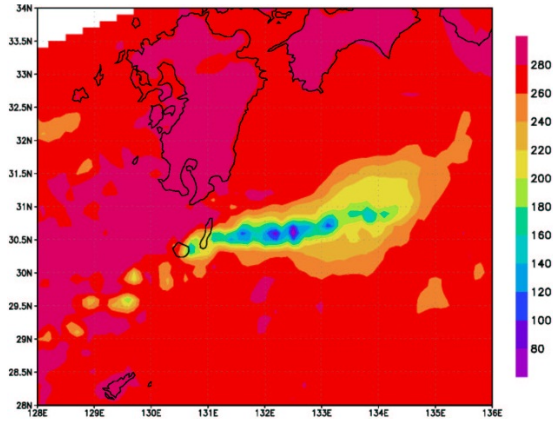

Mie Scattering by each particle

$$\sigma_{sc} = Q_{sc}\pi r^2,\ \ Q_{sc}\ is\ function\ of\ \ \mathrm{Re}(n_c)$$

$$\sigma_{ab} = Q_{ab}\pi r^2,\ Q_{ab}\ is\ function\ of\ \ \mathrm{Im}(n_c)$$

$$where\ \ x = 2\pi r / \lambda$$

$$n_c : complex\ index\ of\ refraction$$

Complex Index of Refraction

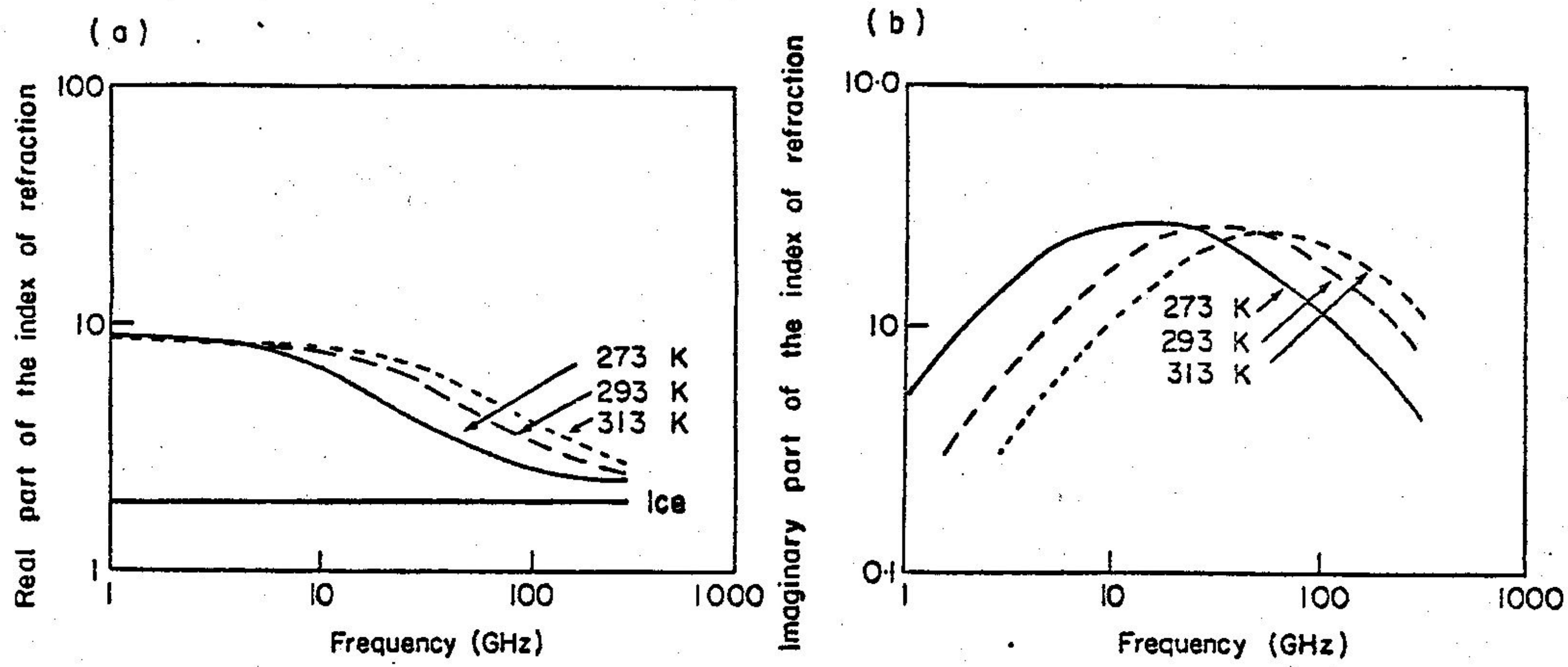

Emission& scattering By liquid water particles

Only Scattering By frozen water particles

Satellite Observation (TRMM)

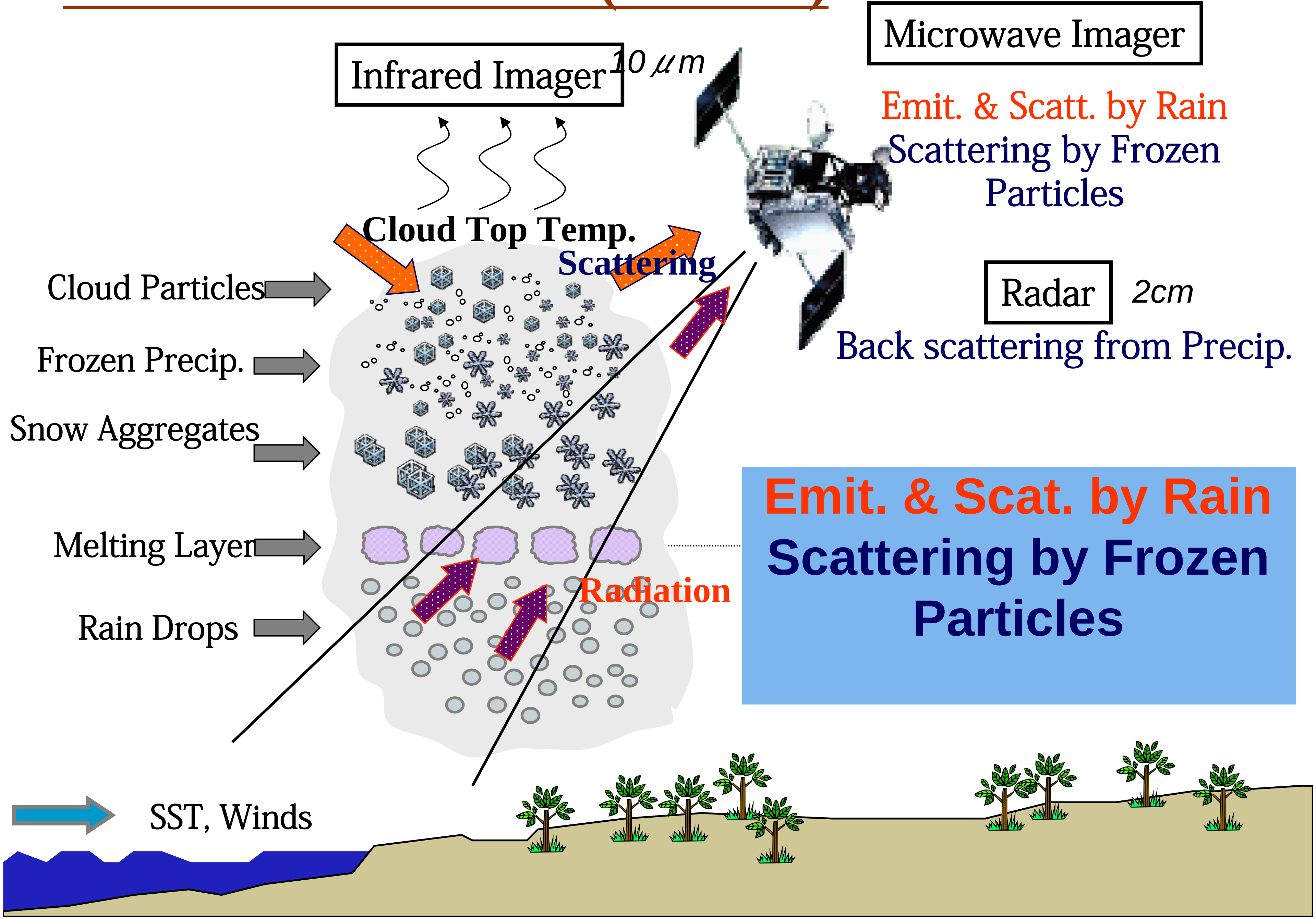

Emit. & Scat. by Rain
Scattering by Frozen Particles

Surface Emissivity

- Surface Emissivity is > 0.9 over dry land, 0.4~0.7 over sea
- Surface Emissivity over sea depends surface wind speed, SST.
- Surface Emissivity over land depends on snow coverage, soil moisture, vegitation, etc.

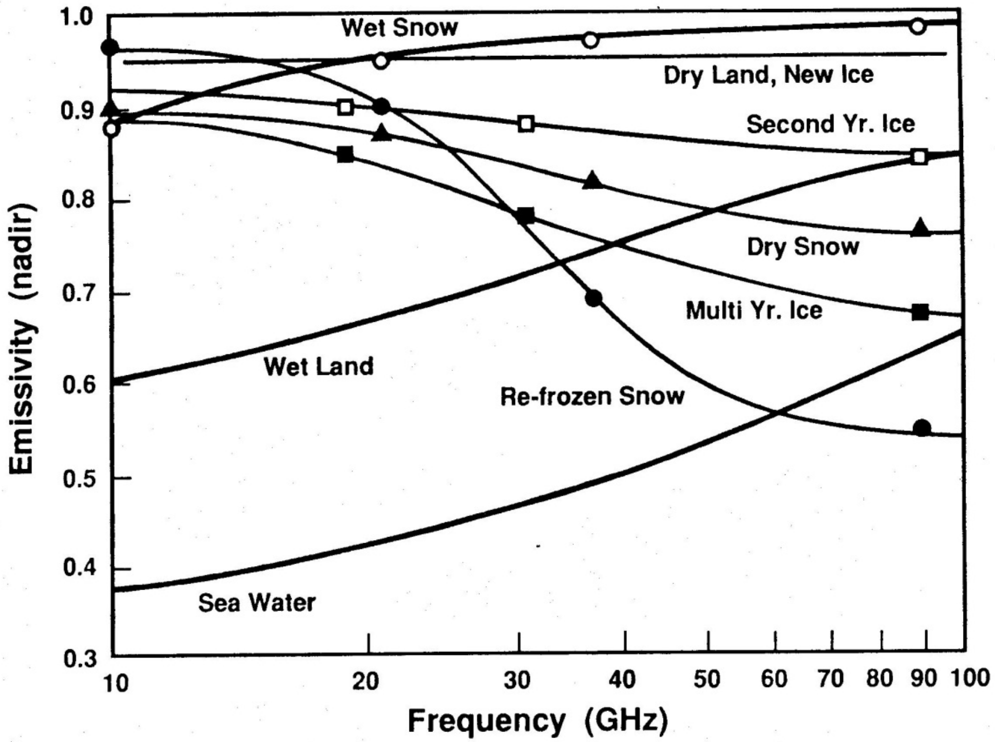

$$T - TB \approx (1 - \varepsilon_s) T e^{-2\tau/\mu},$$

$$when\ T \approx T_s$$

Heavy Precipitation observed with TRMM sensors
(MCS near Southern Kyushu, Jun. 13, 1998)

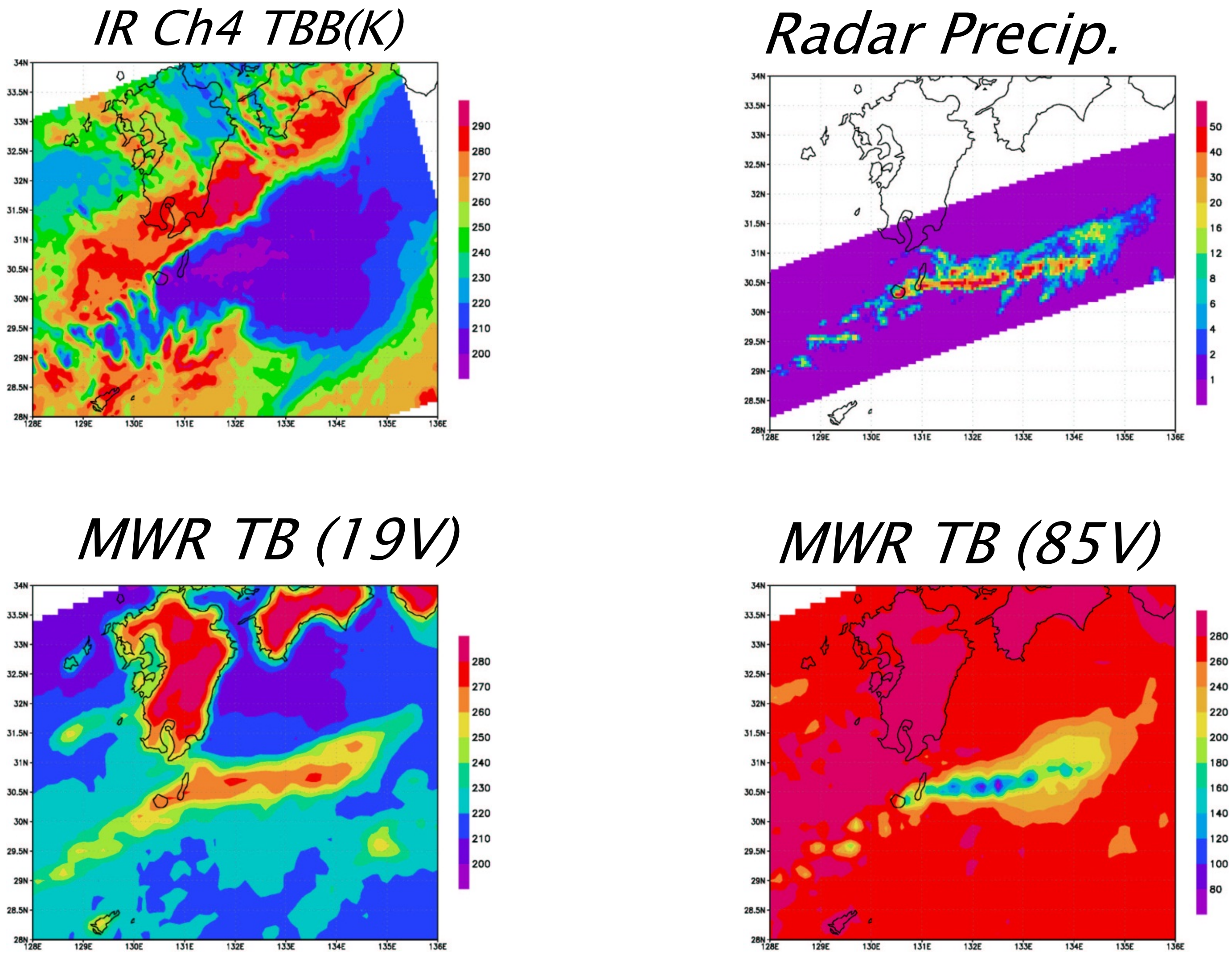

Surface physical observable from MWR

Sea Ice

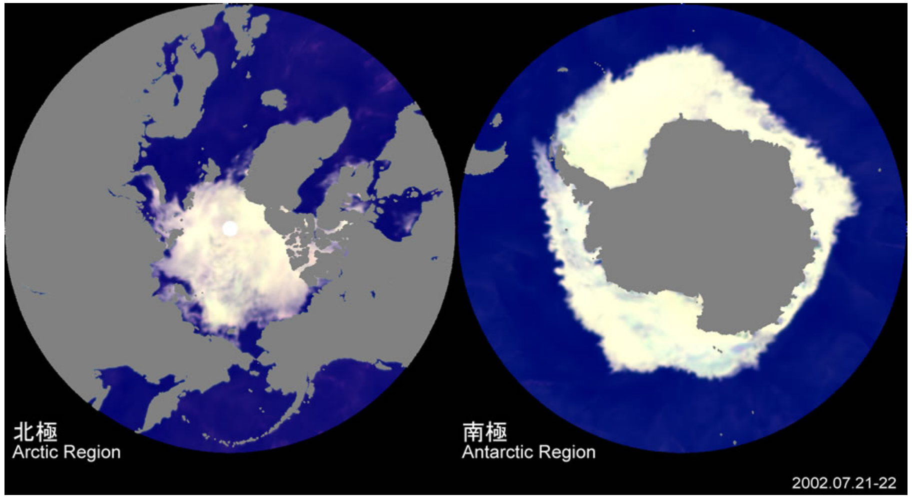

SST (including cloudy area)

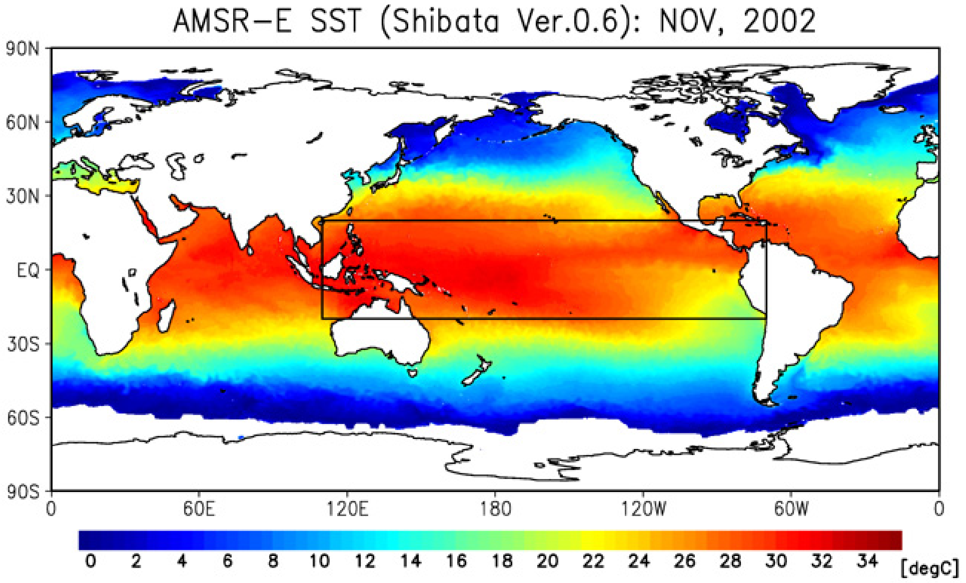

MWR TB sensi
Saturation (over

- TB becomes close to Temp as optical thickness increases (saturation)

$$T - TB \approx (1-\varepsilon_s)Te^{-2\tau/\mu},$$

$$when\ T \approx T_s$$

- After saturation TB decreases mainly due to scattering.
- TB at Higher Frequencies are more sensitive to rain intensity. So saturation occurs at weaker intensity.

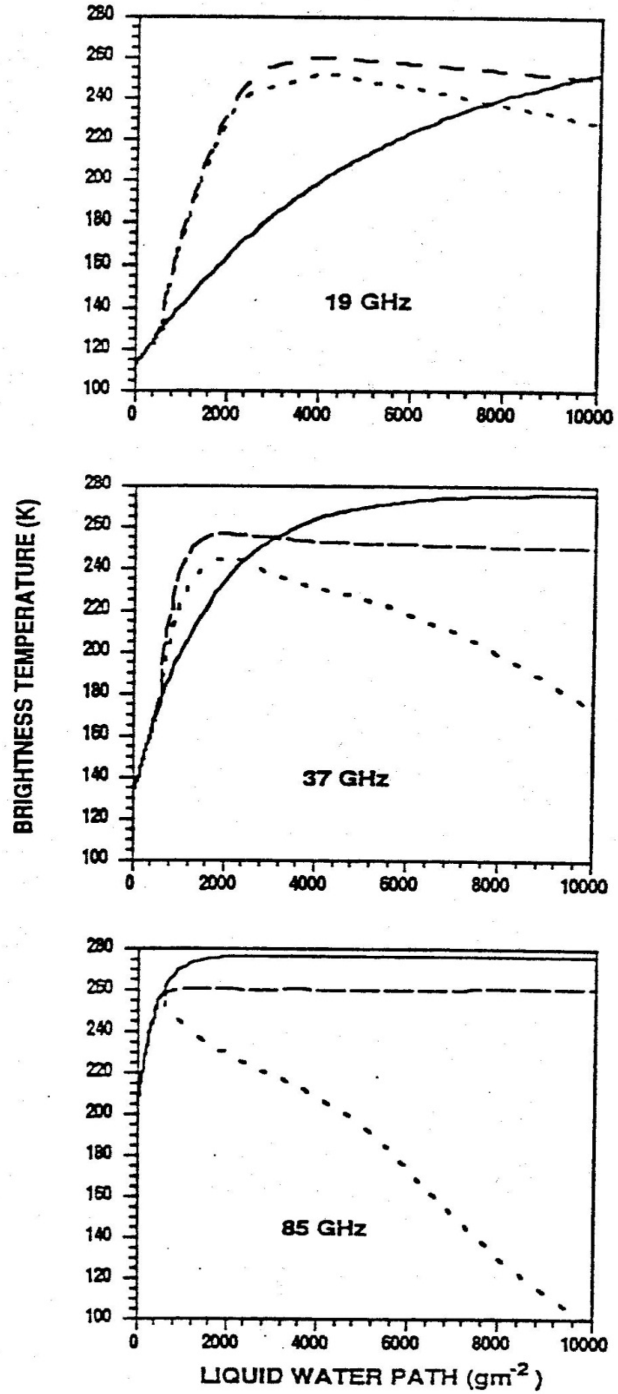

Physical Basis of Microwave Precip. Retrival

- **Over Land:**
  Scattering by frozen particles
  (Higher Freq.)

- **Over Ocean:**
  Scattering
  (Higher Freq.) +
  Emission from Rain
  (Lower Freq.)

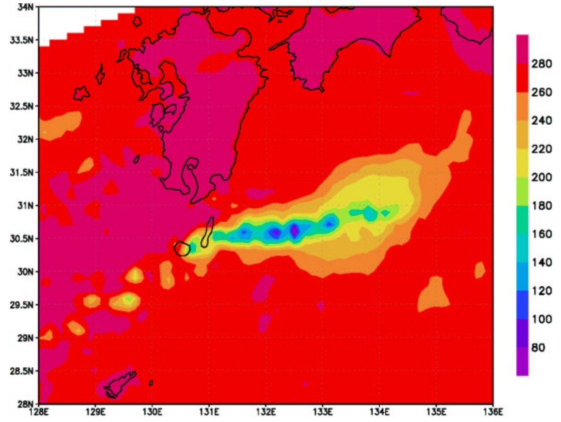

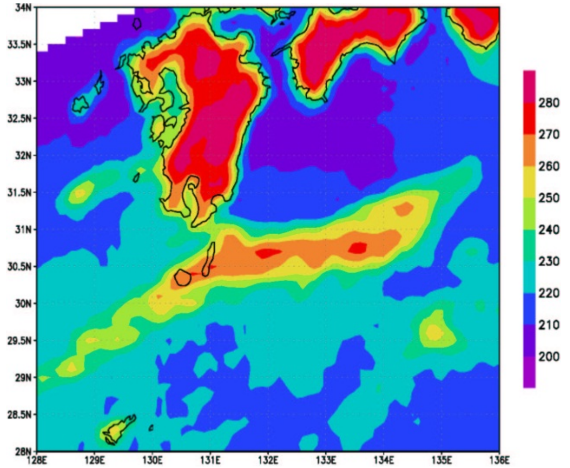

TRMM Microwave Imager (TMI)

Frequency : 10.7 & 19.4 & 21.3 & 37.0 & 85.5 GHz

Resolution : 38.3 & 18.4 & 16.5 & 9.7 & 4.4 km

Swath : 760 km

TRMM

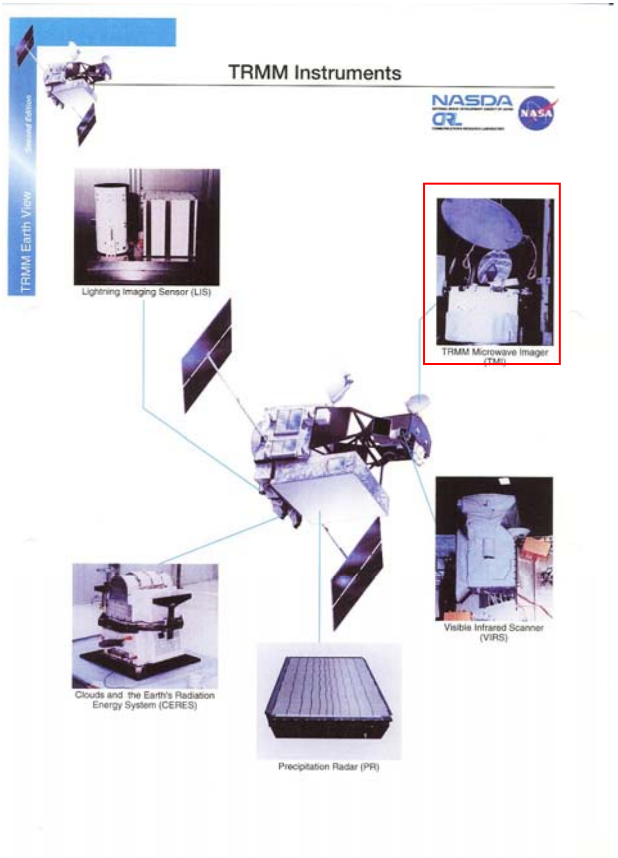

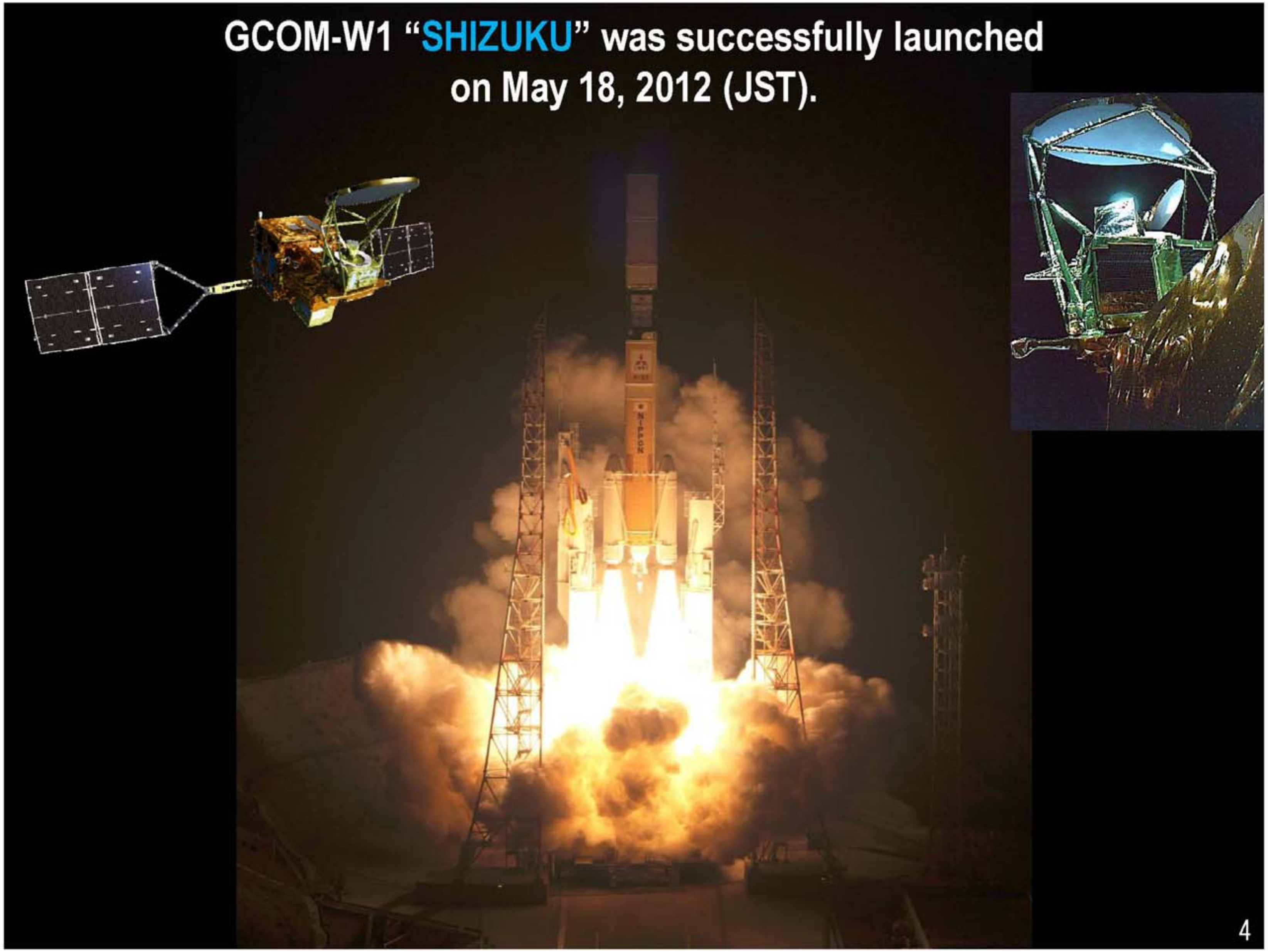
GCOM-W1 "SHIZUKU" was successfully launched
on May 18, 2012 (JST).
4

GCOM-W1 "SHIZUKU" was successfully launched on May 18, 2012 (JST).

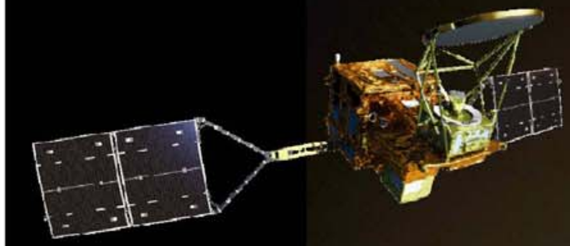

MAJOR CHARACTERISTICS OF AMSR2

Freq (GHz) :	6.925 /7.3	10.65	18.7	23.8	36.5	89.0
IFOV (km) :	35x62	24x42	14x22	15x26	7x12	3x5

Swath width :1450 km

DMSP SSMIS

- SSMIS: conically scanning MWR with a 53.1 degree and a swath width of 1707 km.
- **Center Frequencies(GHz)**
  19.35 22.235
  37.0 91.665 150.0
  183.31+/-1 183.31+/-3
  183.31+/-7
- **Polarization**
  V/H V
  V/H V/H H
  H H H
- **IFOV (km x km)**
  73x47 73x47
  41x31 14x13 14x13
  14x13 14x13 14x13

SSMIS (2003~)

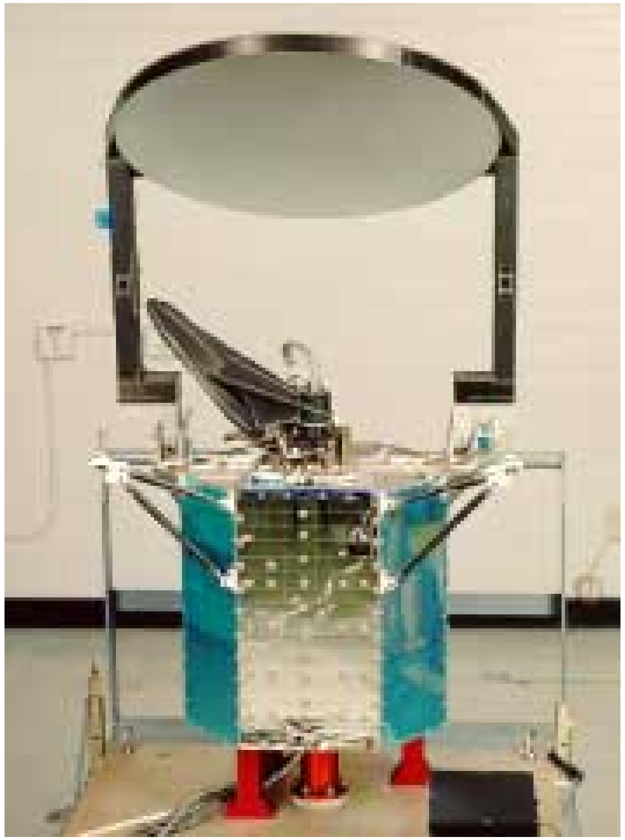

GPM Reference Concept

OBJECTIVE: Understand the Horizontal and Vertical Structure of Rainfall and Its Microphysical Element. Provide Training for Constellation Radiometers.

OBJECTIVE: Provide Enough Sampling to Reduce Uncertainty in Short-term Rainfall Accumulations. Extend Scientific and Societal Applications.

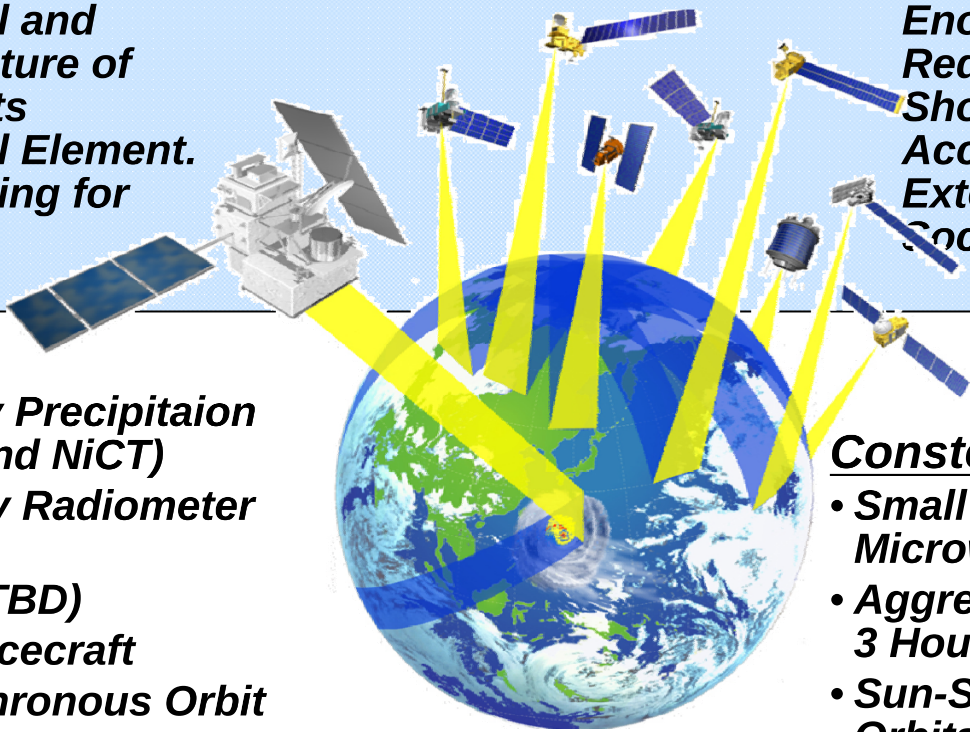

<u>Core Satellite</u>

- ***Dual-frequency Precipitaion Radar (JAXA and NiCT)***
- ***Multi-frequency Radiometer (NASA)***
- ***H2-A Launch (TBD)***
- ***TRMM-like Spacecraft***
- ***Non-Sun Synchronous Orbit***
- ***~65° Inclination***
- ***~407 km Altitude***
- ***~5 km Horizontal Resolution***
- ***250 m / 500m Vertical Resolution***

<u>Constellation Satellites</u>

- ***Small Satellites with Microwave Radiometers***
- ***Aggregate Revisit Time, 3 Hour goal***
- ***Sun-Synchronous Polar Orbits***
- ***500~900 km Altitude***

<u>Precipitation Validation Sites</u>

- ***Global Ground Based Rain Measurement***

<u>Global Precipitation Processing Center</u>

- ***Capable of Producing Global Precipitation Data Products as Defined by GPM Partners***

Microwave Radiometer Measurements

Passive Microwave Precipitation Retrieval

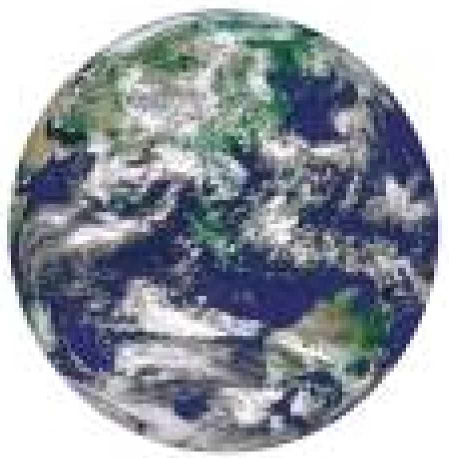

Outline

- Introduction
- Conventional Algorithm
  – Forward Calculation (precip cloud models)
  – Retrieval Part
  – Validation (TRMM PR)
- New over-land algorithm
  – MWI Indices for Over-land Algorithm
  – Validation (TRMM PR)
- Summary

Global Rainfall Map Processing System at JAXA/EORC

Near real time and high-resolution global rainfall map based on satellite observation

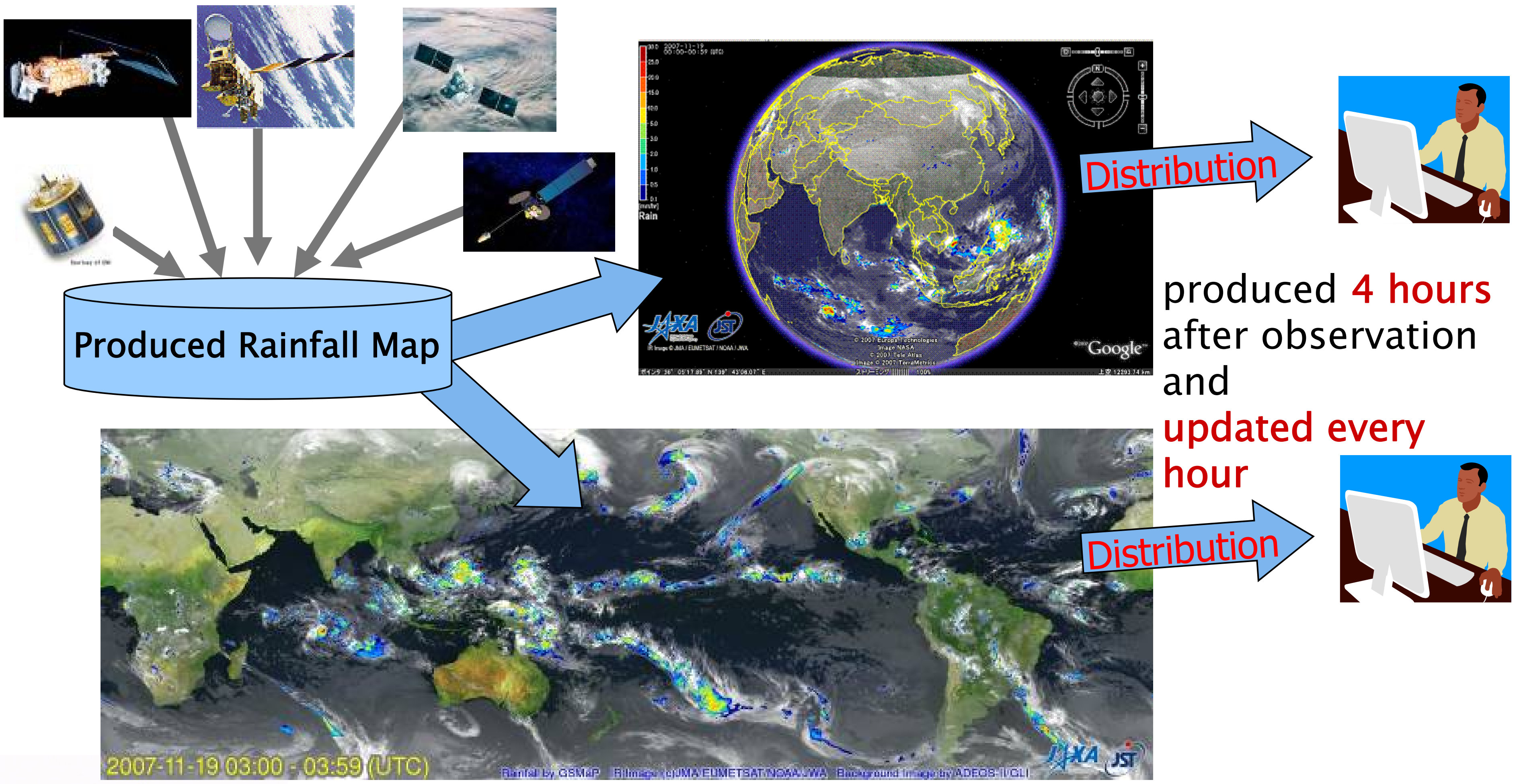

http://sharaku.eorc.jaxa.jp/GSMaP/

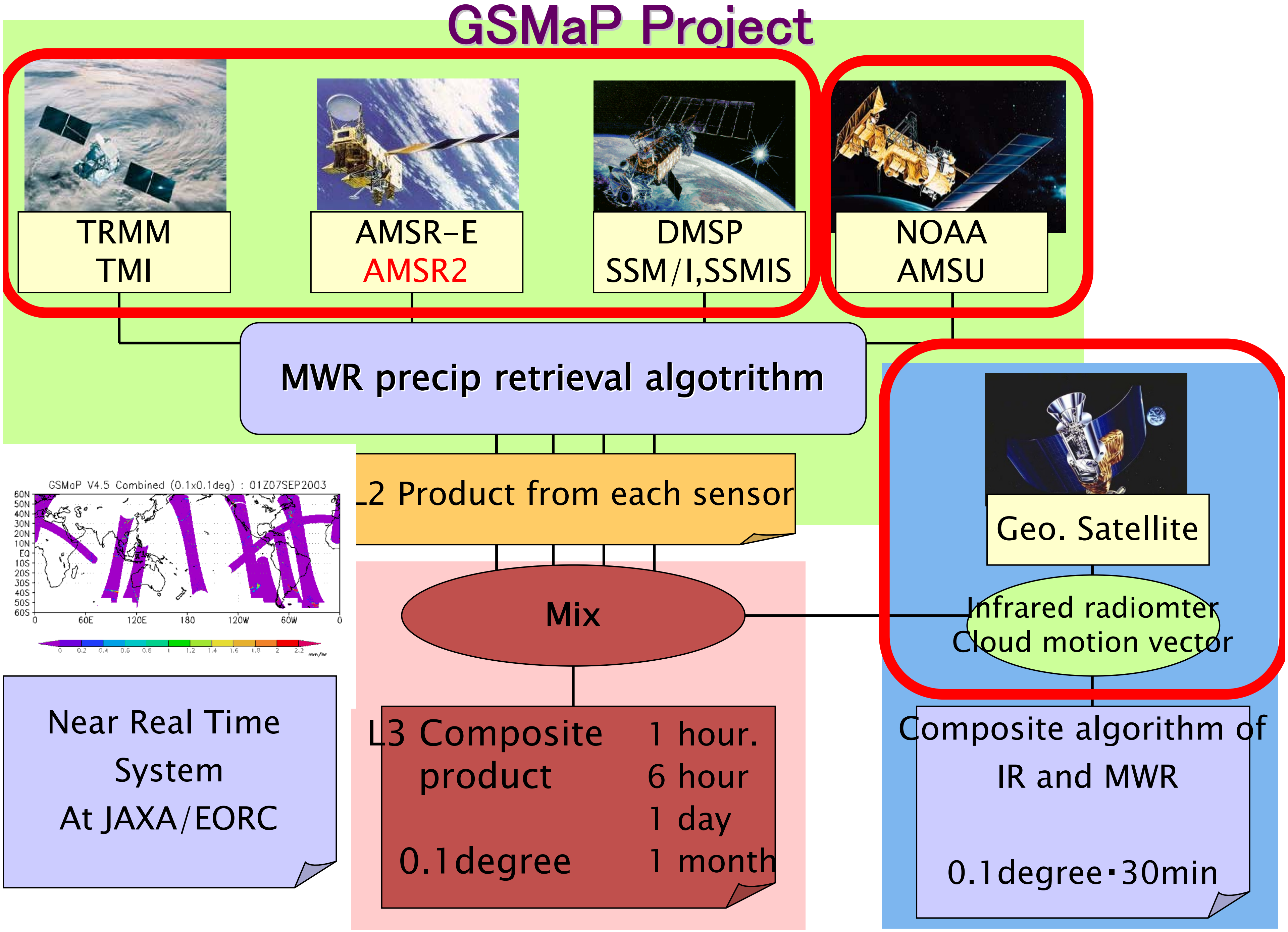
GSMaP Project
TRMM
TMI
AMSR-E
AMSR2
DMSP
SSM/I,SSMIS
NOAA
AMSU
MWR precip retrieval algotrithm
L2 Product from each sensor
GSMaP V4.5 Combined (0.1x0.1deg) : 01Z07SEP2003
Geo. Satellite
Infrared radiomter
Cloud motion vector
Mix
Near Real Time
System
At JAXA/EORC
L3 Composite
product
0.1degree
1 hour.
6 hour
1 day
1 month
Composite algorithm of
IR and MWR
0.1degree・30min

Conventional Algorithm

Forward Calculation
Retrieval Part
Validation (TRMM PR)

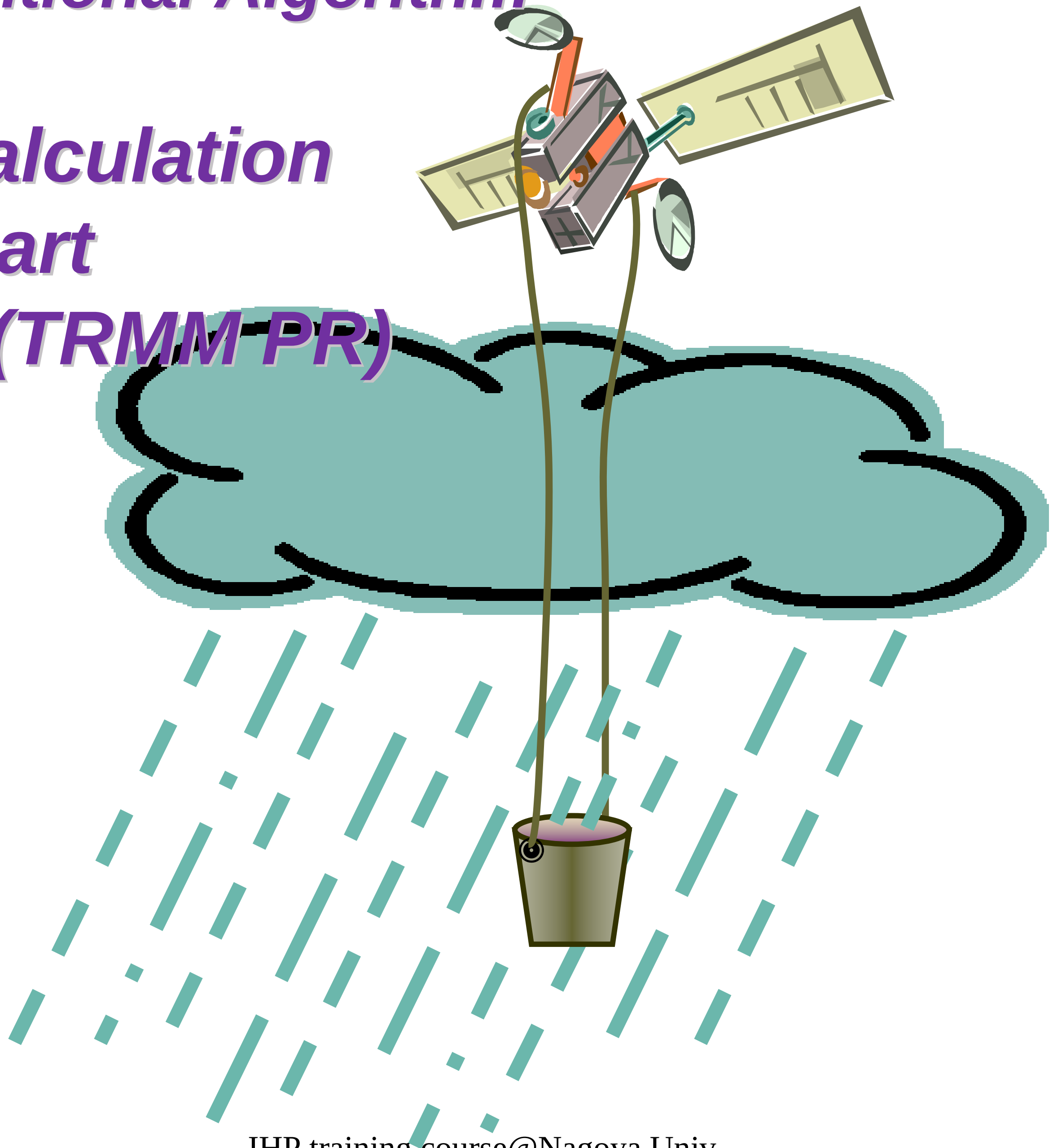

Physical Basis of Microwave Precip. Retrival

- **Over Land:**

  Scattering by frozen particles

  (Higher Freq.)

- **Over Ocean:**

  Scattering

  (Higher Freq.) +

  Emission from Rain

  (Lower Freq.)

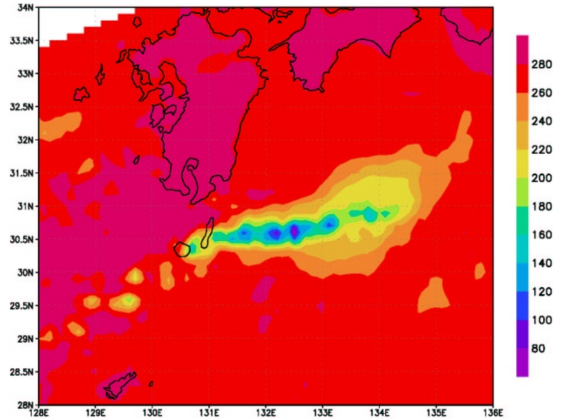

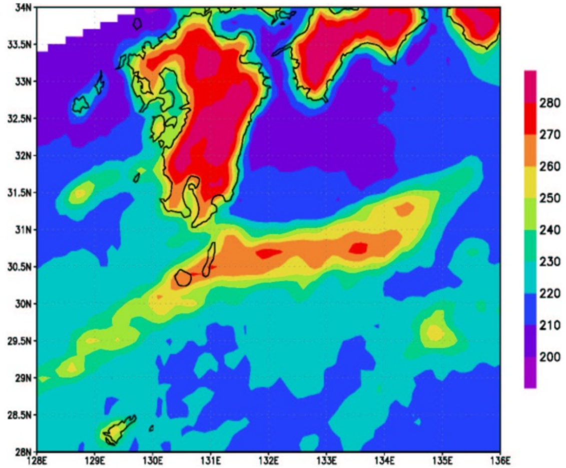

Basic Idea of the Retrieval Algorithm

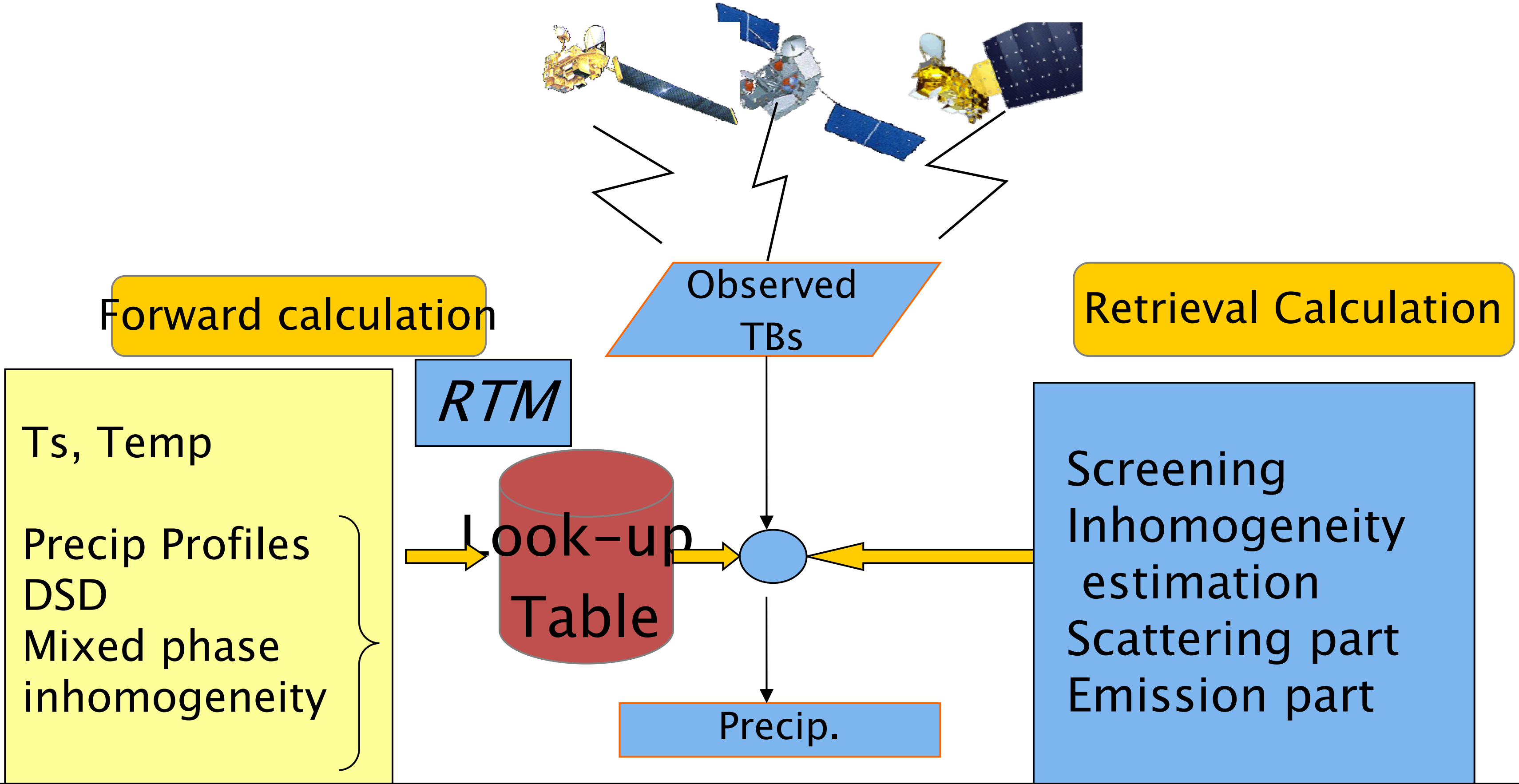

Find the optimal precipitation that gives RTM-calculated TBs fitting best with the observed TBs:
PCT37, PCT85 (land)
TB10v,TB19v, TB37v, PCT37, PCT85 (sea)

Fig.1

Parameters for RTM calculation

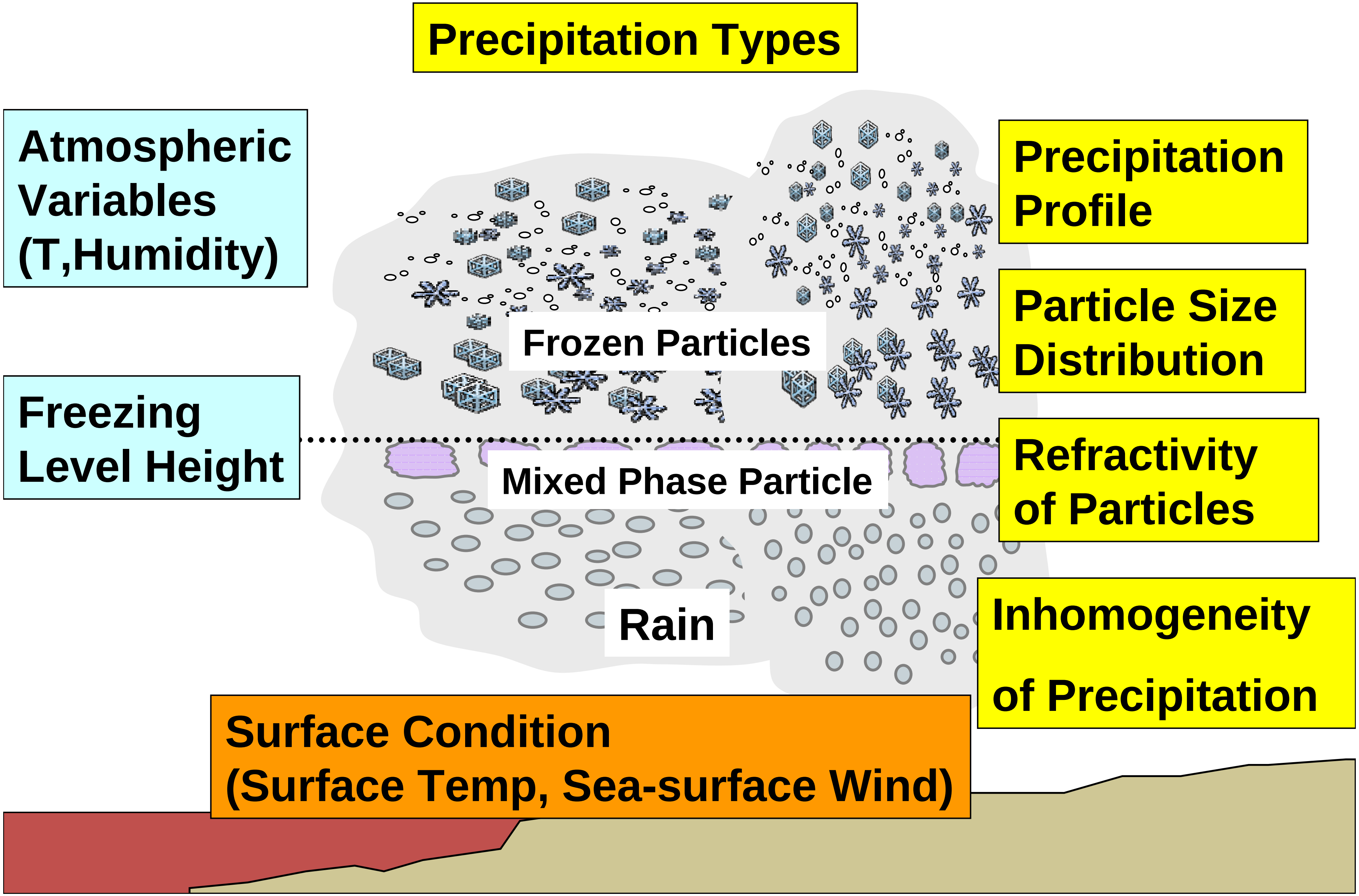

Basic Idea of the Retrieval Algorithm

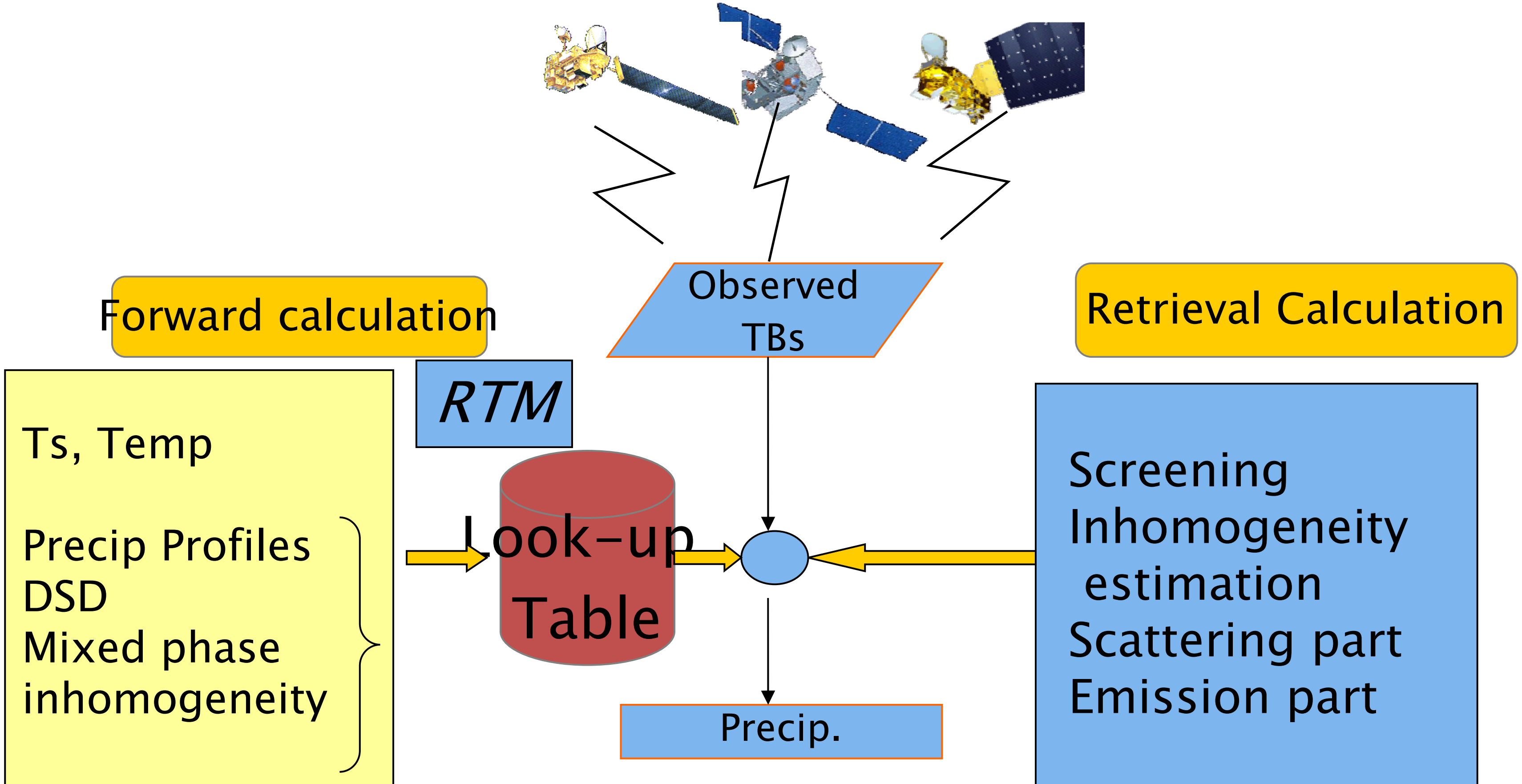

Find the optimal precipitation that gives RTM-calculated TBs fitting best with the observed TBs:
PCT37, PCT85 (land)
TB10v,TB19v, TB37v, PCT37, PCT85 (sea)

Basic Idea of the Retrieval Algorithm

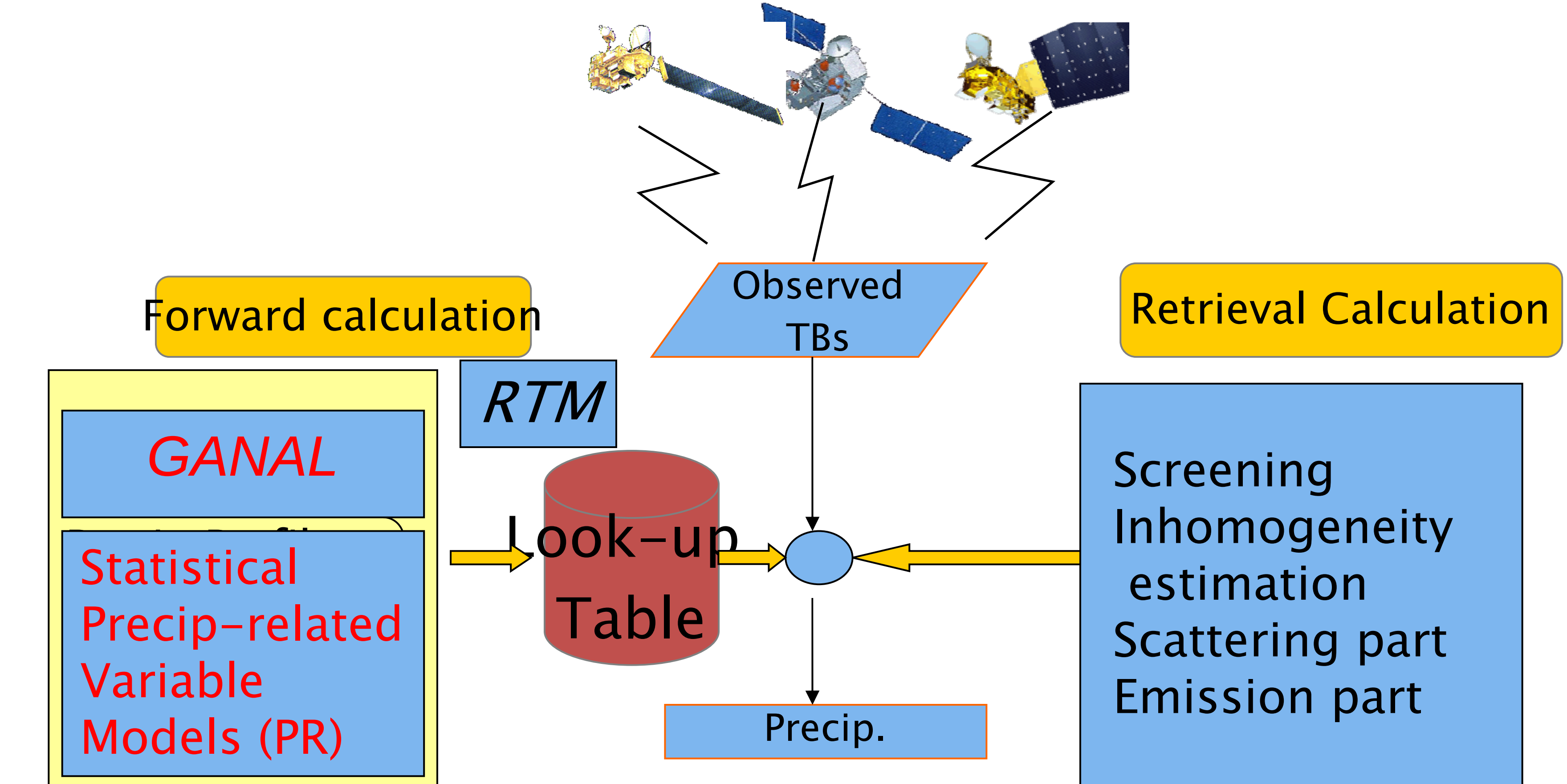

Find the optimal precipitation that gives RTM-calculated TBs fitting best with the observed TBs:
PCT37, PCT85 (land)
TB10v,TB19v, TB37v, PCT37, PCT85 (sea)

Parameters used in the Algorithm: Atmospheric & surface variables

- **Atmospheric variables (Temp,FLH), surface variables(Ts, SSW, SST)**

are derived from the Global Analysis data of JMA

Temperature bias of GANAL against sonde

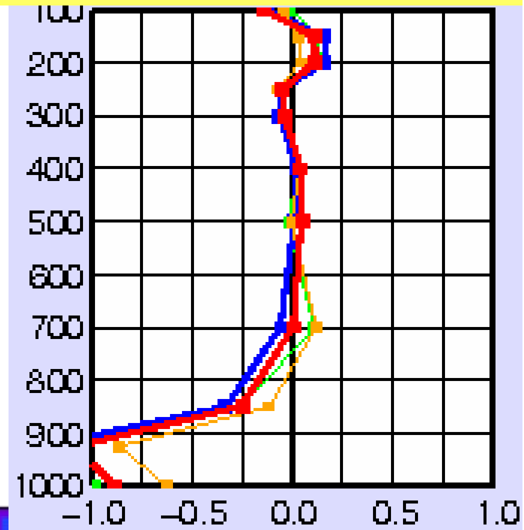

Freezing Level Height for Jan.1, 2003

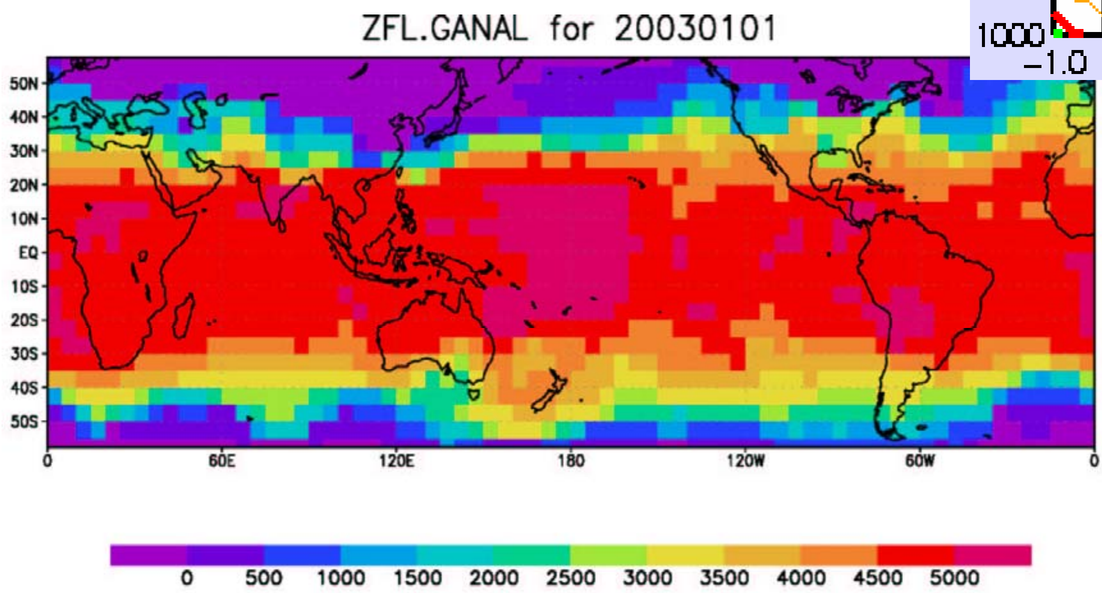

Precipitation Profile Model

Precip type classification

Data base

10 types (land 6, sea 4) are classified from TRMM PR data (2.5 deg, 3 monthly)

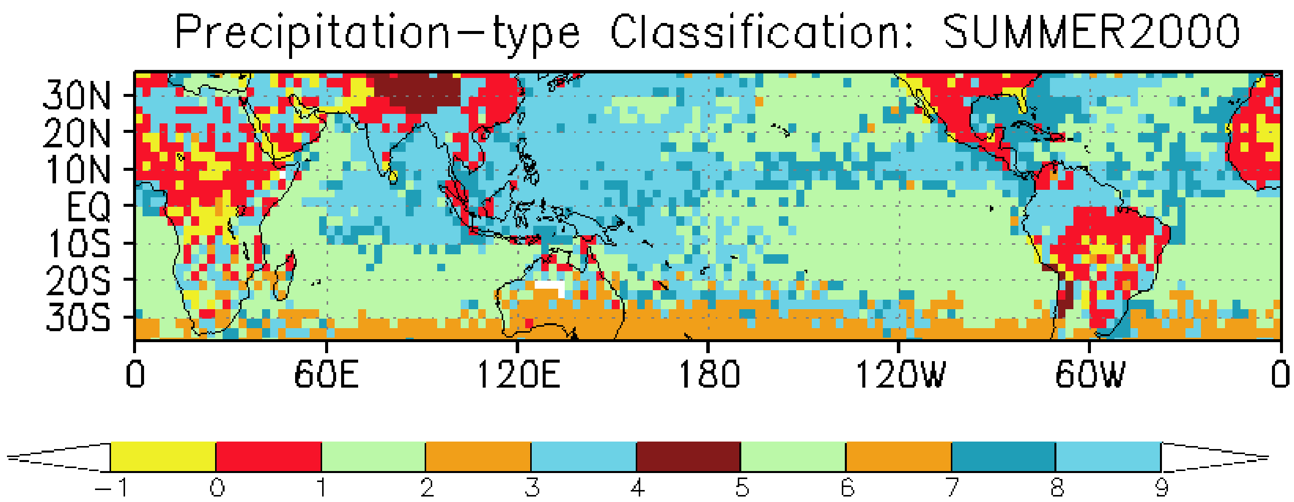

Precip Profile

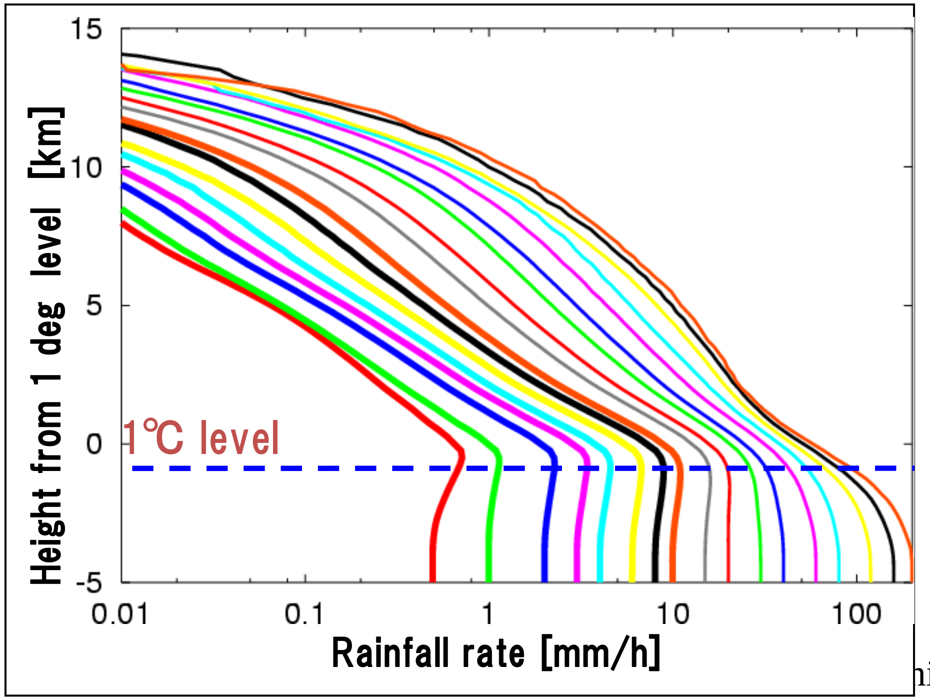

(land) 0: thunderstorm, 1: shower, 2: shallow, 3: frontal rain, 4: organized rain 5: highland
(sea) 6: shallow 7:frontal rain, 8:transit, 9:organized rain

Precip profile data base

Example:

TRMM PR averaged preciptation profiles for each type, surface precip, conv/stra

Particle Size Distribution

DSD for rain: Kozu model (2A25 average distribution calibrated with averaged epsillon)
epsillon =1 for stratiform rain

$$N(D) = N_0 D^{\mu} \exp(-\Lambda D)$$

PSD for frozen particles: Marshall-Palmer distribution

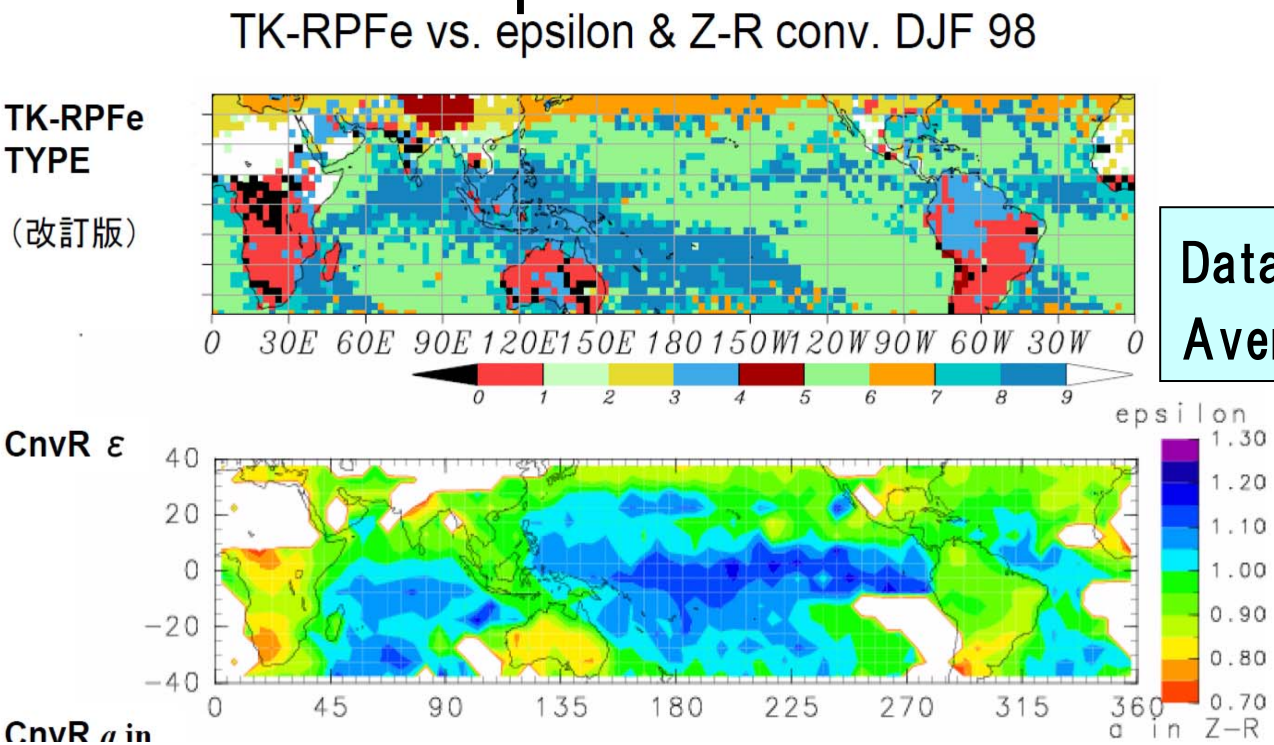

Data base of conv. Epsillon
Averaged for each precip type

Nishitsuji (Mixed-Phase) Model for Stratiform Rain

On the basis of the filed experiment, the following parameters are modeled

- Volume liquid water fraction（Pw)
- shape parameter of the dielectric constant (U)
- DSD parameter (B) is a function of Pw
- Density $\rho = \sqrt{\ }$ Pw
- Fall velocity Magono-Nakamura(1965) for snow and Foot and Du Toit for rain

$$\frac{\varepsilon_s - 1}{\varepsilon_s + U} = P_w \frac{\varepsilon_w - 1}{\varepsilon_w + U} + P_i \frac{\varepsilon_i - 1}{\varepsilon_i + U} + P_a \frac{\varepsilon_a - 1}{\varepsilon_a + U}$$

$$N(D) = N_0 10^{-Ba} \quad (m^{-3} mm^{-1}) \quad \text{(a : radius in cm)}$$

Pw and U profile

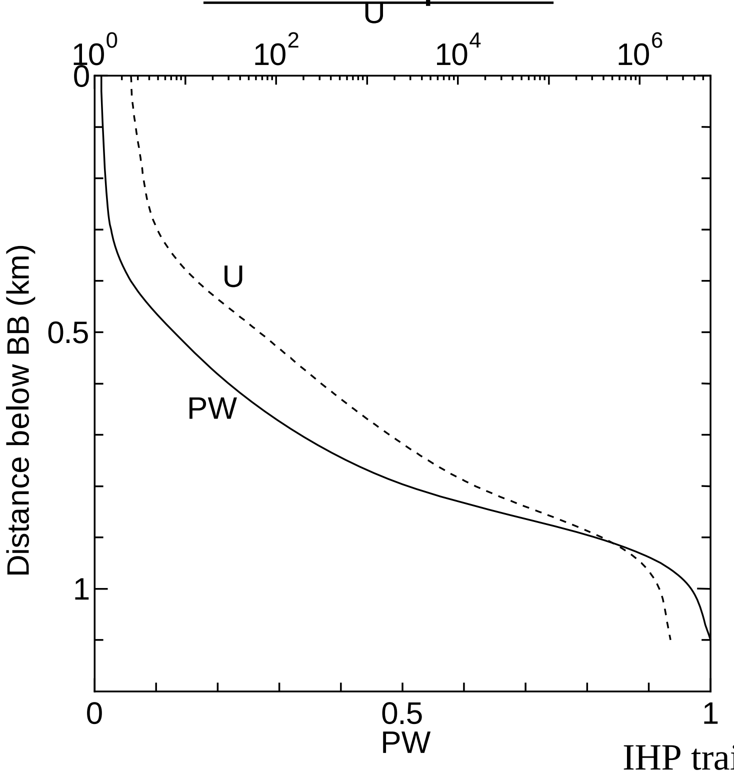

Relationship between B and Pw

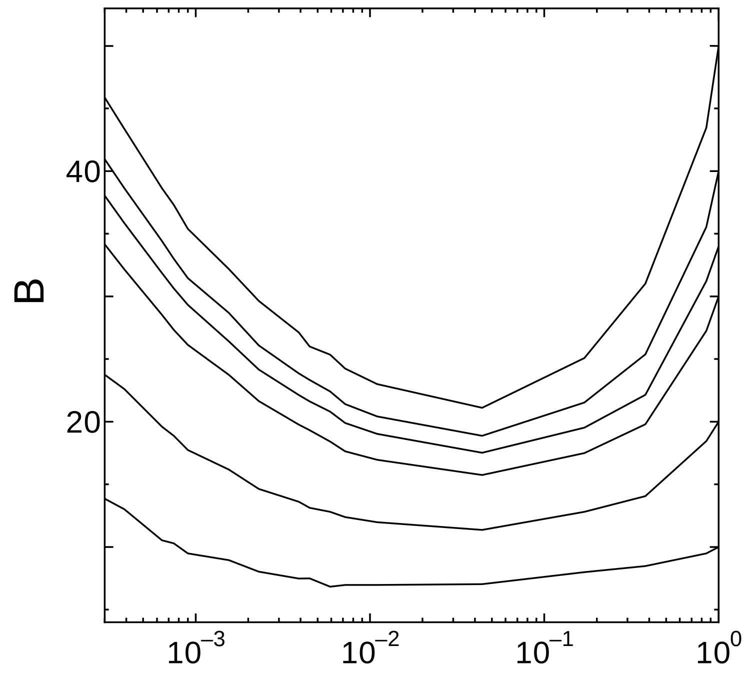

LUT calculation (1)
TBs for homogeneous precip

$$\mu \frac{dTB(\tau,\mu,\varphi)}{d\tau} = TB - (1-\omega_0)T(\tau) -$$

$$\frac{\omega_0}{4\pi}\iint P(\tau,\mu,\varphi,\mu',\varphi')TB(\tau,\mu',\varphi')d\mu' d\varphi'$$

$$where\ \mu = \cos\theta, \tau = \int K_{ab} + K_{sc} dz, \omega_0 = K_{sc}/(K_{ab}+K_{sc}),$$

P *is phase function*

Radiative Transfer Code (Liu,1998)

- One-dimensional model (Plane-parallel)
- Mie Scattering (Sphere)
- 4 stream approximation
- Calculate TBs for homogeneous, convective & stratiform precip with each precip types.

Basic Idea of the Retrieval Algorithm

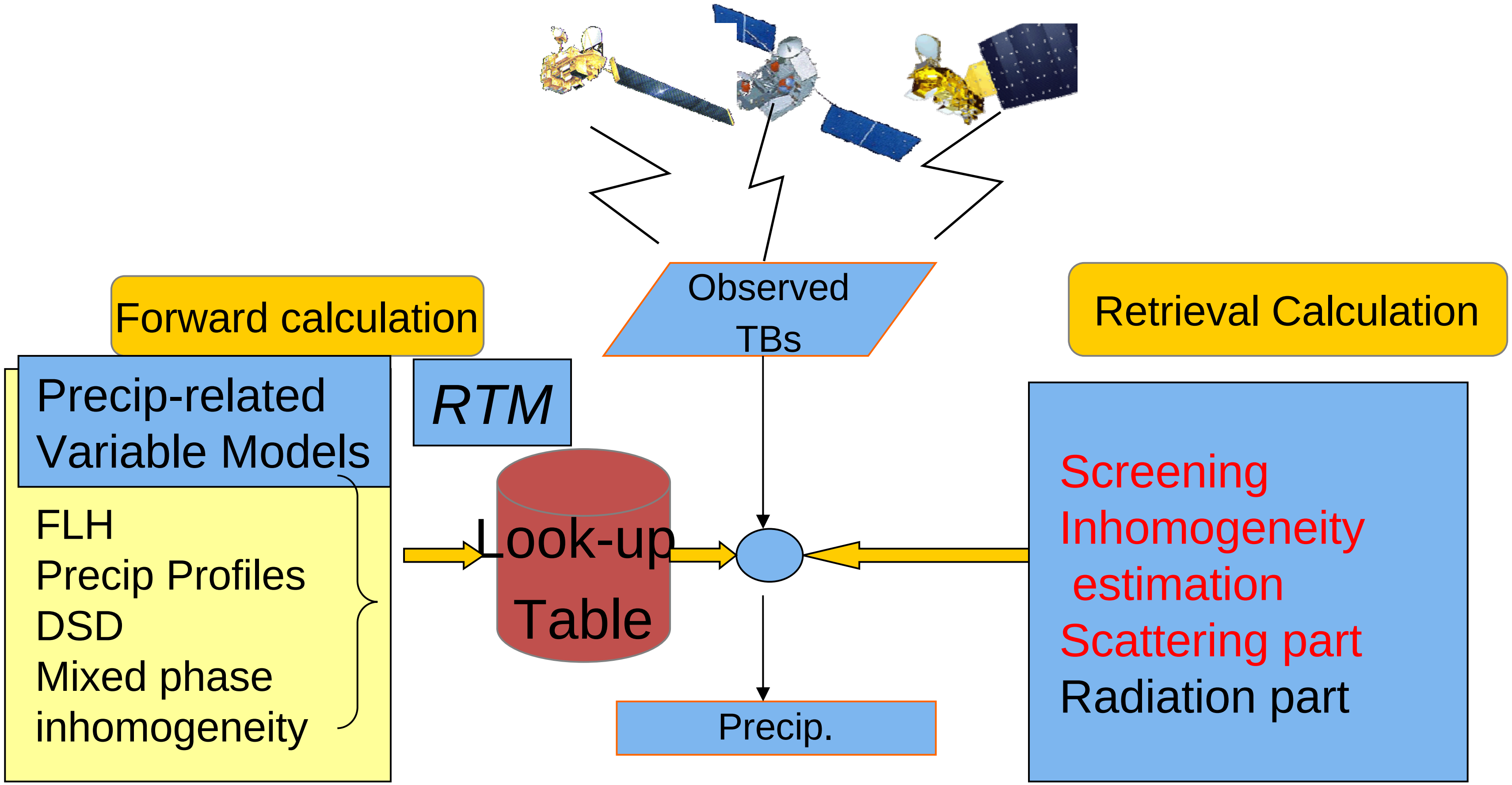

Find the optimal precipitation that gives RTM-calculated TBs fitting best with the observed TBs:
PCT37, PCT85 (land)
TB10v,TB19v, TB37v, PCT37, PCT85 (sea)

Flow of the retrieval part

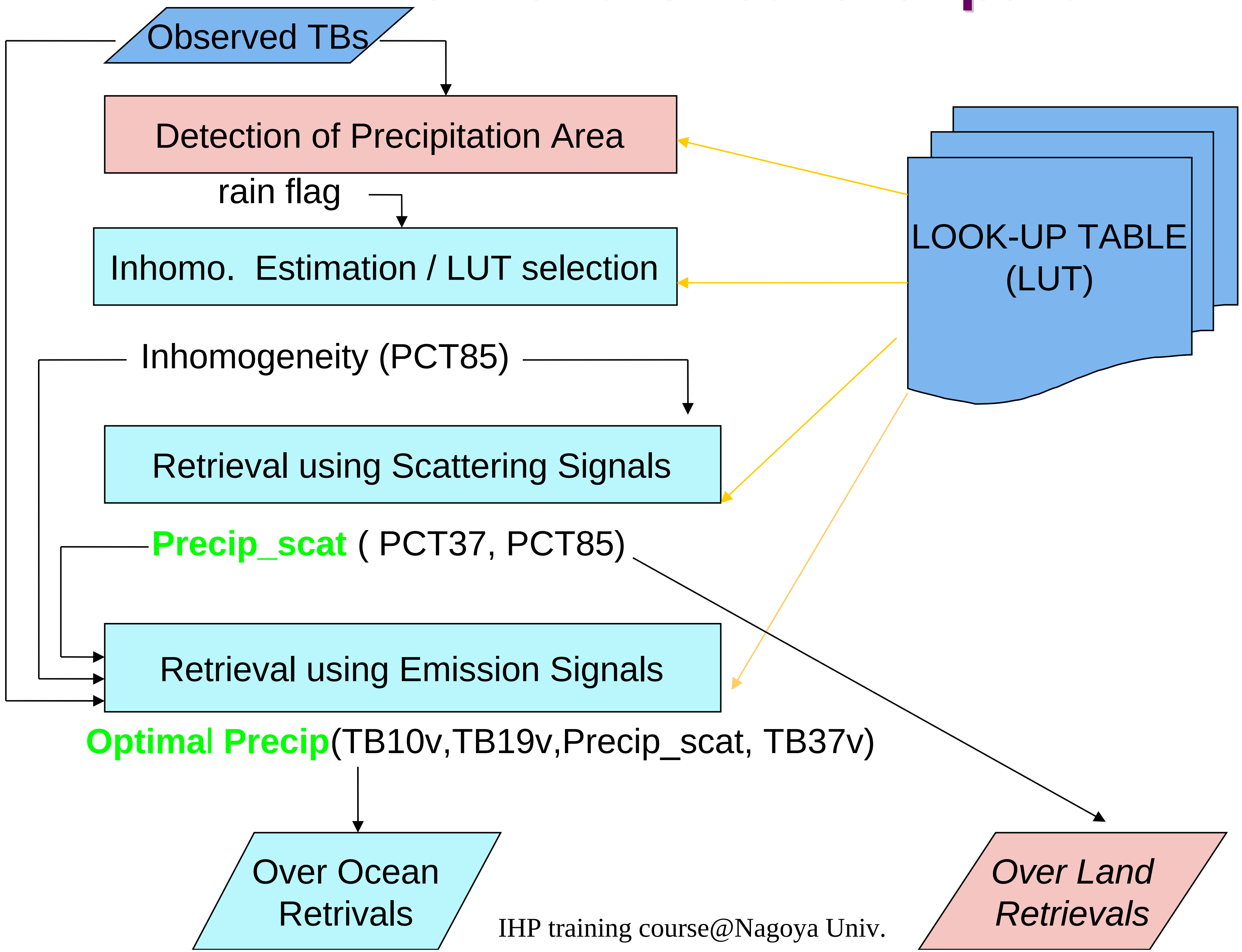

Screening Algorithm over land（Seto et al., 2005）

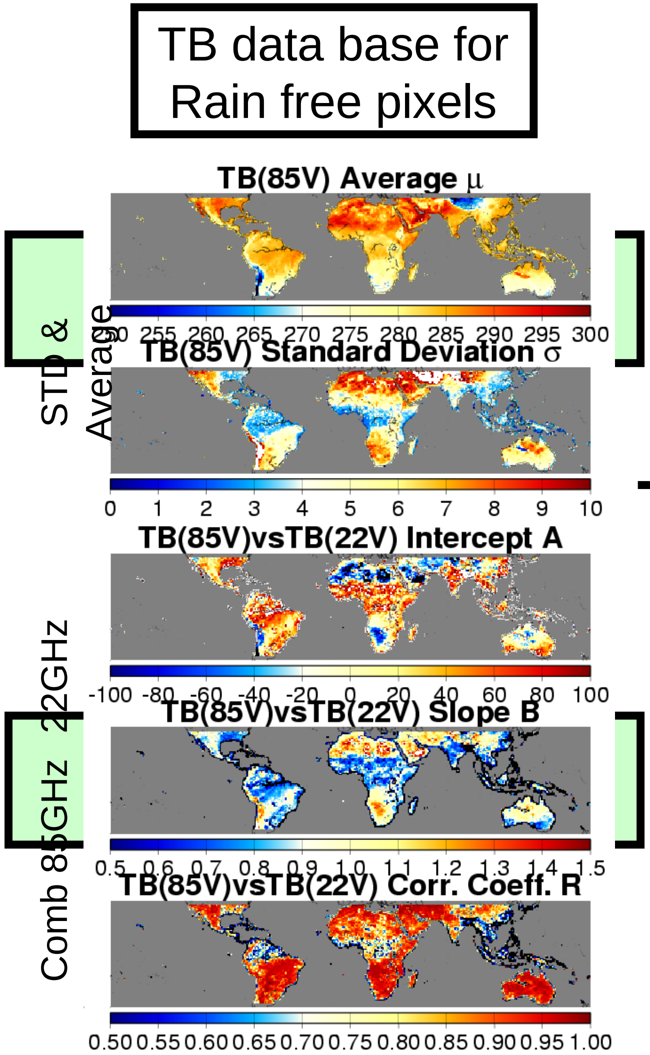

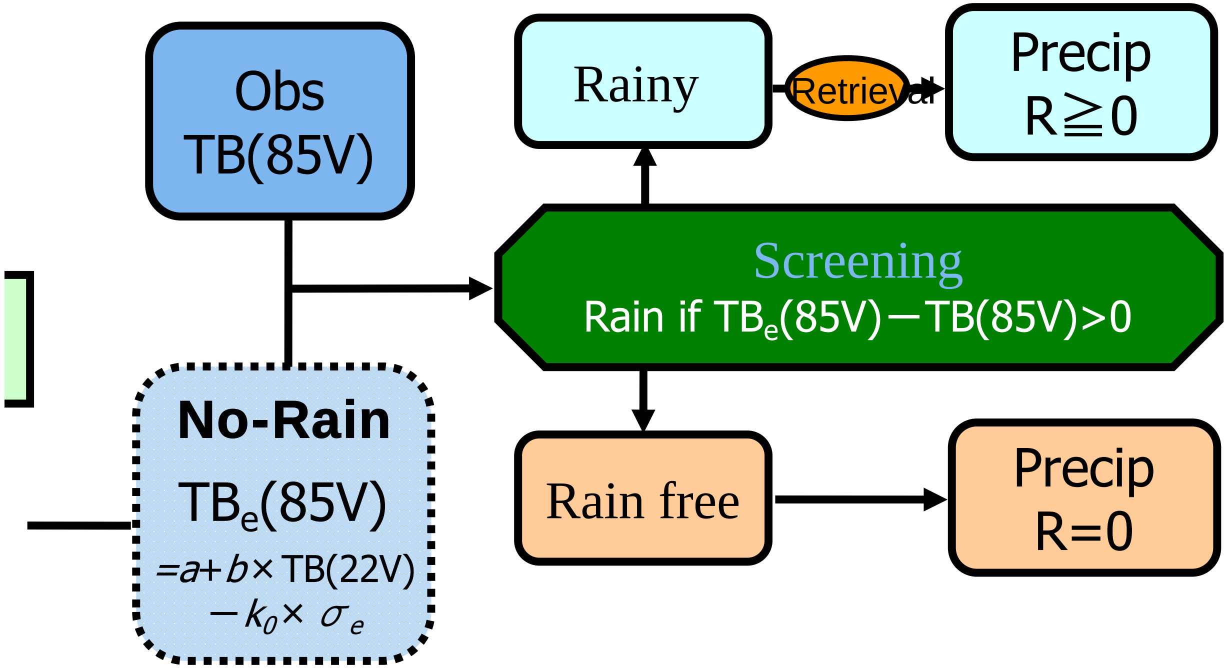

Results

Accuracy is improved compared to GPROF

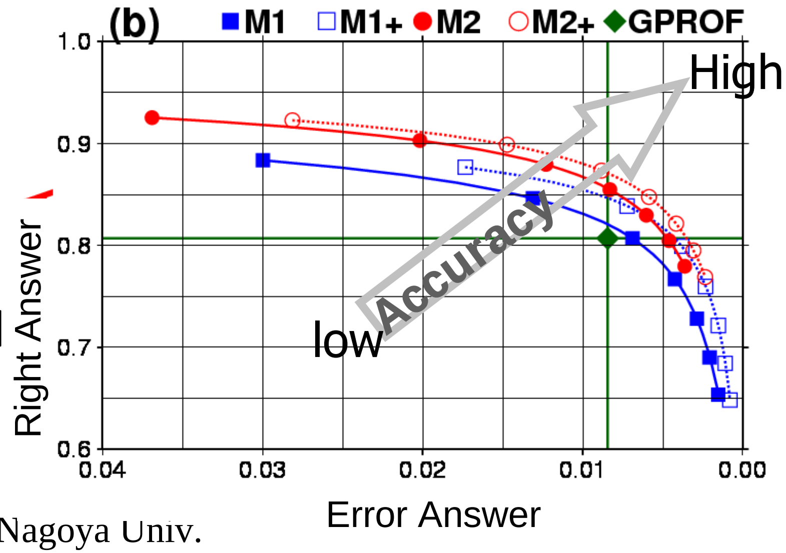

Flow of the retrieval part

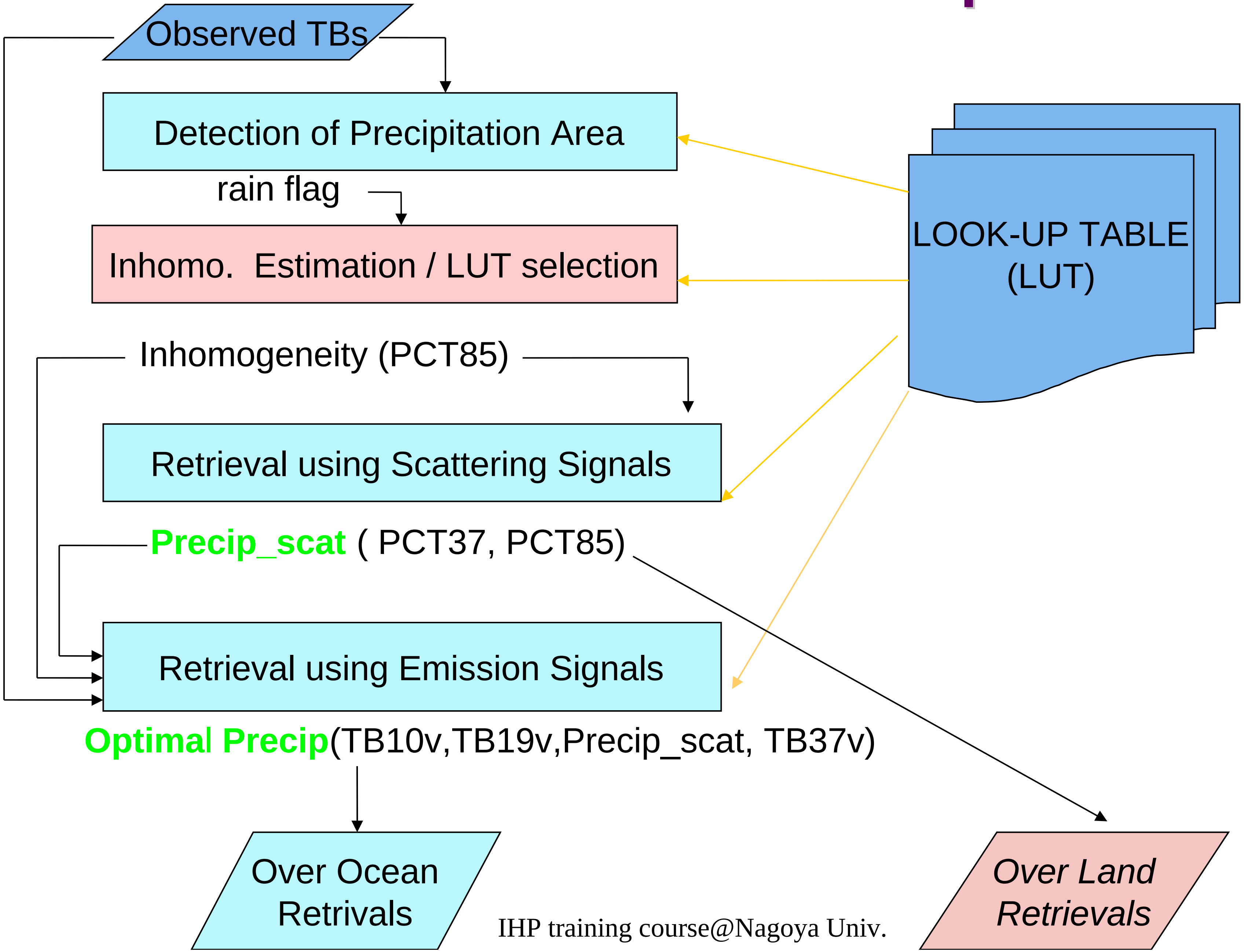

LUT calculation (2): LUTs for inhomo precip

- The calculated TBs are converted into TBs for inhomogeneous precip with Aonashi and Liu’s method (2000).
- LUT used for retrieval is weighted average of convective & stratiform TBs.

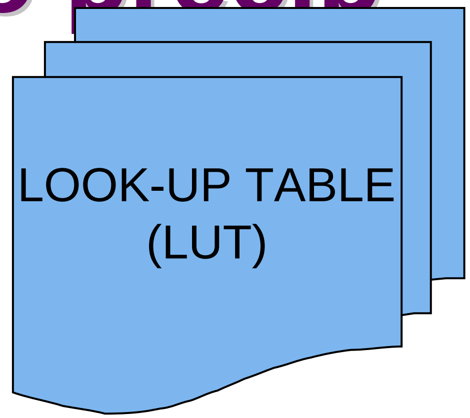

- STD of Log(Pr) is estimated from STD of Log(rain85) statistically (Kubota et al, 2008)

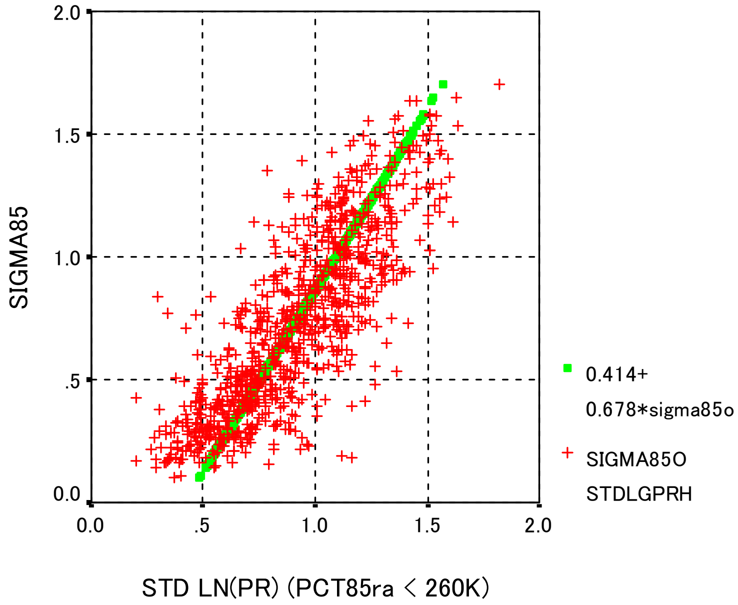

Flow of the retrieval part

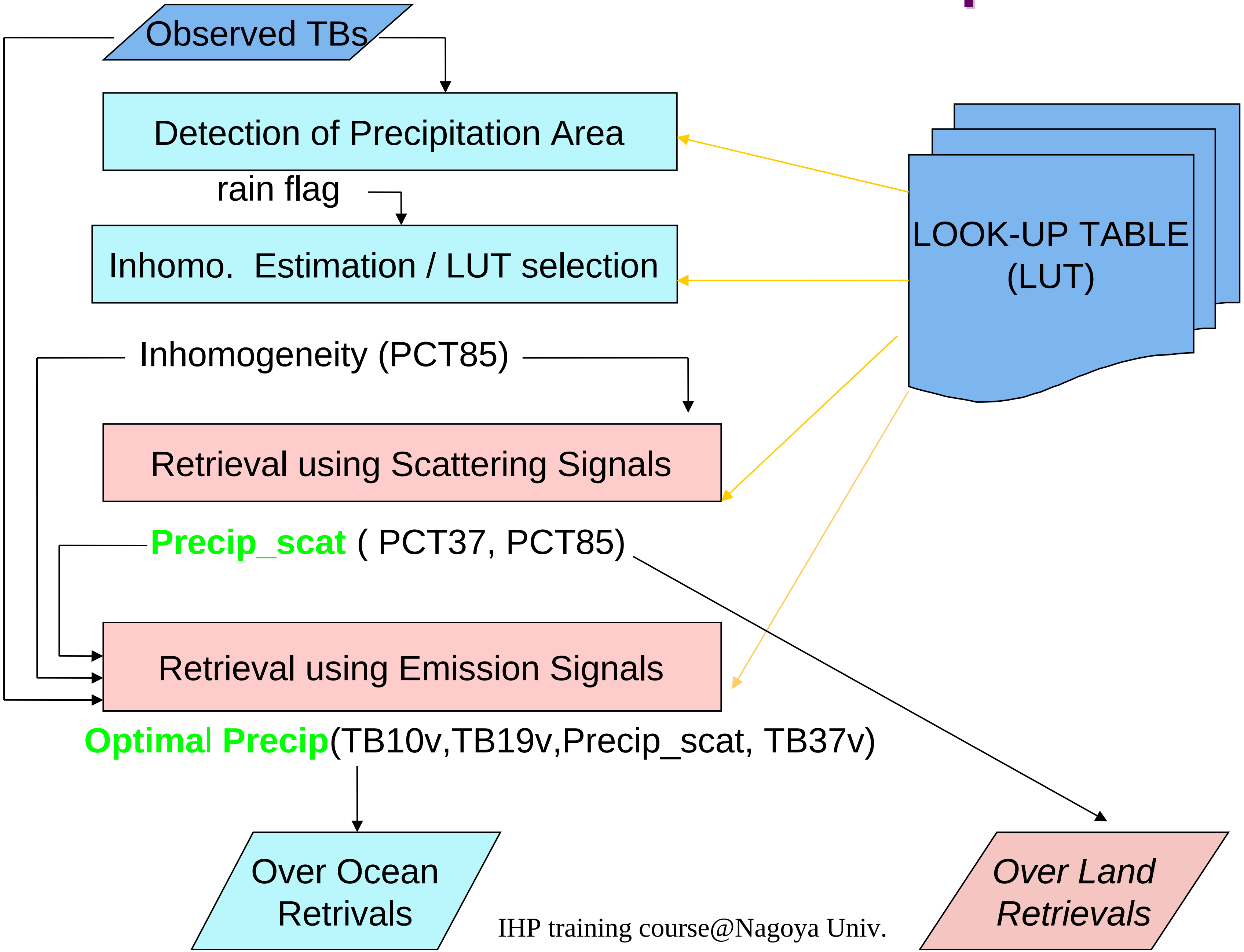

Cyclone Nargis (May, 2008)

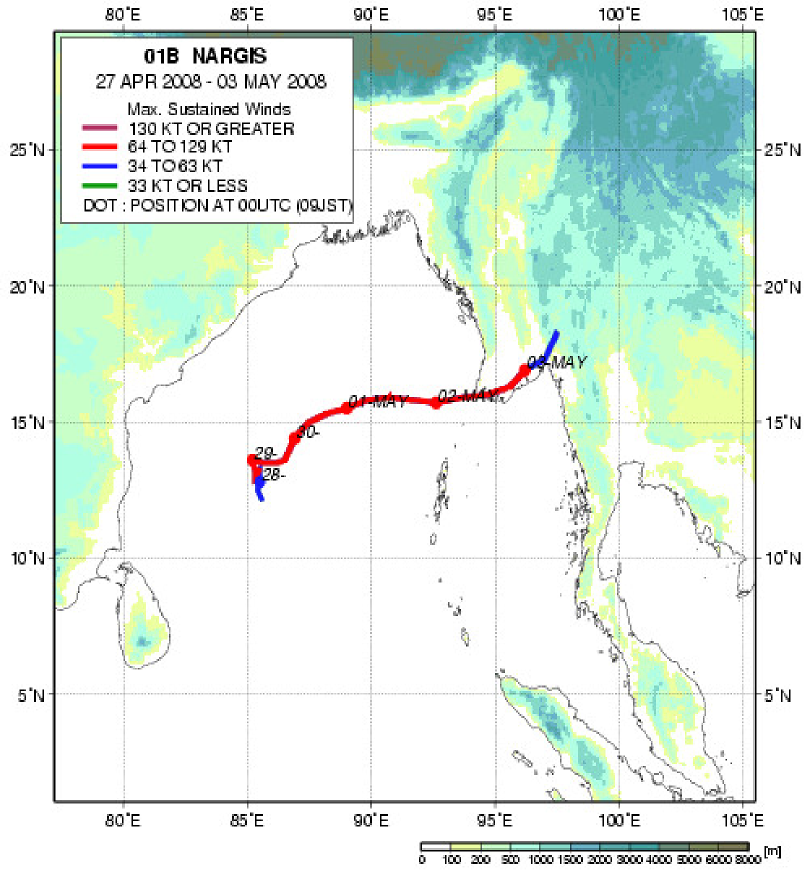

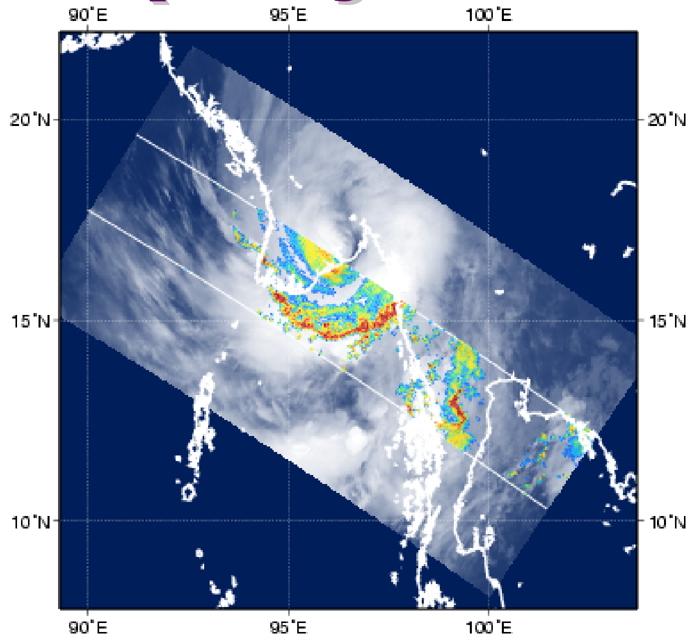

IHP training course@Nagoya Univ.

PR and TMI precipitation (OP59618)

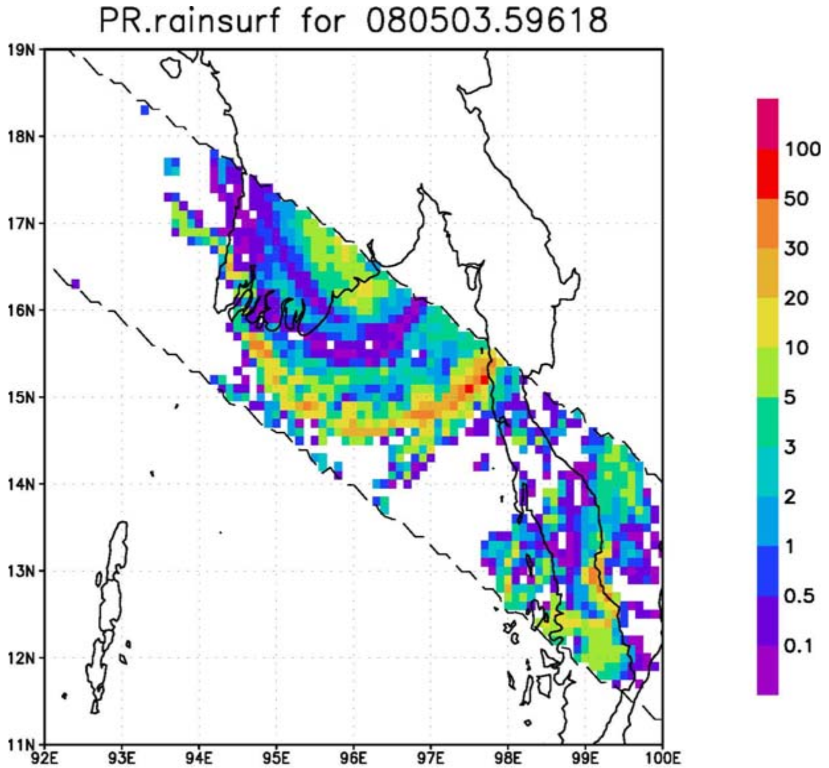

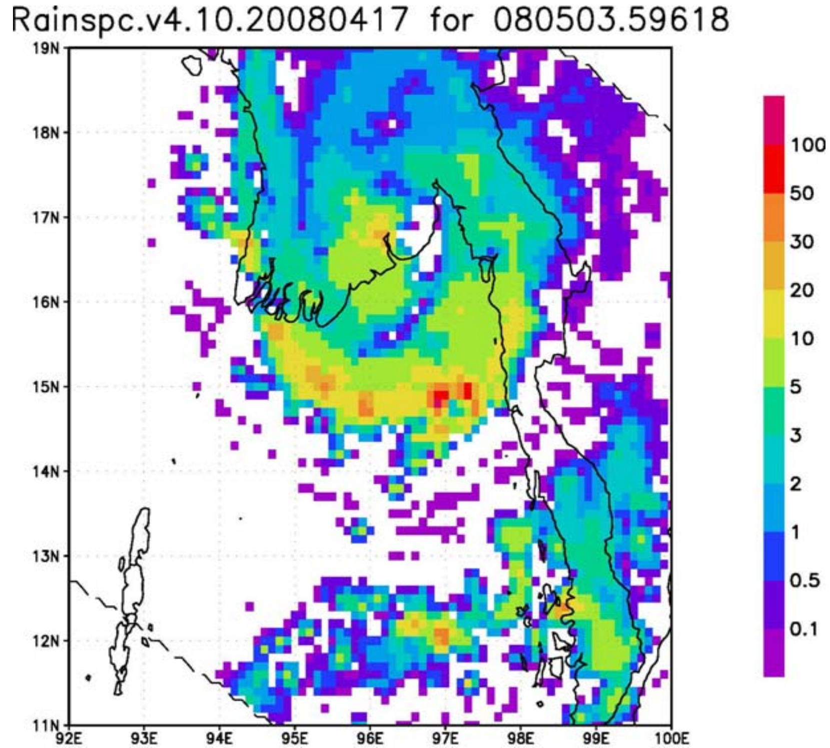

Rainspc.v4.10.20080417 vs PR rainsurf over Sea for Jan,Apr,Jul,Oct 1998

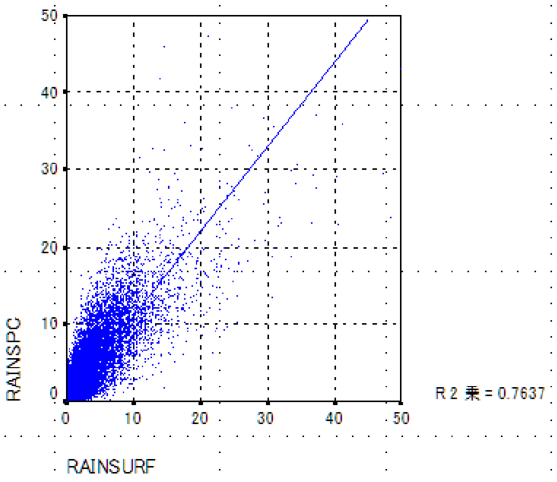

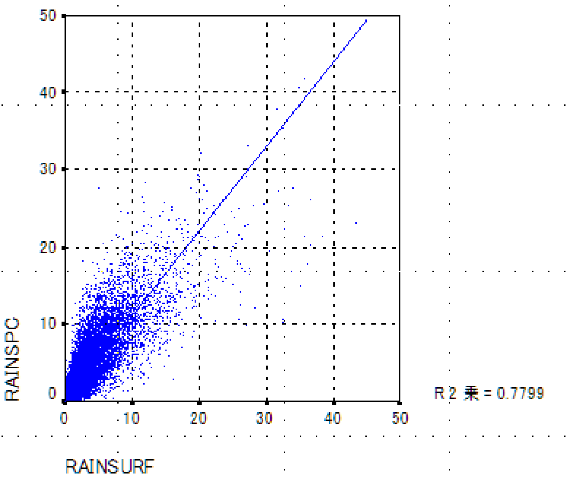

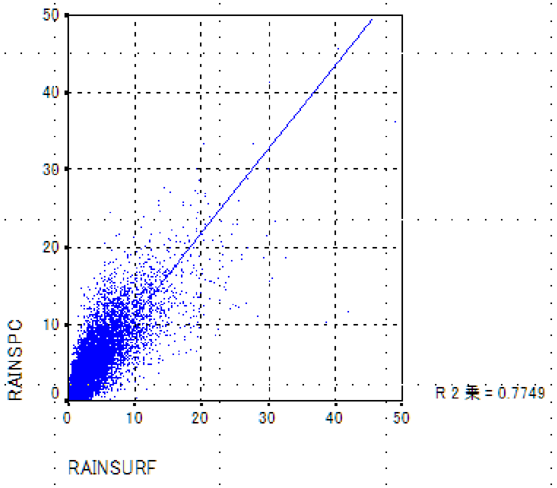

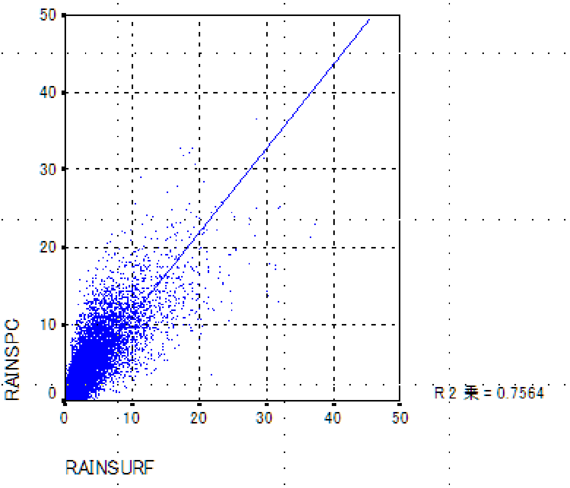

Rainspc.v4.10.20080417 vs PR rainsurf over LAND for Jan,Apr,Jul,Oct 1998

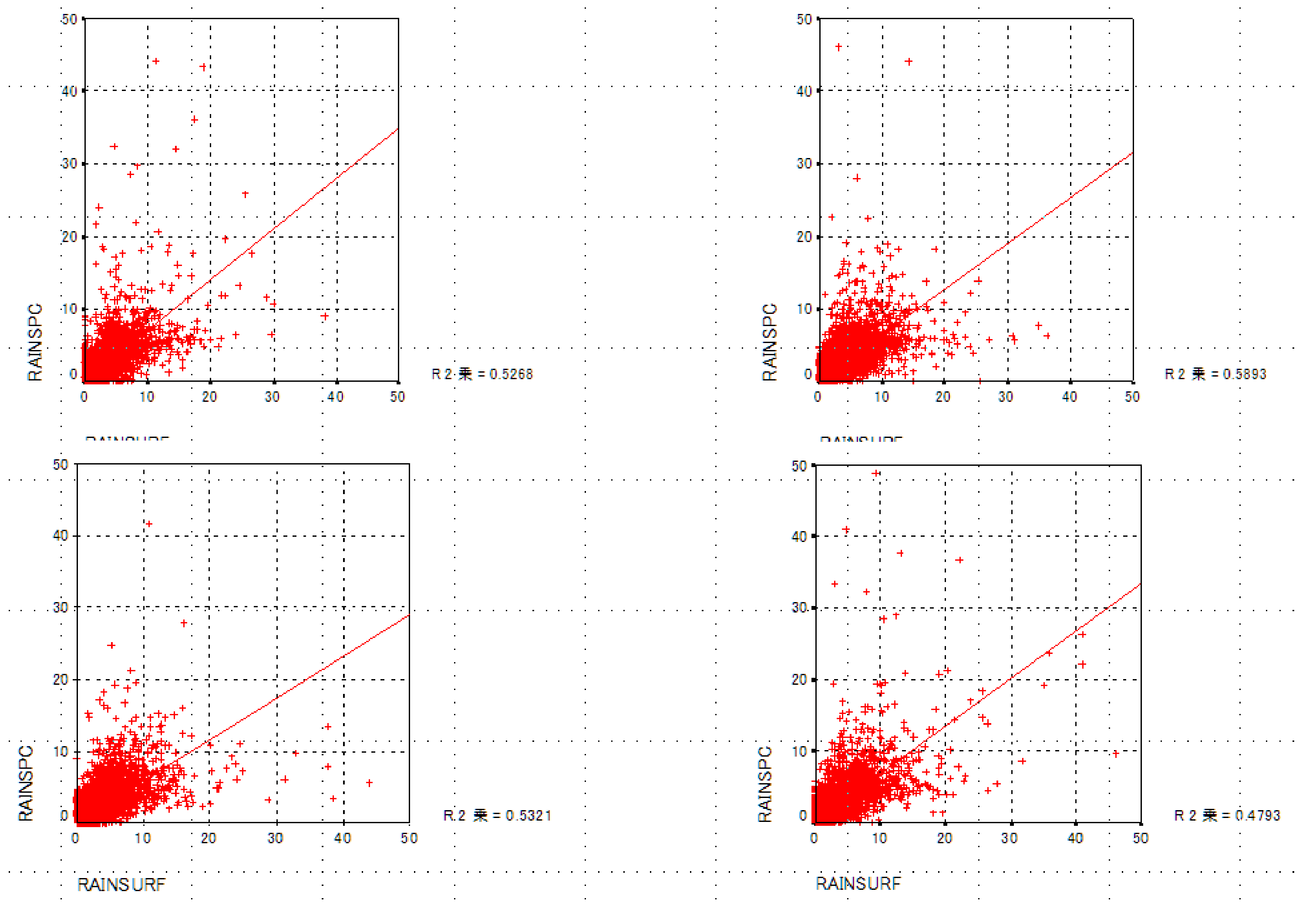

Basic Idea of the Retrieval Algorithm

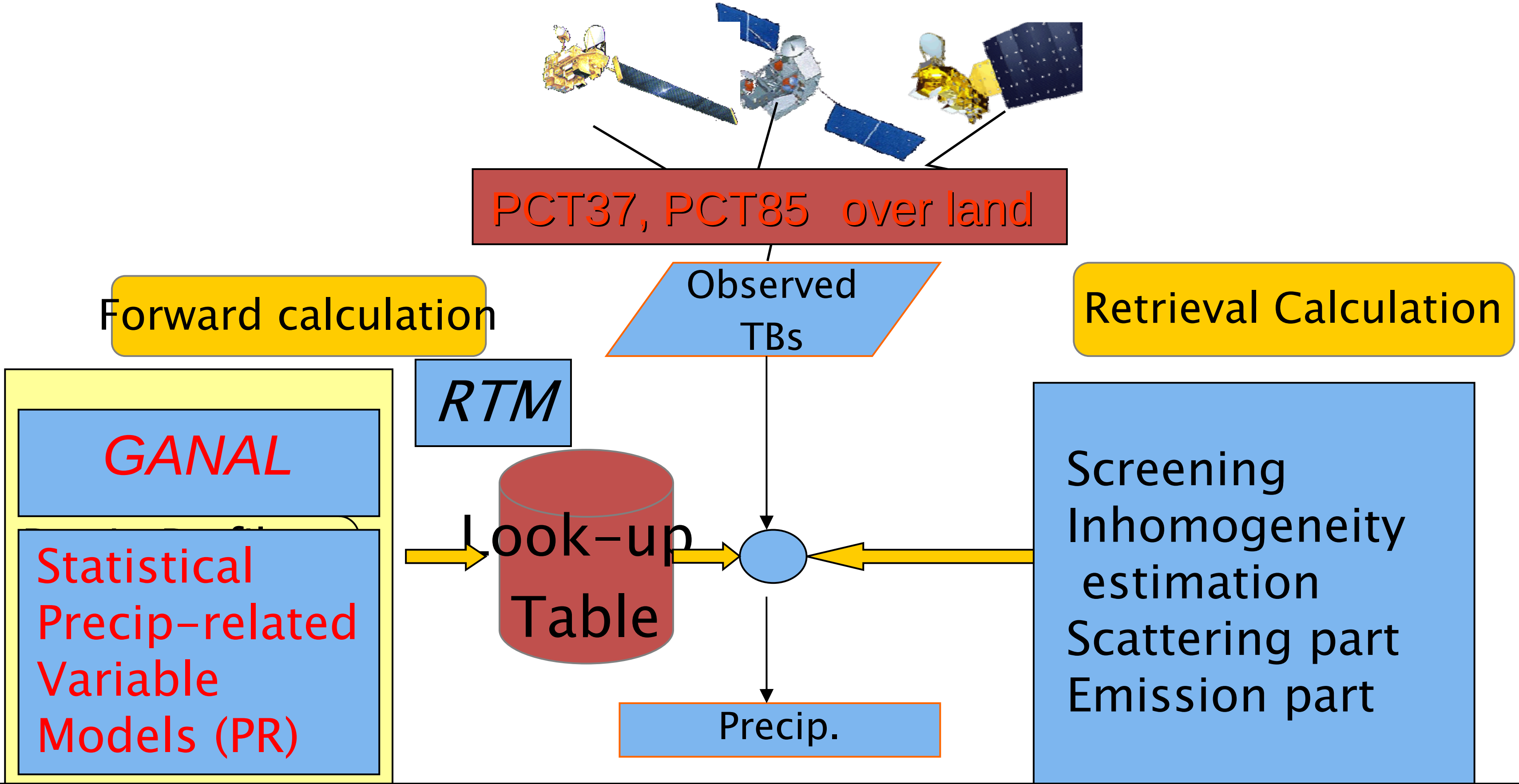

Find the optimal precipitation that gives RTM-calculated TBs fitting best with the observed TBs:
PCT37, PCT85 (land)
TB10v,TB19v, TB37v, PCT37, PCT85 (sea)

MWI indices for Over-Land algorithm

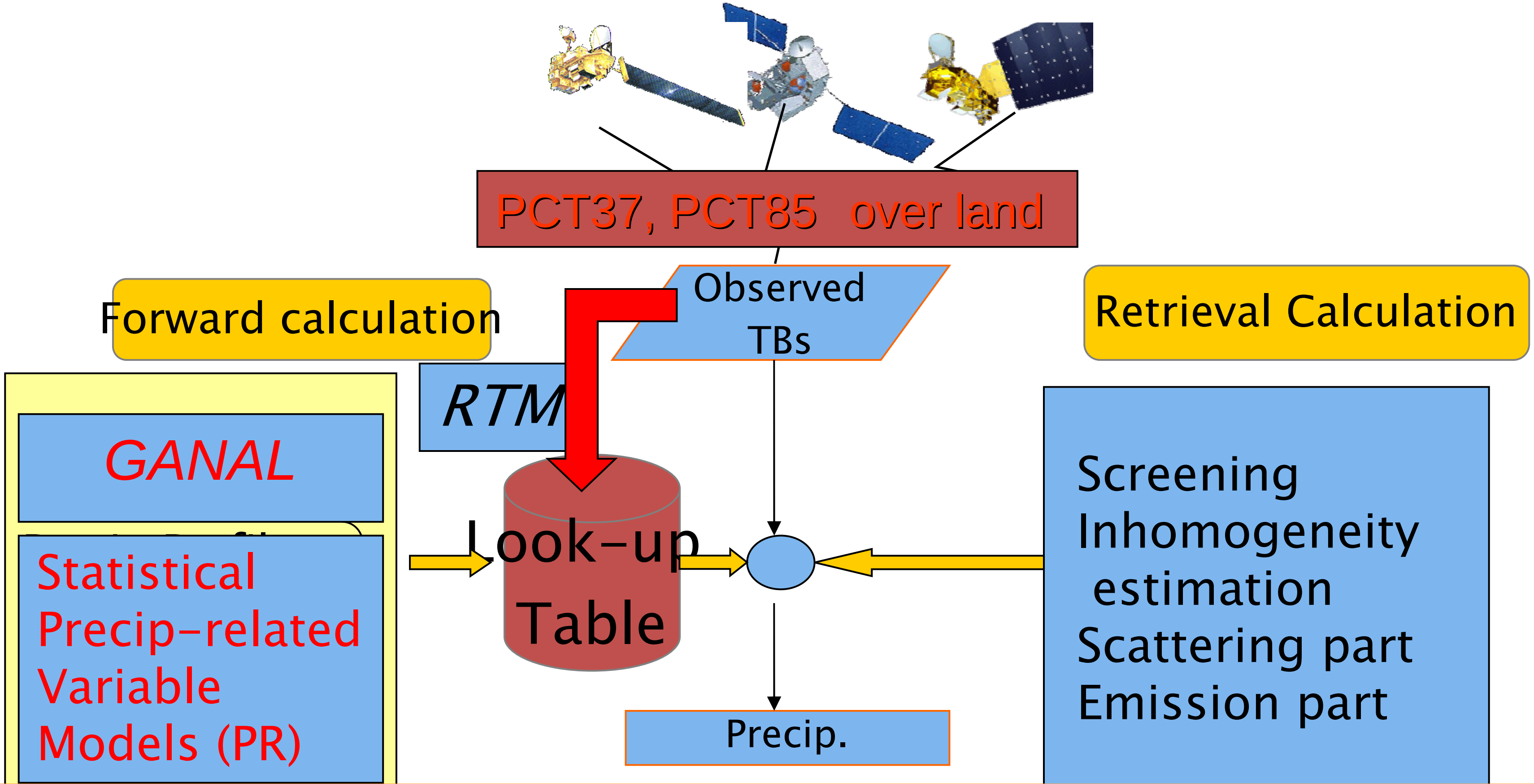

A priori information error is assumed to be the main cause of the retrieval bias.

Introduction of MWI indices which the retrieval bias depends on.

Correction LUT based on the above dependency.

Summary of forward calculation experiments

- **Sensitivities of TB depressions to precip variables**

Freq (GHz)	Depth of frozen precip	PSD of frozen particles	Non-spherical Particles	Freezing level height (FLH)	DSD of rain
85	◎	◎	◎	○	×
37	○	○	×	◎	○

- TB85 depression was very sensitive to frozen precip properties (Dtop, PSD, shapes)
- TB37 depression was sensitive to FLH and Rain DSD in addition to frozen precip properties.

Index of Dtop, R8537

- R8537 expressed as ratio of precipitation retrieved from TB85 (Rain85) to TB37 (Rain37) using the conventional GSMaP algorithm.

- TMI R8537 increases with Dtop estimated from PR.

Retrain.v4.10.20080417
match-up data (Land '98)

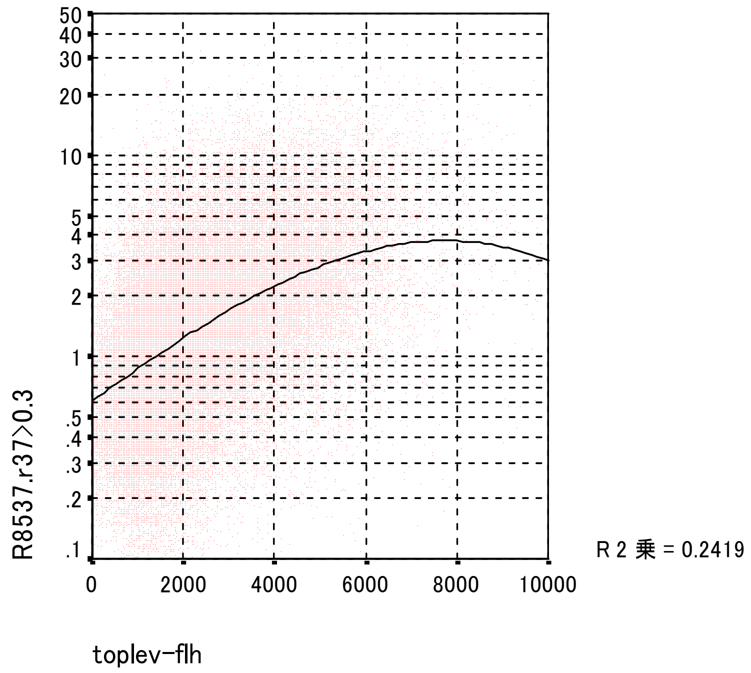

Index of FLH: PCT37 with no rain

- *For each rainy pixel, PCT37 with no rain (PCT37nr) is derived from surrounding no rain pixels.*
- *GANAL tends to over (under)estimate PCT37nr over cold (hot) regions.*

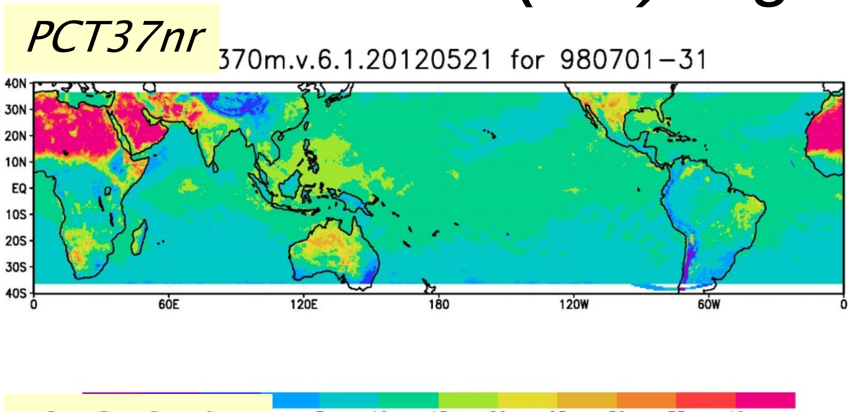

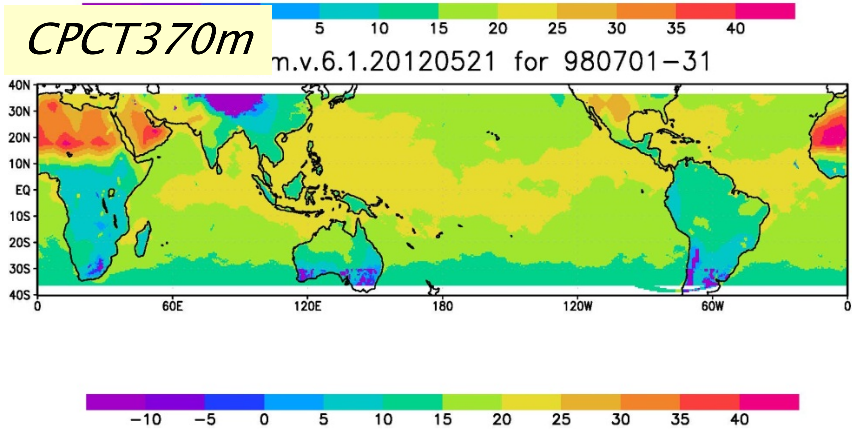

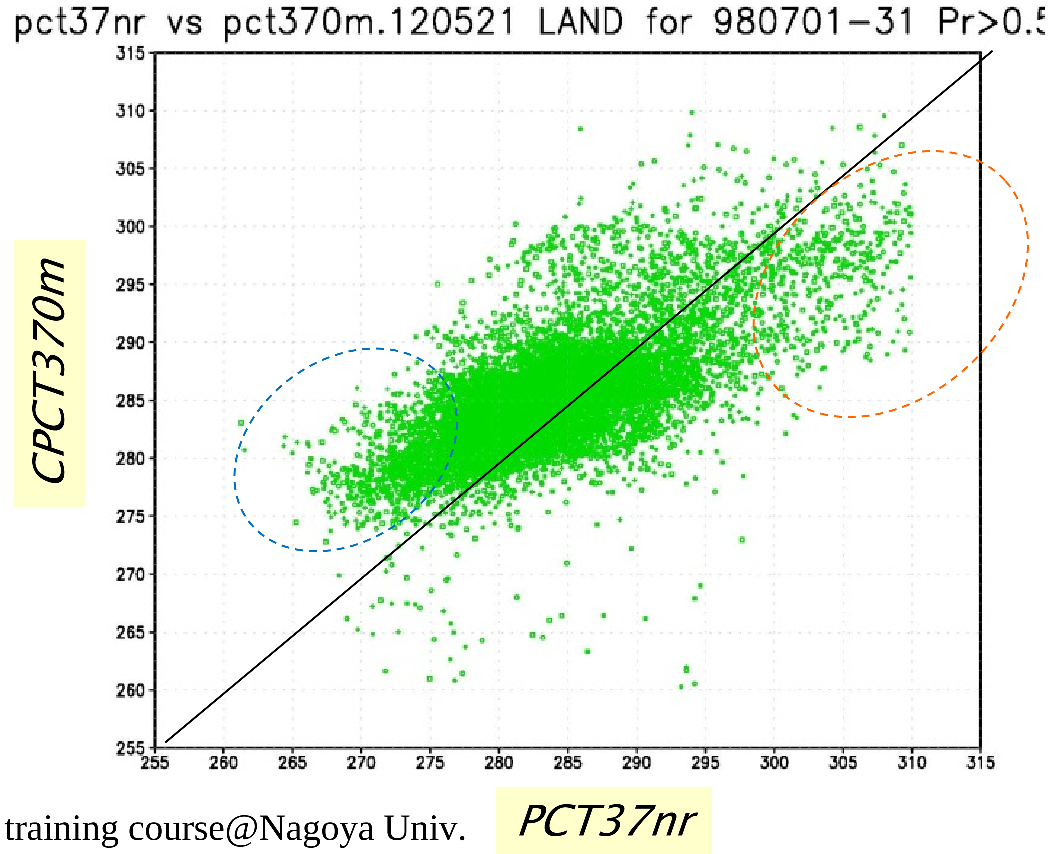

New Over-Land Algorithm: Statistical correction of LUTs using (PCT37nr,R8537)

- TRMM data sets for 1998 are classified by (R8537,PCT37nr) .
- Linear fitting coefficients between Rain37, Rain85 and PR surface precipitation rates.

Rain85 vs PR rainsurf depending on R8537 (1998, over Land)

R8537
> 2.1

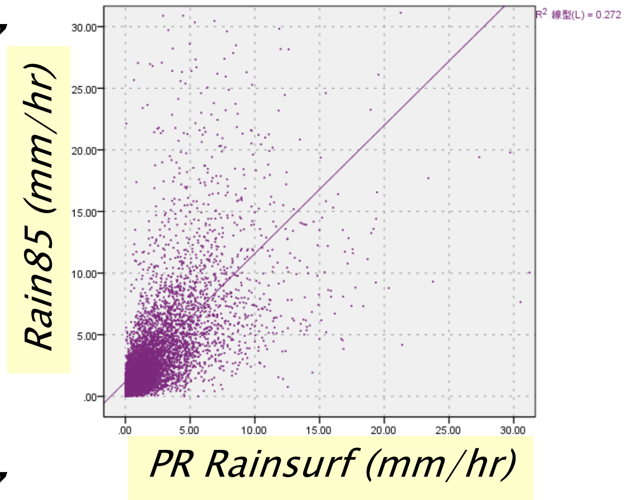

R8537
1.4–2.1

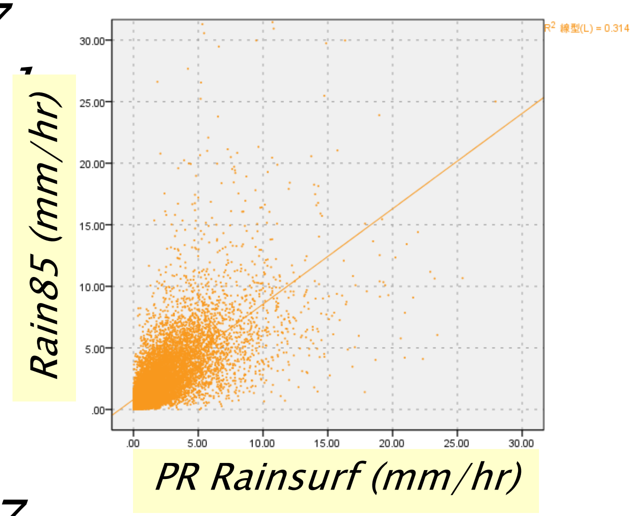

R8537
0.7–1.4

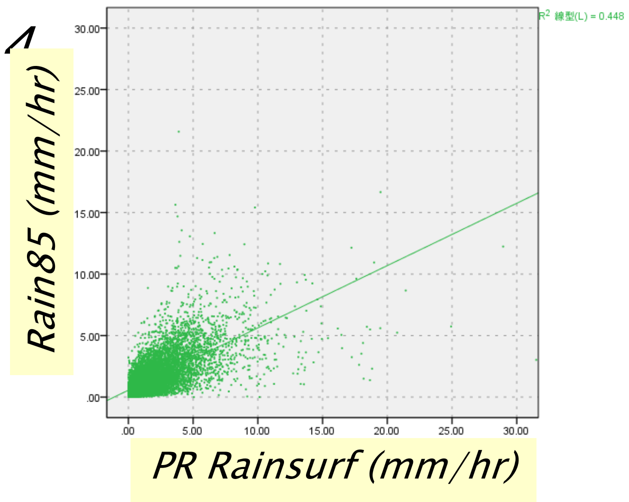

R8537
< 0.7

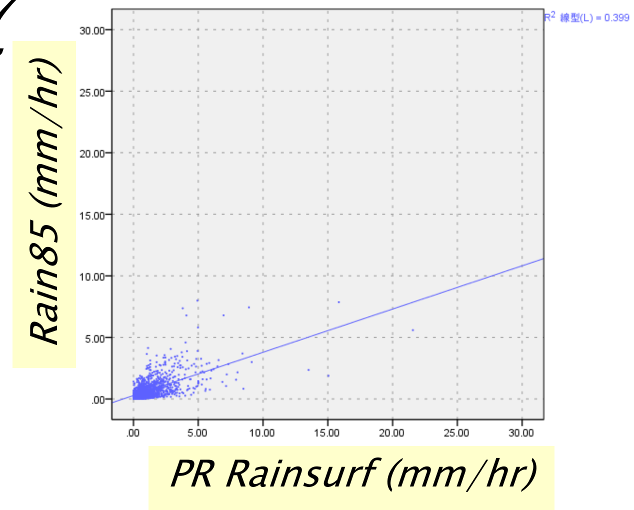

Retrieval bias of Rain85 is mainly due to Dtop error

Rain37 vs PR rainsurf depending on PCT37nr (1998, over Land)

PCT37nr > 300 K

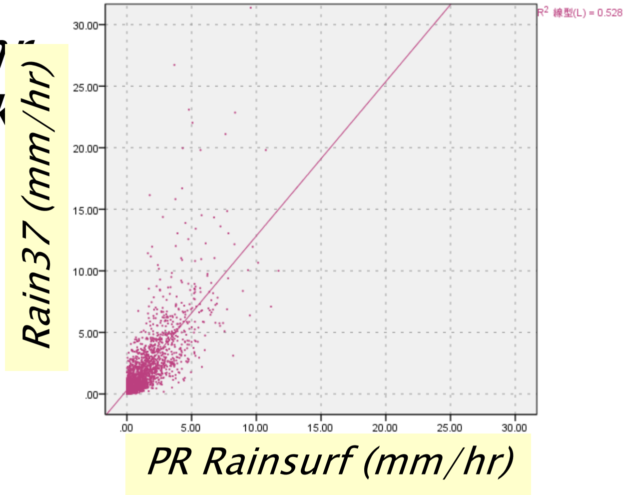

PCT37nr 290-300 K

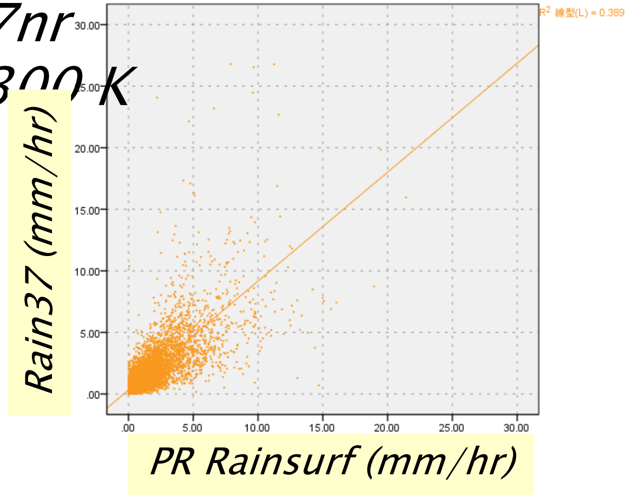

PCT37nr 280-290 K

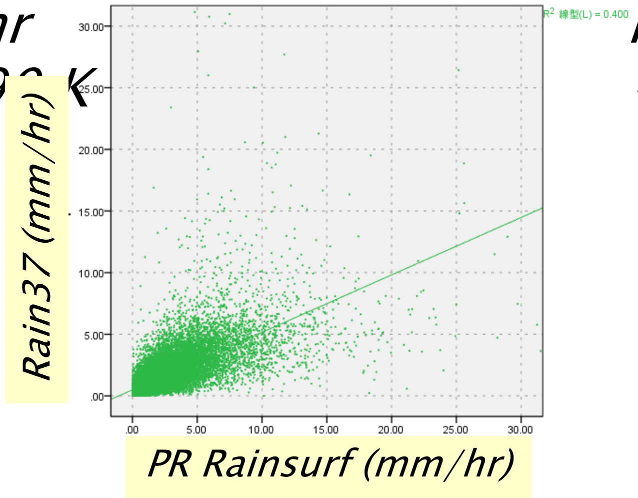

PCT37nr < 280 K

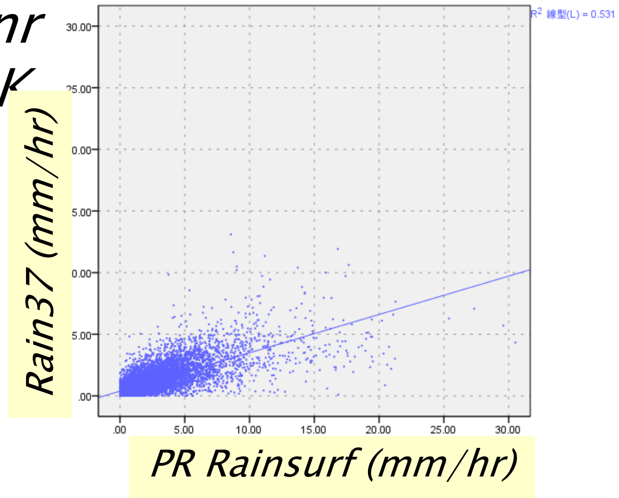

Rain37 vs PR rainsurf depending on dPCT37nr
PCT37nr ~(280-290 K) (1998, over Land)

dPCT37nr > 5 K

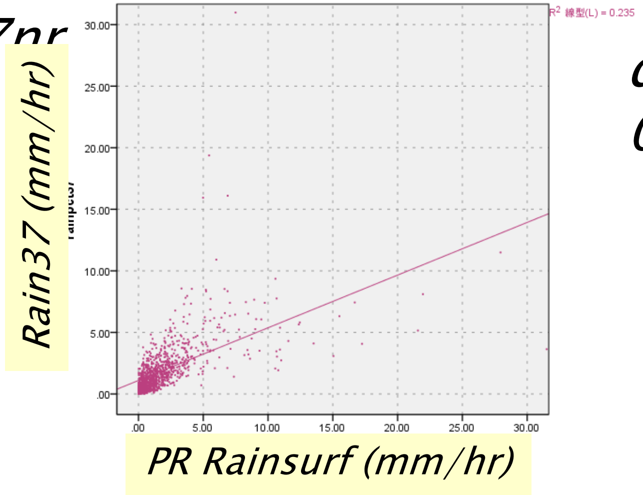

dPCT37nr 0–5 K

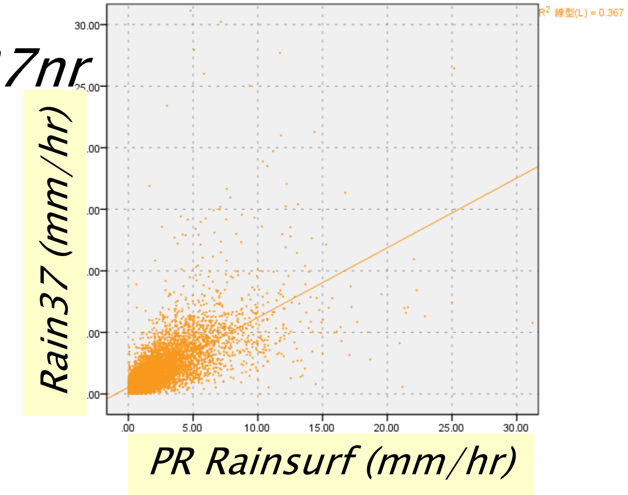

dPCT37nr −5 – 0 K

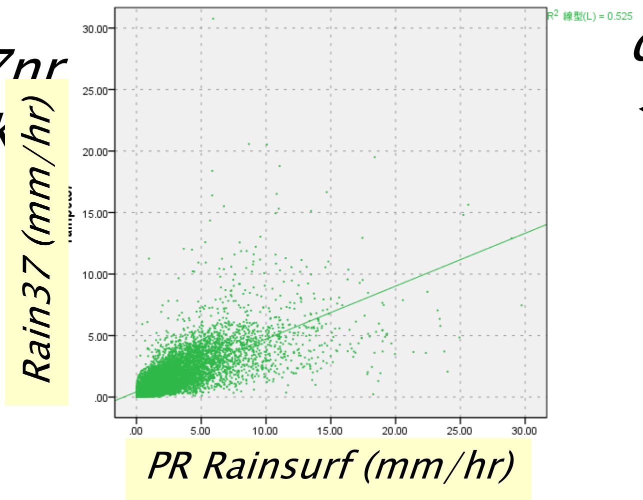

dPCT37nr < −5 K

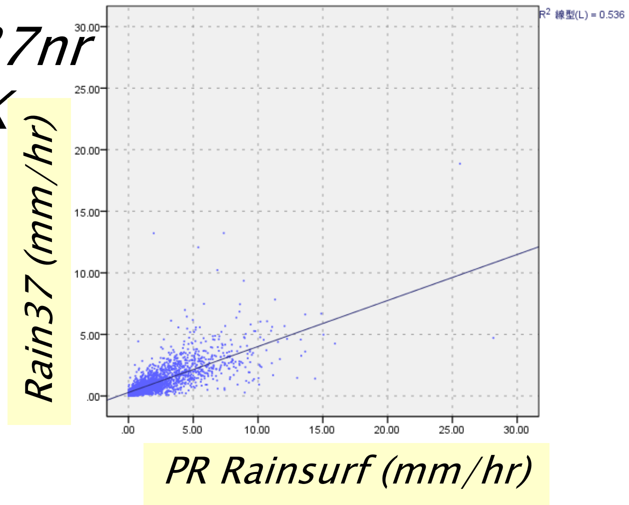

dPCT37nr=(PCT37nr−CPCT370m)

Rain37 vs PR rainsurf depending on PCT37nr

dPCT37nr= (-3 ~ +3 K)(1998, over Land)

dPCT37nr= (PCT37nr– CPCT370m)

PCT37nr > 300 K

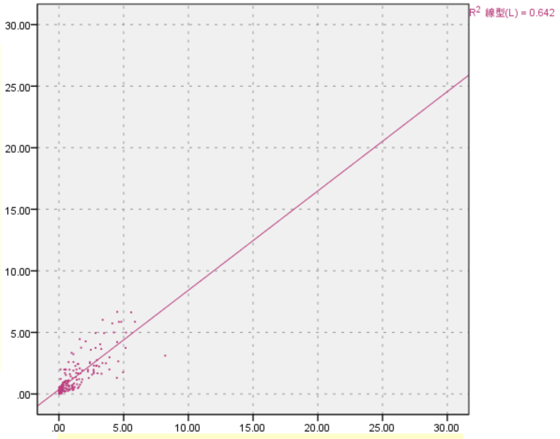

PCT37nr 290–300 K

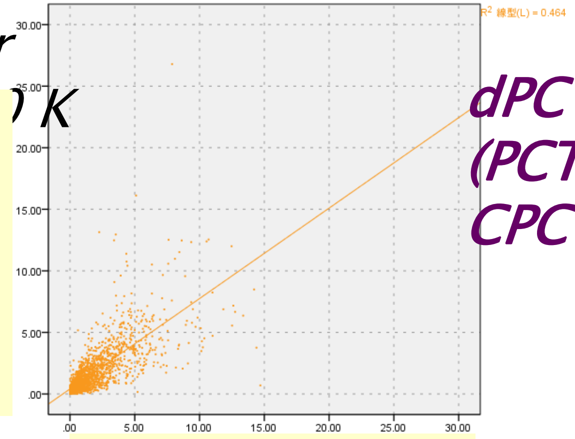

PCT37nr 280–290 K

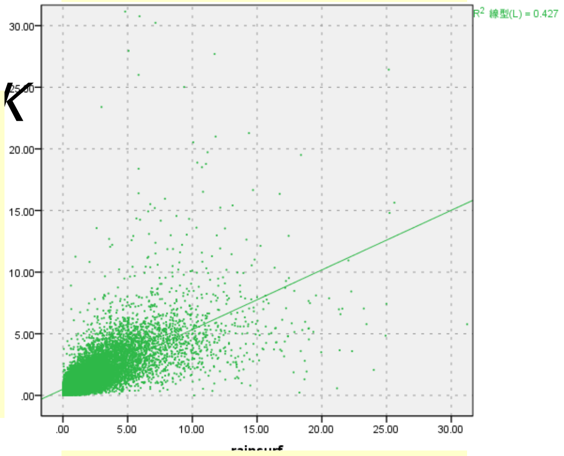

PCT37nr < 280 K

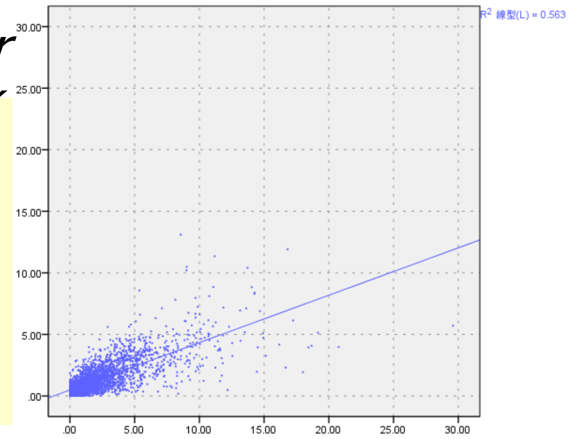

Forward calculation error is main cause of Rain37 biases.

Validation Results

Over-land retrieval for 2004

Comparison of over-land retrievals Rainsurf vs.Rainspc over Land (Jul. '04)

Conventional Algorithm	*New Algorithm*

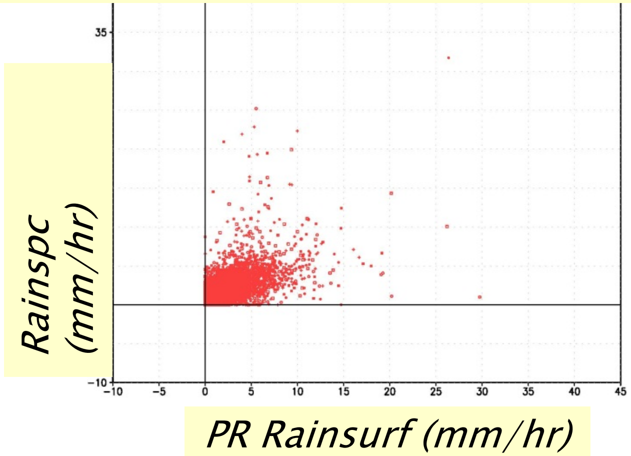

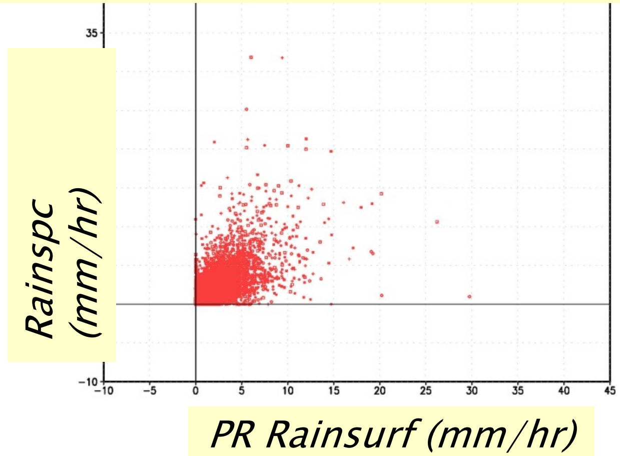

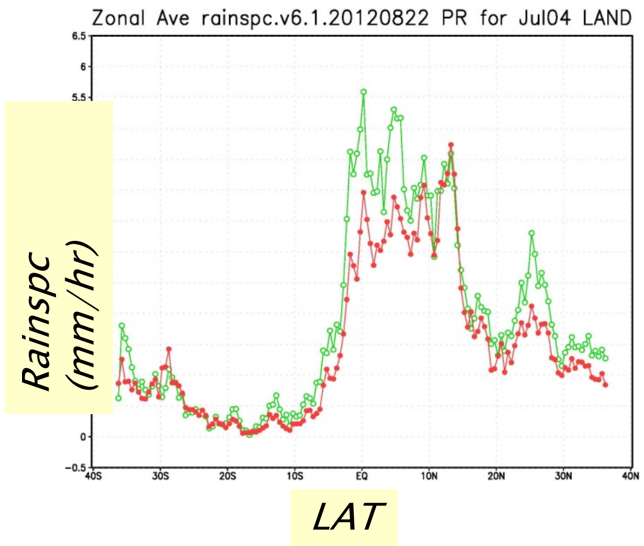

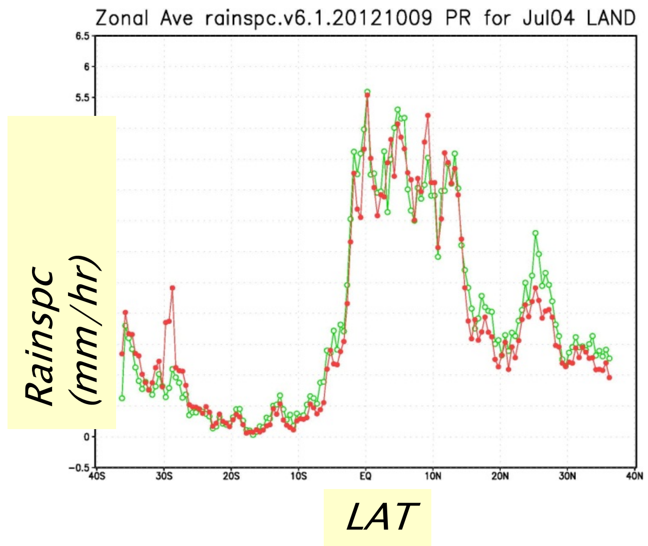

Comparison of over-land retrievals

Rainsurf vs.Rainspc over Land (Jul. '04）

Conventional Algorithm | *New Algorithm*

PCT37nr
> 300 K

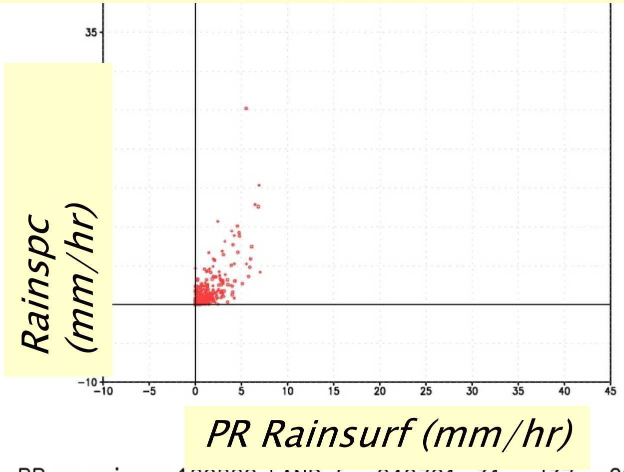

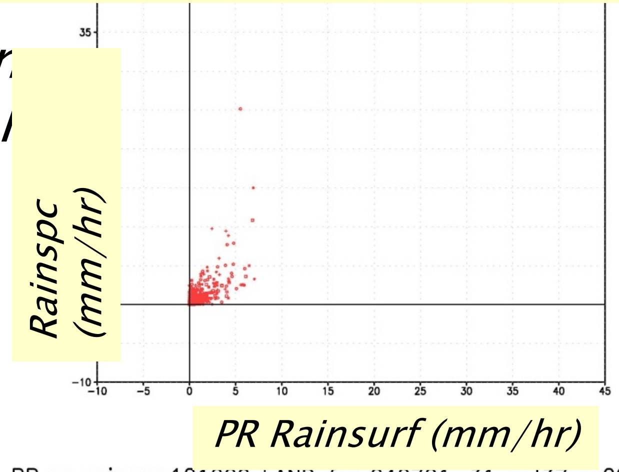

PCT37nr
290-300 K

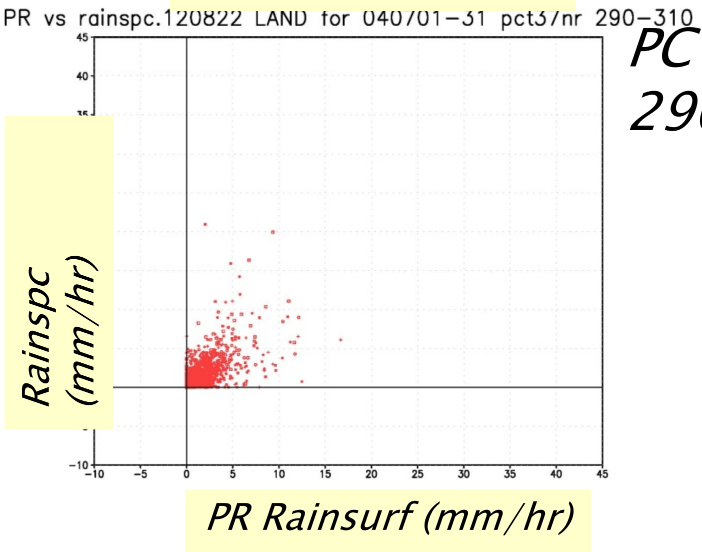

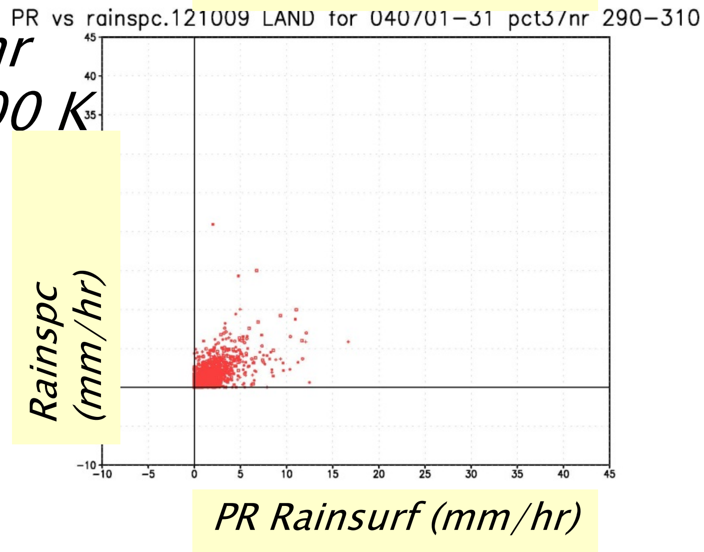

Comparison of over-land retrievals

Rainsurf vs.Rainspc over Land (Jul. '04)

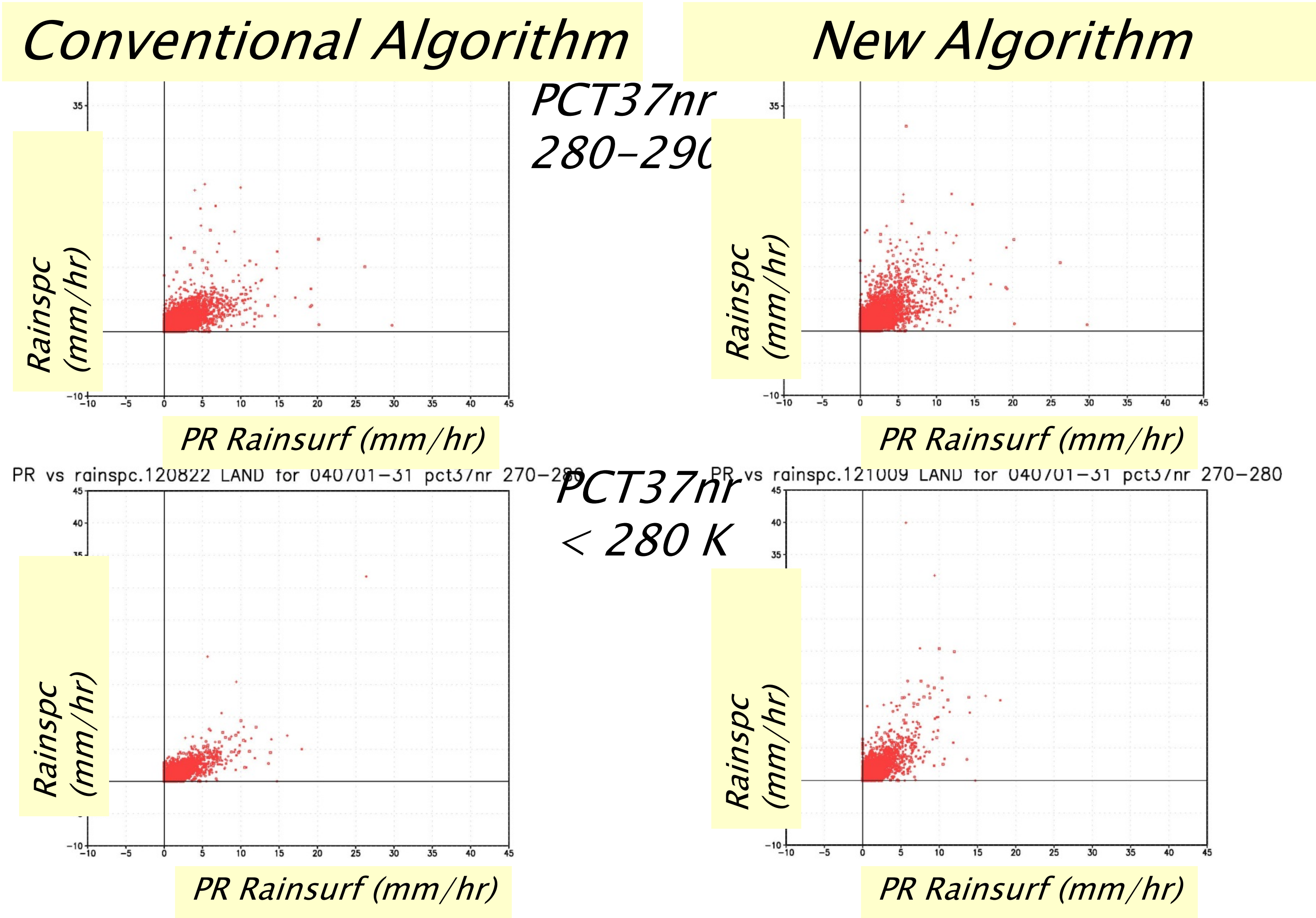

Daily precip (mm/day) of rain37 and their difference from PR rainsurf: over land for Jul. ‘03

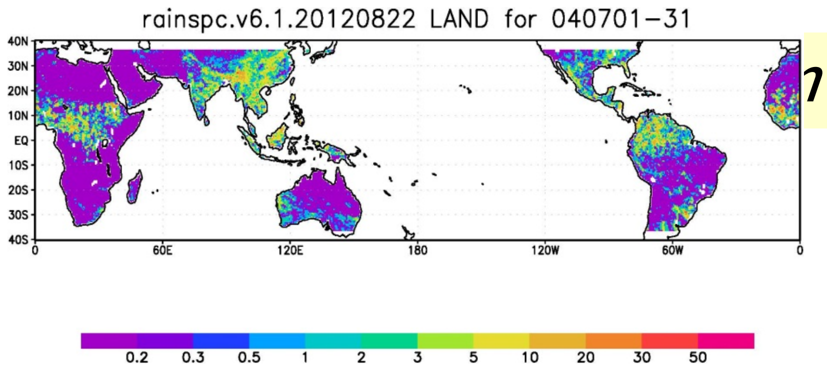

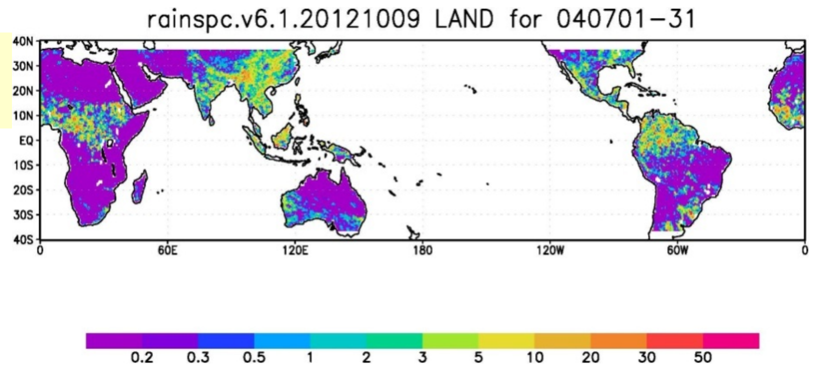

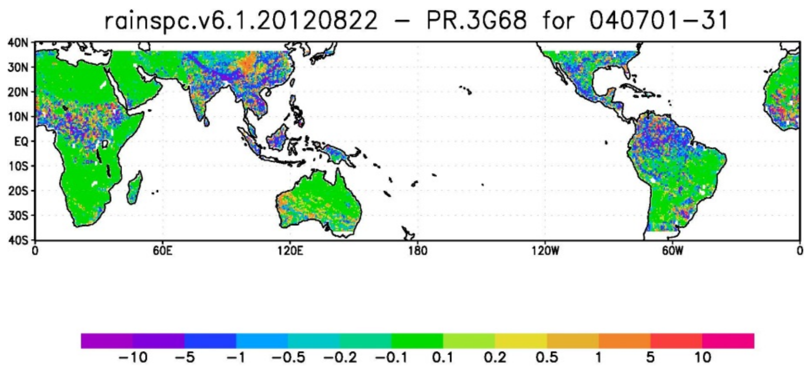

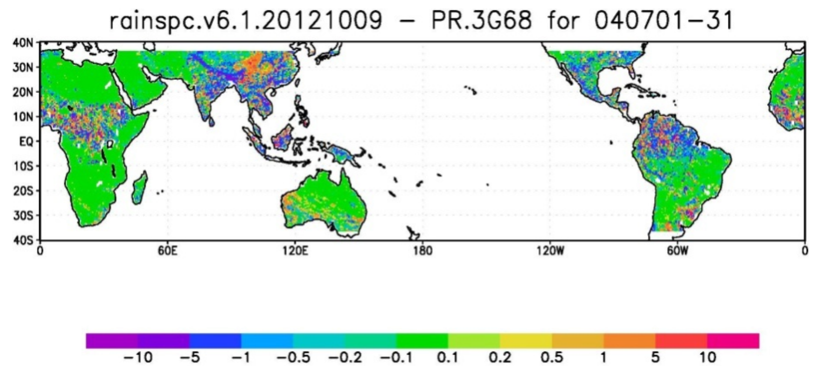

Summary

- Conventional Algorithm
  - Forward Calculation (precip cloud models)
  - Retrieval Part
  - Validation (TRMM PR)
- New over-land algorithm
  - MWI Indices for Over-land Algorithm
  - Validation (TRMM PR)
- Future directions

Orographic Rainfall
(Shige & Taniguchi, 2010)

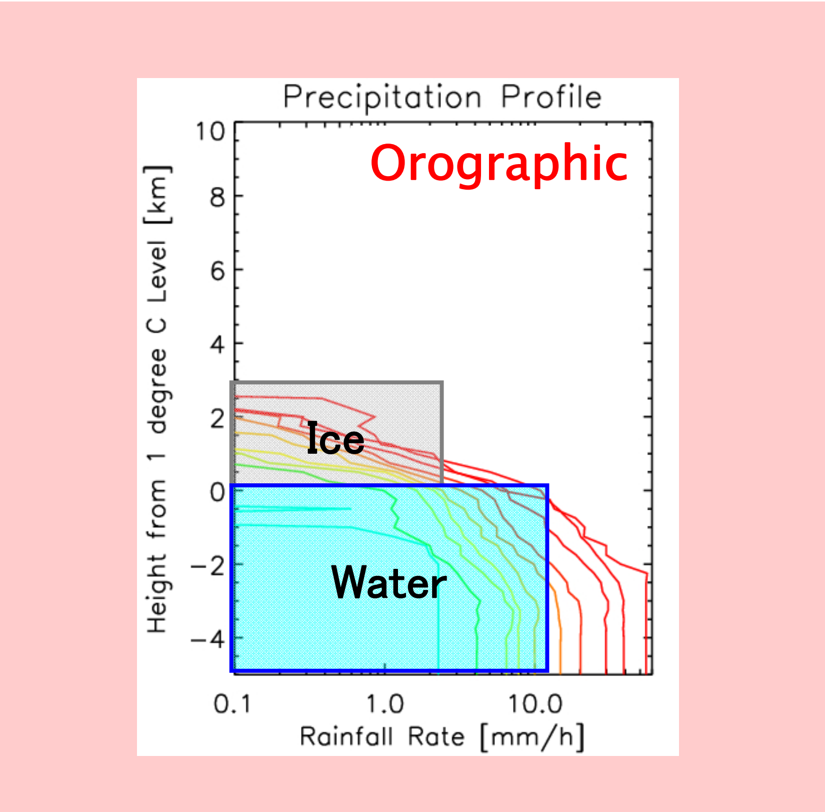

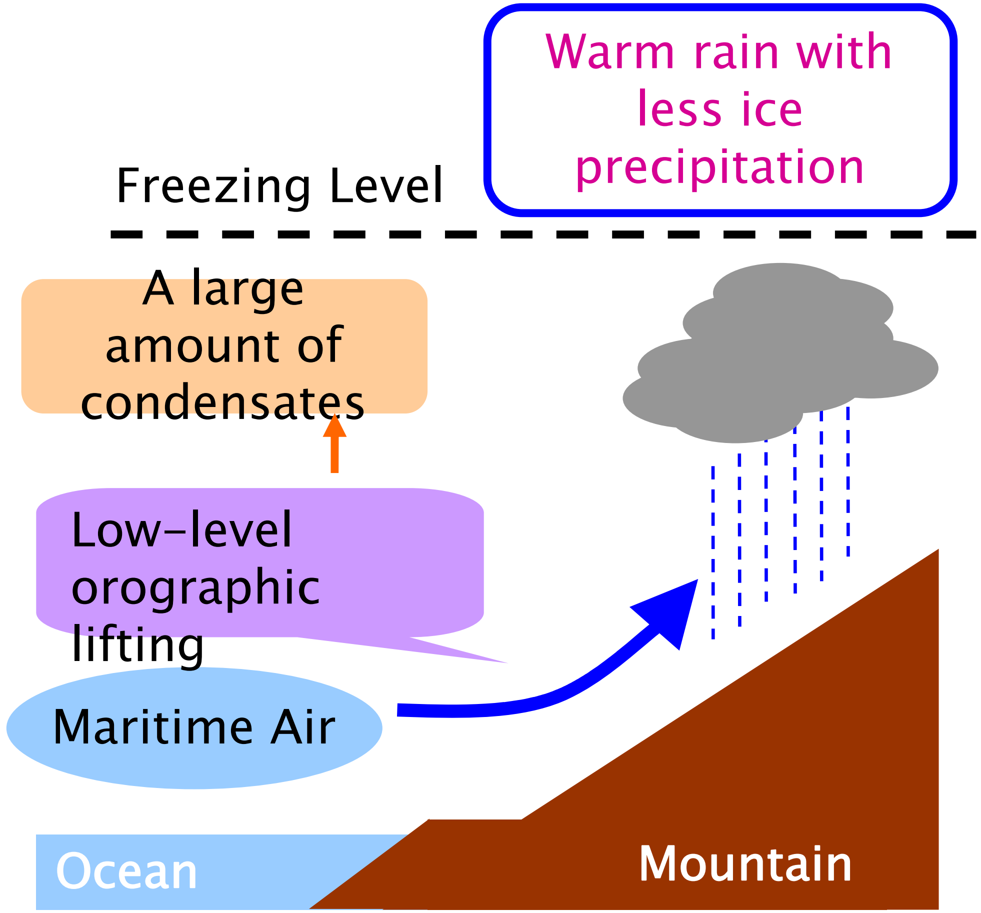

Microwave Radiometer Measurements

Data Assimilation using

Microwave Radiometer Data

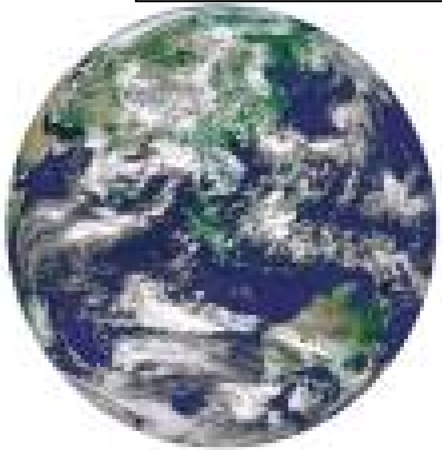

Outline

- What is “Data Assimilation”?
- Ensemble-Based Variational Assimilation Method (EnVA)
- EnVA to Incorporate Microwave Imager Data into a Cloud-Resolving Model

- Summary & Discussion

Definition of Data Assimilation

NWP forecasts

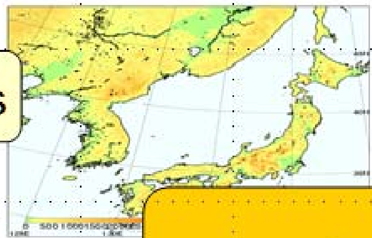

Observed data

Assimilation

Analysis technique in which the observed information is accumulated into the model state by taking advantage of consistency constraints with the model equations

Other Observations

Analysis data

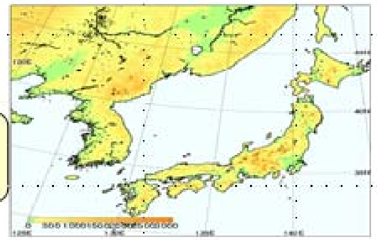

Need for Statistical Approach

- Historically, DA started with interpolation of the observed data.
  - Interpolation is not appropriate in practice.

- Use of first guess of previous NWP forecast or NWP constraints.

- Need for statistical approach to produce analysis data:
  - Represent mathematically the error of the observation, the NWP first guess, and constraints.
  - Find optimal values that minimize the analysis error.

Modeling of the errors

- Observation error ε^{o}=Y-H(Xt)

  where observation (Y) and the model counterpart H(X)

- First guess & analysis error ε^{f}=Xf – Xt, ε^{a}=Xa-Xt

where Xf,Xa are First guess & analysis of the model state

$$P^{f} = (\varepsilon^{f} - \bar{\varepsilon}^{f})^{t} (\varepsilon^{f} - \bar{\varepsilon}^{f})$$

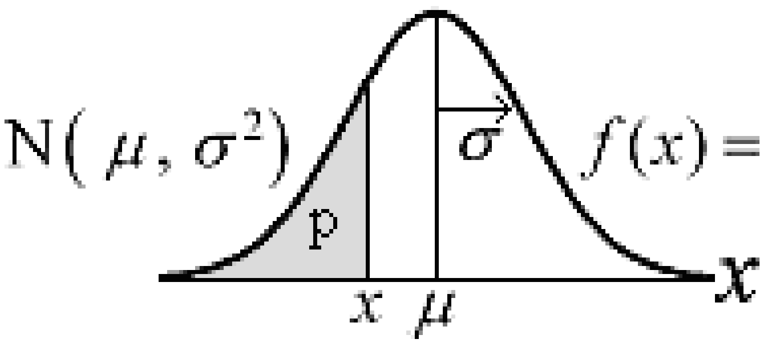

$$f(x) = \frac{1}{\sqrt{2\pi}\sigma} \exp\left(-\frac{(x-\mu)^2}{2\sigma^2} \right)$$

Bayes' rule (conditional PDF)

- Conditional PDF of X given obs. Y:

$$P_{rof}(X\,|\,Y) \propto P_{rof}(Y\,|\,X)P_{rof}(X)$$

- If errors are Gaussian:

$$P_{rof}(Y\,|\,X) = P_{rof}(\varepsilon^{o})$$

$$\propto \exp\{-0.5(Y - H(X))^{t} R^{-1}(Y - H(X))\}$$

$$P_{rof}(X) = P_{rof}(\varepsilon^{f})$$

$$\propto \exp\{-0.5(X - X^{f})^{t} P^{-f}(X - X^{f})\}$$

- The maximum likelyhood state is the one minimizes the cost function J:

$$J:(X - X^{f})^{t} P^{-f}(X - X^{f}) + (Y - H(X))^{t} R^{-1}(Y - H(X))$$

Simple Example

- We have a temperature observation T^o with STD σ^o, given first guess T^f with STD σ^f.
- The maximum likelyhood state is the one minimizes the cost function J:

$$J : \frac{1}{\sigma^{f2}}(T - T^f)^2 + \frac{1}{\sigma^{o2}}(T - T^o)^2$$

$$\partial J / \partial T = \frac{2}{\sigma^{f2}}(T - T^f) + \frac{2}{\sigma^{o2}}(T - T^o)$$

$$\partial J / \partial T = 0 \;\rightarrow T^a = \frac{(T^o / \sigma^{o2}) + (T^f / \sigma^{f2})}{(1/\sigma^{o2}) + (1/\sigma^{f2})}$$

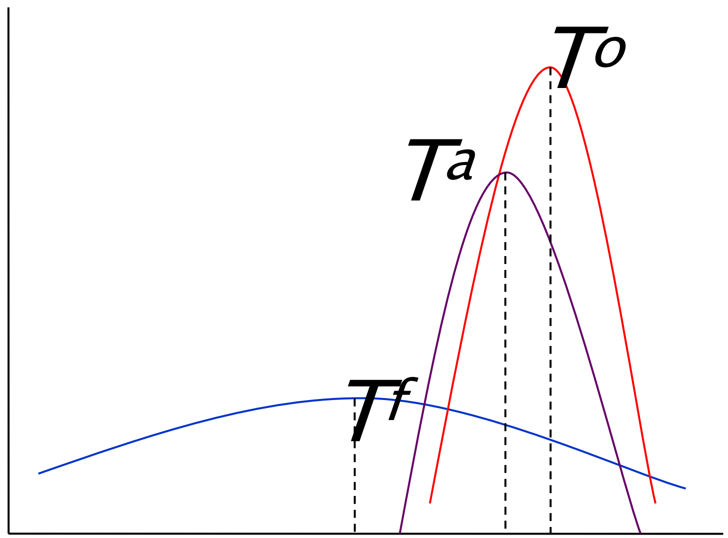

Basic idea of EnVA

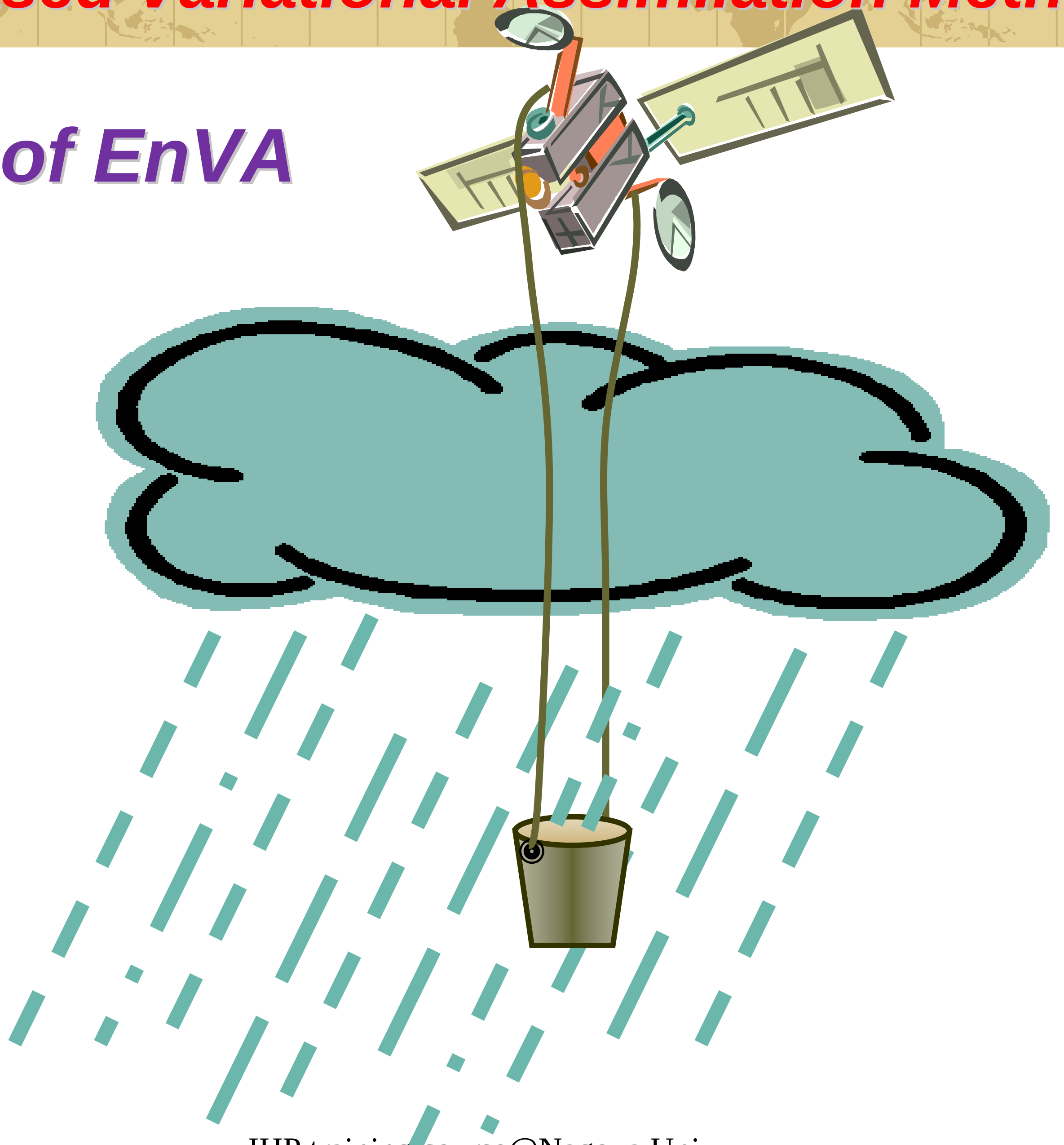

Goal: Data assimilation of MWI TBs into CRMs

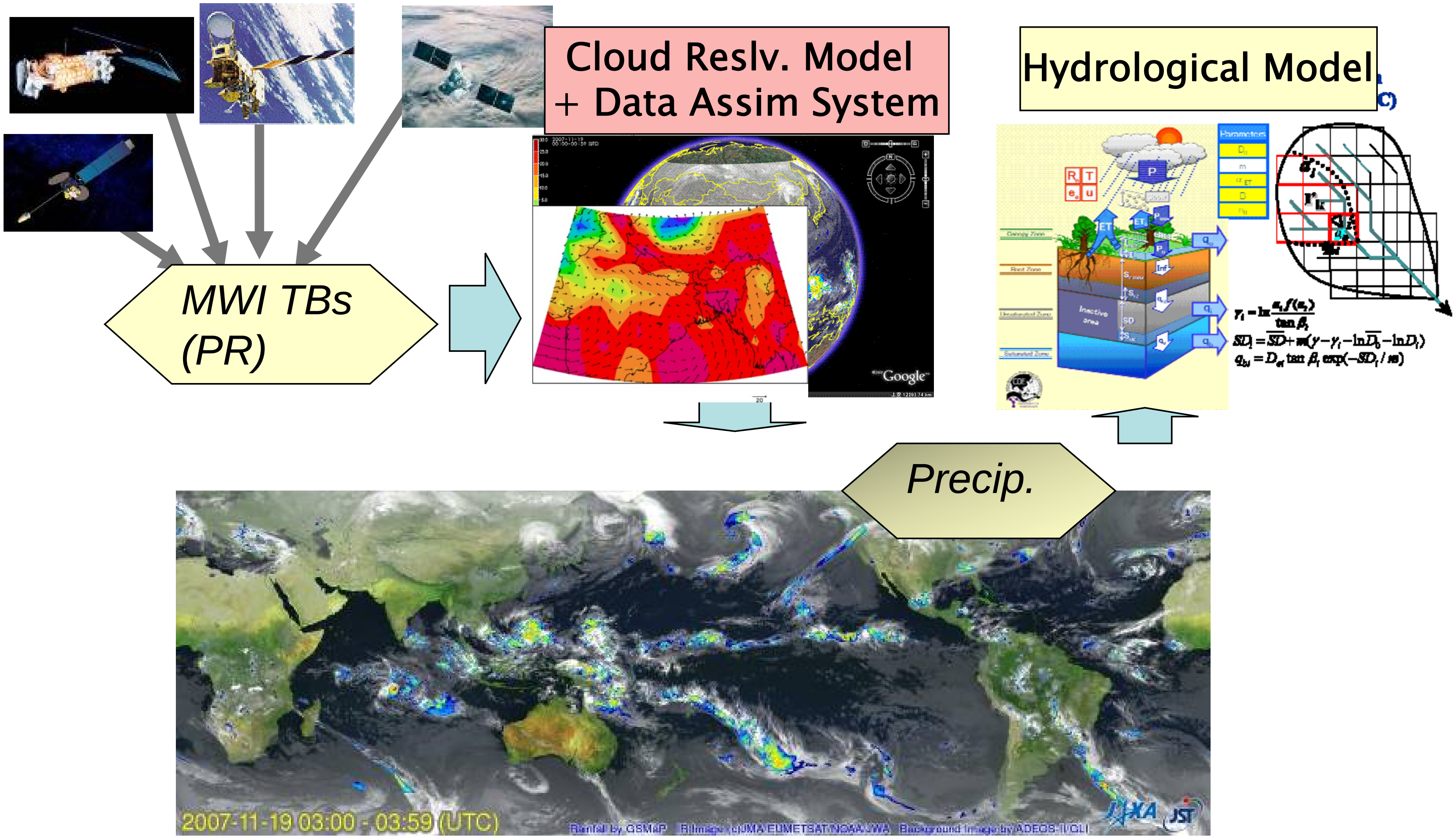

Cloud-Resolving Model used

JMANHM (Saito et al,2001)

- Resolution: 5 km
- Grids: 400 x 400 x 38
- Time interval: 15 s

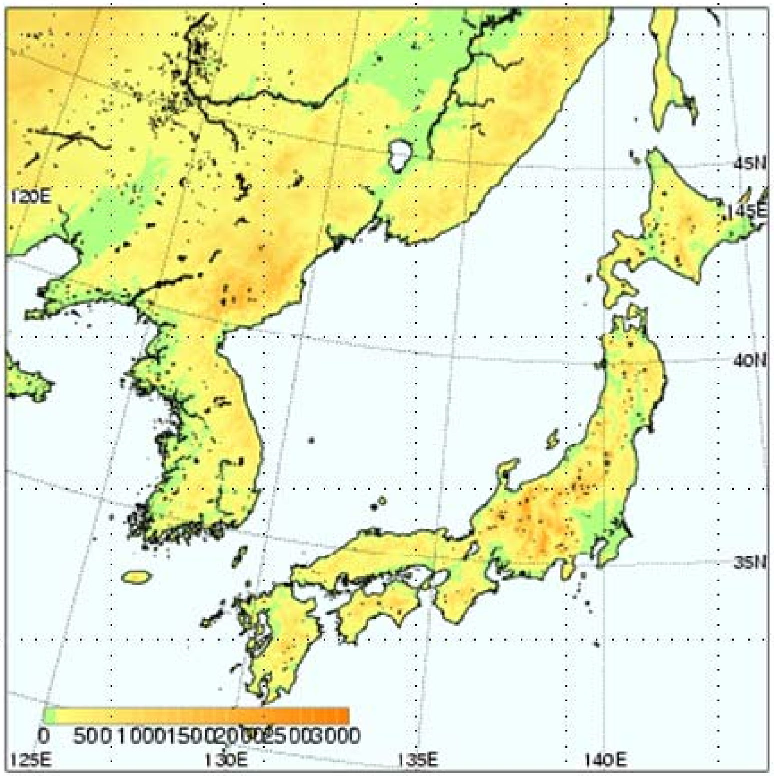

Explicitly forecasts 6 species of water substances

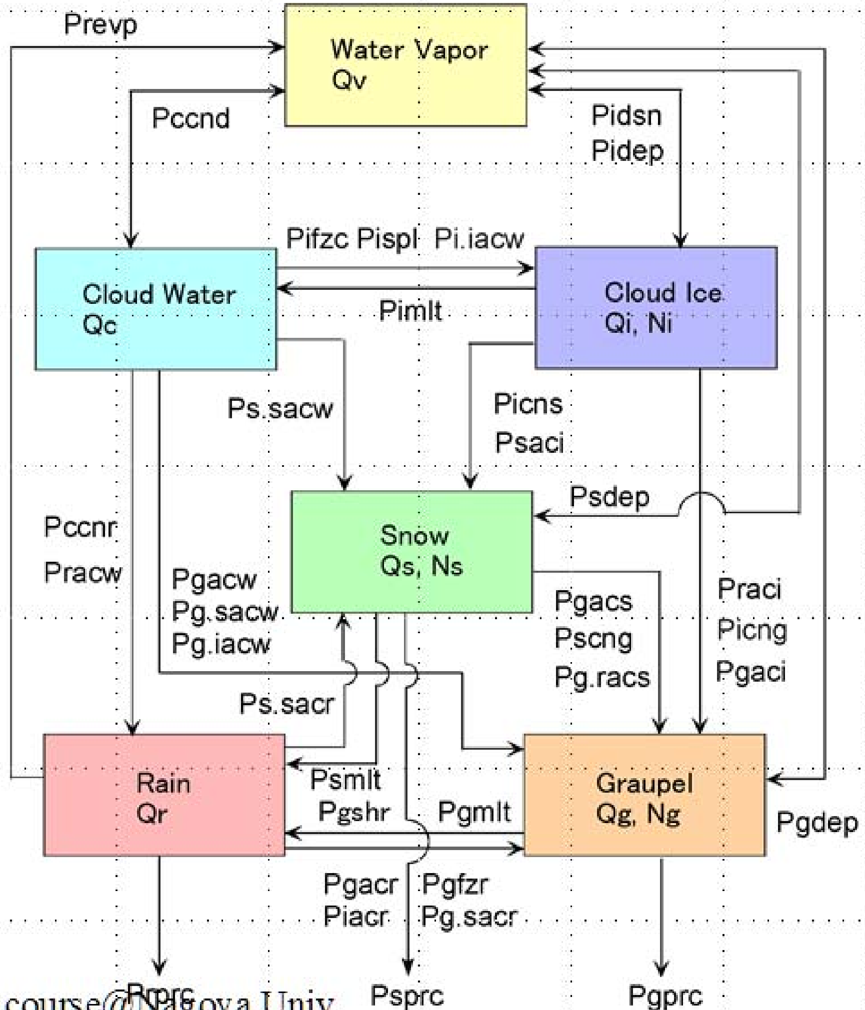

Basic Idea of Ensemble-based assimilation

Estimating first-guess error with Ensemble forecasts

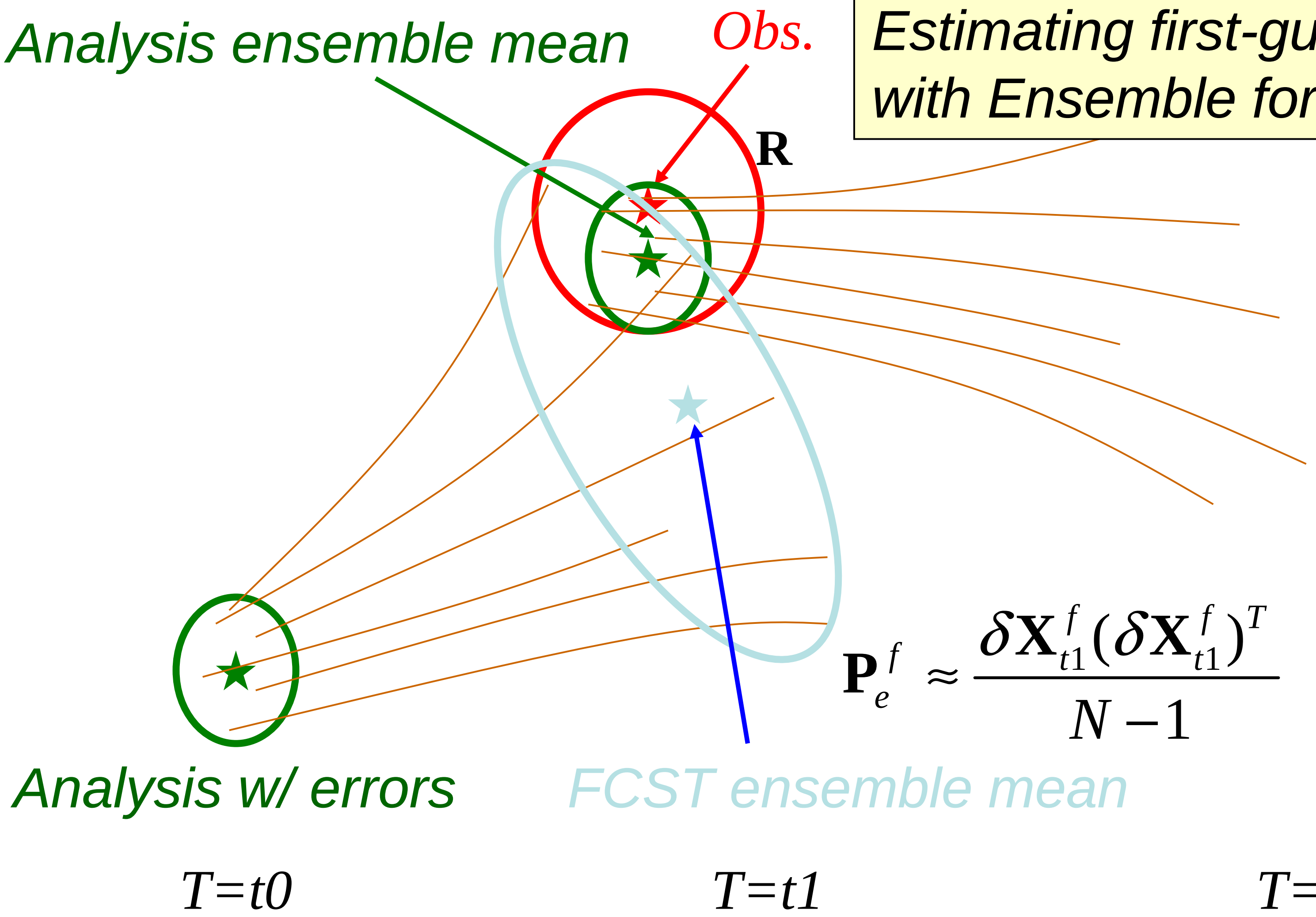

$$\mathbf{P}_e^f \approx \frac{\delta \mathbf{X}_{t1}^f (\delta \mathbf{X}_{t1}^f)^T}{N-1}$$

Why Ensemble-based method?:

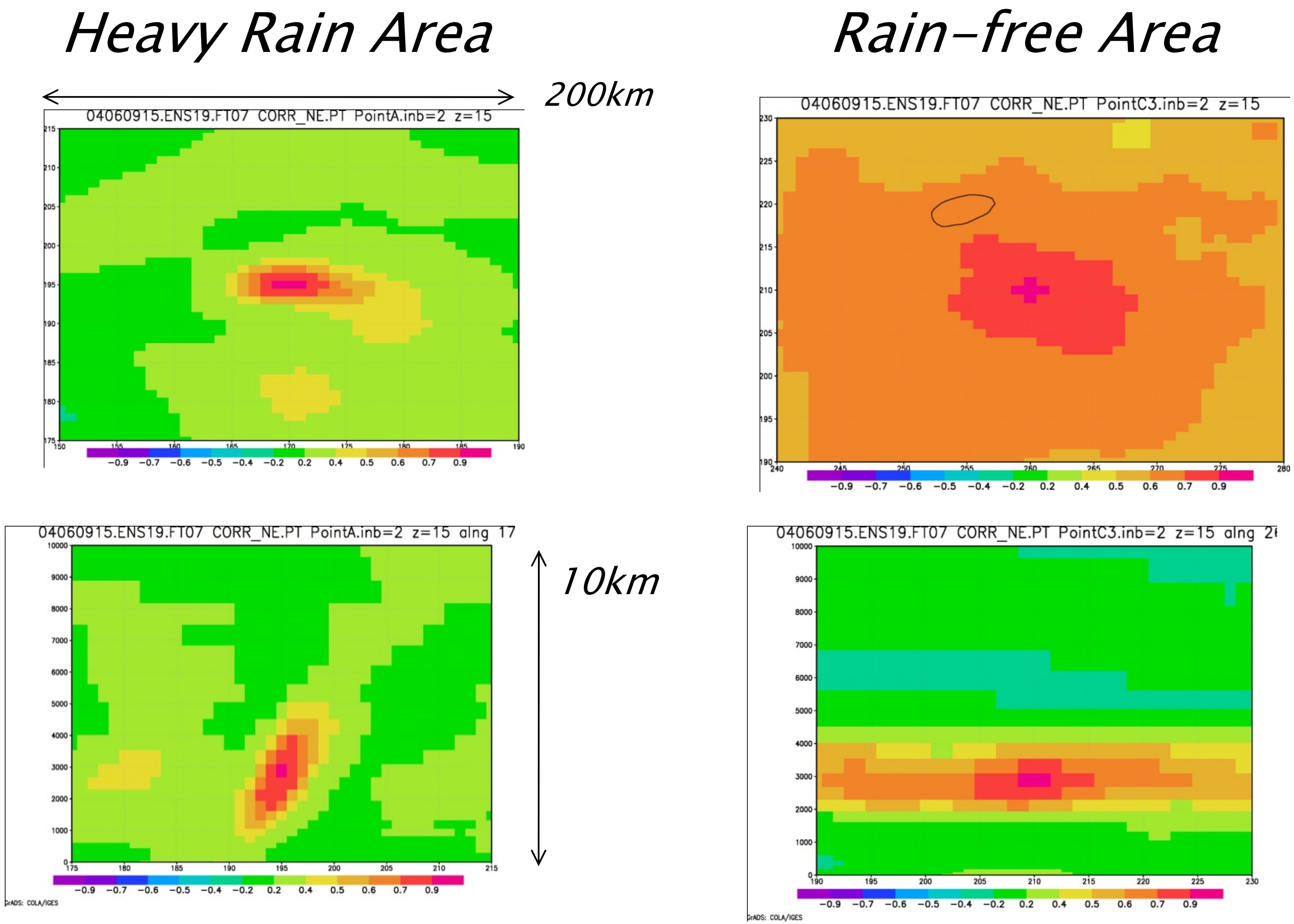

Ensemble forecast error corr. of PT (04/6/9/22 UTC)

Why Ensemble-based *method?:*

To estimate the flow-dependency of the error covariance

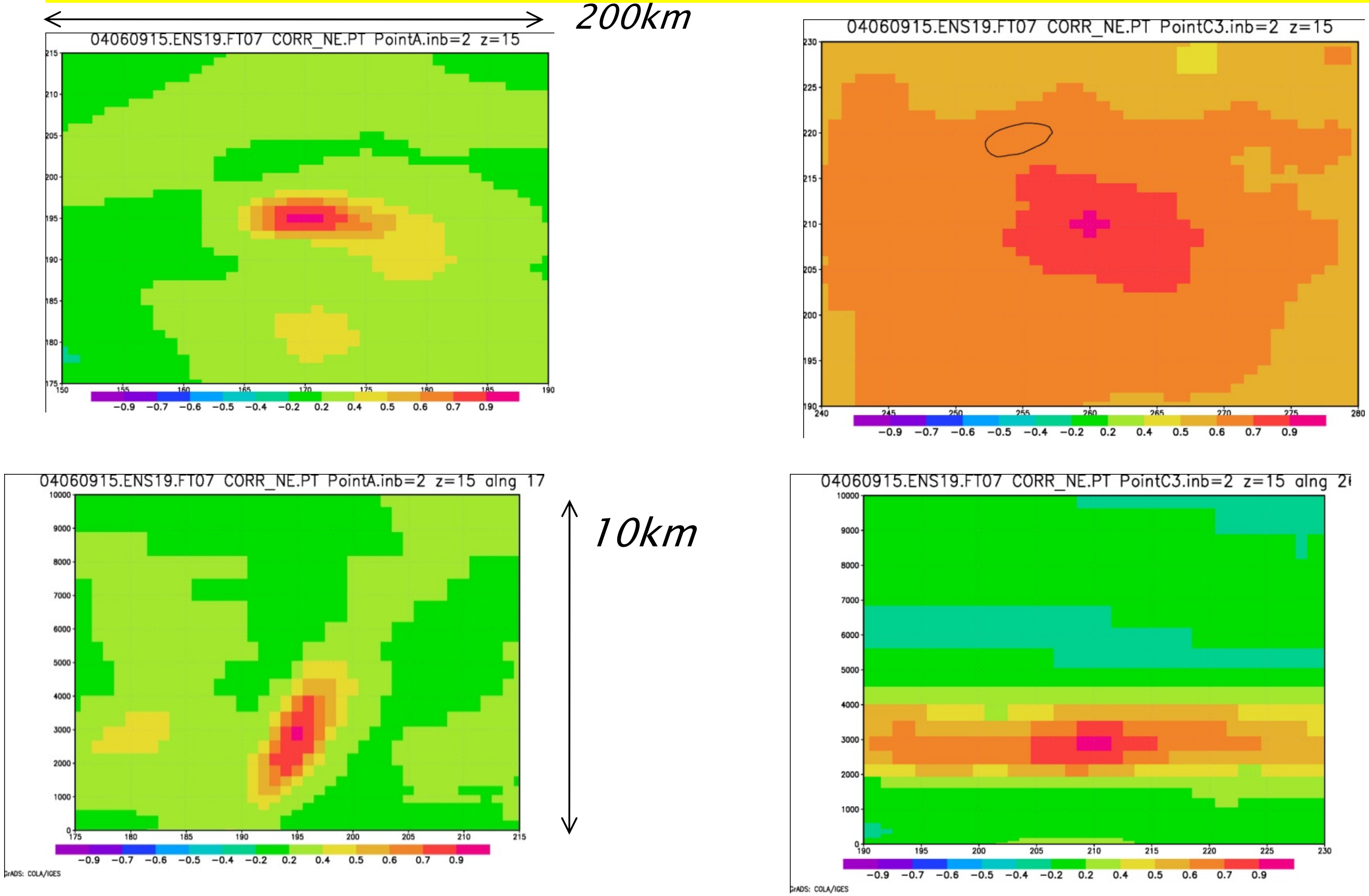

Ensemble forecast error corr. of PT (04/6/9/22 UTC)

EnVA: min. cost function in the Ensemble forecast error subspace

- Minimize the cost function with non-linear Obs. term.

$$J_x = 1/2(\vec{X} - \overline{X}_f)P_f^{-1}(\vec{X} - \overline{X}_f) + 1/2(Y - H(\vec{X}))R^{-1}(Y - H(\vec{X}))$$

- Assume the analysis error belongs to the Ensemble forecast error subspace （Lorenc, 2003):

$$\vec{X} - \overline{X}^f = \mathrm{P}_e^{f/2} \circ \Omega \qquad \Omega = [\vec{w}_1, \vec{w}_2, ,,,,, \vec{w}_N]$$

$$P_e^{f/2} = [\vec{X}_1^f - \overline{X}^f, \vec{X}_2^f - \overline{X}^f, ,,, \vec{X}_N^f - \overline{X}^f]$$

- Forecast error covariance is determined by localizatior

$$\mathrm{P}^f = \mathrm{P}_e^f \circ \mathrm{S}$$

- Cost function in the Ensemble forecast error subspace：

$$J(\Omega) = 1/2\, trace\{\Omega^t S^{-1} \Omega\} + 1/2\{H(\vec{X}(\Omega)) - Y\}^t R^{-1}\{H(\vec{X}(\Omega)) - Y\}$$

Why Variational Method ?

To address the non-linearity of TBs

MWI TBs are non-linear function of various CRM variables.

- TB becomes saturated as optical thickness increases:

$$T - TB \approx (1-\varepsilon_s)Te^{-2\tau/\mu},$$
$$when\ \ T \approx T_s$$

- TB depression mainly due to frozen precipitation becomes dominant after saturation.

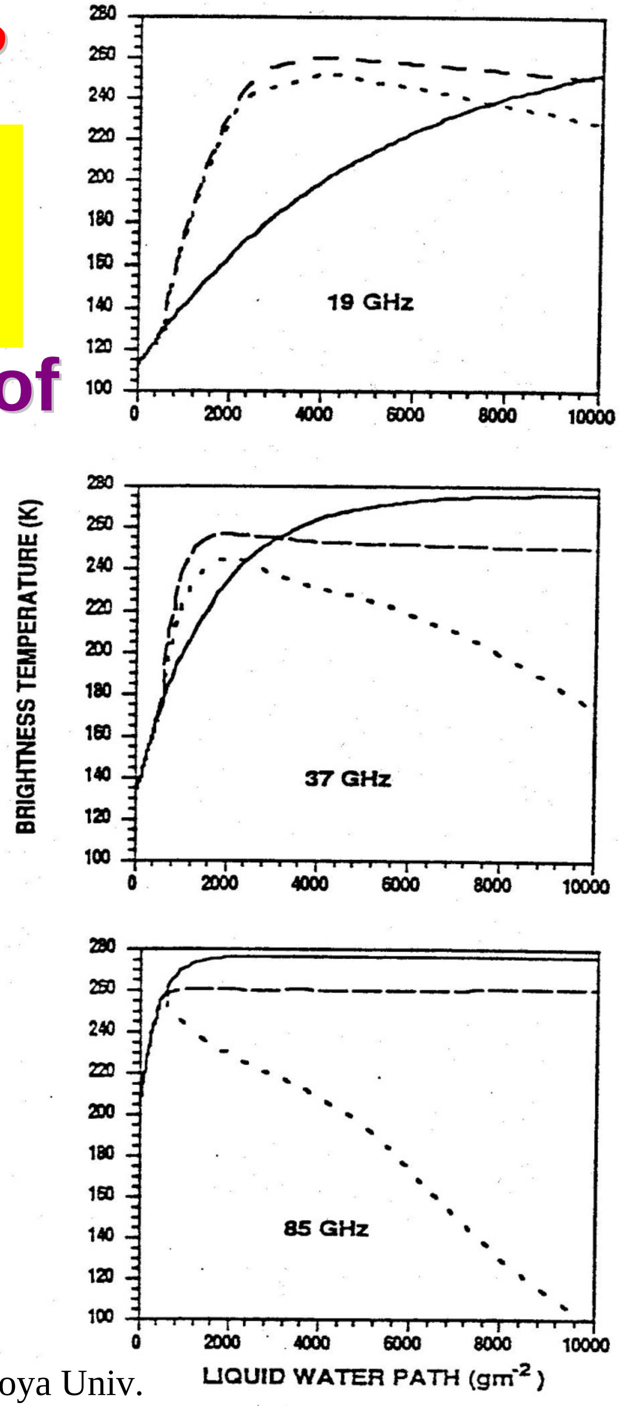

Detection of the optimum analysis

- Detection of the optimum Ω_a, w_a by minimizing J where Ω is diagonalized with U eigenvectors of S :

  $$\chi_i(m) = 1/d_m \{U^t \Omega\}_i(m)$$

- Approximate the gradient of the observation with the finite differences about the forecast error:

  $$\partial H(\vec{X})/\partial\Omega \sim \{H(\vec{X} + \alpha\delta p_i^f) - H(\vec{X})\}/\alpha$$

- To solve non-linear min. problem, we performed iterations.
- Following Zupanski (2005), we calculated the analysis of each Ensemble members, $\vec{X}_i^a$ from the Ensemble analysis error covariance.

EnVA to incorporate MWR TBs into a CRM

Problems in EnVA for CRM
Displacement error correction
Application results

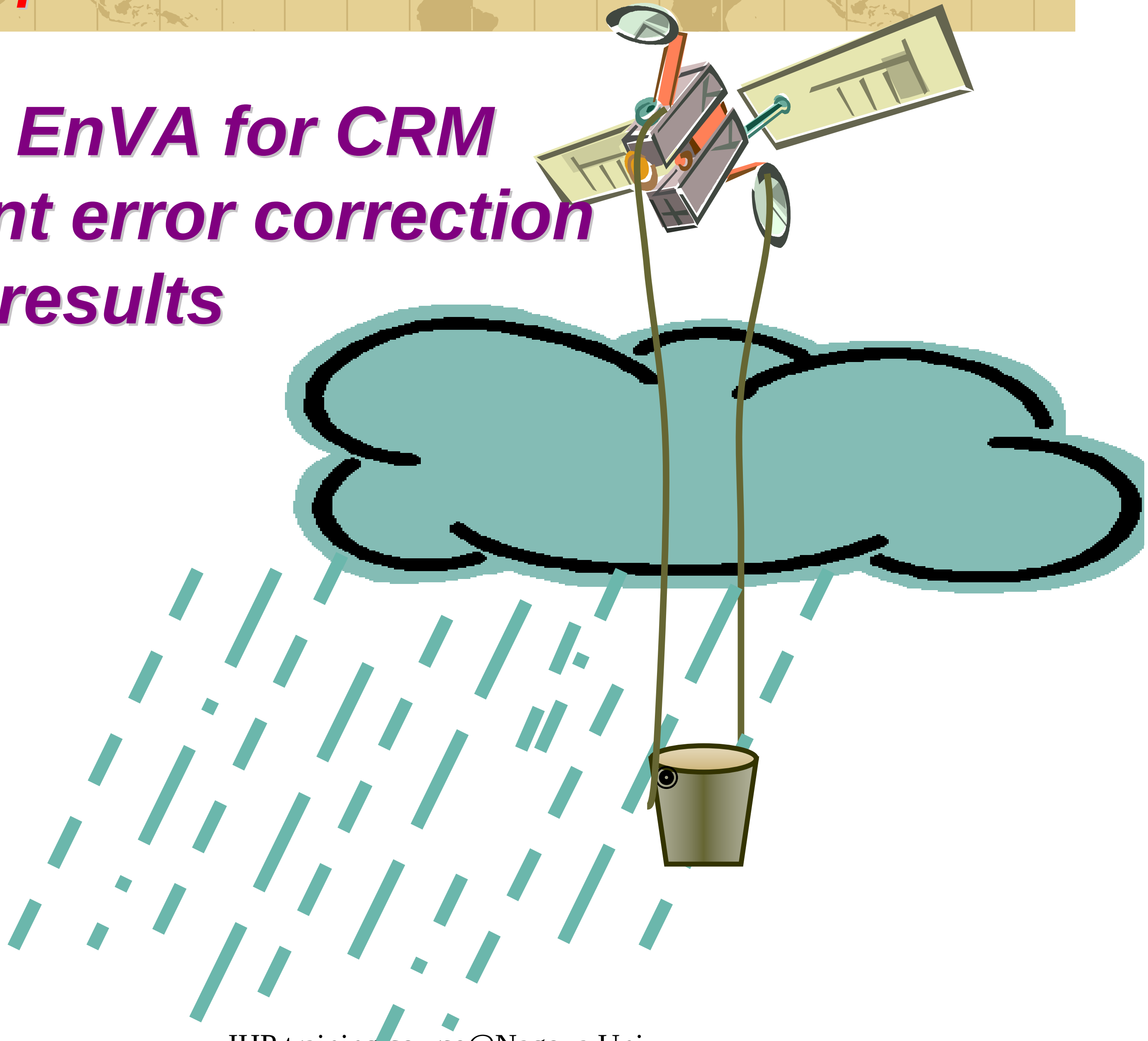

Problem in EnVA (1): Displacement error

- **Large scale displacement errors of rainy areas between the MWI observation and Ensemble forecasts**

- **Presupposition of Ensemble assimilation is not satisfied in observed rain areas without forecasted rain.**

AMSRE *TB18v* (2003/1/27/04z)

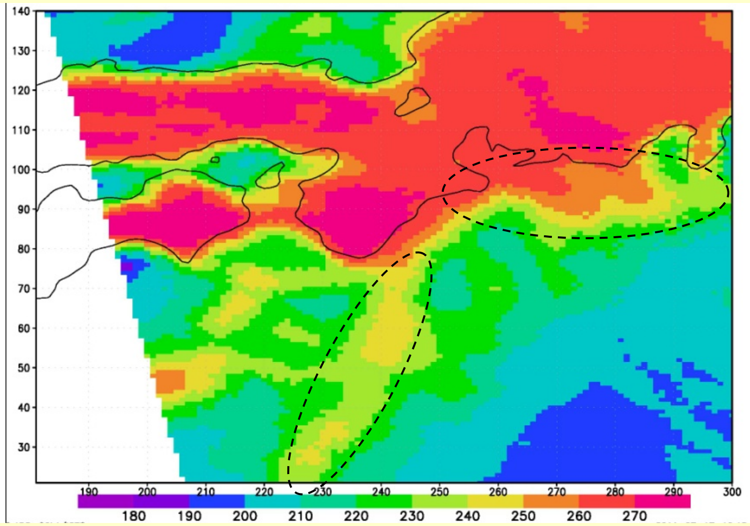

Mean of Ensemble Forecast (2003/1/26/21 UTC FT=7h）

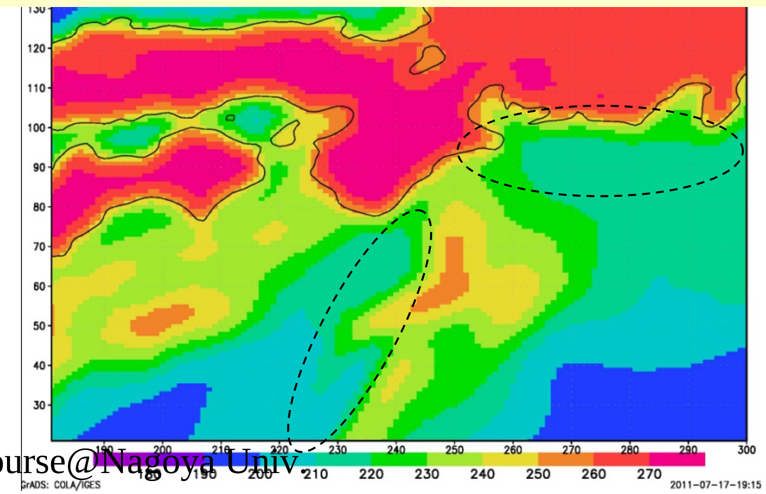

Presupposition of Ensemble-based assimilation

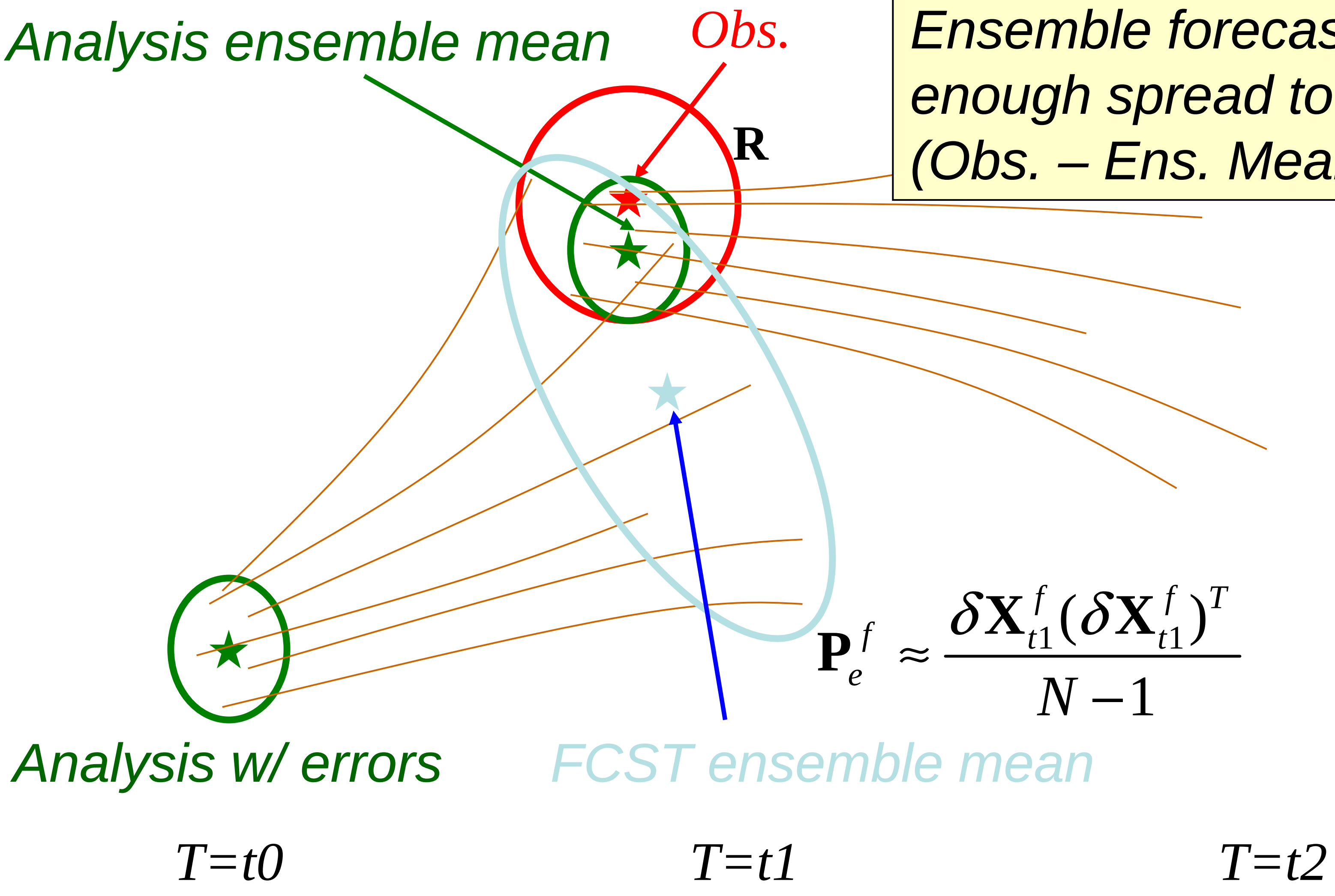

Ensemble forecasts have enough spread to include (Obs. – Ens. Mean)

$$\mathbf{P}_e^f \approx \frac{\delta \mathbf{X}_{t1}^f (\delta \mathbf{X}_{t1}^f)^T}{N-1}$$

Ensemble-based assimilation for observed rain areas without forecasted rain

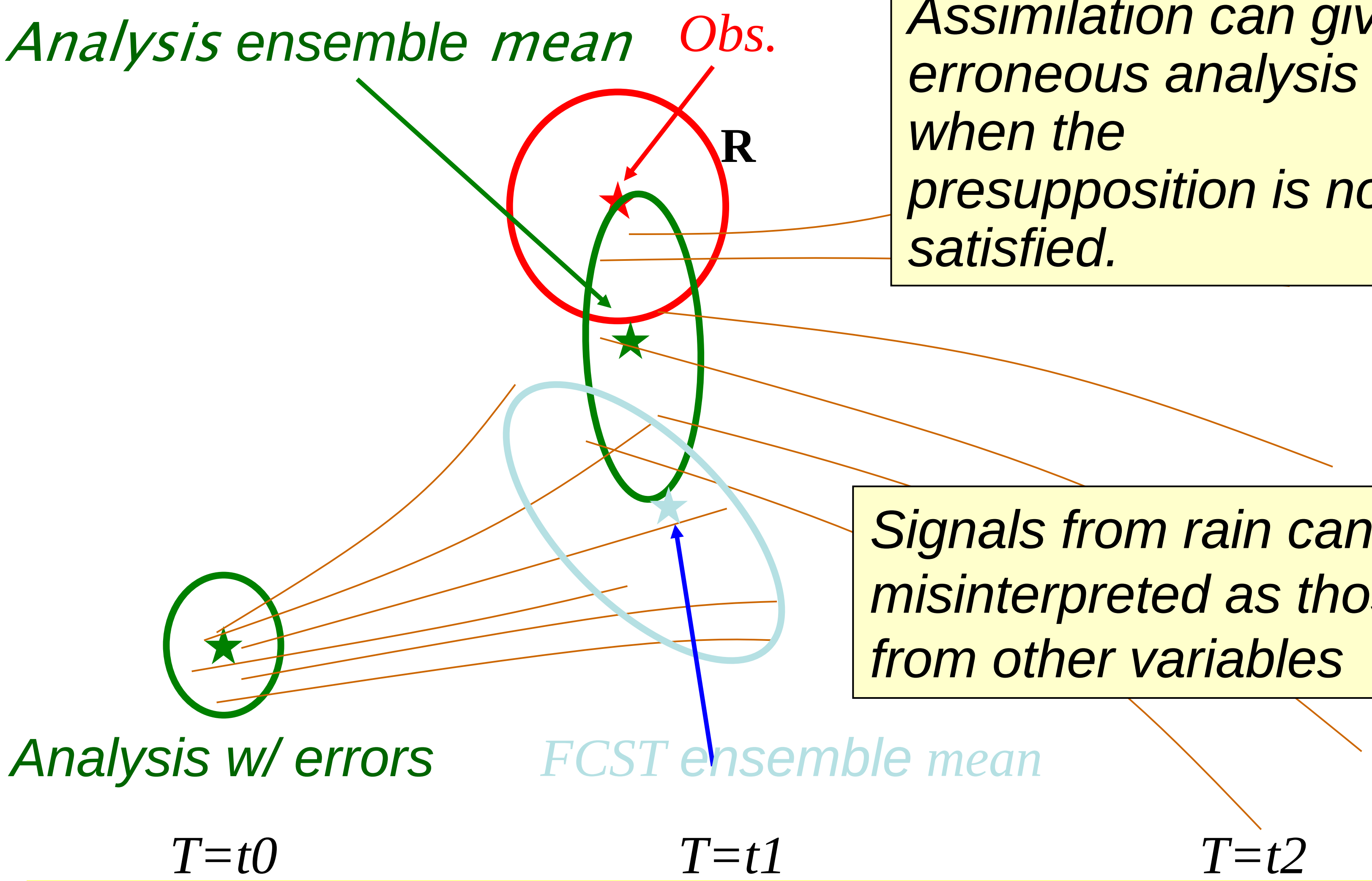

Assimilation can give erroneous analysis when the presupposition is not satisfied.

Signals from rain can be misinterpreted as those from other variables

Displacement error correction is needed!

Displacement error correction (DEC)+EnVA

- Methodology
- Application results for Typhoon CONSON (T0404)
  - Case
  - Assimilation Results
  - Impact on precipitation forecasts

Displaced Ensemble variational assimilation method

In addition to $\vec{X}$, we introduced $\vec{d}$ to assimilation.

The optimal analysis value maximizes :

$$\arg\max P(\vec{X}, \vec{d} \mid Y, \bar{X}^f)$$

$$P(\vec{X}, \vec{d} \mid Y, \bar{X}^f) = P(\vec{d} \mid Y, \bar{X}^f) P(\vec{X} \mid \vec{d}, Y, \bar{X}^f)$$

Assimilation results in the following 2 steps:

1) DEC scheme to derive $\vec{d}^a$ from $P(\vec{d} \mid Y, \bar{X}^f)$

2)EnVA scheme using the DEC Ensembles to derive $\vec{X}^a$ from $P(\vec{X} \mid \vec{d}^a, Y, \bar{X}^f)$

Problem in EnVA (1): Displacement error

- Large scale displacement errors of rainy areas between the MWI observation and Ensemble forecasts

- Presupposition of Ensemble assimilation is not satisfied in observed rain areas without forecasted rain.

AMSRE *TB18v* (2003/1/27/04z)

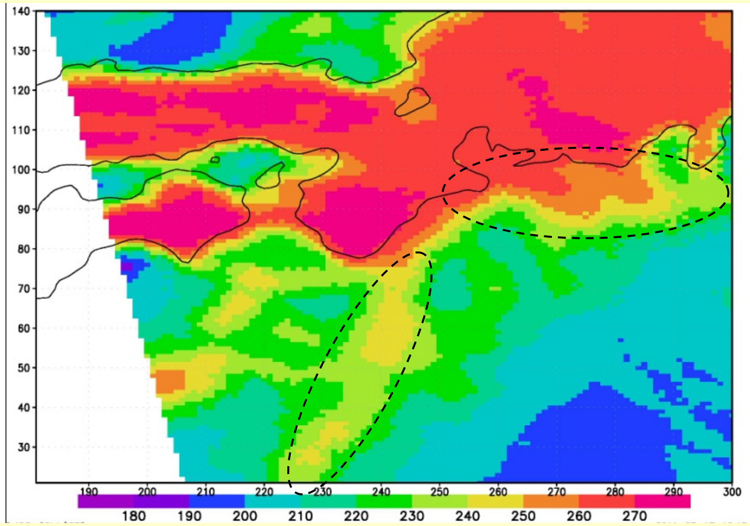

Mean of Ensemble Forecast (2003/1/26/21 UTC FT=7h）

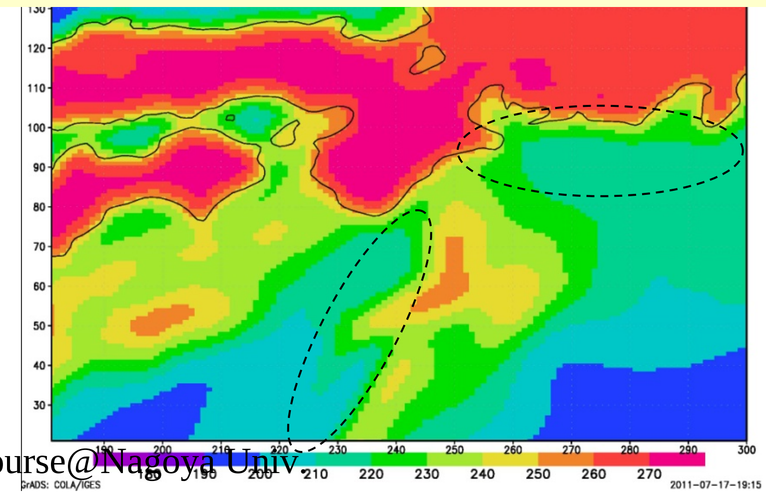

Assimilation method

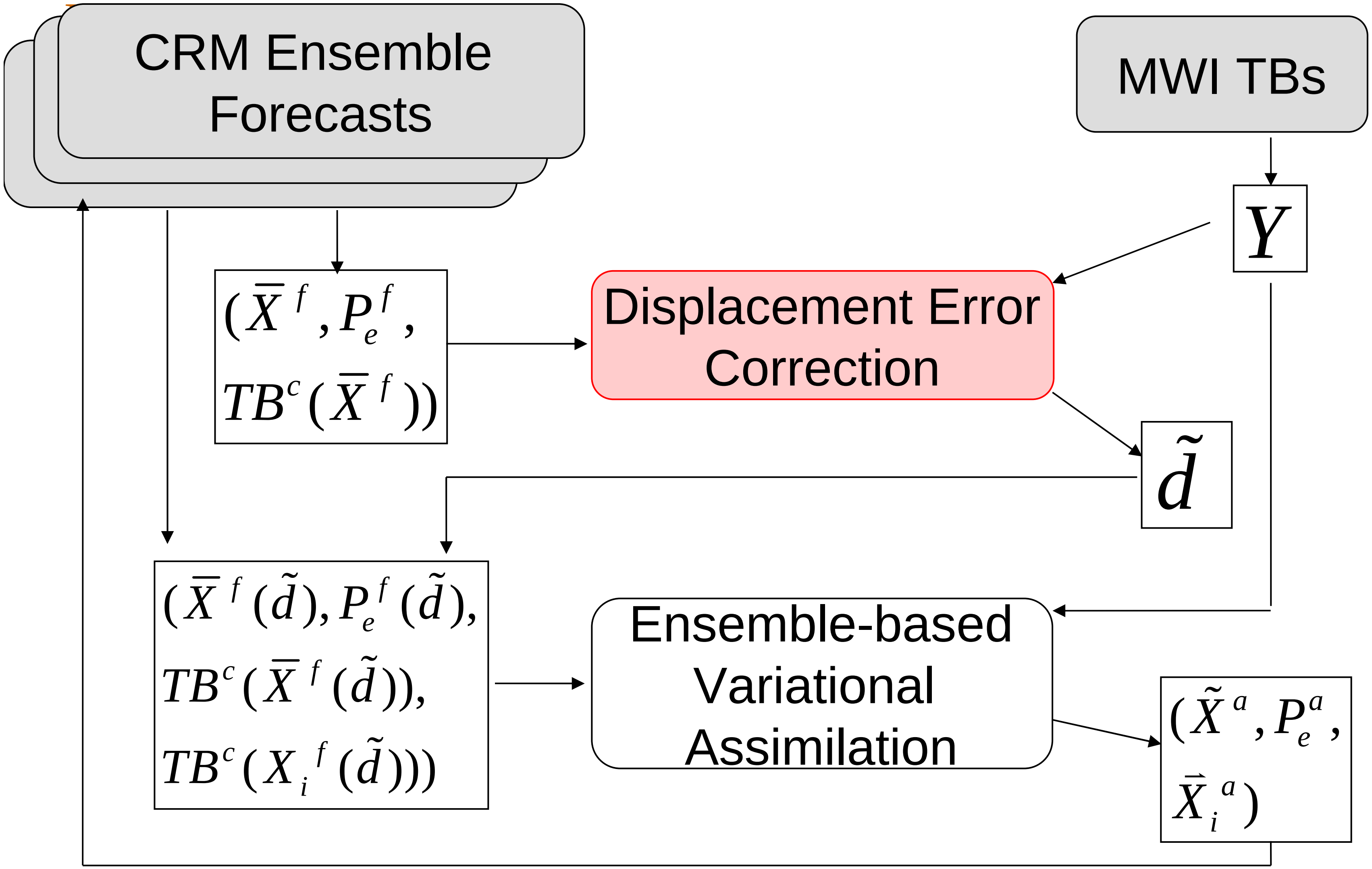

DEC scheme: min. cost function for d

- Bayes' Theorem

$$P(\vec{d}\,|\,Y,\bar{X}^f) = P(Y,\bar{X}^f\,|\,\vec{d})P(\vec{d})/P(Y,\bar{X}^f)$$

- $P(Y,\bar{X}^f\,|\,\vec{d})$ can be expressed as the cond. Prob. of Y given $\bar{X}^f(\vec{d})$:

$$P(Y,\bar{X}^f\,|\,\vec{d}) = \exp\{-1/2\,(Y - H(\bar{X}^f(\vec{d}))^t R^{-1}(Y - H(\bar{X}^f(\vec{d}))\}$$

- We assume Gaussian dist. of $P(\vec{d})$: $P(\vec{d}) = \exp\{-(\left|\vec{d}\right|^2/2\sigma_d^2)\}$

where σ_d is the empirically determined scale of the displacement error.

- We derived the large-scale pattern of $\tilde{d}$ by minimizing J_d (Hoffman and Grassotti ,1996) :

$$J_d = \frac{1}{2}(Y - H(\bar{X}^f(\vec{d})))^t R^{-1}(Y - H(\bar{X}^f(\vec{d})))\} + \left|\vec{d}\right|^2 \Big/ 2\sigma_d^2$$

Detection of the large-scale pattern of optimum displacement

- We derived the large-scale pattern of $\tilde{d}$ from J_d, following Hoffman and Grassotti (1996) :

$$J_d = \frac{1}{2}(Y - H(\overline{X}^f(\vec{d})))^t R^{-1}(Y - H(\overline{X}^f(\vec{d})))\} + \left|\vec{d}\right|^2 \Big/ 2\sigma_d^2$$

- We transformed $\vec{r}$ into the control variable in wave space, $\vec{d}$ using the double Fourier expansion.

- We used the quasi-Newton scheme (Press et al. 1996) to minimize the cost function in wave space.

- we transformed the optimum $\vec{r}$ into the large-scale pattern of $\vec{d}$ by the double Fourier inversion.

Assimilation method

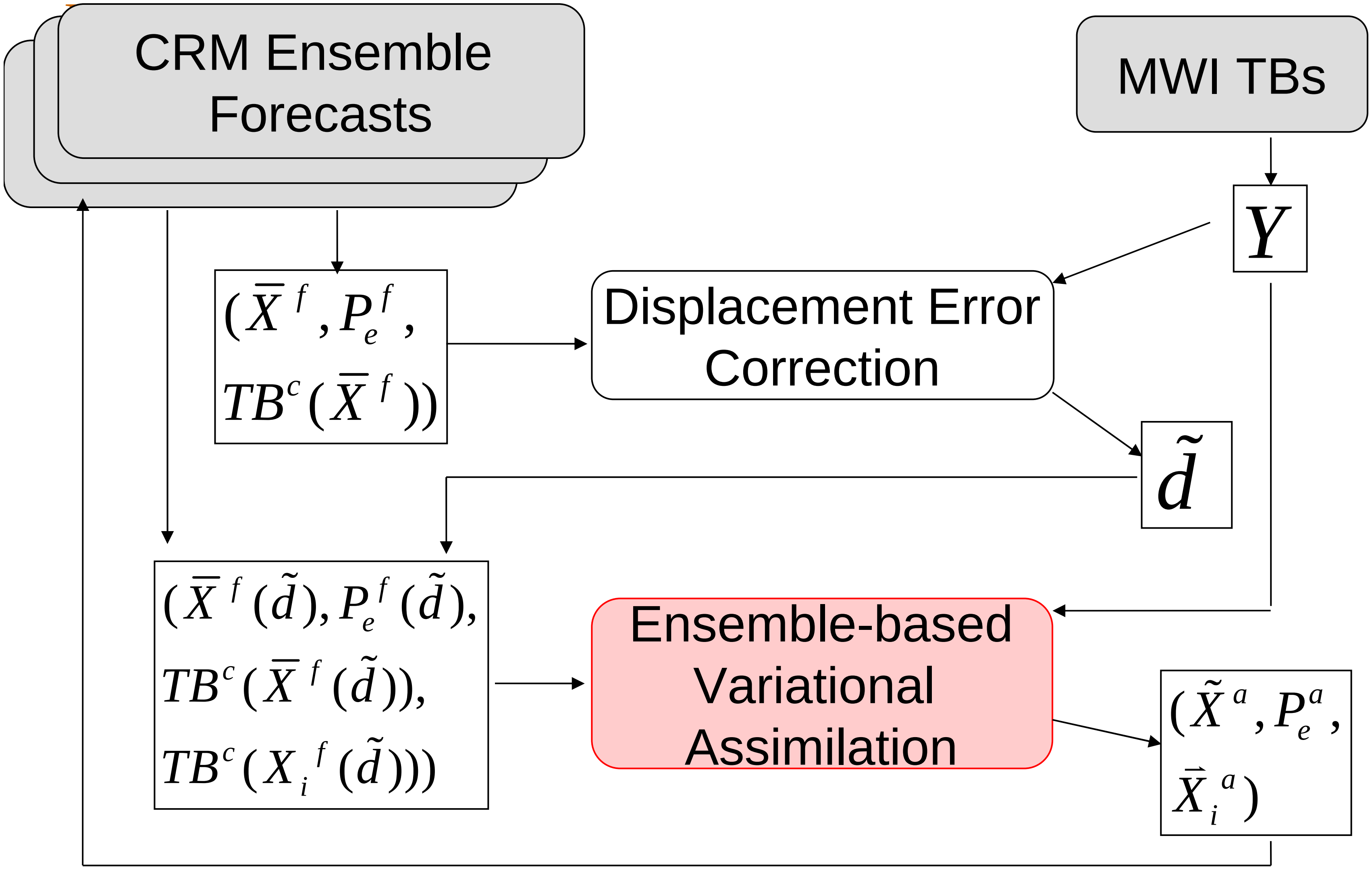

Case (2004/6/9/22 UTC) TY CONSON

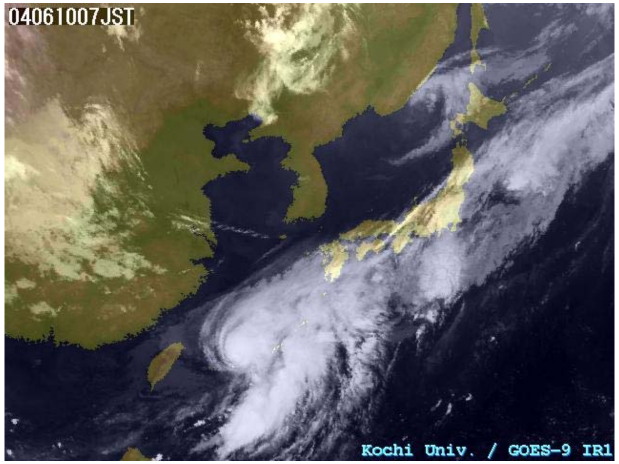

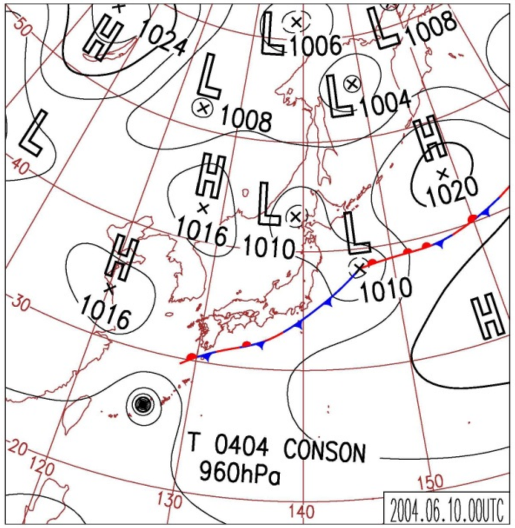

TMI TB19v

RAM (mm/hr)

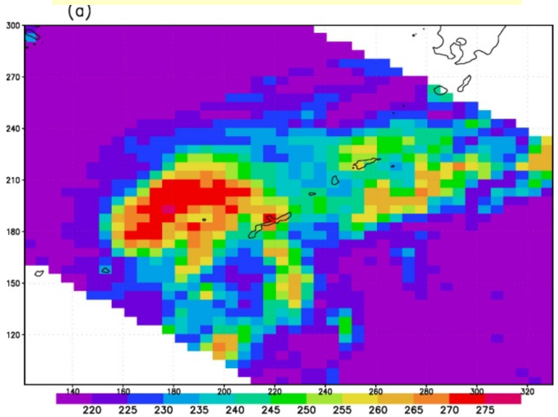

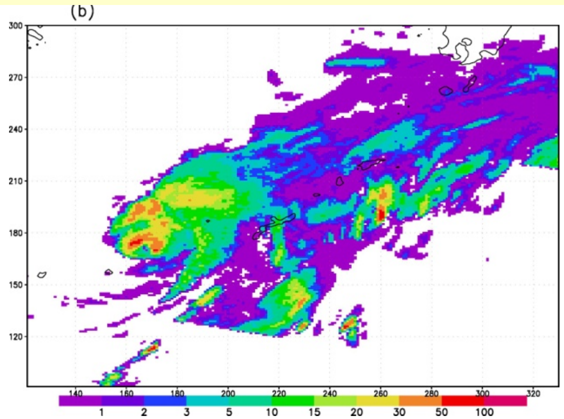

Case (2004/6/9/22 UTC) TY CONSON

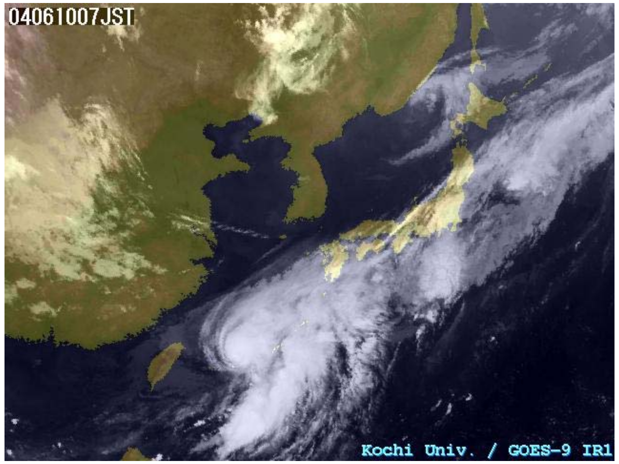

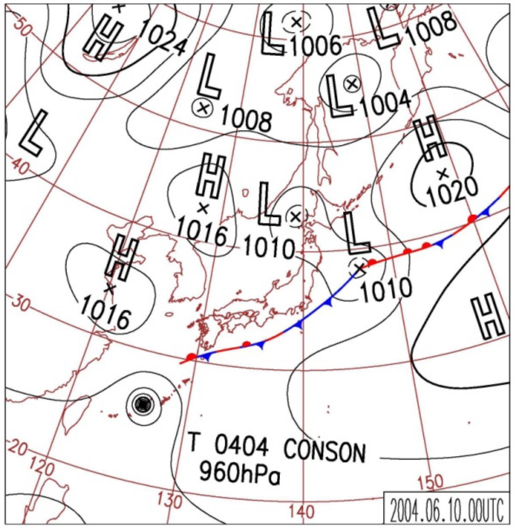

Assimilate TMI TBs (10v, 19v, 21v) at 22UTC

RAM (mm/hr)

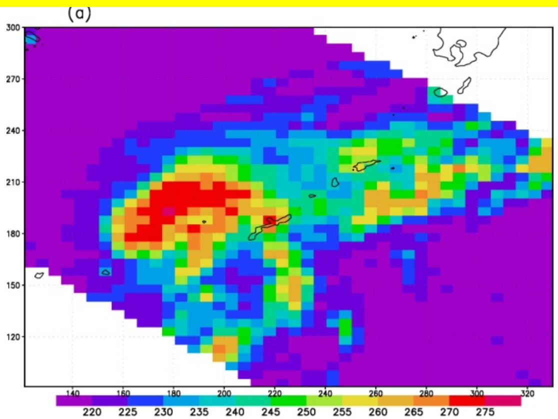

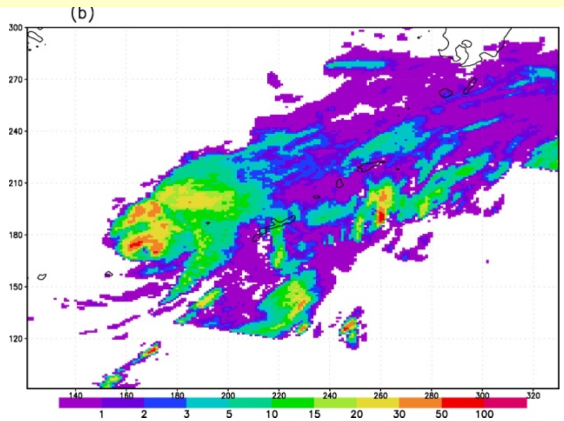

Ensemble Forecasts & RTM code

Ensemble forecasts

- 100 members started with perturbed initial data at 04/6/9/15 UTC (FG)
- Geostrophically-balanced perturbation (Mitchell et al. 2002) plus Humidity

Ensemble mean (FG)
Rain mix. ratio

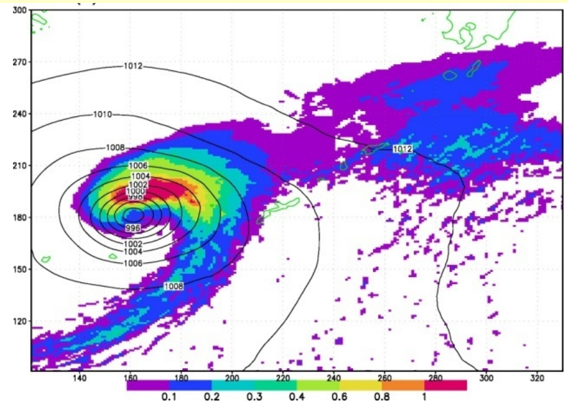

RTM: Guosheng Liu (2004)

- *One-dimensional model (Plane-parallel)*
- *Mie Scattering (Sphere)*
- *4 stream approximation*

TB19v cal. from FG

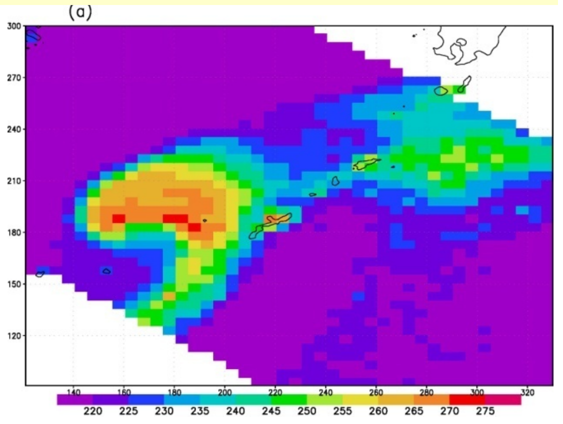

TB19v from TMI and CRM outputs

FG : First guess

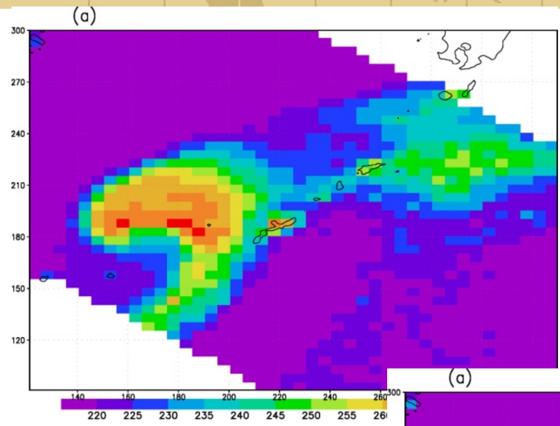

DE : After DEC

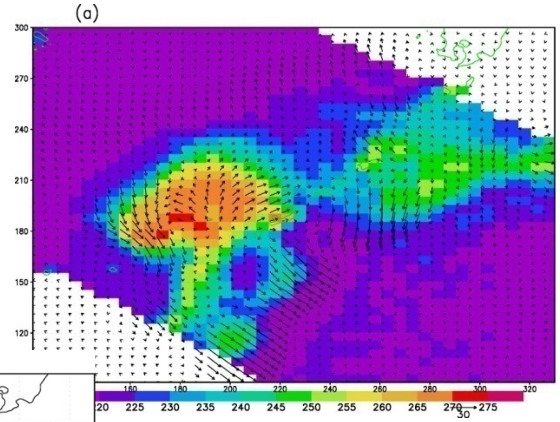

TMI

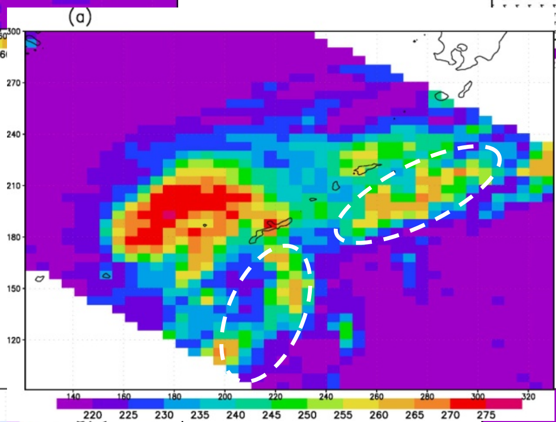

ND: NoDE+ EnVA

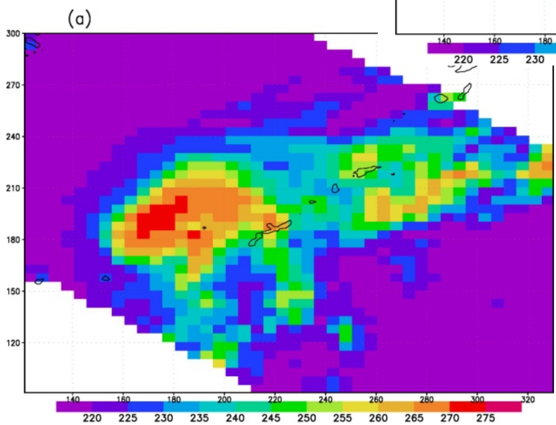

CN : DE+ EnVA

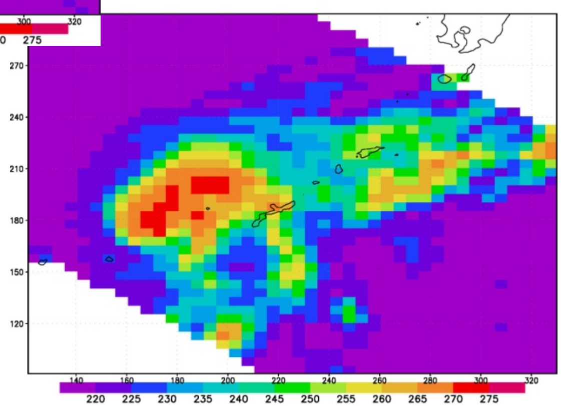

RAM and Rain mix. ratio analysis (z=930m)

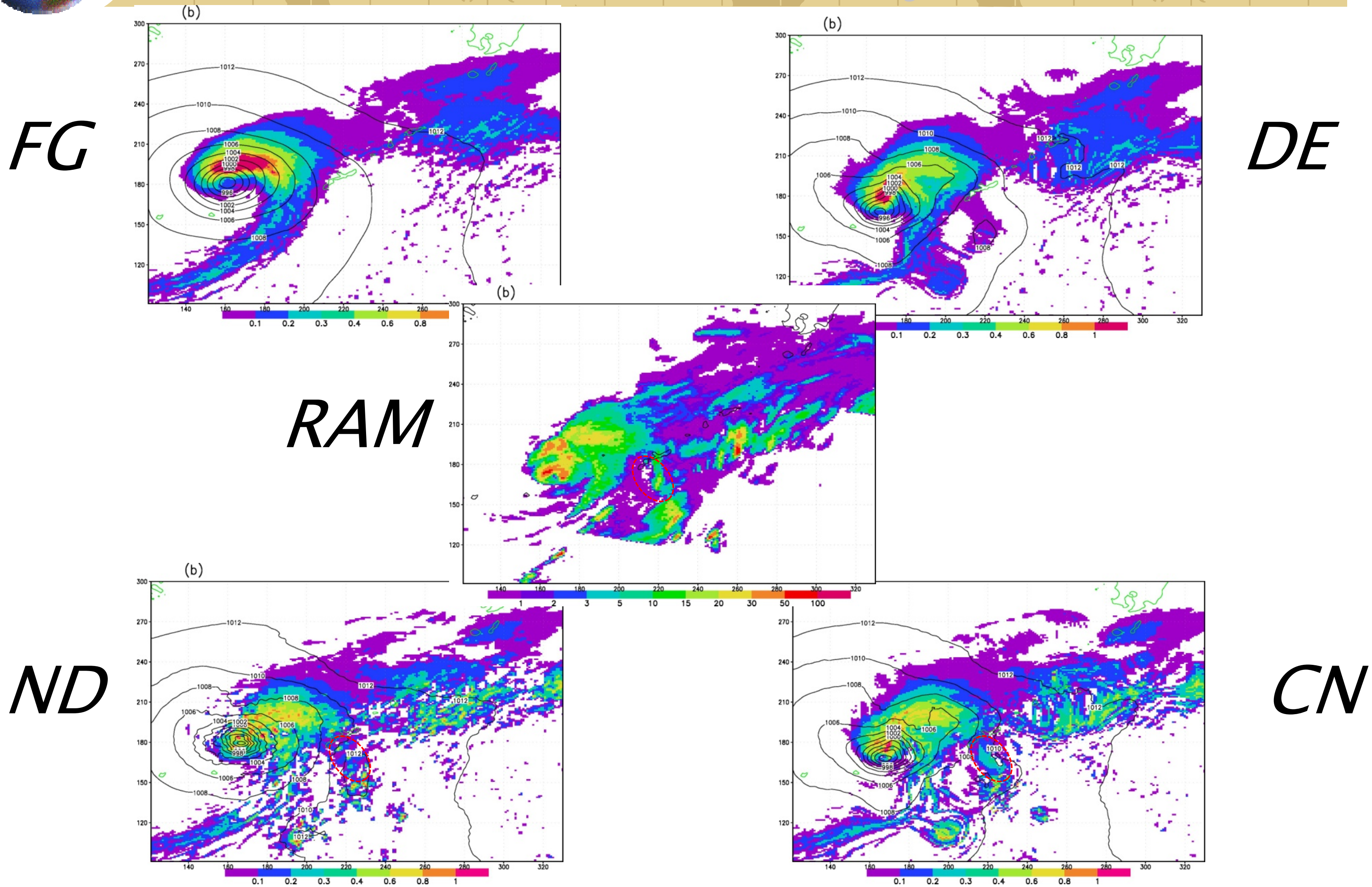

RH(contours) and W(shades) along N-S

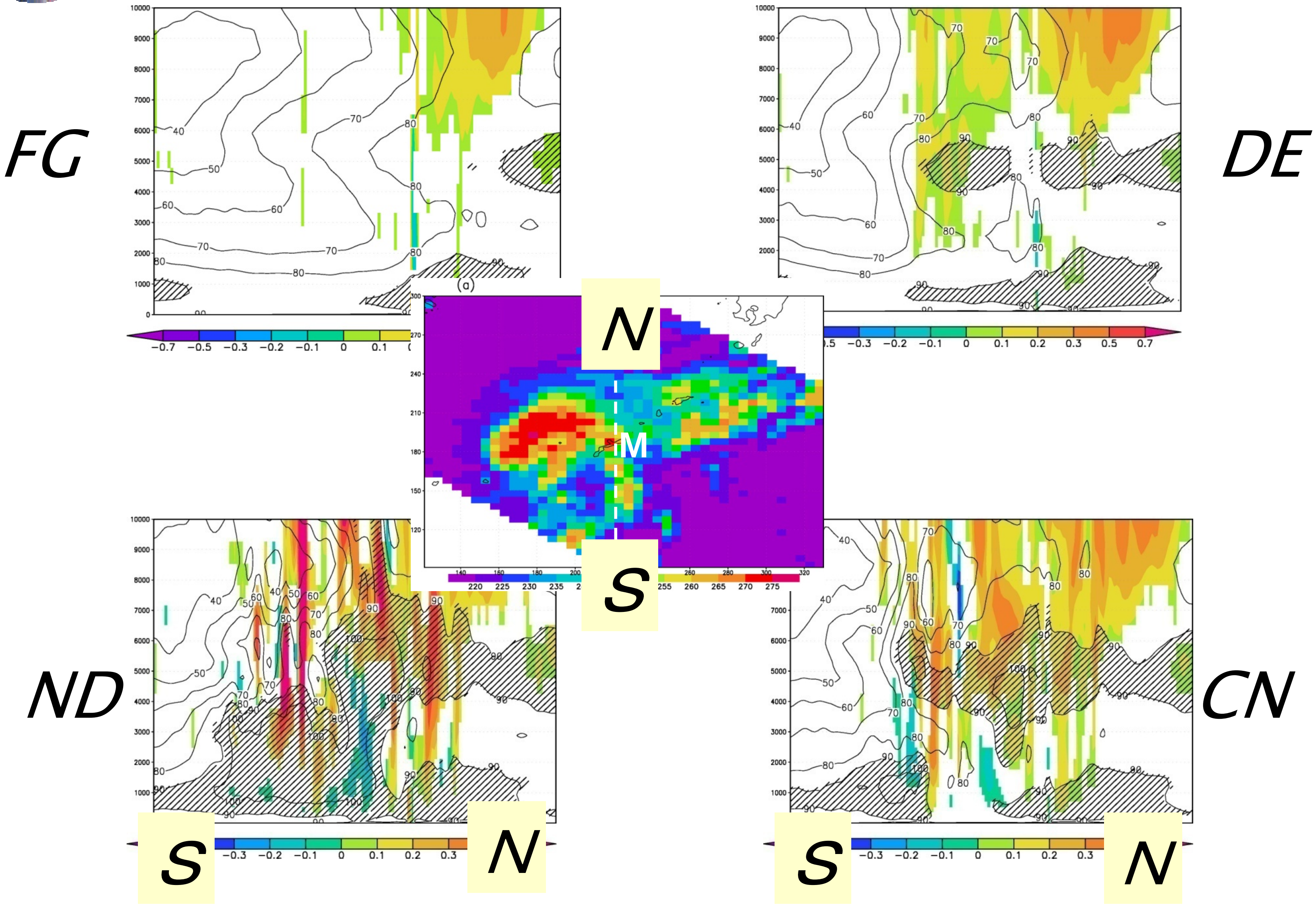

Hourly Precip. forecasts (FT=0-1 h) 22-23Z 9t

FG

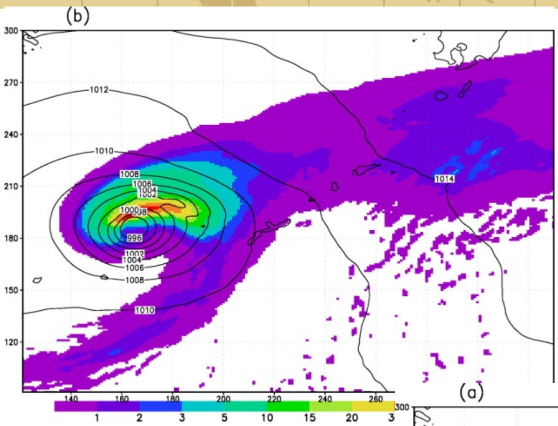

DE

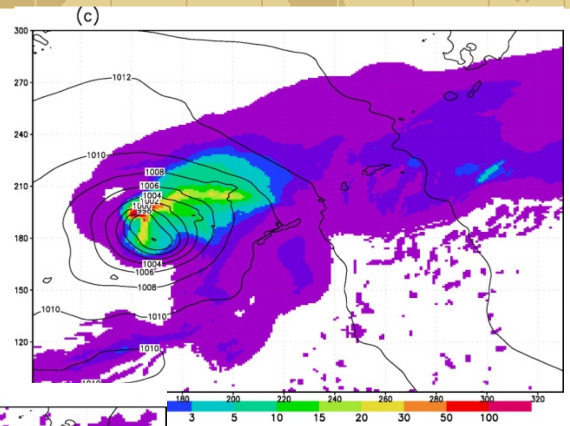

RAM

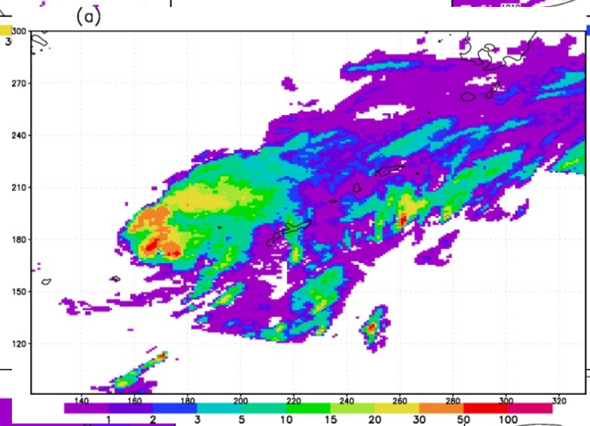

ND

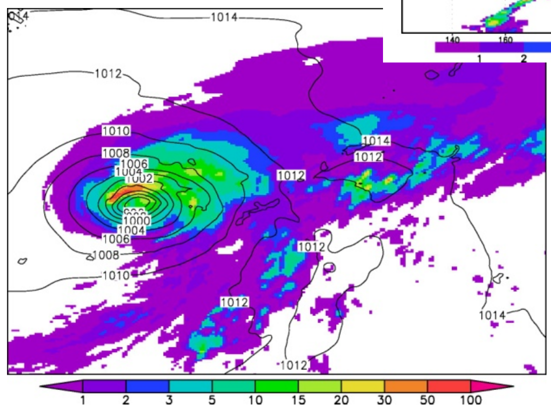

CN

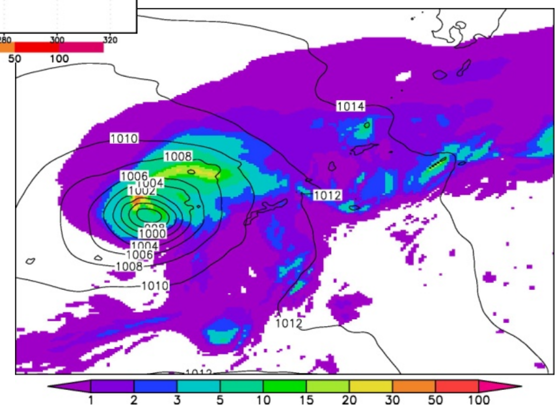

H Forecasts (FT=3-4 h) 01-02Z 10th

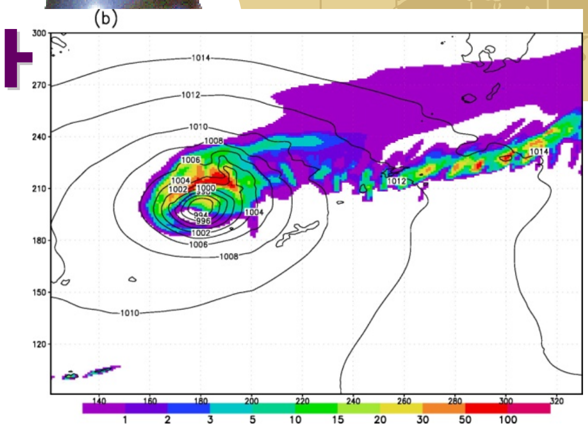

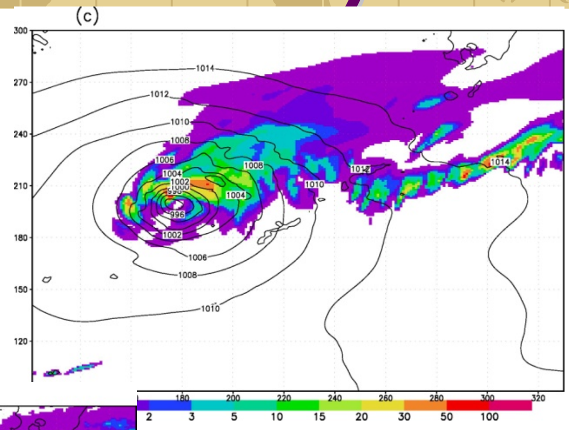

DE

RAM

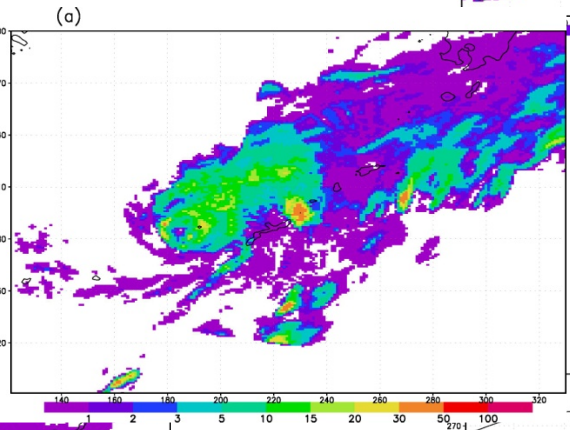

ND

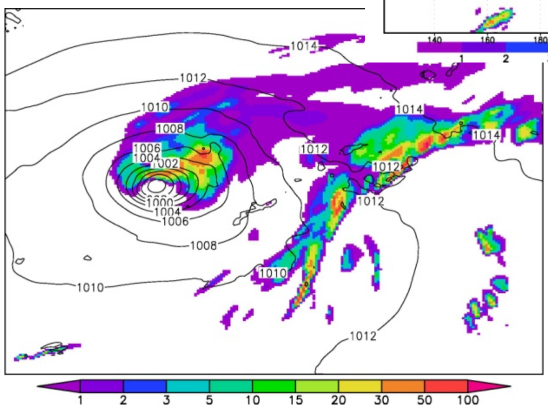

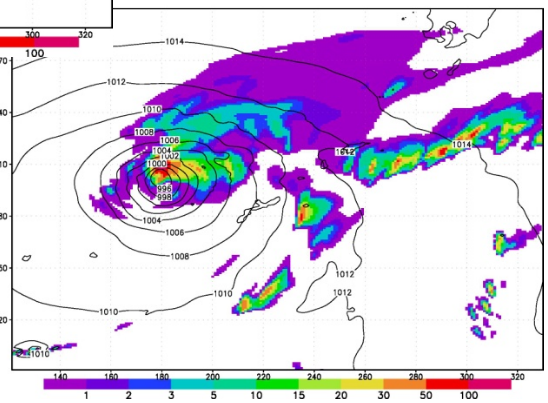

CN

Summary

- Ensemble-based data assimilation can give erroneous analysis, particularly for observed rain areas without forecasted rain.
- In order to solve this problem, we developed the Ensemble-based assimilation method that uses Ensemble forecast error covariance with displacement error correction.
- This method consisted of a displacement error correction scheme and an Ensemble-based variational assimilation scheme.

Summary

- We applied this method to assimilate TMI TBs (10, 19, and 21 GHz with vertical polarization) for a Typhoon case (9th June 2004).
- The results showed that the assimilation of TMI TBs alleviated the large-scale displacement errors and improved precip forecasts.
- The DEC scheme also avoided misinterpretation of TB increments due to precip displacements as those from other variables.

Problem in EnVA (2): Sampling error

Forecast error corr. of W (04/6/9/15z 7h fcst)

200 km

200 km

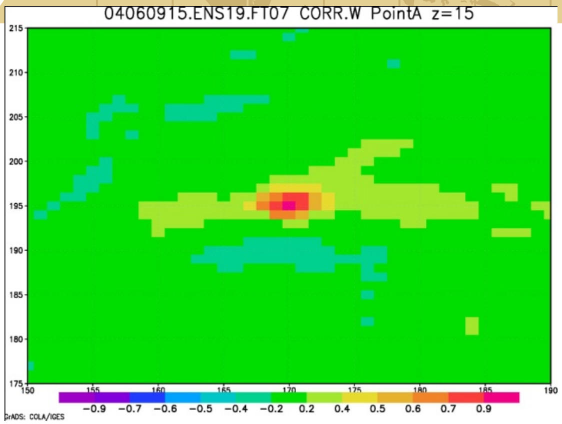

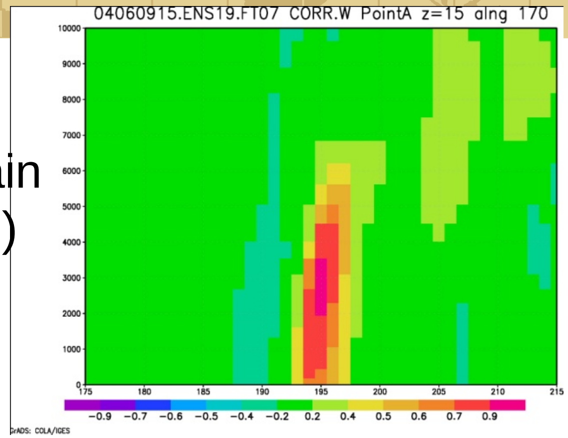

Heavy rain
(170,195)

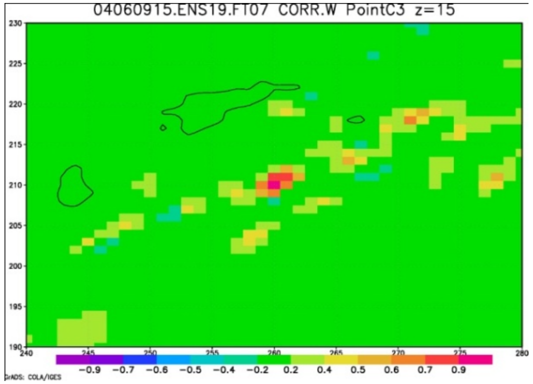

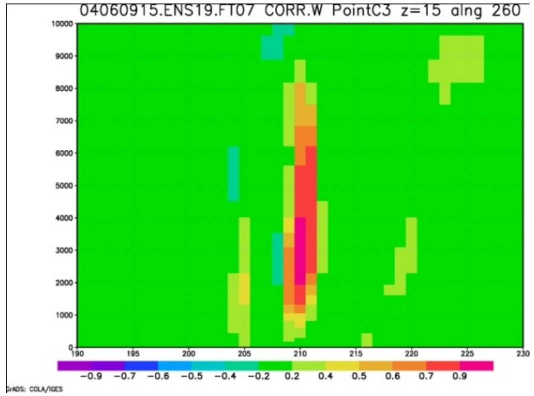

Weak rain
(260,210)

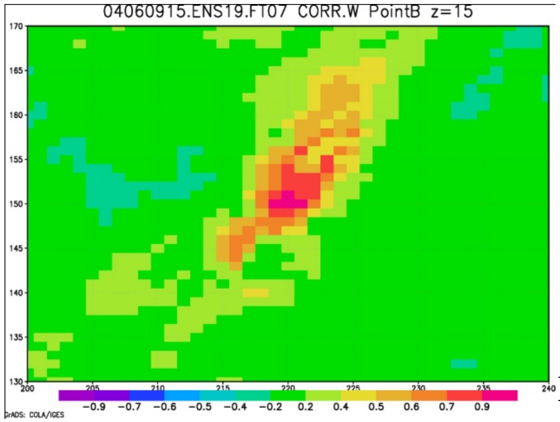

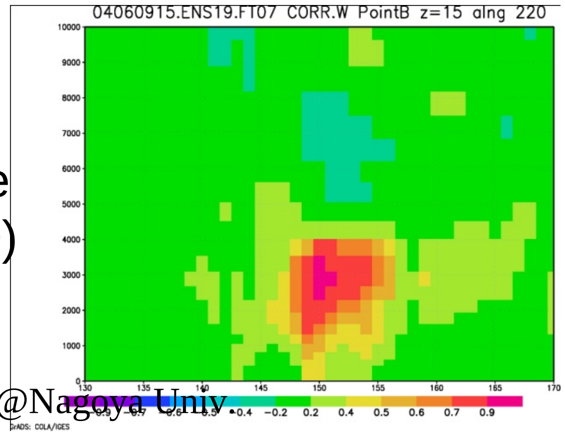

Rain-free
(220,150)

Problem in EnVA (2): Sampling error

Forecast error corr. of W (04/6/9/15z 7h fcst)

200 km

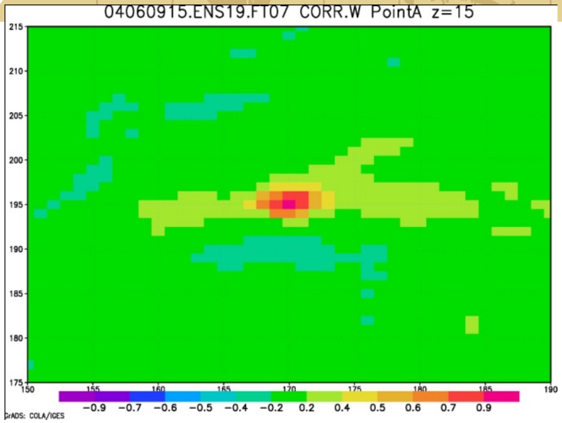

Heavy rain
(170,195)

200 km

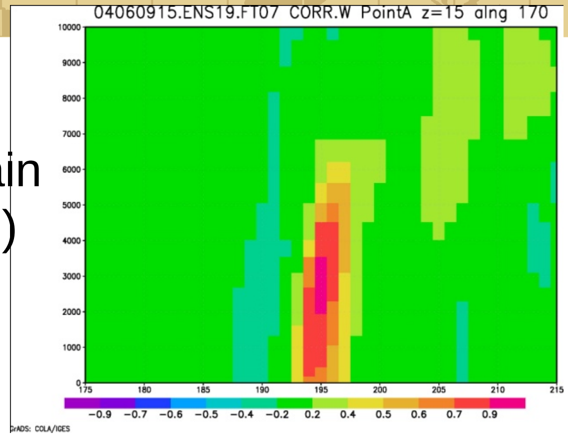

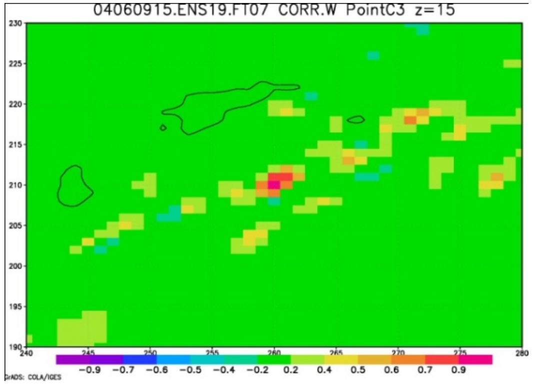

Weak ra
(260,210

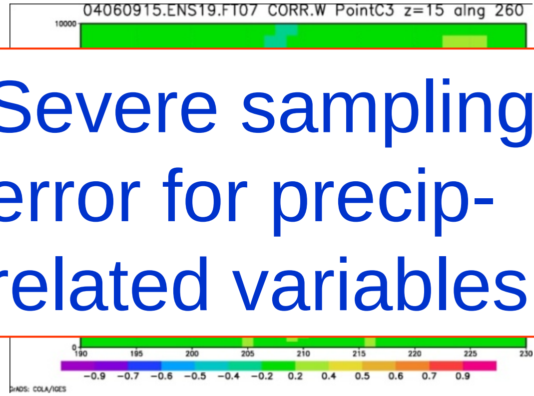

Severe sampling error for precip-related variables

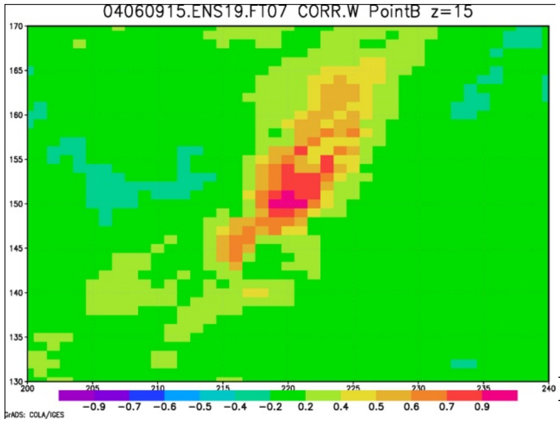

Rain-free
(220,150)

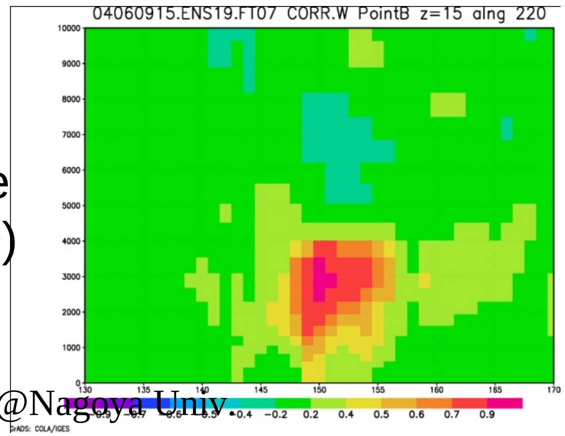

Thank you for your attention.

Combined use of radar and radiometer for precipitation retrieval

Hirohiko Masunaga

Hydrospheric Atmospheric Research Center, Nagoya University

Combined sensor retrieval: Outline

- Introduction
  - Microwave remote sensing
    - A useful window of atmosphere
  - Radar and microwave radiometer
    - Why not using them together?
- Algorithm description
  - How it works and how it is helpful.
- Toward future applications
  - From TRMM to GPM

Introduction

Different bands for different targets

- Visible light
  - Atmospheric particle scattering
    - Cloud and aerosol optical properties
- Infrared radiation
  - Cloud top temperature
  - Molecular absorption
    - Temperature and humidity sounding
    - Other gaseous compositions (e.g., CO_2)
- Microwave
  - Sensitive to liquid water when particles are large
    - Precipitation retrieval
  - Oxygen and water vapor absorption
    - Temperature and humidity sounding

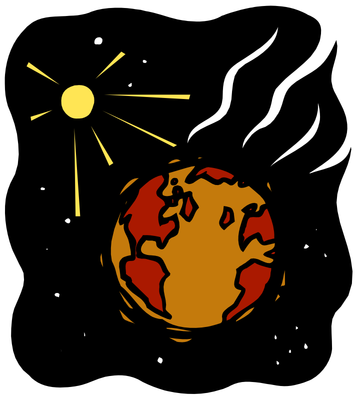

Atmospheric Transmittance

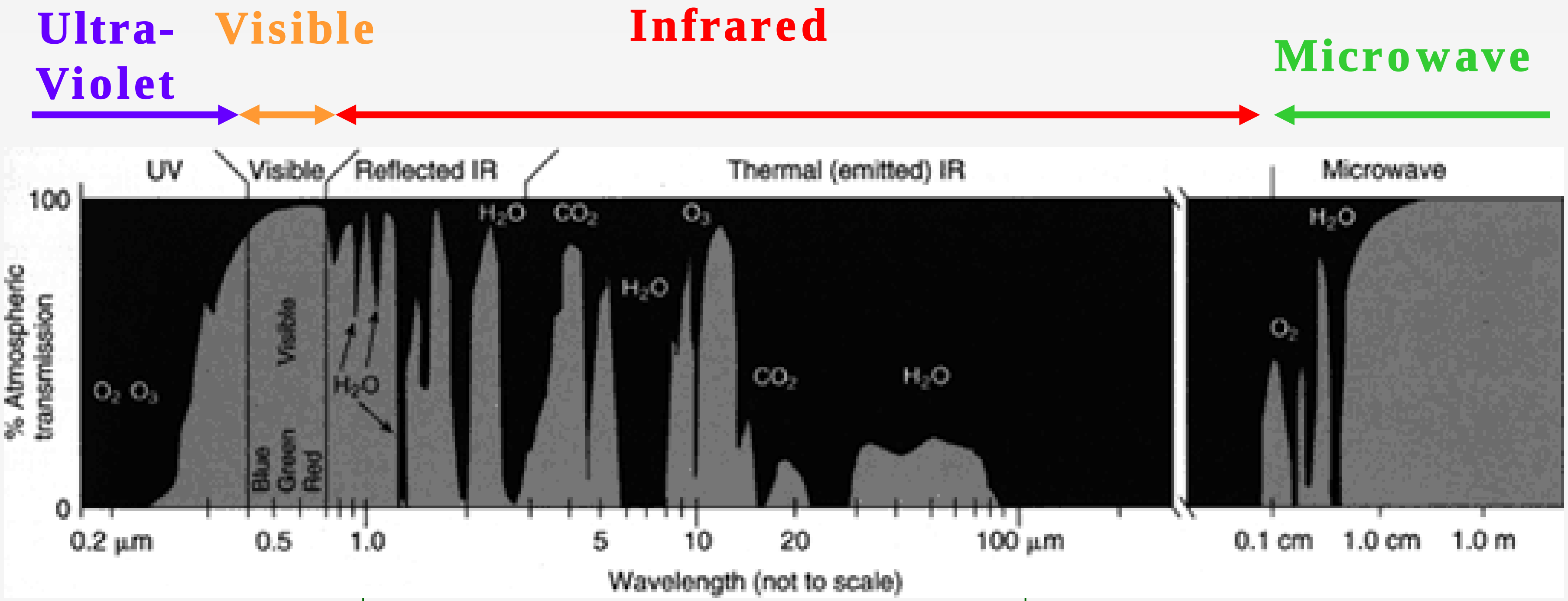

1/1000mm **Wavelength** **1/10mm**

http://earthobservatory.nasa.gov

Microwave spectrum of atmosphere

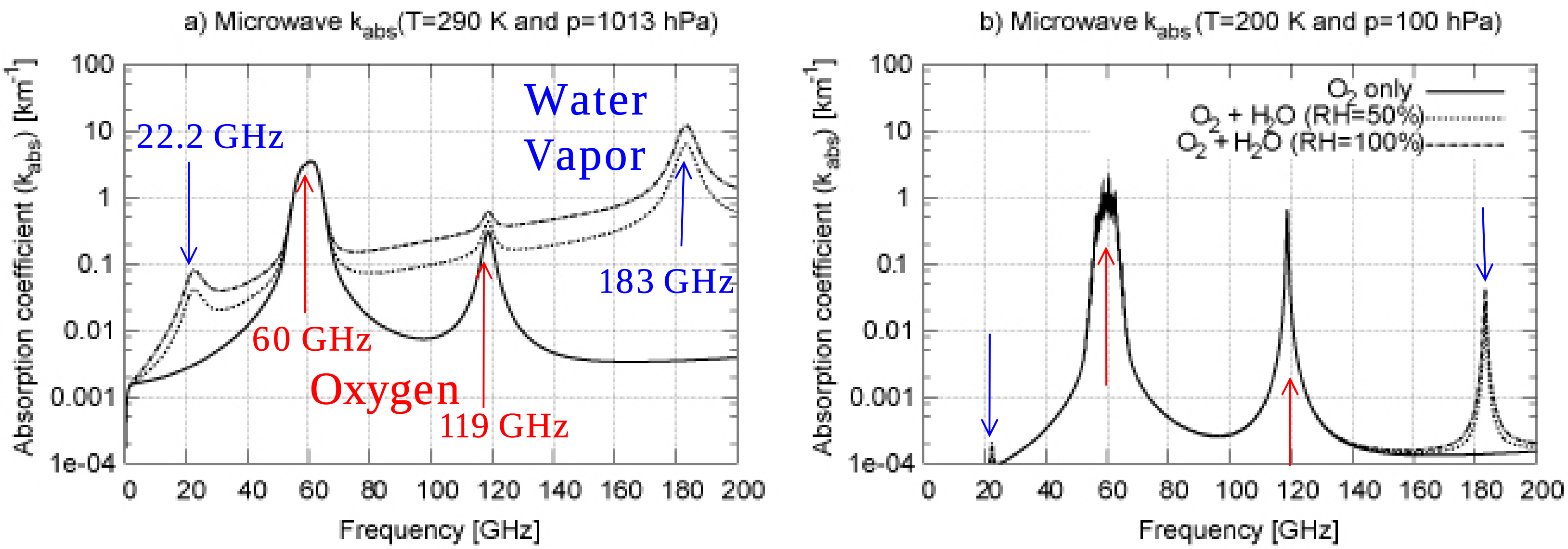

Passive versus Active sensors

- Passive remote sensors
  - Measure natural-origin radiation
    - Imager, radiometers, and sounders
  - Observe two-dimensional plan view.
    - Except for sounders, which measure vertical profiles as well.
  - Relatively inexpensive

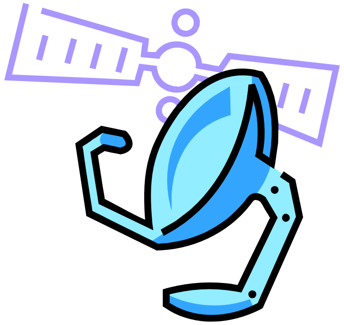

- Active remote sensors
  - Send electromagnetic pulses and detect the strength and temporal delay of back-scattered signal.
    - Radars and lidars
    - c.f., scatterometers
  - Observe three dimensional structure
  - Tend to be expensive

Radar and radiometer observations

Typhoon Cimaron (2006) observed by the Tropical Rainfall Measuring Mission (TRMM) satellite
http://trmm.gsfc.nasa.gov/publications_dir/extreme_events.html

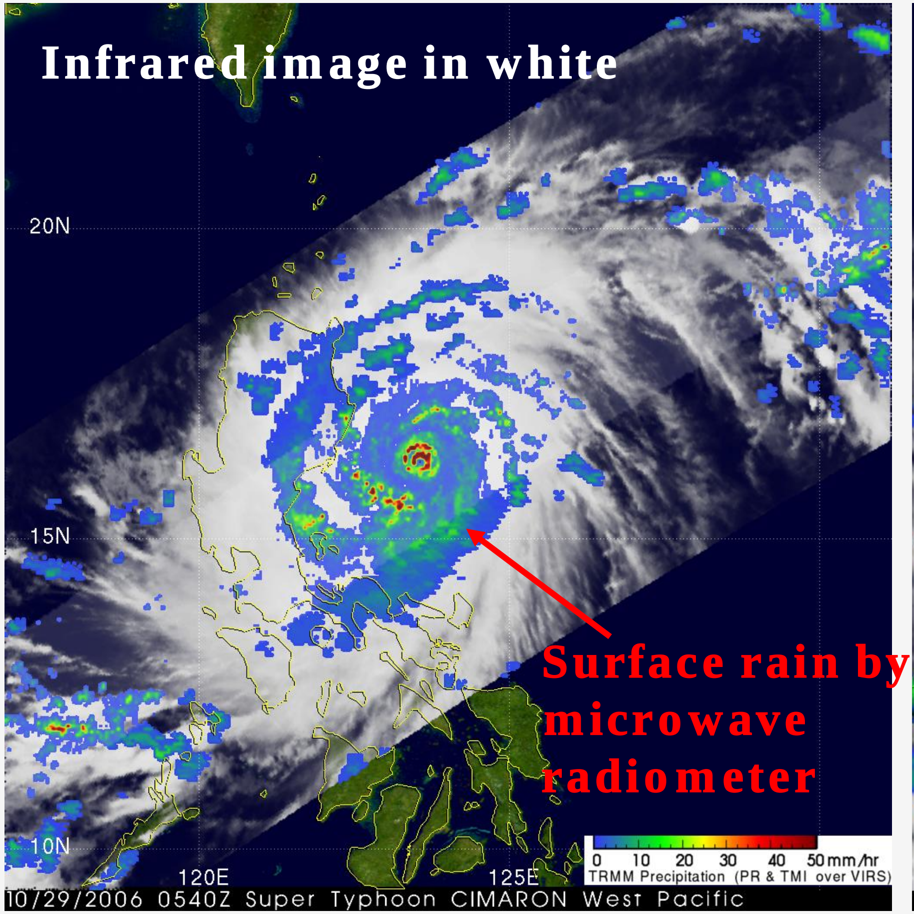

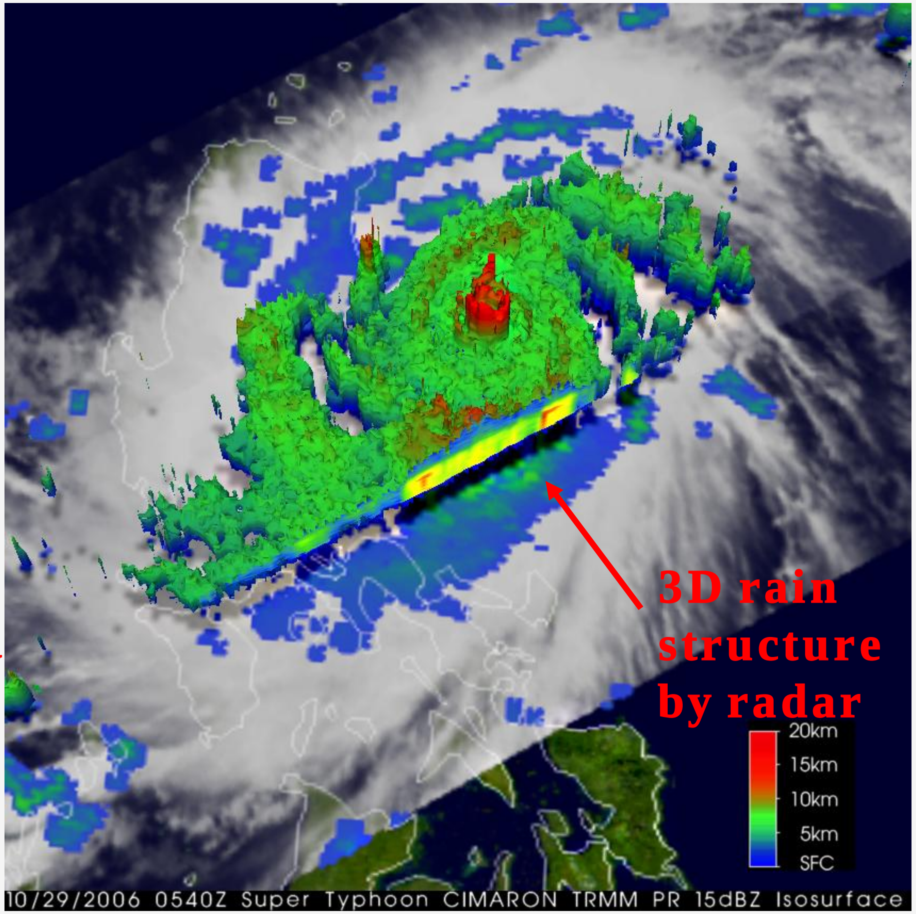

Radar measurement principles

- Radar : Radio Detecting and Ranging
  - Observes back-scattered echo from rain drops.
  - Sensitive to large rain drops but insensitive to small ones.
    - Depends strongly on the drop size distribution (DSD).
    - Rain rate could vary with your choice of Z-R relation.

$$P_r = \frac{C}{r^2} Z \exp\underbrace{\left(-2\int_0^r k_a \rho dr \right)}_{\text{Attenuation}}$$

Pr: Received power

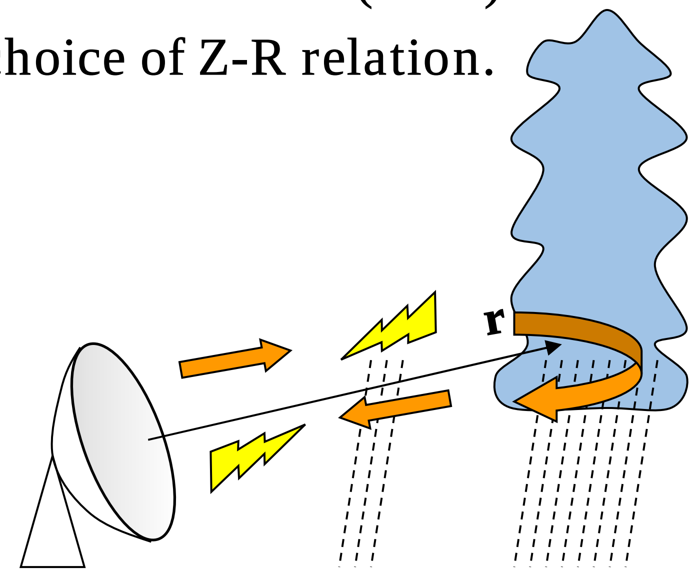

Reflectivity factor

$$Z = \int D^6 N(D) dD$$

N(D): Rain drop size distribution (DSD)

Radiometer measurement principles

- Microwave radiometer: a scanning "radio telescope"

$$\frac{dT_b}{d\tau} = -T_b + (1-\omega)T_w + \omega\int P(\Omega,\Omega')T_b' d\Omega'$$

extinction

thermal emission

particle scattering

- ω~0 (w/o scattering)
- Clouds and rainfall emit thermal radiation brighter than the background surface emission.
- Typical of low frequency channels (10,19GHz etc)

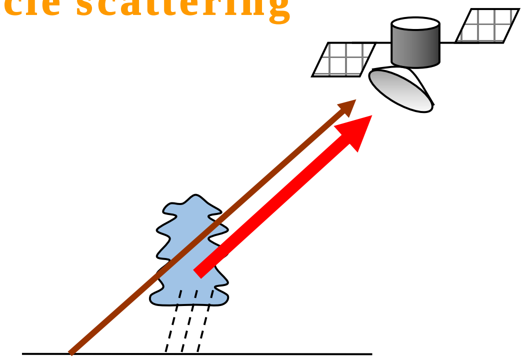

- ω~1 (scattering only)
- Scattering by precipitation particles shields from the background surface emission.
- Typical of high frequency channels (89GHz etc.)

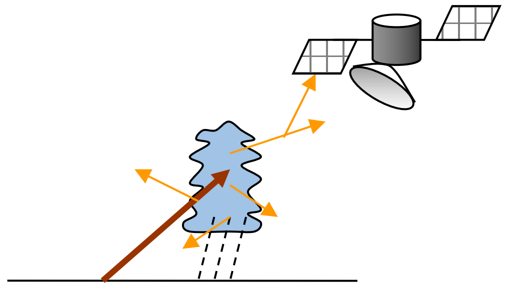

Microwave imagery: 6GHz

http://sharaku.eorc.jaxa.jp/AMSR/index_j.htm

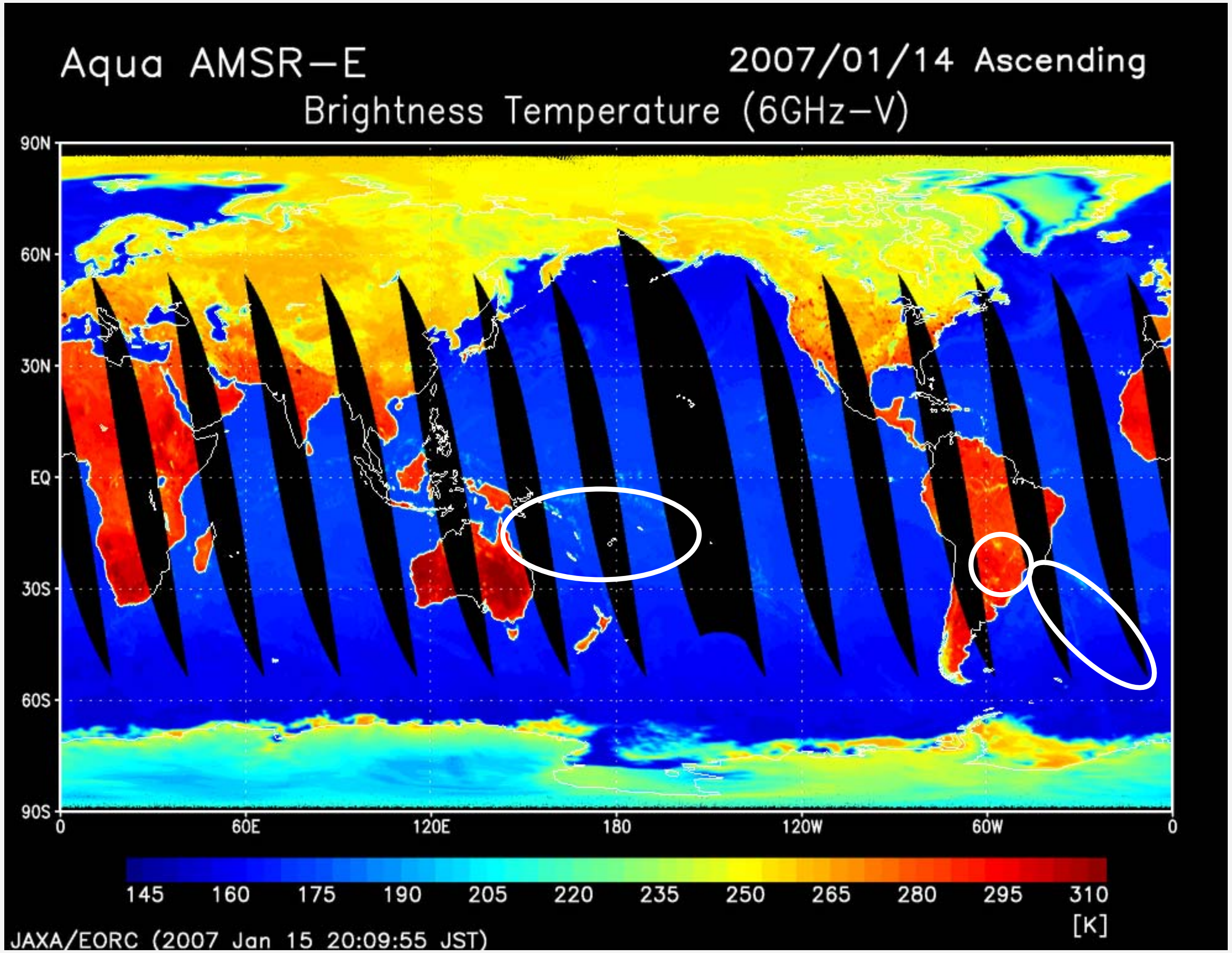

Microwave imagery: 36GHz

http://sharaku.eorc.jaxa.jp/AMSR/index_j.htm

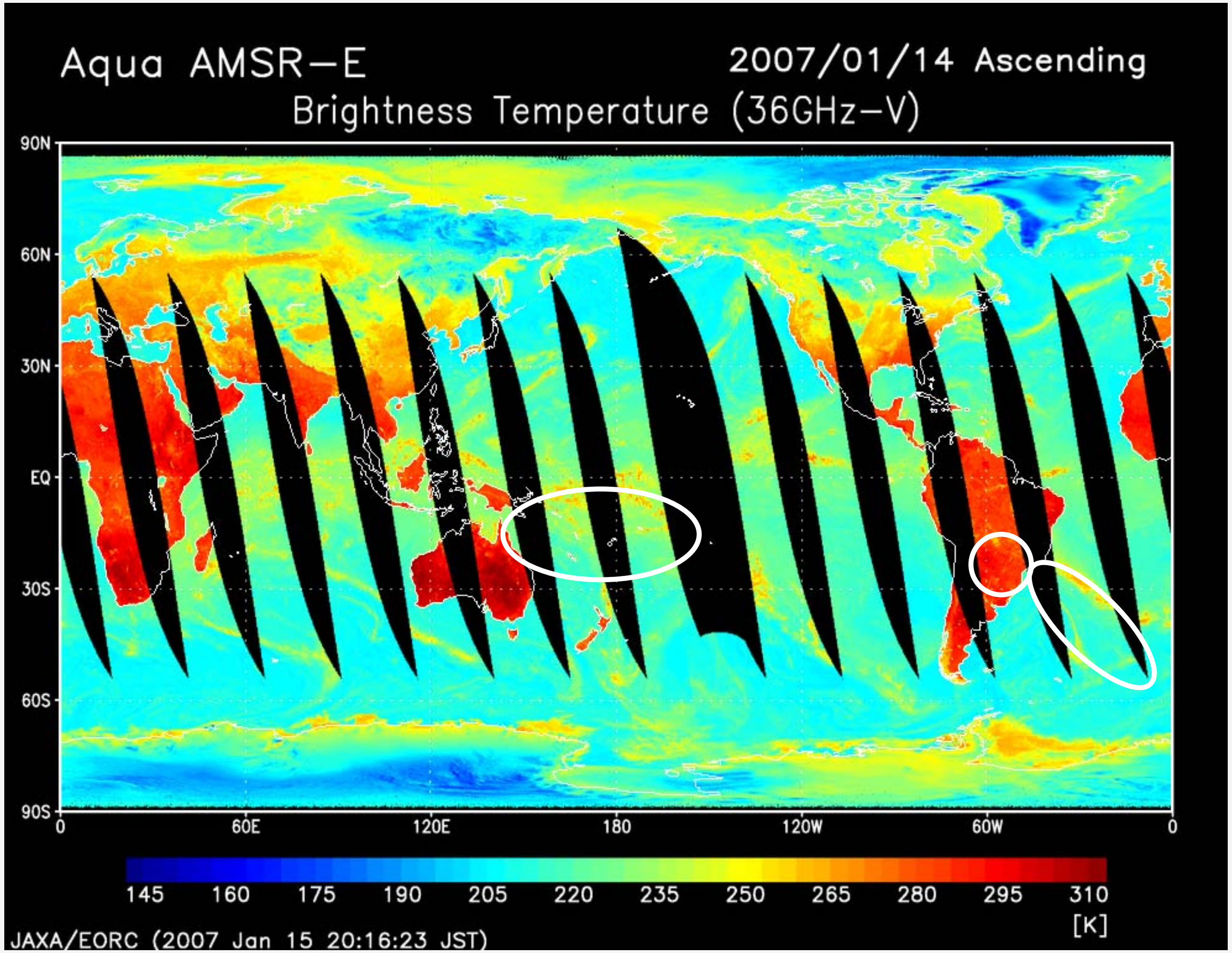

Microwave imagery: 89GHz

http://sharaku.eorc.jaxa.jp/AMSR/index_j.htm

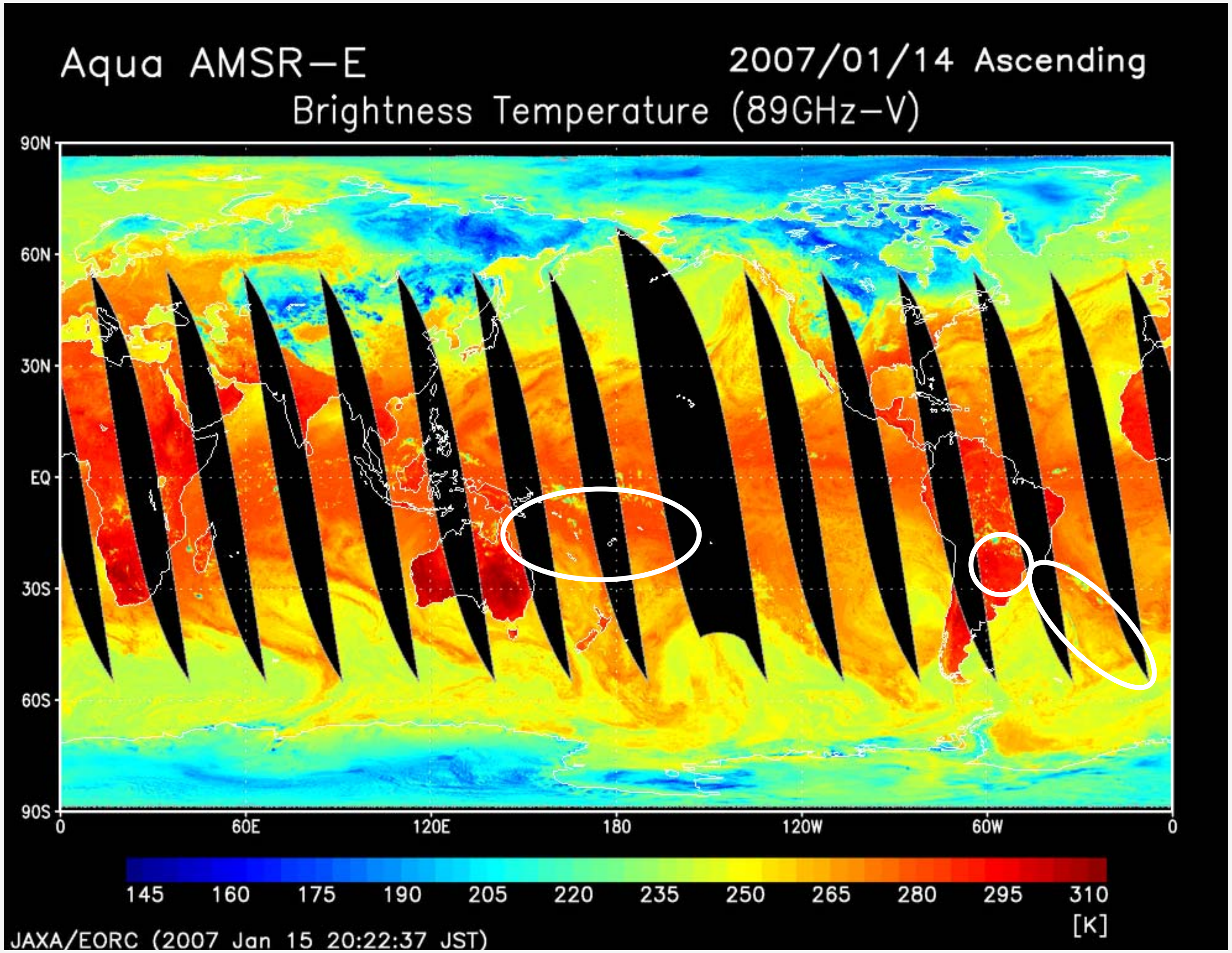

Microwave imagery: Retrieved rainfall

http://sharaku.eorc.jaxa.jp/AMSR/index_j.htm

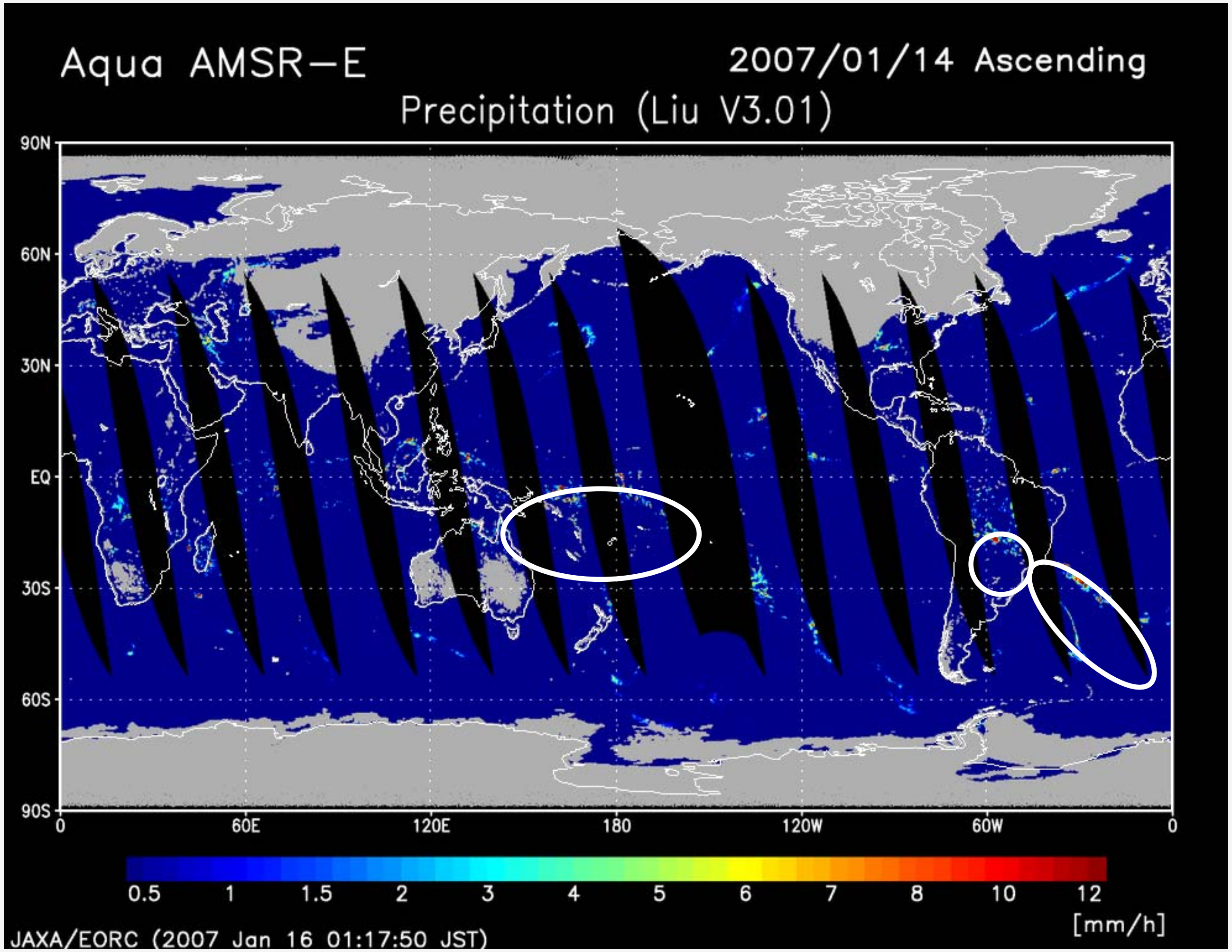

Satellites with radar and radiometer onboard

- Tropical Rainfall Measuring Mission (TRMM)
  - Precipitation Radar (PR)
    - Ku-band (13.6 GHz) radar
  - TRMM Microwave Imager (TMI)
    - 9 channels from 10 GHz to 85 GHz
  - Visible/Infrared Scanner (VIRS) etc.
  - In operation since late 1997
- Global Precipitation Measurement Mission (GPM)
  - Dual-frequency Precipitation Radar (DPR)
    - Ku- (13.6 GHz) and Ka-band (35.5 GHz) radar
  - GPM Microwave Imager (GMI)
    - 13 channels from 10 GHz to 183 Ghz
  - To be launched in 2014.

TRMM satellite scanning geometry

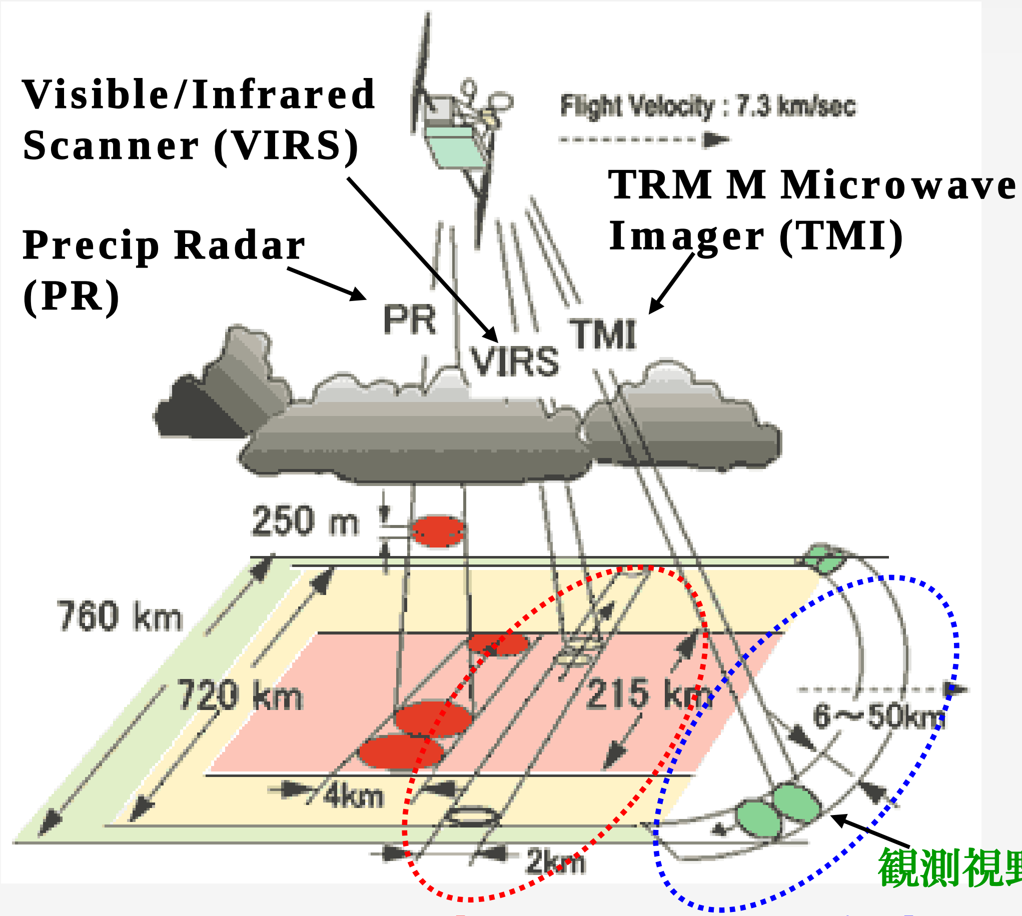

観測視野（FOV)

Cross-track scan (VIRS and PR)

Conical scan (TMI)

http://www.eorc.jaxa.jp/TRMM/channel/index_j.htm

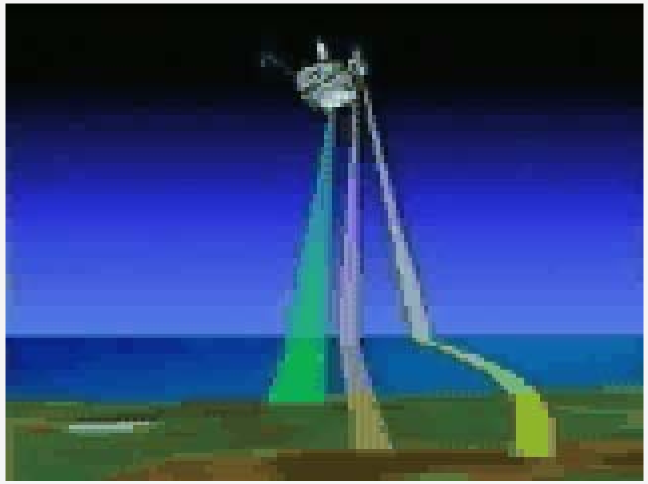

Algorithm description

Existing combined sensor algorithms

- TRMM standard combined algorithm (2B31)
  - Haddad, Z. S., E. A. Smith, C. D. Kummerow, T. Iguchi, M. R. Farrar, S. L. Durden, M. Alves, and W. S. Olson, 1997: The TRMM 'day-1' radar/radiometer combined rain-profiling algorithm. *J. Meteor. Soc. Japan*, ***75***, 799–809.
- GPM standard combined algorithm
  - Grecu, M., W. S. Olson, and E. M. Anagnostou, 2004: Retrieval of precipitation profiles from multiresolution, multifrequency active and passive microwave observations. *J. Appl. Meteor.*, **43**, 562–575.
  - Grecu, M., L. Tian, W. S. Olson, and S. Tanelli, 2011: A robust dual-frequency radar profiling algorithm. *J. Appl. Meteor.Clim.*, **50**, 1543–1557.
- Goddard Profiling (GPROF) algorithm module
  - Masunaga, H., and C. D. Kummerow, 2005: Combined radar and radiometer analysis of precipitation profiles for a parametric retrieval algorithm. *J. Atmos. Oceanic Technol.*, **22**, 909–929.
  - Munchak, S. J., and C. D. Kummerow, 2011: A Modular Optimal Estimation Method for Combined Radar-Radiometer Precipitation Profiling, *J. Appl. Meteor.Clim.*, **50**, 433-448.

Flowchart

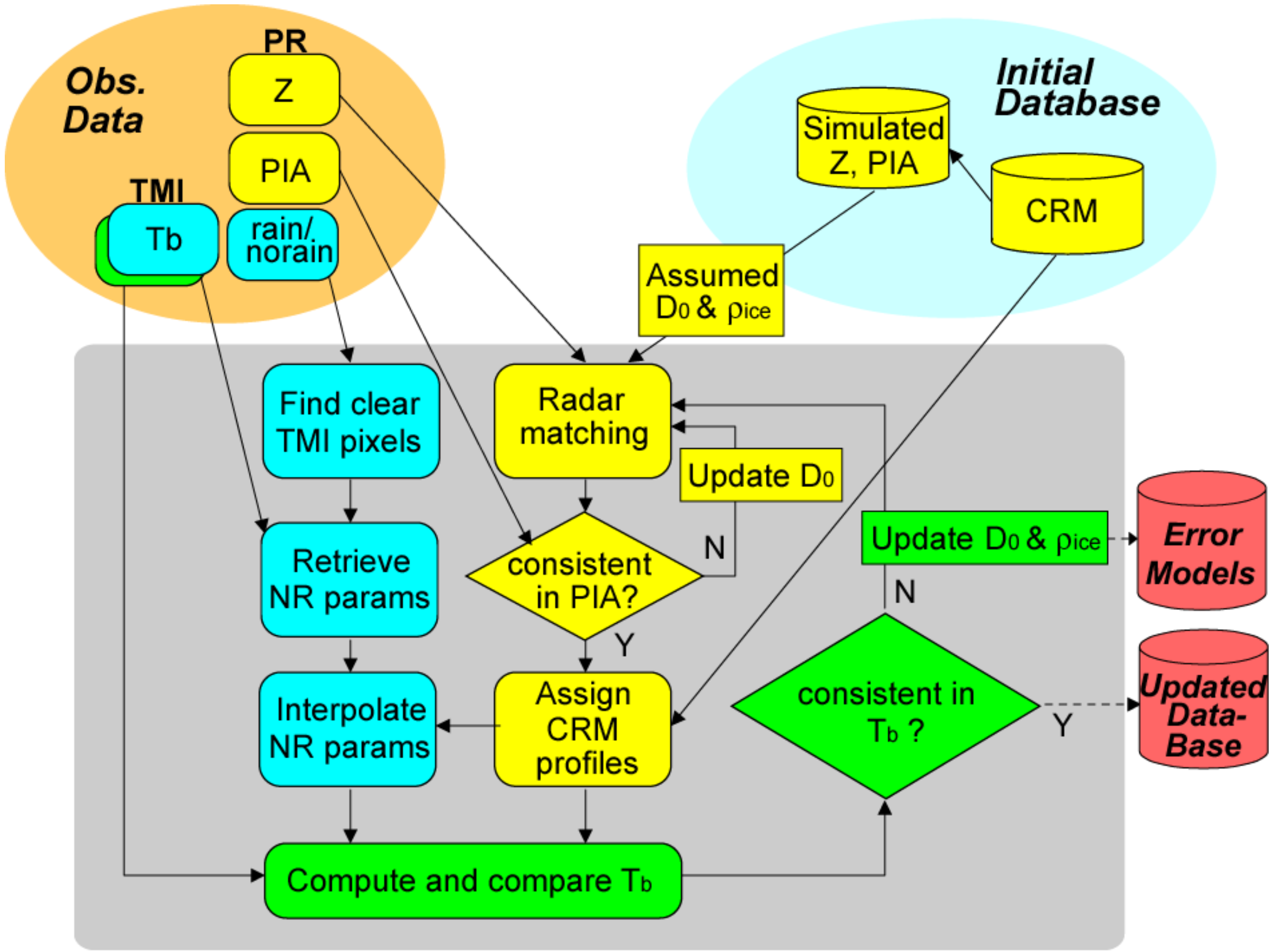

Obs. Data
PR
Z
PIA
rain/ norain
TMI
Tb
Initial Database
Simulated Z, PIA
CRM
Assumed D0 & ρice
Find clear TMI pixels
Radar matching
Update D0
Retrieve NR params
consistent in PIA?
N
Y
Update D0 & ρice
Error Models
N
Interpolate NR params
Assign CRM profiles
consistent in Tb ?
Y
Updated Data-Base
Compute and compare Tb

Flowchart

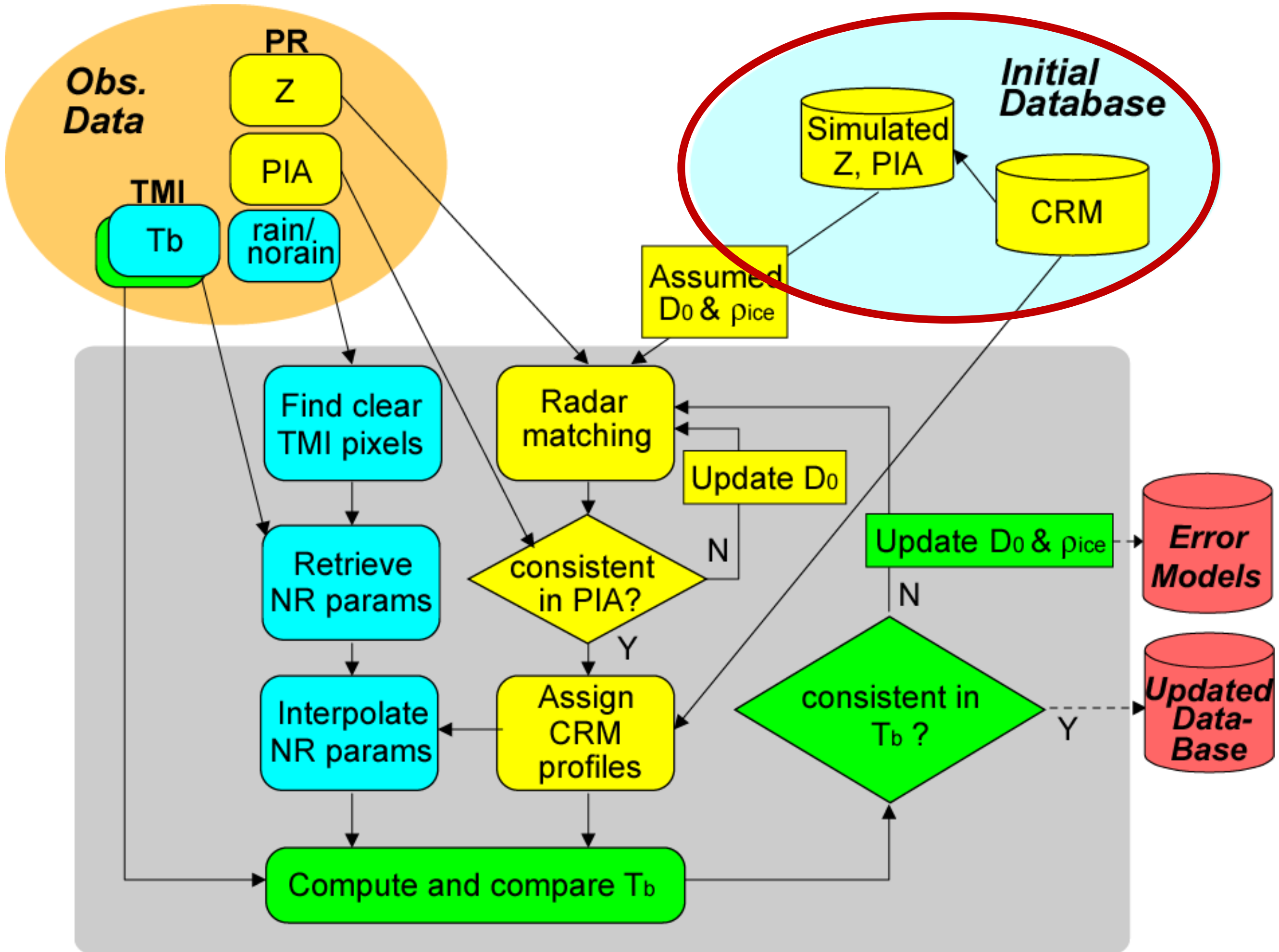
Obs. Data
PR
Z
PIA
rain/ norain
TMI
Tb
Initial Database
Simulated Z, PIA
CRM
Assumed D0 & ρice
Find clear TMI pixels
Radar matching
Update D0
Retrieve NR params
consistent in PIA?
N
Y
Update D0 & ρice
Error Models
N
Interpolate NR params
Assign CRM profiles
consistent in Tb ?
Y
Updated Data-Base
Compute and compare Tb

Initial CRM database

- Cloud-Resolving Model (CRM) database
  - Goddard Cumulus Ensemble Model (GCE) and UW-Nonhydrostatic Modeling System.
  - About 30 snapshots from different simulations
    - Tropical convection & squall line
    - Hurricane
    - Mid Atlantic cold/warm frontal rain
    - Extra-tropical cyclone
    - …
  - 20,000+ pixels for each snapshot

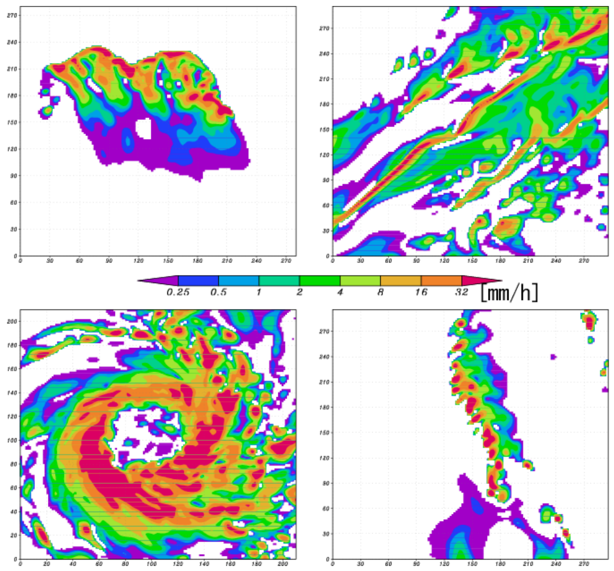

Flowchart

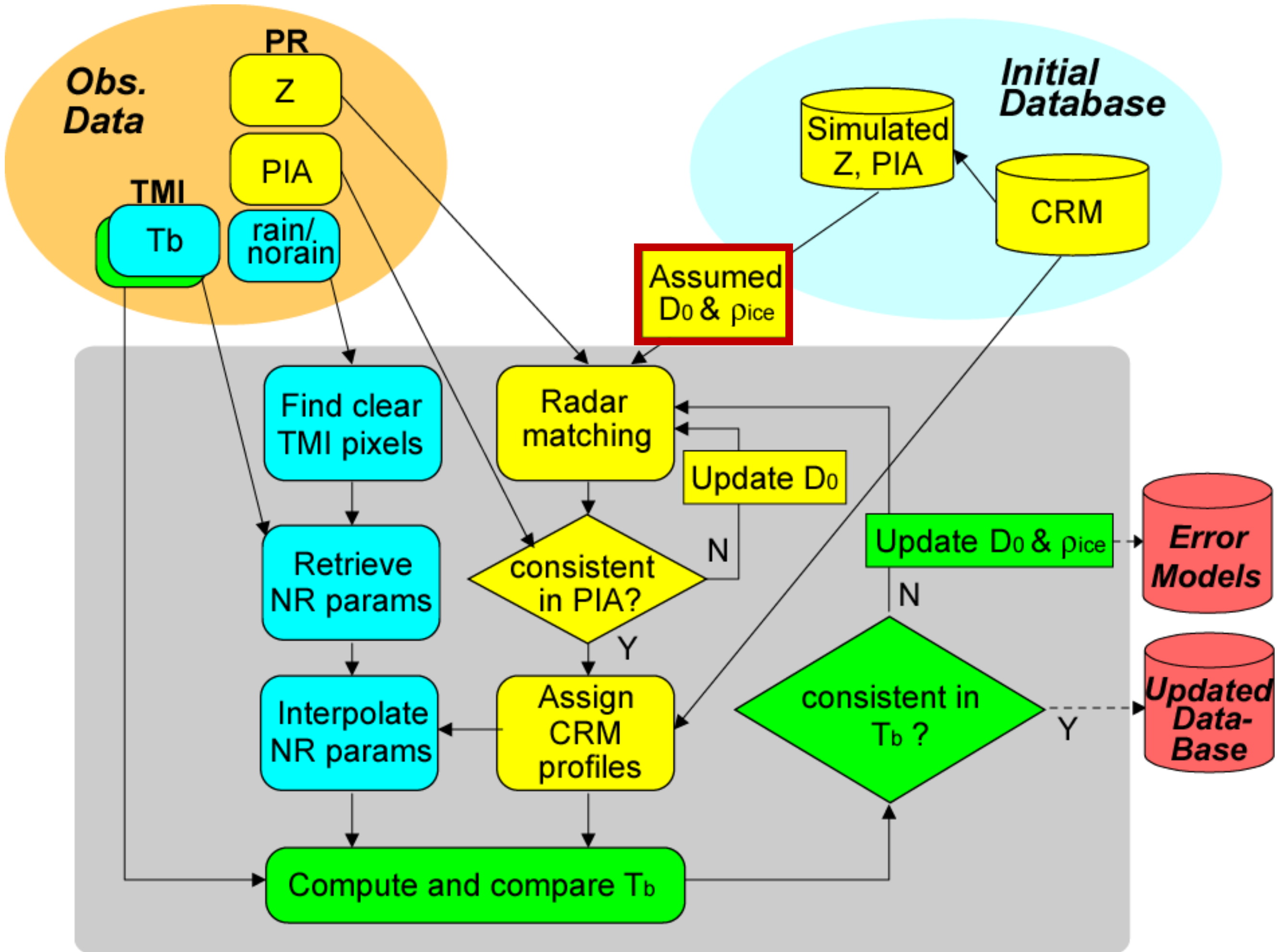

Obs. Data
PR
Z
PIA
TMI
Tb
rain/ norain
Initial Database
Simulated Z, PIA
CRM
Assumed D0 & ρice
Find clear TMI pixels
Radar matching
Update D0
Retrieve NR params
consistent in PIA?
N
Y
Update D0 & ρice
Error Models
N
Interpolate NR params
Assign CRM profiles
consistent in Tb ?
Y
Updated Data-Base
Compute and compare Tb

Raining parameters -1

- DSD assumption
  - The initial assumption is same as adopted by the PR operational (2A25) algorithm.
  - Allow D0 (median volume diameter) to change +/-3 and +/-6mm around the initial value when adjusting DSD.

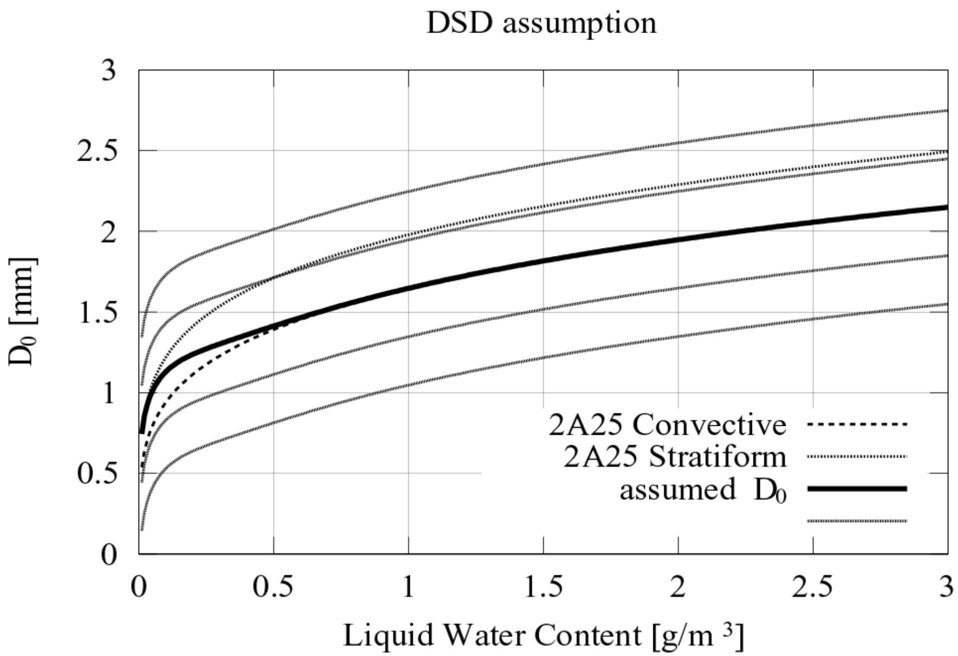

Flowchart

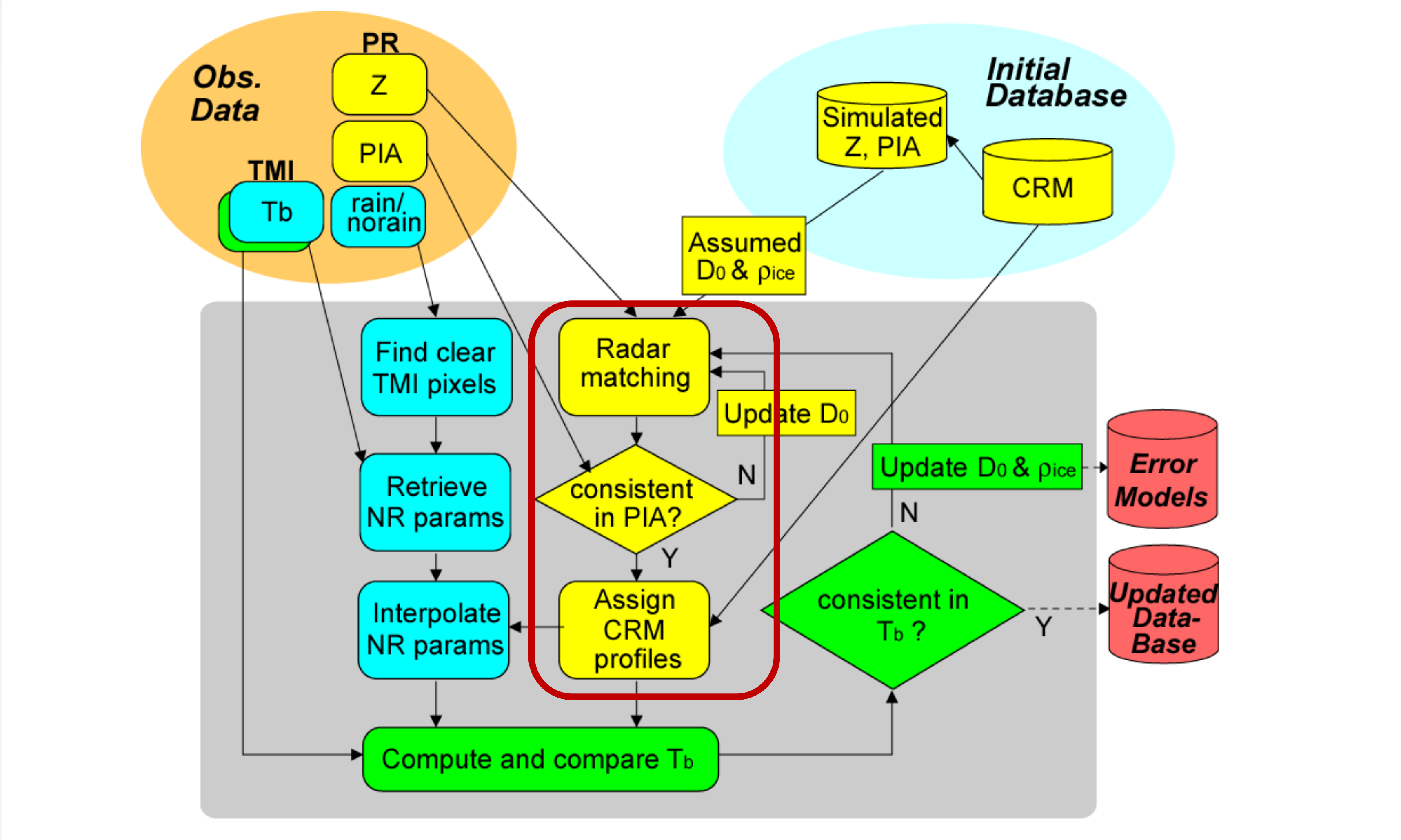

Obs. Data
PR
Z
PIA
TMI
Tb
rain/ norain
Initial Database
Simulated Z, PIA
CRM
Assumed D0 & ρice
Find clear TMI pixels
Retrieve NR params
Interpolate NR params
Radar matching
Update D0
consistent in PIA?
N
Y
Assign CRM profiles
Update D0 & ρice
Error Models
N
consistent in Tb ?
Y
Updated Data-Base
Compute and compare Tb

Raining parameters -2

- PR retrieval
  - Find the best-fit CRM profile in the radar reflectivity (Z) space.
- PIA adjustment
  - Parallel to the TRMM Radar algorithm
  - Path-integrated attenuation (PIA) is used when reliable.
  - The best solution is sought under the constraint of PIA by varying the DSD model.

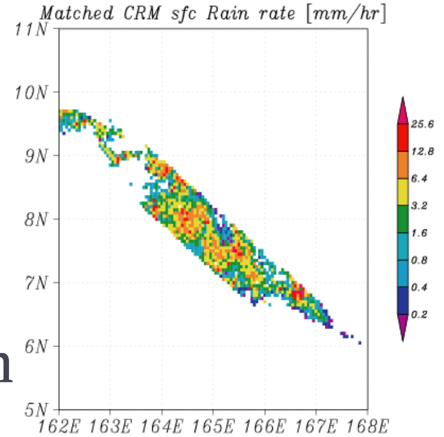

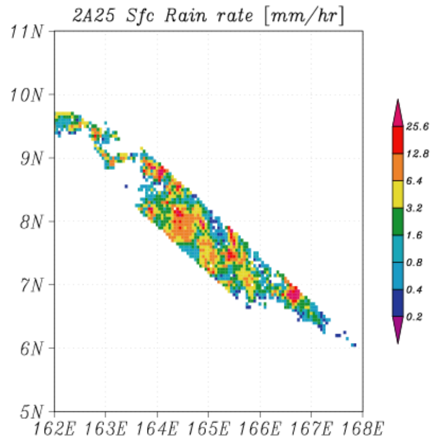

Flowchart

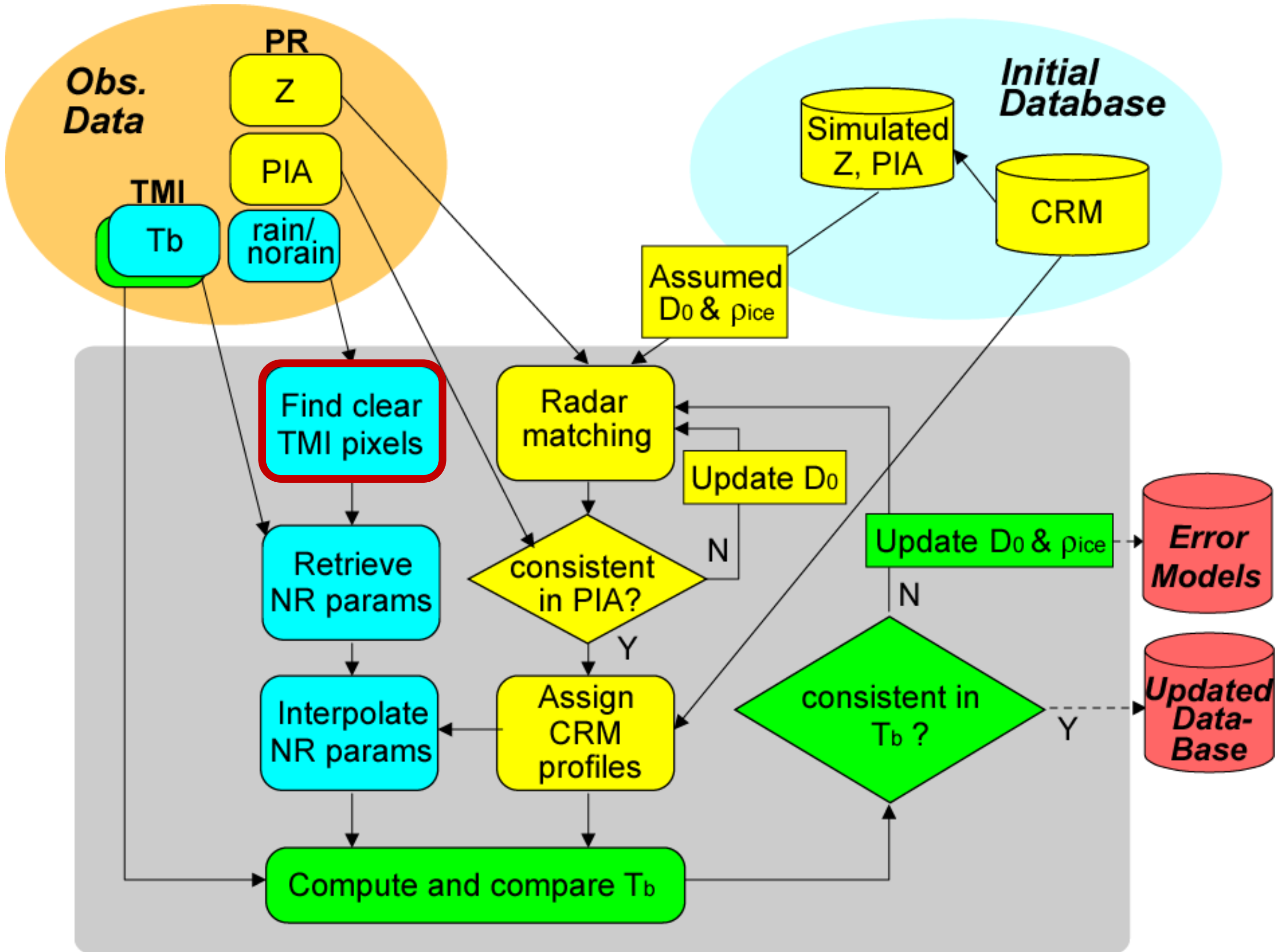

Obs. Data
PR
Z
PIA
TMI
Tb
rain/ norain
Initial Database
Simulated Z, PIA
CRM
Assumed D0 & ρice
Find clear TMI pixels
Radar matching
Update D0
Retrieve NR params
consistent in PIA?
N
Y
Update D0 & ρice
Error Models
N
Interpolate NR params
Assign CRM profiles
consistent in Tb ?
Y
Updated Data-Base
Compute and compare Tb

Identifying rain-free TMI FOVs

- Find PR pixels located within a given TMI 19-GHz FOV.
- If none of these PR pixels contains a rainfall signal, the TMI footprint is defined as "rain free".

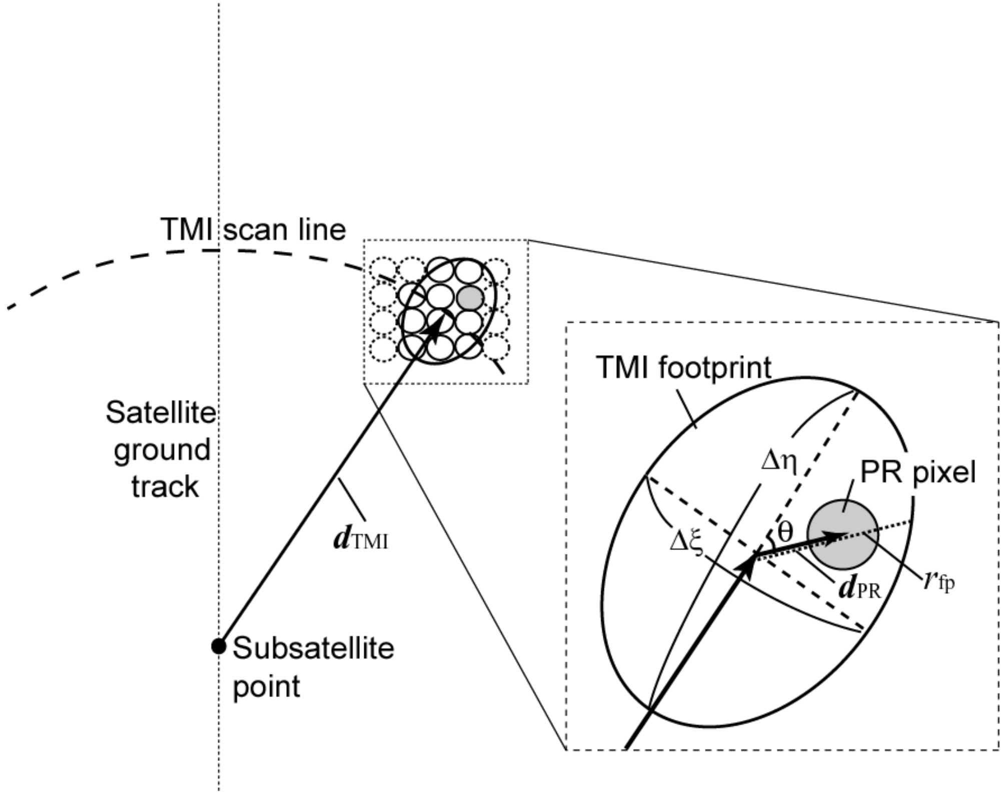

Flowchart

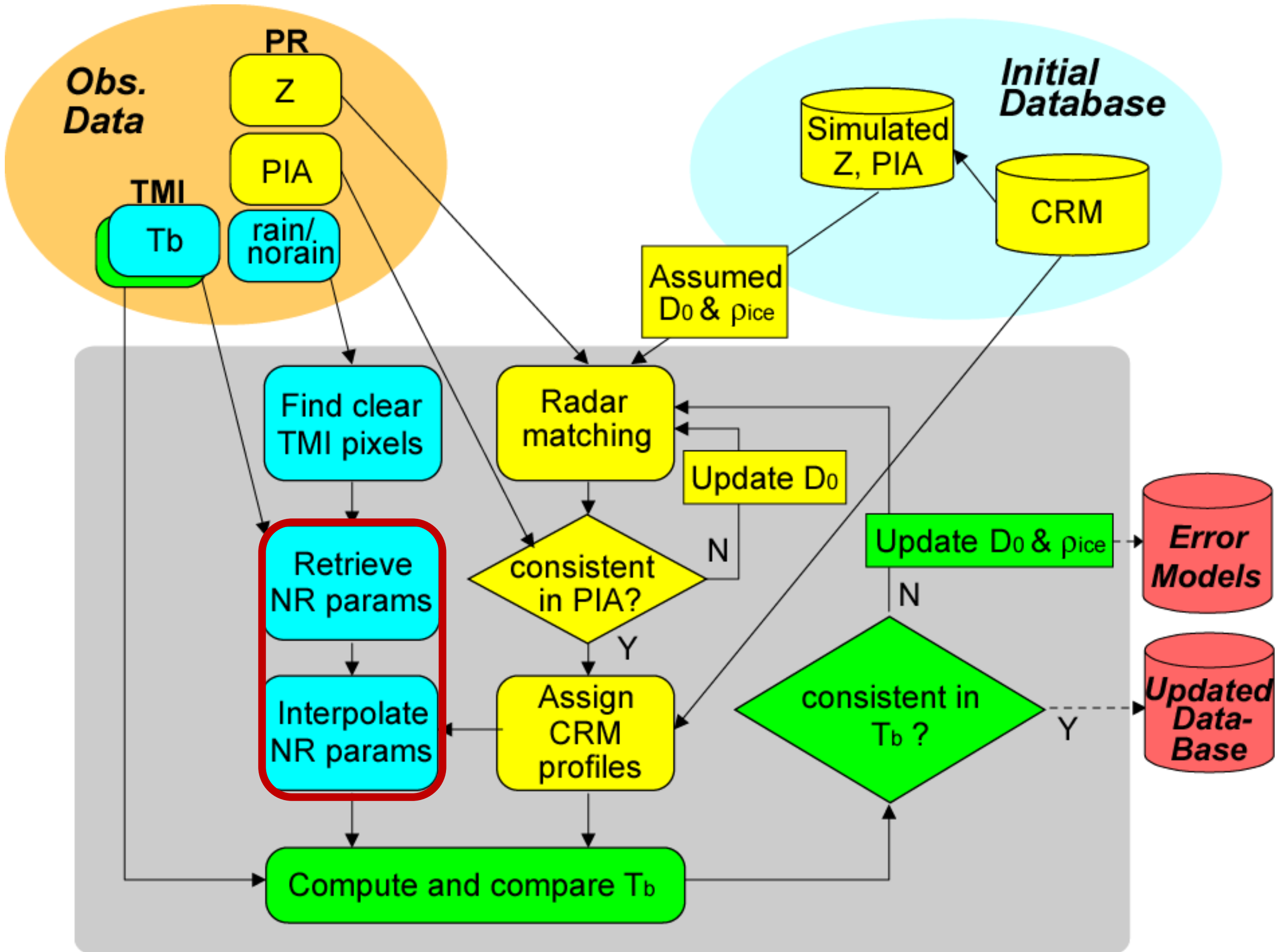

Obs. Data
PR
Z
PIA
TMI
Tb
rain/ norain
Initial Database
Simulated Z, PIA
CRM
Assumed D0 & ρice
Find clear TMI pixels
Radar matching
Update D0
Retrieve NR params
consistent in PIA?
N
Y
Update D0 & ρice
N
Error Models
Interpolate NR params
Assign CRM profiles
consistent in Tb ?
Y
Updated Data-Base
Compute and compare Tb

Nonraining parameters

- Retrieve nonraining parameters (water vapor, surface wind, cloud water, and SST) for rain-free TMI footprints.
- WV and CLW are also derived for raining PR pixels from PR-matched CRM profiles.
- The complete fields of the non-raining parameters are obtained by spatial interpolation.

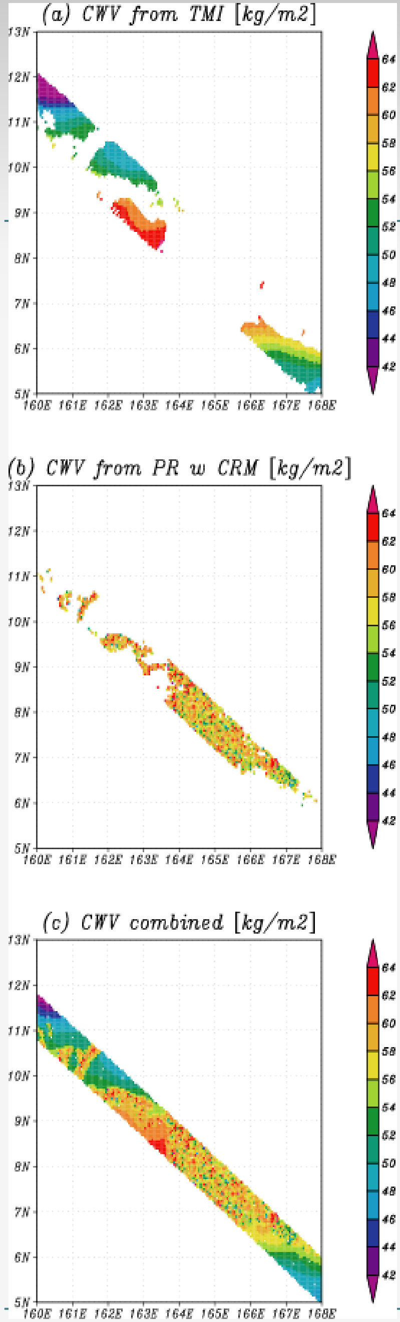

Flowchart

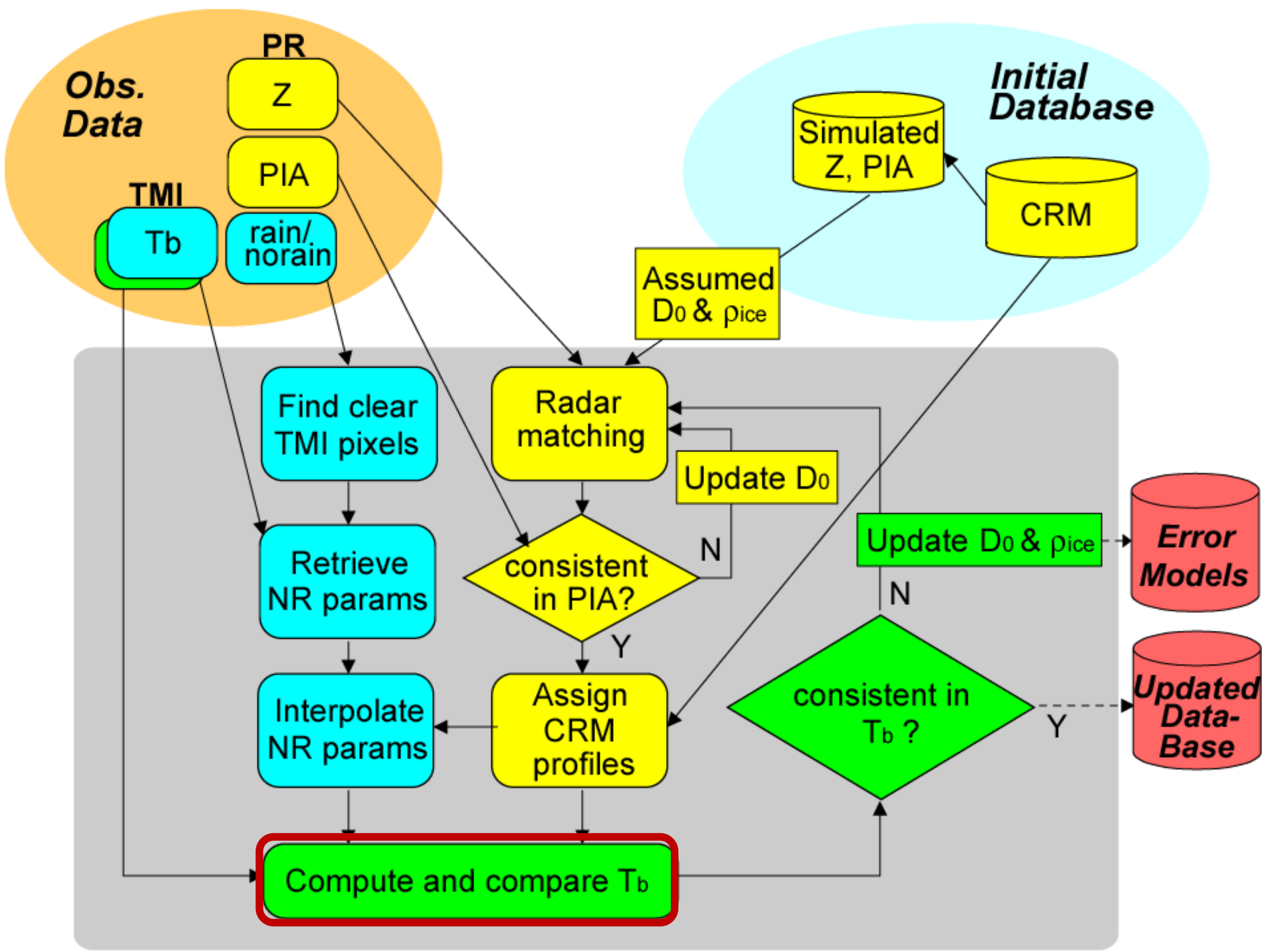

Obs. Data
PR
Z
PIA
rain/ norain
TMI
Tb
Initial Database
Simulated Z, PIA
CRM
Assumed D0 & ρice
Find clear TMI pixels
Radar matching
Update D0
Retrieve NR params
consistent in PIA?
N
Y
Update D0 & ρice
N
Error Models
Interpolate NR params
Assign CRM profiles
consistent in Tb ?
Y
Updated Data-Base
Compute and compare Tb

T_b computations -1

- Compute brightness temperatures
  - The 3-D structure of all the raining and nonraining parameters are available from the previous steps.
  - Microwave brightness temperature is computed for comparison with TMI measurements.
  - A slant TMI sight line intersecting neighboring columns is taken into account.
  - Beam convolution is applied with a 2-D Gaussian beam pattern.

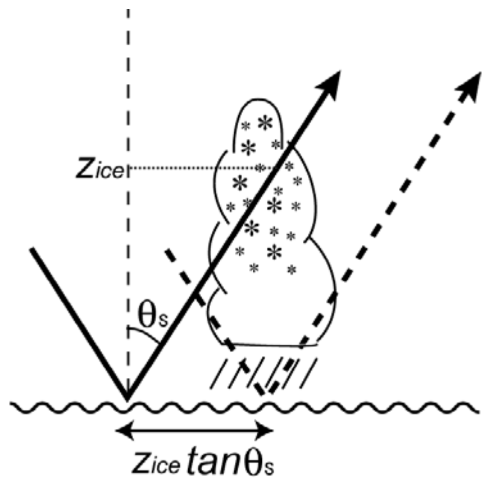

T_b computations -2

- PR-retrieved precipitation profiles exhibit biases in the computed T_b with the initial assumptions.

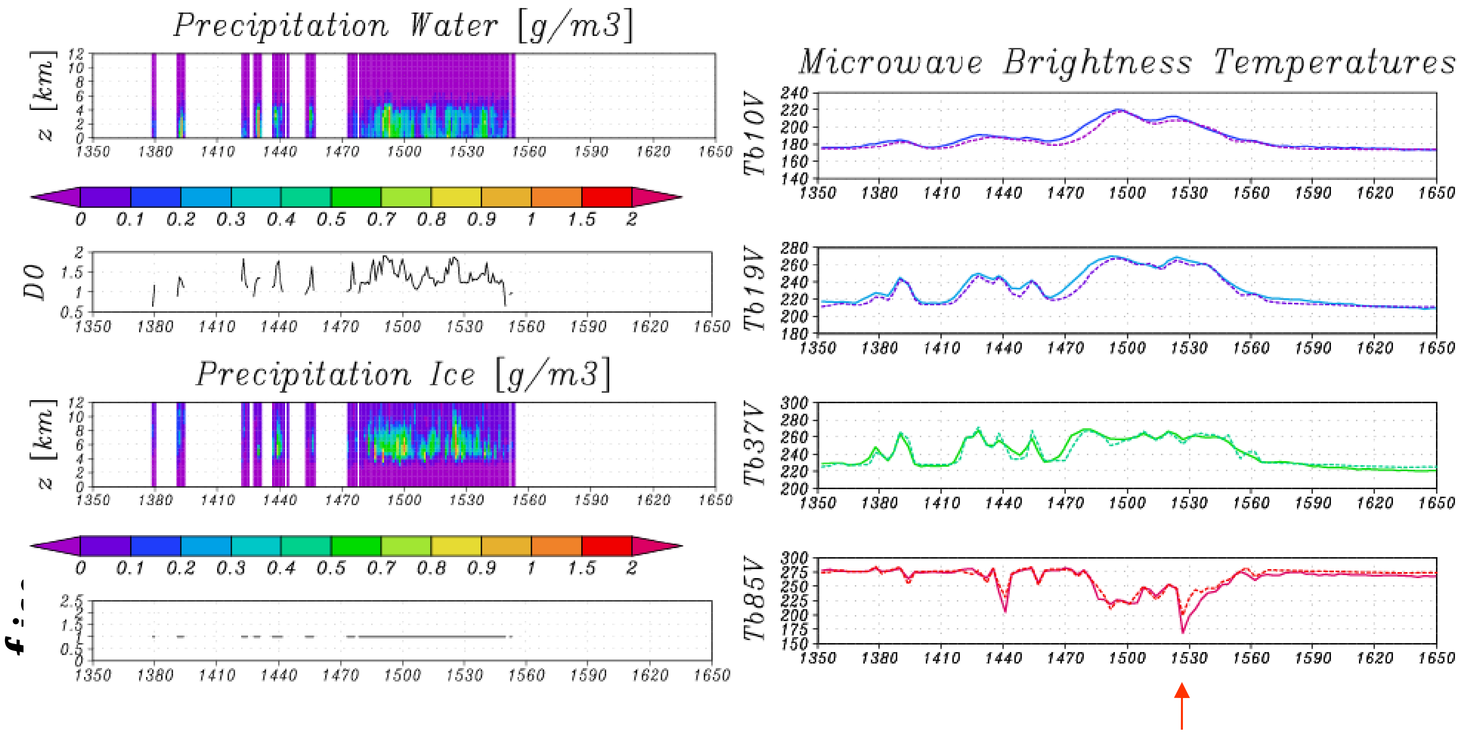

Flowchart

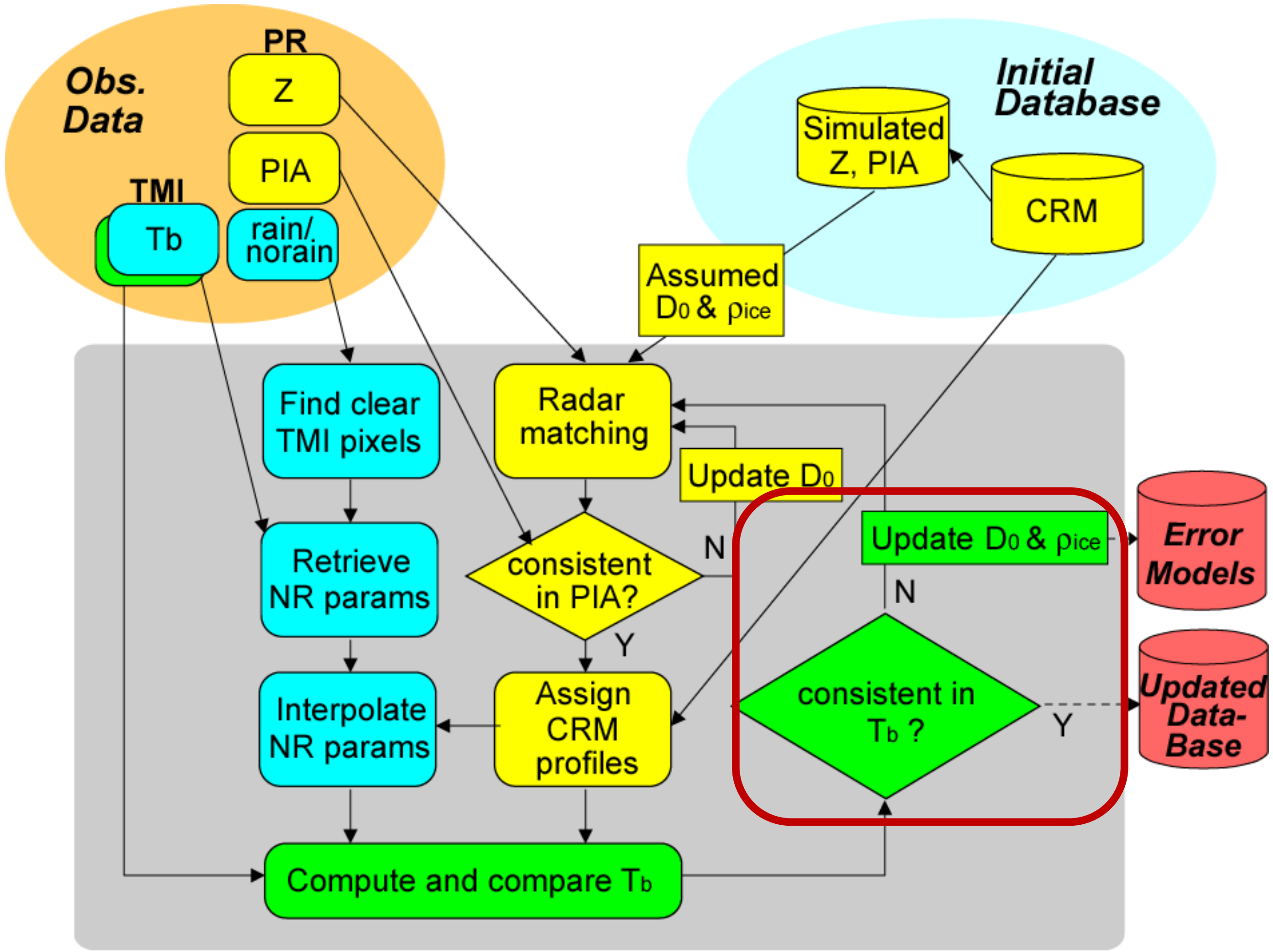

Obs. Data
PR
Z
PIA
TMI
Tb
rain/ norain
Initial Database
Simulated Z, PIA
CRM
Assumed D0 & ρice
Find clear TMI pixels
Radar matching
Update D0
Retrieve NR params
consistent in PIA?
N
Y
Update D0 & ρice
N
Error Models
Interpolate NR params
Assign CRM profiles
consistent in Tb ?
Y
Updated Data-Base
Compute and compare Tb

Updating assumptions -1

- Discrepancy in brightness temperatures
  - A larger (smaller) D_0 results in a colder (warmer) Tb in the emission channels through the underestimation (overestimation) of rain water.
  - A higher (lower) ice-particle density (or fluffiness) results in a colder (warmer) Tb in the scattering channels.
- Adjustment of DSD and ice-density models
  - Modify D_0 and f_{ice} (relative factor multiplied to the original ice-density model) and iterate the retreival.

Updating assumptions -2

- DSD and ice-density models are adjusted so that the bias in Tb is minimized.

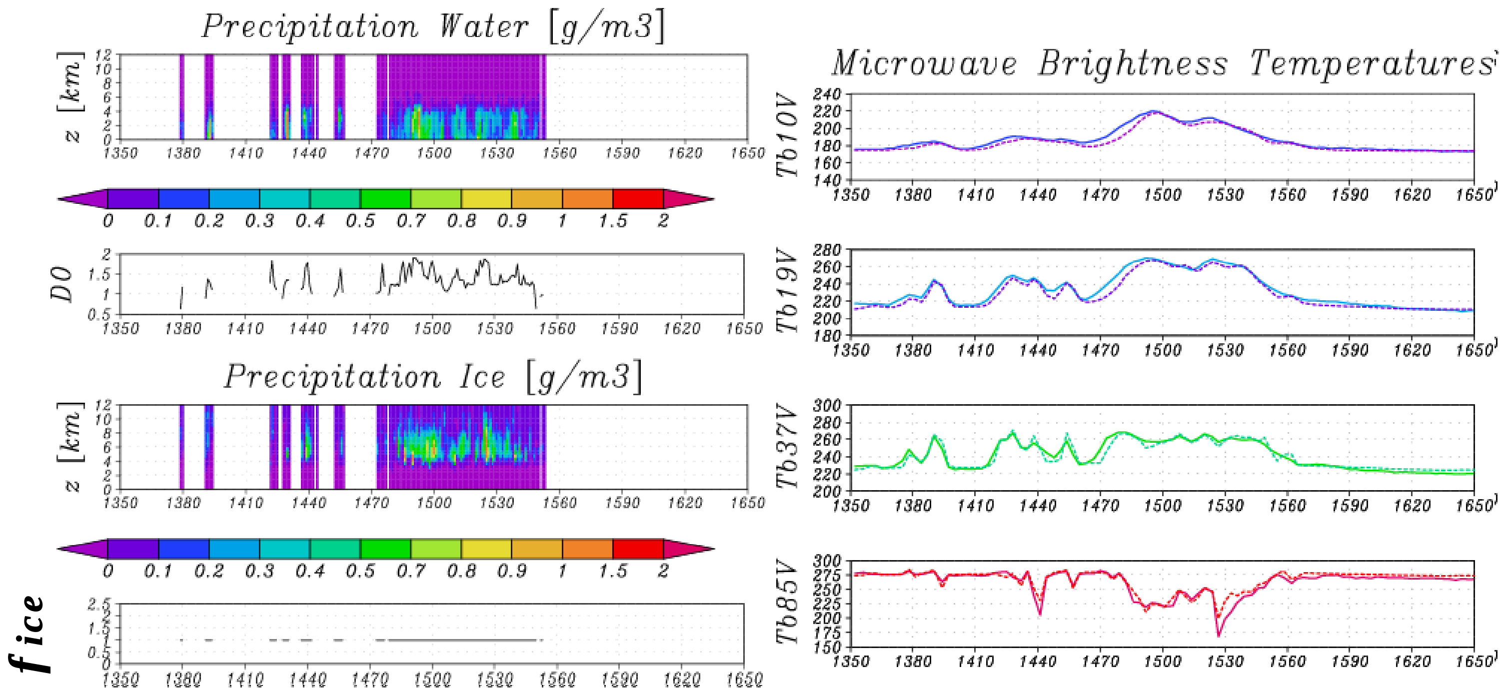

Global application - PR results

- Correlation with the PR operational (2A25) rain

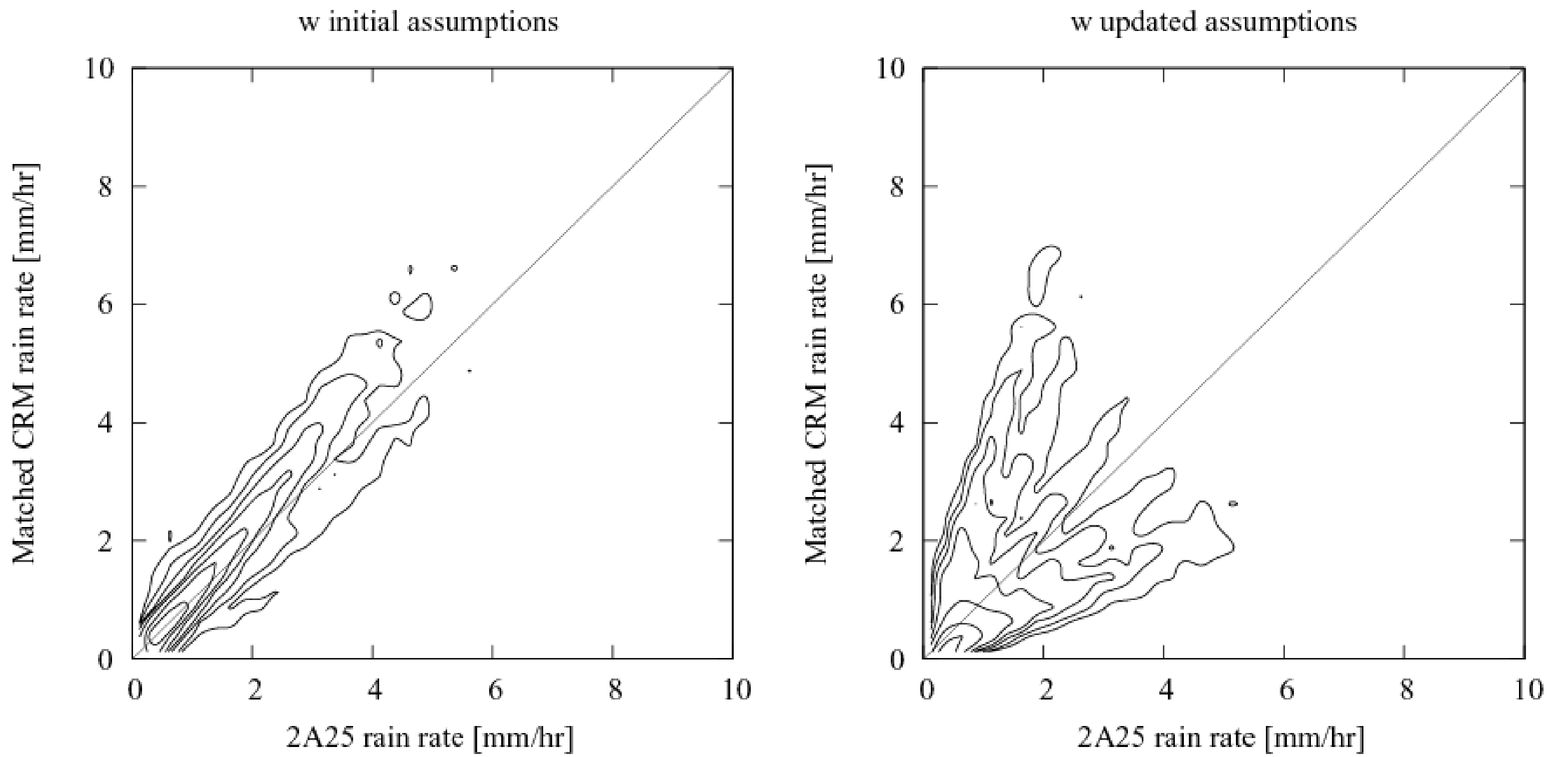

Global application - TMI results

- Statistics of computed/observed Tbs

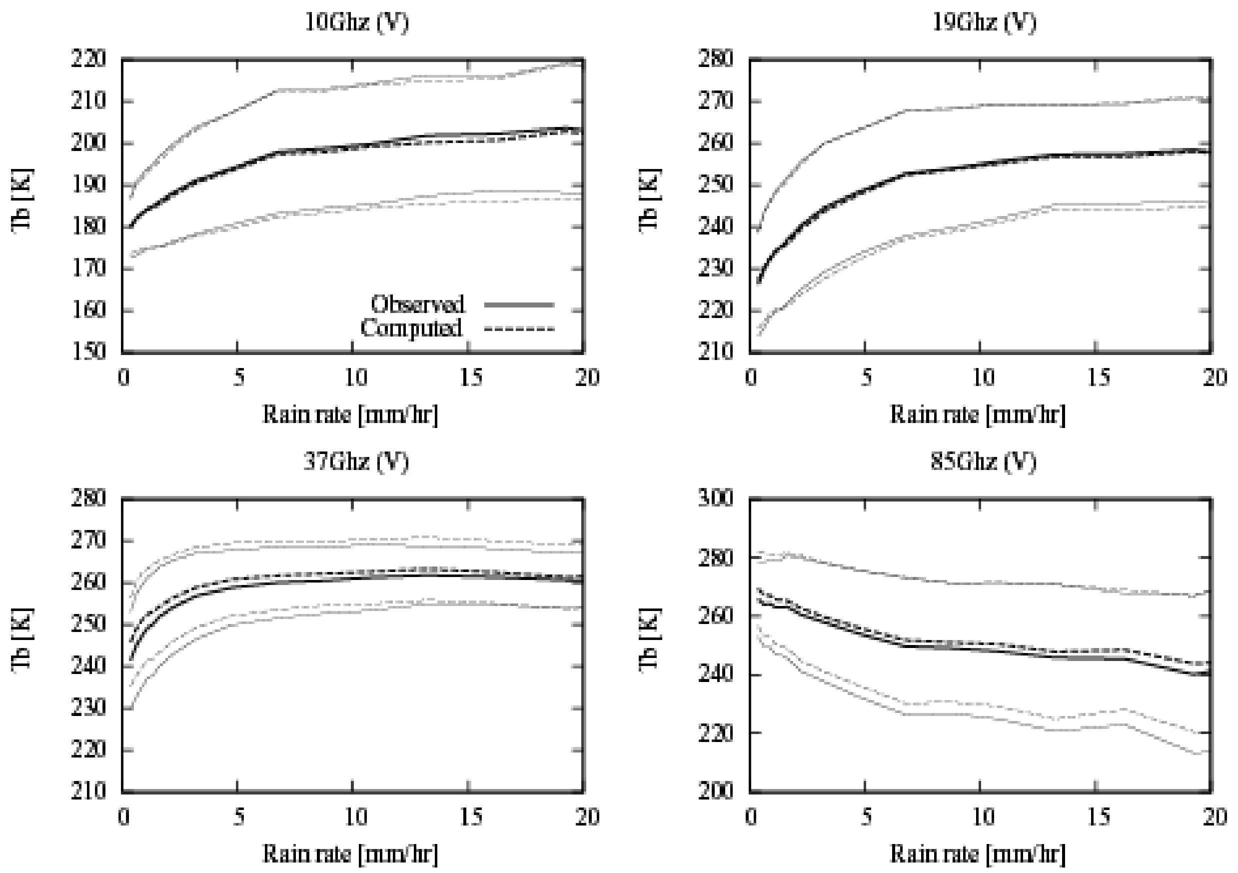

Global application - TMI results

- RMS error in T_b before/after updating assumptions.

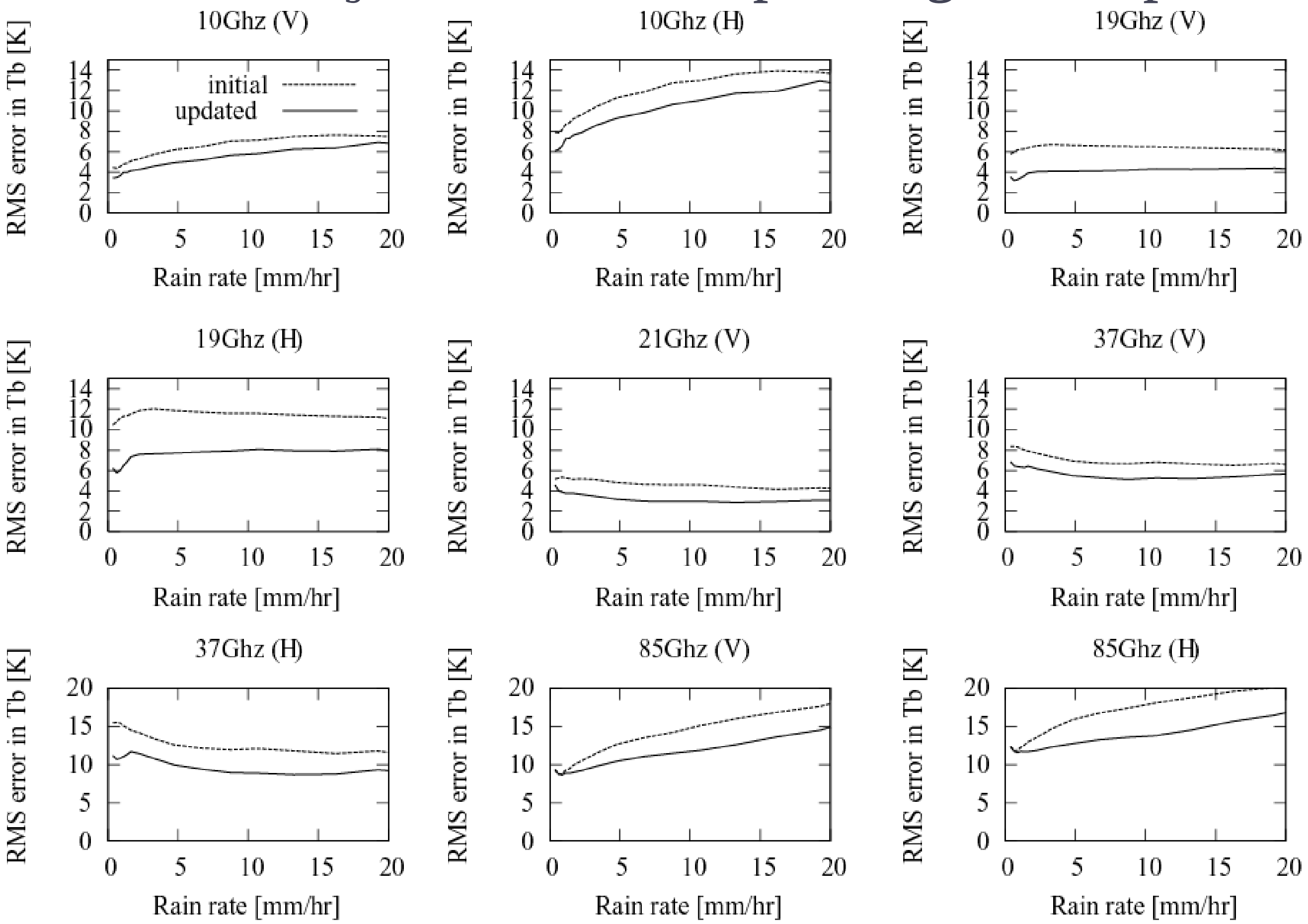

Global application - DSD model

- D0 as a function of surface liquid water content

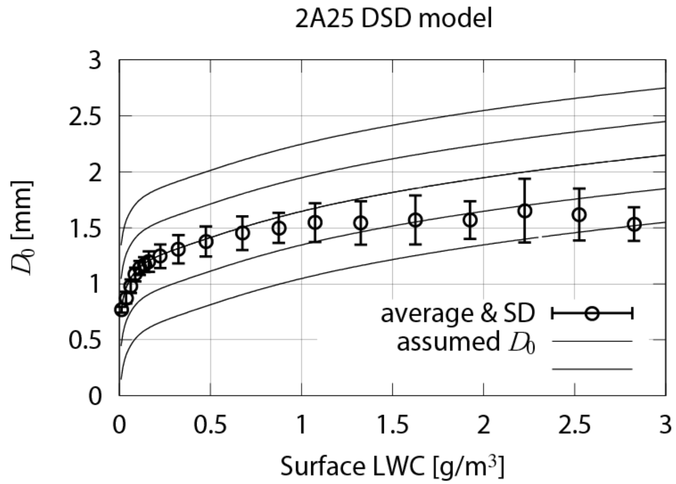

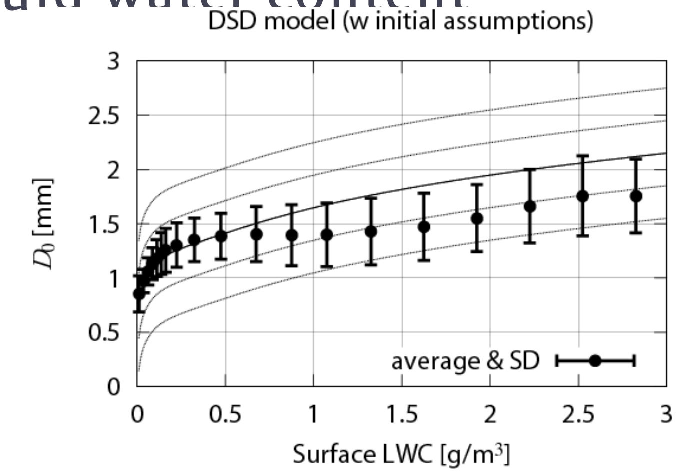

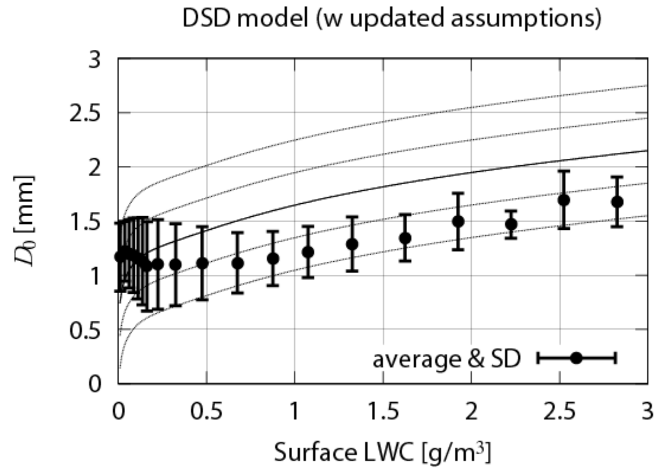

- PR PIA adjusts DSD only for heavy rainfall.
- TMI Tb adjusts DSD over the entire range of rainfall.

Summary – algorithm description

- Combined radar and radiometer algorithm
  - The **radar module** retrieves a full 3D rainfall structure but is susceptible to uncertainties in DSD assumptions
  - The **radiometer module** helps constrain the rain rate uncertainties in the radar retrieval.

Radar Module

Detailed profiling of precipitation profiles

Radiometer Module

Constrains uncertainties underlying the radar retrieval

Toward future applications

Global Precipitation Measurement (GPM)

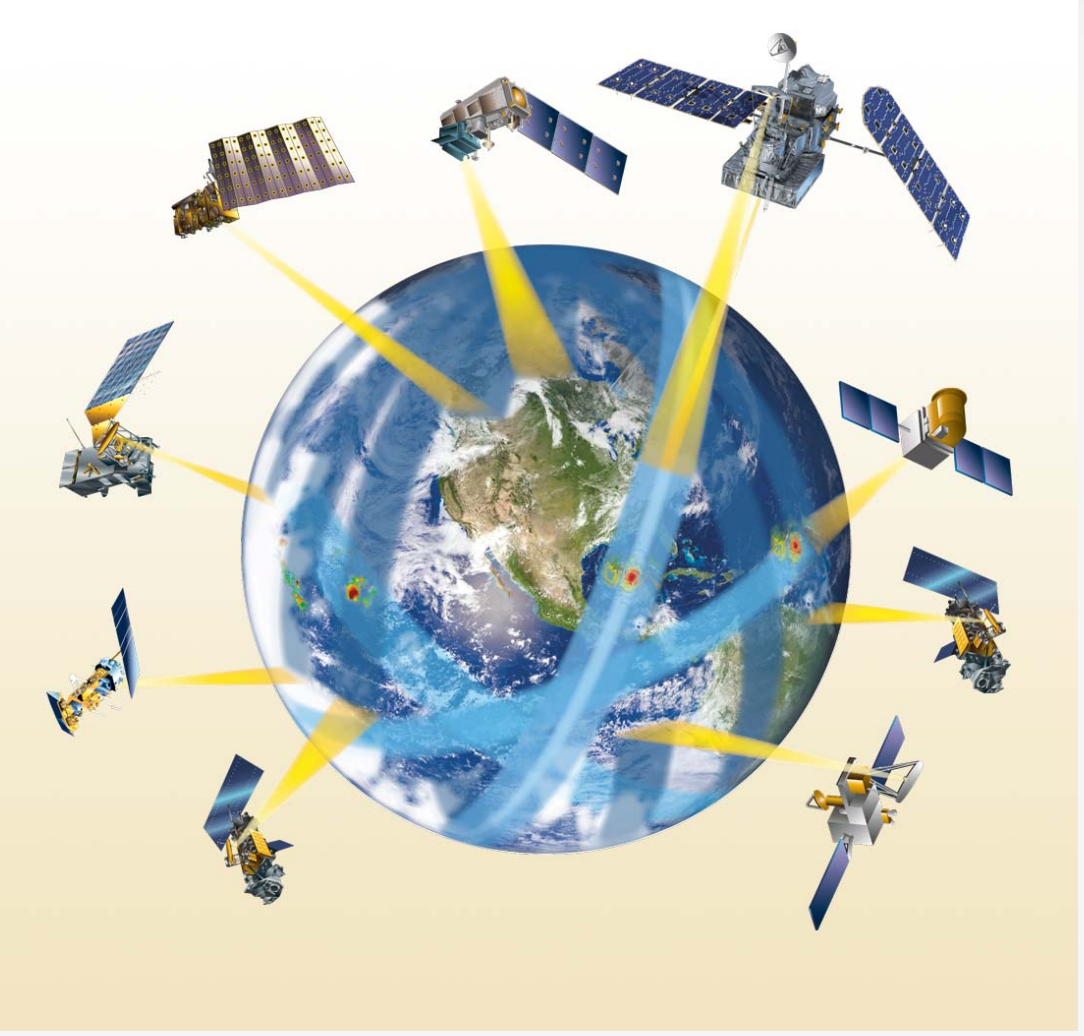

Combined algorithm in the GPM era

- Combined radar and radiometer algorithm
  - The **radar module** retrieves a full 3D rainfall structure but is susceptible to uncertainties in DSD assumptions
  - The **radiometer module** helps constrain the rain rate uncertainties in the radar retrieval.
- GPM
  - Consists of the core observatory and multiple constellation satellites.
    - Only the core satellite carries both radar and radiometer.
    - Other satellites have radiometers or sounders.
  - A combined algorithm runs with the core observatory.
    - Core satellite retrievals improves the constellation rainfall algorithm through an *a prior* database.

Flowchart

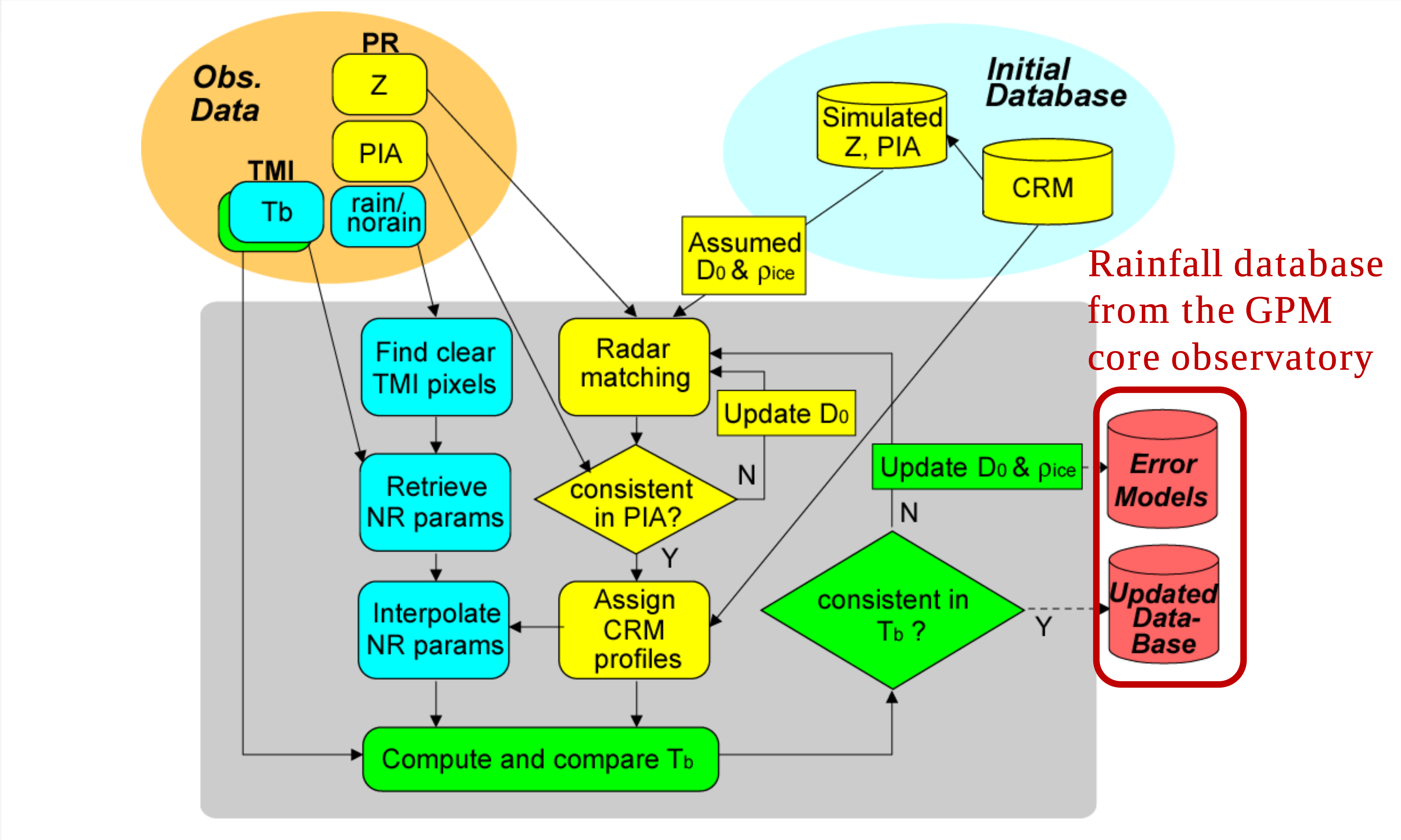
Obs. Data
PR
Z
PIA
TMI
Tb
rain/ norain
Initial Database
Simulated Z, PIA
CRM
Assumed D0 & ρice
Find clear TMI pixels
Radar matching
Update D0
Retrieve NR params
consistent in PIA?
N
Y
Update D0 & ρice
N
Error Models
Interpolate NR params
Assign CRM profiles
consistent in Tb ?
Y
Updated Data-Base
Compute and compare Tb
Rainfall database from the GPM core observatory

Global Precipitation Measurement (GPM)

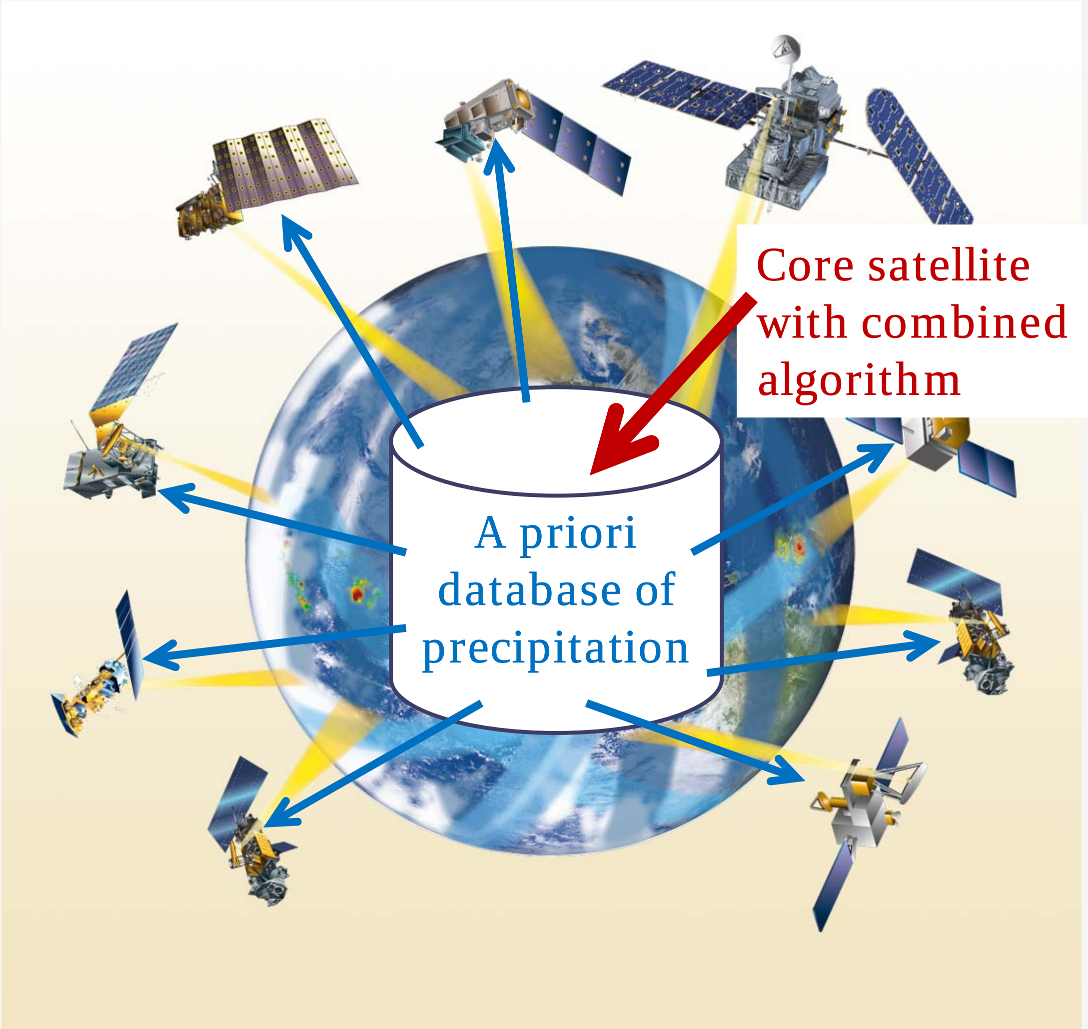

Precipitation Measurement from Space and its Applications

Ground Validation of Rain Data (1)

Hiroshi Uyeda

Hydrospheric Atmospheric Research Center, Nagoya University

Introduction

Tropical Rain Measuring Mission (TRMM) has been providing rain data since 1998 for tropical region and subtropical region. TRRM rain data in tropical sea with little rain data is valuable. Even on land, TRRM rain data is valuable for understanding characteristics of rain in the region where less rain gauge data and weather radar data are available.

TRMM daily rain data as 3B42 provides climatological characteristics of rain in the region where less rain gauge data is available. Recent development of Doppler radar observation in developing countries still requires past data of rain for understanding the current variation of rainfalls .

Studies on characteristics of rain revealed by comparison of TRMM data and rain gauge data would be a good example of study on characteristics of rain. Comparison of rain gauge data and TRMM rain data over Bangladesh will be introduced.

TRMM 3B42 underestimates rainfall amount in the moist region during the monsoon period. This is related to the not tall convection in the moist environment. Analyses of TRMM rain radar data revealed that not tall convections provide large amount of rain even the cloud height is relatively low comparing with thunder clouds in pre-monsoon in Bangladesh.

Introduction

Understanding the vertical structure of precipitation systems, dynamical characteristics of severe storms will be next target to study with Doppler radar. Recent development of Doppler radar network in Bangladesh and preliminary results obtained by the Bangladesh Meteorological Department Doppler radar will be introduced. Numerical simulation of the fast moving system observed by the Doppler radar will be introduced.

Furthermore, X-band polarimetric radar network of Ministry of Land, Infrastructure Transport and Tourism, Japan will be introduced briefly showing a heavy rain case, in order to have a view on next generation radar.

Through these works merit of TRMM measurement of rain and expectation to GPM will became clear.

First comparison of weather radar and TRMM PR was made in GAME/HUBEX (Huaihe River Basin Experiment).

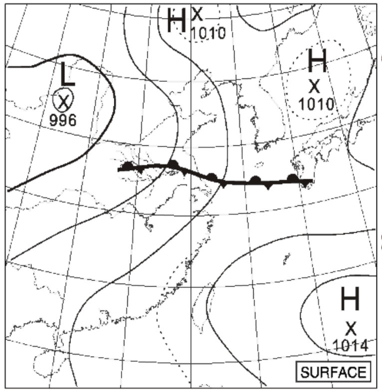

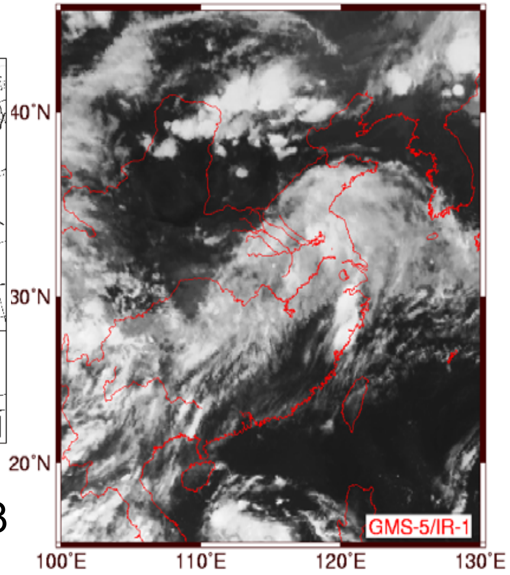

20JST 29 June 1998

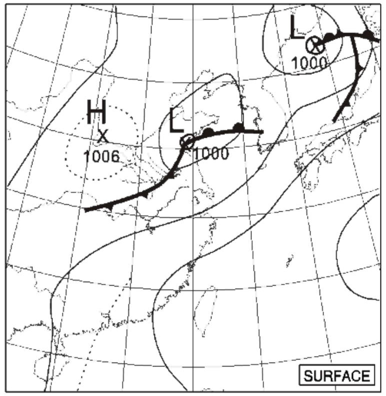

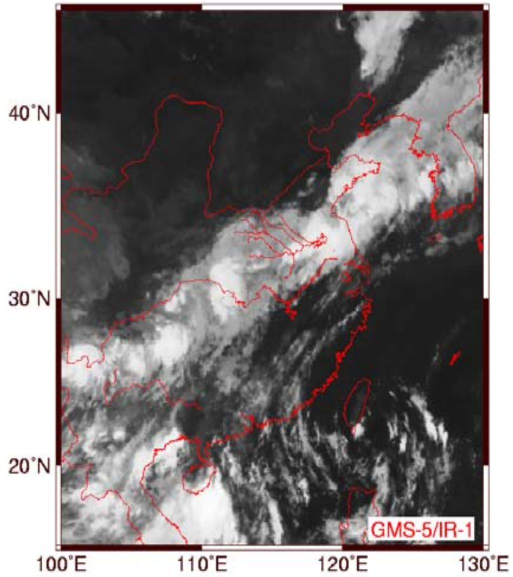

08JST 2 July 1998

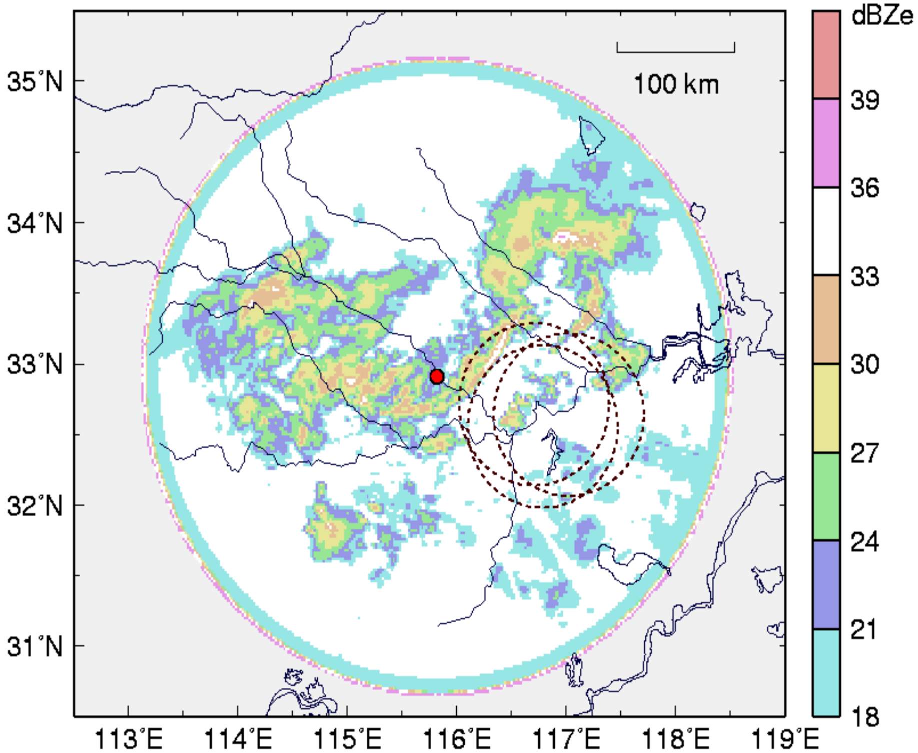

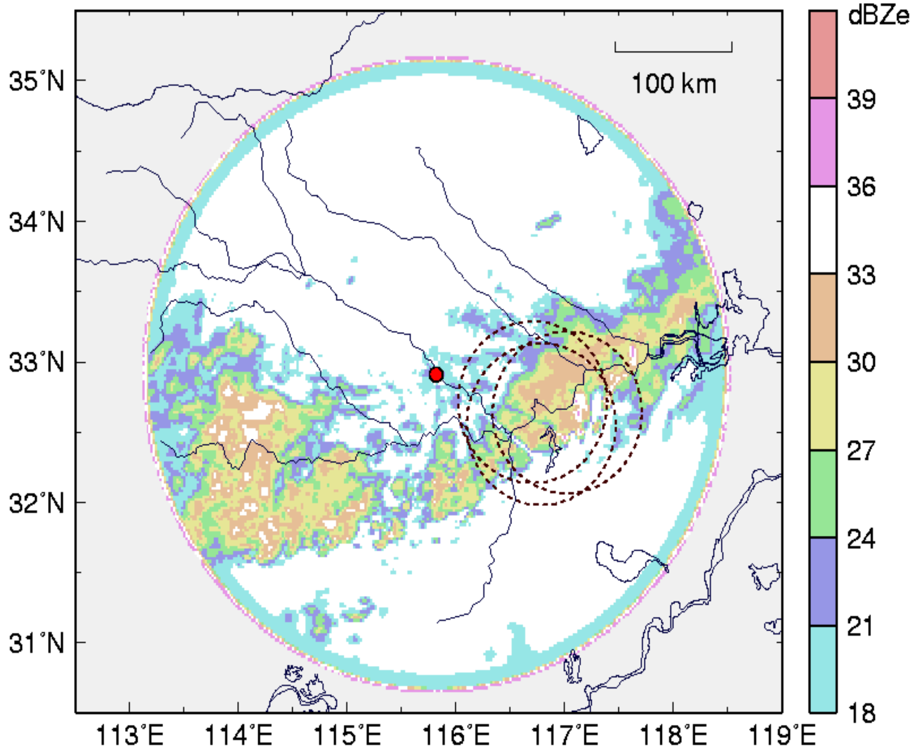

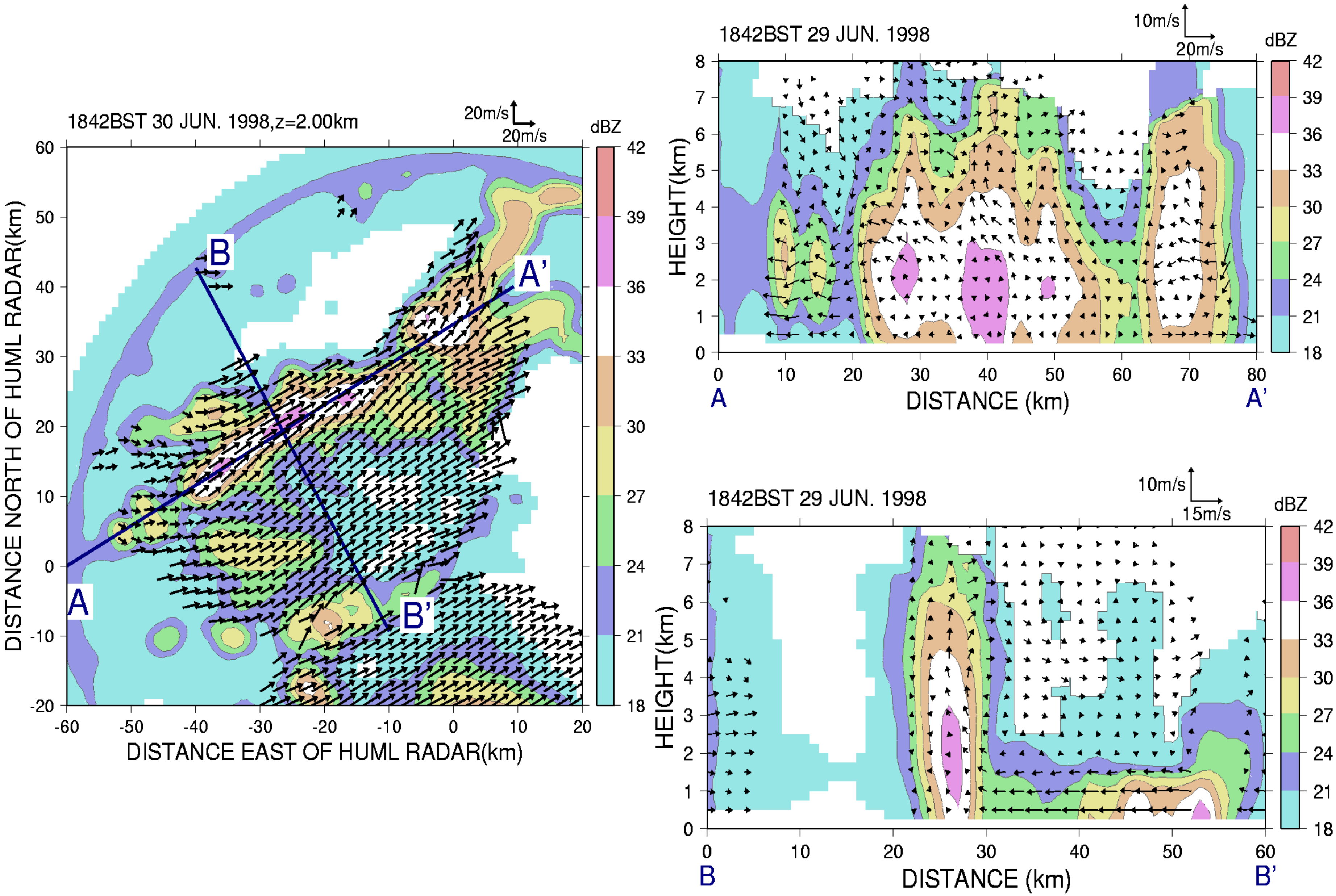

1842BST 30 JUN. 1998,z=2.00km
20m/s
20m/s
dBZ
DISTANCE NORTH OF HUML RADAR(km)
DISTANCE EAST OF HUML RADAR(km)
A
A'
B
B'
1842BST 29 JUN. 1998
10m/s
20m/s
HEIGHT(km)
DISTANCE (km)
1842BST 29 JUN. 1998
10m/s
15m/s
HEIGHT(km)
DISTANCE (km)

前坂 剛

GAME/HUBEX (Huaihe River Basin Experiment)

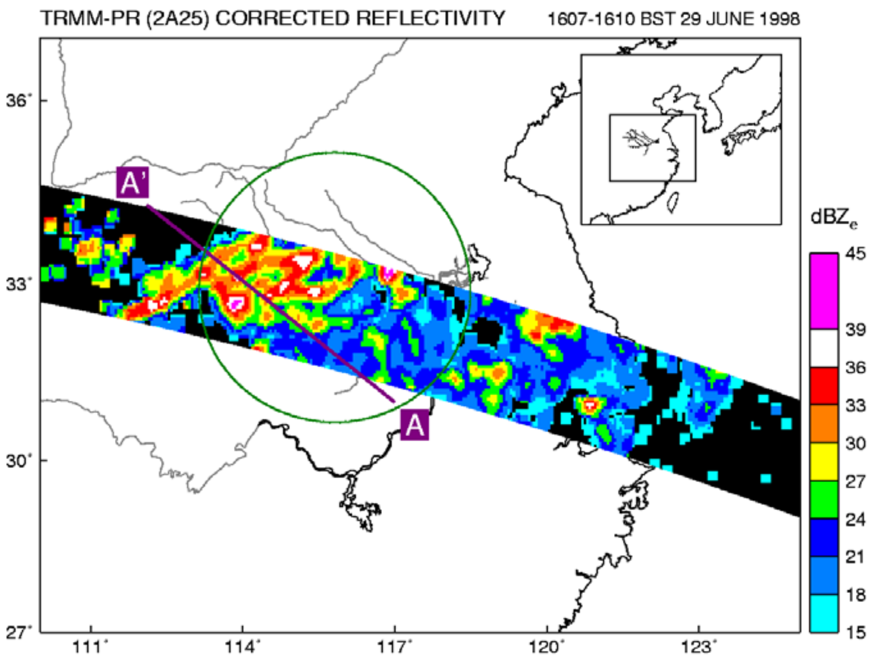

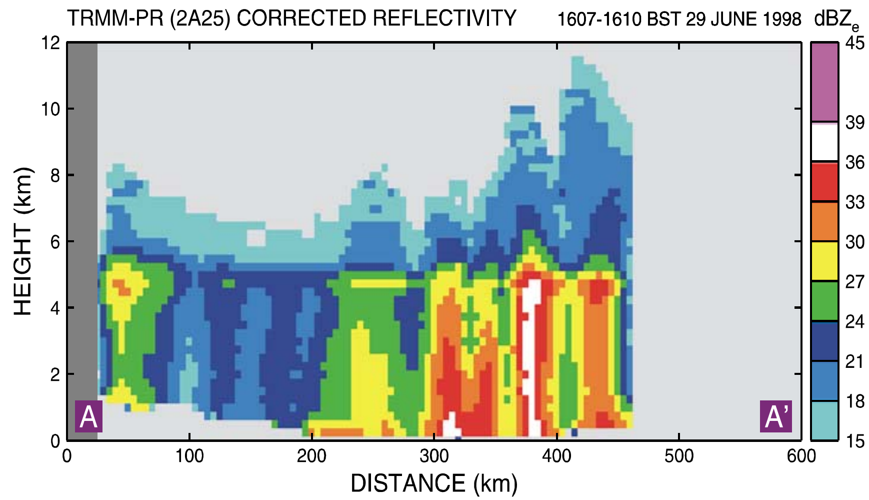

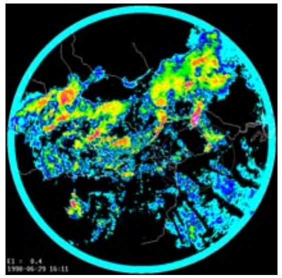

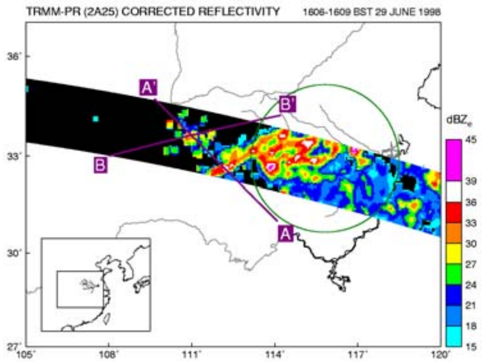

1607-1610 BST 29 JUN. 1998

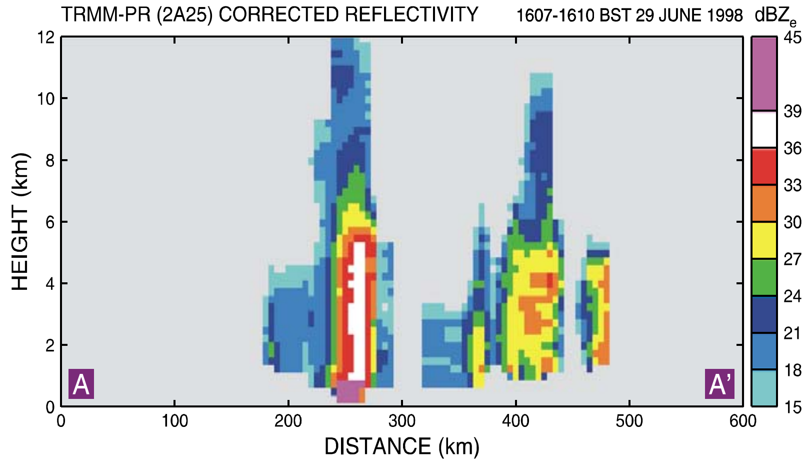

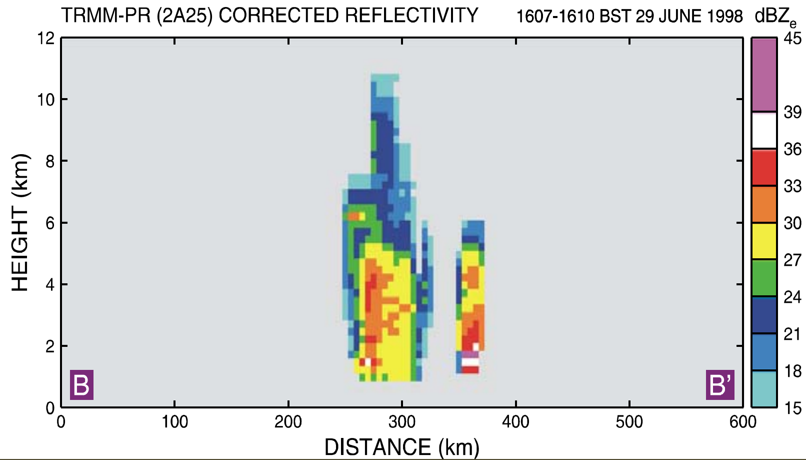

Rainfall in Bangladesh as an Example

Characteristics of TRMM derived rainfall in the SAARC region: Preparation to utilize GPM data in South Asia

Hiroshi Uyeda
and
Rafi Uddin (BUET)
Md. N. Islam (SMRC)

Target Area

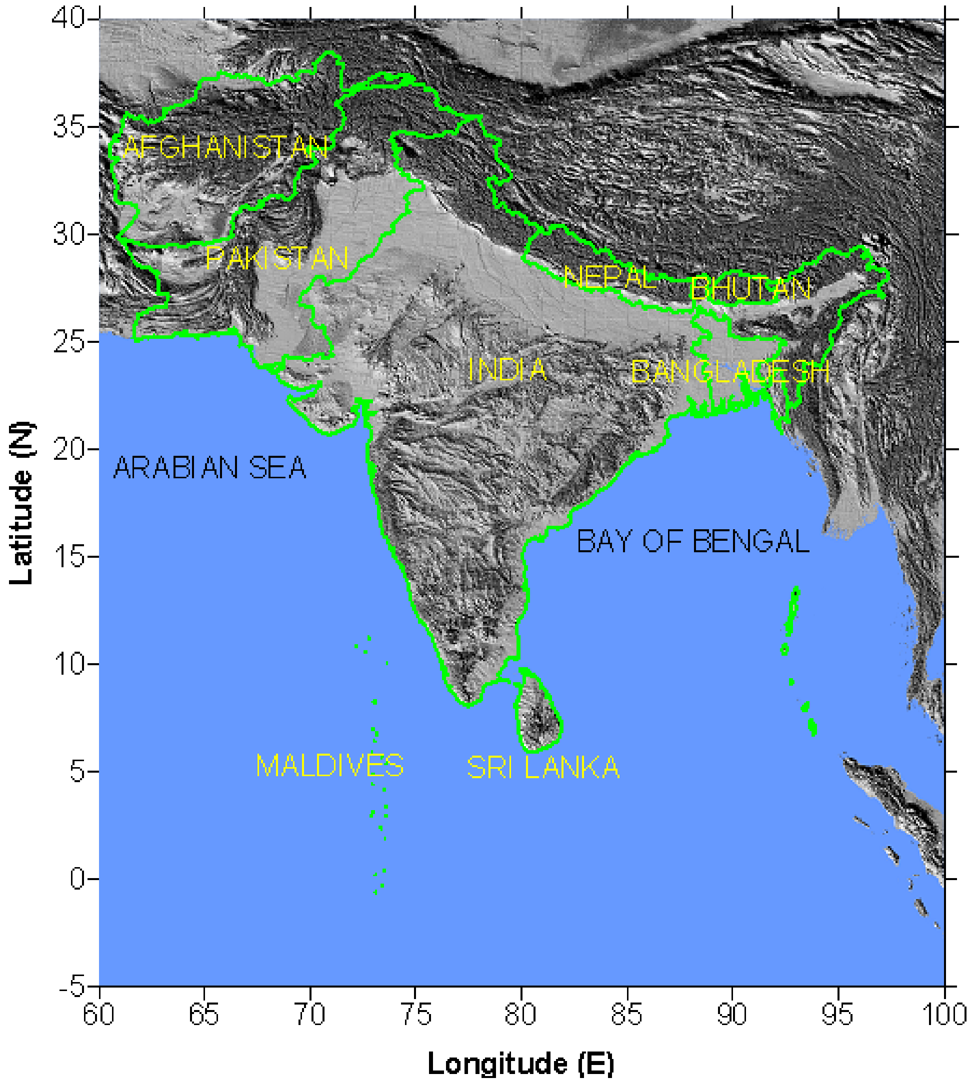

Map of the SAARC region.

SAARC (The South Asian Association for Regional Cooperation)
Bangladesh, Bhutan, India, Maldives, Nepal, Pakistan, Sri Lanka and **Afghanistan**.

The SAARC region has unique characteristics that there is a large geographic variation within a short range.
The spatiotemporal distribution of rainfall in the SAARC domain varies in different rainy periods.
Utilization of TRMM data for understanding the rainfall climatology and interseasonal variation of monsoon rainfall in this region is important.
Long-term TRMM products in estimating exact rainfall are the preparation to utilize GPM products in different sectors including climate change impact studies, agriculture and water management.

Research Group

PI: Hiroshi Uyeda
Hydrospheric Atmospheric Research Center,
Nagoya University

CI-1: Md. Nazrul Islam
Synoptic Division,
SAARC Meteorological Research Centre,
Dhaka-1207, Bangladesh
→King Abdulaziz University Jeddah, KSA

CI-2: Md. Rafi Uddin
Department of Physics,
Bangladesh University of Engineering
& Technology,
Dhaka-1000, Bangladesh

TRMM Data Analyses (Precipitation)

Rain Gauge Data (SAARC Area)

CI-3: Md. Abdul Mannan
Storm Warning Centre
Bangladesh Meteorological Department
Agargaon, Dhaka-1207, Bangladesh.

BMD Doppler Radar Data Analyses

CI-4 : S. M. Quamrul Hassan
Storm Warning Centre
Bangladesh Meteorological Department
Agargaon, Dhaka-1207, Bangladesh.

SAARC: South Asian Association for Regional Cooperation
BMD: Bangladesh Meteorological Division

Characteristics of Rainfall in Bangladesh

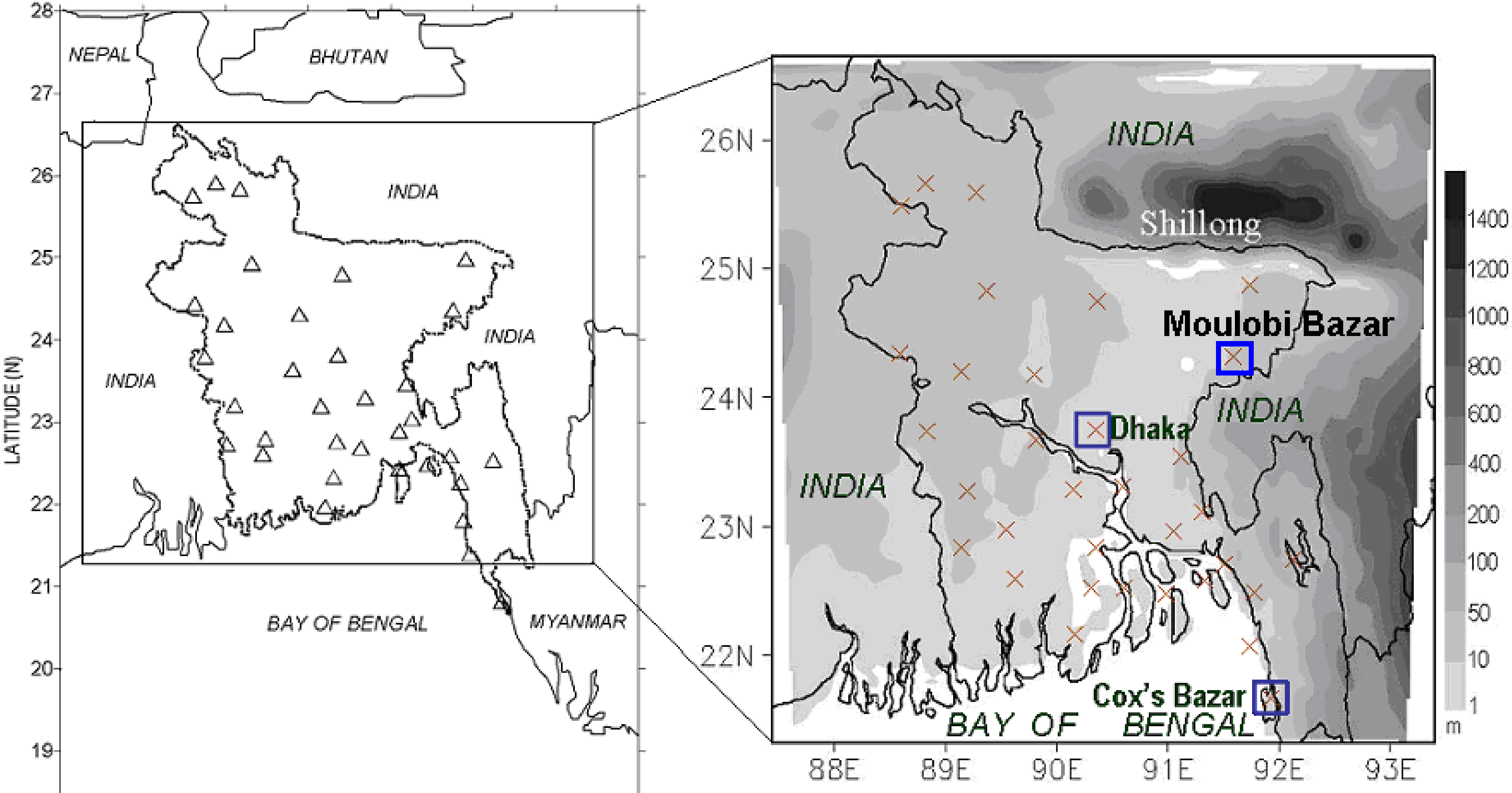

Rain Gauge and Dhaka Radar

The triangles (left panel) and cross (right panel) represent the rain-gauge location in Bangladesh. Square box represents radar locations. Gray shade represents elevation in m.

Characteristics of Rainfall in Bangladesh

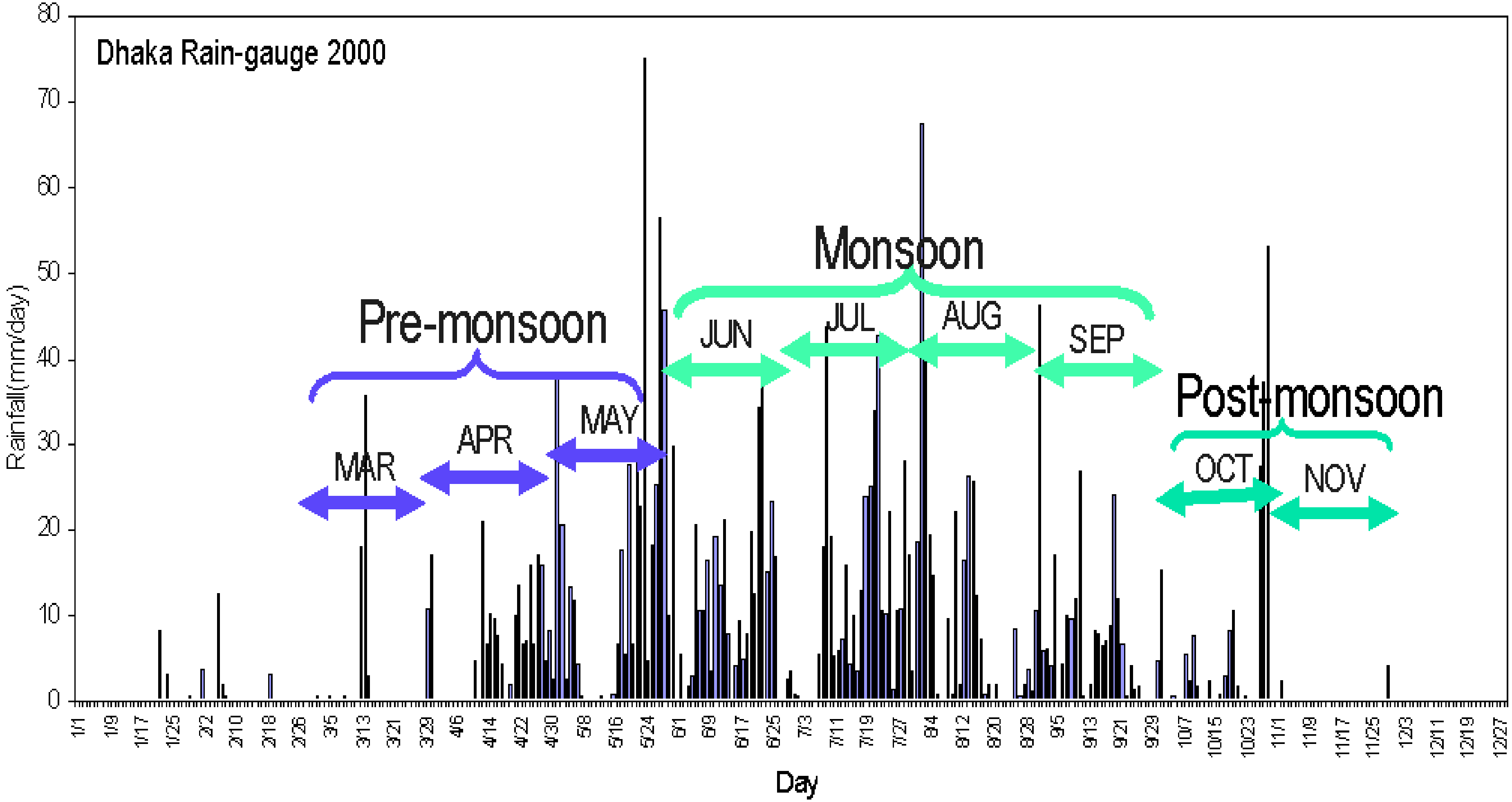

Rain-gauge rainfall at Dhaka station in 2000 in different rainy periods.

Point-to-point comparison of Daily Rainfall (mm) determined by Rain-gauge (left of + mark) and TRMM-3B42 (right to + mark) (Data used: March-Nov)

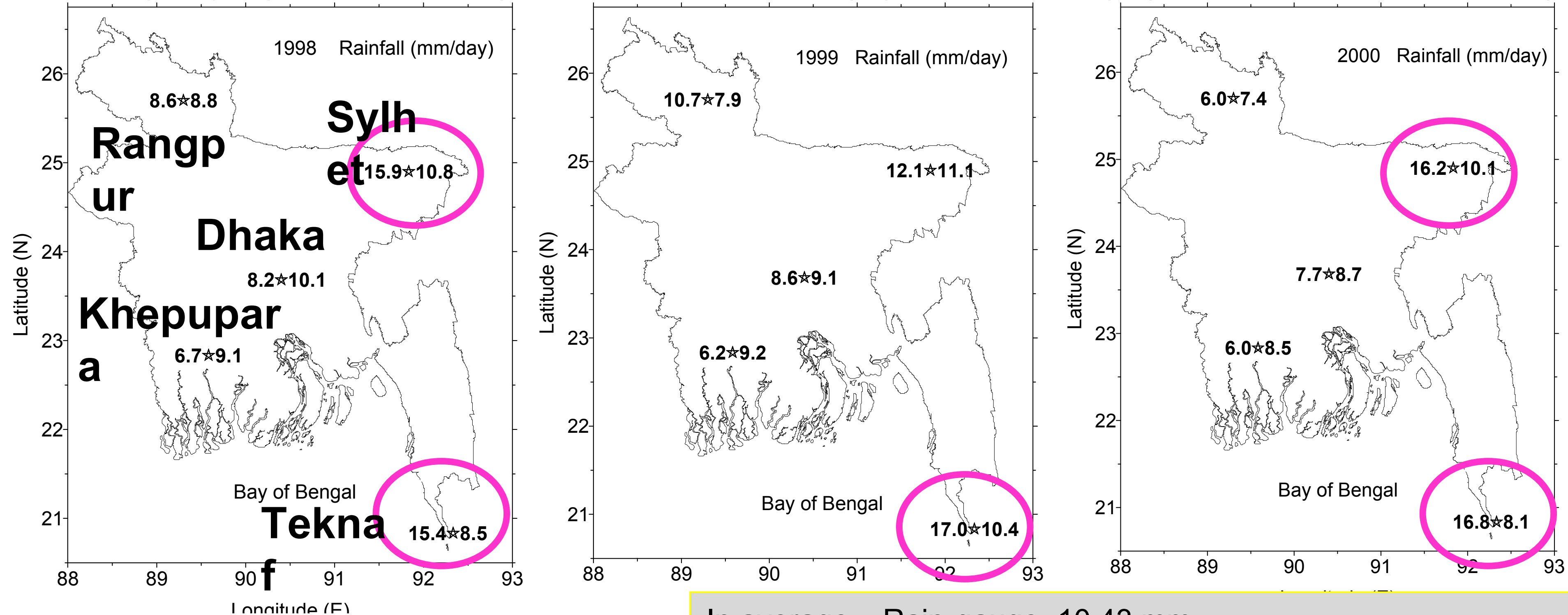

In average Rain-gauge=10.43 mm
TRMM=9.13 %=87.47

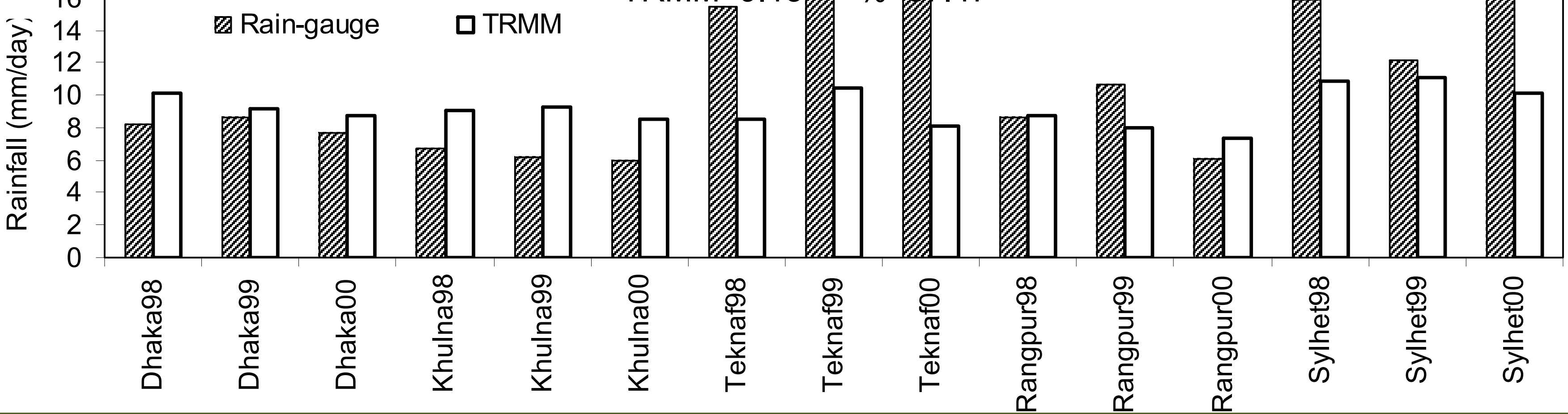

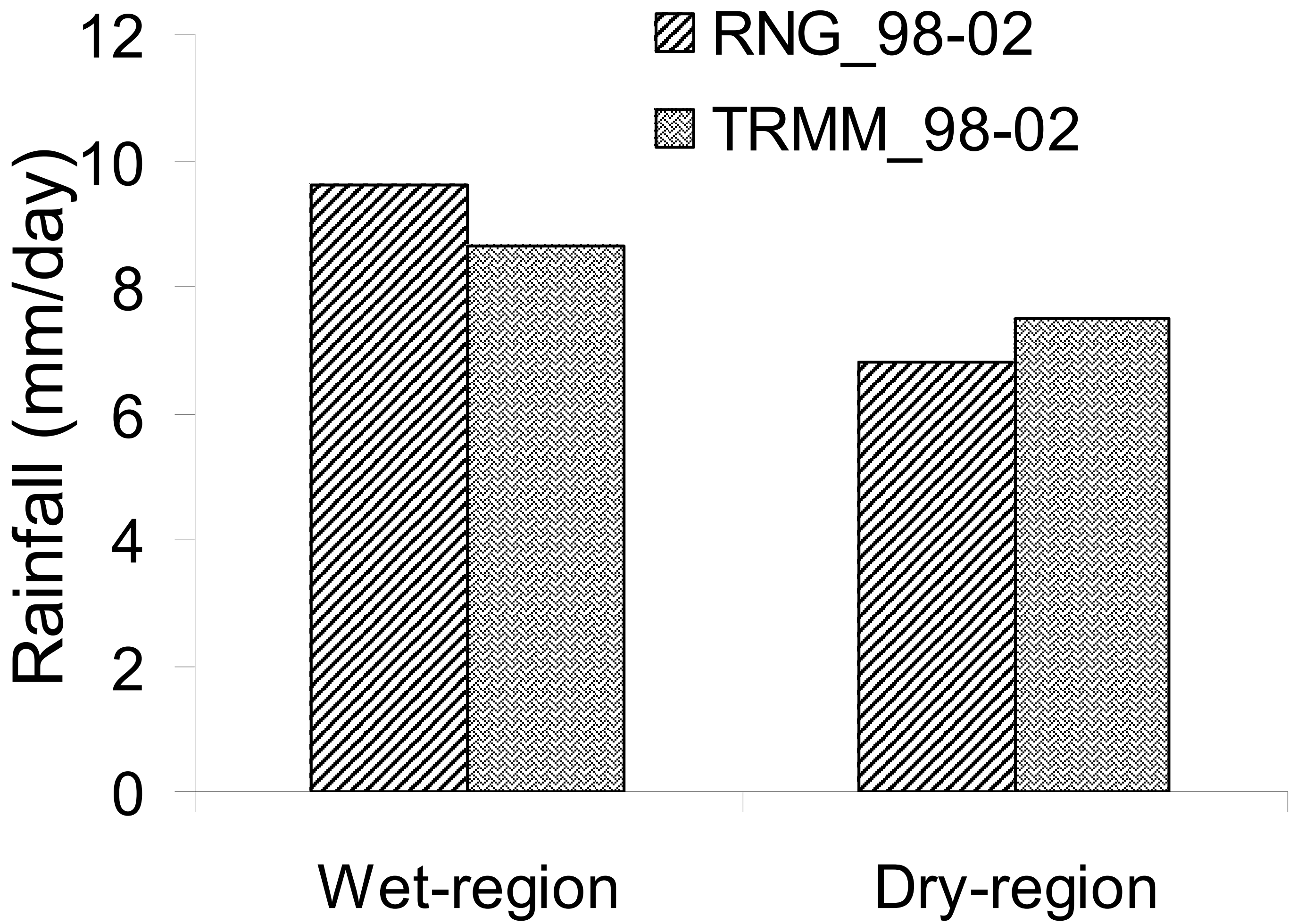

Fig. 11. Rainfall (mm/day) averaged for the wet region (high humidity) and the dry region (low humidity). Data averages for 17 stations in the wet region and 14 stations in the dry region throughout Bangladesh from 1998 to 2002.

M.N. Islam, H. Uyeda / Remote Sensing of Environment 108 (2007) 264–276

Characteristics of Rainfall in Bangladesh

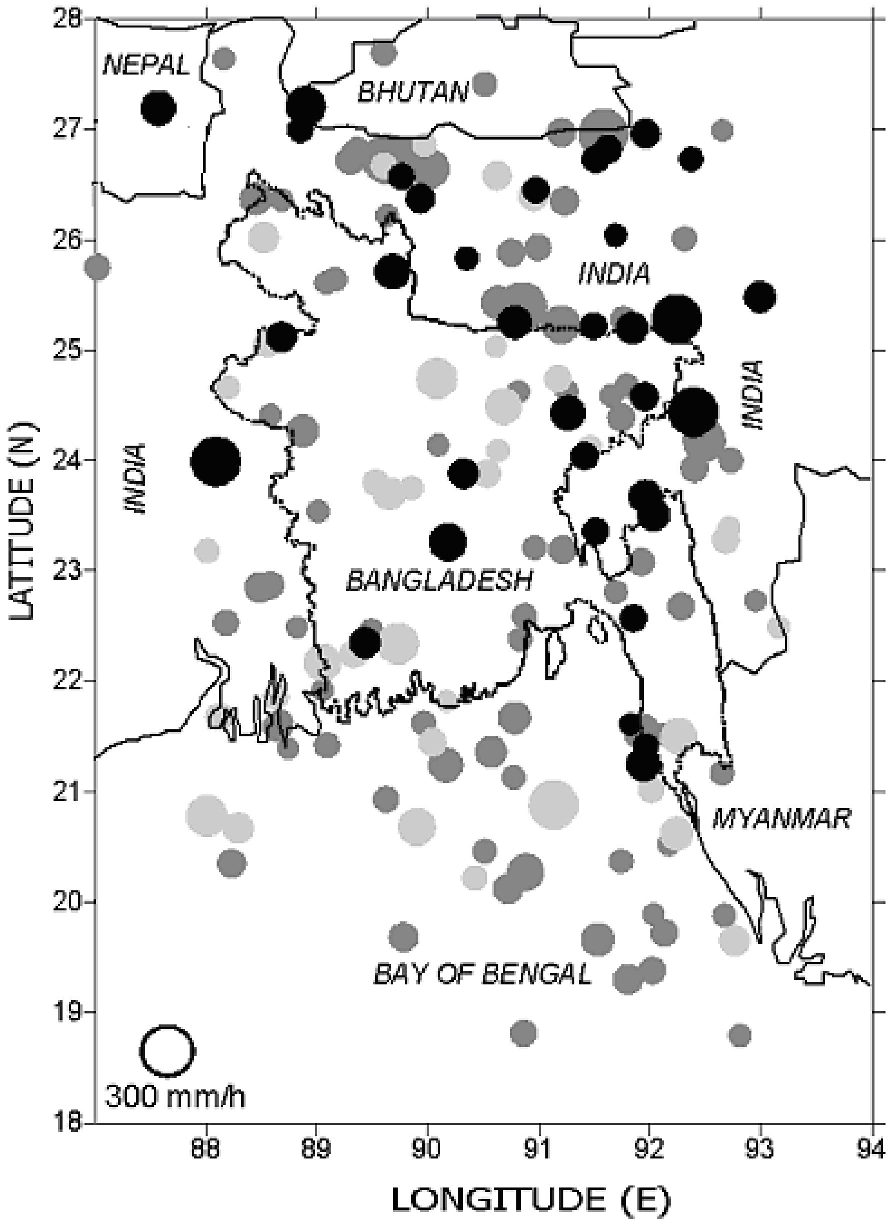

Distribution of the locations of maximum rain rates in April (dark closed circle), July (medium dark closed circle), and October (light dark closed circle). The open circle at the lower left of the panel represents the size of rain rate.

Characteristics of Rainfall in Bangladesh

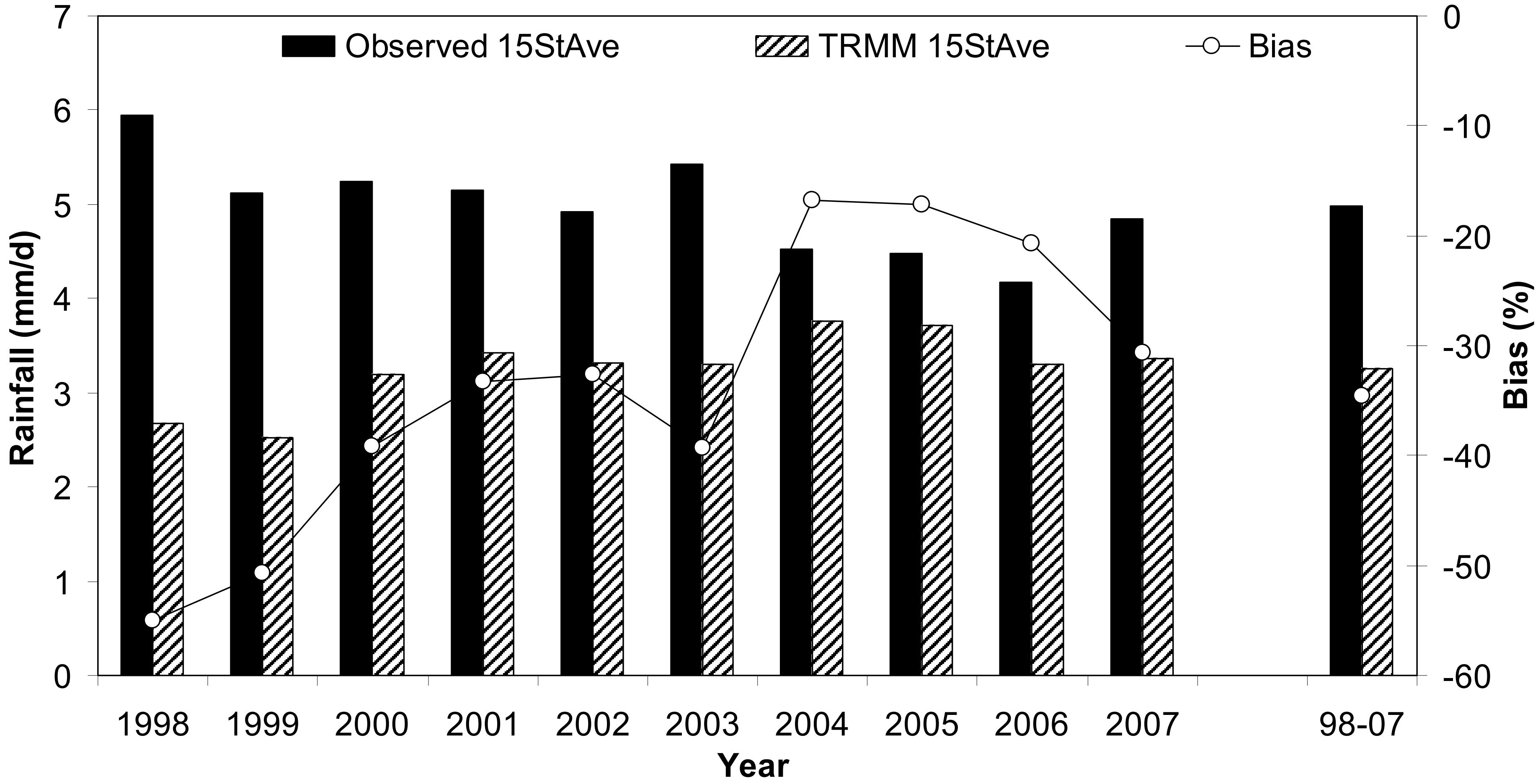

Annual rainfall and bias obtained from TRMM and rain-gauge data over Nepal. Rainfall and bias are averaged for 15 stations.

Characteristics of Rainfall in Bangladesh

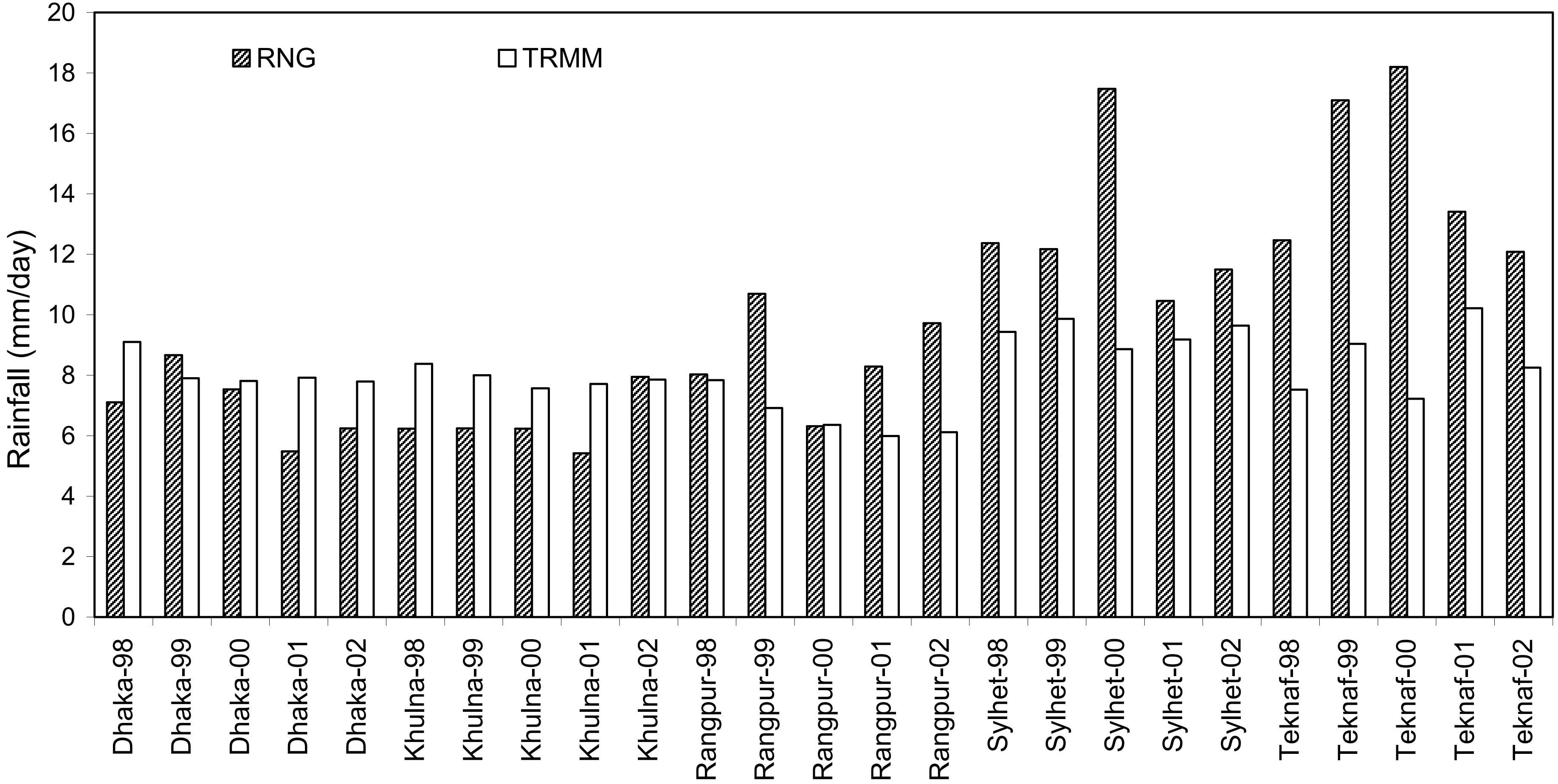

Fig. 4. Rainfall (mm/day) measured from TRMM 3B42 and rain-gauge (RNG) data for a 5-year (1998-2002) period at each selected station.

M.N. Islam, H. Uyeda / Remote Sensing of Environment 108 (2007) 264–276

Characteristics of Rainfall in Bangladesh

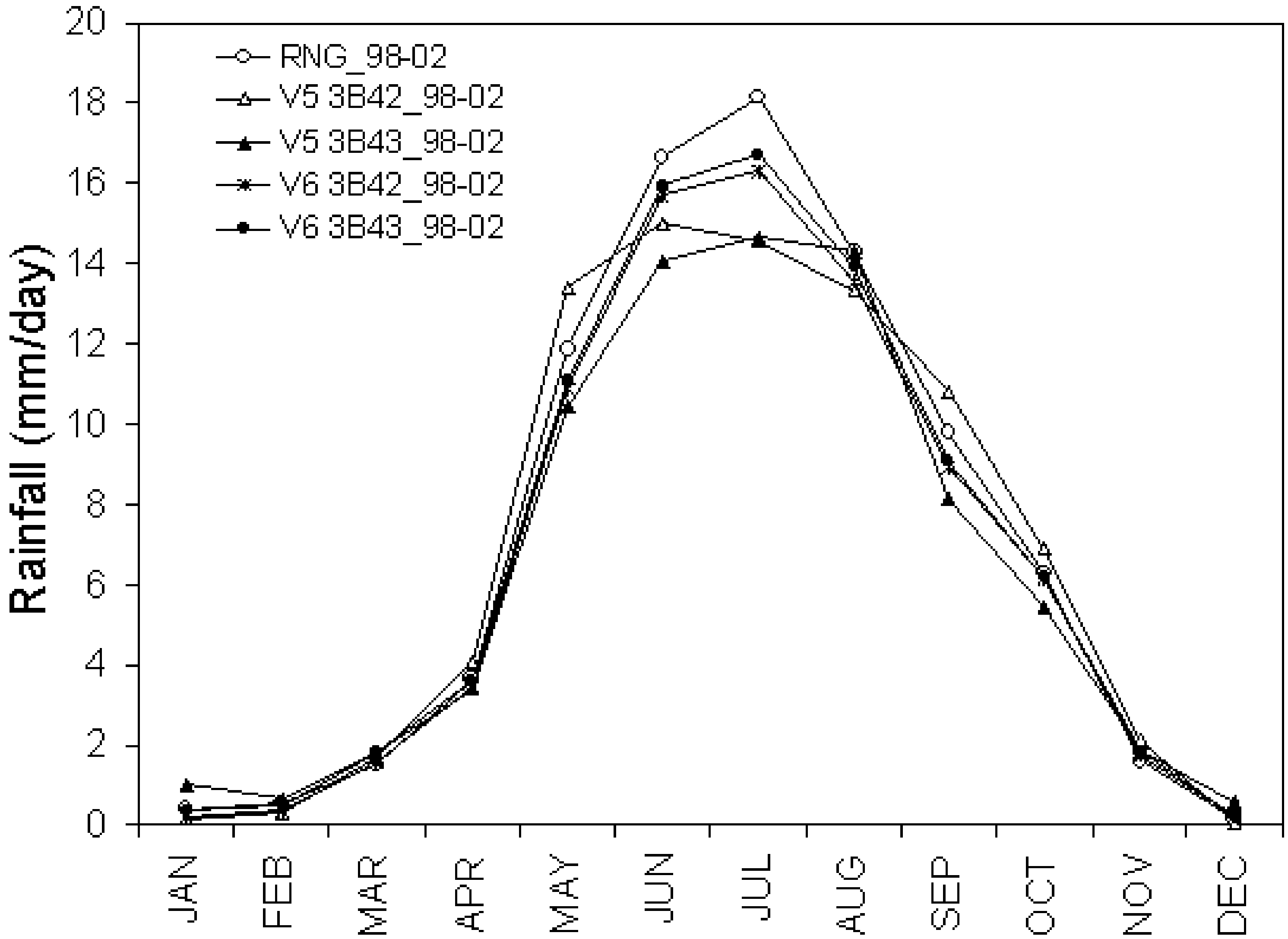

Seasonal cycle of rainfall in Bangladesh obtained from TRMM products and rain-gauge.

Characteristics of Rainfall in Bangladesh (TRMM PR)

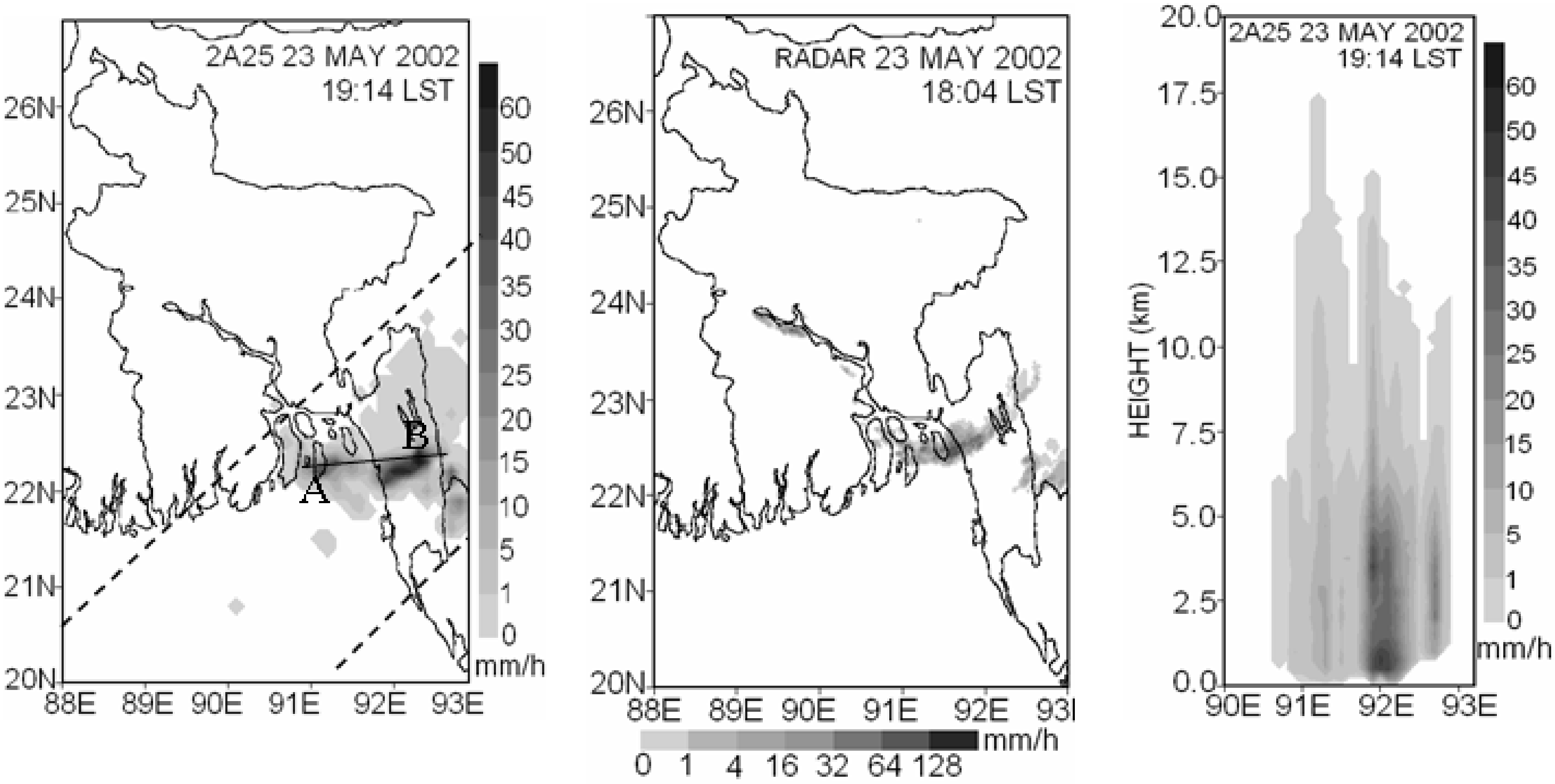

TRMM 2A25 overpass on 25 May 2002 (left panel), Dhaka radar PPI scan (middle panel), and vertical extension of 2A25 precipitation field (right panel) along line AB in left panel.

Characteristics of Rainfall in Bangladesh (TRMM PR)

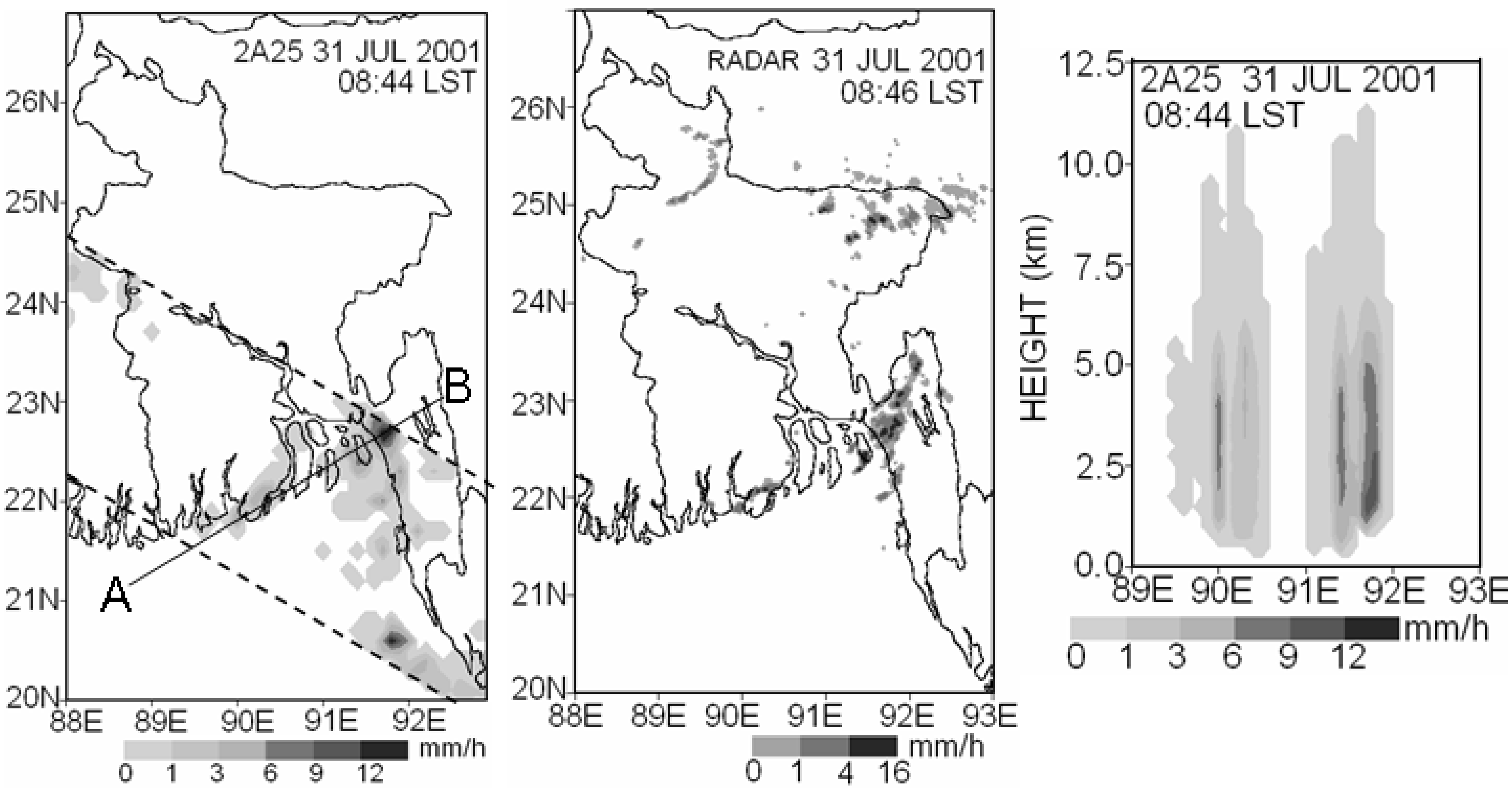

Same as the previous figure except for the case in July 2001.

Characteristics of Rainfall in Bangladesh (Rain Gauge + TRMM)

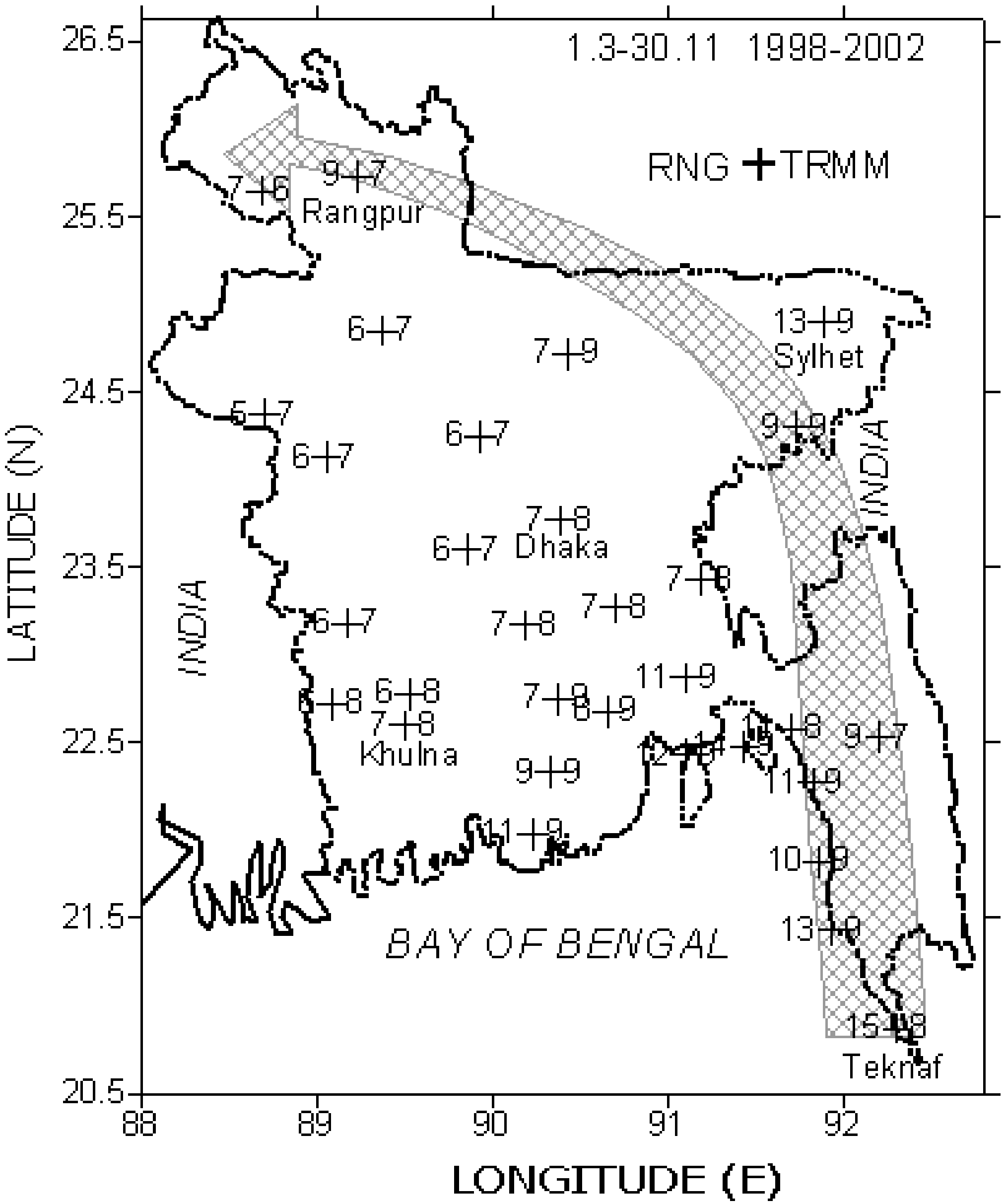

Rain Gauge + TRMM

TRMM under estimates rainfall amount in the moist region.

Daily rainfall averages from 1 March to 31 November for 1998-2002 at rain-gauge sites (plus mark).

Status data of rain rate [BMD Radar]

Status	Rain Rate (R) (mm/h)
1	$1 \leq R < 4$
2	$4 \leq R < 16$
3	$16 \leq R < 32$
4	$32 \leq R < 64$
5	$64 \leq R < 128$
6	$R \geq 128$

Characteristics of precipitation systems [BMD Radar]

Precipitation systems are classified as Arc-, Line- or Scattered-types according to their shape by analyzing six years (2000-2005) radar data of Bangladesh Meteorological Department (*Rafiuddin et al., 2007: MSJ autumn meeting, Sapporo*).

1. Arc type

Having arc shape leading edge and behind has stratiform region (it looks like squall line type)

2. Line type

Having linear shape echo (sometimes having linear echo in-between week echoes)

3. Scattered type

Not well organized small individual echoes distributed in certain area

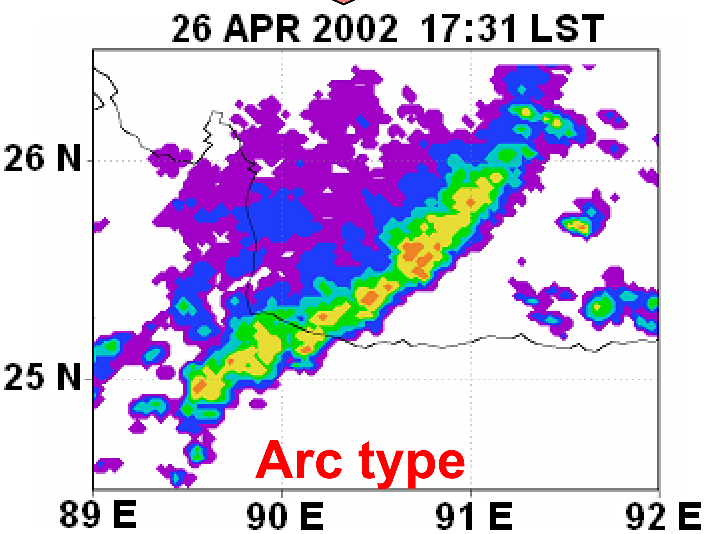

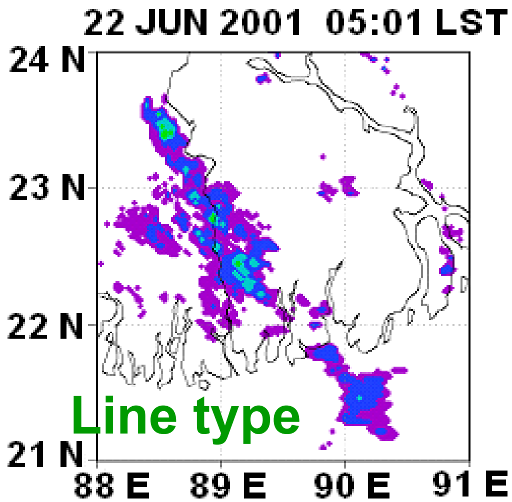

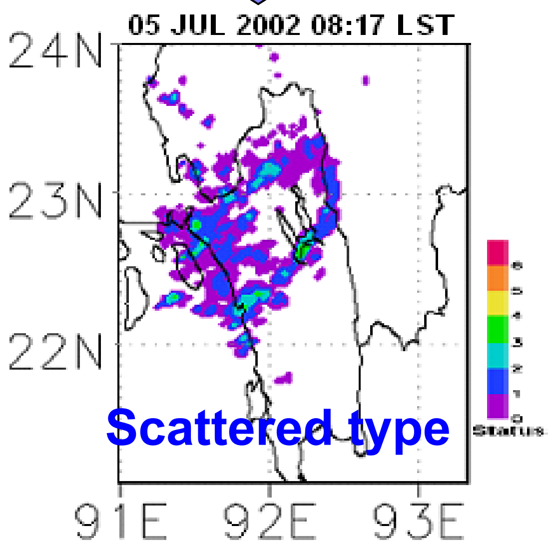

Scattered systems

Scattered systems have wide areal coverage (SWAC) and development of this type of system is ~97% in monsoon.

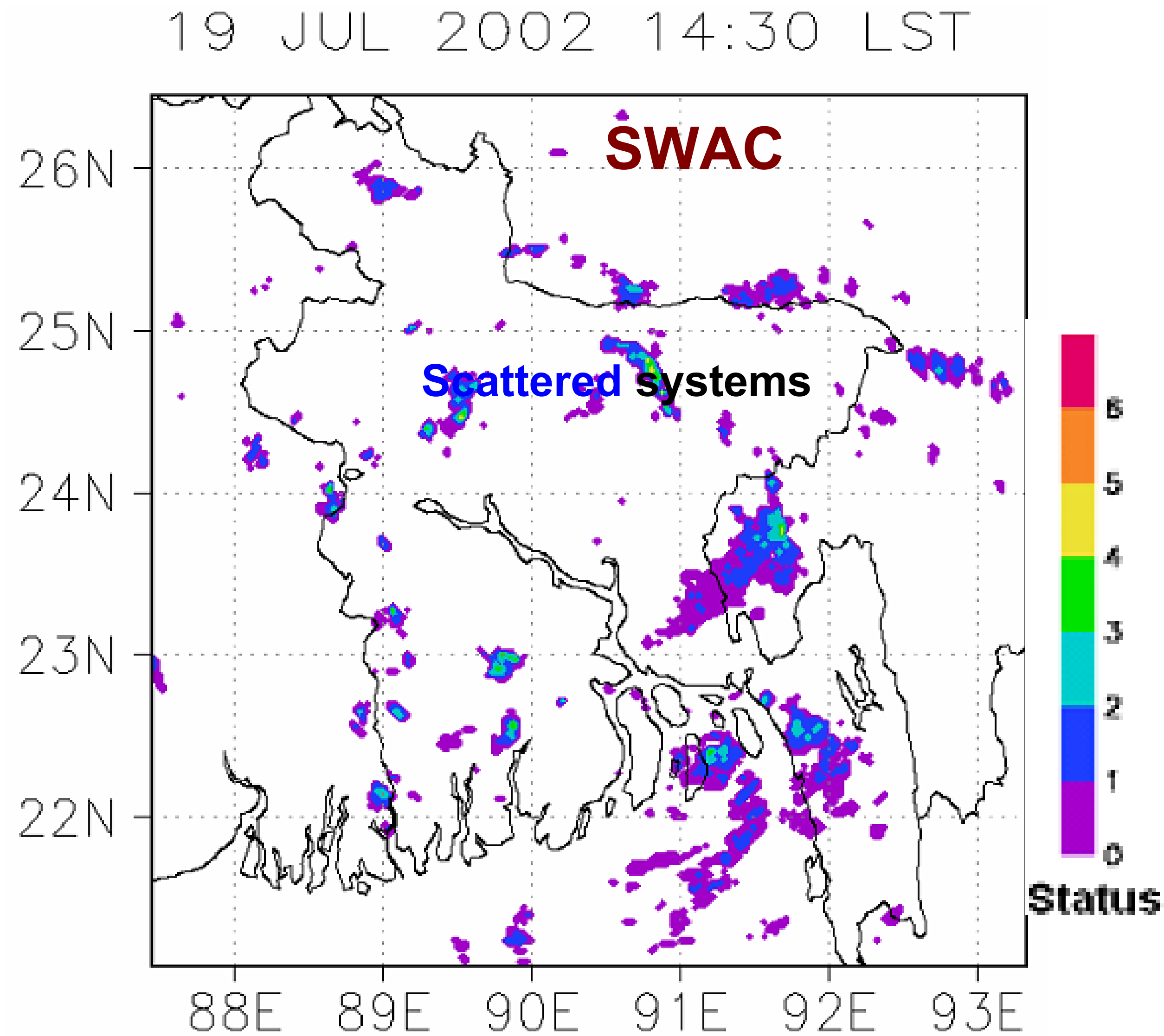

Data number analyzed

Interannual variation of the occurrence number of systems types in different years (2000-2005)

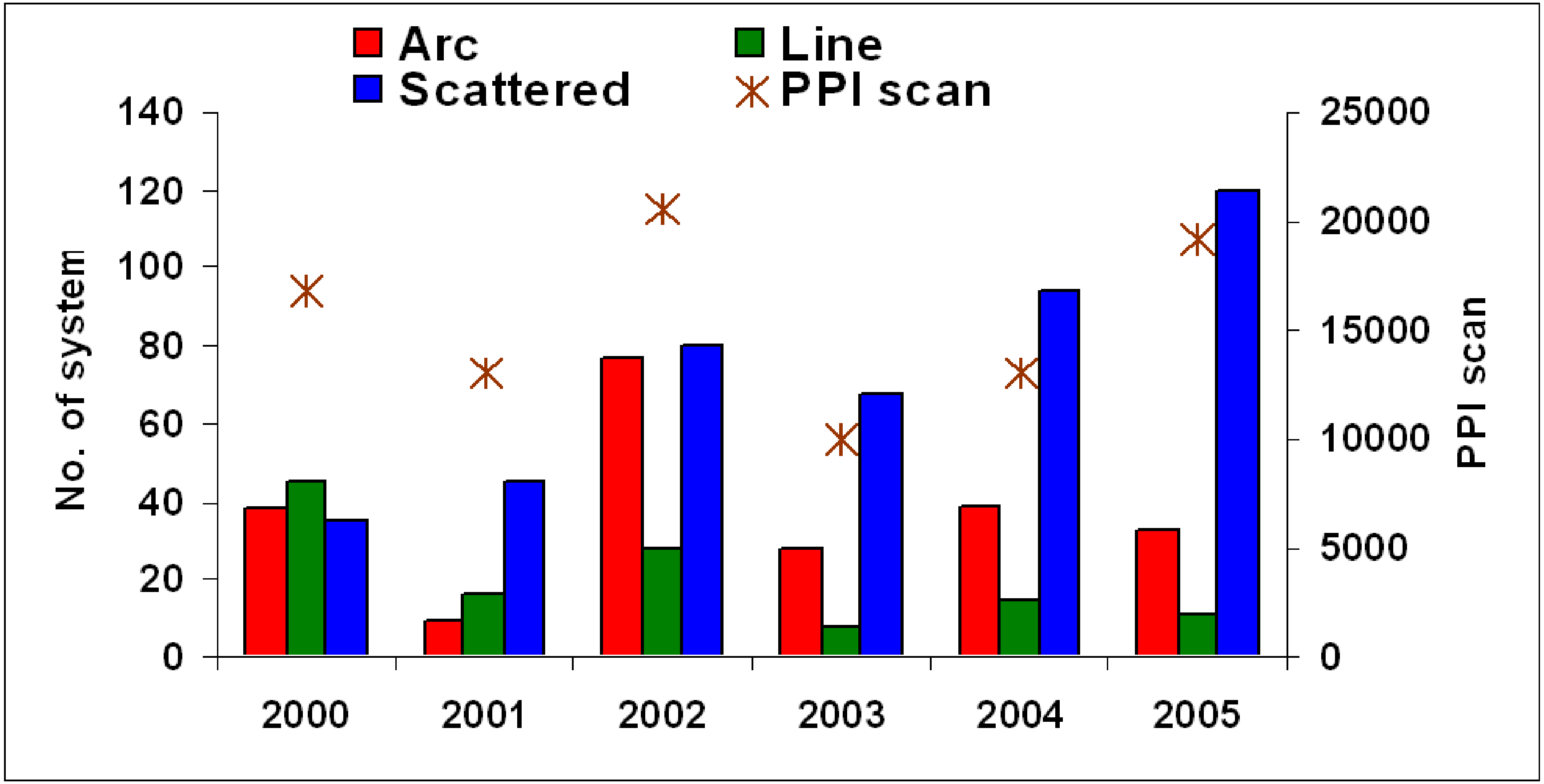

Schematic illustration of pre-monsoon and monsoon precipitation systems

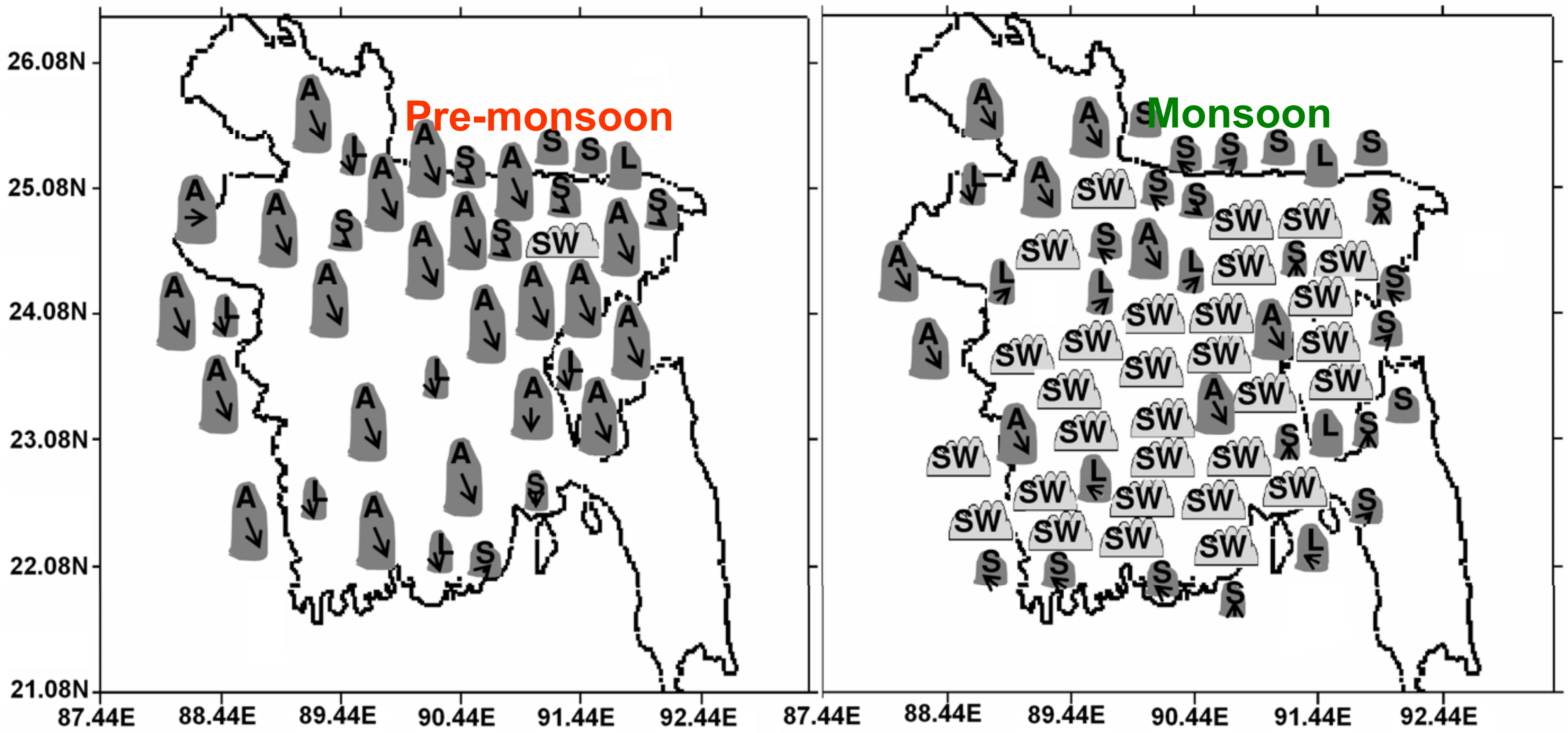

Schematic illustration of pre-monsoon (left panel) and monsoon (right panel) precipitation systems developing in and around Bangladesh. The symbols A, L, S, and SW represent arc-, line-, scattered-type systems, and SWAC, respectively.

Rainfall and Precipitation Type

RAINFALL SEASON

RAINY SEASON (98%) March-November

DRY SEASON (2%) December-February

PRE-MONSOON (20%)
March-May

Systems have Short Length, Short Lifetime, Intensified, Fast Moving

MONSOON (62%)
June-September

Systems have Long Length, Long Lifetime, Less-intensified, Slow Moving

Post-MONSOON (16%)
October-November

System characteristics are almost same as Monsoon

Above definitions to subdivide Rainy Season are based on Month. Sometimes Monsoon ONSET is either Delayed or Prompt from Normal. Therefore, we are interested to divide Rainy Season based on the characteristics of Convection Systems. Also for Model Parameterization vertical profiles of Convection Systems developed in different rainy periods are important.

Islam and Uyeda (2005), IEEE 2nd TRMM Con., Korea

Data to be analyzed

YEAR	RADAR	COX'S BAZAR RADAR	MAULOBI BAZAR RADAR	RAIN-GAUGE	TRMM DATA
1998	N/A	N/A	N/A	MAMJJASON	MAMJJASON
1999	N/A	N/A	N/A	MAMJJASON	MAMJJASON
2000	MAMJJASON	N/A	N/A	MAMJJASON	MAMJJASON
2001	MAMJJASON	N/A	N/A	MAMJJASON	MAMJJASON
2002	MAMJJASON	N/A	N/A	MAMJJASON	MAMJJASON
2003	MAMJJASON	N/A	N/A	MAMJJASON	MAMJJASON
2004	MAMJJASON	N/A	N/A	MAMJJASON	MAMJJASON
2005	MAMJJASON	N/A	N/A	MAMJJASON	MAMJJASON
2006	MAMJJASON	N/A	N/A	MAMJJASON	MAMJJASON
2007	MAMJJASON	MAMJJASON	N/A	MAMJJASON	MAMJJASON
2008	MAMJJASON	MAMJJASON	N/A	MAMJJASON	MAMJJASON
2009	MAMJJASON	MAMJJASON	MAMJJASON	MAMJJASON	MAMJJASON
2010	MAMJJASON	MAMJJASON	MAMJJASON	MAMJJASON	MAMJJASON
2011	MAMJJASON	MAMJJASON	MAMJJASON	MAMJJASON	MAMJJASON
2012	MAMJJASON	MAMJJASON	MAMJJASON	MAMJJASON	MAMJJASON

The data collected and to be collected for the periods.

Summary

◎ We would extend our studies on types of precipitation systems over Bangladesh by using BMD Doppler radar and TRMM data.

◎ TRMM data, rain gauge data and BMD Doppler radar data will be used to reveal characteristics of rainfalls over SAARC Area.

◎ These studies would contribute to utilize GPM products.

Topography around Bangladesh and radar coverage

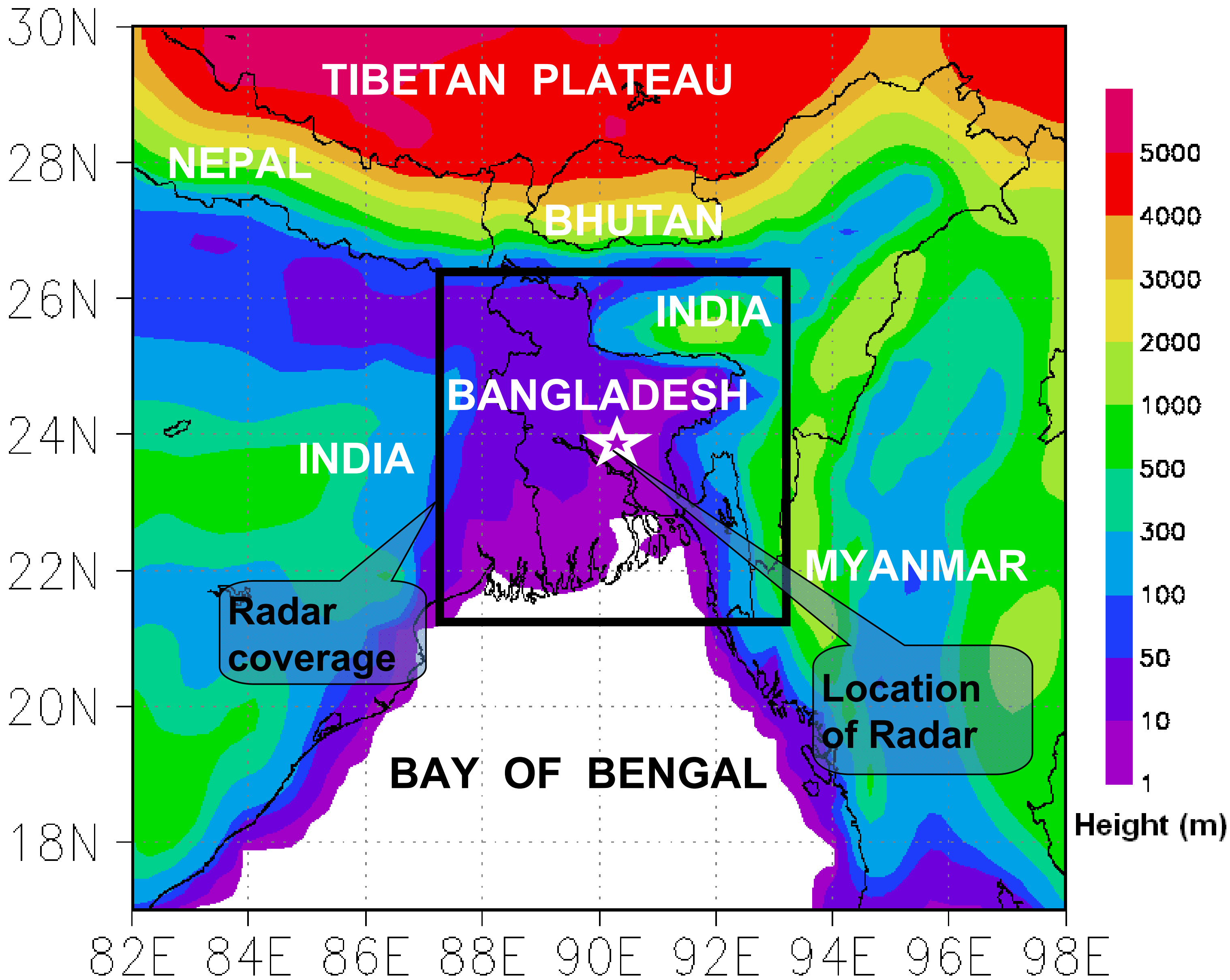

Model Description

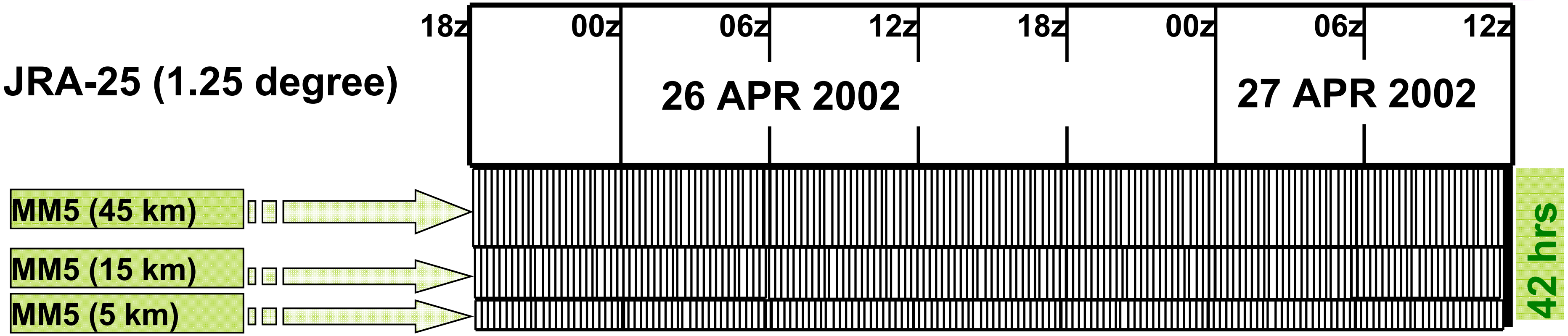

Domain 1 (D1)	(61 x 58)
Domain 2 (D2)	(142 x 130)
Domain 3 (D3)	(289 x 247)
Moisture scheme	Simple ice
Cumulus scheme	Grell
PBL	MRF

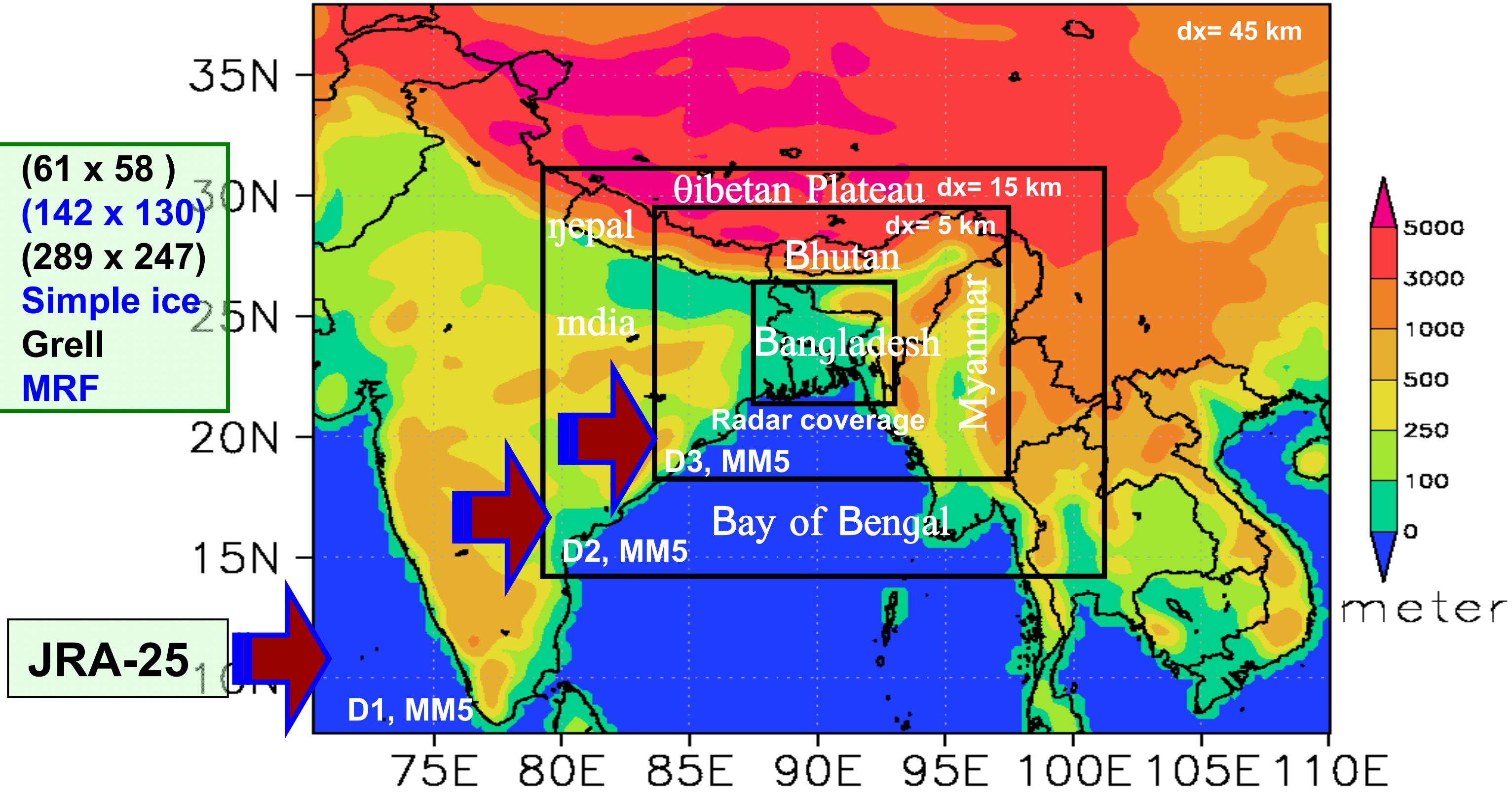

MM5 design for simulation

Number of domain		3 (D1, D2 & D3)
Domain 1 (D1)	(61 x 58)	
Domain 2 (D2)	(142 x 130)	
Domain 3 (D3)	(289 x 247)	
Horizontal grid size		D1: 45 km, D2: 15 km & D3: 5 km
Moisture scheme		Simple ice
Cumulus scheme		Grell
PBL		MRF
Integration time		42 hours
Initial & boundary		JRA-25 (1.25 degree, 6 hrly)

Results and Discussion (Arc type)

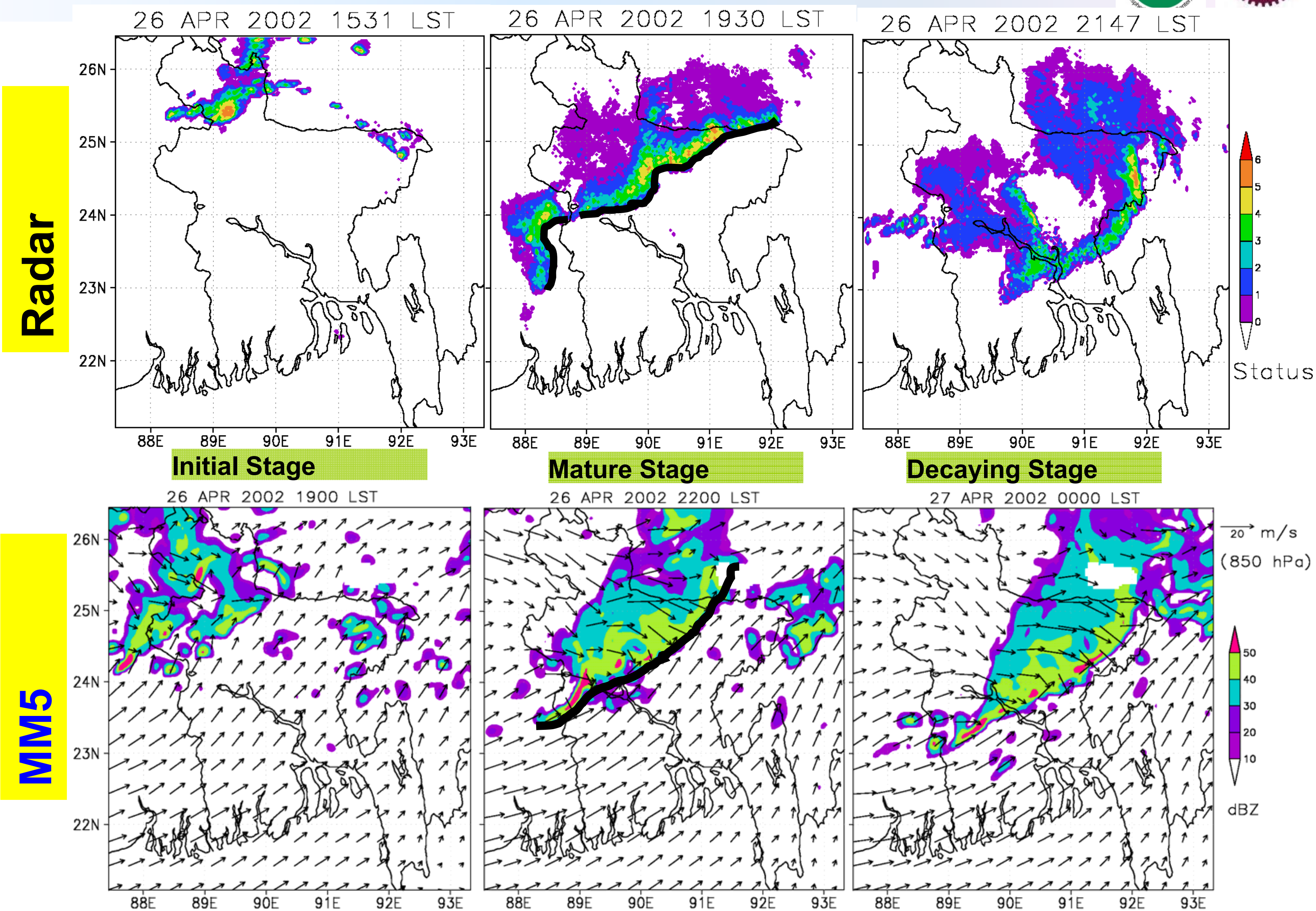

Results and Discussion (Storm motion)

Radar

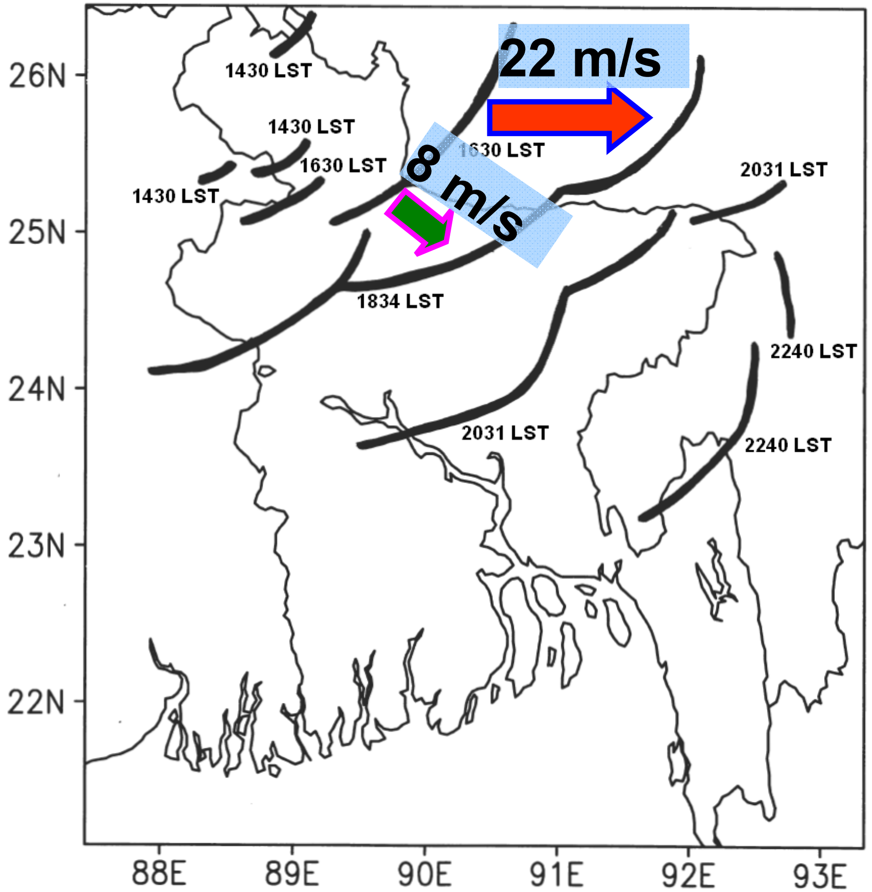

MM5

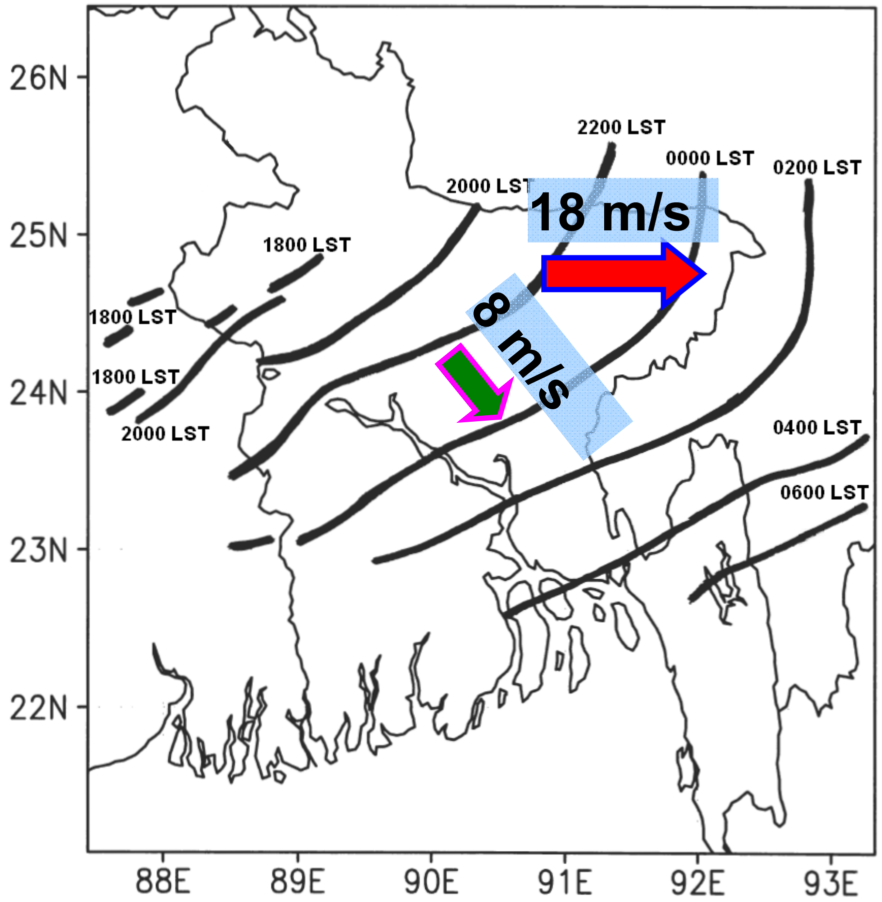

Results and Discussion (T, Wind, Ref., at 925 hPa)

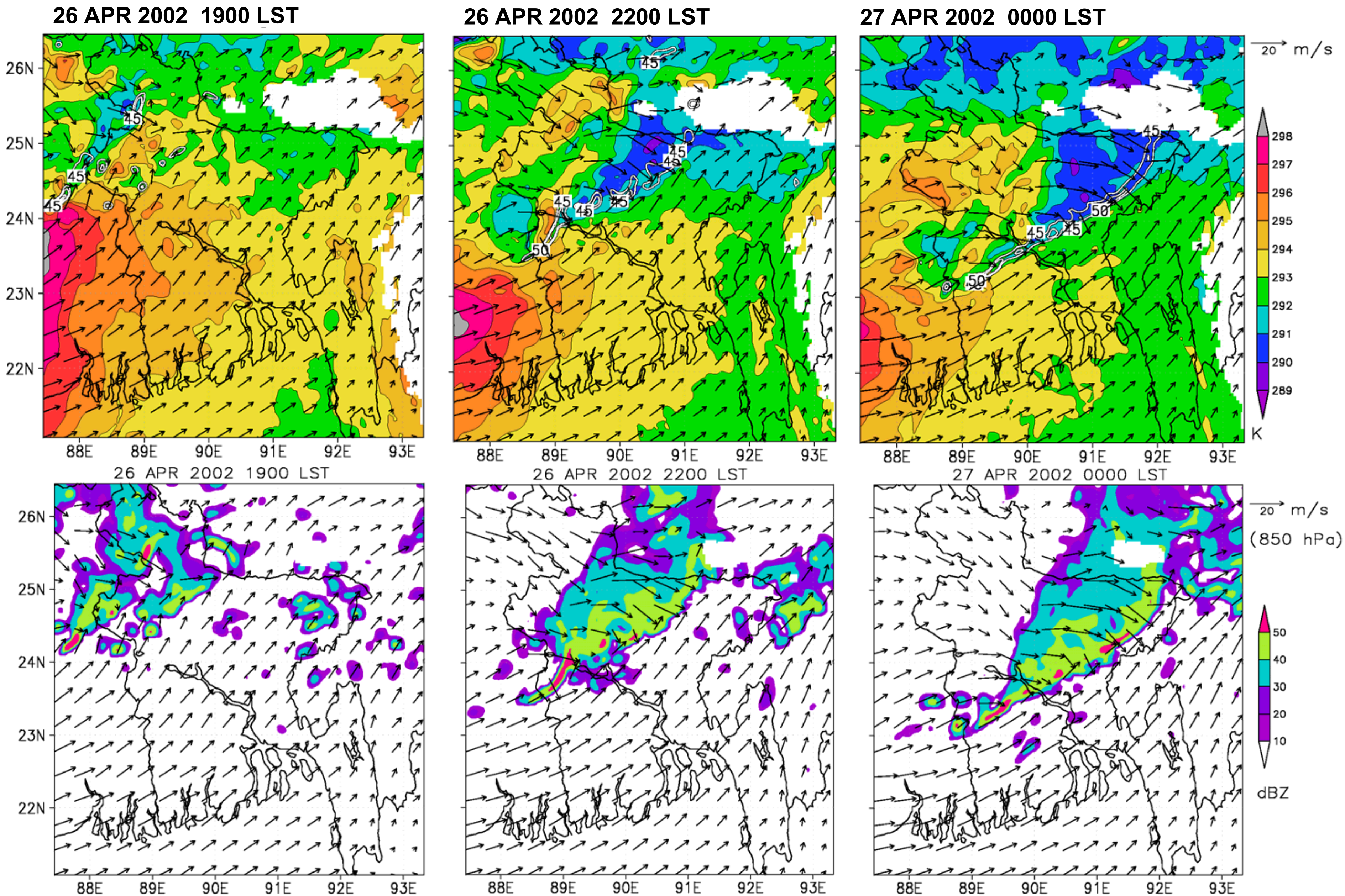

Results and Discussion (RH, Wind, Ref., at 925 hPa)

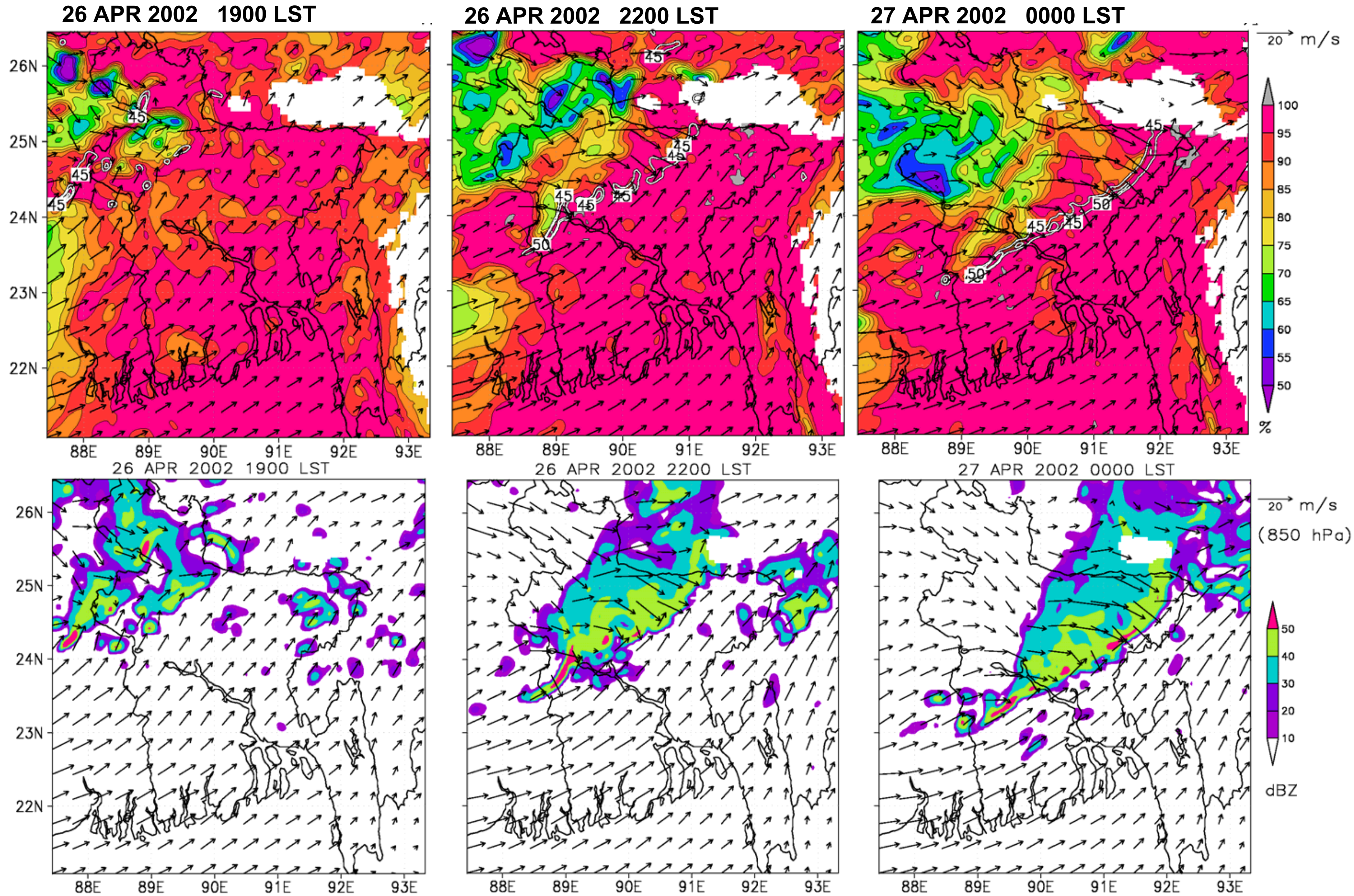

Results and Discussion (Environment ahead Arc)

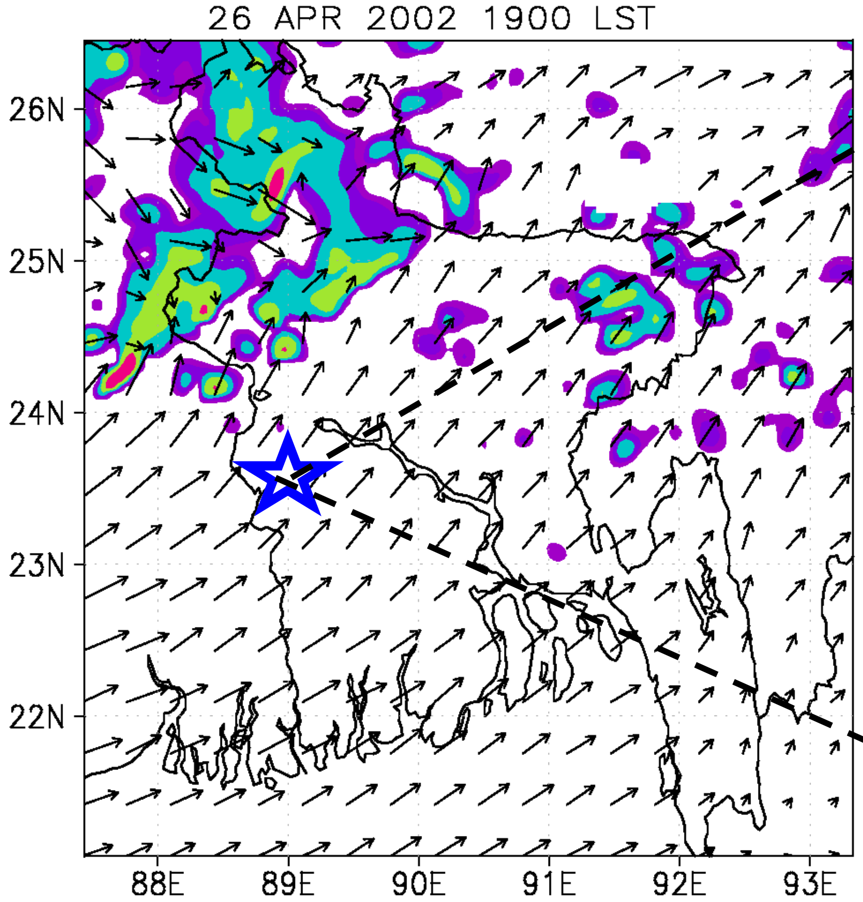

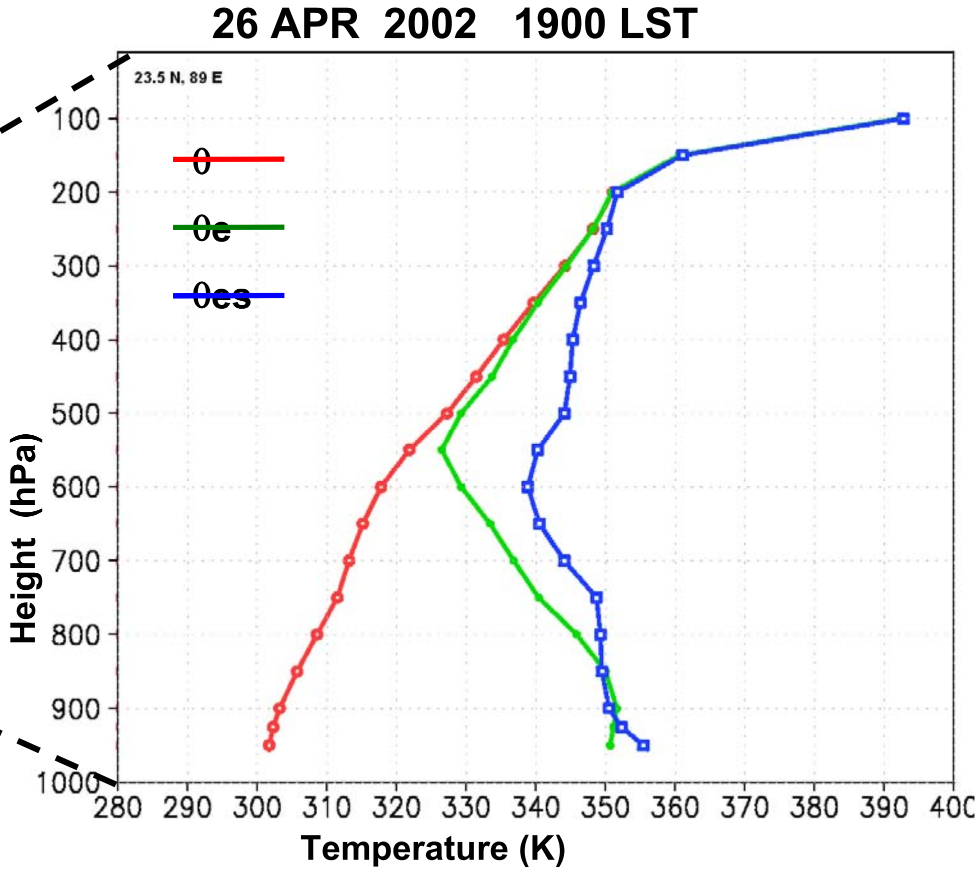

Results and Discussion (Environment ahead Arc)

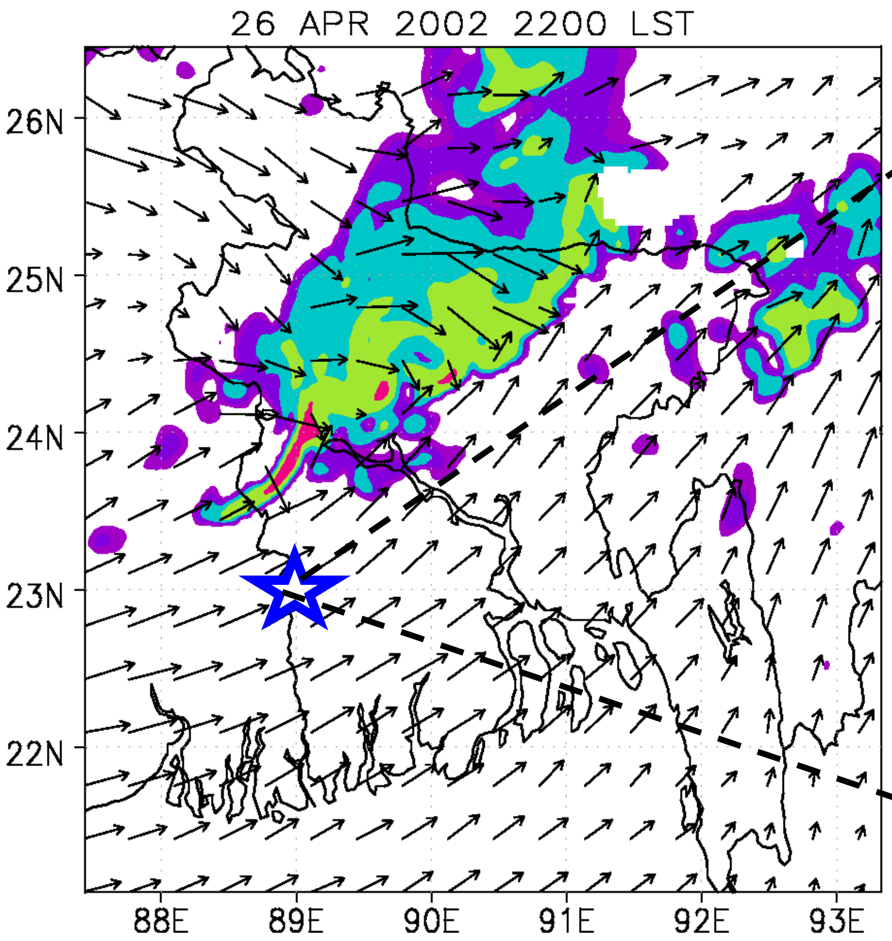

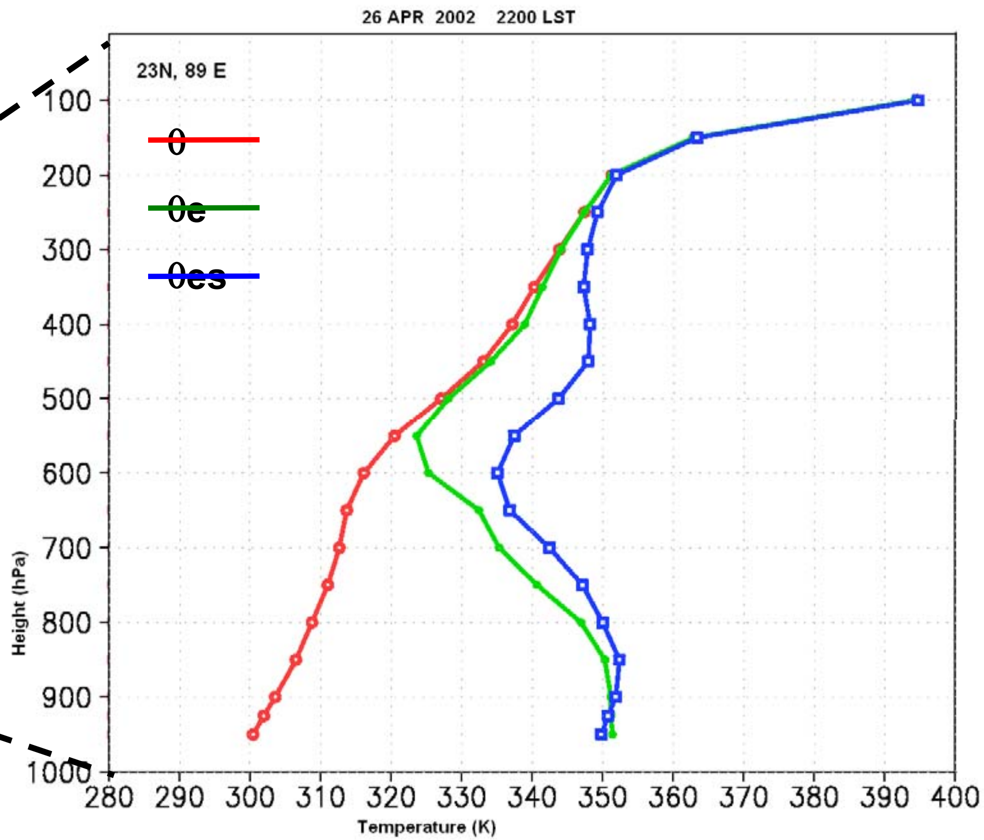

Conclusions

- Shape and southeast-ward propagation of the Arc type system are simulated well by MM5.
- Simulated characteristics (shape, length, propagation speed and direction) are very close to radar observation.
- New and intense cells of the asymmetric squall line are developed in high temperature southwestern region.
- The low level (~ 1 km) southwesterly (moist air from Bay of Bengal) has an important role for the development of new cells.
- Strong outflow from the stratiform region (northeastern part) makes the system move fast.

Future works

- **Vertical structure of the systems:**
  Cloud resolving model (1 km)
  BMD Doppler radar
  TRMM - GPM
- **Understanding the scattered type:**
  Cloud resolving model (1 km)
  Polarimetric radar observation
- **Evaluation of GPM precipitation type:**
  BMD Doppler radar will be useful.

CReSS 1 km run:
"Development of an Arc-Shaped Precipitation System During the Pre-monsoon Period in Bangladesh"
by Rafiuddin, H. Uyeda and M. Kato
Journal of Meteorology and Atmospheric Physics (2012)

(MAP-D-12-00042R1)
"Development of an Arc-Shaped Precipitation System During thePre-monsoon Period in Bangladesh"

M. Rafiuddin et al., Figure 1

Simulation by using Cloud Resolving Model, CReSS (Cloud Resolving Storm Symulator)

Rafiuddin et al.
2012

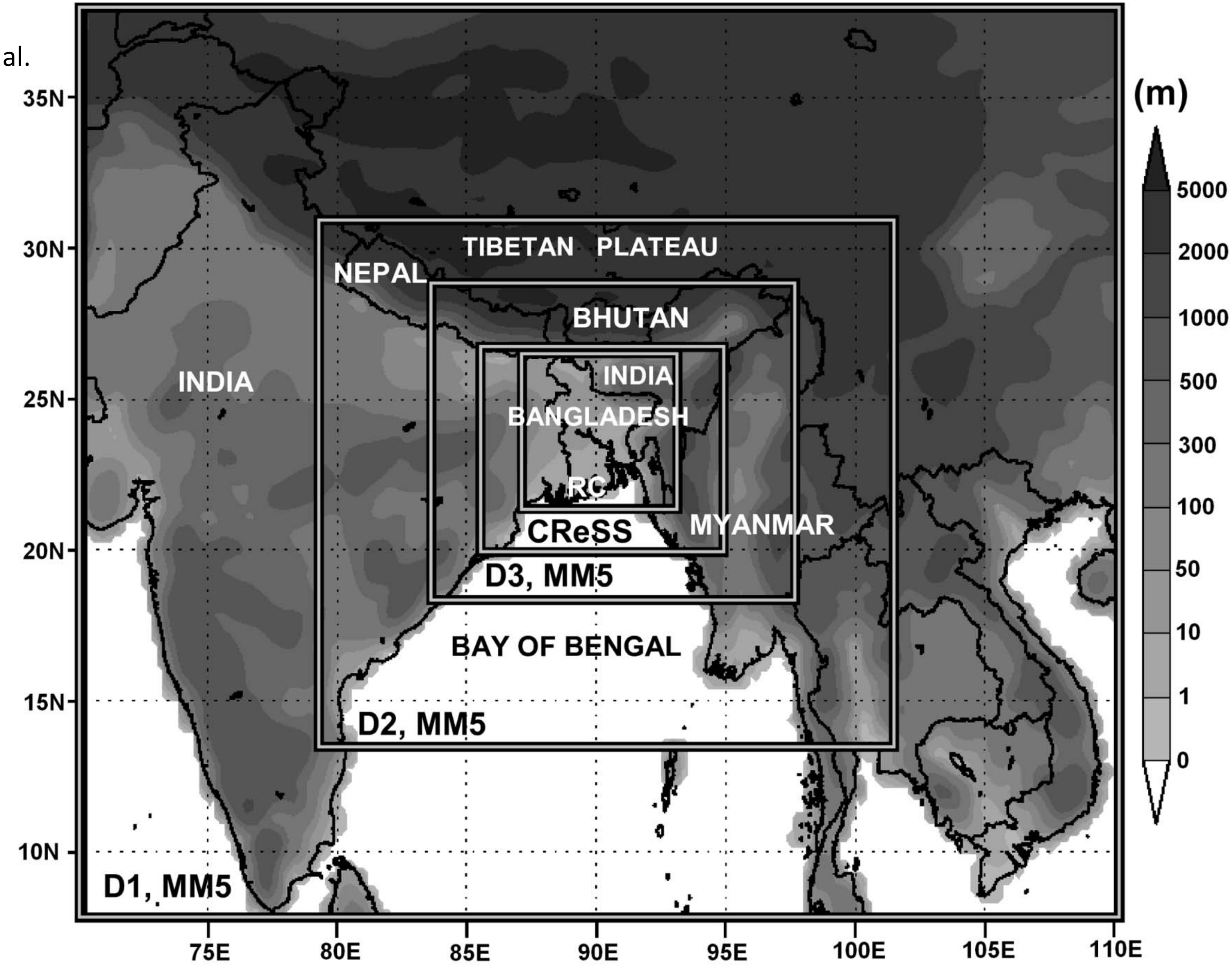

M. Rafiuddin et al., Figure 2

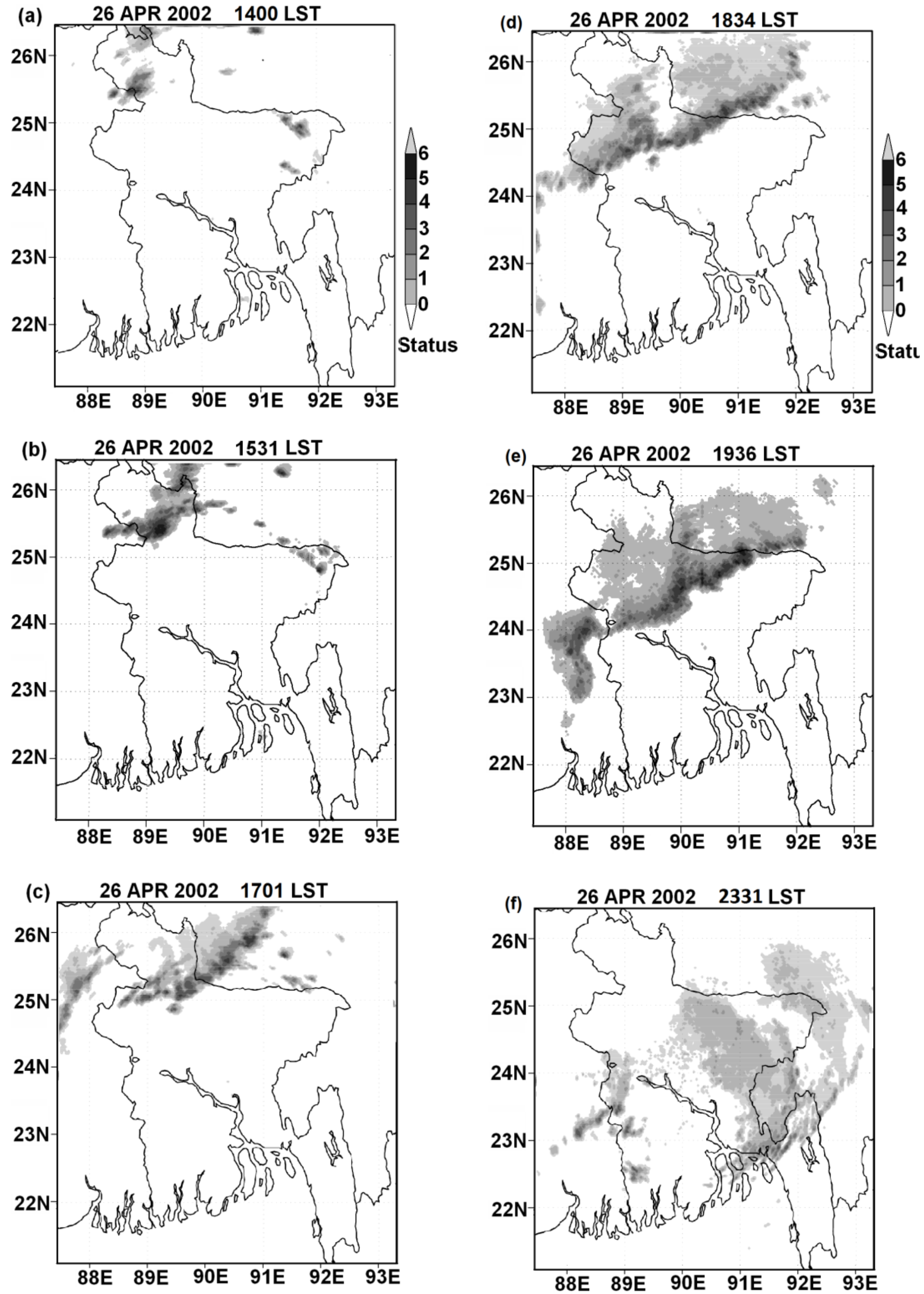

M. Rafiuddin et al., Figure 3

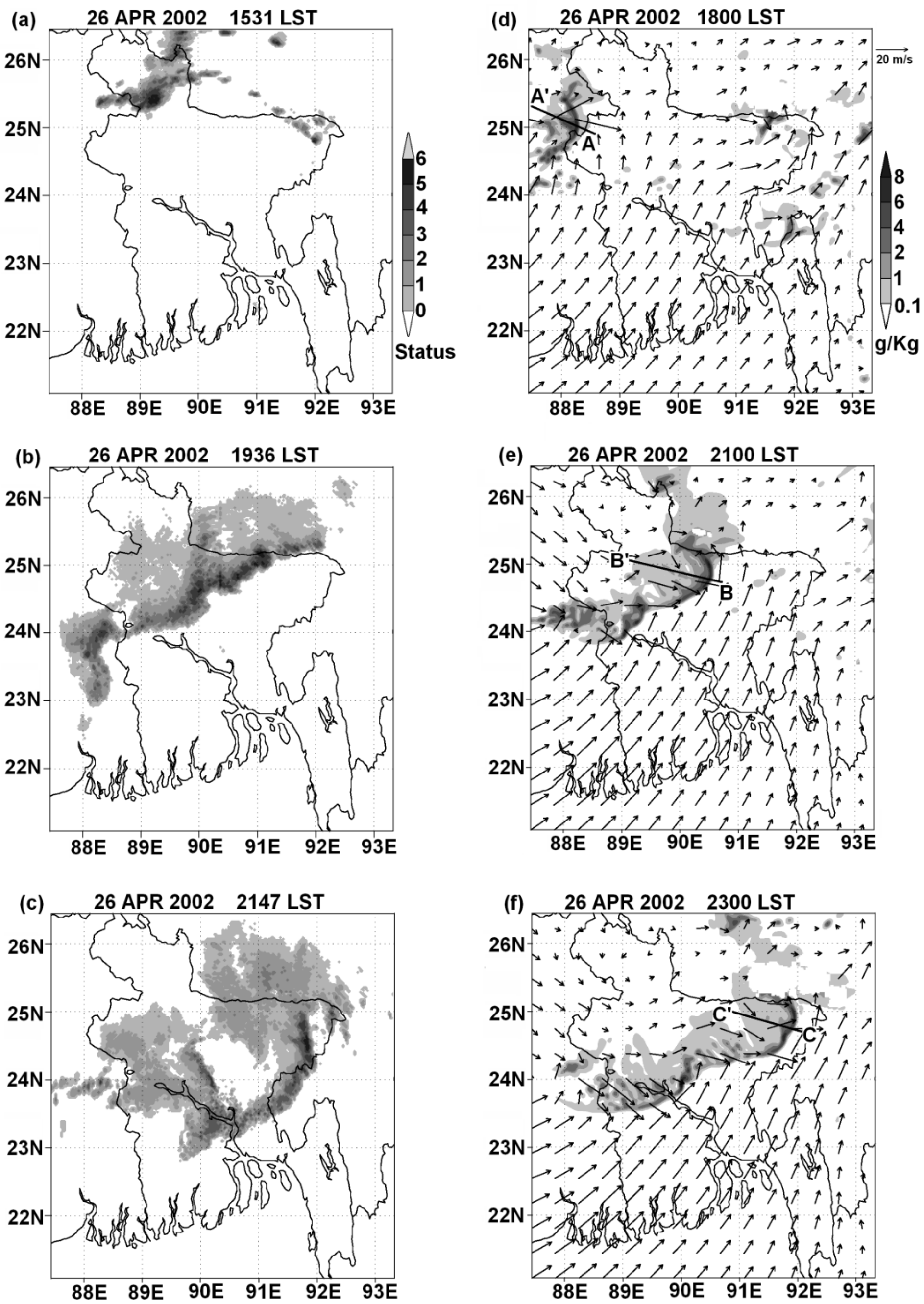

M. Rafiuddin et al., Figure 4

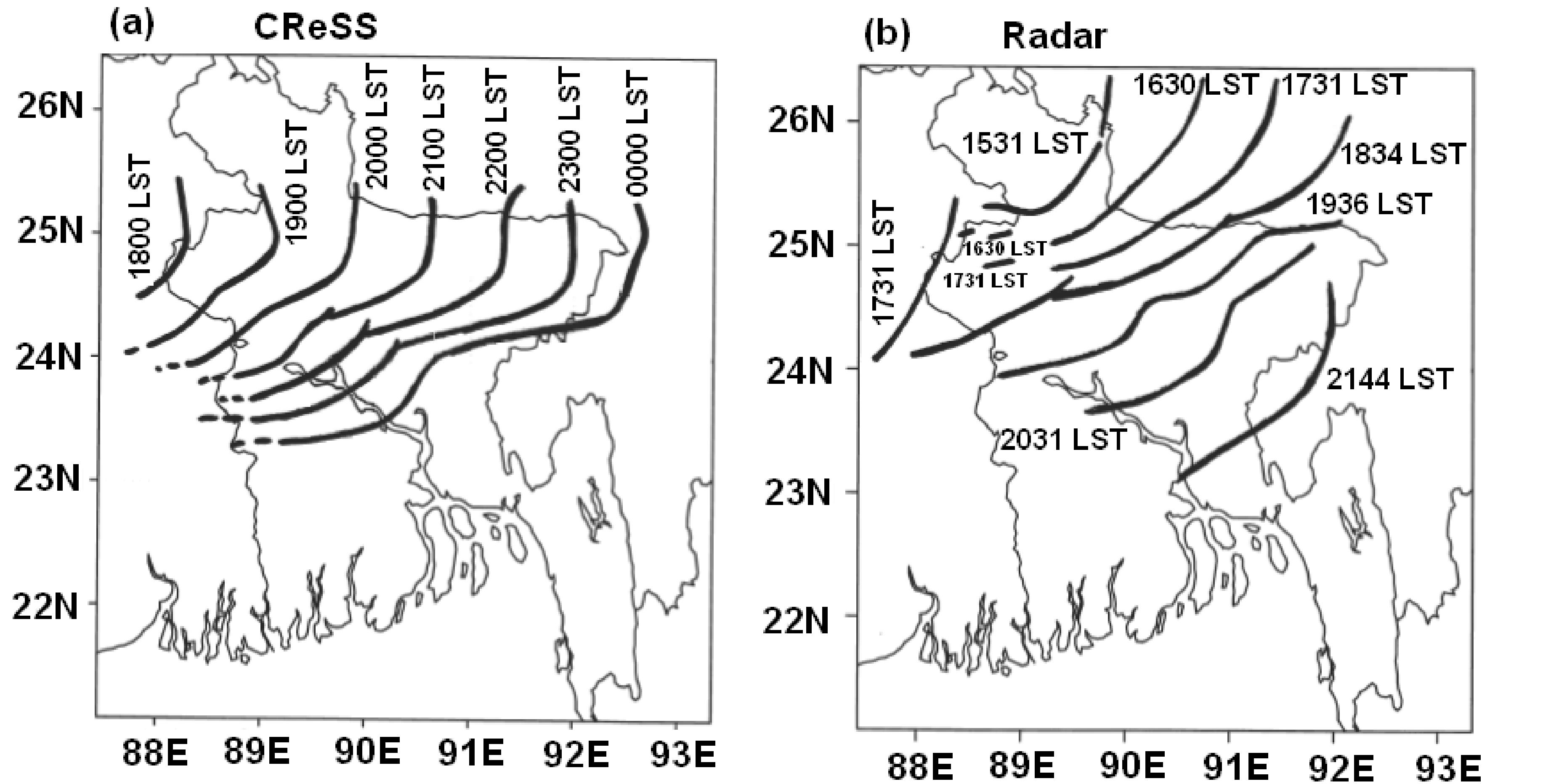

M. Rafiuddin et al., Figure 5

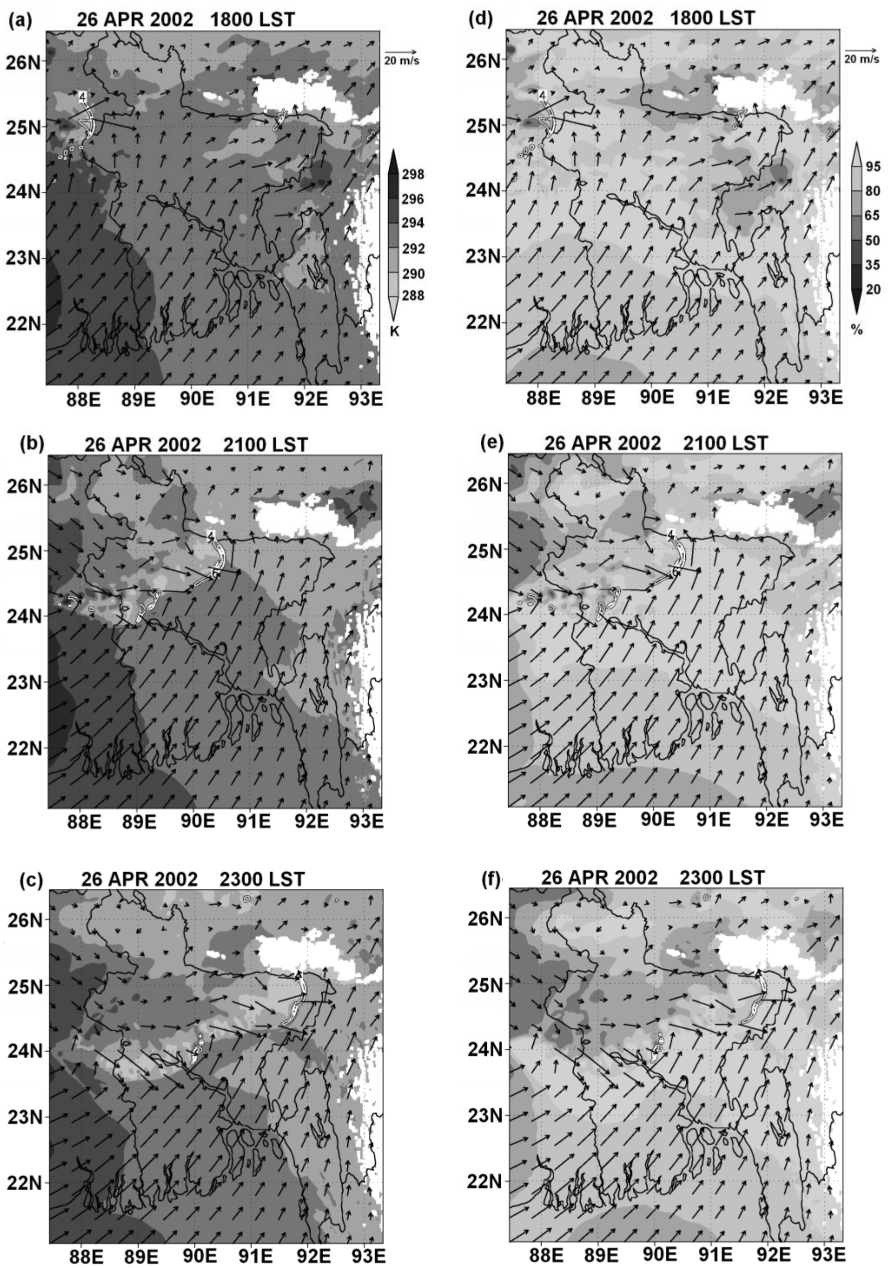

M. Rafiuddin et al., Figure 6

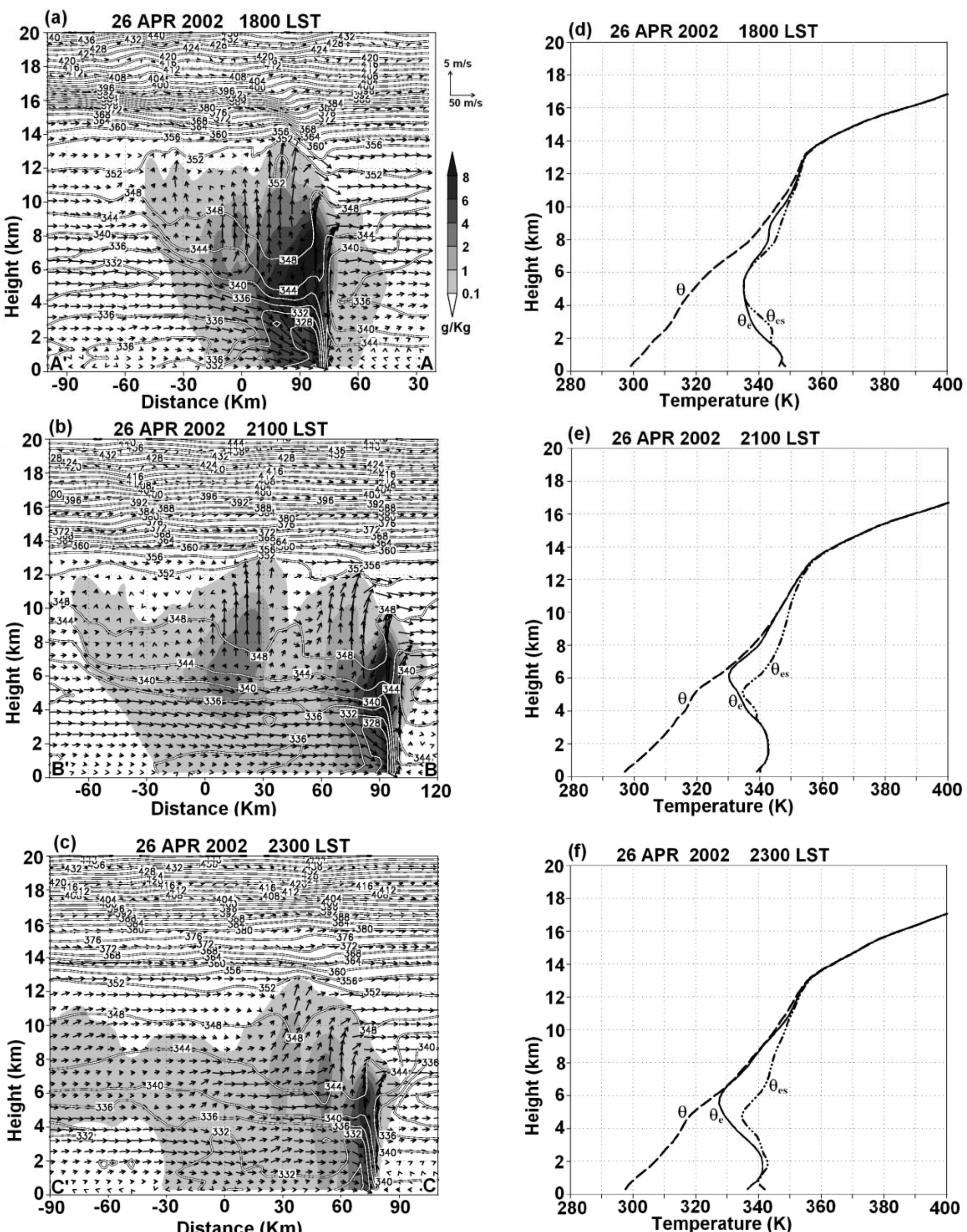

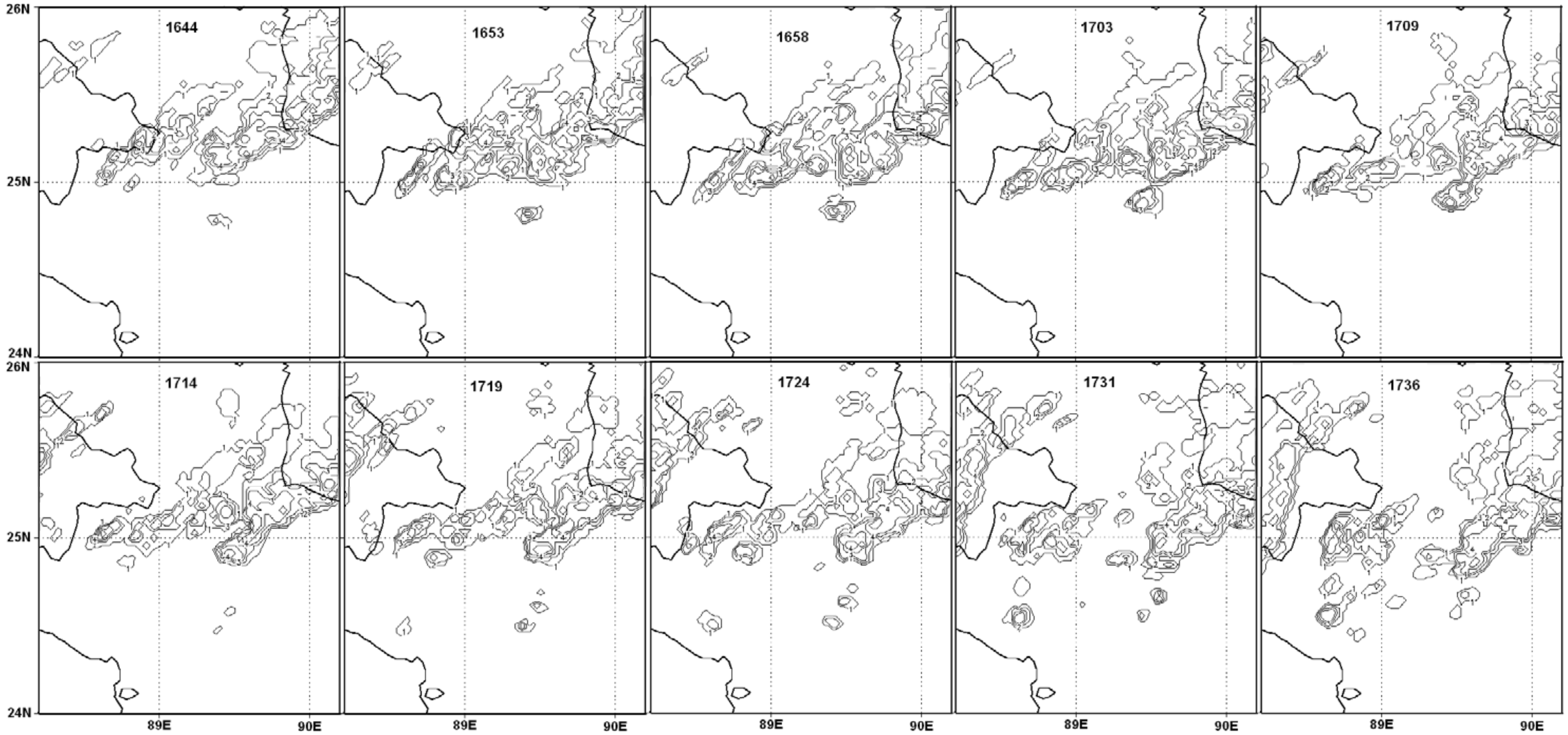

Fig. 8 Time series of cell development observed by radar.

M. Rafiuddin et al. Figure 9

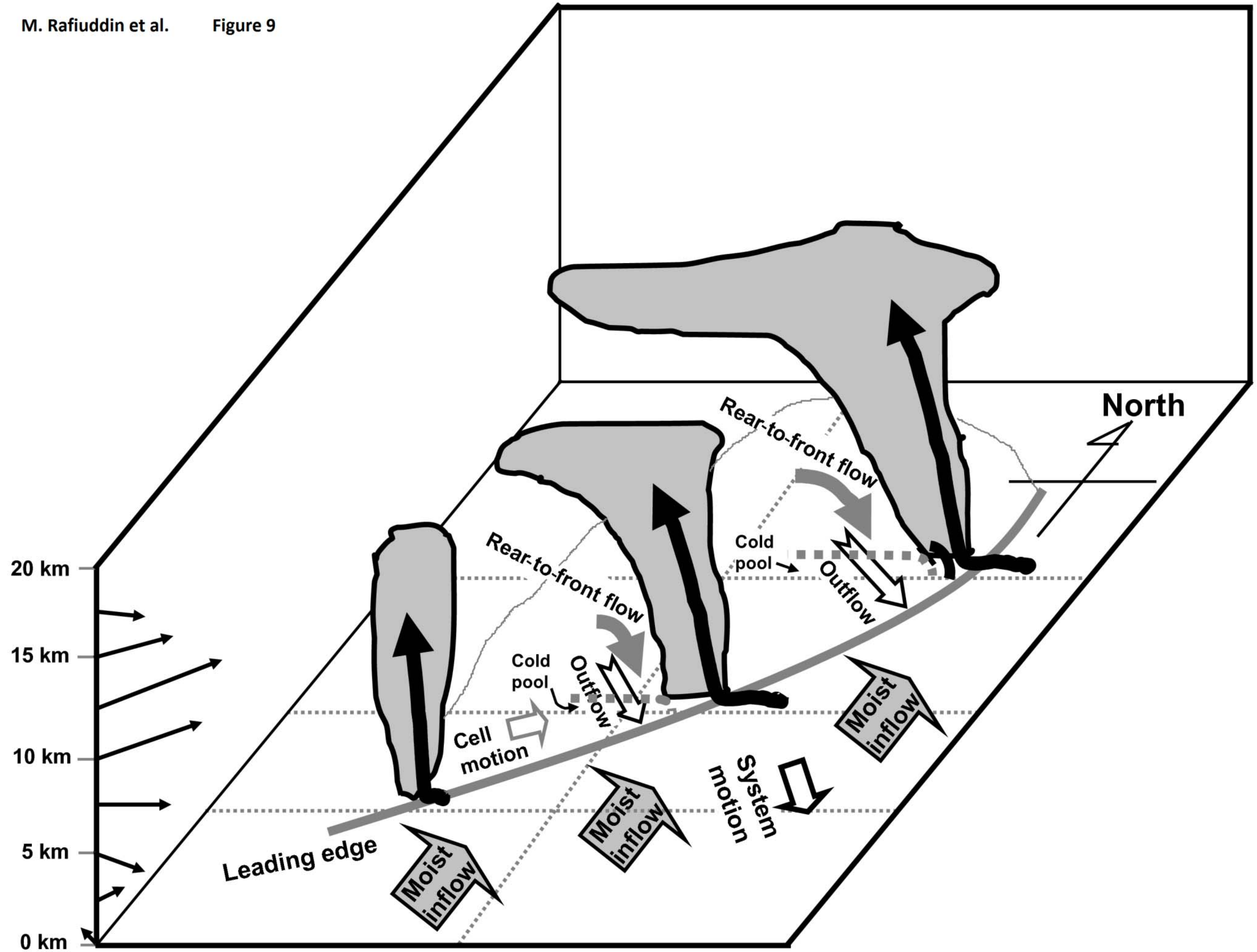

Coverage Area of BMD's Radar in Bangladesh

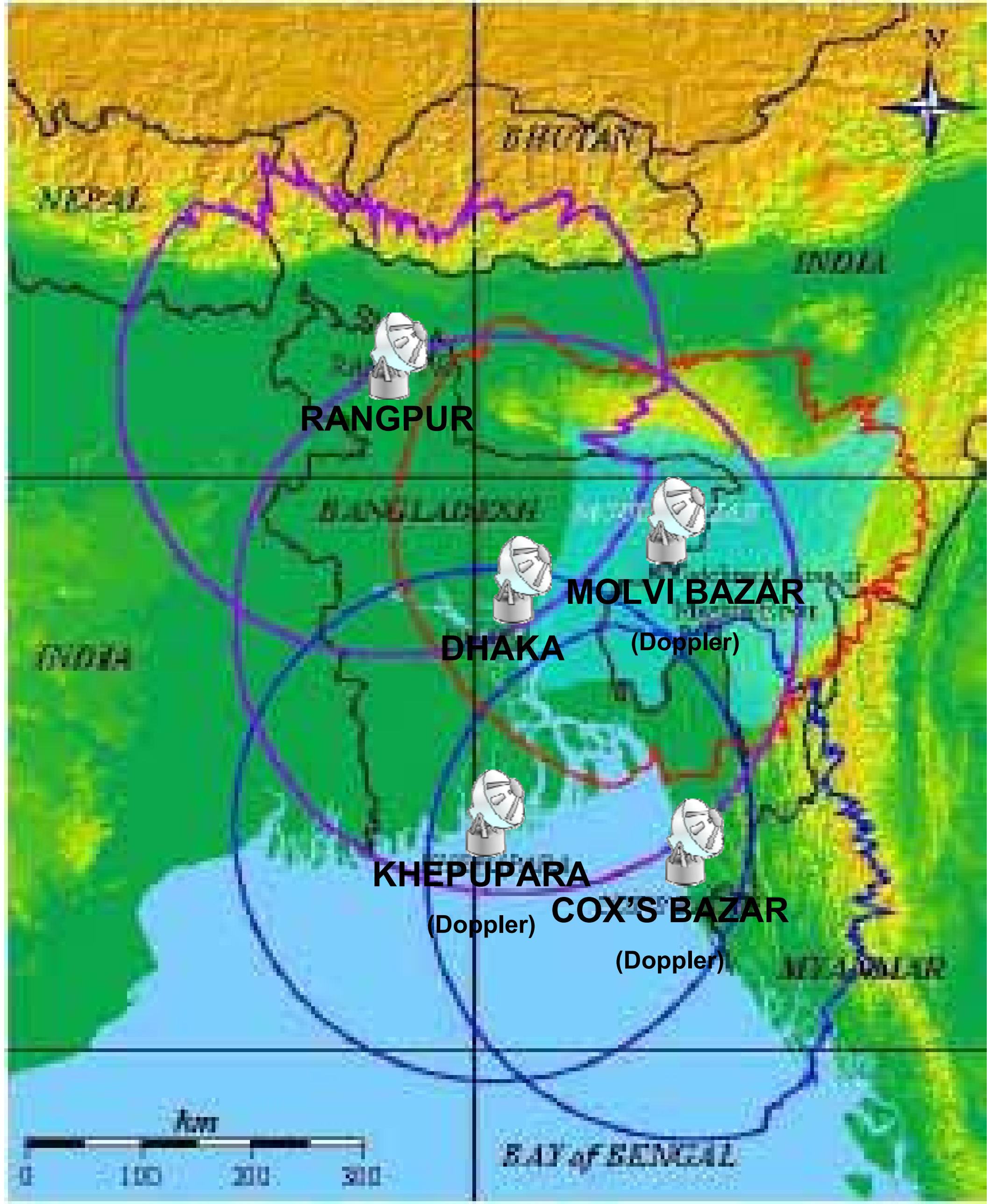

No. of Radar in Bangladesh: 5

(Doppler = 3, Convectional = 2)

To study the structure of precipitation system TRMM PR data will be used.

In order to understand the time variation of precipitation system, Cox's Bazar Doppler radar data will also be used with TRMM PR data.

Cox's Bazar Doppler Radar Specifications

Radar Type : S-band weather radar

Location : 91.9764 E, 21.4340 N

Radar Height : 117 meter

Frequency : 2847 MHz (~3 GHz)

PRF1 : 720 Hz

PRF2 : 576 Hz

Rotational Speed: 6 Deg/s
(24 deg/s for long range)

Elevation angle : 0, 1.5, 3, 4.5, 6, 9, 12, 15 Deg
(0, 1.5, 3 deg for long range)

Radar Range : 200 km
(for long range 440 km)

Operation Hour : 02-03 UTC, 05-06 UTC,
08-09 UTC, 11-12 UTC

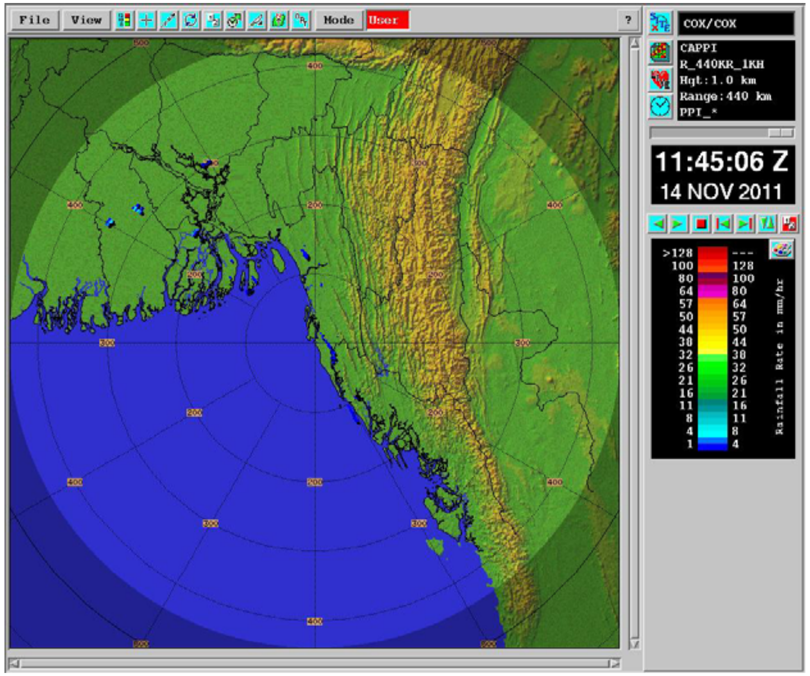

Case of 5 June 2007 [TRMM PR]

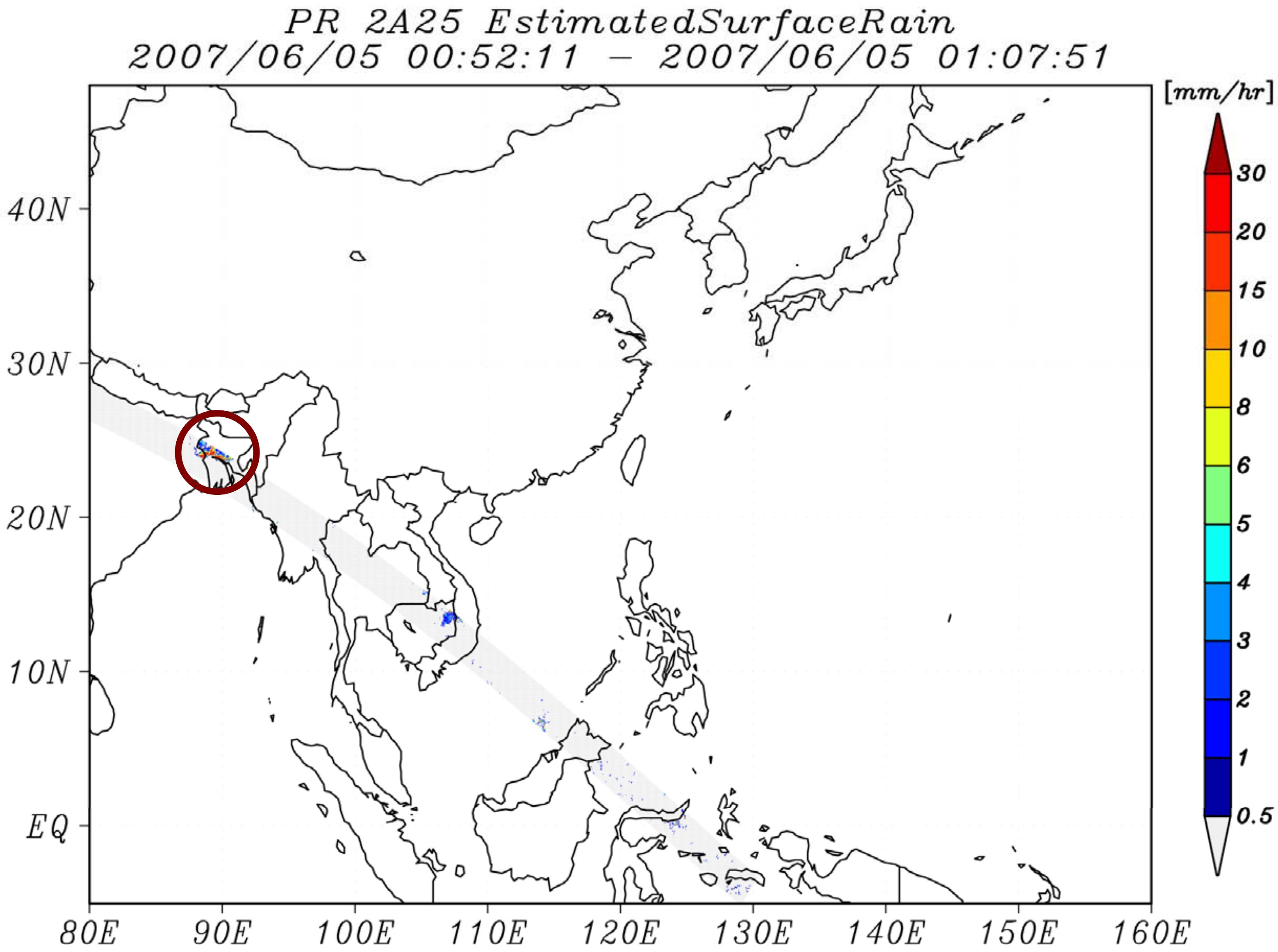

Case of 5 June 2007 [TRMM PR and Cox's Bazar Radar]

TRMM PR

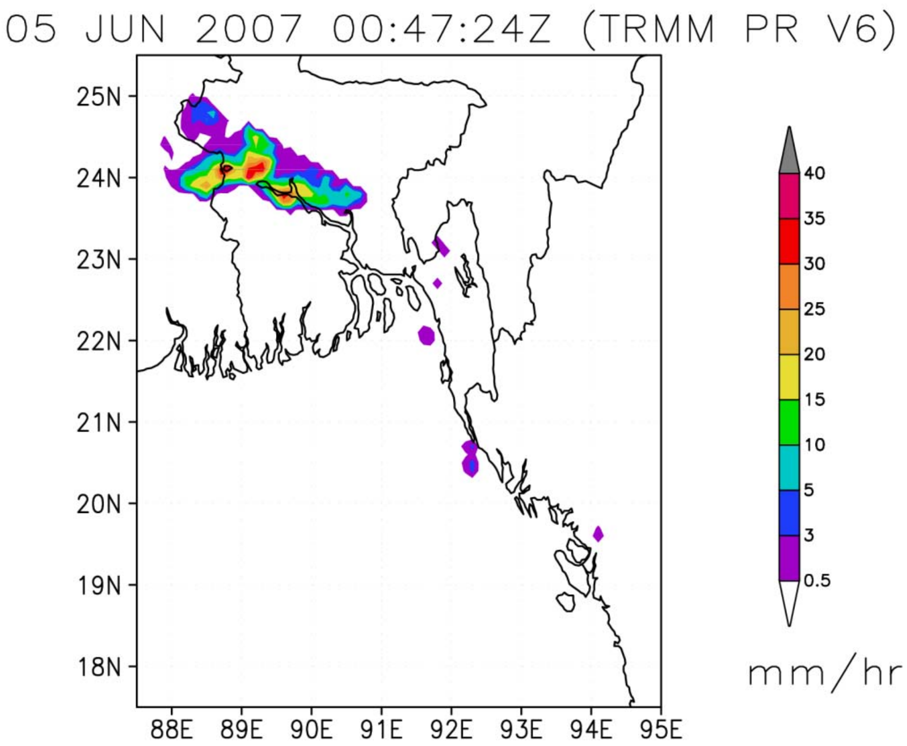

Cox's Bazar Doppler radar

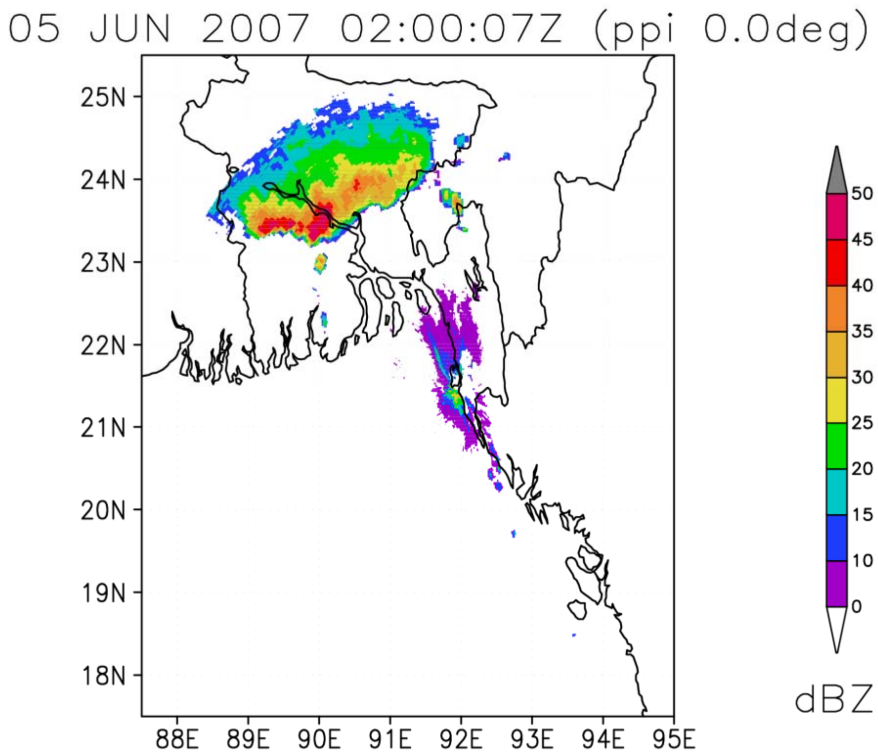

Case of 5 June 2007 [TRMM PR: Vertical Cross Section]

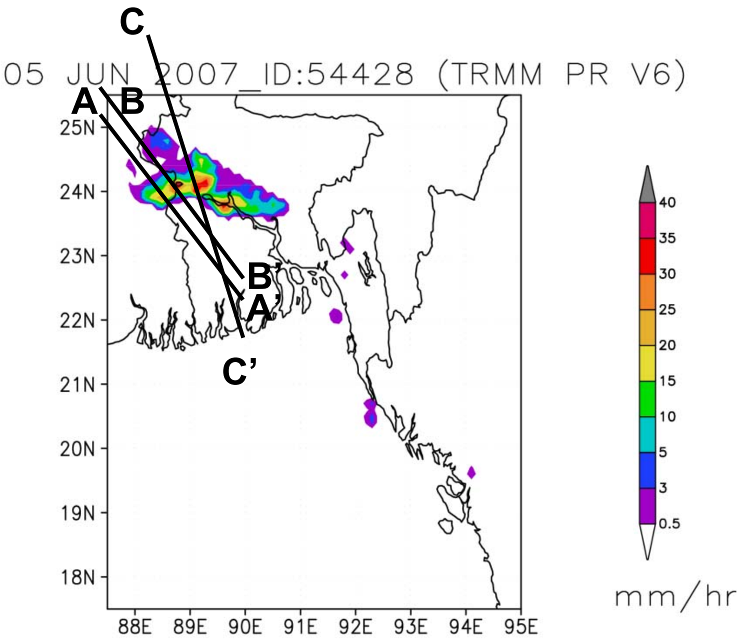

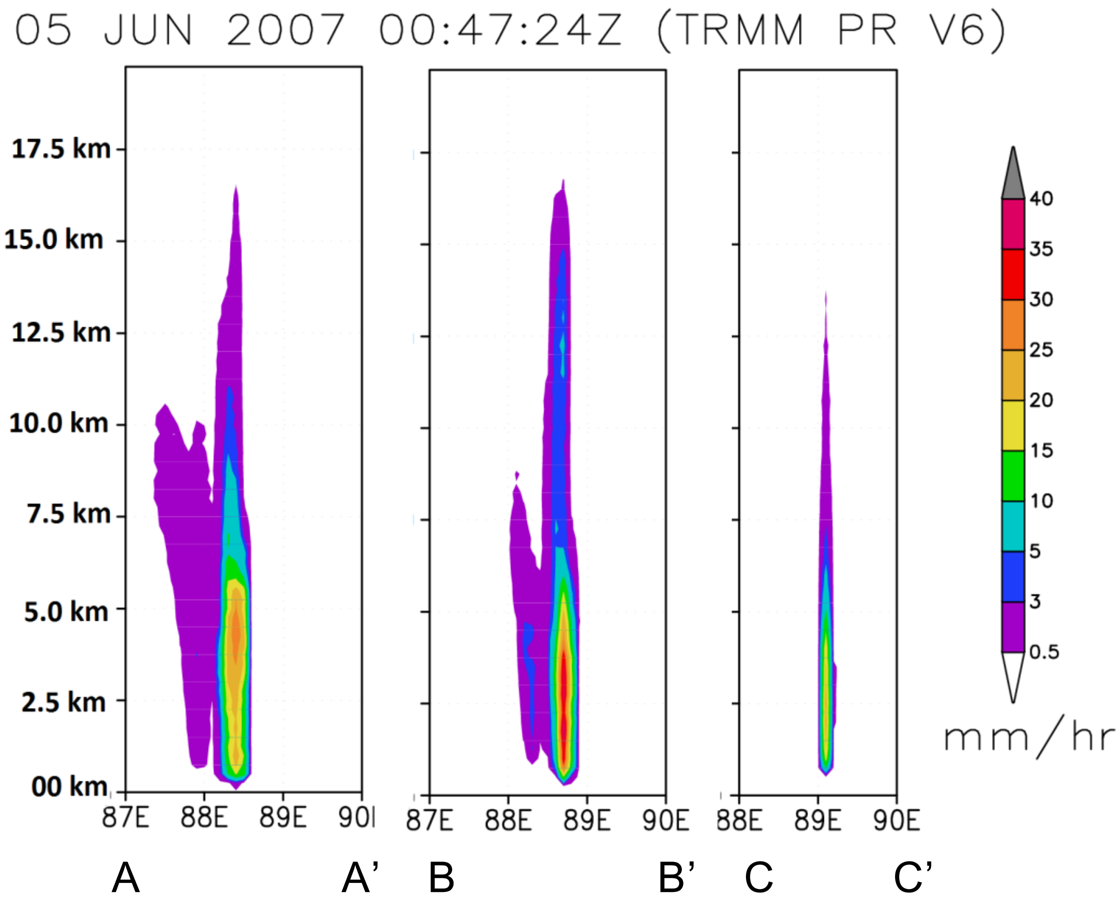

Case of 5 June 2007 [Reflectivity (PPI)]

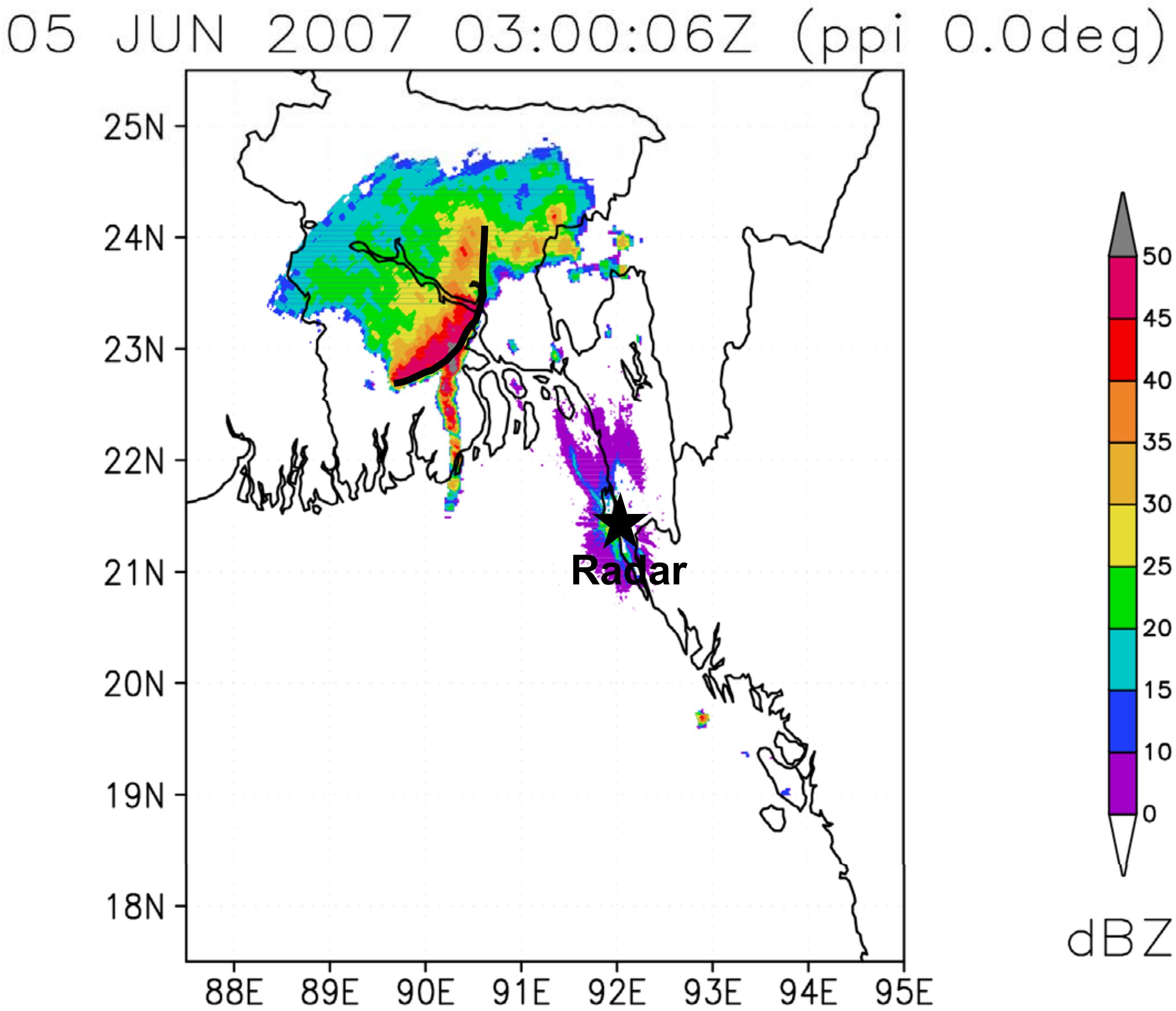

Case of 5 June 2007 [Reflectivity (PPI)]

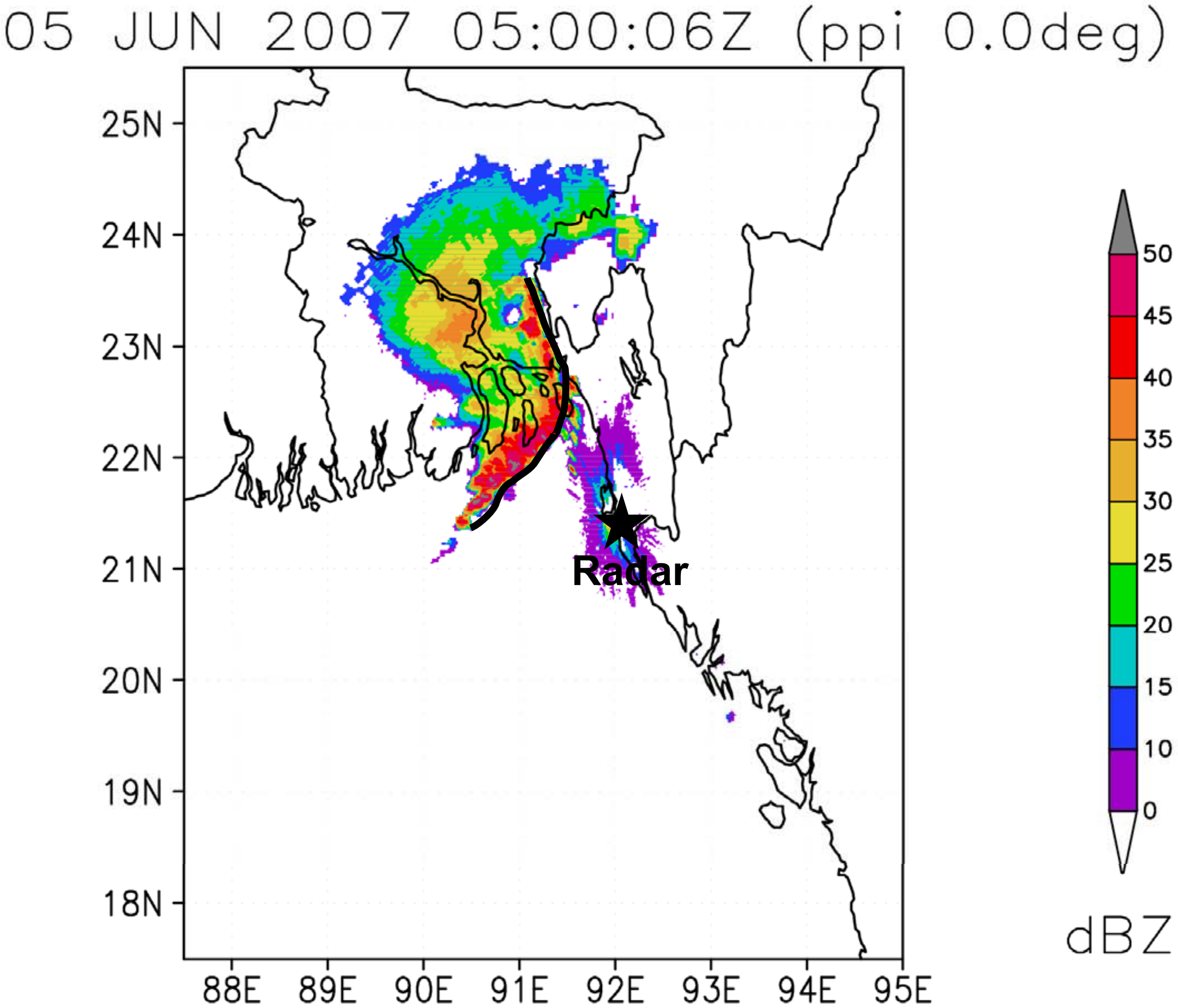

Case of 5 June 2007 [Reflectivity (PPI)]

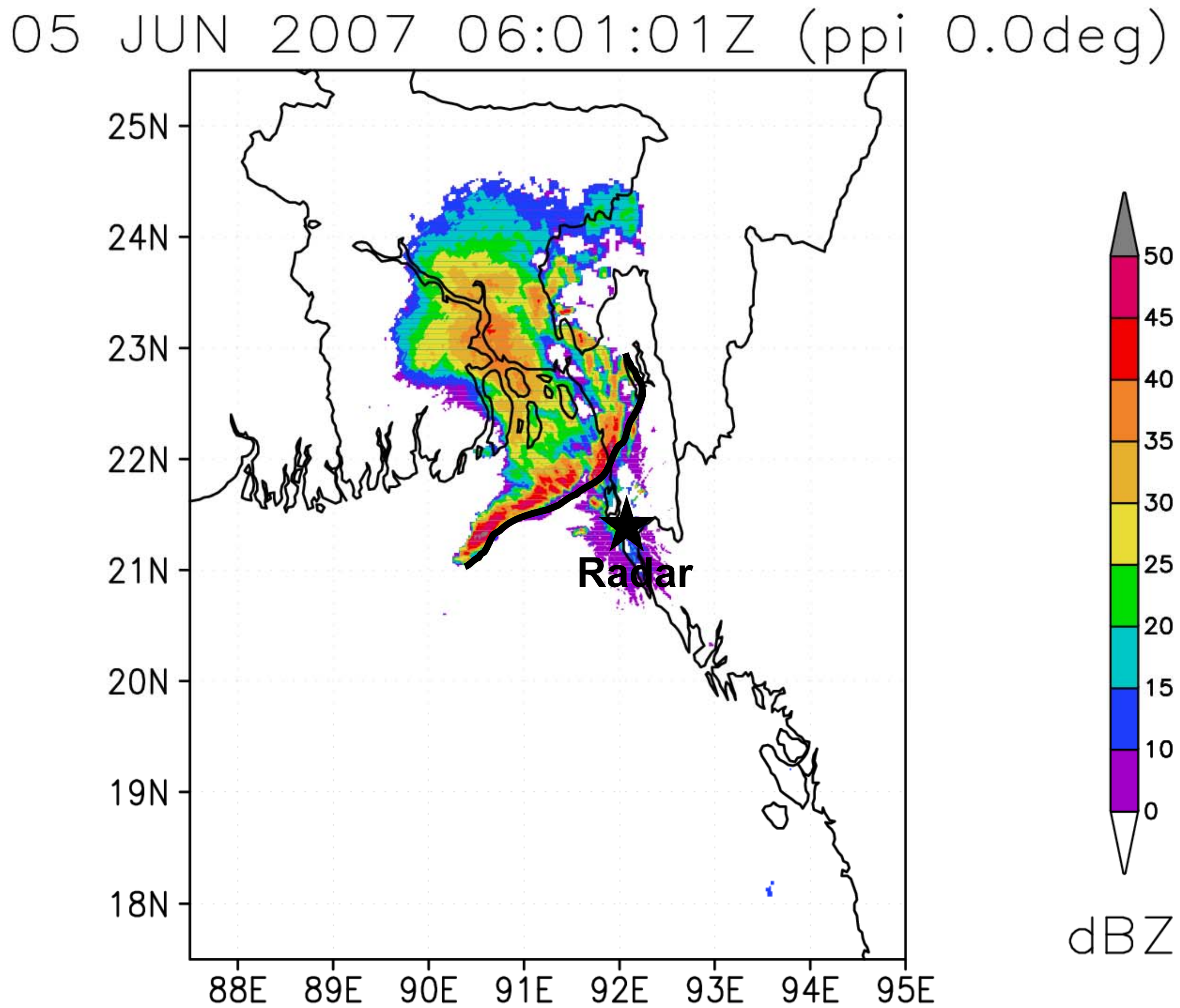

Case of 5 June 2007 [Tracking of Convective Line]

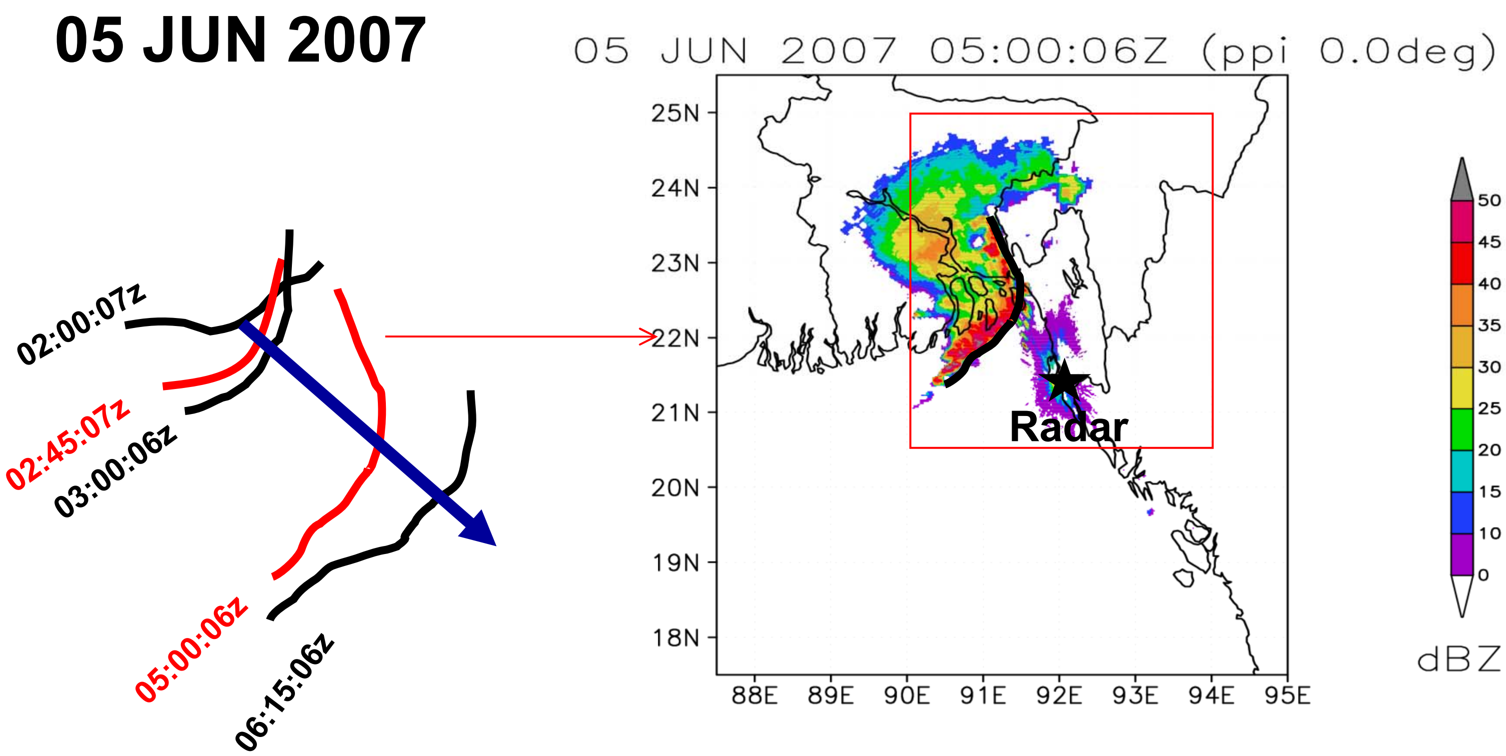

Propagation speed of system = ~ 18 m/s

Case of 5 June 2007 [Reflectivity (CAPPI)]

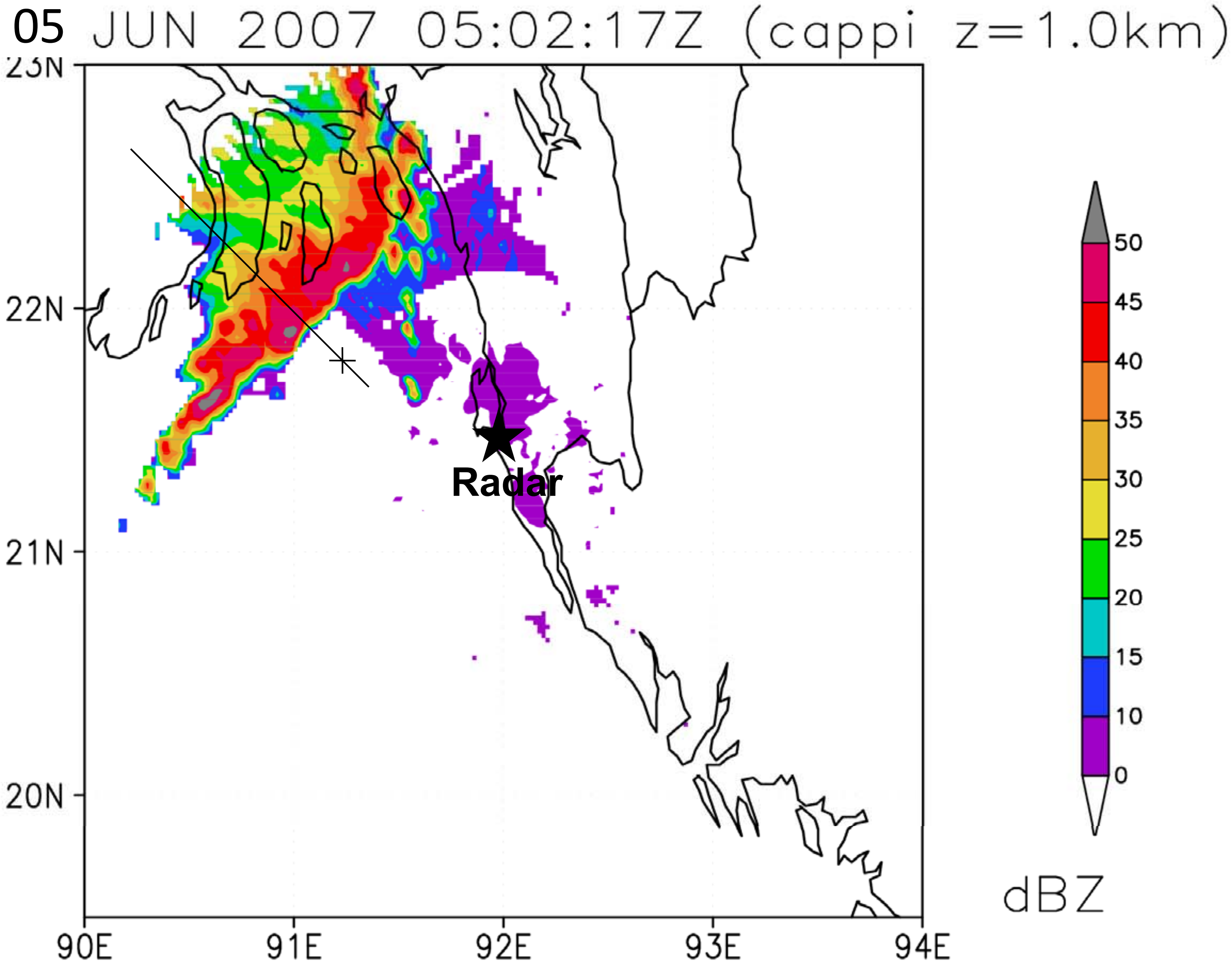

Case of 5 June 2007 [Doppler velocity (CAPPI)]

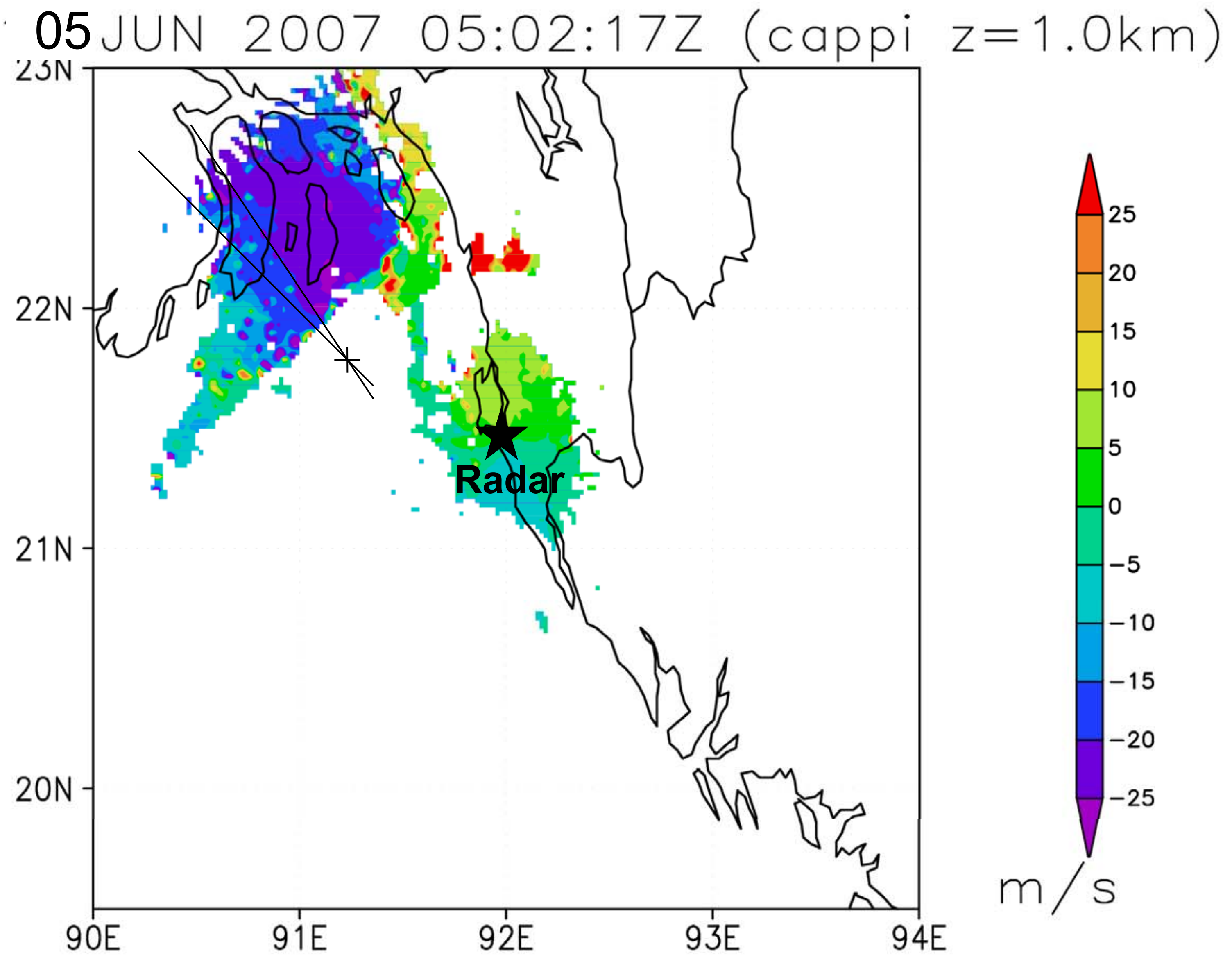

Case of 5 June 2007 [Reflectivity (Vertical Cross-section)]

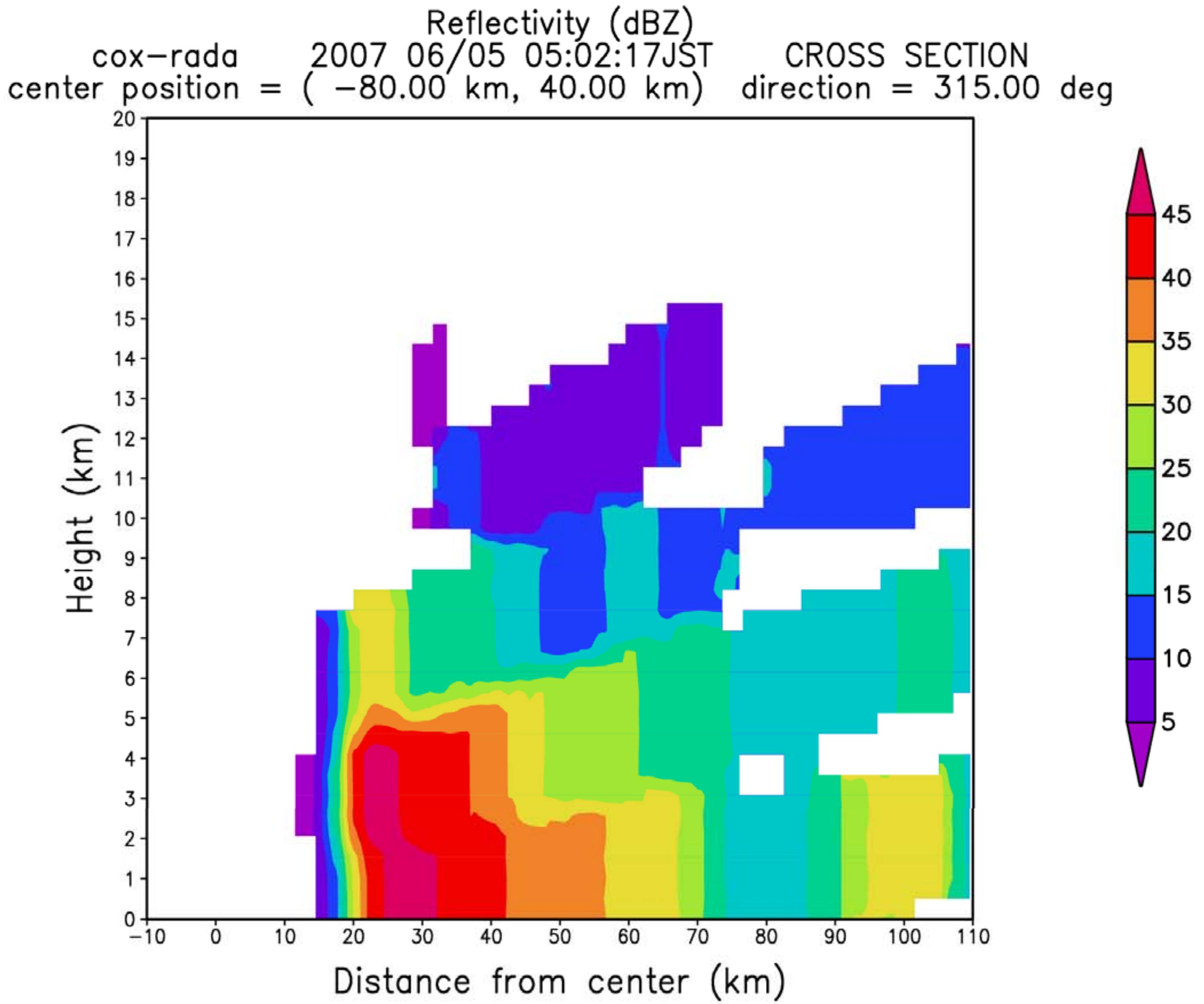

Case of 5 June 2007 [Velocity (Vertical Cross-section)]

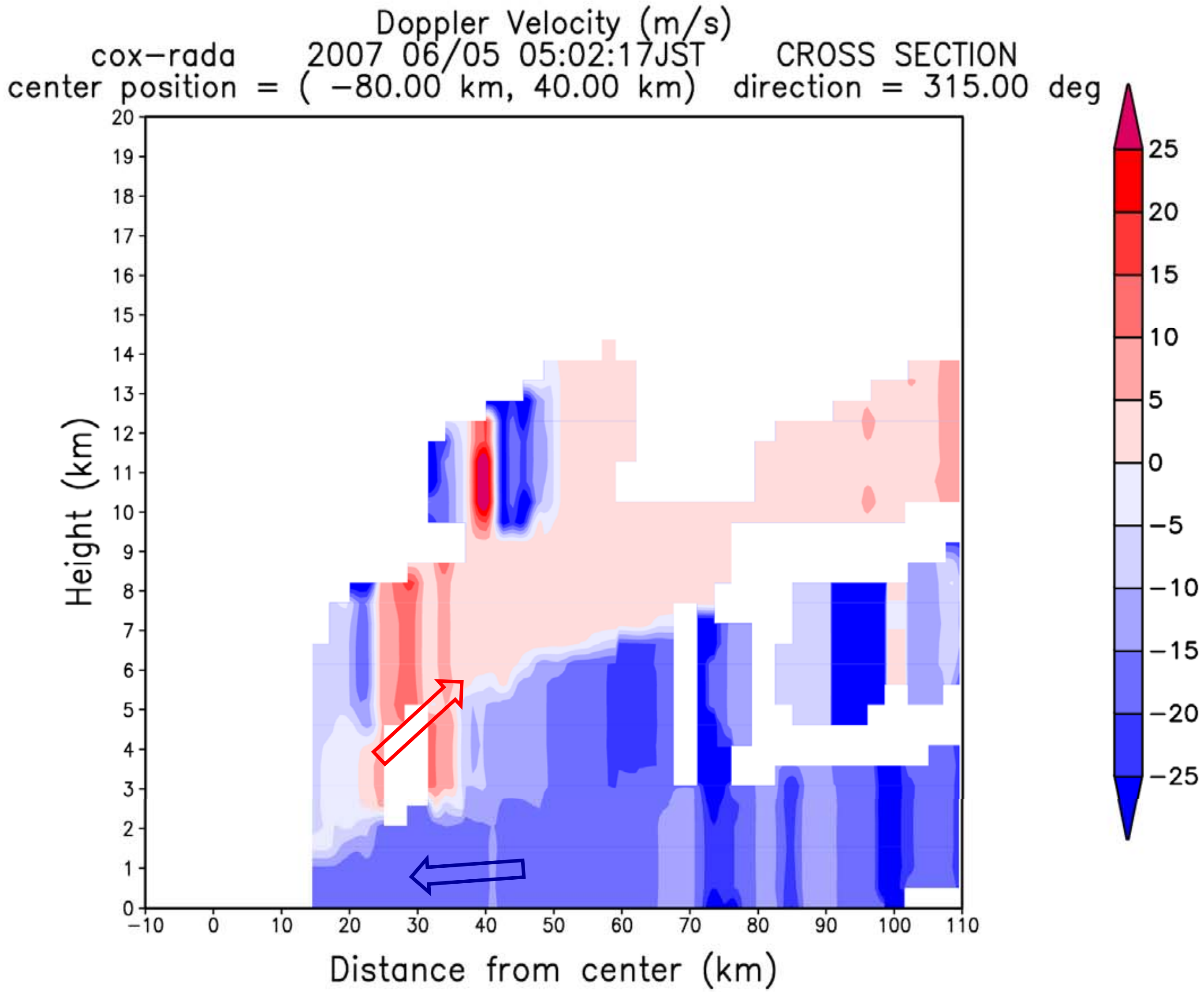

Case of 5 June 2007 [Velocity (Vertical Cross-section)]

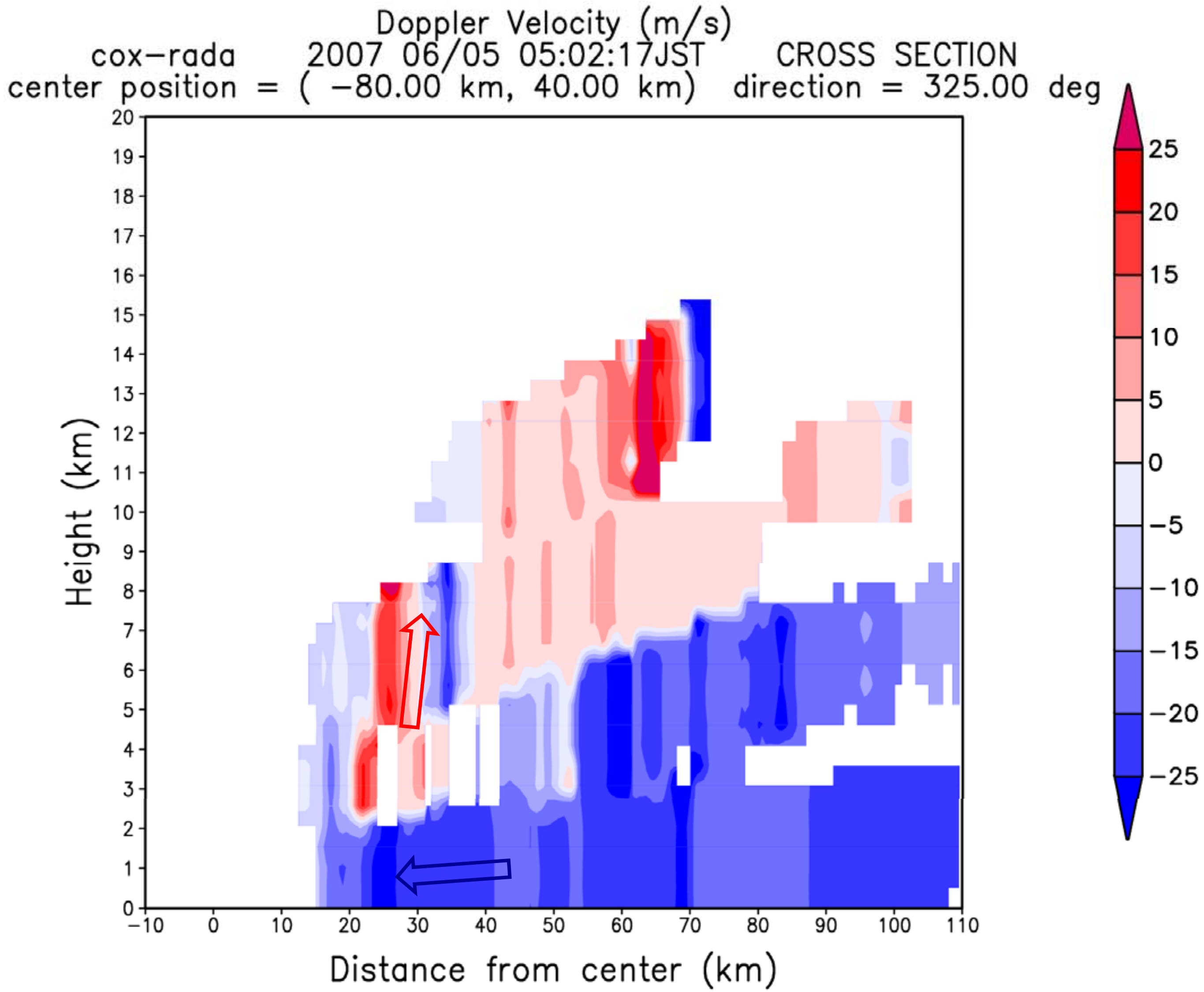

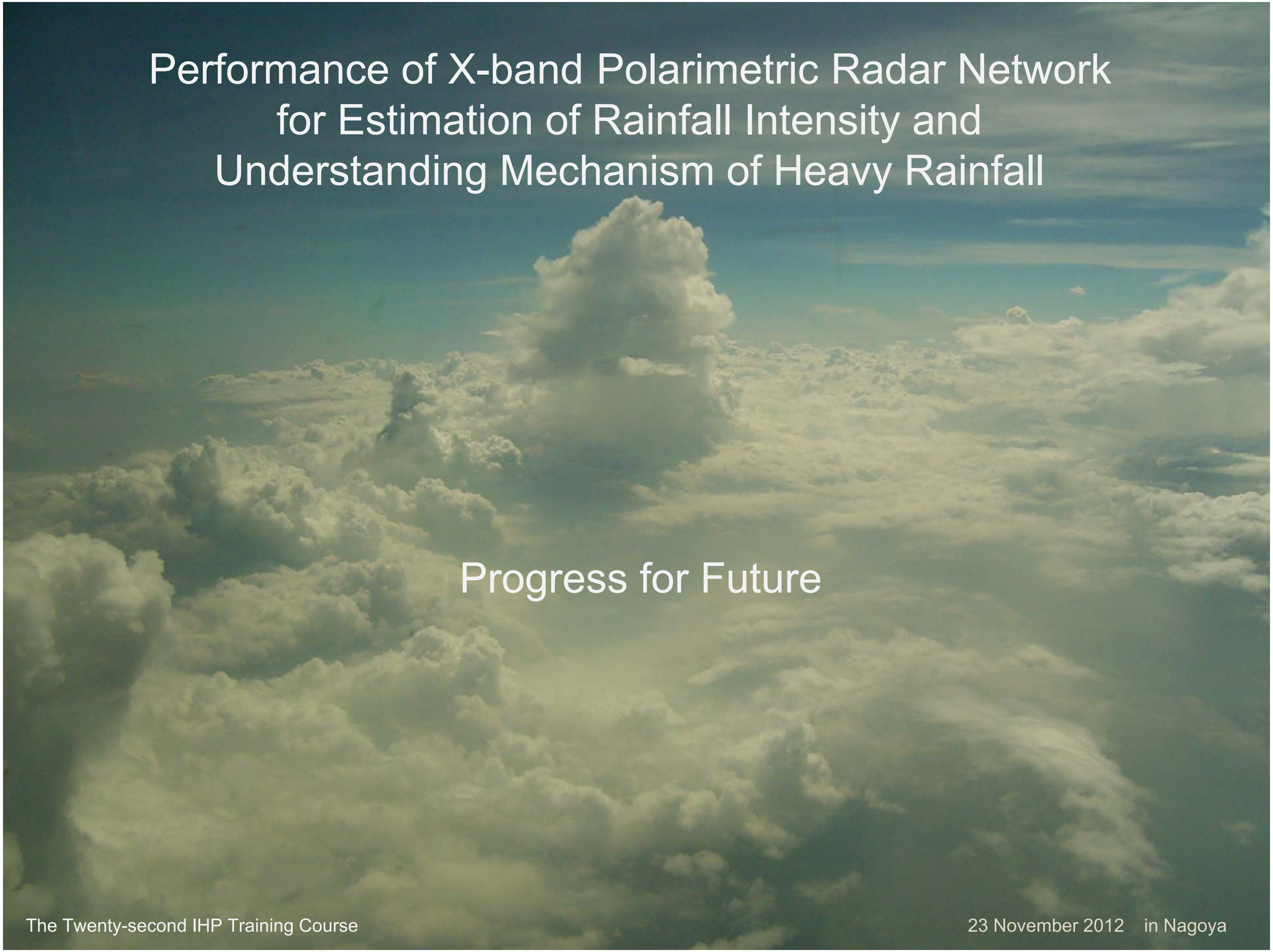
Performance of X-band Polarimetric Radar Network
for Estimation of Rainfall Intensity and
Understanding Mechanism of Heavy Rainfall
Progress for Future
The Twenty-second IHP Training Course
23 November 2012 in Nagoya

Radar Network in East Asia

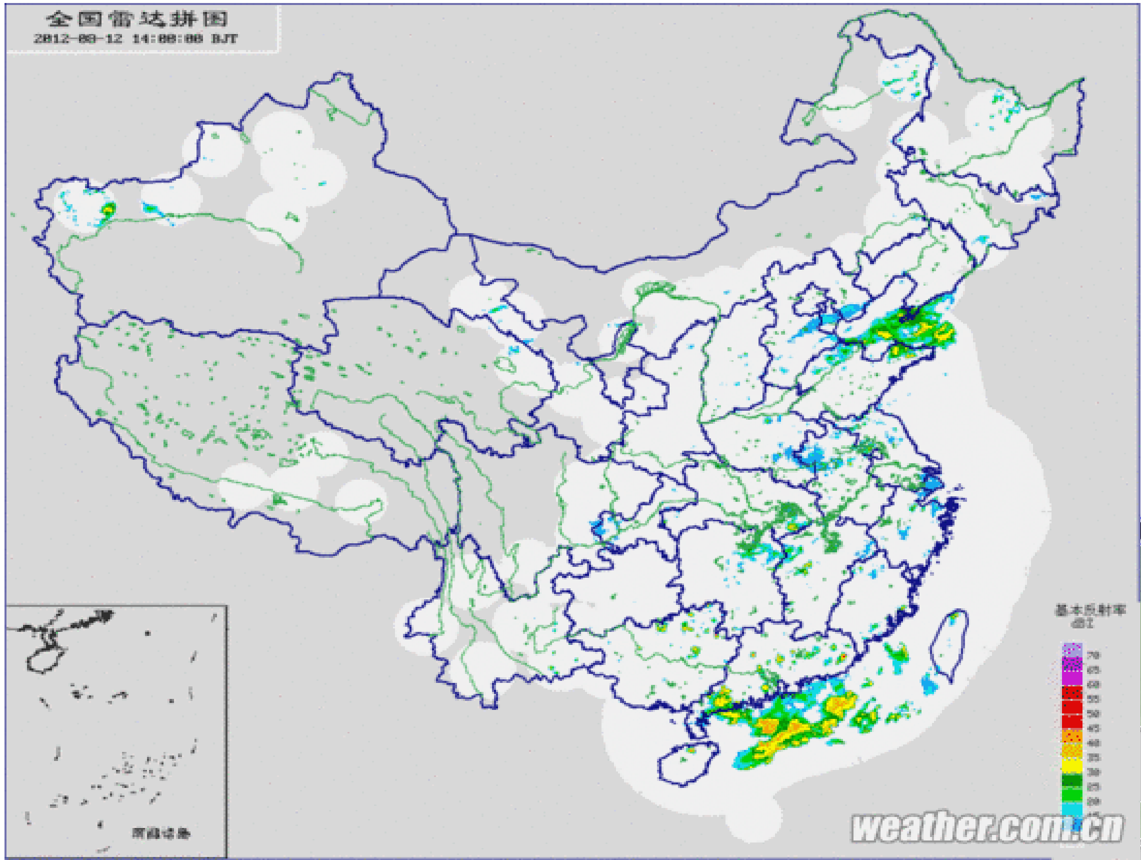

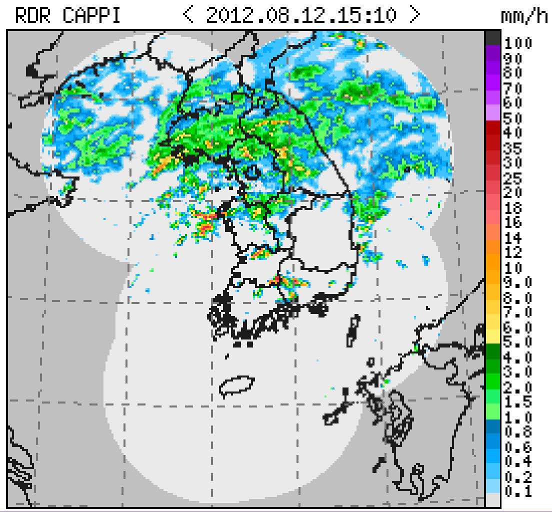

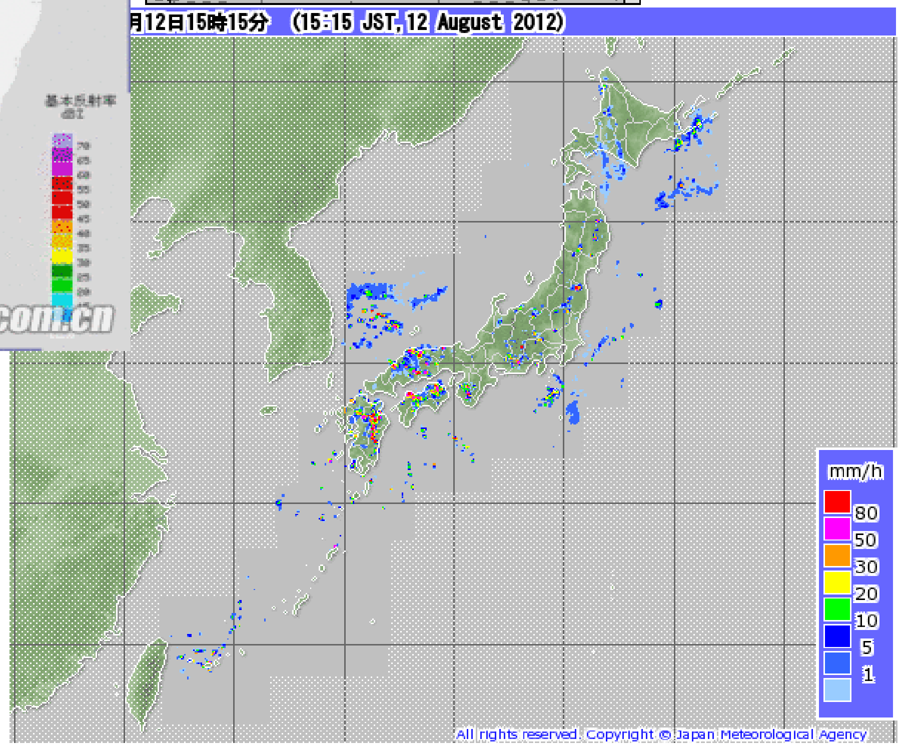

~ 0615 UT
12 August 2012

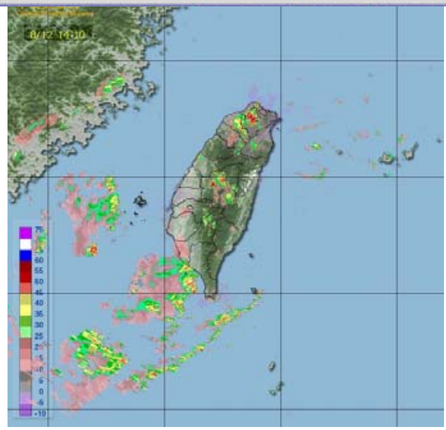

Doppler Radar → Polarimetric (MP) Radar

Recently, X-band polarimetric radar network has been constructed in Japan for monitoring and prediction of heavy rainfall in urban area.

Performance of X-band polarimetric radar for estimation of rainfall intensity and identification of precipitation particle type has been verified.

Progression:

Research in Japan

・Dual-polarization Radar

1987 C-band Public Works Research Institute
1991 X-band Hokkaido University
1995 X-band NIED

・Polarimetric Radar (measures Phase Shift)

2000 X-band (W-band) NIED
2001 C-band CRL (present NICT) [COBRA]
2007 X-band Nagoya University

For operational use in Japan

2010 X-band MLIT (Ministry of Land, Infrastructure, Transport and Tourism) [X-RAIN]

* Main target is heavy rainfall in urban area.

Frequency	9375 MHz, 9415 MHz
Band width	4 MHz
Amplifier	Solid-state
Peak power	200 W
Pulse width	1 μs (short pulse) 1～64 μs (long pulse)
PRF	2000 Hz (normal) 20000 Hz
Antenna diameter	2.0 m
Beam width	1.2 deg.
Observation parameters	Z_H, v, σ_v, Z_{DR}, $\rho_{HV}(0)$, Φ_{DP}, K_{DP} LDR_{HV} , LDR_{VH}
Observation range	64 km

Polarimetric Radar

Illustrate by Kouketus

Polarimetric Parameters

＜Received Signal Power＞
- Radar Reflectivity (Z_h)
- Differential Reflectivity (Z_{dr})
- Correlation Coefficient (ρ_{hv})

＜Phase Shift＞
- Differential Phase Shift (K_{dp})

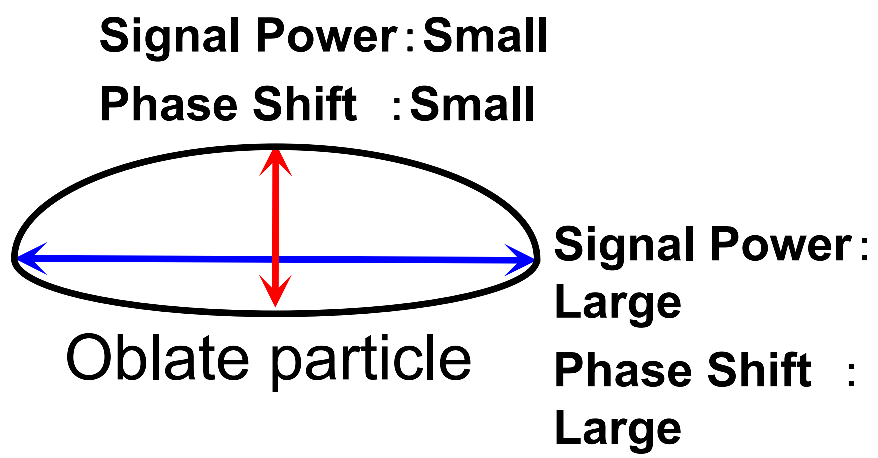

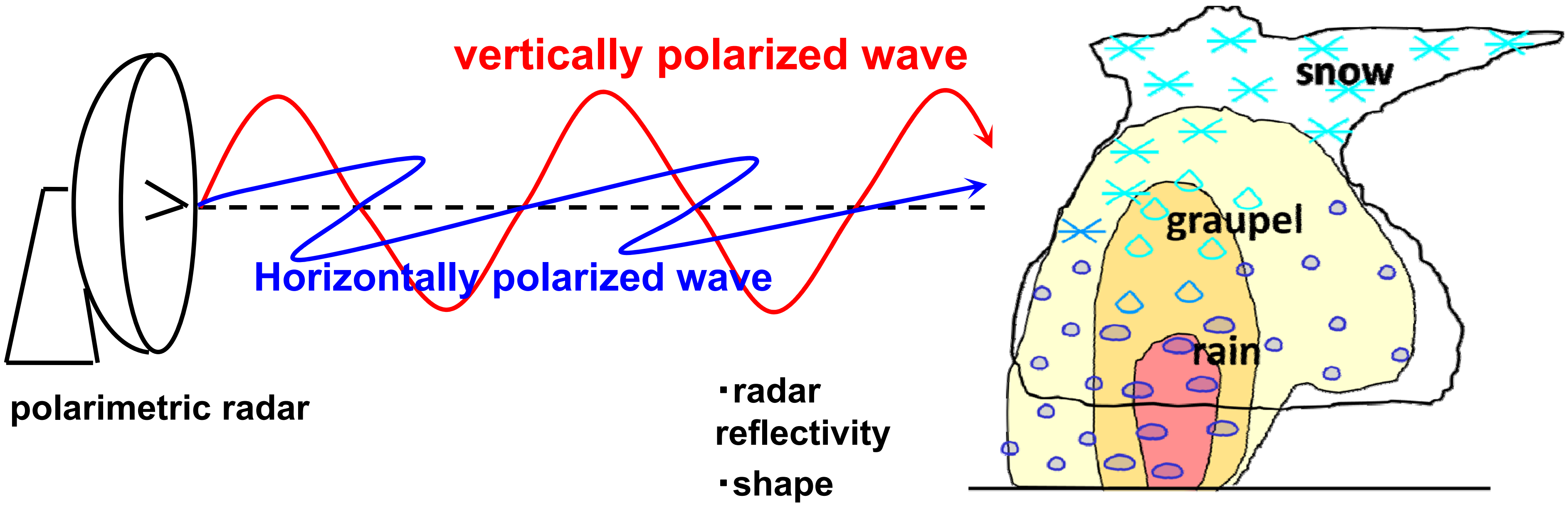

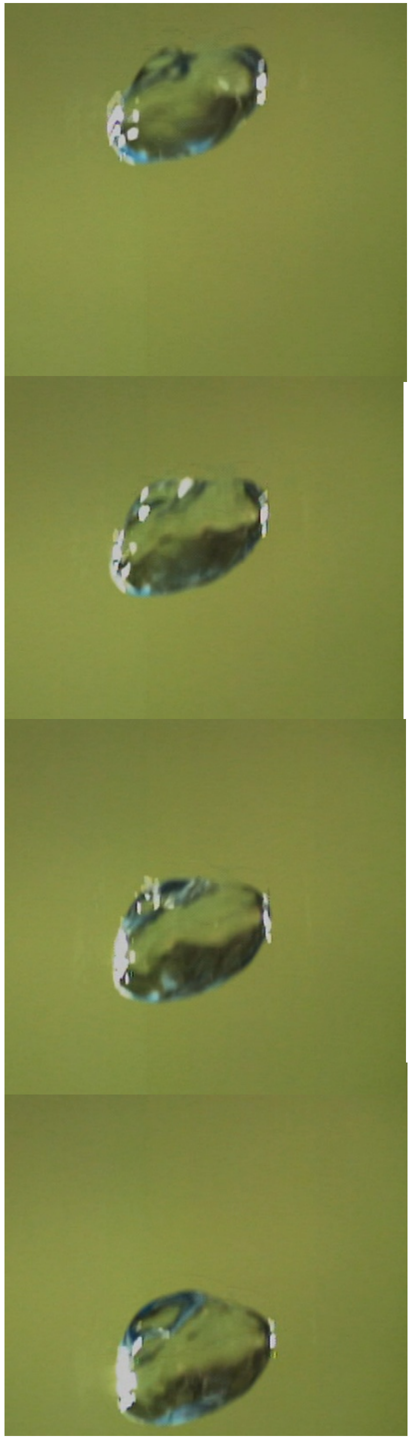


雨の物語
~日本最多雨　大台ヶ原の四季~

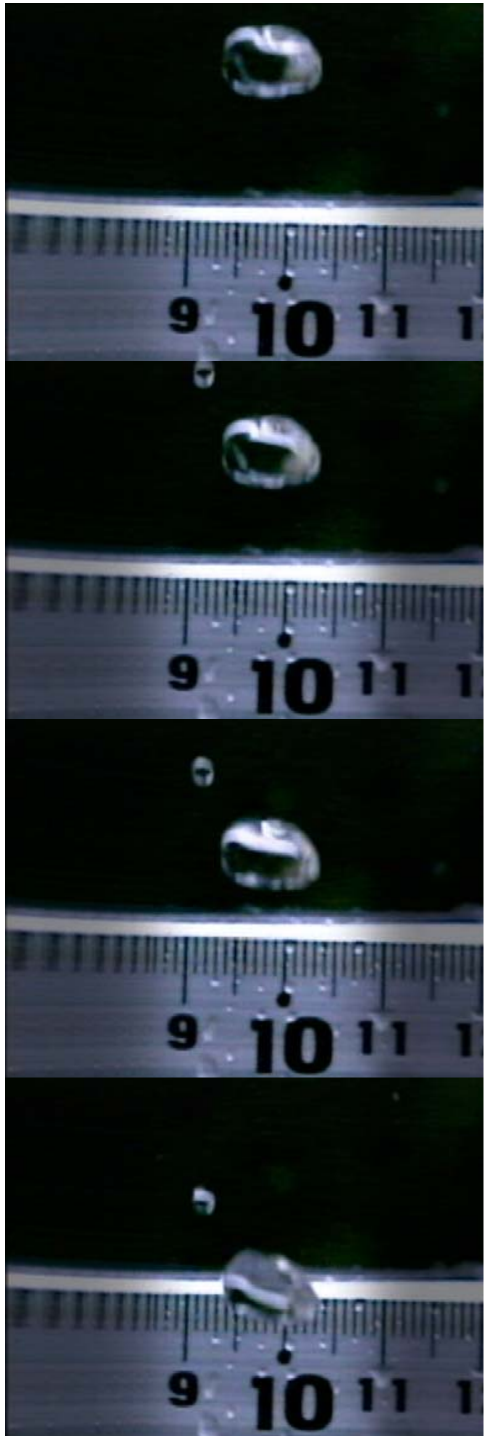

Polarimetric Parameters (1) : Z_h and Z_{dr}

● Radar Reflectivity: Z_h (=$10\log_{10} Z_h^*$)

$$Z_h^* = \int N(D)\, D^6 \, dD$$

Z_h^* : reflectivity factor of **horizontal** wave

D : Diameter N(D) : Particle size distribution

- Proportional to **fifth power of diameter**
- Proportional to **particle Size distribution**

Small

(e.g. drizzle)

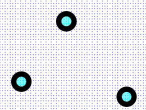

Large

(e.g. heavy rain, hail)

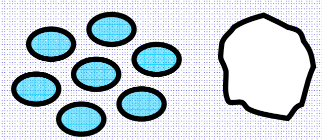

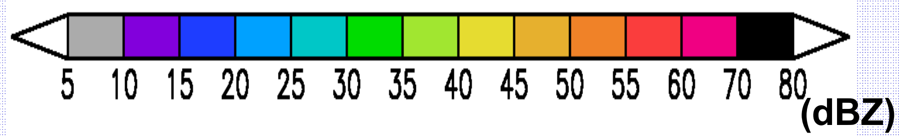

● Differential Reflectivity: Z_{dr}

$$Z_{dr} = 10\log_{10}\left[\frac{Z_h^*}{Z_v^*}\right]$$

Z_h^* : reflectivity factor of **horizontal** wave

Z_v^* : reflectivity factor of **vertical** wave

reflectivity factor : small

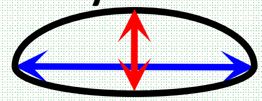

reflectivity factor : large

- **oblate shape → Z_{dr} > 0**
- **spherical shape → 0**
- **prolate shape → Z_{dr} < 0**

graupel, hail

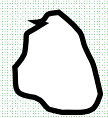

drizzle

large rain drop, ice crystal

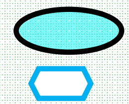

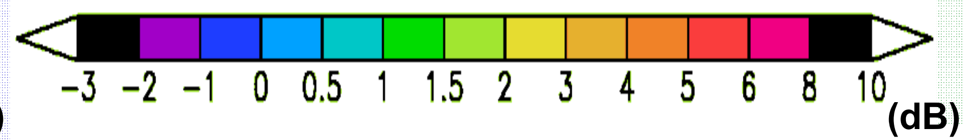

Polarimetric Radar

Polarimetric Parameters

＜Received Signal Power＞

・Radar Reflectivity (Z_h)

・Differential Reflectivity (Z_{dr})

・**Correlation Coefficient (ρ_{hv})**

＜Phase Shift＞

・**Differential Phase Shift (K_{dp})**

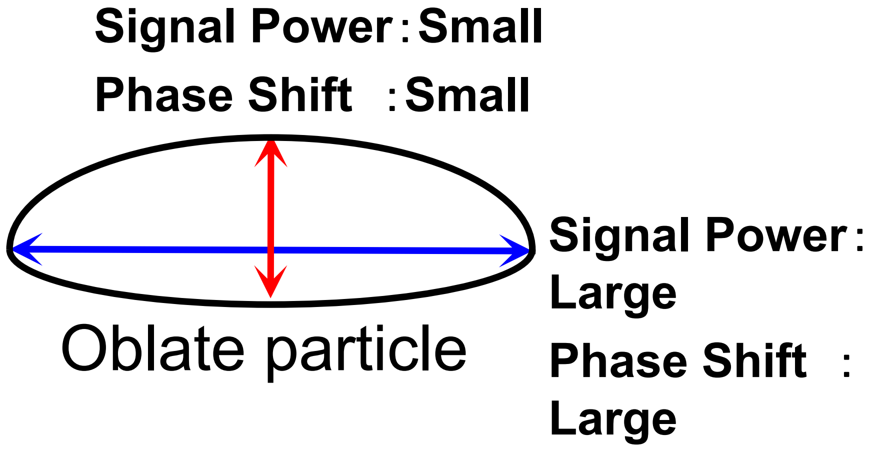

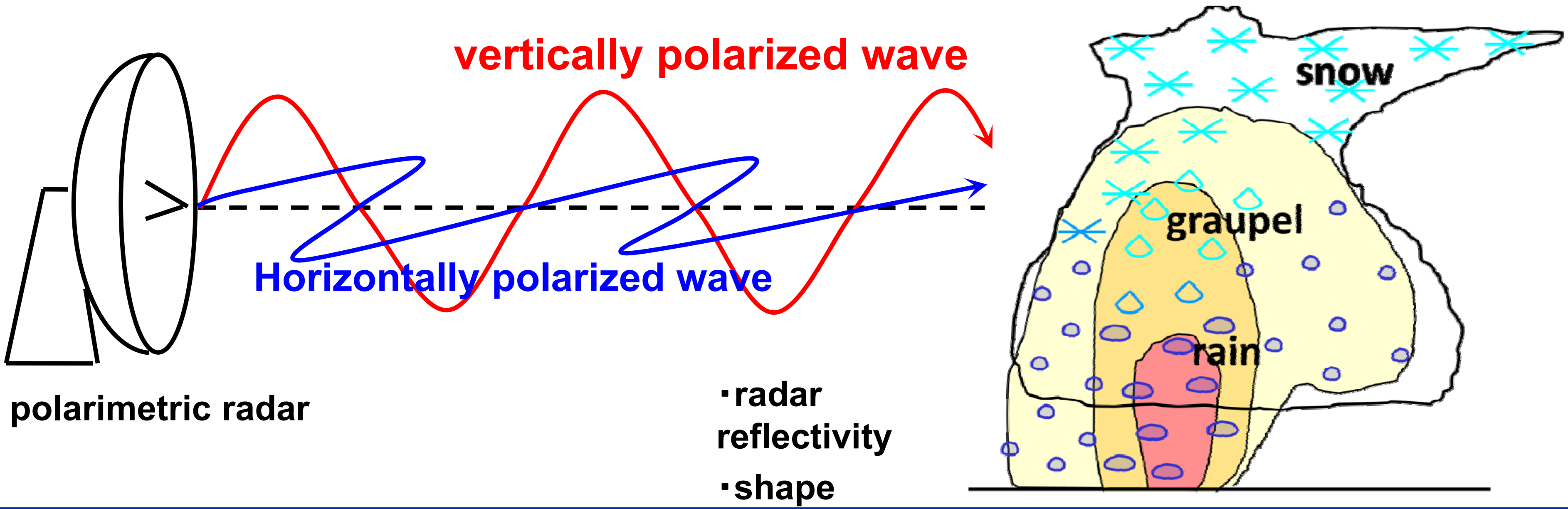

Polarimetric Parameters (2) : ρ_{hv} and K_{dp}

●Correlation Coefficient: ρ_{hv}

$$\rho_{hv} = \frac{|\langle n s_v s_h \rangle|}{\langle n|s_h|\rangle^{\frac{1}{2}} \langle n|s_v|\rangle^{\frac{1}{2}}}$$

s_h : signal power of **horizontal** wave

s_v : signal power of **vertical** wave

- **homogeneous shape → high (～1.0)**
- **inhomogeneous shape → low**
- **wet (melting) ice → very low (<0.95)**

※low SNR → low value

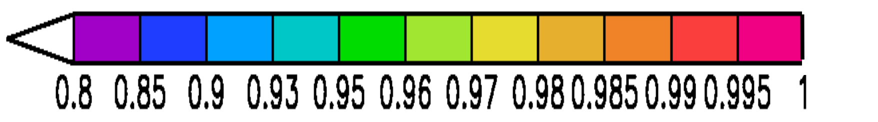

●Differential Phase Shift: K_{dp}

$$K_{dp} = \frac{1}{2}\frac{d\Phi_{dp}}{dr}$$

Φ_{dp} : differential phase

r : range

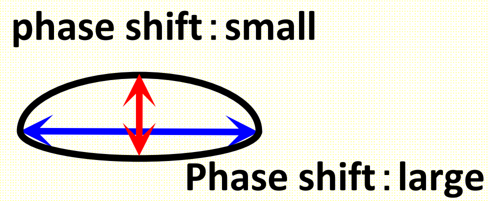

- **oblate particle → K_{dp} is large.**
- **Large water content → K_{dp} is large.**

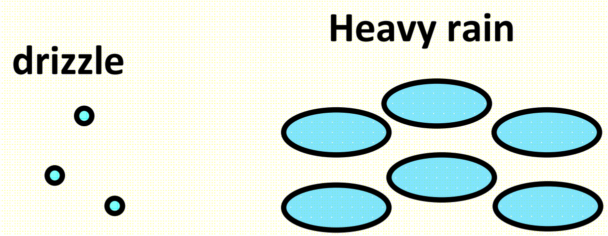

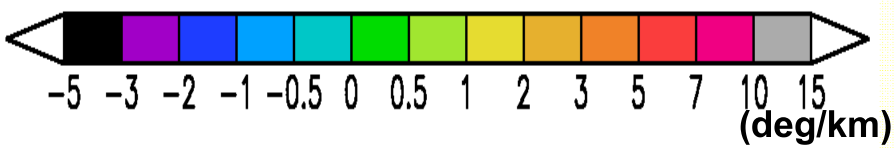

X-band MP Radar Network (Nagoya Area) of WDMB, MLIT

MILT (Ministry of Land, Infrastructure, Transport and Tourism)

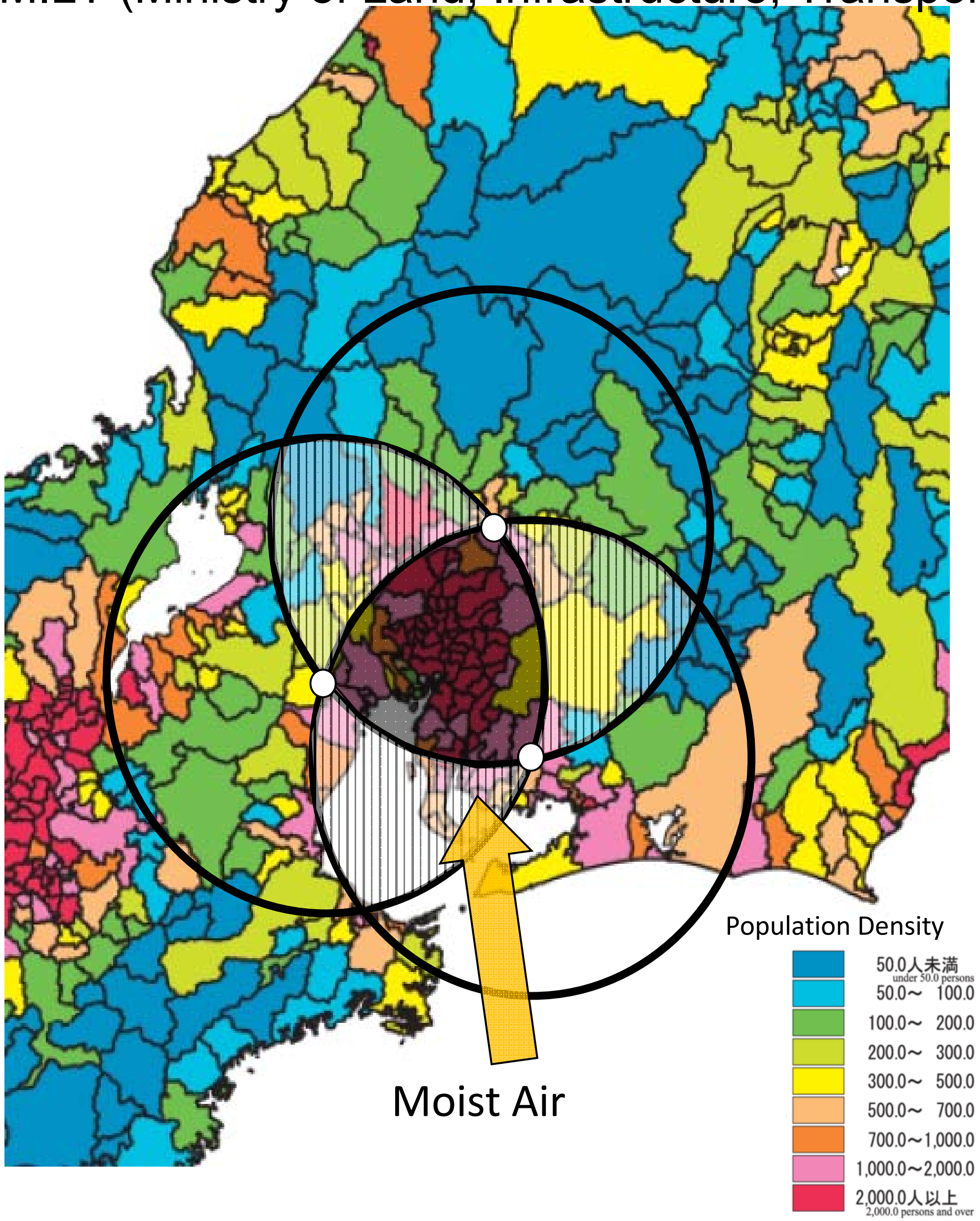

Heavy Rainfall Case (2008/8/29)

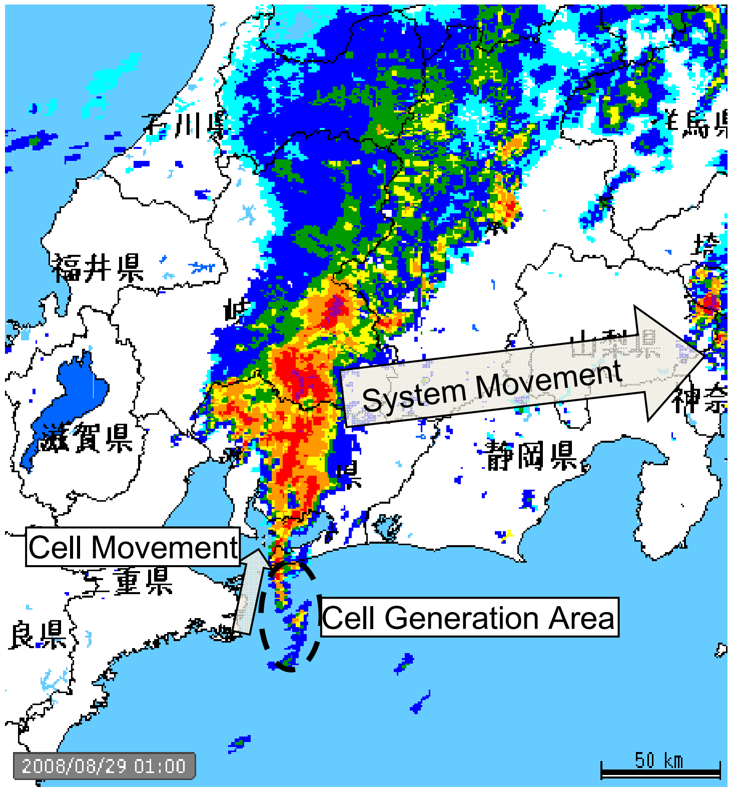

in 2010
- Tokyo Aria (2)
- Nagoya Area (3)
- Osaka Area (4)
- Hokuriku Area (2)

in 2011
- 13 more MP Radar

X-band polarimetric radar network of MLIT

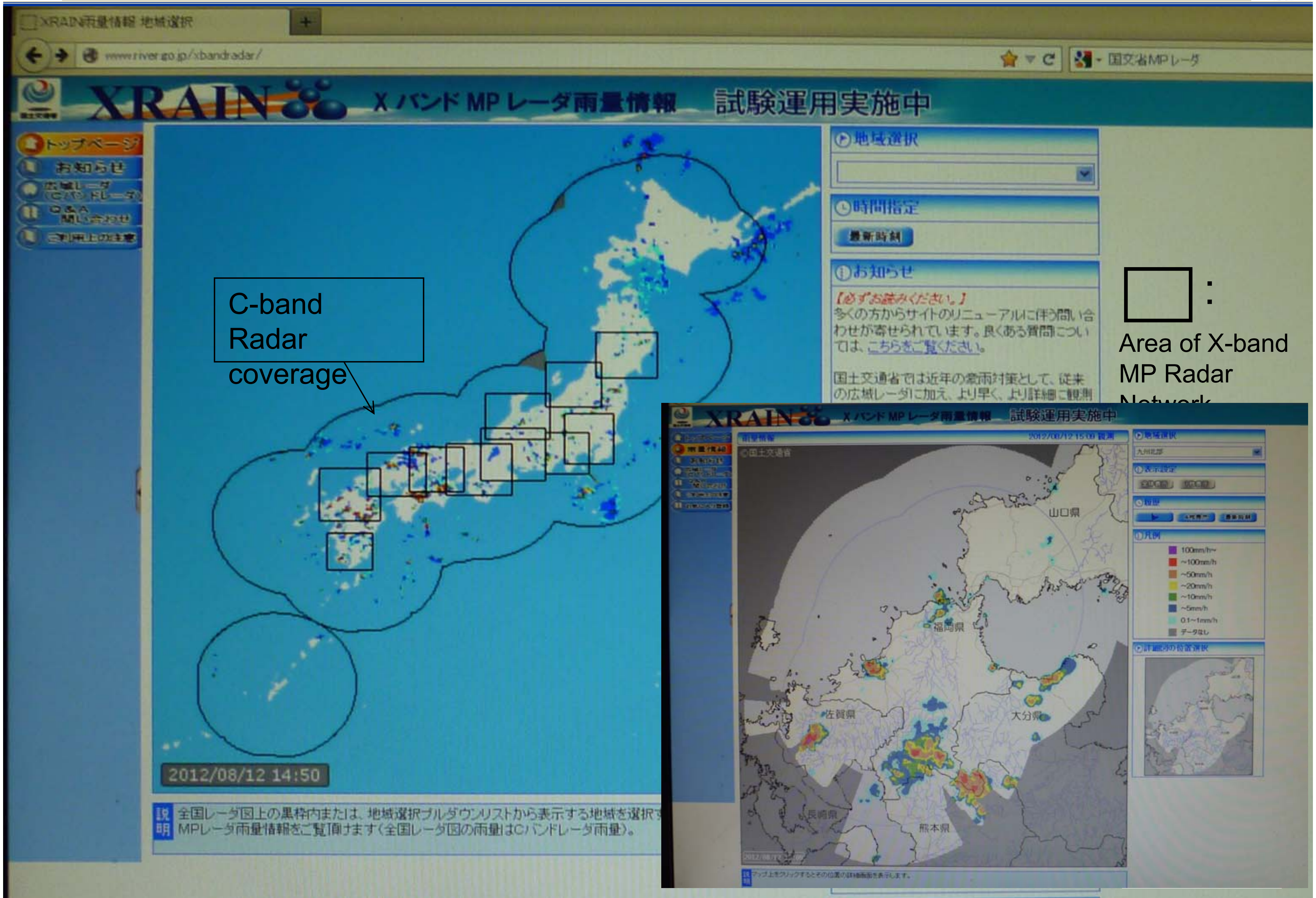

An Example of heavy rainfall in Nagoya Area

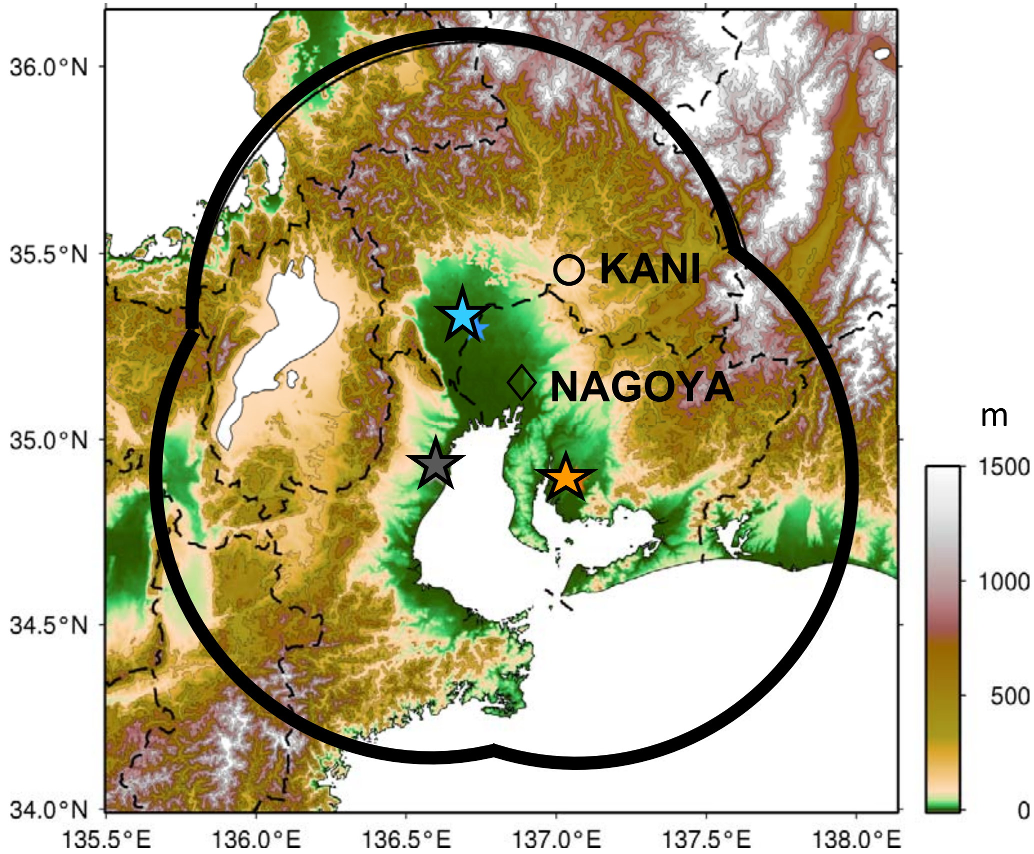

☆ : X-band MP Radar (at Bisai)
☆ : X-band MP Radar (at Suzuka)
☆ : X-band MP Radar (at Anjo)

Heavy Rainfall in Kani:
300 mm in half a day on 15 July 2010

MLIT X-band MP Radar

Range	80km
Mode	PPI (12EL, 5 min.)
Resolution	150m (in radial) 1.2°（Beam width）

Observation Parameters

- Z_h : Reflectivity
- Z_{dr} : Differential Reflectivity
- Φ_{dp} : Differential Phase
- K_{dp} : Differential Phase Shift
- ρ_{hv} : Correlation Coefficient
- Doppler Velocity

3D Cartesian Coordinate

Hoizontal Resolution	1 km
Vertical Resolution	250 m

Estimation of Rainfall Intensity and Hourly Rainfall Amount

River Bureau (Ministry of Land, Infrastructure, Transport and Tourism)

⇩ X-RAIN Data

Research Consortium for X-RAIN

Z_{DR} : Differential Reflectivity

K_{DP} : Specific Differential Phase

Volume Scan Data (every 5 minutes)

⇩

CAPPI at 1 km (1 km × 1 km × 250 m)

⇩

<For Weak Rainfall>

$Z_{DR} \sim 0$ (dB), $K_{DP} \sim 0$ (deg/km), $Z_H > 0$ (dBZ)

$Z = BR^{\beta}$

Z (mm^6m^{-3}) , R (mm/h)

B and β are constants

<For Strong Rainfall>

$Z_{DR} > 0.5$ (dB), $K_{DP} > 0.5$ (deg/km),

$Z_H > 40$ (dBZ)

$R = c\,(K_{DP})^a \times 10^{(0.1 \times b \times Z_{DR})}$

⇩

Accumulated rainfall amount (Hourly Rainfall)

(Use 12 planes at 1 km)

Accumulated Rainfall Amount

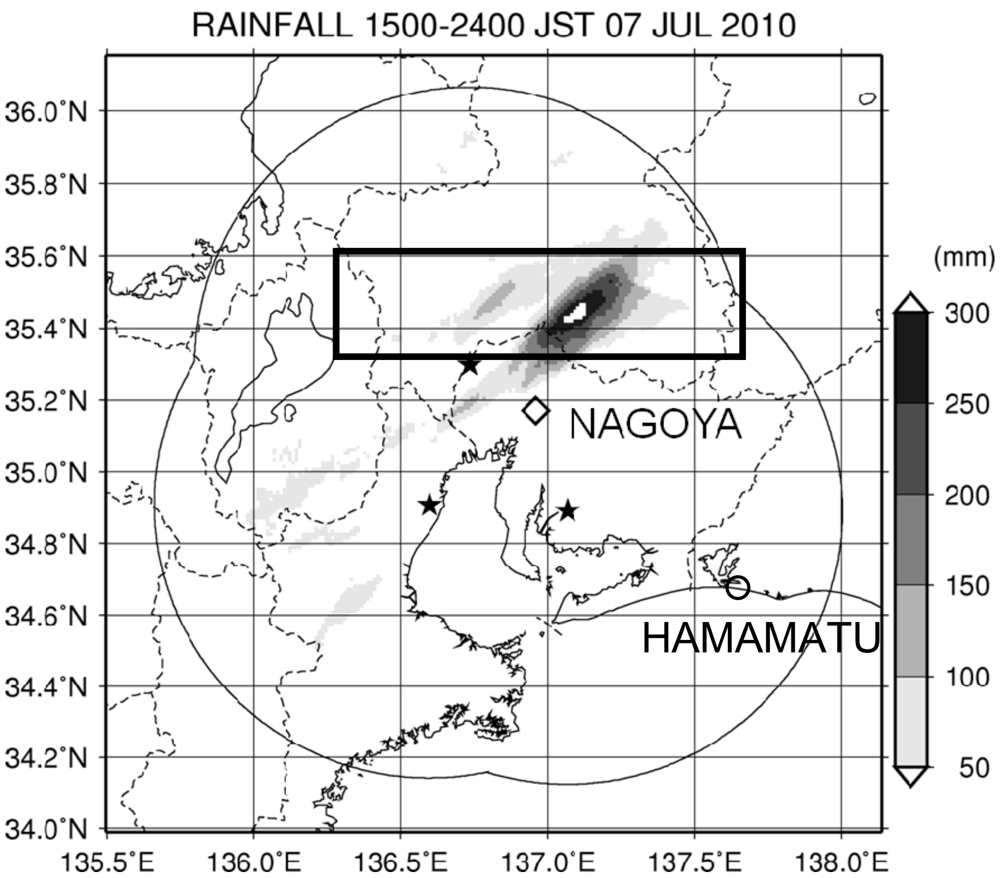

Accumulated rainfall amount from 15 to 24 on 15 July 2010 estimated by MILT X-band MP radar.

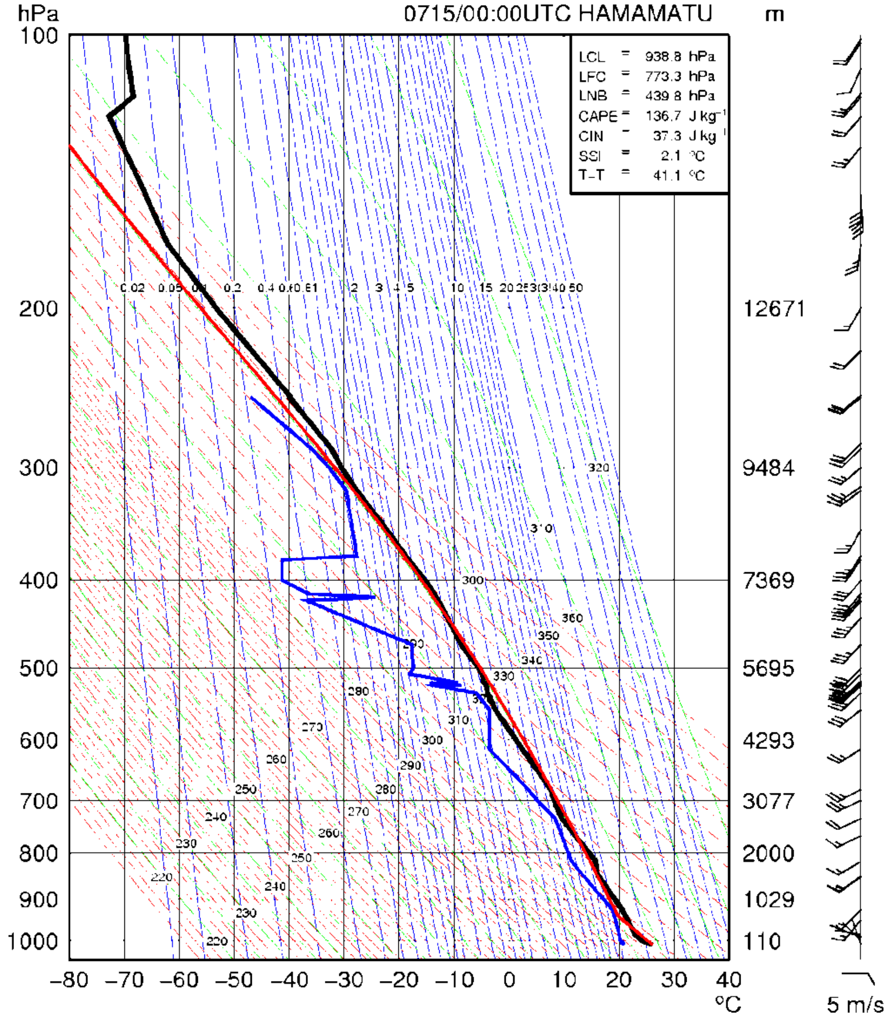

Time Variation of the Precipitation System

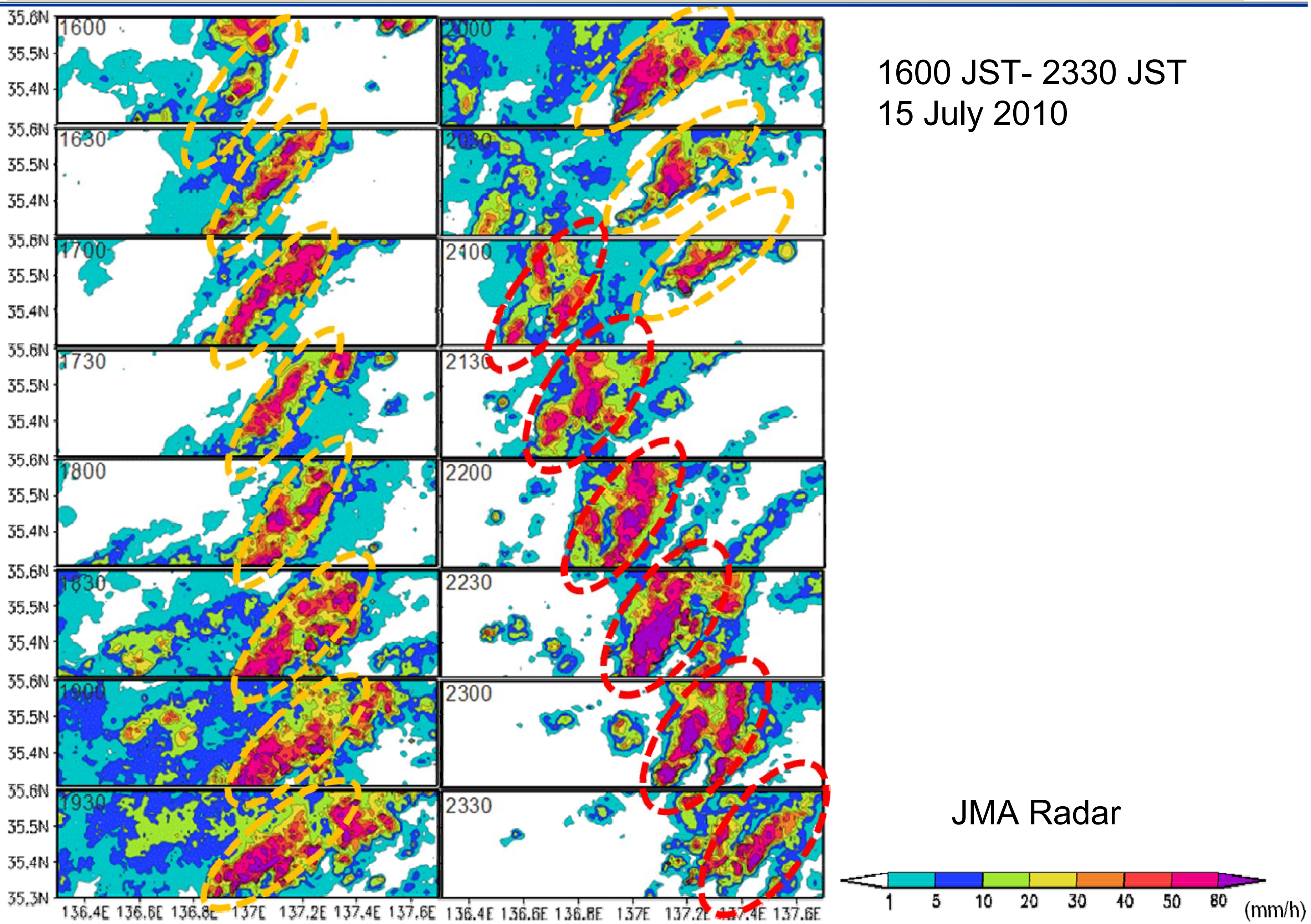

1600 JST- 2330 JST
15 July 2010

JMA Radar

Estimation of Rainfall Intensity

Convective Region（Strong Rainfall）

Threshold (MLIT)

$K_{dp} \geqq 0.1$ deg/km

$Z_h \geqq 30$ dBZ

Threshold（This Study）

$K_{dp} \geqq 0.1$ deg/km

$Z_h \geqq 25$ dBZ

$R = 25.5 \times K_{dp}^{0.815} \div 12$ （mm/5min）

Stratiform Region（Weak Rainfall）

Bringi and Chandraseker (2001)

$R = 0.0365 \times Z^{0.625} \div 12$ （mm/5min）

$Z = 10^{0.1 \times Z_h}$

<u>Height：1 km</u>

Rainfall in 5 min.

Calculate for each grid
(1 km x 1 km x 0.25 km)

Threshold of Z_h in Estimation of Rainfall Intensity with K_{DP}

The threshold of $Z_h \geqq 30$ dBZ makes under estimation of rainfall intensity without using K_{DP}.

$Z_h \geqq 30$ dBZ

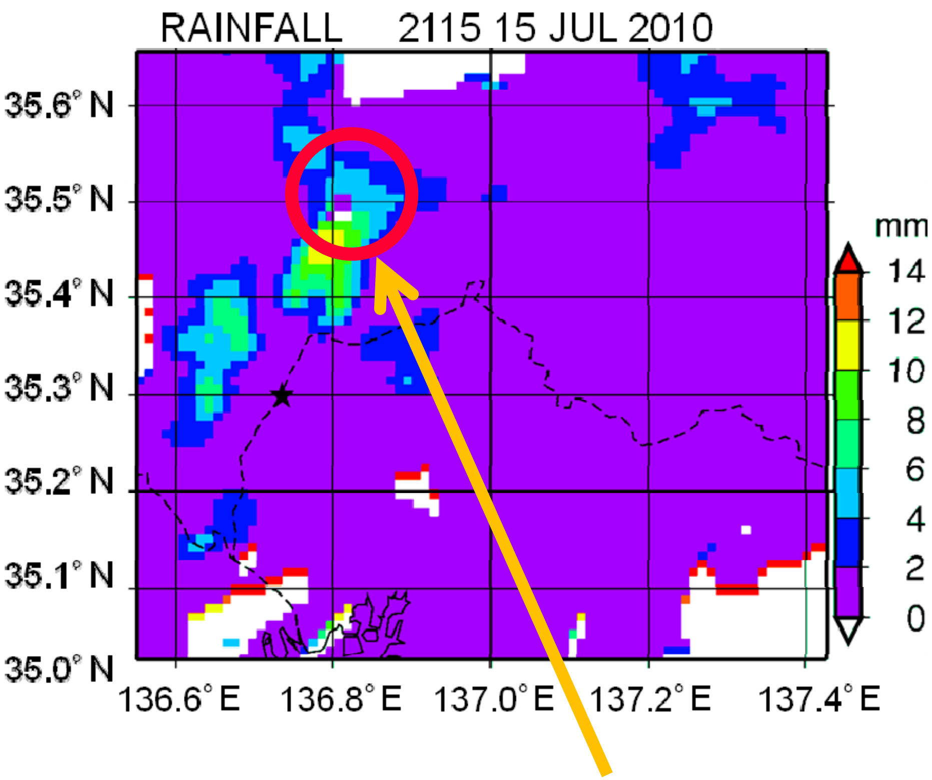

$Z_h = 28$ dBZ

$Z_h \geqq 25$ dBZ

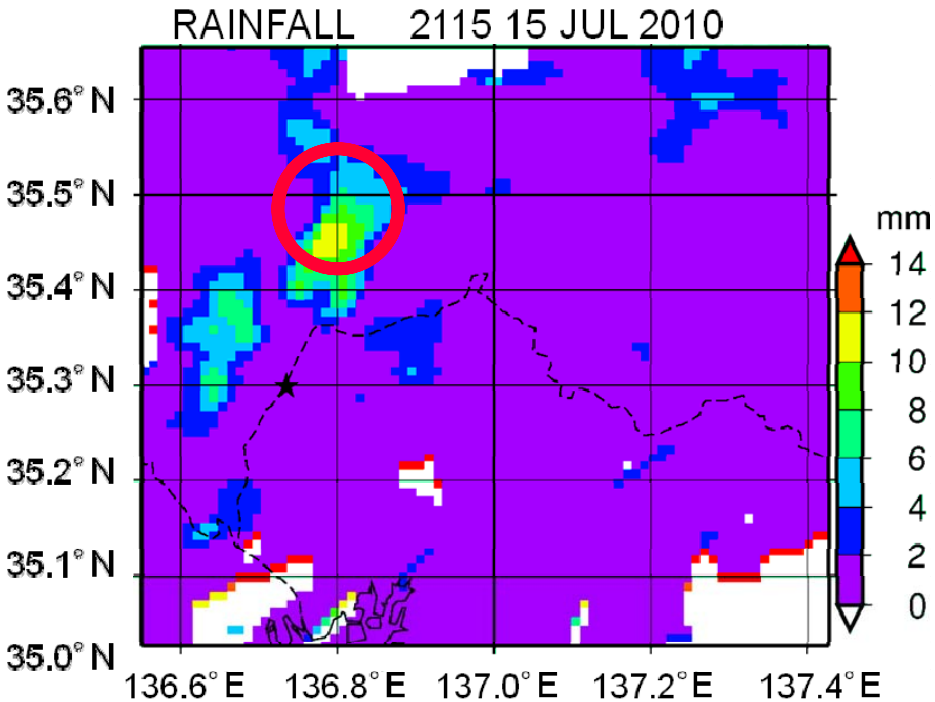

Scatter Diagram of of Z_h and R (estimated with K_{DP})

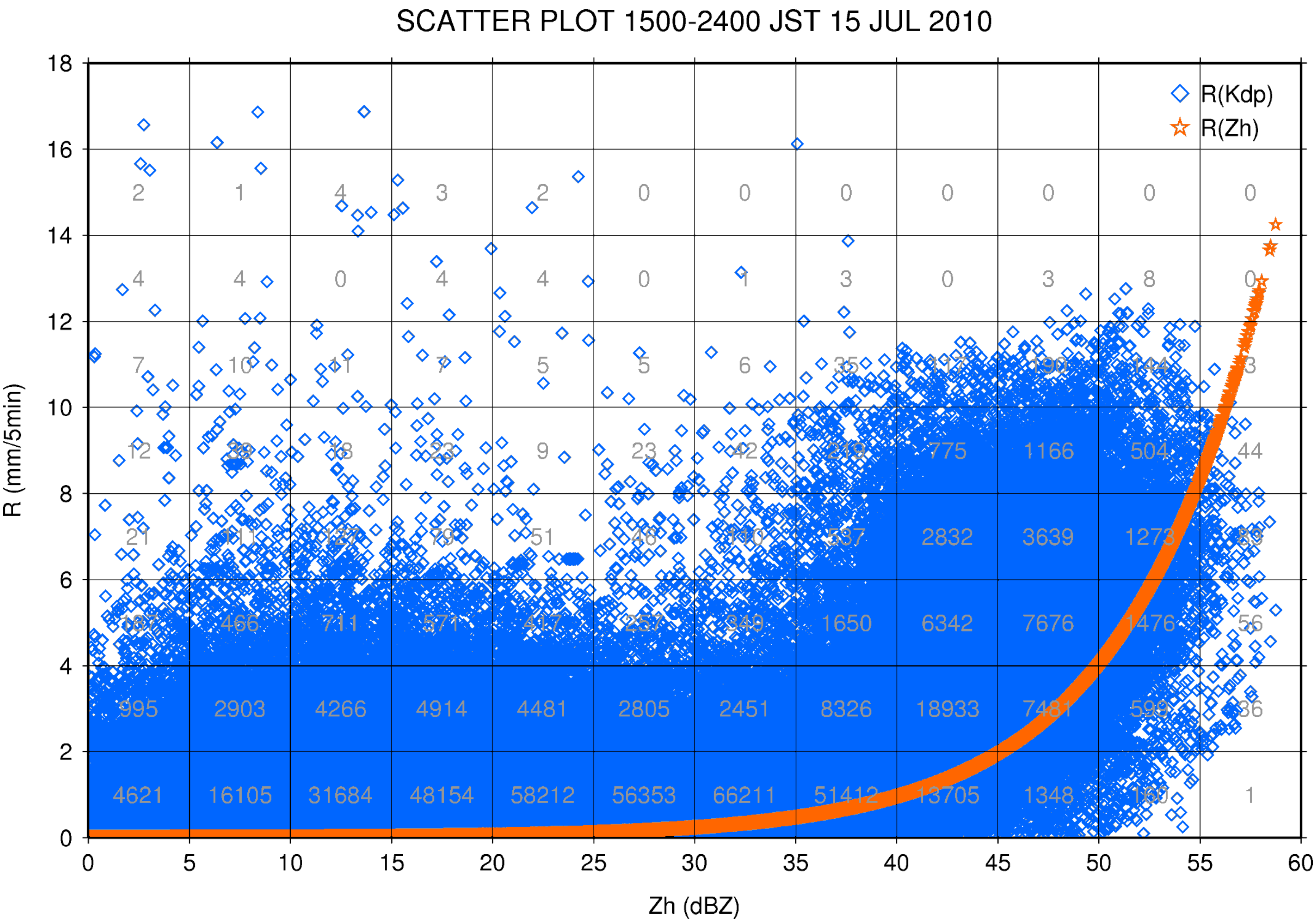

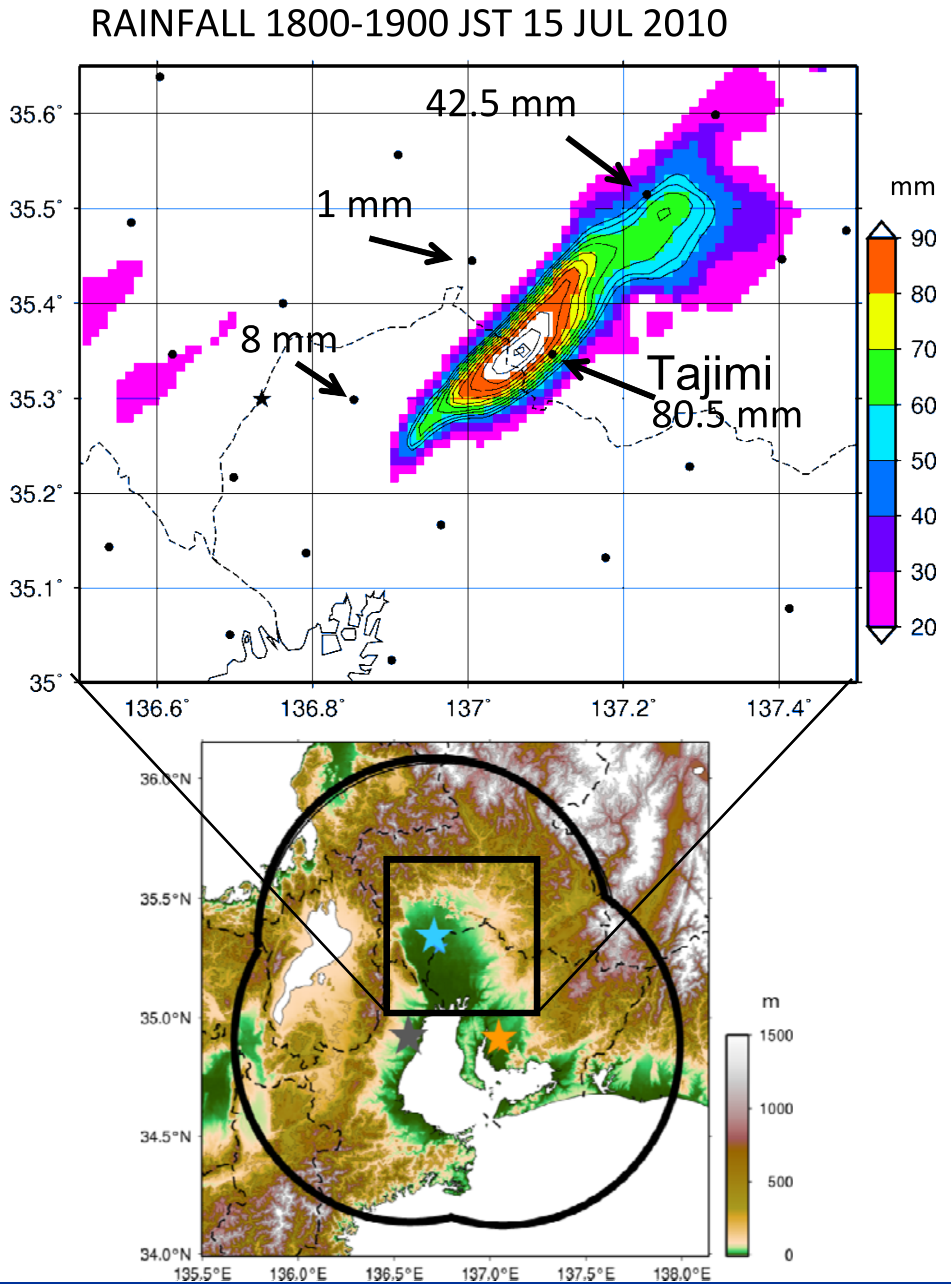

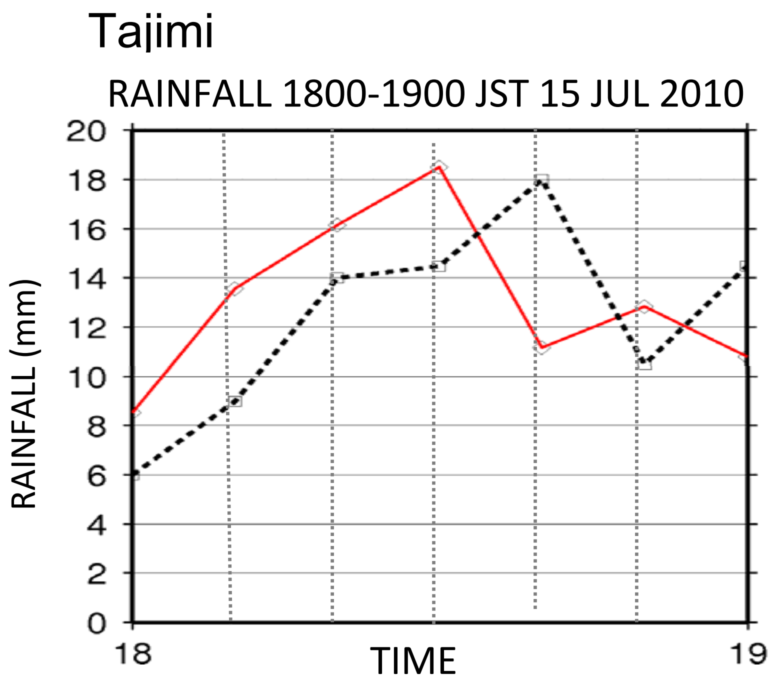

1 hour Accumulated Rainfall

—— : MP radar	83 mm
----- : Rain gauge	80.5 mm

Extraction of Cell

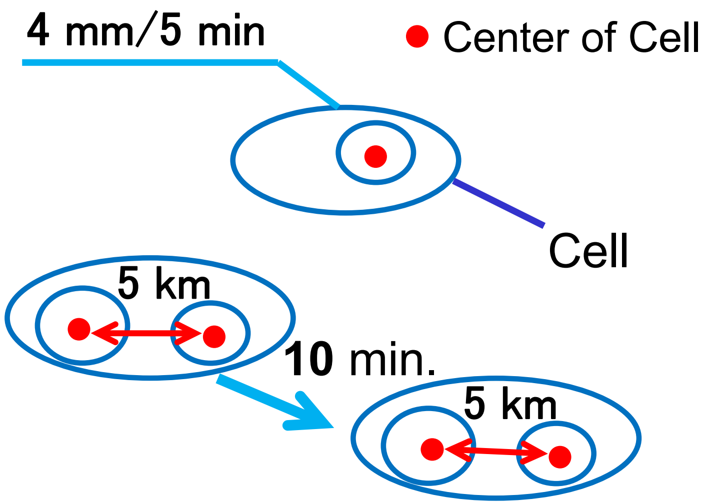

Draw contours every 4 mm/5 min

↓

Identify a cell with maximum rainfall intensity.

Extraction of Cell Group

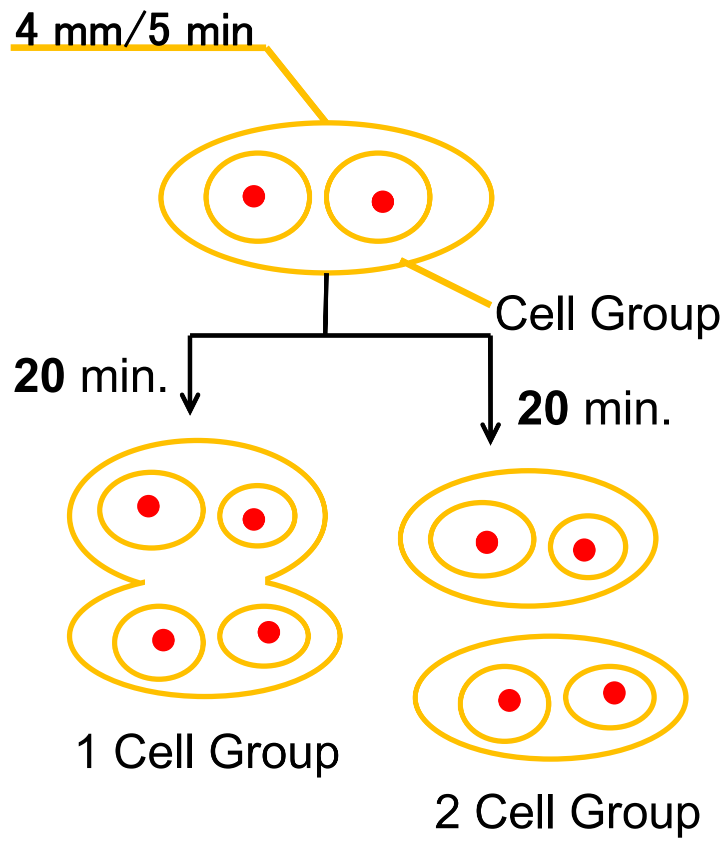

Identification was made by eye.

Identification of Cell Group

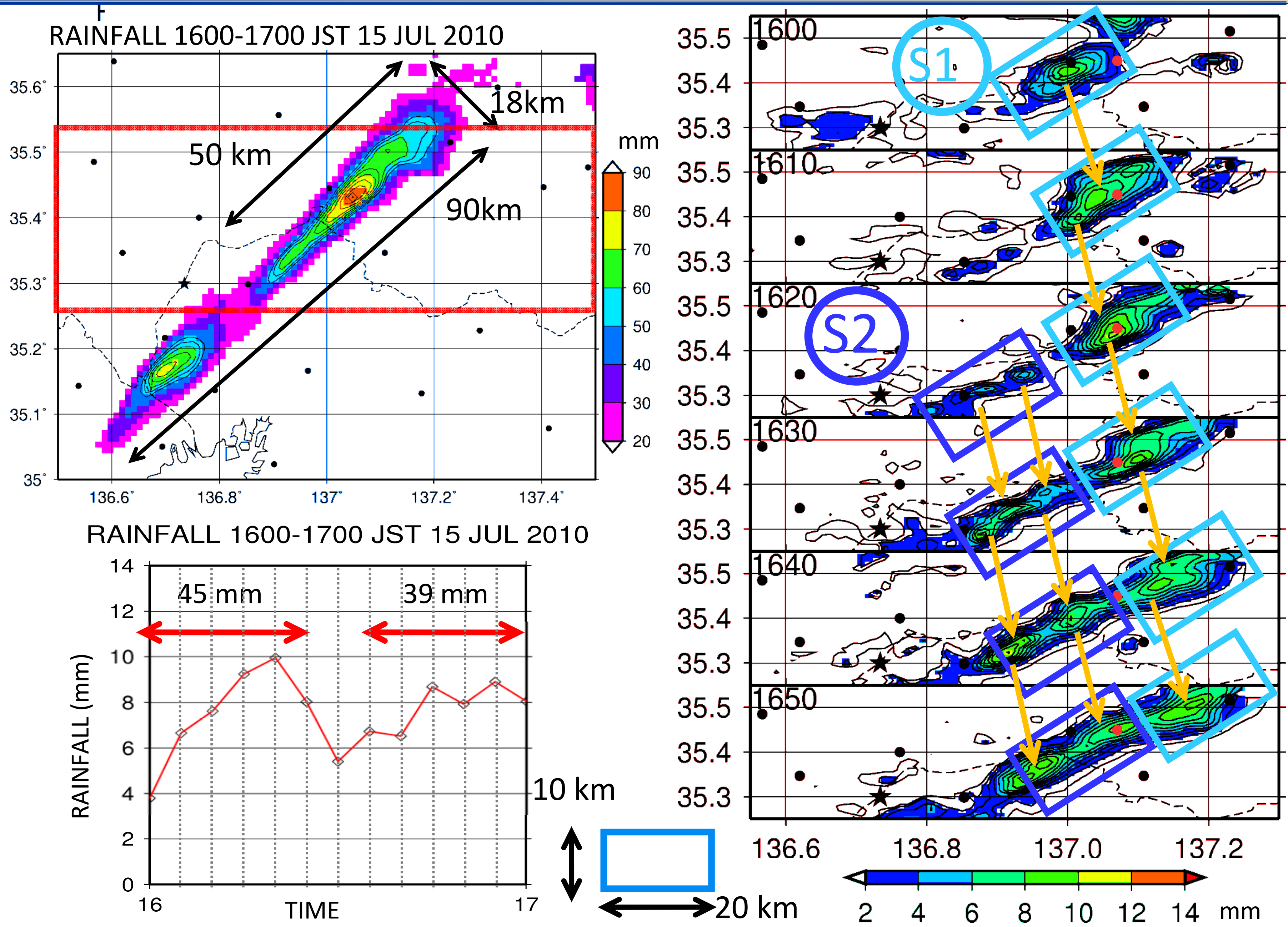

Accumulated Rainfall Amount (Stationary System S)

S1

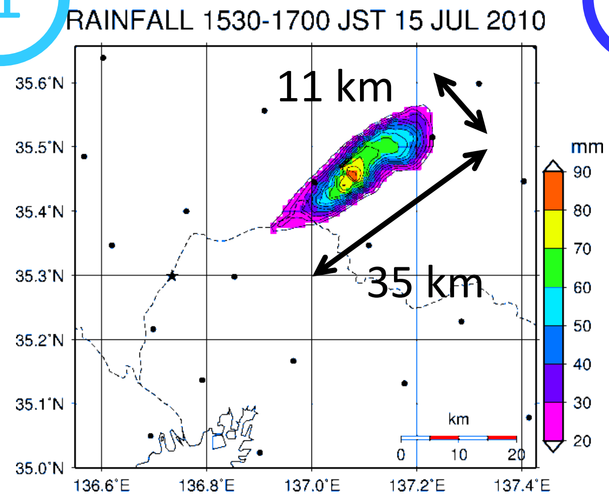

Max.: **84 mm**

S2

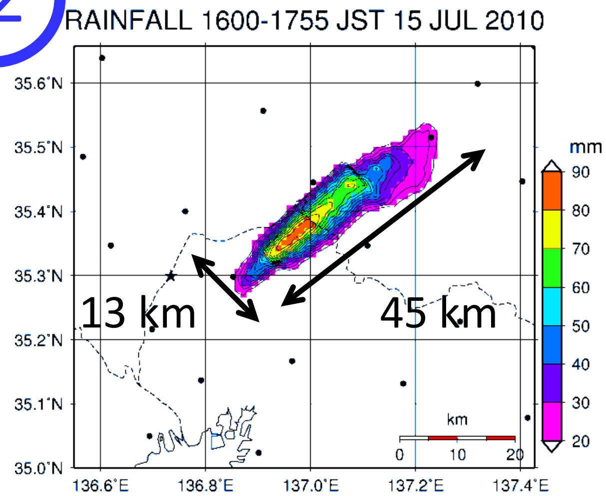

Max.: **85 mm**

Tracking and Accumulation Mehod

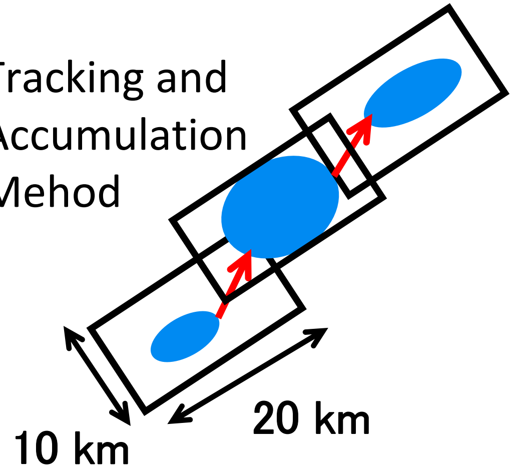

S: Stationary

S3 was not tracked.

S4

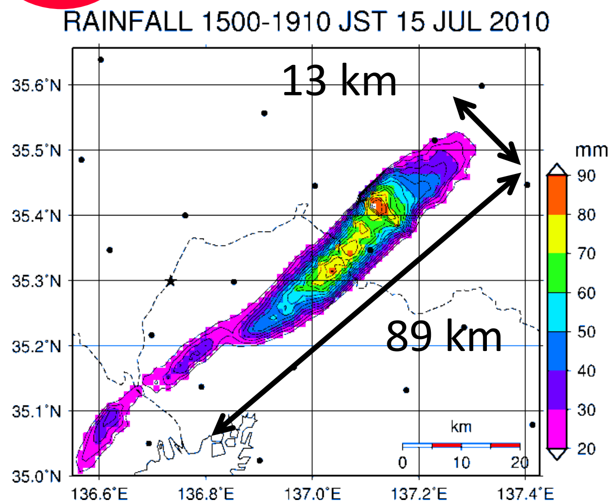

Max.: **90 mm**

S5

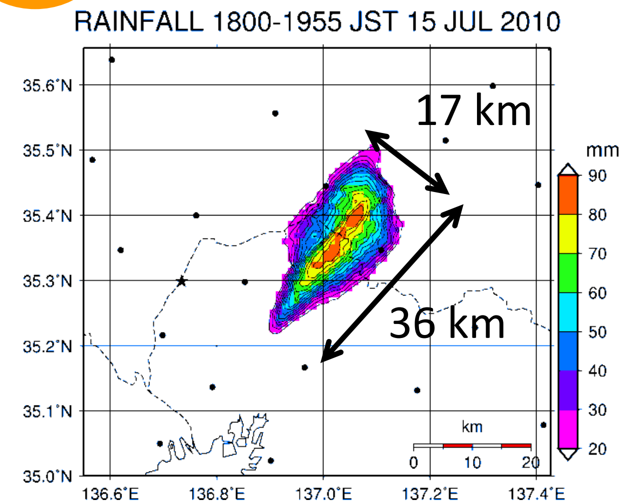

Max.: **85 mm**

S6

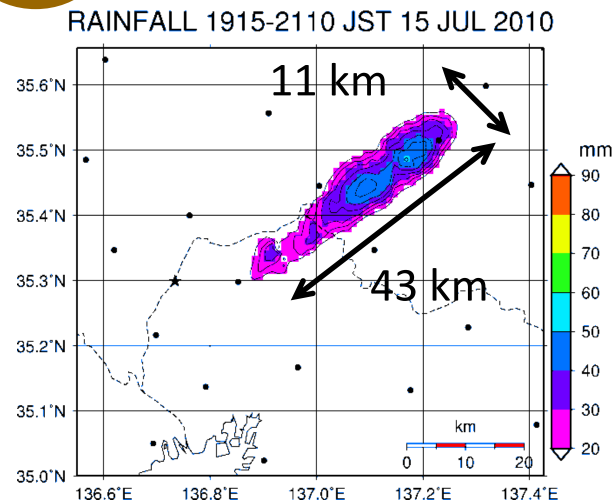

Max.: **52 mm**

Accumulated Rainfall Amount (Fast Moving System F)

F1

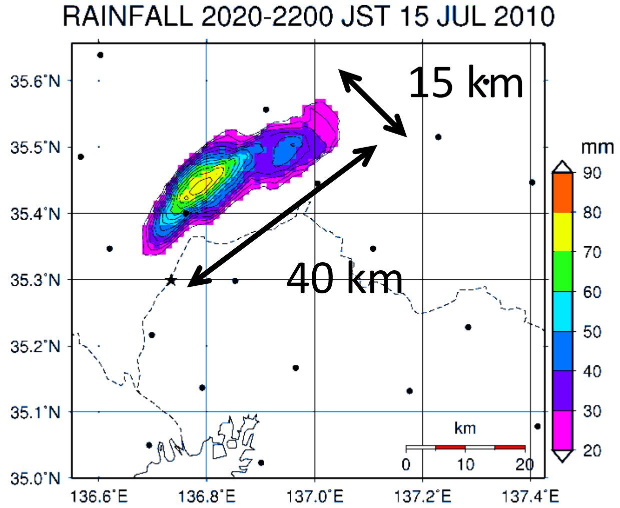

Max. : 78 mm

F2

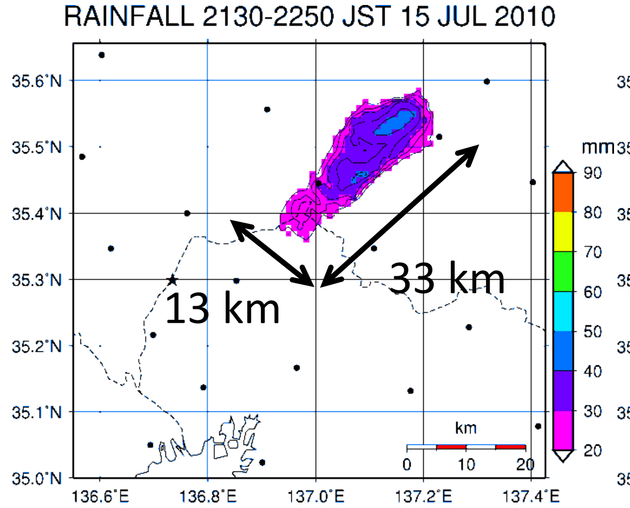

Max. : 49 mm

F3

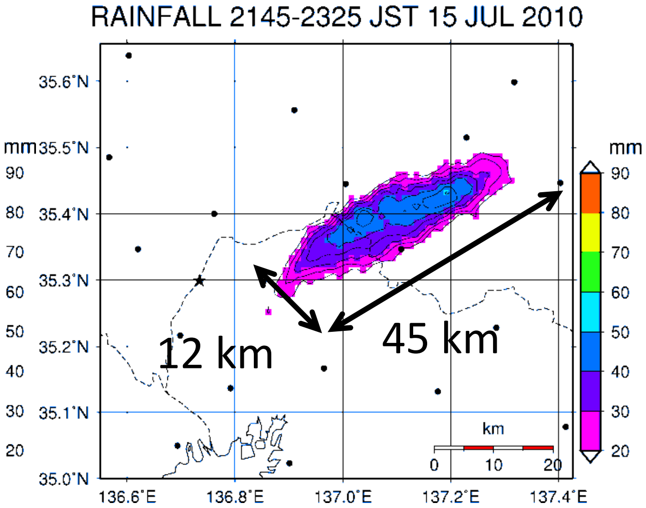

Max. : 51 mm

F: Fast moving

Characteristics of Cell Group

Cell Group	Duration（min.）	Width (km)	Length (km)	Aspect Ratio	Max. Rain (mm)	Number of Cell	Max. Rain in Cell (mm)
S1	15:30～17:00 (95)	11	35	0.31	84	4	45
S2	16:00～17:55 (120)	13	45	0.29	85	8	39
S3	15:50～17:55 (75)	*	*	*	*	5	*
S4	17:15～19:10 (240)	12	89	0.13	90	9	36
S5	18:00～19:55 (120)	17	36	0.47	85	10	38
S6	19:15～21:10 (120)	11	43	0.26	52	5	23
F1	20:20～22:00 (105)	15	40	0.38	78	4	69
F2	21:30～22:50 (85)	13	33	0.39	49	4	16
F3	21:45～23:25 (105)	12	45	0.27	51	5	43

Characteristics of Cell Group
(Accumulated Rainfall Amount > 20 mm)

Elongated Shape
- Width : 11～17 km
- Length : 33～89 km

Orientation : SW - NE

Formation Process of Heavy Rainfall Area

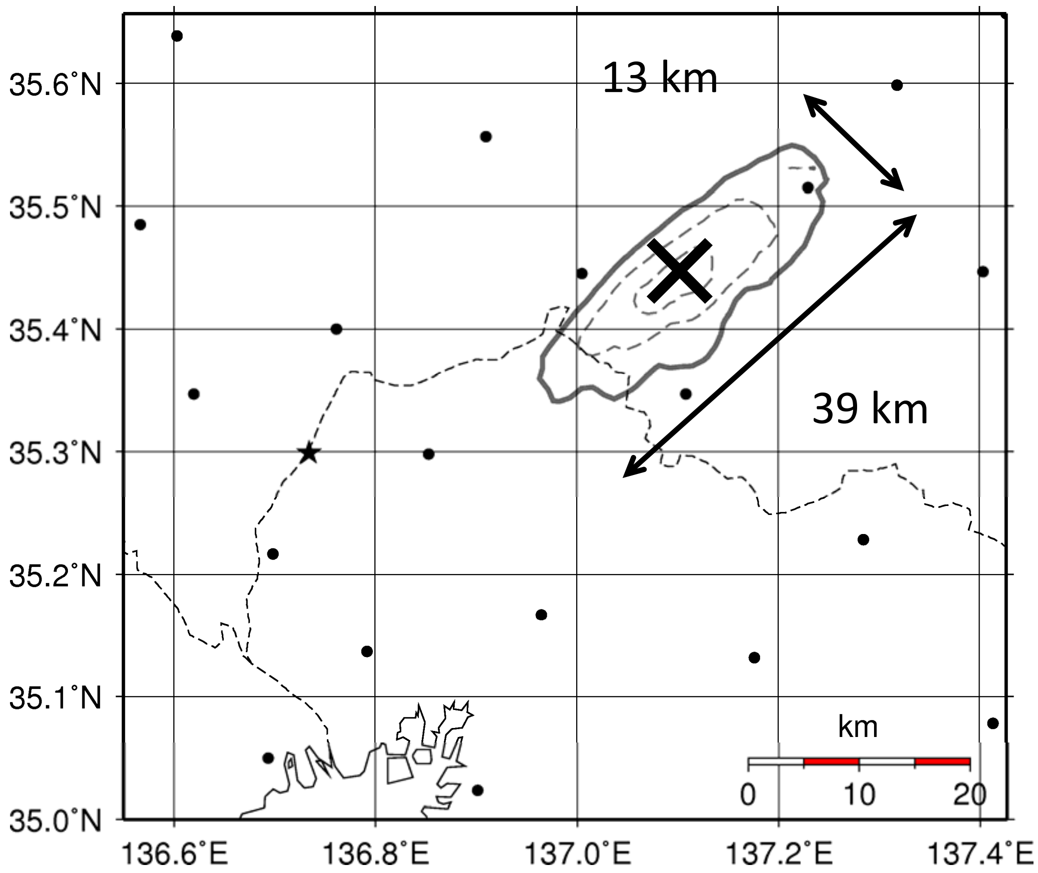

✕ : **322 mm**

Accumulated Rainfall Amount in 9 hours

— : 200 mm

--- : 250 mm and 300 mm

Formation Process of Heavy Rainfall Area

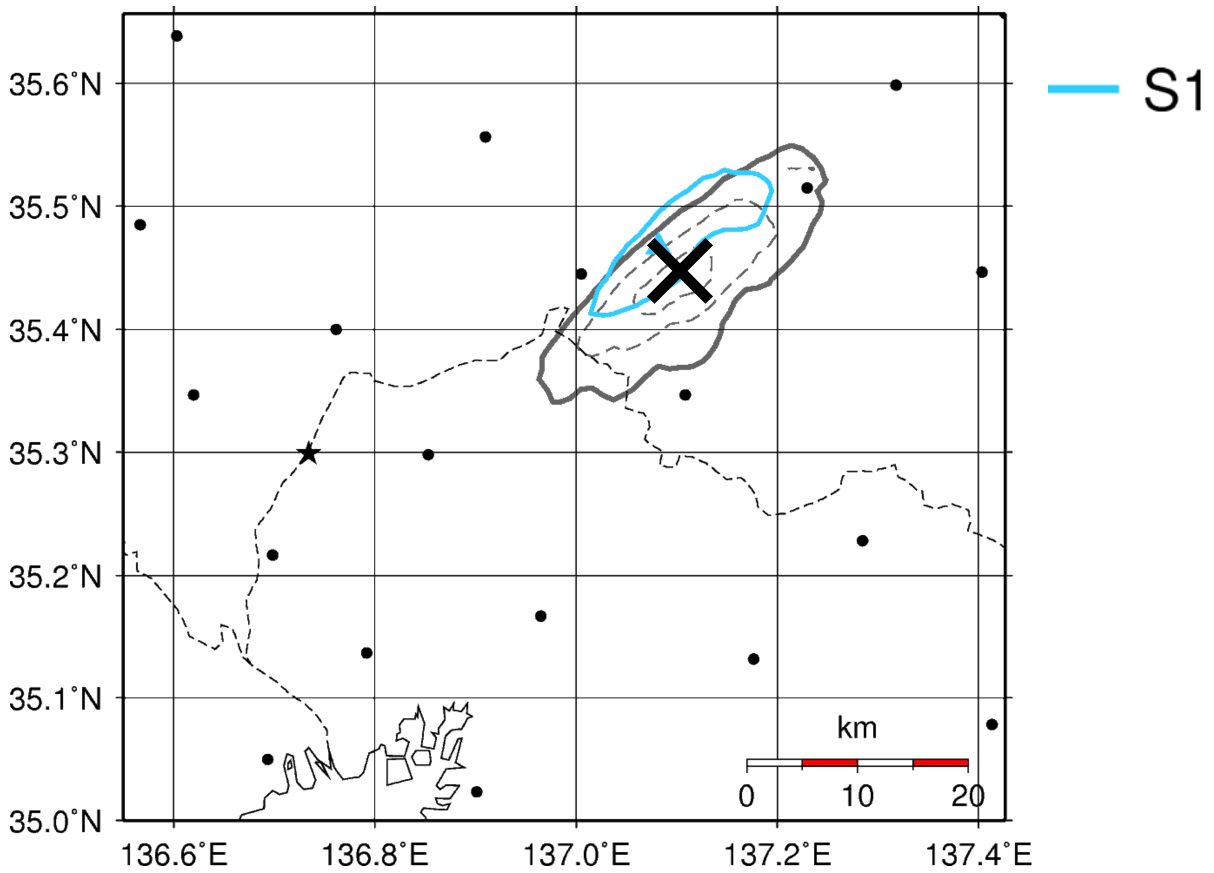

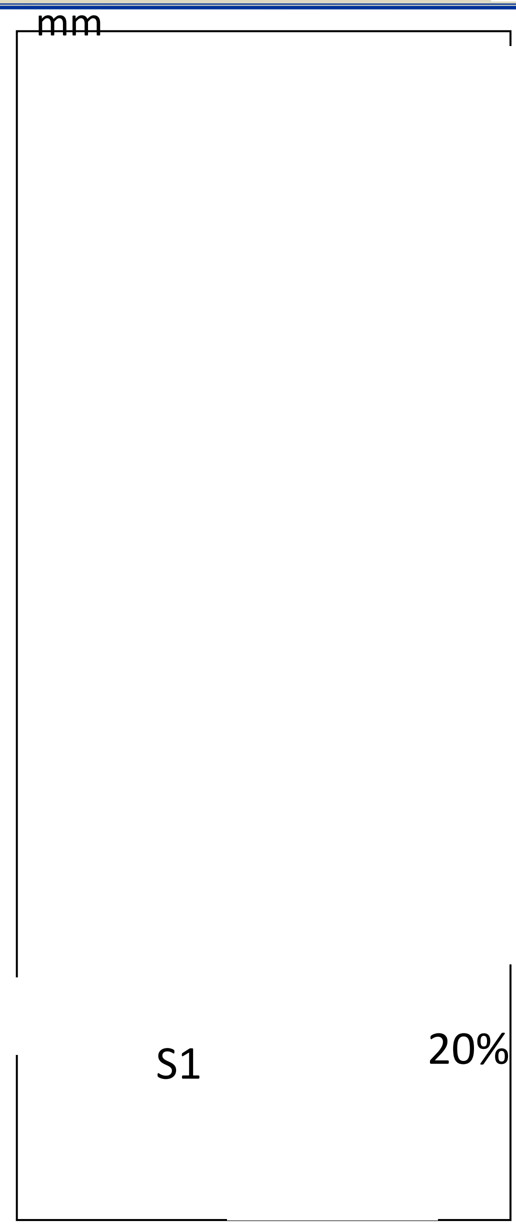

$$\text{Contribution Rate} = \frac{\text{Rainfall amount of each Cell Group}}{\text{Max. of Accumulated Rainfall Amount}} \times 100$$

△: The point of maximum rainfall amount

S1～S6 : 50 mm
F1～F3 : 40 mm

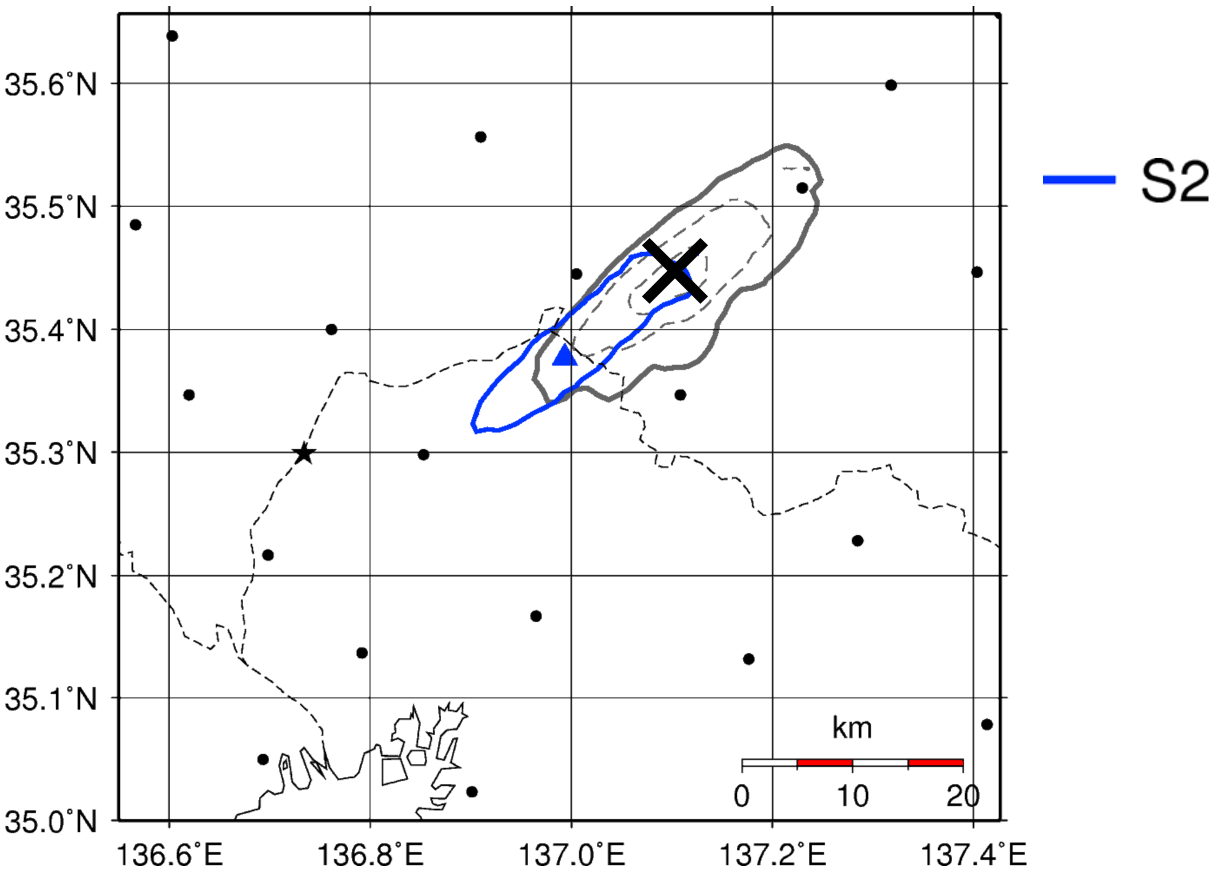

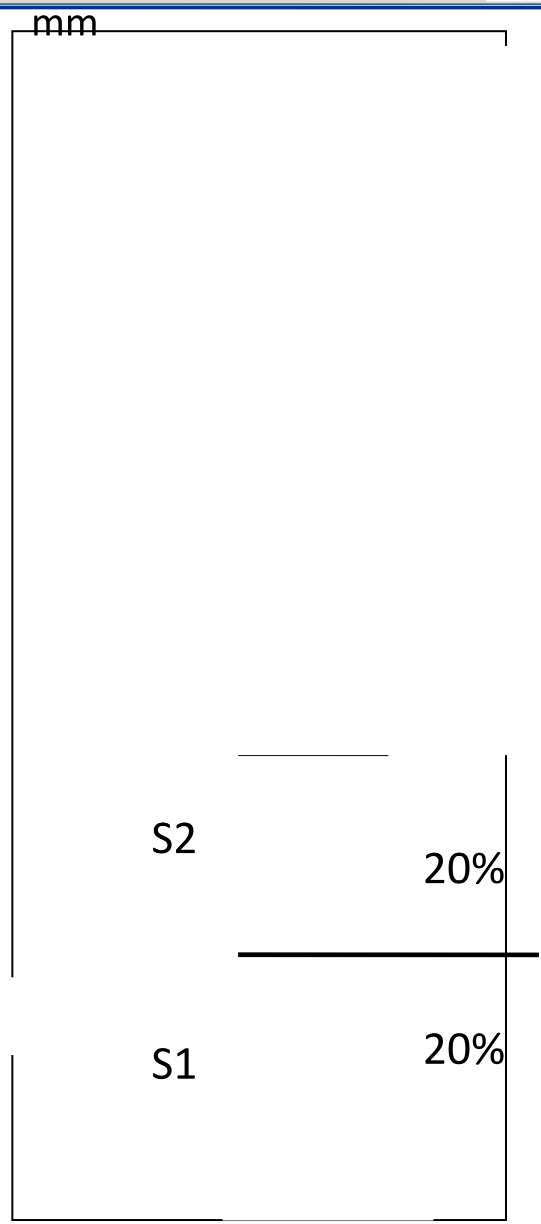

$$\text{Contribution Rate} = \frac{\text{Rainfall amount of each Cell Group}}{\text{Max. of Accumulated Rainfall Amount}} \times 100$$

△: The point of maximum rainfall amount

S1～S6 : 50 mm

F1～F3 : 40 mm

Formation Process of Heavy Rainfall Area

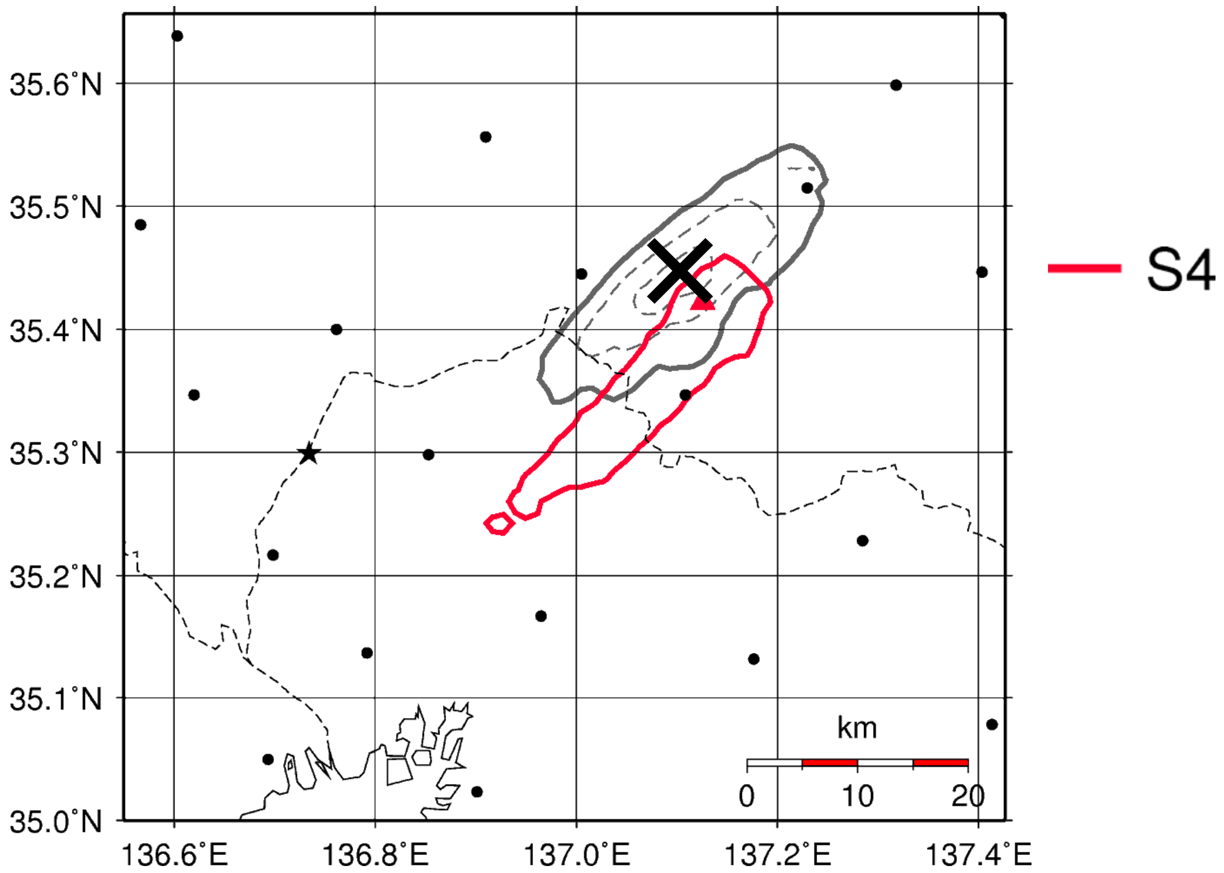

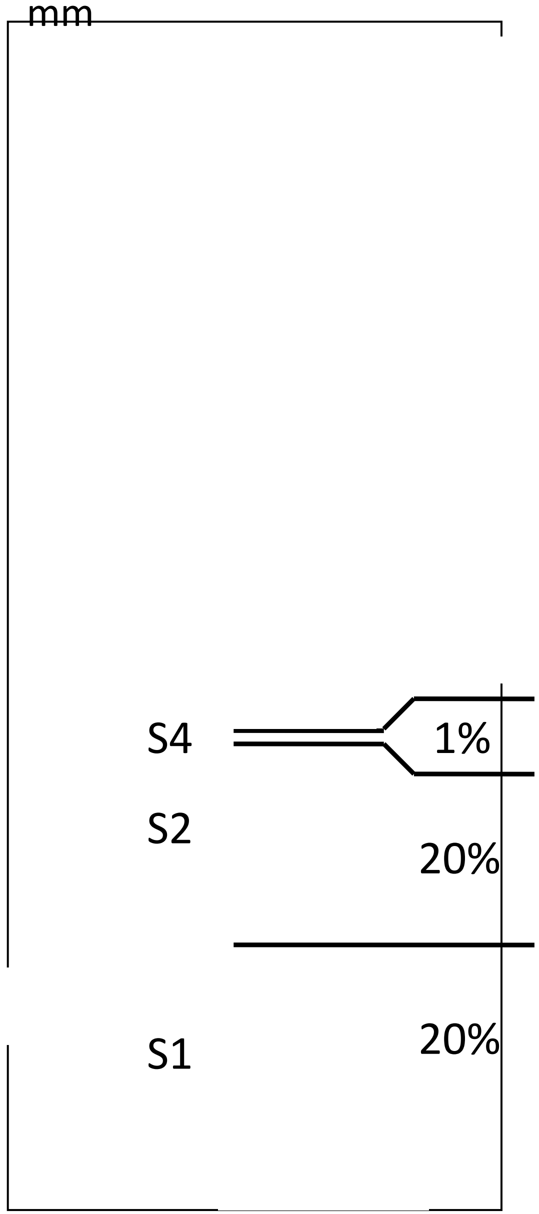

$$\text{Contribution Rate} = \frac{\text{Rainfall amount of each Cell Group}}{\text{Max. of Accumulated Rainfall Amount}} \times 100$$

△: The point of maximum rainfall amount

S1～S6 : 50 mm

F1～F3 : 40 mm

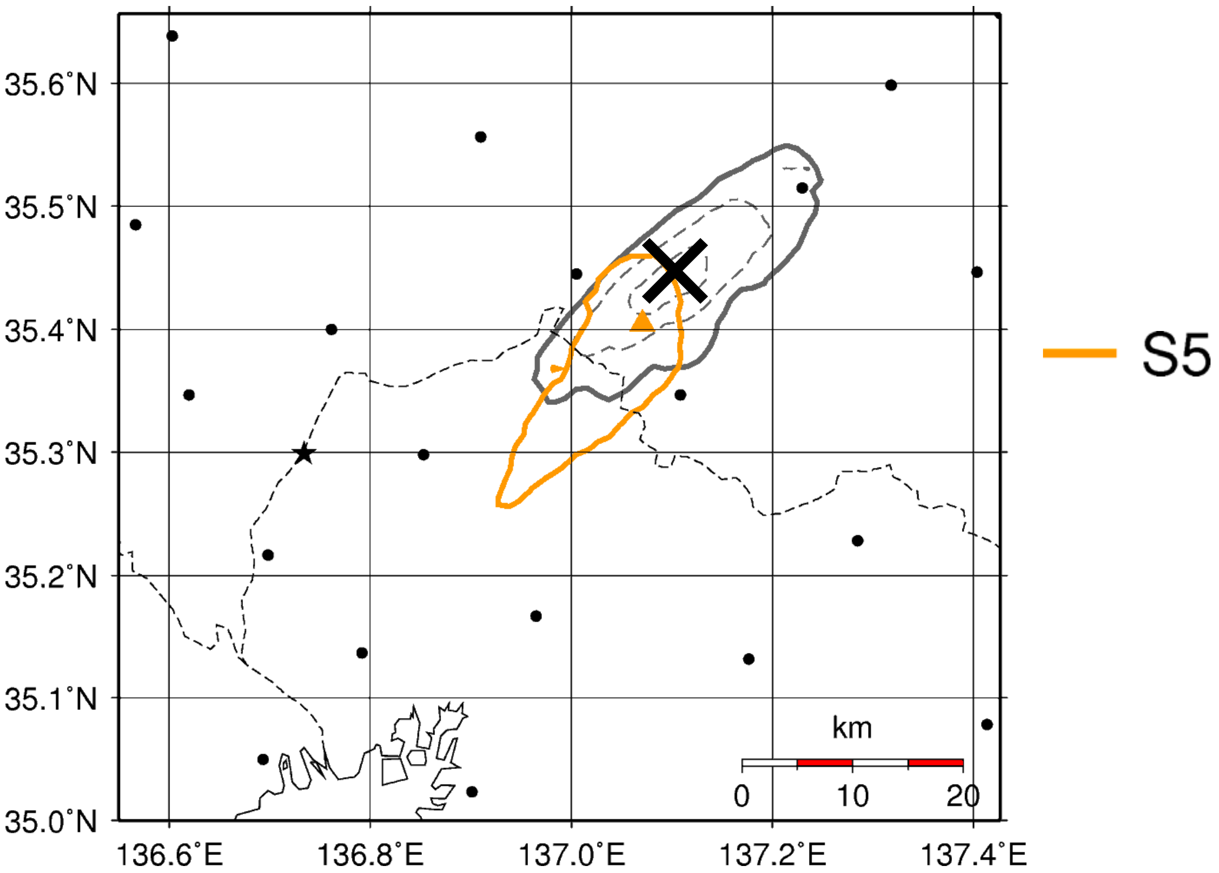

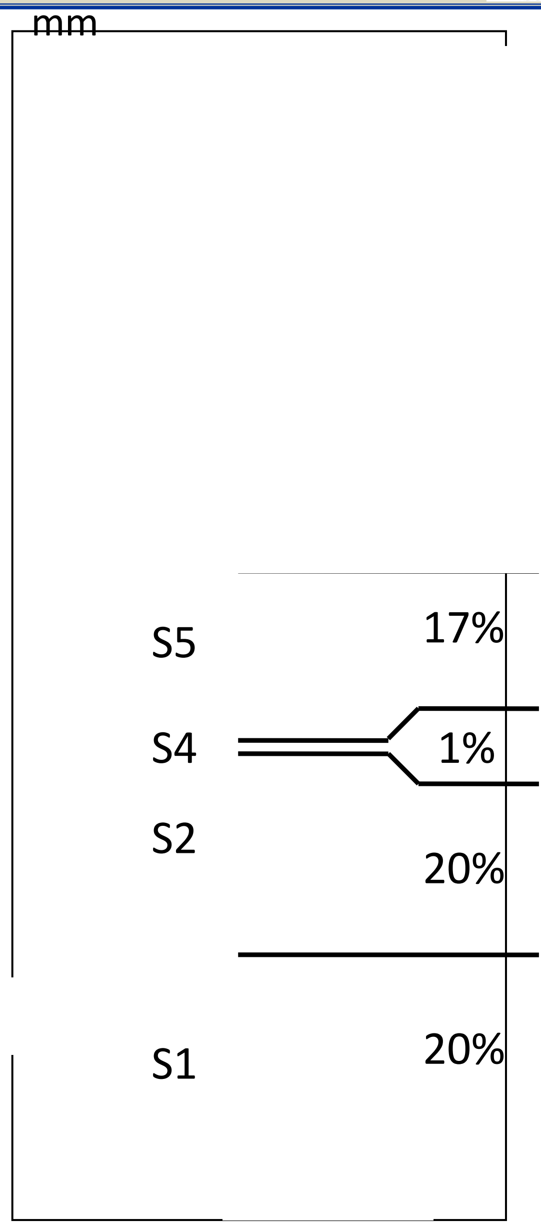

$$\text{Contribution Rate} = \frac{\text{Rainfall amount of each Cell Group}}{\text{Max. of Accumulated Rainfall Amount}} \times 100$$

△: The point of maximum rainfall amount

S1～S6 : 50 mm

F1～F3 : 40 mm

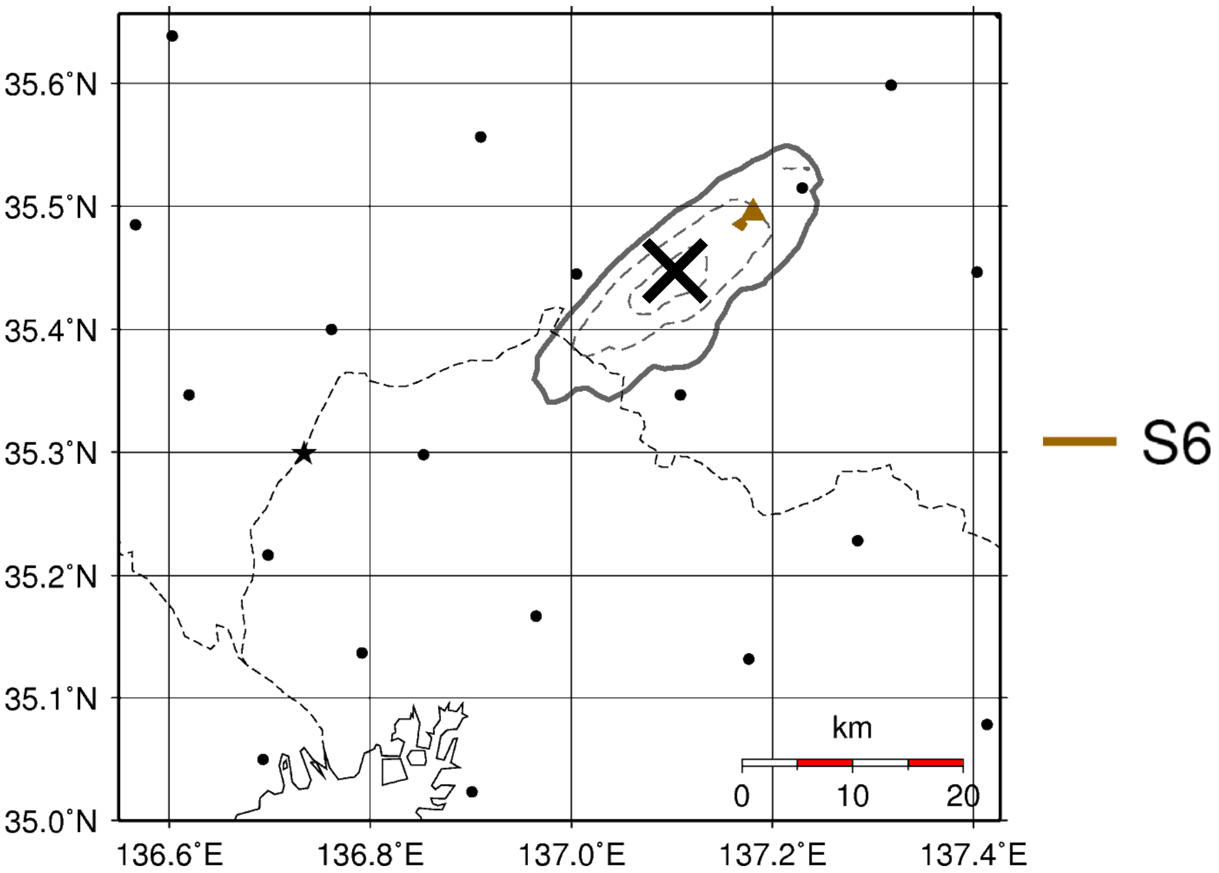

$$\text{Contribution Rate} = \frac{\text{Rainfall amount of each Cell Group}}{\text{Max. of Accumulated Rainfall Amount}} \times 100$$

△: The point of maximum rainfall amount

S1～S6 : 50 mm

F1～F3 : 40 mm

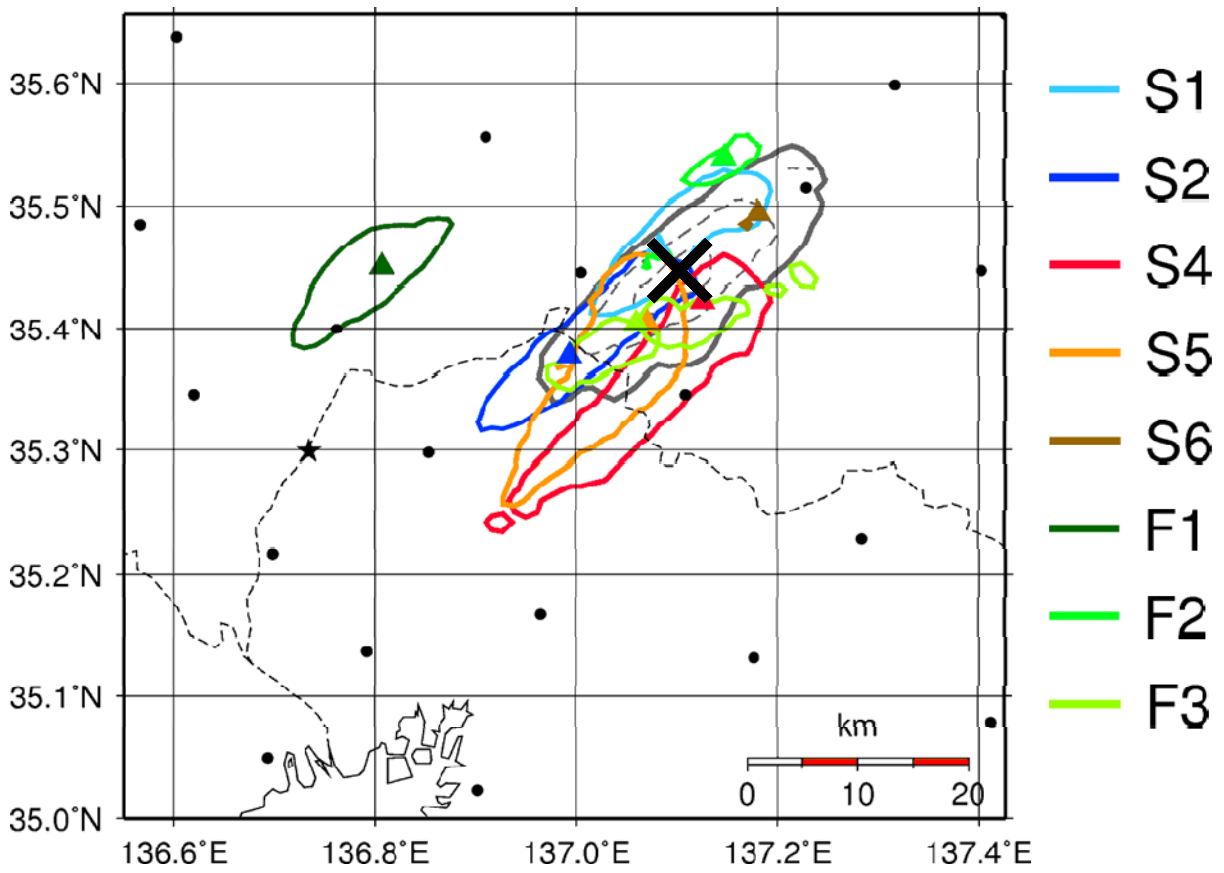

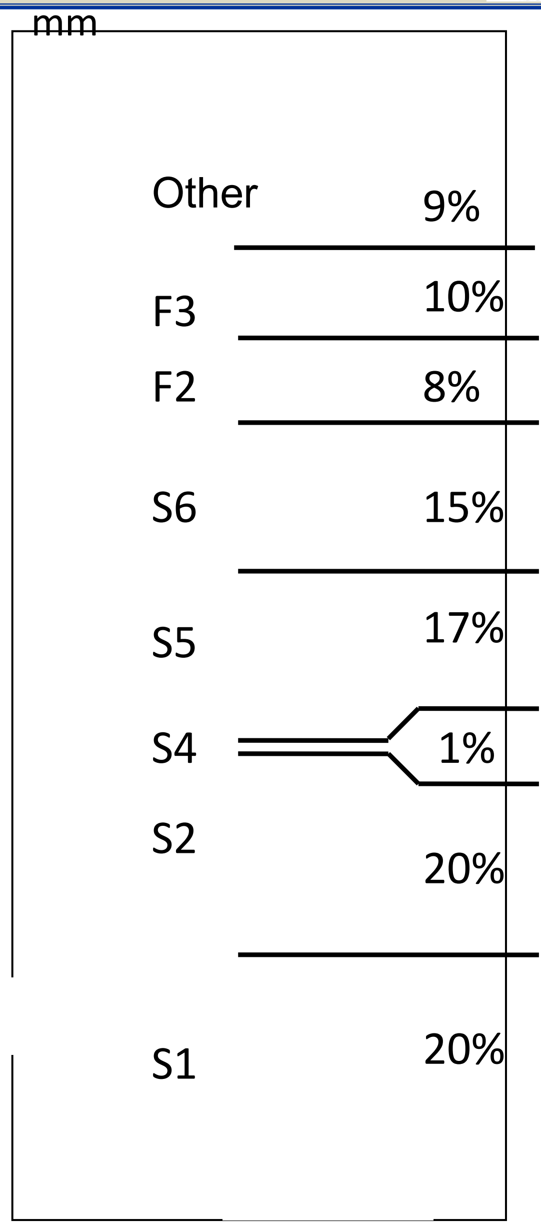

$$\text{Contribution Rate} = \frac{\text{Rainfall amount of each Cell Group}}{\text{Max. of Accumulated Rainfall Amount}} \times 100$$

△: The point of maximum rainfall amount

S1～S6 : 50 mm

F1～F3 : 40 mm

Formation Processes of Heavy Rainfall Area

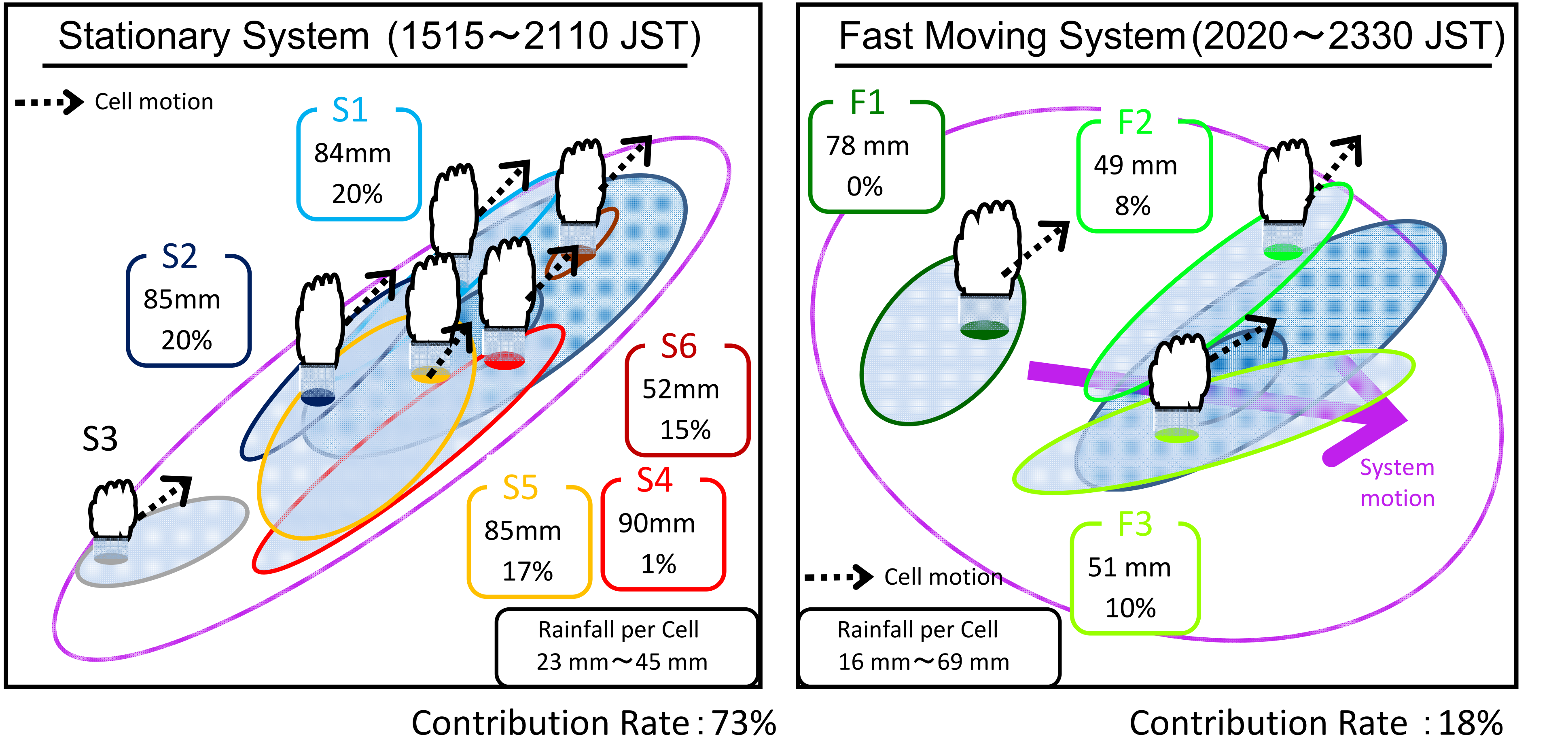

Merit: Identify cell and cell group with rainfall amount in mm.

→ Track in mm and integrate in mm. (Useful for statistical studies.)

Problems: time resolution, attenuation, ground clutter and solid precipitation

Ongoing Studies and Research Plan

- Studies on structure of thundercloud
- Hydrometeor classification [Pis4-017 Oue]
- Assimilation of X-band polarimetric radar data into cloud resolving model (CReSS) [Pis4-015 Kato]

- Statistics of convective cell and precipitation systems
- Improvement of radar system

- Field experiment on Genesis of tropical cyclone in Palau (2013 – 2014)

Hydrometeor Classification

Input parameters

Z_h Z_{dr} K_{dp} ρ_{hv} — polarimetric radar

T (temperature) — sounding, surface

Hydrometeor Classification

(Liu and Chandrasekar, 2000)

Output hydrometeor categories

1)Drrizle  2)Rain 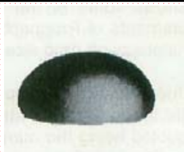

3)Wet (Melting) Snow 4)Dry Snow  5)Ice Crystal 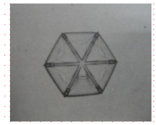

6)Dry Graupel 7)Wet (Melting) Graupel 

8)Small Hail 9)Large Hail 10)Rain and Hail 

Example of Hydrometeor Classification

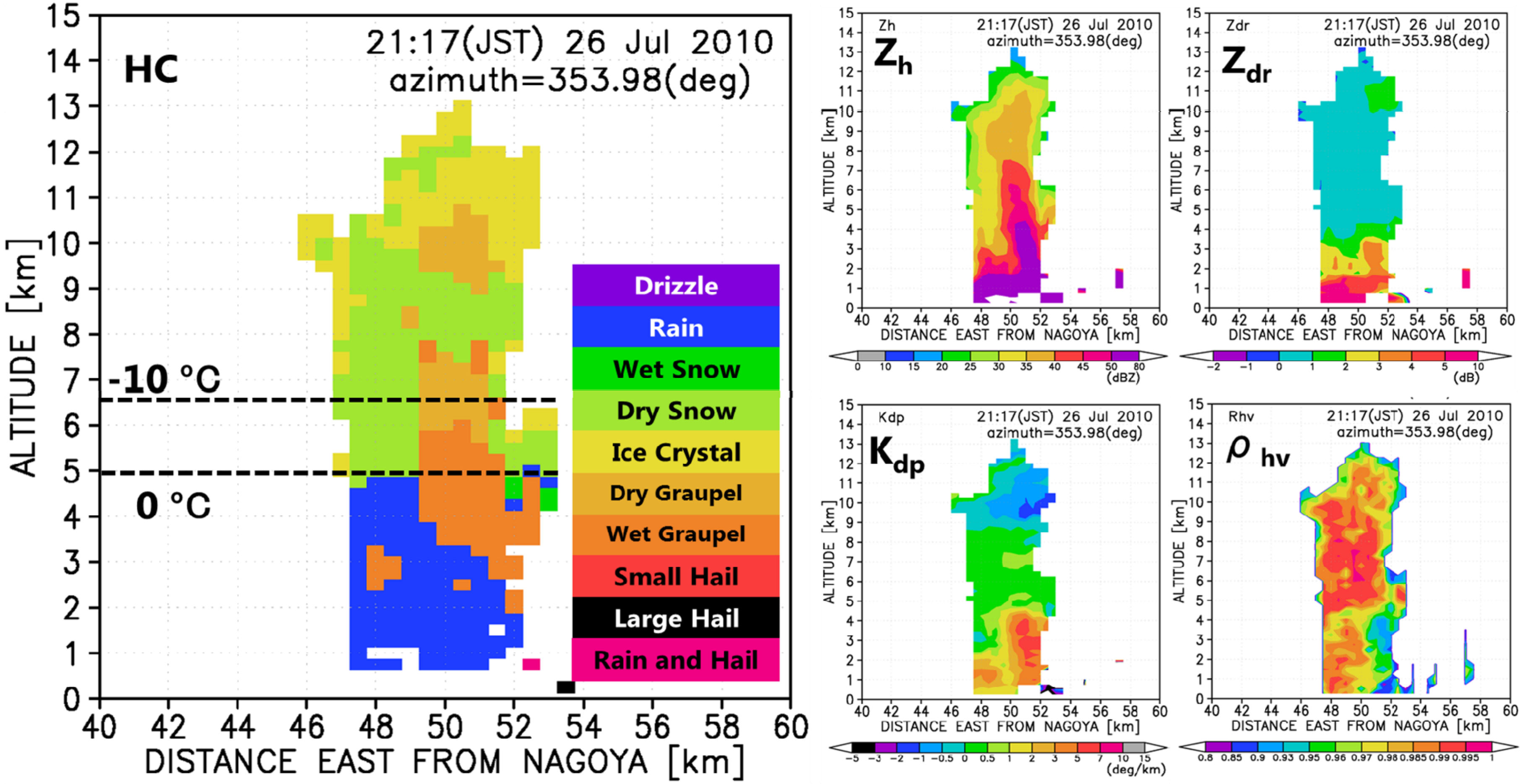

Summer Thundercloud near Nagoya

Identification of graupel!

CAPPI of Radar Reflectivity (X-band MP Radar of MLIT)

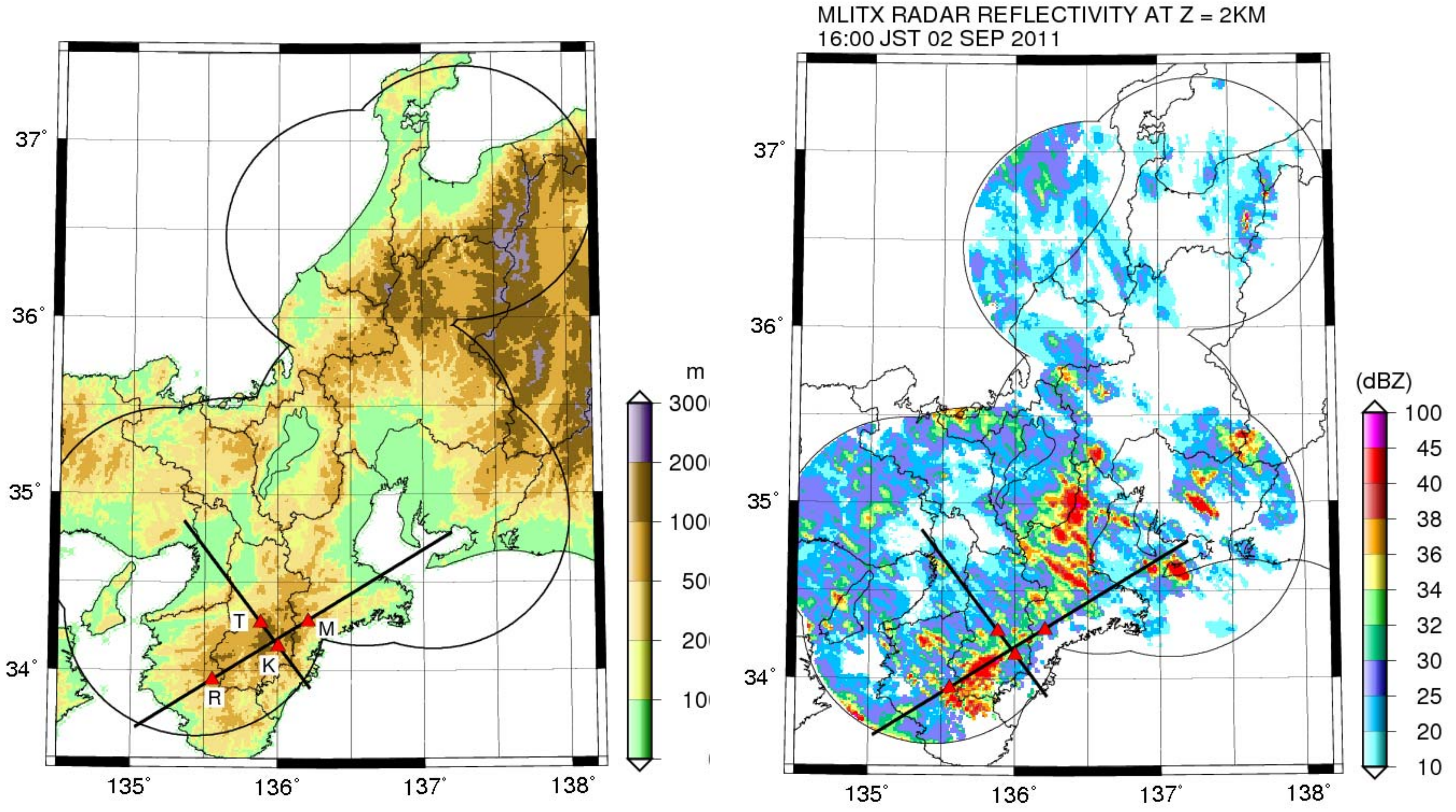

Every 5 minutes volume-scan radar data will provide characteristics of heavy rainfall associated with typhoon.

Problems on Heavy Rainfall

Area of Disaster Strikes	Disasters in recent problem	Expected Disaster Response
Metropolis	Urban River Flooding Sewage Overflow Flooded Underground	Monitoring Short-term Forecasting Warning
(Covered by Monitoring System)	Critical Rainfall Amount (50 mm in one hour)	
River Basin Dam Long-distance Transportation Highway	Critical Rainfall Amount (∼200 mm in one day)	
Mountains	Landslide Deep-seated Landslide Landslide Dam Failure	Monitoring Forecasting Short-term & Long-term Warning
	Critical Rainfall Amount (1,000 mm in a few days and 50 mm in one hour)	

Heavy Rainfall

Typhoon

Utilize Radar Data

S-band and C-band Doppler Radar + X-band Polarimetric Radar
High-resolution Regional Model + Radar Data Assimilation

For Future (Field Experiment in Palau)

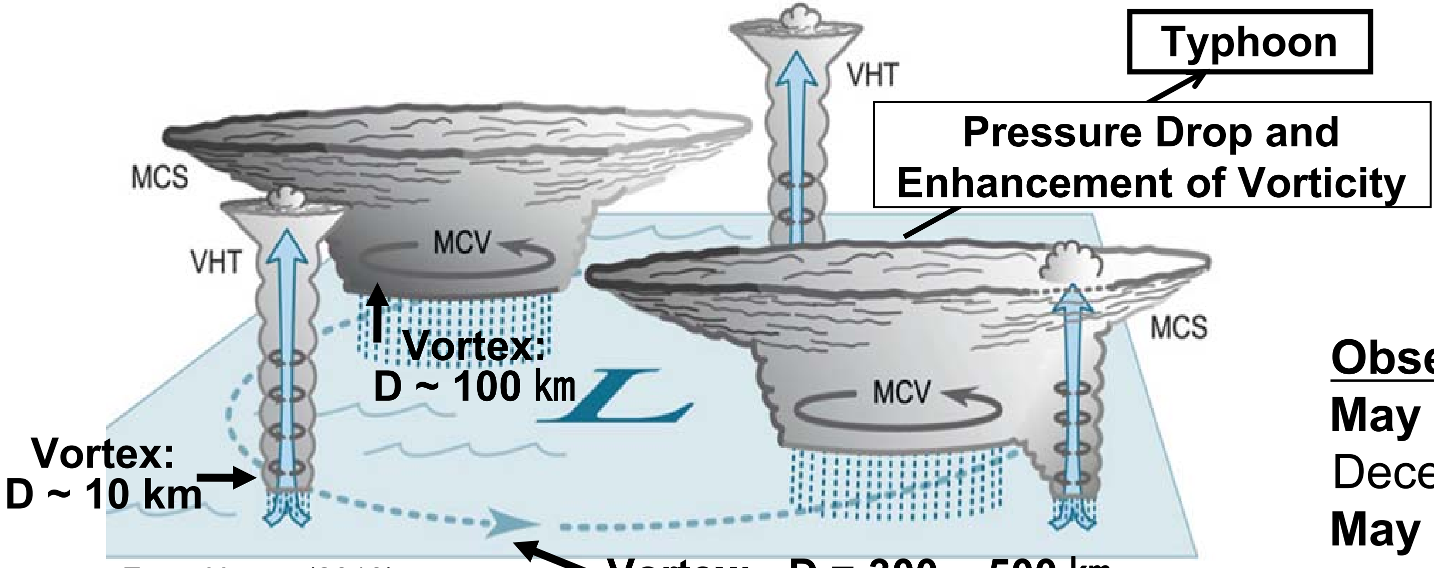

From Houze (2010)

Observation Year

May & June 2013
December 2013
May & June 2014

Cloud Particle Sonde Observation

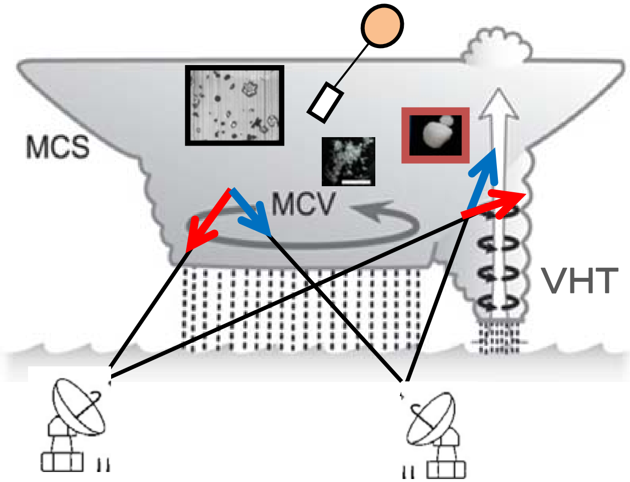

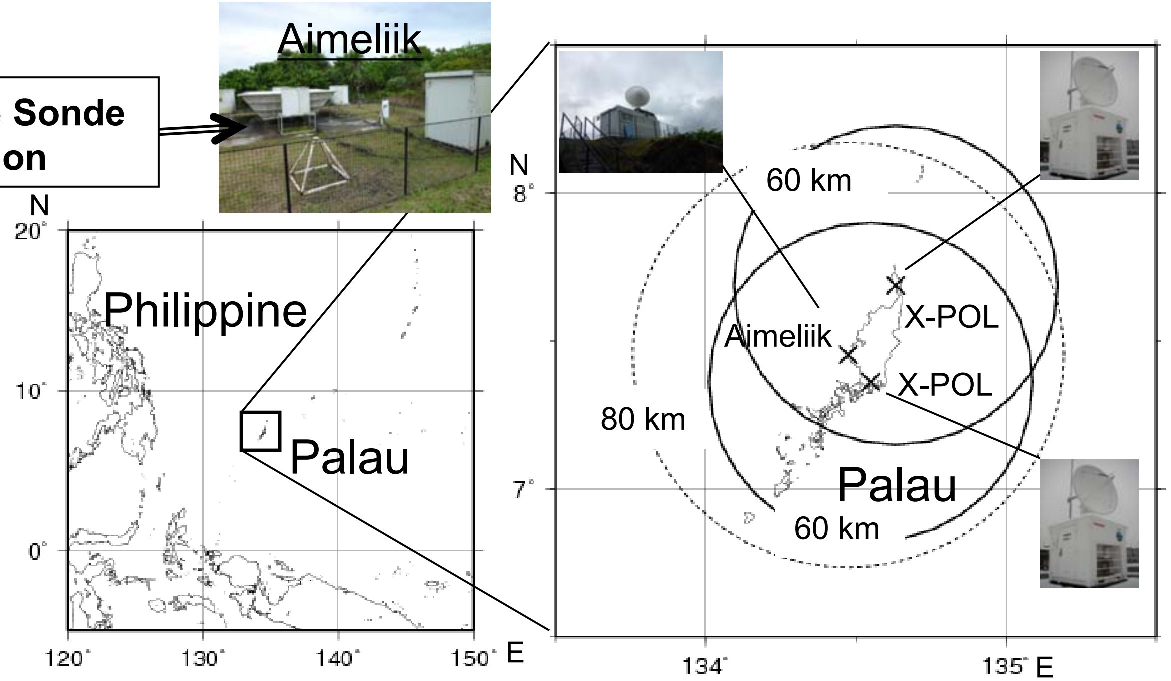

Comparison between radar and HYVIS

- using **RHI** data (high resolution in vertical direction)
- comparing **polarimetric variables** (Z_h, Z_{dr}, K_{dp} and ρ_{hv}) and **particle t**

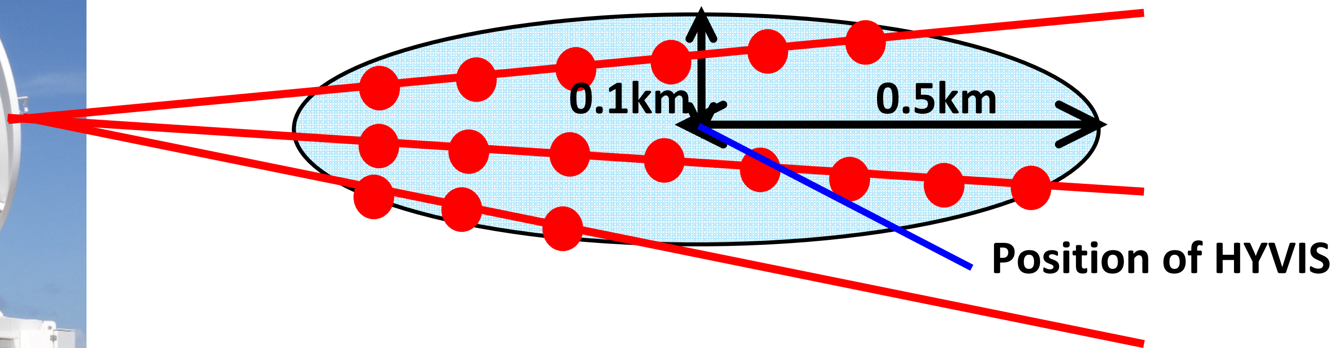

polarimetric variables: averaged spatially ↑

Kouketsu 2012

▼The list of comparison

HYVIS No.	Date of RHI (JST)	Height of HYVIS	Temperature
No. 2	16:05 June 1	About 5,800m	-5.5℃
No. 3	21:35 June 2	(About 9,400m)	(-27.5℃)
No. 5	02:47 June 14	About 9,400m	-25.5℃

Data

- X-band polarimetric radar (X-pol): installed at Aguni Island
- Hydrometeor Videosonde (HYVIS): launched from Aguni Island

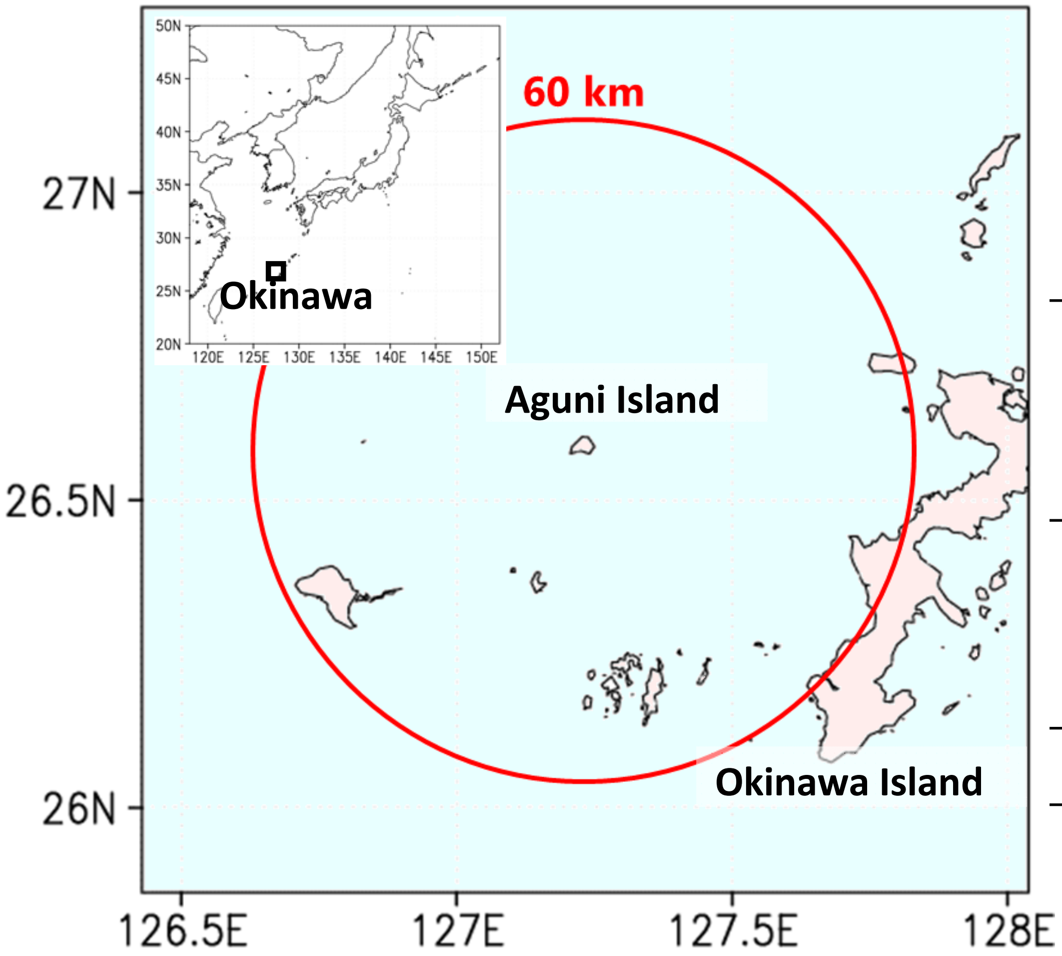

●X-pol observation

location	Aguni Island, Okinawa
Observational period	From May 23 to July 13, 2011※
Maximum range	60km
parameters	Z_h, Z_{dr}, K_{dp} and ρ_{hv}
Scan mode	PPI（15 elevations, every 6 minutes） RHI（arbitrarily）
range gate	150m
Beam width	1.2°

※missing data from May 27 to 29

HYVIS

HYVIS = **Hy**drometero **Vi**deo**s**onde

・**two** types of cameras : **close-up** and **microscopic** cameras

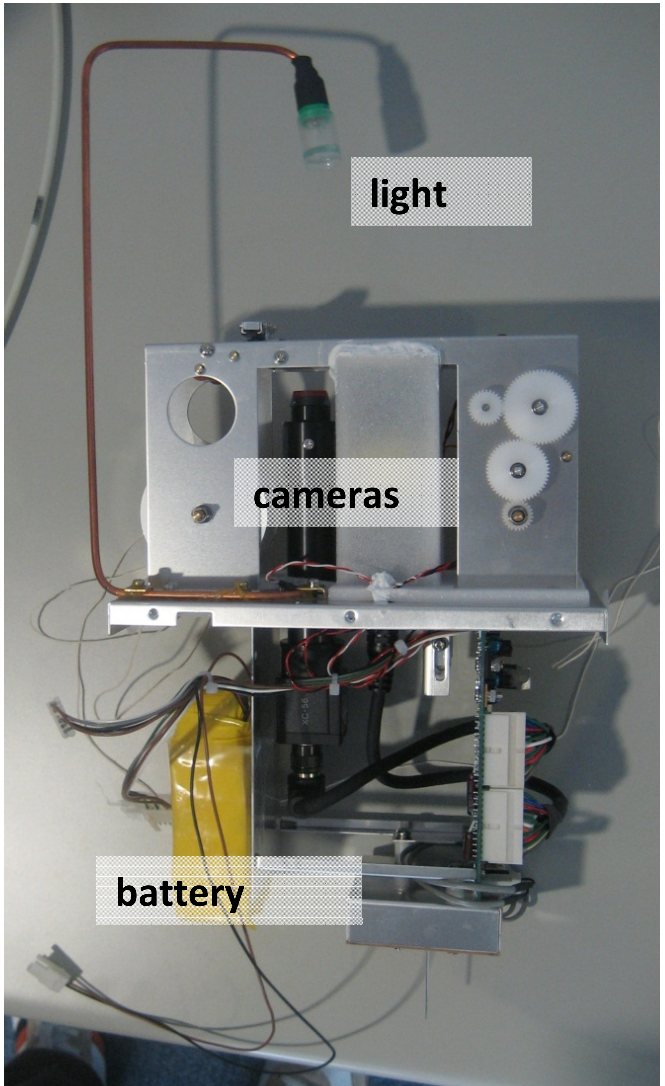

HYVIS Observation

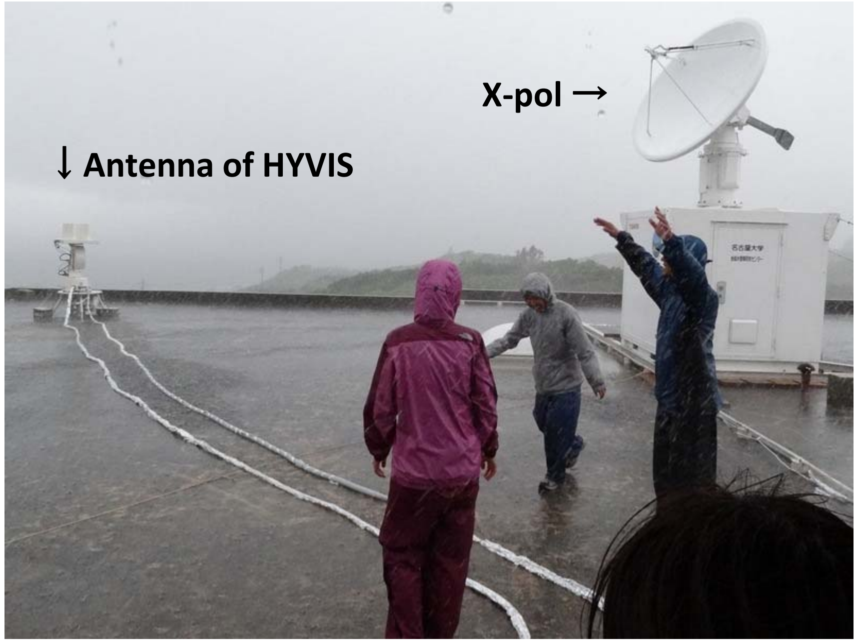

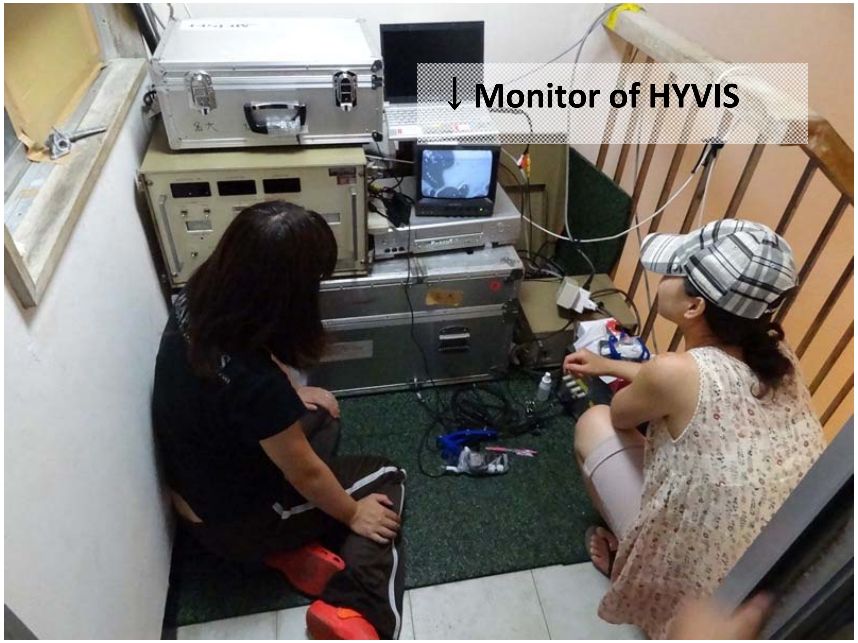

Preparation of launch

Launch of HYVIS

HYVIS

HYVIS = **Hy**drometero **Vi**deo**s**onde

・**two** types of cameras : **close-up** and **microscopic** cameras

Image of Close-up Camera

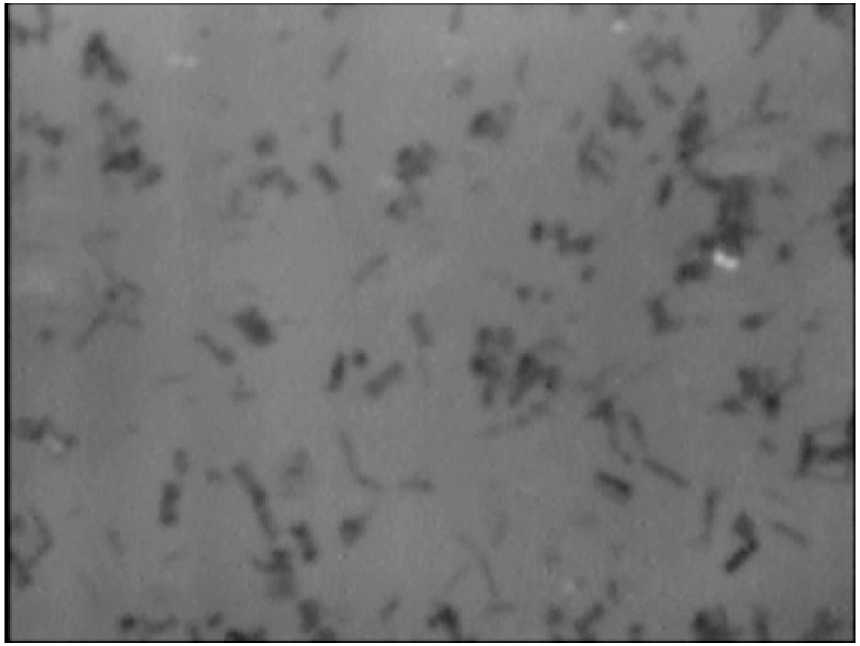

9mm

Image of Microscopic Camera

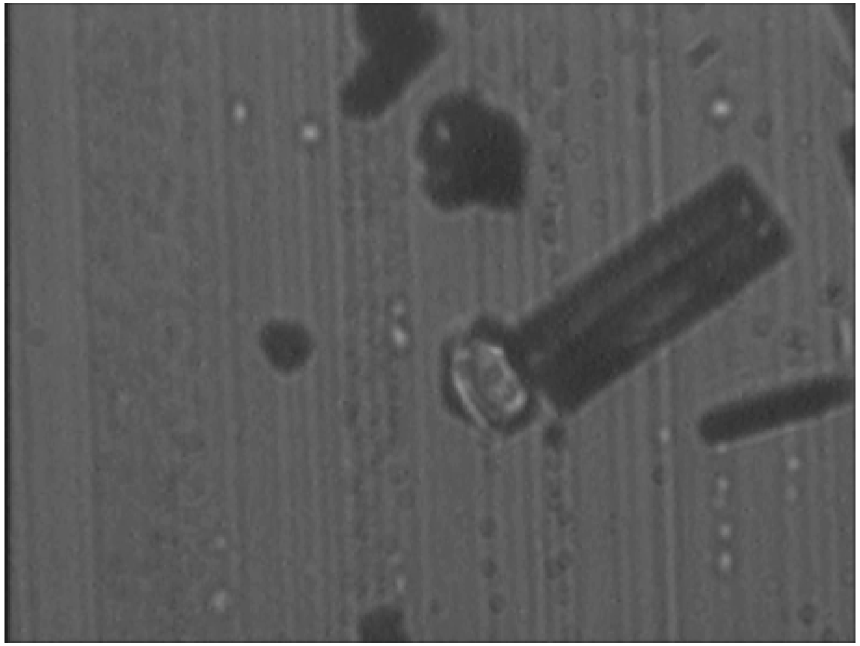

1.4mm

Result: HYVIS #2 (June 1, 2011)

Z_h (CAPPI: z = 2 km)

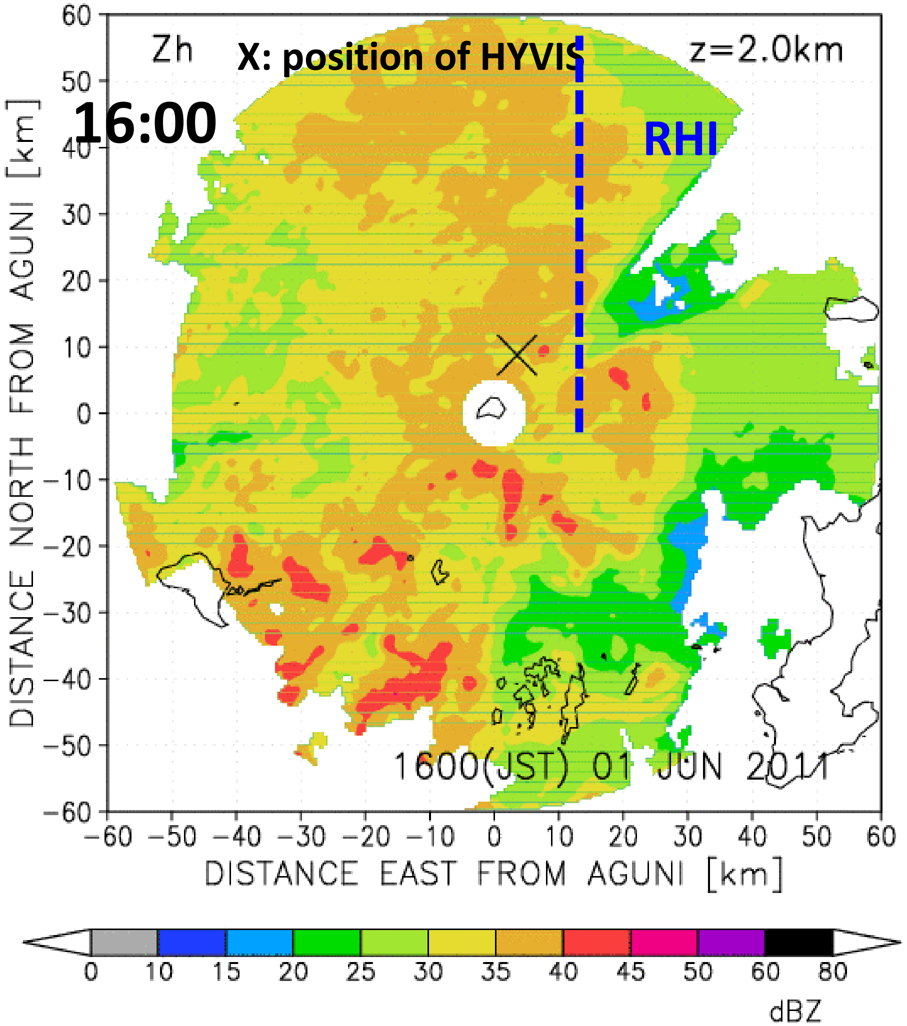

Z_h (RHI: AZ = 26°)

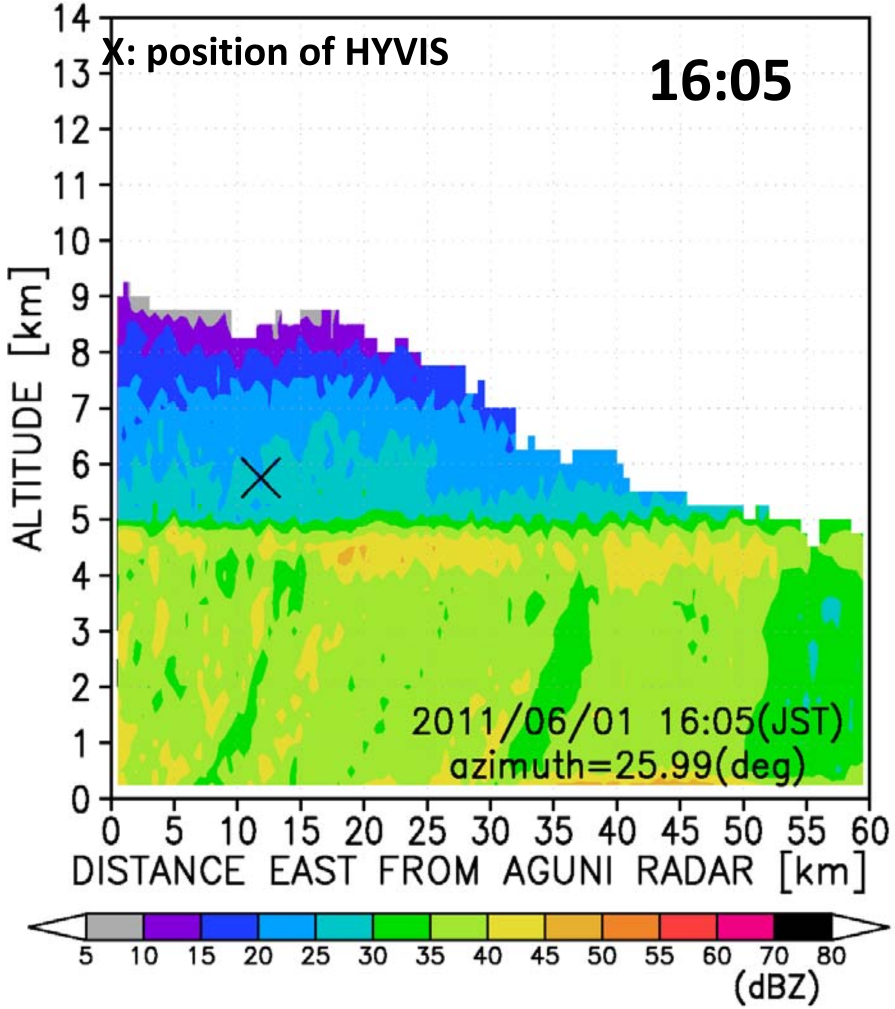

Result: HYVIS #2 (June 1, 2011)

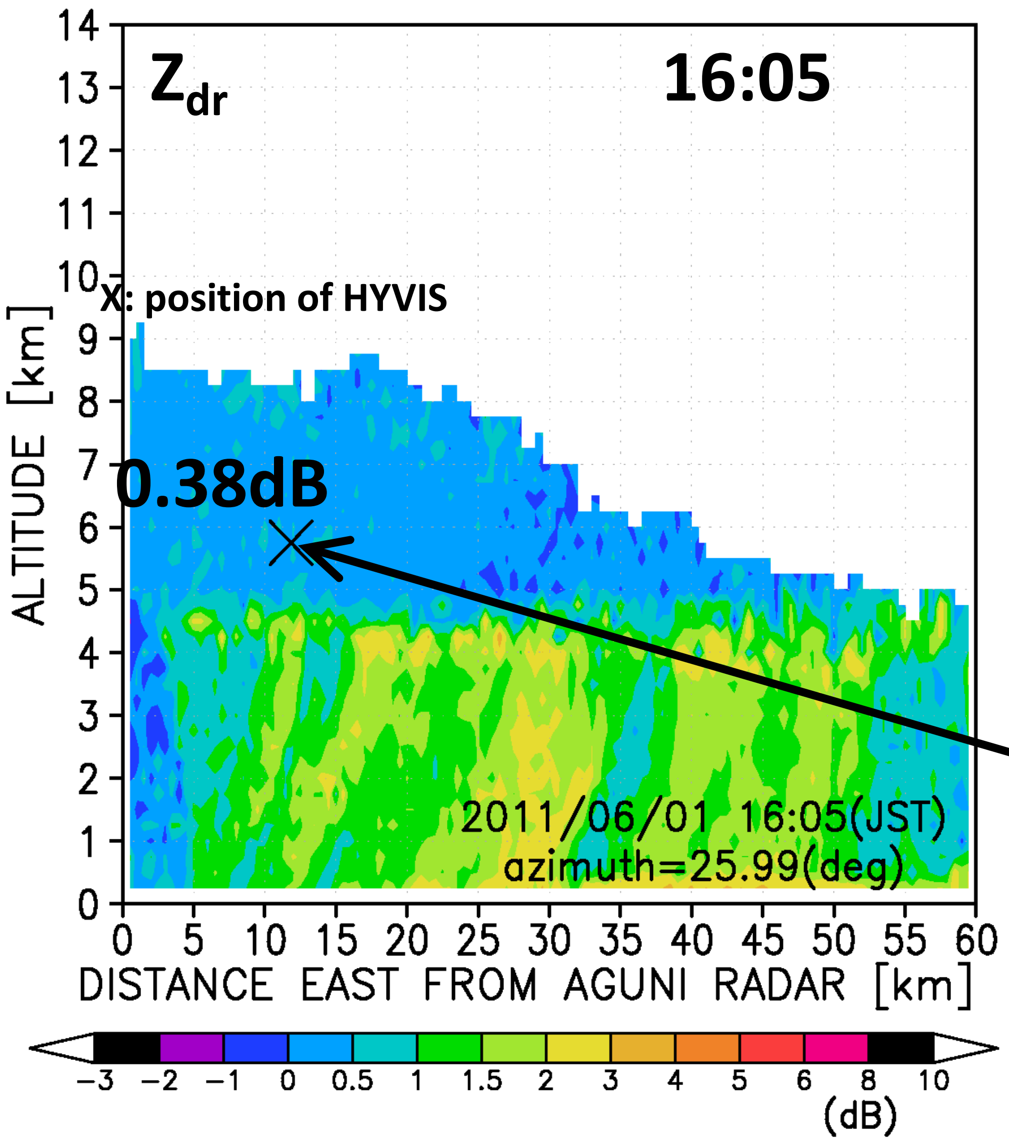

Z ≒ 5,800 m

Particle type: column

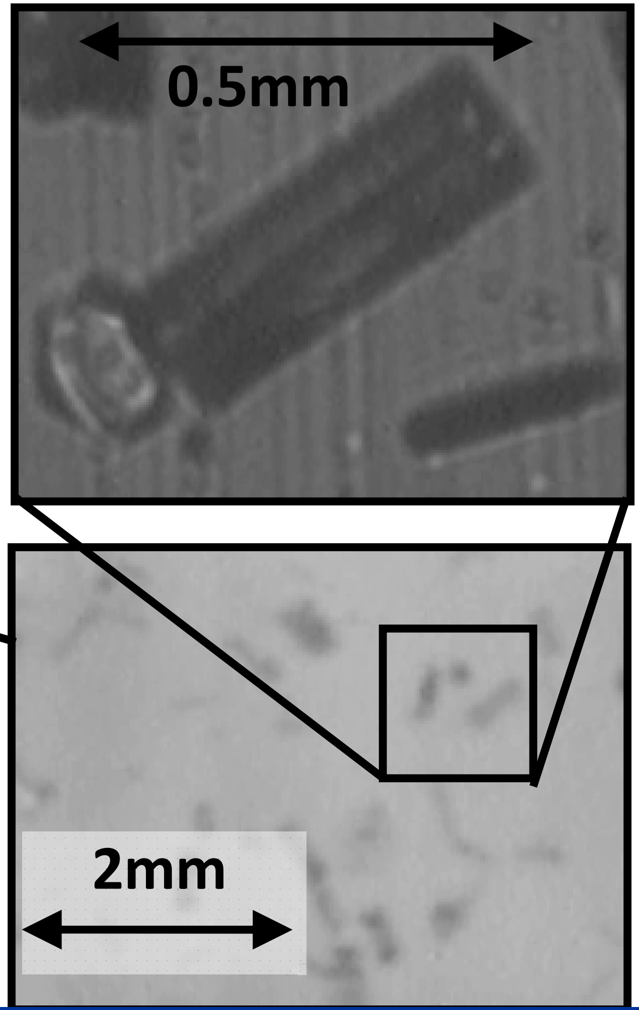


Thank you !

Global
Precipitation
Measurement

Global rain map (1)

Takuji Kubota

Earth Observation Research Center (EORC)
Japan Aerospace Exploration Agency (JAXA)

International Hydrological Programme
Precipitation Measurement from Space and its Applications
The Twenty-second IHP Training Course
22 November 2012 @ HyARC, Nagoya University

Contents

- Multi-satellite rainfall Product
  - Global rain map = Products merged from various sensor data from satellites, in addition to other resources (e.g, rain gauges)
  - Global Precipitation Measurement (GPM)
  - Global Satellite Mapping of Precipitation (GSMaP)
  - Brief algorithm flow & Validation
- GSMaP application
  - Cyclone “Nargis”
  - 2011 Thailand floods
- GSMaP data handling
  - How to Get the GSMaP Online Data
  - Data format

Single-satellite products


GPM
Global Precipitation Measurement
JAXA
衛星名
全衛星
GPM Core
NOAA-N19
GCOM-W1
MetOp-B
DMSP F19
Megha-Trop
NPP
DMSP F20
0
30
60
90
120
150
180 min
INDEX

Multi-satellite products


GPM
Global Precipitation Measurement
JAXA
衛星名
全衛星
GPM Core
NOAA-N19
GCOM-W1
MetOp-B
DMSP F19
Megha-Trop
NPP
DMSP F20
0
30
60
90
120
150
180 min
INDEX

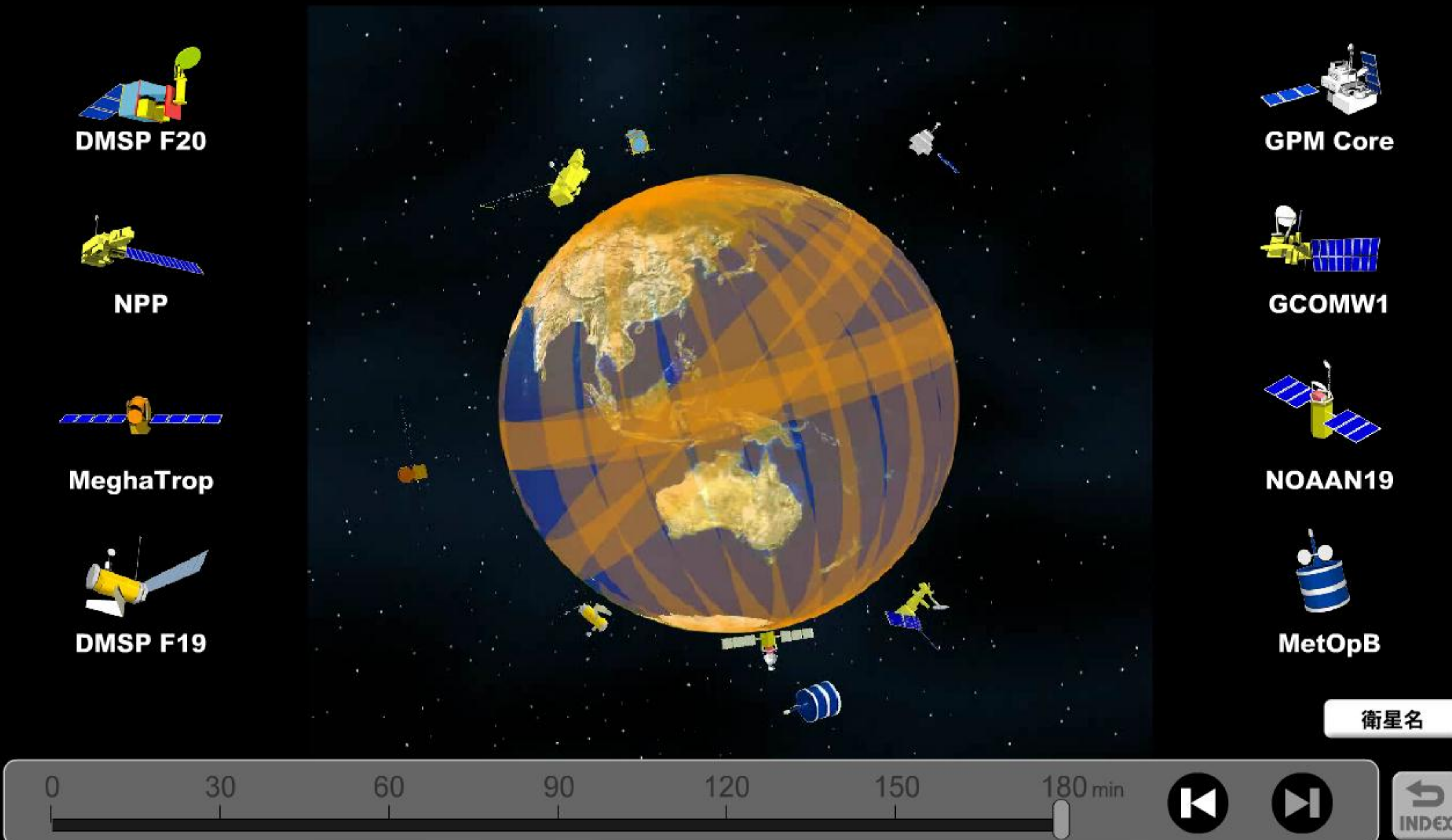
DMSP F20
NPP
MeghaTrop
DMSP F19
GPM Core
GCOMW1
NOAAN19
MetOpB
衛星名
0
30
60
90
120
150
180 min
INDEX

Orbit of Various Satellites

TRMM/GPM-core satellites are flying non-sun-synchronous orbit, which has low inclination angle, in order to observe diurnal variation of tropical rainfall.

Sun-Synchronous orbit
Observation condition will be constant at same location

× cannot capture differences depending on local time
× Least observation frequencies at equatorial area

TRMM/GPM-core's orbit
Local time of observation will be changing as time go on.

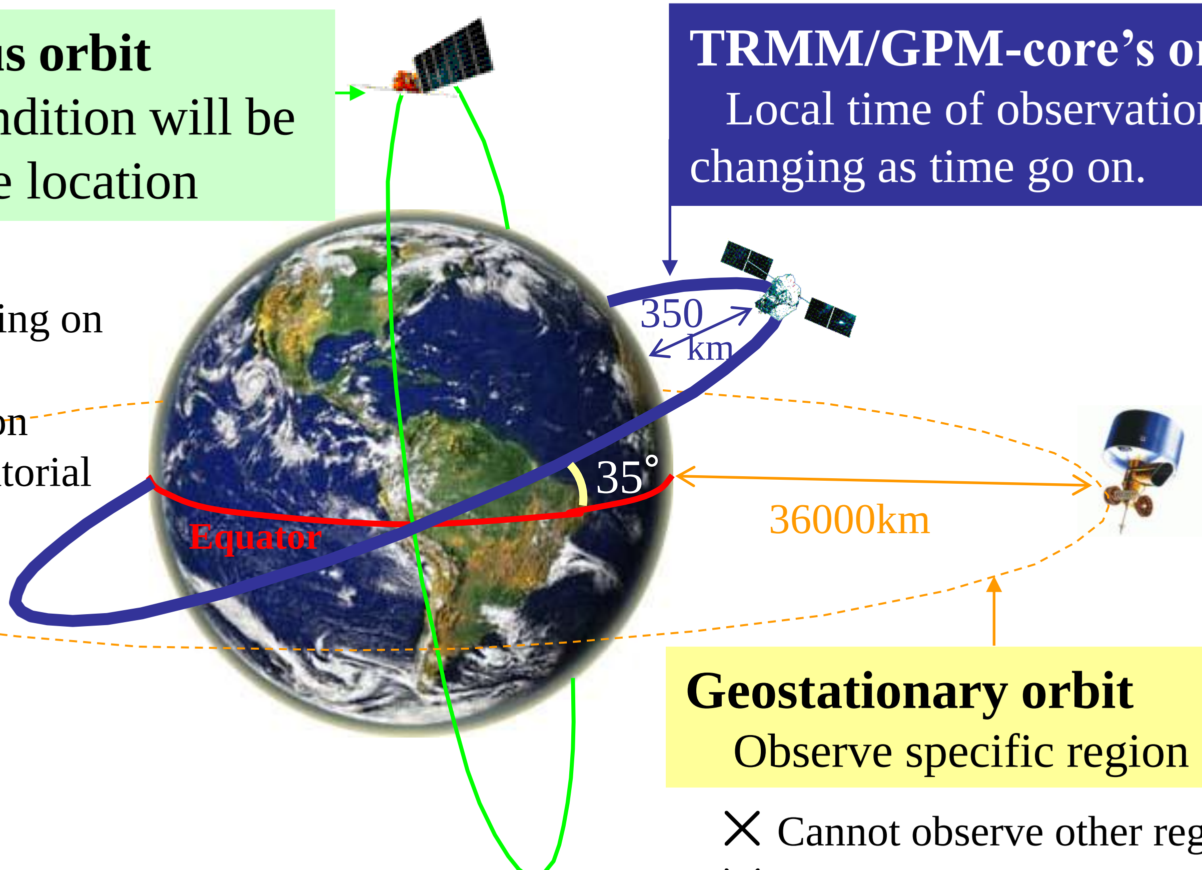

Geostationary orbit
Observe specific region at anytime

× Cannot observe other region
× Horizontal resolution will be worse

Global rainfall map

Products merged from various sensor data from satellites, in addition to other resources (e.g, rain gauges) can be useful for users → Global rain map

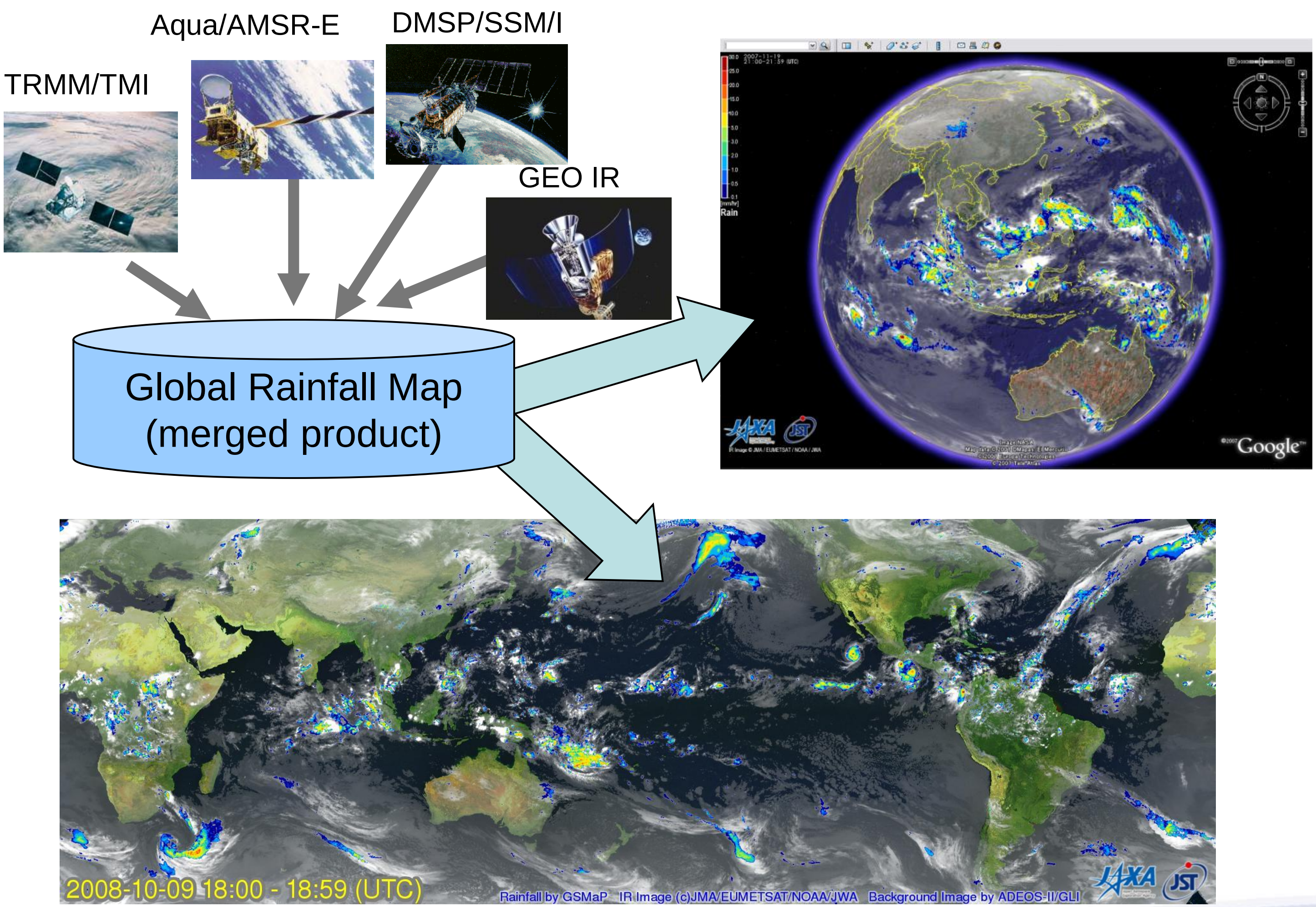

Rainfall Measurement from Space

Active sensor

A remote sensing system that transmit its own electromagnetic energy, then measures the properties of the returned radiation.

Radar; Radio Detection And Ranging

Precipitation Radar (PR)
TRMM/PR, GPM/DPR

Passive sensor

A remote sensing system that relies on the emission of natural levels of radiation from the target.

GCOM-W1/ AMSR2 instrument

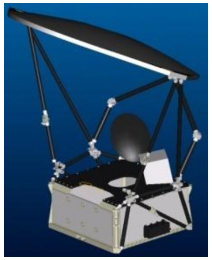

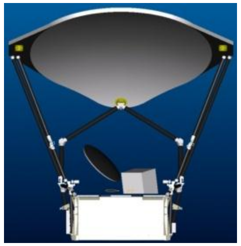

Global Satellite Mapping of Precipitation (GSMaP)

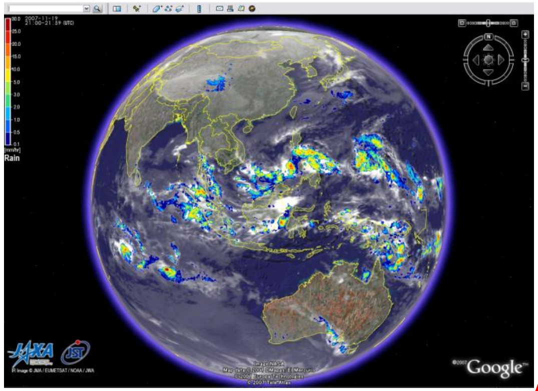

Microwave radiometers (conical scan)

Sensor	SSM/I	TMI	AMSR-E	SSMIS	Windsat	AMSR2	GMI
Satellite	DMSP series (~F15)	TRMM	Aqua	DMSP series (F16~)	Coriolis	GCOM W1	GPM
Provider	DoD, U.S.	NASA	JAXA	DoD, U.S.	NASA	JAXA	NASA
周波数 [GHz]	19.35 - 85.5	10.65 – 85.5	6.93 – 89.0	19.35 – 183.3	6.8 – 37.0	6.93 – 89.0	10.65 – 183.3
観測幅 [km]	1400	700	1450	1700	1000	1450	890
Antenna size [m]	0.61	0.61	1.6	0.61	1.8	2.0	1.2


DMSP series


TRMM


Aqua

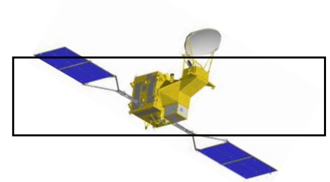
GCOM-W1

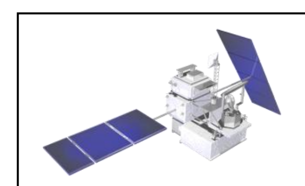
GPM Core

AMSU/MHS

- AMSU(Advanced Microwave Sounding Unit) is carried by NOAA KLM satellites (NOAA 15(-K), 1998-; NOAA 16(-L), 2000-; NOAA 17(-M), 2002-)
- MHS (Microwave Humidity Sounder) is similar to AMSU-B, and carried by NOAA 18, 19, Metop-A, Metop-B

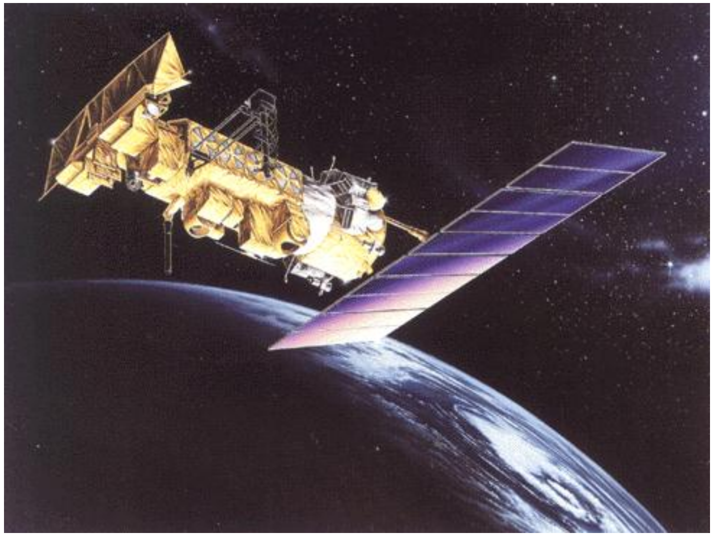

Observation swath: 1650km
Footprint size of AMSU-B/MHS: 16km at nadir, but it changes according to observation directions.)

http://amsu.cira.colostate.edu/

http://www2.ncdc.noaa.gov/docs/klm/html/c3/sec3-4.htm

Channel	MSU	AMSU-A	AMSU-B
1	50.30	23.8	89.0
2	53.74	31.4	150.0
3	54.96	50.3	183.3±1
4	57.95	52.8	183.3±3
5		53.6	183.3±7
6		54.4	
7		54.9	
8		55.5	
9		57.2	
10		57.29±.217	
11		57.29±.322±.048	
12		57.29±.322±.022	
13		57.29±.322±.010	
14		57.29±.322±.0045	
15		89.0	

(GHz)

Operational geostationary satellites

- GOES, METOSAT, MTSAT, FY-2, INSTAT, COMS... carries Infrared (IR) sensor

GEO = Geostationary Earth Orbit

http://www.wmo.int/pages/prog/sat/globalplanning_en.php

Observation of Precipitation from the Satellite

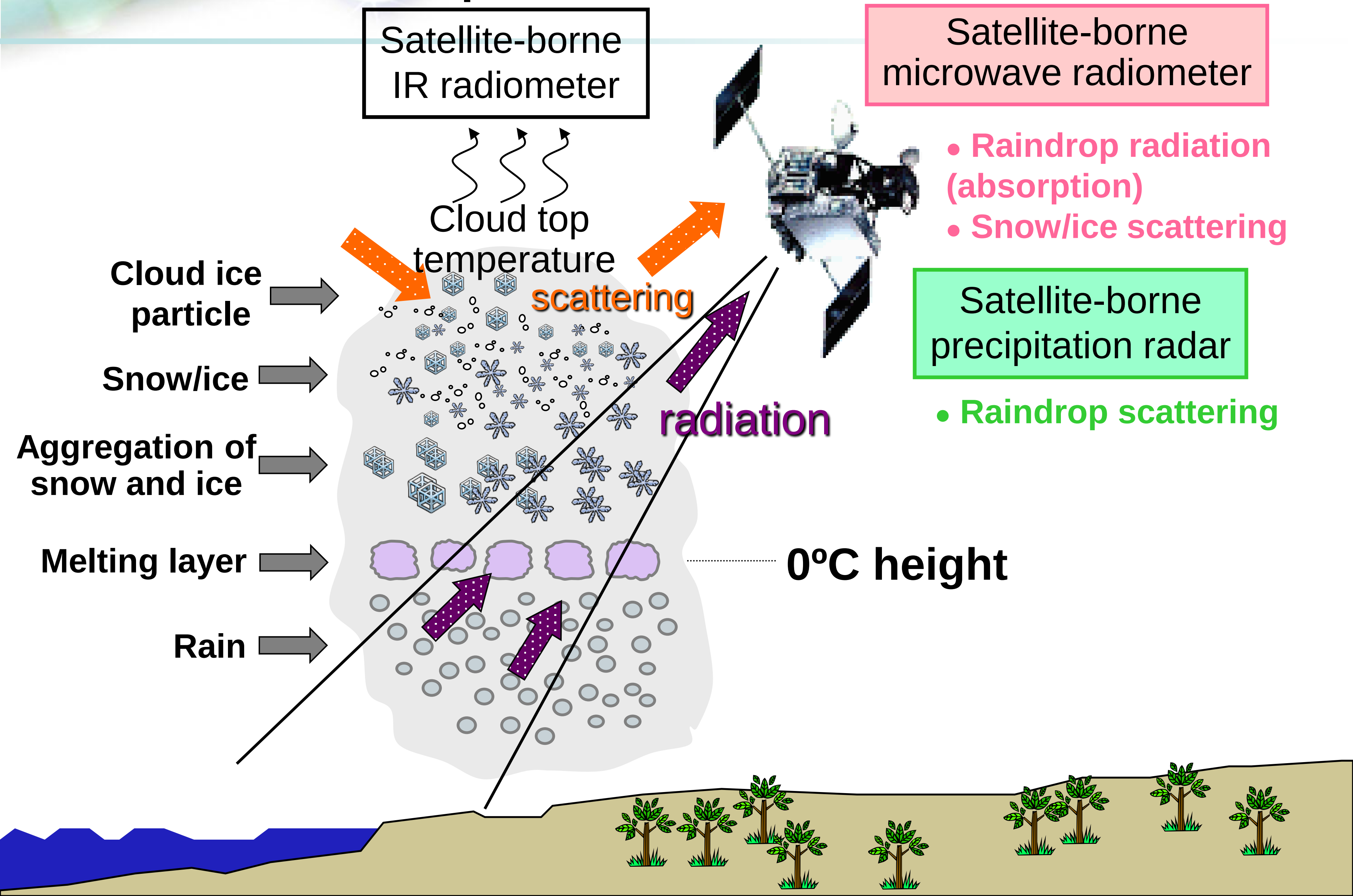

Precipitation characteristics observed by the space borne sensors

Typhoon MORACOT (8 Aug. 2009)

(a) Precipitation radar

Back scattering from rain drops

High accuracy

Narrow swath width

(b)Infrared radiometer:

Cloud top information

Not related to surface precipitation rates

(c)Microwave radiometer(19GHz):

(d)Microwave radiometer(85GHz):

Directly measures emission from rainfall & scattering from snow/ice over the ocean

Directly measures scattering from snow/ice over the land

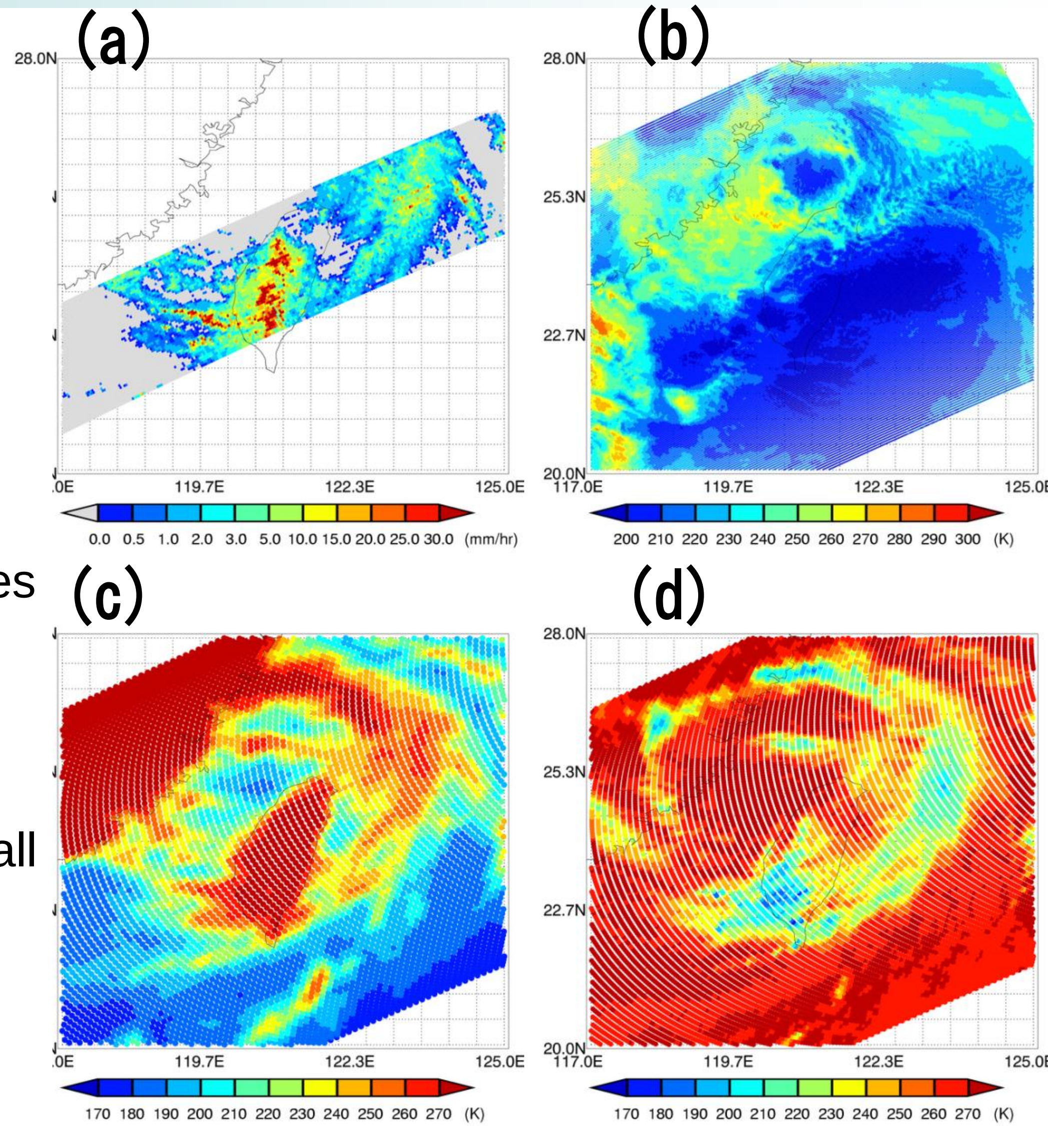

It is important to combine the data from different frequencies to retrieve precipitation

Strength and Weaknesses of Each Sensor

- Each sensor has strength and weaknesses.
  - Microwave passive sensor has
    - Very good correlation to precipitation
    - Emission not useful over land
    - No operational estimates over frozen surfaces
    - The major draw back is temporal sampling due low earth orbit satellite (LEO)
  - Infrared (IR) sensor has
    - Excellent sampling from Geostationary Earth Orbit (GEO) satellites
    - Weak instantaneous relationship to precipitation
    - Weak mean relationship outside 40 degree
  - → Blended Microwave-IR approach

Ground rain gauge distribution

Distribution of rain gauge in GPCC Monitoring Product
Provided by Global Precipitation Climatology Centre (GPCC)
http://gpcc.dwd.de

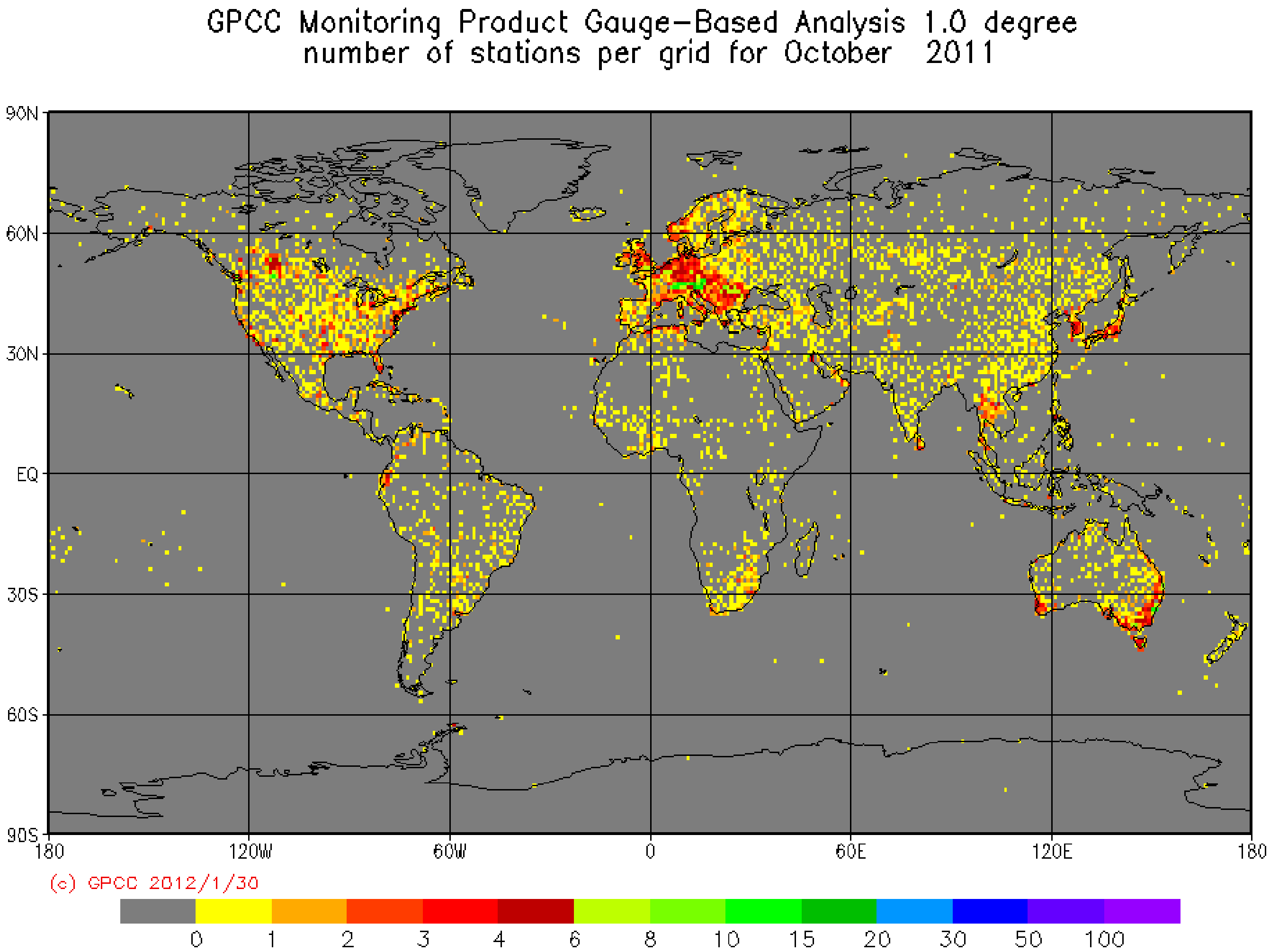

Weaknesses of Other Approaches

- Rain gauge
  - Wind losses, evaporation, and side-wetting and splashing
  - Sparse (in particular) at Tropics
  - Latency (availability)
- Surface-based radar
  - Small observation area with beam blockage by surface features
  - Calibration uncertainties
  - Anomalous propagation
- Numerical prediction model
  - Difficulty in model representation of precipitation
  - Initialization errors

TRMM impact on global rainfall map

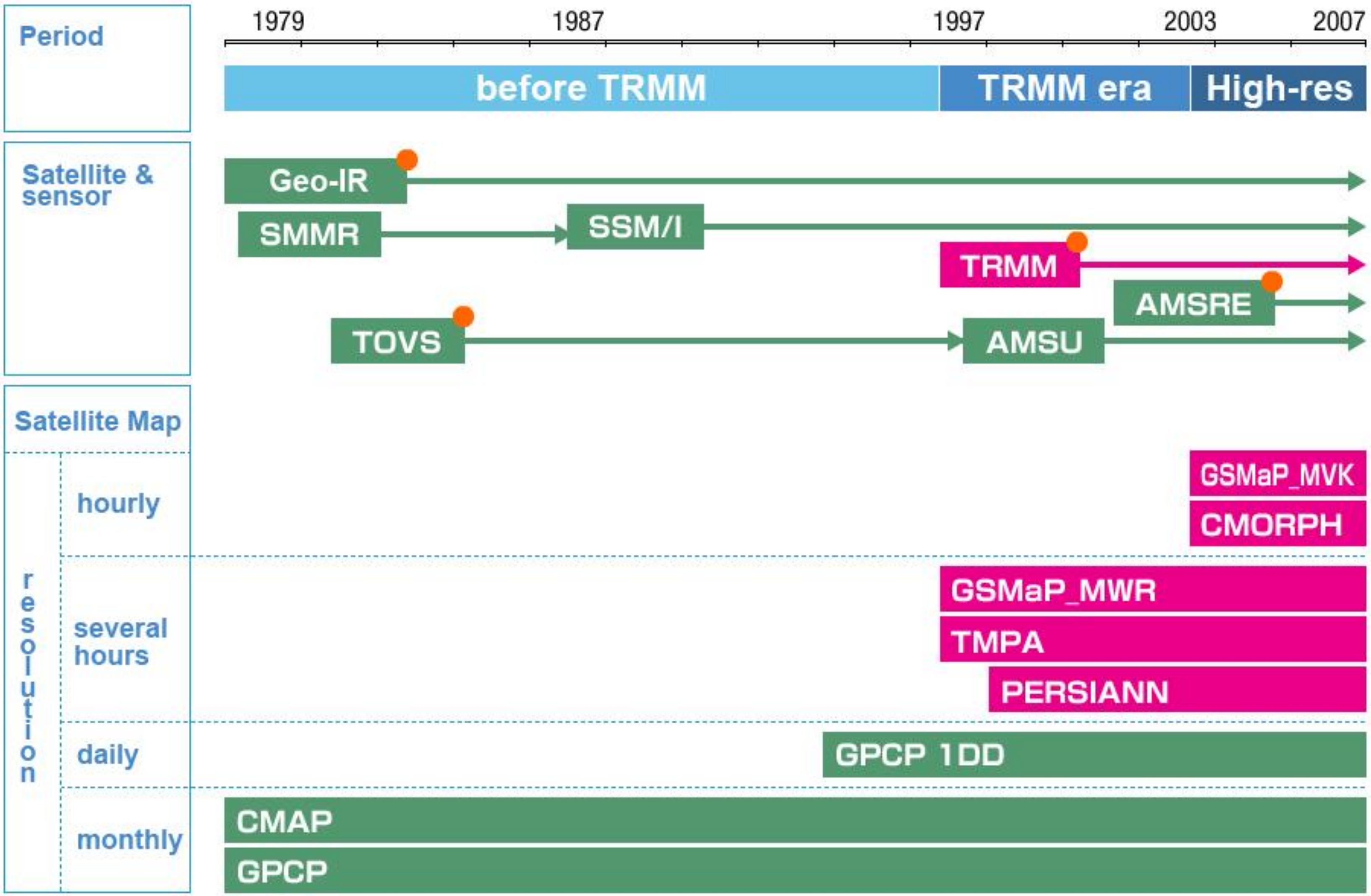

Major satellite global rainfall map before TRMM

Product (organization)	Hori. res.	Temp. res.	NRT (delay)	Data source and major characteristics
GPCP (WCRP/GEWEX) http://cics.umd.edu/~yin/GPCP/main.html	2.5 deg	1-month	×	Merge satellite (IR,SSM/I,TOVS/MSU) with gauge data
GPCP 1DD (NASA/GSFC) http://precip.gsfc.nasa.gov/	1 deg	1-dy	×	Merge satellite (IR,SSM/I, TOVS/MSU) with gauge data
CMAP (NOAA/CPC) http://www.cpc.ncep.noaa.gov/products/global_precip/html/wpage.cmap.html	2.5 deg	5-dy	× (1-dy)	Merge satellite (IR,SSM/I, TOVS/MSU) with gauge data.

- Main objectives are to obtain global climatology, and temporal and vertical resolutions are coarse.
- Calibrated satellite (IR and microwave sensors) data over land by ground-based rain gauges.

Major satellite precipitation map after TRMM (1/2)

Product (organization)	Hori. res.	Temp. res.	Data latency	Data source and major characteristics
CMORPH/QMORPH (NOAA/CPC) http://www.cpc.ncep.noaa.gov/products/janowiak/cmorph_description.html	~8 km	3-hr (CMORPH)	18-hr	Merging passive microwave sensors (radiometer/sounder) estimated rainfall & whose features are transported via spatial propagation information by IR. Not use rain gauge data.
	0.5 deg	3-hr (CMORPH)		
	~8 km/ 0.25 deg	30-min (QMORPH)	3-hr	Real-time version of CMORPH. Using forward propagation only. Not use rain gauge data.
PERSIANN (UCI/HyDIS) http://hydis8.eng.uci.edu/persiann/	0.25 deg	1-hr	2-day	Calibration and training IR estimated rainfall using microwave sensor (radiometer & sounder) rainfall. Not use rain gauge data.
NRL Blended (NRL) http://www.nrlmry.navy.mil/sat-bin/rain.cgi	0.25/0.1 deg	3-hr	3-hr (image only)	Blending IR estimated rainfall and passive microwave sensors. Not use rain gauge data.
Hydro-Estimator (NOAA/NESDIS) http://www.orbit.nesdis.noaa.gov/smcd/emb/ff/auto.html	4~6 km	30-min~ 3-hr	10-min (local)	Regional IR estimated rainfall calibrated by numerical weather prediction and ground-based radars.

Major satellite precipitation map after TRMM (2/2)

Product (organization)	Hori. res.	Temp. res.	Data latency	Data source and major characteristics
TRMM TMPA 3B43/3B42/3B42RT (NASA/GSFC) http://trmm.gsfc.nasa.gov/	0.25 deg	1-month (3B43)	1-month	Combine passive microwave sensors (radiometer /sounder) & IR estimated rainfall. Direct use of monthly rain gauge.
	0.25 deg	3-hr (3B42)	1-month	Combine passive microwave sensors (radiometer /sounder) & IR estimated rainfall, indirect use of monthly rain gauge.
	0.25 deg	3-hr (3B42RT)	10-hr	Real-time version of 3B42. Not use rain gauge data.
GSMaP MWR/MVK/NRT (JAXA) http://sharaku.eorc.jaxa.jp/GSMaP/index.htm	0.25 deg	1-/24-hr (MWR)	Not in real-time	Merging microwave radiometer rainfall using PR indirect information. Not use rain gauge data.
	0.1 deg	1-hr (MVK)	2-3 days	Combine MWR and whose features are transported via spatial propagation information by IR, combinational use of Kalman filtering approach. Not use rain gauge data.
	0.1 deg	1-hr (NRT)	4-hr	Real-time version of MVK. Using forward propagation only. Not use rain gauge data.

- higher temporal/horizontal resolution products are available due to improvement in rainfall estimation by microwave radiometer, increase of satellite sensors, improvement in horizontal resolution
- Increase of products distributed in near real-time

Two types of the global precipitation map

- IR-based Approach (Ex. GPCP)
  - Uses mainly direct conversion of the brightness temperature at IR wavelength to precipitation rate
  - Generally, the lower temperature, the higher rain rate
  - It is generally true
- Moving Vector Approach (Ex. CMORPH)
  - Propagate the rainy pixels with the atmospheric motion vector
  - Advantage: Relatively high score
  - A possible main source of error of this type of technique is that the advection vector is the only process that describes the temporal variation of the precipitation process.

Two types of the global precipitation map

- IR-based Approach (Ex. GPCP)
  - Uses mainly direct conversion of the brightness temperature at IR wavelength to precipitation rate
  - Generally, the lower temperature, the higher rain rate
  - It is generally true
- Moving Vector Approach (Ex. CMORPH)
  - Propagate the rainy pixels with the atmospheric motion vector
  - Advantage: Relatively high score
  - A possible main source of error of this type of technique is that the advection vector is the only process that describes the temporal variation of the precipitation process.

Global Precipitation Measurement (GPM)

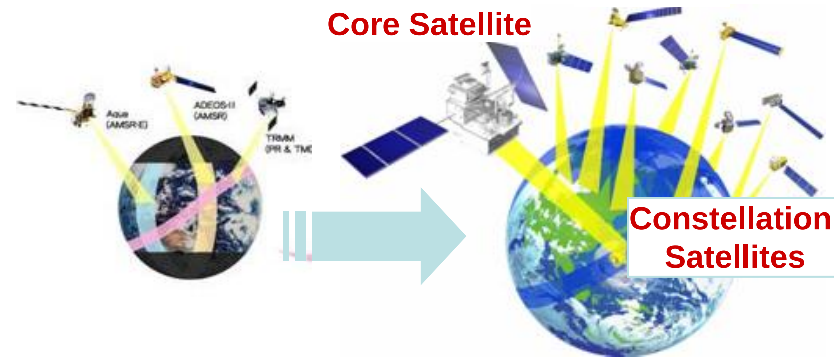

- GPM: An international satellite mission to be launched by JAXA and NASA in 2014 for precipitation measurements worldwide

Core Satellite (JAXA, NASA)

Dual-frequency precipitation radar (DPR)

GPM Microwave Imager (GMI)

- **Precipitation with high precision**
- **Discrimination between rain and snow**
- **Adjustment of data from constellation satellites (The core satellite will fly in non-sun-synchronous orbit.)**

(launch in 2014)

Constellation Satellites (International Partners)

Microwave radiometers

Microwave sounders

- **Global precipitation every 3 hours**

(launch around 2014)

- ➢ Improve the accuracy of both long-term and short-term weather forecasts
- ➢ Improve water resource management in river control and irrigation systems for agriculture

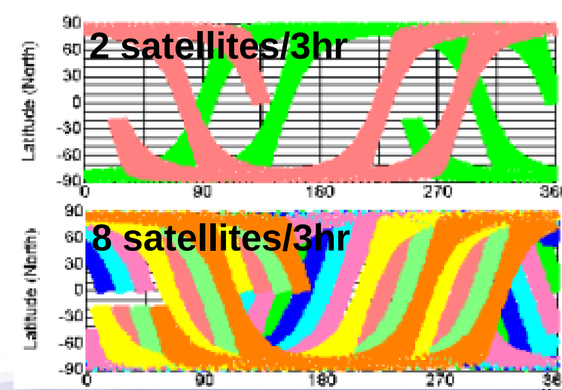

"DPR" aboard GPM core satellite

(launch in 2014)

Dual-frequency precipitation radar (DPR) consists of
-Ku-band (13.6GHz) radar : KuPR
(similar to TRMM/PR)
and
-Ka-band (35.5GHz) radar : KaPR

The DPR was developed by JAXA and NICT.

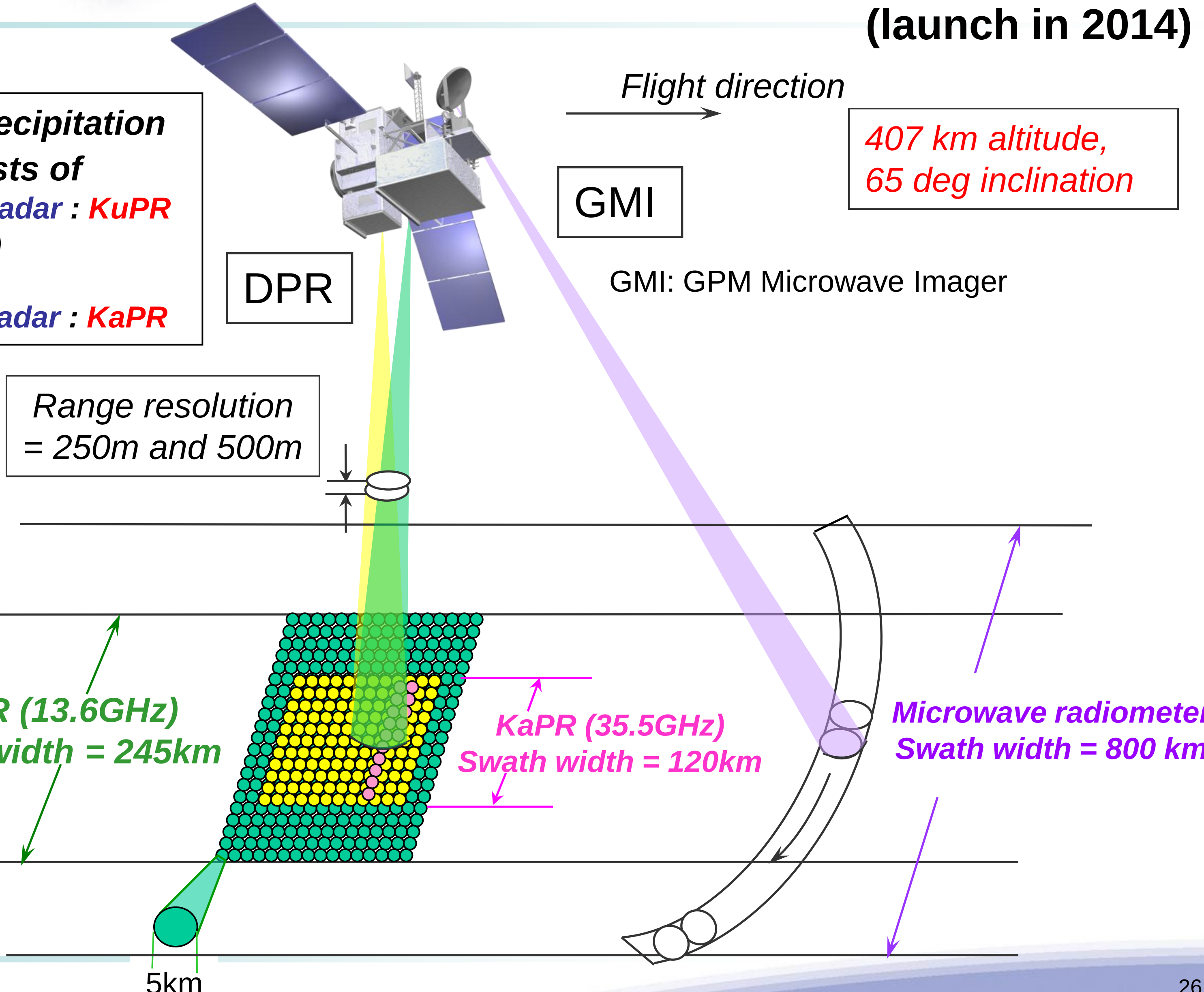

Animation of GPM Core satellite

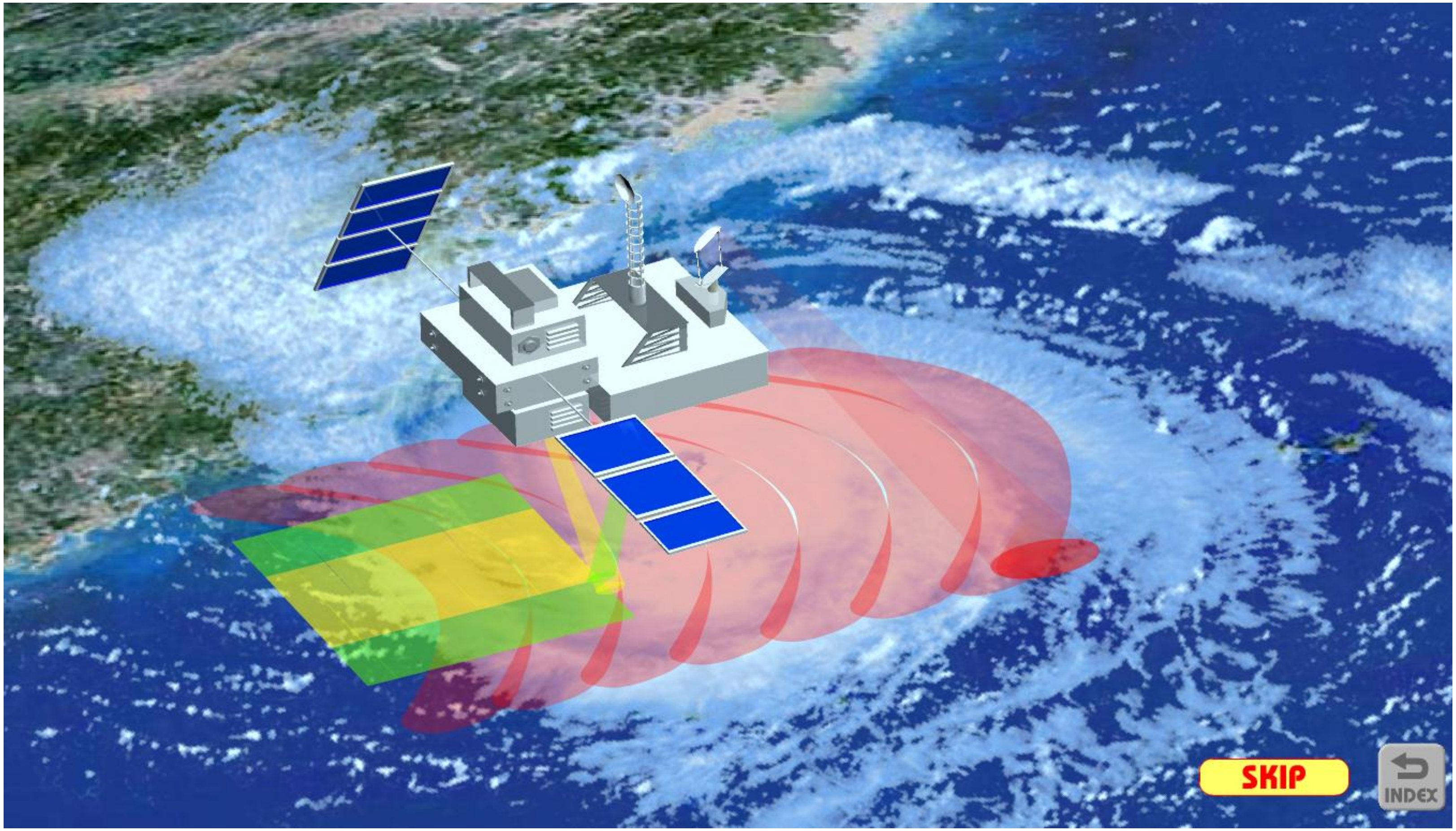

Photo of DPR instruments

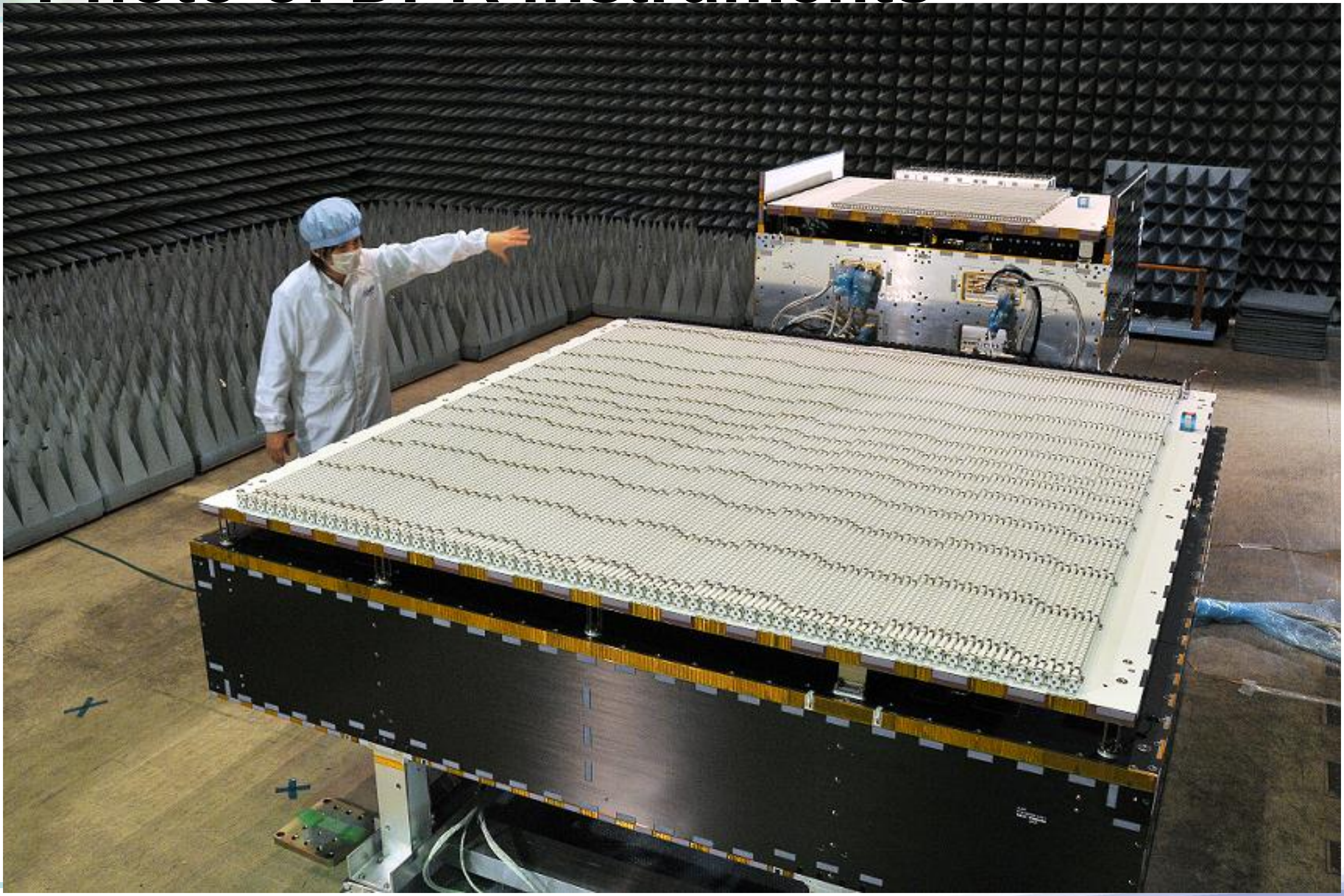

Current status

- Mechanical and Electrical integration to GPM has finished in May 2012.
- Comprehensive Performance Test (CPT) is in progress.

Credit: NASA

Role of DPR in GPM mission

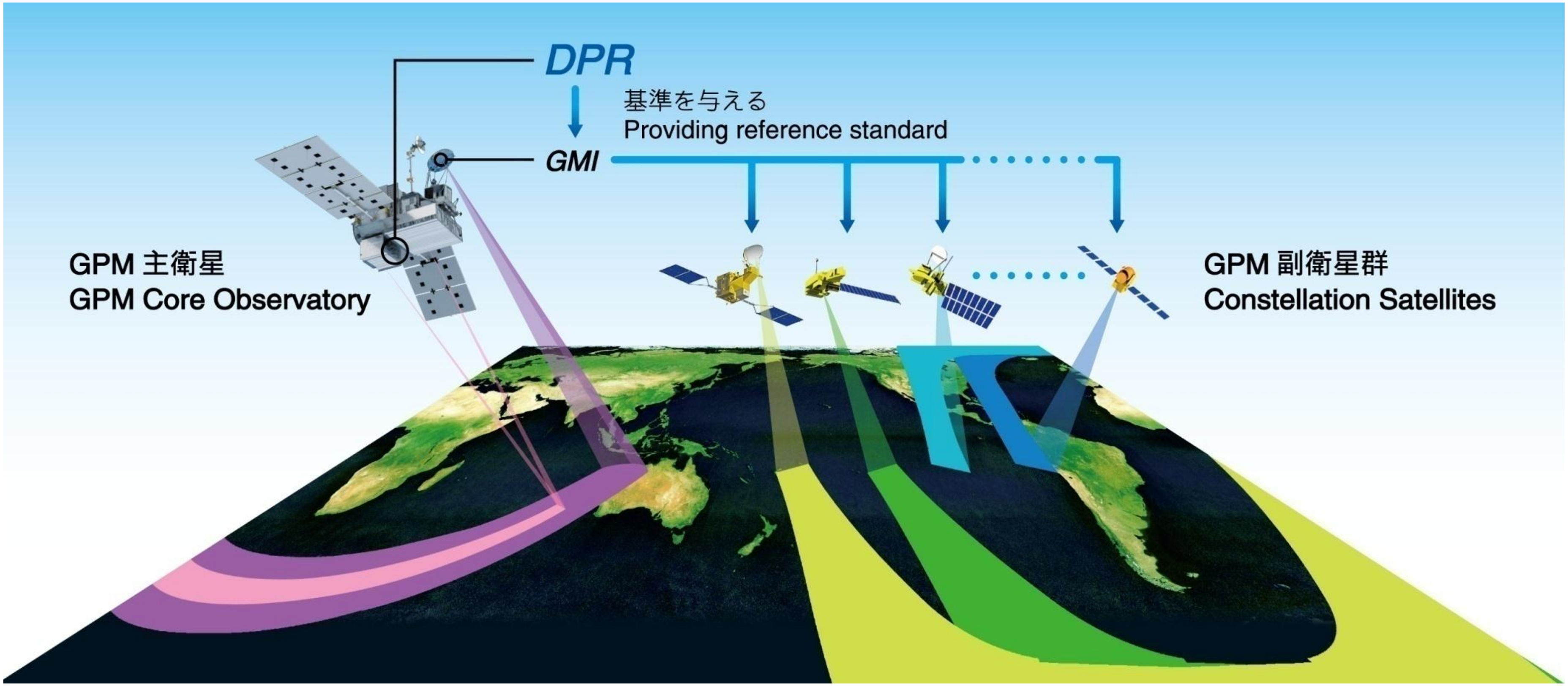

GPM core satellite and TRMM are flying non-sun-synchronous orbit, while Constellation Satellites are flying in non-sun-synchronous orbits.

Multi-satellite rainfall product by JAXA (GSMaP)

As a prototype of JAXA GPM product, we have started to release hourly global rainfall data (0.1x0.1deg. lat/lon) in near real time (about four hours after observations) and visualize the latest data quickly.

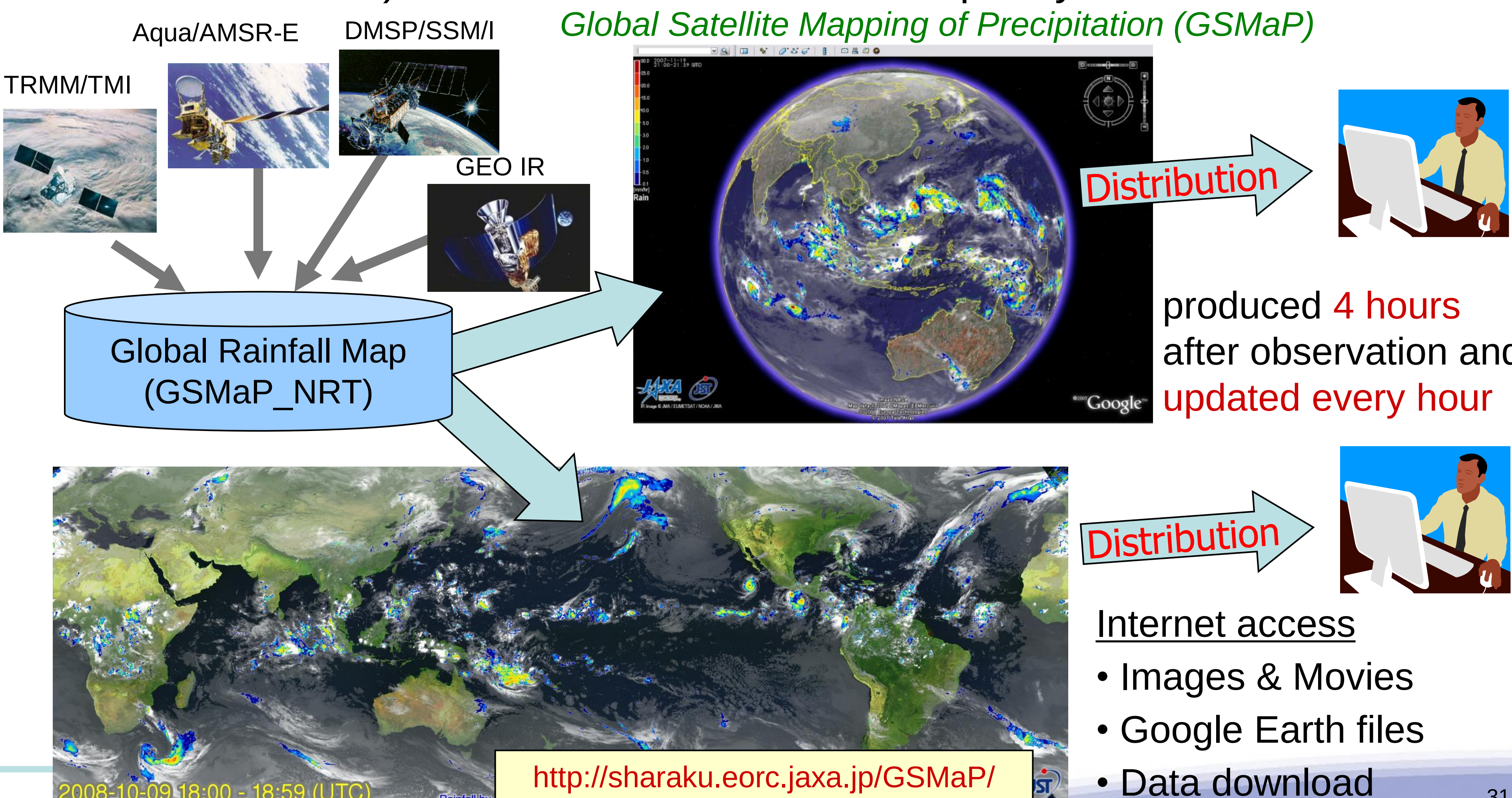

Production of GSMaP by Multi-satellite Data

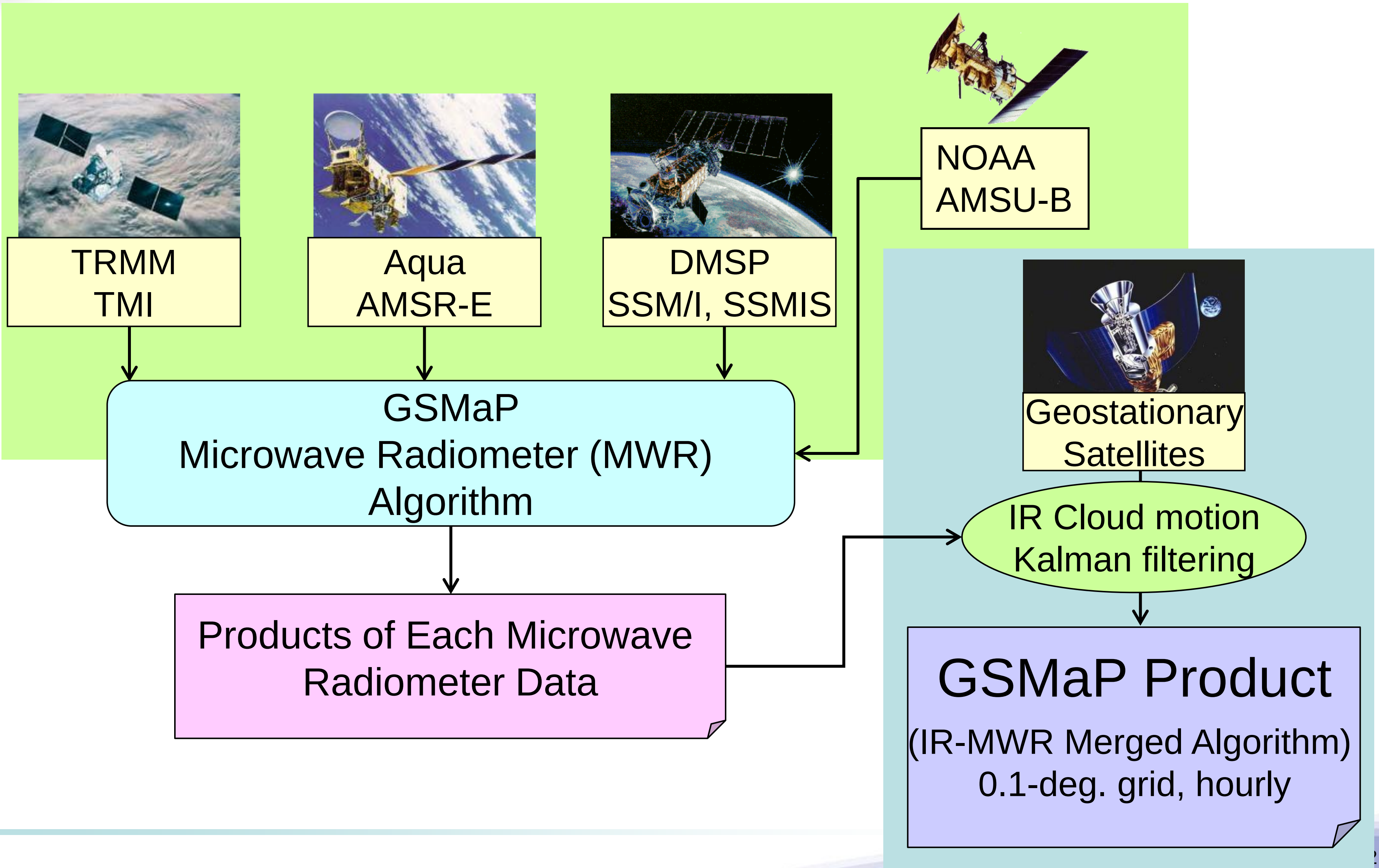

GSMaP approach - Hybrid approach -

- Combination of the moving vector and GPCP type method
  - We have decided to combine each method (sampling from both world).

  That is…..

  1. Propagates the rainy pixels on the moving vector derived from the successive IR images
  2. And then, optimally estimates the rain rate from the brightness temperature at IR wavelength

- What is the best way to realize this?
  - Global precipitation mapping is a sequential process.
  - So, the Kalman filter is the best way to do this.

GSMaP

- Kalman filter method
  - Refine precipitation rate on Kalman gain after propagating the rain pixel
  - The Kalman gain is determined from the database on the relationship between the IR Tb and surface rain rate.

Typhoon 200507/BANYAN (hourly)

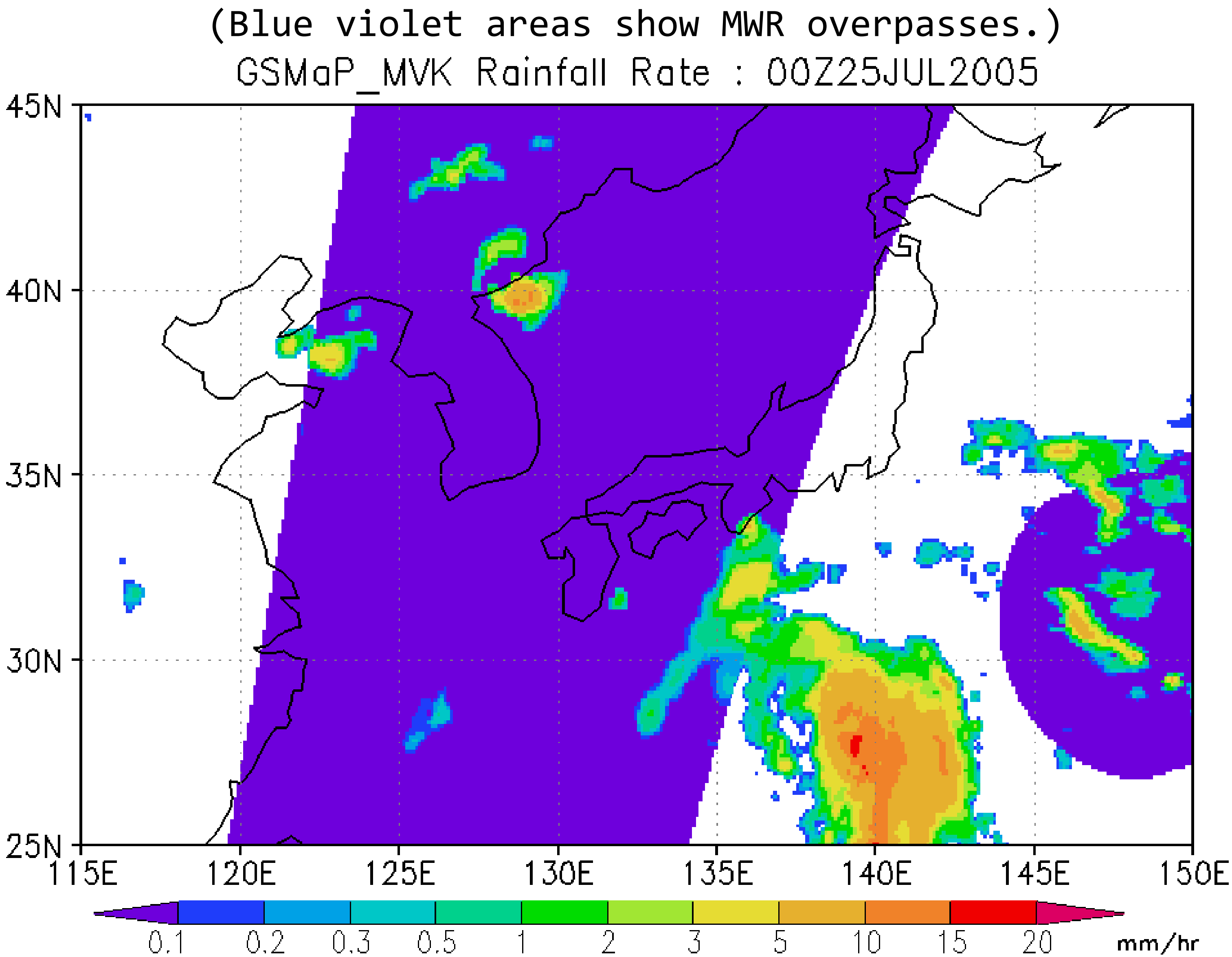

Validation of GSMaP products

- GSMaP Algorithm details will be provided by Prof. Ushio (Osaka Univ.)'s lecture, (in addition to Dr. Aonashi (MRI/JMA)'s lecture)

- So, I move on to a topic about validation of the GSMaP products

Comparison with the ground–radar (COBRA)

Comparison of TMI retrievals (GSMaP_TMI) with COBRA data for four selected overpasses during June 2004 (0.25 x 0.25 deg.)

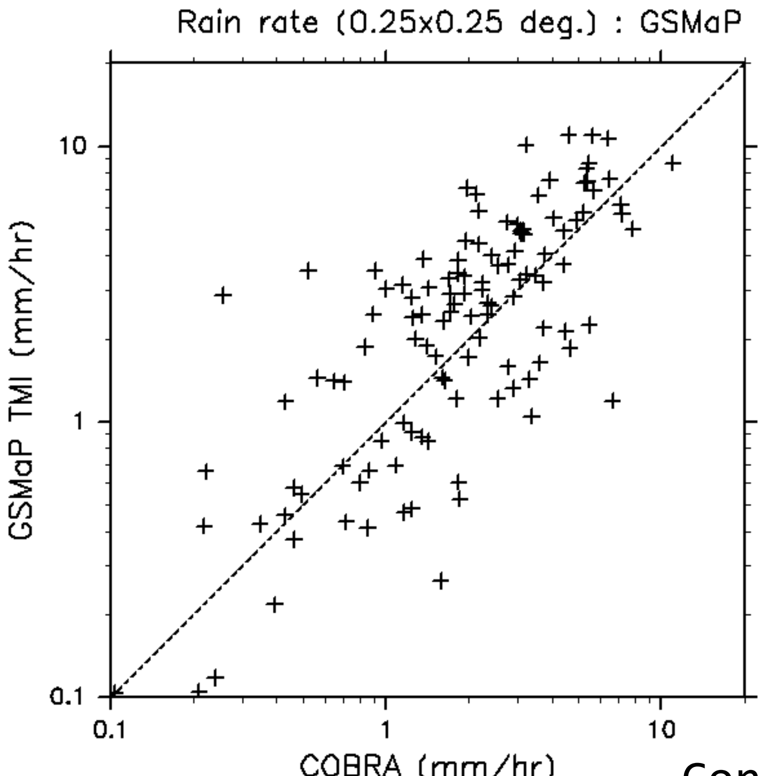

NICT Okinawa Bistatic Polarimetric Radar (COBRA)
C-band(5340 MHz)
10 minute cycle

A field campaign of observing precipitation in Okinawa, Japan during rainy season of 2004 (okn-baiu04)

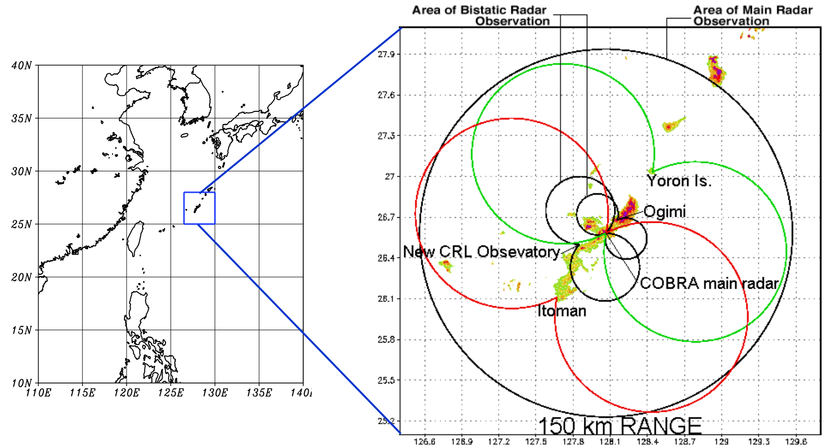

Correlation : 0.82
RMSE(mm/hr) : 1.37

(Kubota et al. 2007)

Validation using JMA Radar-AMeDAS analyssis

GSMaP_NRT (26 July 2009) Radar-AMeDAS

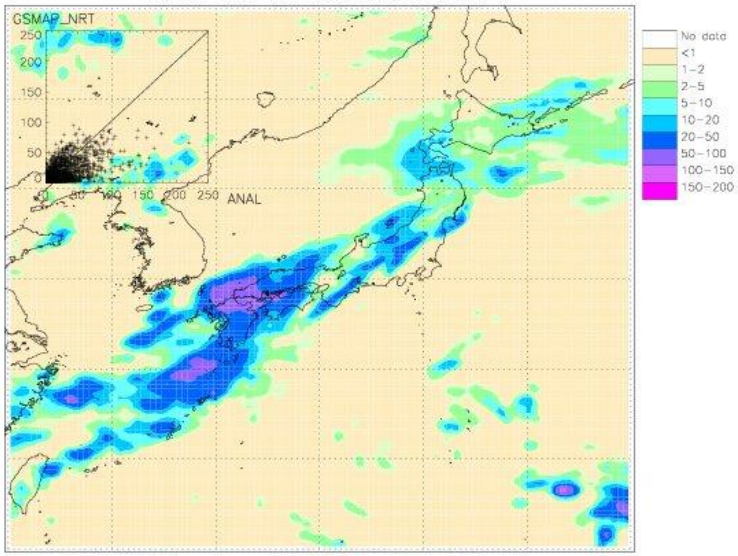

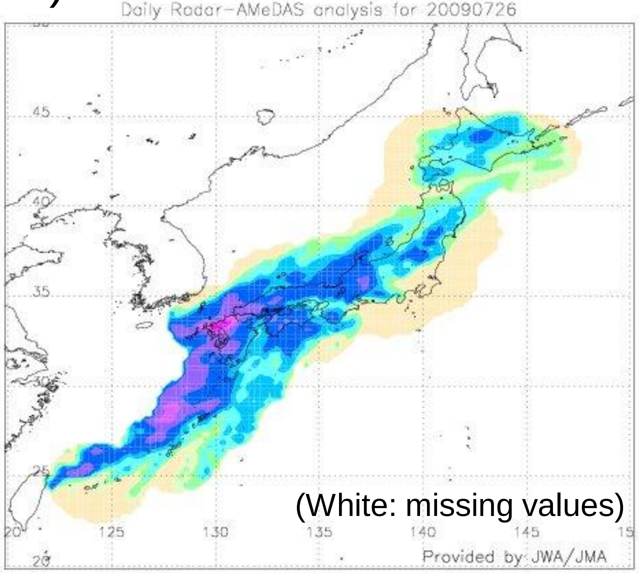

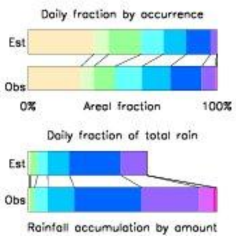

GSMAP_NRT

Observed	<1	≥1
<1	642	214
≥1	423	1783

Verification statistics for 20090726 n=3062 Verif. grid=0.25° Units=mm/day

	Analysed	GSMAP_NRT
# gridpoints raining	2206	1997
Average rain	15.2	9.5
Conditional rain	21.1	14.6
Rain volume (mm•km²x10⁶)	29.4	18.4
Maximum rain	220.0	93.8

Mean abs error = 10.1
RMS error = 18.2
Correlation coeff = 0.648
Frequency bias = 0.905
Probability of detection = 0.808
False alarm ratio = 0.107
Hanssen & Kuipers score = 0.558
Equitable threat score= 0.351

Comparisons in daily averaged rainfall estimates around Japan with 0.25 x 0.25 deg. resolution with reference to the gauge-calibrated ground radar dataset (JMA Radar-AMeDAS precipitation analysis).

Example : Heavy rain in 14 Jul 2010

http://www-ipwg.kugi.kyoto-u.ac.jp/IPWG/sat_val_Japan.html

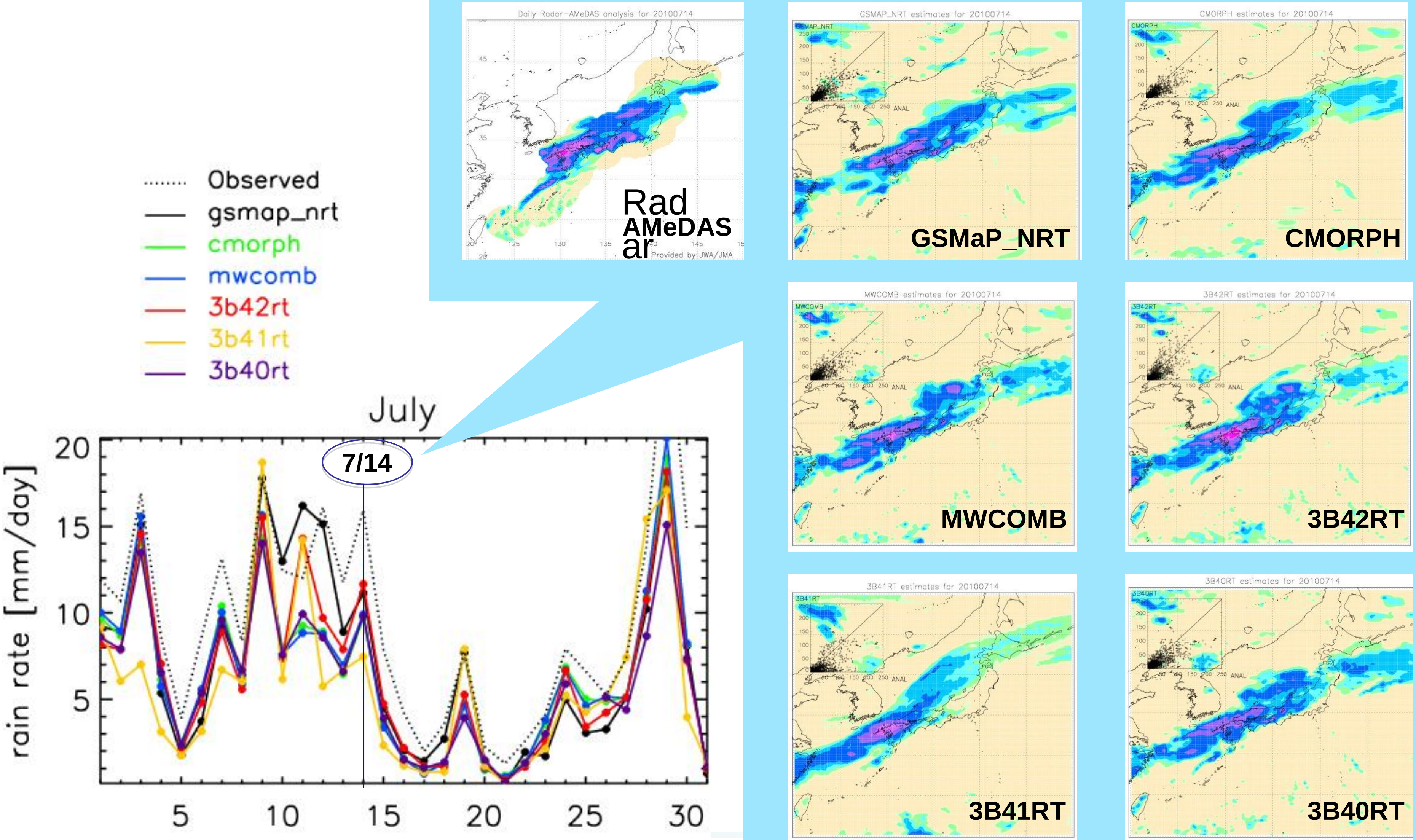

Validation results around Japan during 2004

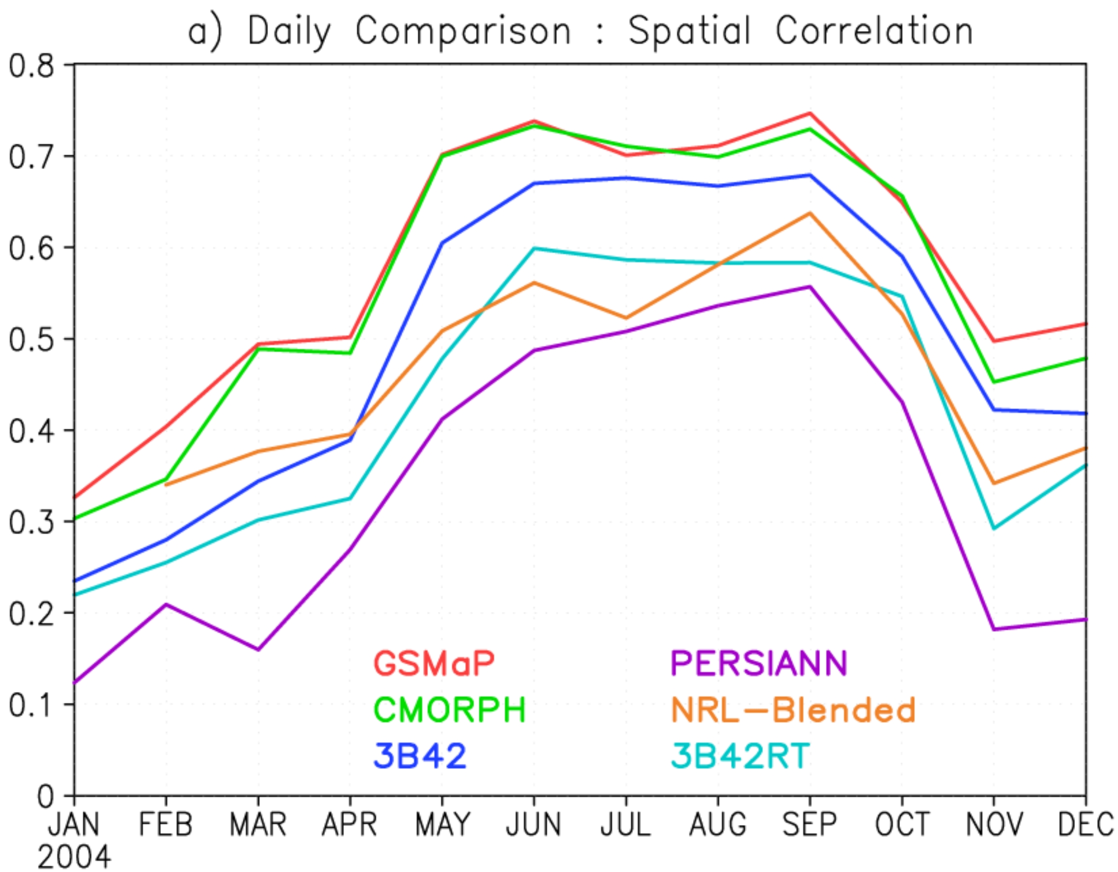

Monthly averaged time series of correlation coefficients with daily estimates around Japan during 2004.

Horizontal resolution:
0.25x 0.25 latitude/longitude.

Reference: JMA Radar-AMeDAS precipitation analysis

6 satellite products:
GSMaP
TMPA 3B42RT and 3B42 (Huffman et al. 2007)
CMORPH (Joyce et al. 2004)
PERSIANN(Sorooshian et al. 2000, Hsu et al.1997)
NRL-Blended (Turk and Miller 2005, Turk and Mehta 2007)

Better during the warm season,
related to false rainfall signals over surface snow,
consistent with validation results in other regions (e.g., Ebert et al. 2007)

Kubota et al. (2009, JMSJ)

http://www.bom.gov.au/bmrc/SatRainVal/validation-intercomparison.html

Collaboration in IPWG

The GSMaP joins the International Precipitation Working Group (IPWG) validation activities.

- We validates various satellite estimates around Japan.
- Our GSMaP products are validated in U.S.(J. Janowiak), Australia (E. Ebert), South America (D. Vila), and Japan every day.

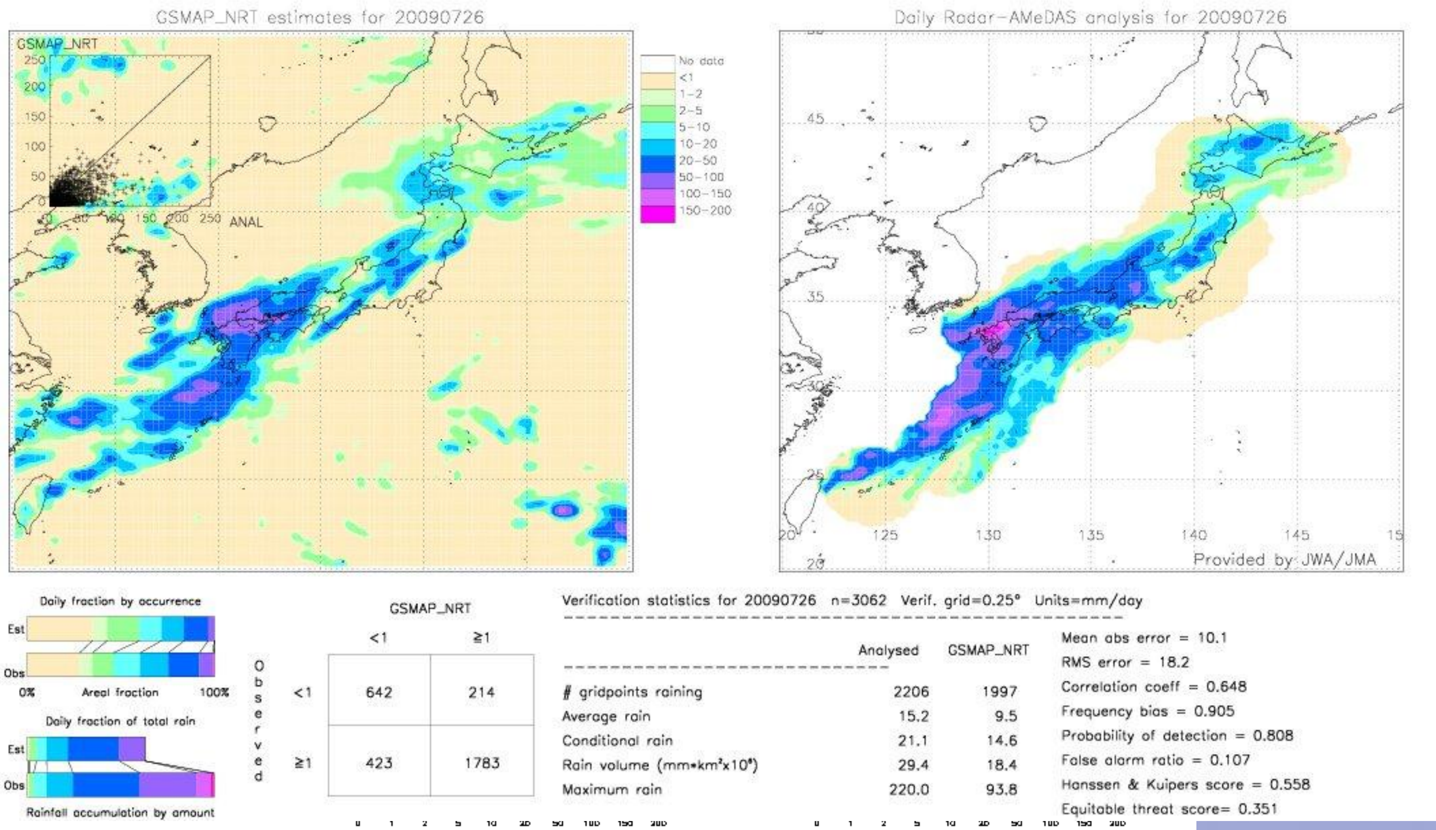

Comparison of GSMaP and Rain-gauge

- 1-minute accumulation gauge data in Bangladesh (provided by Prof. Terao's group) is used in comparison.
  - Possible problem in differences between 0.1degree averages (GSMaP) and station data.
- Peaks of rainfall by GSMaP are well correspond to that of rain-gauge for most of cases, while GSMaP shows lower rainfall rates compared to rain-gauge.
- Short-lived rainfall events, in which rain areas are not detected by the microwave observation, may not be detected by GSMaP algorithm.

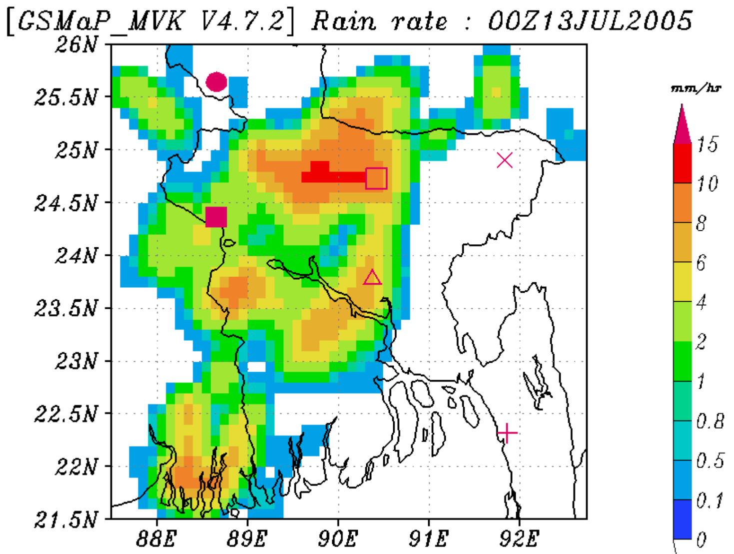

Rainfall by GSMaP_MVK (13-15 July 2005). Dhaka is denoted by △.

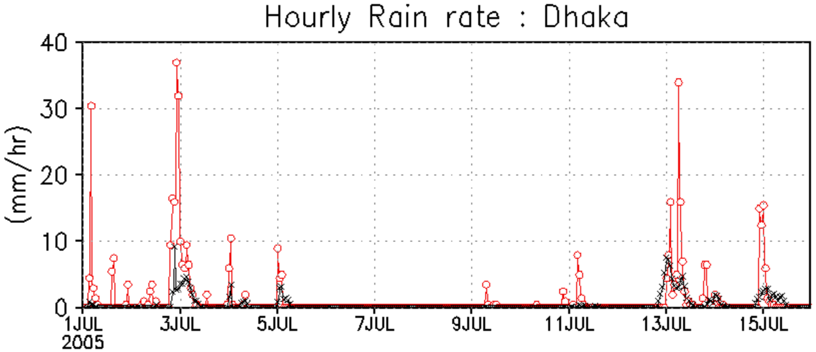

Hourly rainfall series of rain gauges in Dhaka (red) and GSMaP_MVK (black).

Advantages of GSMaP Products

- Advantages of GSMaP are;
  - faster availability within 4-hours; and
  - globally homogeneous rainfall distribution in hourly and 0.1 degree resolution (about 10-km resolution).
- GSMaP will be effectively used for;
  - rainfall over the ocean where no ground observation is available;
  - rainfall events in large temporal scale; and
  - rainfall events in large horizontal scale.

Disadvantages of GSMaP Products

- GSMaP will NOT be useful for;
  - rainfall events in smaller horizontal scale than resolution of microwave observation (a few ten kilometers),
  - rainfall events in shorter time scale than microwave observation frequency (several hours); and
  - flash flood whose lead time is less than satellite data transmission/processing time (4-hours in case of GSMaP near-real-time version).
  - rainfall/snow events over surface snow
- GSMaP tends to show lower rain rates over the land compared to gauge observation, while rainfall peaks are well captured.
  - There are some works to calibrate GSMaP to ground observation in order to apply to operational use.

Multi-satellite product: Application

Rainfall observations by the GSMaP

Global rainfall image with cloud images on 0UTC, 3rd May 2008

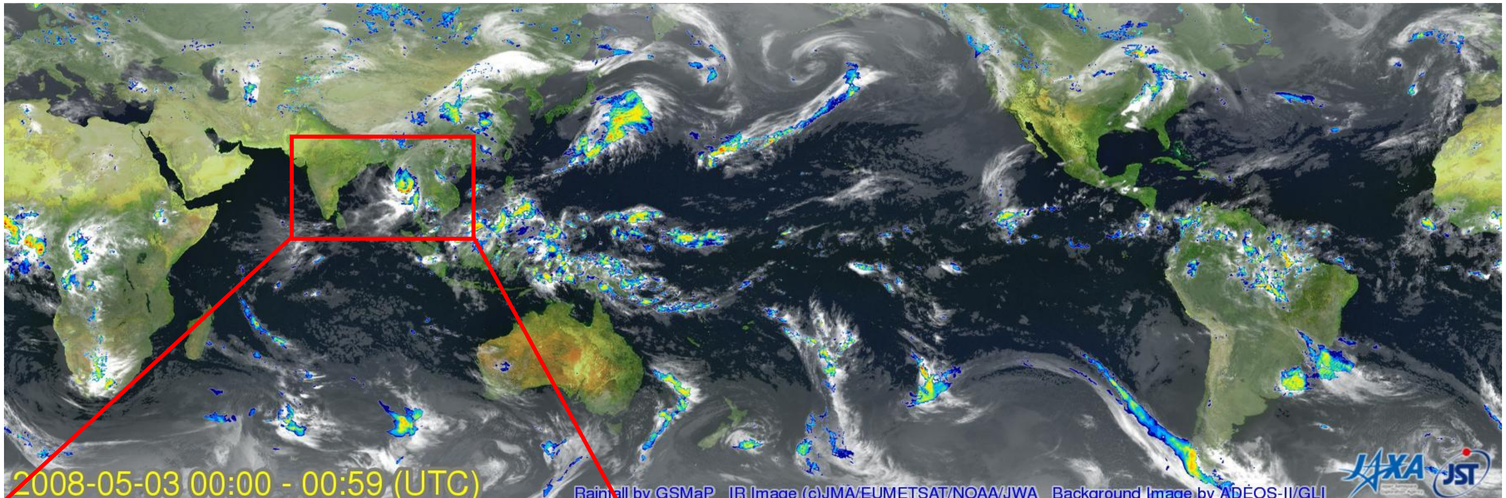

Movie from 28th April to 3rd May 2008 for cyclone "Nargis"

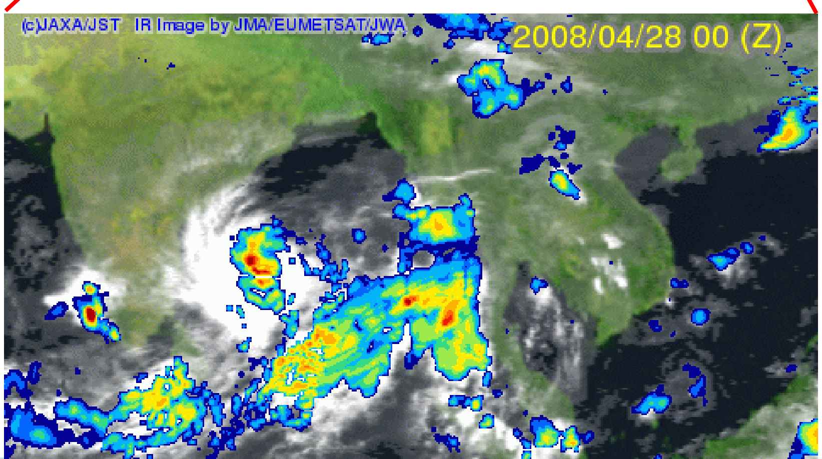

Movie from 11th to 16th November 2007 for cyclone "Sidr"

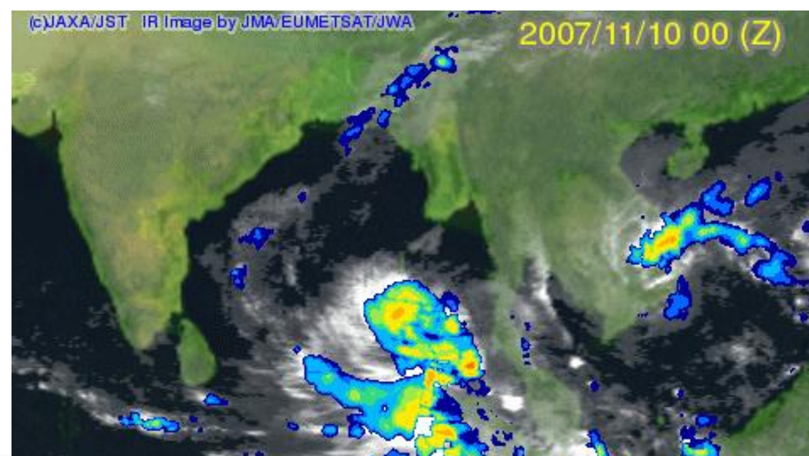

Accumulated rainfall amount

Accumulated rainfall amount, calculated by the GSMaP_NRT (mm)

a) 27April and 3 May 2008 for the cyclone "Nargis"

b) 10 and 16, November 2007 for the cyclone "Sidr"

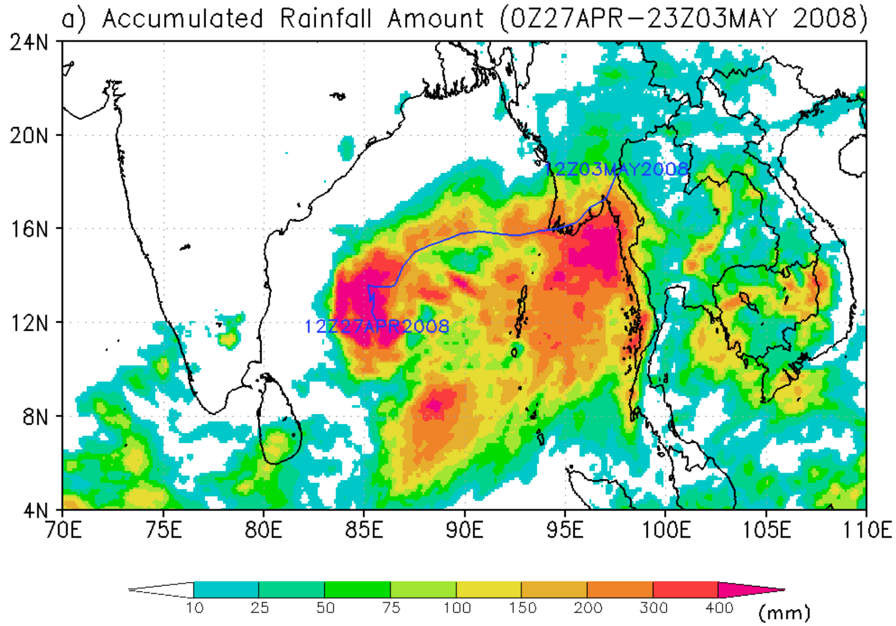

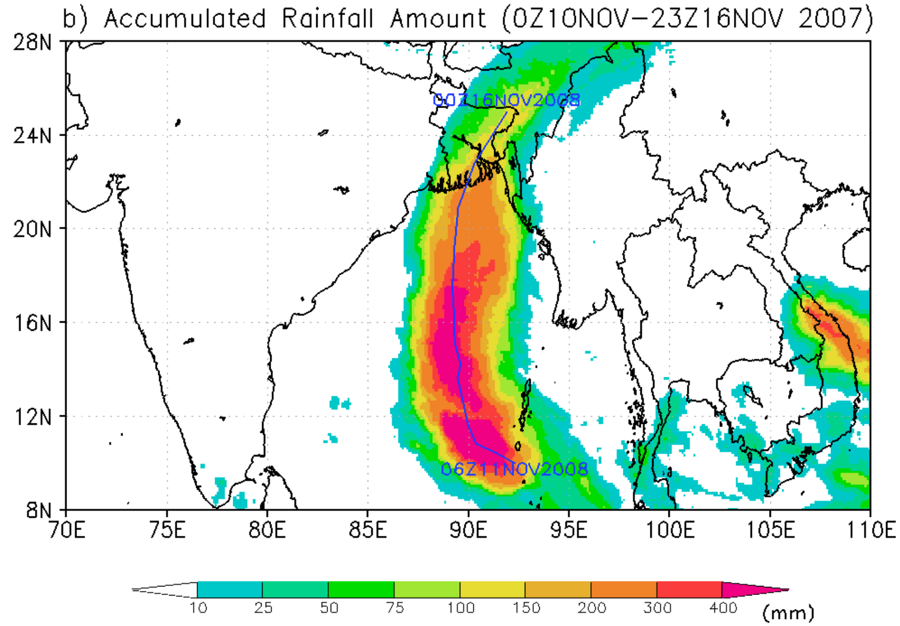

Movie of daily rainfall for Nargis

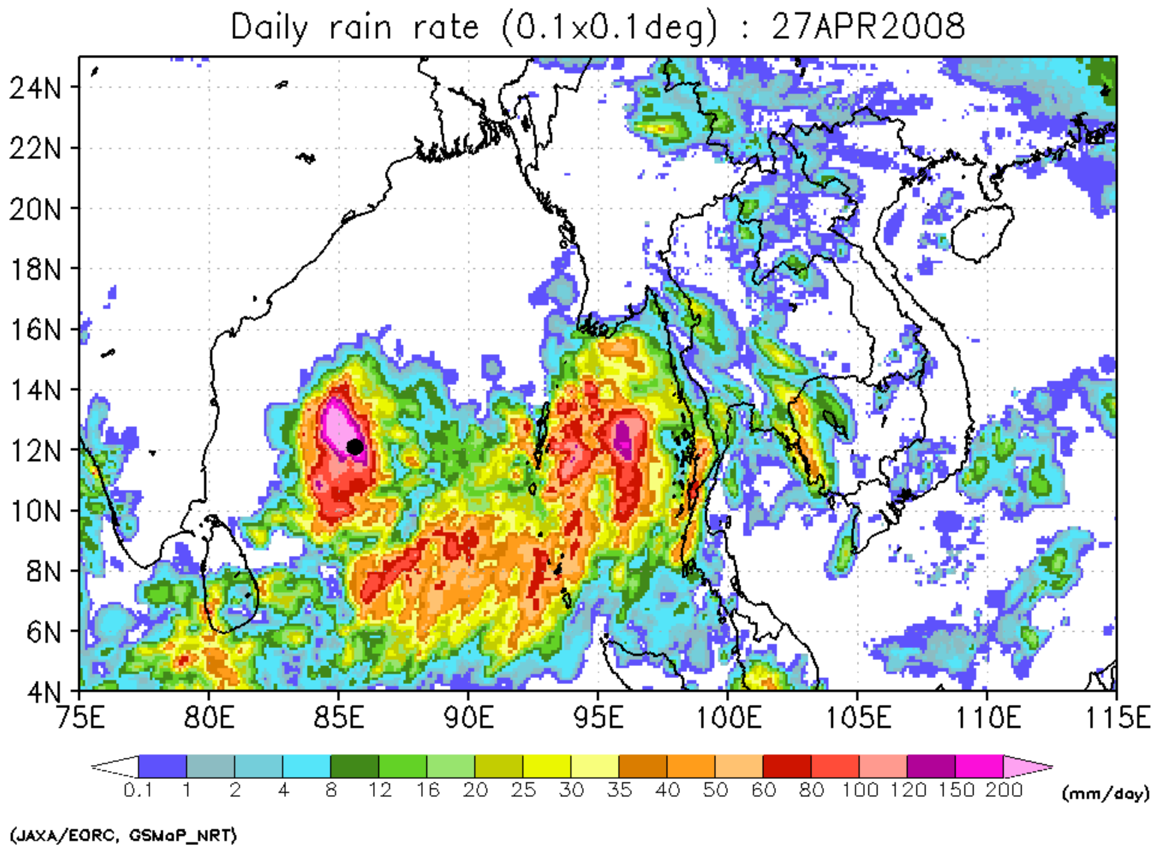

Black circles: Center positions of the cyclone

Period: 27th April 2008 – 3rd May 2008

Daily rainfall amount: 2nd May 2008

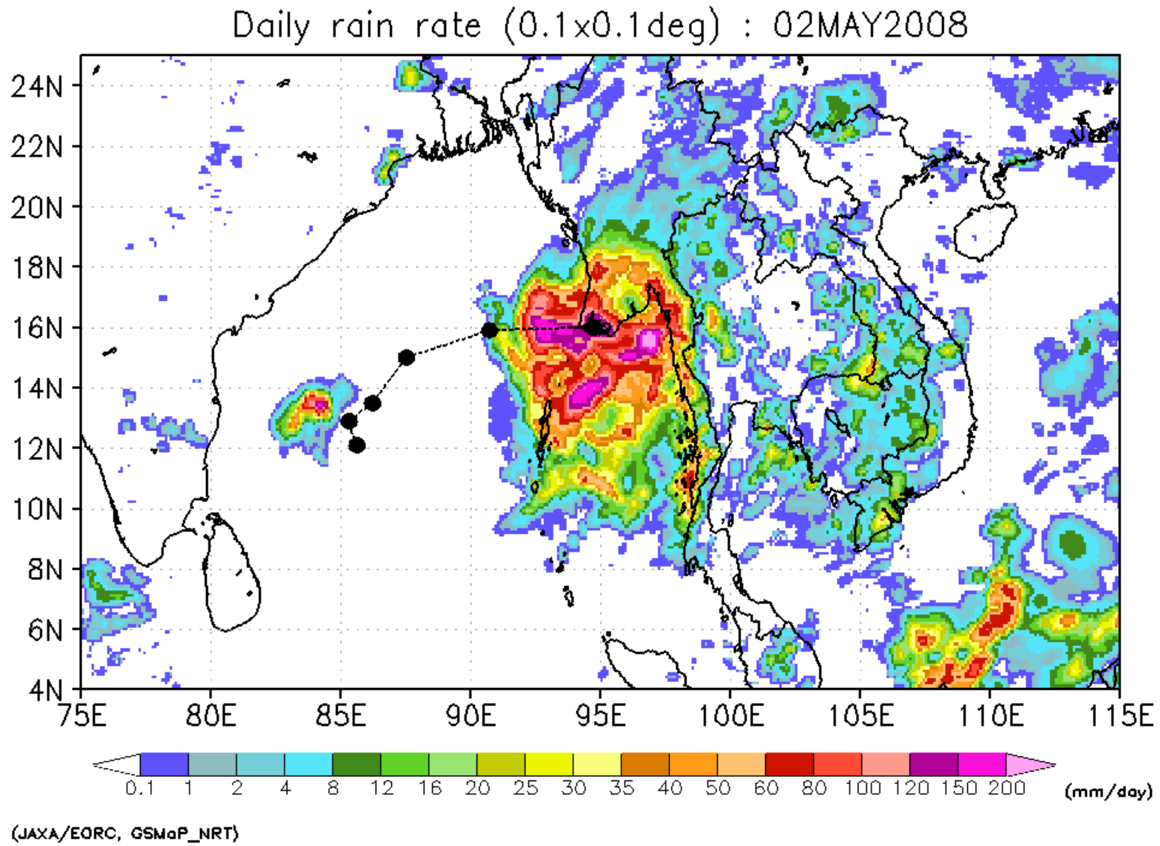

Black circles: Center positions of the cyclone

Date : 2nd May 2008

Accumulated rainfall amount

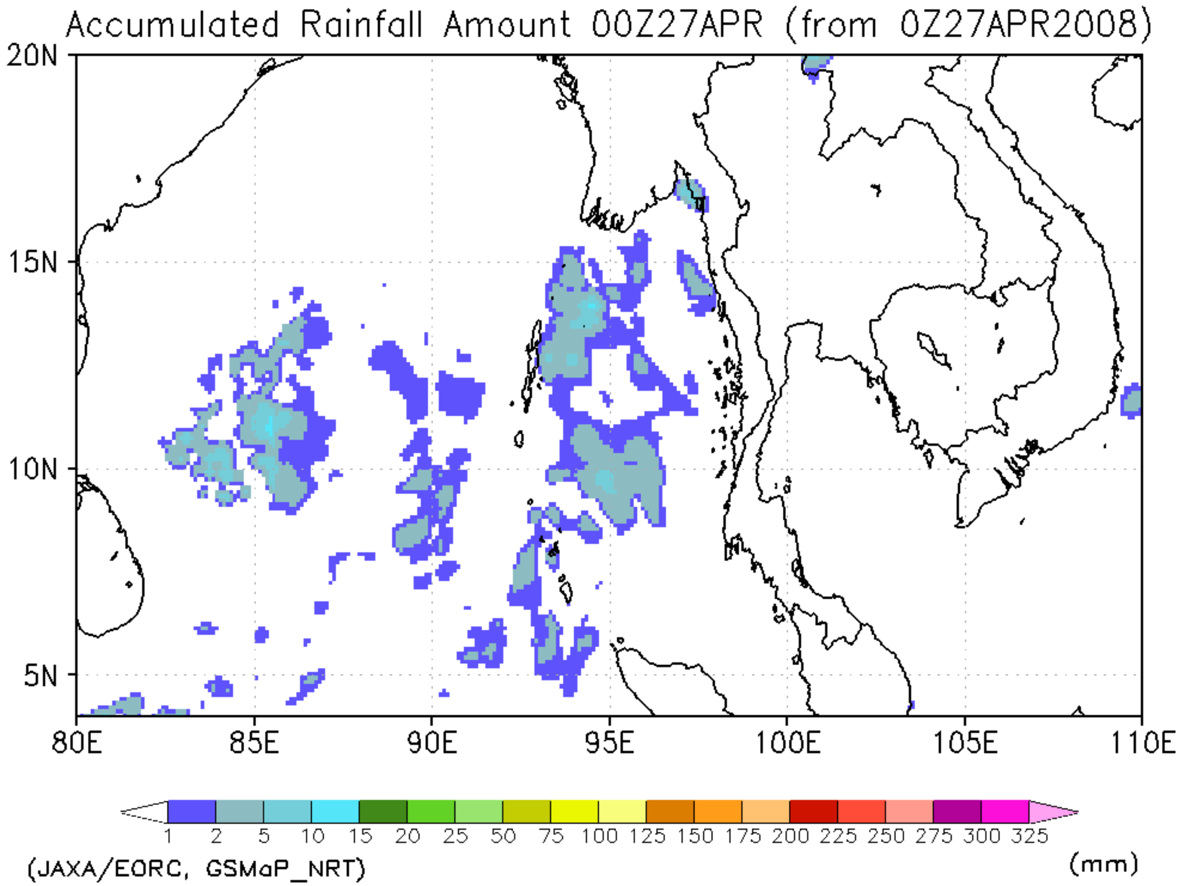

Rainfall amount accumulated from 27th April 2008

Rainfall amount during 8days

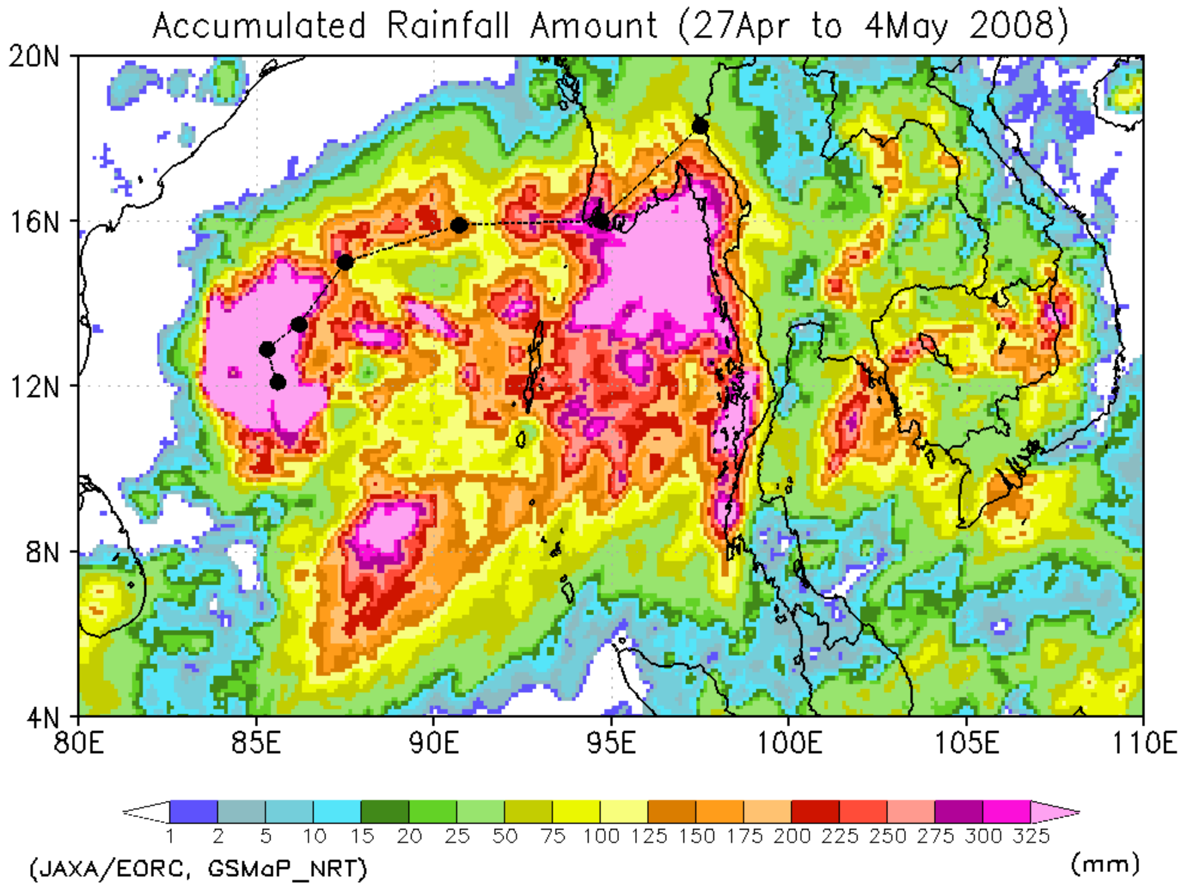

Rainfall amount accumulated from 27th April 2008 to 4th May 2008. Black circles: Center positions of the cyclone.

2011 Thailand floods

Severe flooding occurred during the 2011 rainy season in Thailand, and caused serious economic damages and losses due to flooding.

(Photos: Flooding at AIT)

Oct. 2011 around SE Asia

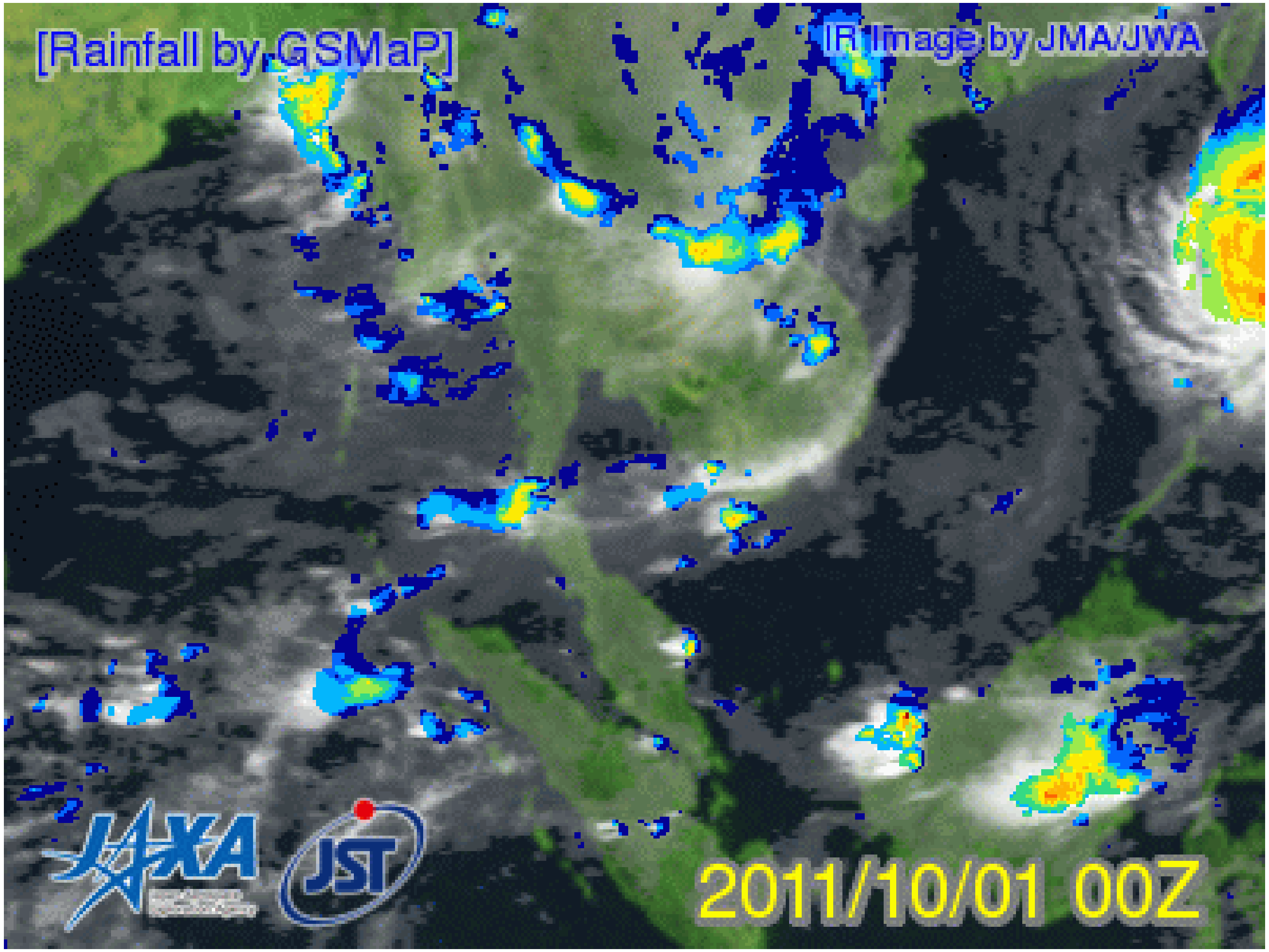

Acculated rainfall amount using GSMaP_NRT Jun-Sep 2011

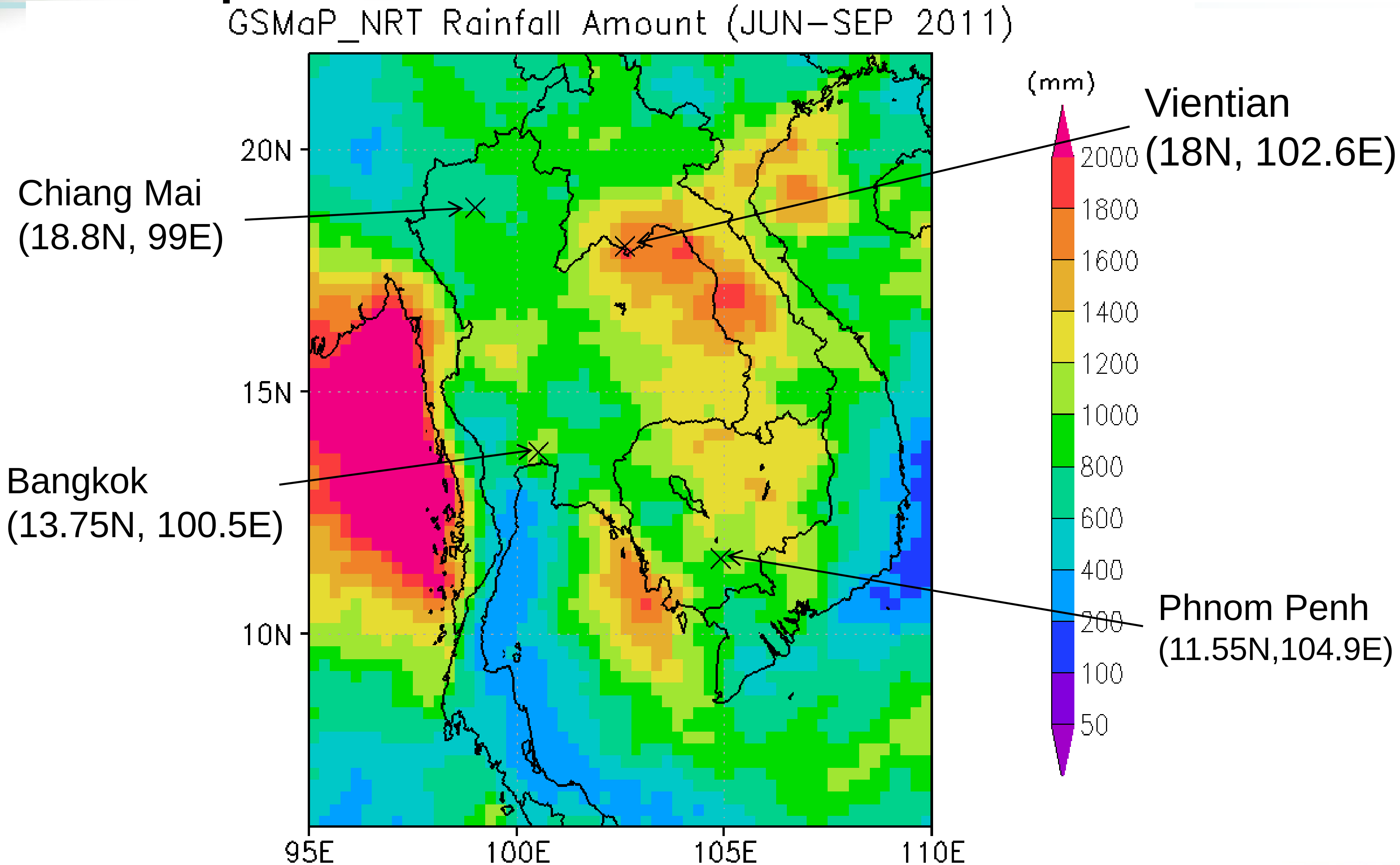

Rainfall variability of several cities

Rainfall variability during March-October by the GSMaP_NRT (15-day-running mean)

Bangkok

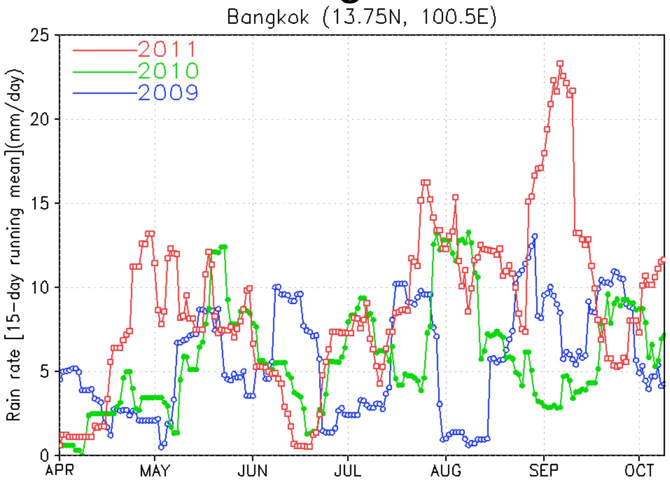

Chiang Mai

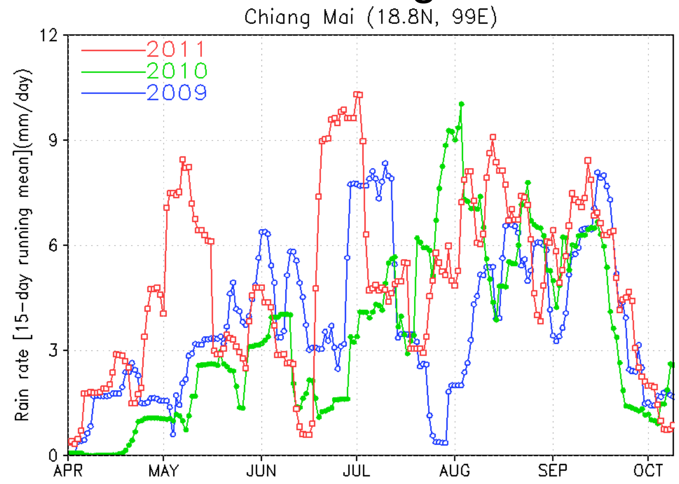

Vientian

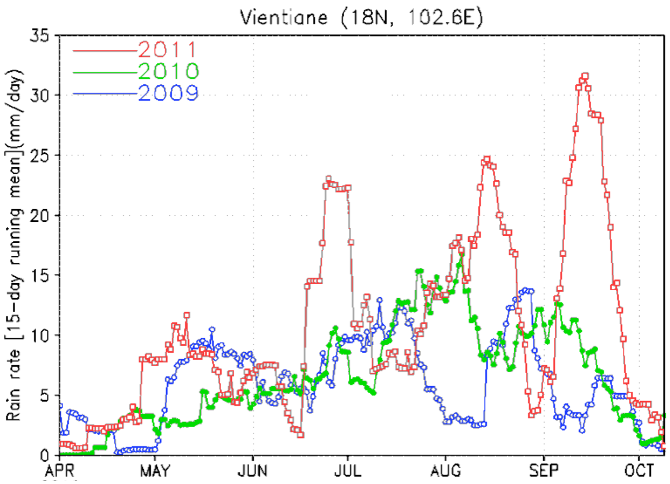

Phnom Penh

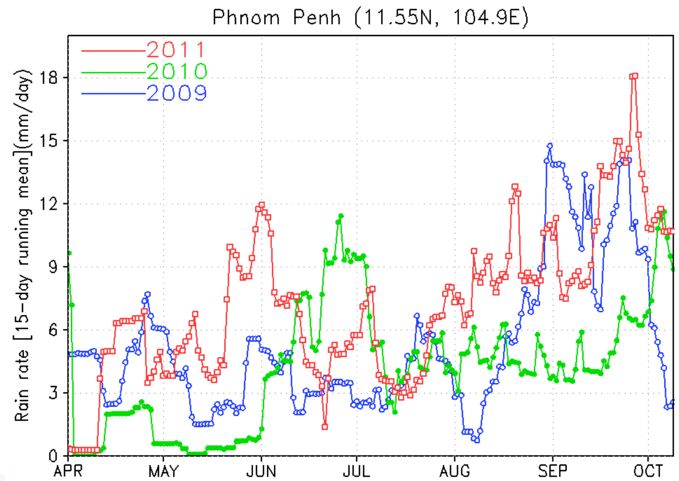

Comparison to rain amount in 2010

Acculated rainfall amount
during Jun-Sep 2010

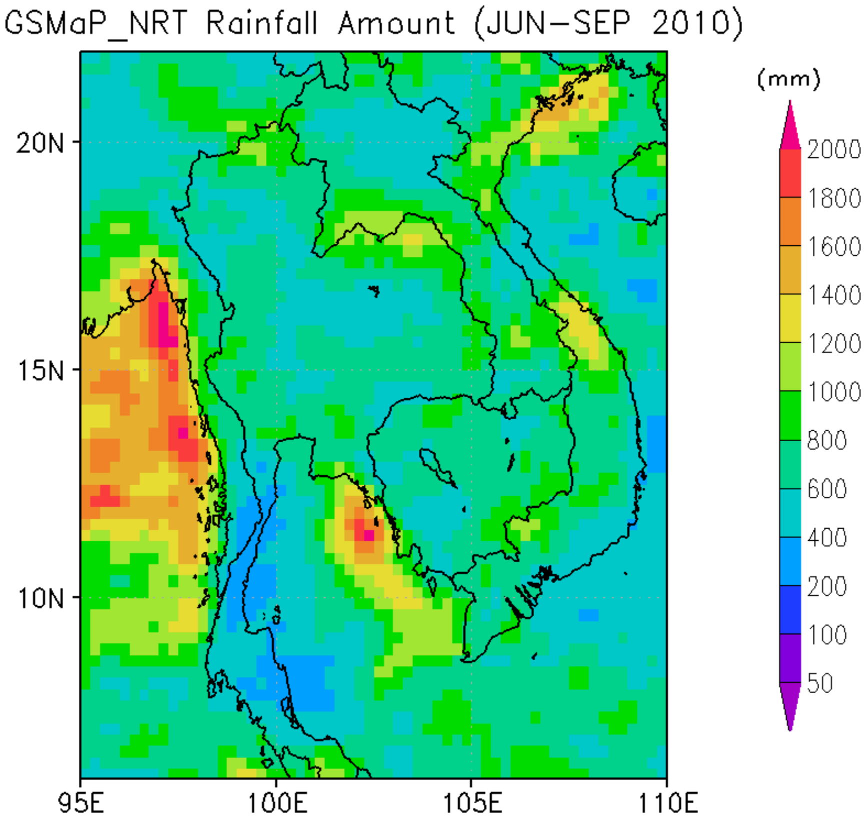

Ratio of R_{2011}/R_{2010}
during Jun.-Sep.

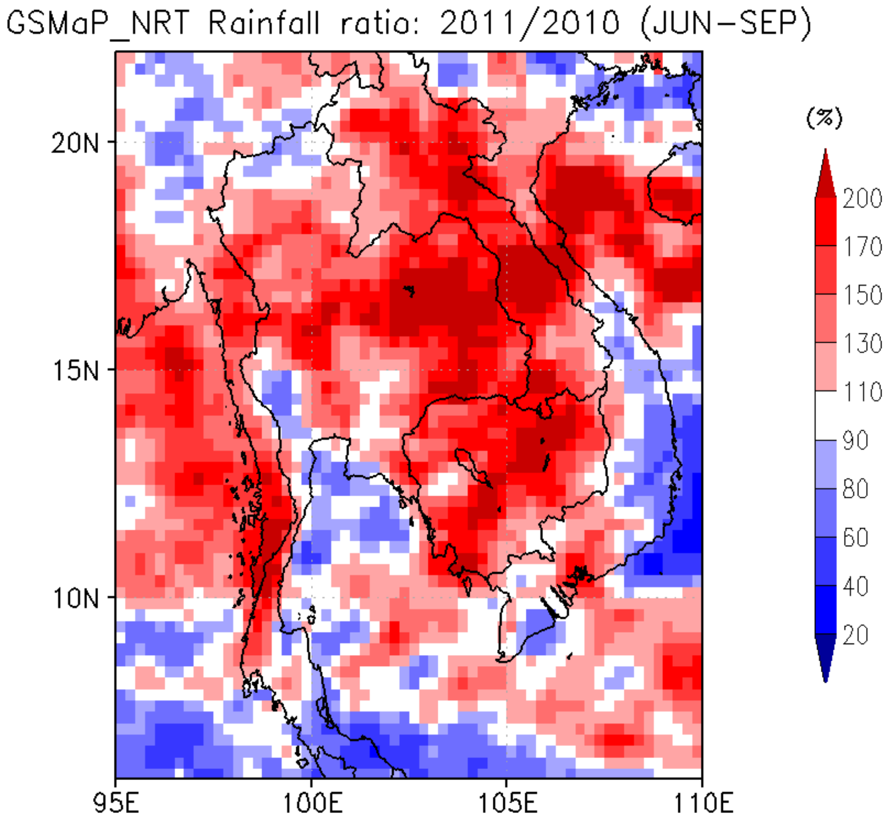

Monitoring of Chao Phraya River basin

Chao Phraya River

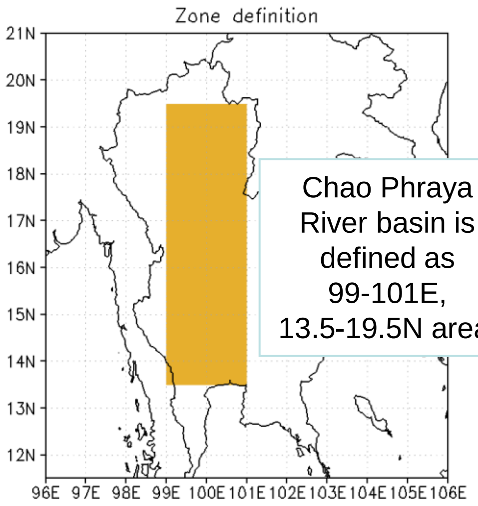

Chao Phraya River basin is defined as 99-101E, 13.5-19.5N area.

Rainfall variability over Chao Phraya River basin by the GSMaP_NRT (15-day-running mean)

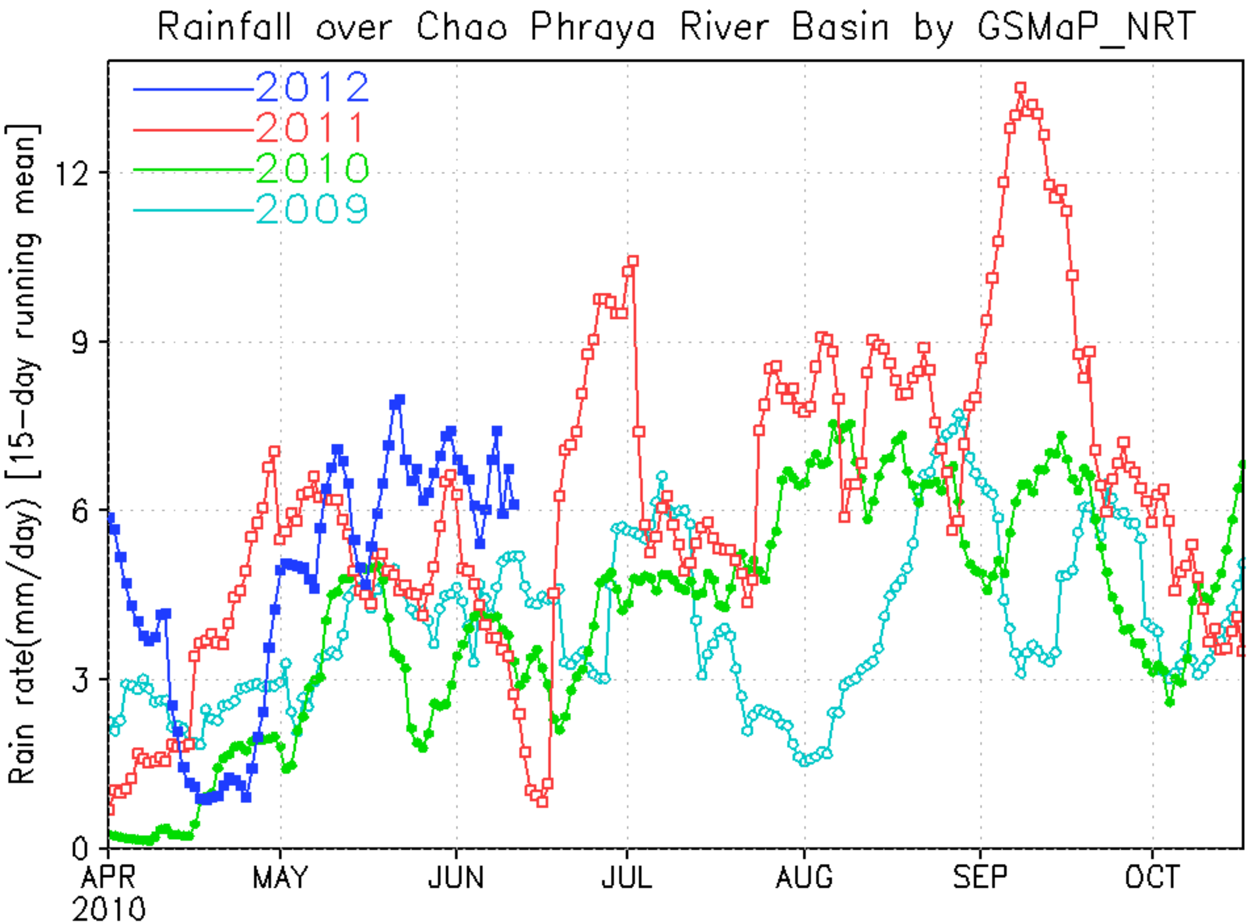

Analysis of Chao Phraya River basin (1)

Chao Phraya River

http://upload.wikimedia.org/wikipedia/commons/3/35/Chaophrayarivermap.png

Zone definition of Chao Phraya River basin

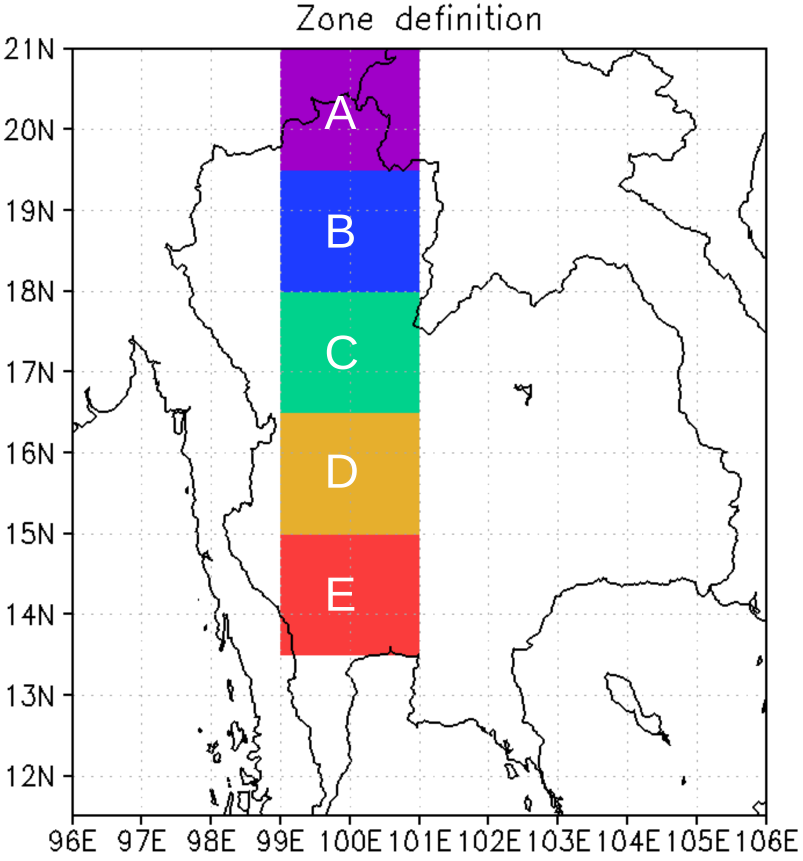

Analysis of Chao Phraya River basin (2)

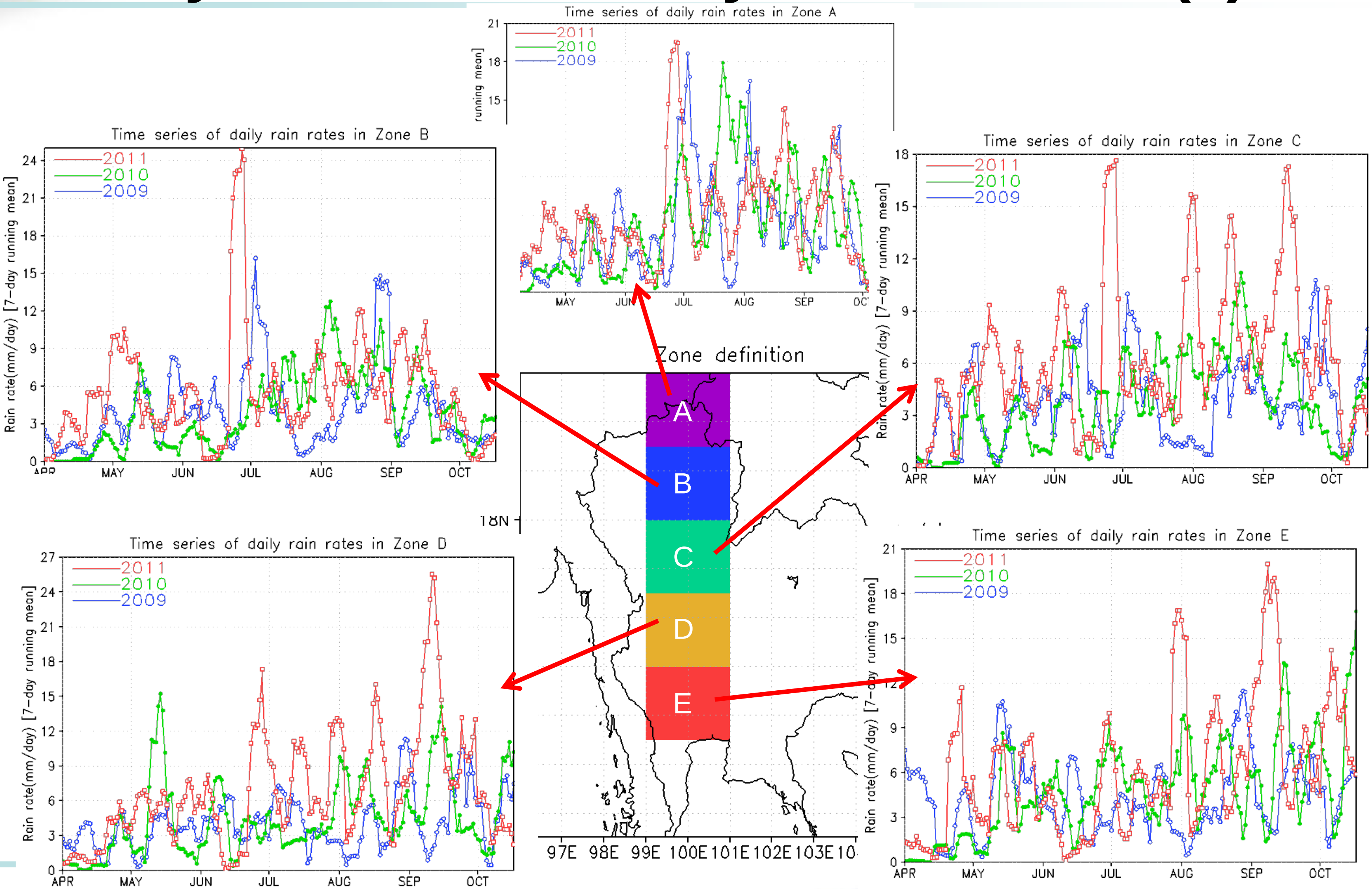

GSMaP data handling

How to Get the GSMaP Online Data

- GSMaP_NRT (NRT:Near-real-time) by JAXA/EORC
  - http://sharaku.eorc.jaxa.jp/GSMaP/index.htm
  - Period: Oct. 2008-Now
  - Availability within 4-hours
- GSMaP_MVK (post-processing version) by JAXA/EORC
  - GSMaP Standard version (Version 5.212)
  - Period: Mar. 2000-Nov. 2010

GSMaP_NRT: Near-Real-time Data

- JAXA's site
  - Data will be archived about 4 hours after observation.
    - Ex., Data of 00:00-0:59UTC will be put at about 5 UTC.
  - FTP
    - ftp hokusai.eorc.jaxa.jp
  - When you want to use GSMaP data, please send your information from http://sharaku.eorc.jaxa.jp/GSMaP/index.htm
  - Binary & Text files
    - 3600 x 1200 pixels
    - longitude-latitude elements corresponding to a 0.1 x 0.1 degree grid that covers the global region from 60N to 60S.

GSMaP Products in GIS-Format

- Collaboration with Sentinel Asia under APRSAF
  - GSMaP rainfall data can be displayed overlaying other infromation in GIS format (GeoTIFF) for flood warning through Sentinel Asia web site developed by JAXA/SAPC.

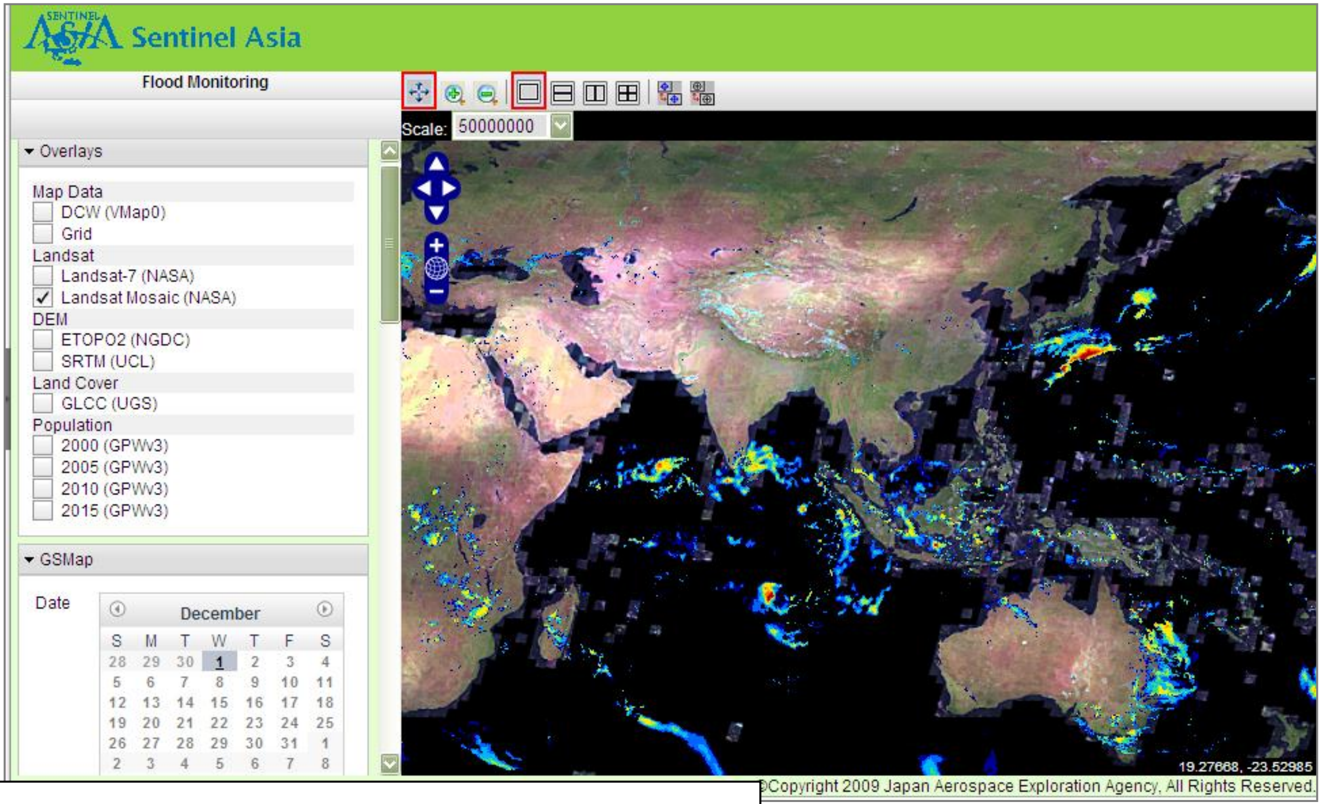

http://dmss.tksc.jaxa.jp/sentinel/

JAXA/EORC GPM site

http://www.eorc.jaxa.jp/GPM/index_e.htm

Summary

- Multi-satellite rainfall Product
  - Global rainfall map = Products merged from various sensor data from satellites, in addition to other resources (e.g, rain gauges)
  - Global Precipitation Measurement (GPM)
  - Global Satellite Mapping of Precipitation (GSMaP)
  - Brief algorithm flow & Validation
- GSMaP application
  - Cyclone “Nargis”
  - 2011 Thailand floods
- GSMaP data handling
  - How to Get the GSMaP Online Data
  - Data format

Sizes of Cloud/Precipitation Particles

Typical rain drop and cloud drop

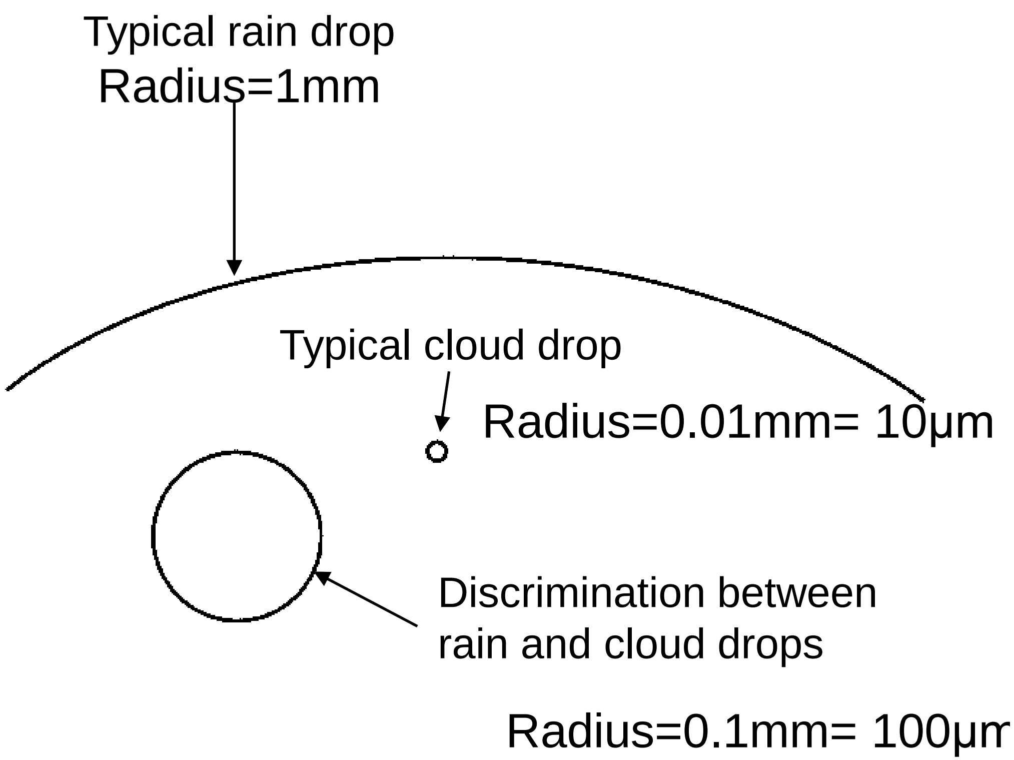

(drawn based upon Takeda 2005)

Snow crystals

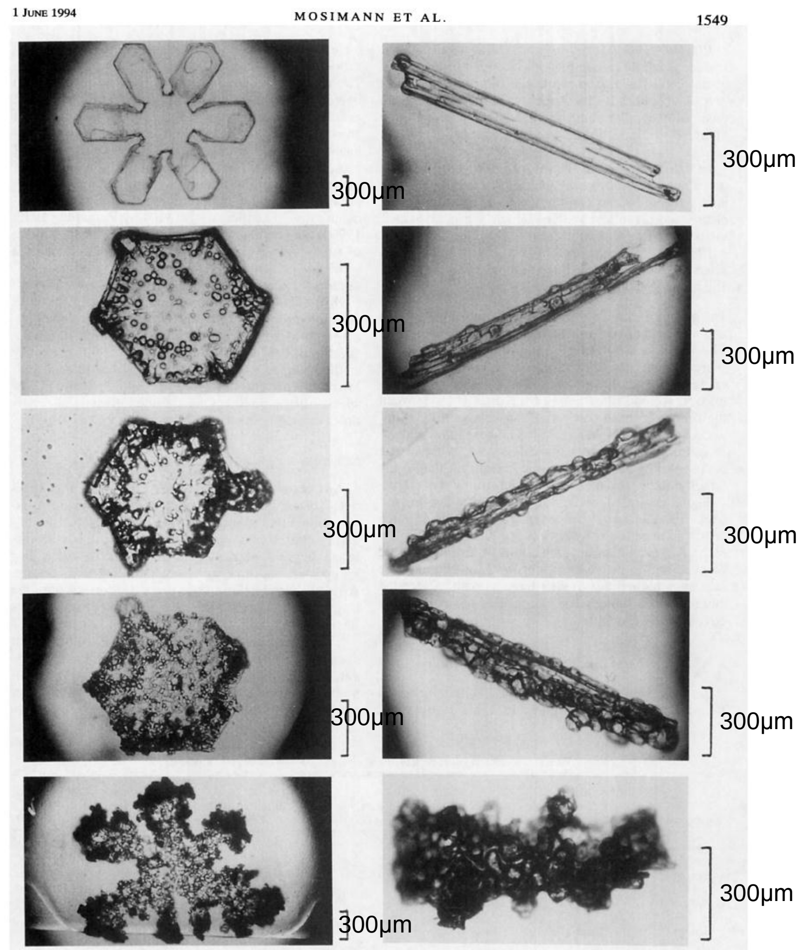

Fig. 1. Photographs of snow crystals representing the first five riming categories from top to bottom riming 0, 1, 2, 3, and 4. Left column: planar crystals; right column: long column and needle crystals. The scale to the right of each photo has a length of 300 μm.

(Mosimann et al. 1994)

Microwave bands

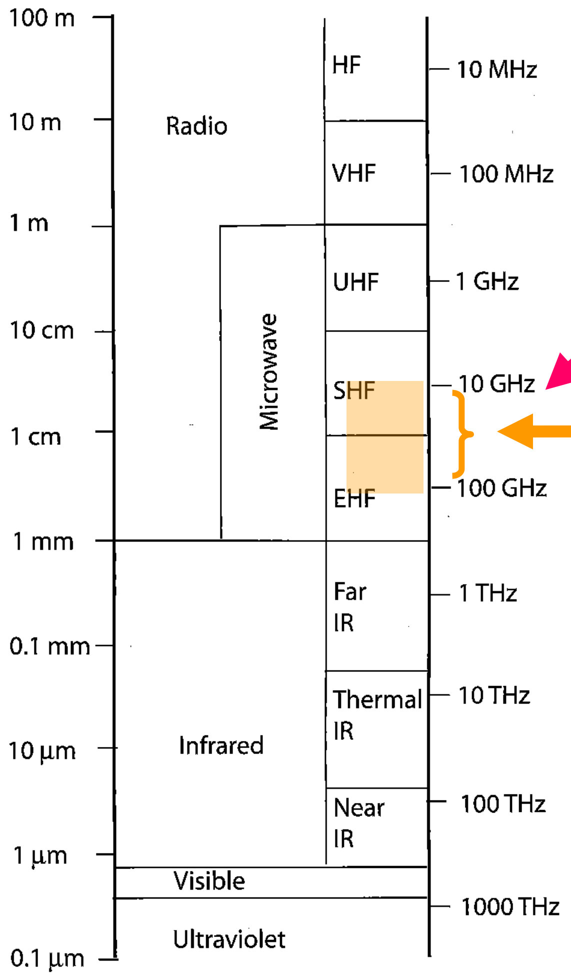

Fig. 3.1: The electromagnetic spectrum.

13.8 GHz
TRMM/PR
(active sensor)

10, 19, 24, 37, 89 GHz
GCOM-W/AMSR2
(passive sensor)

Utility of Microwave Band:
Transparency of Clouds
(< 100GHz)

Electromagnetic waves at microwave frequencies penetrate deeply into clouds or go through clouds, and thereby provide information about the cloud interior.

Global Precipitation Mapping

Tomoo Ushio

Osaka University, Osaka, Japan

INTRODUCTION

Scientific and Social Significance of the global precipitation map

- Global rain map in daily to hourly scale
- Climate change assessment
  - Monitor variations in rainfall and rain areas associated with climate changes and global warming
- Improvement in weather forecasts
  - Data assimilation in numerical prediction systems
- Flood prediction
- Water resource management
  - River, dam, agricultural water, etc.
- Other applications
  - Agriculture, etc.

Precipitation measurement from space?

Remote Sensing from space using electromagnetic waves

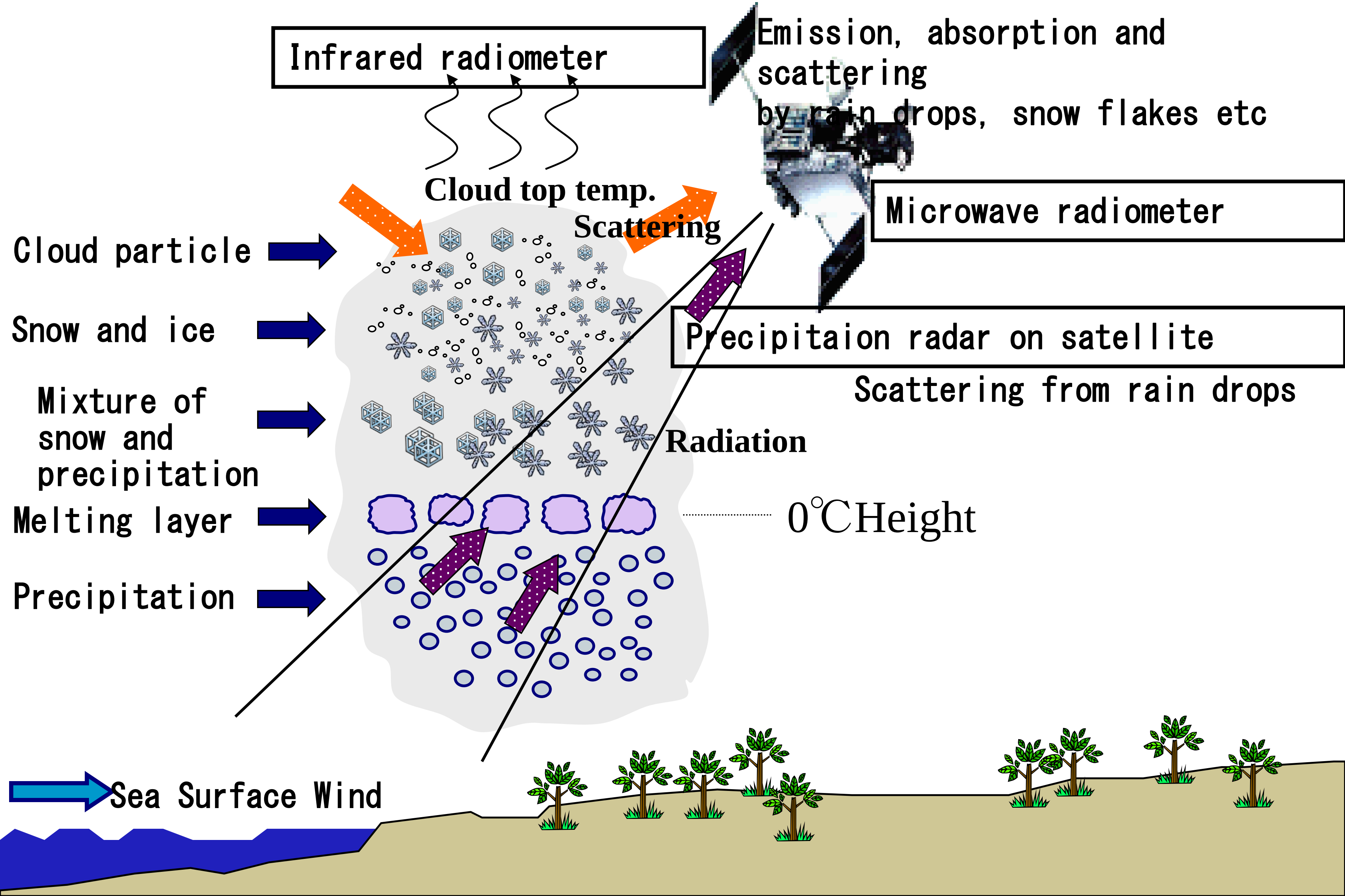

Precipitation characteristics observed by the space borne sensors

(a) Precipitation radar
Back scattering from rain drops
High accuracy
Narrow swath width

(b) Infrared radiometer:
Cloud top information
Not related to surface precipitation rates

(c) Microwave radiometer(19GHz):
(d) Microwave radiometer(85GHz):
Directly measures the emission from precipitation particularly in low frequencies

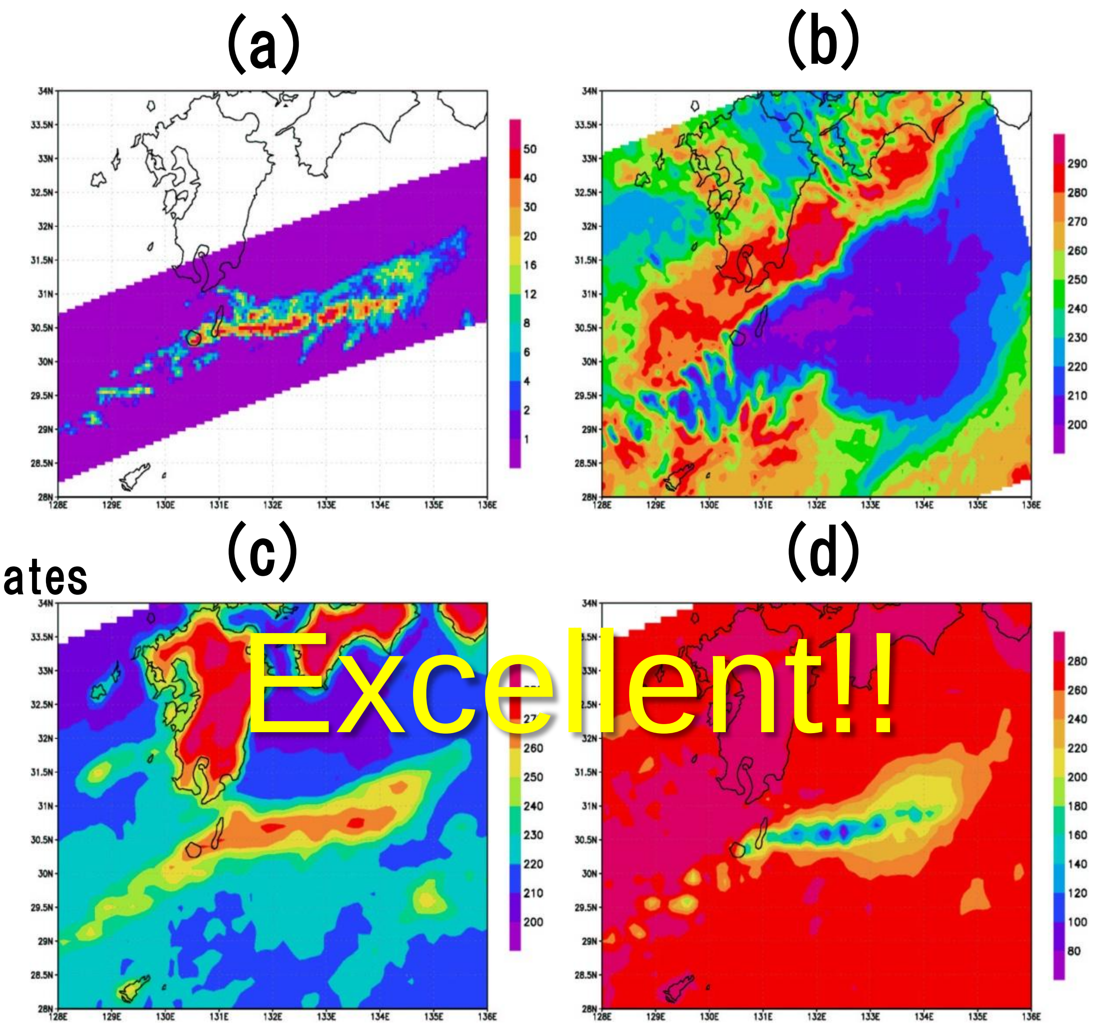

Global Precipitation Product

TRMM
TMI

Aqua
AMSR-E

ADEOS-II
AMSR

DMSP
SSM/I

Microwave radiometer algorithm

Product from each sensor

Geo. Satellite

Infrared radiomter
Cloud motion vector

Mix

Composite product

0.5degree

30 min.
6 hour
1 day
1 month

Composite algorithm of IR and MWR

0.1degree・30min

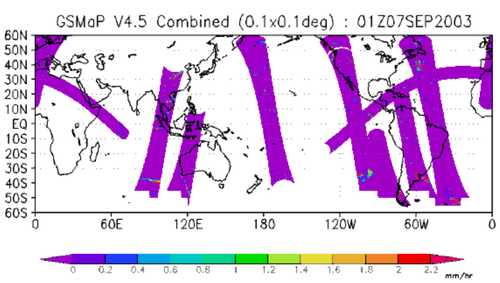

TRMM/TMI, Aqua/AMSR-E, ADEOS-II/AMSR, DMSP/SSMI (F13, 14, 15)による1時間のデータ

6 hourly MWR combined map

TMI

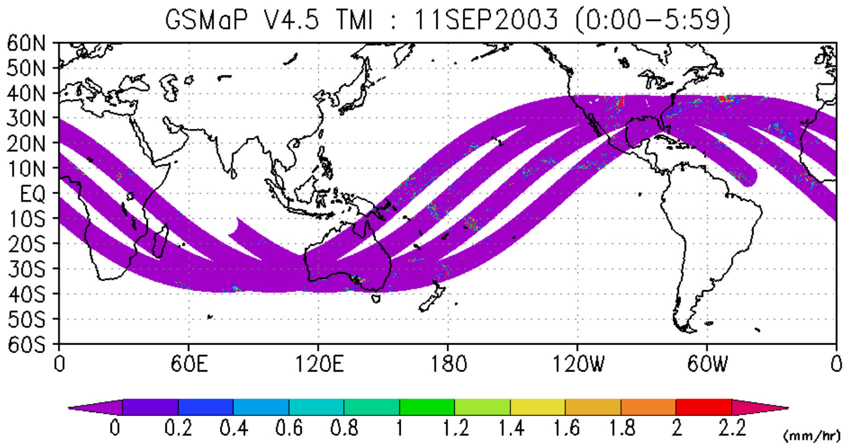

AMSR & AMSR-E

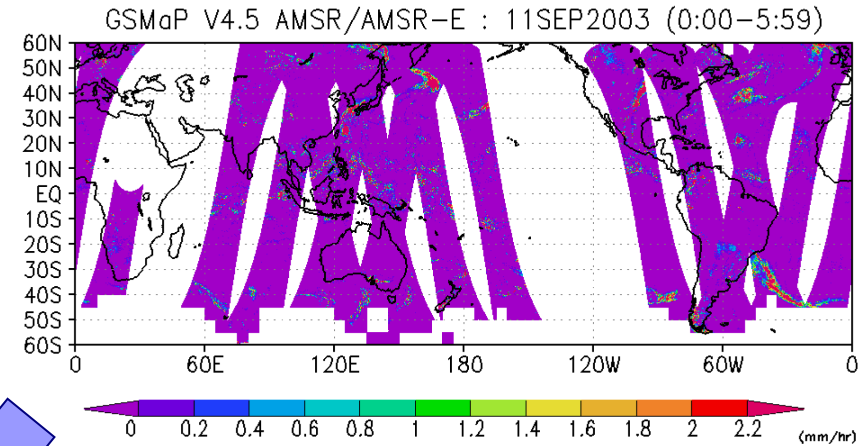

Combined
6 hourly

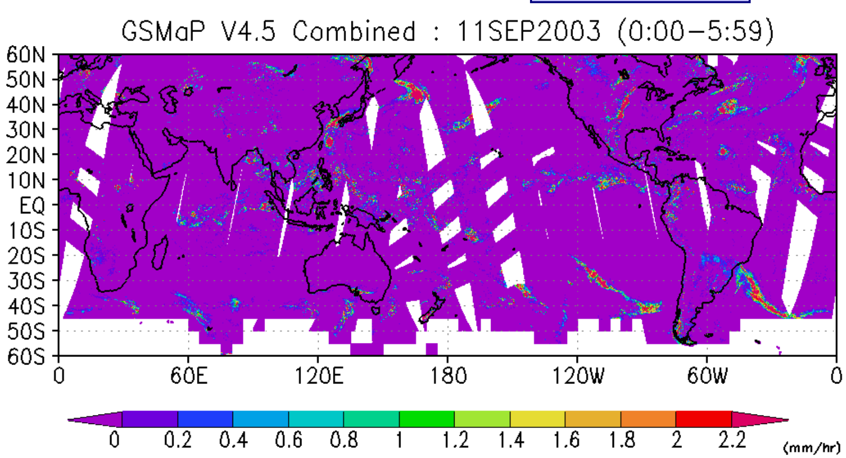

SSM/I （F13, F14, F15）

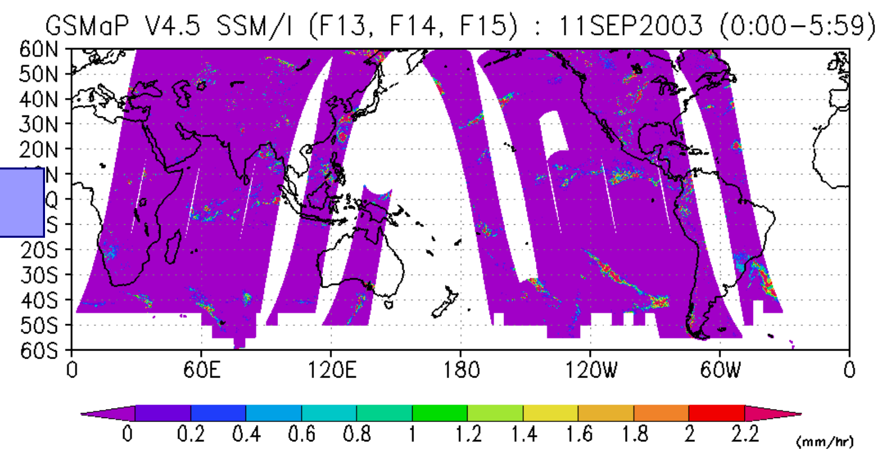

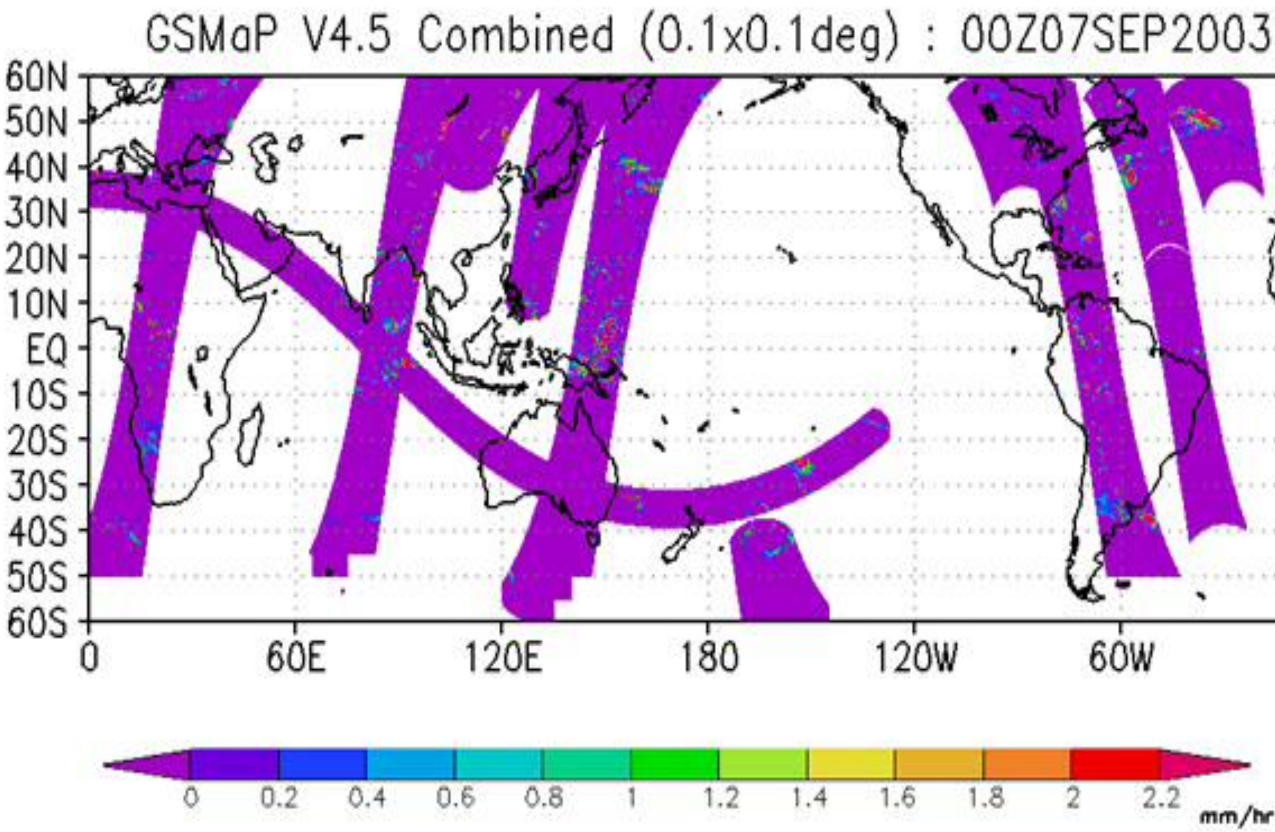
GSMaP V4.5 Combined (0.1x0.1deg) : 00Z07SEP2003
60N
50N
40N
30N
20N
10N
EQ
10S
20S
30S
40S
50S
60S
0
60E
120E
180
120W
60W
0
0
0.2
0.4
0.6
0.8
1
1.2
1.4
1.6
1.8
2
2.2
mm/hr

Global Precipitation product

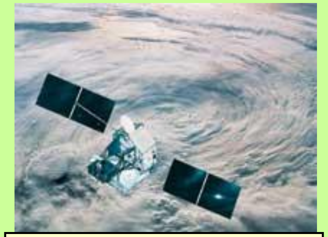
TRMM
TMI


Aqua
AMSR-E


ADEOS-II
AMSR


DMSP
SSM/I

Microwave radiometer algorithm

Product from each sensor


Geo. Satellite

Infrared radiomter
Cloud motion vector

Mix

Composite product
0.1degree

1 hour
6 hour
1 day
1 month

Composite algorithm of
IR and MWR

0.1degree･30min

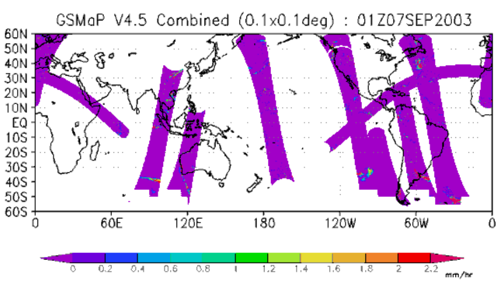

TRMM/TMI, Aqua/AMSR-E, ADEOS-II/AMSR, DMSP/SSMI (F13, 14, 15)による1時間のデータ

How can we get a global precipitation map with temporal resolution of 3 hours or less?

- Infrared radiometers (IR)
  - can provide information on cloud top layers (not precipitation)
  - Can ensure a global coverage with high temporal resolution (> 30 min) due to the geo-synchronous orbit (GEO)

- Microwave radiometers (MW)
  - Can detect cloud structure and precipitation with high spatial resolution
  - The major draw back is temporal sampling due low earth orbit satellite (LEO)

↓

- The LEO-MW and GEO-IR radiometry are quite complementary for monitoring the highly variable parameters like precipitation.

Global High Time/Space Resolution Precipitation Map

- CMORPH (CPC Morphing) – NOAA
- PERSIANN (Precipitation Estimation from Remotely Sensed Information using Artificial Neural Networks) - University of California Irvine
- TRMM 3B42 – GSFC, NASA
- TRMM 3B42rt – GSFC, NASA
- NRL Blended - Naval Research Laboratory
- NESDIS Hydro Estimator (STAR) - NOAA
- Eumetsat Multi-Sensor Precipitation Estimates(MPE)

GLOBAL SATELLITE MAPPING OF PRECIPITATION (GSMAP)

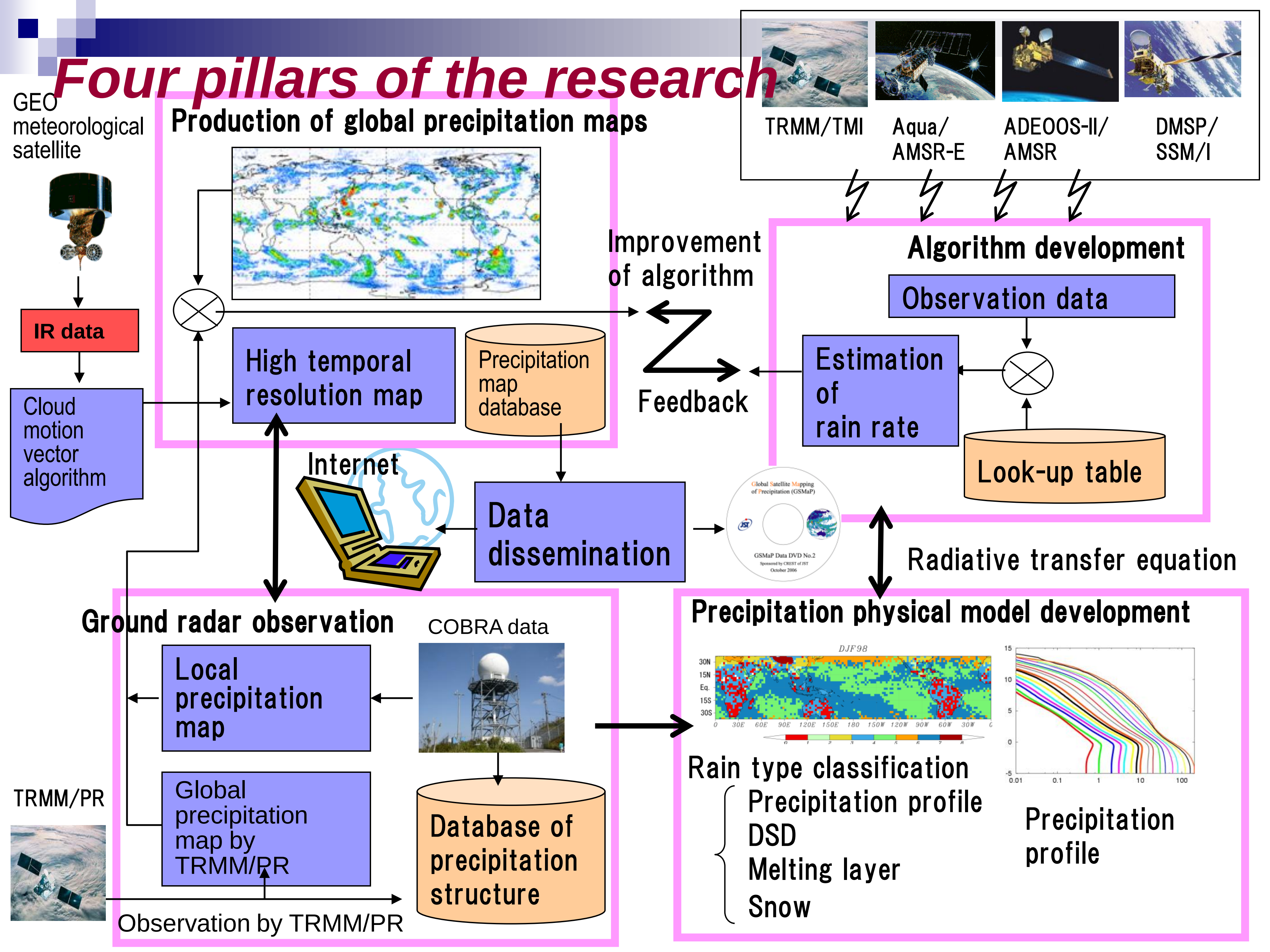

Four pillars of the research
TRMM/TMI
Aqua/ AMSR-E
ADEOOS-II/ AMSR
DMSP/ SSM/I
GEO meteorological satellite
IR data
Cloud motion vector algorithm
Production of global precipitation maps
High temporal resolution map
Precipitation map database
Improvement of algorithm
Feedback
Algorithm development
Observation data
Estimation of rain rate
Look-up table
Internet
Data dissemination
Global Satellite Mapping of Precipitation (GSMaP)
GSMaP Data DVD No.2
Radiative transfer equation
Ground radar observation
COBRA data
Local precipitation map
Global precipitation map by TRMM/PR
Database of precipitation structure
TRMM/PR
Observation by TRMM/PR
Precipitation physical model development
DJF98
Rain type classification
Precipitation profile
DSD
Melting layer
Snow
Precipitation profile

Global Precipitation Product

TRMM
TMI

Aqua
AMSR-E

ADEOS-II
AMSR

DMSP
SSM/I

Microwave radiometer algorithm

Product from each sensor

Geo. Satellite

Mix

Infrared radiomter
Cloud motion vector

Composite product

0.5degree

30 min.
6 hour
1 day
1 month

Composite algorithm of IR and MWR

0.1degree･30min

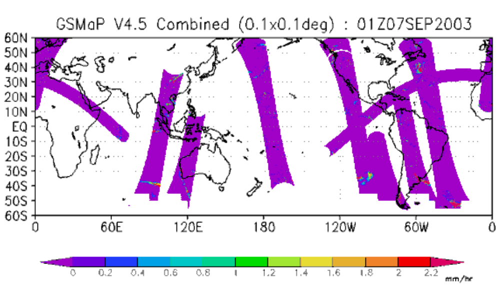

TRMM/TMI, Aqua/AMSR-E, ADEOS-II/AMSR, DMSP/SSMI (F13, 14, 15)による1時間のデータ

Basis of Rain Rate Retrieval by Microwave Radiometers

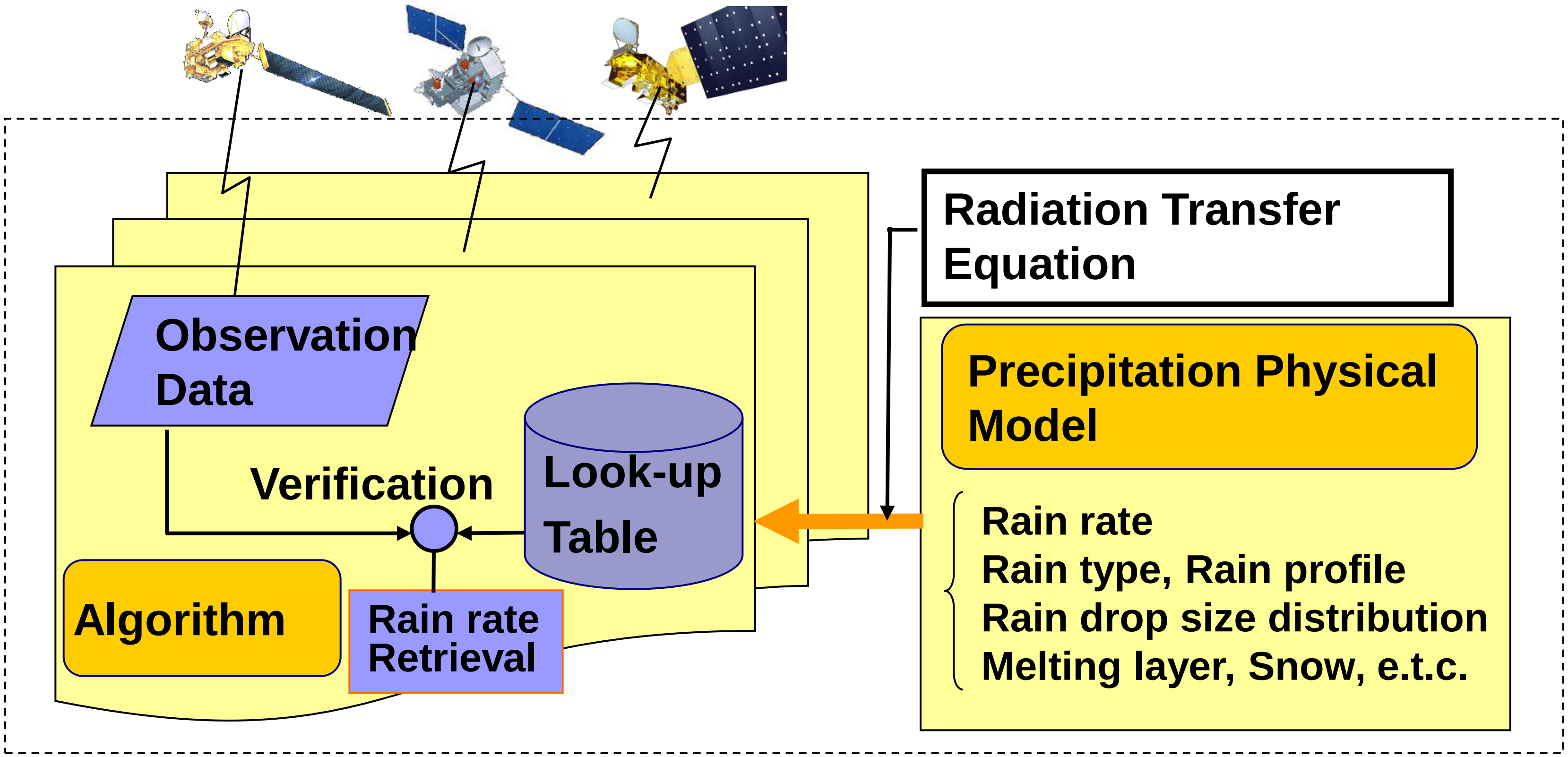

- Satellites observe the brightness temperature, integration of radiation and scattering power.
- The relation between rain rate and brightness temperature is tabulated by assuming precipitation physical model and calculating the radiative transfer equation. The rain rates giving the nearest brightness temperature values to the observed ones are considered to be the most appropriate estimation.

Flow Diagram of GSMaP MWR Algorithm

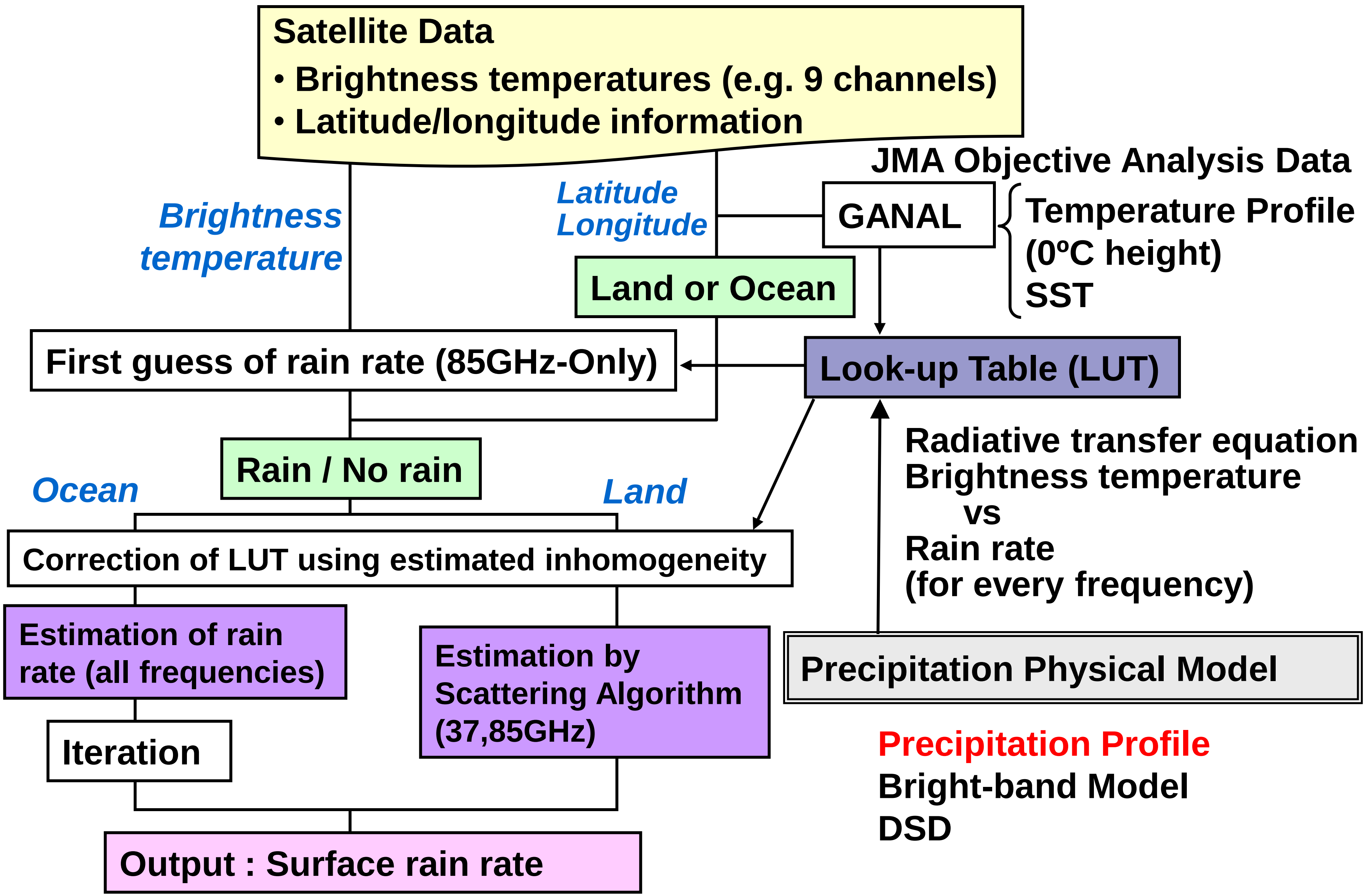

Approach of the GSMaP project

- We use the Aonashi Algorithm to retrieve rainfall rate.
- The sensors for the analysis are TMI, AMSR-E, AMSR, SSMI (F13, 14, 15).

Name	Data available
TRMM (TMI)	Jan. 1998 to Dec. 2005
Aqua (AMSR-E)	Jan. 2003 to Oct. 2005
ADEOS-II (AMSR)	Apr. 2003 to Oct. 2003
DMSP (SSMI:F13, F14, F15)	Sep. 2003, July. 2005 and several

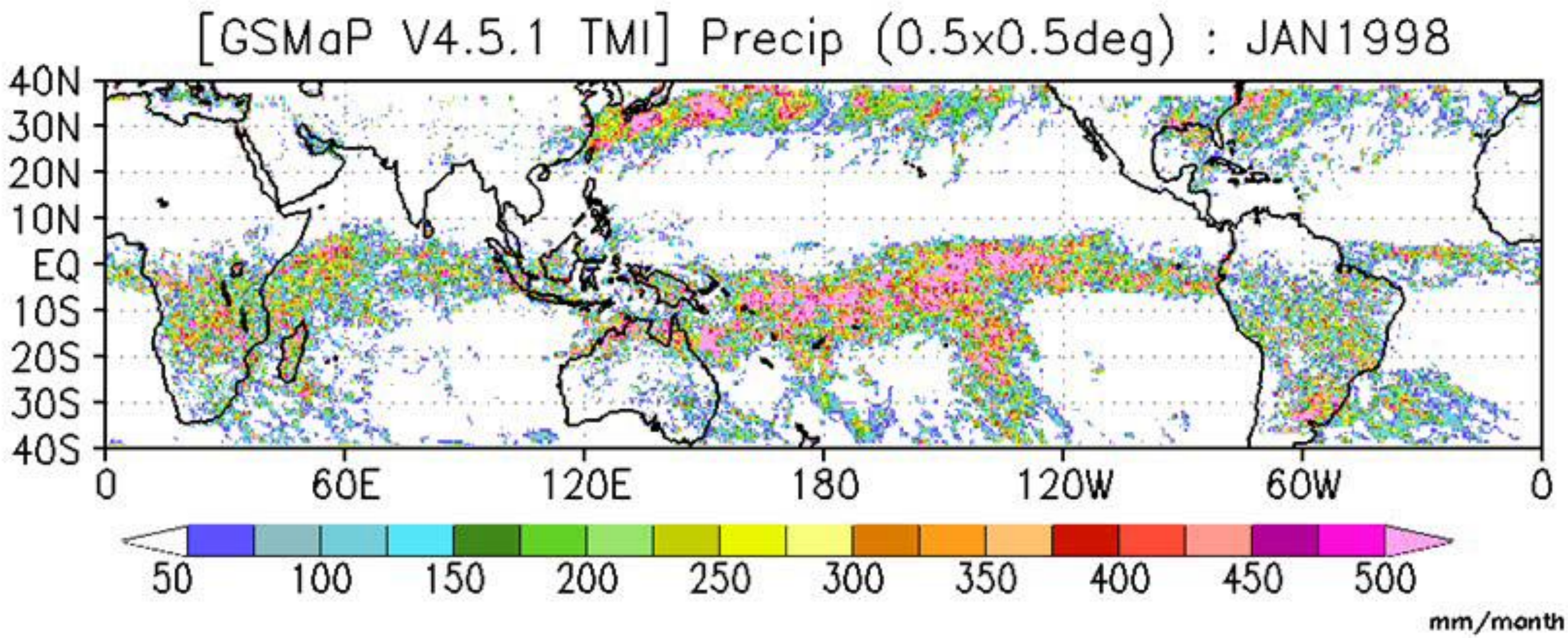
[GSMaP V4.5.1 TMI] Precip (0.5x0.5deg) : JAN1998
40N
30N
20N
10N
EQ
10S
20S
30S
40S
0
60E
120E
180
120W
60W
0
50
100
150
200
250
300
350
400
450
500
mm/month

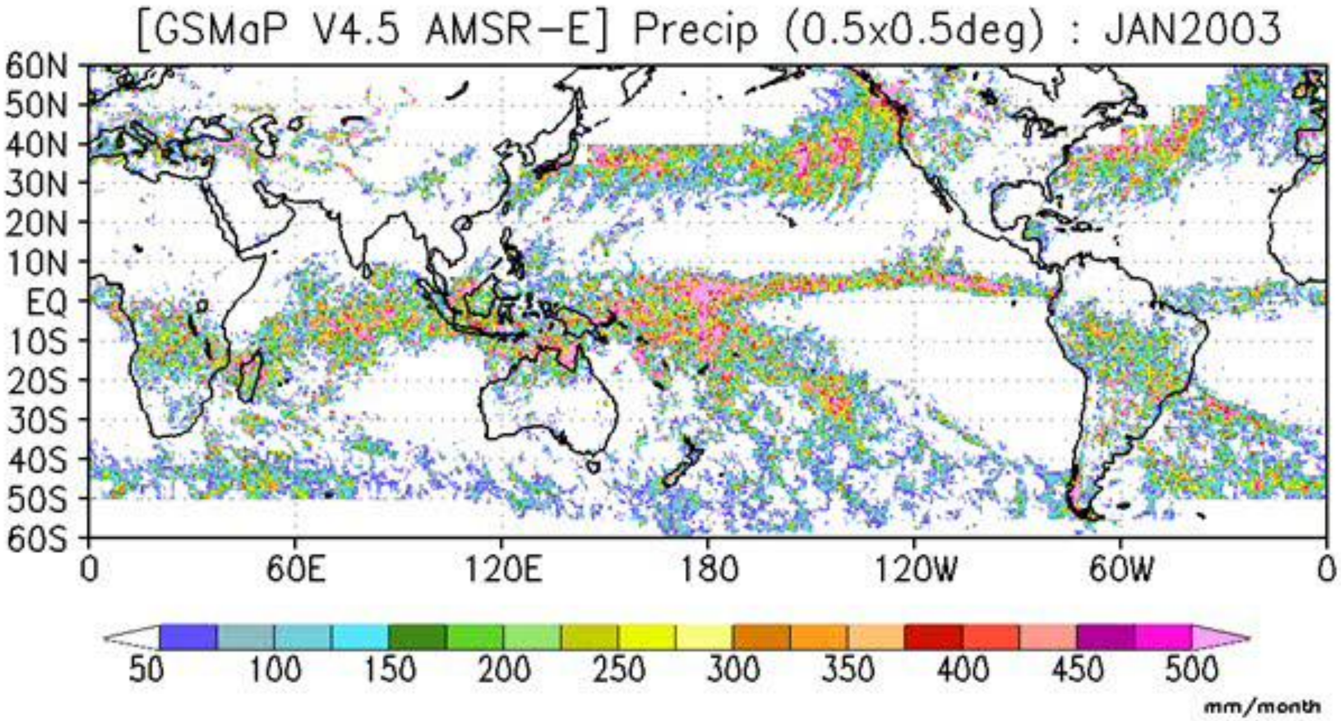
[GSMaP V4.5 AMSR-E] Precip (0.5x0.5deg) : JAN2003
60N
50N
40N
30N
20N
10N
EQ
10S
20S
30S
40S
50S
60S
0
60E
120E
180
120W
60W
0
50
100
150
200
250
300
350
400
450
500
mm/month

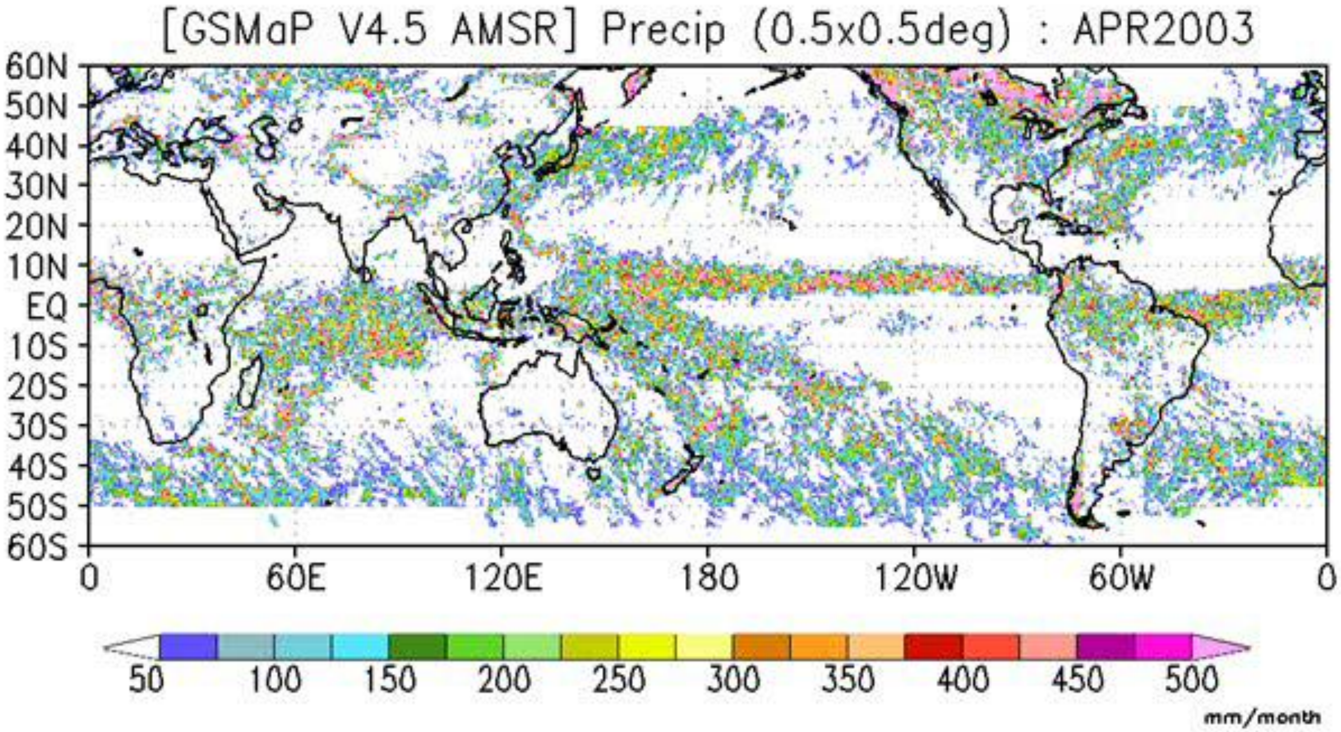
[GSMaP V4.5 AMSR] Precip (0.5x0.5deg) : APR2003
60N
50N
40N
30N
20N
10N
EQ
10S
20S
30S
40S
50S
60S
0
60E
120E
180
120W
60W
0
50
100
150
200
250
300
350
400
450
500
mm/month

Monthly precipitation accumulation from DMSP/SSMI (F13, 14, 15) for Sep. 2003

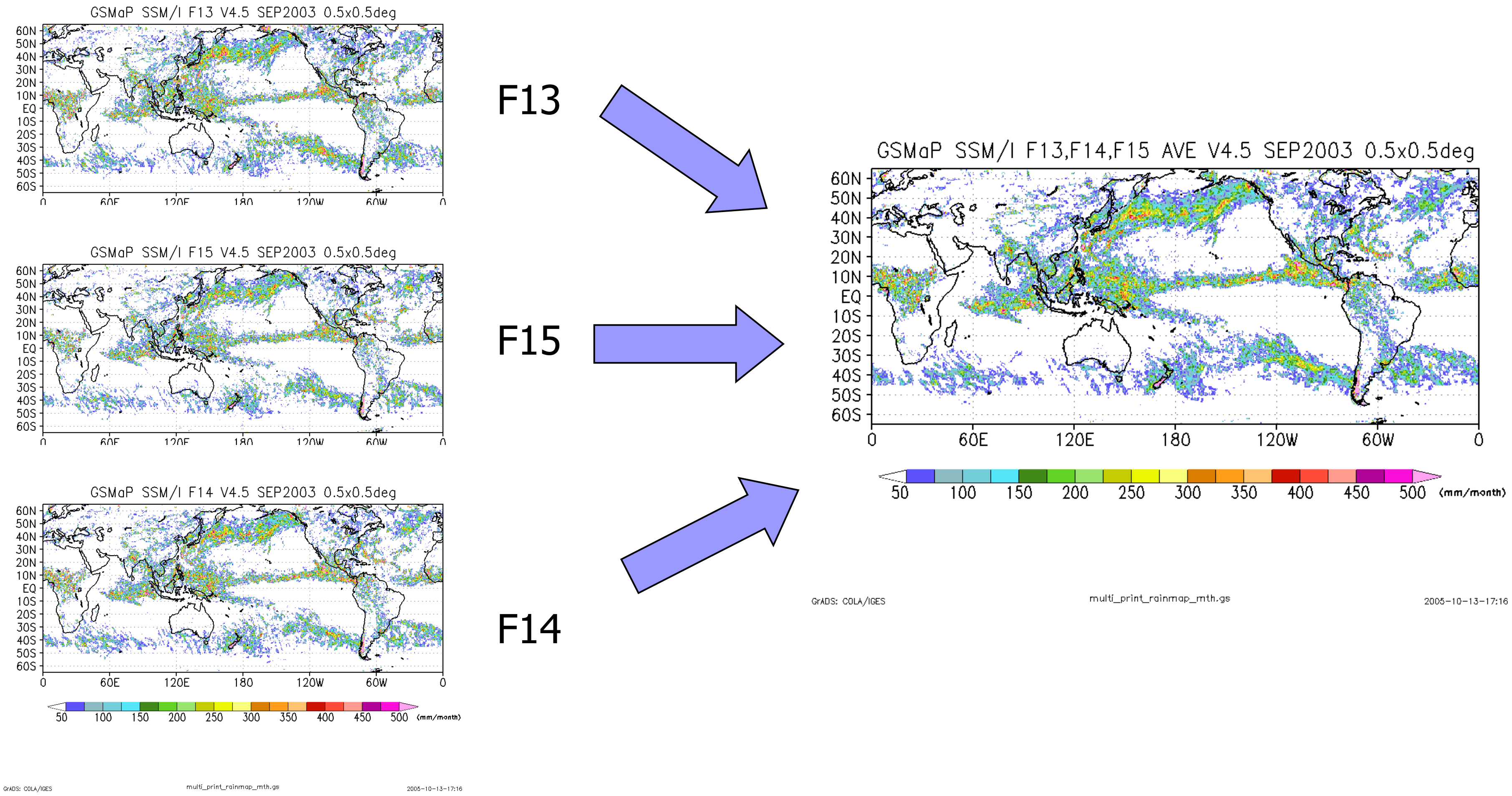

Integrated 6-hour microwave radiometer precipitation map (GSMaP_MWR)

MWR(TMI+AMSR+AMSR-E+F13, 14, 15 SSM/I)

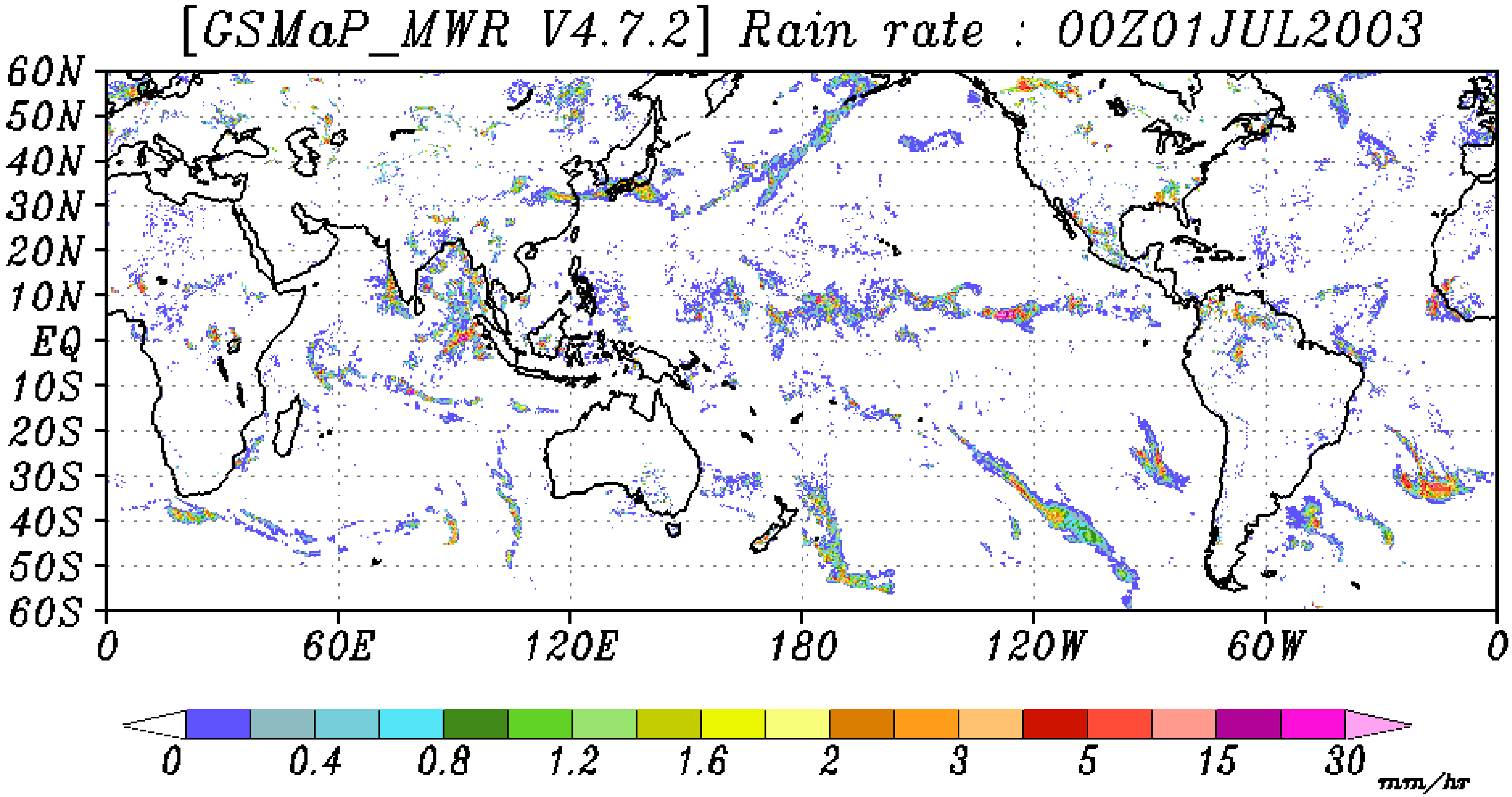

Comparison of monthly rain rates by ground-based rain gauge (GPCC) with GSMaP_MWR

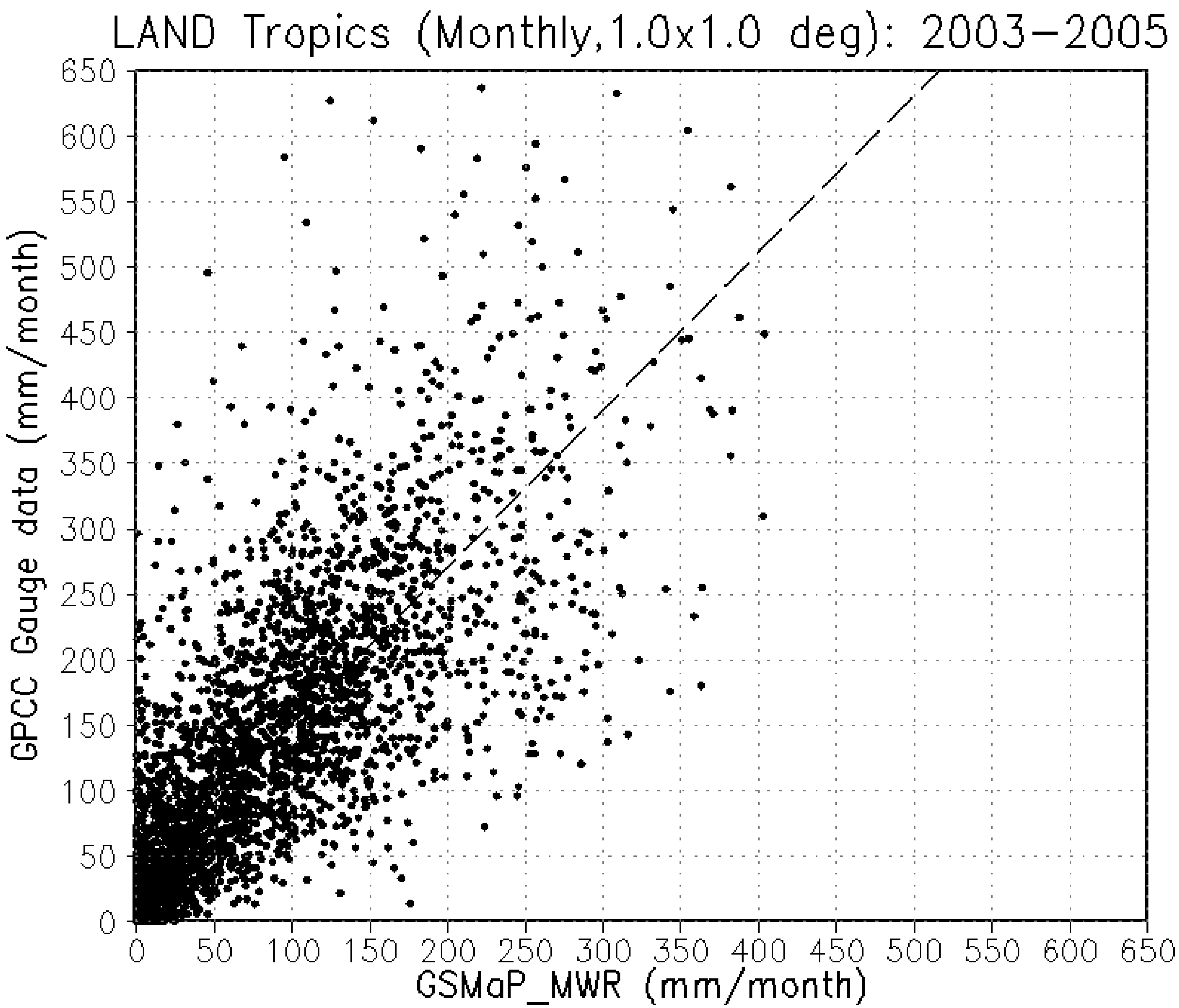

- **GPCC Monthly Precipitation (Monitoring) Product** （Rudolf et al. 2005）
  - ground-based rain gauge
  - about 7000 rain gauges in the world
  - 1.0゜ ×1.0゜
  - monthly average

- Analysis method
  - Tropical Area（20S～20N）
  - There are at least 2 rain gauges in the 1.0゜ ×1.0゜
  - 2003-2005

Regression line : y=1.20 x + 30.8 (mm/month)　Correlation coefficient : 0.79

If we need a global precipitation map with higher resolution, how should we do?

- Solution
  - ????

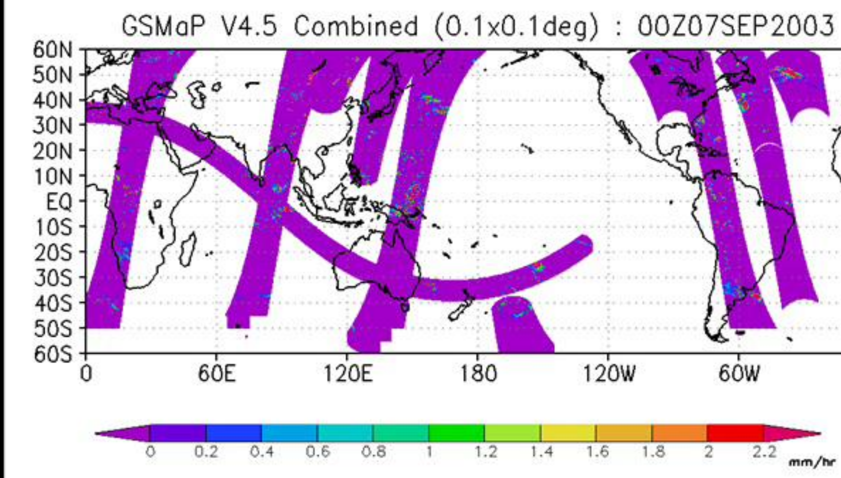

Global Precipitation product

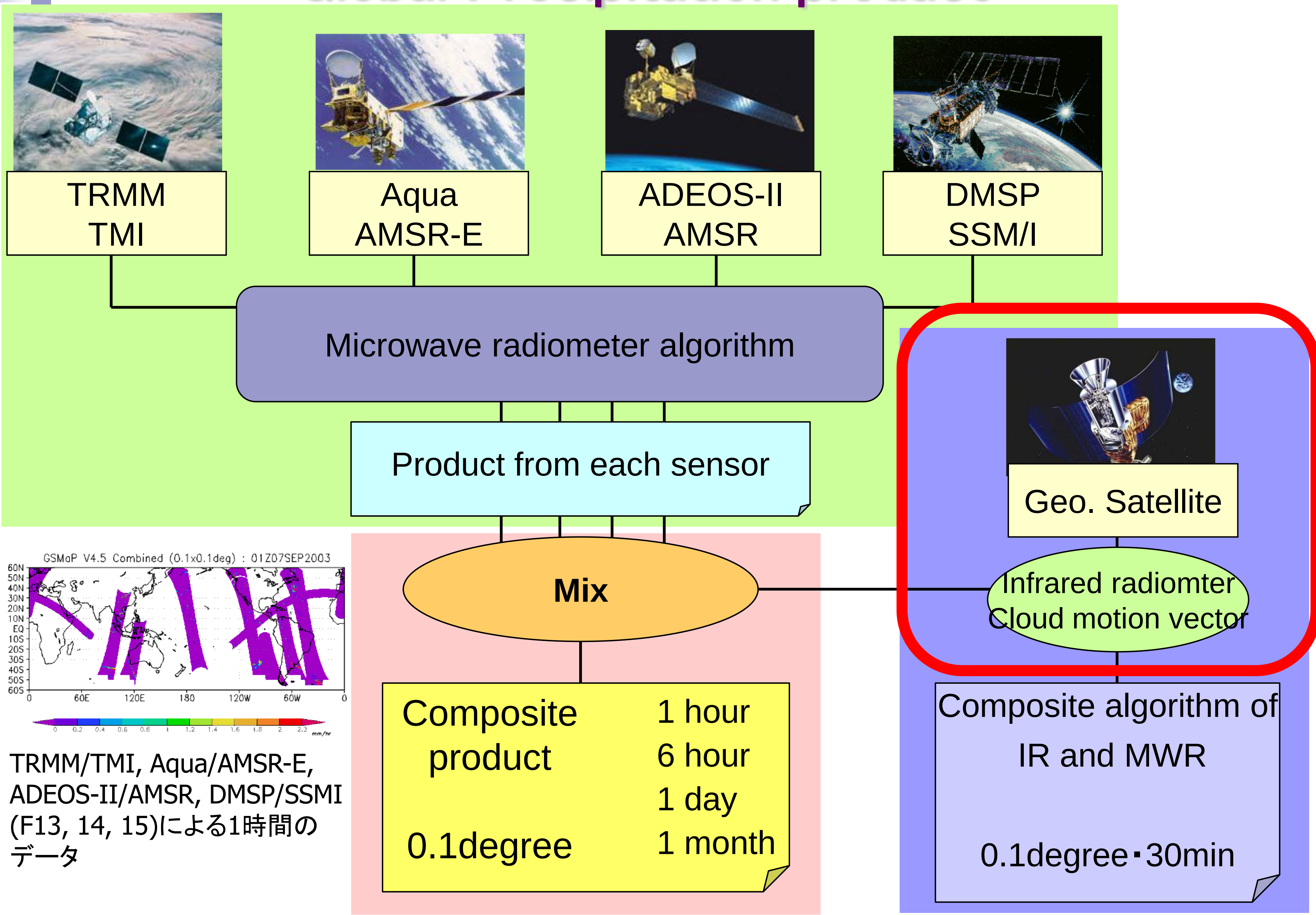

TRMM/TMI, Aqua/AMSR-E, ADEOS-II/AMSR, DMSP/SSMI (F13, 14, 15)による1時間のデータ

Approaches

- There are so many products to realize the 3 hours or less resolution.

- What is the GSMaP approach?

How do we combine the MWR and IR data?

- Combination of the moving vector and Kalman filtering method

- The moving vector method was introduced by Joyce et al. [2004].
  - Joyce R., J. Janowiak, P. Arkin, and P. Xie, CMORPH: A method that produces global precipitation estimates from passive microwave and ifrared data at high spatial and temporal resolution, J. Hydrometeorology, 487-503, 2004
  - Advantage
    - MWR based approach (not Tb but cloud motion)
    - Fast processing time
  - Disadvantage
    - Not include the developing and decaying process of precipitation

New!!

- Kalman filter approach
  - Refine precipitation rate on Kalman gain after propagating the rain pixel
  - The Kalman gain is determined from the database on the relationship between the IR Tb and surface rain rate.

What is the Kalman Filter?

- **Example (Simple Gaussian form)**
  - **Assumption**
    - **All error form Gaussian noise**
  - **Estimated value**

$$x_e, \sigma_e^2$$

  - **Measurement value**

$$x_m, \sigma_m^2$$

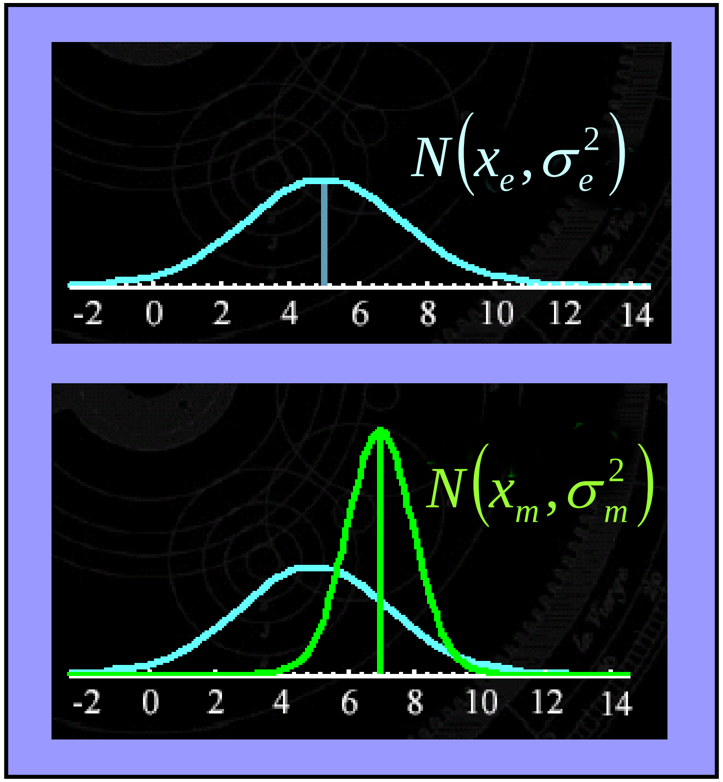

What is the Kalman Filter?

- **Example (Simple Gaussian form)**
  - **Optimal variance**

$$\frac{1}{\sigma^2} = \frac{1}{\sigma_e^2} + \frac{1}{\sigma_m^2}$$

  - **Optimal mean**

$$x = \left[\frac{\sigma_m^2}{\sigma_e^2 + \sigma_m^2}\right] x_e + \left[\frac{\sigma_e^2}{\sigma_e^2 + \sigma_m^2}\right] x_m$$

$$x = x_e + \boxed{\left[\frac{\sigma_e^2}{\sigma_e^2 + \sigma_m^2}\right]} \boxed{\left(x_m - x_e\right)}$$

$$x = x_e + K i$$

Innovation

Kalman gain

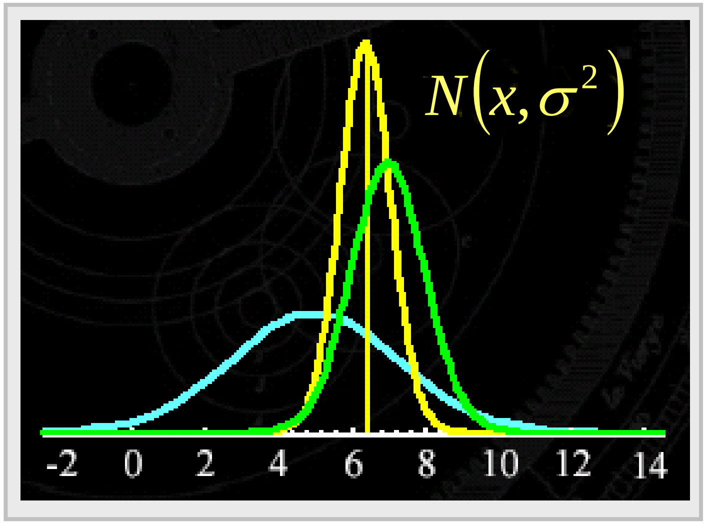

State and observation equation used in Kalman filter

$$x_{k+1} = x_k + \sigma w \qquad (State\ \ Equation)$$

$$y_k = Hx_k + \sigma v \qquad (Observation\ Equation)$$

x_k : Rain rate at time k

y_k : Infrared Tb

x_{k+1} : Rain rate at time k+1

w : System noise

v : Observation noise

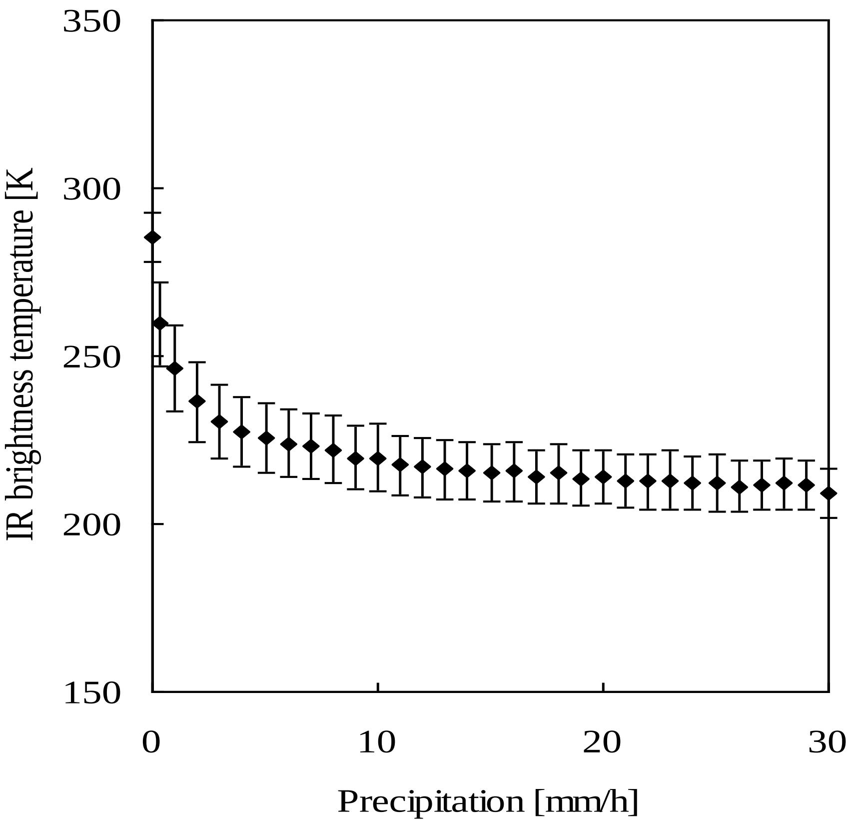

Kalman Filter

Predicted rain rate $\bar{x}$

$$\alpha = \frac{\sigma_w^{\ 2}}{\sigma_v^{\ 2}}$$

IR Tb y

Obs. Noise σ_v

Refinement

$$\hat{x} = \bar{x} + K\left(y - \bar{x}\right) \qquad K = \frac{\sqrt{\alpha^2 + 4\alpha} - \alpha}{2}$$

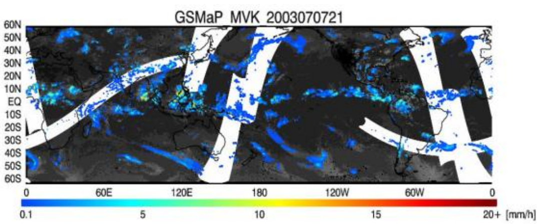

GSMaP $\hat{x}$

Prediction

$$\bar{x}' = \hat{x}$$

System Noise σ_w

Predicted rain rate $\bar{x}'$

Production of high temporal (1 hr)/high spatial (0.1°×0.1°) resolution precipitation map (GSMaP)

Algorithm flow to predict the movement of raining areas by applying the cloud motion vector of the past 1 hour estimated from the IR cloud image

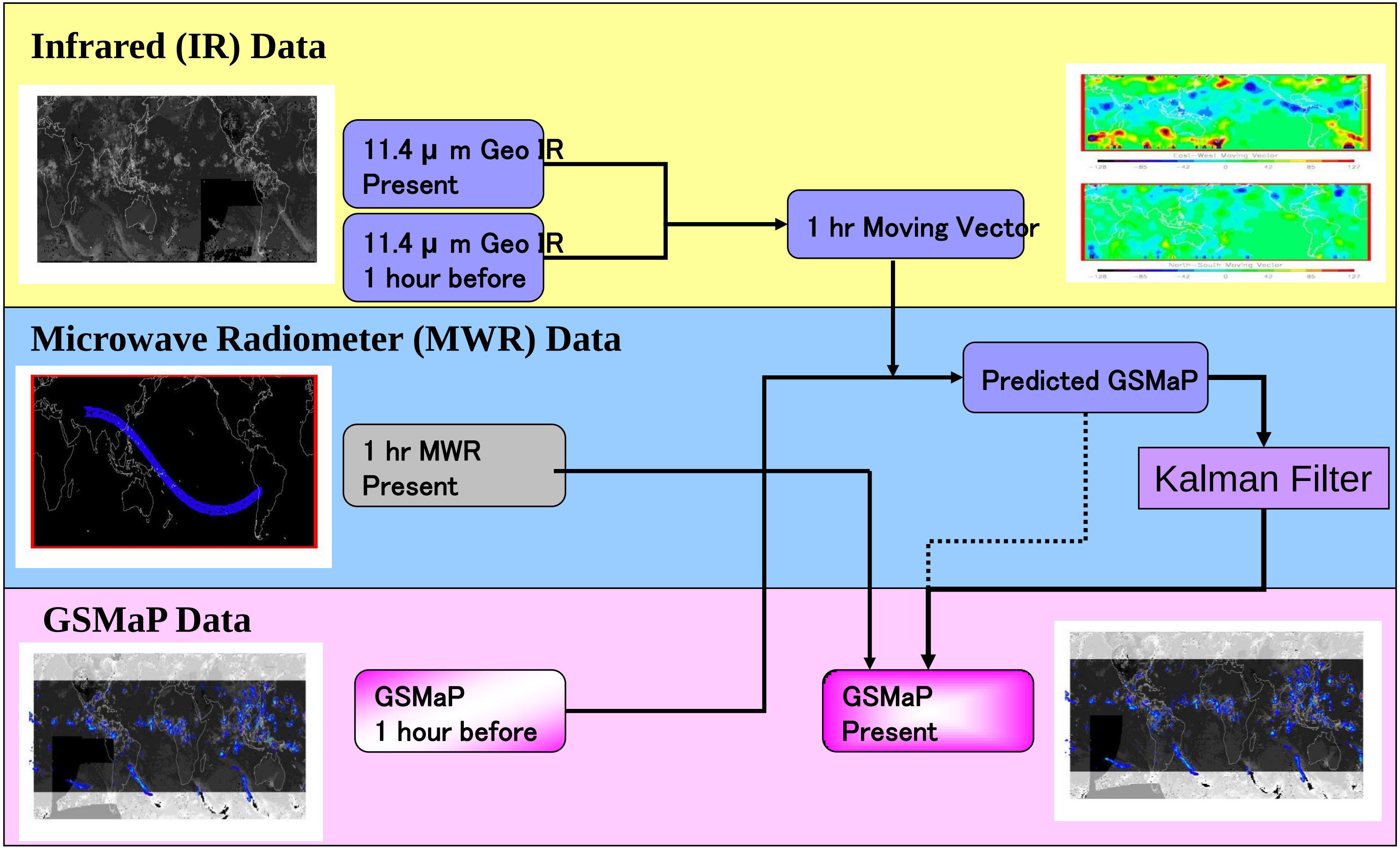

Backward process

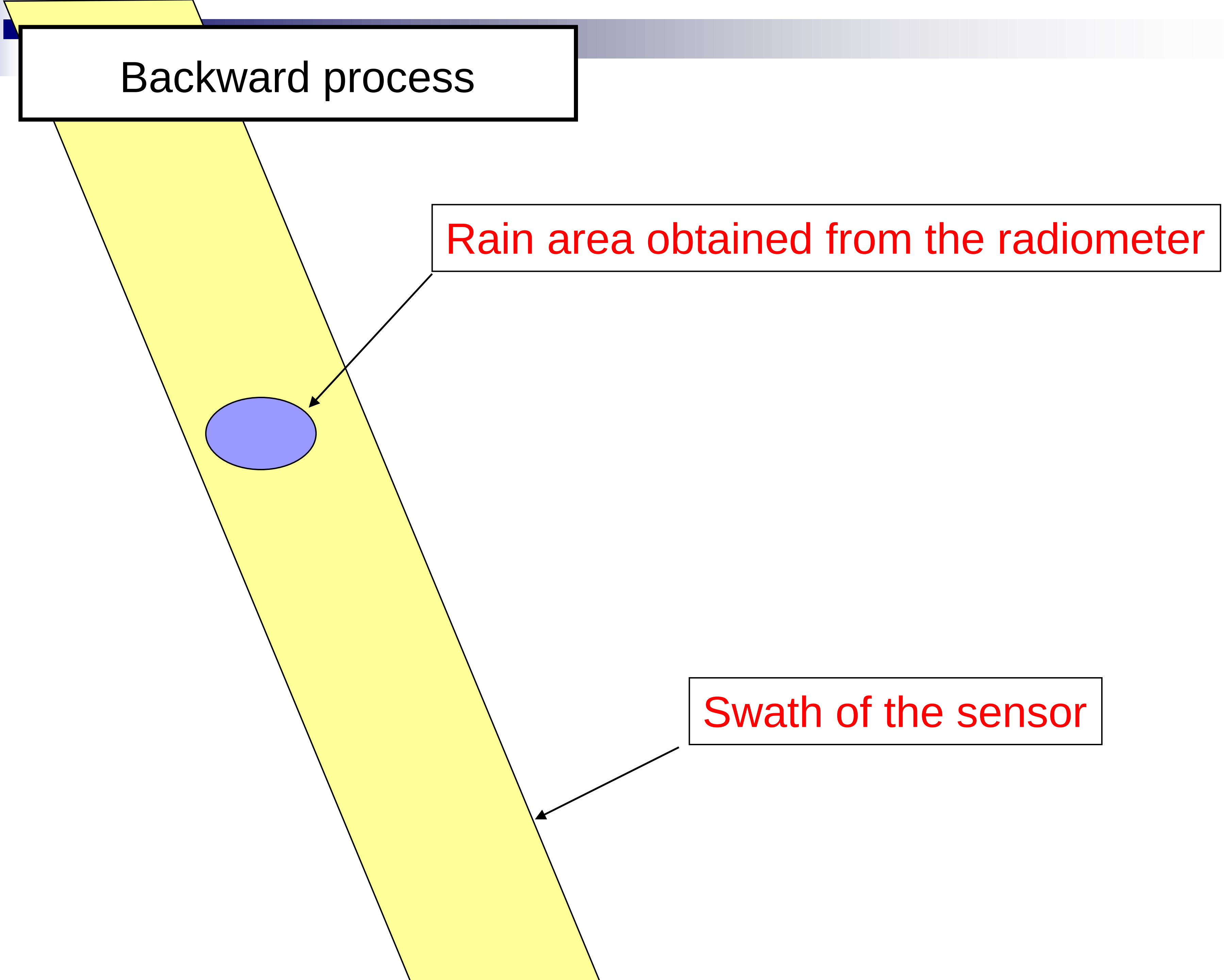

Backward process

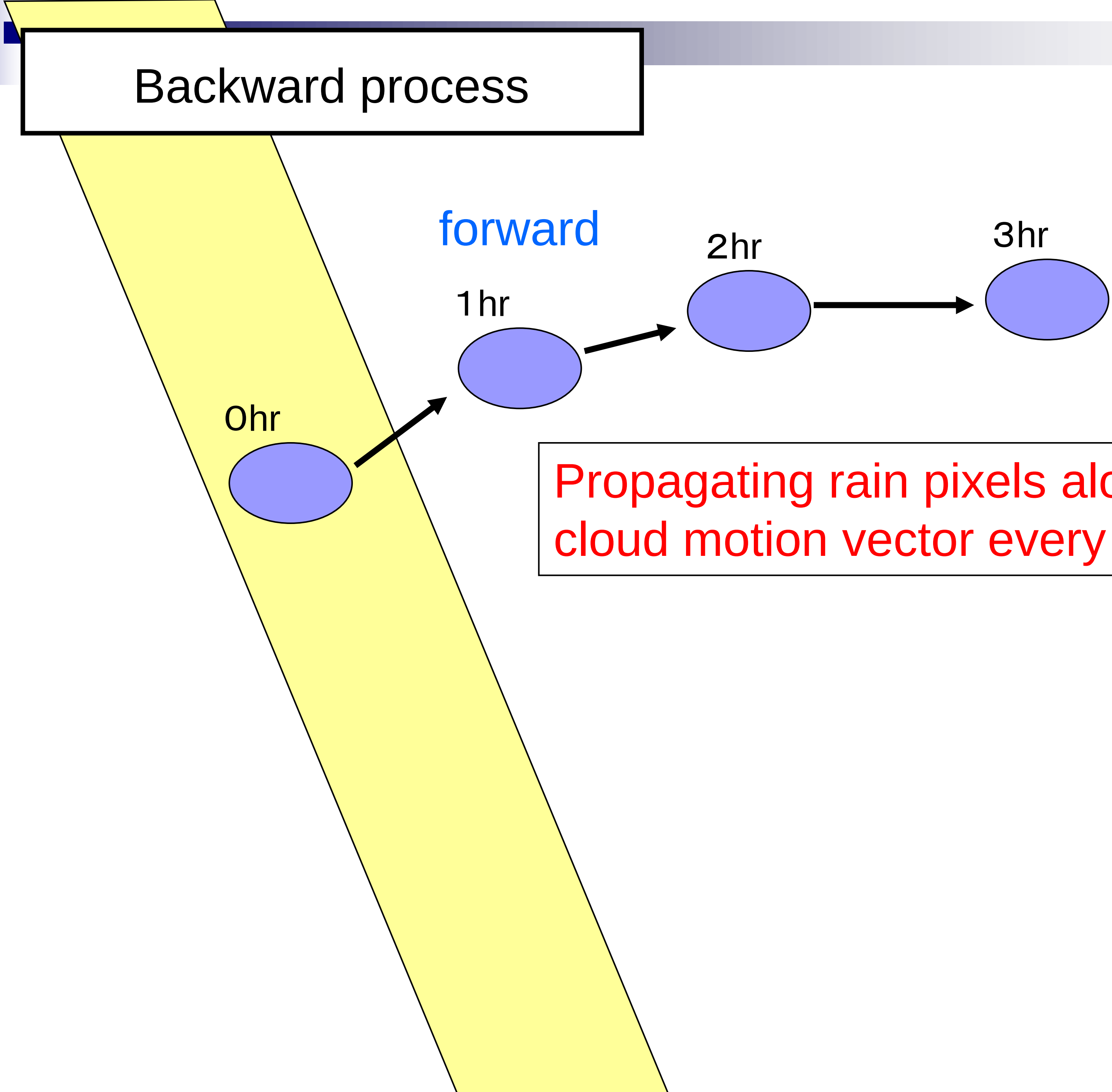

Propagating rain pixels along with cloud motion vector every hour

Backward process

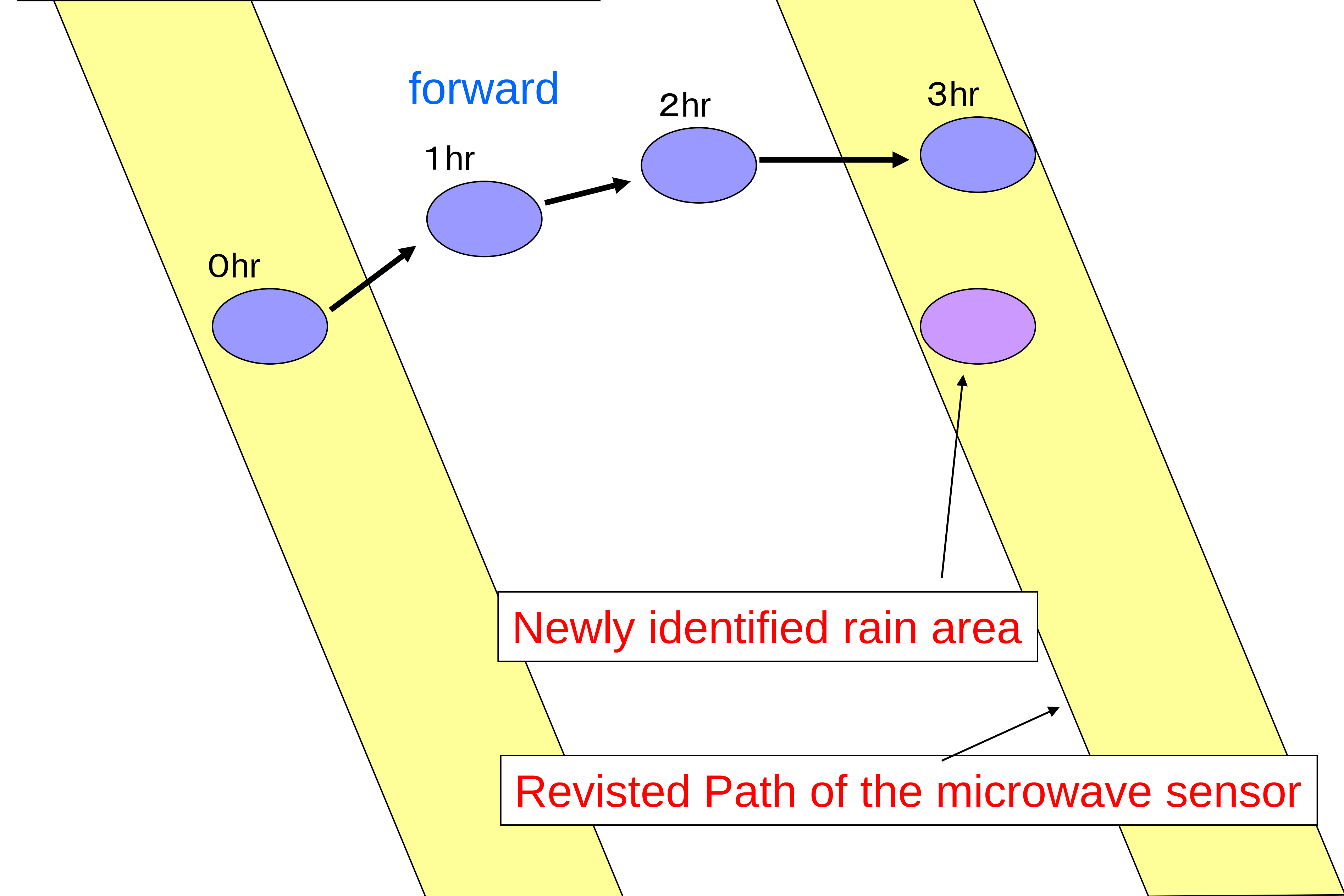

Backward process

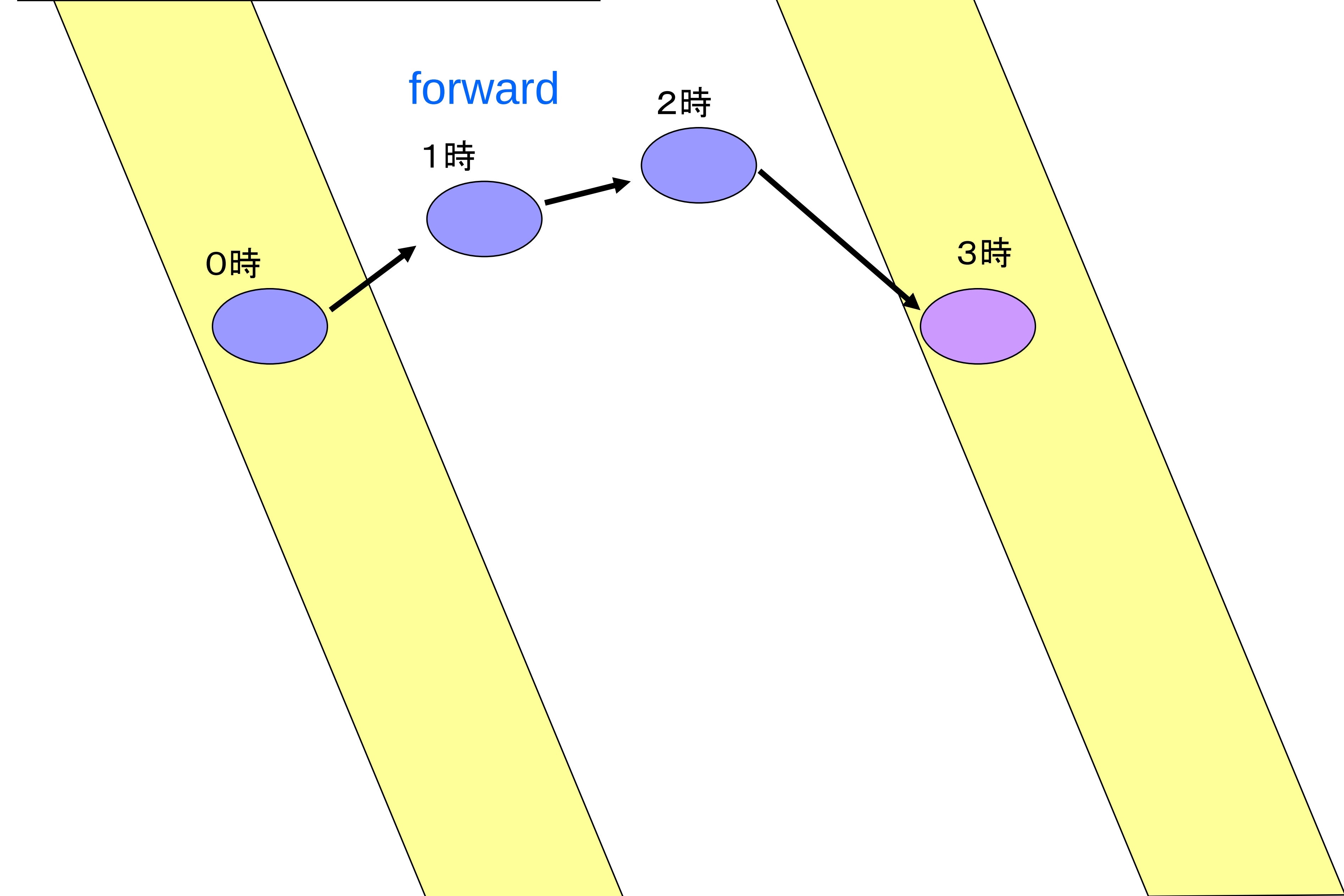

Backward process

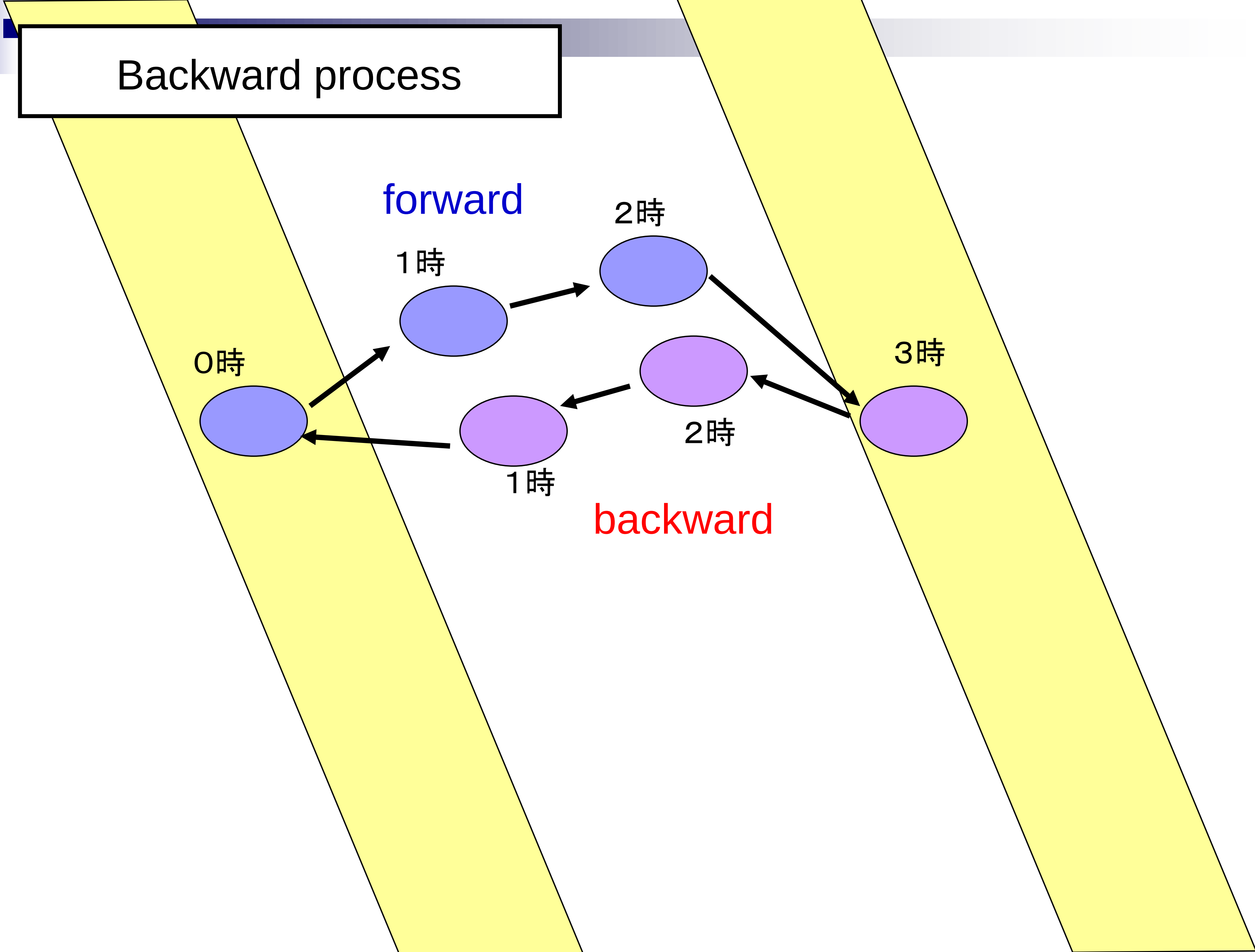

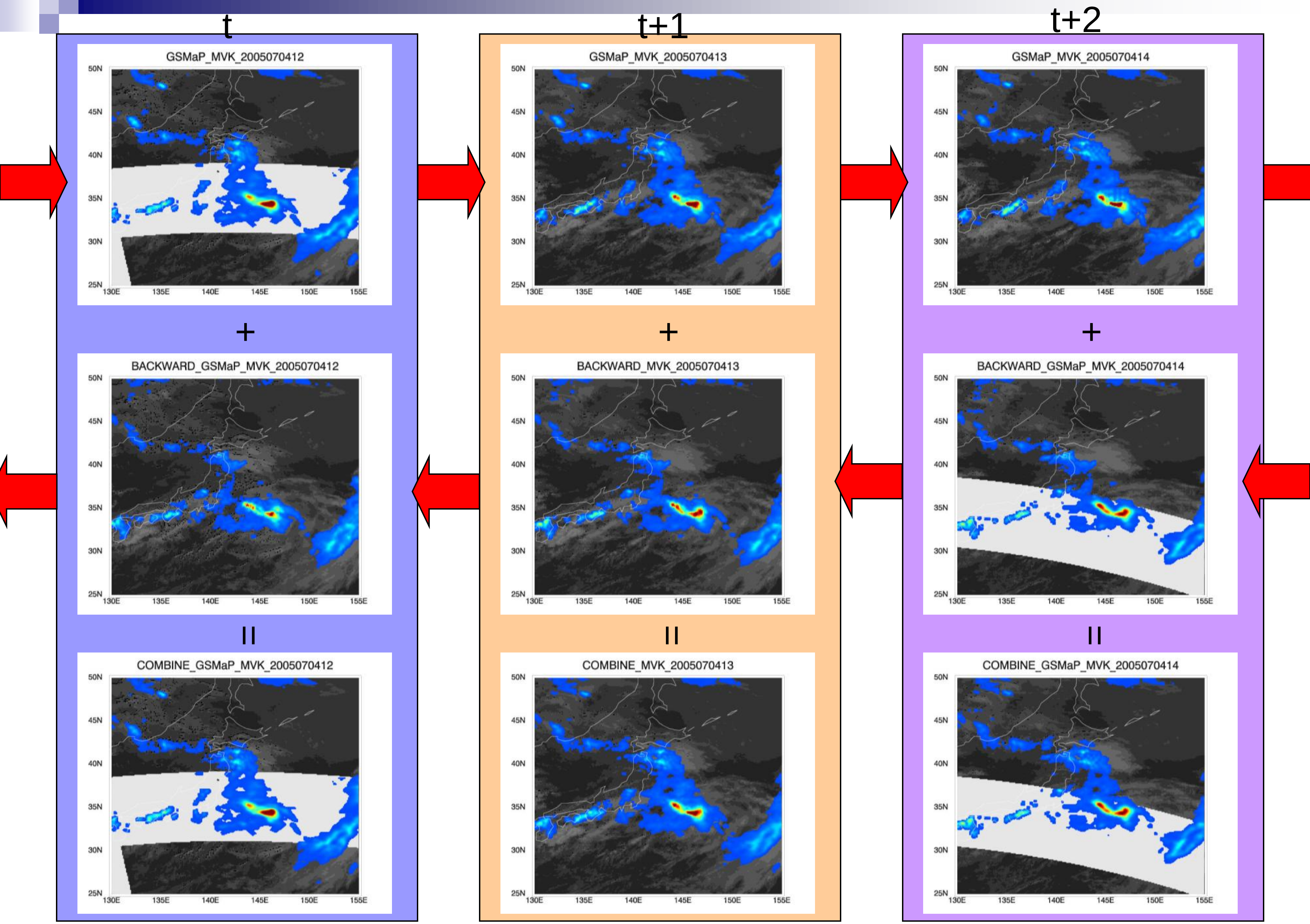

t
t+1
t+2
GSMaP_MVK_2005070412
GSMaP_MVK_2005070413
GSMaP_MVK_2005070414
+
BACKWARD_GSMaP_MVK_2005070412
BACKWARD_MVK_2005070413
BACKWARD_GSMaP_MVK_2005070414
=
COMBINE_GSMaP_MVK_2005070412
COMBINE_MVK_2005070413
COMBINE_GSMaP_MVK_2005070414
50N
45N
40N
35N
30N
25N
130E
135E
140E
145E
150E
155E

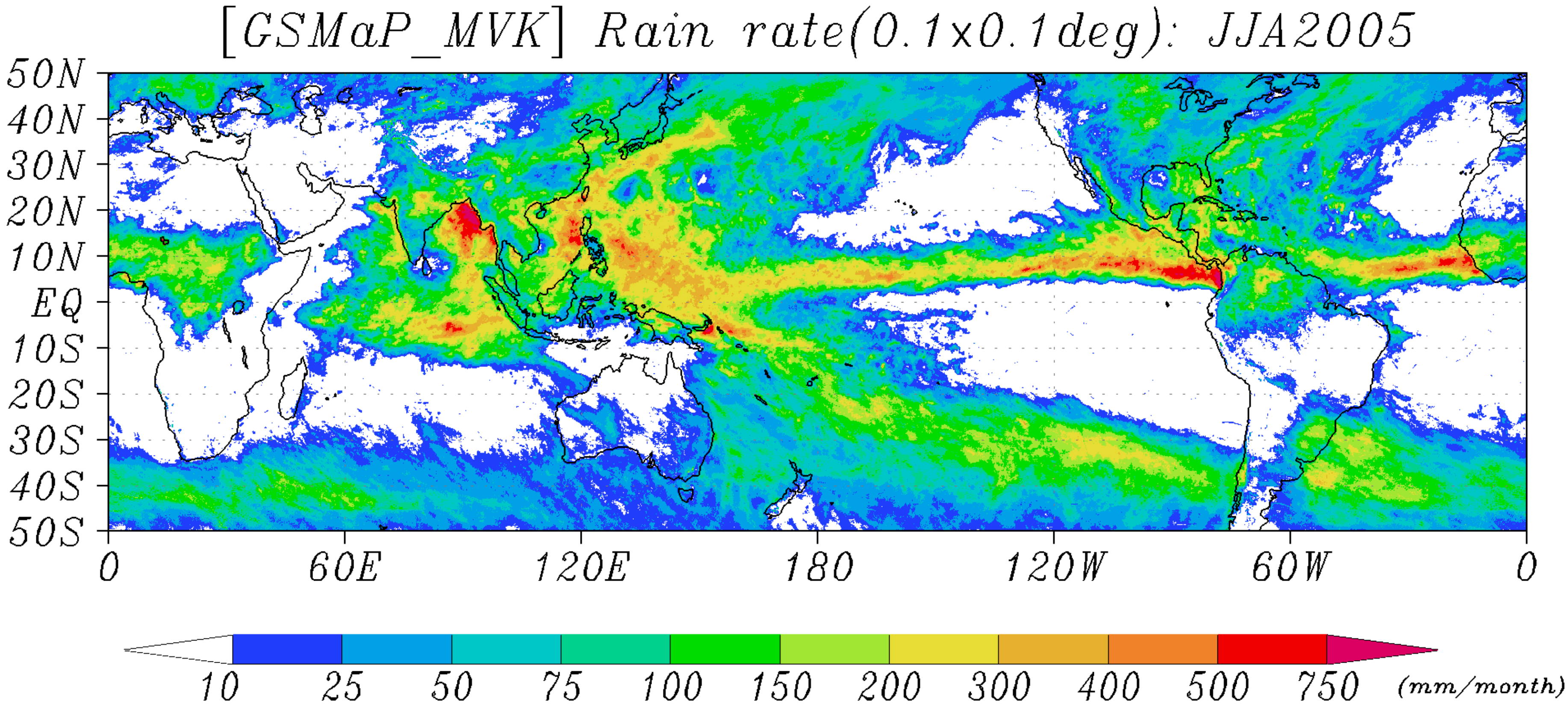
[GSMaP_MVK] Rain rate(0.1x0.1deg): JJA2005
50N
40N
30N
20N
10N
EQ
10S
20S
30S
40S
50S
0
60E
120E
180
120W
60W
0
10
25
50
75
100
150
200
300
400
500
750
(mm/month)

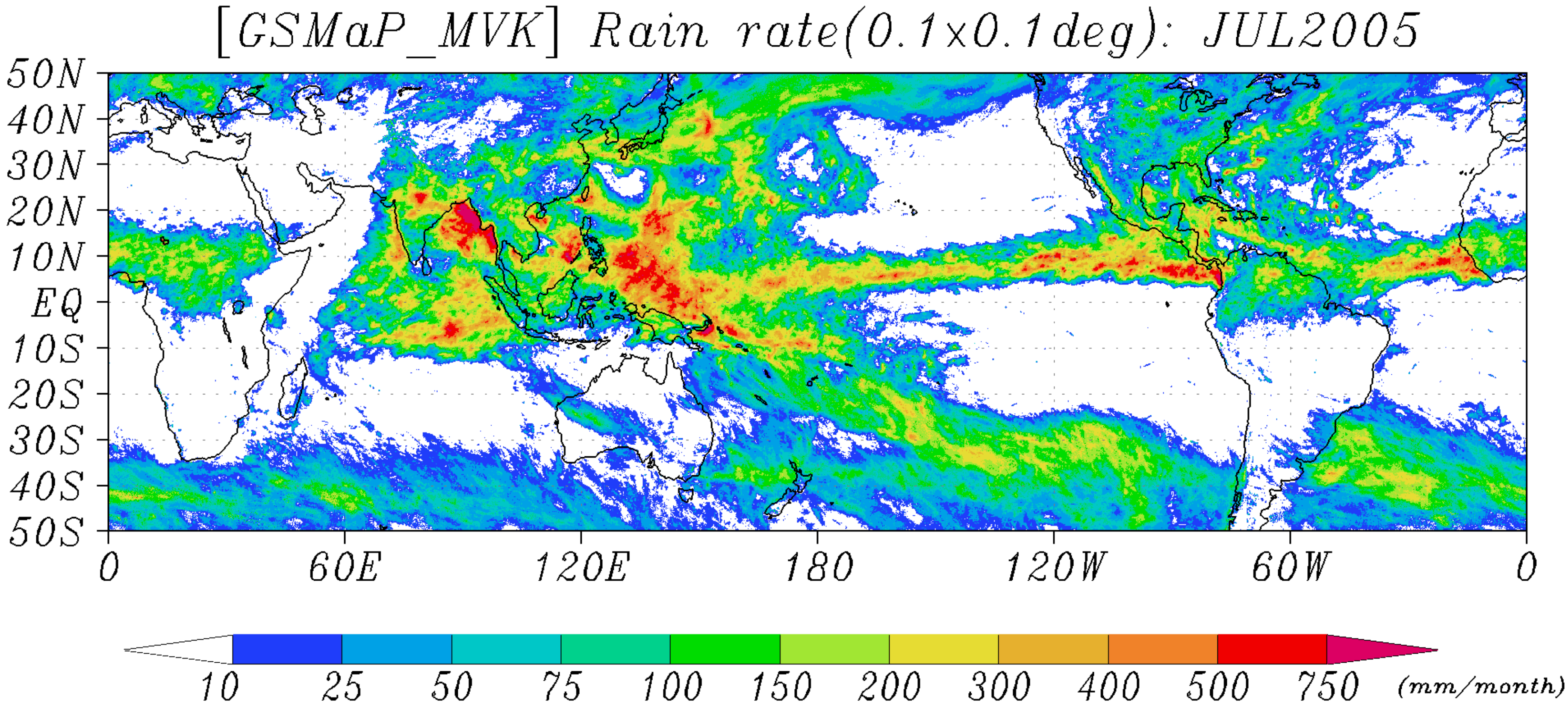
[GSMaP_MVK] Rain rate(0.1x0.1deg): JUL2005
50N
40N
30N
20N
10N
EQ
10S
20S
30S
40S
50S
0
60E
120E
180
120W
60W
0
10
25
50
75
100
150
200
300
400
500
750
(mm/month)

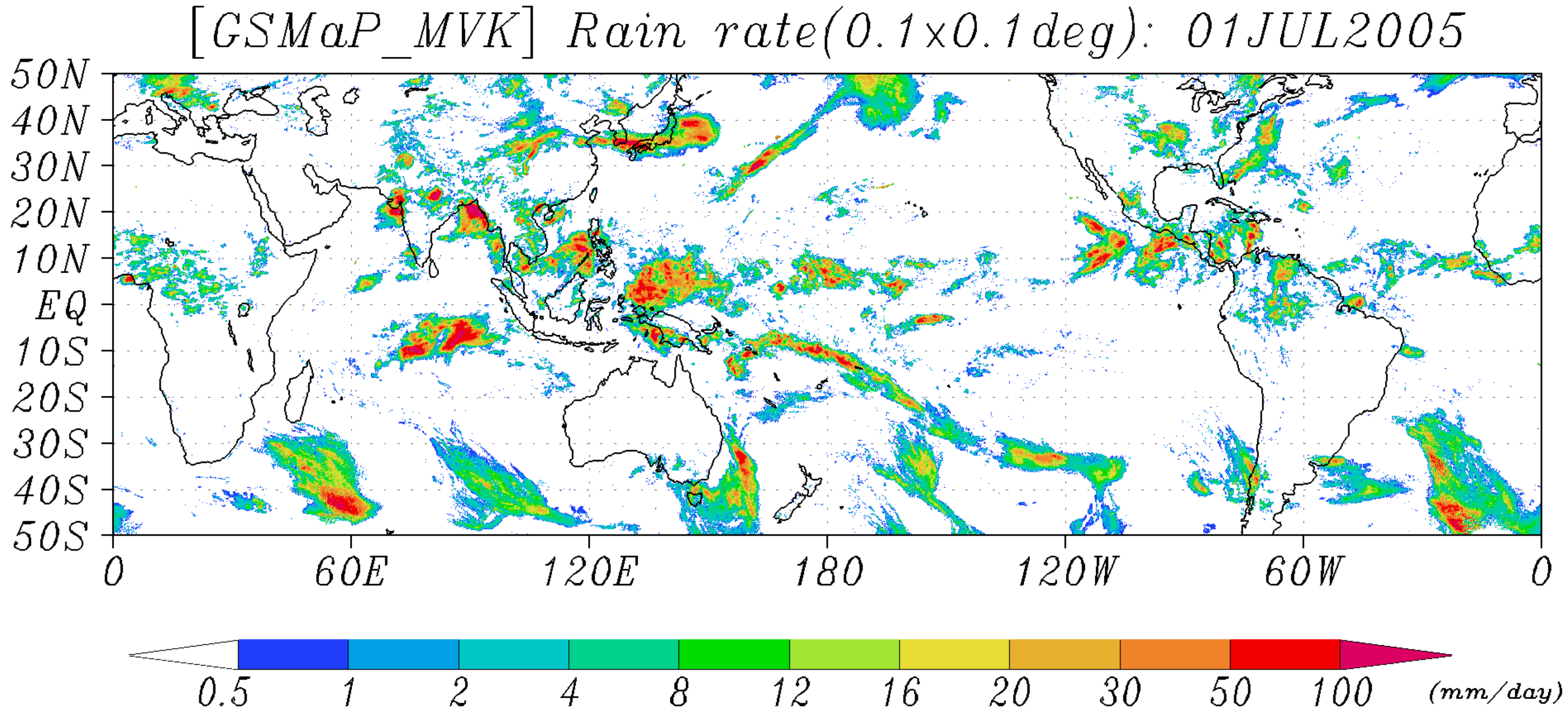
[GSMaP_MVK] Rain rate(0.1x0.1deg): 01JUL2005
50N
40N
30N
20N
10N
EQ
10S
20S
30S
40S
50S
0
60E
120E
180
120W
60W
0
0.5
1
2
4
8
12
16
20
30
50
100
(mm/day)

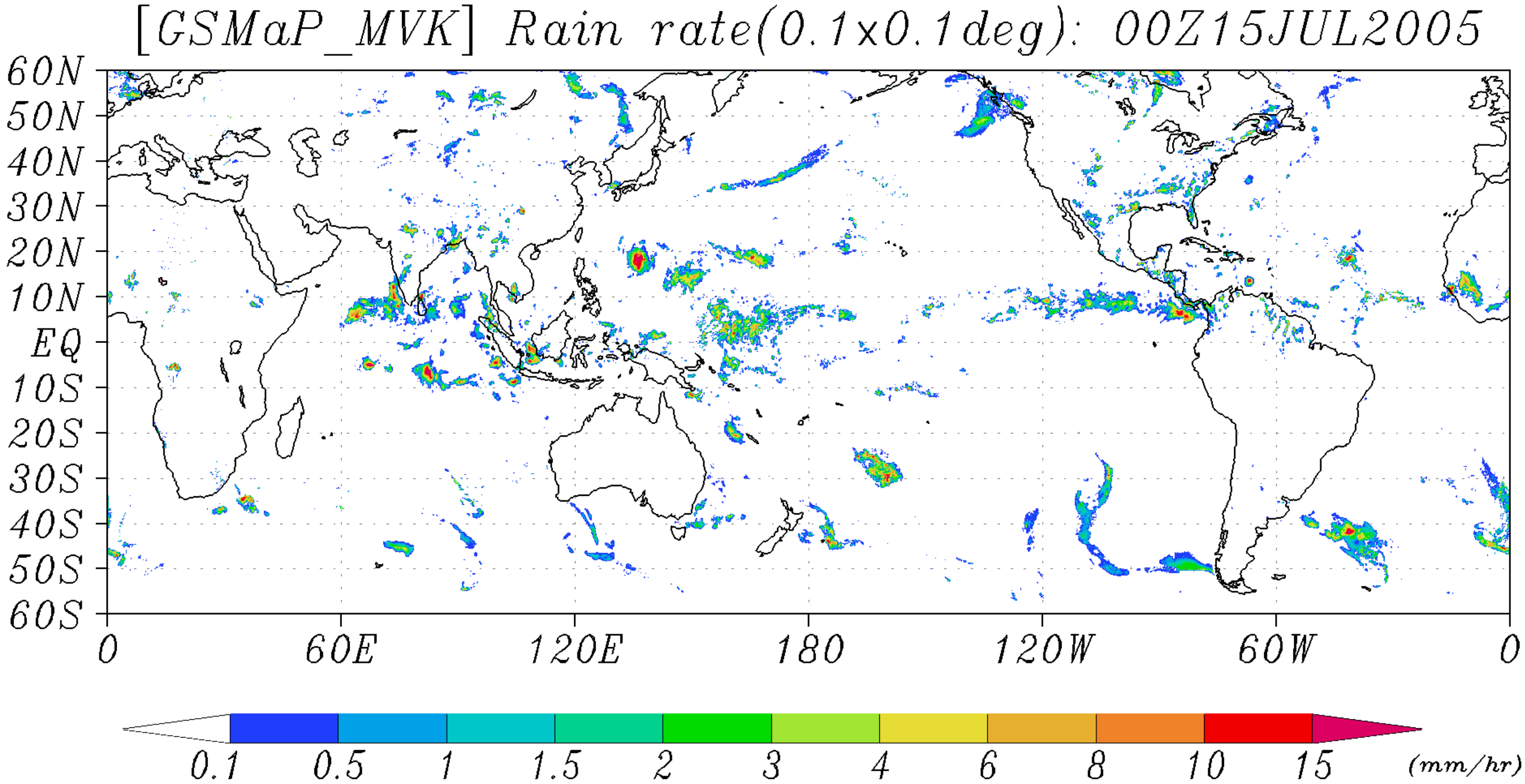
[GSMaP_MVK] Rain rate(0.1x0.1deg): 00Z15JUL2005
60N
50N
40N
30N
20N
10N
EQ
10S
20S
30S
40S
50S
60S
0
60E
120E
180
120W
60W
0
0.1
0.5
1
1.5
2
3
4
6
8
10
15
(mm/hr)

Combined global precipitation map

-MW radiometer + cloud motion vector with Kalman filter-

(0.1˚ , 1 hour, 8-10 July 2005)

MVK: MWR(TMI+AMSR+AMSR-E+F13, 14, 15 SSM/I)
+IR Cloud Motion Vector +Kalman Filter

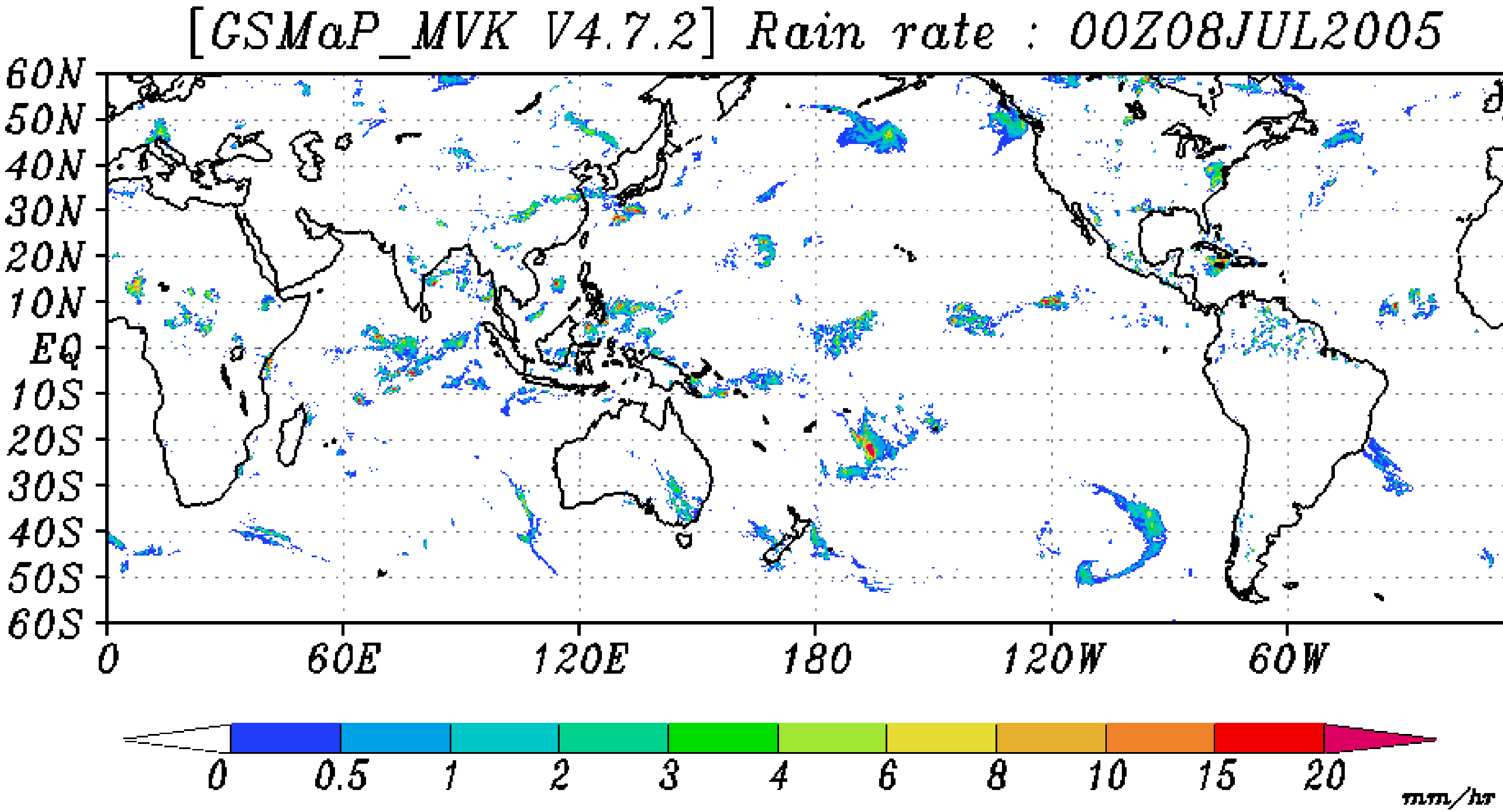

赤外・マイクロ波放射計 複合アルゴリズムによる降水量(2005年7月9～10日)

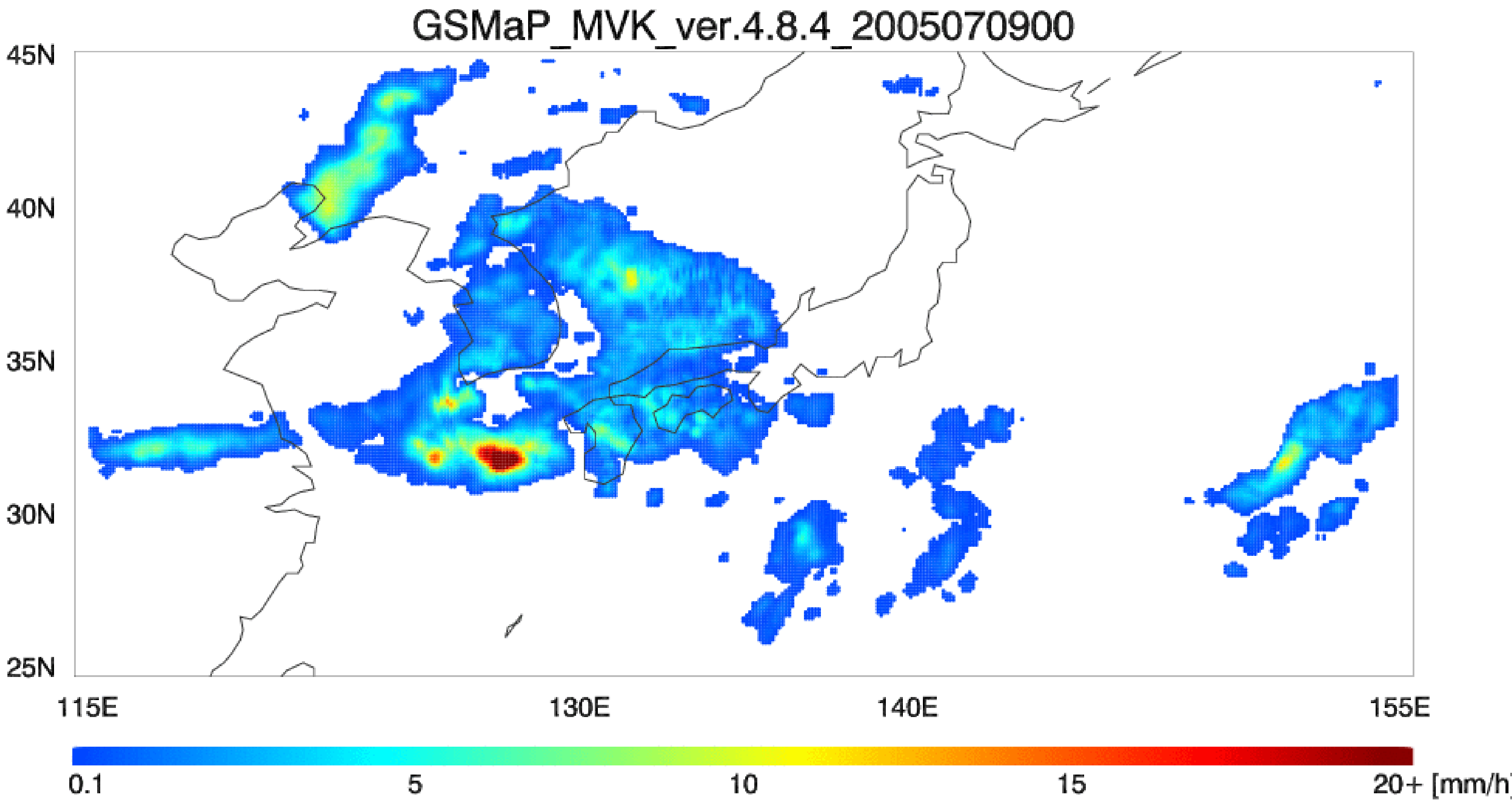

赤外・マイクロ波放射計 複合アルゴリズムによる降水量（台風200507号/BANYAN）

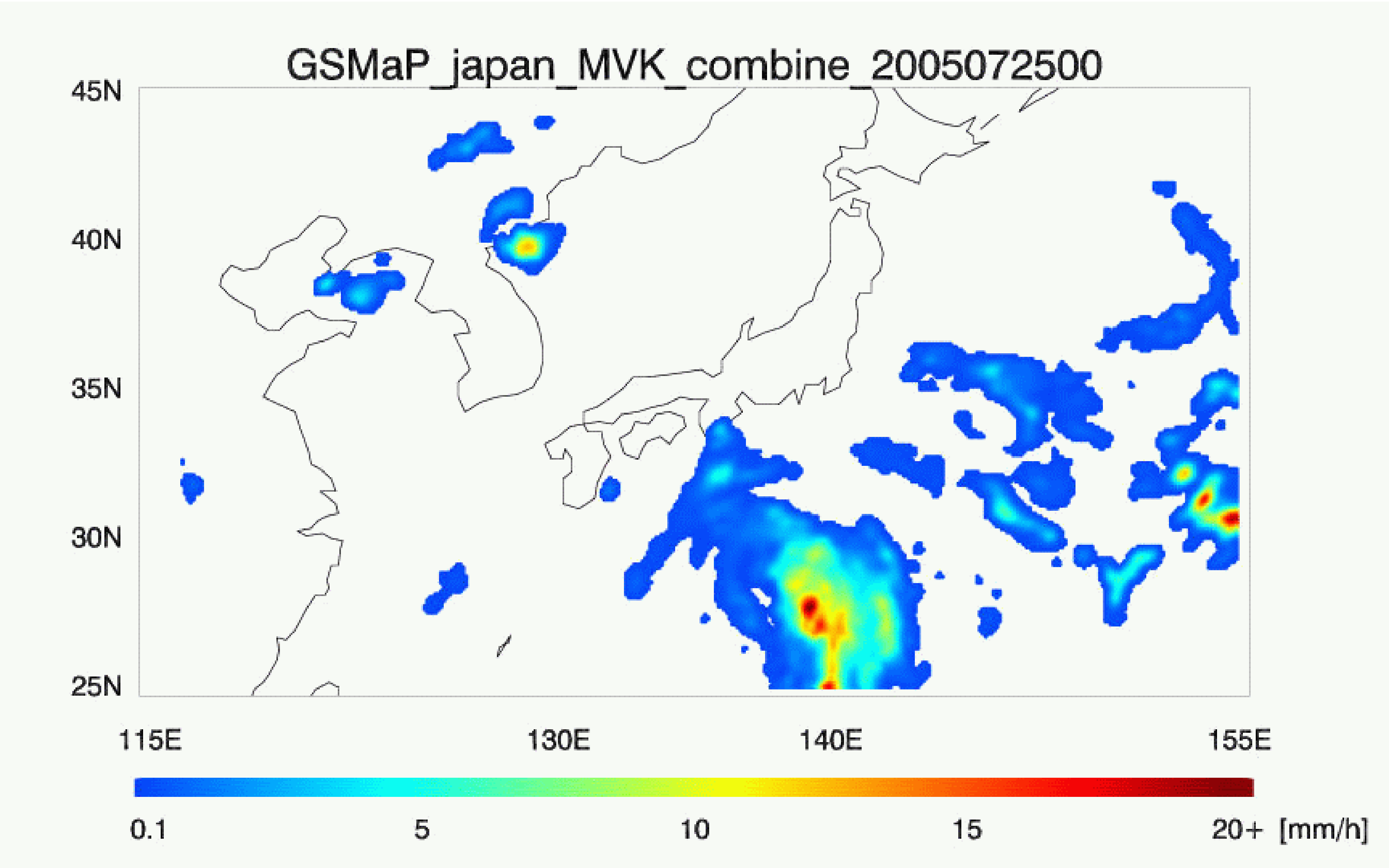

Correlation between radar and the GSMaP product as a function of the past microwave satellite overpass

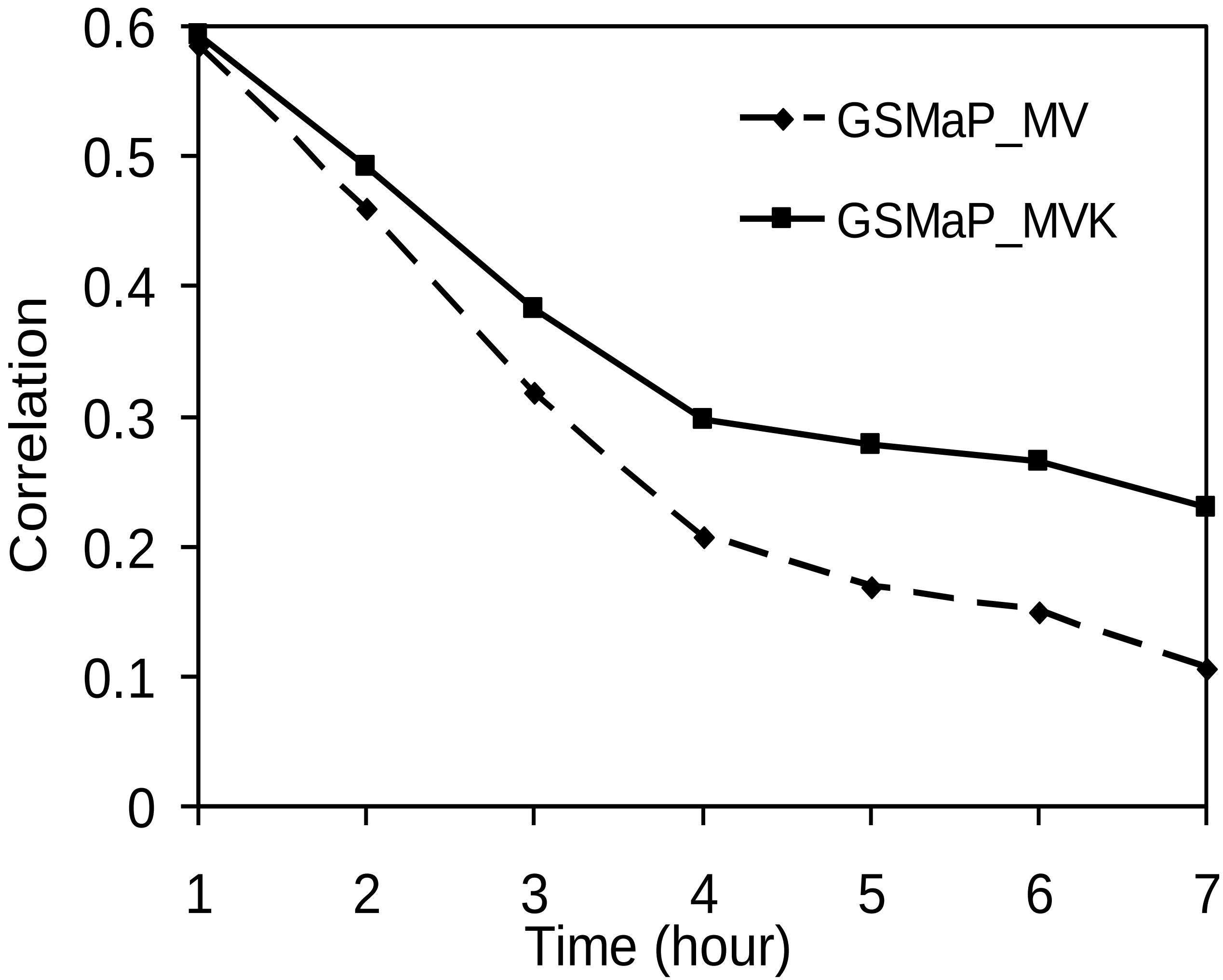

VALIDATION OF THE PRECIPITATION PRODUCTS

Hurricane Katrina – August 2005

TRMM 3B42, CMORPH, NRL, PERSIANN

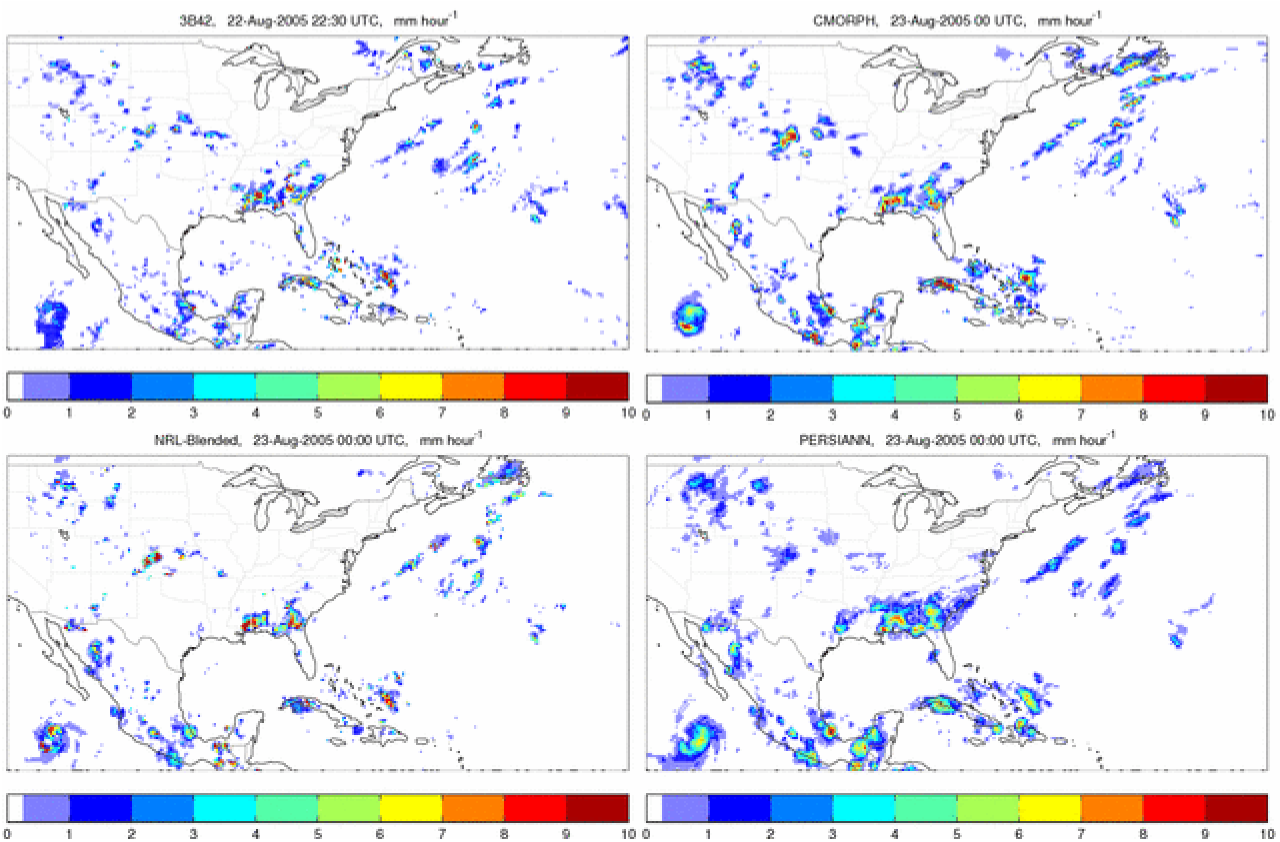

These products are very impressive, but how good are they really?

It is important to evaluate these new high resolution precipitation products to understand their errors and to identify a path to a consensus product that can be combined with gauge observations and other appropriate information and used for scientific and social applications

Program for the Evaluation of High Resolution Precipitation Products (PEHRPP)

- A comprehensive hypothesis-based collaborative effort to understand the capabilities and characteristics of these new HRPP (High Resolution Precipitation Products)
- Hypotheses:
  - HRPP errors can be characterized by comparing them to independent observations from rain gauges and radars.
  - Errors of and differences between HRPP are meaningful, in that they can be systematically related to precipitation characteristics and/or algorithm methodology.
  - Improved HRPP can be derived by combining products or methods based on the observed errors and differences.
  - HRPP spatial and temporal variability is realistic on scales appropriate for scientific studies (e.g., hydrology).
  - Numerical weather prediction forecasts of precipitation can be used to improve HRPP in some locations and times (e.g., high latitudes).
- Sponsored by the International Precipitation Working Group (Working Group of CGMS) with broad voluntary participation

PEHRPP Consists of 4 Suites of Activities

Suite 1: Continental/Regional Comparisons

- Large areas, long (continuous) time periods
- Daily/0.25° x0.25° areas

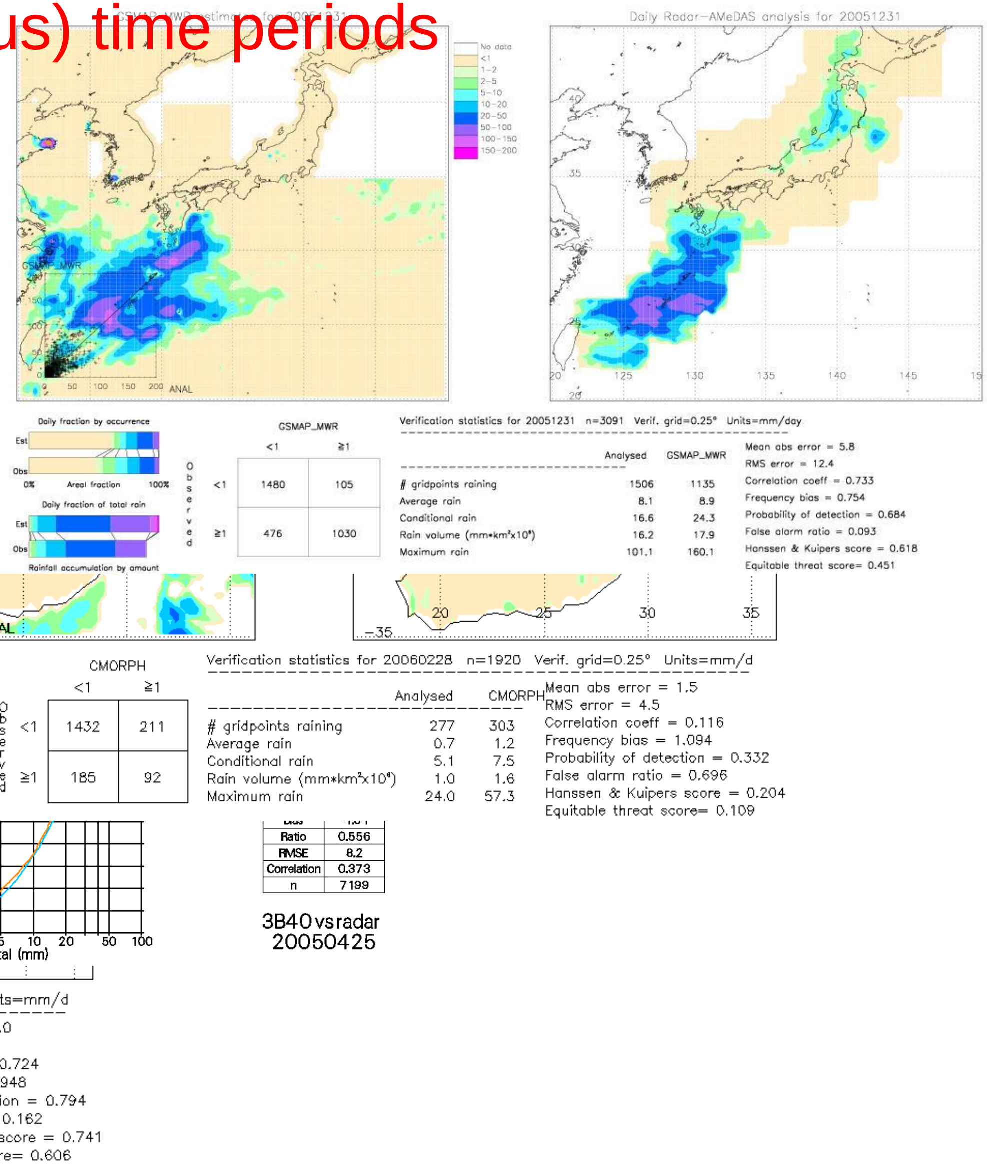

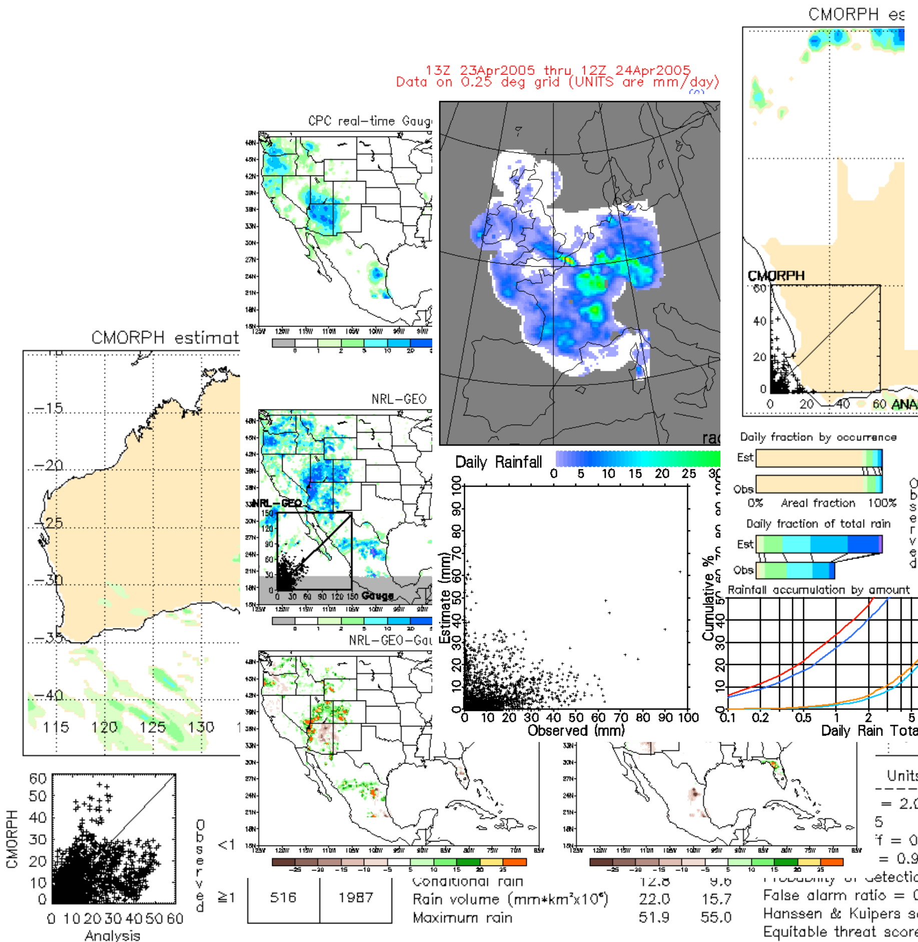

Current/Proposed PEHRPP Suite 1 Validation Sites

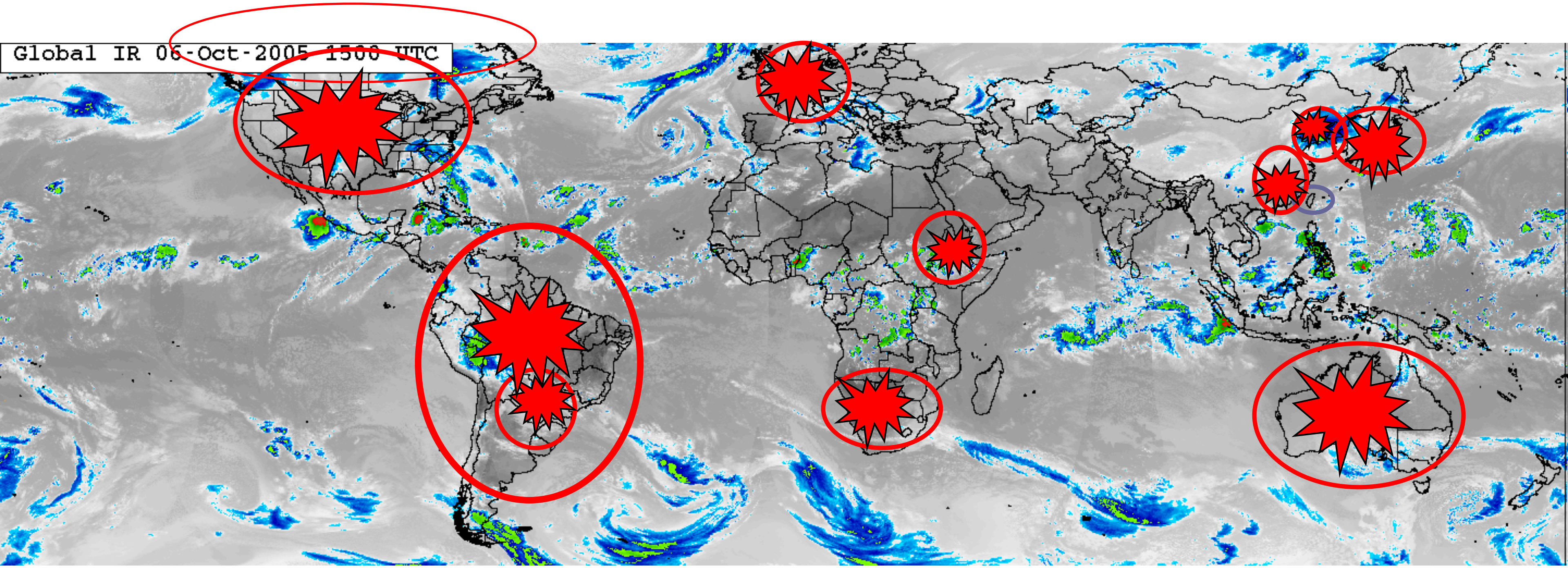

Original:
Australian continent (Ebert), CONUS (Janowiak), UK/Europe (Kidd)

New:
South America (Vila), S Africa (Pegram), Korea (Sohn), Taiwan (Jou), Japan (Ushio), Ethiopia/Sub-Saharan Africa (Dinko), Guangdong (Liang)…

Validation

GSMaP_MVK

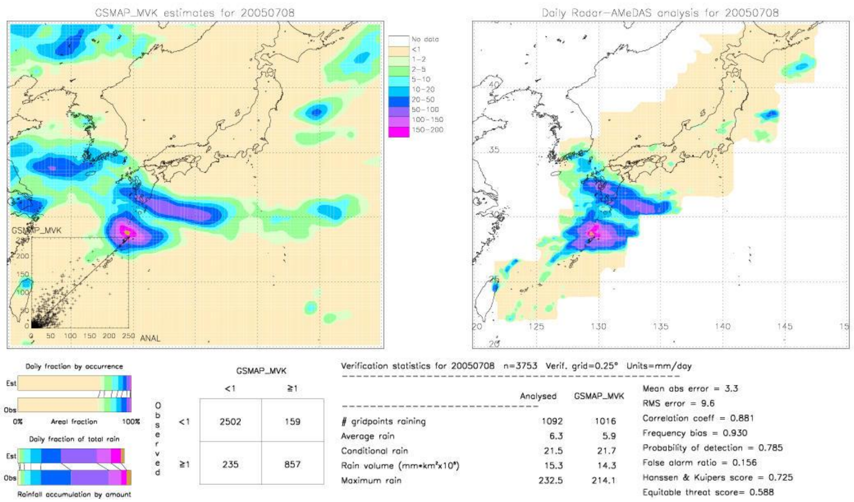

GSMaP_MWR

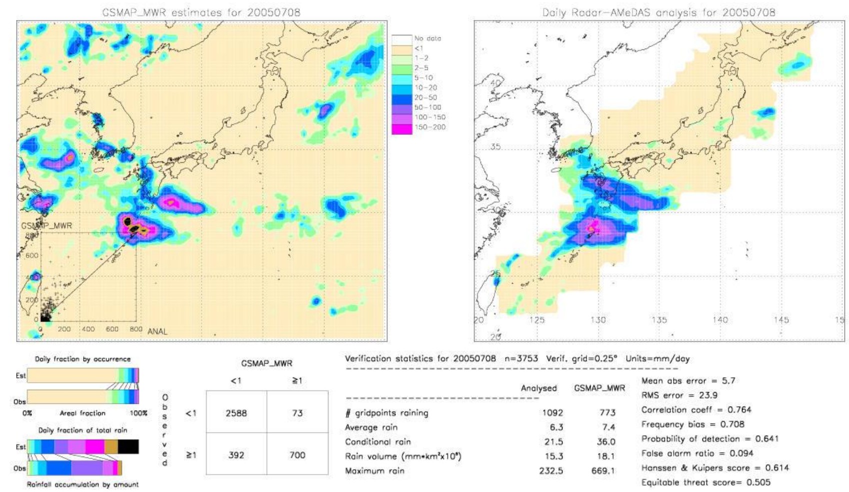

CMORPH(NOAA/CPC)

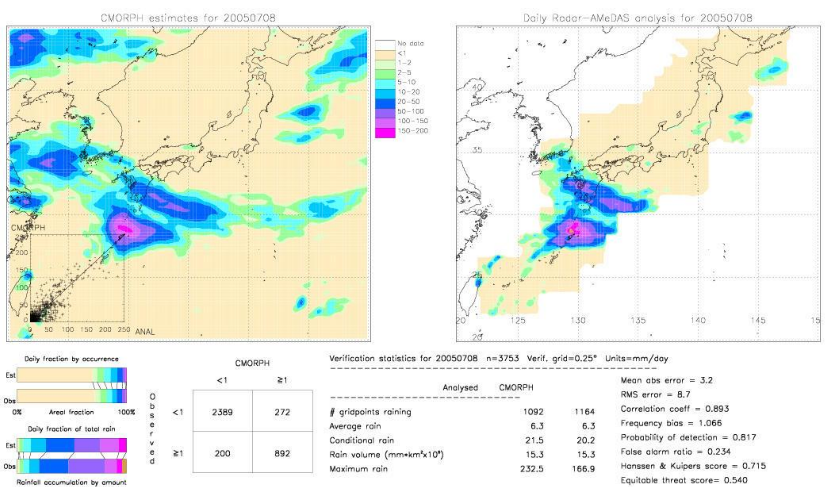

3B42RT(NASA)

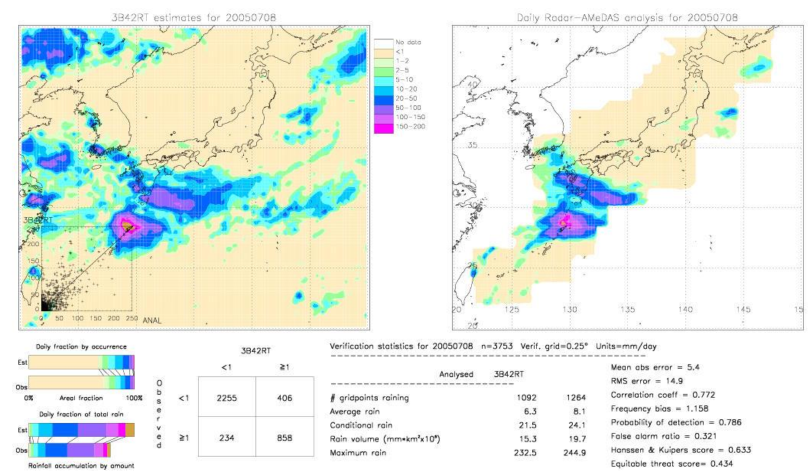

Example of validation of GSMaP_MVK using Radar-AMeDAS (8 July 2005)

GSMaP_MVK

Radar-AMeDAS

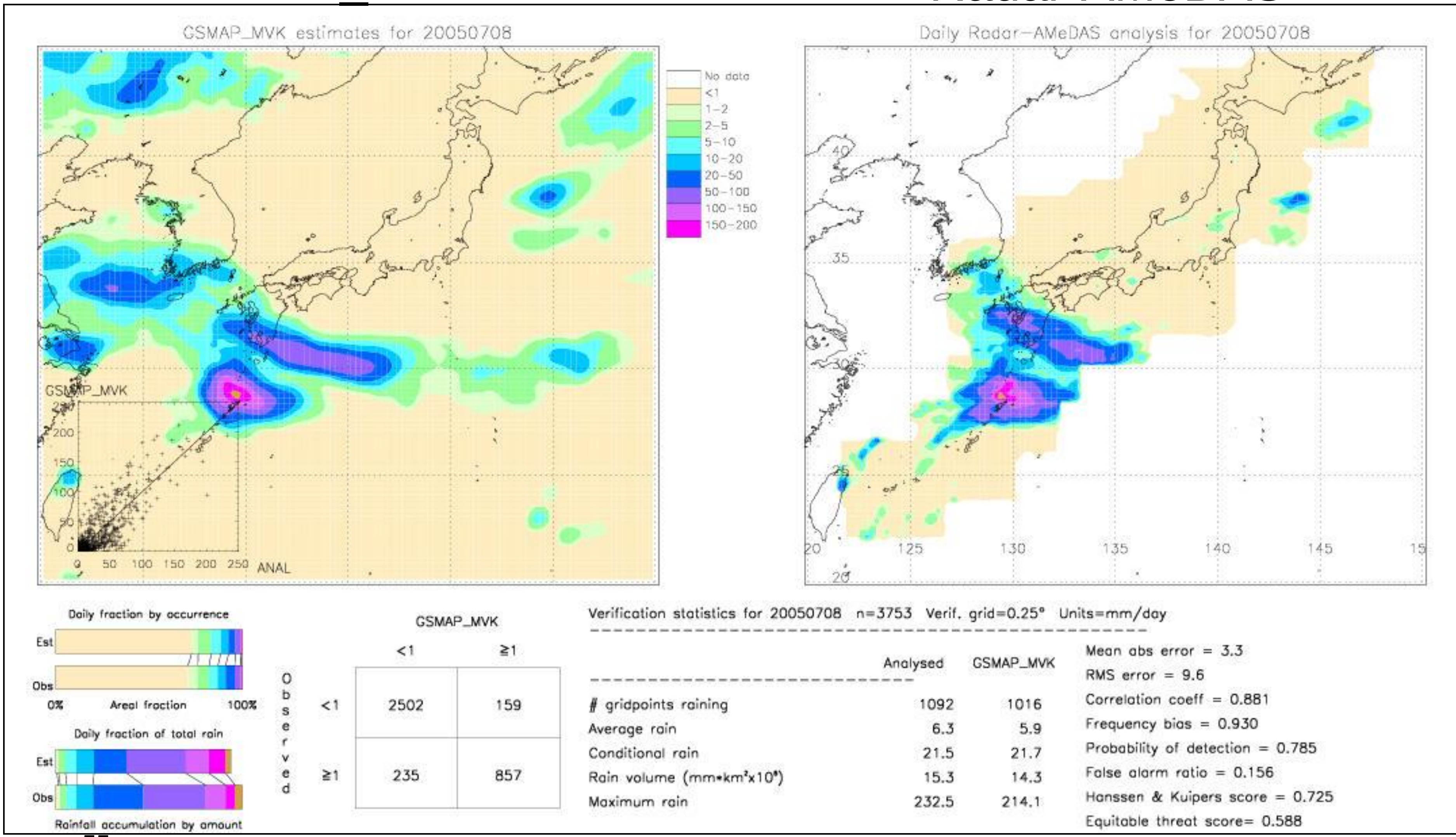

Evaluation of various high resolution precipitation map using Radar-AMeDAS rain map

Daily variation of correlation coefficient (0.25° ×0.25°)) July, 2005

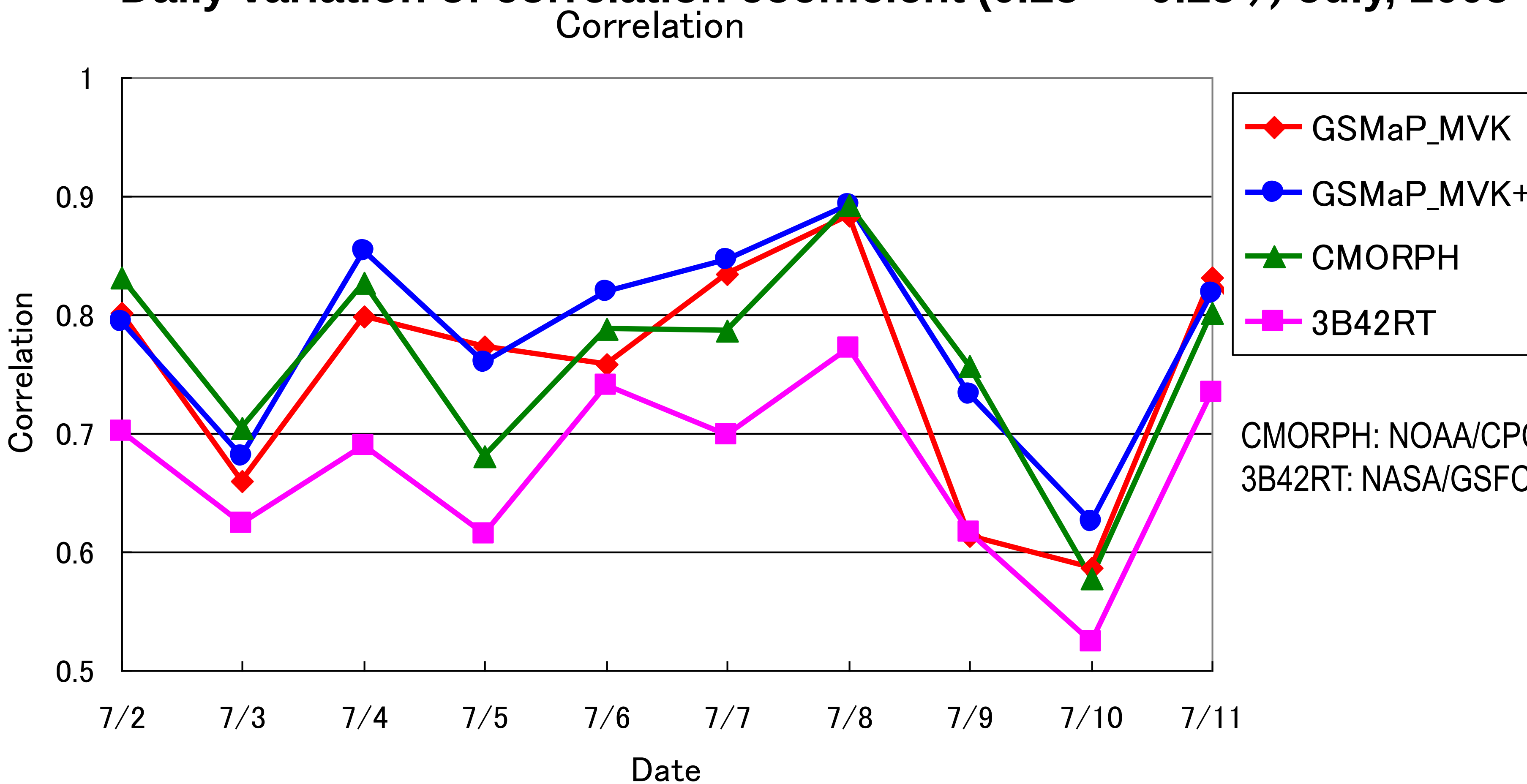

CMORPH: NOAA/CPC
3B42RT: NASA/GSFC

GSMaP_MVK shows high correlation with Radar-AMeDAS throughout the period.

GSMaP_MVK+, produced by adding NOAA AMSU rain rates to GSMaP_MVK, shows particularly high correlation.

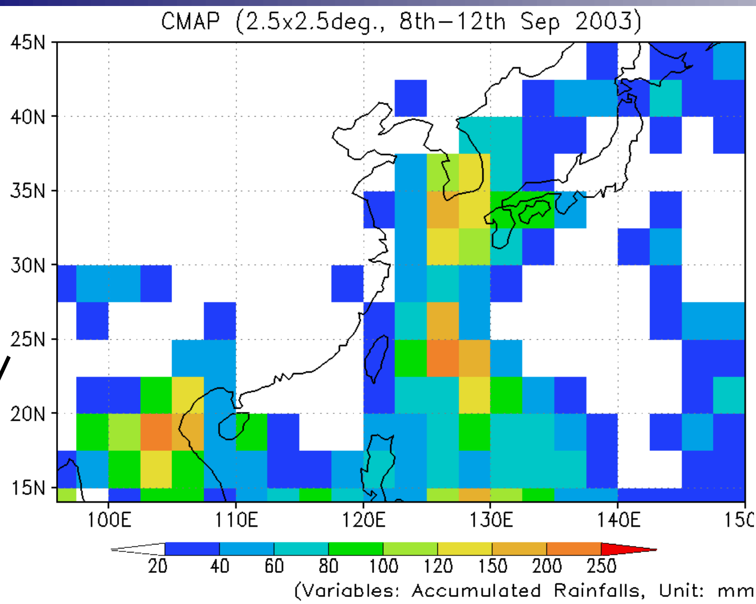

CMAP
(NOAA/
CPC)

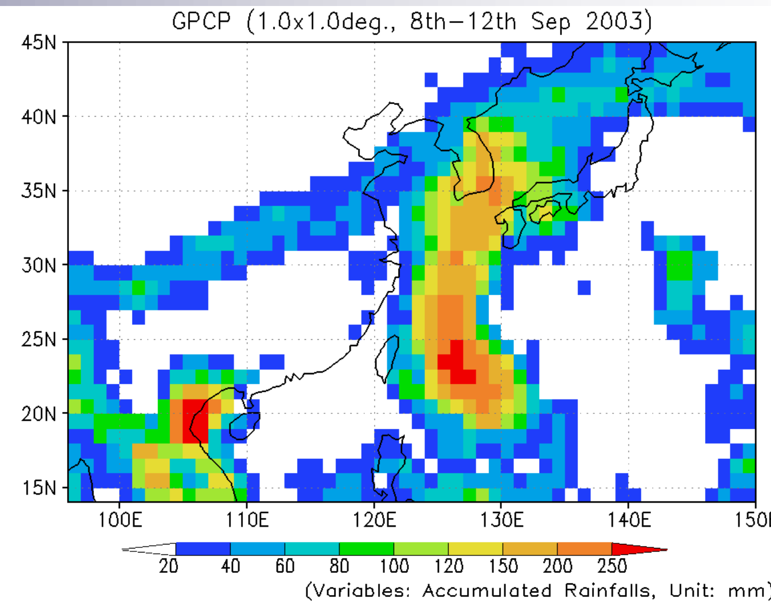

GPCP
Daily
(NASA/
GSFC)

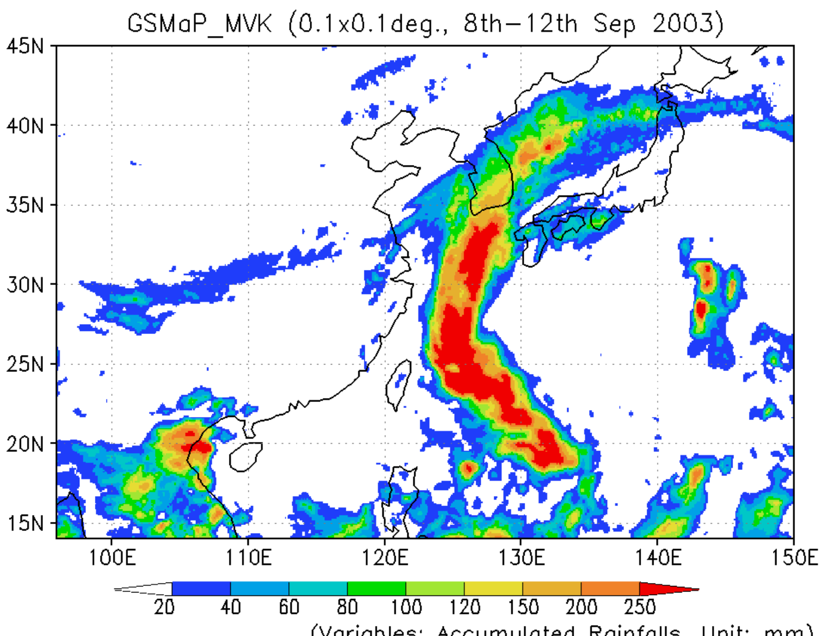

GSMaP

降水マップの比較

(8-12 Sept. 2003)
(左上):CMAP, 2.5° 格子
(右上):GPCP Daily, 1.0° 格子
雨量計と衛星推定雨量
(IR, SSM/I, TOVS)複合
(左下):GSMaP, 0.1° 格子
衛星推定雨量(TMI, AMSR-E, SSM/I)のIR補間

REAL TIME SYSTEM FOR APPLICATION

Construction of System for Near-Real-Time Global Rainfall Maps by GSMaP algorithms

JAXA/EORC has started to release global rainfall data in near real time (about four hours after observations) on the Internet using GSMaP algorithms.

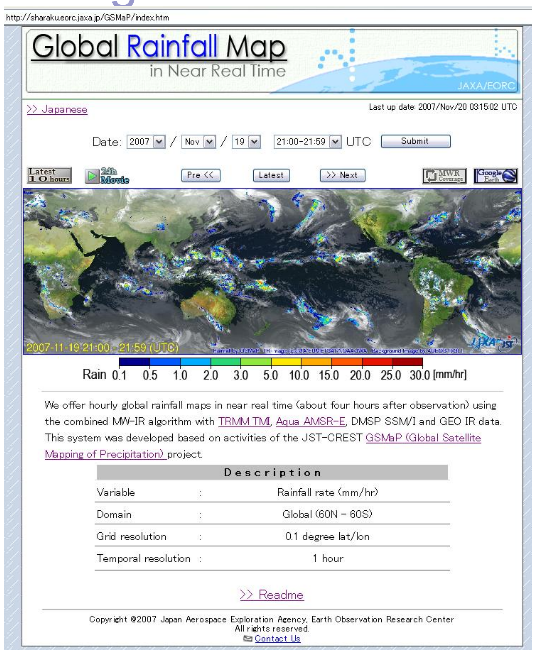

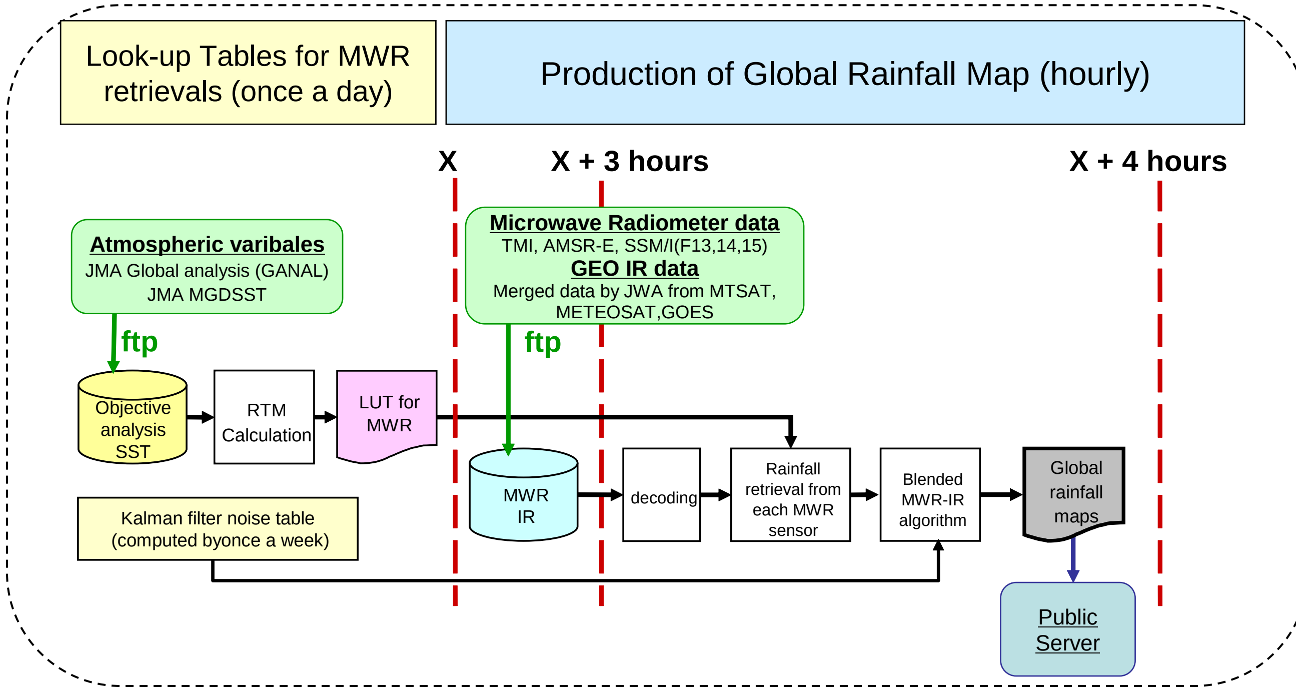

GSMaP NRT System in JAXA/EORC

Global Rainfall Map in Near Real Time by JAXA/EORC
http://sharaku.eorc.jaxa.jp/GSMaP/

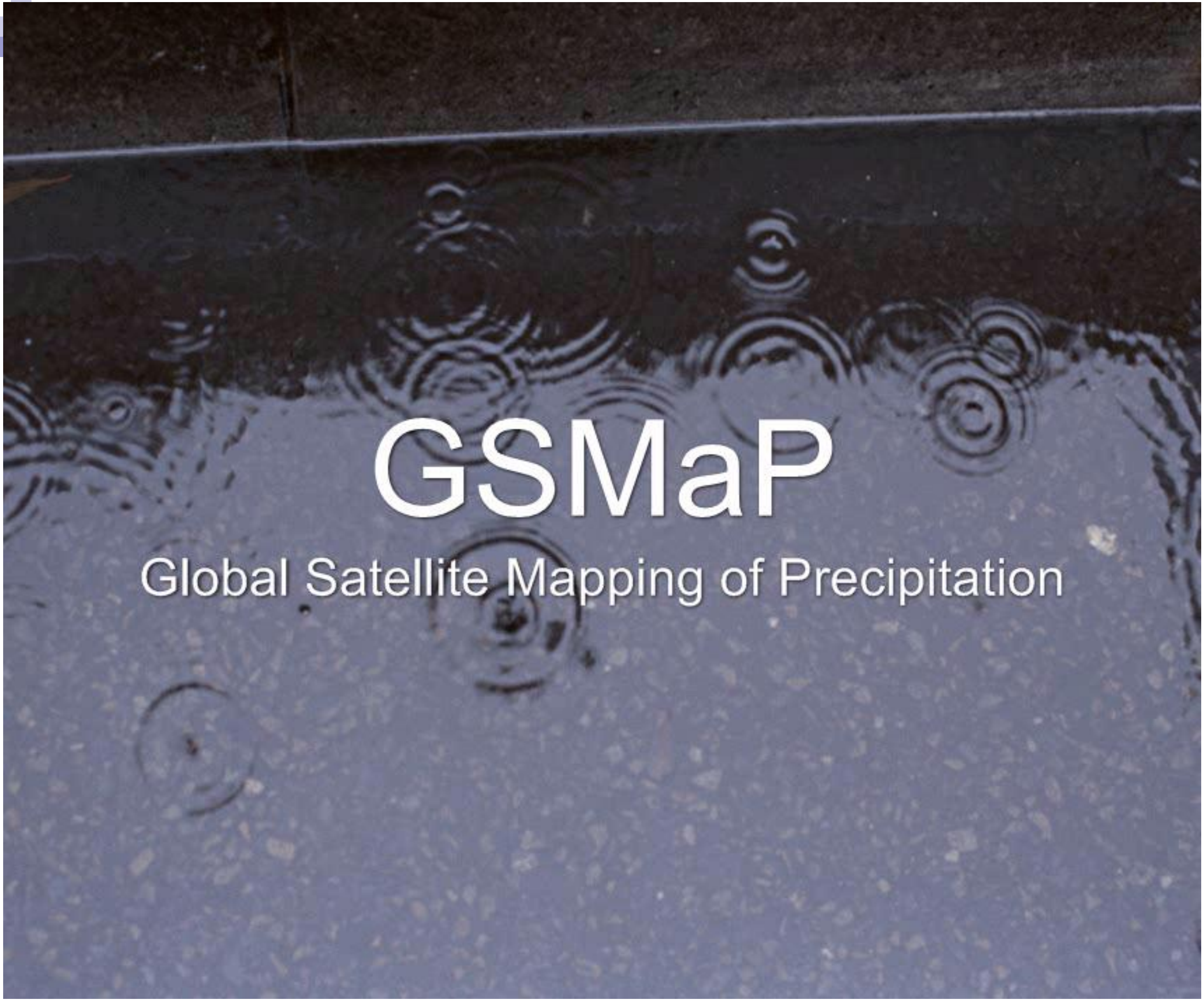
GSMaP
Global Satellite Mapping of Precipitation

Six hourly animation

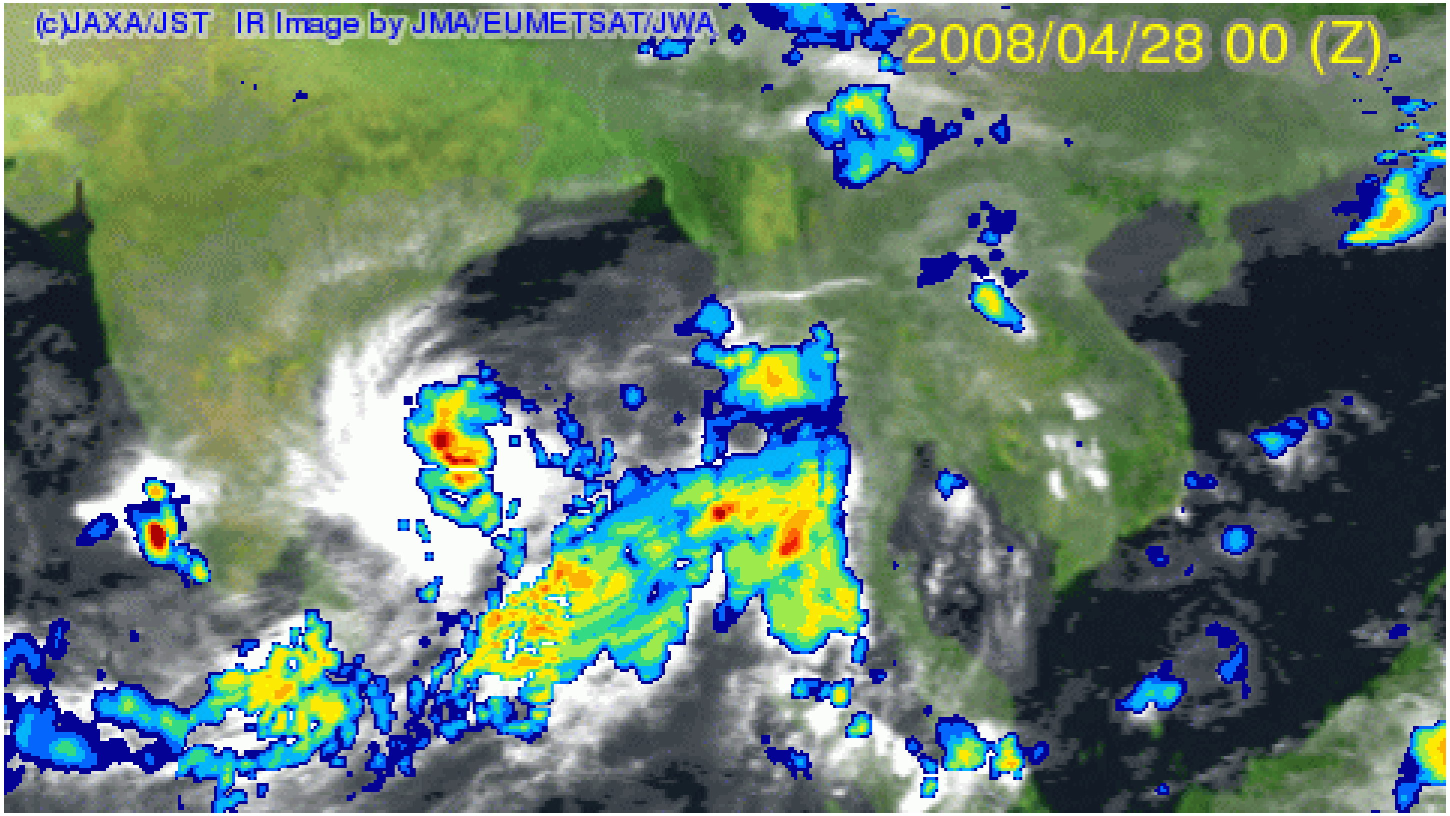

Accumulated rainfall amount from Apr. 27 to May 5

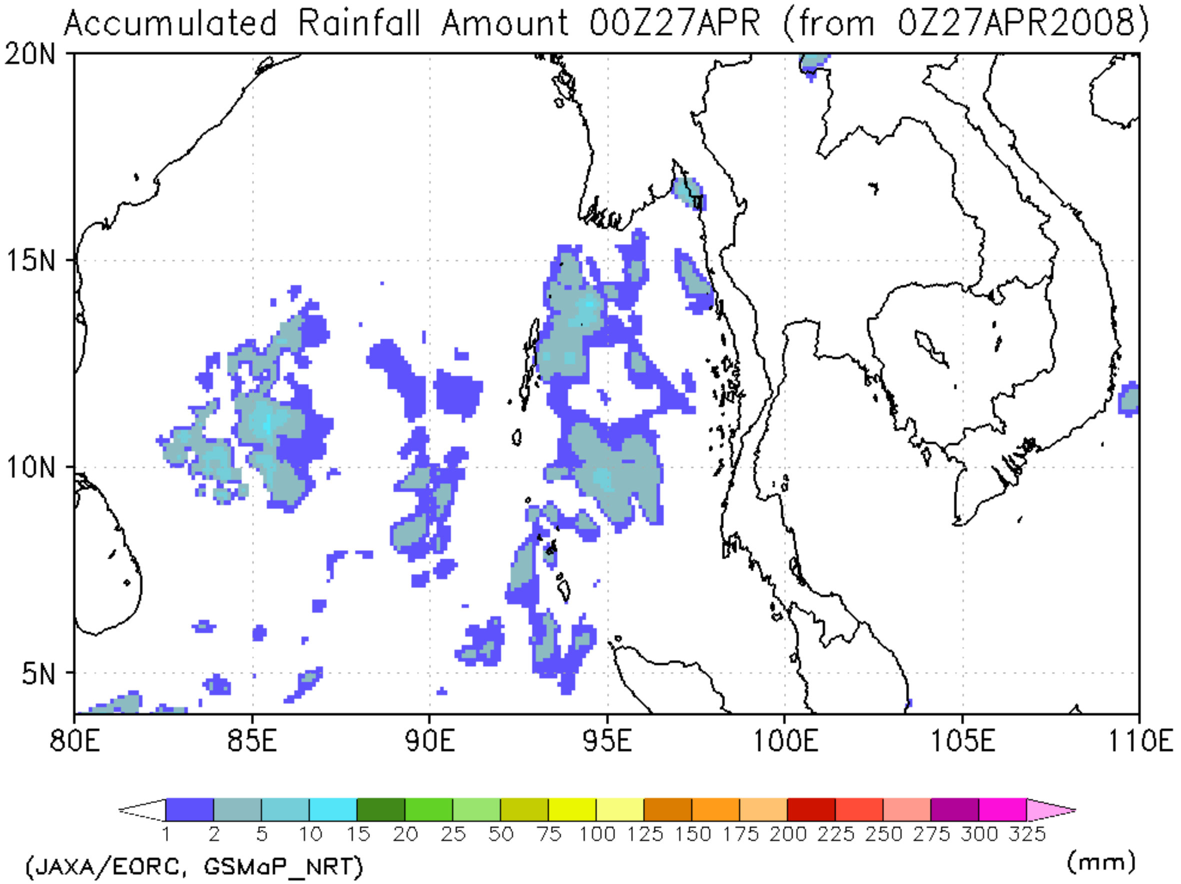

Reference

- Ushio, T., K. Sasashige, T. Kubota, S. Shige, K. Okamoto, K. Aonashi, T. Inoue, N. Takahashi, T. Iguchi, M. Kachi, R. Oki, T. Morimoto, and Z-I. Kawasaki, A Kalman Filter Approach to the Global Satellite Mapping of Precipitation (GSMaP) from Combined Passive Microwave and Infrared Radiometric Data, J. Meteor. Soc. Japan, Vol. 87A, 2009

Summary

- Needs for IR and MWR integration method are described.

- Some of the high resolution products are introduced.

- GSMaP_MVK product was introduced.

Precipitation measurement in global warming era

Kenji Nakamura
Hydrospheric Atmospheric Research Center
Nagoya University

International Hydrological Programme
Precipitation Measurement from Space and its Applications
The Twenty-second IHP Training Course
18 November - 1 December, 2012

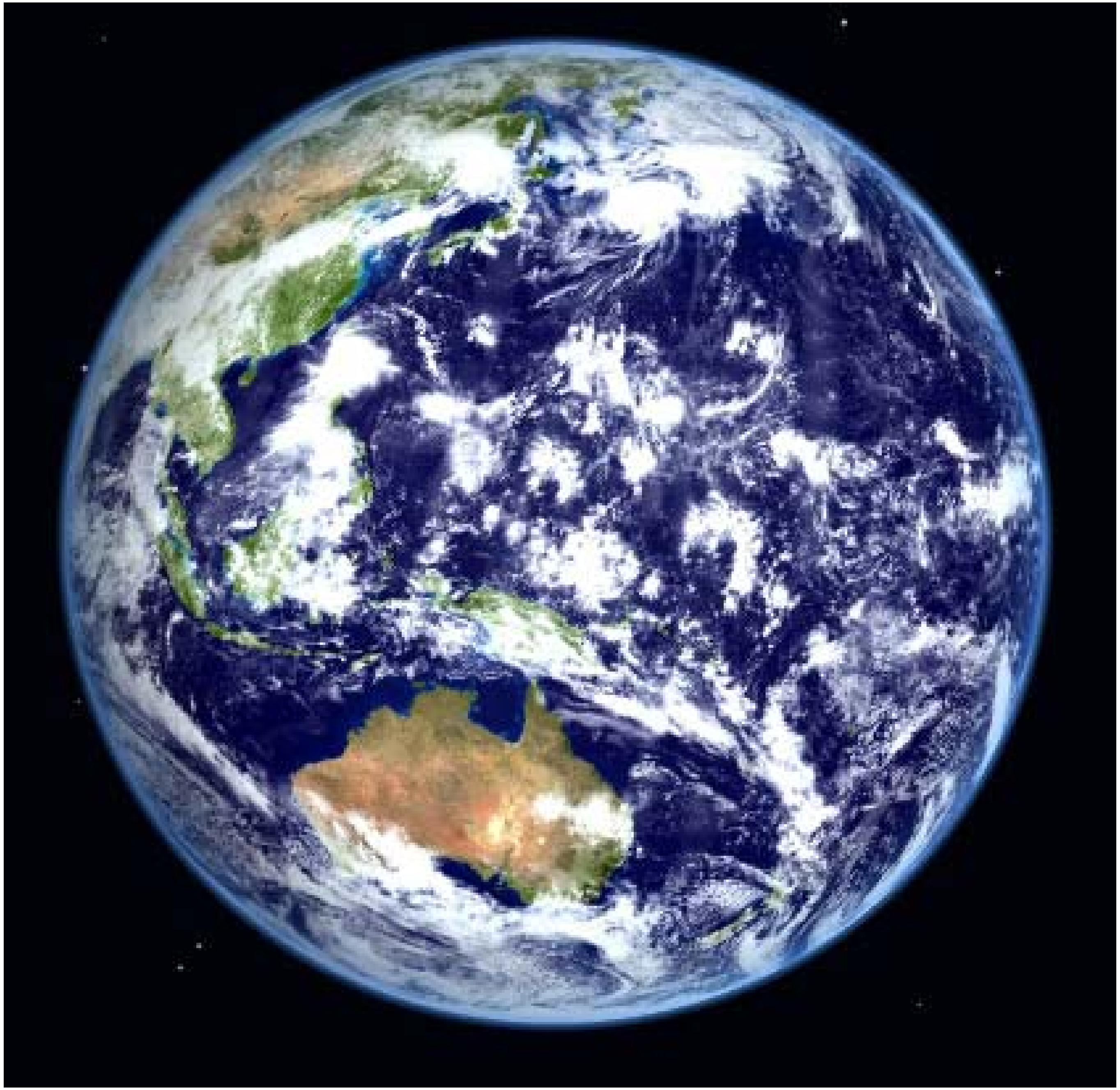

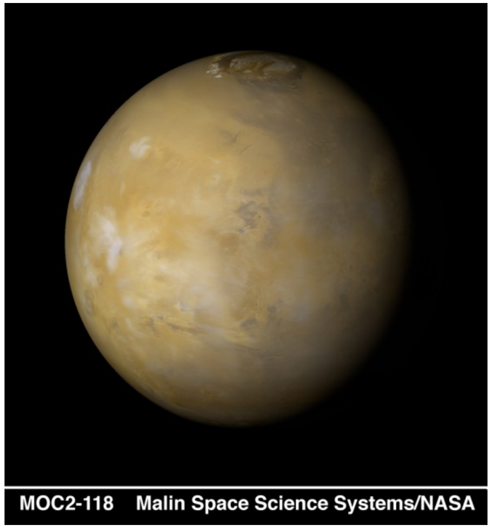

Mars

Venus

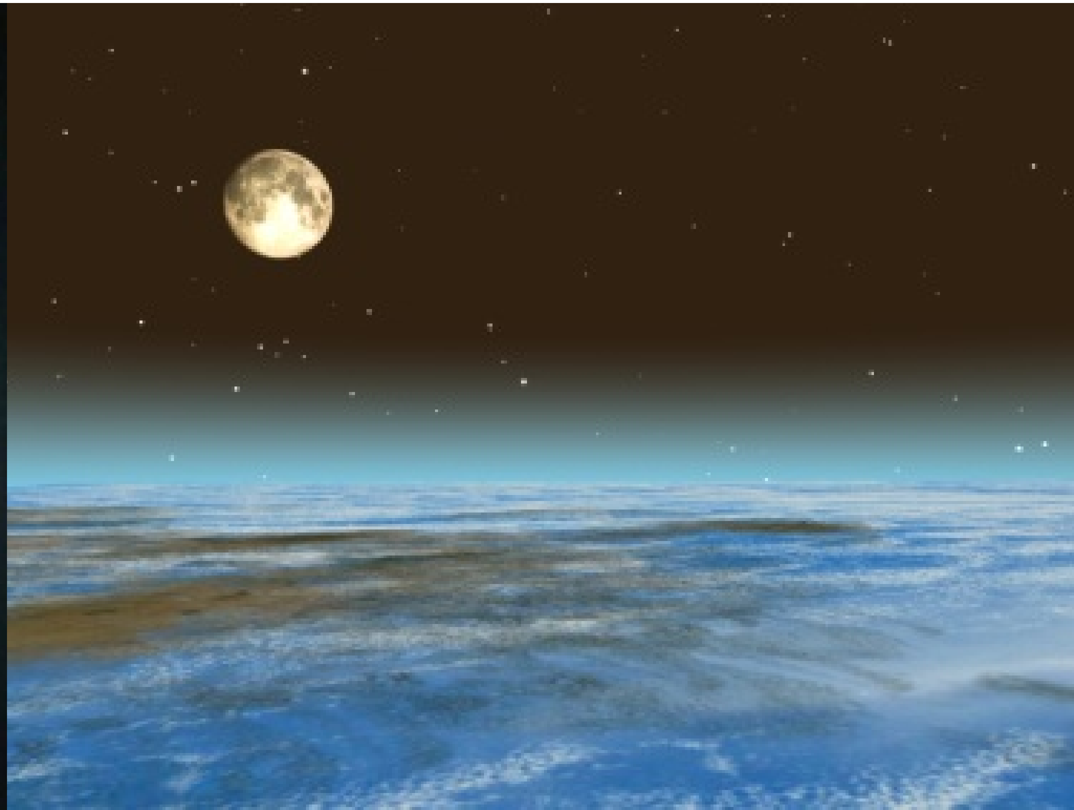

Eclipse by Earth.
Thin atmosphere

（http://www.jaxa.jp)

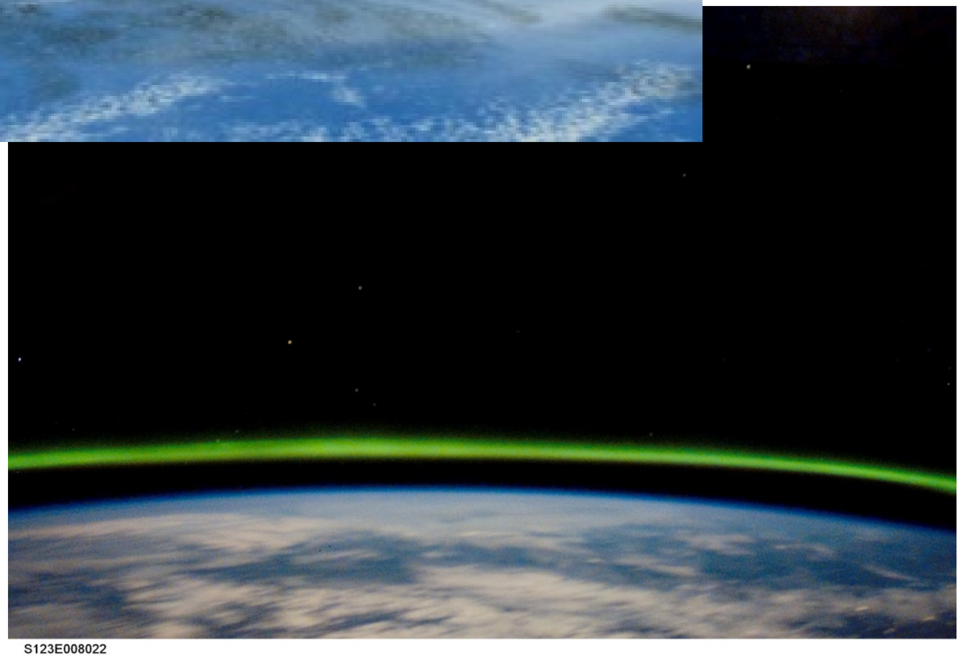

Aurola at 100-150km height. Green light is from atomic oxygen.

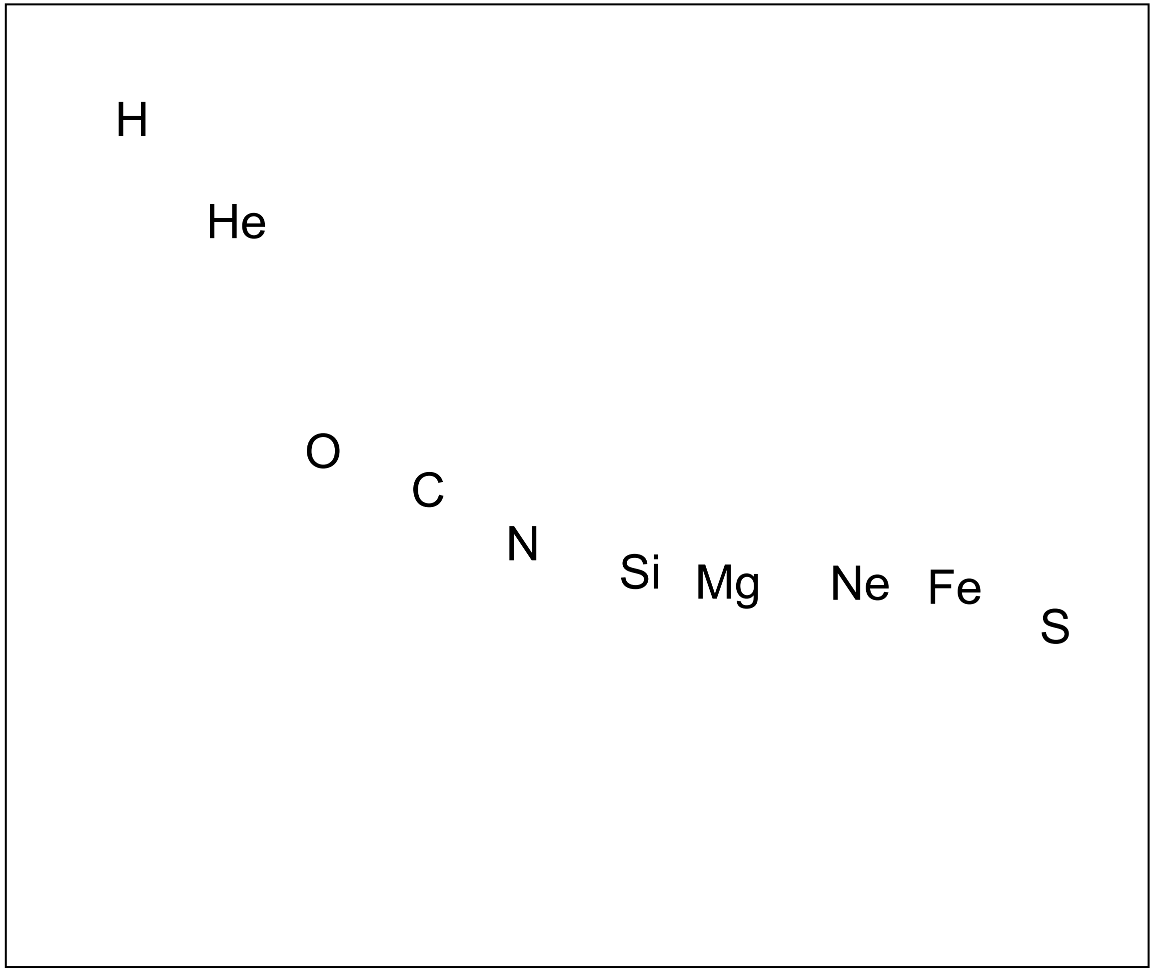

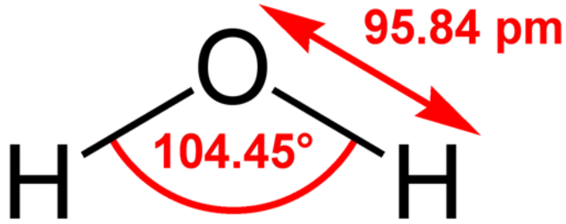

Water molecule

Electric diple

Hydrogen bond

- High melting, boiling temperature
- Large heat capacity
- High capability to solve materials
- Ice is lighter than water
- etc.

Number density of elements in solar system relative to 1 M hydrogen atoms.

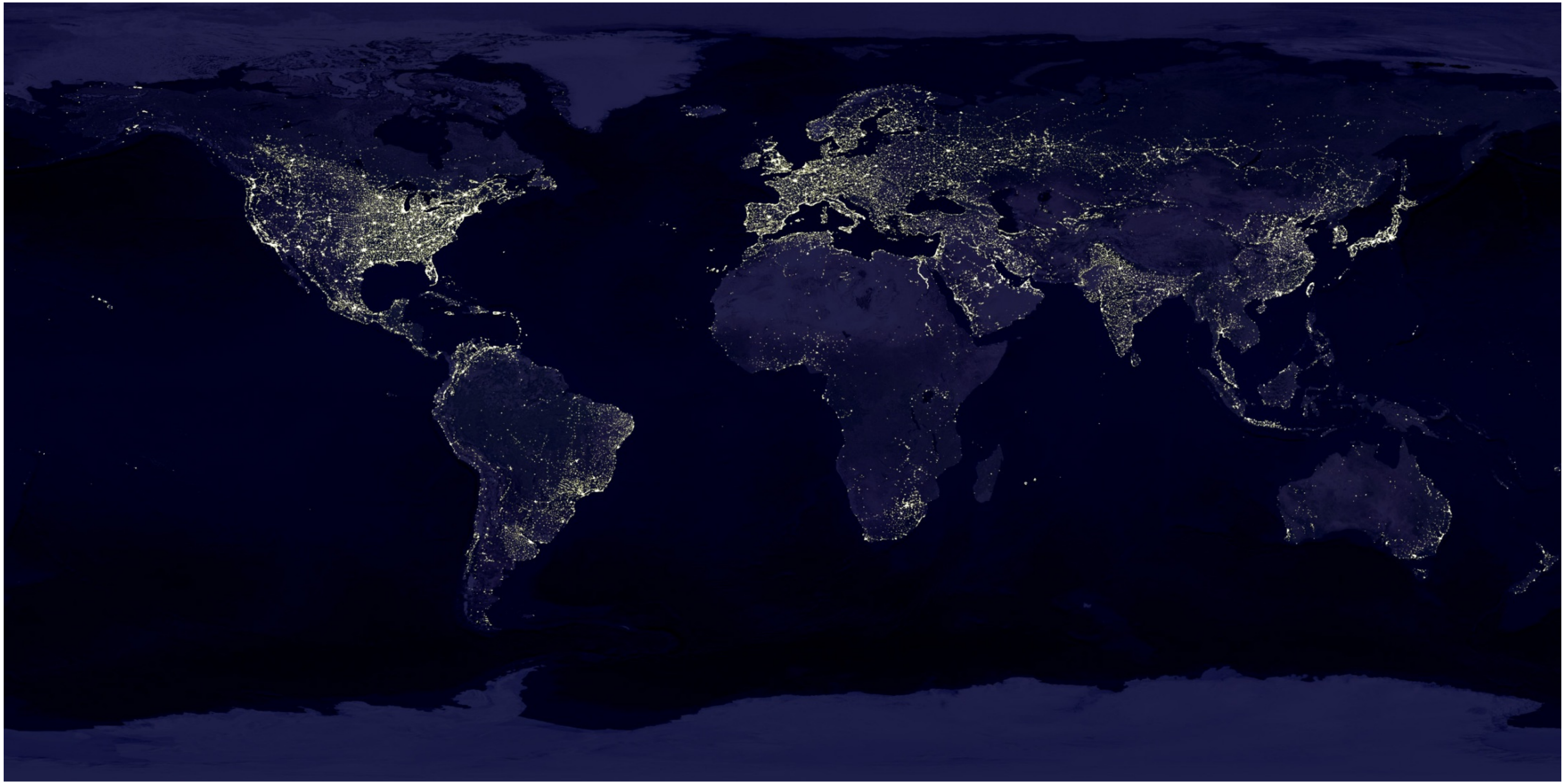

（from NASA website）

(from NASA website)

OZONE HOLE

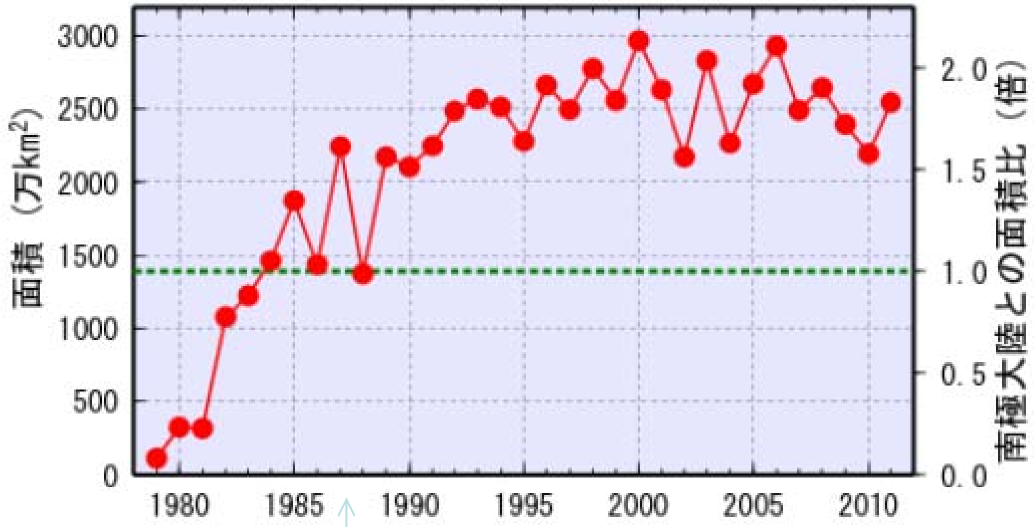

Monreal protocol

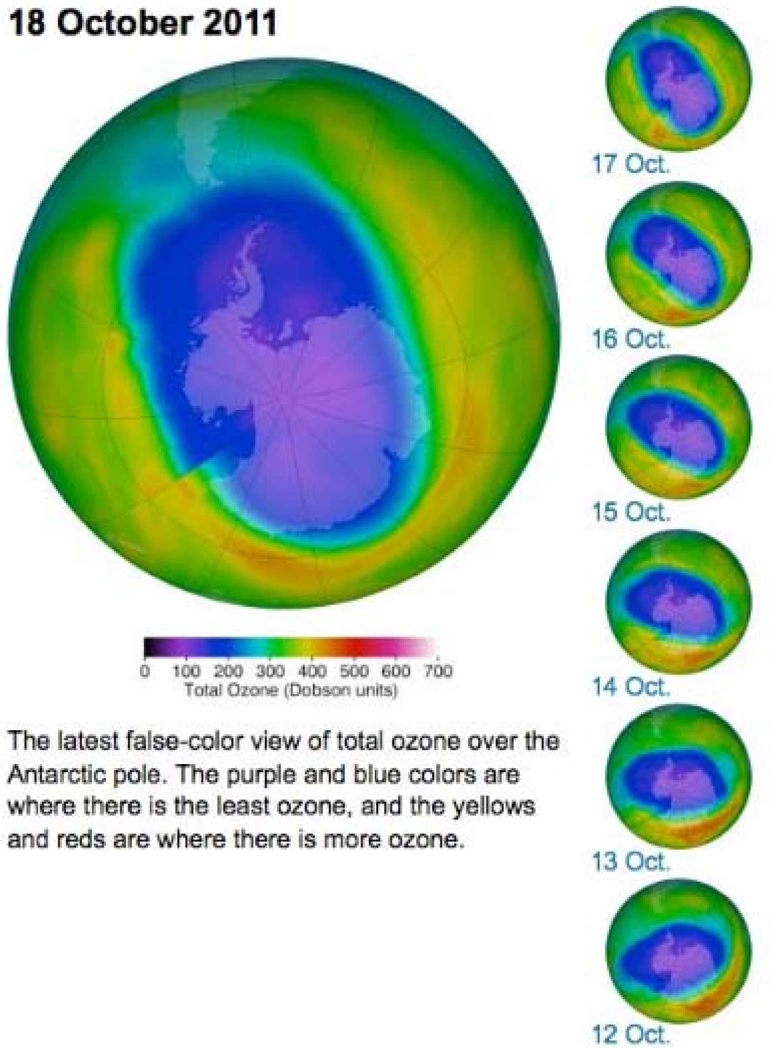

The latest false-color view of total ozone over the Antarctic pole. The purple and blue colors are where there is the least ozone, and the yellows and reds are where there is more ozone.

http://photozou.jp/photo
/

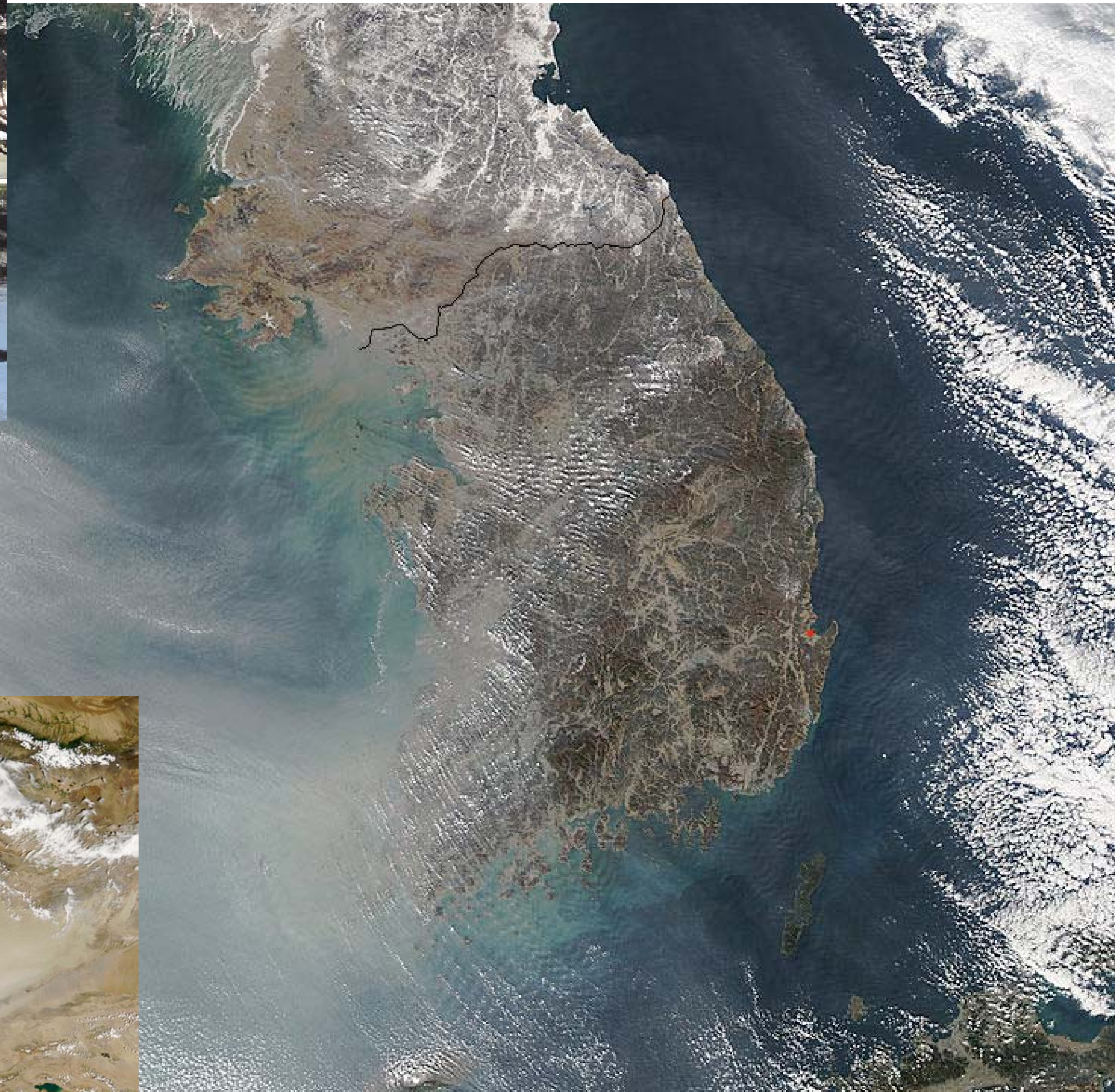

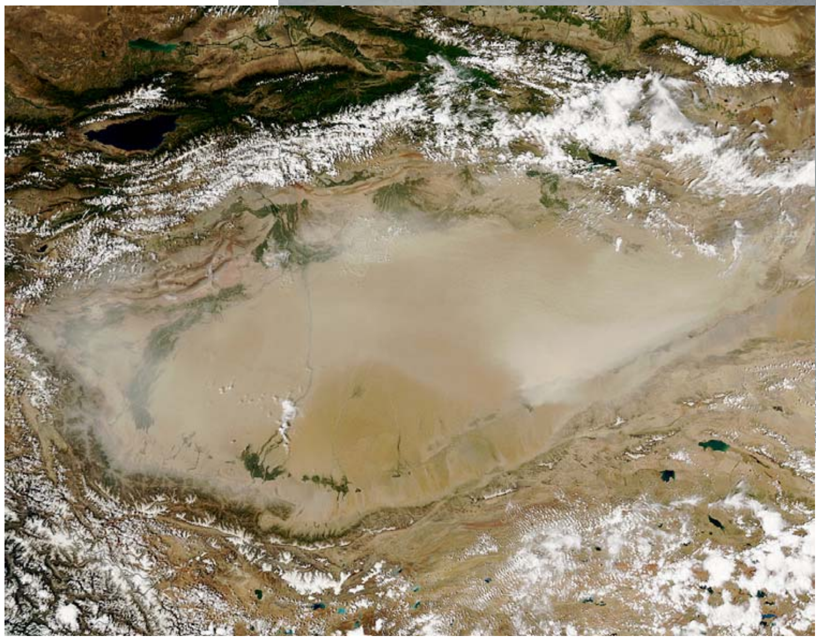

Long range transport of dust, aerosol

北極海の海氷密接度分布

2007年9月24日
Aqua/AMSR-E(アクア/アムサー・イー)

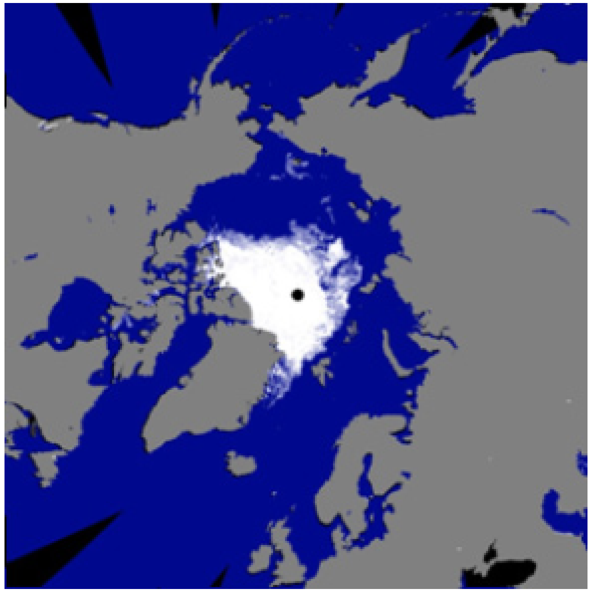

2012年8月24日
「しずく」/AMSR2(アムサー・ツー)[検証中]

Arctic Ice distribution

(from JAXA website)

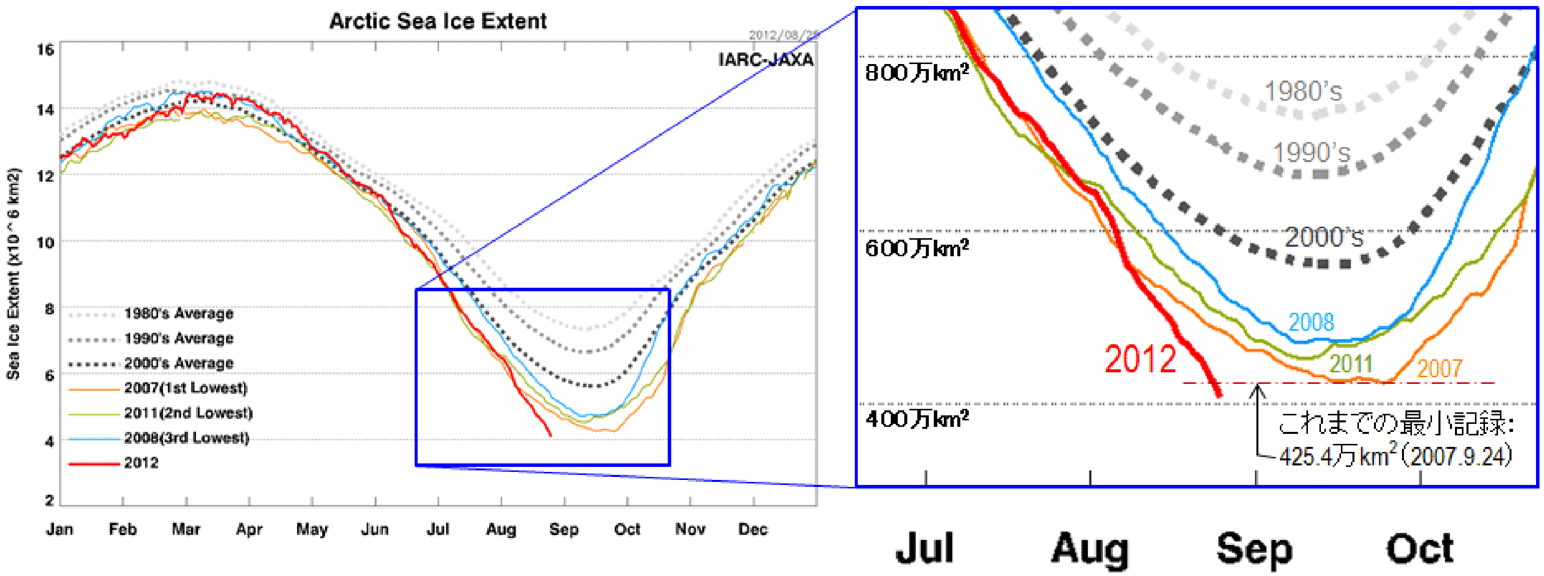

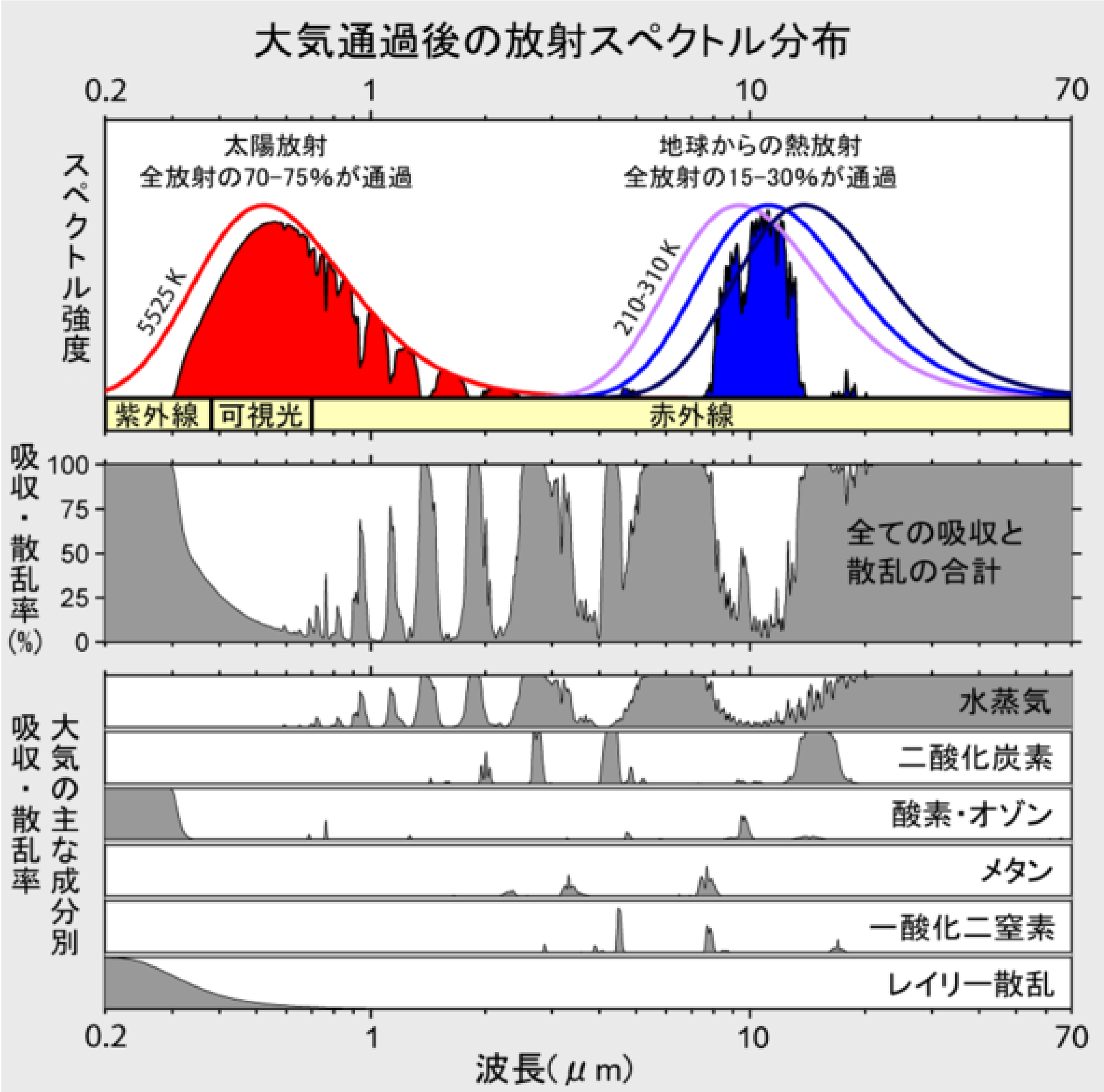

Spectra of incoming short waves and outgoing long waves (Wikipedia）

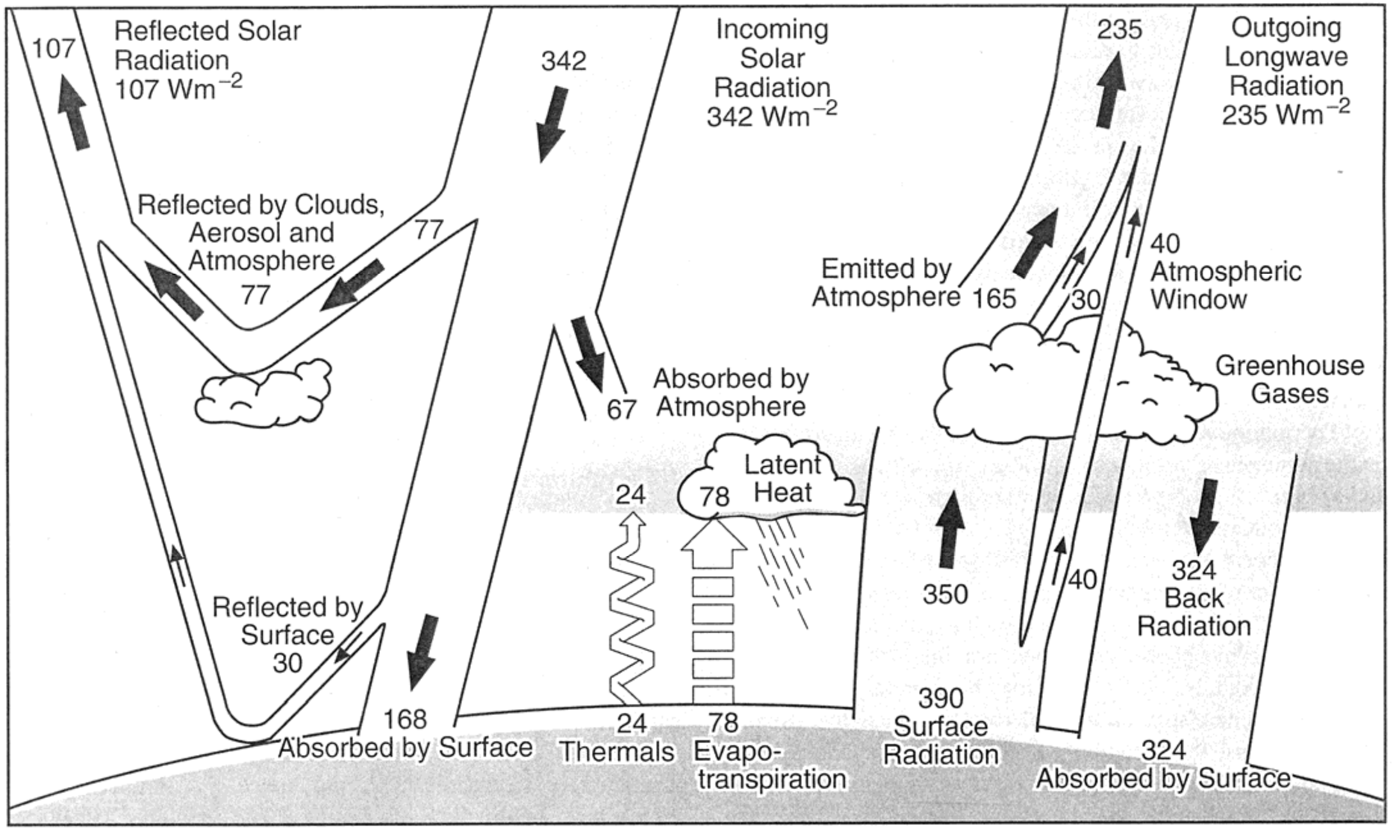

Energy budget of Earth surface（IPCC AR3）

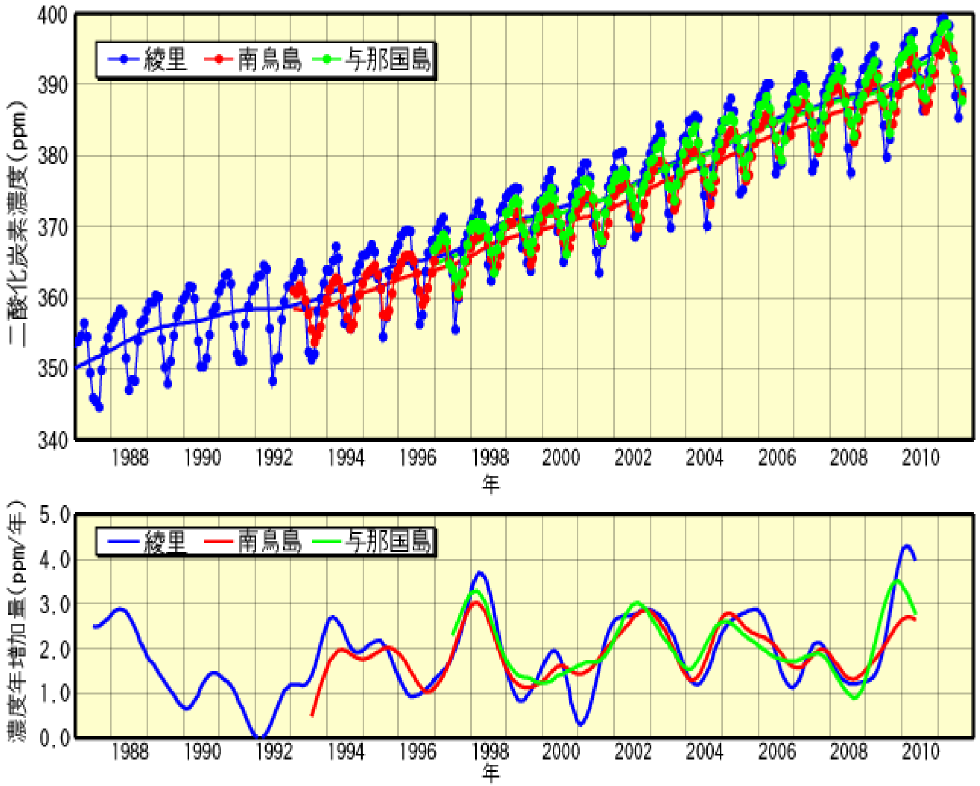

気象庁の観測点での大気中の二酸化炭素濃度(月平均値)と濃度年増加量の経年変化

Increase of CO_2

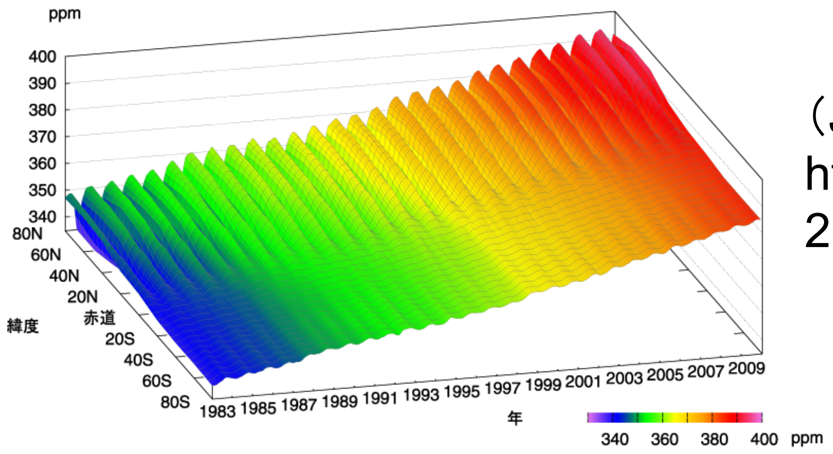

緯度帯ごとに平均した大気中の二酸化炭素濃度の変動

（JMA、http://ds.data.jma.go.jp/ghg/kanshi/ghgp/21co2.html）

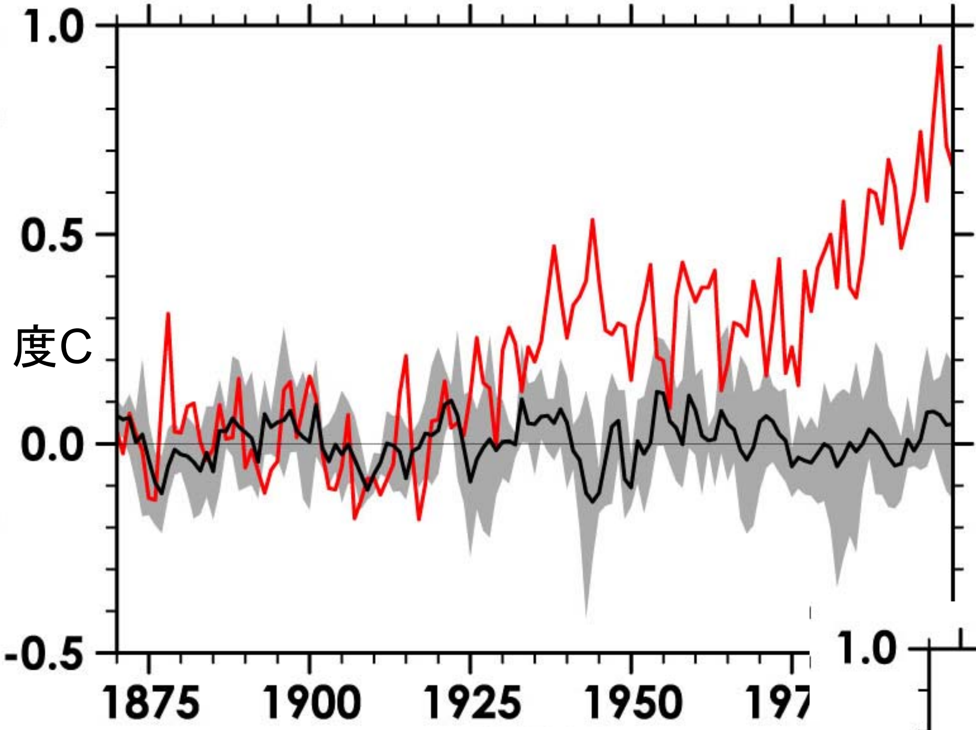

With CO_2 increase

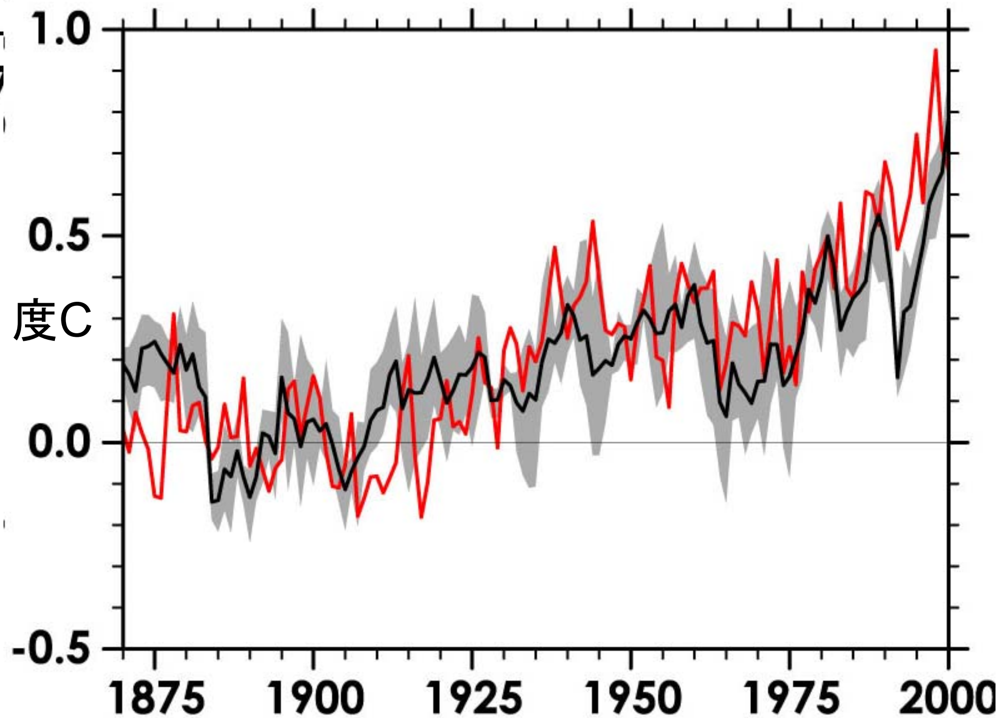

El Chichon：1982
Pinatubo：1991

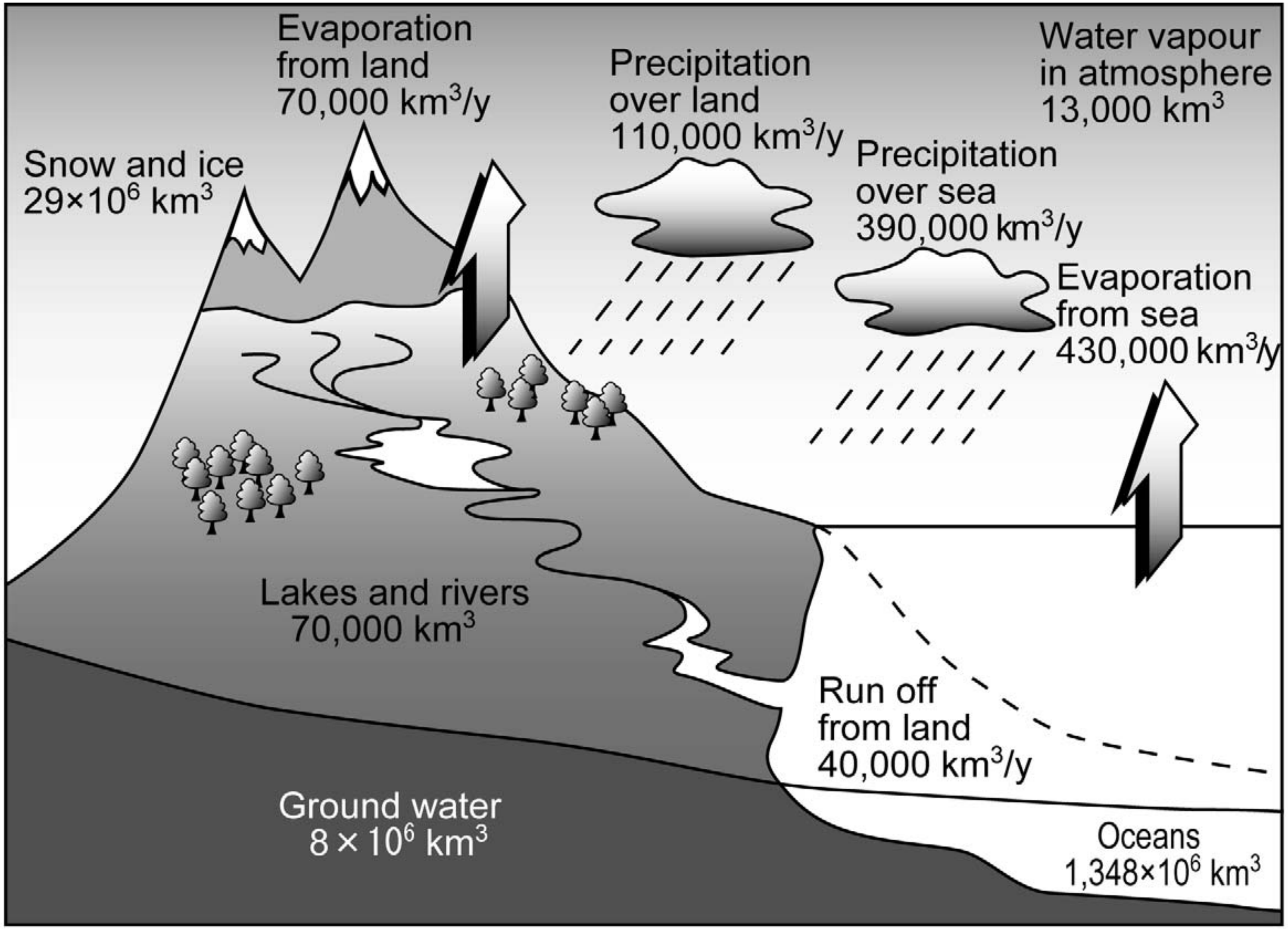

The amount of water

（Reference： ENCYCLOPEDIA of HYDROLOGY AND WATER RESORCES,1998)

Greenhouse effect

$T_g = 2^{(1/4)} T_a \sim 1.2\ T_a$

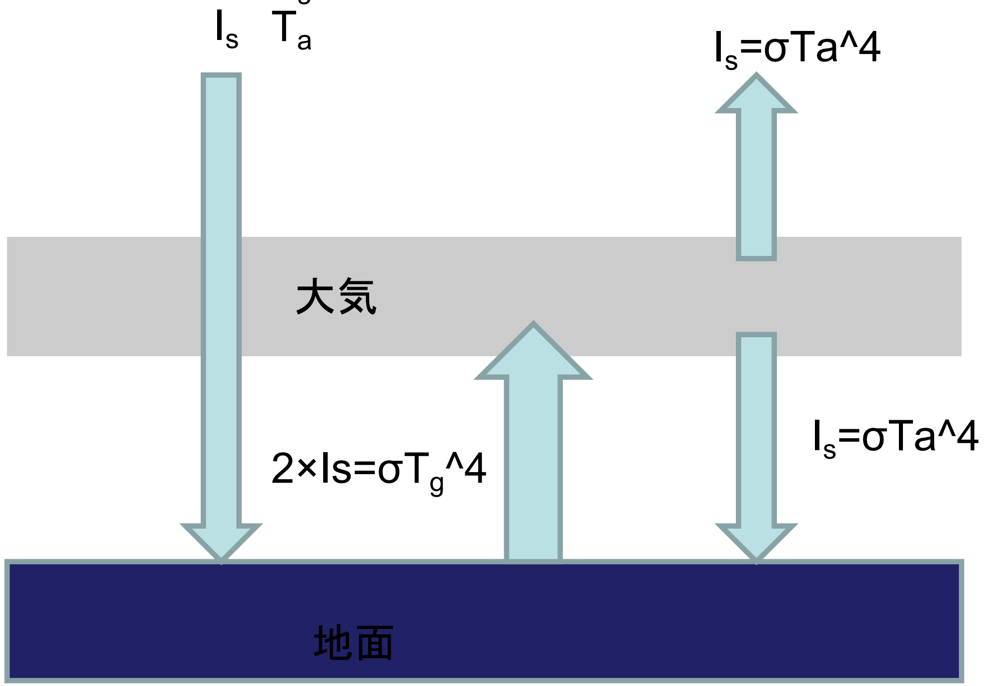

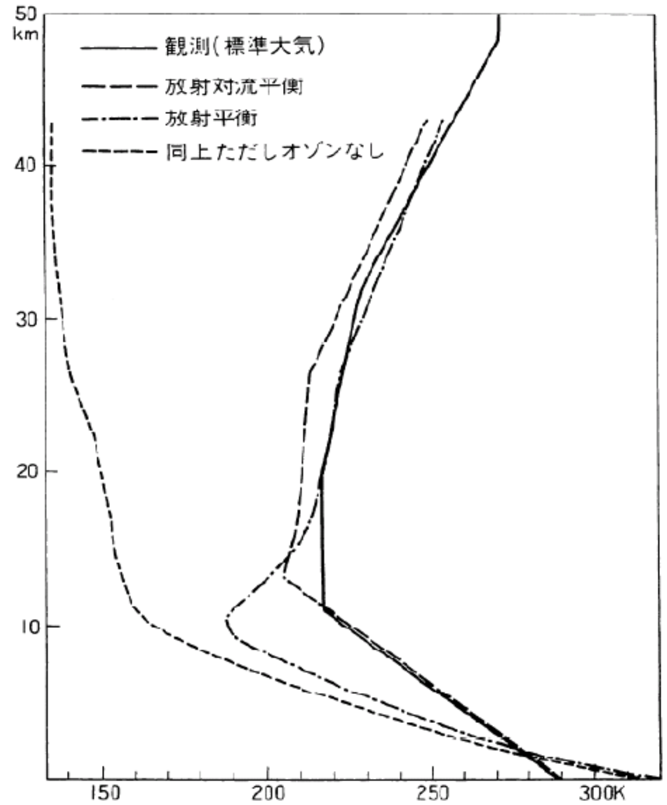

Atmospheric temperature profile in radiative-convective equiliburium state (Manabe and Stricker, 1964)

Demonstration of a meteorological observation balloon with helium.

The balloon inflates in upper air, and the temperature lowers.

Water vapor condensates, and produces clouds and precipitation.

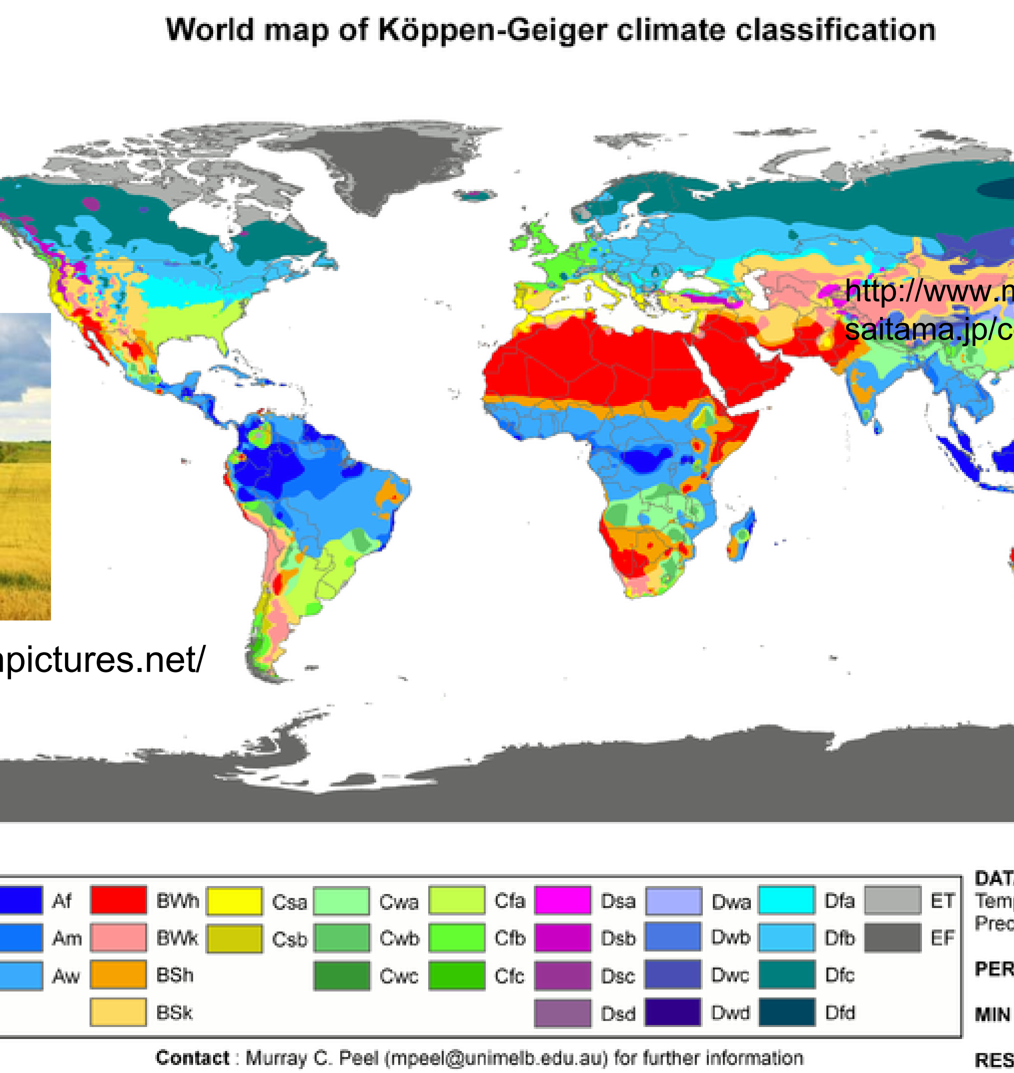

http://www.minumatanbo-saitama.jp/contest.htm

http://www.publicdomainpictures.net/

http://image.search.yahoo.co.jp

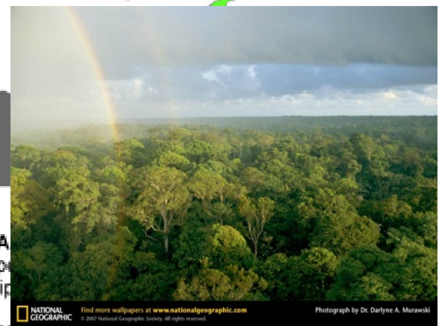

Climate category (Wikipedia)

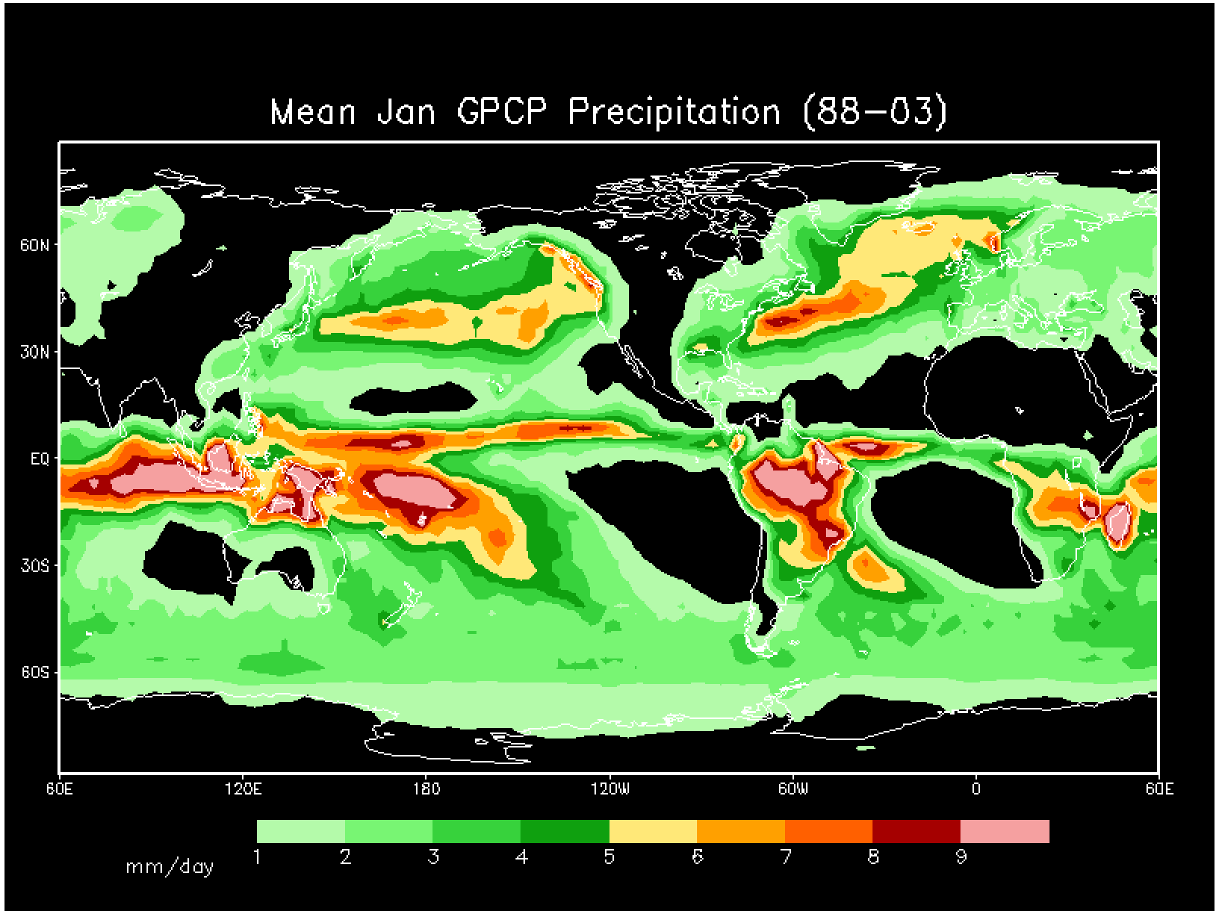

Month and pentad beginning 1979; 2.5° global coverage.

Mean annual cycle (above) and global mean precipitation (below)

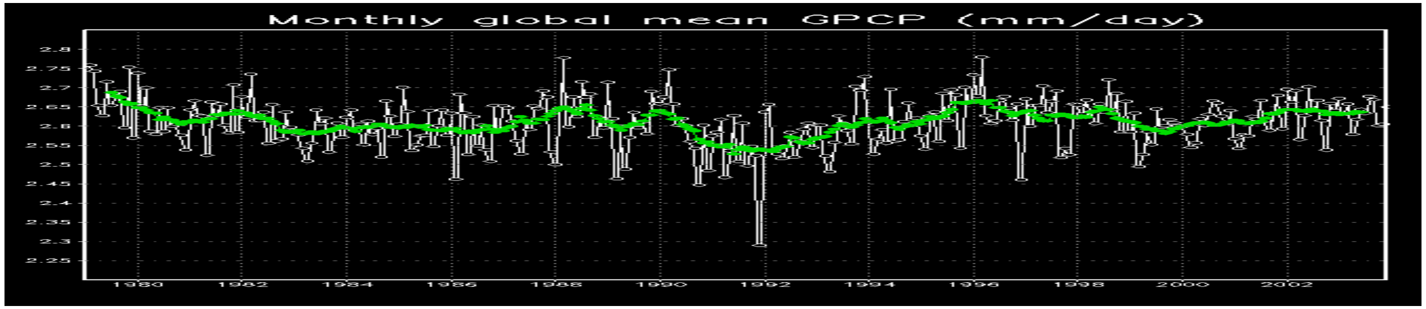

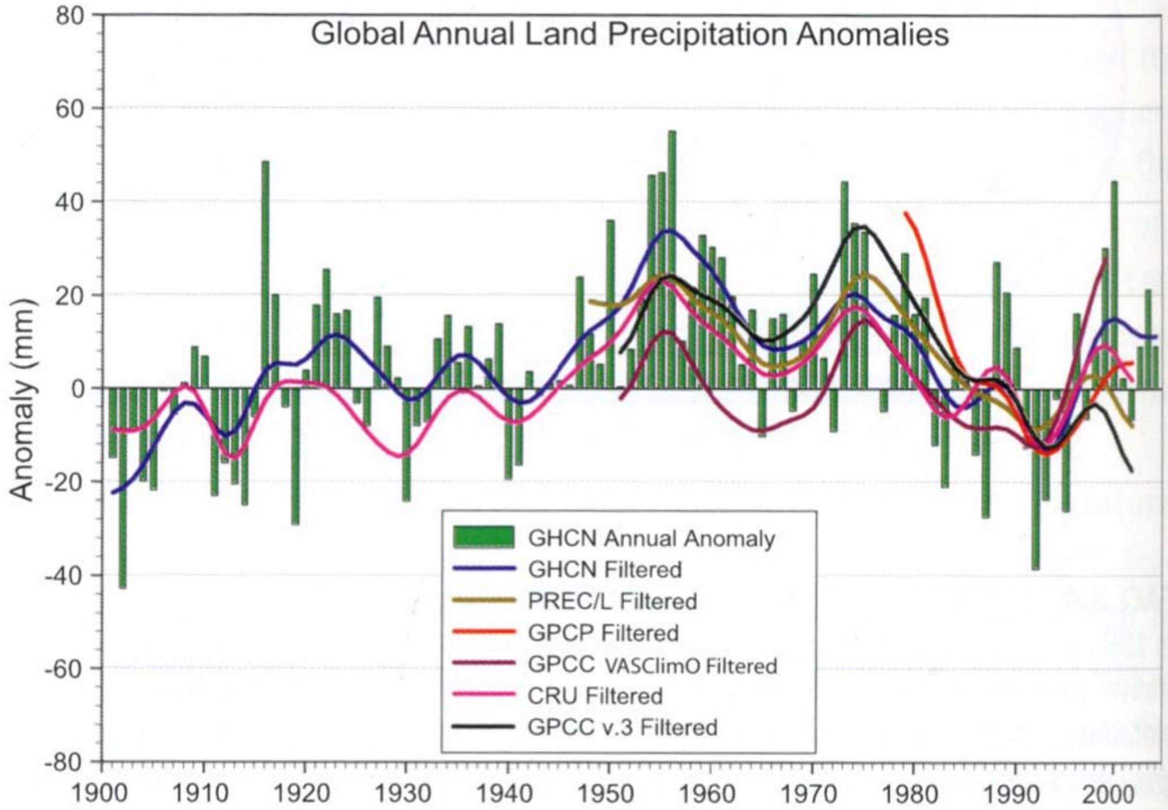

Figure 3.12. *Time series for 1900 to 2005 of annual global land precipitation anomalies (mm) from GHCN with respect to the 1981 to 2000 base period. The smooth curves show decadal variations (see Appendix 3.A) for the GHCN (Peterson and Vose, 1997), PREC/L (Chen et al., 2002), GPCP (Adler et al., 2003), GPCC (Rudolf et al., 1994) and CRU (Mitchell and Jones, 2005) data sets.*

“CLIMATE CHANGE 2007”, (CAMBRIDGE UNIVERSITY PRESS), Figure 3.12.

Figure 3.14. *Precipitation for 1900 to 2005. The central map shows the annual mean trends (% per century). Areas in grey have insufficient data to produce reliable trends. The surrounding time series of annual precipitation displayed (% of mean, with the mean given at top for 1961 to 1990) are for the named regions as indicated by the red arrows. The GHCN precipitation from NCDC was used for the annual green bars and black for decadal variations (see Appendix 3.A), and for comparison the CRU decadal variations are in magenta. The range is +30 to −30% except for the two Australian panels. The regions are a subset of those defined in Table 11.1 (Section 11.1) and include: Central North America, Western North America, Alaska, Central America, Eastern North America, Mediterranean, Northern Europe, North Asia, East Asia, Central Asia, Southeast Asia, Southern Asia, Northern Australia, Southern Australia, Eastern Africa, Western Africa, Southern Africa, Southern South America, and the Amazon.*

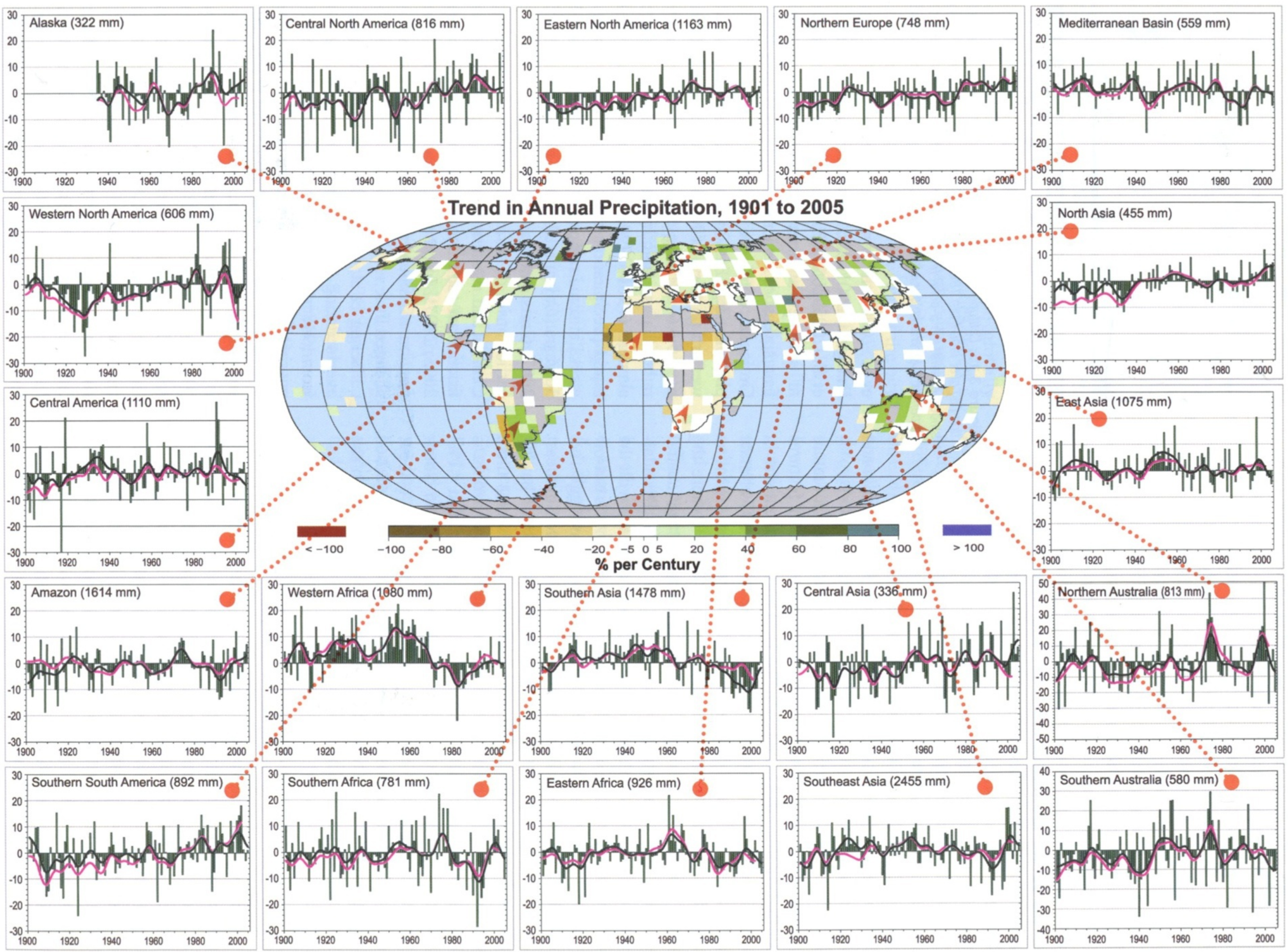

“CLIMATE CHANGE 2007”, (CAMBRIDGE UNIVERSITY PRESS), Figure 3.14.

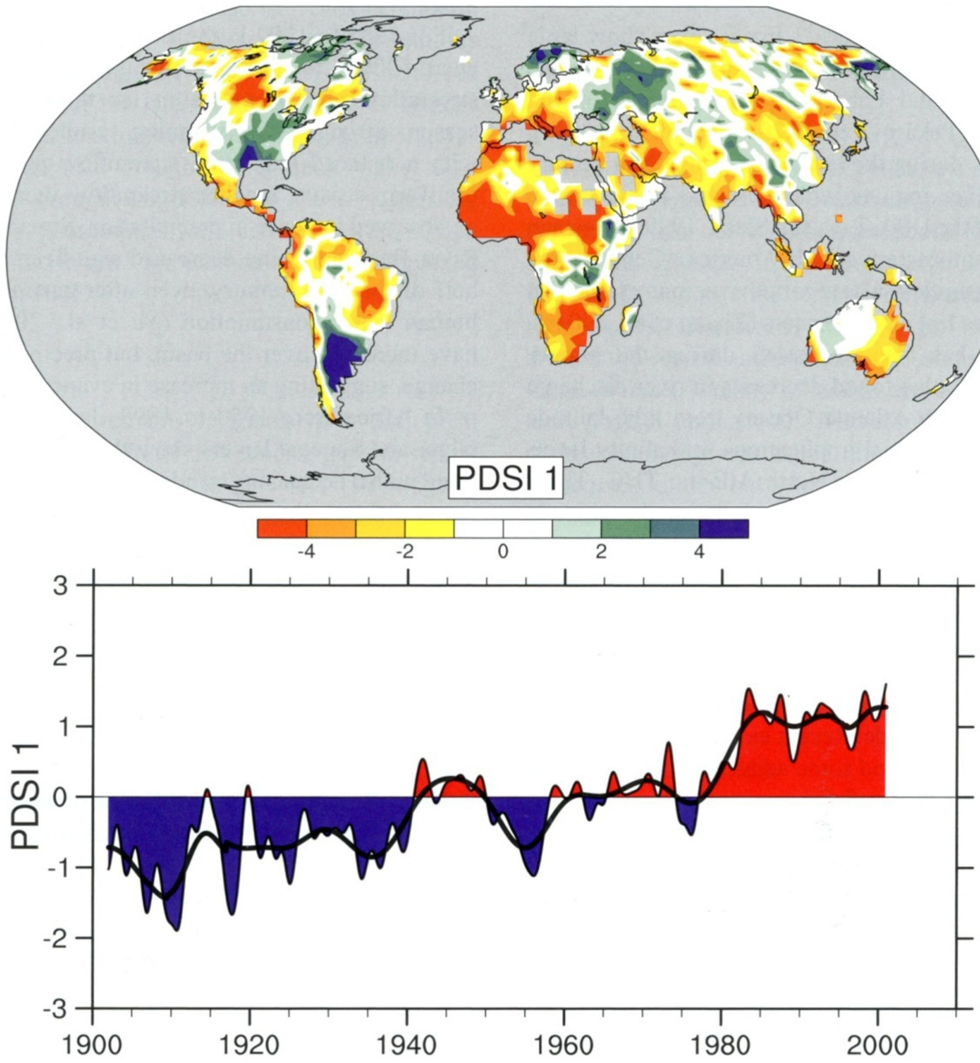

FAQ 3.2, Figure 1. *The most important spatial pattern (top) of the monthly Palmer Drought Severity Index (PDSI) for 1900 to 2002. The PDSI is a prominent index of drought and measures the cumulative deficit (relative to local mean conditions) in surface land moisture by incorporating previous precipitation and estimates of moisture drawn into the atmosphere (based on atmospheric temperatures) into a hydrological accounting system. The lower panel shows how the sign and strength of this pattern has changed since 1900. Red and orange areas are drier (wetter) than average and blue and green areas are wetter (drier) than average when the values shown in the lower plot are positive (negative). The smooth black curve shows decadal variations. The time series approximately corresponds to a trend, and this pattern and its variations account for 67% of the linear trend of PDSI from 1900 to 2002 over the global land area. It therefore features widespread increasing African drought, especially in the Sahel, for instance. Note also the wetter areas, especially in eastern North and South America and northern Eurasia. Adapted from Dai et al. (2004b).*

“CLIMATE CHANGE 2007”, (CAMBRIDGE UNIVERSITY PRESS), FAQ 3.2, Figure 1.

Tropical Rainfall Measuring Mission: TRMM

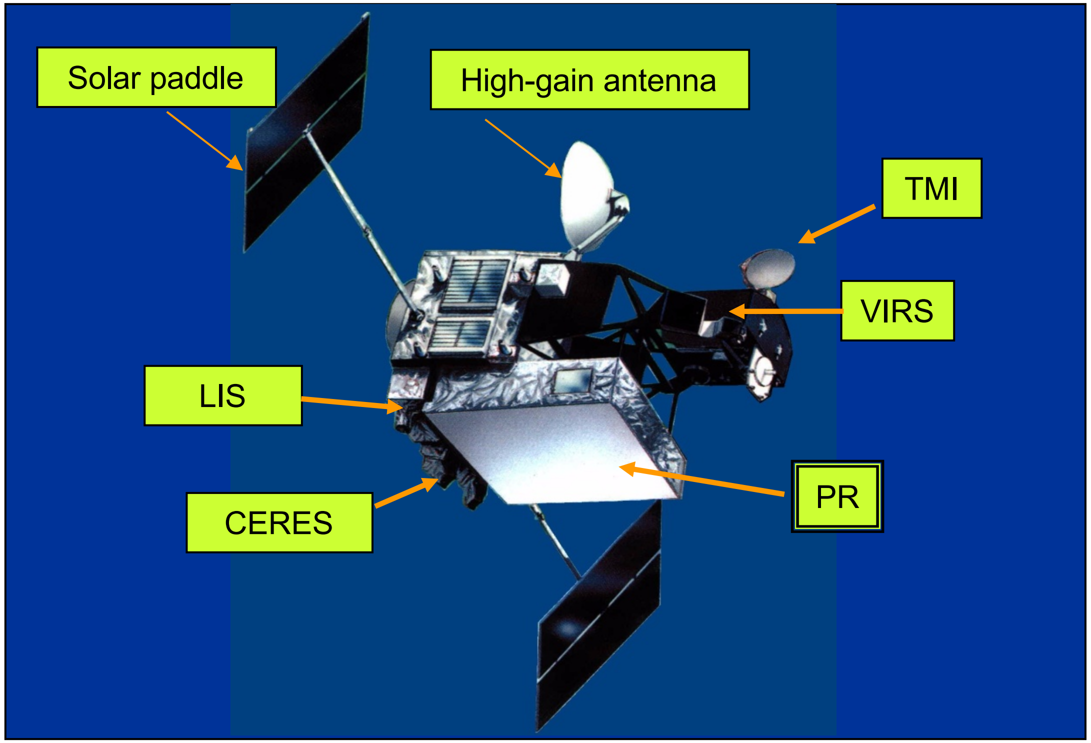

Orbit Altitude Inclination	Circular（Non-Sun Synchronous） 350km (402.5km since Aug. 2001) (±1.25km) 35 deg.
Sensor	**Precipitation Radar (PR)** TRMM Microwave Imager (TMI) Visible and Infrared Scanner (VIRS) Clouds and the Earth's Radiation Energy System (CERES) Lightning (LIS)

- ɔbservation of tropical rainfall (ðriving engine of global atmosphere)
- ʊʃ-əapan joint mission (əapanː PR, Launch, ʊʃː Bus, 4 sensors, operation)
- Launched in ŋov., 1997. ʃtill under operation
- First space-borne precipitation radar developed by CRL and ŋaʃða

NASDA
NATIONAL SPACE DEVELOPMENT AGENCY OF JAPAN
COMMUNICATIONS RESEARCH LABORATORY

Global Rain Distribution

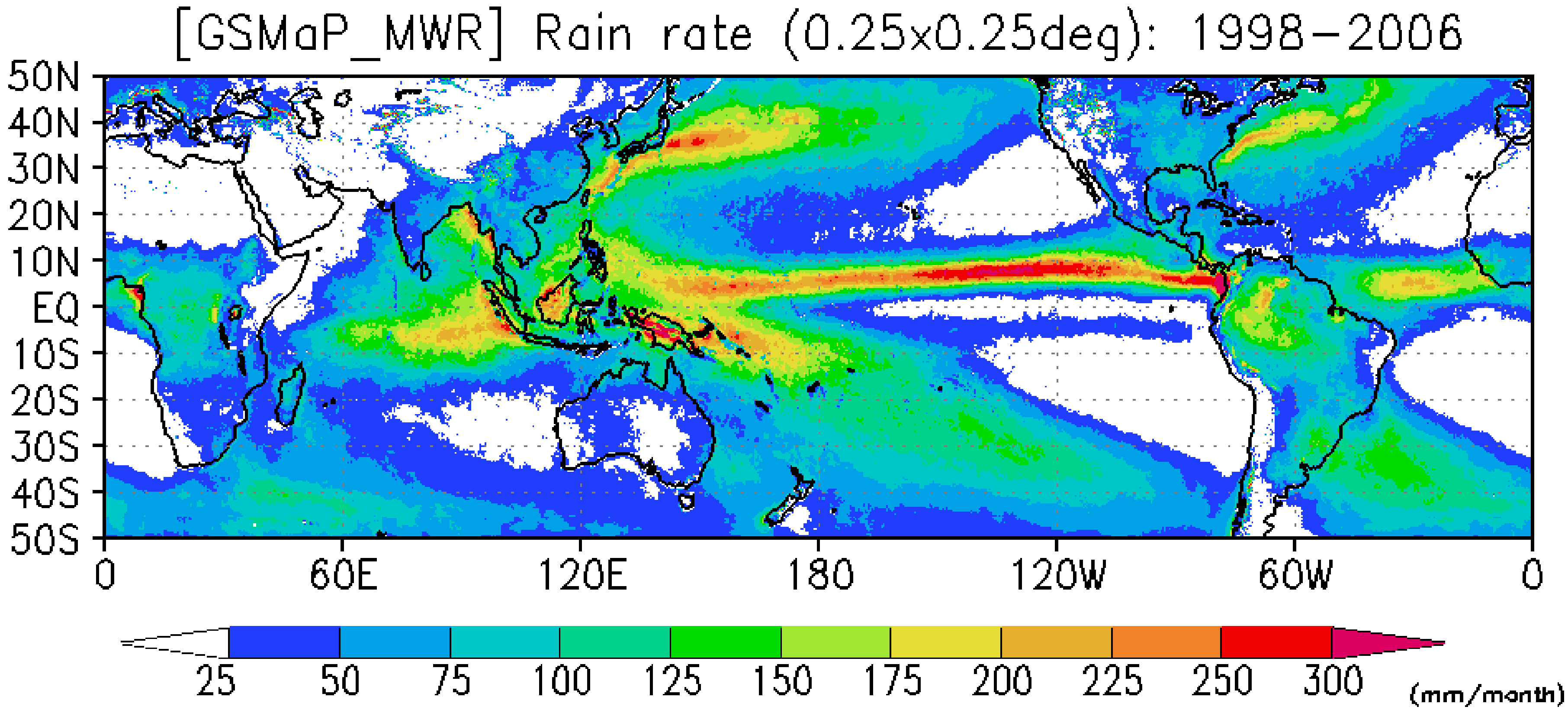

(JAXA wetsite)

Global Monthly Accumulated Rain by TRMM/PR
(Estimated Surface Rain 1997/12 – 2010/05)

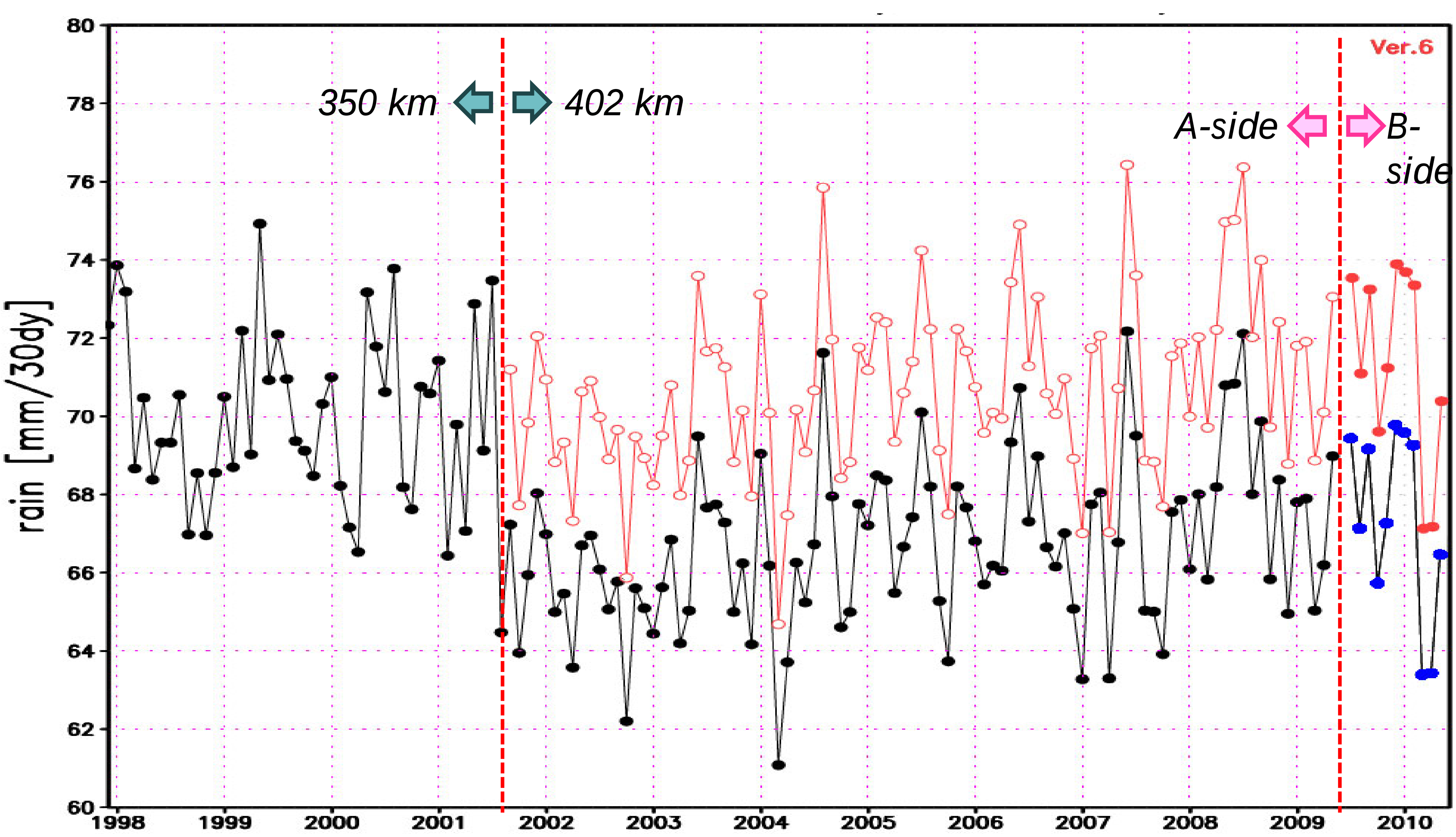

- *The total decrease in PR e_surface rain by altitude change is estimated to be 5.90% on average in a global scale.*
- *Data continuity was kept by calibration for B-side H/W.*

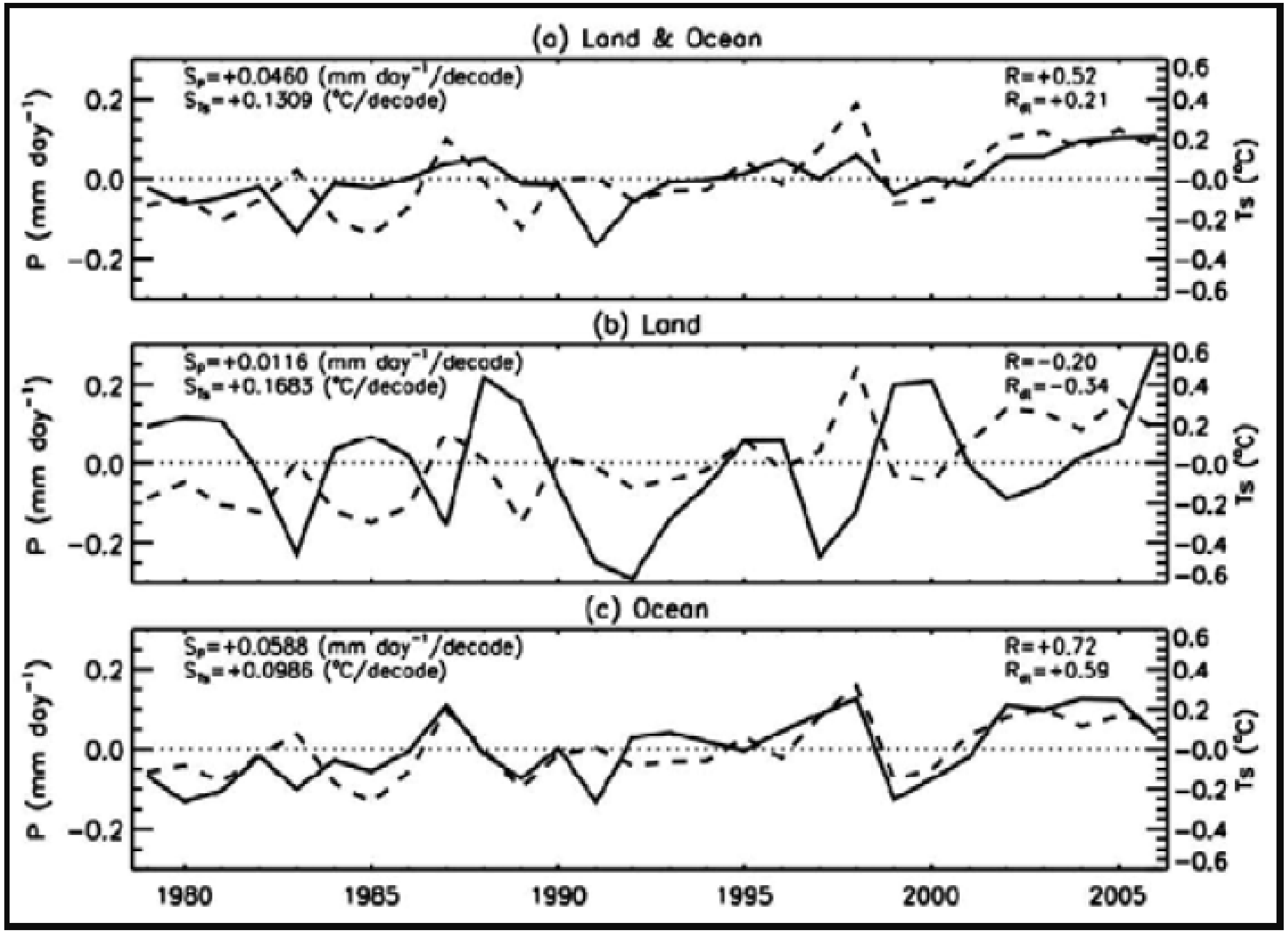

Tropical (25S–25N) annual mean precipitation (solid lines) and temperature (dashed lines) anomalies. Sp and STs denote linear changes for precipitation and temperature anomalies, respectively. R and Rdt represent the correlations between precipitation and temperature anomalies with and without the respective linear changes.

(Adler et al., 2008)

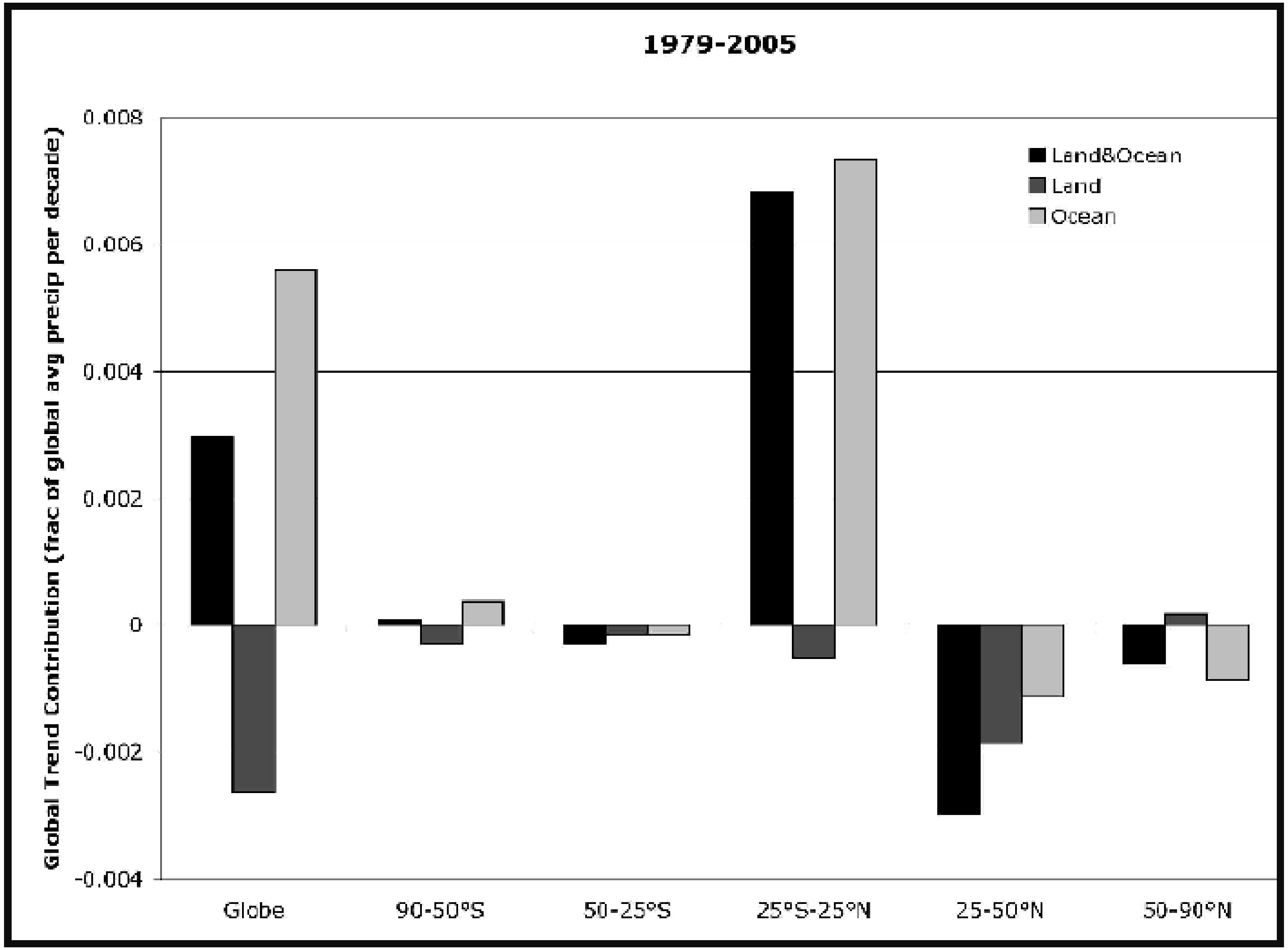

Volume contributions to long-time change/linear fit during 1979–2005.

(Adler et al., 2007)

Examples of regional precipitation system characteristics

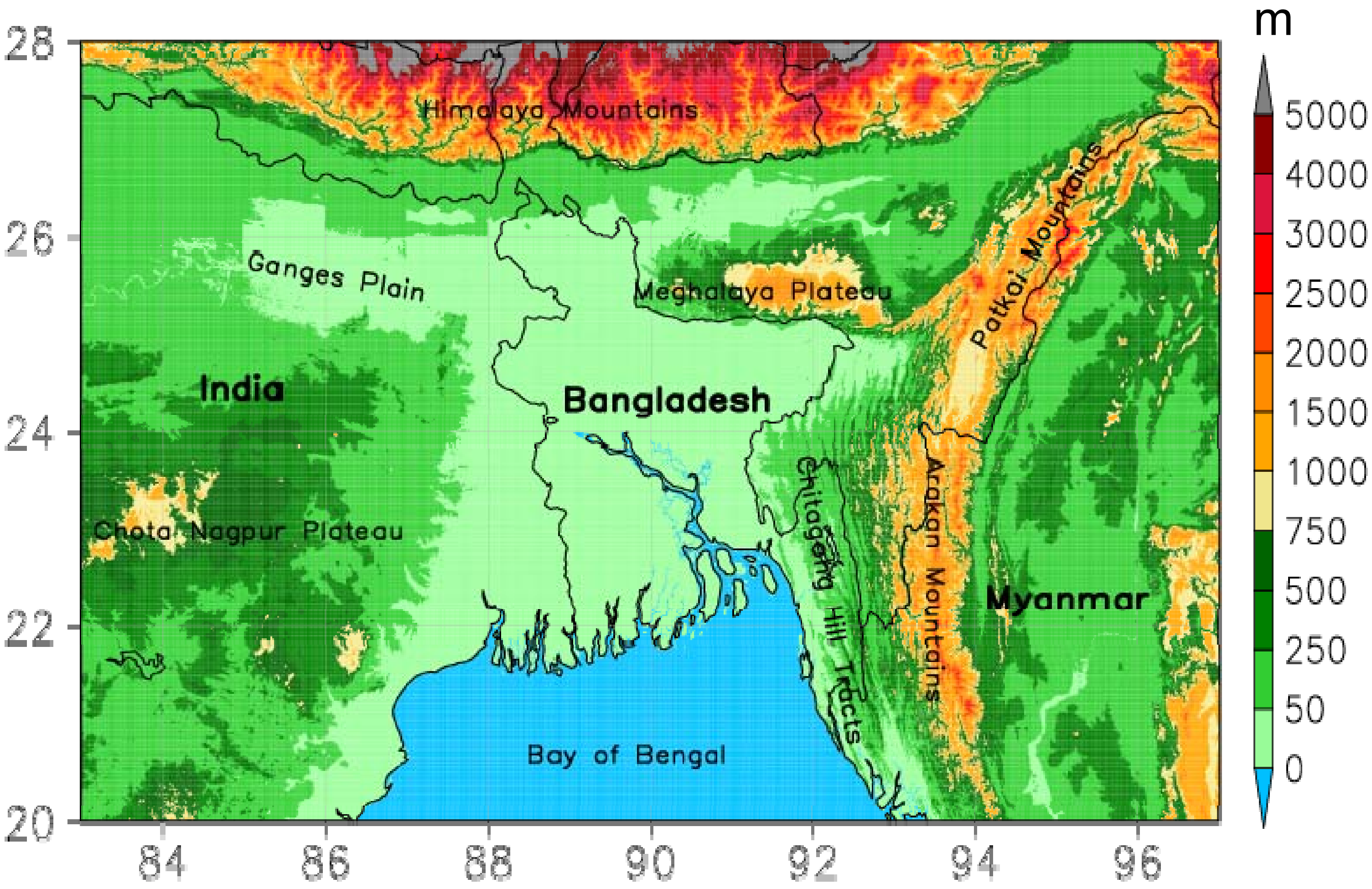

Rainfall Distribution

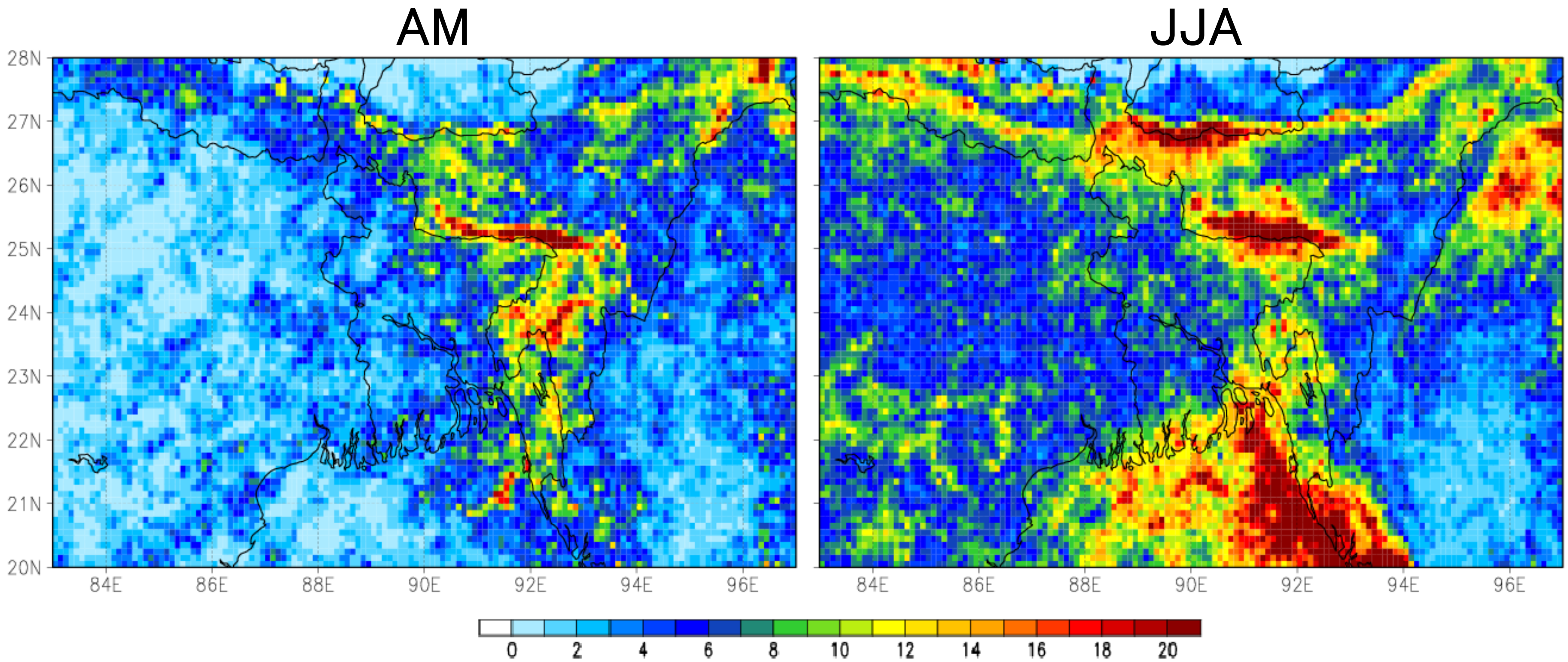

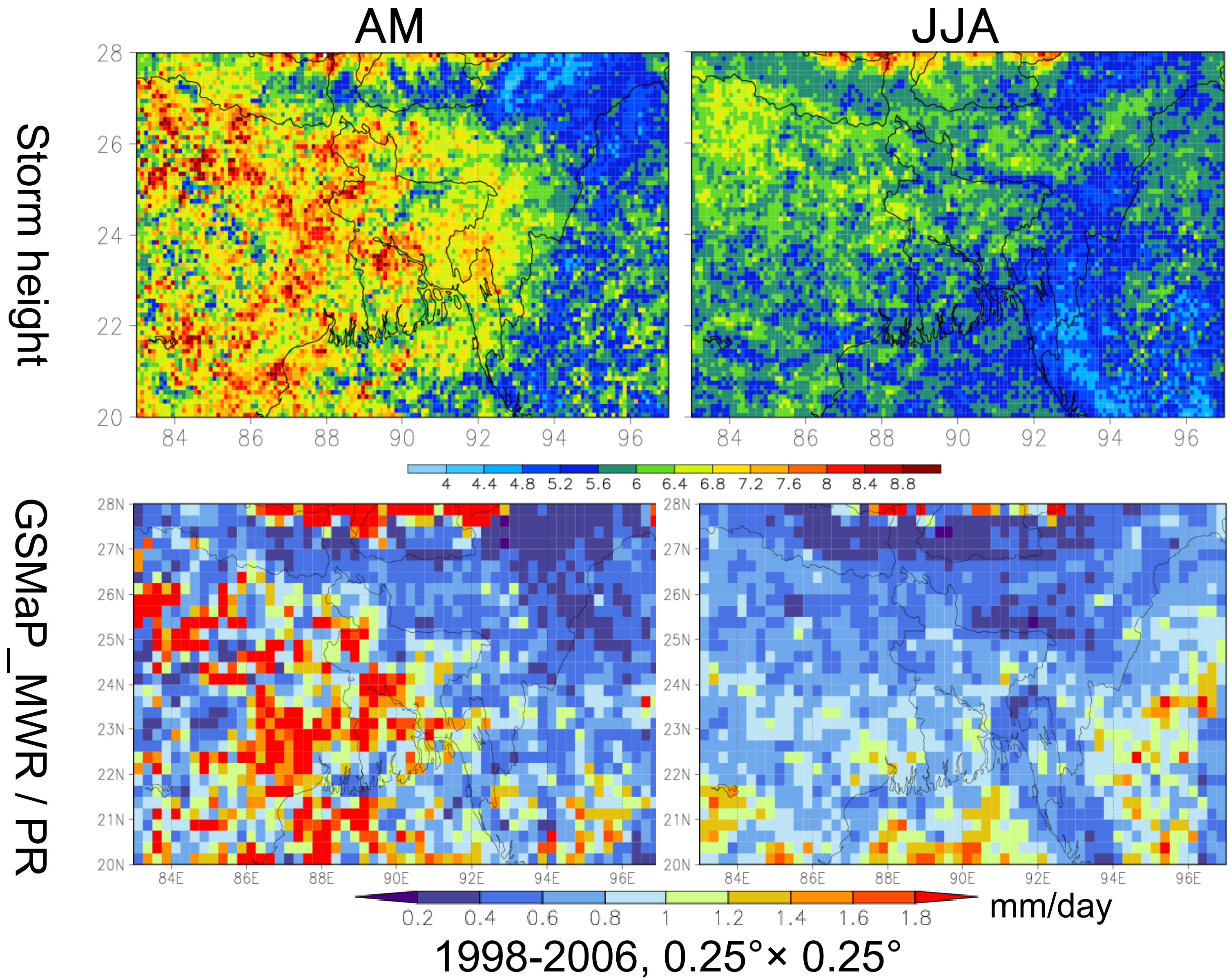

AM
JJA
Storm height
28
26
24
22
20
84
86
88
90
92
94
96
4 4.4 4.8 5.2 5.6 6 6.4 6.8 7.2 7.6 8 8.4 8.8
GSMaP_MWR / PR
28N
27N
26N
25N
24N
23N
22N
21N
20N
84E
86E
88E
90E
92E
94E
96E
0.2 0.4 0.6 0.8 1 1.2 1.4 1.6 1.8
mm/day
1998-2006, 0.25°× 0.25°

- AM
  - Strong intensity up to high altitude
  - Decrease intensity at the near surface
- JJA
  - Weak rain at high altitude
  - Continues to increase from top to the near-surface.

Vertical profile of area-averaged (89-91E, 23-25N) conditional rain rate.

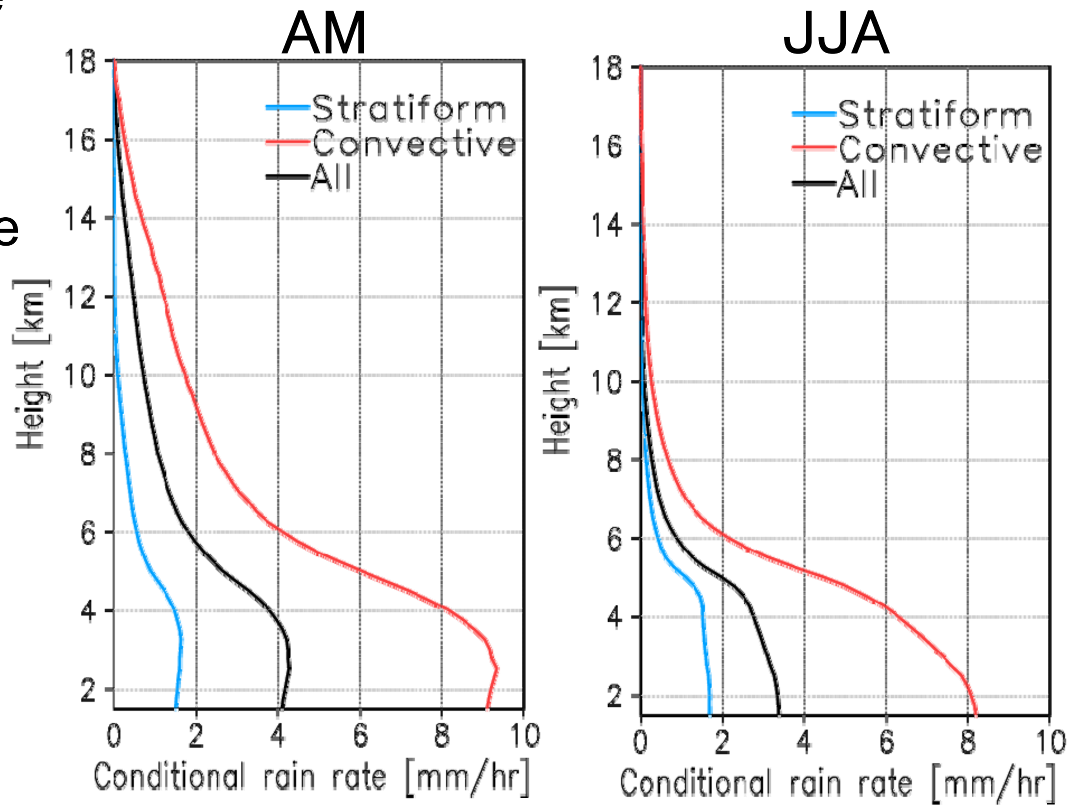

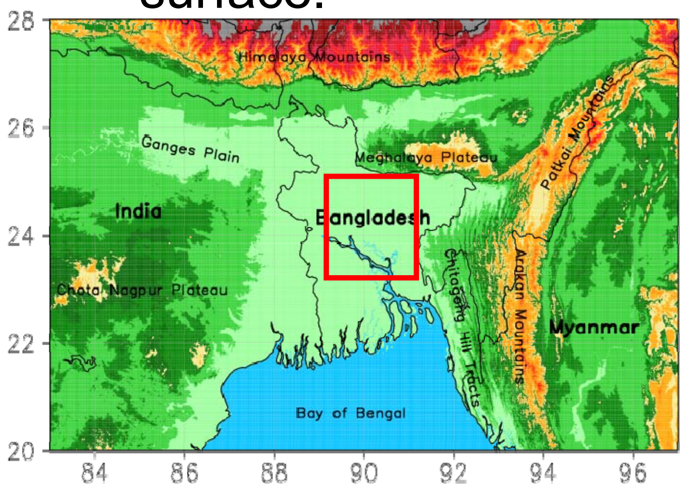

Atmospheric fields (AM)

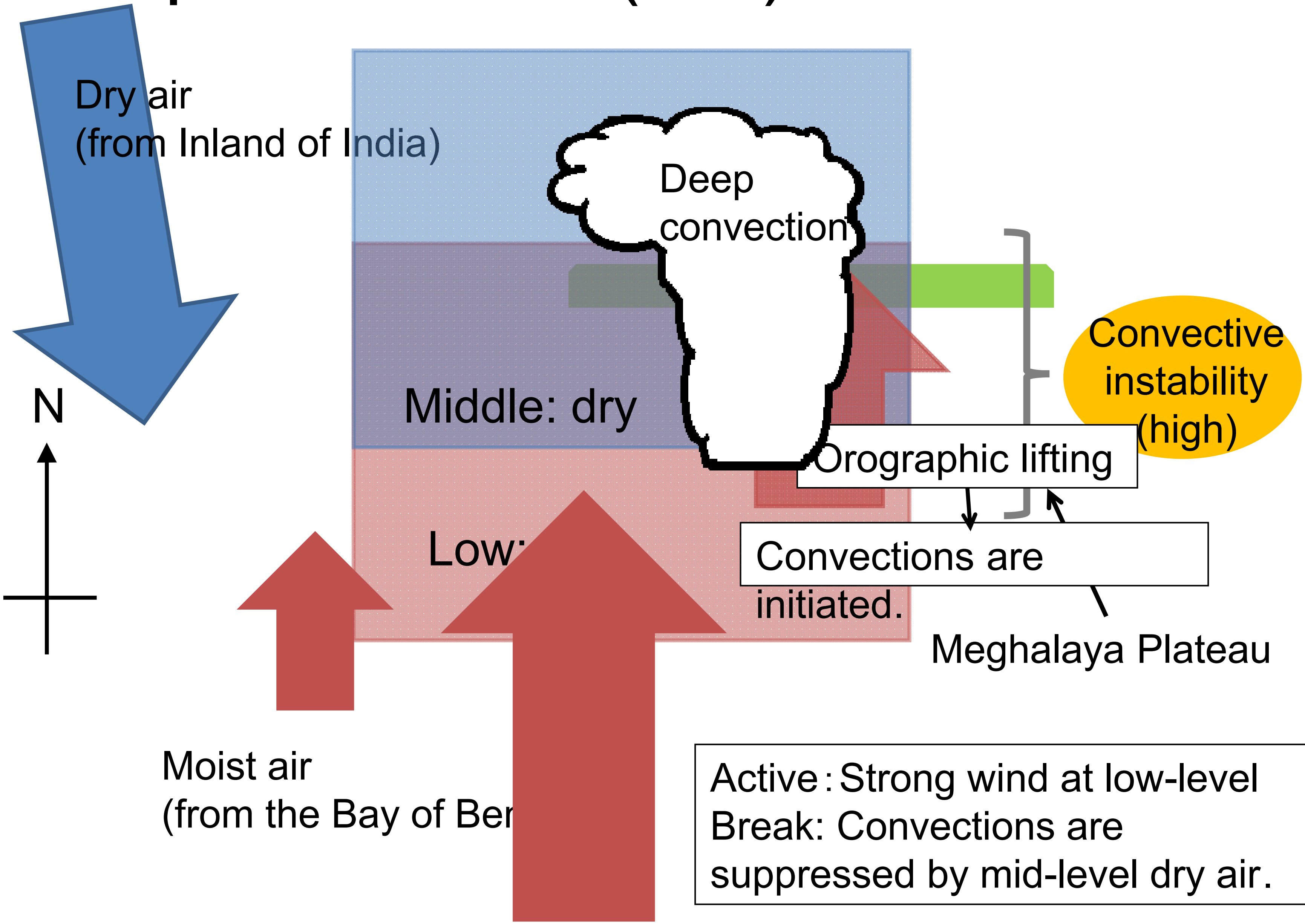

Active：Strong wind at low-level
Break: Convections are suppressed by mid-level dry air.

Atmospheric fields (JJA)

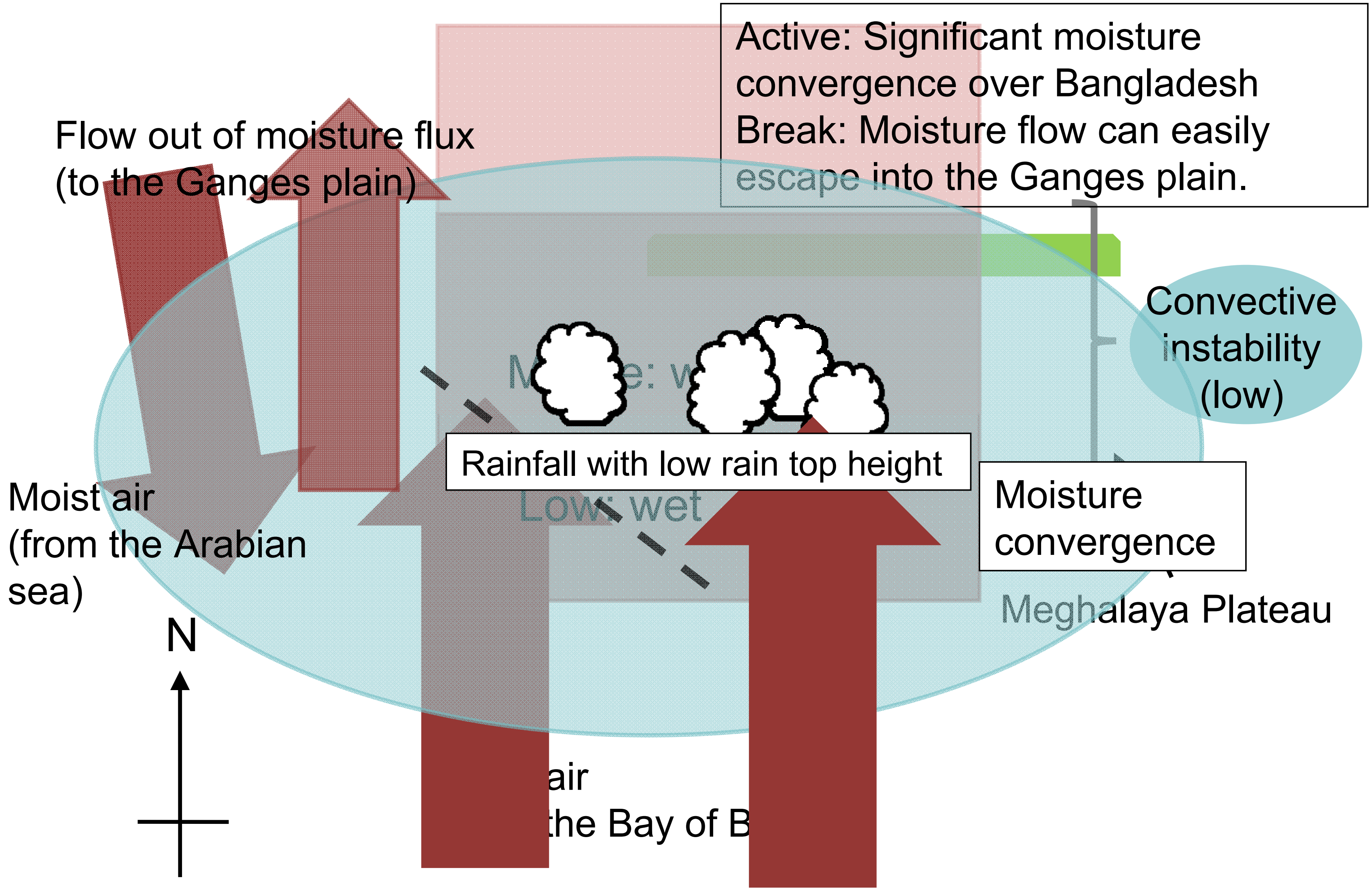

Topography

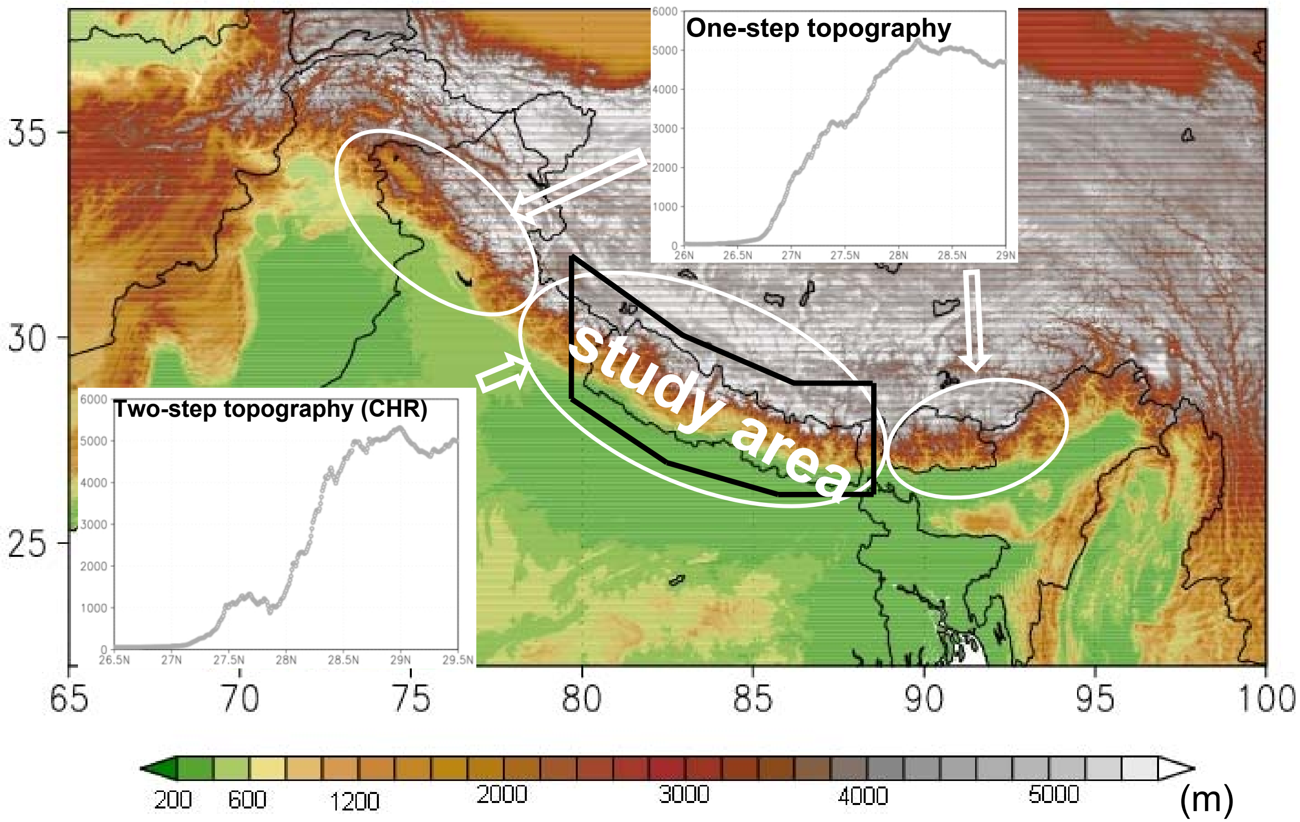

Central Himalaya Region (CHR): Three sub-parallel ranges

First topographic barrier → Sub Himalayas (Siwalik Range) (400-1,200 m MSL)

Major topographic barrier → Lesser Himalayas (1,200-3,000 m MSL)

→ Great Himalayas (> 3,000 m MSL)

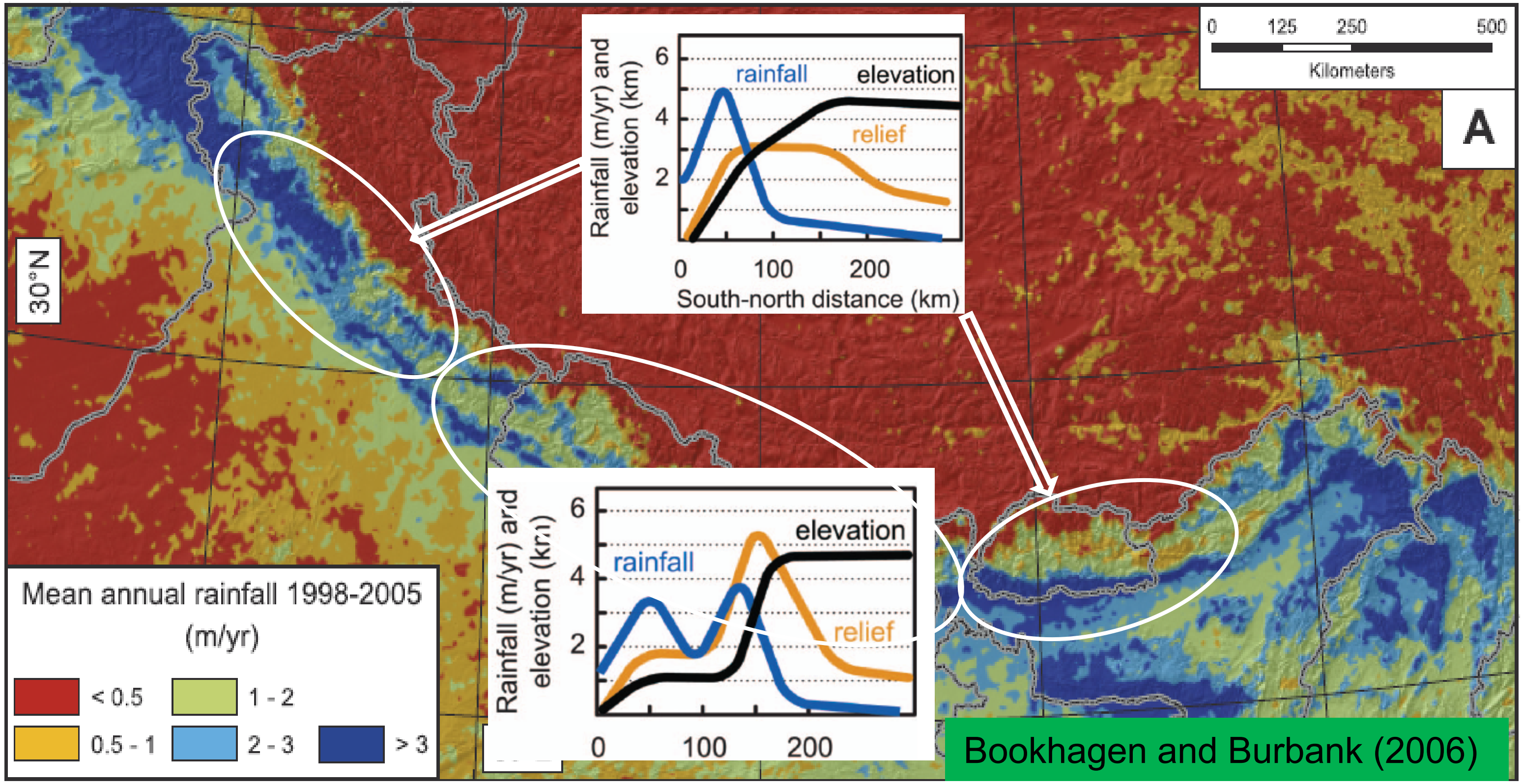

Purpose

To explore the impact of two-step topography in the central Himalayas and the associated rainfall processes.

Horizontal distribution of rainfall

Contours: 500, 2000 and 4000 m AMSL

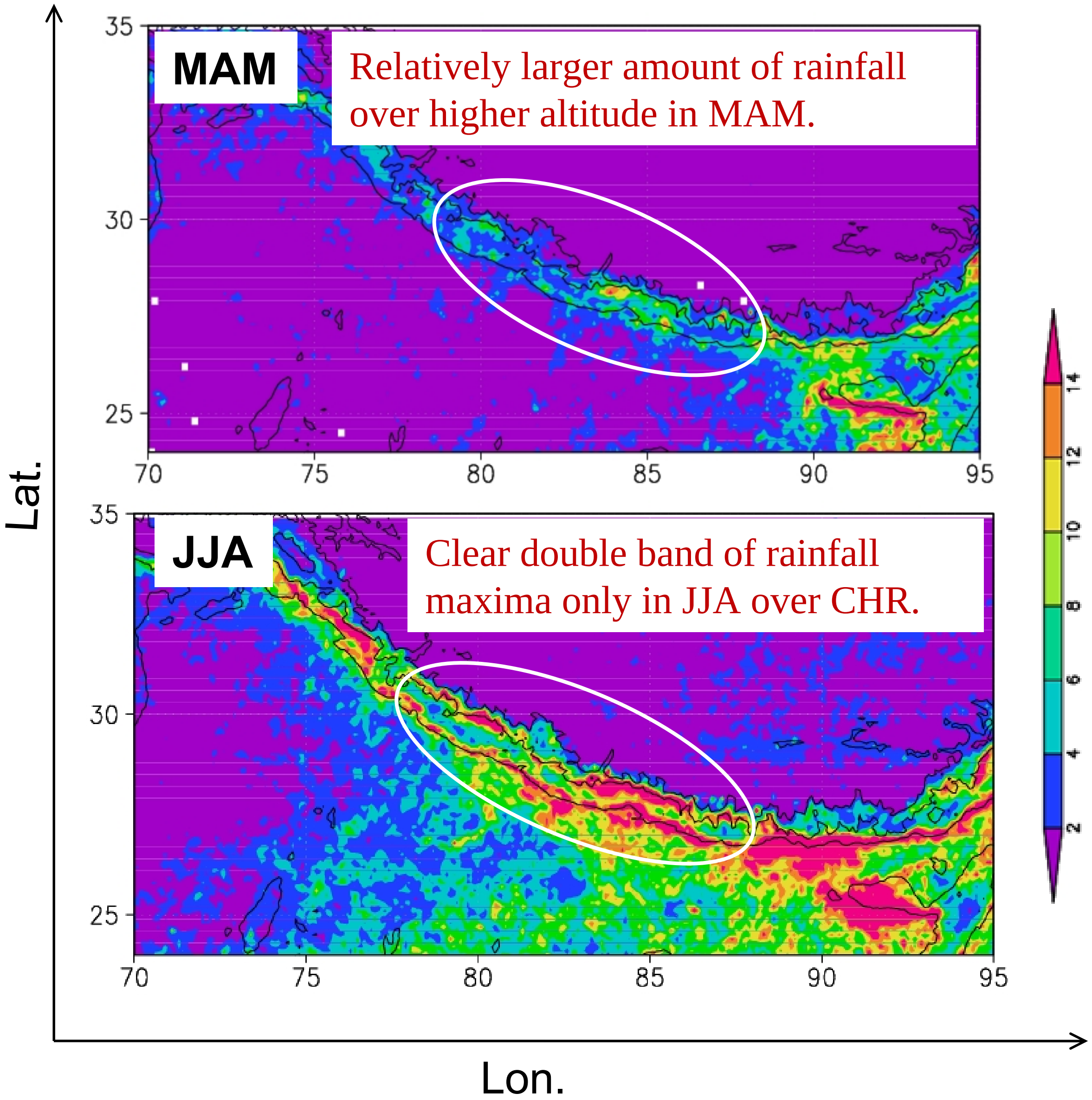

Rain characteristics in JJA

Rain conditioned rain rate: Near-surface rain rate greater than 0 mm/h.
Rain frequency: Number of rain sample normalized by total number of sample.

Rain cond.
RR

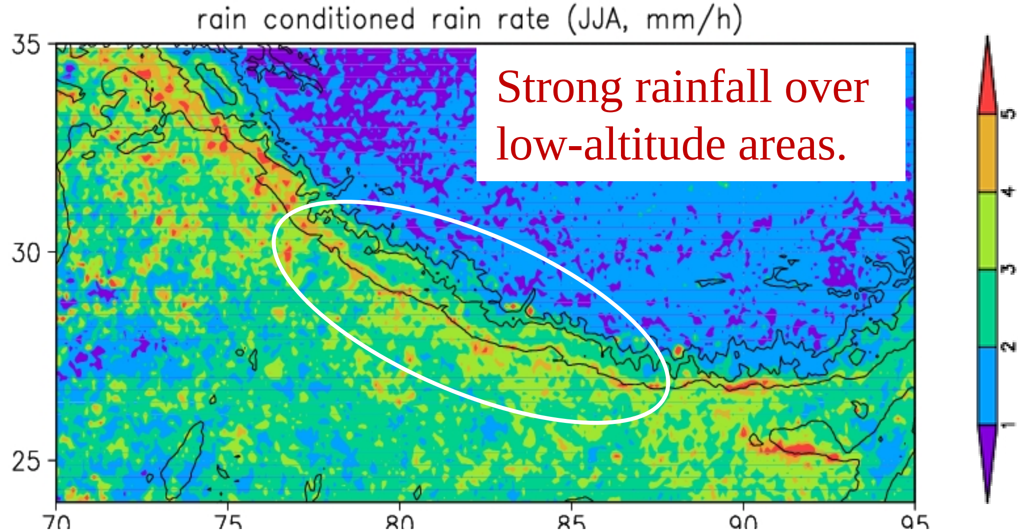

JJA

Frequency

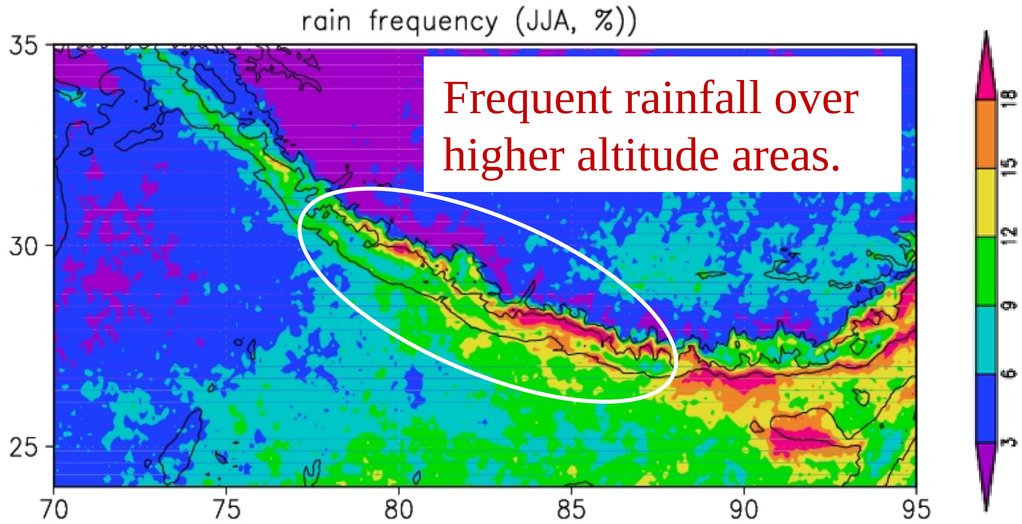

Rain Characteristics in JJA

Area averaged analysis:- Rainfall characteristics are averaged for each 200 m altitude interval up to 5,000 m MSL.

- Double rainfall peaks
- Primary peak (~500 m AMSL): Rain conditioned rain rate is dominant.
- Secondary peak (~2,100 m AMSL): Frequency is dominant.

❖ Storm height is approximately 6 km AMSL, with clear peak near the top of the slope and a small peak at the bottom.

Dry and wet periods

Definition: Wet (dry) phase when daily rainfall over Himalayan foothills (82^0-90^0E and 26^0-27.5^0N) is more (less) than 0.5 standard deviation from the average of July-August for each year for a minimum of three consecutive days (Singh and Nakamura, 2010).

No. of wet days: 83 Average wet days: 7.55
No. of dry days: 144 Average dry days: 13.09

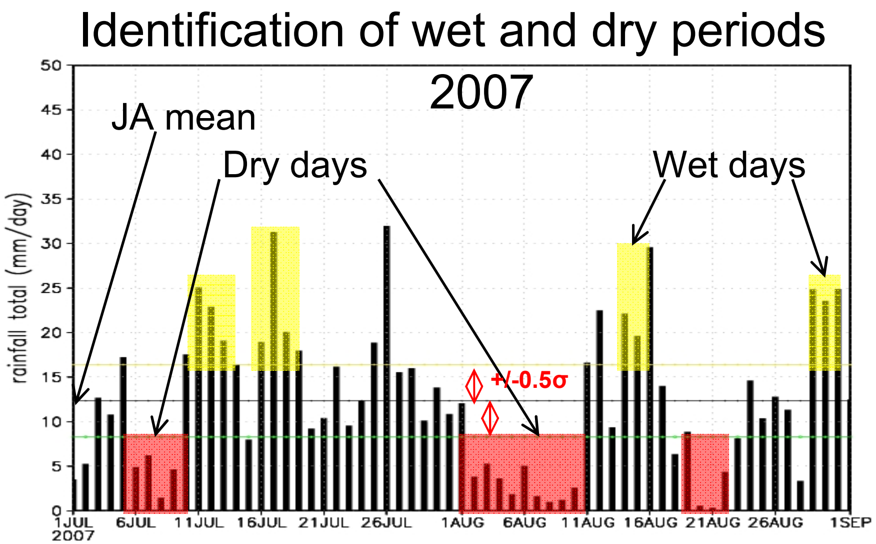

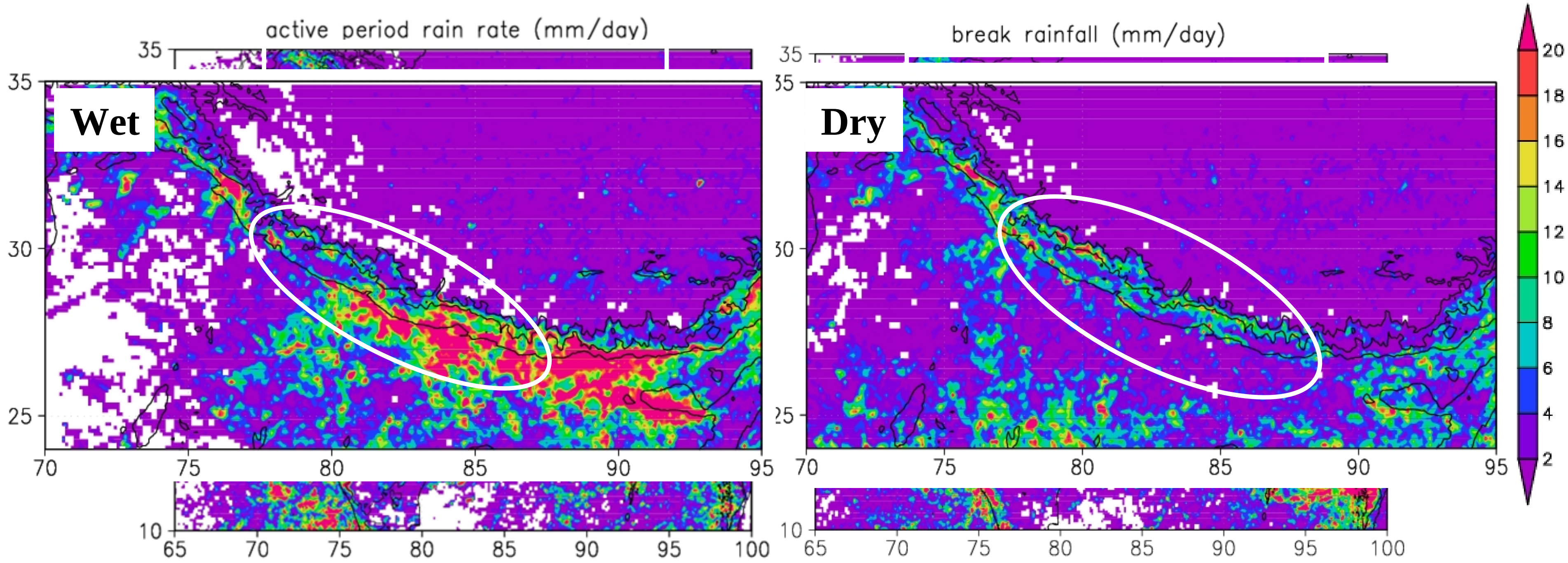

Rain type

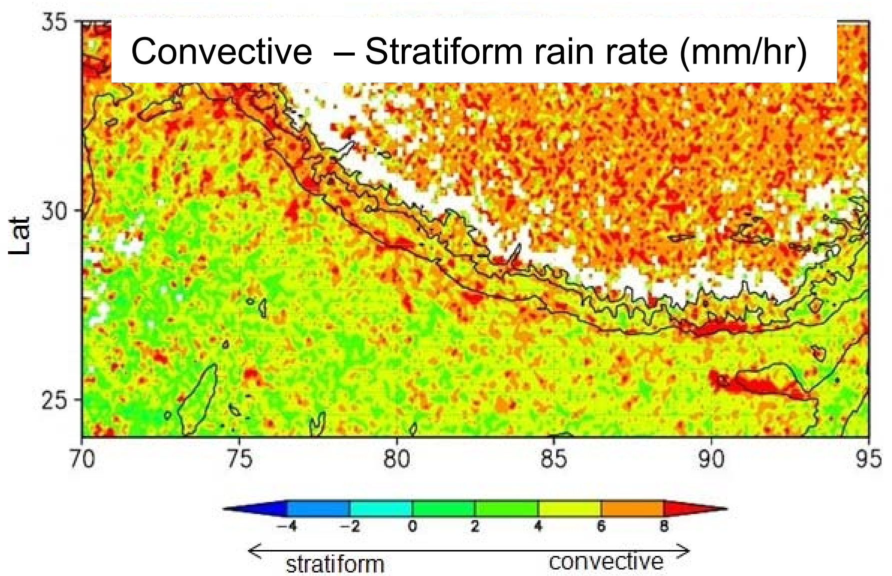

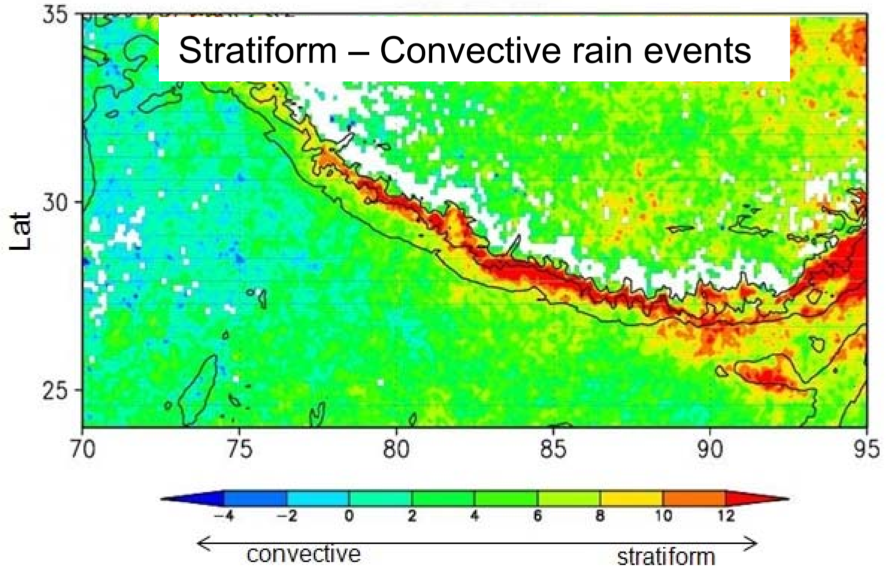

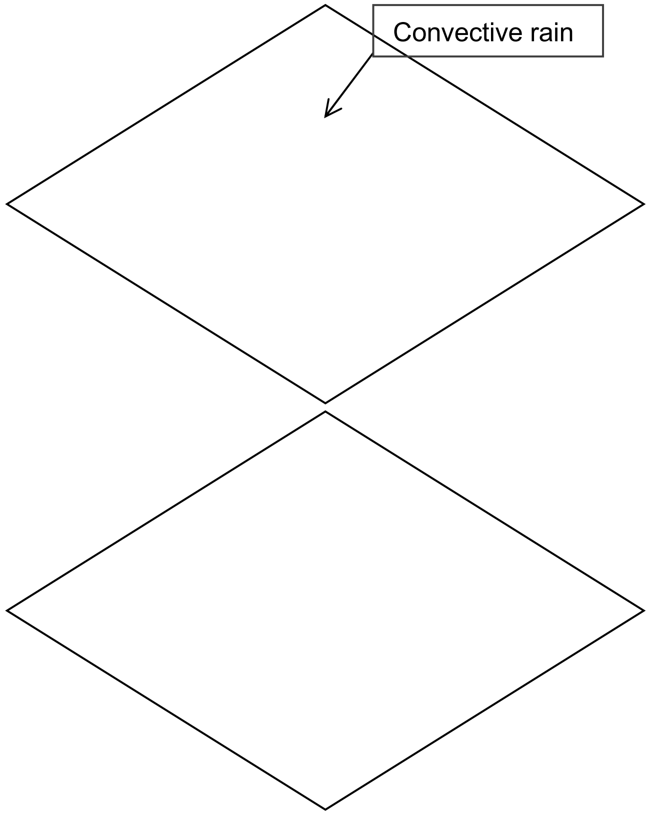

- Intense convective rainfall over the foothills
- High frequency of stratiform rainfall over higher elevation

Rain characteristics

Rain rate

Rain percentage

Rain total (mm/day)

Rain fraction (%)

Elevation (m) ⟶

Rain-cond. rain rate

Rain frequency

Rain-cond. Rain rate (mm/hr)

Rain frequency (%)

Elevation (m) ⟶

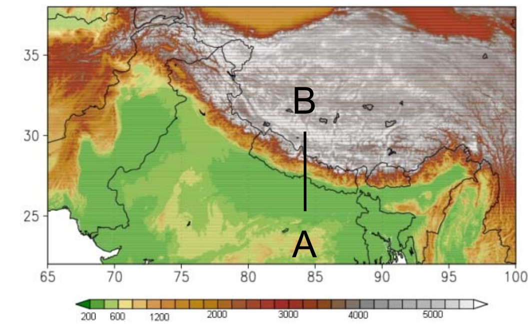

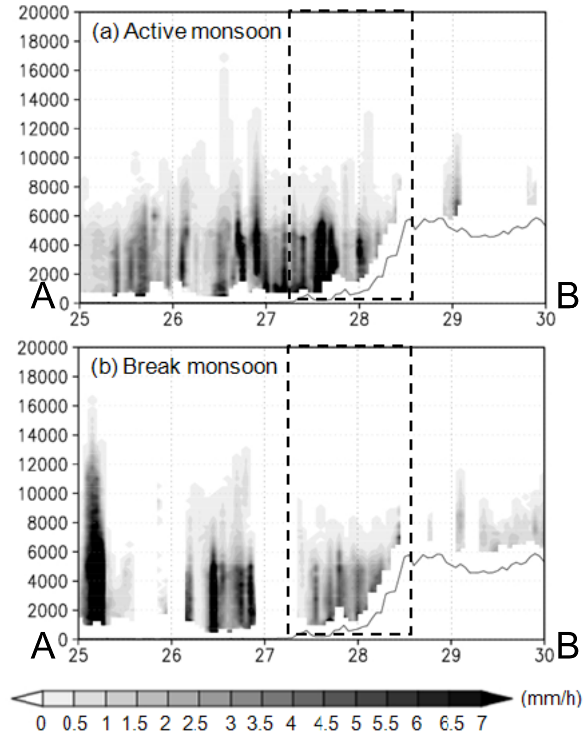

Active: Shallow systems with intense rain
Break: Shallow systems with weak rain

- ❖ Lower elevation: Wet phase rainfall dominant
- ❖ Higher elevation: Dry phase rainfall dominant

Atmospheric stability (84.5°E)

Shaded: Equivalent potential temperature (K)
Vector: Horizontal wind (m/s)
Contour: Specific humidity (gm/kg)

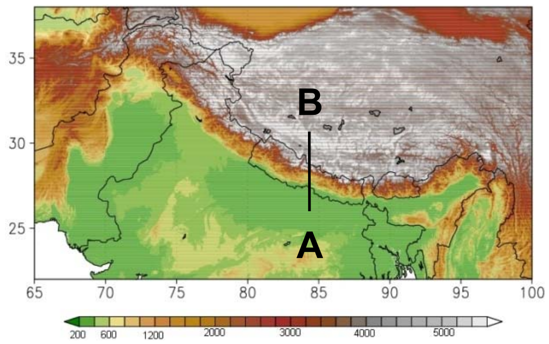

- ❖JJA: atmospheric stability is higher.
- ❖MAM: Convective instability

- ❖Distributions are remarkably similar to each other except for horizontal wind.

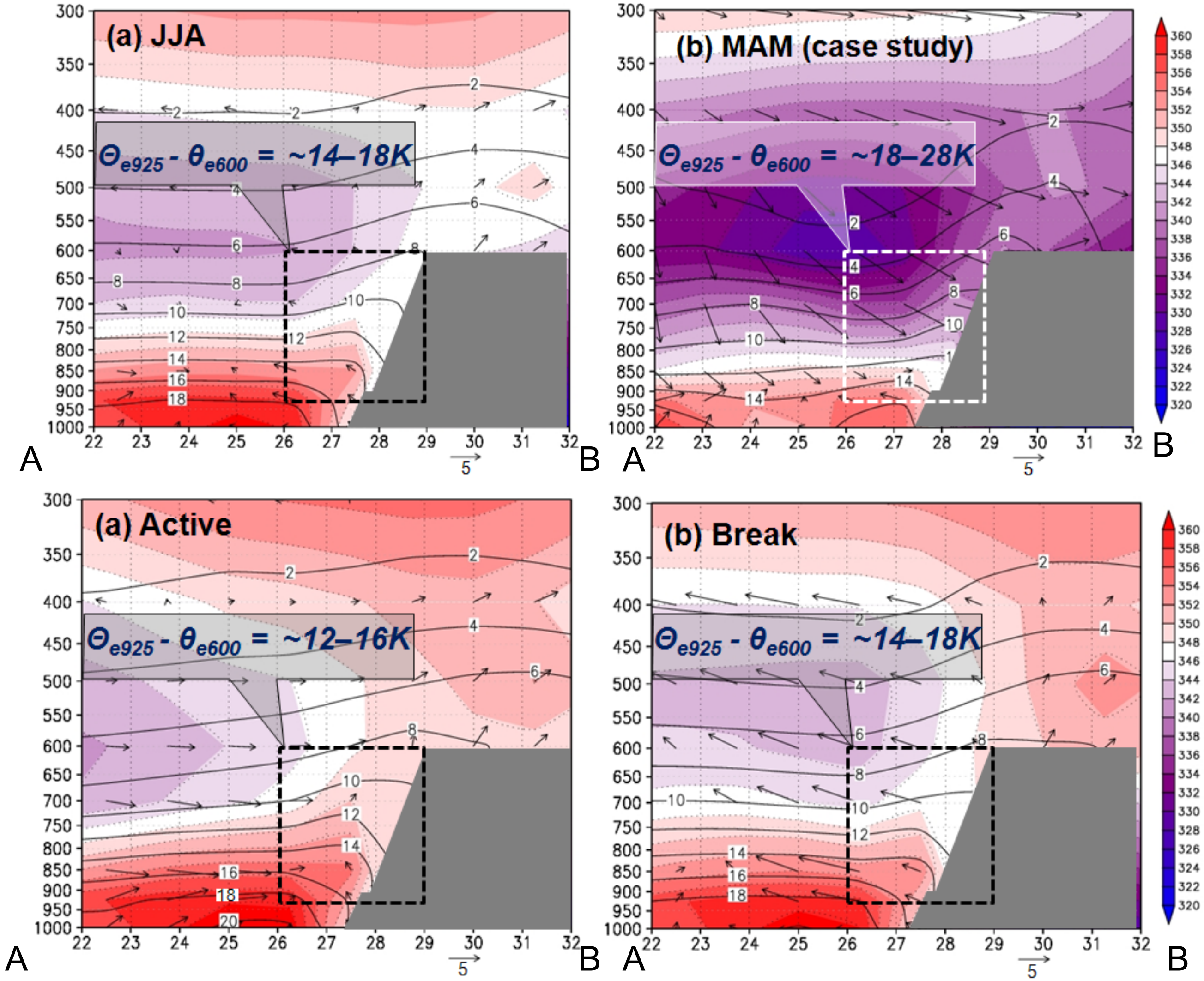

Summary of the precipitation system characteristics over southern slope of Himalayas

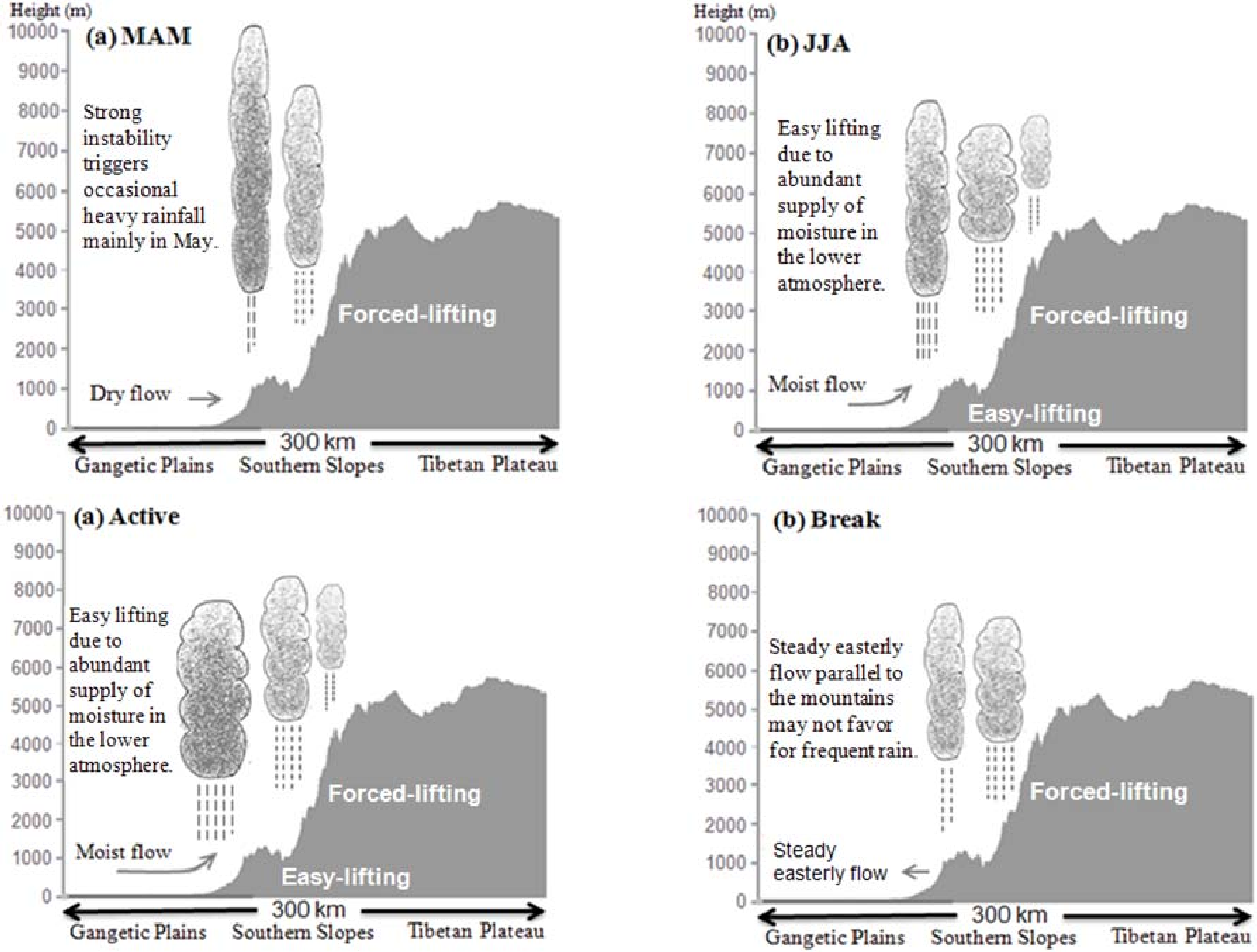

Bangladesh

- Clear pre-monsoon and monsoon season
- Difference in atmospheric stability due to wind systems.
- Pre-monsoon and monsoon difference
- Active and break difference.

Nepal

- Strong topography effect causing local differences
- Difference in atmospheric stability due to wind
- Pre-monsoon and monsoon difference
- Active and break difference.

GFAS Global Flood Alert System (GFAS) – Streamflow

Applicability and potential of satellite-based data for flood analysis

~Experiences of ICHARM through development & application of Integrated Flood Analysis System (IFAS) and Rainfall-Runoff-Inundation (RRI) Model ~

Kazuhiko FUKAMI, Seishi NABESAKA, Takahiro SAYAMA, Mamoru MIYAMOTO and Ai SUGIURA

International Centre for Water Hazard and Risk Management under the auspices of UNESCO (UNESCO-ICHARM), Public Works Research Institute (PWRI), Japan

IFAS

IFNet International Flood Network

ICHARM

Trend of water-related disasters by type of hazard

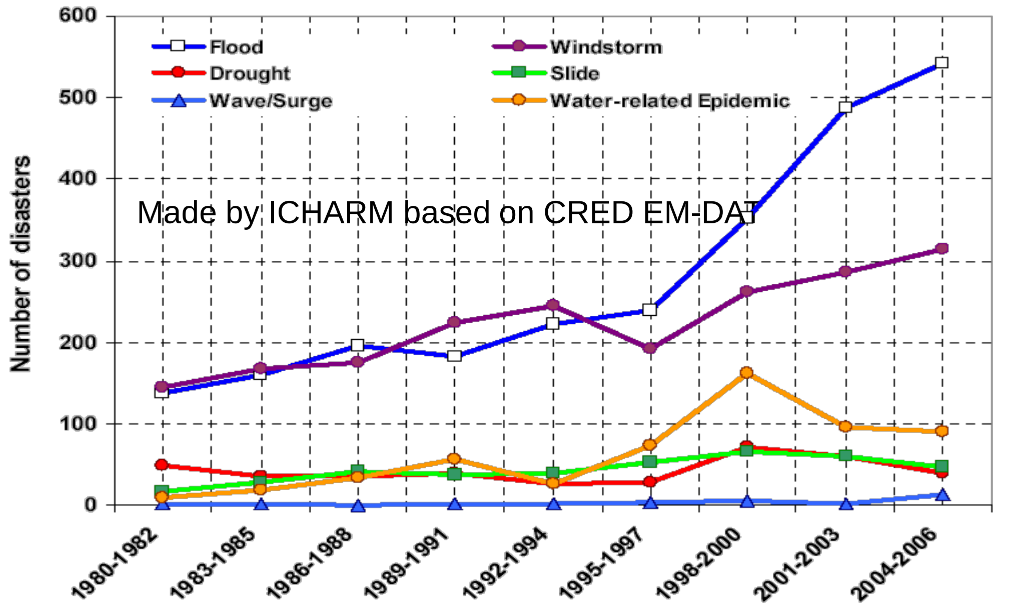

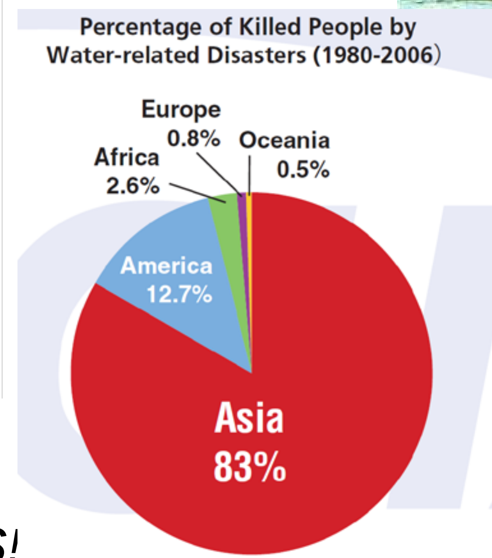

Increase of vulnerability + climate change?

Flood warning can reduce casualties!

China Floods		Bangladesh Storm Surges		Myanmar Nargis	
Year	Death Tolls	Year	Death Tolls	Year	
1931	3 700 000 (400 000*)	1970	300 000	2008	138 000
1954	30 000	1991	139 000		
1998	3 700	2007	4 200		

- Integrated flood risk management
  - Flood warning
  - Hazard and risk analysis based on “data”
- Climate change impact analysis and adaptation

Problems of flood forecasting system installation in poorly-gauged river basins

- Difficulty to get real-time hydrological data in the upstream of a transboundary river basin
- Insufficient of implementation and maintenance of ground-based real-time hydrological observation stations, such as raingauge and river discharge gauging station with data transmission system.
- Lack of the data required for creation of a flood forecasting model such as altitude, land use, river channel network, etc.
- Difficulty of the expense burden which is needed for a flood forecasting system installation
- Insufficient framework to enhance technical capabilities

Rainfall observation by hand

Houses built along a river

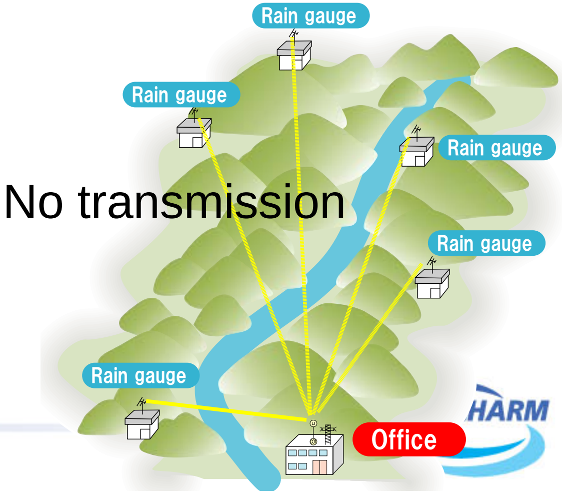

Possible approaches…

In any case, in-situ hydrologic monitoring is always VERY important. But it may require very long time to implement any sufficient network system …

- Community-based approach
  - Simple on-site warning devices, etc.
- Empirical & statistical approach using limited hydrologic (rainfall, water level and/or streamflow) data
- To start from the utilization of global earth observation data such as satellite-based rainfall and globally-available GIS data, and to improve in-situ hydrologic observational network, step by step or gradually, depending upon the availability of resources
- If you have enough resources now, then you can make a fully-packaged system immediately…

ICHARM

Concept of development IFAS
&
Introduction of satellite-based rainfall data

IFAS was developed originally by a joint research (FY2005-2007)among the following:

International Centre for Water Hazard and Risk Managemennt (ICHARM)
Public Works Reserch Institute (PWRI)
CTI Engineering Co., Ltd.
NIPPON KOEI Co., Ltd.
IDEA Consultants, Inc.
Yachiyo Engineering Co., Ltd.
Pacific Consultants Co., Ltd.
Tokyo Kensetsu Consultants Co., Ltd.
NEWJEC Inc.
CTI Engineering International Co., Ltd.
Infrastructure Development Institute (IDI)
Kokusai Kogyo Co., Ltd.

IFAS

ICHARM

Integrated Flood Analysis System (IFAS)

Flood runoff analysis system with satellite-based rainfall & global GIS information

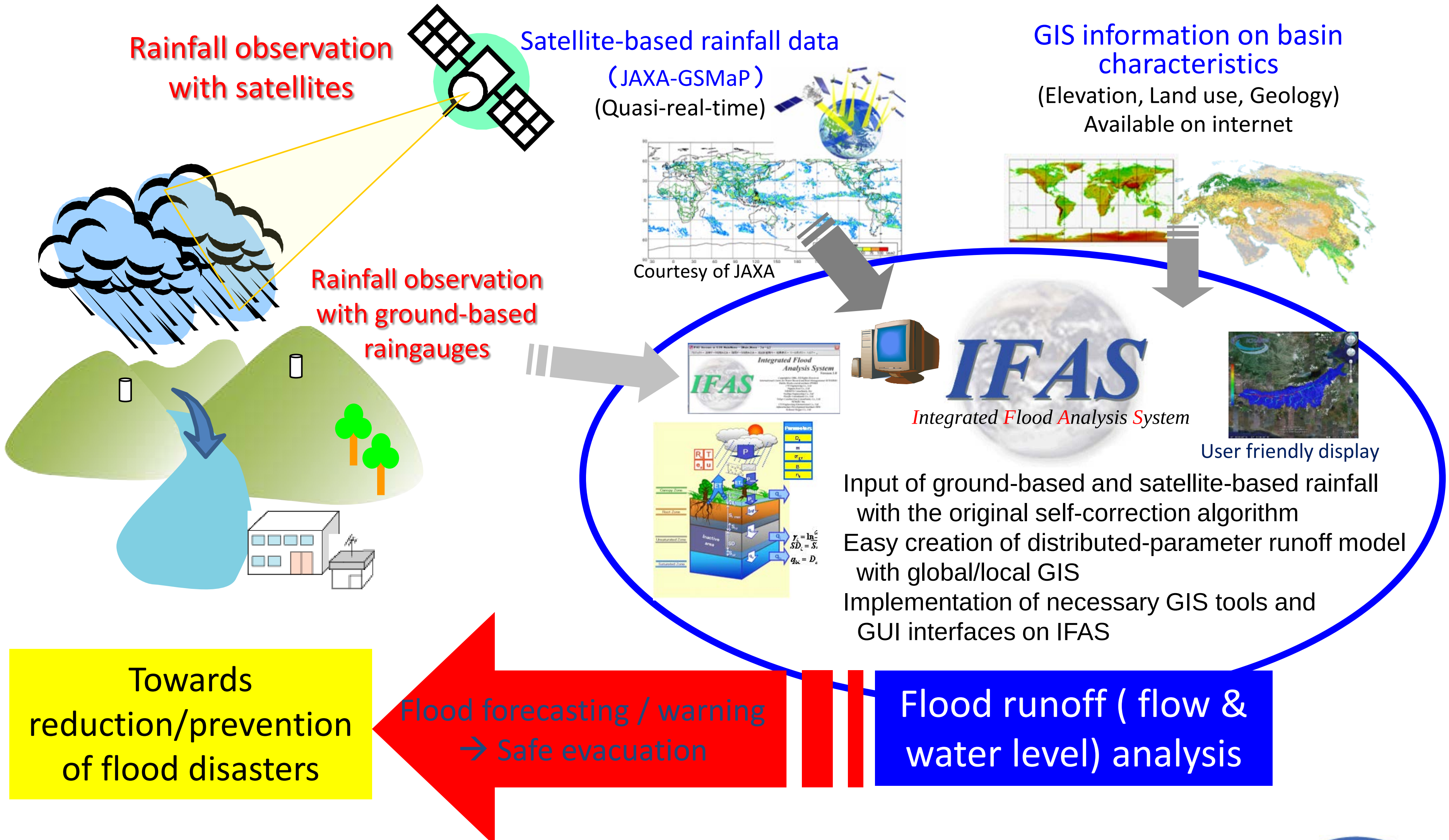

Outline of IFAS

Satellite-based rainfall or
Local data (Ground rainfall)

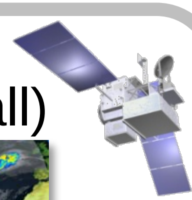

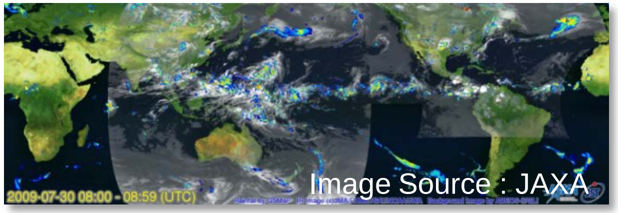

Global GIS datasets
Elevation data, Land use data, etc.

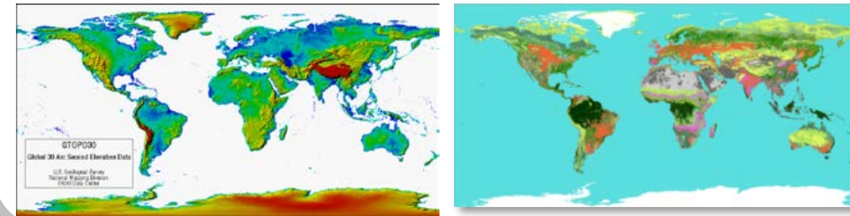

IFAS (Integrated Flood Analysis System)

Data input

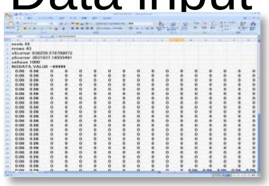

Model creation

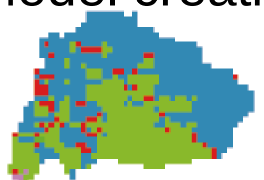

Run-off analysis

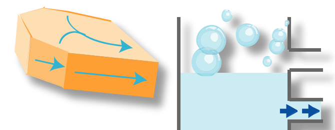

Output

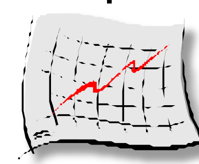

Calculation of river discharge

Runoff Analysis Engine : PWRI Distributed hydrological model (PDHM Ver.2)

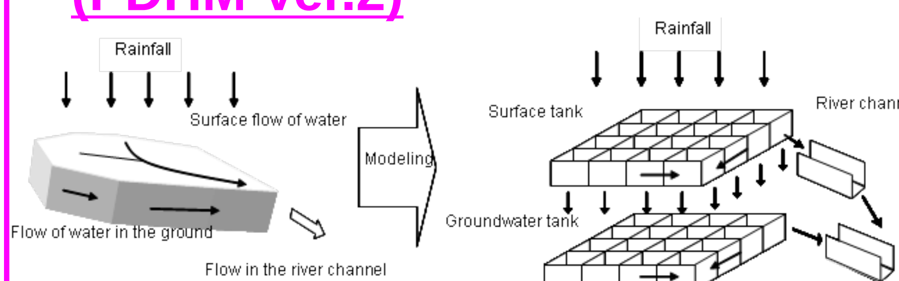

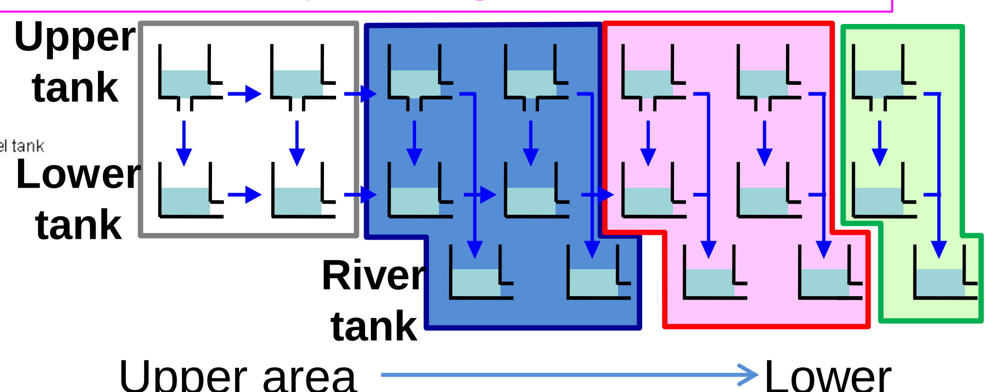

GFAS - Rainfall

http://gfas.internationalfloodnetwork.org/gfas-web/

Rainfall information
from observation satellites

Data Obtainment
Data Processing
Data Dissemination

Website: Maps, Data
E-mail delivery:
Heavy Rain Notice

Flood Forecasting and Warning
by using GFAS information

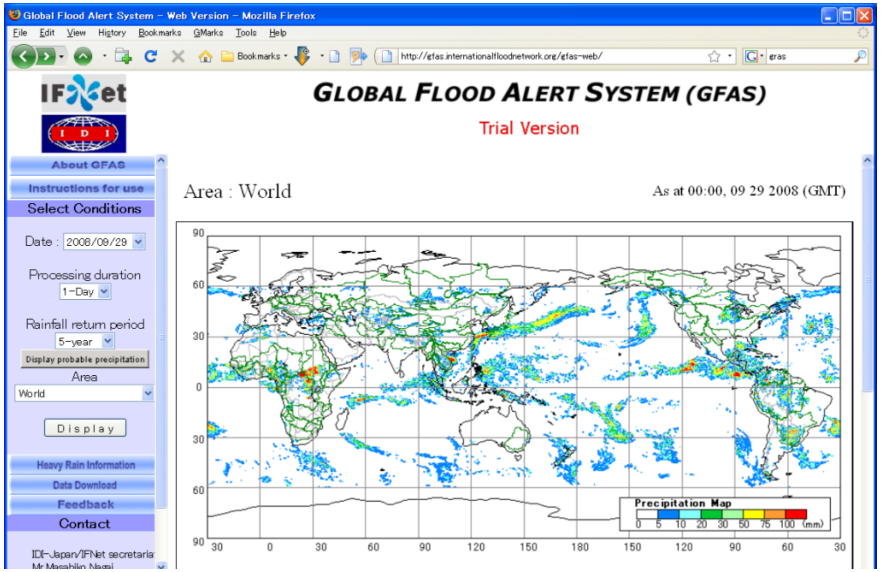

Real-time Rainfall Map (every 3 hour)

Heavy rainfall identification → alert

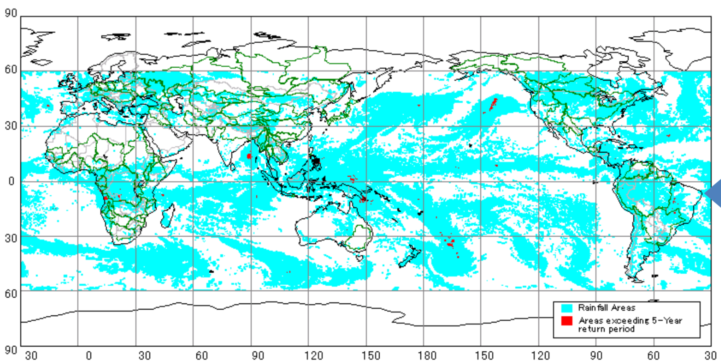

Real-time estimation of rainfall areas

Exceeding 10- (or 5-) Year Return Period

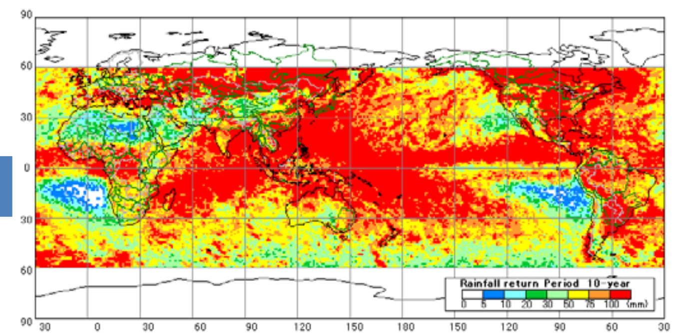

Pre-analyzed rainfall distribution
exceeding 5 or 10-year return period

ICHARM

Satellite-based rainfall data

- There is no necessity for installation and maintenance of a rain gauge or transmission equipment .
  - Ground-based rainfall data are indispensable to get highly-accurate flood runoff analysis and forecast.
- Almost the worldwide coverage and a consistent accuracy are obtained.
- Resolution (time and space) and observation accuracy are low compared with properly-distributed ground-based rainfall data.

Product name	3B42RT	CMORPH	**GSMaP_NRT**
Developer and provider	NASA/GSFC	NOAA/CPC	JAXA/EORC
Coverage	N60° - S60°		
Resolution	0.25°	0.25°	**0.1°**
Resolution time	3 hours	3 hours	**1 hour**
Time lag	10 hours	15 hours	**4 hours**
Coordinate system	WGS		
Historical data	Dec 1997-	Dec 2002-	Dec. 2007～
Sensors	TRMM/TMI Aqua/AMSR-E AMSU-B DMSP/SSM/I IR	Aqua/AMSR-E AMSU-B DMSP/SSM/I TRMM/TMI IR	TRMM/TMI Aqua/AMSR-E ADEOS-Ⅱ/ AMSR SSM/I IR AMSU-B

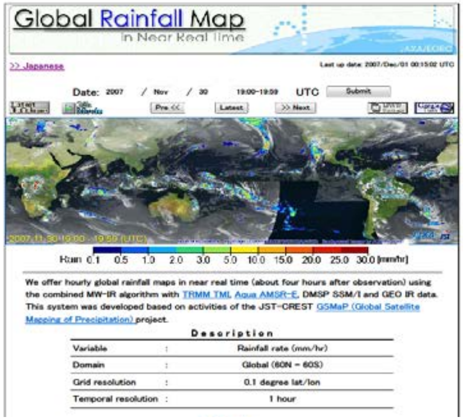

GSMaP_nRT

http://sharaku.eorc.jaxa.jp/GSMaP/index.htm

Algorithm for self-correction of satellite-based rainfall data without any ground-based rainfall data

Moving fast →Underestimation

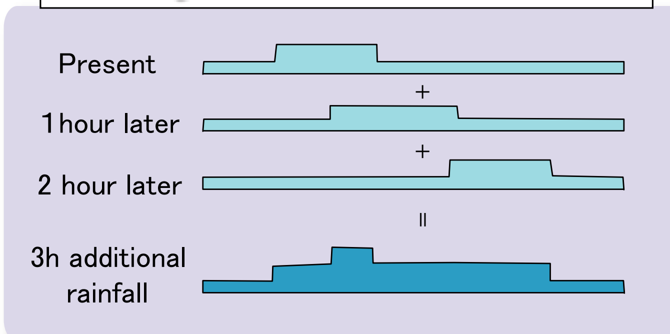

Small spatial variance of cumulative rainfall on a certain scale

Moving slowly → Better coincidence

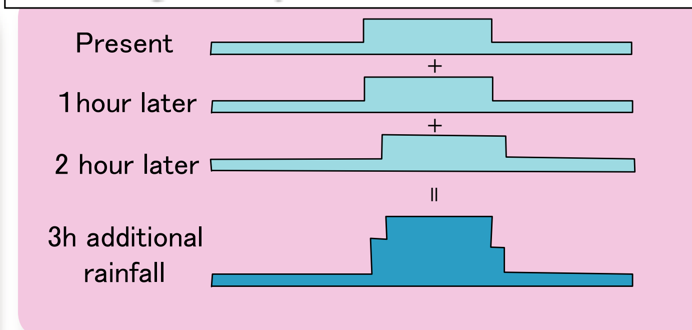

Large spatial variance of cumulative rainfall on a certain scale

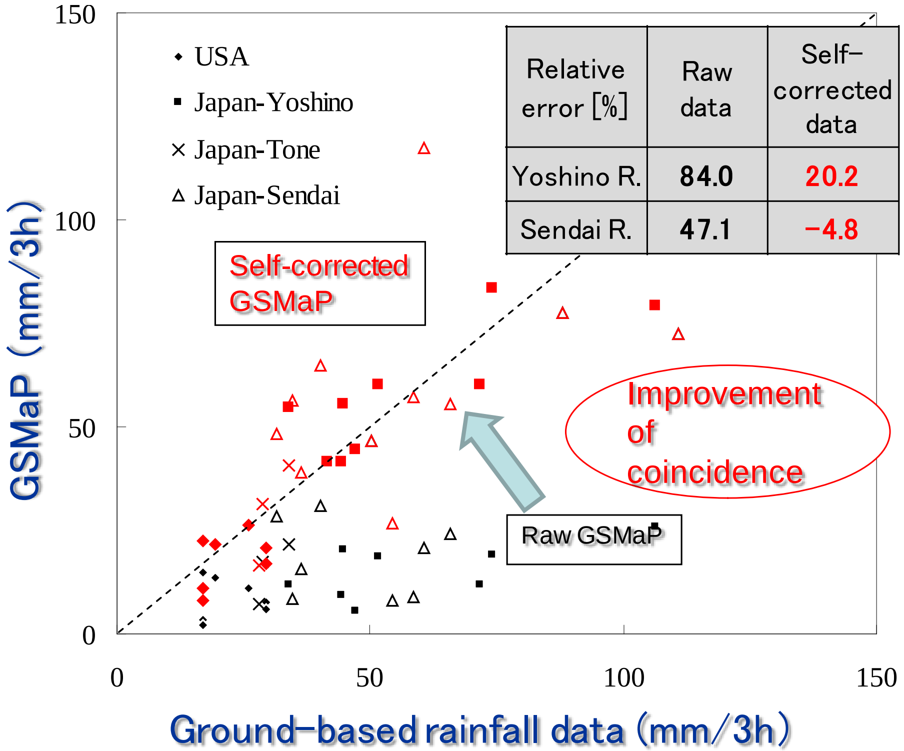

Relative error [%]	Raw data	Self-corrected data
Yoshino R.	84.0	20.2
Sendai R.	47.1	−4.8

A hypothesis on the reason why this self-correction is empirically effective.

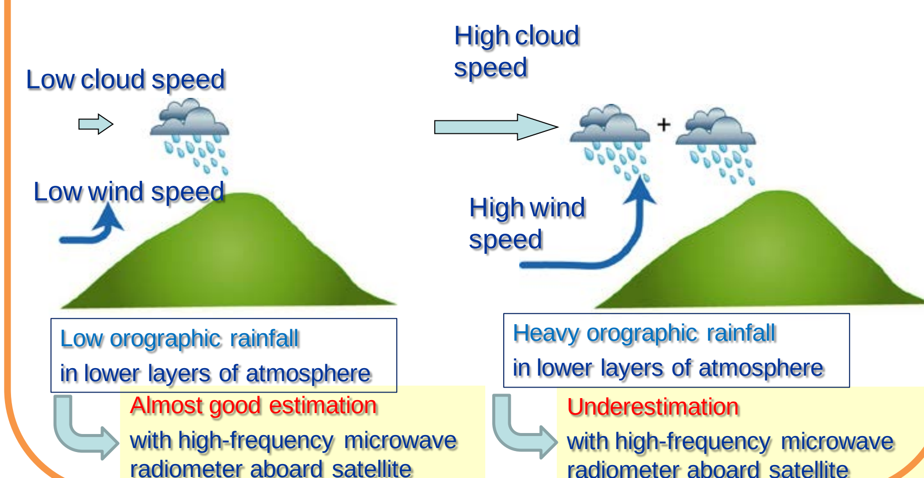

ICHARM

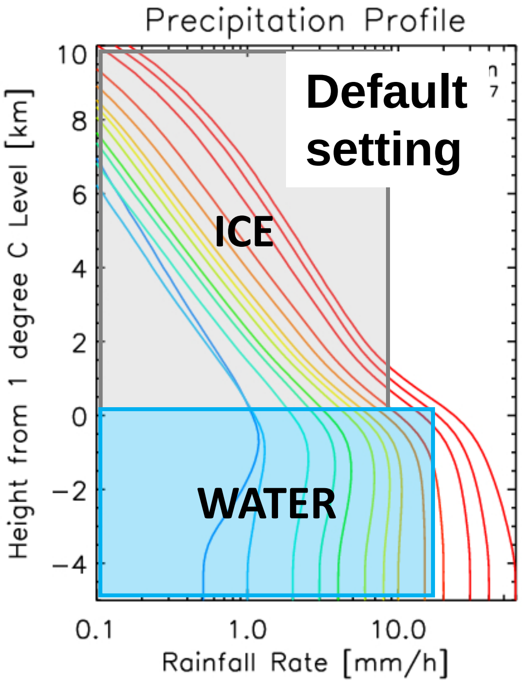

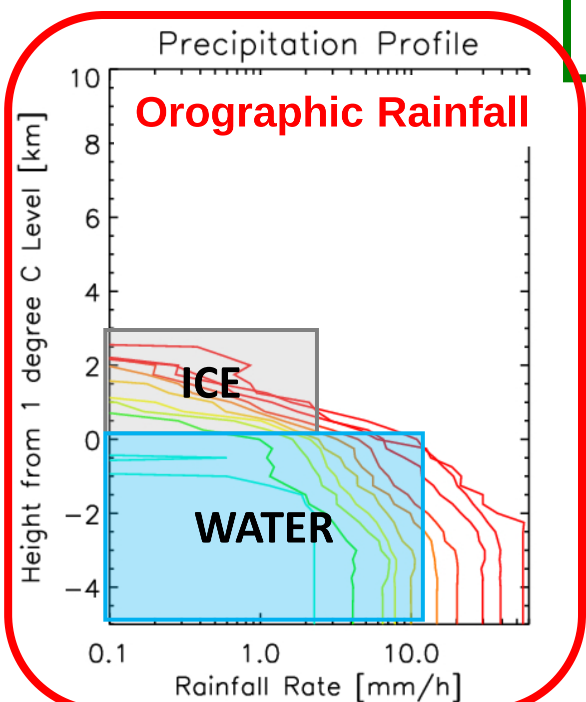

Look-up table:
Relationship between microwave brightness temperatures (Tbs) and rain rates

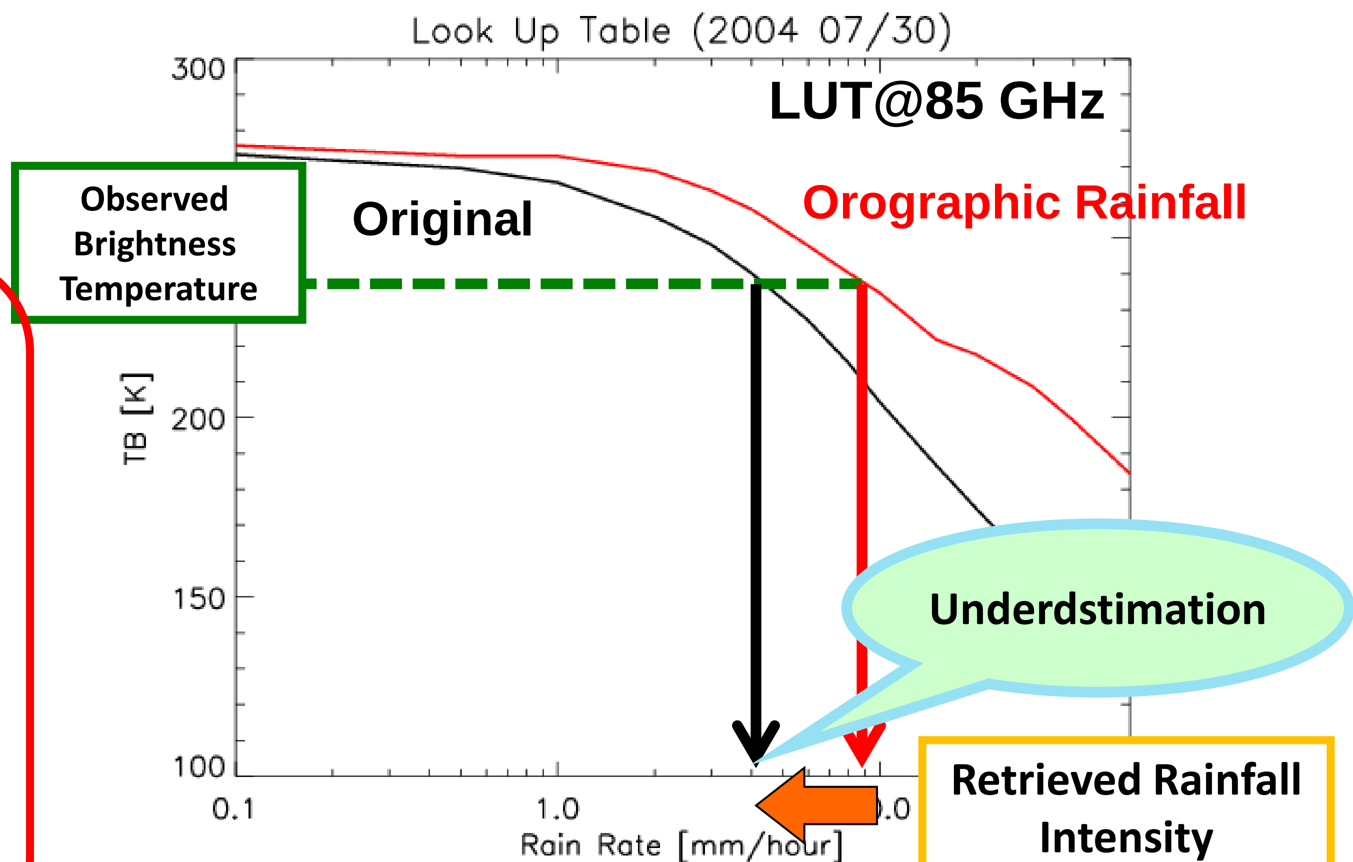

From Taniguchi and Shige (2011) and Ashiwaki(2010)

Effect of the ICHARM's self-correction method of satellite-based rainfall

- Self-corrected GSMaP_nRT can effectively reduce the degree of underestimation for heavy rainfall data **without any real-time ground-based rainfall data.**
- **IFAS implements this self-correction method.**

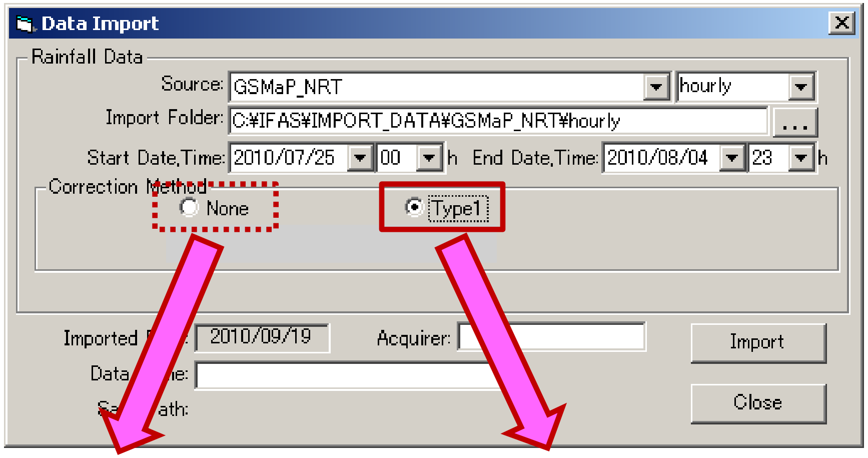

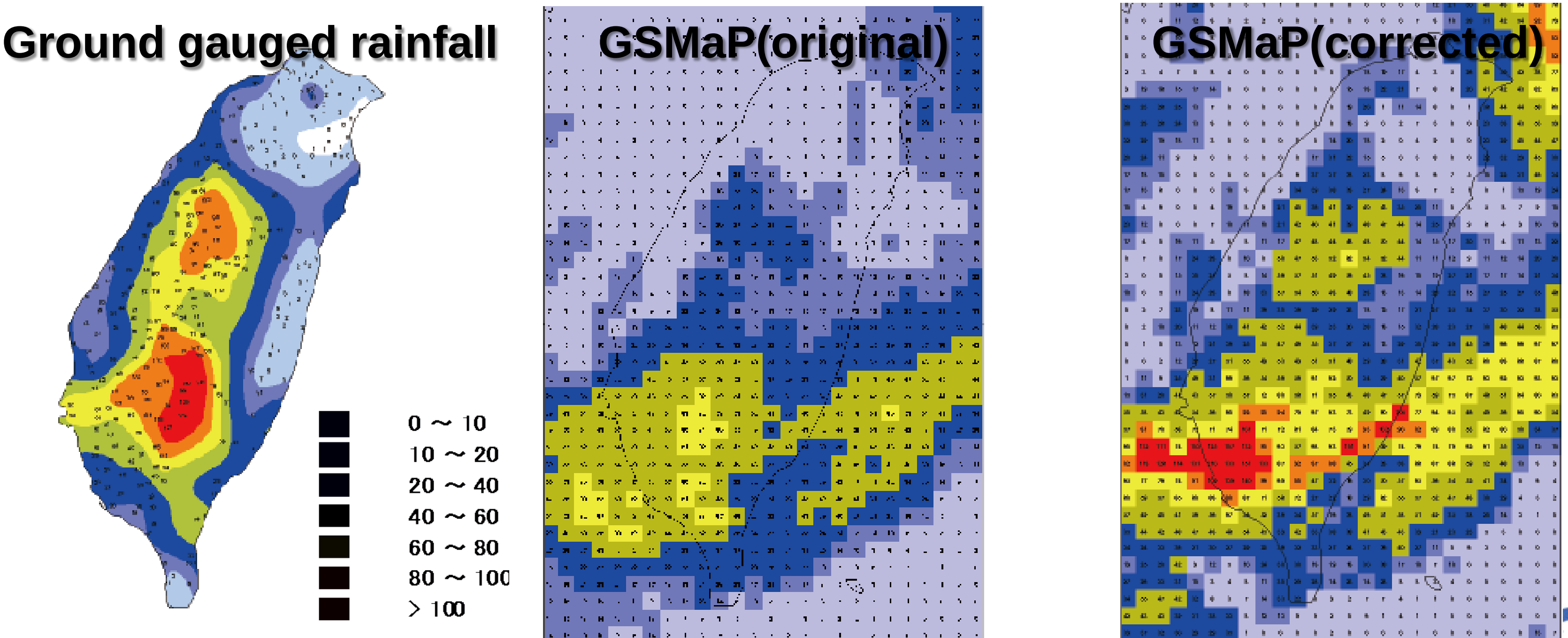

Typhoon No.8 in 2009 (Typhoon Morakot)
Rainfall distribution in Taiwan (3-hour cumulative rainfall)

Main features of IFAS:

Not only ground-based but also satellite-based rainfall data area applicable

Distributed-parameter flood runoff model creation using global GIS data

With limited historical / real-time hydrological databases in poorly-gauged rivers

All-in-one package for GIS data analyses

Free download for the executable program from ICHARM-IFAS website
http://www.icharm.pwri.go.jp/index.html

Prompt and efficient implementation of flood analysis and forecasting system even in poorly-gauged rivers
and
step-by-step improvement of accuracy
with the **enhancement of in-situ hydrological observational network**

ICHARM

Default runoff analysis models on IFAS

- Three types of distributed hydrological models
  - PWRI Distributed Hydrological Model (PDHM Ver.2) (simplified for flood events, below)
    - Suzuki, Terakawa & Matsuura (1996), Inomata & Fukami (2007), IFAS Ver.1.2 Manual (2009)
  - PWRI Distributed Hydrological Model (PDHM Ver.1) (for flood & long-term flows)

    3-layer model for wide availability from low to high flows

    - Yoshino, Yoshitani & Horiuchi (1990) → released in IFAS Ver.1.3
  - BTOP Model (for a variety of hydrological conditions)
    - Takeuchi, Hapuarachchi, Zhou, Ishidaira & Magome (2008) → upon special request

PDHM Ver.2

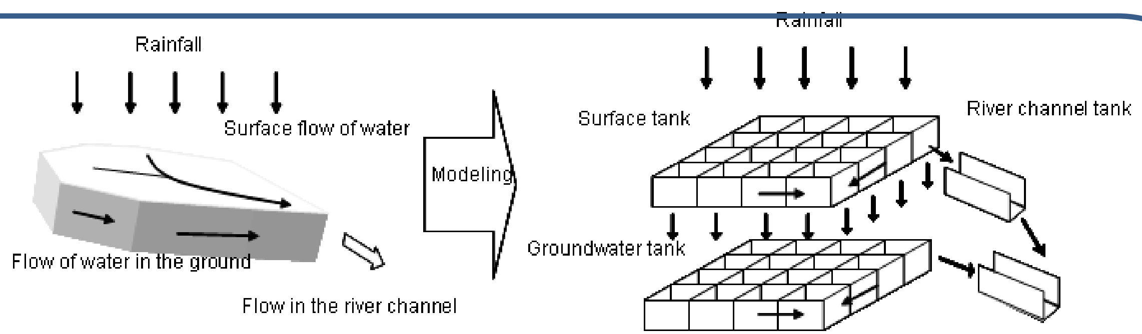

2-layer model for quick flood runoff simulation

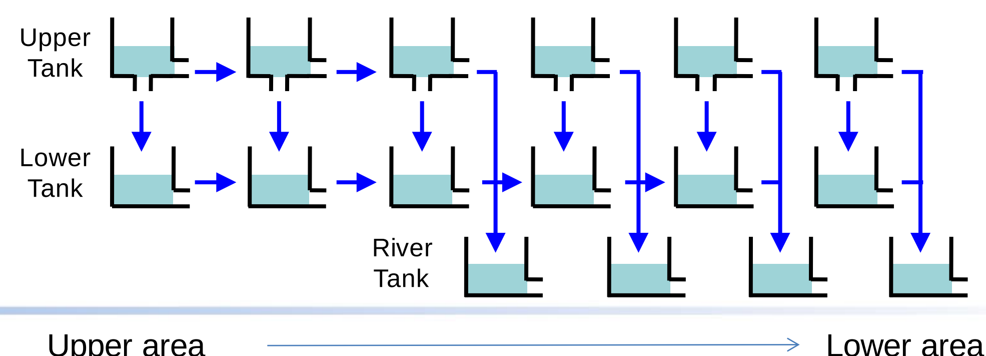

Runoff Analysis Model on IFAS (PDHM Ver.2)

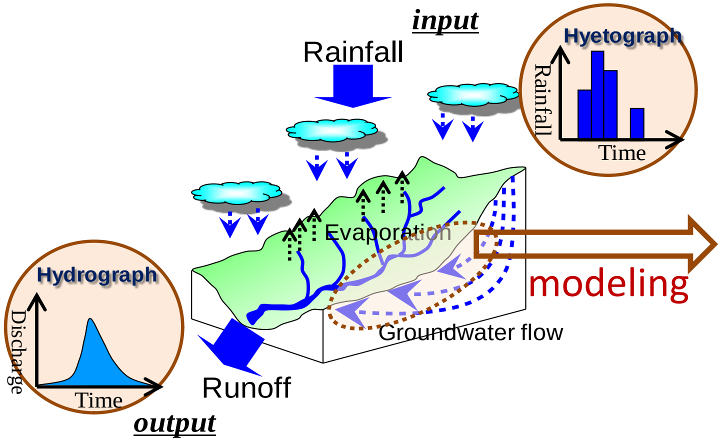

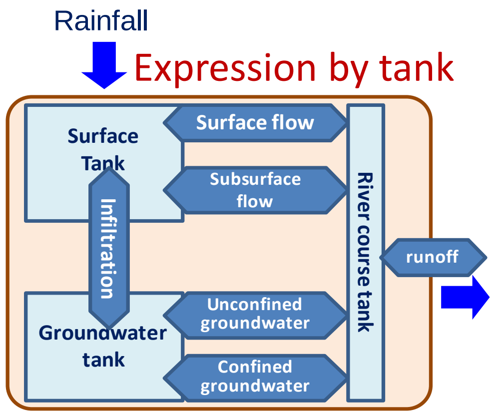

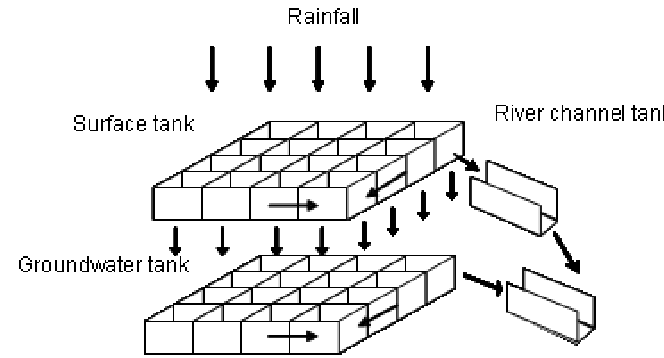

Surface Tank (Upper tank)

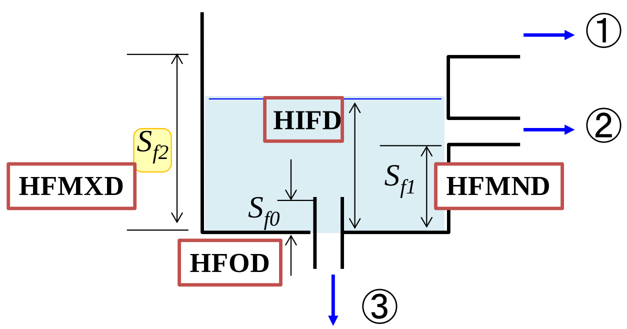

①Surface flow: $L\frac{1}{N}(h-S_{f_2})^{\frac{5}{3}}\sqrt{i}$ SNF

②Subsurface flow: $\alpha_n A f_0 (h-S_{f_1})/(S_{f_2}-S_{f_1})$ FALFX

③Infiltration: $Af_0(h-S_{f_0})/(S_{f_2}-S_{f_0})$ SKF

Groundwater Tank (Lower tank)

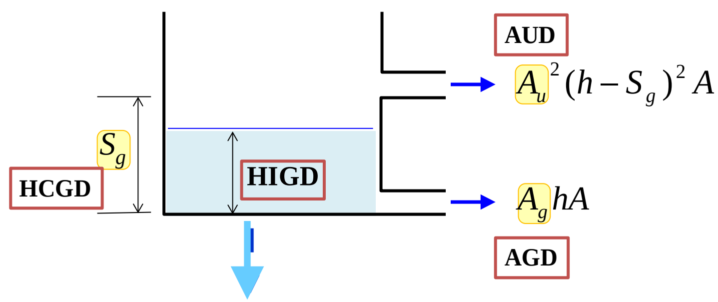

It is possible to set α as groundwater loss.

Parameters of upper tank varies by land cover (forest, bush and meadow, cropland, urban & water)

River Course Tank

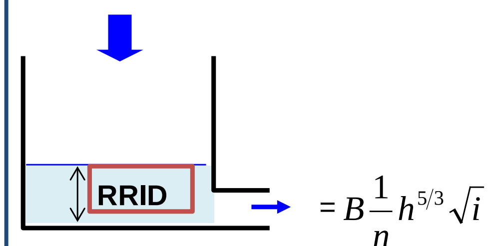

Even if you have no cross-section data of river channels, it is possible to calculate flood flow in steep river channels through the Manning Formula with the assumption or wide rectangular channels.

Flood runoff simulation model creation using global GIS data

Import data

Type	Product	Provider
Elevation	Global Map(Elevation data)	ISCGM
	GTOPO30	USGS
	Hydro1k	USGS
Land use	GLCC	USGS
	Global Map(Land cover)	ISCGM
	Global Map(Land use)	ISCGM
Geology	Geology	CGWM
Soil type	Soil Texture	UNEP
	Soil Water Holding Capacity	UNEP
	Soil Depth	GES

Example of elevation data of a each cell and a river channel network

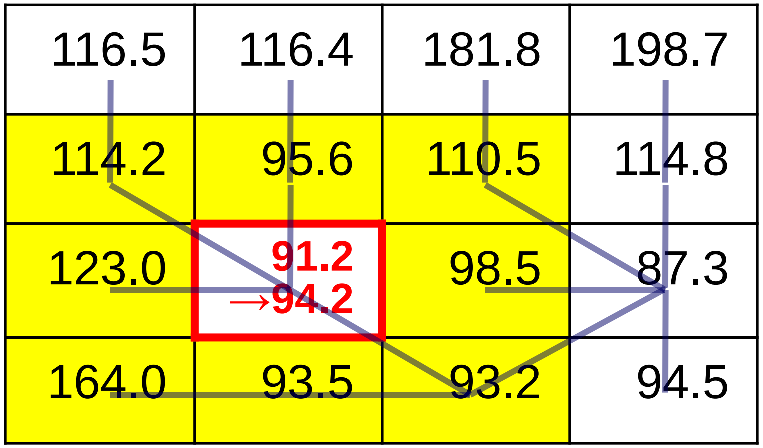

Modify elevation until all sells are decided their flow directions

Creation of River channel network and basin shape based on elevation data

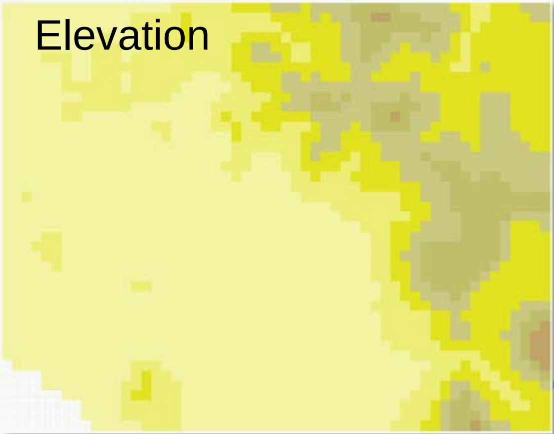

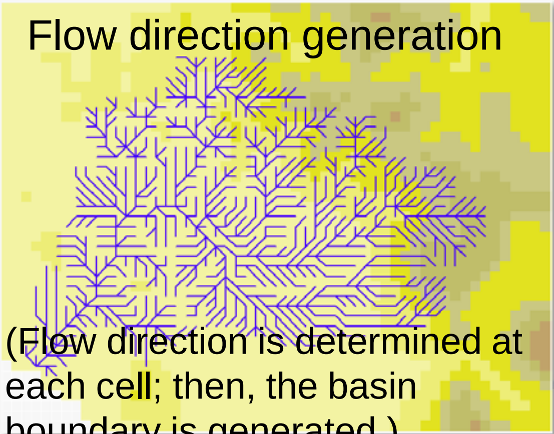

(Flow direction is determined at each cell; then, the basin boundary is generated.)

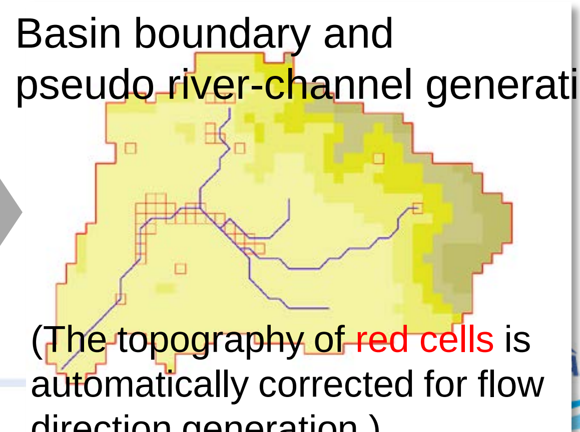

(The topography of red cells is automatically corrected for flow direction generation.)

Parameter estimation using GIS data [surface / groundwater

1. Import GIS data → 2. Distribute GIS data into some classes → 3. Input value for each tank → 4. Set value for each cell

GIS data

Land use/Land cover

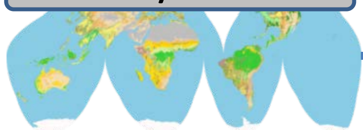

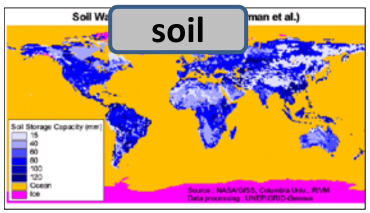

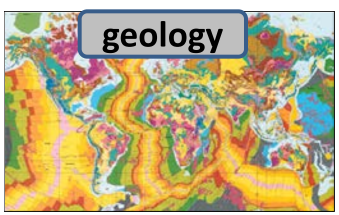

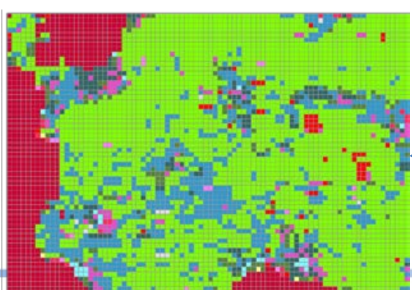

Imported GIS data

Land use classification (GlobalMap)	Surface parameter	Infiltration capacity	Rough -ness	○○
Broadleaf Evergreen Forest	1	0.0005	0.7	…
Broadleaf Deciduous Forest				
Needleleaf Evergreen Forest				
Needleleaf Deciduous Forest				
Mixed Forest				
Tree Open				
Shrub	2	0.00002	2	…
Herbaceous				
Herbaceous with Sparse Tree/Shrub				
Sparse vegetation				
Bare area (gravel, rock)				
Bare area (sand)				
Cropland	3	0.00001	2	…
Paddy field				
Cropland / Other Vegetation Mosaic				
Mangrove				
Wetland				
Urban	4	0.000001	0.1	…
Snow, ice	5	0.00001	2	…
Water bodies				

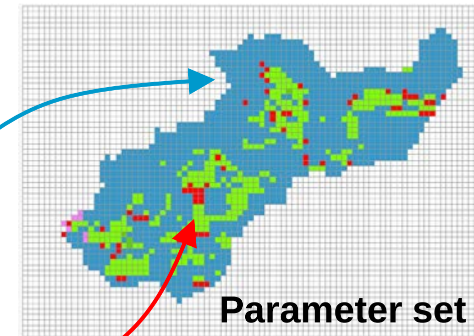

- ◆IFAS has already set default parameter.
- ◆Each parameter reflects local condition.

River course model parameter estimation using Cell type classification

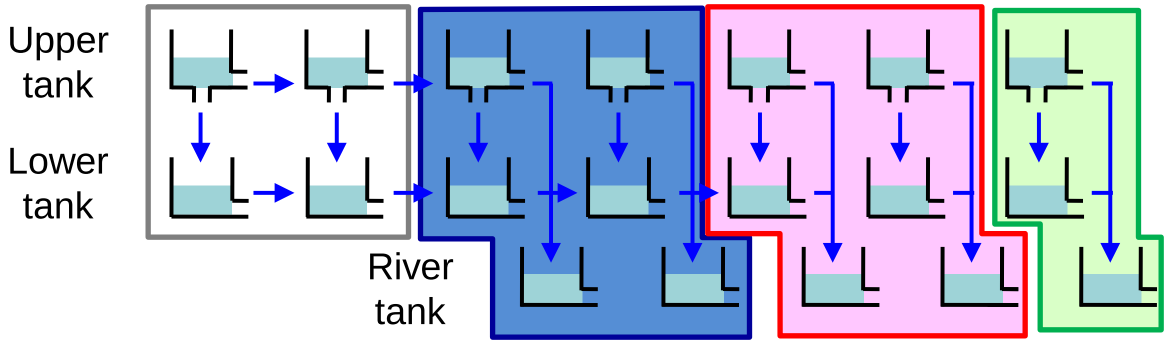

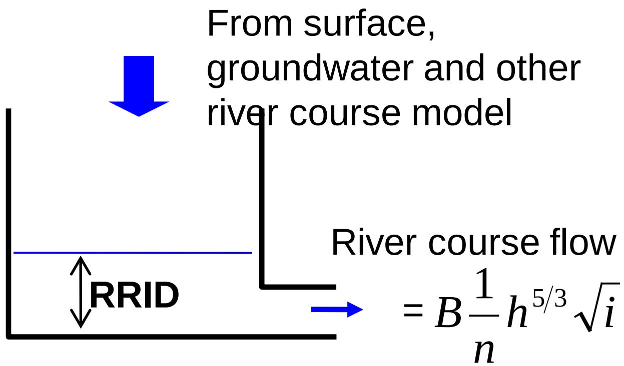

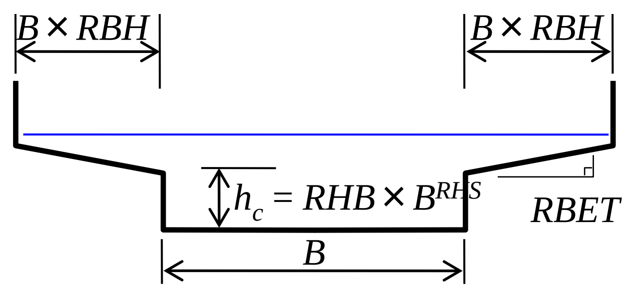

Upper area → Lower area

	Cell type 0	Cell type 1	Cell type 2	Cell type 3
Number of upper cell (default)	1～2	3～4	5～64	65～
Constant of Resume law	-	6	7	8
Manning roughness coefficient	-	0.07	0.05	0.035
…	-	…	…	…

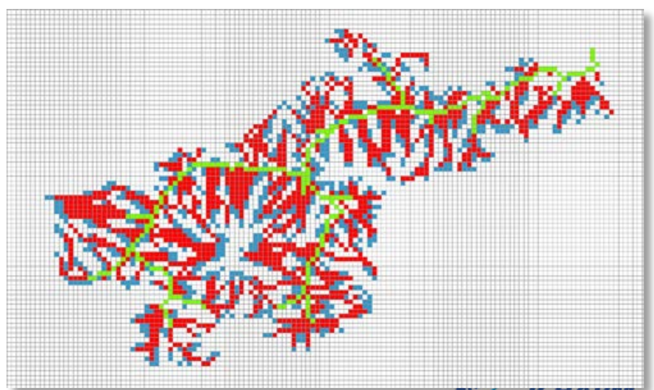

Cell type3 routing by the Kinematic waving method. (displayed as a main river channel)

Consideration of flood control regulation with dam operation in IFAS

1) Fixed release-rate operation

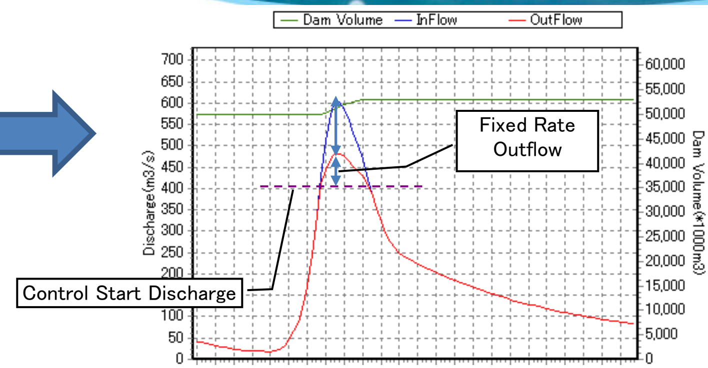

2) Fixed release-value (amount) operation

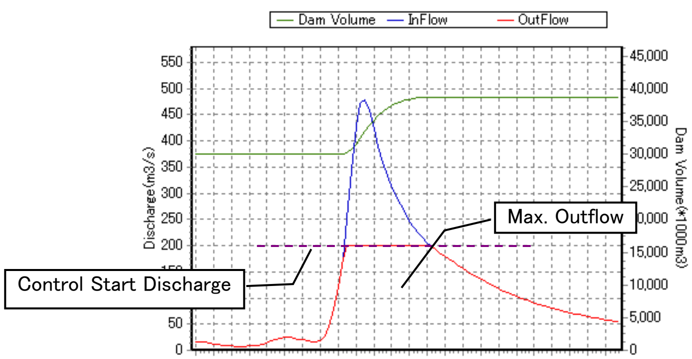

3) Fixed-rate and fixed-value releasing operation

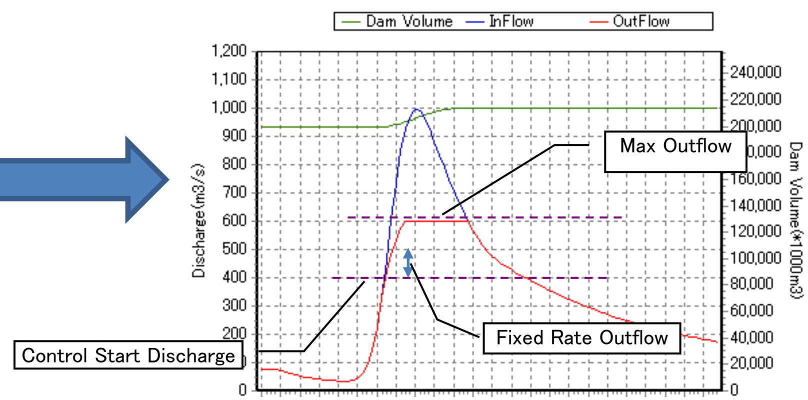

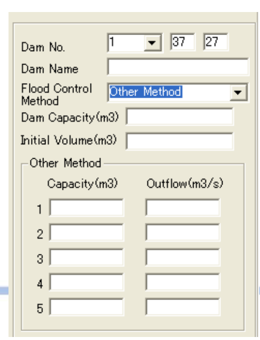

4) Arbitrary regulation-curve-based operation

(up to five storage levels)

Interface display

Main display

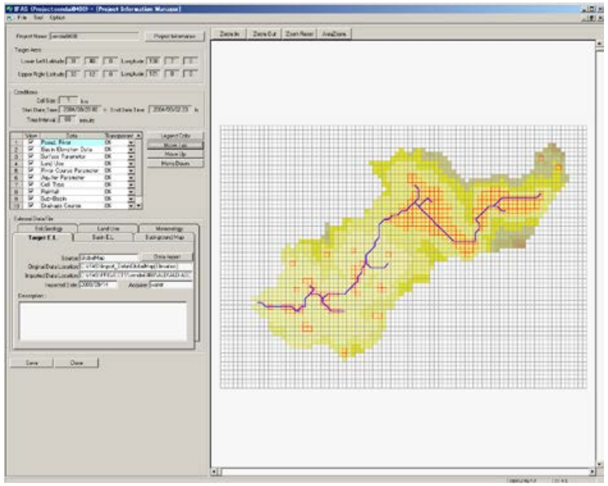

Edit display of rainfall data

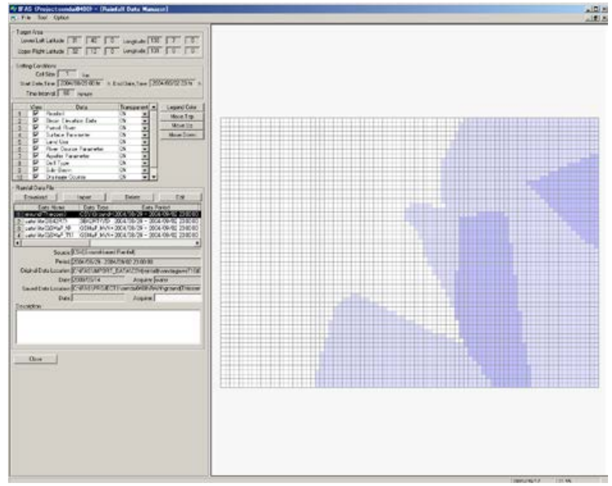

Setting display of parameter

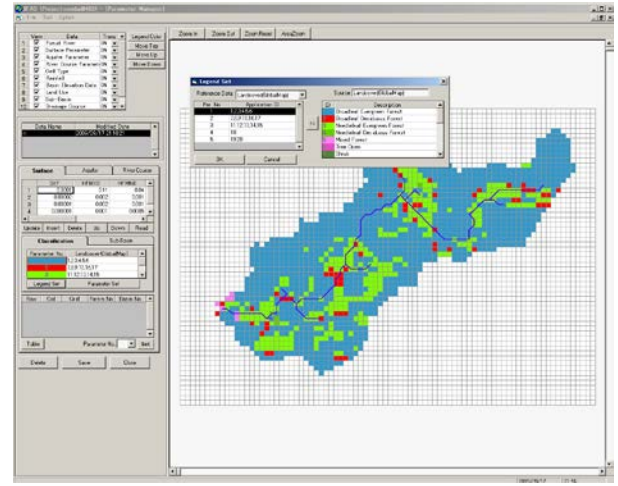

Calculation result

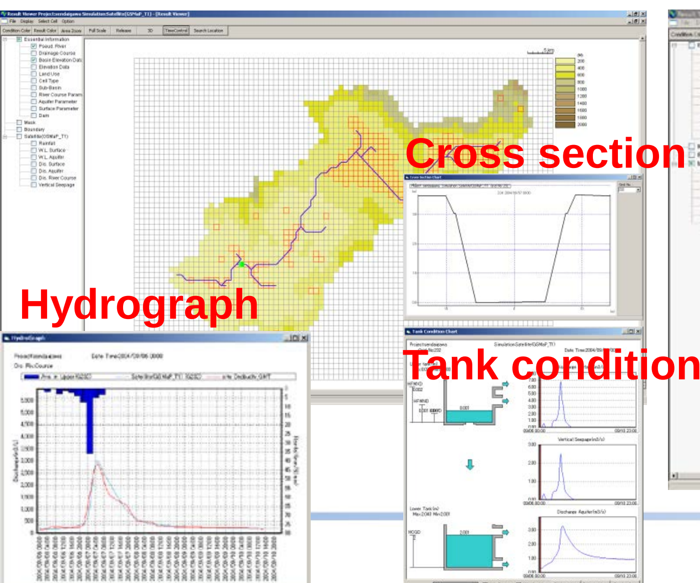

Calculation (Plane view)

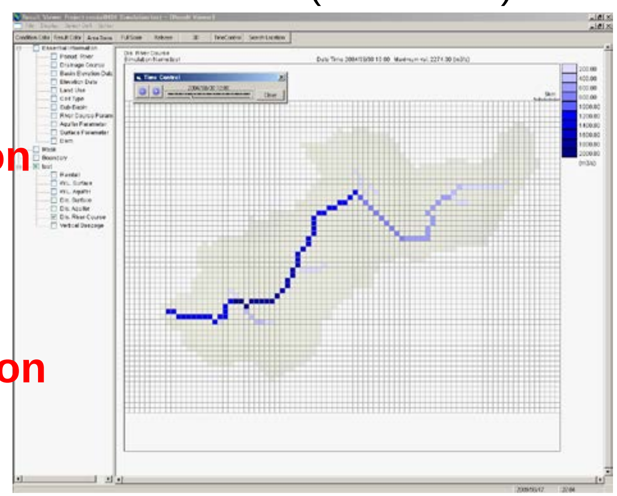

Plane view on Google Map

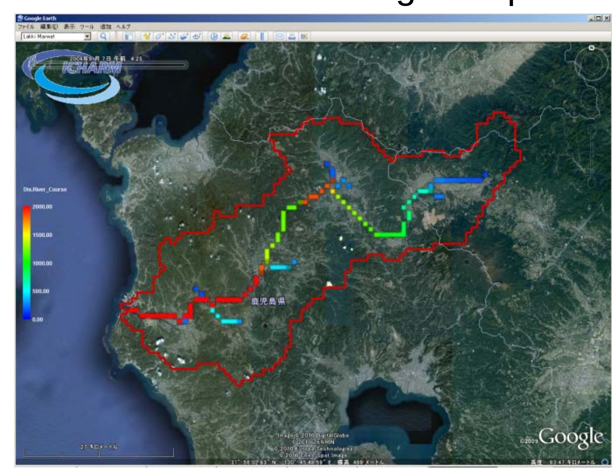

New functions in IFAS ver1.3 prototype

- Automatic download function every hour for storing satellite-based rainfall
- Modification of self-correction method for GSMaP
- Implementation of 3-tank hydrological model (PDHM Ver.1)
- Effect of loss into deep groundwater
- Simple real-time calibration method of calculated discharge
- Each time-step data storing function for the state of each tank
- Automatic early warning system (alert window & e-mail)

New IFAS-extra-module for Automatic Warning System (IFAS Ver.1.3) (automatic incremental simulation for each time step and alert window & e-mail)

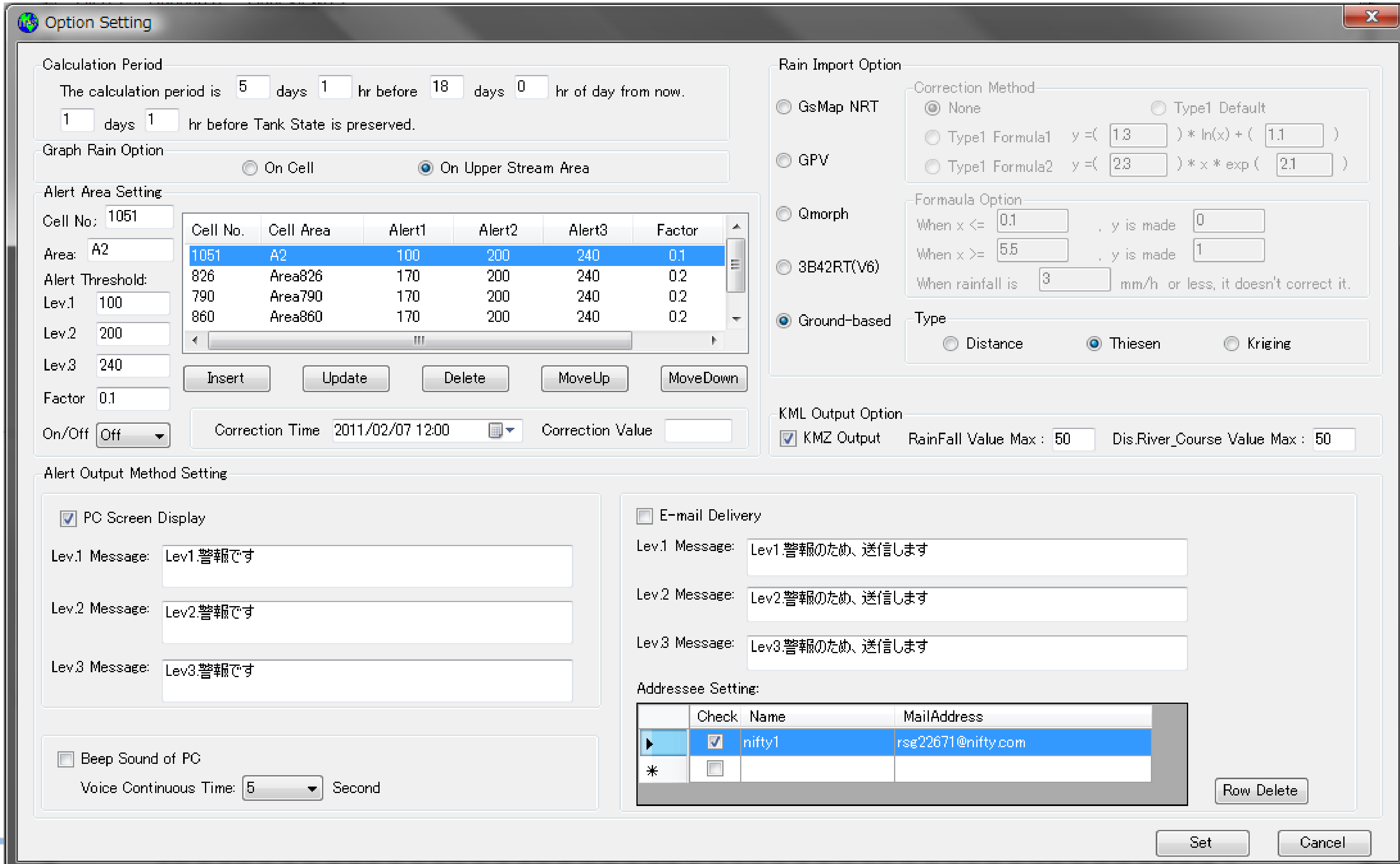

Potential applications of IFAS

- Tool for fundamental GIS & hydrologic data analysis
  - Delineation of river basin boundary, river channel network, basin characterization, etc.
  - Rainfall analysis (temporal and spatial distribution) in poorly-gauged river basins with satellite-based and ground-based data
- Flood hazard/risk assessment & integrated flood management
  - Flood runoff analysis for extreme events
  - Flood hazard/risk identification and hazard mapping
  - Implementation of flood forecasting / warning system, coupled with not only ground-based telemetry data but also radar-derived and/or satellite-based rainfall data
- Water resources assessment and management
  - Long-term hydrologic analysis → drought monitoring / warning

Examples of IFAS applications to flood runoff analyses / forecasting, their achievements and problems

IFAS-based runoff analysis: Sendai River, Japan

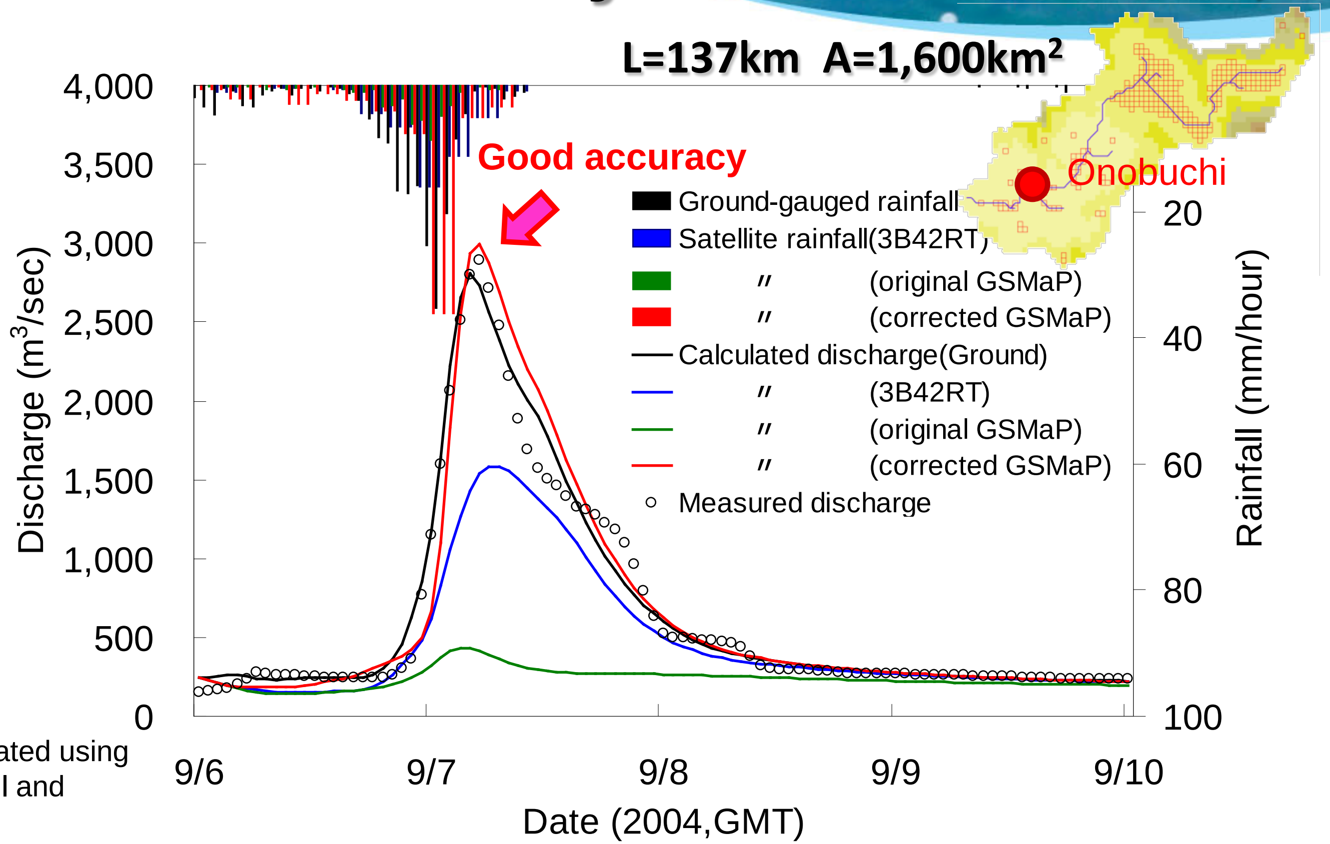

Parameters are calibrated using ground-gauged rainfall and measured discharge

- A flood-runoff event analysis in the Sendai River basin of Japan was very accurately reproduced with IFAS using the ICHARM's self-corrected satellite-based rainfall data without any in-situ ground-based rainfall data, in spite of the under-estimation of rainfall rate in its original GSMaP product.

IFAS-based runoff analysis: Chindwin River, Myanmar

A=27,420km²

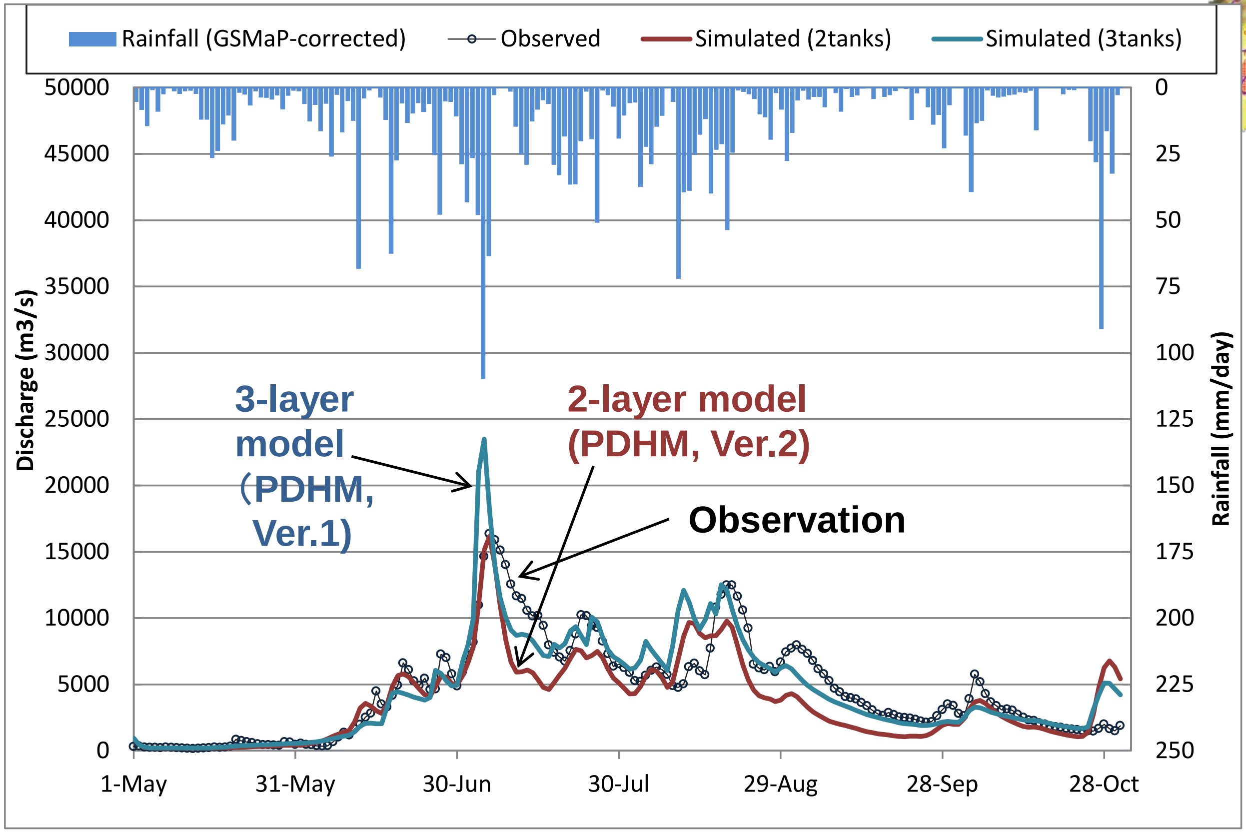

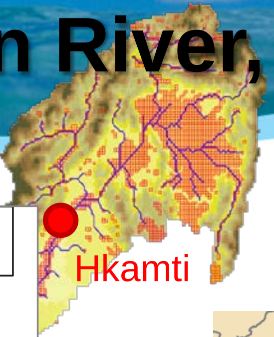

Tributary of ***Irrawaddy***

Parameters are calibrated using self-corrected GSMaP and observed discharge.

- The 2-tank model (PDHM Ver.2) reproduced the 1st major flood peak level and the other major flood peak timings well, but low flows were much underestimated.
- The 3-tank model (PDHM Ver.1) reproduced both major flood peaks (timing and level) and their recessions better. The 1st major flood peak level seems overestimated, but this may show the possibility of inundation in the upstream of the gauging station.

Flood runoff analysis in Dungun River, Malaysia

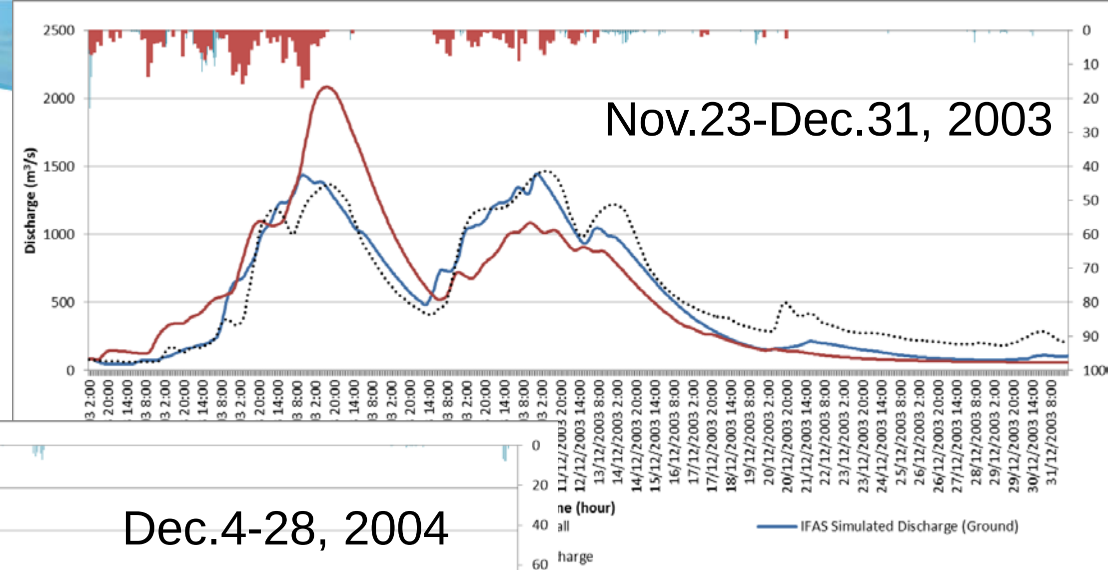

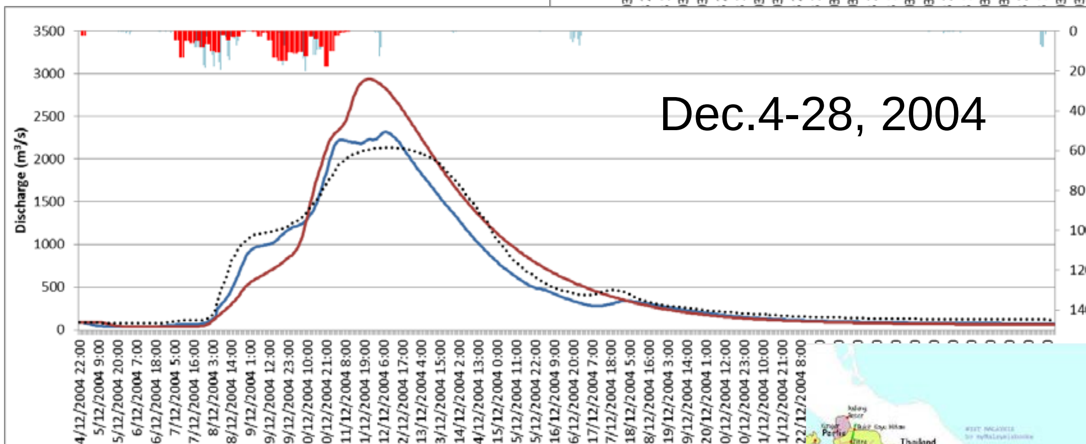

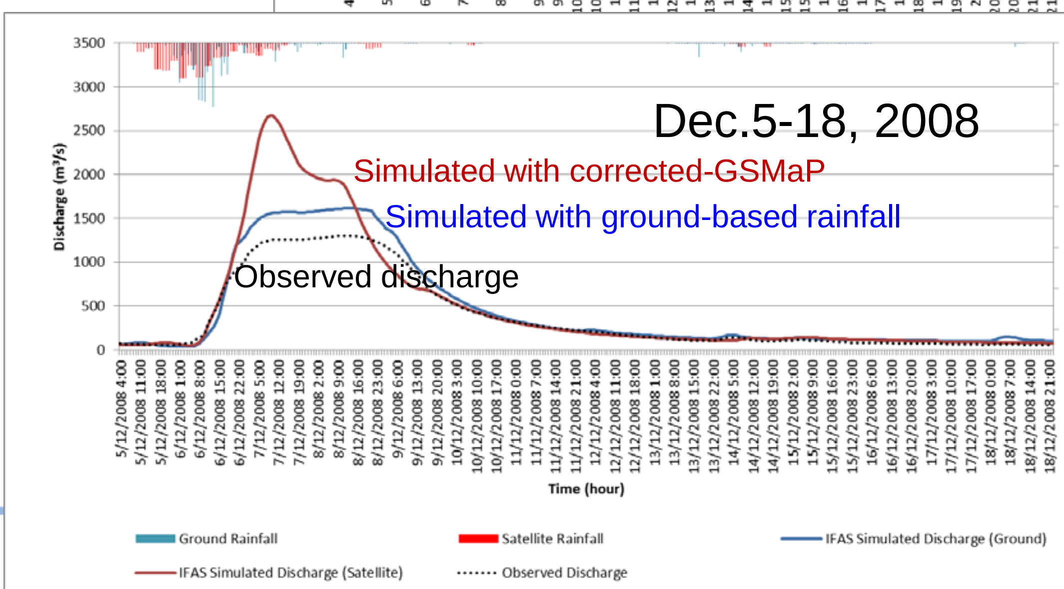

Catchment area = 2,500km^2

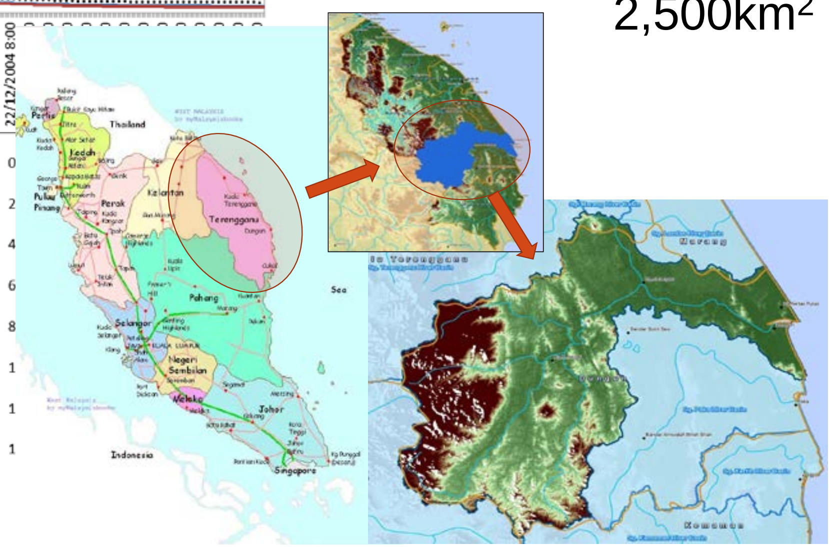

UNITEN, DID & ICHARM

IFAS-based runoff analysis: Kikuchi River, Japan

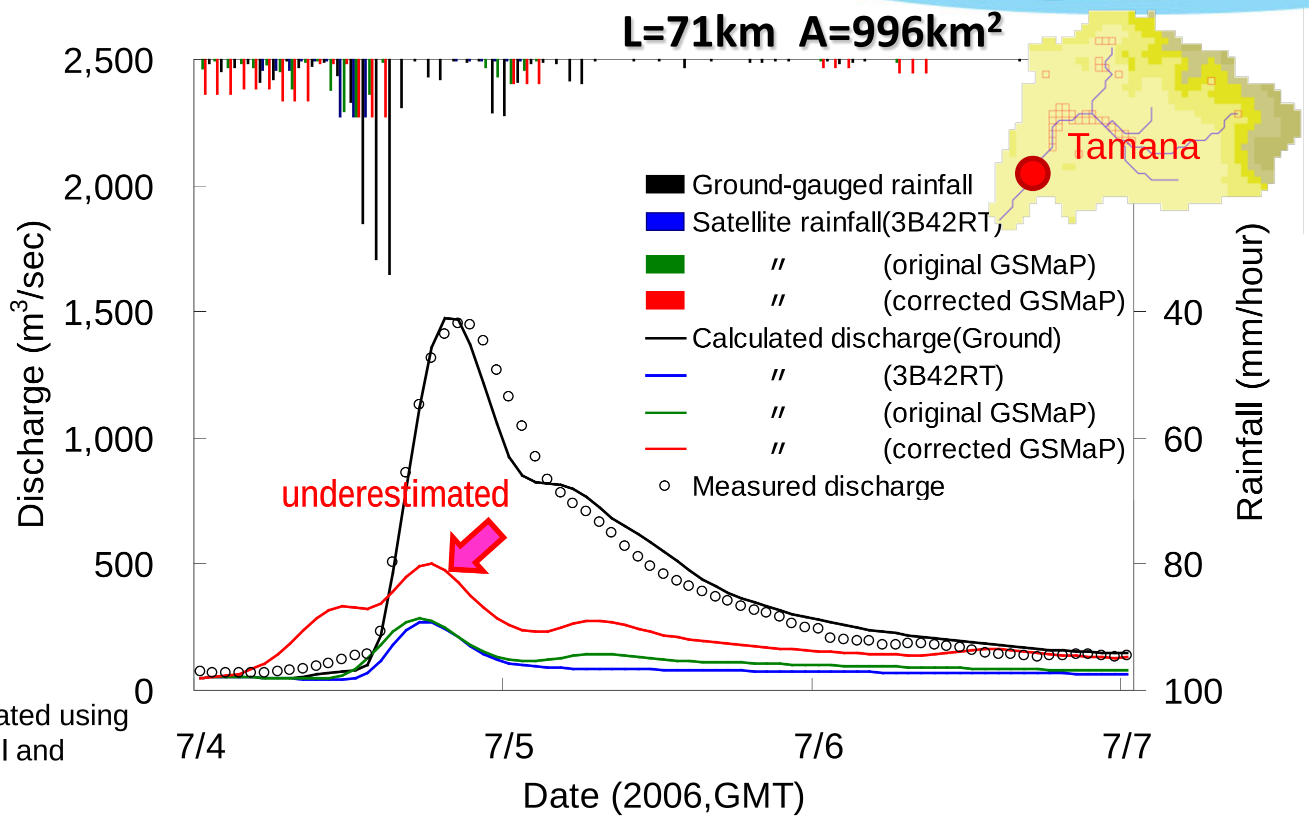

Parameters are calibrated using ground-gauged rainfall and measured discharge

Why was the self-correction of GSMaP unsuccessful for this case?

Difference of frequency of Microwave (MWR) observation

successful case : Sendai river

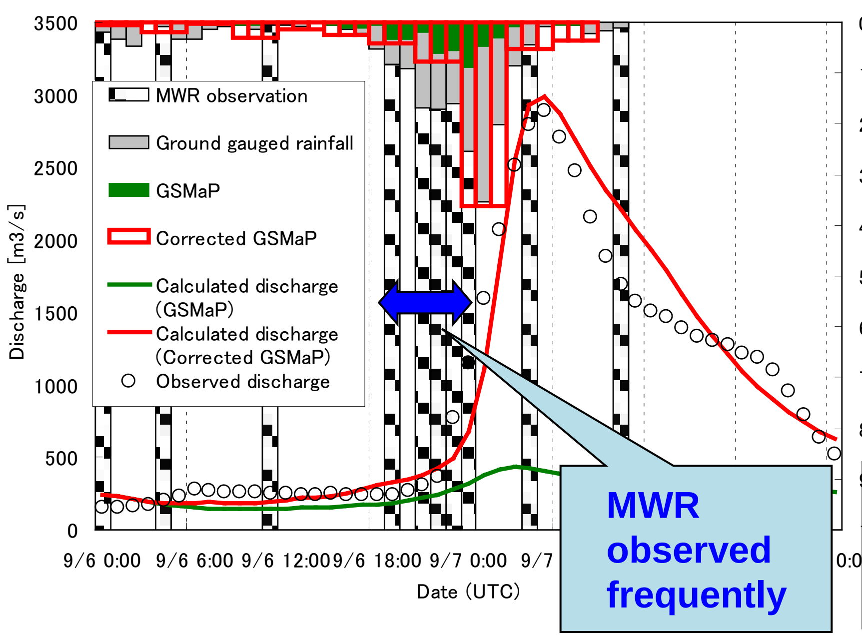

unsuccessful case : Kikuchi river

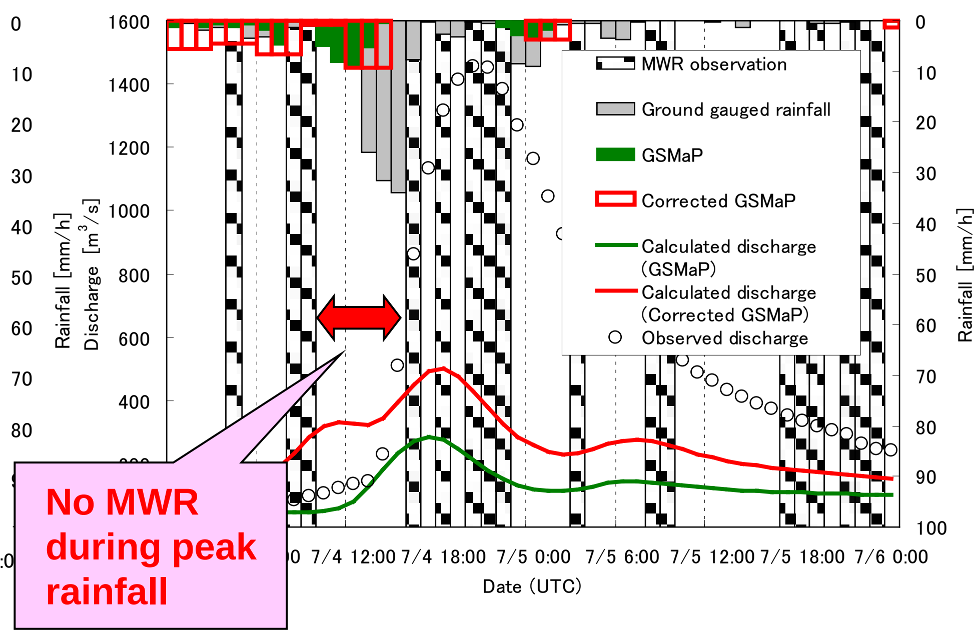

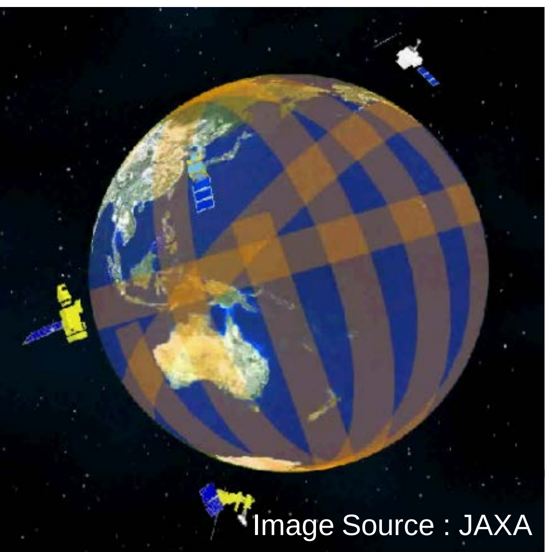

Accuracy of rainfall distribution depends on the frequency of MWR observations

(& accuracy of IR-based motion vectors)

Ozawa et al (2010)

← Image of microwave observation

- MWR obs. is once a few hours on average, but not always guaranteed.
- During no MWR period, rainfall field is transferred by IR-based motion vector.

Global Precipitation Measurement (GPM)

Current Observation System:
TRMM and other orbital Satellites, and 5 Geostationary Satellites

Core Satellite

Dual Frequency Radar
Multi Frequency Radiometer

✧Observation of rainfall with more accurate and higher resolution

✧Adjustment of data from constellation satellites

JAXA (Japan)
Dual frequency Radar, Rocket
NASA(US)
Satellite Bus, Micro-wave gauging measurement

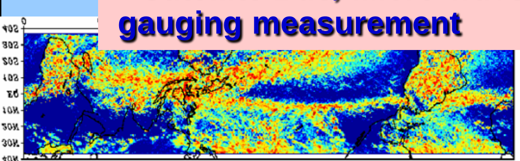

8 Constellation Satellites

Satellites with Micro-wave Radiometers

✧More frequent Observation

Cooperation：
NOAA(US),NASA(US),ESA(EU), China, Korea and others

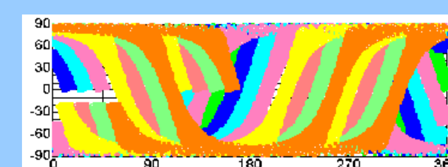

–Earth heating Phenomena
–Study of Climate Change
–Improvement of forecasting system

Global Observation every 3 hours

- IWRM
- Flood Forecasting
- Forecasting of crop productivity

Flood in Pakistan, 2010

- Heavy rain from late July due to monsoon which brought inundation wide-area in the Indus river and affected about 20 million people.
- In the KP province, “flash flood” brought most of the number of deaths in this flood event.
- In Peshawar, it rained 274mm/day (over 2 times as the highest record before)
- GSMaP underestimated. → The ICHARM’s self-correction-based or Thiessen-polygon-based corrections were conducted.

Province	Deaths	Injured	Houses Damaged	Villages Affected	Population Affected
BALOCHISTAN	48	102	75,261	2,604	*672,171
Khyber Pakhtunkhwa	1,154	1,193	200,799	2,834	4,365,909
PUNJAB	110	350	500,000	3,132	8,200,000
SINDH	186	909	1,058,862	7,277	6,988,491
AJ&K	71	87	7,108	No info	245,000
Gilgit Baltistan	183	60	2,830	No info	81,605
FATA	86	84	4,614	Awaited	Awaited
Total	1,838	2,785	1,849,474	15,847	20,553,176

** Additional 600,000 IDPs from Sindh are living in Balochistan*

Table updated from NDMA, 06 September 2010

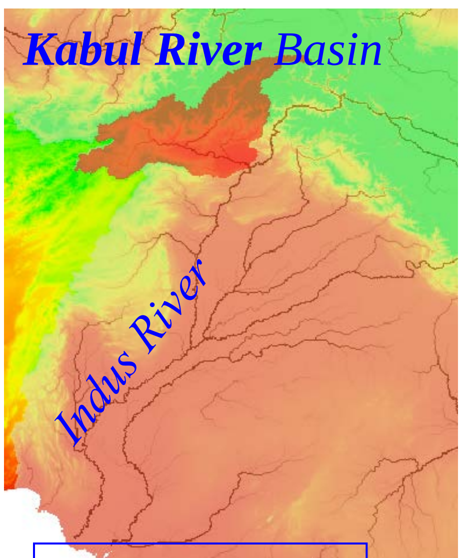

Area: 92,600 km^2
Length: 700 km

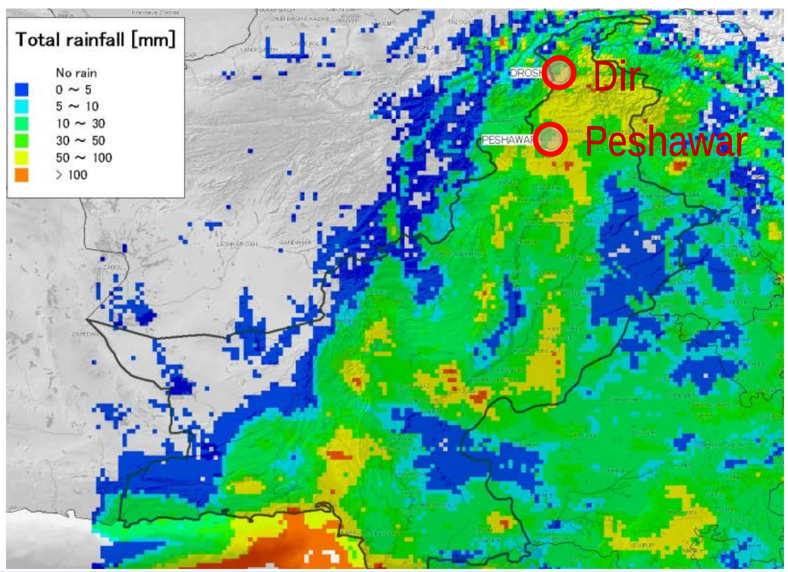

GSMaP_NRT(total amount: 7/27~31)

IFAS-based runoff analysis: Kabul River, Pakistan

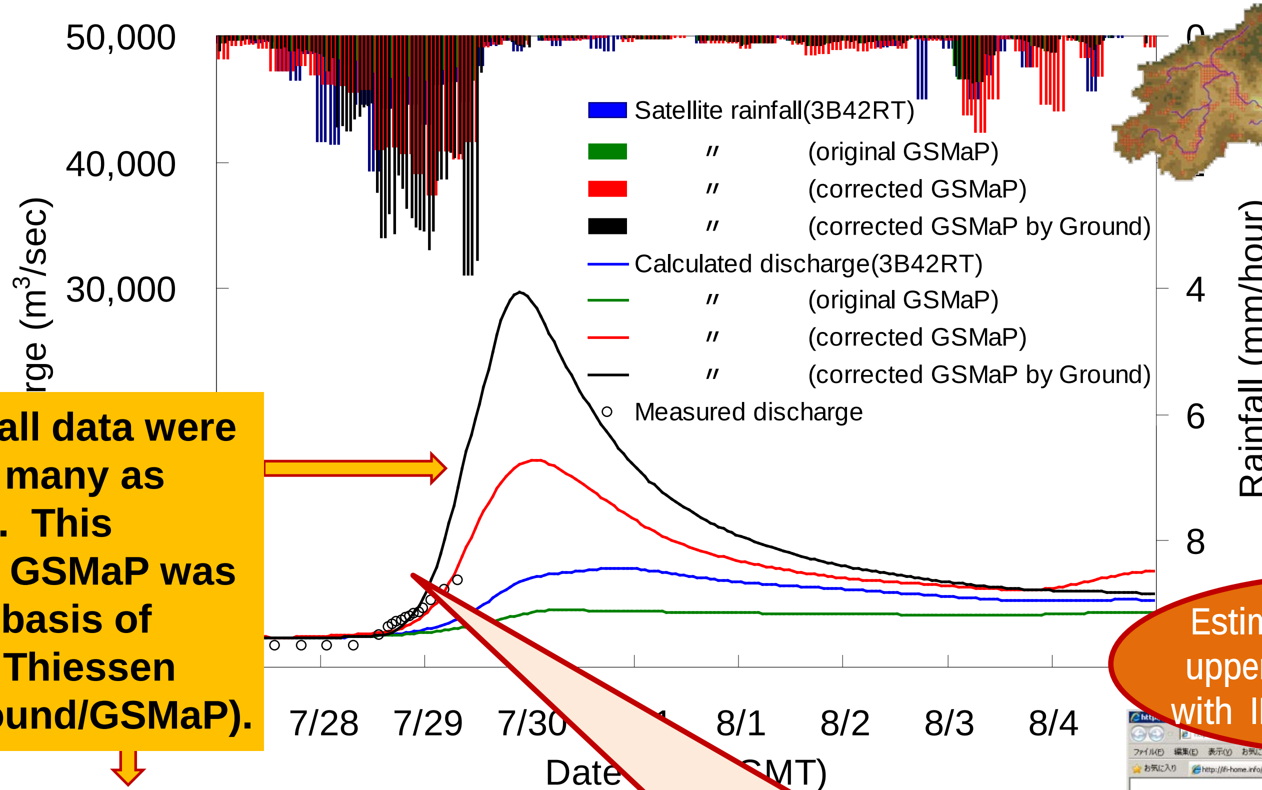

Calculated by
Default parameter

Ground rainfall data were 2~7 times as many as GSMaP ones. This correction of GSMaP was made on the basis of each ratio of Thiessen polygon (Ground/GSMaP).

Estimated hydrographs in upper & middle Indus river with IFAS were on IFI-home

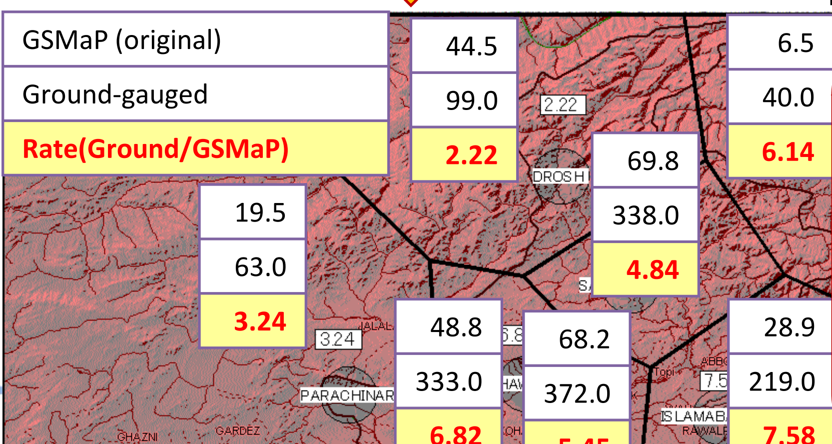

Alghouth the runoff simulation with ICHARM's self-correction algorithm without any ground-based rainfall data seemed best, this does not necessarily mean the truth. In any case, this shows the high potential of satellite-based runoff simulation.

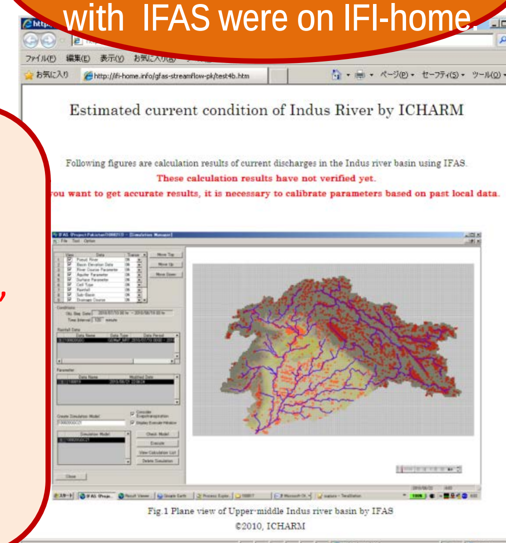

Comparison between satellite-based inundation extent and inundation simulations with another ICHARM's Rainfall-Runoff-Inundation (RRI) Model for Pakistan flood, August 2010

Runoff-inundation simulation can **interpolate <u>missing</u> satellite-based information** on flood inundation area caused by flash flood.

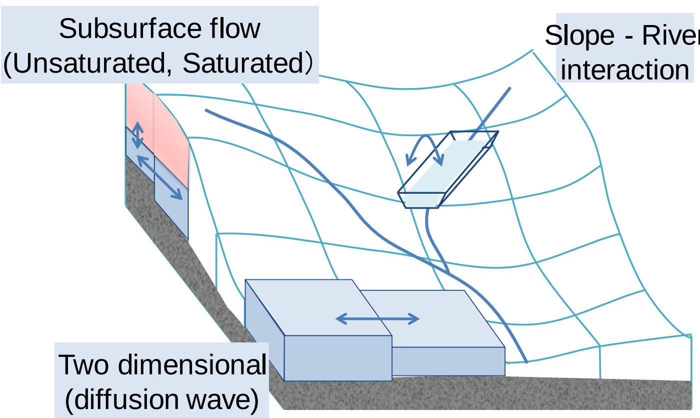

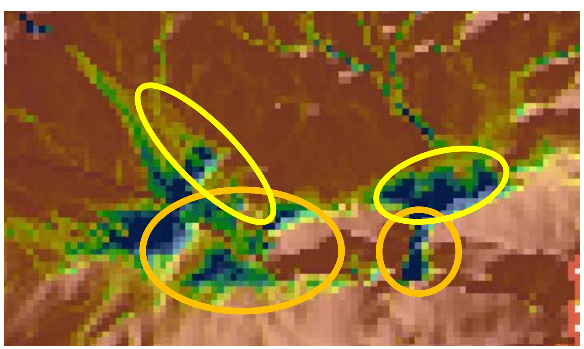

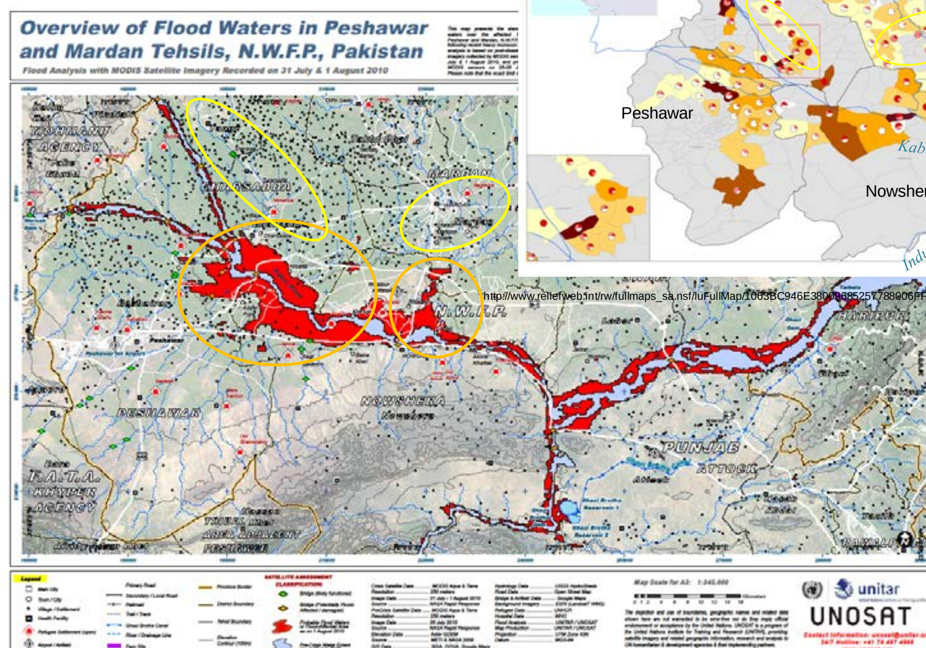

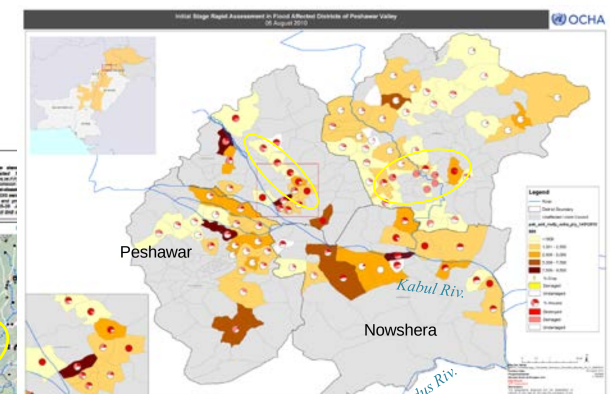

http://www.reliefweb.int/rw/fullmaps_sa.nsf/luFullMap/1003BC946E3800...B5257788006FF75B/$File/map.pdf?OpenElement

Sayama et al. (2011)

Rainfall downscaling & forecasting with different initial conditions

Ushiyama et al. (2011)

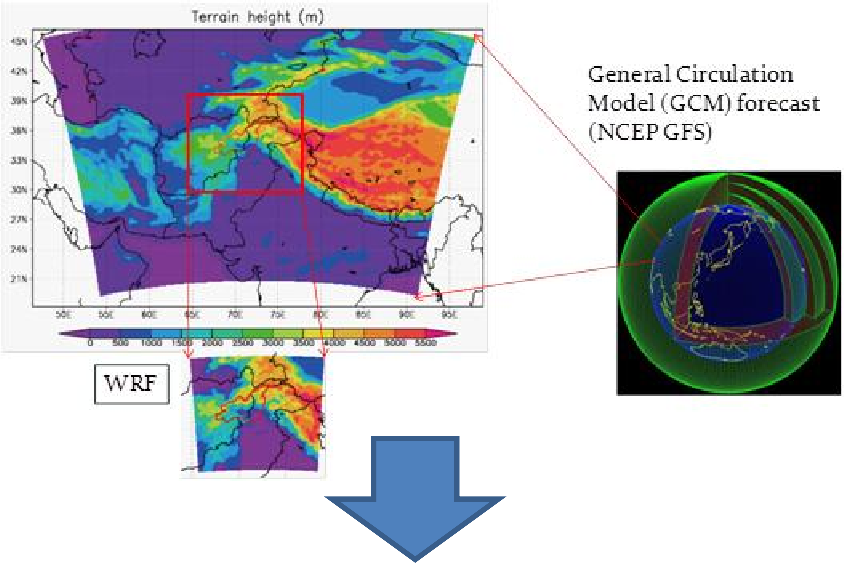

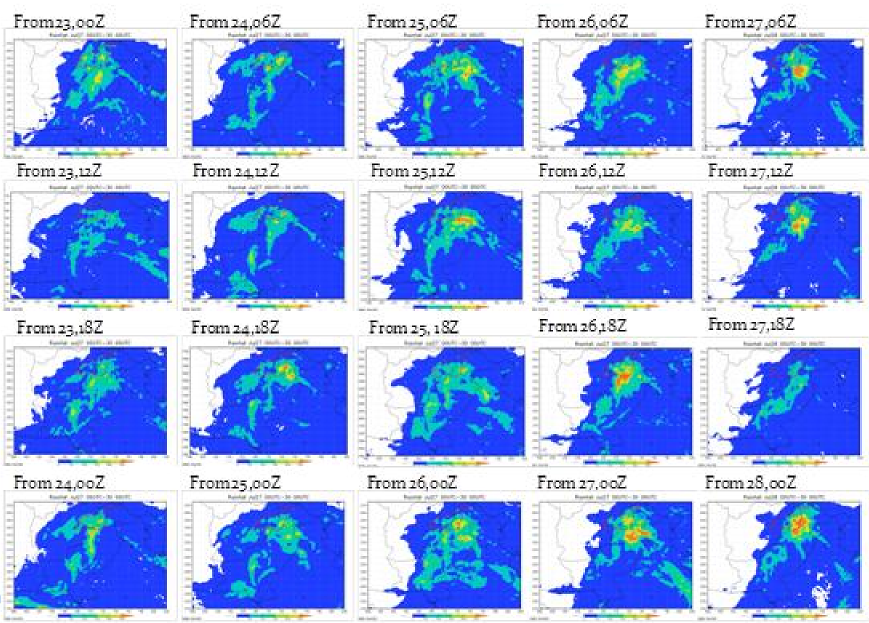

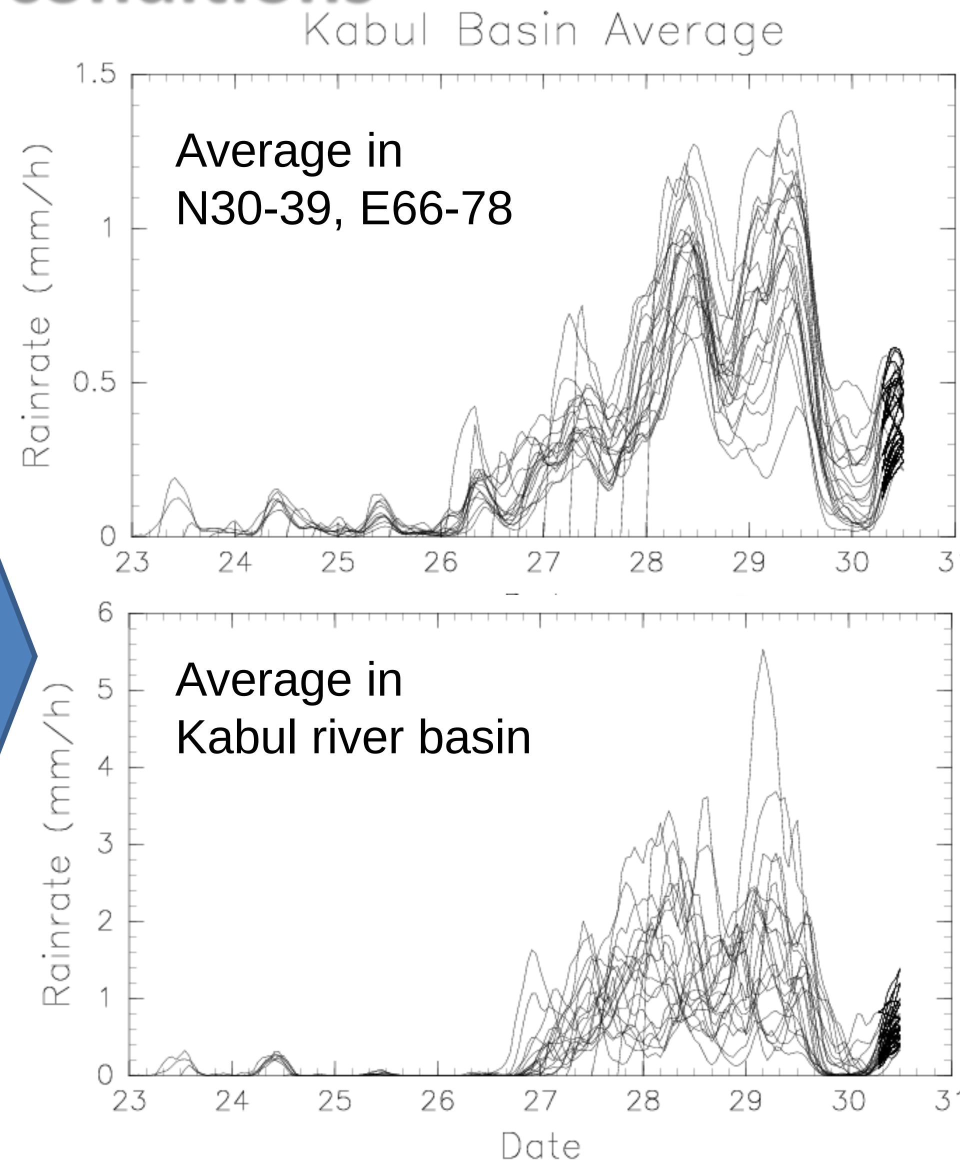

Ensemble of rainfall forecast with WRF

Ensemble inundation forecast with RRI Model

Hydrograph at Kabul
Frequency distribution by 13 members

Inundation probability
The ratio of members which maximum water depth exceed 1m.

Forecast at July 26
(23 00Z -26 00Z)

Input predicted rainfall of 13 members.

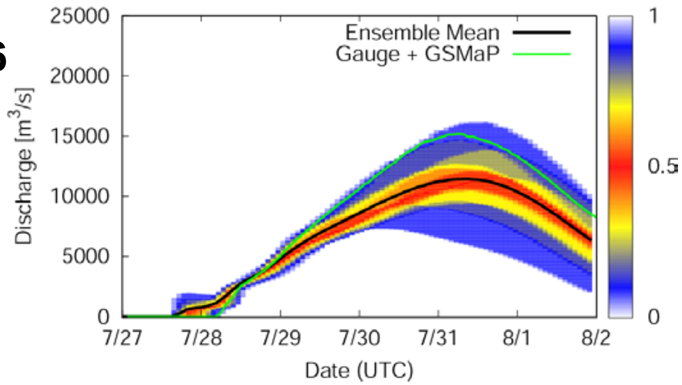

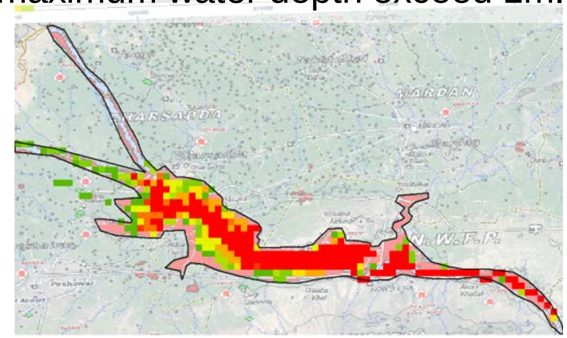

Forecast at July 27
(24 00Z -27 00Z)

✓ Ensemble members with initial condition before the beginning of rainfall gave better ensemble mean and probability range.

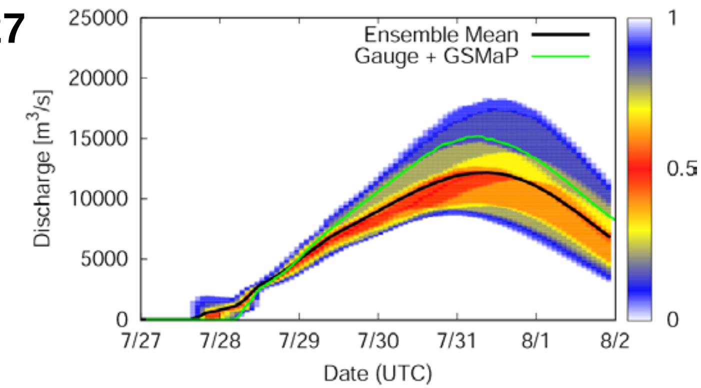

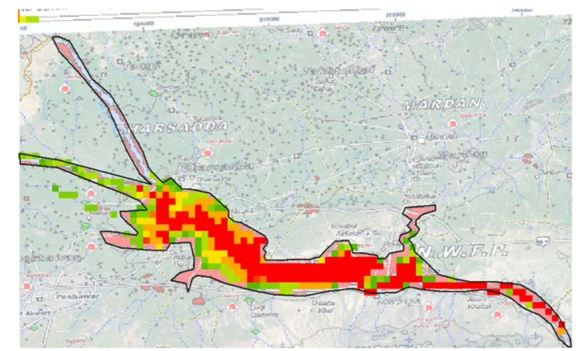

Forecast at July 28
(25 00Z -28 00Z)

✓ Ensemble members with their initial conditions during the rainfall period had large variance.

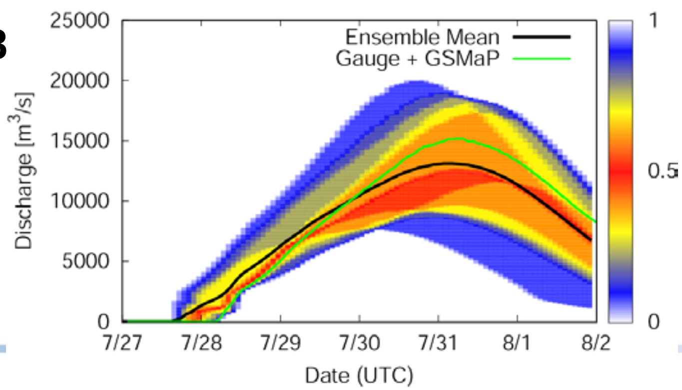

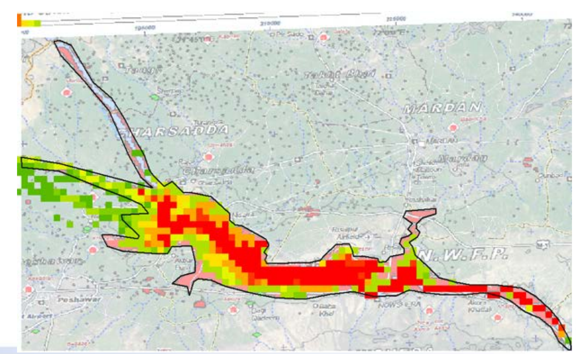

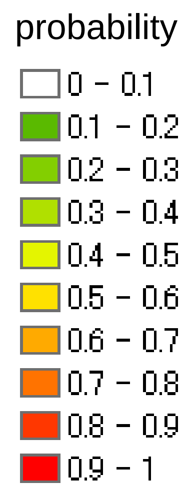

Ushiyama et al. (2011)

Development of another new-generation hydrology / hydraulics coupled model for large-scale river basins

~ Rainfall-Runoff-Inundation (RRI) Model and its high potential ~

ICHARM

ICHARM

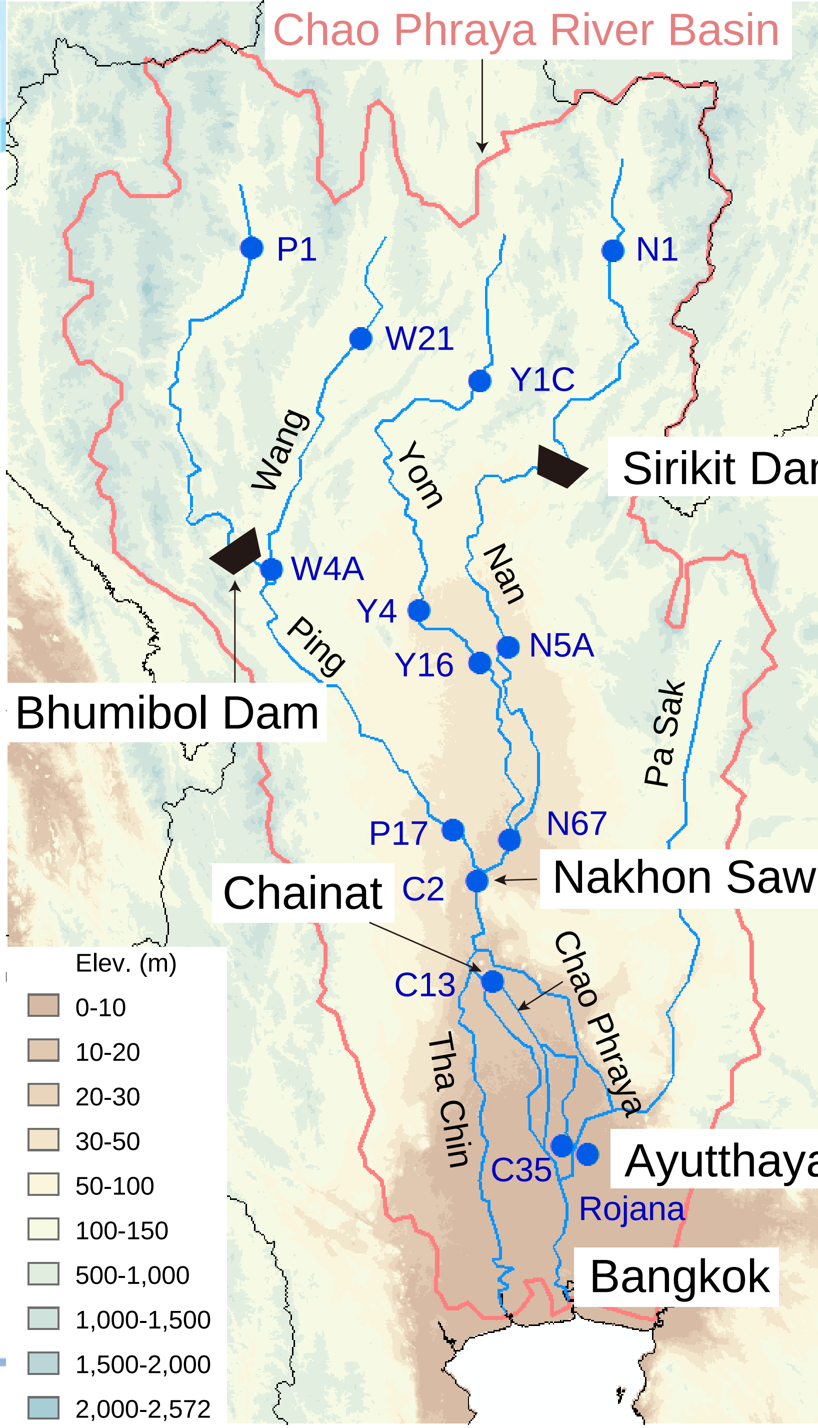

Chao Phraya River Basin

Area	160,000km^2
Length	800 km
Slope	1/50,000 ~ 60,000 (Ayutthaya – River Mouth)
Dam	Bhumibol : 13.5 Billion m^3 Sirikit : 9.5 Billion m^3

Outline of 2011 Thailand Flooding

Rainfall	May - Oct. : 1372 mm (140% of Ave.) Five typhoons and tropical low pressure systems
Peak Discharge	4,680 m^3/s on Oct. 14, 2011 (5,960 m^3/s in 2006)
Inundation Vol.	Approx. 10,000 km^2, 10.0 Bill. m^3
Damage	Deaths and missing : 678 Affected people : 1.35 Million Damage and loss : 45.7 Bill. USD

ICHARM

Rainfall-Runoff-Inundation Model (1/3)

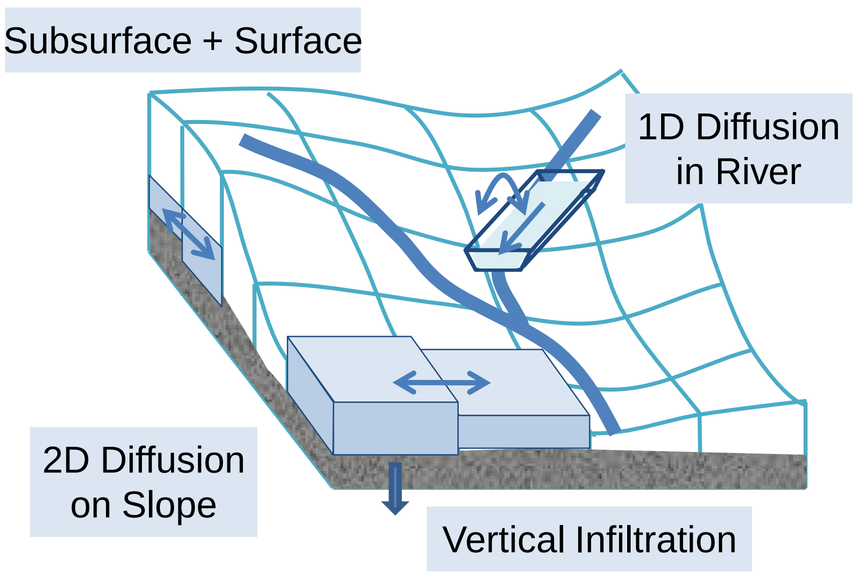

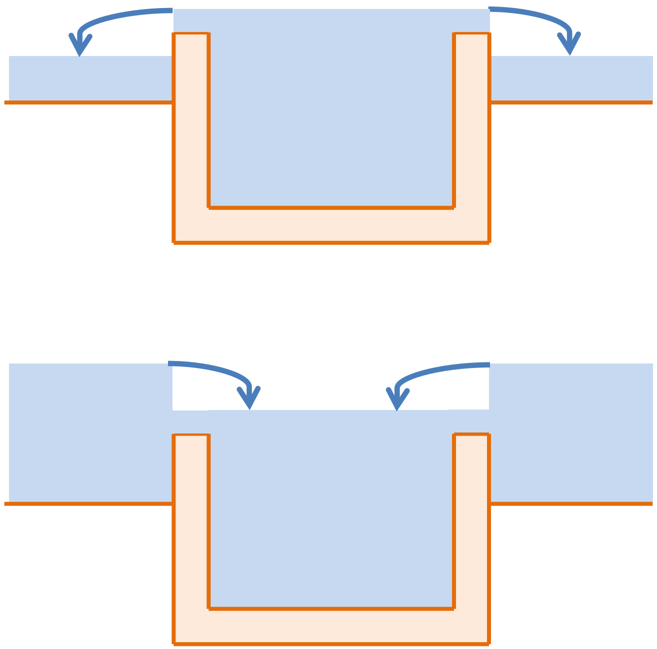

- Diffusion Wave Approximations
  - 1D in River
  - 2D on Slope
- Subsurface flow
  - Vertical Infiltration with Green Ampt
  - Saturated Subsurface + Surface Flow

- Rectangular river cross sections
  - Width, Depths, Levee heights can be assigned for each river grid-cells
- Over-topping and step-down formulae are used to compute the interactions between water in river and on slope
- Water depth and discharge boundary conditions can be wet at any grid-cell

Sayama, T. et al.: Rainfall-Runoff-Inundation Analysis of Pakistan Flood 2010 at the Kabul River Basin, *Hydrological Sciences Journal*, 57(2), pp. 298-312, 2012.

Rainfall-Runoff-Inundation Model

Subsurface + Surface

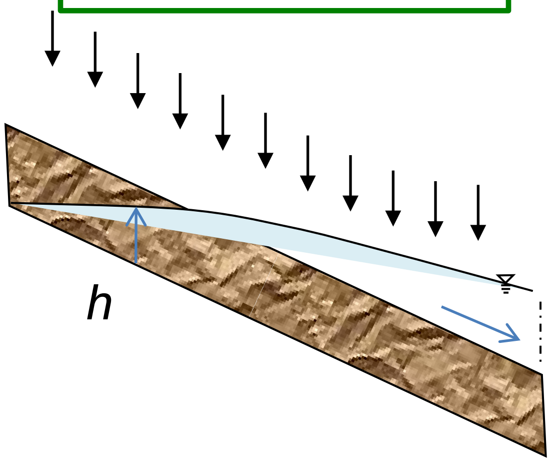

Vertical Infiltration

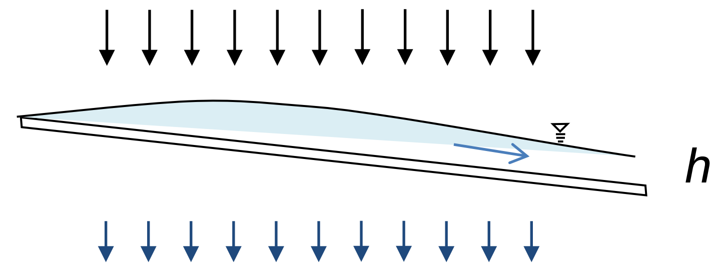

Infiltration : Green Ampt Model

$$q_x = \begin{cases} -kh\dfrac{\partial H}{\partial x}, & (h \le d) \\ -\dfrac{1}{n}(h-d)^{5/3}\sqrt{\left|\dfrac{\partial H}{\partial x}\right|}\,\mathrm{sgn}\left[\dfrac{\partial H}{\partial x}\right] - k(h-d)\dfrac{\partial H}{\partial x}, & (d < h) \end{cases}$$

Takasao & Shiiba (1981)

$$f = k_v\left[1 + \frac{(\phi - \theta_i)S_f}{F}\right]$$

$$q_x = -\frac{1}{n}h^{5/3}\sqrt{\left|\frac{\partial H}{\partial x}\right|}\,\mathrm{sgn}\left[\frac{\partial H}{\partial x}\right]$$

Rainfall-Runoff-Inundation Model (2/3)

Typical Distributed R-R Model

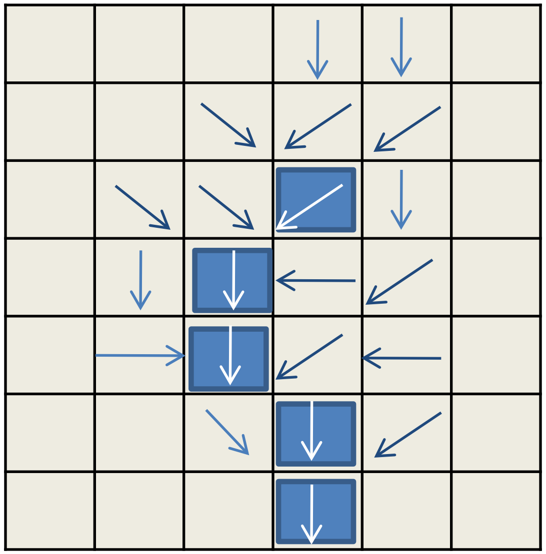

2D Diffusion Model --- Slope of water level controls flow direction and velocity (RRI)

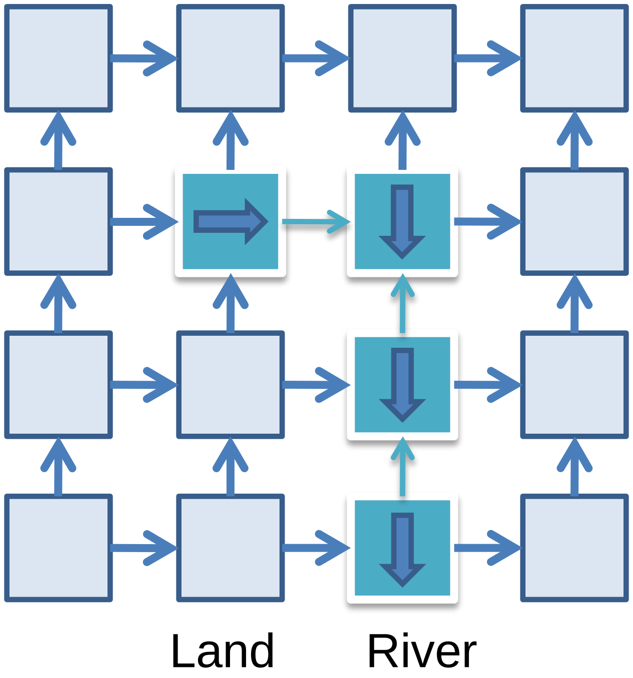

Rainfall-Runoff-Inundation Prediction of Thailand Flood 2011 (conducted on 2011/10/14)

Simulation Domain : 163,293 km^2
Grid Size : 60sec (1776 x 1884 m)
Simulation Period :
2011/07/01 0:00 (UTC) – 2011/11/30 0:00 (UTC)
Input Rainfall:
✓2011/07/01 0:00 (UTC) – 2011/11/8 0:00 (UTC)
3B42RT (Satellite Based Rainfall)
(Every 3hours, Spatial Resolution: 0.25 deg)
✓2011/11/8 6:00 (UTC) – 2011/11/15 12:00 (UTC)
JMA- GSM Weekly Weather Forecasting
（Forecasting Lead Time: 8 days, Update every 12 hours）
✓2011/11/15 15:00 (UTC) – 2011/11/30 0:00 (UTC)
(Previous year's 3B42RT rainfall in the same period)

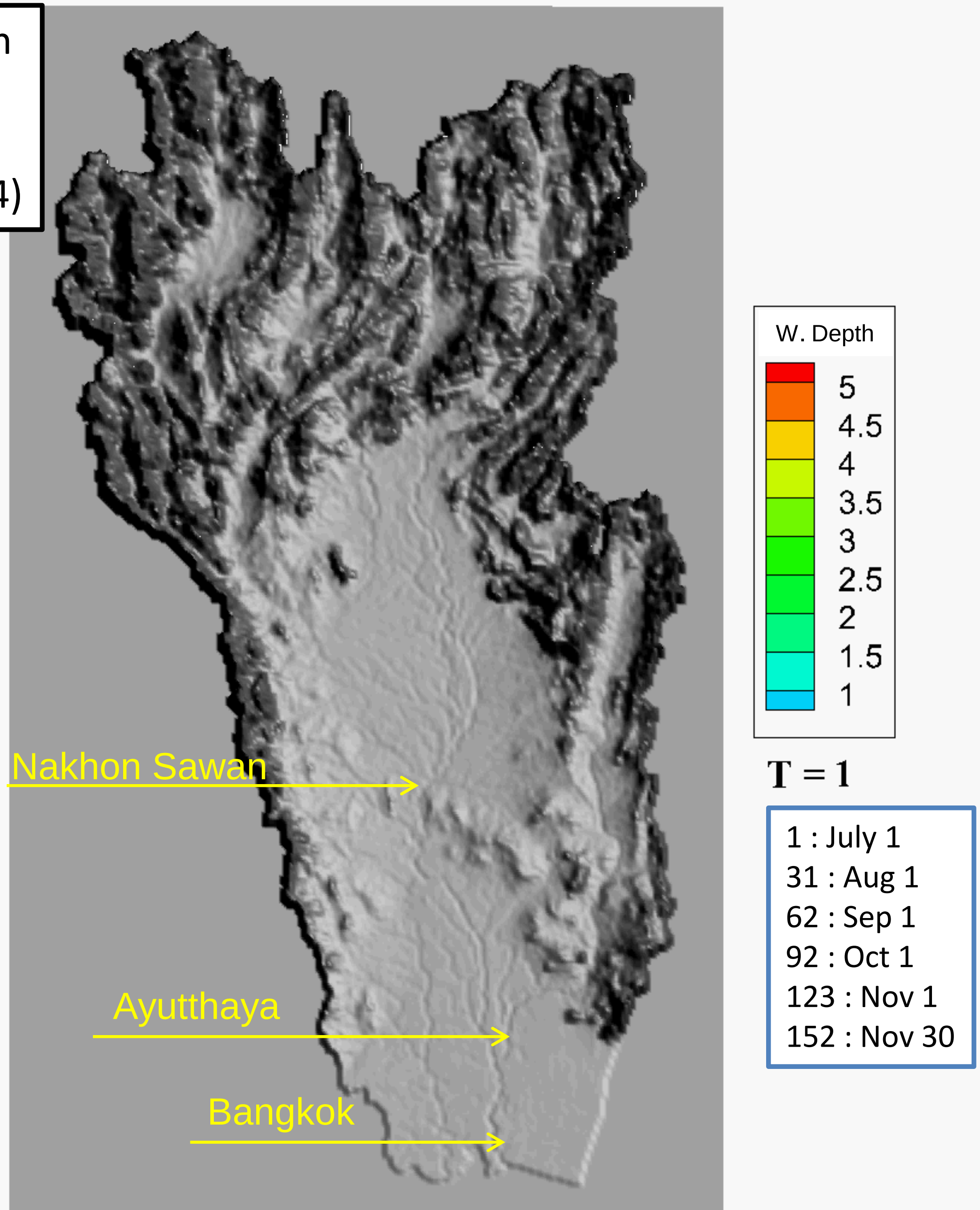

http://www.icharm.pwri.go.jp/news/news_j/111024_thai_flood_j.html

Emergency response-type prediction (Lv1) and Post flooding simulation with more local data (Lv2)

	Lv1		Lv2	
入力降水量	衛星雨量＋予測雨量		地上雨量補正後の衛星雨量	
蒸発散量	考慮なし		流域一様 (4 mm/d) で設定	
ダム	考慮なし		ダムモデルの導入	
下流端境界条件	河床勾配 ＝ 動水勾配を仮定		天文潮位	
河道断面	流域面積の関数として設定		断面情報をもとに設定	
パラメータ	山地	平野	山地	平野
n [$\mathrm{m}^{-1/3}\mathrm{s}$]	0.3	0.3	0.35	0.35
d [m]	0.3	-	0.3	-
k [m/s]	0.1	-	0.1	-
k_v [cm/h]	-	0.2	-	0.06
ϕ	-	0.471	-	0.475
S_f	-	0.273	-	0.316
F_{limit} [m]	-	0.4	-	0.4
n_{river} [$\mathrm{m}^{-1/3}\mathrm{s}$]	0.03	0.03	0.03	0.03

注 1） Lv1 のパラメータは Case 4 の値を表示

注 2） Case 1 と 3 は斜面粗度 n を 0.15 [$\mathrm{m}^{-1/3}\mathrm{s}$]，Case 1 と 2 は河道粗度 n_{river} を 0.015 [$\mathrm{m}^{-1/3}\mathrm{s}$] に設定した．

注 3） k_v，ϕ，S_f は Green Ampt モデルのパラメータであり Lv1 は Silty Clay Loam，Lv2 は Clay に相当[11]．

注 4） F_{limit} は積算鉛直浸透量の最大値．

Sayama et al. (2012)

River Discharges

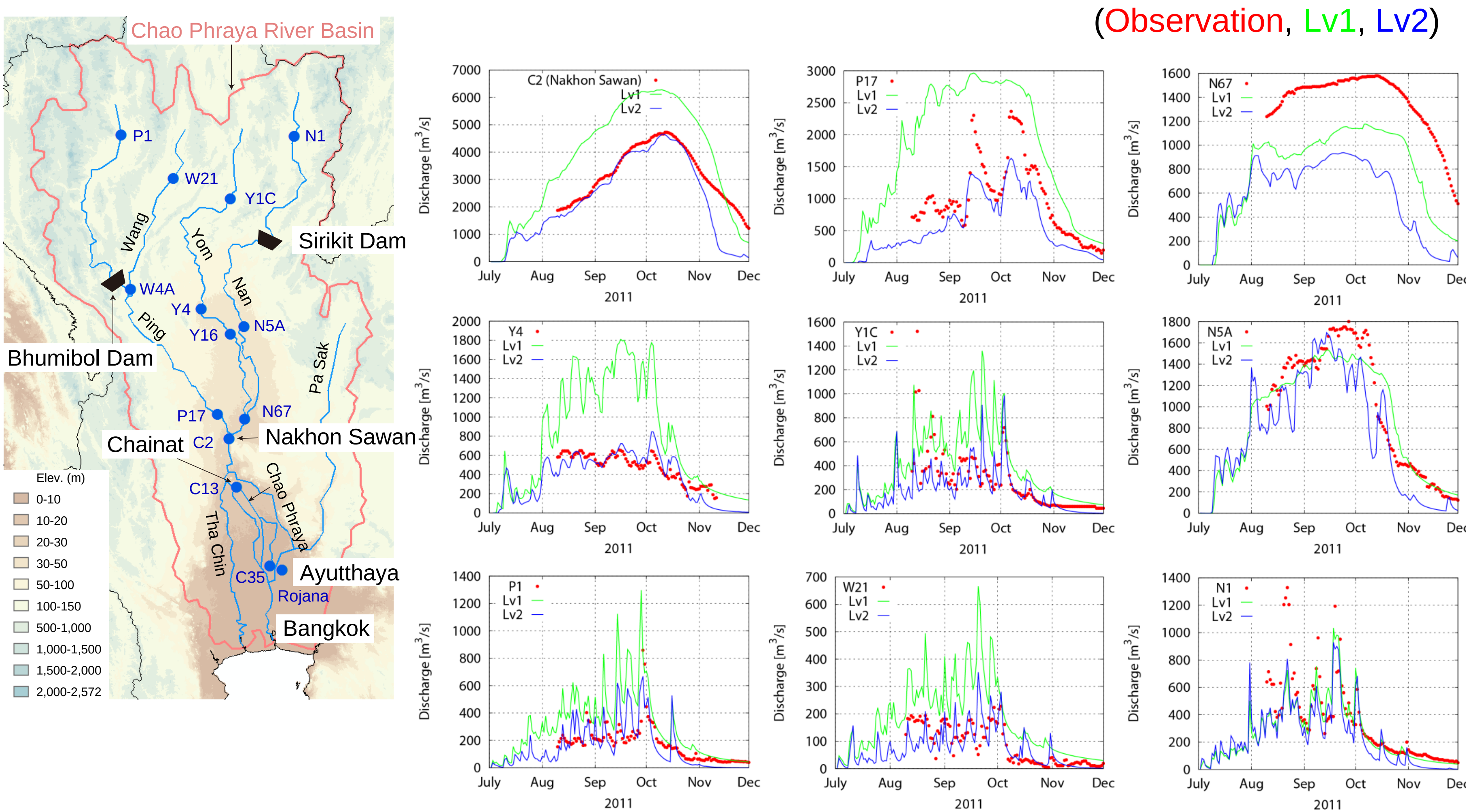

Emergency response-type prediction (Lv1) and post flooding simulation with more local data (Lv2)

Sayama et al. (2012)

Peak water levels

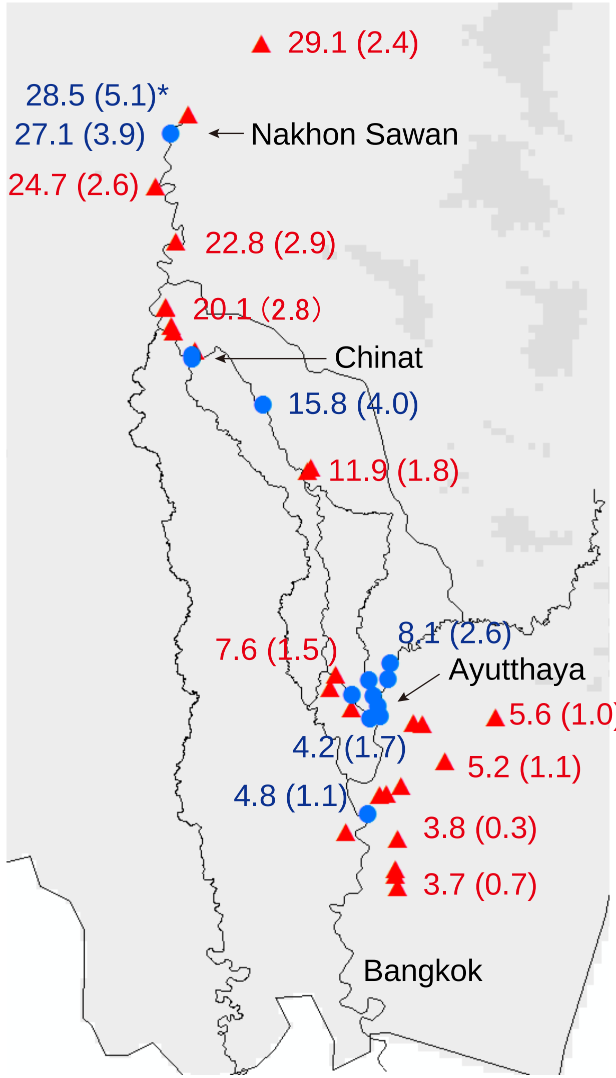

Red: Land, Blue: River Peak water level
(Reduced water level by the end of November)

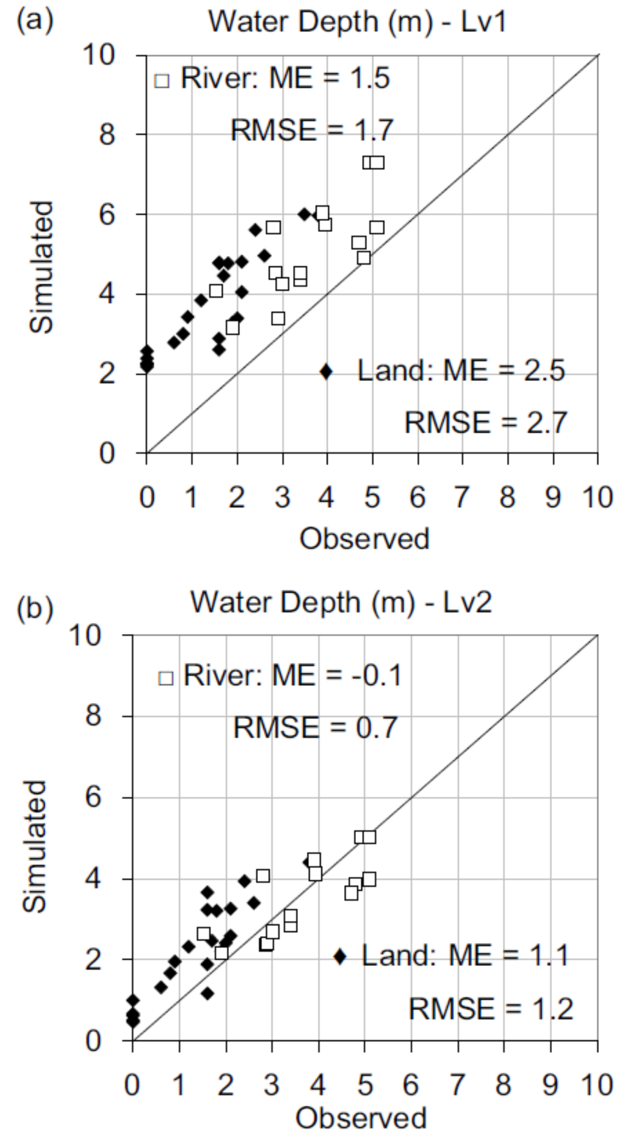

Sayama et al. (2012)

Inundation extents

F: $$\frac{IA_{obs} \cap IA_{sim}}{IA_{obs} \cup IA_{sim}}$$

- Lv2 slightly under-estimates inundation extents
- Water levels in river and on floodplain become independent, becomes difficult to simulate

Spatial distribution of cumulative rainfall during July and October 2010

(a) Satellite-based rainfall for Lv.1 (NASA-3B42RT), (b)Satellite-ground-coupled rainfall for Lv.2

(Yellow plots show the locations of the ground-based rainfall stations used for the modification)

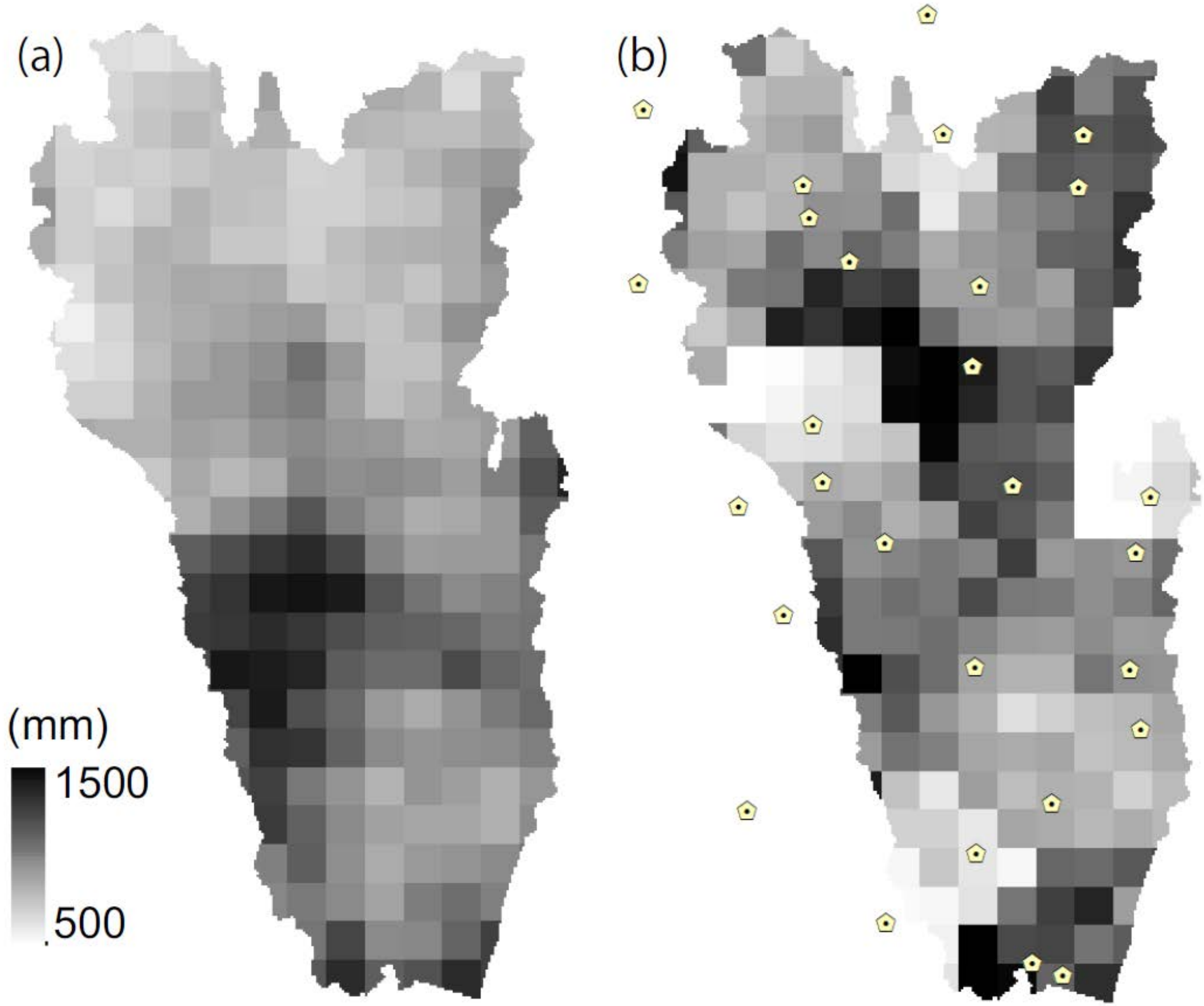

Cumulative and daily basin-averaged rainfall from July to December 2011

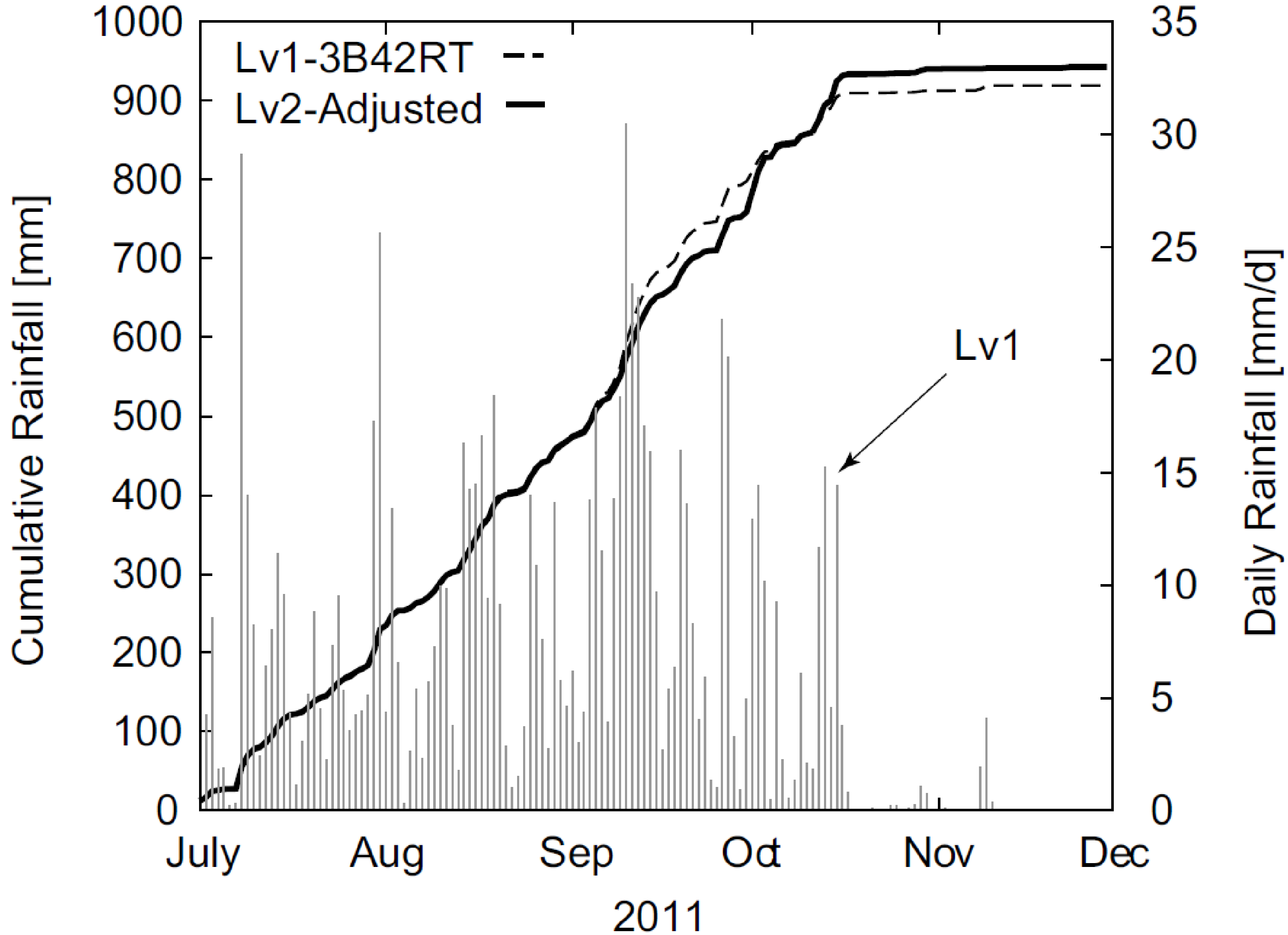

Effect of different input information (sensitivity analysis)

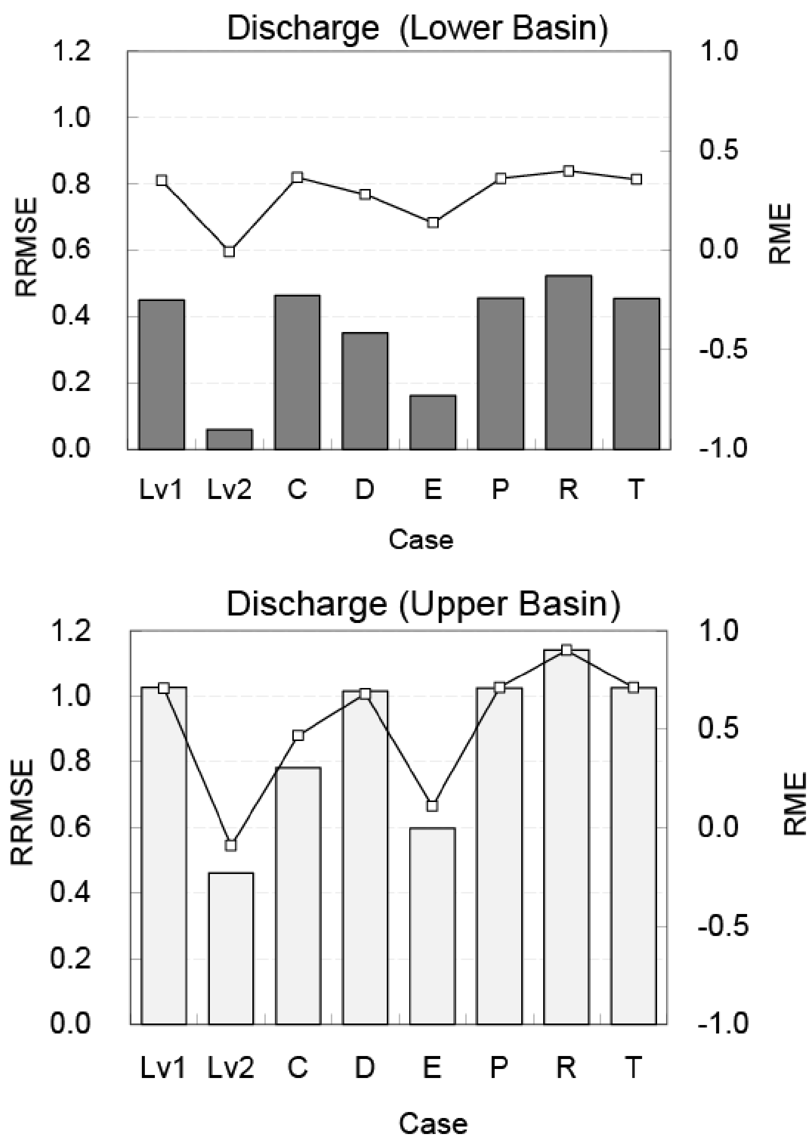

Errors in simulated river discharges with different types of input updates from Lv1

Lv 2: All
C: Cross section
D: Dam
E: ET (Evapotranspiration
P: Parameters
R: Rainfall
T: Tide

Overestimation in Lv1 was primary due to the ignorance of ET !

Ongoing projects
for practice and operation

UNESCO Project (2 years: 2012-14)
Strategic Strengthening of Flood Warning and Management Capacity of Pakistan

United Nations
Educational, Scientific and
Cultural Organization

A. Strategic Augmenting of Flood Forecasting and Hazard Mapping Capacity

A-1 Development of Indus IFAS

A2- Floodplain and Hazard Mapping of Lower Indus

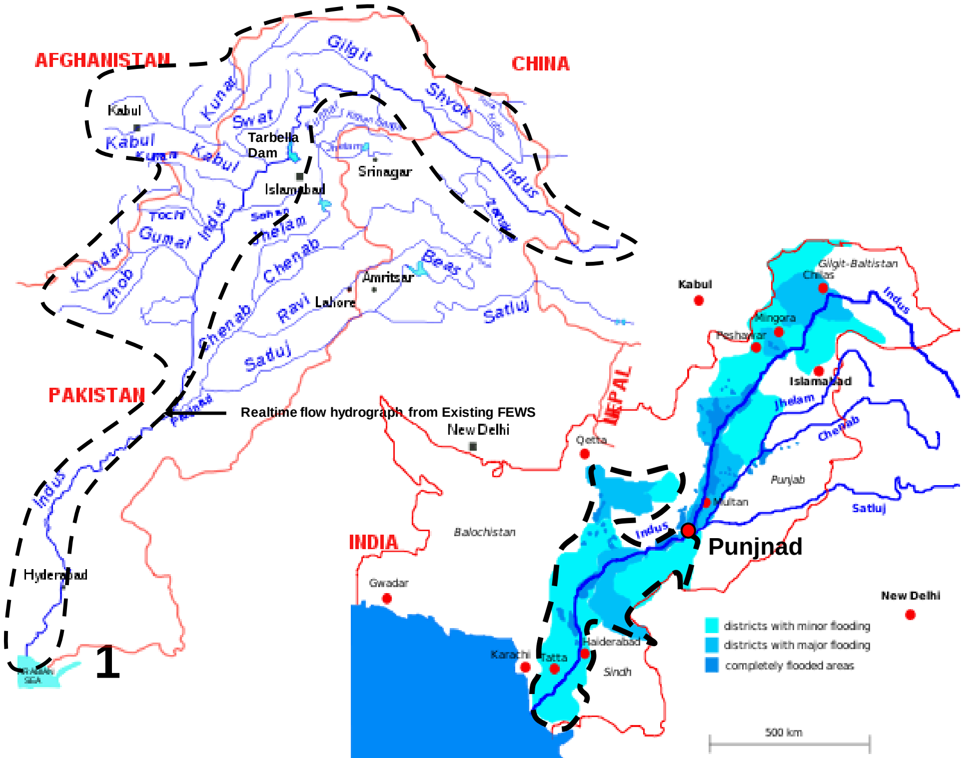

B. Knowledge Platforms for Sharing Transboundary Data and Community Flood Risk Information

B1. International Networking for Sharing of Transboundary Data

B2. Knowledge platform for timely national, provincial and district level data sharing

C. Capacity Development for Flood Forecasting and Hazard Mapping

- Master's Degree training at ICHARM for PMD, SUPARCO and FFC on flood forecasting/warning, hazard mapping and integrated flood management
- A short training course at ICHARM on IWRM and integrated flood management
- Training workshops in Pakistan conducted by UNESCO Islamabad

Example of Implementation Project for flood early warning system with satellite-based information

ADB-RETA 7276 in Indonesia to implement IFAS-based flood forecasting and warning system for the Bengawan Solo River

(FY2009-2012)

JST-JICA SATREPS Project on Research and Development for Reducing Geo-Hazard Damage in Malaysia caused by Landslide & Flood

(FY2011-2015)

Flood in Dec.2007

Training Workshop with BBWS Solo in March, 2010

Major target river basin for flood: Kelantan River

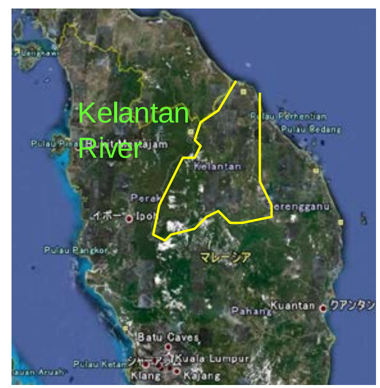

Wide-range analysis: IFAS

High-res. analysis: GETFLOWS

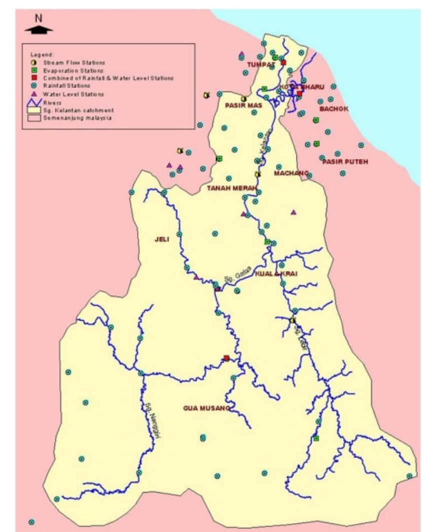

Dissemination activities
and
final remarks

ICHARM Website to download IFAS (IFAS-PDHM Ver.1.2 & 1.3β)

http://www.icharm.pwri.go.jp/index.html

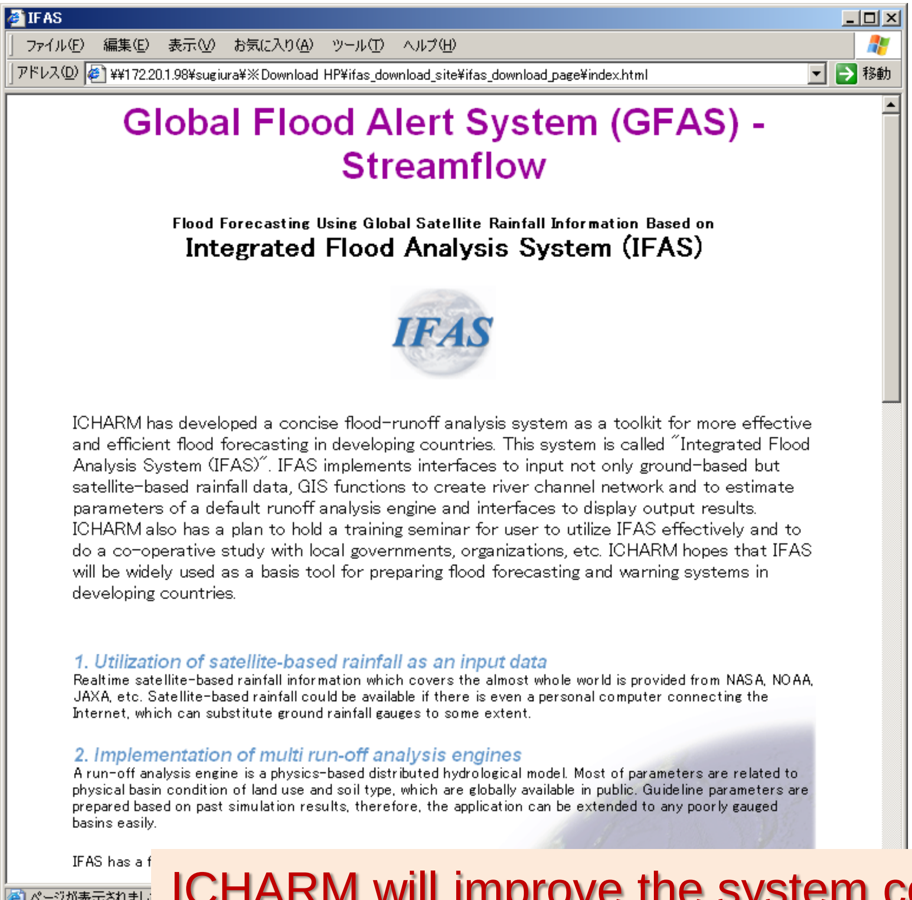

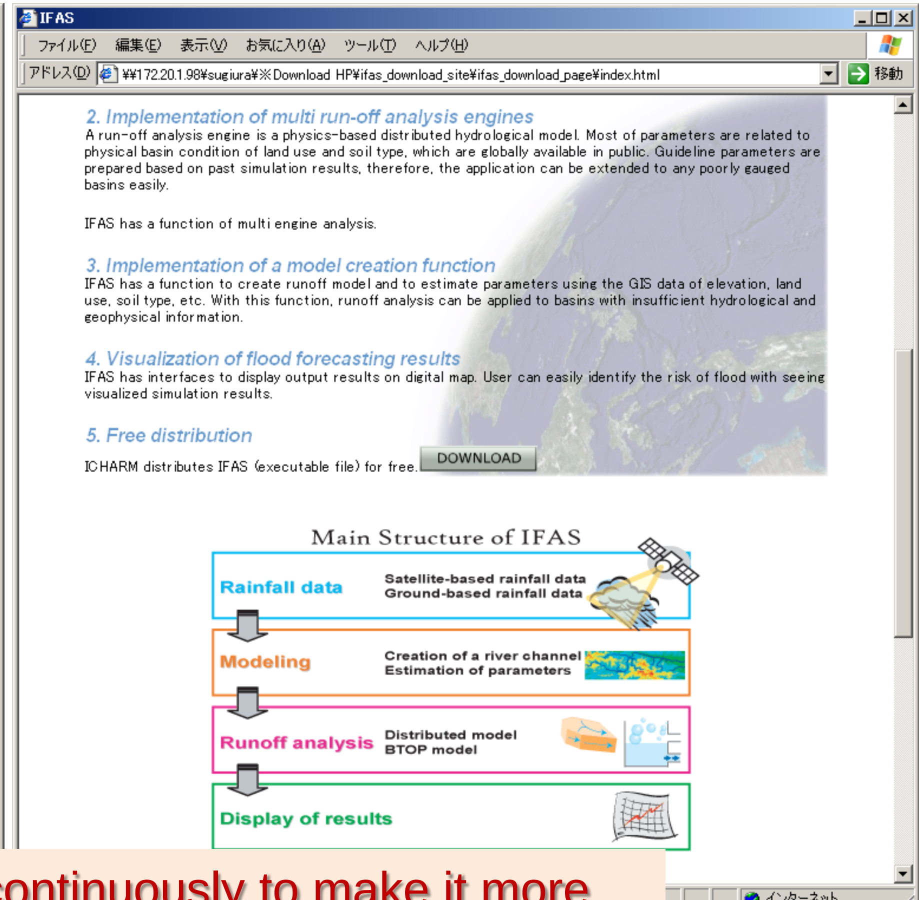

ICHARM will improve the system continuously to make it more user-friendly software and contribute to flood mitigation at local communities.

ICHARM

IFAS Training workshops (2008 – 2011)

- Purpose of the training course

  To build capacities to undertake hydrological prediction/forecasting in relatively ungauged basins using satellite-based rainfall.

Program

•Remote Sensing of Precipitation from Space (JAXA)
•Introduction of river administration in Japan
•Introduction of Global Flood Alert System
•Operating procedures for IFAS
•Validation method of satellite-based rainfall
•Current conditions and problems in each country

- International Workshop on Application and Validation of GFAS

  2008: Ethiopia, Zambia, Cuba, Argentina, Bangladesh, Guatemala, Nepal (7countries)

  2009: India, Indonesia, Viet Nam, Bangladesh, Nepal, Laos (6countries)

- IFAS Seminars in overseas (sponsored by ADB, JAXA, UNESCAP, UNESCO-IHP,etc.)

  Nepal (2009), Indonesia, Myanmar, Vietnam (2010),

  Pakistan, Vietnam, India (2011), Iran, Vietnam and Indonesia(2012)

- Training seminars at ICHARM Master Course & JICA short courses

IFAS to enhance local ownership of flood forecasts & in-situ hydrological observation network on the ground

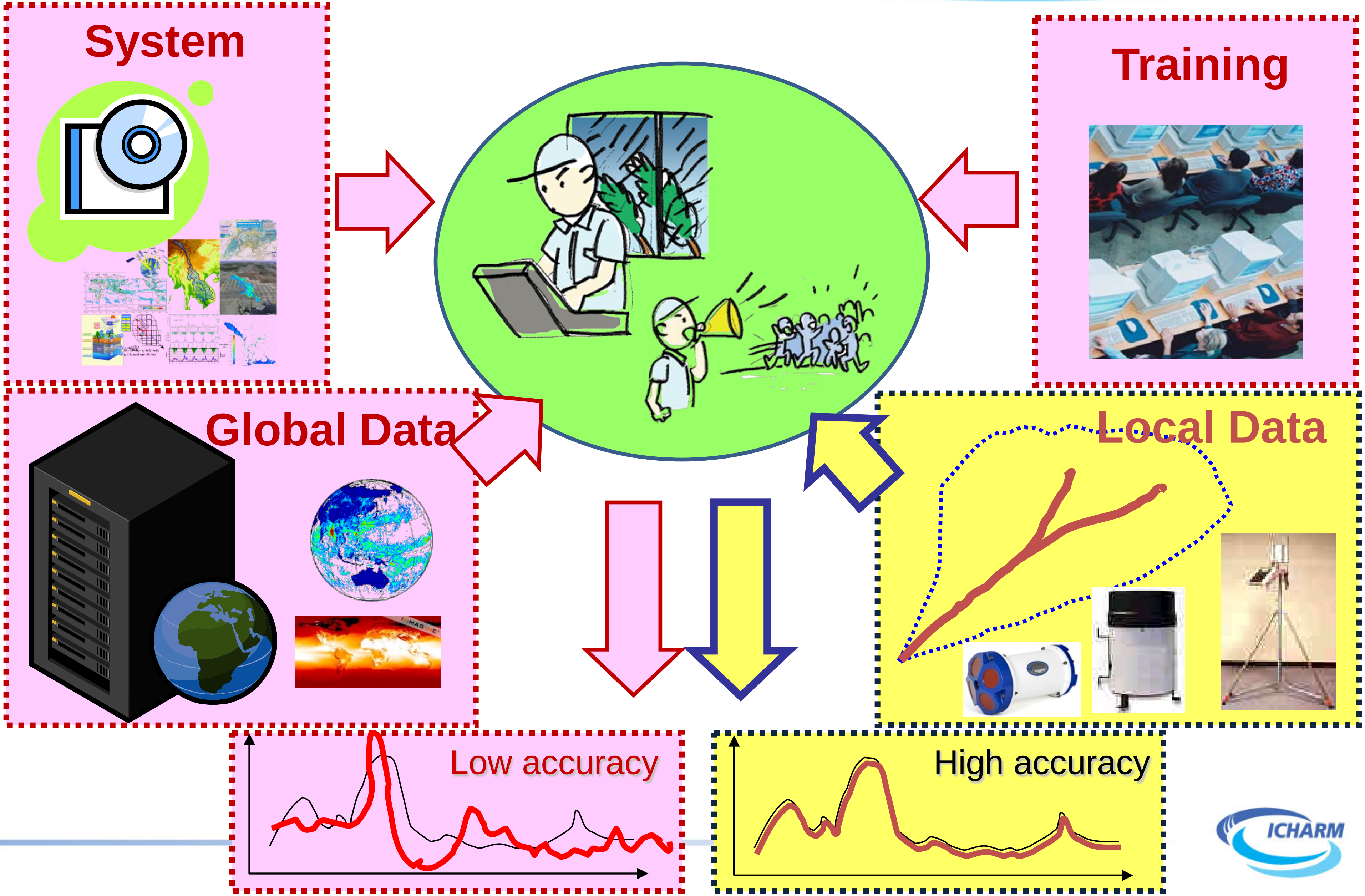

Conclusion (1/2)

- The combination of satellite-based rainfall information, global GIS data and IFAS (Integrated Flood Analysis System), as a practical toolkit for local users, especially in poorly-gauged river basins to integrate all those global information easily, has very high potential to promptly & efficiently implement flood analysis & forecasting system, in consideration with further step-by-step improvements in the future.
- RRI model has also high potential for large-scale flood and inundation hazard forecasting and mapping in poorly-gauged river basins, although the RRI model has not been designed for simple operational use.
- Key minimal information can be acquired through satellite-based and global-GIS-based IFAS / RRI simulations even if the accuracy is not enough from the perspective of the exact coincidence of hydrograph, water level and/or flooding area.

Conclusion (2/2)

- On the other hand, it should be also noted that, without any in-situ (ground-truth) data, such integrated information & analysis cannot be assured, verified nor improved.
- It is, therefore, indispensable to couple satellite, global GIS and possibly numerical meteorological simulation data with in-situ (geographical, geophysical and hydrologic) data in order to improve the quality (accuracy) of the integrated information & analysis and to upgrade the range & depth of application, which will lead to the establishment of local ownership of flood forecasting and warning.